PNNL-14168

Pacific Northwest
National Laboratory
Operated by Battelle for the
U.S. Department of Energy

Capstone Depleted Uranium Aerosols: Generation and Characterization

Volume 1. Main Text

Attachment 1
of
Depleted Uranium Aerosol Doses and Risks:
Summary of U.S. Assessments

M. A. Parkhurst,
Principal Investigator
F. Szrom
R. A. Guilmette
T. D. Holmes
Y. S. Cheng
J. L. Kenoyer
J. W. Collins
T. E. Sanderson
R. W. Fliszar
K. Gold
J. C. Beckman
J. A. Long

October 2004

Prepared for the U.S. Department of the Army
under a Related Services Agreement
with the U.S. Department of Energy
under Contract DE-AC06-76RL01830

DISCLAIMER

PACIFIC NORTHWEST NATIONAL LABORATORY
operated by
BATTELLE
for the
UNITED STATES DEPARTMENT OF ENERGY
under Contract DE-AC06-76RL01830

Printed in the United States of America

Available to DOE and DOE contractors from the
Office of Scientific and Technical Information,
P.O. Box 62, Oak Ridge, TN 37831-0062;
ph: (865) 576-8401
fax: (865) 576-5728
email: reports@adonis.osti.gov

Available to the public from the National Technical Information Service,
U.S. Department of Commerce, 5285 Port Royal Rd., Springfield, VA 22161
ph: (800) 553-6847
fax: (703) 605-6900
email: orders@ntis.fedworld.gov
online ordering: http://www.ntis.gov/ordering.htm


This document was printed on recycled paper.
9/2003

PNNL-14168

Capstone Depleted Uranium Aerosols: Generation and Characterization

Volume 1. Main Report

M. A. Parkhurst,[a] Principal Investigator
F. Szrom[b]
R. A. Guilmette[c]
T. D. Holmes[d]
Y. S. Cheng[e]
J. L. Kenoyer[f]
J. W. Collins[b]
T. E. Sanderson[f]
R. W. Fliszar[g]
K. Gold[g]
J. C. Beckman[f]
J. A. Long[f]

October 2004

Prepared for the U.S. Department of the Army
under a Related Services Agreement
with the U.S. Department of Energy
under Contract DE-AC06-76RL01830

Pacific Northwest National Laboratory
Richland, Washington 99352

(a) Pacific Northwest National Laboratory
(b) U.S. Army Center for Health Promotion and Preventive Medicine
(c) Lovelace Respiratory Research Institute, currently of U.S. Army, Aberdeen Test Center
(d) Lovelace Respiratory Research Institute
(e) Pacific Northwest National Laboratory, currently of Dade Moeller & Associates, Inc.
(f) U.S. Army, Aberdeen Test Center, Aberdeen Proving Ground
(g) U.S. Army, TACOM-Armament Research, Development, and Engineering Center

Summary

Armor-piercing, depleted-uranium (DU) munitions were used by the U.S. Armed Forces on the battlefield for the first time during the 1991 Gulf War Operation Desert Storm (ODS).[a] Although the U.S. Army has conducted periodic impact tests on armored targets, the tests involved only limited sampling to characterize the aerosols that form when DU penetrators impact and perforate targets. As a consequence, the available data were insufficient for performing human health risk assessments. To remedy this, the U.S. Department of Defense (DoD) committed to obtaining more complete data about aerosols generated by the impact and perforation of armored vehicles by DU munitions to support a revised and updated personnel exposure assessment and human health risk characterization. The program arising from this commitment is the Capstone DU Aerosol Characterization and Risk Assessment Program consisting of two separate components. The first is the Capstone DU Aerosol Study, in which DU aerosols were generated through perforation of armored target vehicles, and the chemical and physical properties of aerosols generated were characterized. The study methods and results are presented in this report. The second component of the program is the Human Health Risk Assessment, documented in the *Human Health Risk Assessment of Capstone Depleted Uranium Aerosols* (Guilmette et al. 2004).

S.1 Purpose

Under a program jointly sponsored by the Office of the Special Assistant for Gulf War Illnesses, Medical Readiness and Military Deployment (OSAGWI)[b] and the U.S. Army, the Army Heavy Metals Office provided oversight to the Capstone DU Aerosol Study, which was designed to quantify and characterize DU aerosols inside, on, and near Abrams tanks and Bradley Fighting Vehicles (also referred to as Bradley vehicles) struck by large-caliber DU (LC-DU) penetrators. This report, which documents the Capstone study, is the sourcebook of data from which reasonable and appropriate data could be selected for assessing exposure and characterizing human health risks to personnel who were exposed to aerosols during the Gulf War/ODS or potentially could be exposed to aerosols in future military activities. These data are expected to fill many gaps in available aerosol knowledge, thereby helping risk assessors to better estimate the health risks from DU aerosols to affected personnel.

The aerosol data derived from this study provides the basis for modeling input parameters by summarizing the bounds and characteristics of typical aerosols generated by perforating armored vehicles with LC-DU penetrators. The test results will be used to update the human health risk characterizations for OSAGWI Gulf War/ODS exposure scenarios, and to determine if changes in personnel protective measures are warranted to reduce risks to DoD personnel in the future.

S.2 Investigation Team

An independent subject matter expert from Pacific Northwest National Laboratory (PNNL) directed the Capstone DU Aerosol Study. The project staff, known as the Capstone test team, consisted of Army health physicists and engineers from the Aberdeen Test Center (ATC), Aberdeen Proving Ground (APG), Maryland; the U.S. Army Center for Health Promotion and Preventive Medicine (USACHPPM),

(a) ODS is used to differentiate the 1991 Gulf War from the 2003 Operation Iraqi Freedom.
(b) The OSAGWI organization currently is referred to as the Deployment Health Support Directorate.

Aberdeen Proving Ground–Edgewood Area, Maryland; and the U.S. Army Tank-Automotive and Armaments Command, Armament Research, Development and Engineering Center (TACOM-ARDEC), Picatinny Arsenal, New Jersey. Collaborators from outside the Army included health physicists, aerosol specialists, and instrument engineers from Lovelace Respiratory Research Institute (LRRI), Los Alamos National Laboratory (LANL), and PNNL.

An Army steering committee (the Depleted Uranium Research–Integrated Process Team [DUR-IPT]) guided the overall test objectives and test implementation. The U.S. Army Medical Command (MEDCOM) developed a set of Data Quality Objectives (DQOs) for the specific information to be derived from this testing program. An independent nine-member peer review panel provided technical feedback on the project plans and the draft report.

S.3 Study Overview

The Capstone DU Aerosol Study involved the development of scenarios to determine an upper bound on aerosol concentrations and to quantify other aerosol characteristics from actual firing incidents and from possible future engagements. The field tests, which incorporated two target vehicles and various firing angles, were divided into phases so the investigators could separately focus on circumstances 1) that were similar to Gulf War/ODS actions (retrospective exposure scenarios) and 2) that simulated possible future actions (prospective exposure scenarios). The study focused on the quantities and characteristics of aerosols and residues 1) generated inside the vehicles at the time of impact, 2) collected inside the vehicles during and after settling had occurred, and 3) collected outside vehicles struck by DU penetrators. The series of field tests was designed to collect aerosol data for input to radiological and chemical health risk assessments, thereby enabling investigators to estimate a range and an upper bound of aerosol concentrations, and their associated characteristics, that would be generated from shot lines similar to those that occurred during the Gulf War/ODS and those that might occur during future conflicts.

Four field-test phases were conducted at the ATC DU Containment Facility (“Superbox”), which is a 25.6-m (84-ft) diameter, half-sphere vessel/dome with auxiliary components and facilities that protect the environment by containing contaminants generated from targets impacted by DU (or non-DU) munitions (see Figure S.1). Phase-I tests fired at a ballistic hull and turret (BHT) version of an Abrams tank (without DU armor) and recreated shot lines from the Gulf War/ODS as well as simulating possible future firing incidents. Phase-II tests fired at a Bradley vehicle, primarily recreating experiences from the Gulf War/ODS. An Abrams tank BHT with DU armor was used as the target in the Phase-III tests, while Phase-IV testing was performed in conjunction with a congressionally mandated testing program that used an operational Abrams tank with DU armor as the target. Phases III and IV simulated possible future firing incidents. Each phase featured specific vehicle configurations and scenarios that defined the instrument setup in and around the vehicles and the target impact points needed to achieve specific entry and exit angles for observation and collection of data.

The munition used for all shot tests in Phases I, II, and III was a LC munition with a DU penetrator. The Phase-IV test used a variety of munitions, only one of which was a DU munition, which was specifically relevant to the Capstone study. The projectiles were fired from a fixed-gun position. In addition to the selection of shot lines, priorities in testing included preserving instrumentation and maximizing generation of aerosol to establish upper and lower bounds of aerosol production from the stated scenarios.

To preserve unique and expensive instrumentation and to ensure data acquisition, instrumentation was strategically located to limit damage from expected fragmentation and shielding was provided as further protection.

For each field test phase, the relevant target vehicle was prepared, instruments were set up, shots were fired, air samples were recovered, targets were repaired, and the Superbox was cleaned. The field testing parameters were adjusted with field experience to improve their effectiveness in representing actual combat field experience. Air sampling, contamination surveys, personal monitoring of recovery entry personnel, pressure and temperature measurements, impact observations, recovery observations, and observation of aerosol resuspension with recovery activities were all documented.

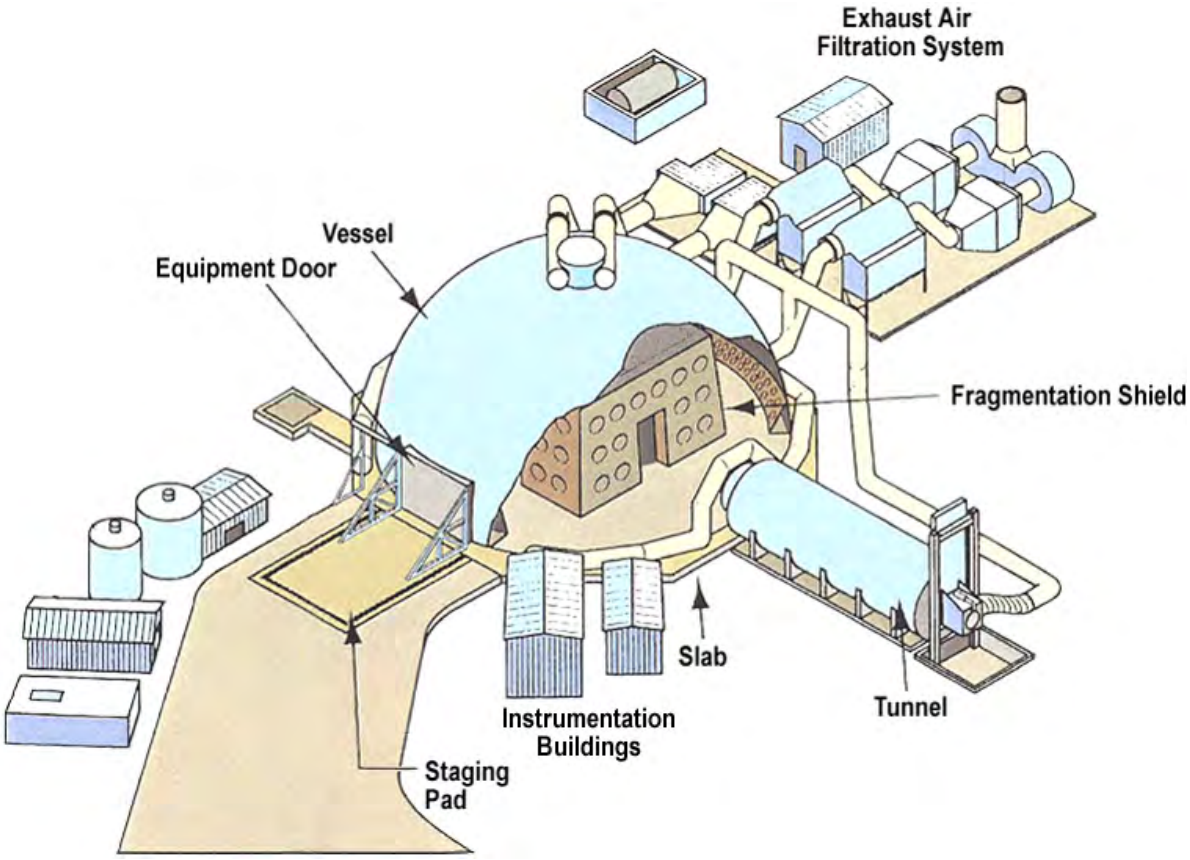

Figure S.1. Superbox: ATC DU Containment Facility

The aerosol collection system used during the testing program was designed to function in an environment in which high temperature and pressure transients occur, to survive damage from fragments, and to provide sample collection redundancy, confidence in timing, adequate flow rates, and sufficient sample collection for chemical analyses of selected samples. Aerosols were collected inside the vehicle as a function of time, position, and shot line; outside the vehicle as aerosols and as deposited material; and in sufficient quantity to allow for characterization in terms of uranium concentration, particle size, and other chemical and physical parameters.

Stainless steel filter cassettes, cascade impactors (CIs), a five-stage cyclone, and a moving filter sampler were used to collect aerosols samples inside the vehicle. Sampling arrays that paired filter cassettes with CIs for eight separate sampling times provided an effective means of containing and operating the samplers. An engineering software program remotely controlled the operation of these air samplers. Limited sampling was also conducted outside the vehicle using large-volume CIs to collect aerosols created by armor perforation and deposition trays to collect particulate matter deposited by gravitational sedimentation. Wipes of the interior and exterior surfaces were taken to determine the quantity of deposited material.

All samples were evaluated for uranium by measuring their radioactivity. Samples obtained primarily from the cyclone sampler, but also from most other sampler types were selected for additional chemical and physical analyses. These analyses measured uranium and non-DU element concentrations, and evaluated particle morphology, DU oxide phases, particle size distribution, and solubility in lung fluid — characteristics that provide the basis for input to computer models to assess chemical and radiological doses from inhalation and ingestion of DU.

S.4 Study Results

Twelve LC-DU munitions were fired at BHT versions of an Abrams tank and a Bradley vehicle. One LC-DU munition was fired at an operational Abrams tank. These shots successfully simulated retrospective and prospective trajectories through armored vehicles. Each of the shots hit the target vehicle in the area intended, and none caused excessive loss of air samplers. As a result, an extensive and comprehensive data set was obtained from the many samples recovered. Results and generalizations about the tests are related to 1) physical aspects of the field tests, 2) uranium concentration in the aerosols, and 3) physical and chemical characteristics of the aerosols. Generalizations related to physical parameters include the following:

- Field tests were performed to the satisfaction of the project team. The researchers found the Army's Superbox and support staff to be well qualified to conduct field tests in which LC-DU munitions were fired at target vehicles. The facility was large enough to allow appropriate configuration of target vehicles for aerosol sampling and sample recovery.

- The vehicle and shot line variations were effective for determining an upper bound for aerosol concentrations and for quantifying other aerosol characteristics from actual firing incidents and possible future incidents. The use of the vehicle BHTs accommodated placement for many air samplers and relative ease of access.

- Temperature and pressure pulses in the crew compartments were brief. The temperature pulse lasted from about 0.2 to 4.6 sec, and the pressure pulse lasted for milliseconds.

- Immediately after each vehicle perforation, tiny DU fragments underwent rapid oxidation, disappearing within 1 to 2 sec. These fragments, referred to as "fireflies," were visible on high-speed videotape.

- The amount of penetrator erosion varied with test phase. The Bradley vehicle armor caused the least penetrator erosion, and the Abrams DU armor caused the most. (In this context, erosion refers to the removal of surface layers as the penetrator perforated armor. Higher erosion rates lead to a higher quantity of uranium in the aerosol.)

- The filter cassette, CI, and cyclone samplers performed well under the adverse environmental conditions in the tests. Shielding was necessary to minimize fragment hazard and enhance sampler survivability. The initial filter medium used in the filter cassettes was too sensitive for the environmental conditions and was replaced by a Teflon-based medium that was sufficiently durable.

- A shielded moving filter (MVF, inlet unshielded) successfully collected aerosols immediately after impact on five of the shots. This was especially useful because the other sampler types did not begin operating until 5 sec post-shot. The moving filter provided 1) a means for estimating the initial aerosol concentration immediately after impact and 2) an independent comparison with the data obtained using the filter cassettes that began operating 5 sec post shot.

DU aerosol mass concentrations inside the vehicles were analyzed as a function of time beginning 5 sec after perforation and at sequential time intervals post shot. DU concentrations varied with shot and with crew position within the vehicle. Deposition occurred as particles settled on vehicle surfaces and some dispersed through open hatches or other structures. A summary of the mean DU concentrations (time-standardized) as measured by the IOM filter cassettes (in grams per cubic meter [g/m^3]) by vehicle configuration are listed in Table S.1.

Table S.1. Mean DU Aerosol Mass Concentrations Over Time

Shot Description	Mean DU Concentration (g/m^3)				
	10 sec	**30 sec**	**1 min**	**30 min**	**1 h**
Retrospective Scenarios					
• Abrams BHT—crossing hull through turret; no ventilation	11	9.0	6.0	0.11	0.057
• Bradley BHT—crossing turret or passenger compartment; no ventilation	3.0	2.7	2.2	0.13	0.049
Prospective Scenarios					
• Abrams BHT—crossing turret; no ventilation	8.8	7.9	5.7	0.15	0.064
• Abrams BHT—crossing turret into breech; no ventilation	16	12	6.4	0.020[(a)]	0.029
• Abrams BHT—fired into DU armor; no ventilation	10	7.9	4.2	0.049	0.017
• Abrams tank—fired into DU armor; with operating ventilation	0.092	0.14	0.22	0.011	--[(b)]

(a) Samplers for both shots showed similar pattern in large reduction from 1 min; most 30 min DU concentrations were lower than at 1 h.
(b) Averages not extrapolated past last sample.

Generalizations related to the DU aerosol concentrations include the following:

- Initial radiological data were analyzed assuming that the uranium in the aerosols was in secular equilibrium with its immediate short-lived progeny. This assumption was tested and found to be

incorrect for most sample types and particle sizes. A procedure to adjust for the progeny disequilibrium was developed to ensure that the uranium in these aerosols was not underestimated.

- Based on the sampling results of the moving filter, the highest measured uranium concentration in a perforated Bradley BHT was 1.1 g/m^3 (1.1E+06 µg/ m^3). This peak occurred 7 sec post shot. The highest concentrations in a perforated Abrams BHT ranged from 2.3 to 6.0 g/m^3 in a vehicle without DU armor and 8.2 to 9.1 g/m^3 in a vehicle with DU armor. In each case for which MVF data were collected, the peak occurred within the first 13 sec post shot.

- The peak DU aerosol concentration measured by the filter cassettes in the BHTs occurred during the first sampling interval, which began 5 sec post shot and lasted from 10 to 30 sec. (In the Abrams tank, the DU concentration in the 1 min sample was greater than in the 10 sec sample, probably because of less initial dispersion of aerosol into the driver's position where the samples were collected.)

- The highest mean DU aerosol concentrations within the Abrams and Bradley BHTs and the Abrams tank as shown in Table S.1 were the following:

  - Abrams BHT hull shot (conventional armor) – 11 g/m^3
  - Abrams BHT turret-crossing shot (conventional armor) – 8.8 g/m^3
  - Abrams BHT turret-crossing into breech shot (conventional armor) – 16 g/m^3
  - Abrams BHT shot fired into DU armor – 10 g/m^3
  - Abrams tank (with ventilation) shot fired into DU armor – 0.22 g/m^3
  - Bradley BHT turret and passenger compartment shots – 3.0 g/m^3

- The Abrams tank, in which samples were collected in an equipped and operational vehicle instead of a BHT, most closely represents actual tank conditions. As such, it may provide a better estimate of DU aerosol concentrations in an Abrams tank perforated through DU armor than similar shots to the BHT. However, few samplers operated during this single test, making firm conclusions difficult.

- An extensive database of analyzed wipe samples was developed that provides upper bounds on surface deposition inside and outside the vehicle and provides qualitative information about the amount of uranium potentially available for resuspension. Uranium on the wipe media and on the cotton gloves used to evaluate the quantity potentially available for hand-to-mouth transfer will be useful when assessing the ingestion pathway of uranium intake.

Generalizations related to the other physical and chemical parameters of the aerosols include the following:

- The percentages of uranium mass in the total mass of aerosol collected in the cyclone samples varied as follows:

  - 38 to 54% in the Abrams BHT/hull shot, conventional armor
  - 43 to 72% in the Abrams BHT/turret shots, conventional armor

- 60 to 72% in the Abrams BHT/turret shot, DU armor
- 18 to 29% in the Bradley BHT/passenger compartment shots.

- As expected, particle size distributions decreased as a function of time as settling occurred. The particle size distributions were analyzed using unimodal and bimodal models. The bimodal model provided a better fit for many of the samples, but neither approach modeled a significant number of samples well. Use of the actual size distribution data may be preferable to using activity median aerodynamic diameters when using the Capstone data in human health risk assessments.

- Exterior air sampling yielded ranges of uranium concentrations and particle size distributions. Because the aerosols generated by target perforation were confined within the Superbox, use of these data to estimate exterior source term will overestimate DU aerosol concentrations.

- The predominant uranium oxide phase consisted of U_3O_8/UO_3. Its presence increased as particle size decreased while the percentage of U_4O_9, which was highest with the large particles, decreased as particle size decreased. A small amount of $UO_3 \cdot 2H_2O$ (schoepite) was detected in several cyclone stages and in backup filter samples.

- The particles obtained from the cyclone residues and from other samples evaluated under a scanning electron microscope had a complex, heterogeneous structure. The uranium particles displayed many different shapes, from spheres to grain-appearing structures to fractured appearances. These different shapes suggest the likelihood that the DU particles were formed by several different mechanisms.

- The *in vitro* dissolution rates most closely resembled Type-M (a moderate rate of dissolution) absorption behavior. More than half of each sample (about 58 to 99%) fit the Class-Y (halftime of >100 days) clearance category. These samples also contained a Class D (half-time of <10 days) function ranging between 1 and 36%. Several samples also contained a Class-W (intermediate) component.

- Besides the predominance of uranium, other metals present in the cyclone aerosols consisted primarily of aluminum and iron. Aluminum varied the most by phase and was highest in Phase-II samples and lowest in Phase-III samples. Other major constituents included titanium (alloyed with DU in the penetrator), zinc, and copper.

- Some data were collected even though they were outside the main scope of the project. These data, which were subjected to a preliminary analysis, are presented and may be useful to specific assessments.

S.5 Conclusions

During the course of this project, the Capstone DU Aerosols Study successfully generated, collected, and evaluated DU aerosols from firing DU munitions at an Abrams tank BHT and a Bradley vehicle BHT. Priority was placed on characterizing DU aerosols within crew compartments during the first 2 h post shot. An analysis of aerosols during recovery activities 2.5 to 4 h post shot added to the timeline during which air samplers were collecting samples, at least intermittently. Samplers also operated outside the vehicles after each shot to collect and size aerosol particles near the vehicles. An extensive database was acquired from which exposure may be characterized and human health risks may be assessed to update previous efforts related to exposure by Gulf War/ODS personnel and to apply to assessments and characterizations of potential future engagements.

The interior aerosol source term was well characterized over time for the various retrospective and prospective shots. The BHTs provided sufficient space to contain the sampling configurations described in this report. However, scaling from the BHTs to operational vehicles may not be straightforward because of differences in air volume and surfaces available for deposition. The Abrams tank shot (PIV-4) and the ventilation tests provide additional information to assist in scaling.

Physical and chemical characterization of the DU aerosols was extensive. Aerosol composition, particle size, morphology, and *in vitro* dissolution properties over a wide gamut of interior samples has led to a greater understanding of the properties of these materials and helps bracket the range of expected characteristics. Their heterogeneous nature was identified through scanning electron microscopy, and the ramifications of such heterogeneity on particle size distributions and *in vitro* dissolution were demonstrated in the variability in these results. In spite of the depth of evaluation already conducted, more data are contained in the report than the project team had opportunity to thoroughly evaluate. These activities are left to other investigators.

Overall, the project results have greatly expanded our understanding of DU aerosol concentrations and properties resulting from perforation of armored vehicles with LC, kinetic-energy, DU munitions. The comprehensive data set arising from the project will support analysis of human health risk assessments for both retrospective and prospective exposure scenarios. The data generated is applicable for assessing human health risks associated with various DU exposure scenarios related to personnel in, on, or near vehicles during perforation or entering vehicles immediately or well after perforation.

Acknowledgments

The Capstone depleted uranium (DU) Aerosol Study was conducted under the auspices of the U.S. Army Heavy Metals Office. It was financially supported by the Office of the Special Assistant for Gulf War Illnesses, Medical Readiness and Military Deployment and by the U.S. Army. The Depleted Uranium Research-Integrated Process Team (DUR-IPT) was charged with project oversight. Mr. Michael Los, a DUR-IPT member from the Assistant Secretary of the Army (ASA) for Acquisition, Logistics and Technology, US Army Heavy Metals Office, was the Army lead for the project and the point of contact between the DUR-IPT and the project team. Additional organizations directly contributing to its performance included the Army Surgeon's Office, the PEO-GCSS, USACHPPM, MEDCOM, AMC, ARDEC, ATEC, OSD, and others.

A very long list of people from many organizations supported this test in one capacity or another and whose efforts are truly appreciated by the authors. Some of those providing the most support included the following:

*Aberdeen Test Center (ATC), Aberdeen Proving Ground, Maryland***:** Jesse Meerdink, Bruce Taylor, Dana Blankenbiller, Kathy Burns, Gina DiMarco, William McMillan, Greg Heinz, David Butler, James Stauffer, Jeff Adams, Chris Thomas, David Bryner, and Stella Woosley.

*US Army Center for Health Promotion and Preventive Medicine (USACHPPM)***:** Gordon Lodde, Dr. Gerald Falo, P. Mark Moscato, David P. Alberth, Robyn Lee, David Morrow, Thomas Beegle, Angel Christman, Karl Kroeck, Lorus Miller, and the radiological counting lab staff.

*Pacific Northwest National Laboratory (PNNL)***:** Technical staff—Chuck Soderquist, Norma Van Houten, Bruce Arey, Evan Jenson, Orville T. Farmer, III, Lori Darnell, Dr. Kenneth Krupka, John Glissmeyer, Dr. Richard Traub, and Dr. Larry Thomas; Publications staff—Cary Counts, Susan Ennor, Jean Cheyney, Zontziry Pritchett, Rose Urbina, Trina Russell, and Barbara Wilson.

*Lovelace Respiratory Research Laboratory (LRRI)***:** Dr. Mark Hoover, currently of the National Institute of Occupational Safety and Health (NIOSH), Tim Krenik, and Jun Gao.

*Aberdeen Research Laboratory (ARL)***:** Dr. Lee Magness and Dr. Bill Bruchey.

Abrams Live-Fire Program: Lawrence Kravitz, Doug Blankenbiller, and Mark Ryzyi.

Battlefield Damage Assessment and Repair: Robert Gehr, SSG James Ables, and MSG Richard Collins.

*DUR-IPT Members***:** In addition to their IPT duties, several of the DUR-IPT specifically provided additional guidance and other project assistance. COL Eric Daxon (now retired) of MEDCOM helped us understand the Army's vision for this project. Dr. David Case, previously assigned to OSAGWI, now at SAIC, provided comments and technical feedback regarding test plans, data analysis and the draft report at opportune junctures. LTC Mark Melanson ensured the availability of his technical staff to support the many contributions they made to the overall project. Norman Harrington, Development Test Command, helped facilitate field testing arrangements and lent his onsite support.

In addition to organizational support, we want to acknowledge Dr. Paul Baron of NIOSH for providing the Andersen cascade impactors used for collection of aerosols outside the target vehicles. Without these, we would not have been able to collect aerosols exterior to the vehicle with air samplers capable of particle size separation.

And finally, we wish to thank the independent peer reviewer panel who contributed richly to project guidance by reviewing and commenting on our test plans, our first field test and sample handling procedures, and the draft version of this report. This team of peer reviewers was led by Dr. Roy Reuter and included (in alphabetical order) Dr. Paul Baron, Dr. John Doull, Dr. Rogene Henderson, Dr. David Hoel, Dr. Morton Lippmann, Dr. Paul Strickland, Dr. Arthur Upton, and Dr. Wes Van Pelt.

Working Group Authors

The Capstone Aerosol Characterization Working Group authors and team members were responsible for planning and conducting the Capstone field tests and aerosol characterization. These authors are listed below along with a short statement of their areas of expertise specifically relevant to this study.

Ms. Mary Ann Parkhurst	Project Manager, Health Physicist Specializing in Depleted Uranium
Ms. Frances Szrom	Certified Health Physicist, Specializing in Depleted Uranium
Dr. Raymond A. Guilmette	Health Physicist, Radiation and Inhalation Toxicologist, Dose Assessor, Aerosol Scientist
Mr. Thomas D. Holmes	Electronics Engineer, Equipment Specialist
Dr. Yung-Sung Cheng	Theoretical and Experimental Aerosol Scientist
Mr. Judson L. Kenoyer	Certified Health Physicist, Certified Industrial Hygienist, Aerosol Scientist
Mr. John W. Collins	Health Physicist Specializing in DU
Mr. T. Ellory Sanderson	ATC Vulnerability Test Engineer
Mr. Richard W. Fliszar	Health Physicist, Industrial Hygienist, Specializing in DU
Dr. Kenneth Gold	Scientist/Engineer, Specializing in Munitions Applications of Scanning Electron Microscopy and X-Ray Diffraction
Mr. John C. Beckman	Health Physicist, NRC License Compliance, Specializing in Field Operations
Ms. Julie A. Long	Document Control and Engineering Assistant

Contents

Volume I. Main Report

Figures

Tables

Abbreviations and Acronyms

ACGIH	American Conference of Governmental Industrial Hygienists
AD	aerodynamic diameter (also known as aerodynamic equivalent diameter, AED)
AMAD	activity median aerodynamic diameter
AMC	Army Materiel Command
APFSDS	Armor Piercing Fin-Stabilized Discarding Sabot
APG	Aberdeen Proving Ground, Maryland
ARDEC	U.S. Army Armament Research, Development and Engineering Center
ARL	Army Research Laboratory
ASTM	American Society for Testing and Materials
ATC	Aberdeen Test Center
ATEC	Army Test and Evaluation Command
BDAR	Battlefield Damage, Assessment, and Repair
BFV	Bradley Fighting Vehicle
BHT	ballistic hull and turret
bse	backscatter electron mode
BW	baseline wipe
C	Centigrade
cfm	cubic feet per minute
CI	cascade impactor
cm	centimeter(s)
CV	combat vehicle
CY	cyclone
DoD	U.S. Department of Defense
DOE	U.S. Department of Energy
DQO	data quality objective
DU	depleted uranium
DUR-IPT	Depleted Uranium Research – Integrated Process Team
EC/NBC	environmental control/nuclear, biological, chemical ventilation system
ECD	effective cutoff diameter
EDS	energy dispersive spectroscopy
EOD	Explosive Ordnance Disposal
EPA	U.S. Environmental Protection Agency
ES&H	environment, safety, and health
F	uranium mass fraction in first peak of bimodal distribution
FS	filter sampler

GSD	geometric standard deviation
GPS	gunner's primary sight
h	hour(s)
HCl	hydrochloric acid
HEPA	high-efficiency particulate air (filter)
HF	hydrofluoric acid
Hi-Vol	high-volume Staplex sampler, abbreviated in sample identification as HV
HNO_3	nitric acid
HRTM	Human Respiratory Tract Model
HVAC	heating, ventilation, and air conditioning
ICP-AES	inductively coupled plasma – atomic emission spectroscopy
ICP-MS	inductively coupled plasma – mass spectrometry
ICRP	International Commission on Radiological Protection
ICSD	Inorganic Crystal Structure Database
IMP	impactor (cascade impactor)
IOM	Institute of Occupational Medicine, used as an abbreviation for filter cassettes
IW	impact wipe
keV	kiloelectron volt(s)
KPA	kinetic phosphorescence analysis
L	liter(s)
Lpm or L m^{-1}	liter(s) per minute
LANL	Los Alamos National Laboratory
LC	large-caliber (referring to depleted uranium munition)
LRRI	Lovelace Respiratory Research Institute
MCE	mixed cellulose ester
MEDCOM	U.S. Army Medical Command
mg	milligram(s)
min	minute(s)
mL	milliliter(s)
mm	millimeter(s)
MMAD	mass median aerodynamic diameter
msec	millisecond(s)
MVF	moving filter
NATO	North Atlantic Treaty Organization
NBC	nuclear-biological-chemical
NIOSH	National Institute of Occupational Safety and Health
NIST	National Institute of Standards and Technology
NRC	U.S. Nuclear Regulatory Commission
NRPB	National Radiological Protection Board

ODS	Operation Desert Storm (1991 Gulf War)
OSAGWI	Office of Special Assistant for Gulf War Illnesses, Medical Readiness, and Military Deployment
PAPR	powered air purifying respirators
PEO-GCSS	Program Executive Officer for Ground Combat and Support Systems
PFDB	parallel-flow diffusion battery
PMP	polymethylpentene (filter support ring)
PNNL	Pacific Northwest National Laboratory
POC	point of contact
ppm	parts per million
psig	pounds per square inch gauge
PTFE	polytetrafluoroethylene (filter support membrane)
PTP-ESP	point-to-point electrostatic precipitator
PVC	polyvinyl chloride
QA	quality assurance
QC	quality control
R^2	correlation coefficient
RADIAC	Radiation Detection, Indication, and Computation Instruments
RH	relative humidity
RSO	Radiation Safety Office(r)
SCBA	self-contained breathing apparatus
sec	second(s)
SEM	scanning electron microscopy
SEM/EDS	scanning electron microscopy/energy dispersive spectrometry
SF_6	sulfur hexaflouride (tracer used in ventilation rate measurements)
SOP	standard (or standing) operating procedure
SP/QAP	Sampling Protocols and Quality Assurance Plan
SUF	synthetic ultrafiltrate
TACOM-ARDEC	Tank-automotive and Armaments Command, Armament Research, Development & Engineering Center
TEM	transmission electron microscope
TIMS	thermal ionization mass spectrometry
TRU	transuranic
U	uranium
µm	micrometer(s)
USACHPPM	U.S. Army Center for Health Promotion and Preventive Medicine
U_xO_y	uranium oxide phase, typically UO_2, U_3O_8, UO_3, or $UO_3 \cdot 2H_2O$
VDC	**v**olts direct current
XRD	x-ray diffraction

Glossary

Abrams Main Battle Tank – A full-tracked, armored, land combat vehicle with a 105-mm (M1) or 120-mm (M1A1/M1A2) gun operated by a four-man crew consisting of a commander, gunner, loader, and driver. The Abrams tank is the principal weapon of tank battalions of the Army during all types of combat operations.

aerodynamic diameter (AD) or aerodynamic equivalent diameter (AED) – AD and AED are both used to describe the diameter of a sphere, in μm, of unit density (1 g/cm^3) that has the same terminal settling velocity in air as the particle of interest. A 1-μm-AED particle has 1000 times the volume of a 0.1-μm-AED particle. Discussion of AED measurements refers to individual particles.

aerosol – An assemblage of liquid or solid particles suspended in a gaseous medium long enough to be observed and measured; generally about 0.001-μm to 100-μm AED.

ballistic hull and turret (BHT) – A production Abrams or Bradley structure without any operational components. The turret is mounted on the hull via a race ring, but no other internal or external components are present (i.e., no power train, fire control system, ventilation system, etc). A BHT may contain a gun, road wheels, and track if the specific test requires these. A BHT is typically used to reduce test costs when an operational vehicle is not required to meet test objectives.

breech – The rear part of the bore of a gun, especially the opening that permits the projectile to be loaded at the rear of the bore.

bioassay – An analysis of body fluids, tissue, or excreta to determine the absence, the degree, or presence of specific materials. Used as an index of radioactivity in the body.

Bradley Fighting Vehicle – A full-tracked, medium-armored fighting vehicle that provides protected, cross-country mobility and vehicular-mounted firepower to infantry/cavalry units. The Bradley Fighting Vehicle System family consists of an infantry and a cavalry version, which differ primarily in the number of passengers carried and placement of ammunition.

catch plate – A backstop consisting of stacked armor plates and other materials positioned behind the target, and designed to capture the residual penetrator.

chemical composition – The elemental makeup of a chemical compound.

deposition tray – An object with a specific dimension (usually 100 cm^2) that passively collects formerly aerosolize material that has since deposited on surfaces.

dissolution rate – The rate of change of a solid into a liquid form by immersion in a fluid of suitable chemical composition or character.

Data Quality Objective – A systematic strategic planning tool based on the scientific method that identifies and defines the type, quality, and quantity of data needed to satisfy a specified use.

depleted uranium – Depleted uranium (DU) is the primary material used in the large-caliber penetrators fired at vehicle targets in this study. Uranium is considered depleted if it contains a smaller component of the uranium-235 isotope (approximately 0.2 percent for U.S. munitions) than natural uranium, which contains about 0.7 percent uranium-235. DU, which is mostly uranium-238, is less radioactive than natural uranium.

DU cone sample – A pile of DU oxide powder resembling a cone (point side up)

environmental control/nuclear-biological-chemical ventilation system (EC/NBC) – A ventilation system found on the Abrams Main Battle tank that conditions air for breathing (filtering out nuclear, biological, and chemical agents) as well as personal heating and cooling as required, while crew members are wearing protective suits and masks. The EC/NBC system on the Abrams tank also provides positive air pressure within the turret and driver's locations to prevent diffusion of NBC contaminants.

fireflies – Nickname of tiny DU fragments created immediately after vehicle perforation that undergo rapid oxidation and burn out very quickly.

first responder Soldiers who enter damaged vehicles after DU perforation to evacuate personnel.

glacis – Sloped portion of a tank turret.

hull – Armored structure primarily containing the power train, road wheels, and track to provide vehicle mobility.

inhalable fraction – The fraction of aerosolized material of a particular size (usually particles 100 μm or less aerodynamic equivalent diameter) available for intake via the respiratory tract.

LabVIEW – A computer engineering controller program used to remotely start, stop, and monitor pressure aerosol monitoring instrumentation.

large-caliber DU munitions – Rounds with large-caliber depleted uranium penetrators that are fired from the Abrams platform (M1A1 and M1A2 series tanks). These heavy metal, long-rod penetrators use kinetic energy to penetrate a target.

Level I – Crewmembers in, on, or near an armed vehicle at the time of DU perforation or first responders who enter the vehicle within minutes of perforation.

Marple cascade impactor – A personal cascade impactor consisting of several stages used to separate particle sizes. Marple impactors used in this test had a nominal flow rate of 2 Lpm through an 8-stage (34-mm-diameter) unit capable of collecting particles ranging from about 0.5 to 20 μm AED.

particle mass concentration – The mass of particulate matter or material in a unit volume of air, usually expressed in $\mu g/m^3$, mg/m^3, or g/m^3.

particle size distribution – The number concentration of particles as a function of particle diameter, usually aerodynamic diameter, and expressed in micrometers, μm.

particle morphology – The appearance or shape of a particle, usually characterized by parameters such as shape, volume, and surface area.

penetration – Used here to convey the piercing of the armor by the DU penetrator that may or may not enter a turret, driver, or passenger (Bradley) compartment.

perforation – Used here to convey the breach by the DU penetrator through vehicle armor into the turret, driver, or passenger (Bradley) compartment.

quality assurance – An integrated system of management activities involving planning, implementation, assessment, reporting, and quality improvement to ensure that a process, item, or service is of the type and quality needed and expected by the customer.

quality control – The overall system of technical activities that measure the attributes and performance of a process, item, or service against defined standards to verify that they meet the stated requirements established by the customer, operational techniques, and activities that are used to fulfill requirements for quality.

respirable fraction – The fraction of aerosolized material of a particle size (usually particles 10 μm or less aerodynamic equivalent diameter) available for intake and deposition into the deep lung.

scenario – An outline of a projected chain of events, which as related to the Capstone field tests, includes the selection of target vehicle, trajectory angle, and sampling equipment. Scenarios were developed to evaluate aerosols created from retrospective actions, such as events that occurred during the Gulf War/ODS, and possible prospective events.

shot line – A munition's trajectory (attack azimuth and elevation) and impact point relative to a target.

solubility – The ability of a substance to form a solution with another substance. Normally lung or tissue fluid is considered the fluid of choice for evaluation of residence time of a chemical in the body with regard to inhalation intake.

source term – The amount of radionuclide or chemical released from a source or site to the environment over a specific period for use in dose assessment or exposure assessment.

spall liner – Kevlar panels bolted to the inner walls of the passenger compartment in the Bradley vehicle, designed to capture fragments from vehicle perforation that could injure the crew or damage internal vehicle components.

Superbox – A state-of-the-art containment facility that can accommodate a fully loaded combat vehicle for testing purposes. The facility has an air filtration system with 99.97 percent removal efficiency for particles 0.3-μm AED and greater efficiencies for all other particle sizes. There is a thick steel fragmentation shield inside the vessel to contain fragments within the vessel wall.

turret – Revolving armored structure (located on top of the tank hull) that primarily houses the main gun and fire control system.

wipe sample – A type of sample (wipe or smear) that collects readily removable surface radioactivity in which moderate pressure is applied to a collection substrate when wiping a surface suspected of contamination over a known area. The wipe sample can then be assessed with standard radiation detectors, and is usually expressed in units of disintegrations per minute per 100 cm^2 (dpm/100 cm^2).

1.0 Introduction

The 1991 Gulf War (Operation Desert Storm [ODS]) was the first time that armor-piercing, depleted-uranium (DU) munitions were used on the battlefield. Many Iraqi tanks and other vehicles were hit and perforated by DU rounds fired by the U.S. contingent of the Coalition Forces. Fratricide incidents also occurred in which 6 U.S. Abrams tanks and 15 Bradley Fighting Vehicles (referred to as Bradley vehicles) were fired upon after having been mistakenly identified as enemy vehicles. In addition to the Soldiers known to have been hit with DU fragments, others participating in certain battlefield actions or recovery activities are presumed to have been exposed to DU aerosols as a result of 1) being in Abrams tanks or Bradley vehicles at the time the vehicles were struck and perforated by one or more DU projectiles, 2) entering DU-perforated vehicles as first responders to recover personnel or equipment, or 3) entering damaged vehicles to gather intelligence and/or assess or repair damage (i.e., performing maintenance or operations work). Other individuals, including those without a clear purpose for entering the vehicles (e.g., trophy hunters or scavengers), may have been exposed to DU residues on vehicle interior or exterior surfaces or from DU aerosols following mechanical or wind resuspension of particulate matter. Other exposure scenarios are possible, and these are discussed in reports by the Office of the Special Assistant for Gulf War Illnesses, Medical Readiness and Military Deployment (OSAGWI) (1998) and U.S. Army Center for Health Promotion and Preventive Medicine (USACHPPM) (2000). The work documented here focused primarily on exposure scenarios that involve personnel who were in the vehicle.

Over the past two decades, the U.S. Army has conducted periodic impact tests on armored targets to determine system survivability and/or the lethality of the impacts. In conjunction with these tests, sampling was performed to characterize the aerosols that formed when DU penetrators impacted and perforated the targets. However, the scopes of these tests and the aerosol monitoring equipment used were limited. The data obtained in Fliszar et al. (1989) for exposure outside of the struck vehicle were sufficiently robust for use in for human health risk assessments. However, the data from the limited number of attempts to measure aerosol generation inside of the struck vehicles at the time of perforation were insufficient for performing human health risk characterizations inside vehicles perforated by DU munitions. To remedy this, the U.S. Department of Defense (DoD) made a commitment to obtain more complete data about aerosols generated by the impact and perforation of armored vehicles by DU munitions. Under a program jointly sponsored by OSAGWI[(a)] and the U.S. Army, the Army Heavy Metals Office managed a study designed to quantify and characterize DU aerosols inside, on, and close to Abrams tanks and Bradley vehicles at the time and shortly after they were struck and perforated by large-caliber (LC) DU penetrators. The program, named the Capstone DU Aerosol Study, was designed to generate data from which personnel exposure assessment and risk characterization could be conducted for exposure scenarios that involved either being in the vehicle at the time the vehicle was struck or being in the struck vehicle shortly after perforation occurred.

The Army selected a scientist from Pacific Northwest National Laboratory (PNNL) as the independent Principal Investigator to direct the Capstone DU Aerosol Study and to work with the Capstone test team, which was composed of Army health physicists and engineers from the Aberdeen Test Center (ATC), Aberdeen Proving Ground (APG), Maryland; USACHPPM, Aberdeen Proving Ground–Edgewood Area,

(a) The OSAGWI organization currently is referred to as the Deployment Health Support Directorate.

Maryland; and the U.S. Army Tank-Automotive and Armaments Command, Armament Research, Development and Engineering Center (TACOM-ARDEC), Picatinny Arsenal, New Jersey. In addition, scientists from Lovelace Respiratory Research Institute (LRRI) and Los Alamos National Laboratory (LANL) were project collaborators, particularly in the areas of aerosol sampling and particle size analysis. This group received guidance concerning overall test objectives and test implementation from an Army steering committee, known as the Depleted Uranium Research–Integrated Process Team (DUR-IPT). The U.S. Army Medical Command (MEDCOM) developed a set of Data Quality Objectives (DQOs) for the specific information to be derived from this testing program.

Peer review was an integral part of the Capstone process. An independent panel of experts in the disciplines of health physics, industrial hygiene, occupational health, inhalation physics, chemical toxicology, radiation biology, aerosol science, and biostatistics was impaneled by the U.S. Army Medical Research and Materiel Command. The function of this panel was to provide an independent scientific and medical review of the data quality objectives and Capstone experimental objectives and to provide technical feedback regarding the field tests and the draft report. The peer reviewers were given access to all aspects of the test. The peer review comments were resolved in a series of joint meetings.

The Capstone DU Aerosol Study focused on the quantities and characteristics of aerosols and residues 1) generated inside the vehicles at the time of impact, 2) found inside the vehicles during and after settling had occurred, and 3) to a lesser extent, found outside vehicles struck by DU penetrators. The Capstone series of tests was designed to estimate an upper bound of the aerosols that would be generated from shot lines similar to those that occurred during the Gulf War/ODS and those that might occur during future conflicts.

Field tests for the program were conducted in four phases at the ATC DU Containment Facility. In Phases I and II, ballistic hull and turret (BHT) versions of an Abrams tank (without DU armor) and a Bradley vehicle were used as targets to recreate experiences from the Gulf War/ODS and simulate possible future incidents. Phases III and IV were designed to simulate possible future conflicts. An Abrams tank BHT (with DU armor) was used as the target in the Phase-III tests. Phase IV was performed in conjunction with a congressionally mandated testing program and used an operational Abrams tank with DU armor as the target. Each phase featured specific vehicle configurations and scenarios that defined the instrument setup in and around the vehicles and the target impact points needed to achieve specific entry and exit angles for observation and collection of data.

Volume I of this report describes the testing program (Chapter 2.0), the methods used to set up and conduct the tests (Chapter 3.0), the test parameters and observations (Chapter 4.0), sample analysis (Chapter 5.0), data analysis by target and shot (Chapter 6.0), conclusions (Chapter 7.0), and references (Chapter 8.0).

Volume II of this report consists of seven appendices (A–G), which contain a) technical data collected during the tests that were used to draw the conclusions discussed in Chapter 7.0 and 2) descriptions of several of the methodologies used to analyze the data. The information contained in each appendix is described below.

- Appendix A—Tables of the uranium masses and concentrations of the various samples collected.

- Appendix B—Tables of the unimodal and bimodal particle size distributions of the aerosols generated.

- Appendix C—X-ray diffraction patterns used to identify uranium oxide phases present.

- Appendix D—Particle morphology micrographs showing relative particle size and providing some general information concerning particle composition.

- Appendix E—The analytical methodology used and the results of the *in vitro* solubility sample analysis.

- Appendix F—Wipe survey data from wipes taken inside and outside the vehicle.

- Appendix G—A description of how the vehicle ventilation rates were evaluated.

2.0 Description of the Testing Program

The Capstone DU Aerosol Study involved a series of shot tests conducted in four phases in which test vehicles were impacted with DU munitions to simulate specific battlefield conditions. These tests, designed to collect aerosol data for input to radiological and chemical health risk assessments, were conducted at the Depleted Uranium Containment Facility (Superbox) located at APG. The test objectives, scenarios simulated (Phases I through IV), test site, and aerosol collection system are described in the following sections.

2.1 Test Objectives

The overall goal of this study was to generate data that will fill gaps in our knowledge about aerosols created inside a vehicle by impact and perforation of armored vehicles by DU munitions. The new data will be used to assess exposure of personnel to these aerosols and to characterize the human health risk to personnel who possibly were exposed to DU during the Gulf War/ODS or who potentially could be exposed in future military activities. The DQO process identified the following three primary questions that need to be answered by the human health risk assessment using data from the Capstone DU Aerosol Study (DQO Memorandum, USACHPPM 2000):

1. *Are the health risks to personnel in, on, or near an armored vehicle, <u>at the time the crew compartment is perforated by DU munitions</u>, high enough to warrant changes in the medical policy, in the medical treatment and medical monitoring, and in personnel protective measures for Soldiers potentially exposed to DU?* Exposure to Soldiers in this group is from inhalation of DU aerosol from the initial perforation and resuspension and from ingestion of DU. These Soldiers also may be exposed from wound contamination or embedded fragments. The Capstone DU Aerosol Study focuses on assessing exposure from inhalation and ingestion for this cohort of soldiers. Soldiers with embedded fragments are being medically monitored by the Veteran's Admininstration.

2. *Are the health risks to personnel who enter (without protective clothing) a perforated armored vehicle <u>immediately after</u> the perforation high enough to warrant changes in the medical policy for treatment, monitoring, or protective measures?* Exposure to this group is from the inhalation of residual aerosols from the initial perforation, resuspended DU, and ingestion of the DU from hand-to-mouth transfer of DU residues on the interior (and exterior) vehicle surfaces.

3. *Are the health risks to personnel who enter (without protective clothing) an armored vehicle <u>well after</u> the vehicle is perforated by DU munitions high enough to warrant changes in the medical policy, in the medical treatment and medical monitoring, and in personnel protective measures for soldiers potentially exposed to DU?* Exposure to this group is from inhalation of resuspended DU and ingestion of DU from hand-to-mouth transfer of DU residues on the vehicle surfaces.

The ultimate goal of the Capstone DU Aerosol Study was to develop a source of aerosol information to be used by human health risk assessors in their retrospective or prospective evaluations of exposures of DoD personnel who are potentially exposed to DU as a result of being in, on, or near a vehicle at the time of perforation or personnel who entered perforated vehicles after they were struck. This source of aerosol

data will form the basis of modeling input parameters by summarizing the bounds and characteristics of typical aerosols generated by perforating armored vehicles.

To accomplish these assessment and characterization objectives, a robust testing protocol was required to enhance the understanding of DU behavior in the air and on surfaces inside and, to a limited extent, outside impacted armored combat vehicles during and shortly after perforation. Vehicles specifically used in this testing program were the Abrams M1A1 tank and the Bradley vehicle.

Perforation of armored vehicles struck by DU munitions generates fragments of DU penetrators and aerosols consisting of DU oxide particles and armor materials. The Capstone DU Aerosol Study specifically focused on collection of aerosols and particles that were deposited on and resuspended inside and outside selected vehicles struck by LC, kinetic-energy DU penetrators. The DU aerosols created were monitored from the time of LC-DU munitions impact to 2 h after perforation. Samples were collected and analyzed for uranium and metal concentrations, chemical composition, particle morphology, particle size distribution, and solubility. These characteristics provide the bases for input to computer models that are used to assess chemical and radiological doses from inhalation and ingestion of DU.

The primary testing effort focused on generating and characterizing DU aerosols and subsequent surface contamination inside Gulf War/ODS-era combat vehicles as they relate to evaluating the possible health effects on the affected Soldiers (Capstone Phases I and II). Additionally, in Phases III and IV, tests focused on current or future vehicle configurations and any incremental change in aerosols generated by DU munitions impact with DU armor. The test results from the Capstone DU Aerosol Study will be used in subsequent studies to update the human health risk characterizations for OSAGWI Gulf War/ODS exposure scenarios (OSAGWI 2000). Risk characterization findings will be particularly relevant for evaluating OSAGWI Level-I exposures, which included personnel who were in, on, or near (i.e., within 50 m of) an armored vehicle at the time it was perforated by LC-DU munitions and "first responders" who entered damaged vehicles after perforation by DU munitions to evacuate personnel. These findings also will be used to determine if changes in DoD doctrine, policies, and procedures are warranted to reduce risks to military personnel in the future.

2.2 Physical Simulation of Scenarios

Scenarios were developed to measure aerosol concentrations and to quantify other aerosol characteristics from actual firing incidents and from possible future engagements. The field tests, which incorporated varying firing angles, were divided into phases so the investigators could separately focus on circumstances similar to 1) Gulf War/ODS actions (Phases I and II) and 2) those of possible future actions (Phases III and IV). Brief descriptions of the four test phases follow.

- **Phase I—Abrams Tank Without DU Armor**

  Some Abrams tanks used in the Gulf War/ODS were equipped with heavy (DU) armor packages and some were not. The six tanks that were struck by DU rounds in the Gulf War/ODS did not involve perforation of heavy armor. Consequently, the Capstone DU Aerosol Study simulations of these Gulf War/ODS incidents used Abrams tank turrets without the heavy armor packages. The test shots received by these vehicles in Phase I were more severe than the shots received during actual Gulf War/ODS incidents. Four of the seven Phase-I shots were crossing shots in which the round was fired at and perforated the side of the turret, and exited through the opposite side. Two of the

remaining three shots purposely were fired into the gun breech to maximize the amount of aerosol generated. In the final Phase-I test, the shot was fired through the hull within the turret basket to more closely represent the upper bound of aerosol production for Gulf War/ODS incidents.

- **Phase II—Bradley Fighting Vehicle**

  The Bradley vehicle is a lightly armored, maneuverable vehicle that is equipped with a medium caliber gun. LC-DU munitions easily penetrate the Bradley's light armor, and they generally traverse the vehicle with little penetrator erosion. During the Gulf War/ODS, 15 Bradley vehicles were struck by DU munitions, and in some cases, there were multiple strikes. Most of the strikes that crossed crew compartments were fired into the Bradley's passenger compartment (rather than through its turret).

  In Phase II of the Capstone DU Aerosol Study, two crossing shots were fired through the passenger compartment and one shot was fired into the gun feeder in the turret (similar to a gun breech shot in an Abrams tank) to simulate the Bradley incidents.

- **Phase III—Abrams Tank with DU Armor**

  Though Abrams tanks equipped with heavy armor received no perforating shots through this armor during the Gulf War/ODS, it was desirable to study aerosol generation and potential aerosol levels that would result from such an incident. In Phase III, two shots were fired into DU armor using munitions specifically loaded to perforate the armor.

- **Phase IV—Operational Abrams Tank with DU Armor**

  In a series of tests that were conducted under a separate program, shots were fired at a fully operational M1A2 Abrams Main Battle Tank equipped with heavy armor and uploaded with aluminum surrogate penetrators rather than DU munitions. Unlike the Phase-I through Phase-III tests, the Abrams Live-Fire tests were performance-based and were not designed specifically to evaluate DU aerosols produced during the tests. However, a small number of aerosol samplers were installed in three of the tests to 1) establish a background, 2) evaluate the DU aerosol created when the armor was perforated by a non-DU munition, and 3) collect the aerosols from firing a DU munition through the heavy armor.

2.3 Test Site

Field tests conducted for the Capstone DU Aerosol Study required a site that was licensed by the U.S. Nuclear Regulatory Commission (NRC) for use of DU and that could support the firing of DU munitions against armored targets. After evaluating possible test sites, the study team selected ATC's Superbox facility located on the Ford's Farm range at APG to carry out the testing program. The Superbox is a 25.6-m (84-ft) diameter, half-sphere vessel/dome with auxiliary components and facilities that protect the environment by containing contaminants generated from targets impacted by DU (or non-DU) munitions. Typical munitions tested at the facility include anti-armor, kinetic-energy rounds and high-explosive warheads. Targets range from small-scale field targets to full-sized vehicles. A thick, steel fragmentation shield about 12 m wide by 12 m long by 7.6 m high (40 ft by 40 ft by 25 ft) inside the vessel ensures that

no munition or target fragments penetrate the vessel walls. The fragmentation shield and vessel are capable of withstanding explosive blasts.

The Superbox incorporates a high-efficiency filtration system that removes contaminants from the vessel. The filtration system draws 30 m^3/sec (64,000 cubic feet per minute [cfm]) of air through ducts located around the bottom perimeter of the vessel. This exhaust train leads to high-efficiency particulate air (HEPA) filters that clean any airborne contaminants before air is released to the atmosphere. Clean air is drawn through a supply train and blown into the top of the vessel. A real-time monitoring system that continuously analyzes the air quality in terms of suspended particulates in the vessel is used to determine when contamination levels following a shot have decreased sufficiently to allow safe entry of workers. During the Capstone tests, the air handling system was turned off before impact and remained off during the 2-h, turret-sampling interval to avoid interference with sample collection.

Figure 2.1 details the various external features of the Superbox, and Figure 2.2 illustrates the floor plan of the facility.

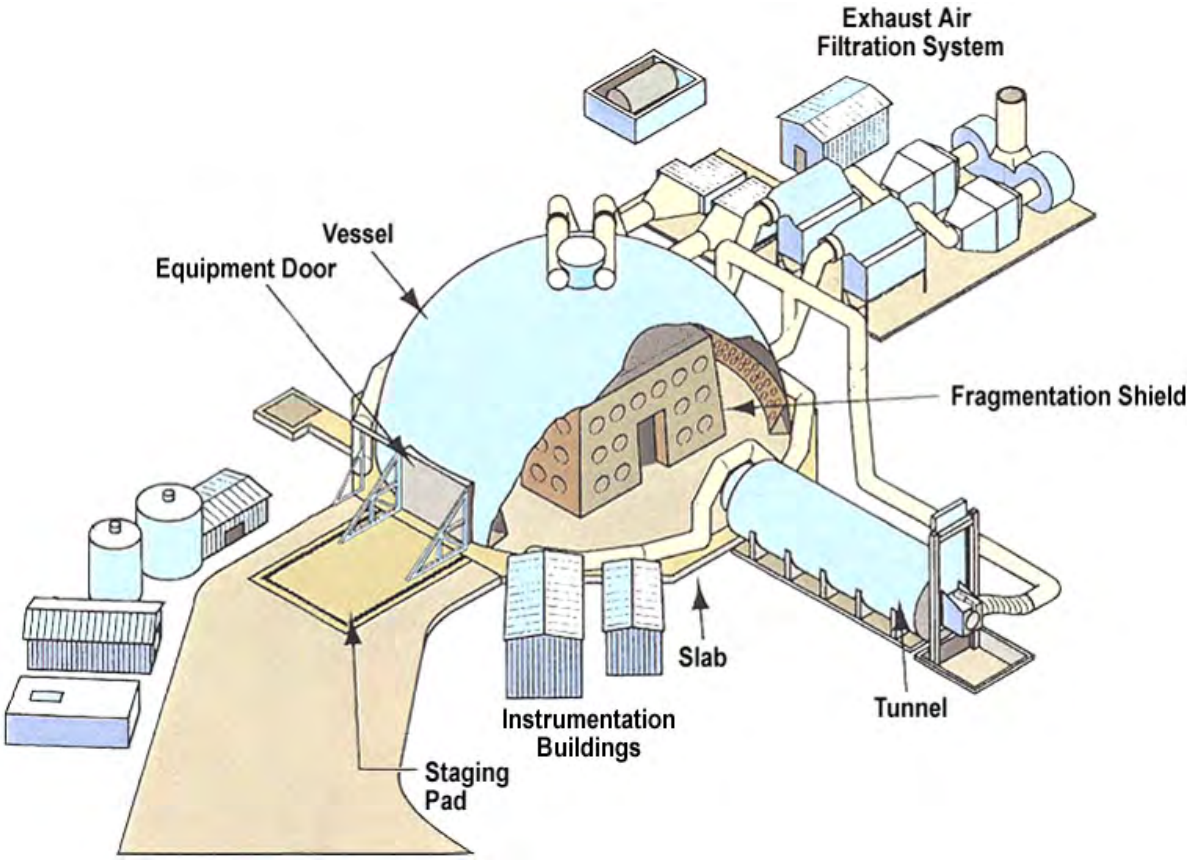

Figure 2.1. Exterior Plan of the Superbox and Auxiliary Buildings

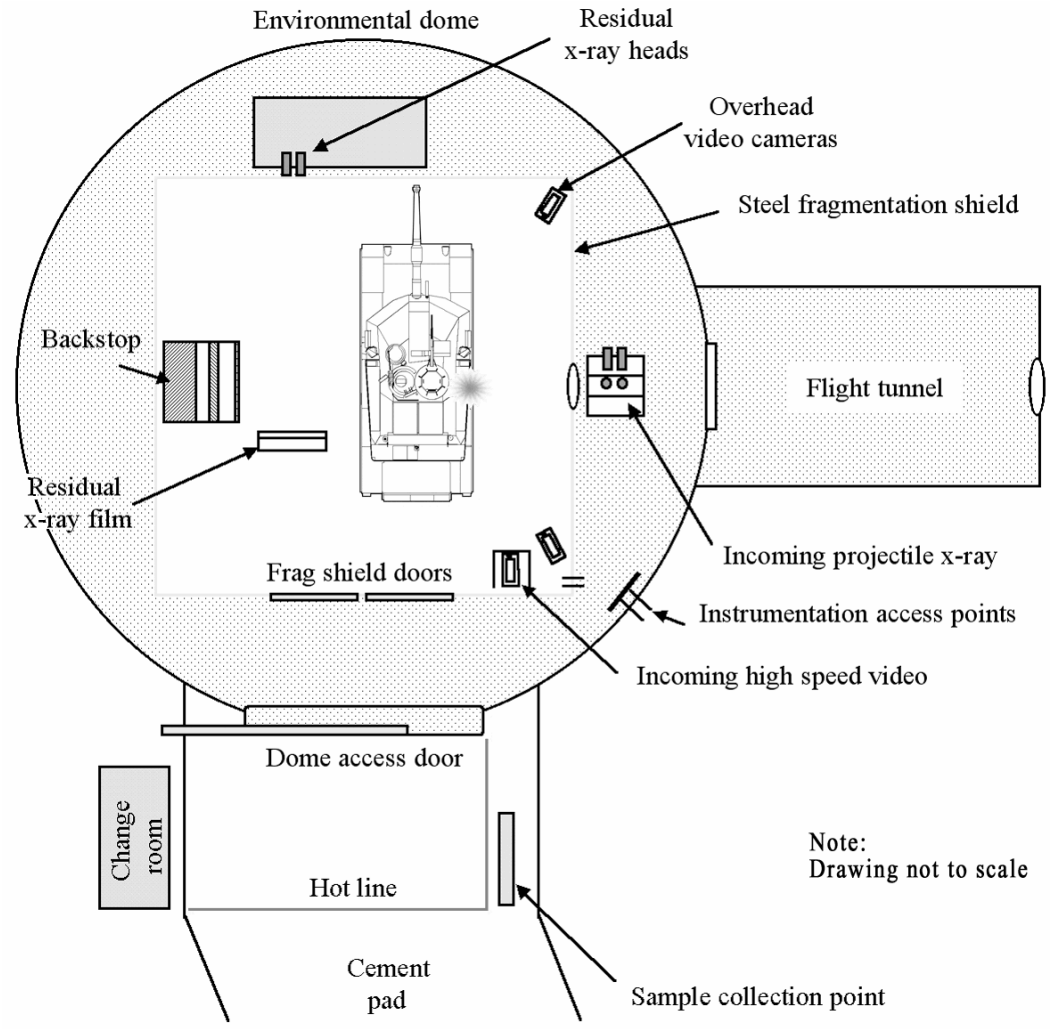

Figure 2.2. Floor Plan of the Superbox and Auxiliary Buildings

2.4 Aerosol Collection and Characterization

It was imperative that an aerosol collection system be designed to 1) function in a high-temperature, high-pressure environment; 2) survive damage from fragments; and 3) provide sample collection redundancy, confidence in timing, adequate flow rates, and sufficient sample collection for chemical analysis of selected samples. Further stipulations were that aerosols be collected:

- inside the vehicle as a function of time, position, and shot line
- exterior to the vehicle as aerosol and as deposited material
- in sufficient quantity to allow characterization in terms of uranium concentration, particle size, and other parameters.

The Capstone DU Aerosol Study was designed to address the primary factors that affect Gulf War/ODS exposure assessments. These factors are listed and prioritized in Table 2.1. The priorities were developed to guide allocation of resources for planning configuration scenarios and analyzing the aerosols collected.

Table 2.1. Test Evaluation Priorities

Priority	Factor Description
1	Interior DU source term
2	Interior DU concentration by particle size distribution over time
3	Lung fluid solubility and dissolution rates by particle size distribution
4	Chemical forms by particle size over time
5	Particle morphology by particle size over time
6	Effect of heating, ventilation, and air conditioning (HVAC) and environmental control/nuclear, biological, chemical (EC/NBC) systems on interior DU concentration by particle size over time
7	Total elemental composition by particle size
8	Resuspension factors from interior and exterior surfaces
9	Transferable DU from interior and exterior surface contamination to hands
10	Exterior source term, including particle size distribution
11	Isotopic uranium ratios by particle size

The bases for performing each type of analysis for the radiological health risk assessments are explained below.

1. *Interior DU source term*: A certain percentage of the penetrator and armor aerosolizes upon impact and perforation. Some of the aerosol created will remain outside the vehicle. The interior source term establishes how much DU aerosol is present inside the vehicle.

2. *Interior DU concentration by particle size distribution over time*: Concentration and the distribution of particle sizes changes as a function of time in this violent environment, and both are needed for dose assessment. The particle size distribution determines where the particles will deposit in the respiratory tract—a key parameter in intake and dose estimation.

3. *Lung fluid solubility and dissolution rates by particle size distribution*: The solubility and dissolution rates of DU aerosols determine the rate at which the DU particles enter body fluids, which in turn influences the chemical and radiological dose.

4. *Chemical forms by particle size over time*: The chemical forms, especially the oxidation phases, of the DU aerosols are an indication of the type of solubility and dissolution rates that can be expected from internalized DU. Evaluation of chemical forms as a function of particle size also indicates whether or not the forms are consistent across particle size ranges.

5. *Particle morphology by particle size over time*: The particle morphology (shape) helps confirm or explain the correlation between the chemical forms and the solubility and dissolution rates. If the chemical forms indicate a different type of solubility or dissolution than is expected, the particle morphology may be useful in explaining the differences.

6. *Effect of HVAC and EC/NBC on interior DU concentration by particle size over time*: The HVAC and environmental control/nuclear, biological, chemical (EC/NBC) overpressure ventilation systems, as well as the fire suppression system and turret blower, will reduce the DU airborne concentration as well as change the particle size distribution. Many of these systems were operational in the armored

vehicles that were hit during the Gulf War/ODS or can be expected to be operational in future battlefield actions. Therefore, evaluation of these systems with respect to DU aerosols inside the vehicle provides information on the clearance of DU aerosols from the vehicle interior. Additionally, operation of the fire suppression system may result in the formation of compounds that not only will influence the settling rate of the aerosol particles but also may affect the solubility and dissolution rate of DU once it is internalized. The risk assessors can then apply an appropriate ventilation rate to calculate the concentration by particle size distribution within a specific time period.

7. *Total elemental composition by particle size*: The elemental composition of the aerosol samples identifies other primary elemental constituents to whom the crewmembers are exposed. The presence of other elemental constituents may influence the solubility and dissolution rate of the isotopes of DU.

8. *Resuspension factors from interior and exterior surfaces*: The majority of personnel exposed to DU are individuals who entered either U.S. vehicles involved in fratricide incidents or damaged Iraqi vehicles. Inhalation is still the predominant route of exposure for these individuals, but the mechanism or action by which DU particles are made airborne is different. Hence, measuring the resuspension of DU particles from surfaces (both exterior and interior) addresses scenarios involving the exposure of these individuals.

9. *Transferable DU from interior and exterior surface contamination to hands:* The "hand-to-mouth" pathway of ingesting residual DU is another exposure route that individuals may have encountered.

10. *Exterior source term, including particle size distribution*: The exterior source term quantifies the amount of DU present outside the vehicle that could lead to exposure. A certain percentage of the DU penetrator aerosolizes upon impact, and the aerosol concentration exterior to the vehicle will be different from the concentration within the vehicle. Although establishing an exterior source term would aid in the evaluation of DU exposure to those individuals adjacent to the vehicle at the time of impact and to the "first responders" (i.e., those who enter the vehicle to assist in personnel and equipment recovery), the test environment conditions complicated the assessment that would have led to establishing the exterior source term. The static air conditions within the Superbox and the undefined aerosol contribution from subsequent penetrator impact with the catch plate were serious drawbacks to determining this source term. However, characterization of particle size distribution of the exterior aerosols was deemed plausible and pursued in this test.

11. *Isotopic uranium concentrations by particle size*: The isotopic uranium concentration by particle size distribution validates that the uranium being collected is primarily DU rather than natural uranium. The total amount of uranium and its isotopic composition in DU (U-238, U-235, U-234, and to a lesser extent, U-236) are needed to adequately assess the health risk.

3.0 Methods

In preparation for the Capstone field tests, targets, munitions, and firing angles were selected to simulate the desired conditions. The study's focus then shifted to designing an air sampling strategy to withstand the impact forces inside the vehicle while meeting the aerosol collection objectives. A customized system integrating sampler configuration, shielding, and computerized control was developed for collection of interior aerosols. Exterior air sampling, though requiring less sophisticated control or shielding, presented its own concerns. To avoid affecting aerosol particle size and settling during the firing tests, the Superbox air handling system was turned off during the sampling period, which extended 2 h post impact. Because the resulting static environment would tend to overestimate aerosol concentrations exterior to the vehicle, its usefulness for source-term calculations was uncertain. Procedures to measure aerosol deposition and resuspension were developed, and a procedure to measure air exchange rates in target vehicles was developed for later extrapolations of aerosol clearance rates in functional vehicles with operating ventilation systems.

This chapter summarizes test preparations and discusses methods used to conduct the firing tests, sample collection, aerosol analysis, and quality assurance (QA).

3.1 Selection of Targets

Target vehicles were selected to match those armored vehicles struck during the Gulf War/ODS for retrospective analyses. A newer vehicle and DU armor were used for prospective analyses. The target selected for Phase I of the testing program was a circa-1991 Abrams tank that was not equipped with DU armor. An infantry version of the Bradley vehicle was the target for Phase II. In Phases III and IV, Abrams tanks equipped with DU-armor packages were used as the target vehicles. With the exception of the Phase IV test, all testing was conducted using BHT structures. The high cost of using operational Abrams tanks and Bradley vehicles precluded their use for these destructive tests, and the test team concluded that aerosols collected inside a BHT would yield adequate data for input into updated human health risk assessments.

The BHTs were actual vehicle structures without instrumentation, wiring, or flammable components. Components normally found inside a combat-ready vehicle, such as communications and fire-control equipment, the EC/NBC ventilation system, the HVAC system, etc., were removed. The breech, which was integral to the testing program, was left in place. Between shots at the same vehicle, the area around the entry and exit holes was removed and replaced with production specification material (armor or other material) for structural integrity and to ensure as clean a condition as possible prior to the next shot.

3.1.1 Abrams Tank (Phase I)

The Abrams Main Battle Tank family consists of several generations of tanks (see Figure 3.1). The two generations that participated in the Gulf War/ODS were the M1A1 without DU armor and the M1A1 with DU armor. The M1A2 series has largely replaced the M1A1 series tanks. The Phase-I turret shots affected only the turret-side armor package, which is similar for the M1A1 and M1A2 series tanks. Therefore, side-armor and projectile interactions for past and future scenarios are expected to be the same.

Figure 3.1. Abrams Main Battle Tank

An M1 series turret was placed on an M1A1 series ballistic hull that had been used in previous ballistic tests at ATC. The hull front armor and side armor skirts were not necessary for the Capstone tests so they were removed to minimize the amount of material for ultimate disposal. These differences were external to the crew compartment and did not compromise the integrity of any shots. The hull was cleaned and decontaminated before being outfitted with the turret. The turret and hull were stripped of wire harnesses and hoses and all other components except for the gun breech and turret basket. While the stripped condition increased the interior air volume compared with an operational vehicle, it also eliminated obstacles to mixing. Vehicle openings were closed or sealed to simulate an intact vehicle and to minimize aerosol loss and interference from external effects

3.1.2 Bradley Fighting Vehicle (Phase II)

The Bradley Fighting Vehicle System family has several vehicle generations and stowage configurations. The M2 is the infantry version, and the M3 is the cavalry version. Each version has an A1 and A2 generation reflecting various system enhancements. Units of each of these versions were impacted by DU munitions during the Gulf War/ODS. The choice between the infantry and cavalry versions was not critical because of their structural similarities. An M2A1 (represented in Figure 3.2) was selected for the Capstone DU Aerosol Study because of its availability. The Bradley vehicle was stripped of all components, wire harnesses, and hoses to provide room for the sampling instrumentation and eliminate unnecessary combustible sources. Because the spall liner is an integral part of the armor design, it was not removed. Vehicle openings were closed or sealed to minimize aerosol loss and interference from external effects.

3.1.3 Abrams Tank with DU Armor (Phase III)

The DU armor test was conducted using a second M1 series turret and replacing the left front armor with DU armor from an M1A1 DU turret. As with the previous M1 turret, this one was stripped of wire harnesses, hoses, and all other components, except for the gun breech and turret basket. The turret was mounted on the Phase-I ballistic hull, which had been decontaminated.

Figure 3.2. Bradley Fighting Vehicle

3.1.4 Operational Abrams Tank with DU Armor (Phase IV)

A fully operational M1A2 Abrams tank was the target for a series of Abrams Live-Fire Vulnerability Tests, a performance-based test that was not designed specifically to evaluate DU aerosols. The M1A2 tank was equipped with DU armor and was uploaded with aluminum surrogate penetrators rather than DU munitions. Mannequins were placed at each crew position, and extensive sampling equipment filled the turret and driver's compartment. The ventilation/filtration system was operating during these tests.

3.2 Munition and Firing Angles

The type of munition used for all Phase-I, Phase-II, and Phase-III shots was a kinetic-energy cartridge with an LC-DU penetrator. The firing angles for the tests were selected from composites of actual Gulf War/ODS shots and from shots expected to penetrate the heaviest armor and other components to enhance the generation of DU aerosol. The test shots were intentionally loaded to perforate the target, and in most cases, the trajectory was designed so that the projectile would exit the target.

Twelve test shots were conducted for Phases I through III over a period of about four months. Phase III was conducted between Phase I and II. The Phase-IV target was struck several times with different types of munitions. The Phase-IV shot with the most relevance to the Capstone study objectives was Phase IV, Shot 4 (PIV-4), which involved an LC-DU munition.

3.2.1 Munition

The munition for all shot tests in Phases I, II, and III was an LC munition, known as an Armor-Piercing Fin-Stabilized Discarding-Sabot (APFSDS) munition, with a DU penetrator. The projectile of this munition included the DU penetrator, a steel-tipped aluminum windshield, and aluminum tail fins. The penetrator is made of 99.25% DU alloyed with 0.75% titanium. The same type of LC-DU munition was selected for all shots to maintain consistency in ballistics and in the probable generation of DU aerosols and particulates. The propellant charges were adjusted to achieve the impact velocities needed to meet the test objectives. LC-DU munitions will be referred to simply as DU munitions in the remainder of this document except where needed to differentiate from smaller caliber DU munitions.

3.2.2 Shot Lines

The extent of DU and target aerosol generated upon impact depends on the thickness of the armor and the other components that are perforated. Considerations of shot lines included analysis of major armor and turret components directly in the path of each shot line. The choice of shot lines for Phases I and II was guided as much as possible by Gulf War/ODS incidents, including those in which multiple impacts occurred.

Another requirement of the Capstone field tests was to acquire data from scenarios that were not directly experienced during the Gulf War/ODS but could occur during future engagements. The test conditions imposed during these tests balanced the following considerations:

- types of shots experienced during the Gulf War/ODS
- possible future scenarios
- preservation of instrumentation
- maximum generation of data
- establishment of upper and lower bounds of aerosol production.

In almost all Gulf War/ODS shots in which U.S. vehicles were perforated through the crew compartment, the shot lines were angled crossing shots (e.g., from left rear to right front, etc.). In some instances, the shots did not cross crew compartments, and these shots would have the least effect on personnel uptake of DU aerosols. For testing purposes, shot lines were selected to simulate the Gulf War/ODS shot lines believed to have had the highest potential for aerosol generation. Additionally, two separate shots into the gun breech of the Abrams tank and one shot into the turret gun feeder of the Bradley vehicle were conducted to enhance the generation of aerosols and provide an estimate of an upper bound of DU aerosol production.

Shot lines for the various tests are summarized below. Drawings of each shot line are presented in Chapter 4.0. The projectiles were fired from a fixed gun position.

- **Phase I:** Shots 1 and 2 were selected as replicates of representative turret-crossing shots, while Shots 3 and 4, (otherwise referred to as Shots "3/4" to indicate that they represented a single event of two shots that were fired minutes apart) were selected to assess the contributions of multiple shots to aerosol production. A turret-crossing shot is represented in Figure 3.3. Shots 5 and 6 were also turret-crossing shots but were selected to establish the upper bound for aerosol production with non-DU armor by firing into the gun breech. Shot 7, a hull shot (Figure 3.4), was chosen to replicate as closely as possible the single shot in the Gulf War/ODS that struck the turret ring and perforated the crew compartment. Phase-I shots are abbreviated PI-1 through PI-7.

- **Phase II:** Shots 1/2 were crossing shots fired minutes apart through the passenger compartment in a single test event (Figure 3.5). This test replicated shots that occurred during the Gulf War/ODS and assessed the DU aerosol contribution from multiple impacts. Shot 3, which was fired into the turret gun feeder, replicated Gulf War/ODS scenarios and was expected to establish an approximate upper bound of aerosol production in the Bradley vehicle. Phase-II shots are abbreviated PII-1/2 and PII-3.

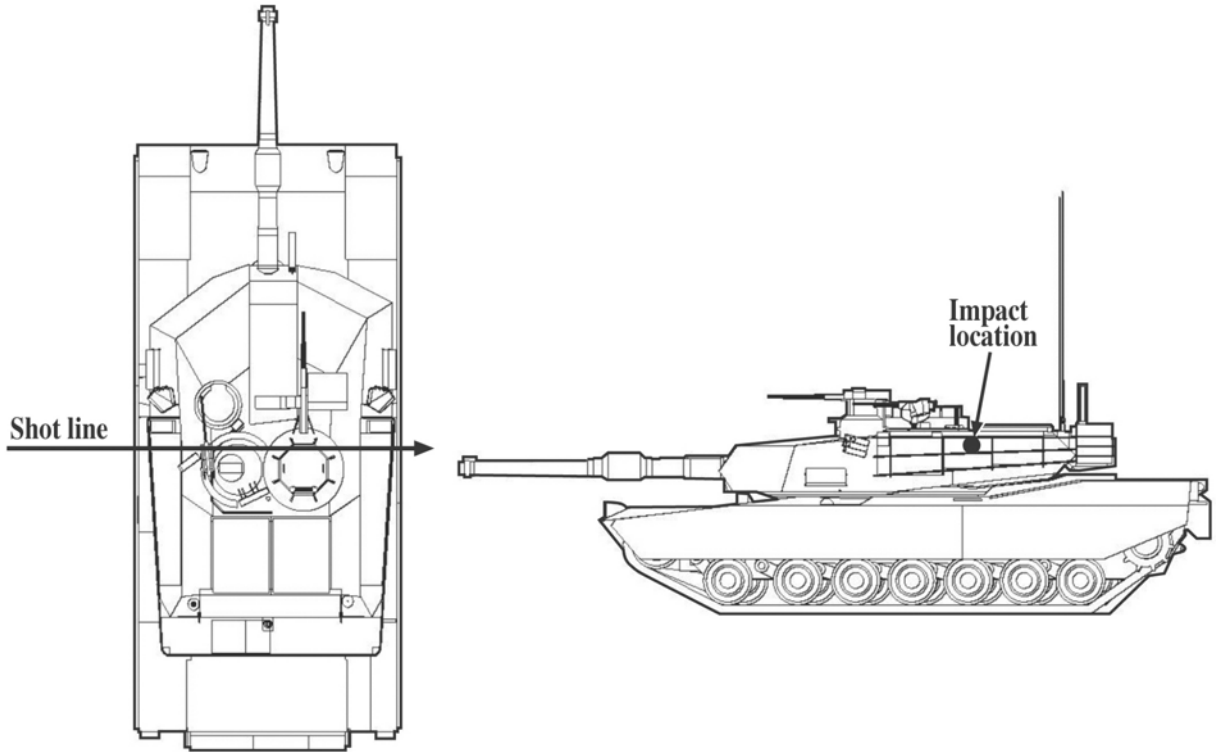

Figure 3.3. Abrams Turret-Crossing Shot Lines

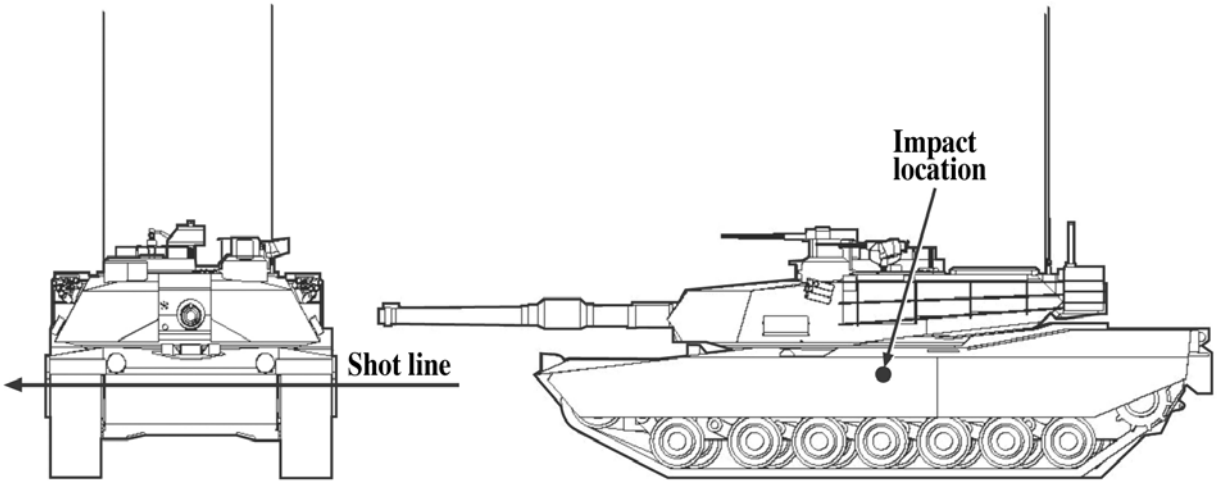

Figure 3.4. Abrams Hull Shot Line

- **Phase III:** Shots 1 and 2 into the front DU armor (Figure 3.6) represented future scenarios and helped to assess the aerosol contributions from the DU armor. Though not pictured in the drawing, the turret was turned to the left to facilitate the shot into the left front armor. Phase-III shots are abbreviated PIII-1 and PIII-2.

- **Phase IV:** In a series of tests using a variety of munition types, an operational vehicle was used as the target. Contamination surveys were conducted for four of these shots, and limited aerosol

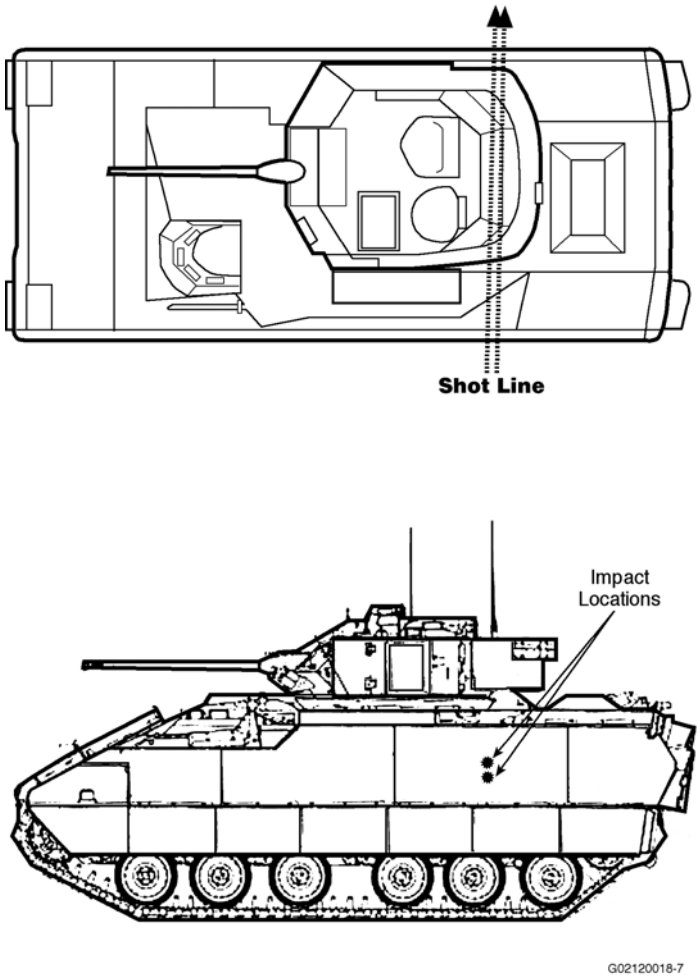

Figure 3.5. Bradley Passenger Compartment Shot Line

sampling was performed during three of the shots. Shot 4, in which a DU munition was fired at the operational vehicle, used a shot line similar to that used in the Phase-III shots and represented the aerosol produced by firing DU munition through DU armor. Phase-IV shots for which aerosol sampling was conducted are abbreviated PIV-1 through PIV-4.

3.3 Equipment Protection

Ballistic events are inherently destructive and cause significant collateral damage from fragments, blast, and pressure effects. However, sample collection, both inside and outside the target, required close proximity of the air samplers to the event. To preserve unique and expensive instrumentation and to ensure data acquisition, protective measures were taken. All instrumentation was strategically located to limit its damage from expected fragmentation. Shielding was provided, particularly for instrumentation installed in the most vulnerable positions near entry or exit points.

Initially, 0.64-cm (0.25-in.)-thick protective steel louvers were used to protect the aerosol samplers from fragments, but some filters were damaged in the first shot, apparently by high pressure and temperature and hot particles. In the second shot, a bottom-hinged flat metal plate covered the louver at the gunner's

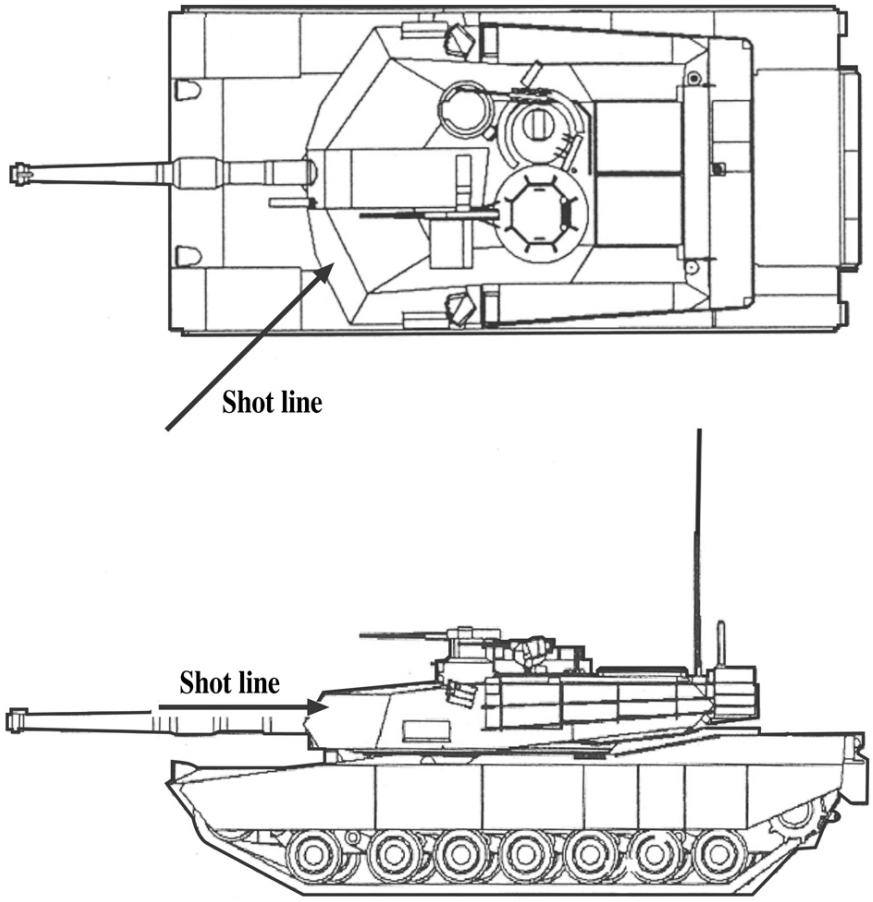

Figure 3.6. Abrams Front-Armor Shot Line

position in an attempt to improve filter survivability; however, this plate, which was released shortly after the shot was fired, offered little or no improvement. Solid steel covers were employed and sample media were changed in subsequent tests to avoid this problem. These covers had drop-down doors that were remotely released 3 sec after impact, and sampling was initiated 5 sec after impact. Figure 3.7 illustrates an air sampler array, a louvered shield, and a closed solid armored cover. The cyclone and moving filter (MVF) samplers were placed in a steel box in the crew compartment to allow for collection of aerosols through sample inlets (see Figure 3.8). These samplers are discussed in Section 3.5.2.

Lexan viewing panels were used to protect photographic equipment placed in the ammunition compartment, the engine compartment, or armored boxes. Interior cables, hoses, and harnesses were protected with metal barriers.

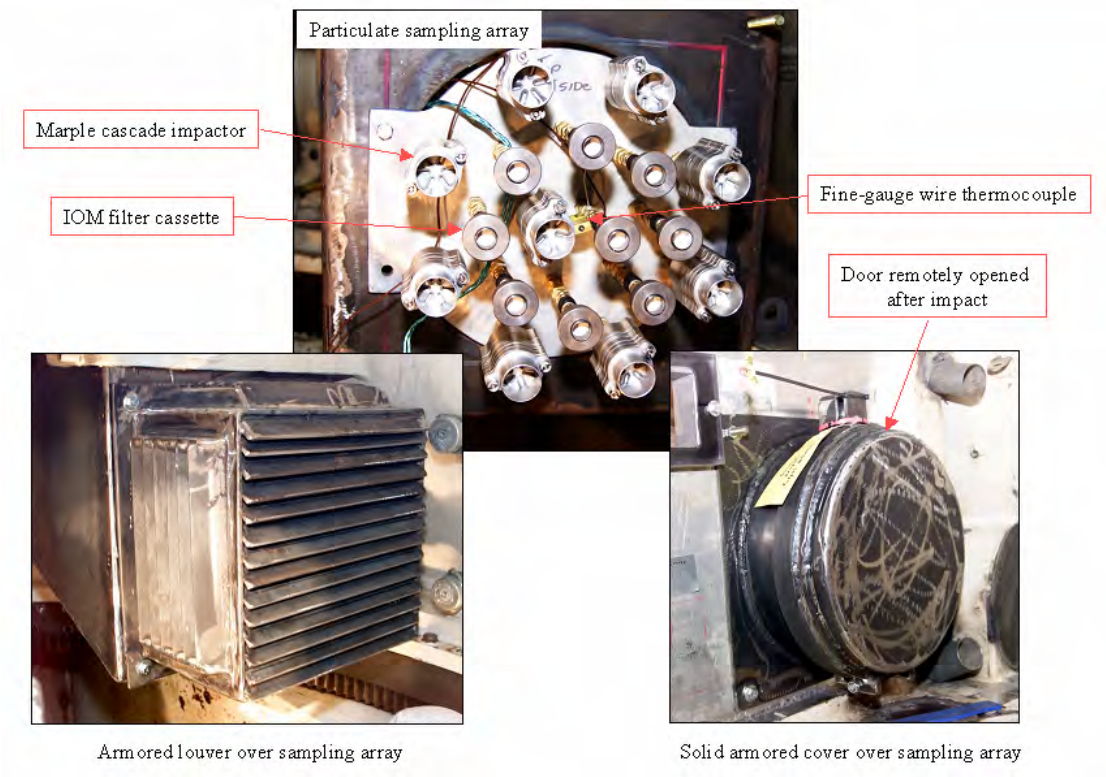

Figure 3.7. Air Sampler Array with Louvered and Solid Armor Shielding (in closed position)

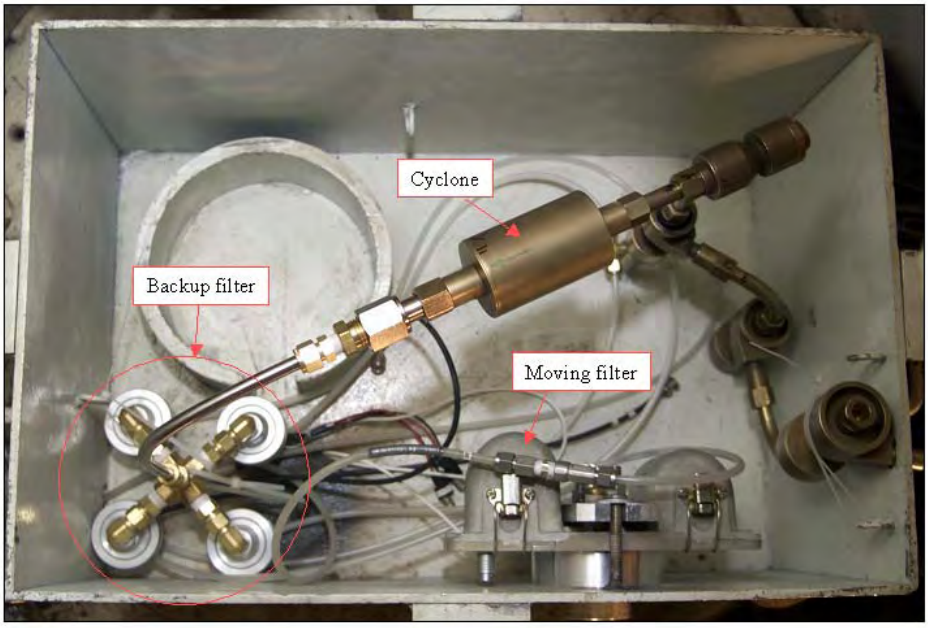

Figure 3.8. Protective Box for Cyclone (with Backup Filter) and Moving Filter

3.4 Superbox and Target Vehicle Operations

The Superbox crew from ATC cleaned the fragmentation shell before testing began. They also decontaminated and repaired the Abrams and Bradley BHT target vehicles between shots. Experienced gunners conducted the test firing operations, and staff from the Superbox facility performed the initial re-entry activities to ensure that the environment was safe for sampler recovery and contamination surveys.

For each field test phase, the relevant target vehicle was prepared, instruments were set up, shots were fired, air samples were recovered, targets were repaired, and the Superbox was cleaned. Each of these activities is described in the following sections.

3.4.1 Vehicle Preparations

Vehicle tracks and ancillary equipment that were not needed during the shot test were removed from the exterior of the target vehicles to minimize the weight and volume of material ultimately requiring disposal. To the extent possible, flammable and combustible materials were removed from the targets. No fuel was present in the BHT.

The vehicle gun was not needed for the field tests and was not attached to the Abrams tank for the first shot in Phase I. An inflated ball was placed in the gun breech to seal the gun position; however, this approach to sealing the gun breech was not effective because of the pressure created by the perforation. For subsequent tests, a gun tube was in place, and a blank shell casing was inserted and sealed into the breech. The gun breech was closed and secured prior to each shot.

The hatches were closed and secured prior to all shots. After the fourth shot, the hatches were bolted down to reduce their chances of opening. As observed from the external remote camera views in the Superbox, one or more hatches popped open during each shot in Phase I and during Shot 2 of Phase III. For those cases in which the hatch remained open, dispersion of aerosol through the hatch was observed on the video monitor.

3.4.2 Instrument Setup

For most, but not all of the tests, temperature and pressure sensors were placed in the vehicle to measure the temperature and pressure pulses within the turret, usually at aerosol sampler locations. The sensors measured the temperature and pressure pulse and their rapid decreases after perforation. An x-ray image of the residual penetrator exiting the vehicle was captured on film for use, if possible, in qualitatively evaluating the extent of penetrator erosion.

A high-speed video camera (nominally 1000 frames per second) was installed inside the bustle and positioned to point into the turret. The camera was installed behind a Lexan shield and was set up to use self-illumination. Real-time video feeds captured exterior and interior views. Two external cameras mounted above the vehicle provided views of the aim point on the side of the turret facing the gun and on the opposite side of the turret. Inside the turret, two cameras mounted near the bustle sides pointed toward the gunner's position. Six lights set up inside the turret to illuminate the interior were lightly shielded. External, remotely operated electrical power was provided for auxiliary equipment (e.g., the sampling gear, x-ray equipment, and video cameras).

3.4.3 Penetrator Catch Plate

The Superbox uses an armor catch plate to stop and contain the penetrator within the fragmentation chamber. DU aerosols are generated exterior to the vehicle due to the impact of the penetrator with the catch plate. Although this impact should not significantly affect the aerosols generated inside the vehicle, it could significantly change the concentration of aerosols generated exterior to the vehicle, thereby skewing the exterior sampling results and leading to over-estimation of external aerosol concentrations and exterior vehicle surface contamination compared to those occurring under actual battlefield conditions.

Several strategies, including the use of a sand catch box, were considered to avoid mixing fragments and aerosols produced by shots through target armor with those generated by the residual penetrator impacting the catch plate. At open-air sites, a sand catch box is commonly used to slow down penetrators and capture ricocheting fragments. The setup of such a structure inside the Superbox was considered but discarded as creating too much contaminated waste. In an attempt to provide a practical and inexpensive alternative (though of uncertain effectiveness) to mitigate this problem, a ballistic polyethylene covering was installed over the catch plate, and an aluminum plate was placed in front of it to limit fragment bounce and movement of aerosols. The ballistic polyethylene survived the first shot, but it became brittle in the cold weather and shattered during the second shot. It was not replaced. The aluminum plate also shattered during PI-7 and was not replaced.

3.4.4 Firing at Target Vehicles

After all equipment was in place and the facility was secured, the test team and equipment operators went to the observation facilities to activate the equipment and watch the results of each shot via the video feed. The gunners fired the DU cartridges from the fixed-position gun mount outside the Superbox. With the exception of PI-3/4, and PII-1/2, only one shot was fired for each test. At least a week passed between tests. In the case of the two-shot test events (PI-3/4 and PII-1/2), the first sampling sequence started with the first shot, continued while the gunners changed the aim point slightly and reloaded. This initial sampling sequence was terminated shortly before the second shot, which was fired 13 to 14 min after the first shot. The second sampling sequence was initiated when the second shot was fired. For single shots, manual startup of the sampler collection system was coordinated with the firing of the shot. Once started, the computer controller automatically switched samplers on and off at the programmed times.

3.4.5 Sample Recovery Operations

The fans controlling HEPA filtration of exhaust air inside the Superbox were turned off just before each shot was fired and remained off for the next 2 h during interior vehicle aerosol monitoring. This step was necessary to restrict airflow within the structure after the shot so the settling rate of particulate matter could be clearly evaluated without external interference. After the last sample collection period, the exhaust airflow was turned on to reduce gross particulate concentrations to levels required for safe entry. In accordance operational Superbox procedures, all personnel involved in initial recovery operations wore full-face masks or supplied-air respirators.

These personnel also wore personal air samplers to assist in the measurement of aerosol that remained in the air at the time of re-entry or that were resuspended by recovery activities. Documentation of

observations inside the tank included notations of any visible penetrator fragments, damage to aerosol samplers and vacuum lines inside the vehicle, and any anomalous damage to or conditions of the vehicle.

3.4.6 Target Repair and Superbox Decontamination

The Superbox underwent extensive cleaning, including power washing, before the Capstone field tests began to reduce the potential of cross-contamination from previous tests. Between Capstone shots, the target was vacuumed using a HEPA vacuum, and the floor was vacuumed to eliminate most removable contamination within the fragmentation shield. Radiation surveys were conducted after cleaning and before each shot to establish uranium levels on the vehicles and in the surrounding area. Baseline measurements were taken using wipes at prescribed positions within the vehicles and the fragmentation shield to establish the new level of background activity before initiating each test shot. The Abrams and Bradley BHTs were repaired as necessary between shots to maintain structural integrity and to cover perforation holes.

3.5 Interior Air Sampling

The Capstone DU Aerosol Study evaluated aerosol characteristics expected to be used as input to update the human health risk characterization for three exposure scenarios initially defined by OSAGWI. These scenarios are described in the USACHPPM Health Risk Assessment Consultation Number 26-MF-7555-00D (USACHPPM 2000) and are repeated here: 1) Level-I personnel consist of those who are in, on, or near an armored vehicle at the time the crew compartment is perforated by DU munitions and first responders; 2) Level-II personnel consist of those who were required to enter or work on perforated armored vehicles to perform military functions; and 3) Level-III personnel consist of all others with possible exposure including personnel downwind of a burning vehicle and curious onlookers. The Capstone DU Aerosol Study was designed to fill the data gaps associated with exposure Levels I and II, which are the foci of the following discussion.

The specific objectives of the aerosol characterization task were to 1) collect aerosolized and deposited particulate material in and around the vehicle, 2) gather physical data about particle size distributions and chemical information about the aerosols that may directly affect solubility rates of respirable aerosol particles in lung or intestinal fluids, and 3) gather information about elemental composition because, in addition to DU and titanium from the penetrator, other metals from armor and target components located along the shot line also were aerosolized.

During and immediately after DU penetration, heat, a pressure wave, the penetrator, fragments of armor and the penetrator, and aerosols are released into the crew compartment. The sampling of aerosols produced by penetration of an armored vehicle by a DU projectile presents complex demands on the design of aerosol sampling systems and sampling strategies. Every effort was made to protect sampling equipment to prevent damage by the actual projectile impact, by flying debris, and/or from hot gases. The characteristics of the aerosols released into the compartment (i.e., the aerosol mass, number of particles, size distribution, composition, morphology, intrinsic solubility) depend on the conditions of the perforation event (e.g., trajectory and route of DU penetration, type of armor penetrated, type of DU penetrator, presence and operating status ventilation and fire suppression systems, status of hatches and other compartment penetrations, etc.). Aerosol concentrations and particle size distributions were expected to be both spatially and temporally dynamic.

Sufficient data from previous sampling of DU aerosols produced from impacts on hard targets suggested that the aerosol concentrations in a test would change rapidly soon after creation of the aerosol. Mass concentrations may change with settling halftimes that are initially on the order of seconds and then minutes. Additionally, because of the possibility of spatial variability in aerosol concentrations within a crew compartment, the sampling strategy had to address temporal and spatial variables, so sampling for each type of these variables was conducted simultaneously.

Real-time instruments were considered but not used because most are delicate electro-optical devices. Their use presented two specific concerns: 1) they might not survive the hostile and violent test environment, and 2) they could not be operated at very high aerosol concentrations. Given these constraints, a moving filter device was chosen to obtain the time-sequence aerosol profile, especially during the initial sampling period. The device was chosen for the following two reasons: 1) the simple design of the device stood a better chance of surviving in the environment, and 2) particles collected on the device's substrates could be used for radioactivity counting.

Overall, the aerosol sampling and characterization plan was designed to obtain data on the following time- and space-dependent variables:

- particle mass concentration
- particle size distribution
- solubility (primarily in lung fluid)
- particle morphology and chemical composition.

The air samplers were operated well below a flow rate limit of 200 Lpm (7 cfm) to ensure that they did not exceed the maximum respiration rate for four crewmembers.

Total mass and particle size distributions of the aerosols were measured as a function of time. Most samplers operated during a specific portion of the total sampling duration so that the change in uranium concentration and particle size distributions over time could be evaluated. Others samplers operated during the entire sampling period to collect an integrated sample. Selected aerosol samples were evaluated for chemical composition, particle morphology, and solubility in simulated lung fluid.

3.5.1 Aerosol Sampler Arrays

Custom-designed arrays of sampling heads were secured to the inside of the target in locations approximating the breathing zones of the commander, loader, gunner, and driver. Each array was designed to support nine 25-mm Institute of Occupation Medicine (IOM) filter cassettes (described in Section 3.5.2.1) and nine cascade impactors (CIs; described in Section 3.5.2.2) mounted with quick-disconnect fittings. The array was configured in a circular pattern on a 36-cm (14-in.) diameter aluminum plate. Each of the nine sampling positions had a filter cassette/CI pair (Figure 3.9), with sampling ports positioned horizontally. The filter cassette numbering system started at the center top, moving in a clockwise direction, with Sampler 9 at the center. The CI numbering system began at the eleven o'clock position and moved in the clockwise direction also, again with Sampler 9 at the center.

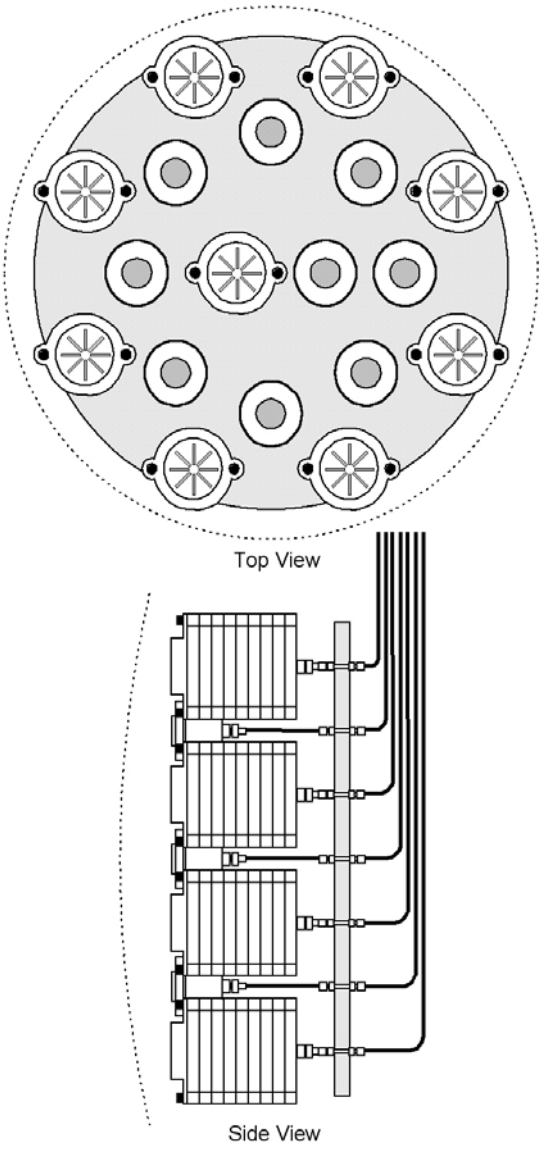

Figure 3.9. Schematic of a Sampler Array

The sampling arrays were protected from fragments by shields previously described. The initial design was a 0.64-cm (0.25-in.) steel shield fabricated with 3.8-cm (1.5-in.)-wide louvers on the front and all four sides. The louvers were intended to provide maximum protection of the samplers from fragment damage while minimizing restrictions to free air exchange between the compartment atmosphere and the shield air volume. Recognizing that shielding the air samplers and providing unimpeded air mixing to the samplers are intuitively contra-variant, the potential influence of creating a dead-space volume was assessed after evaluating the data obtained from Shot 1. A delay in the occurrence of the peak aerosol concentration would have been interpreted as the existence of impeded air mixing within the shield volume. However, the pressure pulse that occurs instantaneously with the shot is believed to have provided sufficient and immediate mixing to decrease the significance of impedance.

3.5.2 Aerosol Collection Instrumentation

Although some modifications were made, samplers used in this analysis were essentially off-the-shelf items that were chosen for their immediate availability and to minimize cost. Samplers used within the vehicle interiors included:

- filter cassettes
- CIs
- a five-stage cyclone coupled with a parallel-flow diffusion battery (PFDB) or backup filter apparatus
- a moving filter (MVF).

The filter cassettes and CIs were positioned within four sampling arrays. Each array was installed near the breathing zone of each of the Abrams crew positions (i.e., the driver's, loader's, commander's, and gunner's positions). Figure 3.10 shows the placement of the arrays during Phase I (with exception of Shots 5 and 6 for which the gunner's array was removed). Figure 3.11 shows a similar illustration for PII-1/2 with the Bradley target vehicle in which the arrays were placed near the commander's position in the turret, the driver's position in the driver's tunnel, and on the back ramp behind the right and left scout positions (labeled as "squad area sampling arrays"). Figure 3.12 shows the same vehicle but with the turret angled for a shot line into the Bradley vehicle's gun feeder. Figure 3.13 represents the configuration used in Phase III in which the turret was angled to receive the shot in the front armor.

The sampler types, their purposes, flow rates, and placements are listed in Table 3.1. Except for the MVF, sample collection began several seconds after the shot was fired to preclude interference from elevated temperatures and the blast pressure.

With respect to spatial sampling, the extent to which mixing of aerosols occurs in the crew compartments as a result of the impact and its short-term turbulence is relevant in evaluating aerosol concentration and inhalation that may be experienced from position to position in the perforated vehicle. Placement of sampler arrays consisting of cassettes and CIs was designed to evaluate the aerosols at the crew locations and near floor level while protecting the samplers from the path of the penetrator. To this end, one sampler array was positioned at each of the following locations in the Abrams turret and driver's compartment for the initial crossing shot lines (see Figures 3.10 and 3.13):

- near the commander's position at approximately shoulder height, with the array extending through the bustle plate

- near the loader's position at approximately shoulder height, with the array extending through the bustle plate

- near the gunner's position at approximately head height and immediately in front of gunner's position in the driver's compartment, which has air exchange with the turret basket, with the array at chest height.

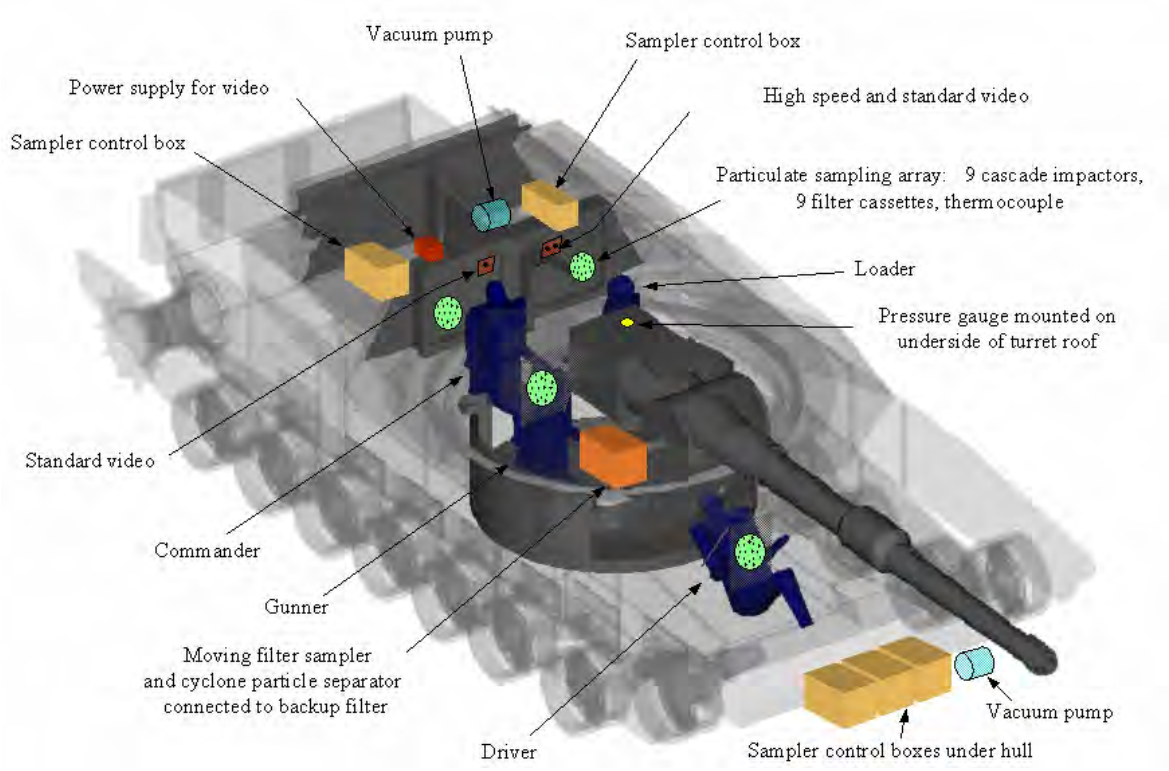

Figure 3.10. Placement of Testing Equipment in an Abrams Tank, Phase I

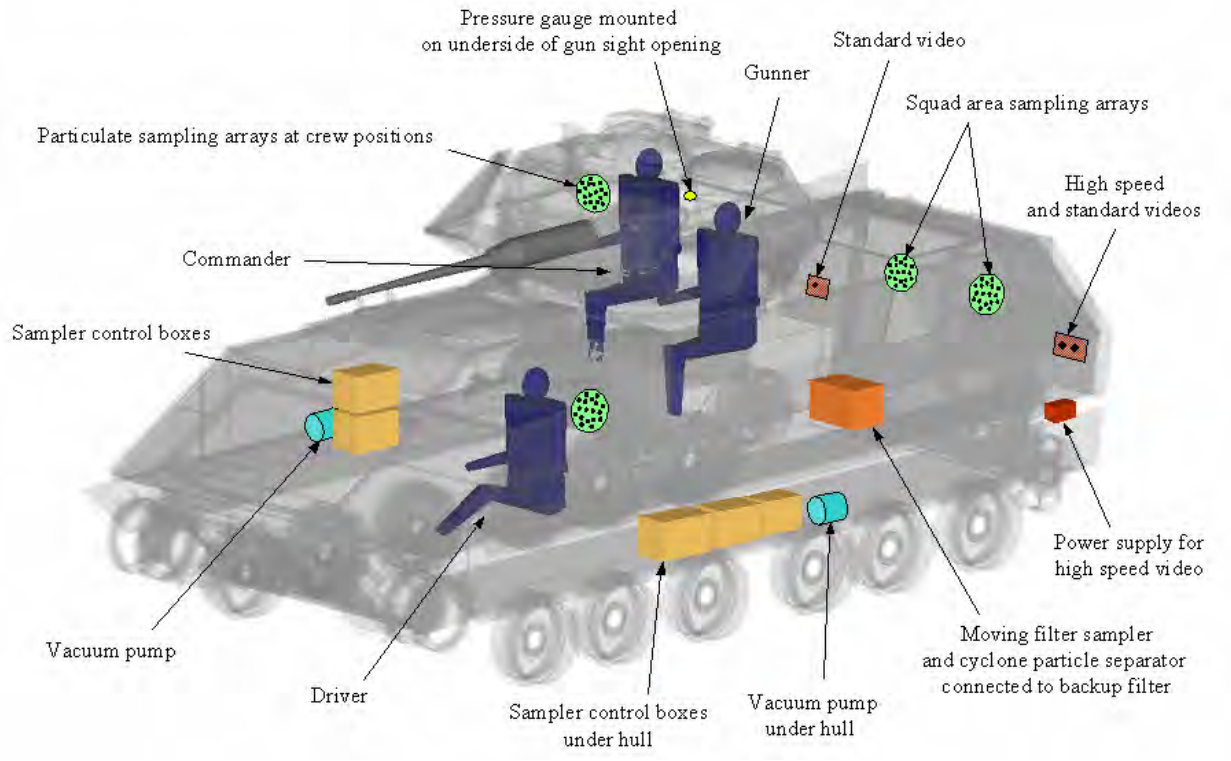

Figure 3.11. Placement of Testing Equipment in a Bradley Vehicle for Crossing Shots

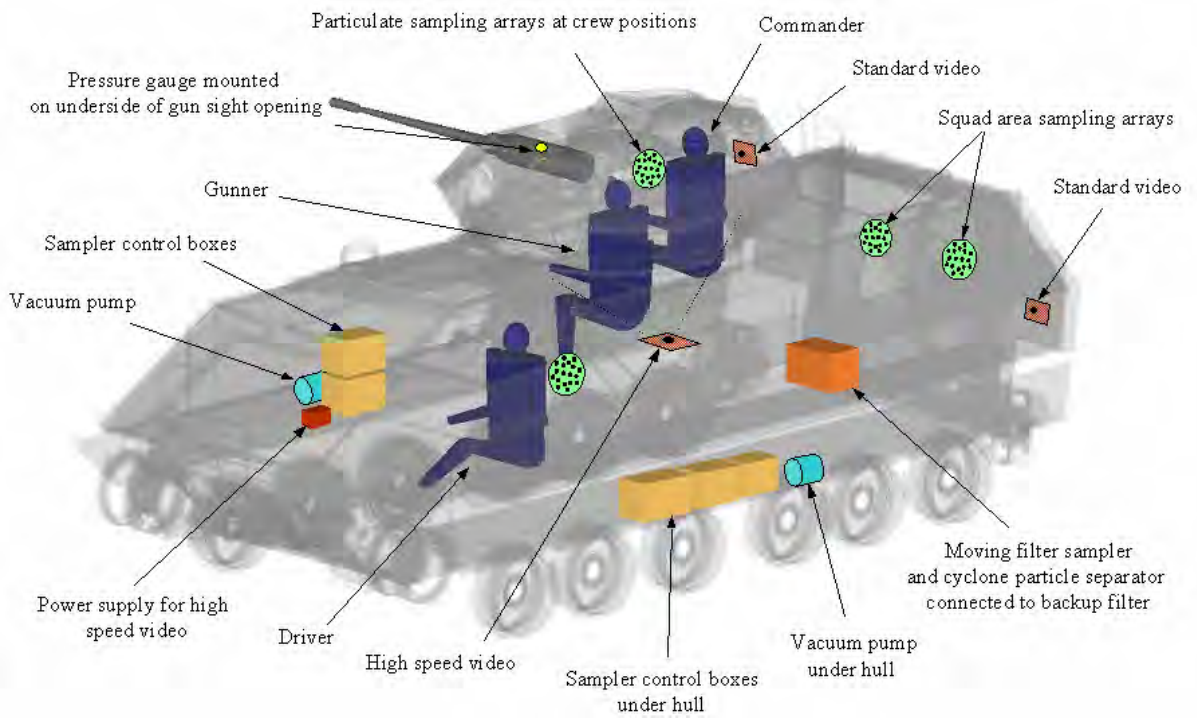

Figure 3.12. Placement of Testing Equipment in a Bradley Vehicle for a Turret Shot

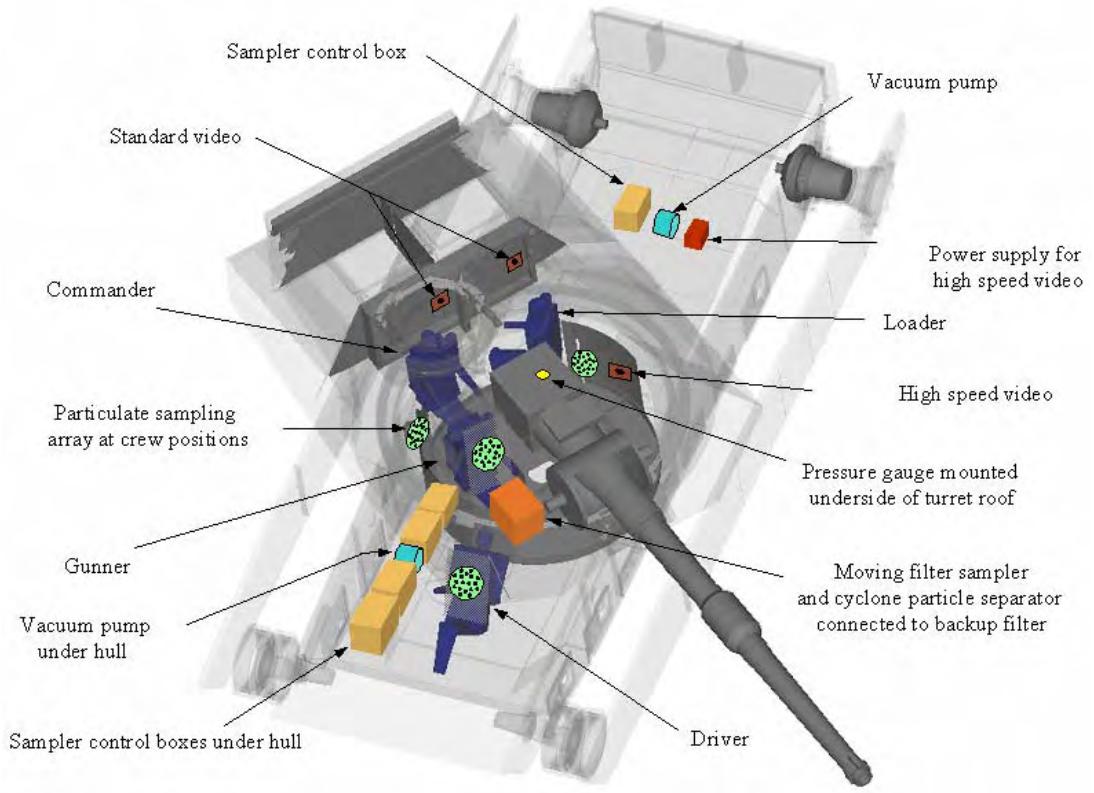

Figure 3.13. Placement of Testing Equipment in an Abrams Tank, Phase III

Table 3.1. Aerosol Sampling in the Crew Compartment

Type of Sampler	Purpose	Flow Rate	Number, Timing, Location
IOM filter cassettes, Supor filter media, later changed to Zefluor; polyvinyl chloride (PVC) backup filter	Time-dependent mass concentration by sequential sampling; chemical composition	2 Lpm per sampler times 4 units at a time →8 Lpm total	Four different interior locations with 8 plus 1 spare sequential sampler; total of 36 filter samplers
Marple CIs, mixed cellulose ester filter medium	Time-dependent aerodynamic particle size distribution, and total mass concentration (Σ stages); chemical composition	2 Lpm times 4 units at a time →8 Lpm	Four interior locations with 8 plus1 spare sequential sampler per location; total of 36 CI samplers
Five-stage SRI aerosol cyclone	Aerodynamic particle size distribution and total mass concentration. Size-selected bulk aerosol samples for chemical composition, particle morphology, and solubility	10 Lpm (nominal) for a single unit (operated between 9 and 13 Lpm)	One unit running continuously for the ~2-h sampling duration
Cyclone backup filter, Teflo, Silver membrane, Zefluor	Particles less than 1.2 μm.	10 Lpm nominal; coupled with exhaust of cyclone train; no additional flow required (operated between 9 and 13 Lpm)	One unit (consisting of 4 filters) running continuously for the ~2-h sampling duration
Parallel-flow diffusion battery (PFDB), Supor	Particle size distribution in the ultrafine range (0.005 to 0.5 μm aerodynamic diameter)	10 Lpm (nominal) for a single unit; the PFDB was coupled to the exhaust of a cyclone train; no additional flow required	One unit (consisting of 7 filtered samples) running continuously for the ~ 2-h sampling duration
Moving filter sampler, AW-19 filter media	High-resolution, time-dependent mass concentration; particle size and morphology	28 Lpm (operated between 19 and 33 Lpm)	One unit running during the first 5 sec, intermittently thereafter per programming

In the Bradley target vehicles, sampling arrays were installed in the following positions (see Figures 3.11 and 3.12):

- in the driver's tunnel behind the driver's seat
- near the commander's position at approximately head height
- on the right side of the back ramp at approximately head height, near a right scout position
- on the left side of the back ramp at approximately head height, near a left scout position.

Additionally, a cyclone was placed on the floor with the inlet about 0.3 m (1 ft) above the floor. The MVF was placed next to the cyclone. Their placement depended on the shot line and predicted survivability locations. To avoid damage to the gunner's array, which was too close to the line of fire, it was removed during shots into the breech.

The sampling intervals and the flow rates based on pressure drops were preset and computer controlled. Most samplers were located behind protective steel shields to increase sampler survival. Sampler array survivability was reviewed for every shot to minimize sample damage while collecting as many samples as possible.

3.5.2.1 Filter Cassettes

Samples for use in determining timed serial mass concentrations of the crew compartment atmosphere were collected using 25-mm SKC IOM stainless steel filter cassettes,[(a)] referred to primarily as IOMs or filter samplers (FSs). A disassembled IOM is shown in Figure 3.14. The filter medium initially selected for the cassettes was Gelman Supor 800 membrane discs,[(b)] which had been demonstrated to create an acceptable pressure drop of 0.8 psi. After the first two shots, during which the samplers closest to the penetration exit holes were damaged, Gelman Zefluor filters[(c)] were substituted and used successfully throughout the remainder of the tests.

Figure 3.14. Disassembled IOM Stainless Steel Filter Cassette

Sampling arrays of these filters were positioned at four locations within the interior of the crew compartment, thus providing time-dependent total concentration measurements at these four locations. The sampling sites were close to the approximate breathing zone for each member of the crew (commander, gunner, loader in the turret, and driver in the hull compartment). Nine filter cassettes (eight time-programmed and one spare or field blank) were arrayed in a circular geometry with CIs (described in Section 3.5.2.2) concentrically paired with the filter cassette at each site. The IOMs operated at a nominal flow rate of 2 Lpm.

(a) SKC Gulf Coast, Inc., Houston, Texas.
(b) Hydrophillic polyethersulfone, Pall Corp., East Hills, New York.
(c) Ultra-thin Teflon-based (PTFE) filters with a polymethylpentene support ring; Pall Corp., East Hills, New York

3.5.2.2 Cascade Impactors

Eight-stage, stainless steel, 34-mm Marple CIs[(a)] (Model 298) were selected to measure particle size distributions over discrete time periods. Several sets of disassembled impactors are pictured in Figure 3.15. The CI inlets were modified to change the standard right-angle inlet to a straight-through configuration to allow the arrays to be installed more efficiently at the crew sampling stations. The nominal cutoff diameter for the first stage of the Marple CI is 21 µm for a flow rate of 2 Lpm. Nominal cutoffs for the other stages are about 15, 10, 6, 3.5, 1.6, 0.9, and 0.5 µm**,** respectively. The substrate selected for the impactors on the basis of immediate availability was a mixed cellulose ester impaction medium of 0.8-µm pore size.[(b)] The backup filter was made of polyvinyl chloride (PVC) and had a 5-µm pore size.[(c)] A silicone-adhesive coating was applied to the first-stage substrate to minimize particle bounce. The CIs operated at a nominal flow rate of 2 Lpm.

During Phase IV, Capstone sampling arrays could not be placed in the vehicle due to Phase-IV test requirements. The primary samplers were the off-the-shelf Marple CIs attached to the uniform of the manikins placed at the driver's and loader's positions (Figure 3.16).

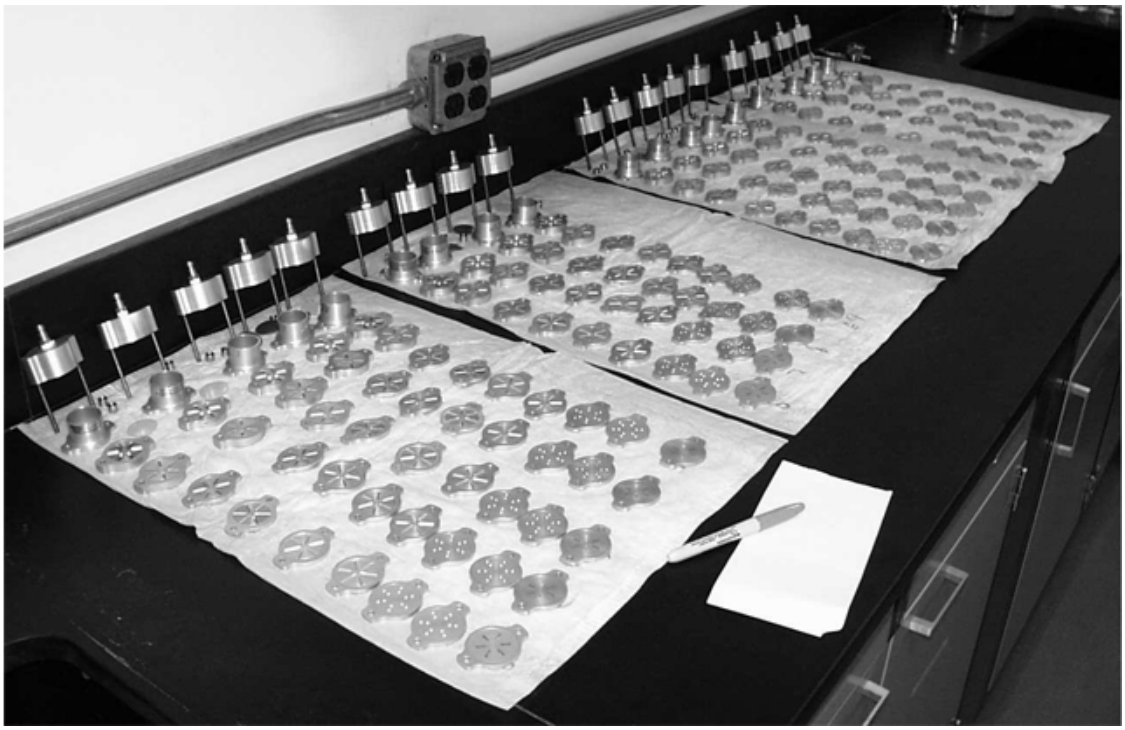

Figure 3.15. Disassembled Marple Cascade Impactors

(a) Andersen Instruments, Inc, Smyrna, Georgia.
(b) SEC-290-MCE; purchased through Andersen Instruments, Inc.
(c) SEF-290-P5; purchased through Andersen Instruments, Inc.

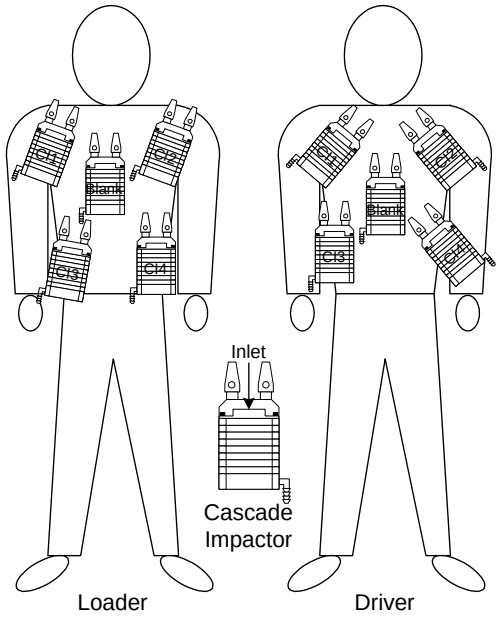

Figure 3.16. Position of Cascade Impactors on Manikins Placed in Target for Phase-IV Tests

3.5.2.3 Five-Stage Cyclone

A five-stage, SRI cyclone train[(a)] (Figure 3.17) collected size-selected aerosol residues for post-test studies (chemical and physical characteristics and *in vitro* solubility). Initial plans called for the cyclone to be operated at a flow rate of 10 Lpm so the cutoff diameter for Stage 1 would be approximately 10-μm aerodynamic diameter (AD), which is the cutoff diameter specified by Phalen et al. (1986) for thoracic deposition. The cutoff diameters for the remaining stages were 4.3 μm for Stage 2, 2.9 μm for Stage 3, 2.0 μm for Stage 4, and 1.2 μm for Stage 5. The actual flow rates were a nominal 14 Lpm and actually ranged from 9.0 to 13.4 Lpm. The cutoff diameters for Stages 1 through 5 at 14 Lpm were 7.8, 3.2, 2.3, 1.2, and 0.7 μm, respectively.

Typically, a backup filter is used on the exhaust of the cyclone to capture aerosol particles that are <1.2 μm AD. However, because of considerable uncertainty regarding the existence of an ultrafine particle fraction in the interior atmosphere, the exit filter was replaced with a Lovelace PFDB during the first shot. This seven-cell, screen-type diffusion battery has a useful range from 0.005- to 0.5-μm AD and collects particles that pass through Stage 5 of the cyclone. The PFDB with Supor filters was flow-matched and calibrated with the cyclone at 14 Lpm. Measurement of both total mass of particles (by gravimetric analysis) and DU concentration (by radiological and chemical analyses) was planned using these ultrafine particle size fractions. The PFDB is a complicated apparatus, and in spite of exceptional efforts to seal all components, a leak may have developed during the first shot. For the remaining tests, the standard backup filter apparatus (actually a set of four filters, nicknamed a “spider”) replaced the PFDB. The backup filter media used included 47-mm Gelman Teflo for PI-2; a combination of Teflo, silver membrane, and Zefluor for PI-3/4; and Zefluor for the remaining shots.

(a) In-Tox Products, Moriarity, New Mexico.

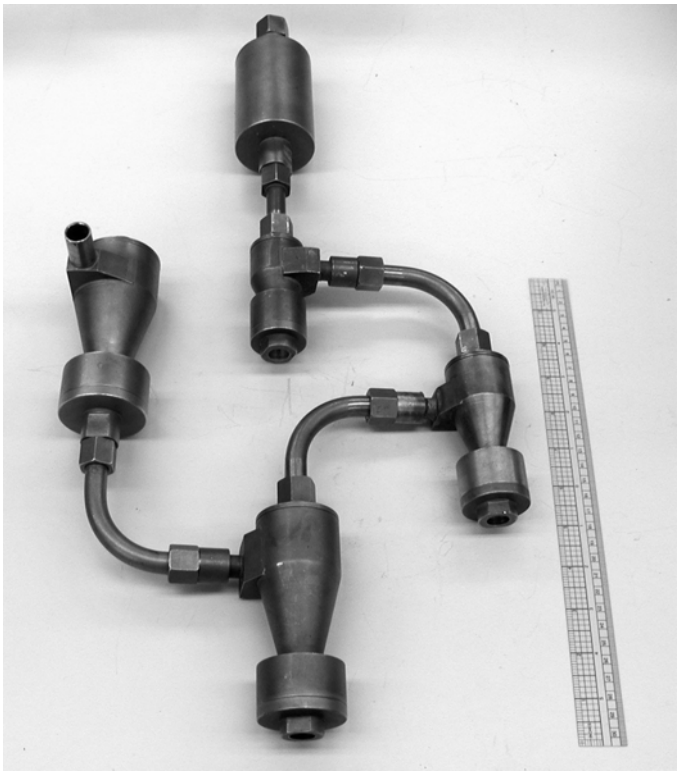

Figure 3.17. Five-Stage SRI Cyclone Train

3.5.2.4 Moving Filter

The Merlin-Gerin auto-advance MVF[(a)] was added to collect aerosols during the first few seconds after impact before the other samplers were activated and during pre-selected sampling time intervals. A schematic and a photograph of the workings of the MVF are shown in Figures 3.18 and 3.19, respectively. The aerosol was pulled through the sampling inlet and collected on the filter through a square aperture that measured about 2.5 cm x 2.5 cm (1 in. x 1 in.) (Figure 3.20). The filter operated in a manner similar to camera film, advancing from one spool to the other. Filter tape,[(b)] which moved under the sampling inlet, collected the aerosol continuously or at programmed intervals. The onboard motor operating at 7 VDC (volts direct current) controlled the speed of the tape. A critical orifice controller maintained the nominal sampling flow rate of 28.3 Lpm. The device was placed inside a stainless steel box with the sampling inlet outside the box. After the test was completed, the tape was cut into 1-in. segments for radiological and chemical analysis.

Two sampling strategies were employed, subsequently referred to as discrete intervals and serial sampling. Discrete interval sampling was only used in PI-1. During the discrete sampling period, the filter was held in place for 5 sec then advanced over a 5-sec period and then held in place for another 5 sec—this sequence (hold-move) was repeated for 1 min. After the first minute of sampling, the

(a) MGP Instruments, Smyrna, Georgia.
(b) Model AW-19, Millipore Corporation, Bedford, Massachusetts.

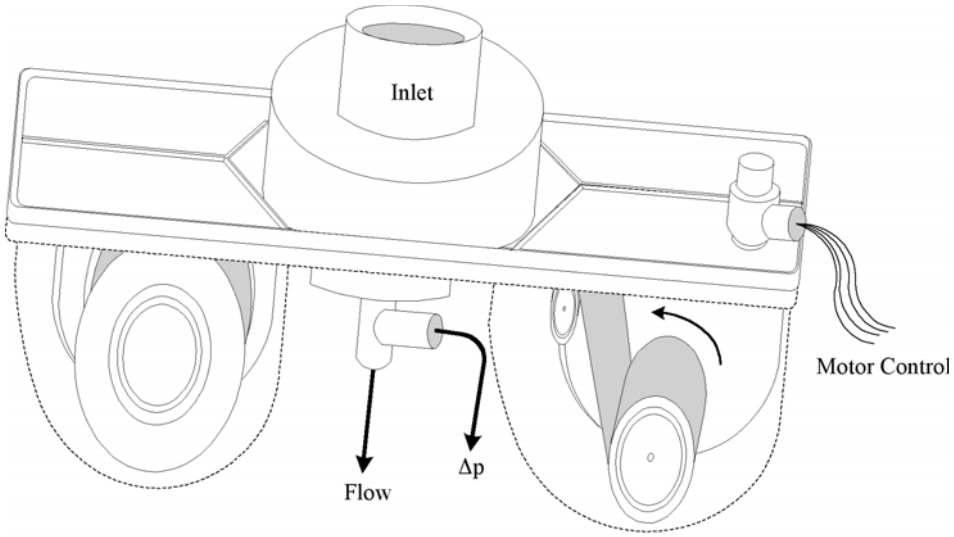

Figure 3.18. Moving Filter Schematic

Figure 3.19. Opened Auto-Advance Moving Filter

hold-move sequence time interval was increased to 15 sec. Clogging at the sampling collection area was encountered with the hold-move strategy, and as a result, the serial sampling strategy was implemented for the remaining shots. The hold-move mass was determined for each sample interval by converting the radioactivity counts to uranium mass and dividing that result by the airflow volume and the sampling time.

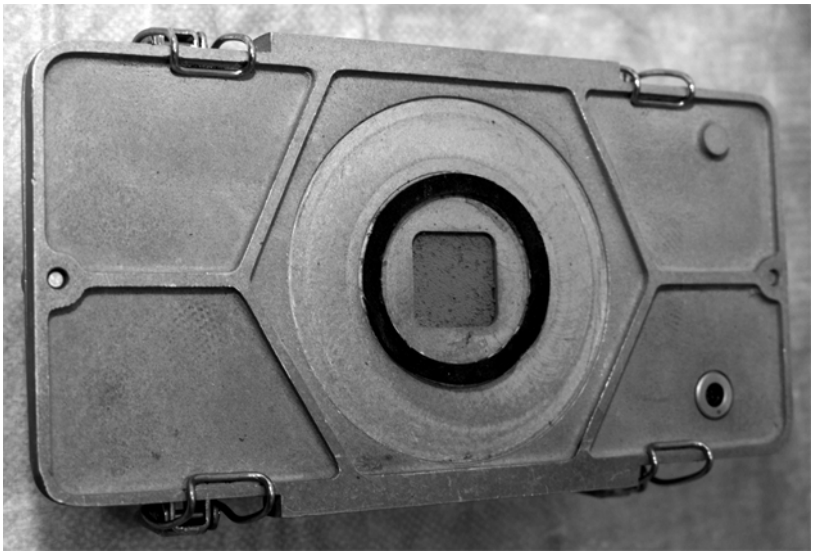

Figure 3.20. Moving Filter Sampling Port

For the serial sampling, the MVF was generally programmed to move at a steady pace of 0.88 cm sec^{-1} (20.9 in. min^{-1}) within each collection interval. The rate of advance for a 2.54-cm (1 in.) segement of filter tape in the MVF was calculated to be 0.0479 min (2.87 sec). The serial sampling concentration on each segment was determined as:

Uranium concentration = Uranium mass collected / (Flow Rate × 0.0479 min).

The computer-controlled interface was programmed to sample for the first 3.5 min post-impact and then for 30-sec periods at intervals of 7, 15, 31, 61, 121 min post-impact.

3.5.3 Sampler Control and Data Collection System

Flow control for the air samplers was provided by five remotely located valve control/pressure monitoring units located inside and around the test vehicle. Four of these units controlled the four sampler arrays. The remaining unit controlled the cyclone and the MVF. The units used to control the sampler arrays were made up of 18 individual modules for flow control and pressure monitoring. The unit controlling the cyclone and moving filter had eight modules. The modules in each of these units consisted of:

- a solenoid valve to turn the flow to the individual samplers on and off
- a critical orifice to regulate the sampler flow rate
- a pressure “snubber” to protect the units against pressure spikes
- a pressure transducer that monitored the active sampler’s change in pressure drop during the test.

This instrumentation was installed in protected or otherwise shielded parts of the vehicle out of the line of fire in the bustle or engine compartment (Figure 3.21). In the case of the Bradley vehicle, control instrumentation for the right and left scouts’ positions was mounted outside the back ramp and was heavily shielded.

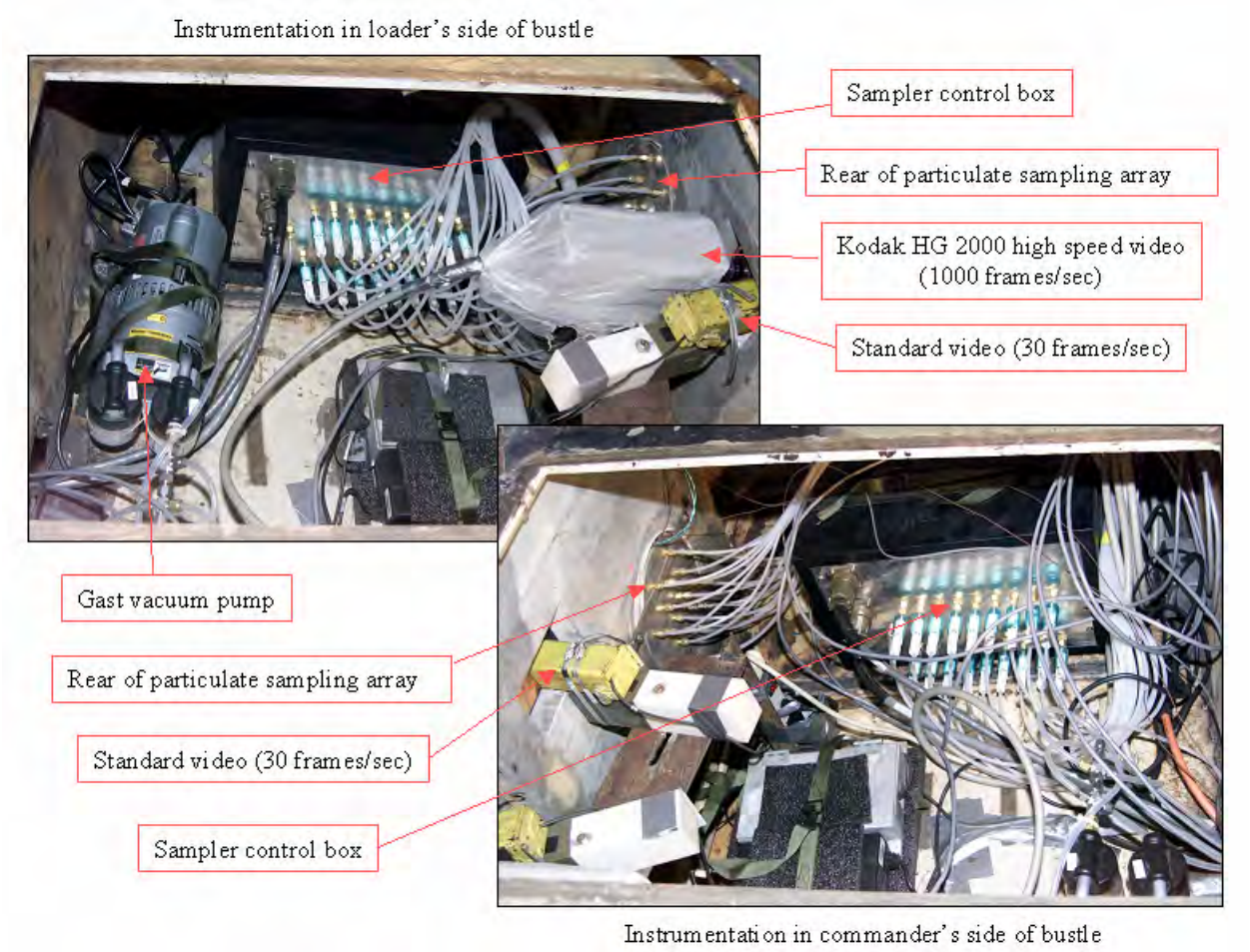

Figure 3.21. Sampler Vacuum and Monitoring Control Instrumentation

The valve control/pressure-monitoring units were connected through 125 ft of power and data cables to a National Instruments[(a)] SCXI computer interface chassis, which contained a SCXI-1200 digitizing module; 5 SCXI-1160/1324, 16-channel relay modules for solenoid valve control; and 3 SCXI-1102B/13008 analog input modules for pressure monitoring. This interface unit was located in a down-range control building and was interfaced with a computer running a customized National Instruments, LabVIEW engineering computer control program. The down-range computer was networked via fiber-optic cables to an up-range computer that controlled the aerosol sampling system at the time of the shot.

Because the accuracy of the aerosol sampling timing sequence was critical, LabVIEW was customized specifically for the Capstone test series to remotely start and stop each aerosol sampler in a predetermined sampling sequence (Figures 3.22 through 3.24). LabVIEW monitored and logged the changes in pressure that occurred during sample collection for each of the active samplers. Using this software, the operator was able to perform calibration and verification checks, operate the system for a controlled experiment, and review results from a past experiment.

(a) National Instruments, Inc., Austin, Texas.

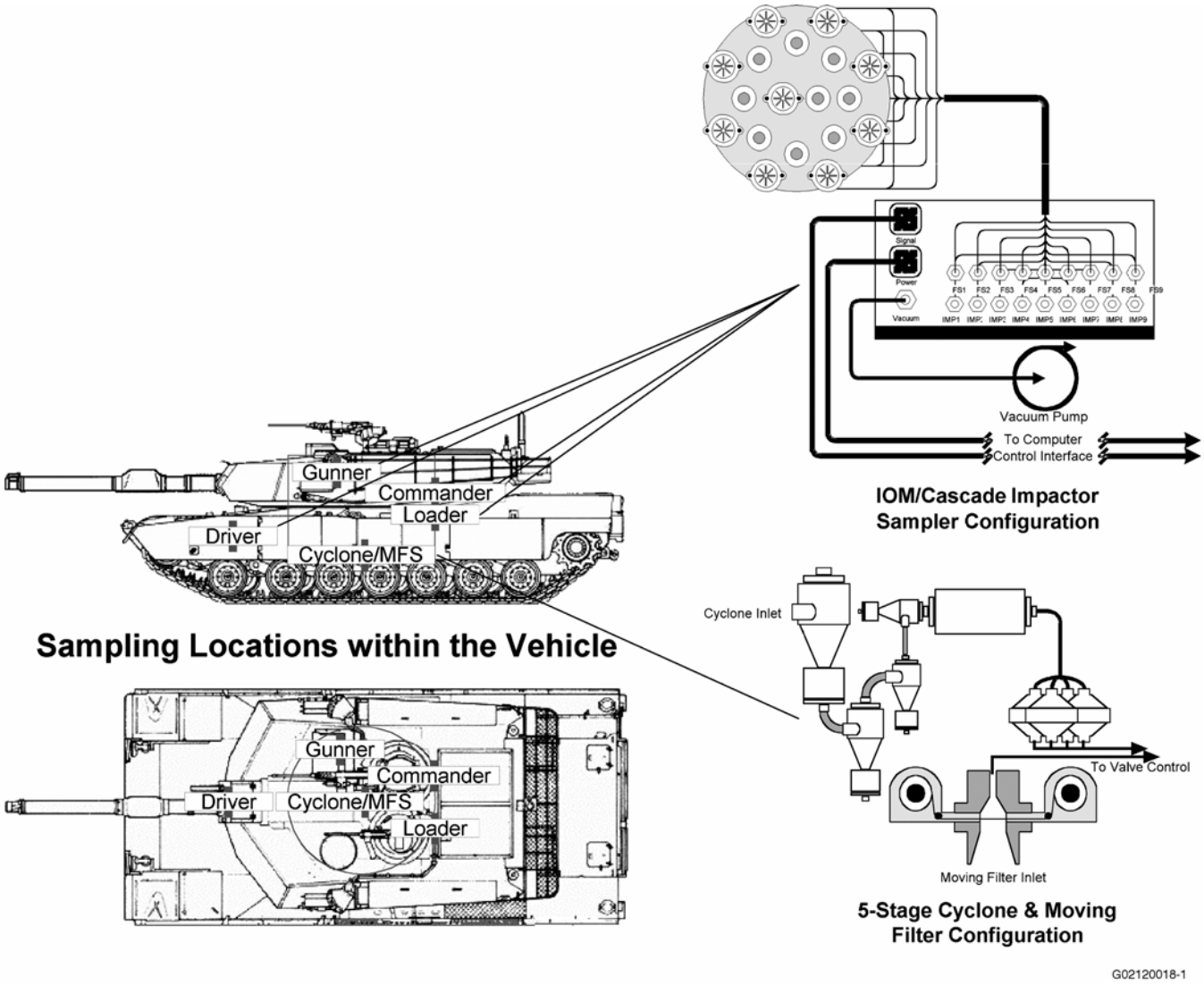

Figure 3.22. Aerosol Sampling Configuration

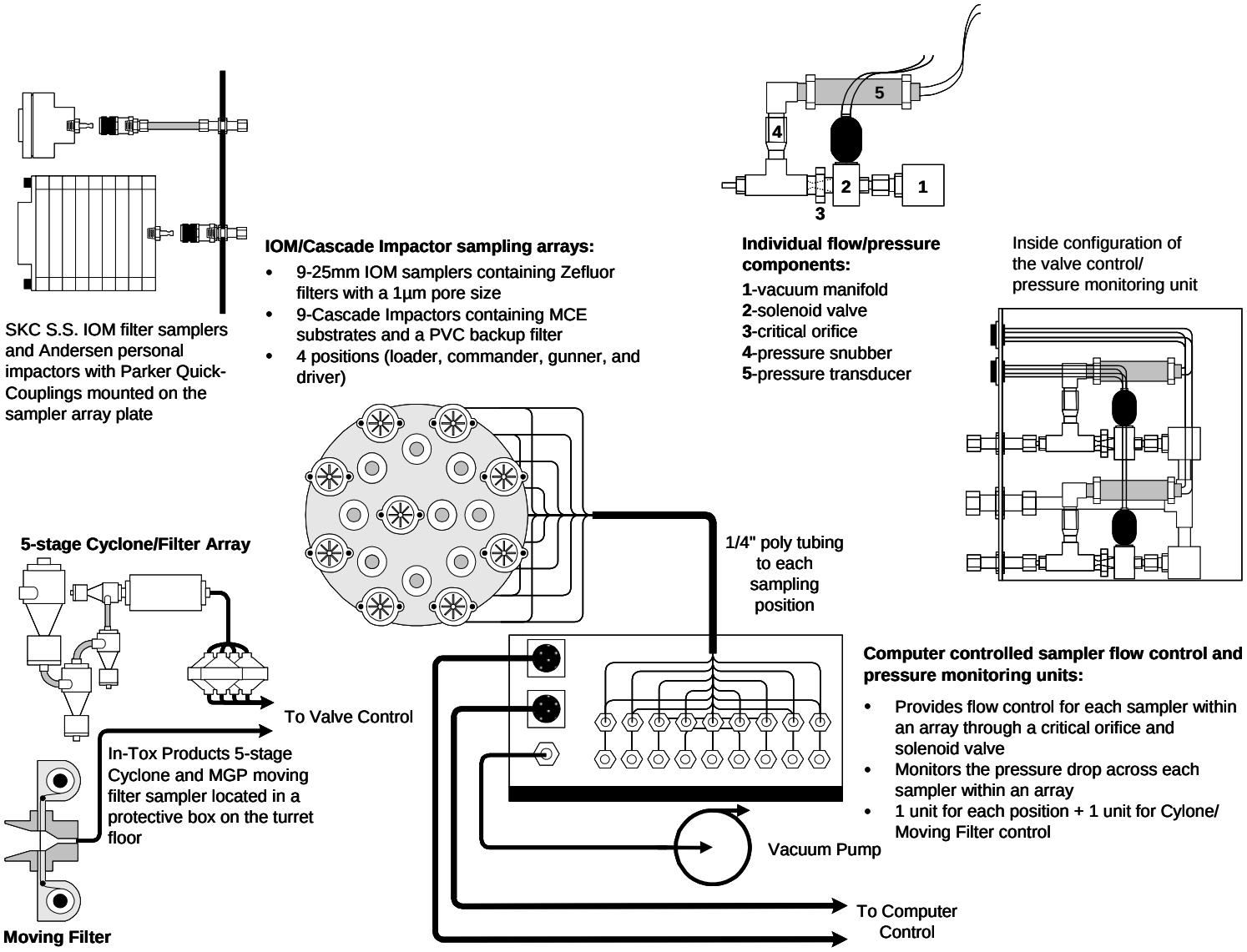

Figure 3.23. Aerosol Sampling Components

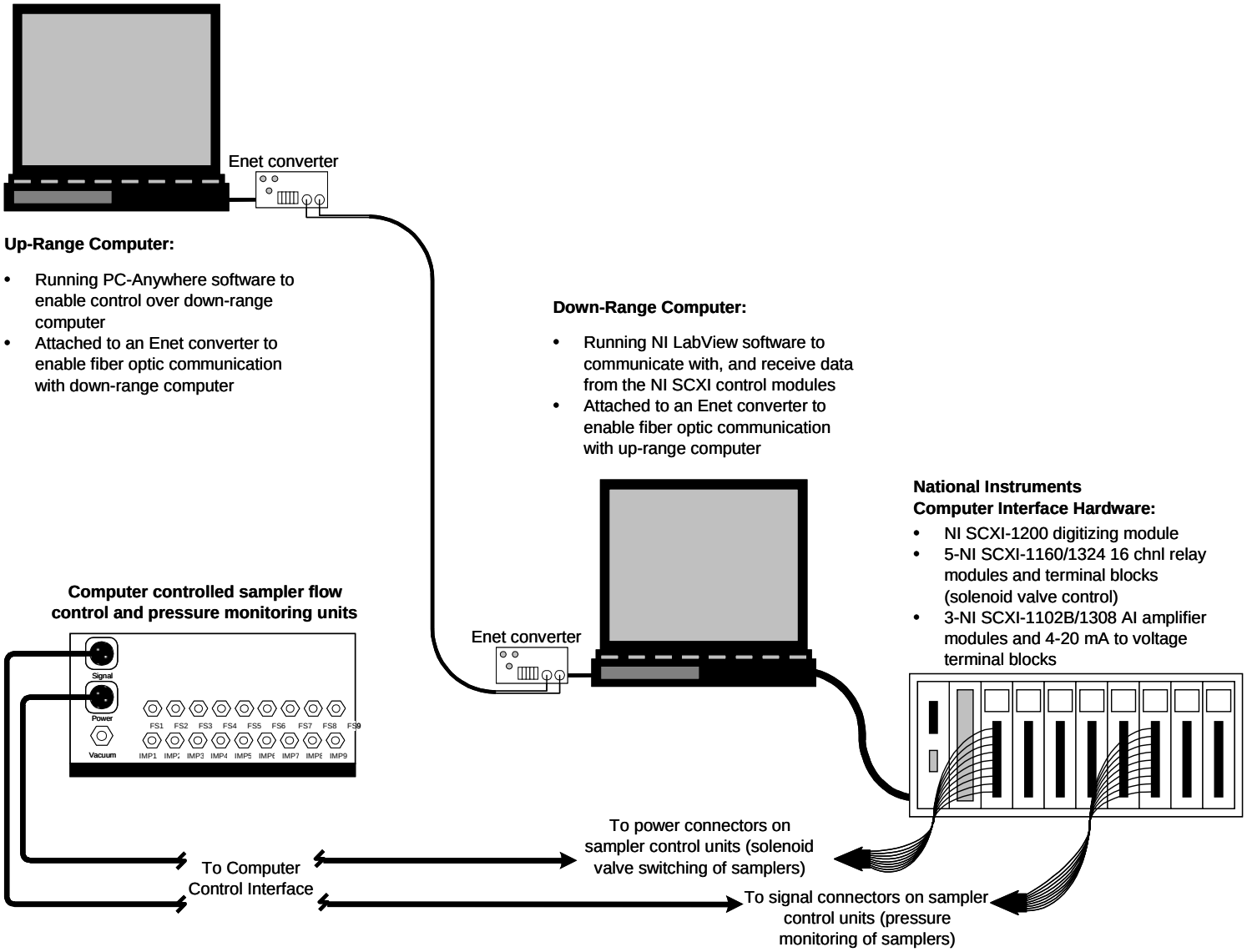

Figure 3.24. Aerosol Sampling Computer Control System

The initiation of sampling was delayed 5 sec after DU penetration to allow temperature and pressure transients to decay. The CIs were operated at the same time and over the same intervals as the respective IOM filters in the arrays at the four crewmember positions. In this way, coupled, time-dependent mass concentrations and particle size distributions were obtained.

Prior to each test shot, the timing sequence for the ATC firing control system was synchronized with the timing sequence for the LabVIEW aerosol sampling and data collection systems. This procedure ensured that samples were collected at the appropriate times. As a QA feature, the pressure drop across each filter was measured to document the exact time that the sample was initiated (i.e., as indicated by the time at which the vacuum was applied to the sampler), any variation in the flow rate of the sampler (i.e., as indicated by fluctuations or interruptions of the pressure on the sampling line), and the exact time that the sample collection was concluded (i.e., the time at which the pressure condition on the sampling line returned to ambient pressure). In addition, the status of the aerosol sampling system was monitored before initiation of each test so that any sampling system failures could be detected and the test could be appropriately delayed until the sampling system was operational.

Each of the 70-plus sampling lines used in the various shots contained the following components, which were connected in series:

- A low-pressure-drop canister filter installed between the aerosol sampler and the control panel. This filter was designed to prevent aspiration of aerosol particles into the control panel if the sampler integrity failed.

- A pressure transducer to provide time-dependent measurement of the pressure drop (ΔP) across the specific sampler. Loss of ΔP indicated sample breach and failure, whereas increasing ΔP suggests progressive loading of the sampler. This was anticipated to be important for the cassette filters obtained at early post-shot times.

- A critical orifice to maintain constant airflow in conditions of changing line resistance.

- A solenoid valve to turn the sampler on and off.

In addition to the IOMs and CIs, the cyclone sampler and the MVF were activated using LabVIEW. The MVF collected samples prior to, during, and after perforation of the target vehicle. Flow rates, total sample volumes, sample masses collected, and the derived uranium concentrations are provided in Appendix A.

3.5.4 Ventilation Rates of Target Vehicles

The ventilation rate, or the speed at which the air in the turret is exchanged, is relevant in the evaluation of aerosol available for inhalation. The ventilation rates created by operation of the EC/NBC conditioned air system, the HVAC, and the fire suppression systems on the dispersion characteristics of aerosols inside armored vehicles are expected to have a significant effect on the rate of aerosol removal. However, their use would have significantly confounded the results relative to the deposition rate of aerosols in still-air environments within the various turrets or crew compartments. Rather than installing one or more of

these systems into the BHT and conducting the firing tests with operating ventilation systems, the air-exchange rates of functioning vehicles were evaluated separately.

The ventilation rates of the Abrams and Bradley target vehicles were measured using a sulfur hexafluoride (SF_6) tracer gas dilution method. Briefly, this method involves introducing a small quantity of the inert tracer gas into the cavity or containment in which the air-exchange rate is to be measured, and the concentration of the SF_6 is measured *in situ* using a dedicated electron-capture gas chromatograph (Model 101 Autotrac; Lagus Applied Technology, Inc.). By serially measuring the concentration of SF_6, the decay rate can be calculated from the equation $I = 1/t \ln(C_0/C_t)$, where t is time of measurement, C_0 and C_t are the initial and final tracer concentrations, respectively, and I is the containment air-exchange rate. This procedure was initiated before the test and operated during and after vehicle penetration. These rates were compared with rates tested in operational Abrams M1, M1A1, and M1A2 tanks and in the Bradley M2A2 under three conditions: 1) with the internal fan off and the hatches closed, 2) with the fan on and the hatches closed, and 3) with the fan off and the commander's hatches open. This comparison was done to determine the effects of the ventilation system and hatch openings on the ventilation rate.

Factors such as hatch position (open vs. closed); operation of the HVAC, NBC, or fire suppression systems; and holes created by the DU penetrators are likely to affect the dynamics of the aerosol cloud initially formed during penetration. To facilitate extrapolation of results to different ventilation environments, it was imperative that the dynamics of air exchange within the crew compartment be characterized. Operational Abrams tanks (M1, M1A1, and M1A2 models) and a Bradley vehicle were tested for air exchange with the hatches open and fans off and with the hatches closed and fans on.

3.5.5 Measured Aerosol Characteristics

Aerosols collected were characterized using a variety of parameters including the uranium mass and particle size distributions. The aerosol settling time was established from uranium concentrations derived from radioactivity measurements as a function of time and space. Aerosols were further evaluated for chemical composition, morphology, and solubility in simulated lung fluid.

3.5.5.1 Aerosol Mass

Analysis of the uranium mass within the crew compartment atmosphere as a function of time (and regardless of particle size) was conducted using the 25-mm IOMs, the 5-stage cyclone, and the MVF. The CIs also are useful for evaluating uranium mass concentrations but are better suited for particle size analysis. The IOM filters were placed in sampling arrays at four separate locations within the interior of the crew compartment, thus providing time-dependent measurements of total uranium concentration (independent of particle size) at the four locations. Because the IOMs and MVF have no pre-cutter to remove large particles, they collect suspended particles of all sizes and represent the total concentration of suspended particulate matter during the active time period sampled.

3.5.5.2 Aerosol Radioactivity

Samples from IOM and CI samplers were evaluated for alpha and beta radioactivity. The beta activity was used as a surrogate measurement of the uranium mass on the sample (see Appendix A for conversion from radioactivity measurements to uranium mass). Normally, CI data are used to determine the mass

median aerodynamic diameter (MMAD), but because the uranium mass on each stage of the CI was calculated from radioactivity measurements, the derived value is actually an activity median aerodynamic diameter (AMAD). Samples from the MVFs also were analyzed for alpha and beta activity. Residues from the cyclone stages and other samples, such as gloves and deposition trays, were analyzed using gamma spectrometry because the sample geometries did not lend themselves readily to gas-flow proportional analysis.

3.5.5.3 Particle Size Distribution and Morphology

Particle size distribution data were obtained using both the CIs and the cyclone stages. Additionally, scanning electron microscopy (SEM) was used to evaluate whether the particles were predominantly crystalline, aggregated, or amorphous based on their morphology, and energy dispersive spectrometry (EDS) provided confirmation of the approximate composition of the particles.

3.5.5.4 Aerosol Settling with Time

Interior vehicle video footage showed airborne particulate matter after perforation. Burning DU fragments may have contributed to aerosol mass for up to 2 sec after perforation. After the initial aerosol cloud was created *in situ*, various removal mechanisms, such as gravitational settling, decreased the mass concentration of airborne particles with time. The relative importance of each removal mechanism and the rate at which it affected the aerosols determined the shape of the concentration-time curve. Frequent data collection was conducted during the first few minutes. The number of sampling intervals possible was ultimately limited by the space available because space limitations restricted the number of samplers and associated equipment that could be placed in the sampling environment.

To protect sensitive samplers from the pressure transient and its potential effects on the calibration of the size-selective samplers (e.g., CIs and cyclones), the timing sequence for the majority of samplers was delayed until after the initial positive pressure transient in the crew compartment had decayed to ambient pressure. The decay of this pressure transient was expected to occur over several milliseconds. Additionally, with reports of “fireflies” (tiny DU fragments undergoing rapid oxidation), sampling delay would protect the filters covered by solid shields from possible burns. Thus, sampling within the crew compartment using IOM and CI samplers was not initiated until 5 sec after impact. The MVF sampler was operating at the time of impact and perforation to obtain initial uranium concentration data.

The PI-1 sampling scheme for the interior crew compartment is listed in Table 3.2. The time sequence was evaluated after each shot and was modified based on a qualitative assessment of the quantity of aerosols collected and aerosol-settling rate. Based on the evaluations after each shot, the sample collection time intervals were reduced in later shots to avoid overloading the filters. For single shots, the start times relative to the shot time remained the same. Actual sample time sequences for each shot are listed in Chapter 5, Table 5.1. The maximum total flow rate for all active samplers was about 75 Lpm, which is well below the amount of air likely to be inhaled by the crew of the armored vehicle.

Table 3.2. PI-1 Sampling Time Sequence

Sampler Started[(a)]	Sampler Stopped[(a)]	Collection Time Interval (t)
5 sec	35 sec	30 sec
35 sec	1 min, 35 sec	60 sec
1 min, 35 sec	3 min, 35 sec	2 min
3 min, 35 sec	7 min, 35 sec	4 min
7 min, 35 sec	15 min, 35 sec	8 min
15 min, 35 sec	31 min, 35 sec	16 min
31 min, 35 sec	63 min, 35 sec	32 min
63 min, 35 sec	127 min, 35 sec	64 min
(a) Relative to the DU munition shot time.		

3.6 Air Sampling Exterior to the Vehicle

Within the Superbox test chamber, where testing was conducted under static air conditions (i.e., the building exhaust ventilation system was turned off during the tests), the aerosols produced by target impact are likely to be less dispersed and, therefore, more highly concentrated than those produced when firing at an outdoor target, where dilution and dispersion effects are more pronounced.

The value of collecting aerosols within the Superbox but outside the target vehicles is complicated by several factors such as the addition of secondary aerosols from impact of penetrator remains into the catch plate and the limited volume within the test facility compared with significant dilution over a large combat area. Measurements of air concentrations within the fragmentation shield would overestimate similar outdoor air concentrations. Nevertheless, limited aerosol monitoring within the confines of the fragmentation shield test chamber, but exterior to the vehicle, was conducted to collect aerosols generated by the impact, determine their particle distributions, and calculate an exterior source term using the data available.

External aerosol monitoring equipment included at least two high-volume samplers and two CIs. Four high-volume Staplex samplers,[(a)] referred to as Hi-Vols, were fitted with 10-cm (4-in.) sampler heads and operated at nominal flow rates of 560 Lpm **(**20 cfm) (Figure 3.25). The filter medium used was 110-mm Whatman-41.[(b)] Except for the Hi-Vol positioned a couple of feet off the ground under the catch plate during the first two shots, the sampler heads were located 1.5 m (5 ft) above the floor at the designated sampling stations surrounding the target vehicle. The Hi-Vols sampled for total particulate aerosols during 1-h baseline evaluations prior to all shots. They were also used to collect total particulates after impact following the first five shots and to assess filter-loading rates in the confines of the Superbox fragmentation shield in consideration of subsequent exterior CI sampling.

The capability to turn the exterior air samplers on and off remotely via a switch panel at a remote building complex was not available until PI-3/4. Therefore, out of necessity, the exterior samplers in PI-1 and PI-2 were manually turned on several minutes before the impact event using an electrical panel located outside the Superbox. For PI-1, the samplers operated from 10 to 30 min after impact. Because the filters

(a) The Staplex Company, 777 Fifth Avenue, Brooklyn, New York.
(b) Ashless filter paper, Whatman, Springfield Mill, United Kingdom.

Figure 3.25. High-Volume Air Sampler

overloaded, the operating times for PI-2 were decreased to a 3 to 7 min time period following impact. With filter overloading still experienced in PI-2, the Hi-Vol samplers operated no longer than 30 sec to 2 min following impact for PI-3 of PI-3/4.

Additionally, two Andersen ambient CIs,[(a)] also referred to as Andersen impactors and abbreviated as external CIs, were used beginning with PI-5 to provide data on particle size distributions (Figure 3.26). These samplers used 81-mm mixed cellulose ester substrates[(b)] and operated at a nominal flow rate of 28 Lpm (1 cfm). Once Andersen impactors and associated filter media were available, they replaced the Hi-Vols as the primary samplers. The Andersen impactors were located 1.5 m (5 ft) above floor level in a horizontal orientation. These samplers were activated 10 sec after impact and generally ran for 2 min during all subsequent shots in all three test phases, except for PI-7 during which they were only run for 1 min following impact; the PIII-2 sampler designated number 1 ran for 5 h. Metal shields were affixed to the sampler test stands to protect the tubing, electrical wires, and samplers during the impact events. In spite of these precautions, damage to the hoses occurred, thus reducing the amount of usable data. Beginning with PI-6, the exterior CIs and the Hi-Vols were angled to face slightly away from the impact point in an effort to reduce the opportunity for fragment damage.

The initial and final flow rate readings for each sampler were recorded to calculate total air volumes. Flow rates and total air volumes are presented in Appendix A.

(a) Anderson Instruments, Inc., Smyrna, Georgia.
(b) Mixed cellulose ester, 20-305/301, purchased from Andersen Instruments, Inc.

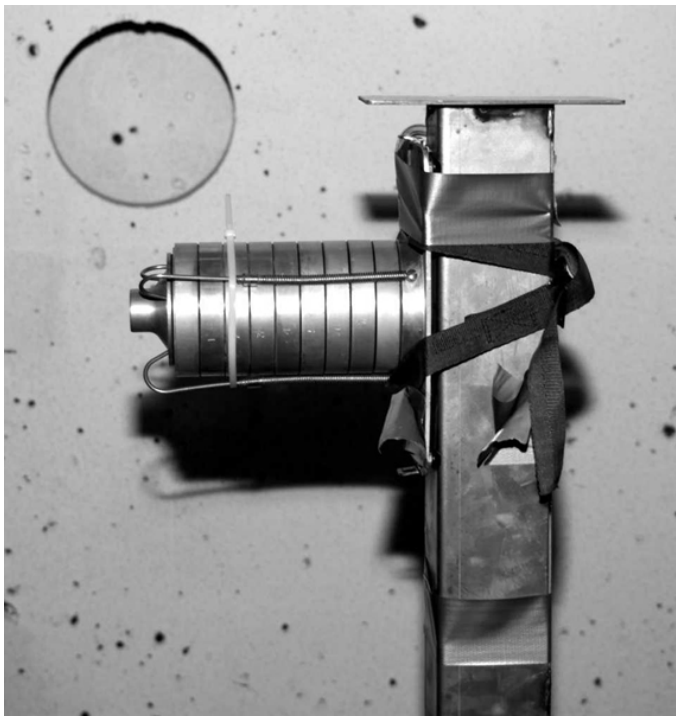

Figure 3.26. Andersen Cascade Impactor

3.7 Aerosol Deposition and Resuspension Sampling

Particulate matter generated by perforation of a target eventually settles onto surfaces both inside and outside the target, thus becoming a source of contamination and exposure to personnel carrying out rescue, recovery, repair, and intelligence-gathering missions. The heaviest particles typically settle first, and the settling process proceeds over time with the lightest particles taking the longest time. The light-to-medium fraction of the deposited material is most likely to be resuspended by mechanical or climatic turbulence. Particles small enough to be resuspended may be internalized by personnel in the area via the inhalation pathway. Surface-to-hand-to-mouth transfers contribute to internalization by way of the ingestion pathway. First responders and the personnel that comprise OSAGWI Levels 2 and 3 are at risk of DU intakes via the inhalation and ingestion pathways.

DoD personnel may be involved in a wide range of activities on damaged vehicles, so these personnel are potentially at risk of exposure when working on vehicles damaged by DU munitions. These personnel may be exposed to similar levels of residual DU uptake as the vehicle crew. However, unlike the exposure scenario for the vehicle crew, individuals with certain specialties may encounter a greater number of damaged vehicles over an extended time period, thereby potentially increasing their chances for exposure to residual DU.

To evaluate deposited particulate material for assessments of potential health risks to personnel in, on, or near armored vehicles after penetration by DU munitions, removable contamination surveys were conducted in and on damaged vehicles. These surveys were performed with wipe samples and deposition trays to collect the deposited material, which was then analyzed to determine its uranium content. The interior and exterior surveys followed a systematic protocol (i.e., samples were taken at predetermined

wipe and instrument-meter reading locations for survey expediency). Additionally, portable radiation survey instruments were used to conduct radiation surveys to evaluate the correlation between instrument responses and the uranium contamination present. Such instrumentation surveys help determine the extent of contamination on surfaces and could be the first indication the soldier has of potential DU contamination.

As with the exterior aerosol sample collection, the value of assessing aerosols deposited and resuspended outside the target vehicles was complicated by several factors such as the possible addition of secondary catch-plate aerosols and fragments and the limited dispersion within the test facility when compared with the significant dilution and dispersion that would occur over a large combat area. The aerosol generation, dispersion, and settling data from tests conducted in the closed Superbox fragmentation shield would overestimate the results obtained from tests or actual events that occur in open-air environments.

The aerosol levels remaining during recovery activities and resuspended by them were evaluated in several limited exercises in which IOM and CI personal air samplers supplemented the worker's occupational air samplers (closed-faced lapel samplers). Cotton gloves worn over protective gloves by selected recovery personnel provided a method to collect the deposited material and qualitatively evaluate the amount available for transfer during recovery activities.

The next sections describe the aerosol deposition (contamination surveys and deposition tray sampling) sampling.

3.7.1 Background and Baseline Sampling

Because uranium is part of the natural radioactive background and DU munitions have been used previously at the Superbox, it was necessary to establish the average background in the facility and any residual radioactivity or contamination associated with the Superbox and the target vehicles. The background radiation originates from naturally occurring radionuclides present in the Superbox building materials, materials used in the Abrams tank and the Bradley vehicle, and the atmosphere surrounding the vehicles. Baseline surveys were performed to determine alpha and beta-gamma activity per 100 cm^2 as well as the ambient gamma exposure rate (μR/h) at reference locations inside the Superbox.

Establishing a background or baseline radiation level in the Superbox proved to be difficult due to the long-term testing of DU munitions within the structure. Therefore, before each scheduled Capstone test, baseline surveys of the facility and the intended target vehicle were conducted. All Phase-I testing was conducted using the same Abrams target, the same Bradley target was used throughout Phase-II testing, and the Abrams hull used for the Phase-I tests was combined with an unused turret for the Phase-III tests. After sampling was completed for the various shots, the vehicle and accessible Superbox structures were decontaminated using Maslin cloth and Nilfisk HEPA vacuum cleaners. After decontamination procedures were complete, surveys were again conducted. The pre-shot surveys were conducted within 24 h of the scheduled shot, usually within 2 to 3 h of the shot and were also useful in evaluating the effectiveness of decontamination efforts. The same sampling technique used for the post-shot surveys was used for the background/baseline surveys.

3.7.2 Interior Vehicle Sampling

Material deposited on surfaces within the vehicle was sampled using wipes and deposition trays to measure the removable fraction of DU and the extent of contamination on surfaces available for hand-to-mouth transfer and resuspension. The removable contamination survey entailed wiping pre-determined and marked areas with 47-mm diameter Defensap wipe test sampling media. Four 100-cm^2 (4 in. by 4 in.) aluminum deposition trays secured with gun tape were used to passively collect deposited material near each crew position. In actuality, the deposition trays had a 1.3 cm (0.5 in.) beveled edge that added approximately 60 cm^2 of area. These edges had about a 45° angle and may have funneled some deposited material to the horizontal surface. All material from the horizontal and beveled surfaces was collected and analyzed.

Interior vehicle sampling for each shot in Phases I and III included at least 30 discrete wipe locations to include both the turret and driver's compartment, 4 deposition trays secured to the floor at or near each of the 4 crew locations, and instrument readings at pre-designated areas. Figure 3.27 depicts an example of typical wipe and deposition tray sampling locations inside the Abrams tank. The numbers represent wipe identifications for the wipe locations.

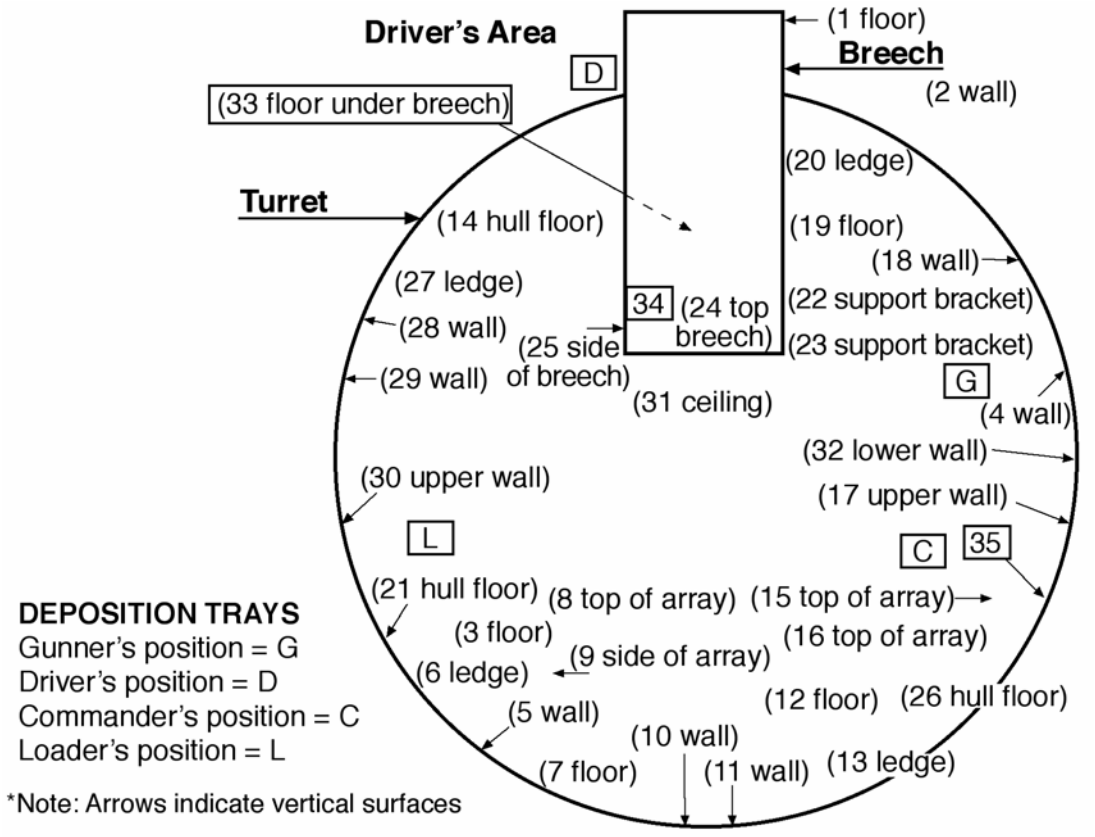

Figure 3.27. Overhead View of Abrams Interior Turret Sampling Locations

Interior vehicle sampling for Phase II included 30 discrete wipe locations to include the turret, the driver's compartment, and the passenger compartment. Four deposition trays were secured to the floor at or near the commander's, driver's, and right and left scouts' locations, and areas designated for instrument

readings. Figure 3.28 shows the typical wipe locations inside the Bradley vehicle. The numbers represent wipe identifications for the wipe locations.

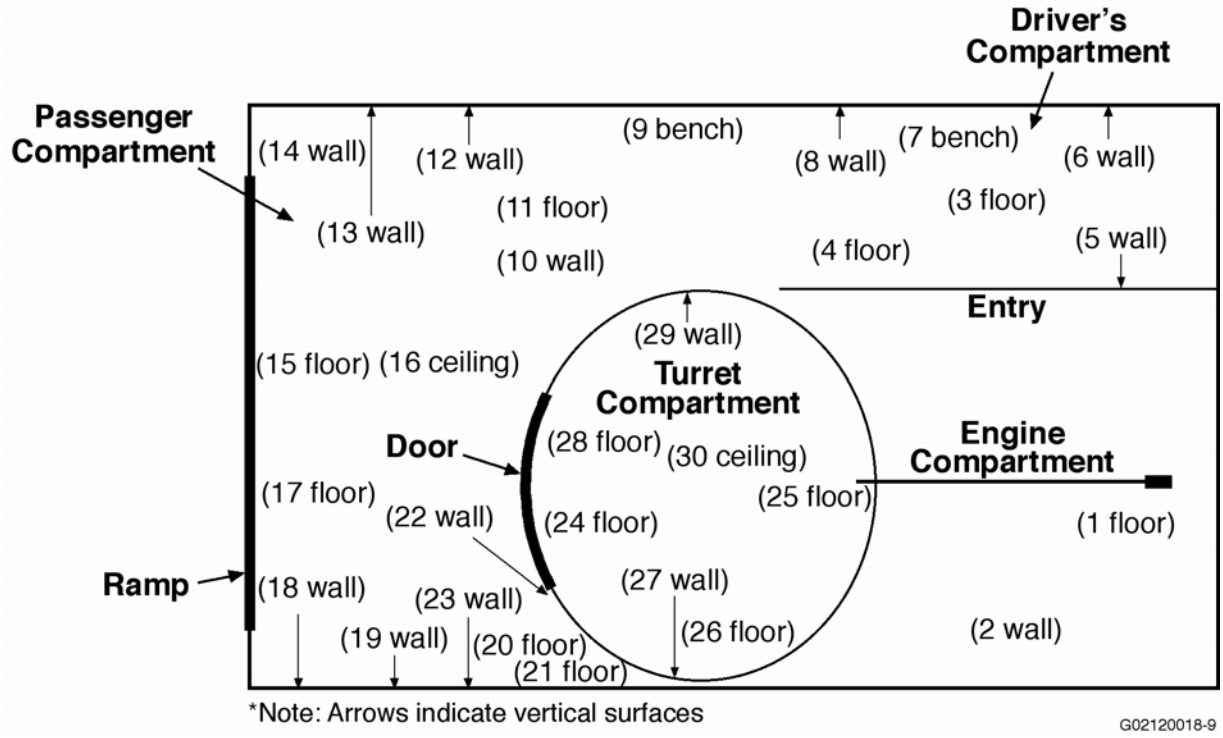

Figure 3.28. Overhead View of Bradley Vehicle Interior Sampling Locations

3.7.3 Sampling Exterior to the Vehicle

Exterior vehicle sampling for Phases I and III included at least 30 discrete wipe locations on and around the target, 4 deposition trays (2 secured to the target vehicle and 2 secured to the fragmentation shield floor), and several designated areas for instrument readings. Several turret configurations of the target vehicle were used during testing: in PI-1 and PI-2, the turret was in a traverse position (gun pointing rearward); in PI-3 through PI-7, the turret was in a combat position (gun pointing forward); and in PIII-1 and PIII-2, the turret was in an angled position. Figure 3.29 shows the typical exterior wipe locations (overhead view) for the Abrams tank in a combat position. The numbers represent wipe identifications for the wipe locations. (Trays C and D were placed on the fragmentation shield floor rather than on the vehicle.)

Exterior vehicle sampling for Phase II included at least 30 discrete wipe locations on and around the target, 4 deposition trays (2 secured to the target vehicle and 2 secured to the fragmentation shield floor), and several designated areas for instrument readings. The turret configuration of the target vehicle was different in the Phase-II shots: for PII-1/2, the turret was positioned so the gun was parallel to driver's line of sight, and for PII-3, the turret was rotated to the left so the gun was perpendicular to the driver's line of sight. Figure 3.30 depicts the overhead view of typical exterior wipe locations for test shots of the Bradley target vehicle in a combat configuration.

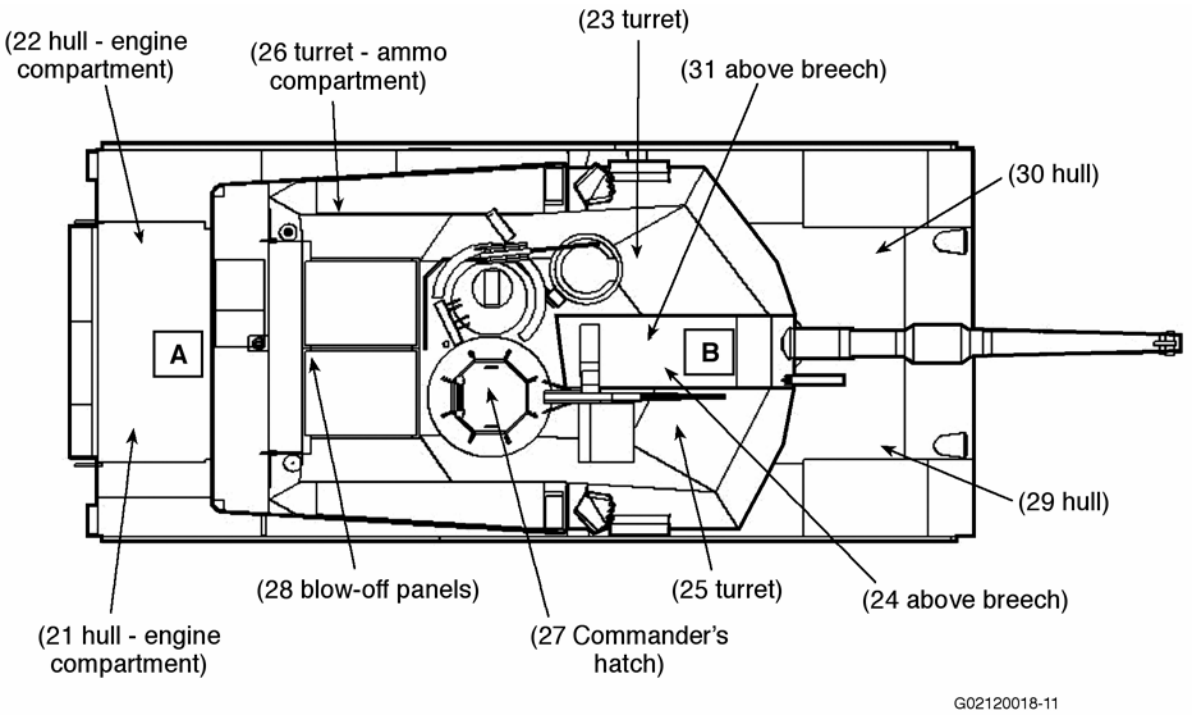

Figure 3.29. Overhead View of Exterior Sampling Locations for the Abrams Target

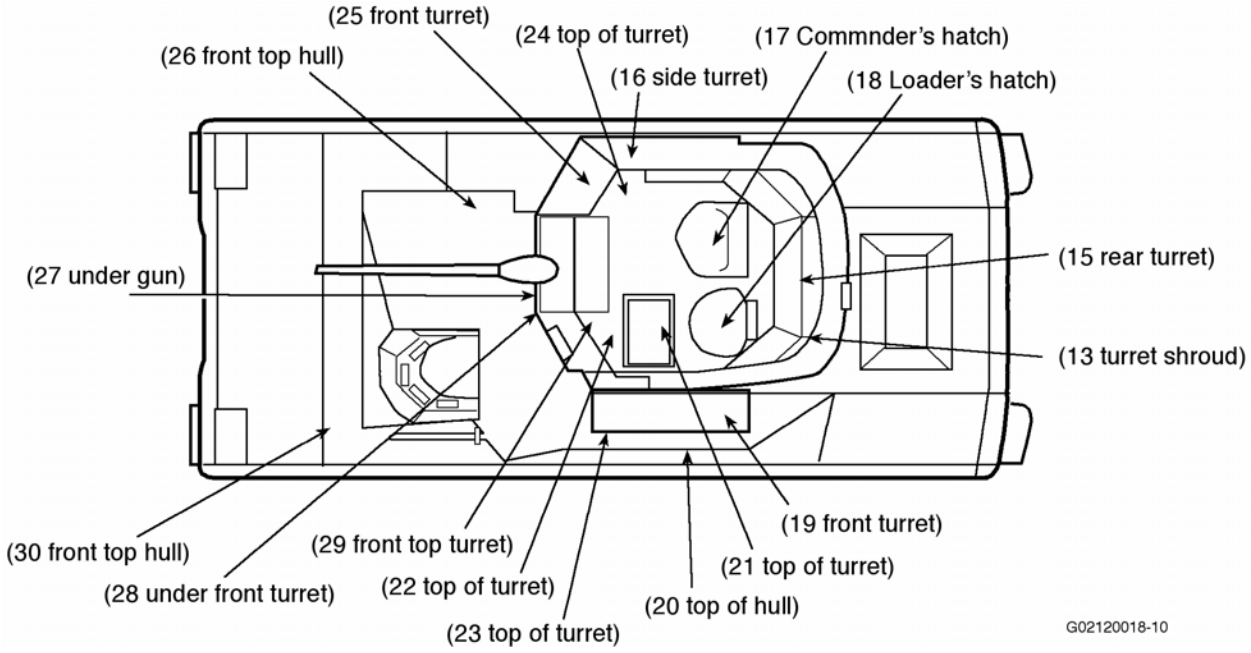

Figure 3.30. Overhead View of Exterior Sampling Locations for the Bradley Target

3.7.4 Aerosols Resuspended During Recovery Activities

In a battlefield situation in which an Abrams tank or a Bradley vehicle is perforated by an LC-DU munition, personnel who enter the vehicle shortly afterward to assist in the recovery of the crew and equipment make up the group designated as first responders. Unless they are wearing respiratory protective equipment, these first responders may inhale aerosols that remain suspended or aerosols that are resuspended by their activities within the vehicle. First responders may also ingest DU from hand-to-mouth transfer of contamination. Evaluations of resuspended DU aerosol concentrations were performed in conjunction with sample recovery activities conducted several hours after impact. This approach was taken to maintain consistency in measuring the aerosol settling within the vehicle during the initial 2 h after the shot and to comply with facility procedures.

To a limited extent, sampling for suspended aerosol concentration was addressed by placing 37-mm Marple personal CIs and IOM filter cassettes on selected recovery personnel. In addition, the transfer of contamination from surfaces to hands was evaluated by analyzing cotton gloves that were worn by recovery personnel over their protective gloves while carrying out specific activities. The cotton gloves were collected and analyzed to provide a measure of DU contamination potentially available for ingestion by responders.

Particle resuspension was evaluated after the initial 2-h aerosol-sampling period for the PI-6 and PI-7 tests. During the 2 h following impact in these tests, the loader's sampling array was shielded and unused. When this period was over and recovery activities could commence, the shield was manually released after the loader's hatch was opened. This opening of the shield was done in a manner to limit or prevent cross contamination of deposited aerosols from outside of the vehicle to the inside and to minimize resuspension from mechanical action before the sample recovery personnel entered. The hatch remained open during sample collection. During the PI-6 recovery activities, the first set of IOM and CI samplers was remotely operated for 20 min to establish a baseline (Table 3.3). The second and third sampler set ran during the contamination survey within the vehicle, which lasted about 35 min. Following the contamination survey, the worker spent between 20 and 40 min photographing the sampler arrays and other structures within the turret and then removing the samplers. The fourth and fifth sampler sets ran for about 15 and 22 min, respectively, while these activities were being conducted. After the samples were removed and the workers exited the vehicle, the sixth through ninth sampler sets ran in increasing time intervals of 2, 4, 8, and 16 min, respectively, to evaluate aerosol concentrations after the mechanical turbulence created by the workers had ceased.

In PI-7, the damage caused by shattering of the aluminum plate (placed in front of the catch plate) forced a change in the recovery sampling procedure. This time, after a 20-min baseline run, the next two sampler sets each ran for 20 min, during which time photography, wipe surveys, and initial sampler retrieval activities were conducted and recovery personnel exited. Sampling intervals were not specifically coordinated with PI-7 recovery activities. A fourth sampler set ran for approximately 10 min during which time no one was present. Sampling was terminated early so damage to the other turret arrays could be evaluated without further delay.

Table 3.3. Sampling During PI-6 Recovery Activities

Collection Time Post-Impact	Elapsed Sampling Time	Recovery Activities
2:35 to 2:55	20 min	Baseline sample prior to recovery activities
2:55 to 3:06	No sample taken	No recovery activities
3:06 to 3:28	22 min	Interior contamination survey
3:28 to 3:42	13 min	Photography survey
3:42 to 3:56	15 min	Air sampler retrieval
3:56 to 4:18	22 min	Continued sample retrieval
4:18 to 4:20	No sample taken	Post-recovery, no activities
4:20 to 4:22	2 min	Post-recovery, no activities
4:22 to 4:26	4 min	Post-recovery, no activities
4:26 to 4:34	8 min	Post-recovery, no activities
4:34 to 4:50	16 min	Post-recovery, no activities

3.7.5 Fragmentation Shield Contribution to Resuspension

Although the Superbox interior was decontaminated prior to the first shot and the floors and lower walls were vacuumed between shots, it was inevitable that DU residues would deposit on the inside of the fragmentation shield during each shot. An attempt to determine how much of this residue could possibly be loosened during the next shot and contribute to the external aerosol formed by the impact was addressed in a separate test conducted between Phases III and II. This test did not involve the use of DU munitions and was called the C4 test because C4 explosive was used.

To simulate actual impact conditions as closely as possible for the C4 test, the Superbox structure was first decontaminated to the same degree as it had been in previous shots, and the exhaust system to the Superbox was shut down to create a static air environment within the test structure. Two pre-test Hi-Vol samplers ran for 1 h to collect baseline air samples. Two external CIs were set up in the sampling locations that had become standard since PI-6. A C4 explosive charge was remotely set off several inches from the surface of the Phase-III target vehicle to simulate a blast similar in magnitude to the blast within the Superbox from the DU test shots. Two external CIs were activated 10 sec after the C4 blast and ran for 2 min. The air filters were subsequently recovered and processed using the same procedures used for the filters collected from the test shots.

3.8 Sample Handling

The majority of aerosol samplers were IOM filter cassettes and Marple CIs. After each shot (or double shot), these samplers, along with the cyclone and the MVF, were removed from the target vehicle. All samplers were transferred to the ATC laboratory for subsequent processing. The IOMs and CIs were conditioned in chambers at 40 to 45% relative humidity and disassembled. Their filters and substrates were weighed, placed into PetriSlides, photographed for documentation, and analyzed for alpha and beta activity. The MVF strips were photographed and then cut into 2.5-cm (1-in.) strips and placed into PetriSlides.

Cyclone residues were weighed and transferred to vials within a few days of each shot. The Phase-I, Phase-III, and PII-1/2 vials were placed under a nitrogen atmosphere on 16 March 2001 to minimize

oxide phase changes. The remaining PII-3 vials were placed under nitrogen within a few days of the shot. The samples were held at ATC prior to their transfer to the USACHPPM laboratory where they were analyzed by gamma spectrometry.

Gloves were collected in clean plastic bags, sealed, labeled, and stored at the ATC laboratory prior to transfer to the USACHPPM laboratory for gamma spectrometry analyses.

The deposition trays were removed from the Superbox by the recovery team, sandwiched between commercially available disposable paper plates, sealed in a large plastic bag, and transferred to the ATC laboratory. At the ATC laboratory, the material on each tray was weighed and transferred to a vial for storage until gamma spectrometry analyses could be performed at the USACHPPM laboratory.

External CI substrates were removed from the Andersen CI samplers, weighed and photographed, and held for transfer to the USACHPPM laboratory where they were analyzed by gamma spectrometry.

A pile of DU oxide powder lodged on a ledge within the Abrams BHT also was collected during recovery operations. This sample was referred to as the "DU cone" sample because it resembled a cone with the point side up.

Following weighing and alpha and beta radioactivity analyses at the ATC laboratory, the various samples were archived or shipped to one of three laboratories (USACHPPM, PNNL, LRRI) for further analyses.

All quality control (QC) data and information were recorded within project documentation. Each sample had a unique identification number, and data obtained from each sample were recorded in appropriate field and project documentation (e.g., field data sheets) along with information describing the sample. An identification label or tag was applied to the sample container. Samples were controlled as much as possible during handling and transfer to preclude misidentification, damage, deterioration, and loss of sample.

3.8.1 Sample Identification

The samples were identified and controlled in a consistent manner to help ensure traceability of samples from the time and place of collection through shipment to other laboratories and to final disposition. The identification strategy of samples taken inside the vehicle included a series of alternating alpha and numeric components separated by hyphens. Each sample had a unique identifier. The sampling designators were as follows:

- Phases 1 through 4: represented by Roman numerals I, II, III, and IV, respectively
- Shot number: numbered 1 through 7; double shots (those performed within a few minutes of each other) were noted as 1/2 and 3/4
- Sample location relative to vehicle: E=external, I=internal
- Position within vehicle: C=commander, L=loader, G=gunner, D=driver; for Phase-II tests on the Bradley vehicle, the pre-stamped G sampler identifiers were used to indicate the right scout and L identifiers were used for the left scout

- Position (programmed time interval) within array: 1 through 9

- Sampler type: FS=IOM filter cassettes, CI=Marple cascade impactor, CY=cyclone, DB=diffusion battery, MV (or MVF)=moving filter, CF=cyclone backup filter, DT=deposition tray, HV=Hi-Vol, E (when used in addition to E for external)=Andersen cascade impactor; P=samplers clipped to recovery team during resuspension tests

- Stage number (for CIs and CYs): 1 through x, where x represents the bottom or lowest stage (CIs have 8 stages and the backup filter, which is designated as Stage 9; the CY has 5 stages).

For example, applying the above sample identification system to the driver's IOM at position 3 from Phase I, Shot 2, yields the following sample number: PI-2I-D3-FS. The Stage-4 CI from the same array and position is identified as PI-2I-D3-CI-4. In discussions where there is little opportunity for confusion, abbreviated sample designations based on phase and shot are used in this report. For example, PI-1 is the shorthand for Phase I, Shot 1.

3.8.2 Gravimetric Analysis

After sampling was completed, the assembled IOM and CI samplers were placed into a chamber with controlled humidity for at least 12 h before disassembling the samplers and reweighing the filters and substrates. At the recommendation of an expert peer reviewer, rather than following the common practice of desiccating the filters before weighing them, the IOM and CI filters were conditioned in a relative humidity (RH) chamber held at ~43% humidity for at least 12 h before taking pre-test weights. The desired RH was achieved using a saturated solution of potassium carbonate dihydrate ($K_2CO_3 \cdot 2H_2O$). Samples were handled only with forceps.

Samples were weighed on one of two Mettler[(a)] M5 electronic balances with sensitivities of ±1 μg. The balances had automatic calibration and linearization features, and their calibration stickers indicated that instruments were within valid calibration dates. Calibrated National Institute of Standards and Technology (NIST) Class S weights in the range of sample weights were weighed before and after each array set of IOMs and before and after each set of CI substrates. The filters were moved across an anti-static cartridge/brush[(b)] to remove static charge prior to weighing. The filters and substrates were placed into PetriSlides, photographed for documentation, counted for radioactivity, and then archived or transferred to one of three chemical laboratories for further analysis.

Although the IOM filters were weighed with little difficulty, the mixed cellulose ester (MCE) substrates used in the CIs proved to be problematic, particularly for the lower stages that collected the finer particles. With almost every CI, at least one of the substrates weighed less after testing despite visual evidence of material collected and detectable levels of radioactivity. This observation led to intense scrutiny of the laboratory weighing procedures in an attempt to identify the cause of the apparent loss of substrate weight. Some improvements were made to the procedures, but nothing seemed to prevent the substrate weight loss. In one test, a second substrate was placed behind Stage 2 on all the CIs. These substrates were in the same macro- and micro-environment as the sample substrates, but were not subjected to aerosol deposition. The expectation was that the post-test weights of these added substrates

(a) Mettler-Toledo International Inc., Greifensee, Switzerland.
(b) Staticmaster with polonium strip, Model 1C2000 from NRD, Inc., Grand Island, New York.

should remain constant if the difficulty resulted from handling in the laboratory. It was postulated that a post-test bias would point to the problem. Or, if the substrate medium underwent a physical reaction that caused its weight to change, the post-test results of the second substrate would remain relatively constant. However, knowledgeable personnel who observed the sample re-weighing process could not make much sense of the erratic results or identify the cause of this effect.

The material collected in the cyclone grit chambers was weighed and transferred to vials. In the last few tests (beginning with Phase II), samples were placed under a nitrogen atmosphere shortly after being weighed to minimize possible sample oxidation. Cyclone residues from previous shots were placed under a nitrogen atmosphere at this time. The sample vials were archived or transferred to the participating laboratories for further analysis.

3.9 Chemical and Physical Composition of Aerosols

The materials found in samples collected during the Capstone field tests were expected to consist predominantly of DU oxides and other metallic particles and oxides in powder form. The materials were recovered either on a filter medium, in a cyclone grit chamber, on a deposition tray, or on a Defensap wipe. Grit chamber residues were transferred to a glass or V-vial for storage and handling.

All samples that readily lent themselves to proportional counting were analyzed for alpha and beta activity at the ATC Health Physics Laboratory. The data from these analyses were used to estimate the uranium mass in these samples. Physical and chemical analyses were conducted on one cyclone sample set from each phase, on one full set of samples from the IOMs, and on several samples from the CIs with backup filters. Additional samples that underwent extensive analysis included several MVF samples, the diffusion battery filters, and a sample (i.e., the DU cone sample) of nearly pure DU oxide from a penetrator fragment that had oxidized *in situ* on a ledge inside the turret, thus forming a small cone-shaped pile of gray powder. Deposition trays, wipes, Andersen impactors, and gloves were analyzed by gamma counting. Several wipe and glove samples underwent chemical analysis as well.

Various samples were selected and evaluated for at least one of the following properties: uranium content, other metals composition, uranium oxide composition, particle size distribution, particle morphology, and solubility in simulated lung fluid.

Cyclone residue samples were split into the following five portions:

- one for USACHPPM for radioanalytical analysis
- three for PNNL for various physical and chemical analyses
- one for LRRI for *in vitro* solubility analysis.

The samples sent to USACHPPM were analyzed by inductively coupled plasma-mass spectroscopy (ICP-MS) to determine the concentrations of uranium and other metals. USACHPPM also used ICP-MS to determine the U-235/U-238 atom ratio in various sample types.

The three samples sent to PNNL were analyzed by:

- x-ray diffraction (XRD) to identify the crystalline solid phases (uranium oxides) present in the sample

- kinetic phosphorimetric analysis (KPA) to measure the uranium content
- inductively coupled plasma-atomic emission spectroscopy (ICP-AES) to measure the concentrations of other metals
- thermal ionization mass spectrometry (TIMS) for isotopic analysis of uranium
- SEM/energy dispersive spectroscopy (EDS) to determine particle morphology and elemental analysis
- selected transuranic analyses of a penetrator fragment.

The sample provided to LRRI was used to analyze the *in vitro* solubility of the residue (primarily uranium oxide) in simulated lung fluid.

The laboratories followed their internal standard QA/QC procedures for these analyses, some of which are briefly described in discussions of the analytical processes.

The analyses completed on each type of aerosol sample and the approximate number of samples used in each analysis is listed in Table 3.4. General descriptions of the analytical procedures are discussed in the next sections.

Table 3.4. Sample Analysis

Sample/Analysis Type	Number Analyzed
IOM Filters Cassettes (and Personal IOMs used by recovery team)	
Gravimetric	368
Alpha/beta activity	368
Alpha/beta activity verification	55
Gamma counts (self-shielding verification)	17
ICP-MS Shot 1 – U + U-235/U-238 ratio and other metals	9
ICP-MS Shots 2 through10 – U and other metals	17
Marple CIs (and Personal CIs used by recovery team)	
Gravimetric	3606
Alpha/beta activity	3606
Alpha/beta activity verification	549
Gamma spectrometry	108
SEM (checking for particle bounce)	3
ICP-MS – 3 impactors for first shot; 1 impactor for 9 shots	108
U + possible U235/U238 ratio	108
Cyclone Residue	
Gravimetric	50
Gamma spectrometry	50
XRD (5 fractions times 4 scenarios)	20
ICP-MS U and other metals, U-235/U-238 ratio	18
ICP-MS other metals	18
KPA – uranium	18
SEM/EDS (5 size fractions per scenario)	19
U/DU ratio (TIMS-best precision)	1
Lung solubility (U by KPA)	15
PFDB (7 filters for first shot only)	
Alpha/beta activity	7
Alpha/beta activity verification	7
Gamma spectrometry	3
ICP-MS – U and other metals	3
SEM	4
Lung solubility	1
Backup Filters	
Gravimetric	48
Alpha/beta activity	56
Alpha/beta activity verification	8
Gamma spectrometry	3
ICP-MS – U and other metals	4
IOM Filters Cassettes (and Personal IOMs used by recovery team)	
XRD	4
SEM	4
Moving Filter	
Alpha/beta activities	530 slices
Alpha/beta activity verification	24
Gamma spectrometry	12
ICP-MS – U and other metals, U235/U238 ratio	12
SEM – 3 selected samples	3

Table 3.4. (contd)

Sample/Analysis Type	Number Analyzed
Wipes	
Alpha/beta activity	1990
Alpha/beta activity verification	65
Gamma spectrometry	12
ICP-MS U only	12
Gloves	
Gamma spectrometry	56
ICP-MS U only	12
Deposition Trays	
Gamma spectrometry	95
Hi-Vols (Exterior)	
Alpha/beta activity	58
Alpha/beta activity verification	5
Andersen (Exterior) CIs - 2 sets x 4 shots; 1 set x 1 shot	
Gamma spectrometry	144
ICP-MS U only	12
DU Cone Oxide	
KPA – uranium	1
ICP-MS – other metals	1
TIMS – U235/238 ratio	1
XRD	1
SEM	1
Lung solubility	1
DU Fragment	
Primary transuranics elements	1
TIMS – U235/238 ratio	1

3.9.1 Radioactivity-Derived Uranium Content

Radioactivity measurements provided a means for nondestructively analyzing the samples and deriving their uranium concentrations. Simultaneous alpha and beta analyses were performed using two proportional counters at the ATC Health Physics Laboratory. Beta and gamma activity measurements were used as surrogate measurements of uranium mass for the majority of the samples collected during the Capstone DU Aerosol Study. Filters and substrates that readily lent themselves to proportional counting were analyzed for alpha and beta activity by this technique. Residues from the cyclone, external Andersen CIs, gloves, and deposition tray materials were analyzed by gamma spectrometry. Samples analyzed by proportional counting and gamma spectrometry were converted to uranium mass based on conversion factors derived from a subset of samples analyzed by both radioanalytical and direct chemical analysis of uranium. Up to 12 samples of each sample type, except for the deposition tray materials, were analyzed for uranium content by ICP-MS at USACHPPM.

An underlying assumption in using beta or gamma activity as surrogates for uranium mass is that the uranium isotopes are in equilibrium with their immediate short-lived progeny. Samples were identified in which secular equilibrium had not been established at the time of the proportional count; therefore, a methodology to correct for disequilibrium was developed. A summary of this methodology and the calculated uranium masses are included in Appendix A.

Uranium masses on the substrates and backup filters of the Marple and Andersen CIs were used in the analysis of particle size distributions, which are listed by phase, shot, and position in Appendix B and are summarized in Section 5.5.

3.9.1.1 Alpha and Beta Radioactivity Analyses

Alpha and beta analyses were conducted simultaneously at the ATC Radiological Laboratory using two Tennelec[(a)] gas-flow proportional counters. Calibration standards used included thorium-230 and technicium-99. The calibration sources were counted daily to establish alpha and beta counting efficiencies. Contributions from background media samples were subtracted from the gross sample counts, and the data were corrected for detection efficiency.

Verification analyses were performed at the USACHPPM laboratory. Approximately 10% of the samples analyzed by the ATC laboratory were also analyzed by proportional counting at the USACHPPM laboratory. USACHPPM alpha and beta verification analyses were conducted on a Tennelec Series II, Model LB5100 gas-flow proportional counter controlled with Tennelec firmware. The calibration standards used included plutonium-238 and strontium-90 sources. The calibration sources were counted daily to establish alpha and beta counting efficiency, and contributions from background media samples were subtracted from the activity analyses. The samples were run for 10 min.

3.9.1.2 Gamma Spectrometry

Gamma spectrometry was conducted at USACHPPM on selected samples using an Ortec high-purity germanium detector with a beryllium window (for low-energy gamma detection) controlled by Canberra software. Instrument efficiencies are calibrated annually at a minimum. A daily instrument QC check is performed using a mixed-point source of cobalt-60, cesium-137, and cadmium-109 to verify energy and efficiency calibrations. The efficiencies were based on the wipe sample geometry. Samples were analyzed from 10 to 50 min depending on previously measured beta activity. Background spectra were collected using blank sample media and containers and were subtracted from sample spectra as part of the gamma-spectrometry analyses. The gamma-ray energies and abundances for immediate short-lived gamma-emitting uranium progeny were obtained from the National Nuclear Data Center at Brookhaven National Laboratory (http://www.nndc.bnl.gov/). Additional details are included in Appendix A.

3.9.2 Chemical Measurement of Uranium

Direct chemical composition of the samples was conducted on a smaller sample set and included quantification of uranium and the evaluation of the oxide phases of uranium present in the various samples. Because of their greater mass, which allowed for multiple analyses, cyclone residues made up the majority of samples analyzed for uranium, other metals, and uranium oxides. Several examples of most sample types, such as IOMs filters, CI substrates, wipes, and gloves, were also analyzed for uranium. These samples were analyzed for uranium using ICP-MS and KPA. The uranium analytical procedures are summarized in the next sections, and the results are presented in Section 5.6.1.

(a) Models 55-HP and LB5100, Canberra Industries, Meriden, Connecticut.

3.9.2.1 Sample Preparation

The USACHPPM chemistry laboratory prepared cyclone residue samples for uranium measurement using a method developed there for analyzing the uranium content in soils. Each cyclone residue sample was dry-ashed and transferred to a Teflon beaker. The sample was digested in a solution of nitric acid (HNO_3) and hydrochloric acid (HCl). The supernate was collected, and the residue material was returned to its beaker and twice dissolved in a solution of HNO_3 and hydrofluoric acid (HF). The initial supernate was combined with these solutions and evaporated to near dryness. The reduced supernate was diluted to 100 mL with deionized water and analyzed using ICP-MS.

To ensure all material was recovered from the filter medium, filter samples that dissolved easily (IOM Supor filters and MCE substrates) were prepared by dissolving them in HNO_3 and hydrogen peroxide (H_2O_2) and diluting the solution to 50 mL with deionized water. Samples were reduced to dryness twice and then re-diluted to 50 mL with deionized water for ICP-MS analysis. The Zefluor, Teflo Teflon-based filters, and PVC filters were leached to remove uranium from their surfaces. The samples were diluted in a 2% HNO_3 solution for ICP-MS analysis. All samples required further dilution from 100-fold to 100,000-fold before being analyzed. The expected dilution factor was predicted based on the gross alpha, gross beta, and gamma spectral analyses.

Because the aerosol samples were not expected to contain much silicon (as occurs naturally in soil samples) or much titanium (only 0.75% of the DU/titanium alloy is titanium [Ti]), PNNL chose a simpler standard digestion process for all samples (cyclone residues, cyclone backup filters, MVF segments, PFDB Supor filters, and the DU cone sample) by dissolving them in HNO_3 and HCl but not in HF. As it turned out, many of the samples did not dissolve completely in these acids, and a substantial amount of residue remained. Following this incomplete dissolution, the samples were centrifuged, and the solids were weighed. The weight percents of the residuals ranged from low levels (3 to 5%) with Phase-III samples to nearly half the initial sample mass (32 to 41%) in Phase-II samples, which probably contained constituents of the Bradley vehicle spall liner. The amount of residues in the Phase-I samples ranged from 5 to 13% for PI-3/4 and 11 to 23% for PI-7. Eight of these solid residuals were digested in an HF solution for further analysis. With the exception of one MVF strip, which was dissolved in HNO_3, filter samples were prepared at PNNL by scraping sample residue off the filters rather than by dissolving the filters or leaching the sample material from them so the samples could be weighed before they were dissolved. Very little residue remained on the filters.

Ultra high-purity reagents and acid-leached glassware were used to avoid contamination of the samples with impurities.

3.9.2.2 ICP-MS Analysis

The USACHPPM chemistry laboratory used a PerkinElmer[(a)] Elan 6000 ICP quadrapole mass spectrometer to measure the uranium content in the aerosol sample solutions. Samples analyzed by ICP-MS included those from the cyclones and one backup filter from PI-3/4, PI-7, PII-1/2, and PIII-2, and PIV-3; the driver's set of IOMs from PI-1; 12 MVF samples, three PFDB filters; and an assortment of CI substrates, personal CI substrates and lapel filter samplers, wipes, and gloves for comparison of direct uranium measurement with the indirect radioactivity-derived uranium results.

(a) PerkinElmer, Inc., Wellesley, Massachusetts.

A laboratory-fortified blank consisting of the blank filter or substrate spiked with a known quantity of natural uranium was prepared for each medium. This fortified blank, a reagent blank, and a medium blank were prepared using the same preparatory procedure as the samples and were analyzed with the samples. Post-digestion duplicates and spikes (a sample spiked with a known quantity of material) were also analyzed to ensure the quality of the analysis. A five-point calibration curve was run, and five replicate readings were taken for each analysis of these samples to establish a standard deviation for the variability in the instrument response of less than 5%.

3.9.2.3 KPA Analysis

The PNNL chemistry laboratory measured uranium in the acidified samples solutions using a Chemchek model KPA-11R uranium analyzer.[(a)] This method quantifies the uranyl ion in solution by measuring its phosphorescence and is specific to dissolved uranium. It is easily reproducible to within a few percentage points. Measured amounts of sample solutions were placed into a quartz cell, and a phosphate complexing agent was added. The mixture in the cell was irradiated with a laser pulse, which caused the uranyl ion to fluoresce. Immediately after the laser pulse (over the next several hundred microseconds), the phosphorescence intensity of the uranyl ion was measured. The uranyl ion concentration was calculated from the decay curve of the phosphorescence. KPA analysis was conducted on samples including cyclone residues and one or two backup filters from PI-3/4, PI-7, PII-1/2, and PIII-2. Additionally, the first MVF slice from PI-1 and from PIII-2, the coarsest diffusion battery filter, and the DU cone sample were analyzed using KPA.

Sample dilutions varied by sample with an initial dilution to 40 mL followed by a further dilution of 0.1 to 20 mL, depending on its uranium concentration. The laboratory QC procedures included use of matrix and reagent spikes, replicate samples, and sample blanks.

3.9.2.4 Isotopic Analysis

Staff at USACHPPM conducted isotopic uranium analysis on uranium samples using ICP-MS, by correcting for mass discrimination of U-235 and U-238 with an isotopically certified uranium standard. This standard was analyzed periodically to verify accuracy and instrument stability. Various QC samples were analyzed with all samples according to USACHPPM laboratory QA procedures. Results of ICP-MS U-235/U-238 atom ratio analyses are included in Section 5.6.2.

In addition to the ICP-MS procedure for evaluating isotopic uranium concentrations, solutions of dissolved DU cone sample and the metal fragment were run at PNNL using TIMS.[(b)] The TIMS procedure provides a more accurate measurement of the uranium isotopic composition and can identify a wider range of uranium isotopes. In this procedure, the samples were dried on a filament, which was then heated, and the mass ratios of the uranium isotopes were measured. Multiple measurements were performed for each isotope, and the results were analyzed to determine the averages and their uncertainties. Results of the TIMS analysis are also provided in Section 5.6.2.

(a) Chemchek Instruments, Inc., Richland, Washington.
(b) Consolidated Electrodynamics Corporation, CEC Model 21-703, no longer available.

3.9.3 Non-DU Metals Composition

To provide a more complete picture of the aerosols formed during the tests, qualitative analyses of other metals also were conducted using two different methods on most of the samples that had been chemically analyzed for uranium content. Staff at USACHPPM analyzed the samples for other metals using ICP-MS, which is very sensitive to most metals. PNNL staff analyzed some of the same samples using ICP-AES analysis to more accurately measure the aluminum, iron, and zinc contents in the samples. Both methods relied on sample solutions prepared for the uranium analysis. These solutions were spiked with several internal standards to calculate a mass response curve across the mass range of interest.

A semi-quantitative ICP-MS analysis was conducted at USACHPPM for non-DU metals in the various samples. This process developed by PerkinElmer involved the use of a single-point calibration curve that analyzes for a broad range of metals and provides results accurate at about the $\pm$20% to 30% level. Instrument calibration standards, three standard blanks, and a spike recovery sample were run prior to aerosol sample analysis to verify instrument stability and process recovery. Five blanks, two matrix spikes, and a sample duplicate were run with each batch. For ICP-MS, results are normalized to internal isotopic standards.

The instrument was calibrated using a series of multi-element aqueous calibration standards: one initial calibration verification and five continuing calibration verifications, all of which were used for instrument calibration and verification throughout the analytical run. A sample solution was chosen at random for each analytical run and prepared for analysis as a dilution test, an instrument duplicate, and an instrument duplicate spike for evaluation of the instrument performance for all analytes analyzed by ICP/MS. A sample preparation blank spike, a matrix spike, and a matrix-spike duplicate were also prepared and analyzed along with the samples at the time of the digestion to ensure acceptable sample analysis and recovery. Reagent spikes and sample spikes were run to evaluate analyte recovery.

The second method used was ICP-AES.[(a)] Although the high concentration of uranium can interfere with the analysis of other metals using ICP-AES analysis, it provides more accurate results than ICP-MS for elements such as iron and zinc, and it also scans for a variety of elements without having to specifically interrogate the sample for individual metals. This method is similar to ICP-MS in that aqueous or solubilized solutions of samples are nebulized, and the aerosol is transported to a radio-frequency, inductively coupled, argon-plasma torch. The optical spectra are dispersed by a grating spectrophotometer, and intensities of the atomic emission lines are detected by phototubes. The photocurrents are then analyzed by computer to determine the concentrations of various elements using appropriate standards to determine the detection efficiency for each element.

A spike solution containing suitable levels of the analytes of probable interest (e.g., aluminum, iron, zinc, chromium, and titanium) was prepared and added to a duplicate aerosol sample at the time of the digestion to ensure acceptable sample analysis and recovery. Reagent spikes and sample spikes were run to evaluate analyte recovery.

Results of the ICP-MS and ICP-AES analysis of primary non-DU metals are presented in Section 5.6.3.

(a) Jarrell Ash Model 61, Thermo Elemental, Franklin, Massachusetts.

3.9.4 Transuranic Elements

As a by-product of the uranium enrichment process, DU is primarily U-238 with lower (depleted) concentrations of U-234 and U-235 than natural uranium. Because previously irradiated fuel was reprocessed through the enrichment process, primarily during the 1960s, some of the process equipment became contaminated with transuranic (TRU) elements from spent fuel. Trace levels of TRU elements will slightly increase the radioactivity content of the DU material.

A 22.5-g fragment from one penetrator was analyzed at PNNL to verify that the concentrations of TRU elements were similar to the concentrations previously measured in U.S. Army DU penetrators. The fragment was dissolved in nitric acid, and the TRU elements were separated from the uranium by anion exchange. A thin, even layer of precipitate from the resulting sample was mounted onto a membrane filter and evaluated using alpha spectroscopy. The alpha spectrometer uses a semiconductor detector to acquire an alpha particle energy spectrum of sample counts. The sample was examined for several radioisotopes including thorium (Th-228, Th-230, and Th-232), neptunium (Np-237); plutonium (Pu-238 and Pu-239/240); and americium (Am-241). Two matrix spikes, a reagent spike, and a blank were analyzed with the fragment sample. Detection limits ranged from 0.1 to 0.5 pCi/g. Results are presented in Section 5.6.4.

3.9.5 Uranium Oxide Composition

Uranium metal particles formed by penetrator perforation through the target vehicles quickly oxidized. The uranium-containing crystalline solids in the aerosol powder formed in the Capstone tests were expected to consist of a mixture of uranium oxide(s). The oxidation sequence of typical uranium products in order from metal to phases of progressively greater oxidization is the following: $U > UO_2 > U_4O_9 > U_3O_8 > UO_3 > UO_3 \cdot 2H_2O$ (known as schoepite). Intermediary combinations of uranium and oxygen also exist. The oxide(s) formed influence the dissolution rate of the material. Uranium in UO_2 is in the +4 valence state and is the least soluble. Uranium in UO_3 is in the +6 valence state and is the most soluble. Those with compositions between UO_2 and UO_3 contain combinations of +4 and +6 valence states.

The crystalline uranium-oxide phases in residues from PI-3/4, PI-7, PII-1/2, and PIII-2 cyclone stages and backup filters and the first MVF slice from PI-1 were identified using standard powder XRD analysis (Jenkins 1989; Cullity 1967) and a Scintag PAD V x-ray diffractometer.[(a)] Samples were prepared for XRD by mixing the sample powders with nitrocellulose glue and transferring each sample slurry to a glass slide. The samples were irradiated with an intense x-ray beam, and the resultant XRD patterns were collected and compared to standard patterns of uranium and various uranium oxides from the JADE+5[(b)] software and the Inorganic Crystal Structure Database (ICSD) XRD pattern library.[(c)] Refer to Appendix C for more details of the instrumentation and procedure used and the XRD patterns from which the oxide phases were identified. A summary of the results is provided in Section 5.6.5.

(a) Scintag, 707 Kifer Rd., Sunnyvale, California.
(b) Manufactured by Materials Data Incorporated, 1224 Concannon Blvd, Livermore, California.
(c) Maintained by Fachsinformationzentrum, Karlsruhe, Herman-von-Helmholtz-Platz 1, D76344 Eggenstein-Leopoldshafen, Germany.

3.9.6 Particle Morphology

Samples used for the analysis of particle morphology were limited to cyclone residues and their backup filters. The particle morphology for selected samples was evaluated using an SEM equipped with an Oxford Links EDS system. A "touch grid" sampling of particles was collected on various substrates (filters, cyclones, films) by physically touching the SEM stubs to the aerosol sample, thus transferring a number of particles to the stubs. The stubs were mounted, SEM images were taken, and EDS was used to analyze selected particles. A particular advantage of this method was that it eliminated the need for aerosol sampling using point-to-plane electrostatic precipitators, additional extractive probes, high-voltage power supplies, etc.

In addition to revealing particle shapes, SEM/EDS helped confirm particle structures, range of physical particle sizes, and elemental composition. Additionally, each micrograph illustrated whether the materials exhibited characteristics of crystalline solids, such as particles with crystal faces, or of aggregates of similar or dissimilar materials. Knowledge of particle structure is useful in identifying possible mechanisms by which the particles were formed. Refer to Appendix D for more details of the instrumentation used and micrographs of selected particles. A summary of the results is presented in Section 5.6.6.

3.9.7 *In Vitro* Solubility

For inhaled uranium compounds, it has been shown that the rapidly dissolved fraction of a uranium aerosol deposited in the lung is absorbed efficiently into the blood where it is transported mainly to the kidneys and bone or is excreted into the urine. The *in vitro* solubility of DU present in the aerosol samples was measured at LRRI using the static dissolution technique described by Kanapilly and Goh (1973) and Eidson and Griffith (1984). The aqueous solvent employed was synthetic ultrafiltrate (SUF; Eidson and Griffith 1984), with a composition based on Gamble's solution, which is a laboratory surrogate for extracellular fluid (Gamble 1967). The basic *in vitro* test for solubility uses a simulated lung fluid as the sample matrix into which the sample is inserted for a period of at least 30 d and as long as 60 d.

Samples identified for *in vitro* solubility analysis included the cyclone residues collected from Stages 2 through 5 and a backup filter from PI-3/4, PI-7, PII-1/2, and PIII-2 (only Stages 4 and 5 collected sufficient sample). Because the particles collected on Stage 1 generally are too large to be considered respirable, only one Stage-1 sample (PI-7) was analyzed for solubility, just to ensure the solubility of this particle size was understood. The coarsest particle fraction of the PFDB filters (the sample without the additional screens) also was evaluated. To achieve some understanding of the solubility as a function of particles suspended with time, five IOM samples from the driver's position in the PI-1 test also were evaluated. The previously mentioned cone-shaped pile of DU oxide also was included in the *in vitro* solubility analysis.

The solutions collected from the solubility analysis were analyzed for uranium using KPA. The analysis of each batch of solvent samples was accompanied by a set of 50-mL SUF samples, three of which were spiked with NIST-derived natural uranium, and two of which were maintained as process QC blanks. These samples were treated along with the experimental samples to provide batch-specific QC. The composition of the dissolution fluid and other details of the procedure are discussed in Appendix E. A summary of the results appears in Section 5.6.7.

3.10 Quality Assurance

The experimental nature of the field-testing portion of the Capstone DU Aerosol Study was conducted in a violent environment in which total control of events was difficult and the cost of conducting the individual tests precluded reruns. Because of the nature of the test action, a significant loss of sampling instrumentation was expected. In light of this expectation, each test was designed with as much sampling overlap as available space allowed. With regard to sample collection and analysis, the analytical aspects of the project were designed with QC and QA in mind to ensure that the results were accurate, precise, complete, and representative. Audits of sample handling, mass measurements, and radioactivity analyses were conducted periodically throughout the study.

3.10.1 Field Sampling

Field sampling was conducted under the auspices of the ATC and was supported by the ATC Radiation Safety Office (RSO) of the Health Physics Support organization. Exterior and non-automated sampling was conducted in accordance with test site re-entry policies implemented at ATC. Initial entries were restricted to selected personnel using protective (anti-contamination) clothing and respiratory protection, when the particulate levels warranted. Protective clothing for later entries was at the discretion of the RSO and in accordance with standard operating procedure at the Superbox.

QA of sample collection was handled in several ways. Precision, with respect to aerosol sample collection, involved consistent sampler handling and control of sampler flow rates. Sampler handling was guided by standard operating procedures tailored specifically for placement and recovery of aerosol samplers used in the tests. Sample flow rates were controlled and recorded by the LabVIEW computer controller to document the pressure drops (which are converted to flow rates) and length of sampling duration. Flow rates of exterior samplers were measured with a digital calibrator before the test to ensure that they were within acceptable limits and, then again, afterward to determine the drop in airflow following sample collection.

The sampling collection arrays were designed to collect samples that were representative of aerosols that present near the breathing zone of the crewmembers. The quantity and characteristics of particulate matter collected by samplers at the commander and loader positions (in Phases I and III) and at the right and left scout positions (in Phase II) were anticipated to be generally similar. However, they are not exact duplicates in relation to the penetration sites, and variability was expected between interior sample locations. If qualitative observation of filters from these samples had suggested very dissimilar environments, then field-sampling procedures would have been revised. Data from the sampling collection arrays indicated that such revisions were not necessary.

Field instruments and equipment were calibrated, as appropriate, to ensure the accuracy of the measurement of field parameters. For sample collection, the primary parameter being monitored was the pressure drop across the filter over time. Flow rates are inferred by the change in pressure, which relates to a change in resistance. A correlation calibration was conducted to confirm this inference. Pressure drops were measured on each sampler before the experiment commenced, and the change in pressure with test sampling time was documented. Except for PI-7, in which fragments destroyed the electrical lines carrying the feedback signal, the pressure drops were measured on a second-by-second basis.

PI-1 and PI-22 (single crossing shots) and PI-5 and PI-6 (single breech shots) were essentially replicate tests. There were no plans to replicate PI-3/4 (double crossing shots) or PI-7 (hull shot) because the cost-benefit of the effort was judged to be questionable at best. PII-1/2 and PII-3 represent different types of shot lines, which may provide general upper and lower bounds on aerosols created in the Bradley vehicle. PIII-1 and PIII-2 were replicate tests. Aside from corrective actions taken as a result of lessons learned during the course of the test, the sampling method remained as constant as possible for each medium and target sampling location to ensure comparability of data over time.

3.10.2 Laboratory Analyses

All laboratories involved in aerosol sample analysis were licensed to work with radioactive materials. Personnel working in these laboratories were qualified by way of training and experience. Radioactive counting analysis was conducted on all samples collected during the test. Samples conducive to alpha/beta counting were analyzed at ATC's Radiological Laboratory, an NRC license compliance facility. USACHPPM's Directorate of Laboratory Radiological Services performed alpha/beta activity verification analyses and gamma spectrometry. Analyses were conducted in accordance with established laboratory QA programs and included periodic instrumentation checks, calibration standards, and the use of medium, reagent, and field blanks as appropriate.

Chemical analyses were conducted on selected samples. QA/QC protocols were selected to ensure that analyses were conducted appropriately. These protocols varied depending on the type of analysis and included verification of the counting data and duplication of selected samples being processed by chemical means and are briefly discussed along with procedures in Section 3.9. The resulting data were checked extensively for proper sample identification, proper data entry, and sensibility of results to identify anomalies caused by error in identification or data entry. Deviations were noted in a master database and were corrected as possible. Chemical analyses were conducted at USACHPPM, PNNL, and LRRI. The USACHPPM Laboratory is an ISO 9001-registered laboratory that routinely provides analytical support to the U.S. Army. PNNL offers expert analytical support of research and development programs for the U.S. Department of Energy (DOE) and other federal agencies. The LRRI laboratory is a former DOE laboratory that specializes in performing respiratory-related research and has extensive experience with solubility testing in lung fluid. Chemical analyses on the aerosols collected during the Capstone tests were performed in accordance with stringent QA/QC instrument and procedural requirements of the laboratories performing the analyses. Examples of some of the QC procedures relating to instrument calibration, sample blanks, and matrix and reagent spikes are included in the discussions of the various types of analyses.

3.10.3 Data Management

Sample custody and data management were controlled in a number of ways to ensure completeness of data, correct transcription between hardcopy and electronic versions of the data, and accurate calculations. Samples were photographed after sampler disassembly and weight measurement activities were completed. This photographic record was useful for reviewing the appearance of samples with unusual aspects and also for verifying sample identification. Laboratory forms containing weights and alpha/beta activity results were reviewed for completeness. They also were reviewed for technical correctness.

Samples transferred from ATC to other laboratories were assigned random number identifiers. The initial and random identifier codes were maintained by ATC.

The laboratories maintained hard copy and electronic analytical data packages for all samples, some of which were later transferred to ATC for storage. After the initial data review, the staff at USACHPPM entered the data sets into a master database using Microsoft Excel[(a)] software. Portions of this database form the basis of the data tables presented in Appendix A. Various project participants also reviewed the data and associated results.

3.10.4 Data Analysis and Interpretation

Meaningful and accurate data and statistical analyses were critical to interpreting the analytical results for the Capstone DU Aerosol Study. Scientists from PNNL, LRRI, and LANL analyzed and interpreted the aerosol data, and PNNL aerosol scientists who were not directly involved in the data analysis verified the calculations used to 1) analyze uranium concentrations as a function of time and 2) derive particle size distributions. Capstone team members reviewed the results of the other aerosol and chemical data analyses.

It was clear from the early planning stages that thousands of aerosol samples would be generated during the course of this study. Because rapid turnaround between sampler disassembly and reassembly was necessary to support the next test shot, the importance of careful sample handling and custody control led to the establishment of procedures to manage the plethora of samples.

Samples were analyzed for uranium using a combination of nondestructive radioactivity counting and chemical analysis. Because of the experimental nature of these tests in which the possible destruction of samplers was a continuing concern, many QA and QC procedures that are standard practices in a laboratory-scale analysis were not practical for this study. However, standard equipment calibration checks, media and matrix blanks, validation studies, and NIST-traceable sources were components of the process used on all relevant samples to ensure the quality of the analytical data. Nondestructive tests were conducted on all samples selected for chemical analysis to provide two measurements of uranium concentration. With the possible exception of the MVF, the characteristics of the samplers selected were well understood.

(a) Microsoft Corporation, Redmond, Washington.

4.0 Test Parameters and Observations

The field portion of the Capstone DU Aerosol Study was conducted in four phases. Phases I, III, and IV were carried out using an Abrams tank as the target vehicle. Phase II was conducted using a Bradley vehicle as the target and took place between Phases III and IV. Most of the test preparations were identical for the 12 separate shots fired during the 10 firing events of Phases I through III. Preparations for Phase IV were primarily the responsibility of the Abrams Tank 2000 Test Directors, and the Capstone team was involved only minimally in that phase. The objective of each of the shots was to collect aerosol samples inside the crew compartment of the target after impact and perforation by an LC-DU penetrator.

This chapter discusses the four phases separately, listing sample collection parameters common for all shots by phase, followed by parameters and observations specific to each shot. Parameters within Phase I that varied by shot are described in subsequent sections. Parameters specific to Phases II through IV follow. Each phase and the shots within each phase are described in the following sections. All shots were conducted at the ATC Superbox Facility. Figures illustrating approximate shot lines and sampling durations are provided for each shot.

Several physical aspects of the field tests also were documented and discussed in Section 4.5. These other physical aspects include temperature, pressure, and relative humidity; presence of tiny burning DU fragments (“fireflies”) immediately after perforation; intact penetrator fragments recovered in the vehicle; survivability of equipment; and ventilation rates.

4.1 Phase-I Test Parameters

Phase-I tests included four crossing shots, two breech shots, and one hull shot into an Abrams tank BHT. Each test event consisted of a single shot except for Shots 3 and 4, which were combined in a single test event. The Phase-I shots were conducted between 9 November 2000 and 1 February 2001. Common parameters for these Phase-I tests are described below.

Target

An Abrams tank BHT was the target in Phase-I tests. The BHT was an actual vehicle structure but without instrumentation, wiring, flammable components, or an engine. The hull had been used in previous field tests and was decontaminated and refurbished to appropriate structural integrity. The turret, which was equipped with conventional armor, had not previously been fired upon. Between tests, the target was decontaminated, armor patches were welded over the entrance and exit holes, and any additional damage with a potential effect on structural integrity was repaired. Hatches were latched prior to firing the munitions.

Air Sampling Equipment

Air sampling equipment consisted of active aerosol samplers and passive aerosol deposition collectors. The majority of active and passive samplers were placed inside the vehicle turret. A few passive samplers were placed on top of the vehicle, and several active and passive samplers were placed exterior to the vehicle but within the Superbox fragmentation shield. After all the samples had been collected, they were transferred from the Superbox staging area to a nearby building for initial decontamination. Samples

were transferred to the ATC Health Physics Laboratory for sampler conditioning followed by analysis of weights and alpha and beta radioactivity counting of the aerosol samples.

Interior Air Sampling Equipment

Sampling arrays were mounted at the driver's, commander's, loader's, and gunner's positions (except for Shots 5 and 6, which did not include an array at the gunner's position). Each sampling array included:

- Nine, 25-mm, IOM filter cassette samplers, operated at a nominal flow rate of 2 Lpm. The filter media varied by shot with Supor (hydrophilic polyethersulfone) used in the initial shot tests. Because some of the filters tore or disintegrated in Shots 1 and 2, Zefluor (Teflon-based) filters were generally used in later tests. Visual inspection of the samplers in their custom carriers was performed after the samples were removed from the vehicle. IOM sampler caps were installed immediately after inspection of the IOM filter media. The caps reduced the potential for personnel contamination and sample loss.

- Nine, 25-mm, 8-stage modified Marple CIs, operated at a nominal flow rate of 2 Lpm. MCE substrates were used in Stages 1 through 8 and the backup filter, identified in the data as Stage 9. These filter media sustained little or no damage.

The IOM and CI samplers were operated in pairs. The first of the pairs was activated 5 sec after the shot was fired to minimize the possibility of damage. The next seven pairs were operated in a specific time sequence with increasing collection time durations. These collection times varied with each shot and were designed to minimize filter overloading. The final sampler pair was a field blank, brought into service only if a previous sampler did not operate. Sampling durations are listed by shot (Tables 4.1 through 4.6) and are summarized in Table 4.7 (see page 4.25) at the end of Phase-I test observations.

Additionally, a Merlin-Gervin moving filter and a five-stage cyclone train, each with a collection port, were placed in a protective metal box on the floor of the turret. The moving filter, which used AW19 as the filter medium, collected aerosols at a nominal flow rate of 28 Lpm (1 cfm) and moved at a rate of 0.88 cm/sec (20.9 in./min). The moving filter was included in the sampling strategy specifically to collect samples during the first 5 sec after the shot was fired because the filter cassettes and the CI samplers were not operated during that initial 5-sec period. The moving filter also was run intermittently to intercept aerosols at certain time increments following the shot. Sampling durations are listed in Table 4.8 (see page 4.27) at the end of Phase-I test observations.

The cyclone collected aerosols at a nominal flow rate of 14 Lpm. A PFDB was connected to the fifth stage of the cyclone during the first shot to collect ultra-fine material on Supor filter media. For the remaining shots, a backup filter arrangement with four parallel filters was connected to the fifth stage of the cyclone. These backup filters were made of PTFE membranes and polymethylpentene support rings. Cyclone samplers usually operated about 2 h post shot. Sampling durations are listed in Table 4.9 (see page 4.28) at the end of Phase-I test observations.

Considerable sampling redundancy was designed into the tests to account for expected sample losses resulting from the violence of the firing action. Although some sample loss occurred in each test (the IOM samplers and the moving filter were the most susceptible), the needed samples were collected successfully for most of the tests.

Interior air sampling equipment was controlled remotely through use of LabVIEW software. Flow rates for each sampler were checked after each installation. Sulfur hexafluoride (SF_6) analysis was conducted before, during, and after each shot to establish the ventilation rate within the vehicle.

Exterior Air Sampling Equipment

Exterior air sampling was conducted within the Superbox fragmentation shield. Hi-Vol air samplers with 10.2-cm (4-in.) diameter Whatman 41 filters operating at a nominal flow rate of 560 Lpm (20 cfm) were placed in the breathing zone at selected positions outside the target. Baseline air samples were collected at these positions for 1 h prior to each shot. The initial plan was to stagger the run times following impact so that aerosol loading on filters could be assessed. Because all available remotely operated electrical lines were used for test aspects of higher priority, sampling run times for the Hi-Vol samplers were controlled manually via outlet boxes located outside the Superbox for the first two shots in Phase I. The sampling positions varied with each test.

Andersen CI samplers, which used 81-cm diameter MCE filters, became available for use from Shot 5 through the end of the test period, so these samplers replaced the Hi-Vol units for post-shot sampling. They operated at a nominal 28 Lpm (1 cfm). Hi-Vol samplers continued to collect the baseline aerosol samples before each shot.

Deposition Trays

Eight deposition trays (see p.3.35 for description) were used: two positioned on the fragmentation shield floor, two positioned on the hull, and four positioned inside the turret.

Contamination Surveys

Interior Removable Contamination

Interior removable contamination was measured by smearing 47-mm diameter Defensap wipes within a defined 100-cm^2 area. Thirty-two discrete wipes were used to collect removable material on interior vertical and horizontal surfaces. Four deposition trays were placed at each crew position. Additionally, for an analysis outside the scope of the Capstone DU Aerosol Study, four additional locations were evaluated to establish a correlation between removable contamination collected by using 47-mm wipes and exposure rate readings using currently fielded Army portable radiation survey instruments.

Exterior Removable Contamination

Exterior removable contamination on the surfaces of the target and the surrounding Superbox was measured by smearing 47-mm diameter Defensap wipes within defined 100-cm^2 areas. Thirty discrete wipes were collected on the target's horizontal and vertical surfaces (10 on the impact side, 10 on the exit side, and 10 on the top of the target). As with the interior wipes, four additional locations were evaluated for removable contamination using 47-mm wipes and currently fielded Army portable radiation instruments.

Personal Monitoring

Entry personnel who conducted contamination surveys and removed air sampling equipment were fitted with personal air samplers and cotton gloves. Each person entering the Superbox wore a 25-mm cassette filter breathing zone air sampler operated at 2 Lpm. Selected entry personnel wore a 37-mm Marple personal CI sampler operated at 2 Lpm. These samplers were worn for the duration of the contamination survey. In addition, to collect removable contamination contacted during their re-entry activities, selected entry personnel wore cotton gloves over their protective clothing.

Pressure and Temperature Measurements

Impulse pressure and temperature sensors were placed inside the turret to record impact blast and temperature for PI-2 through PI-7 shots. The pressure was measured using a PCB piezoelectric 102A15 gauge,[(a)] which sampled at 40,000 measurements per second at a frequency of 40 kilohertz. The gauge mount was welded into a hole in the turret roof directly above the center of the cannon breech. Temperature measurements were taken initially to determine whether damage to the IOM Supor filters was related to temperature. The thermocouples were 0.076-mm diameter, fast-response, K-type probes, and a sampling rate of 100 measurements per second was used. The thermocouples were placed at several crew positions inside and outside the protective sampler array shields.

Pre-Shot Preparations

Prior to the first test shot, a pre-shot event test was conducted to ensure that the sampling equipment and the computer hardware and software functioned as designed when the sampling system was installed inside the BHT and the Superbox. Sampler handling was reviewed, and at the recommendation of a peer reviewer, a decision was made to condition the filters to a relative humidity regime of about 40% rather than desiccating the filters. Additional QC checks also were implemented into sample preparation and analysis at this time. No ammunition was used during the pre-shot event test.

4.1.1 Phase I, Shot 1 (PI-1) Test

The PI-1 test was initiated on 9 November 2000, and the shot was fired at about 1338 h. This test initially was viewed as a Superbox shakedown or pilot test. Because of its success, it was designated Shot 1. The target was in the traverse position (gun facing rear of vehicle), and the LC-DU penetrator successfully impacted the left side of the turret (loader's side) without interacting with the breech (see the shot-line diagrams in Figure 4.1). The penetrator exited the turret and was captured by the backstop. Though there was some sample loss, air samples generally were collected as programmed. Recovery operations included sampler and deposition tray recovery and contamination surveys.

4.1.1.1 Air Sampling

Shot-specific information regarding the interior and exterior samplers includes the following:

Interior Air Samples

- IOM Filter Medium: Supor

(a) PCB Piezotronics, Inc., Depew, New York.

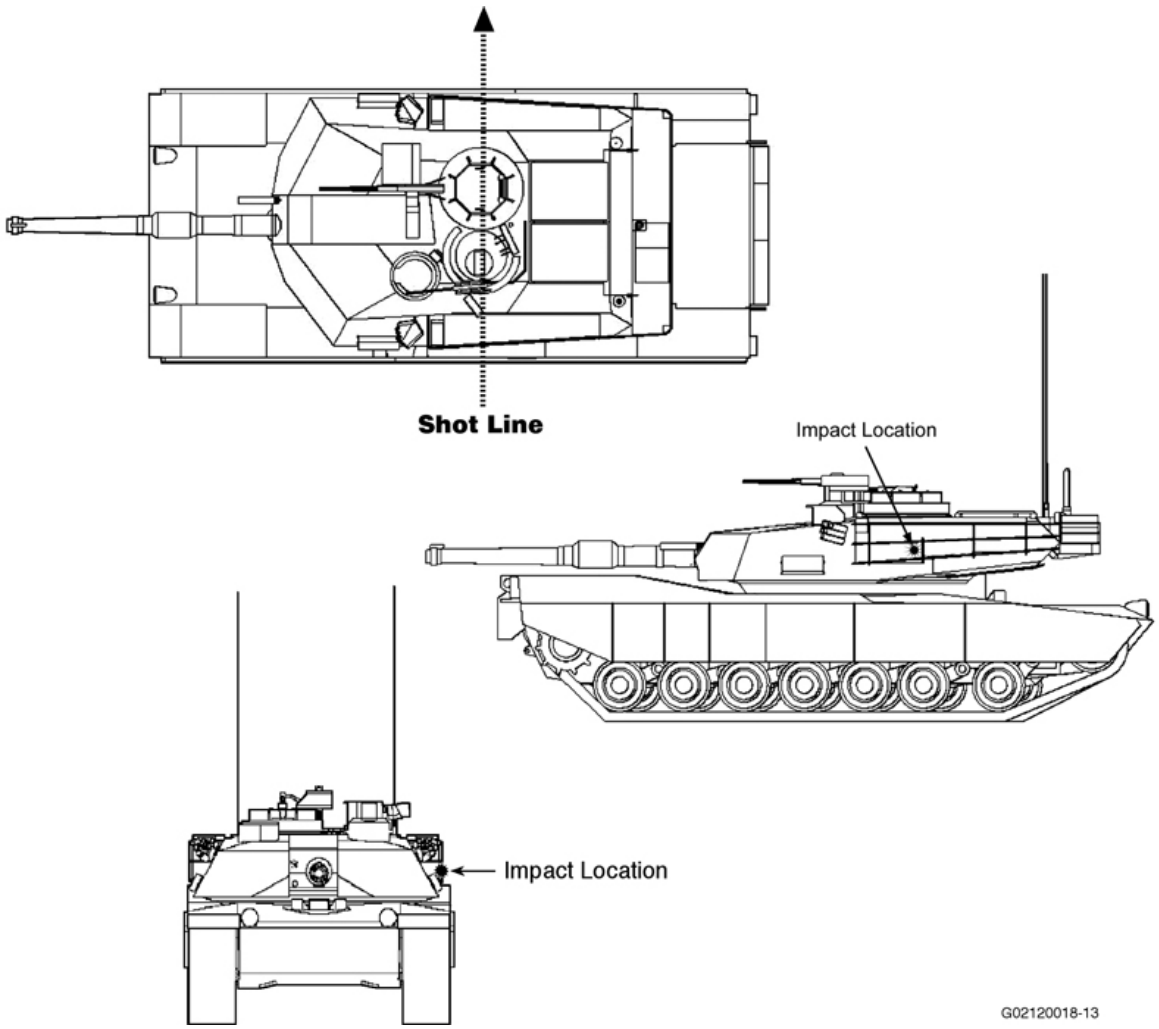

Figure 4.1. PI-1 Shot Line

- Sample Array Shielding: For protection from fragment damage, louver shields were placed over the sampling arrays located at the commander's, gunner's, and loader's positions. No shielding covered the sampling array located at the driver's position.

- Array Sample Times: The IOM and CI samplers began operating 5 sec after impact and followed the time sequence presented in Table 4.1.

Table 4.1. IOM and CI Sample Collection Times for the PI-1 Shot

Sampling Sequence	Collection Interval (+5 sec)	Elapsed Sampling Time
1	0-30 sec	30 sec
2	0.5-1.5 min	1 min
3	1.5-3.5 min	2 min
4	3.5-7.5 min	4 min
5	7.5-15.5 min	8 min
6	15.5-31.5 min	16 min
7	31.5-63.5 min	32 min
8	63.5-127.5 min	64 min

- Moving Filter: The MVF operated from 30 sec before the shot and sampled at this position until 5 sec after the shot. It then advanced to a new position and sampled at that position for 10 sec before moving on to the next position and sampling for 10 sec. It eventually clogged during a stationary phase. See Table 4.8 for the MVF sampling times for Phase-I test shots.

- Cyclone: The protective box containing the cyclone and the MVF was placed on the turret floor between the commander's and the loader's positions. The cyclone, which was fitted with a PFDB for collection of small particles, was started 5 sec after the shot and ran for 2 h, 8 sec. The cyclone was set to operate at 14 Lpm, and the PFDB was flow matched. However, a possible leak in the PFDB test apparatus to which the cyclone was attached may have been responsible for a measured flow rate of 31.4 Lpm.

- Deposition Trays: Eight trays were used: two positioned outside, two positioned on the target, and four positioned inside the target.

Exterior Air Samples

Three baseline Hi-Vol samplers collected total particulate matter within the Superbox, but exterior to the target, for an hour on the morning the test was conducted. Four Hi-Vol air samplers collected particulate matter following the shot. One of these samplers was located to the side of the flight tunnel near the front corners of the fragmentation shield, in front of the target impact point. The second sampler was located to the right (looking from the flight tunnel—see lower side of Figure 2.1), roughly situated along the midpoint of the vehicle (which was turned sideways). The third sampler was placed near the corner behind the target and to the right (looking from the flight tunnel) of the catch plate. The fourth sampler was placed directly below the catch plate and behind the polyethylene sheet that faced the target. The samplers were already operating at the time of impact. The samplers nearest the catch plate operated for 11 min following impact. The remaining samplers operated for 20 and 30 min, respectively, following impact. All were shut off manually from an electrical outlet panel located near the entrance to the Superbox.

The breech of the gun was sealed with an inflatable ball. Hatches were closed and bolted down, and blow-off plates over the bustle were positioned and bolted down.

4.1.1.2 Impact Observations

Immediately after impact, a geyser-like plume that originated in the hull exited through an opening in the rear of the turret, and only thick smoke was visible inside the target. Smoke also was seen exiting the small antenna opening, the gun opening, and other relatively small openings. Although space limitations precluded placing instruments inside the turret, the geyser-like plume from inside the hull (presumed to have been caused by blast overpressure) was observed when viewing a frame-by-frame video replay of the impact event. The hatches appeared to remain closed during impact. The driver's hatch had been removed during target preparations and replaced with a tack-welded metal plate. The tack welds failed, and some aerosol escaped through this partially open hatch covering. The penetrator impacted the target less than 6 in. from exterior survey point Number 3.

The aerosol and smoke initially obscured visibility inside the turret, but after about 2 min, the breech became visible. After about 11 min, the smoke had dissipated noticeably, and first responders later

reported that a portion of the commander's seat had ignited and burned. A frame-by-frame analysis of the video taken during the test verified that a fire had occurred in front of the driver's position where electrical cables led to the bustle. Visibility had improved considerably after about 19 min. The louver shield over the gunner's station appeared to have suffered minor damage, as the horizontal louver rungs appeared slightly bent.

Videotape footage taken inside the target showed the occurrence of a fireball, followed by small flares called "fireflies." The majority of the fireflies (visible small points of light presumably tiny fragments undergoing instantaneous oxidation) within the field of view burned out in less than 1 sec, while one that landed on the loader's louver burned out in less than 2 sec.

Examination of the turret after the test revealed that the commander's position suffered significant fragmentation damage and that a portion of the commander's seat burned. This may have contributed to the reduced visibility observed in the turret. Particulate matter deposited on the plastic shields in front of the camera lenses contributed to the appearance of impaired interior visibility. Also, inside the target, a fragment of the penetrator was observed on the turret/hull ledge below the exit hole. The turret basket screen had been torn loose and apparently had caused damage to some of the samplers but not to the filters or substrates.

4.1.1.3 Recovery Observations

After all of the aerosol sampler collection cycles were completed, the HEPA exhaust system in the Superbox was activated. The fragmentation shield door was kept sealed until the ambient particle air concentration inside the Superbox was within administrative safety limits. Upon opening the door, a layer of gray dust covering the floor of the fragmentation shield was visible.

Interior air samplers: Observations and preliminary conclusions regarding the interior air samplers are listed below.

- Many of the IOM filters from the commander's position and all of IOM filters from the gunner's position appeared to have torn or partially disintegrated. The IOM filters from the loader's position and the driver's position were intact.

- Although most or all of the IOM cassette filters in the commander's and gunner's positions were destroyed by fragment penetration or scorching, perhaps as a result of the temperature/pressure blast, all other samplers survived intact. One IOM filter was dented and detached from its fitting.

- The IOM filters from the loader's and the driver's positions showed fairly even light-brown/gray deposits, which suggests that not only was material recovered, but that the experimental time scheme was reasonably well structured.

- The filters in the first stages of the CI samplers were intact. Some of these filters, as well as some of the IOM cassettes, had large dark particles suggestive of tiny DU fragments on their surfaces.

- The cyclone recovered material in quantities of tens of milligrams.

- The PFDBs collected substantial material, but the radiation detector (pancake probe) did not register readings above background levels for these samples. There was some question about the flow rates and possible sampler leakage.

- The MVF operated for nine separate spots (five stationary, four transitory) at which time it apparently jammed because of the quantity of material recovered. The spots seem to alternate from a dark green for the stationary samples to a lighter greenish brown for the transitory ones. The final spot looked like a cake of beige clay.

External air samplers: All four of the Hi-Vol samplers survived the impact with little to no damage. Only the sampler located underneath the catch plate experienced minor damage, which was easily repairable. Recovery personnel reported that each of the air samplers appeared to have collected a similar quantity of heavy deposit of sample material. When the samplers were reactivated to take post-test flow readings, none of the rotameters moved even though the motors to all of the samplers were operating. Because of the rotameter responses, it is believed that these samples overloaded. When the filters were replaced with unused media, the rotameter readings were similar to the initial readings.

Deposition trays: The deposition trays were measured for beta particle readings and then covered with foam salad plates, secured with tape, and placed into pre-labeled locking plastic bags. Because of the possibility that a static charge associated with this configuration could hinder transfer of all material collected on the deposition trays, this technique for collecting the samples was re-evaluated, and heavy-duty paper plates were used instead for all later shots.

Personnel recovery activities: Two of four recovery staff members (Staff 1 and 3) were designated to wear cotton gloves so that removable contamination residues contacted during their recovery activities could be evaluated. Recovery Staff 1 engaged in recovery activities from 1615 h to 1800 h. During this time, all deposition trays were collected and bagged. Interior wipe samples were collected, and these samples were transferred at the hot line prior to collecting the cotton gloves. The cotton gloves from Recovery Staff 3 were collected at 1635 h, after the exterior instrument survey and the first 15 exterior wipe samples were collected. Recovery Staff 4 collected the remaining 15 exterior wipe samples.

4.1.2 Phase I, Shot 2 (PI-2) Test

The PI-2 test occurred at 1221 h on 29 November 2000. The target was in the traverse position (gun facing rearward), and the LC-DU penetrator impacted the left side of the turret (i.e., the loader's side) and did not interact with the breech (see the shot-line diagram in Figure 4.2). The penetrator exited the turret and was captured by the backstop. Though there was some sample loss, air samples generally were collected as programmed. Recovery operations included sampler and deposition tray recovery and contamination surveys.

Changes from Previous Test

- Beginning with this test, the Superbox was cleaned between tests to minimize carryover of DU debris from one test to the next. Cleaning of the exterior target vehicle and the surrounding area generally consisted of HEPA vacuuming the floor. The target was cleaned by HEPA vacuuming the inside of the crew compartment three times.

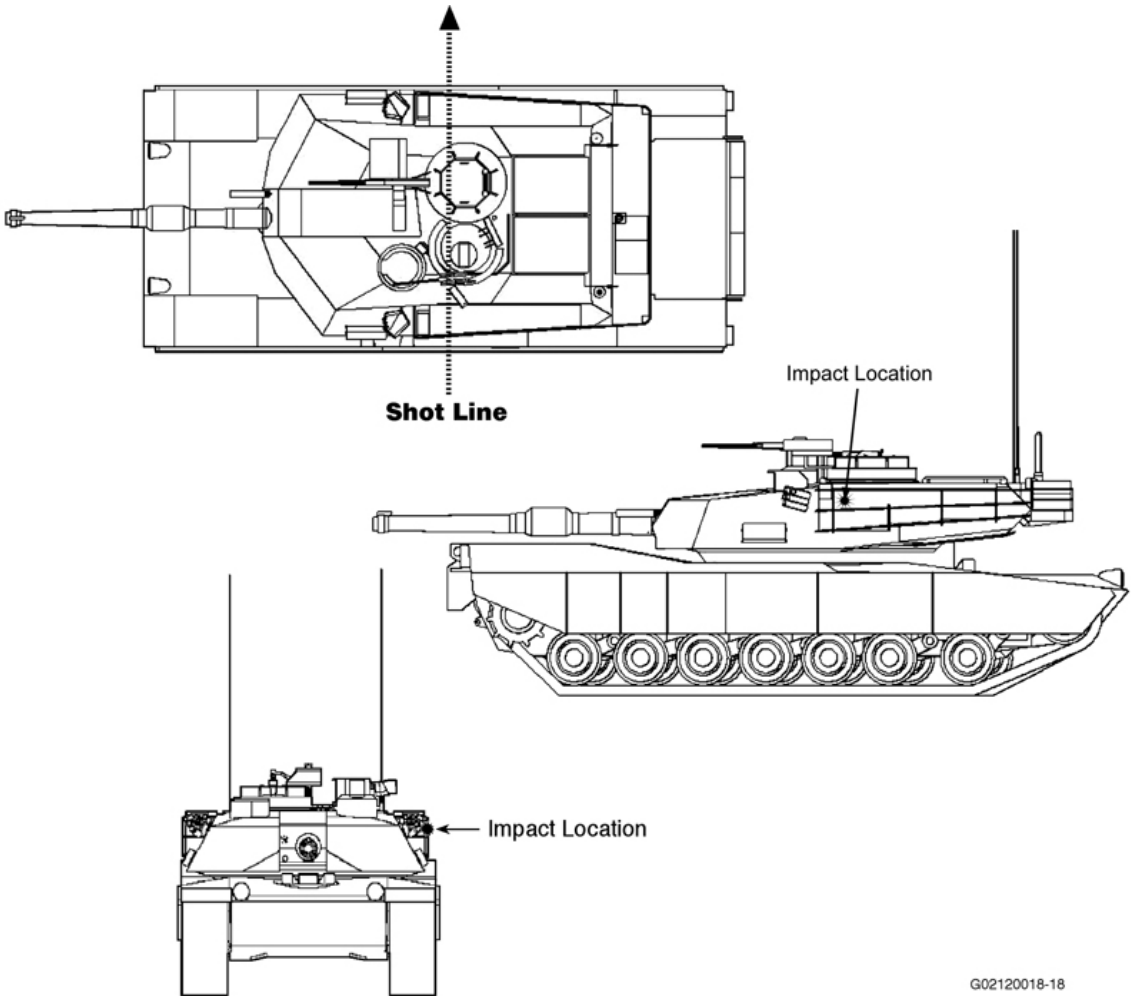

Figure 4.2. PI-2 Shot Line

- Combustible seating pads were removed from the BHT. The section of basket separating the driver's compartment from the crew compartment was installed and secured with hose clamps.

- A gun tube was installed, and the breech was sealed with a spent cartridge shell. The hatches were closed prior to the test, and other openings in the BHT observed in videotapes of the Shot 1 test were sealed.

- The metal cover replacing the driver's hatch was fully welded to prevent it from detaching from the impact blast.

- Four fast-reacting thermocouples were installed inside the turret to measure temperature in the crew compartment following perforation by the penetrator. Two of the thermocouples were positioned to detect temperature outside and inside a louvered shield that was placed to protect a sampling array.

- Four Hi-Vol air filters were installed inside the fragmentation shield. As in the Shot-1 test, three of the samplers were positioned behind the bustle (left, right, and center of the target). The fourth

instrument was positioned below the catch plate and behind the polyethylene sheet that faced the target.

4.1.2.1 Air Sampling

Shot-specific information regarding the interior and exterior samplers includes the following:

Interior Air Samples

- IOM Filter Medium: Supor

- Sample Array Shielding: Louver shields were placed over the sampler arrays located in the commander's, gunner's, and loader's positions. In an attempt to provide better protection for the IOM filters at the gunner's position, a flat metal plate covering the louver at this position was hinged to the bottom of the louver and was tripped shortly after the shot was fired. Unfortunately, this arrangement provided little or no improvement in IOM filter survival. No shielding covered the sampling array located in the driver's position.

- Array Sample Times: Based on the observation that the IOMs at the loader's position may have overloaded during Shot 1 sample collection, the sampling times for the IOMs and the CIs were reduced by 50%. The IOM and CI samplers began operating 5 sec after impact and followed the time sequence presented in Table 4.2.

- Moving Filter: The appropriate filter medium was not available during this shot so the MVF was not used.

- Cyclone: The PFDB used in Shot 1 to collect ultra-fine particles was replaced with a backup filter connected to Stage 5 of the cyclone. The cyclone was started 5 sec post shot and ran for 2 h, 8 min at an average flow rate of 9.9 Lpm.

- Deposition Trays: Eight deposition trays were used: two positioned outside, two positioned on the target, and four positioned inside the target.

Table 4.2. IOM and CI Sample Collection Times for the PI-2 Shot

Sampling Sequence	Collection Interval (+5 sec)	Elapsed Sampling Time (min)
1	0-15 sec	0.25
2	0.5-1 min	0.50
3	1.5-2.5 min	1
4	3.5-5.5 min	2
5	7.5-11.5 min	4
6	15.5-31.5 min	16
7	31.5-79.5 min	48
8	79.5-127.5 min	48

Exterior Air Samples

Four Hi-Vol samplers were located to the right of the impact point: one was located in front of the vehicle, one was in the center near the barrel, one was behind the vehicle near the catch plate, and the last one was located directly underneath the catch plate. Samplers ran from 3 to 7 min following impact. Again, out of necessity, the samplers were manually activated and deactivated.

Temperature and Pressure Measurements

Impulse pressure and temperature inside the turret were measured in this test.

4.1.2.2 Impact Observations

Immediately after impact, the images from the ATC real-time video system revealed only thick smoke in the interior of the target. The breech was barely visible immediately following impact, but it became more visible after about 5 min. The loader's hatch opened partially (approximately three-quarters open) at impact, resulting in the loss of what appeared to be a substantial amount of aerosol from the interior of the BHT.

The target interior cleared more quickly in this test than in the Shot 1 test, probably due to the partially opened loader's hatch. The opening of the hatch upon impact could be due to higher interior pressures resulting from modifications made to the turret after the Shot 1 test (e.g., complete sealing of the driver's hatch plate, use of an empty cartridge case to seal the breech, sealing the antenna port on the turret, use of a better seal on the ready-rack inserts housing the air sampling arrays, and installation of the divider plate in the bustle to prevent air movement throughout the turret).

Review of videotape footage taken inside the target revealed a fireball followed by the appearance of fireflies. The majority of the fireflies within the field-of-view appeared to burn out in about 1.5 sec. The video images also revealed a larger item (probably a steel interior patch welded over the perforation hole after the Shot 1 test) suspended and following the direction of the shot line.

Visibility was much improved within 10 min of impact (i.e., the gunner's louver was visible from the camera port). The metal plate installed over the gunner's louver dropped as intended shortly after impact. The louver appeared to have suffered minor damage (e.g., the horizontal louvers were slightly bent and did not appear to be parallel).

Within 40 min, the interior of the target appeared to be fairly clear while the air within the fragmentation shield but outside the vehicle was fairly smoky (possibly due to the partially opened hatch).

4.1.2.3 Recovery Observations

Interior Air Samplers

Although the metal plate attached to the front of the gunner's louver shield dropped as planned following impact, the design modification was not adequate to prevent damage to the IOM cassette samplers from the temporary heat and pressure pulse phenomenon that occurs for a very short time after impact. All nine of the cassette (IOMs) filters located within the louver at the gunner's station were damaged. The #2

CI was displaced from the driver's sampling array, probably by the impact, and was found on the driver's compartment floor.

Exterior Air Samplers

The external samplers ran from 3 to 7 min. The filter on the sampler located under the catch plate had been blown off. Heavy loading was noted on all the other filters. Little to no movement of the rotameters was again observed although the motors were functioning when the samplers were reactivated to determine post-shot flow rates.

Personnel Recovery Activities: Upon re-entry, the survey team could not find sample location 35 (probably due to the proximity of the munitions exit hole). The survey team used an area near the interior exit hole (near sample location 17) for the exhaustive wipe survey. Exterior sample location 27 on the commander's hatch cover had equipment placed over the 100-cm^2 area before the wipe survey could be performed, possibly changing the quantity of residue at this position.

4.1.3 Phase I, Shots 3/4 (PI-3/4) Test

The PI-3 and PI-4 tests were combined into one event on 7 December 2000 during which two LC-DU penetrators impacted the right (gunner's) side of the turret. This test concluded the series of shots in which penetrators entered the crew compartment through the turret side armor and then exited through turret armor on the side opposite the entry point. The target was in the combat position (with the gun facing forward over the driver's position), and both rounds impacted the turret on the commander's side very close to the aim points, less than 6 in. apart vertically. The gun breech had been sealed with a spent cartridge shell to prevent aerosols from leaving the crew compartment through the muzzle.

The shot lines are diagrammed in Figure 4.3. Firing of the two rounds was separated only by the time required to reload and reset equipment. Shot 3 was fired at 1407 h, and Shot 4 was fired 13 min later at 1420 h. Neither round interacted with the breech, and both rounds penetrated the turret and were captured by the backstop. Though there was some sample loss because of the premature opening of a new shield at the loader's position, air samples generally were collected as programmed. Recovery operations included sampler and deposition tray recovery and contamination surveys.

4.1.3.1 Air Sampling

Shot-specific information regarding the interior and exterior samplers includes the following:

Interior Air Samples

- IOM Filter Media: Because of damage to IOM filters in Shots 1 and 2 (thought to have been caused by the temperature/pressure pulse), Supor continued to be used in Samplers 1, 4, and 7, and Zefluor was used in the remaining IOM samplers.

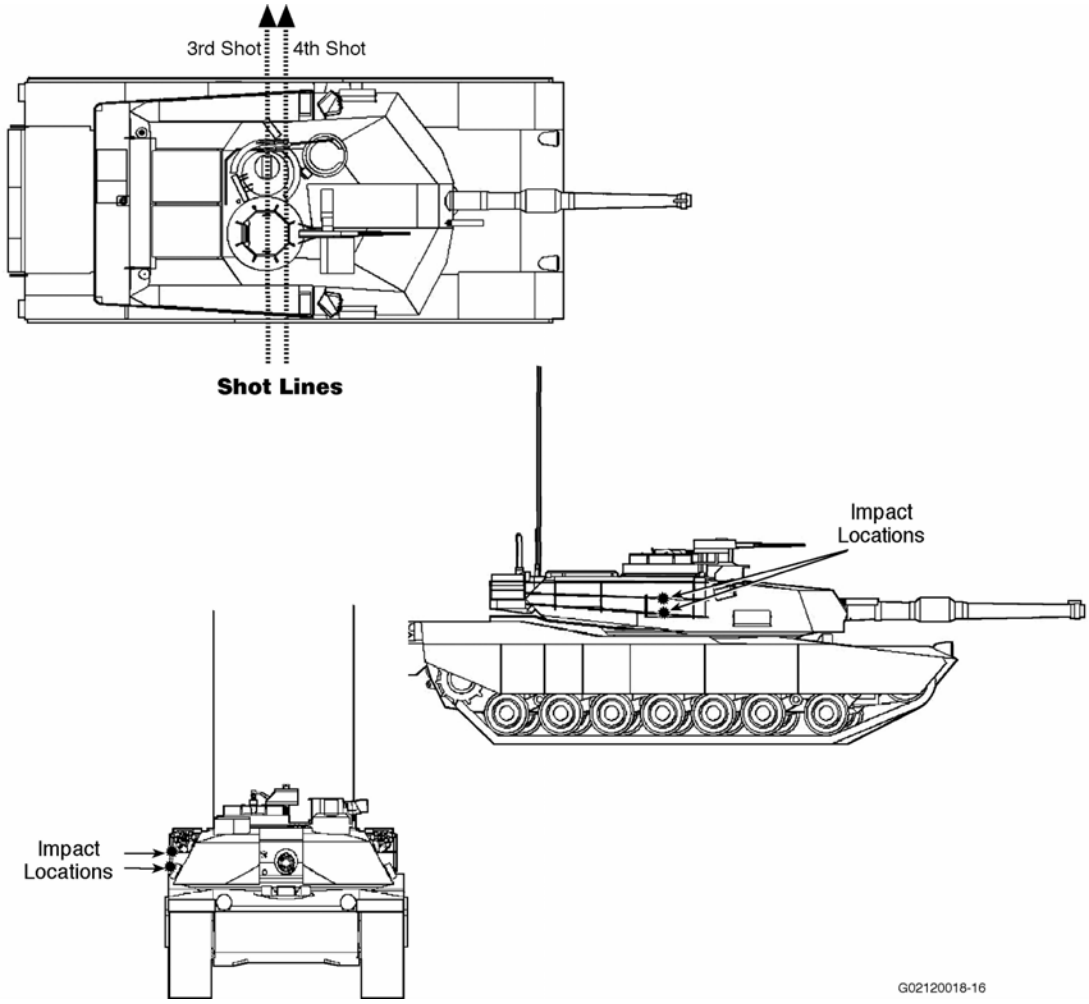

Figure 4.3. PI-3/4 Shot Lines

- Sample Array Shielding: A louvered shield was placed over the gunner's array to ensure that this sample location would intercept aerosols during both shots. Rather than orienting the louvers horizontal to the ground as in the previous shots, the shield louvers for this test were perpendicular to the floor in hopes that this orientation would provide a degree of added protection. The driver's array was unshielded and also would intercept aerosols created during both shots. The arrays at the commander's and loader's positions each were covered with a solid armor shield to be tripped only after Shot 4 had been fired. Pretests of the devices conducted that morning demonstrated that both "active" shields were functioning as designed. During the actual test, the commander's shield released as intended but was not activated until about 5 sec after the samplers were activated). Unfortunately, the loader's shield released prematurely, probably as a result of the Shot 3 impact, and was open before Shot 4 was fired. With the turret turned so that the exit hole (the most vulnerable side to fragment damage) was close to the loader's position, fragments damaged the inlets of two of the CI samplers, and at least half the IOM filters had partially disintegrated.

- Array Sample Times: The sampling times programmed for the first IOM and CI samplers were reduced slightly from the sample durations used in Shot 2. These samplers began operating 5 sec after impact and followed the time sequence presented in Table 4.3.

Table 4.3. IOM and CI Sample Collection Times for the PI-3/4 Shots

Sampling Sequence	Collection Interval (+5 sec)	Elapsed Sampling Time
1	Shot 3: 0-10 sec	10 sec
2	3-3.5 min	30 sec
3	9-10 min	1 min
4	Shot 4: 0-10 sec	10 sec
5	3-3.5 min	30 sec
6	9-10 min	1 min
7	21-23 min	2 min
8	45-49 min	4 min

- Moving Filter: The MVF was activated prior to each shot, and the sampling duration varied. To maximize the filter media available and extend the sampling to cover both shots, the existing roll was taped to a new filter roll. During the course of its movement, the tape holding the two rolls together became dislodged, thus preventing movement of the filter past the first portion of a roll, all of which were sampled before Shot 4 was fired. Twenty sample segments over 1 min of sampling were collected from this portion of the roll.

- Cyclone: A single, five-stage cyclone train with backup filters was used. The cyclone was operated at an average flow rate of 12.7 Lpm for 10 min after Shot 3 and for 1 h, 44 min after Shot 4.

Exterior Air Samples

Three remotely controlled Hi-Vol samplers were used. A non-operating fourth Hi-Vol sampler was positioned next to an operating sampler to assess impaction of particles on the filter. The sampler previously placed beneath the catch plate was eliminated. Samplers ran for 30 sec to 2 min following impact.

Deposition Trays: Eight deposition trays were used: two positioned outside, two positioned on the target, and four positioned inside the target.

Temperature and Pressure Measurements

Impulse pressure and temperature were measured in this test. A different thermocouple from the one was used in Shot 2 and was grounded to reduce noise.

4.1.3.2 Impact Observations

Following Shot 3, the loader's hatch cover quickly raised and lowered twice. The hatch came to rest just above the hatch opening, leaving a crescent shape of light streaming into the vehicle from the lights inside the fragmentation shield. Smoke was seen exiting this hatch up until the second shot was fired. Inside the vehicle, the fireflies dissipated within about a second. The thick smoke, which initially obscured the interior cameras' lenses, cleared enough so that the breech was visible within 7 min. The position of the flag taped to the loader's shield suggested that the shield had dropped prematurely. This premature opening exposed the loader's sampling array to shrapnel, high temperature, and elevated pressure from the second impact. However, because of the coverage provided by the remaining sampling arrays, including the array at the commander's position, which used the same sampling time sequence as the

loader's array, the test team decided that such a possible loss of samples was preferable to terminating the test before the second shot was fired. An x-ray taken suggests that the entire (or very nearly) penetrator exited the vehicle.

The impact of the second shot (Shot 4) again caused the loader's hatch cover to rise and fall and to finally rest again in a slightly offset position that left a crescent-shaped opening. Smoke appeared to exit from the gunner's primary sight (GPS) slot (in which the GPS had been removed) and from the loader's hatch, although the dust in the air within the fragmentation shield from the combination of the two shots made it difficult to confirm this observation. Inside the crew compartment, the fireflies that were produced during perforation were visible for a short time—approximately 1 sec after the first shot and 0.8 sec after the second impact. One relatively large piece of debris was observed on video being propelled in the direction of the shot line. The item was not identified but is believed to be a patch from a previous shot. The crew compartment cleared somewhat within 12 min after the second shot. The shield protecting the commander's array functioned as designed, dropping away when power to the electromagnet closure was deliberately turned off after the second impact.

4.1.3.3 Recovery Observations

Upon opening the Superbox door, it was observed that the floor was covered with a large amount of grayish dust that had to be swept away before entering the structure to open the fragmentation shield. The dust also was visible on surfaces inside the fragmentation shield. The appearance of the holes in the aluminum plate facing the steel catch plate, resulting from the impacts of penetrator fragments, was noteworthy. The residual penetrator material exiting the vehicle tumbled and slapped the aluminum sheet at an angle, leaving elongated openings. The light color of dust on the floor is thought to have resulted from the high concentration of aluminum (from the catch plate) in the aerosol. This action may have created more external aerosols of uranium oxide and aluminum oxide than would normally have occurred.

- Interior Air Samplers: The inlets of the loader's position CIs (#5 and #9) were visibly damaged, one severely. Loader's position IOM filters 1 and 7 were missing, and filters 2, 4, 5, and 9 appeared to have sustained damage. All commander's position samplers and filters appeared to be in good condition. Of the gunner's position samplers, all CI samplers were in good condition, but several of the IOM samplers sustained damage. Sampler 2 had holes; filter 3 appeared to have bubbled; and the sampling head of filter 5 had broken off and detached from the array. All driver's position samplers were in good condition.

- Exterior Air Samplers: Samplers ran as intended. Lighter filter loading than on previous shots was noted. Rotameter responses, however, were still much lower than pre-shot flow rates. The filter blank appeared to be clean.

- Deposition Trays: Deposition tray B, which had been placed on the turret prior to the shots, was found upside down on the floor of the impact side.

4.1.4 Phase I, Shot 5 (PI-5) Test

The PI-5 test occurred at 1218 h on 10 January 2001. The target was in the traverse position (gun facing rearward), and the LC-DU penetrator impacted the right side of the turret (i.e., the commander's side). This shot was the first of two shots designed to impact the breech in what is viewed as a "worst case" for

production of DU aerosols from DU penetrator impacts on non-DU targets. The shot line is diagrammed in Figure 4.4. The penetrator was expected to either completely erode or be retained by the breech. The penetrator impacted the gun breech and traversed it. More robust hatch closures were used to reduce the chance that the hatches would open as a result of internal pressures.

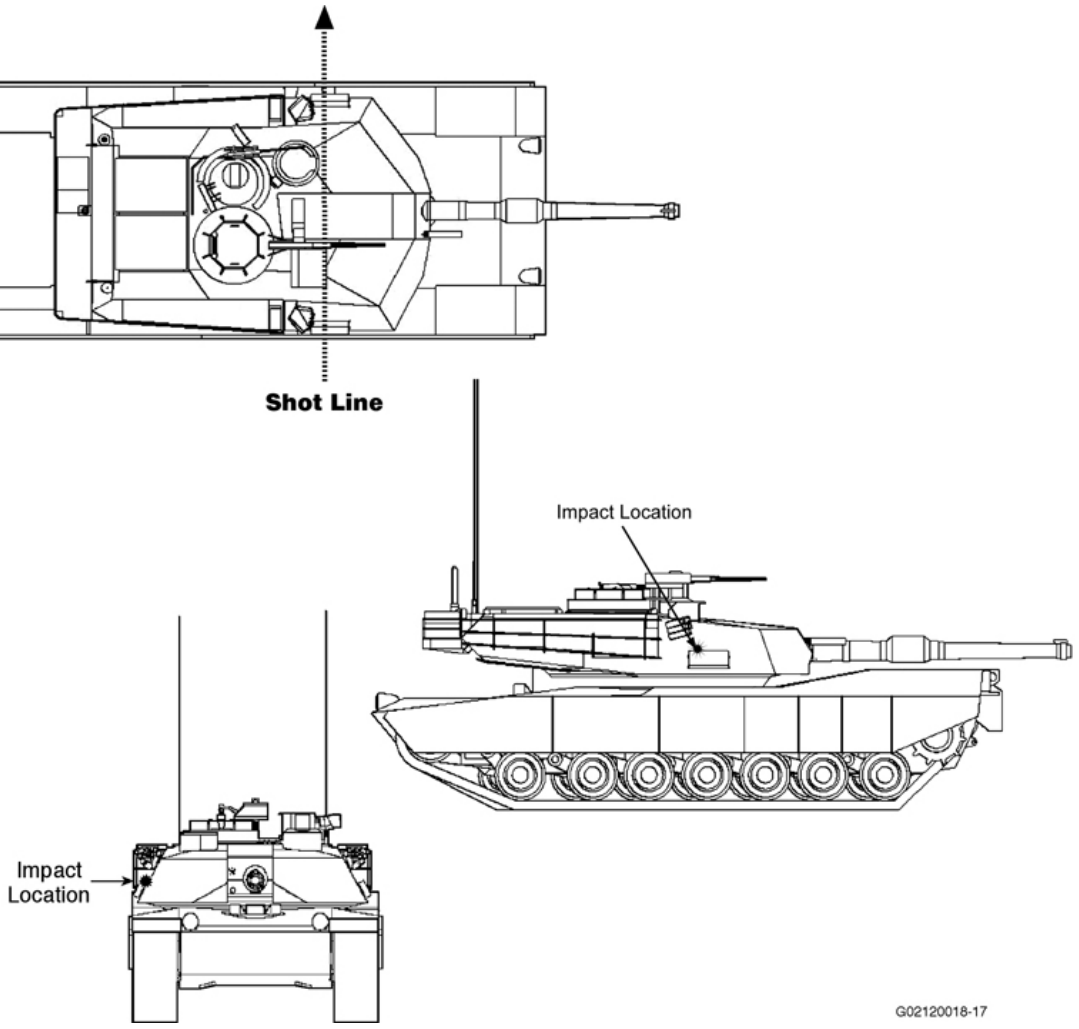

Figure 4.4. PI-5 Shot Line

4.1.4.1 Air Sampling

Shot-specific information regarding the interior and exterior samplers includes the following:

Interior Air Samples

- IOM Filter Medium: Zefluor with PTFE membrane with support
- Sample Array Shielding: Solid shields were placed over the sampler arrays located in the commander's and loader's positions. More robust solenoids were installed than were used previously. These solenoids operated as intended. Because of its close proximity to the breech shot and the probability of damage, the sampler array in the gunner's position was excluded from this

test. The sampler array located in the driver's position was not shielded. Fragments penetrated the vacuum/electric lines of some of the driver's position samples.

- Array Sample Times: Post-impact sampling times were reduced because of the increase in aerosol formation expected as a result of more penetrator erosion and the mass of breech impacted/traversed. The ninth IOM and CI at the loader's station were run for 4 min to collect aerosol levels after the Superbox ventilation system was restarted and particle levels in the fragmentation shield dropped sufficiently to allow re-entry. The IOM and CI samplers began operating 5 sec after impact and followed the time sequence presented in Table 4.4.

Table 4.4. IOM and CI Sample Collection Times for the PI-5 Shot

Sampling Sequence	Collection Interval (+5 sec)	Elapsed Sampling Time
1	0-10 sec	10 sec
2	1-1 min 10 sec	10 sec
3	3-3 min 10 sec	10 sec
4	7-7.5 min	30 sec
5	15-16 min	1 min
6	31-33 min	2 min
7	61-65 min	4 min
8	121-129 min	8 min

- Moving Filter: The suction line for the MVF and cyclone was hit by fragments and did not pull a vacuum.

- Cyclone: The suction line for the cyclone was hit by fragments and did not pull a vacuum.

Exterior Air Samples

Hi-Vol air samplers collected a 1-h baseline total dust sample within the Superbox fragmentation shield. Two were used for post-impact sample collection. For the first time in the test series, two Andersen CI samplers were available to collect post-impact samples. These samplers provide a measure of the exterior particle size distribution. The two sets of Hi-Vol samplers and CIs were set up on two poles with the Hi-Vol sampler above the impactor. The CIs ran for a time period intended to allow for collection of sufficient material for an accurate analysis without skewing the perceived particle size distribution toward smaller particle sizes. One set of samplers (CI and Hi-Vol) was located in front and to the right of the impact point. The filters faced roughly a 45° angle to the catch plate to lessen the possibility of damage to the filters from fragments formed at the time of impact. The other set of samplers was located along the right side of the vehicle near the gun barrel (i.e., the side nearer to the catch plate) and faced the catch plate. Tubing and electrical cords were protected with steel angle irons. The Hi-Vol and CI samplers were operated in tandem, as follows:

- Two Hi-Vol air samplers were remotely operated for 2 min beginning 10 sec after penetrator impact.
- Two Andersen CI samplers (remotely operated)
  - Flow rate: ~28 Lpm
  - Media: 81-mm-diameter MCE

– Sampling time: 2 min beginning 10 sec after penetrator impact. At the time of impact, a fragment sliced the Sampler-2 vacuum line.

Deposition Trays: Eight deposition trays were used: two positioned outside the target, two positioned on the target, and four positioned inside the target.

Temperature and Pressure Measurements

One pressure-measuring device was installed in the roof of the vehicle, and two thermisters were installed inside the turret.

4.1.4.2 Impact Observations

In spite of efforts to reduce the possibility that the hatches would open from the impact, the commander's hatch opened and remained open after impact. A chimney effect of smoke rising from the hatch was visible. The loader's hatch cover also opened and then fell slightly offset leaving a crescent-shaped opening. The majority of interior fireflies burned out within 1 sec. All interior lighting was lost because of the impact. About a minute after impact, there was sufficient clearing to see some light through the loader's hatch opening.

Recovery Observations

Much less dust was present on the fragmentation shield floor than was noted in previous tests.

A small portion of the penetrator broke off and burned in place, producing a small "cone" assumed to be DU oxide directly below the exit point inside the turret. Several other fragments were later found outside the vehicle but within the fragmentation shield. One was approximately 3.8 cm in length. The other two were irregular in shape and about 2.5 cm long.

- Interior Air Samples: Fragments that ricocheted or otherwise hit the power or vacuum lines damaged several samplers located in the driver's compartment. IOM filters 7 and 9 had separated from their supports, and the inlet collar of Impactor 7 had a hole through it. The filters were not damaged.

- A metal fragment hit the intake opening for the MVF. The filter itself was intact, but the suction hose was severed, thus preventing sample collection. Metal fragments also cut the cyclone lines.

- External Air Samplers: A metal fragment cut the vacuum line to the Andersen CI sampler #2 just below the impactor, and DU was embedded in the base in spite of extensive shielding around the sampler. As a result, that sampler did not operate.

- Deposition Trays: The gunner's and driver's position trays were upside down. Exterior deposition tray B, which had been placed on the vehicle, was found upside down and displaced from its original position.

4.1.5 Phase I, Shot 6 (PI-6) Test

The PI-6 test occurred at 1150 h on 24 January 2001. Shot 6 was a mirror image of Shot 5; that is, the target was in the combat position (gun facing forward), but the penetrator impacted the loader's (left) side of the turret rather than the commander's (right) side as in Shot 5. The penetrator was expected to interact with the breech about 10 to 15 cm forward (toward the gun) of the first shot and to completely erode or be retained in the breech. The shot line is diagrammed in Figure 4.5.

This test added the element of particle resuspension caused by sample recovery activities. The array at the loader's position was programmed for sample collection during the recovery phase. This aerosol evaluation was intended to simulate aerosols suspended during activities by battlefield first responders arriving on the scene to remove injured personnel and assess damage to equipment.

By this time in the test sequence, the interior of the turret was extensively pock-marked from fragmentation in previous shots. This condition complicated wipe sampling undertaken to collect removable particulates after the shot.

4.1.5.1 Air Sampling

Shot-specific information regarding the interior and exterior samplers includes the following:

Interior Air Samples

- IOM Filter Medium: Zefluor with PTFE membrane with support

- Sample Array Shielding: A louver shield was placed over the driver's array to protect the samplers. The electrical and vacuum lines also were more completely shielded. Solid shields were placed over the sampler arrays located at the commander's and loader's positions. The commander's array shield operated as intended. To provide information for resuspension analysis, the loader's array shield was opened manually 20 min before actual vehicle re-entry.

- Array Sample Times: Post-impact sampling times were the same as those used in Shot 5, again because of the increased aerosol formation expected as a result of more penetrator erosion and the mass of breech impacted/traversed. The IOM and CI samplers began operating 5 sec after impact and followed the time sequence presented in Table 4.5.

Table 4.5. IOM and CI Sample Collection Times for the PI-6 Shot

Sampling Sequence	Collection Interval (+5 sec)	Elapsed Sampling Time
1	0-10 sec	10 sec
2	1-1 min 10 sec	10 sec
3	3-3 min 10 sec	10 sec
4	7-7.5 min	30 sec
5	15-16 min	1 min
6	31-33 min	2 min
7	61-65 min	4 min
8	121-129 min	8 min

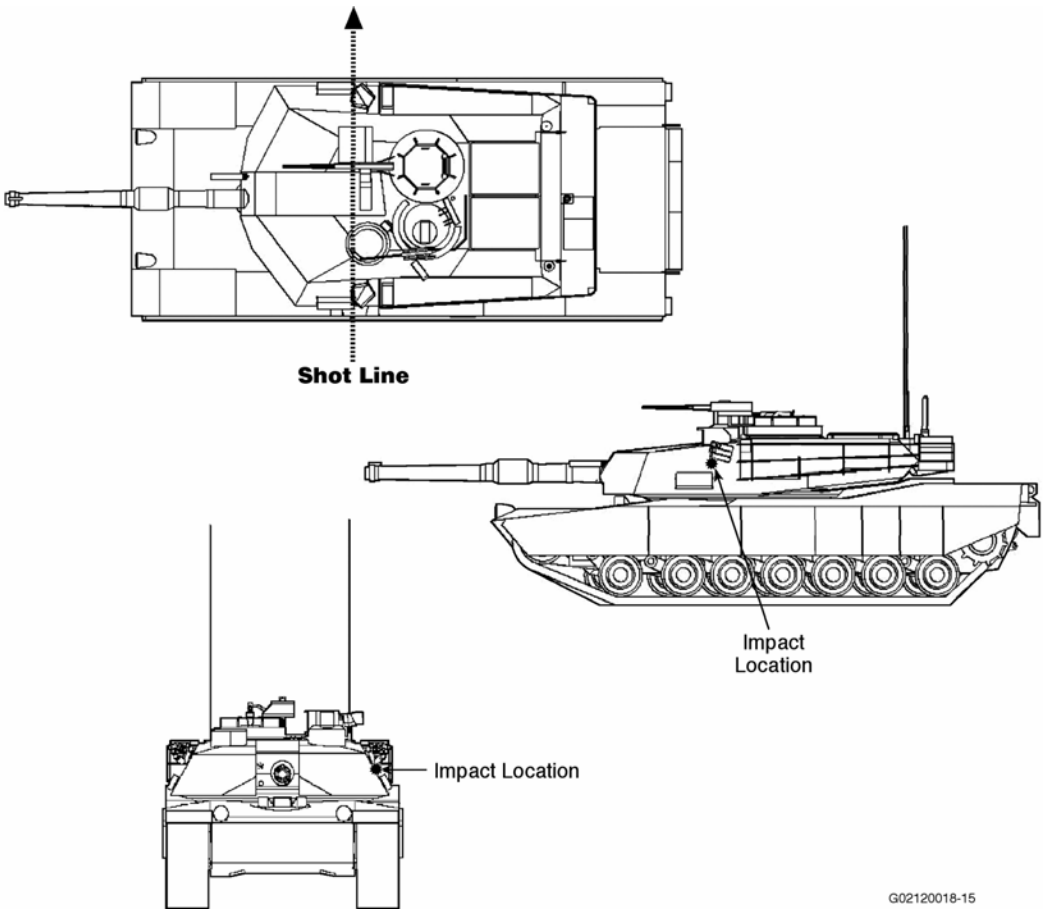

Figure 4.5. PI-6 Shot Line

- Moving Filter: The housing for the MVF and cyclone was further hardened to limit damage to electrical and vacuum lines. Unfortunately, a fragment entered the "protected" inlet line for the MVF, thus damaging the filter and preventing aerosol collection.

- Cyclone: A single five-stage cyclone train with backup filters was run at an average flow rate of 9.0 Lpm for 2 h, 9 min.

- Deposition Trays: Eight deposition trays were used: two positioned outside, two positioned on the target, and four positioned inside the target.

Exterior Air Samples

Hi-Vol air samplers were used to collect baseline measurements only. Two Andersen CI samplers located in front of the impact point on opposite sides of the target were started remotely 10 sec after impact and ran for 2 min.

Additionally, entry personnel involved in sample collection for resuspension analysis were fitted with Marple personal CI samplers that operated at 1 Lpm.

Pressure and Temperature Measurements

One pressure-measuring device was installed in the roof of the vehicle, and two thermisters were installed inside the turret.

4.1.5.2 Impact Observations

The commander's hatch cover opened and remained open after impact. A chimney effect was visible. The loader's hatch cover popped open and remained slightly open. Smoke that was initially visible rising from the vehicle ceased within 8 min. Fireflies within the field-of-view burned out in about 1 sec. Lights inside the turret were protected with Lexan shielding, but only one of the six lights survived the impact; therefore, only low light was available to view the clearing within the turret. The outline of the breech became visible within about 5 min of impact, and visibility further cleared within the next 6 min.

A portion of the penetrator exited the target and struck the aluminum plate and catch plate, leaving a divot in the catch plate.

4.1.5.3 Resuspension Activities

Rather than sample post-impact aerosols, the loader's array remained shielded and unused until vehicle recovery activities were initiated. As soon as the loader's hatch was opened, the loader's shield was manually released, and the first set of IOMs and CIs was activated to measure resuspension as recovery activities commenced. The next sampling sets followed in timed- or activity-related sequences.

After the air monitors indicated that the particulate level within the fragmentation shield was low enough to enter, the loader's hatch was opened and the loader's shield was dropped. Samplers operated sequentially for these activities.

- A 20-min baseline aerosol sample was taken using the first set of samplers before personnel entry/recovery activities began. This was followed by an 11-min interval during which no activities were conducted and no sample was collected.

- The second set of samplers operated for the next 22:39 min (min:sec) during the course of a contamination survey.

- The third sampler set operated for 13:17 min during a photographic survey.

- The fourth sampler set operated for 14:43 min during initial sampler retrieval.

- The fifth sampler set operated for 21:40 min as sampler retrieval continued.

- Following a 1:44 min interval during which no samplers operated, sampler sets 6 through 9 operated after activities in the turret were completed. The sampling periods for these samplers were 2, 4, 8, and 16 min, respectively. Sampling ended 4:50 min post-impact.

4.1.5.4 Recovery Observations

All filter samples appeared to be intact following their removal from the target. Unfortunately, a fragment entered the inlet line for the MVF, thereby damaging the filter and preventing aerosol collection.

Tray A was found upside down and displaced from its initial location. The tray in the loader's position also was found upside down. All other trays were found in their original positions. Post-shot flow rates on the CIs were about half of their pre-shot flow rates.

4.1.6 Phase I, Shot 7 (PI-7) Test

The PI-7 test occurred at 1136 h on 1 February 2001. The target was in the combat position and rested on cribbing that elevated it approximately 1 m off the fragmentation shield floor. The shot line is diagrammed in Figure 4.6. The penetrator impacted the right (loader's) side of the hull, perforated the armor protecting the tracks, pierced the hull armor into the turret basket, and exited the right side of the hull where it shattered the aluminum witness plate and was stopped by the catch plate. A resuspension exercise evaluated aerosols suspended by recovery activities.

4.1.6.1 Air Sampling

Shot-specific information regarding the interior and exterior samplers includes the following:

Interior Air Samples

- IOM Filter Medium: Zefluor PTFE membrane with support

- Sample Array Shielding: The solid shields covering the commander's, loader's, and gunner's positions all operated as intended. The loader's array was activated for resuspension sampling only. A louvered shield protected the driver's array. However, these precautions were not successful in preventing the extensive aluminum plate fragmentation that damaged some of the sampler electrical lines.

- Array Sample Times: Post-impact sampling times for the sampler arrays at the commander's, loader's, and driver's positions again were reduced, but samplers 3 through 7 ran slightly longer than they did during Shots 5 and 6. Because of damage sustained to the feedback wires, second-by-second pressure drop data were not available for this shot. Pre- and post-shot measurements were conducted, and the results were averaged over the sampling duration. The sampler array at the loader's position, which was used to take resuspension samples only, was started a little over 3 h after impact and was operated for 70 min. The IOM and CI samplers began operating 5 sec after impact and followed the time sequence presented in Table 4.6.

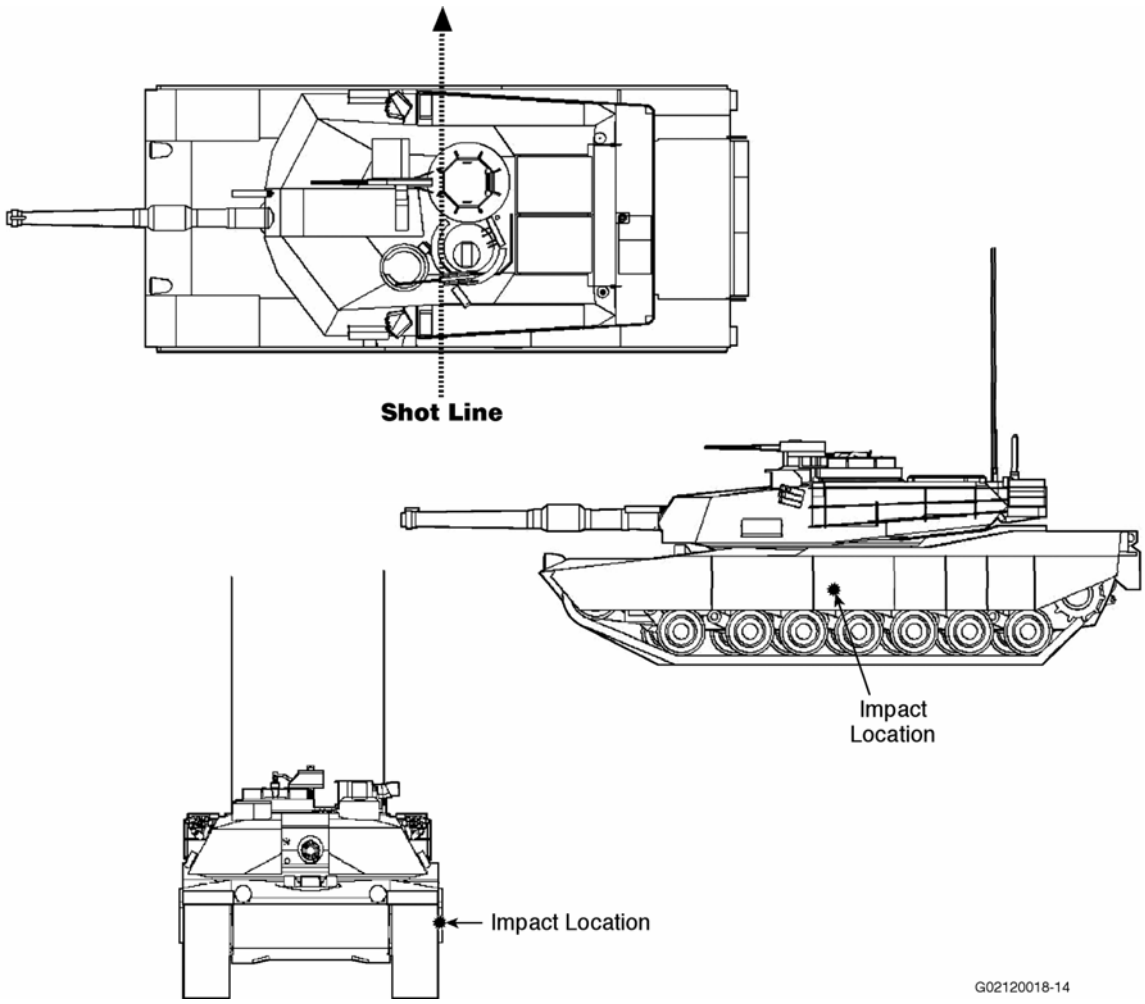

Figure 4.6. PI-7 Shot Line (hull shot)

Table 4.6. IOM and CI Sample Collection Times for the PI-7 Shot

Sampling Sequence	Collection Interval (+5 sec)	Elapsed Sampling Time
1	0-10 sec	10 sec
2	1-1 min, 10 sec	10 sec
3	3-3 min, 15 sec	15 sec
4	7-8 min	1 min
5	Did not run	2 min
6	31-35 min	4 min
7	61-69 min	8 min
8	121-129 min	8 min

- Moving Filter: The MVF did not run because fragments from the aluminum plate severed its electrical lines.

- Cyclone: A single 5-stage cyclone train with backup filters ran for 2 h, 9 min at an average flow rate of 11.5 Lpm.

Exterior Air Samples

Hi-Vol air samplers were used to collect baseline measurements only. Two Andersen CI samplers located in front of the impact point on opposite sides of the target were started remotely 10 sec after impact and ran for 1 min to reduce filter loading.

Additionally, entry personnel involved in sample collection for re-suspension analysis were fitted with Marple personal CI samplers that operated at 1 Lpm.

Deposition Trays: Eight deposition trays were used: two positioned outside, two positioned on the target, and four positioned inside the target.

Pressure and Temperature Measurements

A pressure sensor and thermisters were installed in the turret, but technical problems interfered with data collection. Therefore, limited pressure and temperature data are available for this shot.

4.1.6.2 Impact Observations

The latch released on the commander's hatch cover, but the cover did not open more than about an inch. The loader's hatch had been secured with wedges and remained closed. Smoke was visible around the commander's hatch and from around the gun shield by the barrel. The majority of the fireflies appeared to burn out in about 1 sec. In about 7 min, the outline of the breech was visible. Four minutes later, the air had cleared sufficiently to see the breech.

Upon entry into the Superbox, a layer of gray dust was observed on the floor, and the floor of the fragmentation shield was covered with dust and debris. The penetrator pierced the aluminum witness plate, and then hit the catch plate at an angle and bent. In bending, the penetrator catastrophically shattered the aluminum plate and created numerous shards. One or more of the aluminum shards penetrated five gray bundles of control cables used to operate the samplers. Therefore, real-time feedback of pressures from the samplers at the commander's, gunner's, and driver's positions was lost, and it was not until recovery operations were well underway that the test team learned that electricity had been maintained to most samplers, so aerosols were collected.

4.1.6.3 Resuspension Activities

After the air monitors indicated that the particulate level within the fragmentation shield was low enough to allow entry, the loader's hatch was opened, the loader's array shield was dropped, and the hatch was closed. Samplers operated sequentially but overlapped during these activities. Two sampler sets each ran for about 20 min, during which time photography, wipe surveys, and initial sampler retrieval activities were conducted and recovery personnel exited. A fourth sampler set ran for approximately 10 min after the recovery personnel exited and no one was present. Sampling was terminated at this point so that damage to the other turret arrays could be evaluated without further delay.

4.1.6.4 Recovery Observations

Before removing any samplers, pressure drops through each sampler within the commander's and gunner's sampling arrays were measured. Post-test flow rates in the arrays located at the driver's position

were evaluated later in the laboratory. All samplers believed to have run during the test appeared to have collected some residue except for IOM number 6 at the driver's position. Large particles were visible on several of the IOMs and CIs.

Deposition tray A was found upside down and to the rear of the tank. All other deposition trays remained upright and in their original locations.

The post-test flow rate of the CI located to the left of the impact point was much lower than its pre-test flow rate. It was noted later that there appeared to be a small cut in its vacuum line. The CI located to the right of the impact point had similar pre- and post-test flow rates.

4.1.7 Summary of Phase-I Sample Collection Times

Table 4.7 lists the sampling time sequence during the Phase-I shots for the IOM and CI sampler arrays. The sampling times for the MVF are listed in Table 4.8, and the cyclone sampler collection times are listed in Table 4.9.

Table 4.7. Array Sample Collection Times for Phase-I Shots

Time Sequence Sample Set	Time ON Post Shot (+5 sec) (hh:mm:ss)	Time OFF Post Shot (+5 sec) (hh:mm:ss)	Sample Duration
Shot 1	Samples taken from commander's, driver's, gunner's, and loader's positions.		
1	00:00:00	00:00:30	30 sec
2	00:00:30	00:01:30	1 min
3	00:01:30	00:03:30	2 min
4	00:03:30	00:07:30	4 min
5	00:07:30	00:15:30	8 min
6	00:15:30	00:31:30	16 min
7	00:31:30	01:03:30	32 min
8	01:03:30	02:07:30	64 min
9	Field Blank		
Shot 2	Samples taken from commander's, driver's, gunner's, and loader's positions.		
1	00:00:00	00:00:15	15 sec
2	00:00:30	00:01:00	30 sec
3	00:01:30	00:02:30	1 min
4	00:03:30	00:05:30	2 min
5	00:07:30	00:11:30	4 min
6	00:15:30	00:31:30	16 min
7	00:31:30	01:19:30	48 min
8	01:19:30	02:07:30	48 min
9	Field Blank		

Table 4.7. (contd)

Time Sequence Sample Set	Time ON Post Shot (+5 sec) (hh:mm:ss)	Time OFF Post Shot (+5 sec) (hh:mm:ss)	Sample Duration
Shot 3	Samples taken from driver's and gunner's positions.		
1	00:00:00	00:00:10	10 sec
2	00:03:00	00:03:30	30 sec
3	00:09:00	00:10:00	1 min
Shot 4	Samples taken from commander's, driver's, gunner's, and loader's positions.		
4	00:00:00	00:00:10	10 sec
5	00:03:00	00:03:30	30 sec
6	00:09:00	00:10:00	1 min
7	00:21:00	00:23:00	2 min
8	00:45:00	00:49:00	4 min
9	01:33:00	01:41:00	8 min
Shot 5	Samples taken from commander's, driver's, and loader's positions (gunner's array removed).		
1	00:00:00	00:00:10	10 sec
2	00:01:00	00:01:10	10 sec
3	00:03:00	00:03:10	10 sec
4	00:07:00	00:07:30	30 sec
5	00:15:00	00:16:00	1 min
6	00:31:00	00:33:00	2 min
7	01:01:00	01:05:00	4 min
8	02:01:00	02:09:00	8 min
9	02:24:00 (Loader only)	02:28:00 (Loader only)	4 min
Shot 6	Samples taken from commander's and driver's positions (gunner's array removed).		
1	00:00:00	00:00:10	10 sec
2	00:01:00	00:01:10	10 sec
3	00:03:00	00:03:10	10 sec
4	00:07:00	00:07:30	30 sec
5	00:15:00	00:16:00	1 min
6	00:31:00	00:33:00	2 min
7	01:01:00	01:05:00	4 min
8	02:01:00	02:09:00	8 min
9	Field Blank		
Shot 6	Re-suspension samples taken from loader's position (started 3 h, 35 min post shot).		
1	2:35:00	02:55:00	20 min
No sample taken	2:55:05	3:06:05	(11 min)
2	3:06:06	3:28:45	~23 min
3	3:28:46	3:42:03	~13 min
4	3:42:04	3:56:47	~15 min
5	3:56:48	4:18:28	~22 min
No sample taken	4:18:29	4:20:13	(1:44 min)
6	4:20:14	4:22:13	2 min
7	4:22:14	4:26:13	4 min
8	4:26:14	4:34:13	8 min
9	4:34:14	4:50:13	16 min

Table 4.7. (cont'd)

Time Sequence Sample Set	Time ON Post Shot (+5 sec) (hh:mm:ss)	Time OFF Post Shot (+5 sec) (hh:mm:ss)	Sample Duration
Shot 7	Samples taken from commander's, driver's, and gunner's positions.		
1	00:00:00	00:00:10	10 sec
2	00:01:00	00:01:10	10 sec
3	00:03:00	00:03:15	15 sec
4	00:07:00	00:08:00	1 min
5	00:15:00	00:17:00	2 min
6	00:31:00	00:35:00	4 min
7	01:01:00	01:09:00	8 min
8	02:01:00	02:09:00	8 min
9	Field Blank		
Shot 7	Re-suspension samples taken from loader's position (started ~3 h, 11 min post shot).		
1	03:11:00	03:31:00	20 min
2	03:31:00	03:51:00	20 min
3	03:51:00	04:11:00	20 min
4	04:11:00	04:21:00	9 min, 40 sec

Table 4.8. Moving Filter Sample Collection Times for Phase-I Shots

MVF (time point)	Time ON Post Shot (hh:mm:ss)	Time OFF Post Shot (hh:mm:ss)	Sample Duration[(a)]
Shot 1	Partial sample collected.		
1	00:00:00	00:00:05	5 sec (stationary)
2	00:00:05	00:00:15	10 sec (moving)
3	00:00:15	00:00:30	10 sec (stationary)
4	00:00:30	00:00:50	20 sec (moving)
5	00:00:50	00:01:10	20 sec (stationary)
6	00:01:10	00:01:30	20 sec (moving)
7	00:01:30	00:02:10	40 sec (stationary)
8	00:02:10	00:02:50	40 sec (moving-uncertain)
9	00:02:50	00:03:30	40 sec (stationary, heavily caked)
10	00:03:30	00:04:50	1 min, 20 sec (smeared-uncertain)
11	00:04:50	00:06:10	1 min, 20 sec (smeared-uncertain)
12	00:06:10	00:07:30	1 min, 20 sec (smeared-uncertain)
13	00:07:30	00:10:10	2 min, 40 sec (smeared-uncertain)
14	00:10:10	00:12:50	2 min, 40 sec (smeared-uncertain)
15	00:12:50	00:15:30	2 min, 40 sec (stationary, stuck)
16	00:15:30	00:20:50	b
17	00:20:50	00:26:10	b
18	00:26:10	00:31:30	b
19	00:31:30	00:42:10	b
20	00:42:10	00:52:50	b
21	00:52:50	01:03:30	b
22	01:03:30	01:24:50	b
23	01:24:50	01:46:10	b
24	01:46:10	02:07:30	b
Shot 2	Appropriate filter media not available, so moving filter was not used for Shot 2		

Table 4.8 (cont'd)

MVF(time point)	Time ON Post Shot (hh:mm:ss)	Time OFF Post Shot (hh:mm:ss)	Sample Duration[(a)]
Shot 3	Shot 3 preceded Shot 4 by approximately 13 min		
1	00:00:00	00:56:10	1 min, continuous
Shot 4	Shot 4 was fired approximately 13 min after Shot 3		
1	00:00:00	00:10:00	Did not run
Shot 5	Fragment cut lines, moving filter did not run		
Shot 6	Fragment entered inlet and severed filter, moving filter did not run		
Shot 7	Aluminum shard severed electrical line, moving filter did not run		

(a) Sample duration estimated by planned timing and photographic record.
(b) Filter apparently stuck in #10 position and did not move further. Final sampling increment and total collection time uncertain.

Table 4.9. Cyclone Sampler Collection Times for Phase-I Shots

Cyclone	Time ON Post Shot (+ 5 sec) (hh:mm:ss)	Time OFF Post Shot (hh:mm:ss)	Sample Duration
Shot 1	PFDB attached to cyclone, flow rate up to 31.4 Lpm		
1	00:00:00	02:08:00	2 h, 8 min
Shot 2	PFDB replaced with backup filters, flow rate 9.9 Lpm		
1	00:00:00	02:08:00	2 h, 8 min
Shot 3	Single 5-stage cyclone with backup filters, flow rate 12.7 Lpm		
1	00:00:00	00:10:00	10 min
Shot 4	Single 5-stage cyclone with backup filters, flow rate 12.7 Lpm		
1	00:00:00	01:44:00	1 h, 44 min
Shot 5	Fragment cut lines—cyclone did not run		
1[(a)]	00:00:00	02:09:00	2 h, 9 min
Shot 6	Single 5-stage cyclone with backup filters, flow rate ~9.0 Lpm		
1	00:00:00	02:09:00	2 h, 9 min
Shot 7	Single 5-stage cyclone with backup filters, flow rate ~11.5 Lpm		
1	00:00:00	02:09:00	2 h, 9 min

(a) Suction line penetrated by fragments so there was no flow through the cyclone.

4.2 Phase-II Test Parameters

Phase-II tests included two crossing shots, conducted as a single event, through the passenger compartment and a single shot into the turret compartment of a Bradley vehicle. The field tests were conducted at the ATC Superbox between March 14 and 22, 2001.

Common parameters for the Phase II tests are described below.

Target

A BHT version of a Bradley vehicle was used as the target in Phase-II tests. The BHT hull had not been used previously as a firing target. The turret was stripped of all unnecessary gear including all vehicle electronics and fluids and was refurbished to achieve structural integrity. Between the two events, the BHT was decontaminated, and the holes were patched to ensure structural integrity for the second test.

Interior Air Sampling Equipment

Sampling arrays were located at the driver's and commander's positions. Positions of scouts in a cavalry version or passengers in an infantry version of the vehicle vary depending on the configuration of seats in the particular vehicle. Because the actual crew seating is not absolute, the remaining two sampling positions were selected to best meet testing requirements, including probable survivability and also approximation of the breathing zone of the passengers in the passenger/squad/transport compartment. These two scout arrays were placed flush with the inside of the back ramp. In the sample identification code, the right scout is referred to as the "gunner" position and the left scout as the "loader" position. An elaborate shield structure attached to the backside of the ramp held the arrays in place and protected the wiring and vacuum hoses. As with the Phase-I setup, each sampling array included:

- Nine, 25-mm, Institute of IOM filter cassette samplers operated at a nominal flow rate of 2 Lpm. The filter media was Zefluor (Teflon-based filters).

- Nine, 25-mm, 8-stage modified Marple CIs operated at a nominal flow rate of 2 Lpm. An MCE filter medium was used in Stages 1 through 8, with the smallest sample material collected in a PVC backup filter, which was identified as Stage 9 in the sample data.

The filter cassette and CIs were operated in pairs and were activated 5 sec after the shot was fired to minimize the possibility of damage. Sampling durations are listed by shot (Tables 4.10 and 4.11) and are summarized in Table 4.12 (see page 4.34) at the end of Phase-II test observations.

Additionally, a MVF and a 5-stage cyclone train, each with a collection port, were placed in a protective metal box on the floor of the passenger compartment under the right scout's position. The MVF, which used AW19 as the filter medium, collected aerosol samples at a nominal flow rate of 28 Lpm and moved at a rate of 0.88 cm/sec. The MVF was included specifically to collect samples during the first 5 sec after the shot was fired because the filter cassettes and the CIs were not operated during that initial 5-sec period. The MVF also was run intermittently to intercept aerosols at certain time increments following the shot. Sampling durations are listed in Table 4.13 (see page 4.35).

The cyclone collected aerosols at a nominal flow rate of 14 Lpm. A backup filter arrangement with four parallel filters was connected to the fifth stage of the cyclone. The backup filters were made of PTFE membranes and polymethylpentene support rings.

Interior air sampling equipment was controlled remotely through the use of LabVIEW software. Flow rates for each sampler were checked after each installation. Sulfur hexafluoride (SF_6) analysis was conducted before, during, and after each shot to establish the ventilation rate within the vehicle.

Sample Array Shielding

To protect samplers from fragment damage while allowing unhindered aerosol collection following both shots, louver shields were placed over the sampling arrays located at the driver's and left scout's positions. Solid shields were placed at the commander's and right scout's positions.

Exterior Air Sampling Equipment

Exterior air sampling was conducted within the Superbox fragmentation shield. Samplers were placed in the breathing zone at select positions outside the target. Baseline air samples were collected using Hi-Vol samplers operating at a flow rate of 560 Lpm for 1 h prior to each shot. Andersen CIs with 81-mm diameter MCE filters operated at about 28 Lpm. These samplers were activated about 10 sec after impact and sampled for 2 min.

Deposition Trays

Eight deposition trays were used: two positioned on the fragmentation shield floor, two positioned on the hull, and four positioned inside the turret.

Contamination Surveys

Interior Removable Contamination

Contamination surveys were conducted as described in Phase I. Interior removable contamination was measured by smearing 47-mm-diameter Defensap wipes within a defined 100-cm^2 area. Thirty-two discrete wipes were used to collect loose material on interior vertical and horizontal surfaces. Four deposition trays were placed near each sample array. Additionally, four additional locations were evaluated to establish a correlation between removable contamination using 47-mm wipes and currently fielded Army portable radiation survey instruments.

Exterior Removable Contamination

Exterior removable contamination on the surfaces of the target and the surrounding Superbox was measured by smearing 47-mm-diameter Defensap wipes within defined 100-cm^2 areas. Thirty discrete wipes were collected on the target's horizontal and vertical surfaces (10 on the impact side, 10 on the exit side, and 10 on the top of the target). As with the interior wipes, four additional locations were evaluated for removable contamination using 47-mm wipes and currently fielded Army portable radiation instruments.

Personal Monitoring

Entry personnel who conducted contamination surveys and removed air sampling equipment were fitted with personal air samplers and cotton gloves. Each person entering the Superbox wore a 25-mm cassette filter breathing zone air sampler operated at 2 Lpm. Selected entry personnel wore a 25-mm Marple personal CI operated at 2 Lpm. These samplers were worn for the duration of the contamination survey. No effort was made during Phase II recovery to collect residue samples on cotton gloves.

Other Measurements

Temperature and RH measurements were made inside the target and within the fragmentation shield.

4.2.1 Phase II, Shots 1/2 (PII-1/2) Test

The PII-1/2 test occurred at 1310 h and 1323 h on 14 March 2001, and the two shots were fired 13 min, 41 sec apart. Targeted aim points were several inches behind the turret shroud separated vertically by about 6 in. Both shots were expected to perforate the left (driver's) side of the target and exit through the right side. The target was in combat configuration with the turret gun pointed over the engine. The riring shot lines are shown in Figure 4.7.

The commander's shield was left open to ensure that its samplers would intercept aerosols from both shots. The right scout's shield was closed for the first shot but was released 3 sec after the second shot to intercept aerosols directly created by the second shot and from resuspension of material deposited after the first shot.

The IOM and CI samplers began operating 5 sec after impact and followed the time sequence presented in Table 4.10.

Andersen CIs were activated 10 sec after the first shot and were operated for 2 min. No sampling was performed using the Andersen CIs after the second shot.

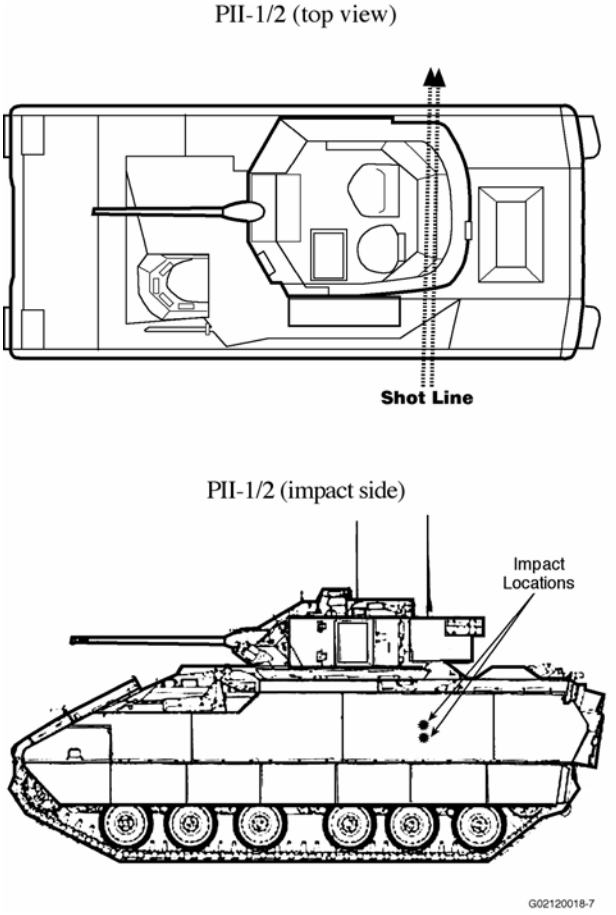

Figure 4.7. PII-1/2 Shot Lines

Table 4.10. IOM and CI Sample Collection Times for the PII-1/2 Shots

Sampling Sequence	Collection Interval (+5 sec)	Elapsed Sampling Time
1	Shot 1: 0-10 sec	10 sec
2	3-4 min	1 min
3	9-11 min	2 min
4	Shot 2: 0-10 sec	10 sec
5	3-4 min	1 min
6	9-11 min	2 min
7	21-25 min	4 min
8	45-53 min	8 min

4.2.1.1 Impact Observations

The hatches on the Bradley vehicle remained closed for both shots. However, beginning approximately 1.5 to 2 min after Shot 1 and continuing until the second shot was fired, a small plume of smoke, apparently from the 25-mm gun barrel shield, streamed out of the target on the right side near the front. Approximately 1 min after the second impact, smoke again was visible from the gun shield area and continued to be visible for at least 5 min. Material that appeared to be fibrous was observed floating in the air outside the vehicle after Shot 2.

The high-speed video showed that glowing fragments (fireflies) were visible for about a second following Shot 1, and that fibrous debris was suspended inside the vehicle. The aerosol obscured images inside the turret after the impact, and visibility did not improve significantly prior to the second shot. The turret shroud/sliding door inside the Bradley vehicle fell or was blown into the passenger compartment apparently as a result of the impact blast. Although not clear enough for certain identification, the video appeared to capture the image of a billowing, swirling dust cloud at the back of the crew compartment.

Following the second shot, the fireflies again were visible for about a second, and the fibrous debris was present. The turret shroud had been blown into the crew compartment again, and a swirling dust cloud appeared to have formed in the compartment. A flame in the upper left hand corner of the ceiling area of the back crew compartment was observed from the left scout camera. This flame was visible for about 45 sec. Some clearing in the crew area was apparent about 6.5 min after Shot 2, and though still not clear, considerable improvement was noted 43 min after the shot.

4.2.1.2 Recovery Observations

During sample recovery efforts, the extent of suspended and deposited fiber debris was unexpectedly heavy. A fiber strand had burned through the MVF media, and small amounts of fibrous material were observed on many of the sampler inlets, though it did not appear that these collections were heavy enough to significantly affect flow rates or otherwise interfere with aerosol collection. IOM samplers had gray-green residues on them. Some of them appeared to have experienced “flaking” of the collected material.

The MVF operated before the shot and sampled at this position until 5 sec after the shot. It then was supposed to advance to a new position and sample at that position for 10 sec before moving on to the next position for a 10-sec sampling period. However, a burning fiber from the spall liner burned through the filter media and prevented this sampling sequence from proceeding. The deposition tray at the loader’s position was upside down.

4.2.2 Phase II, Shot 3 (PII-3) Test

The PII-3 test occurred on at 1204 h on 22 March 2001. The shot was fired into the turret and into the 25-mm gun feeder just left of the cannon to maximize creation of DU aerosol. The turret was positioned at 90° so the barrel would be pointed at the backstop and the penetrator would impact the rear of the turret. The target was in combat configuration with the turret gun pointed over the engine. The rear turret basket was removed so that the first resistance to the penetrator was the rear turret armor. The shot perforated the rear of the turret, passed through the receiver portion of the gun and the trunnion, and then exited the BFV. The shot line is shown in Figure 4.8.

The IOM and CI samplers began operating 5 sec after impact and followed the time sequence presented in Table 4.11.

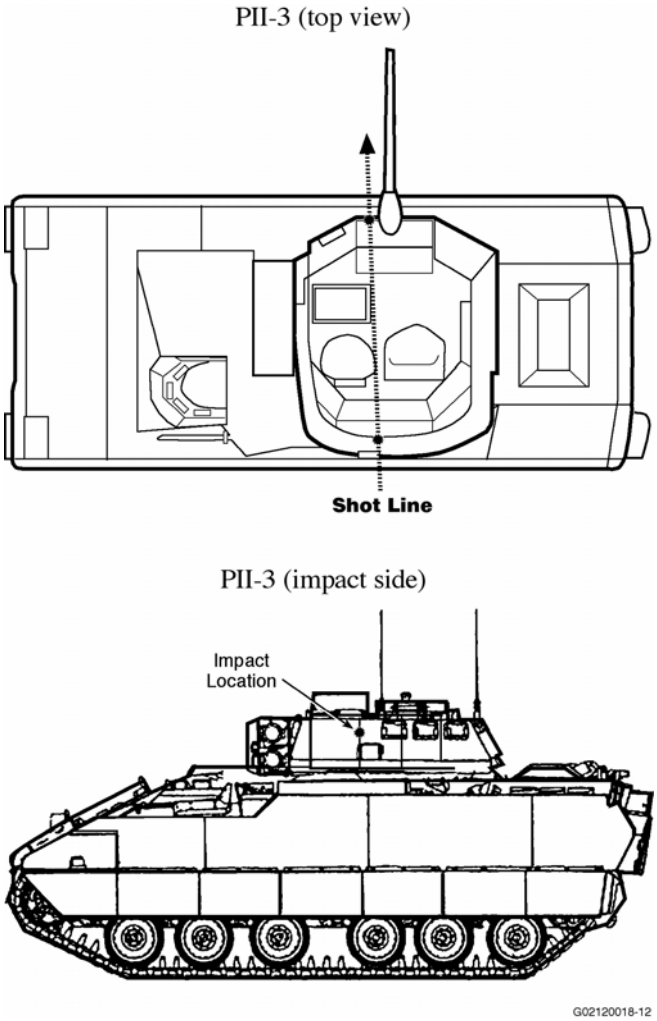

Figure 4.8. PII-3 Shot Line

Table 4.11. IOM and CI Sample Collection Times for the PII-3 Shot

Sampling Sequence	Collection Interval (+5 sec)	Elapsed Sampling Time
1	0-10 sec	10 sec
2	1-1 min, 10 sec	10 sec
3	3-3 min, 15 sec	15 sec
4	7-8 min	1 min
5	15-17 min	2 min
6	31-35 min	4 min
7	61-69 min	8 min
8	121-129 min	8 min

4.2.2.1 Impact Observations

As a result of the impact, the door to the turret shield blew back into the passenger compartment. After impact, the video images from inside the turret were obscured; however, visibility inside the passenger compartment was fairly clear within 12 min of impact. The commander's and gunner's hatches remained closed, but the TOW missile-loading hatch blew open and remained open. Some smoke was visible initially from the gun shield and perhaps from the gunner's hatch shortly after impact. Fireflies produced inside the turret were visible for about 2 sec after impact, and some fibrous material was suspended inside the back crew area. A deposition tray was observed crossing the camera's field-of-view. Within 2 min, the air had cleared considerably; however, there was little improvement over the next 23 min.

4.2.2.2 Recovery Observations

During the shot, some retaining bolts that attached the left scout louver to the rear door broke, but this damage did not appear to affect sampling. The solid shield covering the right scout array did not release as planned. The release pin twisted from the violence of the impact, thereby restricting opening of the shield to about an inch. As a result, these samplers were not expected to collect much material nor would the samples collected be representative of the aerosol concentration in the passenger compartment.

Following sampler recovery, it was noted that all IOMs appeared to have a gray-green coloration on the filters. Some filter residues showed signs of flaking or cracking.

4.2.3 Summary of Phase-II Sample Collection Times

Table 4.12 lists the sampling time sequence during the Phase-II shots for the IOM and CI sampler arrays. The sampling times for the MVF are listed in Table 4.13.

Table 4.12. Array Sample Collection Times for Phase-II Shots

Time Sequence Sample Set	Time ON Post Shot (+5 sec) (hh:mm:ss)	Time OFF Post Shot (+5 sec) (hh:mm:ss)	Sample Duration
Shot 1	Samples taken from commander's, driver's, and left scout positions		
1	00:00:00	00:00:10	10 sec
2	00:03:00	00:04:00	1 min
3	00:09:00	00:011:00	2 min

Table 4.12. (cont'd)

Shot 2	Samples taken from commander's, driver's, and right and left scout positions		
4	00:00:00	00:00:10	10 sec
5	00:03:00	00:04:00	1 min
6	00:09:00	00:11:00	2 min
7	00:21:00	00:25:00	4 min
8	00:45:00	00:58:00	8 min
9	01:33:00	01:49:00	16 min
Shot 3	Samples taken from commander's, driver's, and right and left scout positions		
1	00:00:00	00:00:10	10 sec
2	00:01:00	00:01:10	10 sec
3	00:03:00	00:03:15	15 sec
4	00:07:00	00:08:00	1 min
5	00:15:00	00:17:00	2 min
6	00:31:00	00:35:00	4 min
7	01:01:00	01:09:00	8 min
8	02:01:00	02:09:00	8 min
9	Field Blank		

Table 4.13. Moving Filter Sample Collection Times for Phase-II Shots

MVF (time point)	**Time ON Post Shot (hh:mm:ss)**	**Time OFF Post Shot (hh:mm:ss)**	**Sample Duration**
Shot 1/2	Fragment entered inlet and severed filter, MVF did not run		
Shot 3			
1	00:00:00	00:03:30	3 min, 30 sec
2	00:07:00	00:07:30	30 sec
3	00:15:00	00:15:30	30 sec
4	00:31:00	00:31:30	30 sec
5	01:01:00	01:01:30	30 sec
6	02:01:00	02:01:30	30 sec

4.3 Phase-III Test Parameters

The Phase-III firing tests included two shots into the front heavy armor of the Abrams BHT. The target was in combat position with the turret angled so the penetrator would impact the left front panel. The penetrator was expected to hit the breech and was not expected to exit the vehicle. The tests were conducted between 14 February and 22 February 2001.

The commander's hatch had been removed and replaced with a welded metal cover. The loader's hatch was secured to prevent it from opening.

Common parameters for the Phase-III tests are described below.

Target

A BHT version of an Abrams tank was used as the target in Phase-III tests. The hull used in Phase-I shots was reused in Phase III. All holes from previous shots were patched to ensure structural integrity

for the Phase-III tests. A turret that had not been fired upon replaced the turret used in Phase I. The standard armor package was replaced with a heavy armor package.

Interior Air Sampling Equipment

Sampling arrays were floor level near the driver's, commander's, and loader's position, and at the gunner's positions. Each sampling array included:

- Nine, 25-mm, IOM filter cassette samplers with Zefluor (Teflon-based) filters operated at a nominal flow rate of 2 Lpm.

- Nine, 25-mm, 8-stage modified Marple CIs operated at a nominal flow rate of 2 Lpm. An MCE filter substrate was used in Stages 1 through 8, with the smallest sample material collected in a PVC backup filter, which was identified as Stage 9 in the sample data.

The filter cassette and CIs were operated in pairs and were activated 5 sec after the shot was fired to minimize the possibility of damage. Sampling durations are listed by shot (Tables 4.14 and 4.15) and are summarized in Table 4.16 (see page 4.41) at the end of Phase-III test observations.

Table 4.14. IOM and CI Sample Collection Times for the PIII-1 Shot

Sampling Sequence	Collection Interval (+5 sec)	Elapsed Sampling Time
1	0-10 sec	10 sec
2	1-1 min, 10 sec	10 sec
3	3-3 min, 15 sec	15 sec
4	7-8 min	1 min
5	15-17 min	2 min
6	31-35 min	4 min
7	61-69 min	8 min
8	121-129 min	8 min

Table 4.15. IOM and CI Sample Collection Times for the PIII-2 Shot

Sampling Sequence	Collection Interval (+5 sec)	Elapsed Sampling Time
1	0-10 sec	10 sec
2	1-1 min, 10 sec	10 sec
3	3-3 min, 15 sec	15 sec
4	7-8 min	1 min
5	15-17 min	2 min
6	31-35 min	4 min
7	61-69 min	8 min
8	121-129 min	8 min

Additionally, an MVF and a five-stage cyclone train, each with a collection port, were placed in a protective metal box on the floor of the turret. The MVF, which used AW19 as the filter medium, collected aerosols at a nominal flow rate of 28 Lpm and moved at a rate of 0.88 cm/sec. The MVF was included in the array specifically to collect samples during the first 5 sec after the shot was fired because the filter cassettes and the samplers were not operated during that initial 5-sec period. The MVF also was

run intermittently to collect aerosols at certain time increments following the shot. See Table 4.17 (page 4.42) for the MVF sampling times for Phase-III shots.

The cyclone collected aerosols at a nominal flow rate of 14 Lpm. A backup filter arrangement with four parallel filters was connected to the fifth stage of the cyclone. The backup filters were made of PTFE membranes and polymethylpentene support rings.

Interior air sampling equipment was controlled remotely through the use of LabVIEW software. Flow rates for each sampler were checked after each installation. Sulfur hexafluoride (SF_6) analysis was conducted before, during, and after each shot to establish the ventilation rates within the vehicle.

Sample Array Shielding

Solid shields covered the arrays at the loader's, commander's, and gunner's positions. A louvered shield covered the driver's array. Solid shields were released 3 sec after impact.

Exterior Air Sampling Equipment

Exterior air sampling was conducted within the Superbox fragmentation shield using samplers placed in the breathing zone at select positions outside the target. Baseline air samples were collected using Hi-Vol samplers operating at a flow rate of 560 Lpm for 1 h prior to each shot. Andersen CIs with 81-mm-diameter mixed cellulose ester filters operated at about 28 Lpm. These samplers were initiated about 10 sec after the first impact and continued sampling for 2 min.

Deposition Trays

Eight deposition trays were used in the following positions: two positioned outside, two positioned on the target, and four positioned inside the target.

Contamination Surveys

Interior Removable Contamination

Contamination surveys were conducted as described in Phase I. Interior removable contamination was measured by smearing 47-mm-diameter Defensap wipes within a defined 100-cm^2 area. Thirty-two discrete wipes were used to collect loose material on interior vertical and horizontal surfaces. Four deposition trays were placed in the turret, one at each crew position. Additionally, for an analysis outside the scope of the Capstone DU Aerosol Study, four additional locations were evaluated to establish a correlation between removable contamination using 47-mm wipes and currently fielded Army portable radiation survey instruments.

Exterior Removable Contamination

Exterior removable contamination on the surfaces of the target and the surrounding Superbox was measured by smearing 47-mm-diameter Defensap wipes within defined 100-cm^2 areas. Thirty discrete wipes were collected on the target's horizontal and vertical surfaces (10 on the impact side, 10 on the exit side, and 10 on the top of the target). As with the interior wipes, four additional locations were evaluated

for removable contamination using 47-mm wipes and currently fielded Army portable radiation instruments.

Personal Monitoring

Entry personnel who conducted contamination surveys and removed air sampling equipment were fitted with personal air samplers and cotton gloves. Each person entering the Superbox wore a 25-mm cassette filter breathing zone air sampler operated at 2 Lpm. Selected entry personnel wore a 25-mm Marple personal CIs operated at 2 Lpm. These samplers were worn for the duration of the contamination survey. No effort was made during Phase-III recovery to collect residue samples on cotton gloves.

Other Measurements

Temperature and pressure measurements inside the vehicle were eliminated from this test as a cost-cutting measure. Temperature and RH measurements within the fragmentation shield were taken shortly before the shot was fired.

4.3.1 Phase III, Shot 1 (PIII-1) Test

The PIII-1 test was conducted at 1304 h on 14 February 2001. The target was in combat position with the turret angled so the penetrator would impact the left front panel. The penetrator was aimed to hit the breech and was not expected to exit the vehicle. The shot line is shown in Figure 4.9.

The IOM and CI samplers began operating 5 sec after impact and followed the time sequence presented previously in Table 4.14.

4.3.1.1 Impact Observations

Upon impact, flames erupted and continued for up to 4 sec. The loader's hatch did not appear to have opened, but smoke appeared to seep out from the perimeter of the hatch. Smoke was also visible rising from the GPS unit location. The flames resulted from ignition of a residual amount of hydraulic fluid that remained in the recoil mechanism after pre-test draining. The smoke that resulted from this fire complicated observations and recovery. The air within the turret appeared to begin clearing within 9 min. However, this observation might have been affected by dispersal of the hydraulic fluid on the protective cover in front of the video camera. Fireflies burned out in about 1 sec.

4.3.1.2 Recovery Observations

The recovery team noted that the interior surfaces were covered with a thin layer of an oily residue. Also, the turret interior surfaces, which initially were an off-white color, were discolored to charcoal black. The protective clothing on exiting individuals and wipe samples taken inside showed similar discoloration.

All IOM filters had a dark charcoal-colored residue (though the field blanks showed much less discoloration), and the CI samplers appeared to have visible material on the upper stages. All deposition trays were in their upright positions and appeared to have collected residue.

Prior to the second shot, the BHT was thoroughly cleaned, dried, and inspected. No detectable traces of oily residue remained.

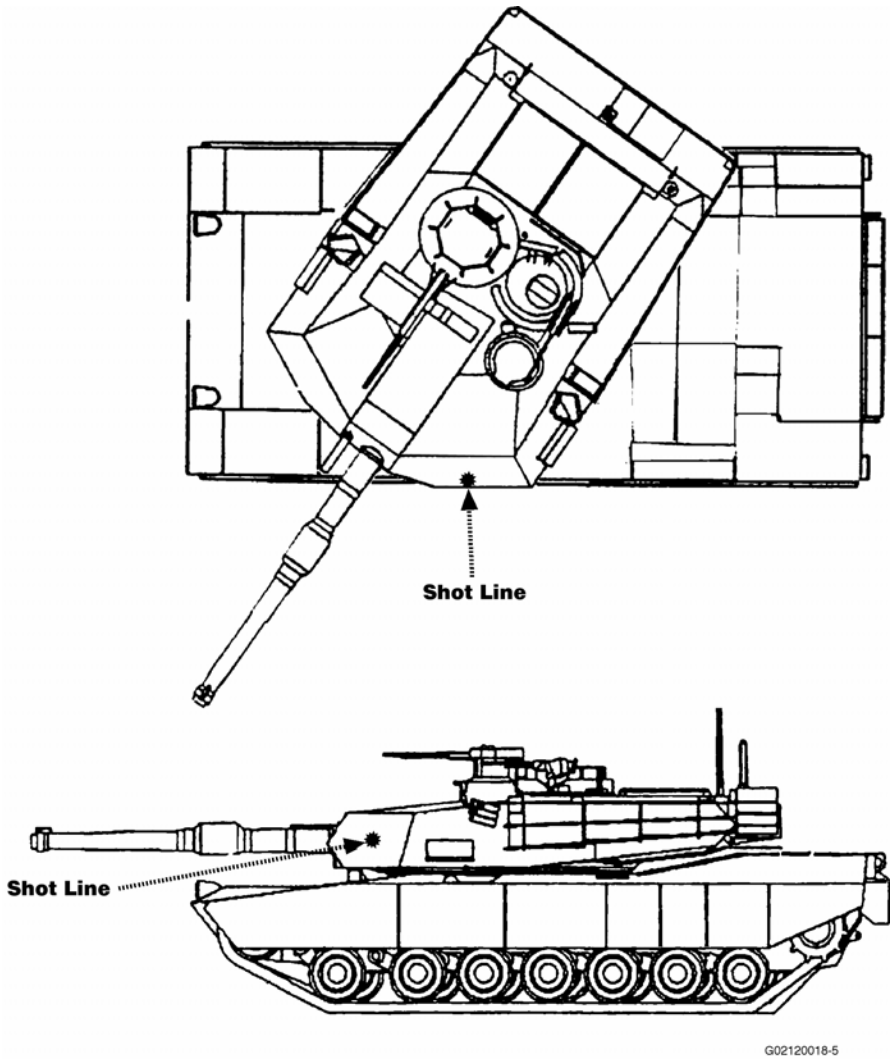

Figure 4.9. PIII-1 Shot Line

4.3.2 Phase III, Shot 2 (PIII-2) Test

The PIII-2 test was conducted at 1149 h on 22 February 2001. The target was in combat position with the turret angled so the penetrator would impact the left front panel. As with the first shot and using a similar shot line, the penetrator was expected to hit the breech and was not expected to exit the vehicle. The shot line is shown in Figure 4.10.

The IOM and CI samplers began operating 5 sec after impact and followed the time sequence presented previously in Table 4.15.

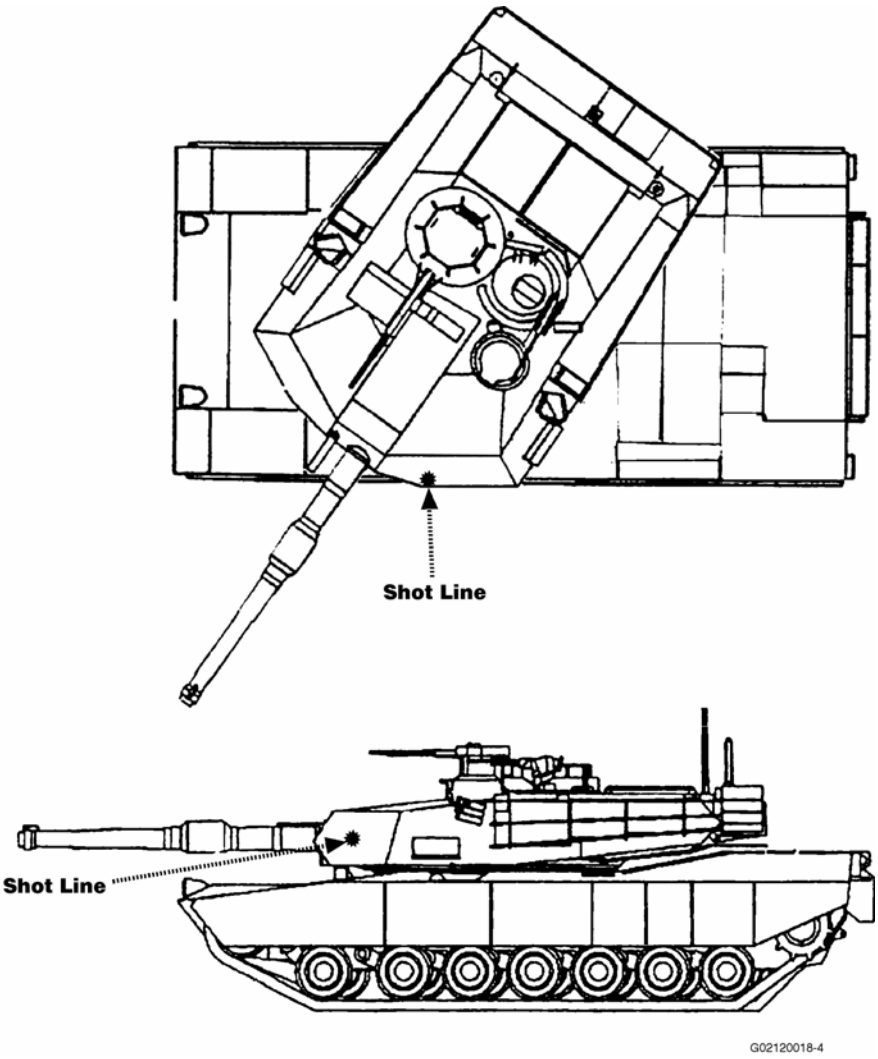

Figure 4.10. PIII-2 Shot Line

4.3.2.1 Impact Observations

Impact was to the left turret front armor, to the right of the impact point for Shot 1. Although the loader's hatch cover was secured prior to the test, it opened several inches upon impact, thus resulting in a chimney effect of smoke rising from the loader's hatch. A slight amount of smoke also was seen rising from the GPS unit location. Visible emission of smoke from the loader's hatch stopped about 9 min after impact.

Most fireflies burned out within the first 1.1 sec and all had burned out after 1.4 sec. The protective cover in front of the interior video camera was severely damaged so interior observations of clearing within the turret were limited.

4.3.2.2 Recovery Observations

The IOM filters collected a gray-green colored residue. Several filter surfaces appeared to have bulged or had waves or wrinkles.

Exterior deposition tray B was found upside down. Other deposition trays remained upright, and none suffered any apparent damage. Interior deposition trays were in upright positions. The deposition tray at the loader's position contained a considerable amount of residue.

Because of a mix-up between the exterior CI power cord and another line, this sample actually ran for 5 h instead for 2 min.

It was noted during sample removal that the seal between the second and third stages of the cyclone seemed loose, suggesting that the aerosol may not have been properly separated by size. Upon opening the cyclone stages, it was observed that there was very little residue collected in Stages 2 and 3. However, residues in the grit chambers of Stages 1, 4, and 5 appeared to be similar to previously collected residues, and the total quantity of sample recovered was similar to the quantity collected during the previous shot. The residues were resuspended and recollected in the laboratory in an attempt to achieve better separation of the particle sizes.

4.3.3 Summary of Phase-III Sample Collection Times

Table 4.16 lists the sampling time sequence during the Phase-III shots for the IOM and CI sampler arrays. The sampling times for the MVF are listed in Table 4.17.

Table 4.16. Array Sample Collection Times for Phase-III Shots

Time Sequence Sample Set	Time ON Post Shot (+5 sec) (hh:mm:ss)	Time OFF Post Shot (+5 sec) (hh:mm:ss)	Sample Duration
Shot 1	Samples taken from commander's, driver's, gunner's, and loader's positions		
1	00:00:00	00:00:10	10 sec
2	00:01:00	00:01:10	10 sec
3	00:03:00	00:03:15	15 sec
4	00:07:00	00:08:00	1 min
5	00:15:00	00:17:00	2 min
6	00:31:00	00:35:00	4 min
7	01:01:00	01:09:00	8 min
8	02:01:00	02:09:00	8 min
9	Field Blank		
Shot 2	Samples taken from commander's, driver's, gunner's, and loader's positions		
1	00:00:00	00:00:10	10 sec
2	00:01:00	00:01:10	10 sec
3	00:03:00	00:03:15	15 sec
4	00:07:00	00:08:00	1 min
5	00:15:00	00:17:00	2 min
6	00:31:00	00:35:00	4 min
7	01:01:00	01:09:00	8 min
8	02:01:00	02:09:00	8 min
9	Field Blank		

Table 4.17. Moving Filter Sample Collection Times for Phase-III Shots

MVF (time point)	Time ON Post Shot (hh:mm:ss)	Time OFF Post Shot (hh:mm:ss)	Sample Duration
Shot 1			
1	00:00:00	00:03:30	3 min, 30 sec
2	00:07:00	00:07:30	30 sec
3	00:15:00	00:15:30	30 sec
4	00:31:00	00:31:30	30 sec
5	01:01:00	01:01:30	30 sec
6	02:01:00	02:01:30	30 sec
Shot 2			
1	00:00:00	00:03:30	3 min, 30 sec
2	00:07:00	00:07:30	30 sec
3	00:15:00	00:15:30	30 sec
4	00:31:00	00:31:30	30 sec
5	01:01:00	01:01:30	30 sec
6	02:01:00	02:01:30	30 sec

4.4 Phase-IV Test Parameters

The M1A2 Abrams Live-Fire Vulnerability Test series followed the Capstone sequence and offered the opportunity to evaluate the aerosols produced in an operational Abrams tank. This test was directed by the Tank 2000 Project Director and had different testing priorities. However, because aerosol collection on a small scale would not interfere with the vulnerability tests, Capstone team participation was approved during the test firings. The Capstone team participated (on a much smaller scale) in the following four of the Live-Fire Tests, which constituted the Capstone Phase-IV field tests:

- PIV-1, a dry run in which a non-DU munition was fired against the DU armor package and did not perforate into the turret/crew compartment. This shot provided contamination survey measurements and an opportunity to test the aerosol equipment placement and function.

- PIV-2, in which a DU munition was fired against the DU armor package and did not perforate into the crew compartment. Only contamination survey measurements were performed during this test.

- PIV-3, in which a non-DU munition was fired against the DU armor package and perforated into the crew compartment. This test provided the opportunity to evaluate DU aerosols generated from the armor alone.

- PIV-4, in which an LC-DU munition was fired against the DU armor package and perforated into the crew compartment. This test is most closely related to the Phase-III shots and provided an opportunity to evaluate differences in aerosol generation and behavior between a BHT and an operational vehicle.

The field tests were conducted at the ATC Superbox between April and July 2001. The aerosol sampling strategy used reflects the very limited area available for placement of air samplers.

Common parameters for the Phase-IV tests are described in the following text.

Target

The target vehicle was an M1A2 Abrams tank with DU (heavy) armor. This tank was operational and uploaded with equipment, mannequins at each crew position, and an abundance of sampling equipment required for the Live-Fire Test objectives. Additional Capstone sampling equipment is detailed below.

Air Sampling Equipment

Interior Air Sampling Equipment

Attached to the coveralls of the mannequins at the loader's and driver's positions: Five, 37-mm, eight-stage standard Marple CIs at each position, operated at a nominal flow rate of 2 Lpm. An MCE substrate was used in Stages 1 through 8, and a PVC backup filter was identified in the data as Stage 9. One CI per position served as a field blank. Live-Fire Test objectives precluded the shielding of control and vacuum lines for these samplers. Vacuum and control lines were positioned where minimal damage was anticipated.

Additionally, an MVF and a five-stage cyclone train, each with a collection port, were placed in small, protective metal boxes in the turret. The MVF, which used AW19 as the filter medium, collected aerosols at a nominal flow rate of 28 Lpm and moved at a rate of 0.88 cm/sec. The MVF was included in the sampling scheme specifically to collect aerosol at the time of perforation. The MVF sample collection was started seconds before the shot and continued for approximately 3.5 min post shot. The CIs were activated approximately 5 sec after impact. The MVF also was run intermittently to collect aerosol samples at time intervals following the shot to coincide with CI samples collected post shot.

The cyclone collected aerosols at a nominal flow rate of 14 Lpm. A backup filter arrangement with four parallel filters was connected to the fifth stage of the cyclone. The backup filters had PTFE membranes and polymethylpentene support rings.

Interior air sampling equipment was controlled remotely through the use of LabVIEW software. Flow rates for each sampler were checked after each installation.

Exterior Air Sampling Equipment

No exterior sampling was attempted because the ventilation/filtration system of the Superbox operated throughout the sampling period.

Contamination Surveys

Interior Removable Contamination

Interior removable contamination was measured by smearing 47-mm diameter Defensap wipes within a defined 100-cm^2 area. Fifteen discrete wipes were used to collect removable material on interior vertical and horizontal surfaces.

Exterior Removable Contamination

Exterior removable contamination on the surfaces of the target and the surrounding Superbox was measured by smearing 47-mm-diameter Defensap wipes within defined 100-cm^2 areas. A total of four aluminum deposition trays (100 cm^2) were used: one on the hull, one on the turret, and two on the fragmentation shield floor.

Personal Monitoring

Entry personnel who conducted contamination surveys and removed air sampling equipment were fitted with personal air samplers and cotton gloves. Each person entering the Superbox wore a 37-mm cassette filter breathing zone air sampler operated at 2 Lpm. Selected entry personnel wore a 37-mm Marple personal CI operated at 2 Lpm.

4.4.1 Phase IV, Shot 1 (PIV-1) Test

The test designated as Shot 1 for Capstone purposes was a test of a non-DU cartridge or explosive not expected to perforate the target vehicle. This test, which was conducted on 12 April 2001, constituted a dry run for placing samplers and monitoring their responses in these tight surroundings. Five CIs were attached to the mannequin at the loader's position, and four CIs were attached to the mannequin at the driver's position. The MVF and cyclone were fit into the driver's compartment. All samplers operated as intended, and their flows and volumes are listed in Table 4.18.

Table 4.18. CI Sampler Flow Rates and Volumes During PIV-1

	Loader			Driver		
Time-point	**ID**	**Flow (Lpm)**	**Volume (L)**	**ID**	**Flow (Lpm)**	**Volume (L)**
0-1 min	IMP1	2.430	2.430	IMP1	2.254	2.254
1-3 min	IMP2	2.574	5.148	IMP2	2.252	4.504
5-9 min	IMP3	2.664	10.658	IMP3	2.516	10.063
25-33 min	IMP4	2.696	21.566	IMP4	2.433	19.467
Blank	IMP5	Field Blank				
0-33 min	Cyclone/FS array	9.95	328.4			
Various	MVF	18.95 Lpm				

4.4.2 Phase IV, Shot 2 (PIV-2) Test

Shot 2 used DU munition fired against the tank armor. The crew compartment was not perforated. This test was conducted on 17 May 2001. No internal air sampling was installed for this shot.

4.4.3 Phase IV, Shot 3 (PIV-3) Test

In Shot 3, a non-DU munition fired at the target perforated into the crew compartment. This test was conducted on 27 June 2001. Five CIs were attached to the mannequin at the loader's position and to the mannequin at the driver's position. The MVF and cyclone were fit into the driver's compartment. All samplers operated as intended, and their flows and volumes are listed in Table 4.19.

Table 4.19. CI Sampler Flow Rates and Volumes During PIV-3

Time-point	Loader			Driver		
	ID	Flow (Lpm)	Volume (L)	ID	Flow (Lpm)	Volume (L)
0-10 sec	IMP1	2.524	0.421	IMP1	2.232	0.372
1 min-1min, 10 sec	IMP2	2.604	0.434	IMP2	2.658	0.443
5 min-5 min, 15 sec	IMP3	2.682	0.670	IMP3	2.544	0.636
25-27 min	IMP4	2.756	5.511	IMP4	2.439	4.878
Blank	IMP5	Field Blank		Field Blank		
0-27 min	Cyclone/FS array	9.85	325.1			
Various	MVF	18.95 Lpm				

4.4.4 Phase IV, Shot 4 (PIV-4) Test

In Shot 4, a cartridge with an LC-DU penetrator was fired at the target. It perforated the DU armor package and entered the crew compartment. This test was conducted on 19 July 2001. Five CIs were attached to the mannequin at the loader's position and to the mannequin at the driver's position. The MVF and cyclone were installed in the driver's compartment. Fragments severed the vacuum lines of the loader's position CI samplers and the MVF lines. Five tiny fragments that collected on loader CIs weighed 0.88, 1.72, 3.0, 8.5, and 24.6 mg. The driver's position CI samplers survived and collected aerosol. The sampler flow rates and volumes are listed in Table 4.20. Samplers for which the vacuum line was severed are noted.

Table 4.20. CI Sampler Flow Rates and Volumes During PIV-4

Time-point	Loader			Driver		
	ID	Flow (Lpm)	Volume (L)	ID	Flow (Lpm)	Volume (L)
0-10 sec	IMP1	2.547	(0.425)[a]	IMP1	2.499	0.417
1 min-1min, 10 sec	IMP2	2.709	(0.451)[a]	IMP2	2.627	0.438
5 min-5 min, 15 sec	IMP3	2.749	(0.687)[a]	IMP3	2.504	0.626
25-27 min	IMP4	2.764	(5.528)[a]	IMP4	2.418	4.836
Blank	IMP5	Field Blank		Field Blank		
0-27 min	Cyclone/FS array	10.0	Line cut			
Various	MVF	5.20	Line cut			

4.5 Physical Data

Measurements and observations of the physical conditions also were collected. These data included the temperature and pressure inside the vehicles following impact, the temperature and RH inside the Superbox before impact, video capture of tiny burning DU fragments (fireflies) generated by the perforation, penetrator fragments found inside the target vehicles, survivability of sampling equipment, and ventilation rates within the vehicles. The reason why a mass balance of the DU was not calculated also is discussed in this section.

4.5.1 Pressure and Temperature

Crew compartment overpressure was recorded on selected shots. The pressure was measured using a PCB piezoelectric 102A15 gauge. The sampling rate was 40,000 measurements per sec at a frequency of 40 kilohertz. The gauge mount was welded into a hole in the turret roof directly above the center of the cannon breech (shown in Figures 3.10 through 3.13). Pressure measurements are presented in Table 4.21 and show that pressures varied considerably between phases and within Phases I and III.

Table 4.21. Pressure and Temperature Peaks

Shot Number	Peak Overpressure psig (gauge)	Peak Temperature °C	Position	Time-to-Temperature Peak
Phase I				
Shot 1	NA[a]	NA	Not measured	Not measured
Shot 2	7.45	NA	NA	NA
Shot 3	3.67	63	Loader – Internal	1350 msec
Shot 4	15.4	52	Commander – External	4600 msec
Shot 5	21.9	89[b]	Commander – Internal	1250 msec
Shot 6	13.9	114	Commander – External	975 msec
Shot 7	10.5	92	Commander – External	741 msec
Phase II				
Shot 1	4.34	36	Loader – Internal	600 msec
Shot 2	5.86	186	Loader – External	Uncertain[c]
Shot 3	6.06	42	Loader – Internal	195 msec
Phase III				
Shot 2	12.5	76	Loader – External	500 msec

(a) NA—not available
(b) Higher temperatures were noted but were believed to have been from noise rather than representative readings.
(c) Start time was not established.

Recorded Phase-I pressures ranged from a low of 3.67 psi on Shot 3 to a high of 21.9 psi on Shot 5. Phase-II pressures were relatively consistent, ranging from 4.34 psi to 6.06 psi. The only Phase-III shot measured reached 12.5 psi. These pressure peaks were instantaneous (i.e., lasting for milliseconds) as the penetrator perforated and exited the vehicle interior.

Temperature measurements were taken in the turret to discern whether damage to the IOM Supor filters was related to temperature. Thermocouples were placed at several crew positions inside (internal) and outside (external) the protective sampler array shields. The thermocouples were 0.076-mm diameter fast-response K-type probes, and the sampling rate was 100 measurements per sec. No attempt was made to characterize the peak temperature around the entry/exit points of the target perforation. The peak temperatures at the point of measurement are probably not the peak temperatures experienced in the turret. Because of the fragile nature of the thermocouples and the violent nature of the event, several channels were routinely lost or the data were unsuitable. Some very transient higher-temperature peaks were recorded and were believed to be either sensor noise or the result of DU fragments burning on or in close proximity to the thermocouples. The results presented in Table 4.21 are from the transducer that provided the most reliable data. These data range from 36º to 89ºC inside the shields and 42º to 186ºC outside the shields. The temperature peaks lasted from 195 to 4600 milliseconds (msec).

4.5.2 Superbox Temperature and Relative Humidity

The temperature and RH inside the Superbox just before the shots were fired were recorded for all but PI-2 and PI-3/4. These data and the date of each shot are listed in Table 4.22. The Phase-I through Phase-II shots were fired between late fall and early spring. The temperature varied between 6ºC (43ºF) and 21ºC (69ºF), and the RH varied between 27 and 76%. The Phase-IV test period spanned the seasons from mid-spring to mid-summer. Temperature and humidity measurements were recorded for PIV-1, during which the temperature was 16ºC (61ºF) with a humidity of 86%, and PIV-4, which recorded a temperature of 37ºC (99ºF) and 40% RH.

Table 4.22. Superbox Temperature and Humidity

Date	Test ID	Temp (ºC/ºF)	%RH
9 Nov 2000	PI-1	21/68.9	50.0
29 Nov 2000	PI-2	Not Measured	Not Measured
7 Dec 2000	PI-3/4	Not Measured	Not Measured
10 Jan 2001	PI-5	7.3/45.2	27.1
24 Jan 2001	PI-6	5.9/42.6	51.7
1 Feb 2001	PI-7	10/50.3	40.1
14 Mar 2001	PII-1/2	13/56.0	39.0
22 Mar 2001	PII-3	14/58.0	47.6
12 Feb 2001	PIII-1	10/50.5	67.0
28 Feb 2001	PIII-2	6.7/44.0	29.0
12 Apr 2001	PIV-1	16/61.0	85.6
17 Jun 2001	PIV-3	Not Measured	Not Measured
19 Jul 2001	PIV-4	37/98.8	40.0

4.5.3 Transient Fireflies

Previous video monitoring inside vehicles perforated by DU penetrators had detected tiny DU fragments that appeared to undergo rapid, almost instantaneous oxidation immediately after the shot occurred. These tiny burning embers were nicknamed “fireflies” by range personnel. Following each Capstone shot, a flash momentarily overloaded the video signal. As the intensity of this illumination subsided, the interior high-speed video camera (1000 frames per sec) captured the firefly phenomenon. The fireflies were visible from just under 1 sec on most shots to a maximum of 1.5 sec. Figure 4.11 shows three photos of this effect occurring during the Capstone PI-2 test. The photo on the left was taken 0.550 sec after impact. The middle photo (cropped vertically to focus on interesting features) was taken from the 0.661-sec frame in which a particle in the lower left of the photo was in the process of disintegrating. The right photo (also cropped vertically) was taken four frames later at 0.665 sec and shows a series of small particles generated by the disintegrating particle.

Figure 4.11. Photographs of Firefly Phenomenon in Sequence

4.5.4 Penetrator Fragments

Fragments of the penetrator were found outside the target vehicles during cleanup after several shots. Only two small fragments were recovered within the Abrams BHT during Phases I through III, both of which were found following the PI-5 shot (Figure 4.12). One of these fragments was weighed before being dissolved for analysis of uranium isotopic ratios and TRU element analysis. Its mass was 22.5 g. Several smaller fragments were recovered from the turret in the PIV-4 test but were not analyzed. Five tiny fragments that collected on PIV-4 CIs weighed a total of 38.7 mg.

In addition to the two fragments from PI-5, a pile of DU oxide powder was found on a ledge just below the penetrator exit hole in the PI-5 shot. This pile, which resembled a cone (pointed end up) and was referred to as the DU "cone" sample, had a measured mass of 4.487 g. There were several much smaller piles of DU oxide that were discovered from the breech shots (PI-5 and PI-6), but they contained too little mass to recover.

Figure 4.12. Penetrator Fragments Inside Vehicle Following Perforation

4.5.5 Survivability of Equipment

Shielding and sampler placement strategies were used to minimize sampler loss due to the penetrator impact and the resulting fragments of eroded penetrator and perforated armor. The strategies generally worked well to protect the samplers, although fragments perforated some filters, vacuum lines, and electrical lines over the course of the field tests. With a few exceptions, IOM and CI samplers survived with negligible damage. IOM filters in positions closest to the penetrator exit holes were most consistently damaged, sometimes appearing to be partially disintegrated, and sometimes bearing holes presumably made by fragments.

The interior lights, though partially shielded, proved most sensitive to damage from the impacts, and in several cases, the remaining light was inadequate to provide sufficient illumination for the video feed. Additionally, debris from the shot routinely fogged the Lexan camera shield, thus obscuring the view somewhat.

Sampler electrical or vacuum lines were severed in several cases, leading to continuous efforts to improve shielding. The sampler most affected by damaged lines was the MVF. Additionally, a fragment entered the "protected" inlet of the MVF on PI-6, and a spall-liner fiber burned through the tape during Shot PII-1/2, preventing the MVF from operating. The performance history of the MVF is documented in Section 5.1.5.

4.5.6 Ventilation Rates

Ventilation rates for operational Abrams tanks are listed in Table 4.23 in units of volume exchanges per hour. The ventilation rates were lowest when the fan was off and the hatches were closed, thus restricting the airflow. Ventilation rates were higher when either the fan was on or the hatch was open. Of the three Abrams tanks, the M1A1 and M1A2 had much lower ventilation rates than the M1 tank (similar to the BHT) when the hatches were closed and the fans were not operating.

An operational Bradley vehicle was tested under three conditions: 1) with the internal fan off and the hatches closed, 2) with the fan on and the hatches closed, and 3) with the fan off and the commander's hatches open. The estimated ventilation rates for the Bradley vehicle are listed in Table 4.2. When the hatches were closed, the ventilation was greater for the Bradley vehicle than for the Abrams tanks. The ventilation rates increased substantially when the fans were operating.

Ventilation rates of the target vehicles before perforation and with the hatches closed (and no fans operating) yielded the volume exchange data presented in Table 4.24. The rates from the Abrams PI-1 through PI-3 shots varied little and ranged from 2.7 to 3.5 exchanges per hour. The ventilation rate from the PI-7 shot was similar to those tested during Abrams Phase III, ranging from 5.55 to 7.15 exchanges per hour. The single Bradley vehicle Phase-II result was considerably higher at 33.9 exchanges per hour. This result is much larger than the results from the operational vehicle except for the readings in the operational vehicle when the fan was on and the hatches were closed.

Table 4.23. Ventilation Rates for Intact, Operational Abrams Tanks and Bradley Vehicles (volumes exchanged per hour)

Fan OFF Hatches Closed	Exchange Rate	Fan ON, Hatches Closed	Exchange Rate	Fan OFF, Hatches Open	Exchange Rate
M1					
1	6.02	1	7.51	1	19.7
2	3.90	2	7.38	2	18.2
3	4.18	--	--	--	--
M1A1					
1	1.17	1	6.59	1	2.96
2	1.09	2	6.58	2	2.86
M1A2					
1	0.27	1	NA	1	4.83
2	0.23	2	NA	2	5.63
Bradley					
1	7.66	1	45.27	1	7.14
2	11.5	2	34.57	2	9.21
NA–not available					

Table 4.24. Pre-Shot Ventilation Rates in BHTs for Phases I, II, and III

Shot	Exchange Rate (volume exchanged per hour)
Phase I (Abrams Tank)	
1	2.98
2	3.49
3/4	2.70
5	NA
6	NA
7	7.15
Phase II (Bradley vehicle)	
1/2	NA
3	33.9
Phase III (Abrams Tank with DU Armor)	
1	5.55
2	6.28
NA—not available	

Post-shot ventilation analysis was not satisfactory. For example, the ventilation rate increased during the first 20 min of monitoring prior to the PI-1 shot. After the shot, the SF_6 concentration increased. This increasing concentration after impact is not explainable physically, and was a consistent observation throughout the course of the testing. Although the reason for this result was not definitively explained, it may have been caused by interference from combustion gases or vapors after the penetrator entered the vehicle.

Approximate total vehicle volumes potentially useful for scaling from the BHT to functional Abrams tanks are:

- Total crew compartment in an Abrams BHT—8.9 m^3 (315 ft^3)
- Total crew compartment in an intact and equipped Abrams—7.1 m^3 (251 ft^3).

Based on these numbers, the volume of the BHT is about 20% greater than the intact (but unoccupied and without ammunition) vehicle. Additional approximate vehicle volumes potentially useful for scaling from the BHT to functional Abrams tanks are:

- Total driver's compartment in an Abrams BHT—0.59 m^3 (20.9 ft^3)
- Total driver's compartment in an intact and equipped Abrams—0.5 m^3 (17.6 ft^3)
- Total air volume in intact Abrams vehicle —7.6 m^3 (268.4 ft^3)
- Four crew members and stowage—0.4 m^3 (14.1 ft^3).

Approximate total vehicle volumes potentially useful for scaling from the BHT to functional Bradley vehicles are:

- Total crew compartment in a Bradley BHT—12.8 m^3 (395 ft^3)
- Total crew compartment in an intact and equipped Bradley—9.5 m^3 (336 ft^3) to 10.0 m^3 (366 ft^3).

Based on these numbers, the volume of the BHT is about 22 to 26% greater than the intact (but unoccupied and without ammunition) vehicle. Additional approximate vehicle volumes potentially useful for scaling from the BHT to functional three versions of the Bradley vehicles are estimated to be:

- M2A2
  - Hull with no crew or stowage—11.1 m^3 (393 ft^3)
  - Hull with crew and stowage—8.5 m^3 (299 ft^3)
  - Turret with no crew or stowage—1.7 m^3 (59 ft^3)
  - Turret with crew and stowage—1.3 m^3 (47 ft^3)

- M3A2
  - Hull with no crew or stowage—same as M2A2
  - Hull with crew and stowage—8.7 m^3 (309 ft^3)
  - Turret with no crew or stowage—same as M2A2
  - Turret with crew and stowage—same as M2A2

- M3A3—similar to M3A2 but with perhaps 0.14 to 0.28 m^3 (5 to 10 ft^3) less interior volume.

4.5.7 Mass Balance

A total DU mass balance analysis was not conducted because of the near impossibility of retrieving the portion of the DU penetrator imbedded in the catch plate. Additionally, breakup of the penetrator created fragments that ricochetted from the vehicle armor and the catch plate and scattered over the floor of the fragmentation shield and even into the disposal trenches. The test team decided that attempts to recover the residual material would not provide sufficiently worthwhile information to justify the use of significant project resources.

5.0 Sample Results

Aerosol samples collected during the field tests were analyzed using a combination of radiological, chemical, and physical techniques to determine their uranium concentrations and to characterize their particle sizes, shapes, and dissolution in lung fluid. The analytical techniques used in these characterizations included gravimetric analysis, radioactivity counting, chemical processing to determine the compositions of various metals, XRD to determine the uranium oxide phases, particle size distributions using CI size partitioning, particle morphology using SEM, and dissolution in lung fluid using *in vitro* evaluations. This chapter discusses the aerosols collected within the crew compartments and exterior to the target vehicles and how the collected samples were analyzed. It also summarizes the chemical composition and particle size distribution of the collected material.

The shot identification, the nature of each shot, the samples successfully collected for each shot (including field blank samplers), whether or not the chemical and physical analyses were performed on the cyclone samples, are summarized in Table 5.1.

Table 5.1. Summary of Nature of Shots, Samplers Operated, and Analyses Conducted[(a)]

Shot	Shot Type	Retro/Pro-spective	IOMs Intact/Total	CIs	Cyclone	MVF	External CIs	Resuspension
PI-1	Turret cross	Prospective	18/36	36	Rad	Yes, Ltd	No	No
PI-2	Turret cross	Prospective	20/36	36	Rad	No	No	No
PI-3/4	Turret cross	Prospective	30/36	36(L)	Chem	Yes, Ltd	No	No
PI-5	Into breech	Prospective	27/27	27	Did not run	No	1	No
PI-6	Into breech	Prospective	27/27	27	Rad	No	2	Yes
PI-7	Into hull	Retrospective	35/36	36	Chem	No	2	Yes
PII-1/2	Scout comp't	Retrospective	36/36	36	Chem	No	2	No
PII-3	Turret	Retrospective	36/36	36	Rad	Yes	2	No
PIII-1	Turret/DU armor	Prospective	36/36	36	Rad	Yes	2	No
PIII-2	Turret/DU armor	Prospective	35/36	36	Chem	Yes	2	No
PIV-1	Baseline	Prospective	no	9	Rad	Yes	no	No
PIV-2	Non-DU; no perforation	Prospective	no	9	Rad	No	no	No
PIV-3	Non-DU; perforation	Prospective	no	9	Rad	Yes	no	No
PIV-4	DU/DU armor	Prospective	no	5 of 9	Did not run	No	no	No

(a) Legend: comp't = compartment; Ltd = limited samples.

Specifically, the table lists columns (from left to right) with the following information:

- test phase and shot number
- location of the trajectory path with notation of shots into the Abrams breech
- whether the shot was intended to simulate a shot from the Gulf War/ODS (a retrospective shot) or a possible future shot (a prospective shot)
- number of IOM filters that survived the test intact over the total number of IOM samplers used
- number of CI samplers used (for which all substrates survived)
- cyclone residue samples selected for radiological analysis only or for additional chemical and physical analysis
- MVF sampler operation; limited (Ltd) sample collection in PI-1 and PI-3/4
- identification of tests that used external CIs and how many
- identification of tests that collected interior resuspension samples using IOM and CI samplers.

5.1 Interior Aerosol Data

Gravimetric and alpha and beta radioactivity analyses were routinely performed on all interior IOM filters and CI substrates. Cyclone samplers underwent gravimetric analysis and were analyzed by gamma spectrometry. The MVF tape segments (cut into 2.54-cm [1-in.] segments) were analyzed for alpha/beta activity.

The following sections discuss the sampler flow data and the mass, radioactivity, and concentration of the IOMs, CIs, cyclone residues, and MVF tape segments.

5.1.1 Flow Data and Integrated Volume Determination

The LabVIEW software recorded the pressure drop across the pressure transducer as the IOM and CI samplers operated inside the target. It also recorded pressure drop information from the cyclone train and MVF sampler. The pressure drops for each sampler were converted to flow rates using a calibration done before each shot. Summaries of flow data from the IOM and CI samplers and the volume of air sampled are presented in Appendix A along with a discussion of flow rate calibration. The CIs are abbreviated "IMP" in tables of flow and volume. Generally, the sampler flows remained relatively constant during the sampling period, although some reduction was observed as the filters loaded with particles (or dust). For example, the beginning and ending flow rates for PI-1 (loader's and driver's arrays), which were run for the longest intervals and generally had the highest mass loadings, are presented in Table 5.2. The sampling time intervals were 30 sec, 1 min, 2 min, 4 min, 8 min, 16 min, 32 min, and 64 min, respectively. Later shots used shorter time intervals to avoid excessive filter loading. The pressure drop changes that occurred over the sampling interval with these samplers were generally similar or higher than with later shots. The flow rate affects the cutoff points for the CIs. Most samplers ran slightly above the nominal 2-Lpm rate. Formulas in the SigmaPlot software used in the particle size analysis accounted for this effect.

Table 5.2. Change in Flow Rates with Sample Collection, PI-1

Loader's Array					
Sampler	Flow Rates (Lpm)		Sampler	Flow Rates (Lpm)	
	Initial	Final		Initial	Final
FS1	2.49	1.82	IMP1	1.92	1.49
FS2	2.45	1.91	IMP2	2.48	2.45
FS3	2.40	1.89	IMP3	2.44	2.03
FS4	2.48	1.88	IMP4	2.55	2.42
FS5	2.36	1.96	IMP5	2.54	2.52
FS6	2.45	2.24	IMP6	2.55	2.53
FS7	2.43	2.16	IMP7	2.49	2.40
FS8	2.46	1.99	IMP8	2.52	2.48
Driver's Array					
Sampler	Flow Rates (Lpm)		Sampler	Flow Rates (Lpm)	
	Initial	Final		Initial	Final
FS1	2.37	2.24	IMP1	2.55	2.55
FS2	2.57	2.47	IMP2	2.39	2.37
FS3	2.60	2.39	IMP3	2.67	2.63
FS4	2.61	2.46	IMP4	2.68	2.66
FS5	2.37	2.23	IMP5	2.58	2.56
FS6	2.56	2.39	IMP6	2.66	2.62
FS7	2.49	2.30	IMP7	2.60	2.56
FS8	2.36	2.16	IMP8	2.65	2.63

5.1.2 IOM Filter Cassettes

The filter cassettes provided the best measure of the change in aerosol mass and uranium concentration within that mass as a function of time for all time periods except for the first 5-sec increment post impact. The MVF was the only sampler operating during that first time increment. Samples were collected over eight time intervals during the 2-h sampling period following impact for a minimum of 10 sec to a maximum of 64 min (sampling times for each shot are provided in Chapter 4.0 and are included in the tables of Appendix A). The filters were weighed and analyzed for alpha and beta radioactivity. All IOM filters were photographed before being counted. Photographs of two sample sets from Phase I illustrate the variations in aerosol color observed (Figure 5.1). The left photograph shows the IOM filters in time sequence (from left to right beginning with the first post impact sample collected) from the PI-2 driver's array. The filter blank is in the lower right corner, and the damage it sustained is visible. The photo on the right side of the figure is from the commander's sampler array for shot PI-6. The two sets cannot be compared directly because the PI-2 samplers operated for longer time intervals than the PI-6 samplers, they used different filter media, and the shot lines were different.

The filter set on the left in Figure 5.2 is from the commander's sampler array for the PI-7 hull shot. The filter set on the right in Figure 5.2 is from the driver's sampler array for shot PII-3. Unlike the PI and PIII samples, the accumulated aerosol collected during PII tended to "cake" and crack. Two of the PIII-2 sample sets are shown in Figure 5.3 (from left to right beginning with the first post impact sample collected) with the driver's position set on the left and the commander's position set on the right. The

samples generally have a similar appearance, but they display some variation in the amount of material collected, especially in the filter blank (lower right-hand corner).

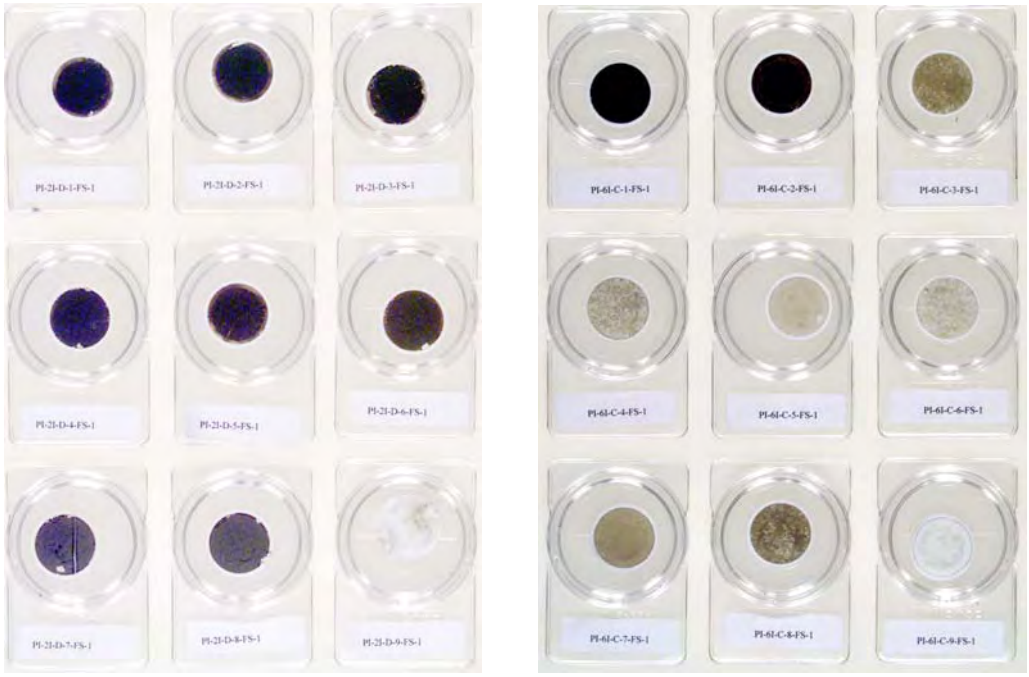

Figure 5.1. Examples of IOM Filter Samples from PI-2 and PI-6, Respectively

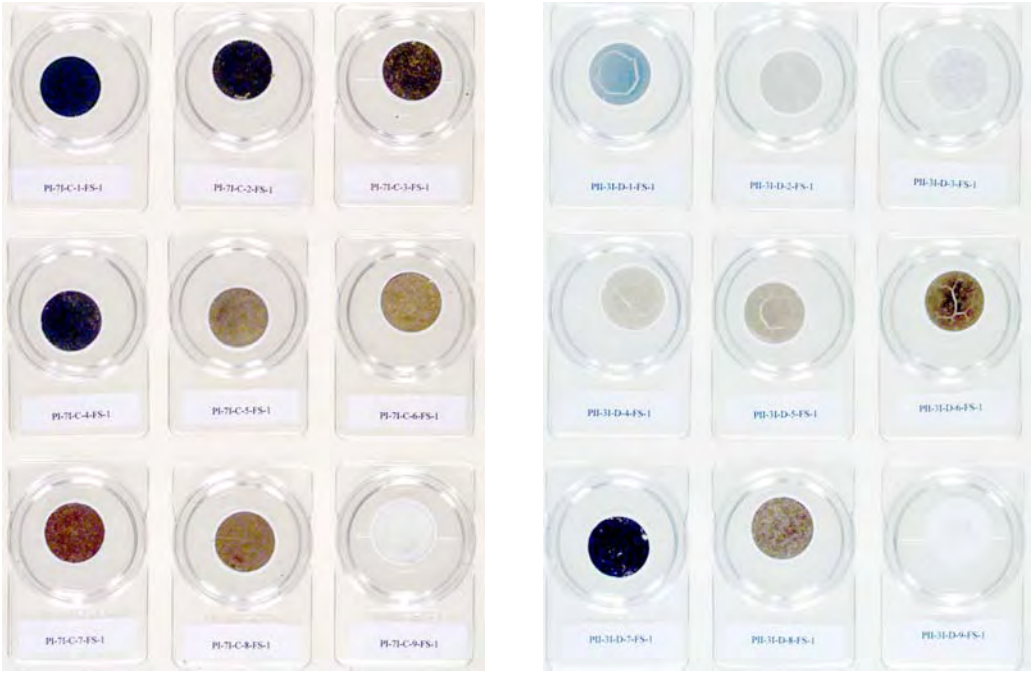

Figure 5.2. Example of IOM Filter Samples from PI-7 and PII-3, Respectively

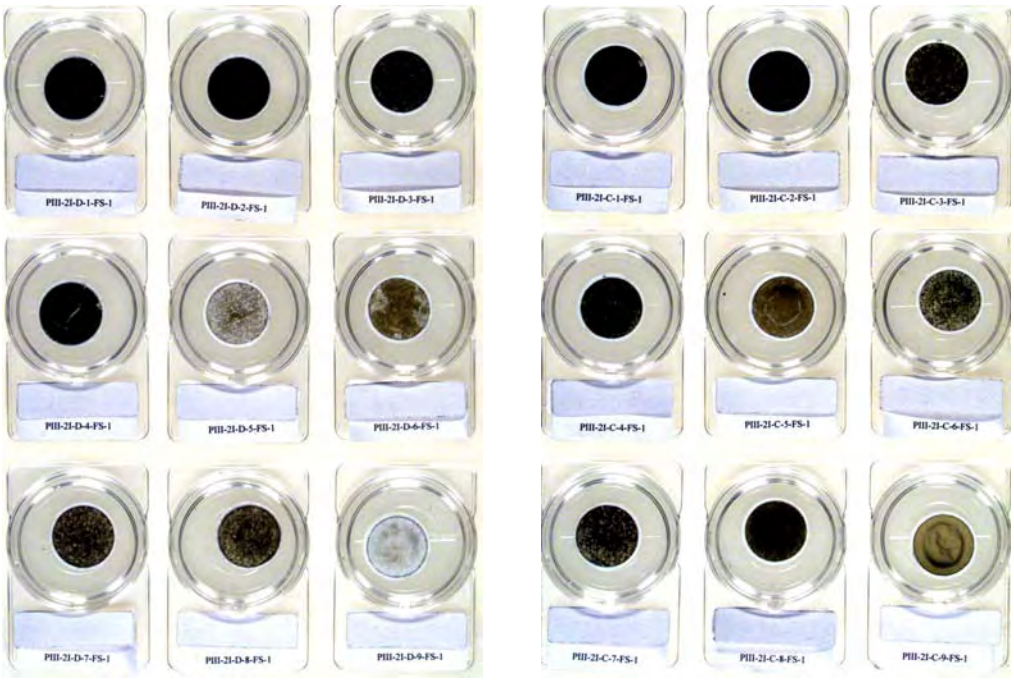

Figure 5.3. Examples of IOM Filter Samples from PIII-2 (Driver's and Commander's Positions)

Most filter samples survived vehicle perforation, but there was extensive damage to the IOMs in the commander's and gunner's arrays in PI-1 and PI-2. About one-third of the Supor filters used in the first two shots were damaged by what was suspected to have been the temperature/pressure pulse from the impact. The IOM filters at the gunner's position proved especially vulnerable in these shots because it was closest to the exit hole. The damage to these filters ranged from minor holes to major disintegration. In contrast to the sample sets shown in Figures 5.1 through 5.3, all the IOM filters from the gunner's sampler arrays were damaged in PI-1 (Figure 5.4). Fragments also appeared to have damaged some of the filters. Any damage causing holes to the filter compromised the flow rate and rendered the sample unsuitable for aerosol analysis.

By the time the PI-3/4 shots were fired, changes to the shielding and to the mix of filter media used improved filter survival. Zefluor filters replaced Supor filters in some of the IOM samplers during PI-3/4 and were used exclusively as the IOM filter medium for the remaining shots. By PI-5, there were no further problems with filter survival. The few remaining problems encountered involved samplers that did not operate.

Several IOM samples were eliminated from analysis because of filter damage, electrical or vacuum lines severed by fragments, or other problems that prevented adequate operation. The following samples experienced one or more of these circumstances and were eliminated from analysis:

- PI-1: All gunner's and commander's array filters
- PI-2:
  - Commander's position filter numbers 2, 6, 7, and 8
  - Driver's position filter number 9 (though it was used as the filter blank for lack of a better choice)
  - Gunner's position filter numbers 1, 2, 3, 4, 6, 7, and 9
  - Loader's position filter numbers 1, 4, 5, and 9

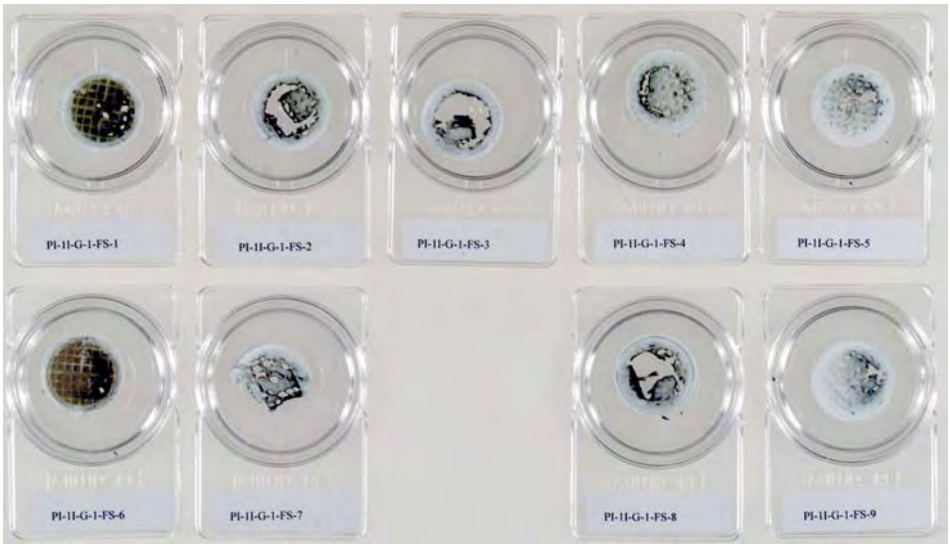

Figure 5.4. Extensive IOM Filter Damage, PI-1

- PI-3/4:
  - Loader's position filter numbers 1, 2, 4, 7, and 9 (filters 1, 4, and 7 were Supor; filters 5, 6, 8, and 9 were Zefluor)
  - Gunner's position filter number 5 sampler head had separated from its stem
- PI-7: Driver's position filter number 5 suffered line damage
- PIII-2: Loader's position filter number 5 was bent, thus preventing a seal with the IOM sampler head.

5.1.2.1 Gravimetric Results

The IOM filter samples were weighed, and their net masses are listed by shot and by time sequence in Appendix A, Tables A.9 through A.18. The mass of material collected on each filter depended on sampling duration as well as aerosol concentrations during the sampling interval. The collected aerosols contained non-DU constituents from the target and the penetrator as well as uranium oxides from erosion and oxidation of the penetrator. Though not analyzed in this report, the total aerosol mass coupled with the radioactivity-derived uranium content provides an indirect measurement of the percentage of uranium in the total aerosol.

5.1.2.2 Radioactivity-Derived Uranium Concentrations

The alpha and beta radioactivity measurements of the IOM samples are presented in Appendix A, Tables A.9 through A.18. Estimates of the mass of uranium on the filters were used in subsequent analysis of uranium concentrations with respect to time. Alpha activity can be used to calculate the uranium where the sample is very thin and alpha particle absorption is minimal. However, to avoid possible underestimation of uranium mass due to alpha particle absorption on the IOM filters, beta activity measurements were used as a surrogate for the amount of uranium in a sample. During the evaluation of beta activity results, it was determined that the short-lived, beta-emitting uranium progeny (Th-234 and Pa-234m) were not in secular equilibrium with the U-238 parent at the time that approximately half the samples were counted. To account for disequilibrium in these samples, the beta activity measurements

were corrected for beta progeny ingrowth and then converted to uranium mass using the methodology described in Appendix A.2.1.5. As part of this methodology, uranium analysis using ICP-MS was performed on a subset of the samples. For samples that were analyzed by both techniques—beta activity counting, which was converted to uranium mass, and uranium mass by ICP-MS—the higher of the two values was reported in the tables in Appendix A and used in the calculations of the uranium mass concentration ($\mu g/m^3$) as described below.

$$Uranium\ Mass\ Concentration\left(\mu g / m^3\right) = \frac{[Sample\ Mass\ (DU\ \mu g) - Field\ Blank\ (DU\ \mu g)]}{[Sample\ Volume\ (L)\ x\ 1.0\ E-3\ m^3 / L]}$$

One-sigma ($\pm 1\sigma$) uncertainties were propagated for the uranium masses and the uranium mass concentrations, which also are listed in the tables in Appendix A. The uranium mass uncertainties varied but typically were in the 20 to 40% range. Uncertainty with regard to the volume of air sampled is believed to be small (within about 3% error) because of the calibrations performed and the control over the pressure drop readout for the samplers. The volume uncertainty is included in the overall propagated of uncertainties for uranium concentrations.

With a few exceptions, each sampler array was set up to run for eight sampling intervals. The ninth IOM/CI pair was a field blank (which pulled no vacuum). Occasionally, a large particle of DU impacted the field blank filter medium and registered a higher uranium mass than would be representative of a sample that pulled no vacuum. Visual inspection of the sample photographs often confirmed the presence of these particles. In these cases and in cases in which the blank filter was damaged, one or more other filter blanks, usually an average of the blanks from the other arrays, was selected as a surrogate field blank to avoid underestimating the uranium present.

Table 5.3 presents a summary of the data derived from this approach using PI-1 at the loader's position. The table lists the time interval during which the sample was collected, the volume of air sampled, and the total mass of uranium and uranium mass concentration. It also presents the midpoint of the sampling time

Table 5.3. Example of Uranium Mass Calculation Process (PI-1, Loader's Array)

Sampling Interval (min)[(a)]	Volume (L)	DU Mass (µg)[(b)]	Graphing Parameters		
			Midpoint (min)	DU Mass Conc. ($\mu g/m^3$)	DU Mass Uncertainty ($\pm 1\sigma$)
0 to 0.5	1.03	17,491	0.25	1.69E+07	5.35E+06
0.5 to 1.5	2.09	12,402	1.00	5.89E+06	1.87E+06
1.5 to 3.5	4.15	11,141	2.50	2.67+E06	8.46E+05
3.5 to 7.5	8.35	10,313	5.50	1.23E+06	3.90E+05
7.5 to 15.5	16.8	5,767	11.50	3.39E+05	1.08E+05
15.5 to 31.5	37.2	2,115	23.50	5.51E+04	1.81E+04
31.5 to 63.5	73.0	1,693	47.50	2.23E+04	7.38E+03
63.5 to 127.5	140	2,864	95.50	1.99E+04	6.47E+03

(a) Beginning 5 sec after impact.
(b) The uranium mass of the field blank was 65 µg.

interval and the average uranium mass concentration in the aerosol in micrograms per cubic meter, both parameters used in plotting settling curves. In this case, the sample collected during the first 5- to 35-sec interval yielded a uranium concentration of 16.9 g/m^3. This aerosol concentration decreased rapidly in the next few minutes as the DU settled out, decreasing to 5.9 g/m^3 in the 35- to 65-sec interval and to 0.3 g/m^3 by the 7.5- to 15.5-min interval. This level further decreased to 0.02 g/m^3 within the 1- to 2-h interval following impact.

The uranium concentrations were plotted as a function of time (midpoints within time intervals), providing a visual display of the reduction in uranium aerosol concentration due to particle coagulation, settling, and plate-out on surfaces, commonly referred to as settling curves (also known as decay curves). A graph of the results of the data in Table 5.3 is shown in Figure 5.5 with the calculated uncertainty intervals related to the mass.

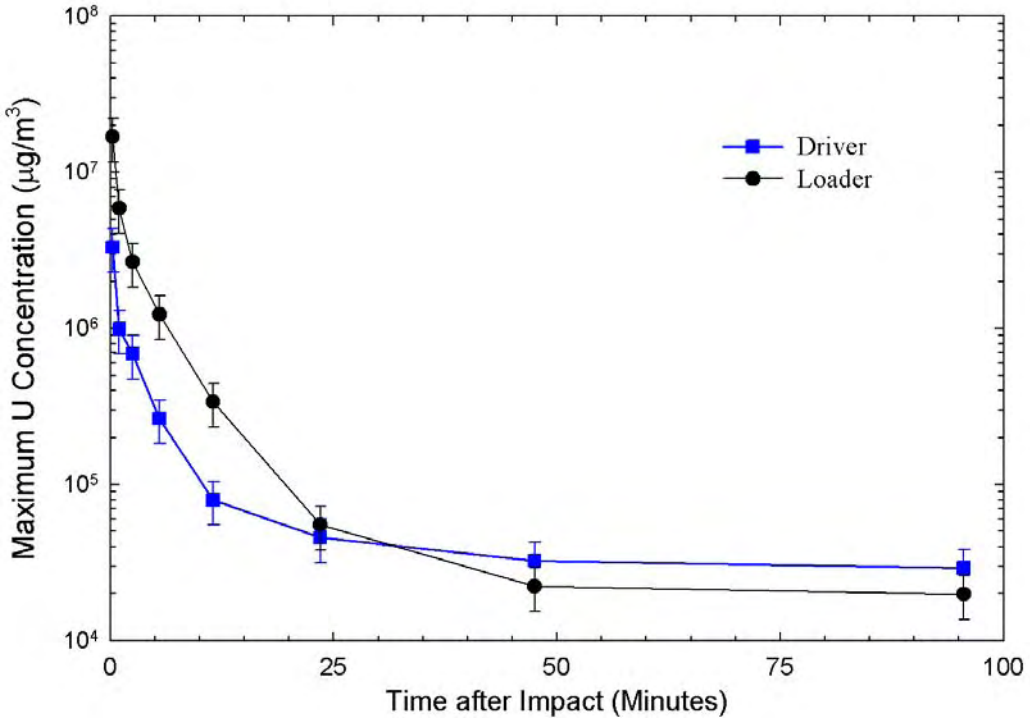

Figure 5.5. Time-Dependent Uranium Aerosol Concentrations, PI-1

Shot-Specific Event Summaries

Short summaries of the observations from each shot are provided in the next sections along with commentary about the graphs where appropriate. Table 5.4 describes the portion of the vehicle perforated, venting observed from hatch covers opening or other leakage of smoke and aerosols, and other comments including information about damage to IOM samplers.

The rest of the shots from Phases I through III are illustrated in Figures 5.6 through 5.14. Lines connect the individual points where full data sets were available and this condition is depicted in the legends with

Table 5.4. Summary of Shot Types, Vehicle Venting, and General Observations

Shot	Shot Type	Vehicle Venting	General Comments
PI-1	Turret crossing	Driver's hatch cover (tack-welded metal plate) opened	Commander and gunner IOMs damaged Longest sample collection duration
PI-2	Turret crossing	Loader's hatch opened	One or more IOM filters damaged at each array
PI-3/4	Turret crossing	Loader's hatch rose and fell	Loader shield opened prematurely, samplers damaged
PI-5	Through breech	Commander's, loader'shatch opened a crack	All IOM filters survived
PI-6	Through breech	Commander's, loader's hatch opened a crack	All IOM filters survived; loader's array used for resuspension
PI-7	Through hull	Commander's hatch raised an inch	Aluminum plate shattered, severed a driver IOM line
PII-1/2	Scout com-partment	Hatches intact, small venting losses	Spall liner fibers visible during recovery operations
PII-3	Through feeder tube	TOW missile loading hatch	Right scout shield opened only partially
PIII-1	Turret/DU armor	Perimeter of loader's hatch, GPS unit	Hydraulic fluid burst into flames, left oily residue on surfaces
PIII-2	Turret/DU armor	Loader's hatch opened briefly, GPS	Nothing noteworthy

a line through the symbol. Incomplete data sets where one or more samples were destroyed or did not run are shown as points only. Error bars were not applied to these sets of four arrays (three for PI-5 and PI-6), but again, the variation in uncertainty ranged from 20 to 40%. The propagation-of-uncertainty values for these data are listed in Appendix A, Tables A.9 through A.18.

Table 5.5 (see p. 5.17) provides uranium concentrations for Phase-I through Phase-III shots at each array as they varied with time. Hyphens where numbers should appear denote filters that were damaged or samplers that did not run. Specific information on these damaged samples or non-operating samplers is provided in Table B.2 and Table C.1. The gunner's array was not used in PI-5 or PI-6 and is therefore listed as not applicable (NA). The loader/left scout array for PI-6 and PI-7 was used to collect resuspended particles when personnel entered the vehicle.

Phase I, Shot 1 (PI-1)

The shot line in the PI-1 test was a side-crossing shot through the turret in front of the loader's and commander's positions. The shot entered from the loader's side and exited through the commander's side. In spite of the presence of the louvered shields, the IOM filters within the commander's and gunner's arrays were damaged by the blast or fragmentation. The impact caused a tack-welded cover over the driver's hatch to detach, and aerosol vented through the hole. In Figure 5.5, the maximum uranium curves for the loader's and driver's positions track relatively well. In the first five sample acquisitions (16 min post shot), the mass concentrations in the driver's position were lower than those obtained in the loader's position. The concentrations equalized with time with the driver's samplers appearing slightly elevated above the loader's samplers, though within the level of uncertainty, after approximately 30 min post impact.

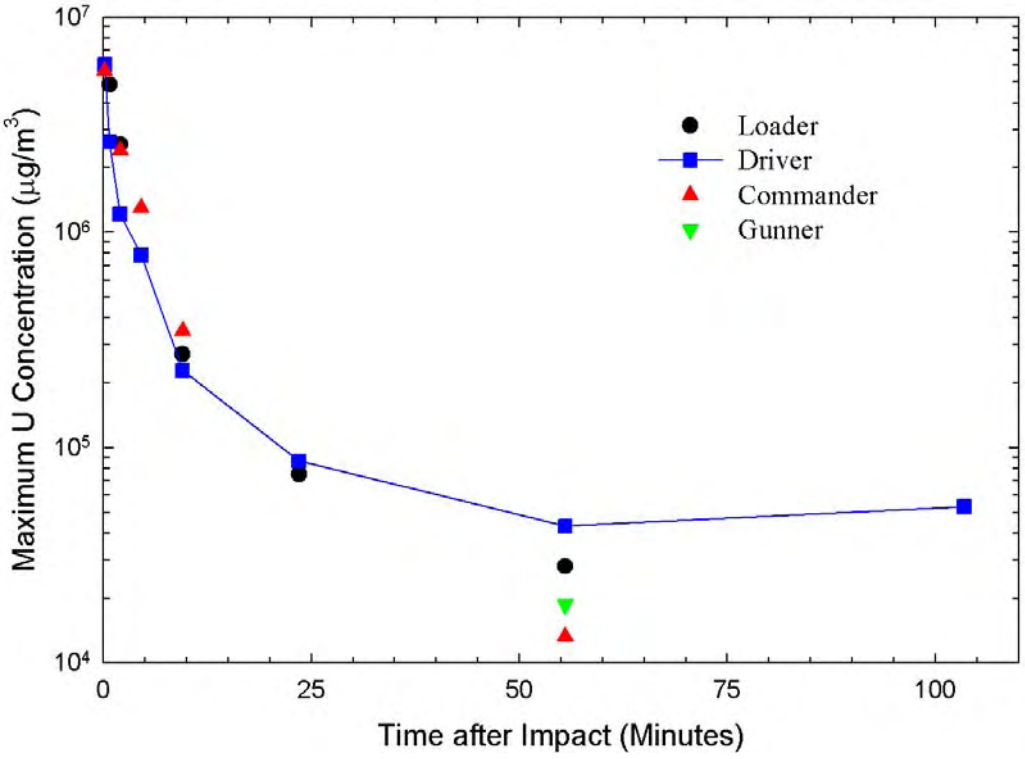

Figure 5.6. Time-Dependent Uranium Aerosol Concentrations, PI-2

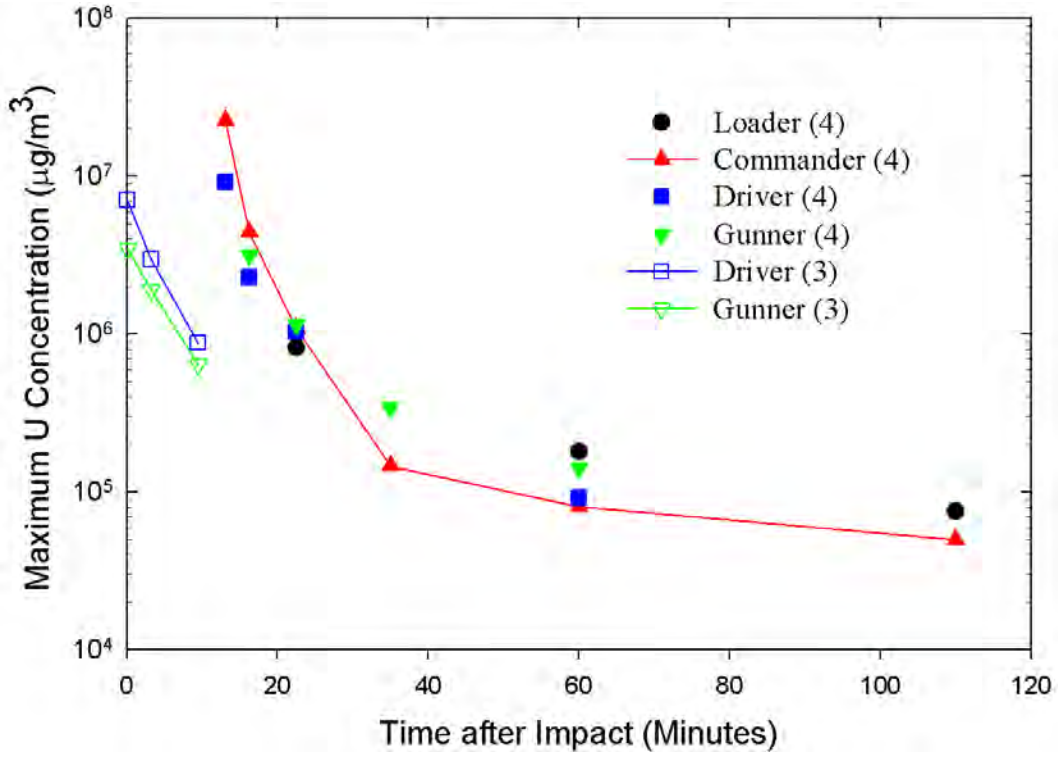

Figure 5.7. Time-Dependent Uranium Aerosol Concentrations, PI-3/4

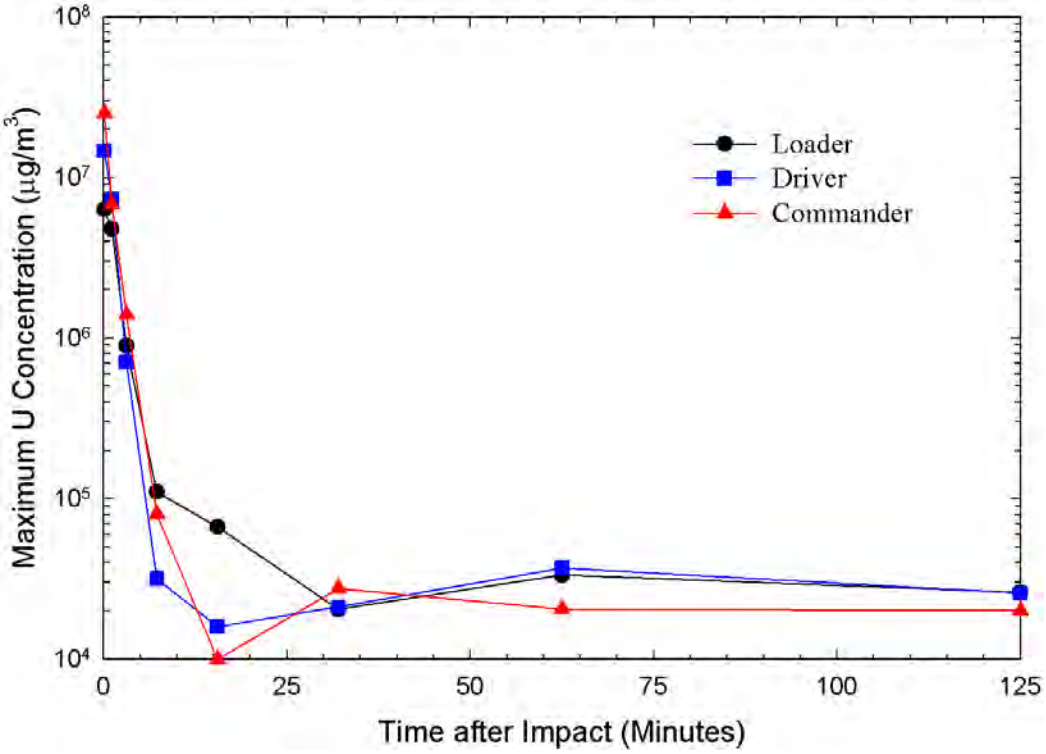

Figure 5.8. Time-Dependent Uranium Aerosol Concentrations, PI-5

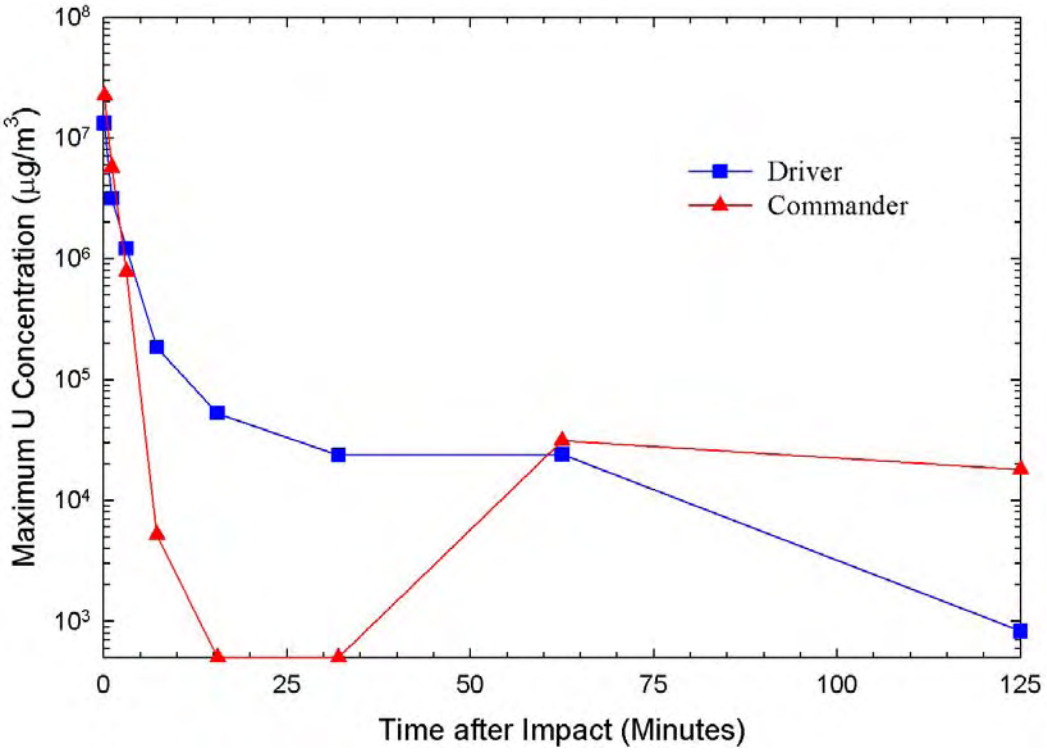

Figure 5.9. Time-Dependent Uranium Aerosol Concentrations, PI-6

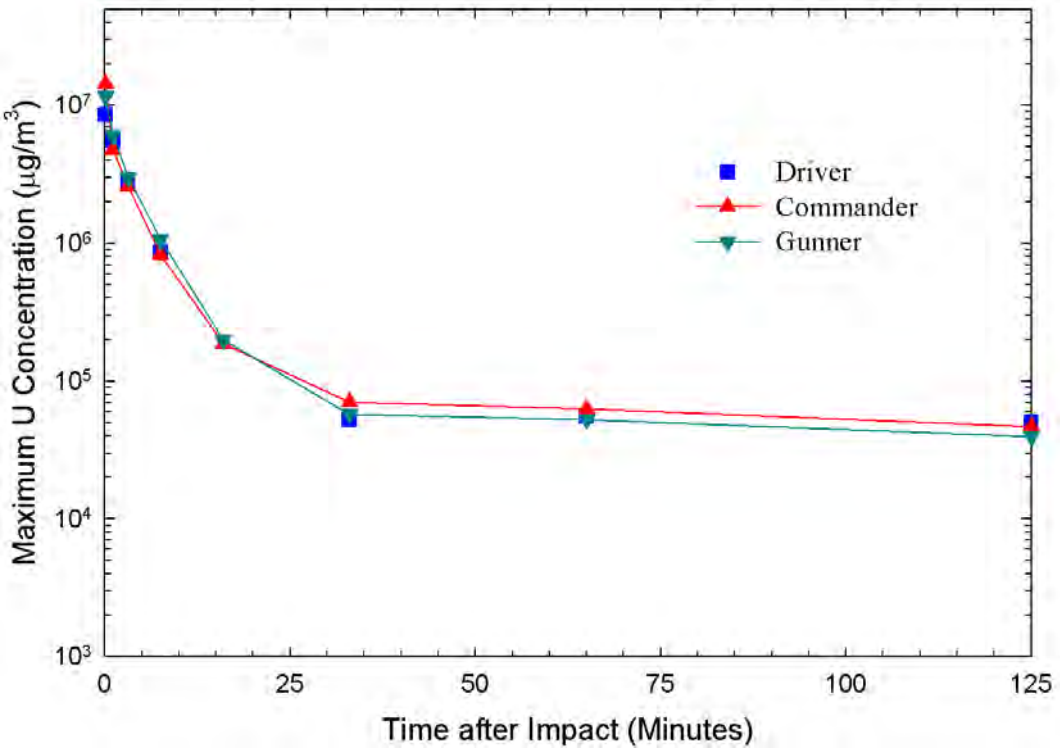

Figure 5.10. Time-Dependent Uranium Aerosol Concentrations, PI-7

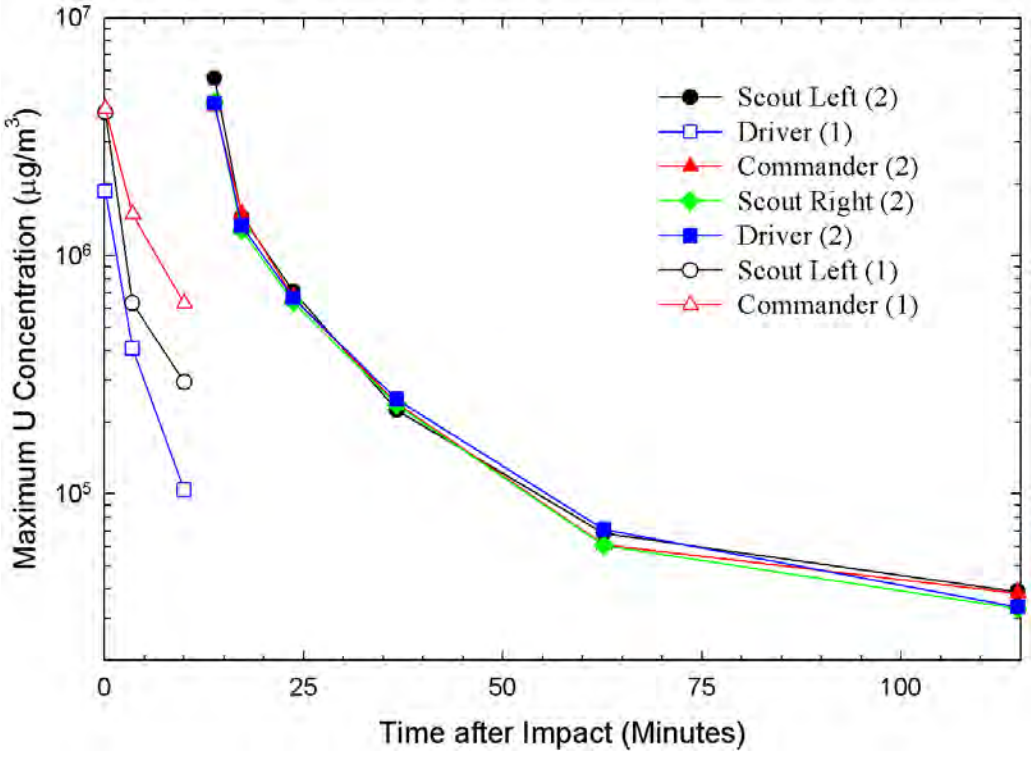

Figure 5.11. Time-Dependent Uranium Aerosol Concentrations, PII-1/2

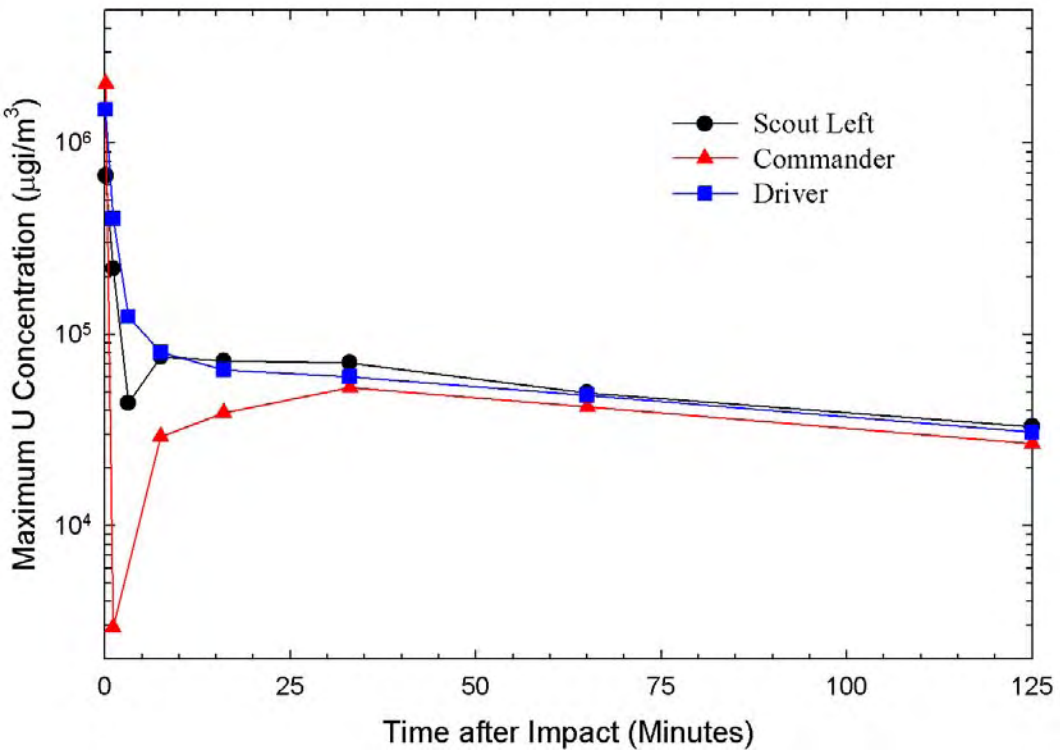

Figure 5.12. Time-Dependent Uranium Aerosol Concentrations, PII-3

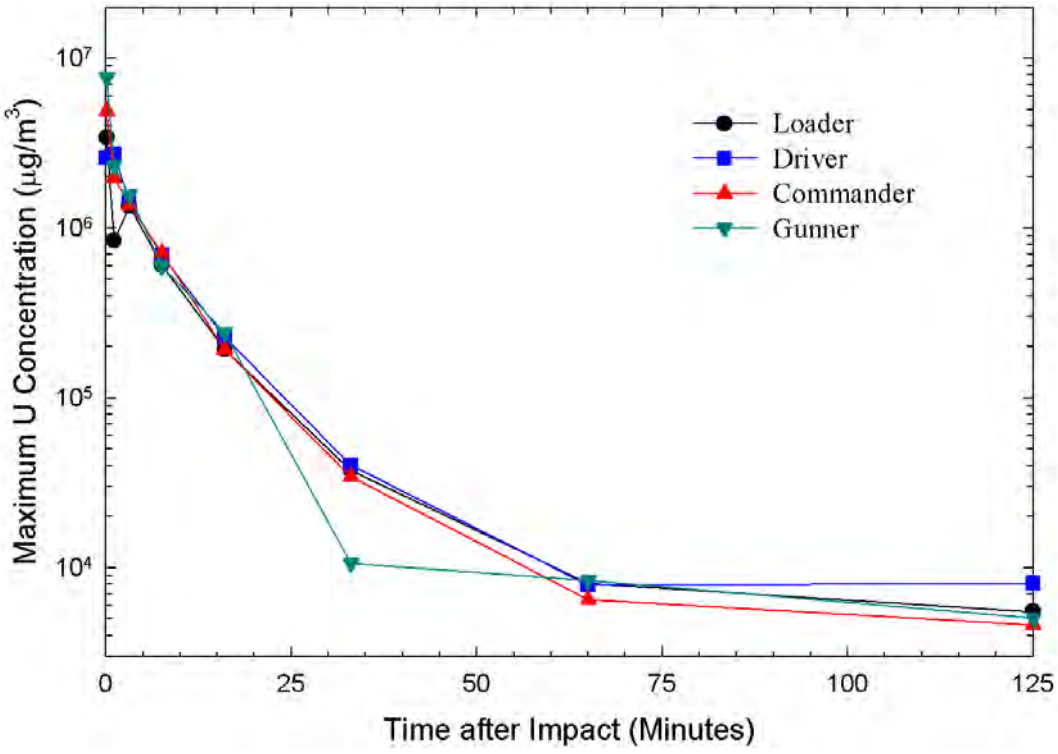

Figure 5.13. Time-Dependent Uranium Aerosol Concentrations, PIII-1

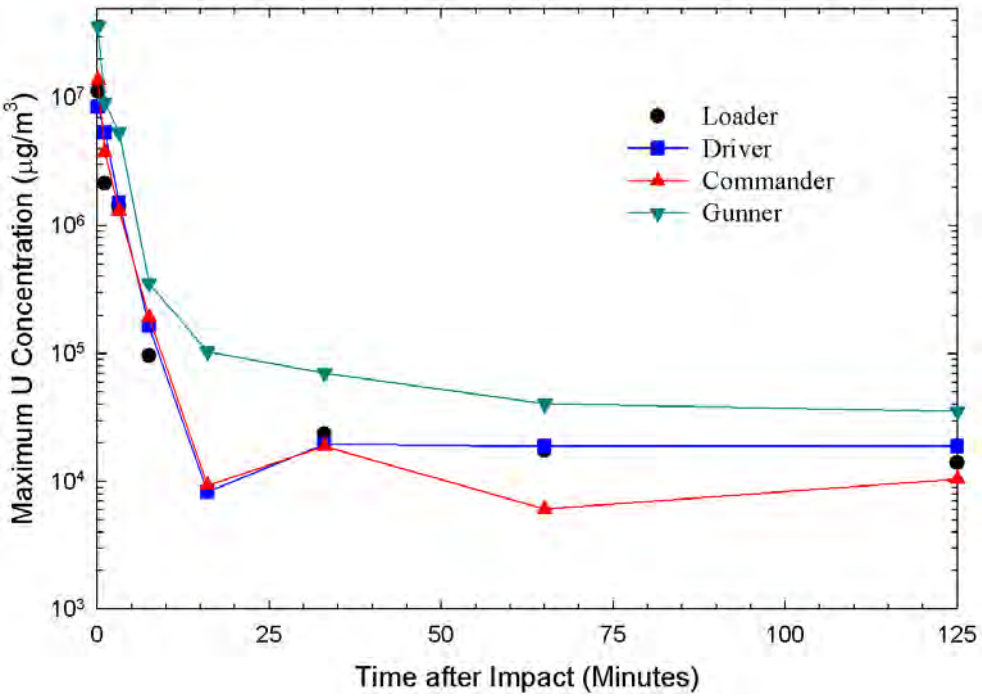

Figure 5.14. Time-Dependent Uranium Aerosol Concentrations, PIII-2

Phase I, Shot 2 (PI-2)

Shot PI-2 used basically the same shot line as PI-1, and its data are plotted in Figure 5.6. In PI-2, a metal drop door was attached to the front of the louver at the gunner's array to improve the chances of IOM filter survival. Although the door dropped as planned following the impact, the design modification was not adequate to prevent damage to the Supor filters from the transient heat and pressure phenomenon that occurs for a very short time after impact. Except for G8 (seventh-time interval), all the IOM filters located within the gunner's array, and several IOM filters at the loader's and commander's arrays and one at the driver's array were damaged. Immediately after impact, the loader's hatch was blown about three-quarters open. Video images showed that some aerosol dissipated through the hatch. It appeared that the first four or five concentrations at the loader's and commander's positions were similar. The initial concentration observed at the driver's array was slightly higher than that at the commander's position. The initial concentration at the loader's station was not available because of a damaged filter, but if the change in concentration with time between the first and second sampler holds, the loader's sampler probably would initially have been the highest of the three arrays by about a factor of two.

Phase I, Shots 3/4 (PI-3/4)

In this turret-crossing set of two shots, the turret was rotated 180º (from the turret position of PI-1 and PI-2) so the penetrator entered the commander's side and exited the loader's side. The shot line was closer to the breech than with the PI-1 and PI-2 shot lines. Following Shot 3, the loader's hatch rose twice and fell back into position. The gunner's and driver's arrays collected aerosol samples following both Shots 3 and 4. After Shot 4, the loader's hatch rose and fell back in a slightly offset position, leaving a crescent-shaped opening.

The commander's array remained covered with a solid shield during Shot 3 and its aftermath, dropping several seconds after Shot 4 was fired. It therefore collected only Shot-4 aerosols (and whatever remained suspended or was resuspended from Shot 3). The graph in Figure 5.7 includes concentrations from both shots in the actual time sequence. The results at the driver's and gunner's arrays track closely with the commander's array. The loader's shield released prematurely either by the impact of Shot 3 itself or shortly thereafter. As a result, it was open when Shot 4 was fired, and filters in several samplers were damaged. Because of this damage, only a few data points from the loader's array are available.

Phase I, Shot 5 (PI-5)

Shot 5 (Figure 5.8) was purposely fired into the breech in an attempt to produce a maximum aerosol concentration in the vehicle. The shot line was a crossing shot that was fired into the commander's side and exited the loader's side. The sampling station at the gunner's position was omitted because it was too close to the shot line. Because of the sampling design, which included the use of solid armor shields with remotely triggered drop doors and Zefluor IOM filters, all filters survived. At the time of impact, the commander's hatch cover opened and stayed open, and the loader's hatch cover popped open but fell back in an offset position, leaving a crescent-shaped opening. The initial concentration was highest at the commander's station. The next highest concentrations (in decreasing order) were at the driver's position and at the loader's position, respectively. The adjusted radioactivity collected on the commander's position C5 filter (15 to 16 min post shot) was at field blank (background) levels. However, its alpha measurement was twice as high as the background alpha level, and its beta measurement was not higher than the field blank. The photograph of the filters suggests that more sample mass was collected on filter C5 than on the field blank, filter C9. This observation was confirmed by the respective weights, but the weight information did not clarify whether the uranium concentration was significantly higher. So, in essence, this number was very low but probably slightly higher than background.

Phase I, Shot 6 (PI-6)

Shot 6 (Figure 5.9) was also fired into the breech in a shot line that crossed the turret from the loader's side to the commander's side. The commander's hatch opened and remained open, and the loader's hatch popped open and remained slightly open. The loader's position was reserved for resuspension sampling after the main aerosol sampling was complete (see Section 5.4 for details). The commander's samples from filters C5 and C6 at the commander's position were at field blank (background) levels. In this case, the alpha measurements were slightly higher for these samples than the field blank levels, but their beta results were similar. Again the photographic evidence and sample weights suggest that more total mass was collected on these filters than on the field-blank filters.

Phase I, Shot 7 (PI-7)

Shot 7 (Figure 5.10) perforated the hull through the lower portion of the turret compartment from the loader's side to the commander's side. The shattering of the aluminum witness plate severely damaged electrical lines, thus preventing relay of a feedback signal on the pressure drops on each sampler. The aluminum fragments were responsible for severing the electrical line to the driver's position D5 sampler. Following impact, the commander's hatch cover opened about an inch. The loader's array was used to measure aerosol that remained suspended in the vehicle after the normal 2-h sampling period and from resuspension during recovery activities. Of the three positions, the initial uranium concentration was

highest at the commander's position, next highest at the gunner's position, and lowest at the driver's position. The range of the differences was about a factor of two.

Phase II, Shots 1/2 (PII-1/2)

In the Bradley vehicle, the sampling positions were adjusted to accommodate the passenger compartment. Sampling positions included the driver's station in the left front of the vehicle, the commander's station inside the turret, and the right scout and left scout stations at the back of the vehicle. The Phase II, Shots 1/2 (Figure 5.11) were side-crossing shots through the passenger compartment just behind the turret shroud. The hatches remained intact, but a small amount of smoke/aerosol exited around the gun barrel shield. Although the shots did not go through the turret, the shroud door between the turret and the passenger compartment was blown off by the impact of the shot. Louver shielding was used over the commander, driver and left scout sampling arrays; they sampled during the entire 2-h period. The sampling array at the right scout's station used a solid shield so the array only sampled during the second shot, which was fired about 13 min after the first shot. The initial mass concentrations after Shot 1 were similar for the commander's and left scout's positions. The concentration observed at the driver's station was considerably lower. Concentrations differed considerably during the next two sample acquisitions, but the settling pattern was similar. After Shot 2, the initial concentration at the left scout's position was slightly higher than the others, which were very close to each other. The subsequent concentration decay curves of the four arrays were almost identical.

Phase II, Shot 3 (PII-3)

During PII-3, the turret was angled so the penetrator could be fired into the gun feeder tube just left of the cannon. The hatches remained closed after firing, but the TOW missile-loading hatch blew open and remained open. Except for the concentration found on the commander's C4 sampler (third time interval), which was at field-blank levels, the curves in Figure 5.12 track very well. The right scout's armored shield released only partly because the release pin twisted, which allowed the sampler to open only about an inch. As a result, the samplers at the right scout's position were not expected to collect much material and were not plotted. However, except for the last two data points, which are quite low, the uranium concentrations collected on these samplers track relatively well with samplers from the other arrays.

Phase III, Shot 1 (PIII-1)

Both Shots 1 and 2 were fired into the DU armor package with the turret angled so the penetrator would impact the left panel. The flames caused by hydraulic fluid (incompletely drained from the gun recoil mechanism) created smoke that briefly escaped from the perimeter of the loader's hatch and from the GPS unit location. The hydraulic fluid left an oily residue on interior surfaces. In spite of this occurrence, the samplers appear to have sampled adequately, and their settling curves track well. Only two points, one in the loader's array and one in the gunner's array, are lower than the rest (for reasons unknown).

The initial mass concentrations followed in this order (from highest to lowest concentration): Gunner > Commander > Loader > Driver (Figure 5.13).

Phase III, Shot 2 (PIII-2)

The same shot line was used in Shot 2 with a slight change in target position. The loader's hatch opened briefly and closed again. Despite the brief opening of the hatch, the concentrations were higher than those of Shot 1 possibly because the droplets of hydraulic fluid in Shot 1 caused more rapid deposition of aerosol. The settling curves are not as uniform as in Shot 1, but they show similar rates of decrease and are relatively similar in shape. The initial mass concentrations followed in the same order (from highest to lowest concentration): Gunner > Commander > Loader > Driver (Figure 5.14).

Summary Table of Uranium Aerosol Concentrations

The uranium concentrations in PI-1 through PIII-2 aerosols are listed in Table 5.5.

Table 5.5. Uranium Concentrations as a Function of Time and Position ($\mu g/m^3$)

Time Interval	Midpoint (min)	Driver	Commander	Gunner/Right Scout	Loader/Left Scout
PI-1					
0-30 sec	0.25	3.31E+06	--	--	1.69E+07
0.5-1.5 min	1.00	9.93E+05	--	--	5.89E+06
1.5-3.5 min	2.50	6.89E+05	--	--	2.67E+06
3.5-7.5 min	5.50	2.65E+05	--	--	1.23E+06
7.5-15.5 min	11.5	7.97E+04	--	--	3.39E+05
15.5-31.5 min	23.5	4.57E+04	--	--	5.51E+04
31.5-63.5 min	47.5	3.26E+04	--	--	2.23E+04
63.5-127.5 min	95.6	2.92E+04	--	--	1.99E+04
PI-2					
0-15 sec	0.125	6.00E+06	5.60E+06	--	--
0.5-1 min	0.750	2.63E+06	--	--	4.85E+06
1.5-2.5 min	2.00	1.22E+06	2.39E+06	--	2.56E+06
3.5-5.5 min	4.50	7.82E+05	1.30E+06	--	--
7.5-11.5 min	9.50	2.28E+05	3.48E+05	--	2.71E+05
15.5-31.5 min	23.5	8.65E+04	--	--	7.52E+04
31.5-79.5 min	55.5	4.32E+04	1.32E+04	1.86E+04	2.81E+04
79.5-127.5 min	104	5.32E+04	--	--	--
PI-3					
0-10 sec	0.083	7.05E+06	--	3.50E+06	--
3-3.5 min	3.25	2.98E+06	--	1.91E+06	--
9-10 min	9.50	8.80E+05	--	6.39E+05	--
PI-4 (Includes residual aerosol from Shot 3, which was fired 13 min before.)					
0-10 sec	0.083	9.21E+06	2.26E+07	--	--
3-3.5 min	3.25	2.28E+06	4.42E+06	3.17E+06	--
9-10 min	9.50	1.04E+06	1.09E+06	1.14E+06	8.19E+05
21-23 min	22.0	~Bkgd	1.46E+05	3.41E+05	--
45-49 min	47.0	9.16E+04	8.06E+04	1.41E+05	1.80E+05
93-101 min	97.0	--	4.96E+04	--	7.52E+04

Table 5.5. (cont'd)

Time Interval	Midpoint (min)	Driver	Commander	Gunner/Right Scout	Loader/Left Scout
PI-5					
0-10 sec	0.083	1.47E+07	2.52E+07	NA	6.29E+06
1-1 min, 10 sec	1.08	7.25E+06	6.81E+06	NA	4.78E+06
3-3 min, 10 sec	3.08	7.13E+05	1.40E+06	NA	8.94E+05
7-7.5 min	7.25	3.18E+04	8.07E+04	NA	1.10E+05
15-16 min	15.5	1.60E+04	~Bkgd	NA	6.68E+04
31-33 min	32.0	2.12E+04	2.78E+04	NA	2.05E+04
61-65 min	62.5	3.72E+04	2.06E+04	NA	3.35E+04
121-129 min	125	2.58E+04	2.01E+04	NA	2.62E+04
144-148 min	146	--	--	NA	2.70E+04
PI-6					
0-10 sec	0.083	1.33E+07	2.25E+07	NA	Resuspension
1-1 min, 10 sec	1.08	3.16E+06	5.71E+06	NA	Resuspension
3-3 min, 10 sec	3.08	1.22E+06	7.86E+05	NA	Resuspension
7-7.5 min	7.25	1.86E+05	5.20E+03	NA	Resuspension
15-16 min	15.5	5.29E+04	~Bkgd	NA	Resuspension
31-33 min	32.0	2.38E+04	~Bkgd	NA	Resuspension
61-65 min	62.5	2.40E+04	3.13E+04	NA	Resuspension
121-129 min	125	8.30E+02	1.81E+04	NA	Resuspension
PI-7					
0-10 sec	0.083	8.56E+06	1.43E+07	1.17E+07	Resuspension
1-1 min, 10 sec	1.08	5.56E+06	4.74E+06	6.07E+06	Resuspension
3-3 min, 15 sec	3.13	2.81E+06	2.59E+06	3.02E+06	Resuspension
7-8 min	7.50	8.74E+05	8.28E+05	1.06E+06	Resuspension
15-17 min	16.0	--	1.86E+05	1.99E+05	Resuspension
31-35 min	33.0	5.27E+04	7.08E+04	5.77E+04	Resuspension
61-69 min	65.0	5.55E+04	6.26E+04	5.26E+04	Resuspension
121-129 min	125	5.09E+04	4.69E+04	3.96E+04	Resuspension
PII-1					
0-10 sec	0.083	1.87E+06	4.15E+06	--	4.00E+06
3-4 min	3.50	4.08E+05	1.49E+06	--	6.32E+05
9-11 min	10.0	1.04E+05	6.31E+05	--	2.95E+05
PII-2 (Includes residual aerosol from Shot 1 fired 14 min before.)					
0-10 sec	0.083	4.37E+06	4.23E+06	4.43E+06	5.56E+06
3-4 min	3.50	1.34E+06	1.50E+06	1.28E+06	1.46E+06
9-11 min	10.0	6.63E+05	6.72E+05	6.40E+05	7.08E+05
21-25 min	23.0	2.50E+05	2.40E+05	2.37E+05	2.26E+05
45-53 min	49.0	7.12E+04	6.13E+04	6.08E+04	6.87E+04
93-109 min	101	3.35E+04	3.82E+04	3.30E+04	3.90E+04
PII-3					
0-10 sec	0.083	1.50E+06	2.05E+06	5.14E+05	6.75E+05
1-1 min, 10 sec	1.08	4.05E+05	2.94E+03	2.77E+05	2.21E+05
3-3 min, 15 sec	3.13	1.24E+05	~Bkgd	1.32E+05	4.38E+04
7-8 min	7.50	8.06E+04	2.92E+04	7.22E+04	7.62E+04
15-17 min	16.0	6.53E+04	3.89E+04	5.43E+04	7.30E+04
31-35 min	33.0	5.99E+04	5.25E+04	4.93E+04	7.11E+04
61-69 min	65.0	4.79E+04	4.19E+04	4.63E+02	4.95E+04
121-129 min	125	3.07E+04	2.69E+04	1.18E+03	3.30E+04

Table 5.5. (cont'd)

Time Interval	Midpoint (min)	Driver	Commander	Gunner/Right Scout	Loader/Left Scout
PIII-1					
0-10 sec	0.083	2.59E+06	4.89E+06	7.67E+06	3.42E+06
1-1 min, 10 sec	1.08	2.72E+06	1.97E+06	2.32E+06	8.45E+05
3-3 min 15 sec	3.13	1.42E+06	1.37E+06	1.56E+06	1.35E+06
7-8 min	7.50	6.96E+05	7.15E+05	5.97E+05	6.08E+05
15-17 min	16.0	2.27E+05	1.93E+05	2.42E+05	1.92E+05
31-35 min	33.0	4.02E+04	3.43E+04	1.06E+04	3.74E+04
61-69 min	65.0	7.94E+03	6.48E+03	8.44E+03	8.12E+03
121-129 min	125	8.07E+03	4.60E+03	5.04E+03	5.53E+03
PIII-2					
0-10 sec	0.083	8.49E+06	1.38E+07	3.62E+07	1.13E+07
1-1 min, 10 sec	1.08	5.32E+06	3.75E+06	9.20E+06	2.15E+06
3-3 min, 15 sec	3.13	1.53E+06	1.30E+06	5.36E+06	1.41E+06
7-8 min	7.50	1.63E+05	1.91E+05	3.56E+05	9.65E+04
15-17 min	16.0	8.29E+03	9.29E+03	1.04E+05	--
31-35 min	33.0	1.95E+04	1.89E+04	7.04E+04	2.38E+04
61-69 min	65.0	1.89E+04	6.10E+03	4.04E+04	1.74E+04
121-129 min	125	1.88E+04	1.05E+04	3.53E+04	1.40E+04

5.1.3 Cascade Impactor Substrates

The CIs provided a measure of particle size as a function of time. Samples were collected over eight time increments for a minimum of 10 sec to a maximum of 64 min within the 2-h sampling period that immediately followed impact. As with the filter cassettes, these CIs were conditioned by placing them in a chamber with a solution to achieve a relative humidity of about 40% to simulate the local ambient humidity. This approach departs from some gravimetric procedures, in which samples are desiccated, usually for 24 h, before being weighed. The total mass and radioactivity-derived uranium mass data are listed by shot in Appendix A, Tables A.19 through A.32. Mixed cellulose ester substrates, which are hydrophilic, were used in the CI samplers. Two photographs from PIII-2 illustrate the appearance of these substrates following sample collection (Figure 5.15). Both sets of substrates were from the gunner's position, beginning with Stage 1 in the upper left and ending with the backup filter at the lower right. The substrates in the left set are from the first time interval (10 sec beginning 5 sec post shot), and those in the right set are from the third time interval (15 sec beginning 3 min, 5 sec post shot). The discoloration in the Stage-9 substrate on the left sample set may reflect differences in elemental composition of particles deposited on this stage.

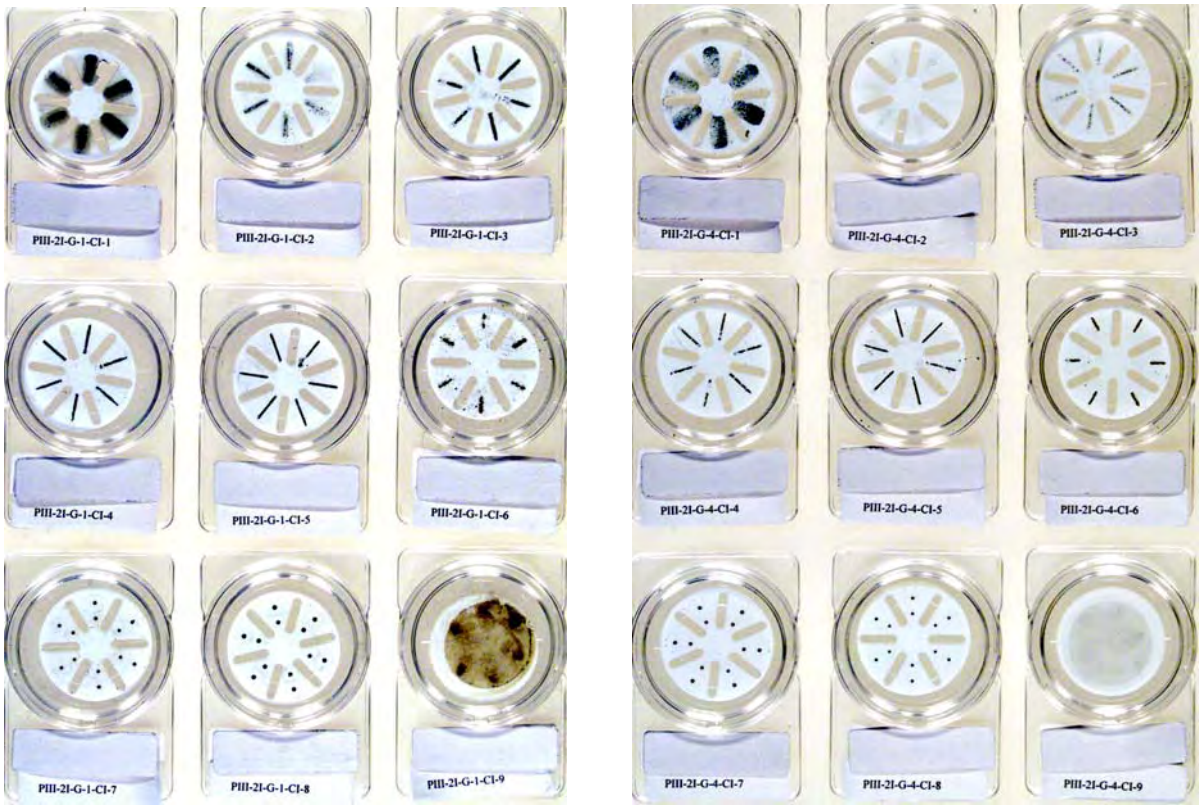

Figure 5.15. CI Substrates Stages 1 Through 8 and Bottom Filter from PIII-2, Gunner's Position

5.1.3.1 Gravimetric Analysis

Many post-test CI substrates weighed less than pre-test weights in spite of various efforts to resolve this difficulty. The weights on the first several stages were usually positive, but negative weight changes were consistently measured on many of the lower stages of the MCE substrates. Cellulose substrates are recognized as being a poor material for gravimetric analysis and are more commonly analyzed by chemical means. In this case, the MCE substrates were selected based on their availability and ease-of-use for radioactivity analysis. Unfortunately, the lack of positive weight changes for a full set of CI stages prevented meaningful evaluation of mass as a function of particle size for these samples. As a consequence, MMAD analysis could not be conducted.

Inconsistencies in water retention and evaporation may be the sole reason for the negative weight changes obtained. However, another hypothesis for the apparent weight losses is that perhaps the temperature/ pressure pulse somehow caused a change in the water retention property of the substrate. To discern whether this suggestion had any merit, one unused and one used substrate that had collected only a small amount of sample material were examined under an SEM. The micrographs taken (Figures 5.16 and 5.17) show some apparent difference in the matrix, but it was uncertain whether this difference was relevant to the issue. It appeared that the center of the used substrate showed less porosity than the unused substrate, as if it melted slightly. Imagining the filter as three concentric circles, the inner circle of the used substrate had a smeared, glazed appearance, almost as if many of the pores in the matrix had

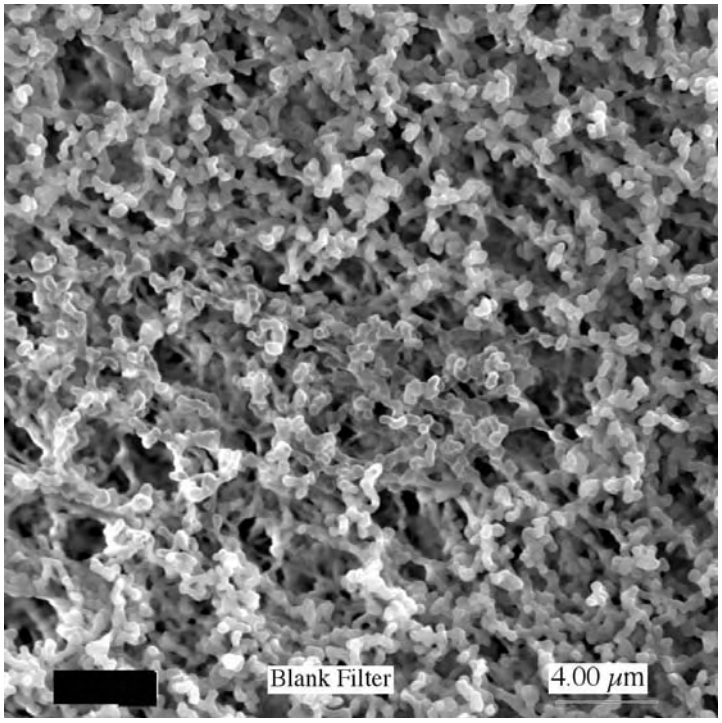

Figure 5.16. SEM Micrograph of an Unused Substrate (Black rectangles in lower edge of photos cover lab notations.)

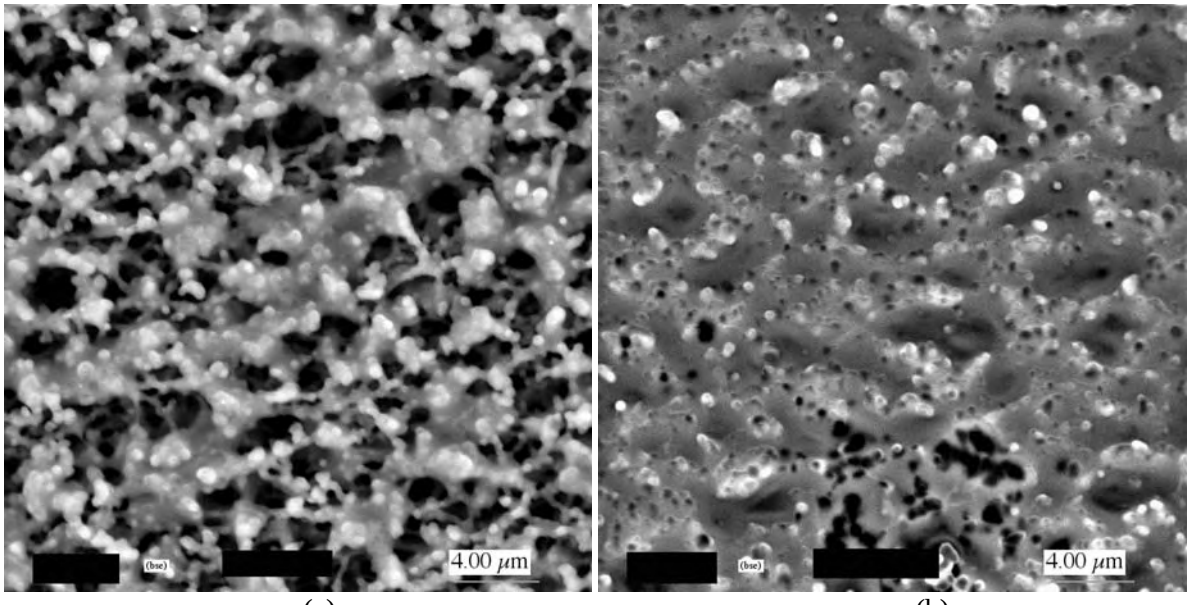

(a) (b)

Figure 5.17. SEM Micrographs of a Post Shot Substrate [Showing Its Fiber Structure in the Transitory Circle (a) and the Center Circle (b)]

been filled in. The middle circle showed a gradation in this characteristic but still appeared to be different than the unused substrate. The outer circle was similar to the unused substrate, though the pores were not

quite as pronounced. The differences observed between the unused substrate and the used substrate do not necessarily explain the negative weights obtained, but they do suggest that there may be a basis for the hypothesis that an event caused by the impact influenced substrate weight.

5.1.3.2 Radioactivity-Derived Uranium Masses

The radioactivity measurements of the Marple CI samples are presented in Appendix A, Table A.19 through A.32. Because it was determined that the uranium in the aerosol was not in secular equilibrium at the time about half of the samples were counted, the calculations of uranium mass based on radioactivity measurements were adjusted for ingrowth. In addition to the radioactivity measurements, a few samples were measured chemically for uranium. The larger mass of uranium derived either from the ingrowth-adjusted activity measurement or measured using a chemical technique was used in the aerosol analyses. The strategy used to calculate uranium mass is presented in Appendix A.

The Marple CI used for sample collection had eight stages plus the final (bottom) filter that collected particulate material. The nominal flow rate of this type of CI was 2.0 Lpm. For each set of CI data (i.e., data obtained during a specific time interval during one shot), the uranium masses on corresponding stages of the field-blank CI were subtracted from the sample CI stages to calculate the net DU in micrograms for each stage.

An example of the uranium mass by stage (rounded to the nearest integer) is presented in Table 5.6, which presents the data set for the PI-1 loader's position using the 5- to 35-sec, post-impact time interval. The table lists the mass of uranium collected on each sample substrate and field blank, the net mass of uranium, and the nominal effective cutoff diameter (ECD, μm) at 2.0 Lpm. These data were used to evaluate aerosol particle size distributions, which are discussed in Section 5.5.

Table 5.6. Example of Uranium Mass on CI Stages, First Sampling Interval, PI-1 (Loader's Array)

Stage #	Nominal ECD (μm)	Uranium Mass (μg)		Net DU (μg)
		Sample	Field Blank	
1	21.3	317	144	173
2	14.8	190	5	185
3	9.8	323	2	321
4	6.0	293	0	293
5	3.5	558	1	557
6	1.55	583	8	575
7	0.93	276	3	273
8	0.53	600	5	595
Bottom Filter	<0.53	859	7	852

5.1.4 Cyclone Stages and Backup Filters

The five-stage cyclone collected sample material for about 2 h beginning 5 sec post impact. As a result, it provided particle size discrimination integrated over the total sampling period and collected sufficient aerosol for various chemical analyses. The cyclone operated for all shots except for PI-5 in which the sampling lines were severed by fragments. The PFDB was connected to the terminal stage for PI-1. Theoretically, it collected particles <0.7 μm at its intended flow rate of 14 Lpm. However, there was some concern about whether the seal between the PFDB and the cyclone was tight**,** and its use was

discontinued. Analysis by SEM later revealed that material on the filters was consistent with collection of very fine particles (0.1 to 0.5 μm) but probably few that would qualify as being in the ultrafine range (less than 0.1 μm). The PFDB was replaced with the four-unit backup filter assembly in all other shots.

The cyclone stage residues were weighed and analyzed by gamma spectrometry because the residue storage containers (glass or V-vials) did not readily lend themselves to proportional counting. The PFDB and backup filters were weighed and alpha/beta counted. After these activities were completed, one cyclone sample set from each phase and the cyclone samples from the hull shot were selected for further analysis. These residues were subdivided and sent to USACHPPM, PNNL, and LRRI for the chemical and physical evaluations described previously in Section 3.9.

The residues collected by each cyclone stage were weighed and transferred to glass or V-vials for further handling and storage. In PIII-2, there was evidence of a poor seal between Stages 2 and 3, and most of the material that should have been collected in Stages 1 or 2 was collected in the Stage 3 grit chamber. The lower stages had collected material, and this material appeared to be similar to the aerosol residues collected in these chambers during previous shots. Even so, it seemed prudent to resuspend the full sample and re-collect it through the cyclone stages. The resuspension and recollection operation was conducted at LRRI where the powder was aerosolized using a Devilbiss dry powder atomizer[(a)] and classified using a five-stage cyclone train similar to the one used in the test. The cyclone was operated at 14 Lpm. Residues collected on the Stage 1 and 2 grit chambers were negligible, although sufficient sample material was collected on Stage 3 for SEM analysis. It is believed that the difference in total weights between the pre-resuspension (left side of column) and the post-resuspension (right side of column) weight is due to losses in the cyclone walls and connecting tubes during the resuspension process.

The cyclone residues underwent gamma spectrometry, and the process of deriving uranium masses from gamma radioactivity data is presented in Appendix A, Section A.2.2. A summary of the total residue mass and the uranium mass are presented by phase and shot and by stage in Tables 5.7 through 5.9. The percentage of mass in each stage is derived solely from the stages within the cyclone and does not include the mass collected on the PFDB or backup filters. The total mass is rounded to three significant figures. Cyclone residues and backup filters from PI-3/4 and PI-7, PII-3, and PIII-2 also were analyzed by chemical methods. Results of these analyses are presented in Section 5.6. Agreement between them was poorer than expected and underscores the difficulty of using gamma spectrometry on these samples to derive uranium masses.

The PFDB filters from PI-1 were collected for other analyses but were not weighed. The four backup filters in the remaining shots were weighed prior to radiological and chemical analyses. They constituted between 0.02 and 0.04% of the weight of the total cyclone-collected sample. The total masses collected by the four backup filters in each shot (except PI-1, which used the PFDB) are listed by phase and shot in Table 5.10. Uranium masses were not calculated for the backup filters because the fit between the beta-derived uranium concentrations and the direct chemistry measurements was not sufficiently robust to apply to the data set.

(a) Devilbiss Co., Somerset, Pennsylvania.

Table 5.7. Phase-I Cyclone Residue Masses

Phase/Shot Total Mass in Stage 1-5	Stage	Total Mass (mg)	% of Mass in Stage	Derived U Mass (mg)	% of U in Total Mass on Stage
PI-1	1	54.0	17.2	29.8	55.2
	2	76.0	24.2	47.7	62.7
Total mass:	3	58.0	18.5	33.1	57.0
314.0 mg	4	71.0	22.6	37.8	53.2
	5	55.0	17.5	32.9	59.6
PI-2	1	34.2	13.4	18.1	52.9
	2	62.5	24.5	32.8	52.1
Total mass	3	35.1	13.8	20.0	57.1
254.7 mg	4	46.7	18.4	26.3	56.3
	5	76.2	29.9	36.8	48.3
PI-3/4	1	46.5	6.6	23.5	50.5
	2	276	39.3	13.3	47.9
Total Mass	3	110	15.6	53.1	48.5
702.8 mg	4	165	23.5	91.4	55.4
	5	105	15.0	44.1	41.9
PI-5 (Did not run)					
PI-6	1	8.53	21.4	5.10	59.8
	2	7.40	18.5	5.27	71.1
Total Mass	3	11.3	28.3	7.01	62.1
39.9 mg	4	9.57	24.0	7.74	80.9
	5	3.10	7.8	<Min Det.	--
PI-7	1	125	20.3	64.1	51.3
	2	191	30.9	124	64.8
Total Mass	3	131	21.3	74.7	56.9
616.8 mg	4	98.1	15.9	65.4	66.7
	5	71.5	11.6	42.5	59.4

Table 5.8. Phase-II Cyclone Residue Masses

Phase/Shot Total Mass in Stages 1-5	Stage	Total Mass (mg)	% of Mass in Stage	Derived U Mass (mg)	% of U in Total Mass on Stage
PII-1/2	1	76.4	12.5	22.2	29.1
	2	158	25.8	59.2	37.4
Total Mass	3	152	24.7	26.0	17.1
613.5 mg	4	144	23.5	49.3	34.2
	5	82.9	13.5	26.8	32.3
PII-3	1	48.0	17.5	0.438	0.91
	2	54.4	19.8	4.25	7.82
Total Mass	3	57.8	21.0	7.64	13.2
274.9 mg	4	57.2	20.8	6.63	11.6
	5	57.5	20.9	8.64	15.0

Table 5.9. Phase-III Cyclone Residue Masses

Phase/Shot Total Mass in Stages 1-5	Stage	Total Mass (mg)		% of Mass in Stage	Derived U Mass (mg)	% of U in Total Mass on Stage
PIII-1	1	29.9		10.0	22.3	74.8
	2	29.1		9.7	42.1	>100
Total Mass 299.85 mg	3	26.1		8.7	40.7	>100
	4	75.5		25.2	22.5	29.8
	5	139		46.4	50.6	36.4
PIII-2	1	(pre) 8.45	(post) 57.8	(post) 29.7	(pre) 1.18	13.9
Total Mass	2	0.957	Trace	--	(pre) 0.108	11.3
194.5 mg	3	132	1.3	0.7	(pre) 107	81.1
	4	88.6	72.5	37.3	(pre) 68.2	77.0
	5	69.5	62.9	32.3	(pre) 56.1	80.1

Table 5.10. Cyclone Backup Filter Masses

Phase/Shot	Total Mass (mg)
PI-2	69.0
PI-3/4	174
PI-5	46.7
PI-6	63.7
PI-7	113
PII-1/2	172
PII-3	53.0
PIII-1	72.5
PIII-2	83.7

5.1.5 Moving Filter

The MVF was included in the aerosol sampling design specifically to collect aerosols within the first few seconds after impact when no other samplers were operating, and to collect sample material at additional programmed intervals, thereby providing concentration measurements redundant to those obtained using the IOM filters but at a higher time resolution. Although the MVF was protected in a metal box, its sampling success was mixed. When the sampler ran, it collected aerosols as intended. However, under the test conditions, several incidents rendered the device ineffective for many of the shots.

A short description of its operation by phase and shot follows:

- PI-1: Worked initially, but the filter tape became clogged with aerosol when programmed to sample for a longer time period.
- PI-2: Filter tape was unavailable.
- PI-3/4: The intent was to run the MVF for 10 min following the first impact and then restart it 5 sec before the second impact, operating it periodically until the end of the second sampling period. However, the tape, which was in two sections that were not connected, separated and recorded only the first 10 min following Shot 3.

- PI-5: A fragment severed the vacuum line, preventing aerosol collection.
- PI-6: A fragment directly entered the inlet, plugging it and preventing aerosol collection.
- PI-7: Fragments from the aluminum witness plate (located in front of the catch plate protecting the facility from damage), which shattered unexpectedly, severed the electrical line to the sampler.
- PII-1/2: Spall liner fibers burned through the filter strip, stopping movement.
- PII-3: Operated as programmed.
- PIII-1 and PIII-2: Operated as programmed.
- PIV-1 and PIV-3: Operated as programmed
- PIV-4: A fragment apparently severed the vacuum line, thereby preventing aerosol collection.

Following sampler recovery, the filter tapes were cut into 2.5-cm segments. Alpha and beta activity were measured for each segment, and the radioactivity-derived uranium masses were calculated (Appendix A, Tables A.33 to A.37). Sampling times, flow rates, volumes, and uranium aerosol concentrations also are provided in the table. Chemical and physical evaluations were conducted on three sample segments (see Section 5.6.1.4).

A photograph of the first several segments of MVF tape from PI-1 (Figure 5.18) distinguishes this sample from the other MVF samples because its operation alternated between stationary and moving intervals in pre-programmed and successively longer time increments (timing sequence provided in Table A.33). In later shots, the filter ran continually during specified intervals. In the photograph of the filter tape from PI-1, the effect of the heavier deposition during stationary cycles is evident in segments 1 and 3 from the left compared to the moving cycle of segment 2 and the edge of segment 4. The scratches on the filter medium in this photograph demonstrate the difficulty in handling this medium without disturbing the collected sample.

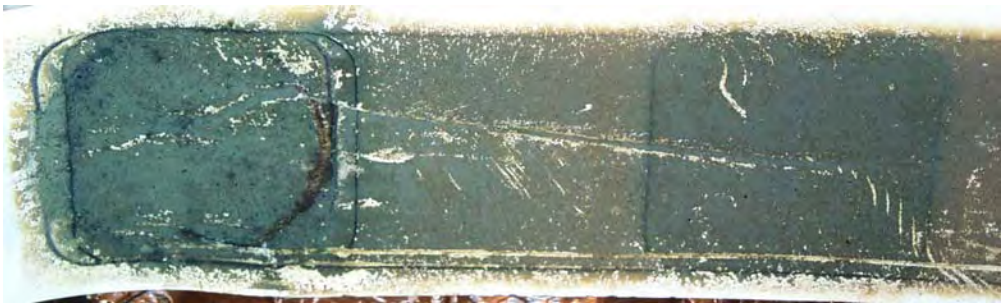

Figure 5.18. Moving Filter from PI-1

After the first few sampling intervals, the sampler became clogged. Consequently, the later data points were not used in the evaluation of the aerosol data. An estimate of the radioactivity-derived uranium collected in the aerosol during the first minute is shown in Table 5.11 in which the initial concentration on

Table 5.11. Aerosol Collected on MVF Tape During Phase I, Shot 1

Time Interval	Volume (Lpm)	Total Aerosol Collected (mg)	Estimated Collection Rate (μg/m^3-sec)
0 to 5 sec—Stationary	1.57	18.2	2.3E+06
5 to 15 sec—Moving	3.13	24.4	7.8E+05
15 to 25 sec—Stationary	3.13	24.1	7.8E+05
25 to 35 sec—Moving[(a)]	1.57	9.17	5.8E+05
35 to 55 sec—Stationary	6.27	26.8	2.1E+05
(a) Best guess on time, differs from programming.			

a per second basis peaked at 2.3 g/m^3 (2.36 x 10^6 μg/m^3) tapering to 0.21 g/m^3 (2.1 x 10^5 μg/m^3) by the end of the first minute.

Four sets of MVF data provided time-sequenced uranium mass concentrations, especially within the initial interval up to 30 sec post impact. These activities were adjusted for ingrowth and converted to uranium masses. These four data sets and the resulting mass concentration plots are discussed in the following paragraphs.

Figure 5.19 shows the uranium mass concentrations as determined by the MVF within the first minute after the impact for PI-3. The amount of filter tape was not adequate to continue the sampling into Shot 4. The data showed a rapid increase of uranium concentration with a peak concentration of 6.02 x 10^6 μg/m^3 occurring 12.9 sec after the sampling started. Also plotted in Figure 5.19 for comparison are uranium concentrations obtained with IOM samplers at the driver's and gunner's sampling arrays. The uranium concentration results for the MVF and IOM samplers are in good agreement despite the fact that the MVF was placed at the floor of the turret. The MVF provided more detailed information on the initial concentration profile.

The uranium mass concentrations for PII-3 as determined by the MVF, which sampled periodically within the 120-min, post-impact sampling period, are shown in Figure 5.20. A rapid increase of uranium concentration with a peak concentration of 1.07 x 10^6 μg/m^3 is apparent about 7.2 sec after the sampling began. Also plotted in Figure 5.20 are uranium concentrations obtained with IOM samplers at the driver's, commander's, right scout's, and left scout's sampling arrays. The uranium concentrations obtained from the MVF samples were at levels between the IOM concentrations obtained at the left and right scouts' positions, especially for the first eight min (a surprising result given that the right scout's shield released only marginally after this shot). This close agreement may be partly because the MVF was placed on the floor of the passenger compartment between the scouts' positions. The relatively open space in the Bradley vehicle may have been responsible for the fairly uniform aerosol concentration from the driver's position to the scouts' positions in the passenger compartment.

The uranium mass concentrations as obtained periodically by the MVF during the 120-min, post-impact sampling period for PIII-1 are shown in Figure 5.21. The data showed a rapid increase of uranium concentration with a peak concentration of 8.17 x 10^6 μg/m^3 at about 7.2 sec after sampling began. There

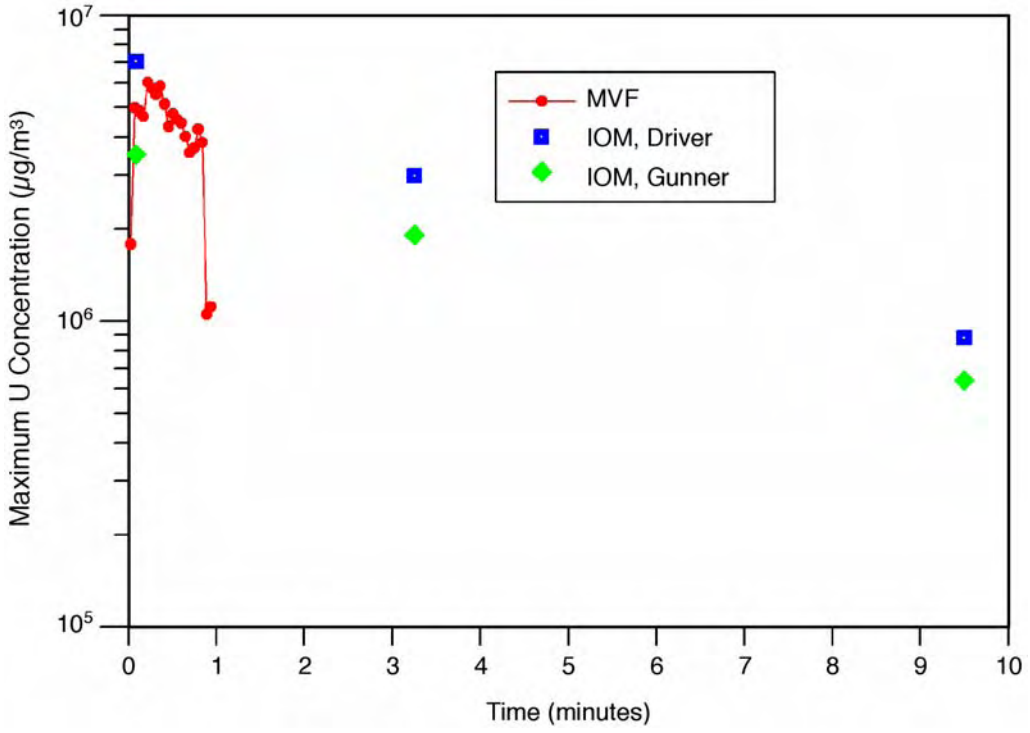

Figure 5.19. Uranium Mass Concentrations as Measured by the MVF and IOM Samplers, PI-3/4

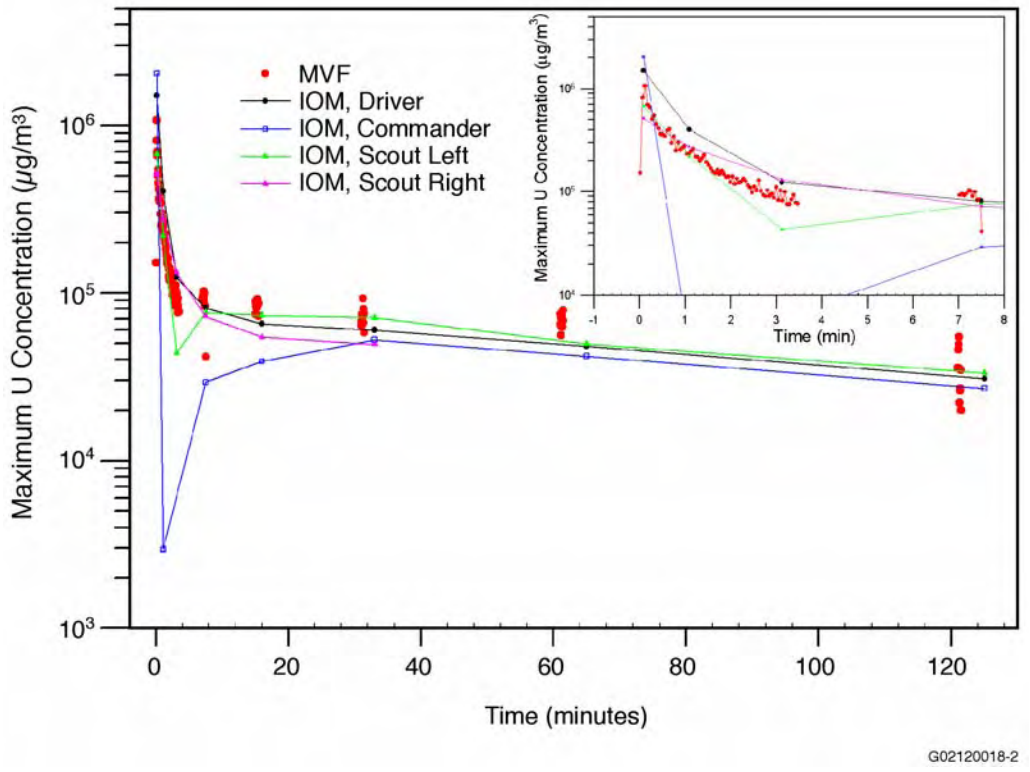

Figure 5.20. Uranium Mass Concentrations as Measured by the MVF and IOM Samplers, PII-3

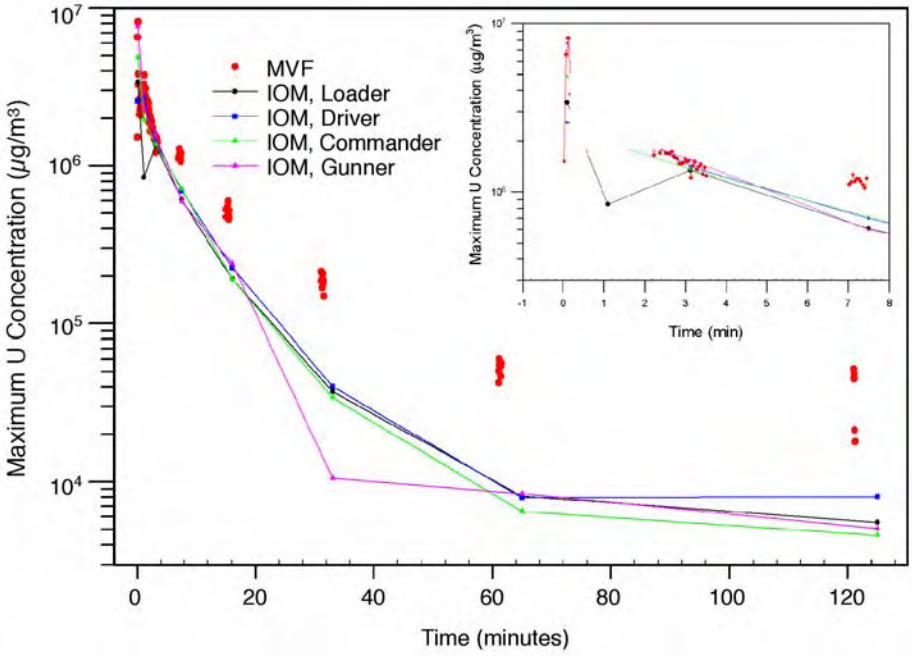

Figure 5.21. Uranium Mass Concentrations as Measured by the MVF and IOM Samplers, PIII-1

was a second and lower peak of 3.76 x 10^6 µg/m^3 at about 73.4 sec. Also plotted in the same figure are uranium concentrations obtained with IOM samplers at the loader's, driver's, commander's, and gunner's sampling arrays. The results are in very good agreement for uranium concentrations for the MVF and IOM filter samplers for the first 3.5 min, but the MVF concentrations were higher by a factor of 0.5 than those obtained by the IOMs afterward. The reason for this difference is not known.

The uranium mass concentration obtained periodically by the MVF during the 120-min post-impact sampling period for PIII-2 is shown in Figure 5.22. The data showed the peak concentration of 9.10 x 10^6 µg/m^3 was reached within 2 sec post impact. Also plotted in the same figure are uranium concentrations obtained with IOM samplers at the loader's, driver's, commander's, and gunner's sampling arrays. The results showed very good agreement in mass concentrations between the MVF and IOM filter samplers, especially at the driver's, loader's, and commander's positions. The IOM concentration obtained at the gunner's position was a factor of 2.5 to 3.5 higher than the other positions.

These limited sets of data showed detailed aerosol concentration profiles that generally agreed with the aerosol concentration data obtained with the IOM samplers. These data indicate that the maximum uranium mass concentrations were reached rapidly in the first few seconds. A summary of the results by shot is provided in Table 5.12.

Three segments (but not the whole tape) of the PIII-2 MVF tape, showing the beginning, middle, and end are shown in the photographs in Figure 5.23. The segments clearly show the change in color of the depositing aerosol with time beginning from the top left, probably related both to change in mass and possibly to change in the aerosol composition. Note that reflected light in the right-hand half of the lowest tape strip lightened this section beyond its actual color.

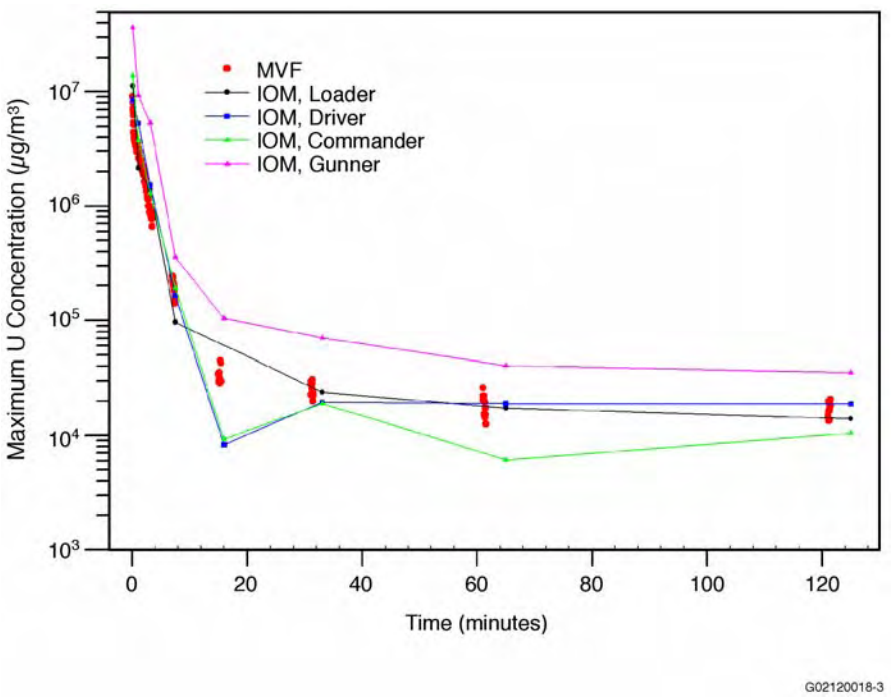

Figure 5.22. Uranium Mass Concentrations as Measured by the MVF and IOM Samplers, PIII-2

Table 5.12. Peak Concentration Reached Immediately after Impact as Measured by the MVF

Phase/Shot	Concentration Peak/Time	Avg. U Conc. First Minute	Avg. U Conc. Over 121.5 min
PI-3	6.02E+06 µg/m^3 (12.9 sec)	4.55E+06 µg/m^3	--
PII-3	1.07E+06 µg/m^3 (7.2 sec)	4.36E+05µg/m^3	1.57E+05 µg/m^3
PIII-1	8.17E+06 µg/m^3 (7.2 sec)	2.99E+06 µg/m^3	1.54E+06 µg/m^3
PIII-2	9.10E+06 µg/m^3 (1.4 sec)	4.53E+06 µg/m^3	1.49E+06 µg/m^3

Figure 5.23. MVF Tape from Three Time Intervals Following the PIII-2 Shot

5.2 Exterior Aerosol Data

Although the lack of ventilation and air movement inside the Superbox is unlike natural ventilation in open-air shots, collected particulate material should provide an upper bound of aerosols dispersed outside the struck vehicle and available for resuspension in the environment and hand-to-mouth transfer. Sampling was conducted to provide a qualitative understanding of the material made airborne by the perforation of the target. It is believed that extrapolating particle deposition and resuspension inside the Superbox to an open-air environment is likely to overestimate this source term.

Hi-Vol samplers were used to collect aerosols external to the target vehicle for baseline and gross estimates of suspended particles near the impacted vehicle. However, the beta radioactivity detected on these filters could not be reconciled with the ICP-MS results that were run on three of these samples. Because these samples may have been misidentified and were not critical to the aerosol evaluations, they were not subjected to further analysis.

Andersen CIs were used to evaluate the suspended particle size distributions. Exterior CI samples using the 81-mm, 8-stage Andersen impactors were obtained for shots beginning with PI-5. The nominal flow rate for this type of sampler is 28 Lpm. With the exception of both units of PI-7, which ran 1 min each, and PIII-2, CI Unit 1, all samplers ran for 2 min. The on-and-off switch controlling PIII-2 CI-1 was incorrectly wired, and the sample ran for 5 h, allowing it to collect much more aerosol material.

Table 5.13 shows an example of the uranium masses derived from gamma spectrometry and presented by stage of the PI-5, CI-1 set of exterior CI substrates and bottom filter. The total uranium masses were collected on the stages and bottom filter of each Andersen CI are listed in Table 5.14. The full data set for external CI flows, volumes, uranium masses, uranium concentrations, and propagation of uncertainties are provided in Appendix A, Table A.39. Variations in the results obtained from samples collected by the two CIs are believed to be related to the difference in proximity of the samplers to the entrance and exit holes. The data identified as “PSB-C4” refers to Superbox C4 test in which a C4 explosive charge was used to create a blast vibration similar to impact testing. This test was conducted after Phase III to evaluate DU oxide deposited on the Superbox fragmentation shield surfaces and could be potentially resuspended during the remaining Phase II shots.

Table 5.13. Example of Exterior Andersen CI Data

Stage	Nominal ECD (µm) at 28.3 Lpm	Derived U Mass (µg)
1	9.0	832
2	5.8	560
3	4.7	81.6
4	3.3	341
5	2.1	260
6	1.1	199
7	0.7	194
8	0.4	188
Bottom Filter	0.25	207

Table 5.14. Exterior Andersen CI Sampling Flow Rates and Uranium Masses Collected

Sample	First CI		Second CI	
	Average Flow Rate (Lpm)	U Mass (mg)	Average Flow Rate (Lpm)	U Mass (mg)
PI-5	27.2	2.86	0[(a)]	--
PI-6	19.5	1.07	20.1	2.30
PI-7	23.5	0.760	29.4	1.62
PII-1/2	28.1	1.37	28.9	1.91
PII-3	27.7	6.02	28.3	6.72
PIII-1	27.0	1.47	27.3	0.486
PIII-2	30.1	62.8	28.7	3.70
PSB-C4E	28.6	0.293	25.2	0.915

(a) A fragment cut the sample line.

5.3 Contamination Surveys, Deposition Trays, and Instrumentation Surveys

Wipe-test surveys to determine removable contamination levels were conducted during each test of the Capstone DU Aerosol Study. Summaries of vehicle interior surface contamination levels are presented in Section 5.3.1.1. Summaries of surface contamination levels exterior to the vehicle are presented in Section 5.3.2.1. Wipe-test samples were collected using a dry wipe technique and wiping a 100-cm^2 area with moderate pressure. Wipe-test sample locations were marked to facilitate sample collection. A sample identification scheme similar to the scheme employed for the aerosol samples was used. Wipe-test samples were collected pre-shot (referred to as baseline wipes) and post shot (referred to as impact wipes) from the same sample location. For example, sample identification, PI-2I-BW-1, is from Phase I (PI), Shot 2, interior (2I), baseline wipe (BW), sample location 1, and PII-1/2E-IW-30, is from Phase II (PII), Shot1/2, exterior (1/2E), impact wipe (IW), sample location 30.

Wipe-test surveys also were performed to determine the effectiveness of the decontamination procedures employed by Battlefield Damage, Assessment, and Repair (BDAR) personnel. These surveys were done post shot, and the sample identifier was appended with an “A” or a “B” to distinguish between the surveys. The “A” survey was done prior to decontamination, and the “B” survey was done after decontamination. Results and diagrams of specific sample locations for each test are included in Appendix F. The uranium mass results, summarized in the following tables and detailed in Appendix F, were derived from ingrowth-adjusted beta activity measurements of the wipe-test samples as detailed in Appendix A. The “NA” notation appears in some of the tables to indicate that the samples were incompletely analyzed before becoming cross contaminated. Pre-shot “baseline” wipe-test results are presented separately and have not been subtracted from the post-shot “impact” wipe-test samples.

Deposition trays were collected from the interior and exterior of the vehicle. Summaries of the total mass and the estimated uranium mass are presented in Sections 5.3.1.2 (interior) and 5.3.2.2 (exterior). The deposition trays were pressed from aluminum sheet metal and had a flat surface area of 100 cm^2 and a beveled lip area of approximately 60 cm^2. They were secured in place with duct tape prior to the shot. In spite of being taped in place, some blew over, and particulate matter on the 100 cm^2 side facing up was collected for analysis. The debris that deposited on the tray was weighed and transferred to vials prior to being analyzed using gamma spectrometry. Four deposition trays had large objects that would not fit into the vial; therefore, these objects were placed in plastic storage bags prior to analysis by gamma spectrometry, and the remaining dust-like debris was placed into a vial. Diagrams of the deposition trays

locations are included in Appendix F. The uranium mass results summarized below were derived from the gamma activity measurements as detailed in Appendix A, Section A.2.2.

Instrumentation surveys, using fielded U.S. Army RADIAC (radiation, detection, indication, and computation) equipment, were performed. Descriptions of the instruments used and the surveys performed are briefly described in Section 5.3.3, and more detailed results are presented in Appendix F.

5.3.1 Vehicle Interior Data

Wipe-test surveys were conducted inside the target vehicle for each shot. These wipe surveys were taken at pre-marked, 100-cm^2 surface locations. Baseline surveys were conducted before each shot (or double shot). In addition, deposition trays positioned near each of the crewmember positions collected deposited material from each shot.

5.3.1.1 Vehicle Interior Wipe-Test Surveys

Pre-shot (baseline) and post-shot average removable uranium mass values and their ranges on interior surfaces are presented in Table 5.15 for each test in which wipes were taken. The lower range values that are negative values (representing statistical variability around zero) in Appendix F are reported as zeros in Table 5.15. The average values in Table 5.15 do not include negative values. Wipe sampling results are not available for those baseline or post-shot periods that are identified as "NA." The locations of the wipes and the data tables on which this summary table is based are provided in Appendix F.

5.3.1.2 Deposition Tray Uranium Mass

Interior deposition trays were placed at the respective crew locations for each shot in Phases I through III. Annotated diagrams in Appendix F identify the placement of these trays Table 5.16 lists the total mass collected on each tray and the mass of uranium in each sample.

Table 5.15. Removable Uranium Mass from Interior Vehicle Surfaces

Phase/Shot	Sampling	Average DU Mass Removed (μg) ± 1σ	Range of DU Mass Removed (μg)
PI-1	Baseline	NA	NA
	Post shot	2,960 (±4,211)	563 to 23,812
PI-2	Baseline	417 (±745)	21 to 4,060
	Post shot	NA	NA
PI-3/4	Baseline	600 (±729)	43 to 3,167
	Post shot	7,560 (±6,073)	937 to 24,311
PI-5	Baseline	275 (±293)	38 to 1,105
	Post shot	NA	NA
PI-6	Baseline	NA	NA
	Post shot	NA	NA
PI-7	Baseline	1,111 (±737)	173 to 2,653
	Post shot	3,617 (±2,842)	727 to 15,044

Table 5.15. (cont'd)

Phase/Shot	Sampling	Average DU Mass Removed (μg) ± 1σ	Range of U Mass Removed (μg)
PII-1/2	Baseline	24 (± 41)	-4 to 165
	Post shot	1,444 (±1,085)	140 to 3,586
PII-3	Baseline	266 (±295)	24 to 1,178
	Post shot	796 (±639)	11 to 2,384
PIII-1	Baseline	99 (±118)	5 to 472
	Post shot	10,052 (±7,750)	518 to 35,026
PIII-2	Baseline	521 (±804)	18 to 3,716
	Post shot	7,780 (±5,285)	1,622 to 22,315
PIV-1	Baseline	3 (±2)	-1 to 7
	Post shot	5 (±4)	-1 to 16
PIV-2	Baseline	9 (±9)	1 to 33
	Post shot	5 (±4)	-1 to 12
PIV-3	Baseline	5 (±5)	-0.4 to 14
	Post shot	22 (±34)	-0.5 to 140
PIV-4	Baseline	1 (±4)	-6 to 8
	Post shot	580 (±448)	17 to 1,340
	Post shot A	1,783 (±4,192)	48 to 16,839
	Post shot B	1,163 (±2,264)	23 to 9,228

Table 5.16. Uranium Mass Collected on Interior Deposition Trays

Interior Deposition Trays (mg/deposition tray)								
	Driver Position		Gunner Position		Commander Position		Loader Position	
Phase/Shot	Total mass	Mass of DU	Total mass	Mass of DU	Total mass	Mass of DU	Total mass	Mass of DU
P1-1	113	33.0	275	29.7	93	54.3	1346	76.8
PI-2	1347	33.0	135	77.6	3209	442	1157	243
PI-3/4	1876	18.8	2854	327	3690	455	2840	648
PI-5	56[a]	28.6	246[a]	171	3721	523	27	17.0
PI-6	3198	853	1729[a]	393	4270[b]	560	656	233
PI-7	219	79.0	3079	258	437	190	1748	187
PII-1/2	387	18.4	378	14.2	1904	10.8	274	45.1
PII-3	86	14.3	71	4.26	149	8.35	79	9.69
PIII-1	185	74.6	130	45.0	3812	534	96950	3460
PIII-2	288	493	361	227	2735	72.5	3797	629

(a) Tray found upside down and may underestimate deposited mass.
(b) A 11.4-g DU fragment was also collected on this deposition tray.

The percentage of uranium within each total sample mass appeared to vary randomly. With the exception of the PIII-2 driver's position, in which the mass of uranium exceeded that of the total recorded mass of

the sample, the percentages of uranium in the total sample mass varied from 0.10% in PIII-1-C to 69.5% in PI-5-G. Only two samples contained less than 1% uranium, and in three samples, the percentages were above 60%. The lowest average results occurred with the Phase-II shots in which the uranium percentages ranged from 0.6 to 16.6%. This result is consistent with the expectation that less of the penetrator would erode and be available for deposition from perforation of a Bradley vehicle.

The individual and combined uranium masses by shot are summarized in Table 5.17. In all of the Abrams shots except for PI-1, at least 700 mg of uranium was deposited on the trays. The highest mass, 4.1 g (4114 mg) from PIII-1, was primarily the result of one sample that contained much more uranium and total particulate matter than the other samples. The next highest was PI-6 in which each of the four trays collected more than 200 mg of particulate matter, and the driver's position tray collected more particulate matter than the others. Deposition from the PI-5 shot (essentially a replicate) was considerably lower and was concentrated at the commander's and gunner's positions.

Table 5.17. Summary of Uranium Masses Collected by Shot on Interior Deposition Trays

Phase/Shot	U Mass (mg/deposition tray)	
	Range in U Mass, mg	**Total U mass, mg**
PI-1	29.7 to 76.8	194
PI-2	33 to 442	796
PI-3/4	18.8 to 648	1449
PI-5	17.0 to 523	740
PI-6	233 to 853	2039
PI-7	79 to 258	714
PII-1/2	10.8 to 45.1	88.5
PII-3	4.26 to 14.3	36.6
PIII-1	3.83 to 3460	4114
PIII-2	72.5 to 629	1422

5.3.2 Vehicle Exterior and Ground Survey Data

Wipe-test surveys were conducted on the exterior of the target vehicle and on the floor nearby for each shot. These wipe surveys were taken at pre-marked surfaces areas of 100 cm^2. Baseline surveys were conducted before each shot (or double shot). In addition, two deposition trays were positioned on the vehicle's exterior and two trays were positioned on the floor on either side of the vehicle to collect deposited material from each shot.

5.3.2.1 Wipe-Test Surveys Exterior to the Vehicle

Pre-shot (baseline) and post-shot average removable uranium mass values and their ranges from surfaces exterior to the vehicle are presented for each test in Table 5.18. The lower range values that are negative values (representing statistical variability around zero) in Appendix F are reported as zeros in Table 5.18. The average values in Table 5.18 do not include negative values. The locations of the wipes and the data tables on which this summary table is based are provided in Appendix F.

Table 5.18. Removable Uranium Mass Collected from Surfaces Exterior to the Vehicle

Phase/Shot	Sampling	Average U Mass Removed (μg)	Range of U Mass Removed (μg) (± 1σ)
PI-1	Baseline	NA	NA
	Post shot	201	0 to 962 (± 192)
PI-2	Baseline	289	5 (± 4) to 1240 (± 247)
	Post shot	2266	166 (± 34) to 9393 (± 1857)
PI-3/4	Baseline	NA	NA
	Post shot	3767	116 (± 24) to 8099 (± 1608)
PI-5	Baseline	243	9 (± 4) to 931 (± 185)
	Post shot	NA	NA
PI-6	Baseline	NA	NA
	Post shot	1755	88 (± 19) to 3761 (± 743)
PI-7	Baseline	92	13 (± 6) to 280 (± 78)
	Post shot	1538	82 (± 23) to 4359 (± 1142)
PII-1/2	Baseline	79	3 (± 0.7) to 408 (± 81)
	Post shot	1213	7 (± 2) to 3665 (± 724)
PII-3	Baseline	428	9 (± 4) to 1879 (± 372)
	Post shot	3553	25 (± 7) to 8076 (± 1603)
PIII-1	Baseline	56	6 (±5) to 225 (± 63)
	Post shot	499	51 (± 15) to 1198 (± 328)
PIII-2	Baseline	182	57 (± 16) to 338 (± 93)
	Post shot	3213	441 (± 82) to 6809 (± 1345)
PIV-1	Baseline	23	0 to 288(± 5)
	Post shot	379	7 (± 2) to 1602 (± 317)
PIV-2	Baseline	96	1 (± 3) to 667 (± 135)
	Post shot A	1659	172 (± 36) to 4303 (± 863)
	Post shot B	556	18 (± 7) to 1855 (± 373)
PIV-3	Baseline	41	5 (± 4) to 181 (± 38)
	Post shot A	670	19 (± 6) to 2478 (± 491)
	Post shot B	261	13 (± 5) to 1408 (± 280)
PIV-4	Baseline	55	1 (± 2) to 214 (± 44)
	Post shot A	380	1 (± 3) to 1294 (± 260)
	Post shot B	422	5 (± 3) to 1262 (± 252)

5.3.2.2 Deposition Tray Uranium Mass

Deposition trays typically were placed on the vehicle (one each on top of the hull and on top of the turret) and on the fragmentation shield floor (one on the impact side and one on the exit side) within the Superbox to collect particulate material deposited outside the vehicle. The survey diagrams in Appendix F indicate the locations of the deposition trays relative to the vehicle. Table 5.19 lists the total mass collected on each tray and the mass of uranium in each sample. The gamma activity data also are listed in Appendix A.

The masses collected in trays on the vehicle are compared in Table 5.20 with the masses collected in trays on the floor. The individual masses are listed by shot along with the average of the two deposition trays on the vehicle and on the floor and the total mass of all four trays. In the majority of cases, the trays on the floor collected more uranium than the trays on the vehicle. The largest deposits occurred with floor trays from shots PI-3/4 and PII-1/2. Generally, each set of trays from PI through PIII collected similar amounts of uranium over the course of the tests.

Table 5.19. Uranium Mass Collected on Exterior Deposition Trays

Exterior Deposition Trays (mg/deposition tray)								
	Position A		Position B		Position C		Position D	
Phase/Shot	Total Mass	Mass of DU	Total Mass	Mass of DU	Total Mass	Mass of DU	Total Mass	Mass of DU
PI-1	57	13.8	132	9.16	39	9.05	434	79.0
PI-1	108	28.0	51	23.5	58	36.9	124	58.0
PI-3/4	208	50.8	249[(a)]	45.4	132	50.8	656	93.4
PI-5	16	7.53	N/A[(a)]	N/A	105	65.4	14	15.1
PI-6	253[(a)]	3.90	34	29.0	8	11.0	37	31.6
PI-7	123[(a)]	1.95	186	62.5	64	16.6	524	32.0
PII-1/2	264	8.07	61	18.1	2467	30.4	2483	234
PII-3	80	17.5	106	34.9	82	19.3	130	45.3
PIII-1	98	9.97	16	6.14	4	3.83	0	--
PIII-2	34	28.8	8	3.77	23	12.7	12	6.45
PIV-1	3	0.079	35	3.13	4	1.66	1	0.0067
PIV-2	150	10.8	118	4.10	383	27.2	386	25.5
PIV-3	14	0.237	7	0.479	106	5.76	82	1.61
PIV-4	0	--	--0	--	32	--	21	--

[(a)] Tray found upside down.

Table 5.20. Summary of Uranium Masses Collected by Shot on Exterior Deposition Trays

U Mass (mg/deposition tray)					
	On Vehicle		On Floor		Total U mass (mg)
Phase/Shot	Range (of 2)	Average	Range (of 2)	Average	
P1-1	9.16 to 13.8	11.5	9.05 to 79	44.0	111
PI-2	23.5 to 28.0	25.6	36.9 to 58	47.5	146
PI-3/4	45.4 to 50.8	48.1	50.8 to 93.4	72.1	240
PI-5	7.53	7.5	15.1 to 65.4	40.3	88.0
PI-6	3.9 to 29	16.5	11 to 31.6	21.3	75.5
PI-7	1.95 to 62.5	32.2	16.6 to 32	24.3	113
PII-1/2	8.07 to 18.1	13.1	30.4 to 234	132.2	291
PII-3	17.5 to 34.9	26.2	19.3 to 45.3	32.3	117
PIII-1	6.14 to 9.97	8.1	3.83	3.83	19.9
PIII-2	3.77 to 28.8	16.3	6.45 to 12.7	9.6	51.7
PIV-1	0.08 to 3.13	1.6	0.007 to 1.66	0.8	4.88
PIV-2	4.1 to 10.8	7.5	25.5 to 27.2	26.4	67.6
PIV-3	0.24 to 0.48	0.4	1.61 to 5.76	3.7	8.09
PIV-4	--	--	--	--	--

5.3.3 Instrumentation Surveys

Instrument surveys using currently fielded U.S. Army RADIAC equipment were performed in conjunction with wipe-test surveys. Details of the various instrumentation surveys are presented in Appendix F. The relationship between the removed beta activity measured on the wipes and the instrument readings are briefly compared below.

Additional wipe-test surveys were performed after the interior and exterior removable wipe-test surveys were completed. A delineated 100-cm^2 area was surveyed with a RADIAC instrument prior to removing DU contamination with five successive wipe-test samples. The wipe-test sample identifier was appended with letters ranging from "a" to "e" to indicate which exhaustive wipe, with "a" being the first exhaustive wipe and "e" being the last exhaustive wipe. After the last wipe test, another instrument reading was taken. The differences in the instrument readings were plotted against the total amount of removable beta activity for the various instruments used. The beta-gamma end-window, and beta-gamma pancake probes were used. There were three interior and three exterior exhaustive wipe locations.

Figure 5.24 shows the relationship between removable DU contamination and beta-gamma end-window probe instrument readings. Figure 5.25 shows the relationship between removable DU contamination and beta-gamma pancake probe instrument readings. Good correlations are observed between the removable beta activity and the beta-gamma pancake probe and between the removable beta activity and the "open" window beta-gamma end-window probe.

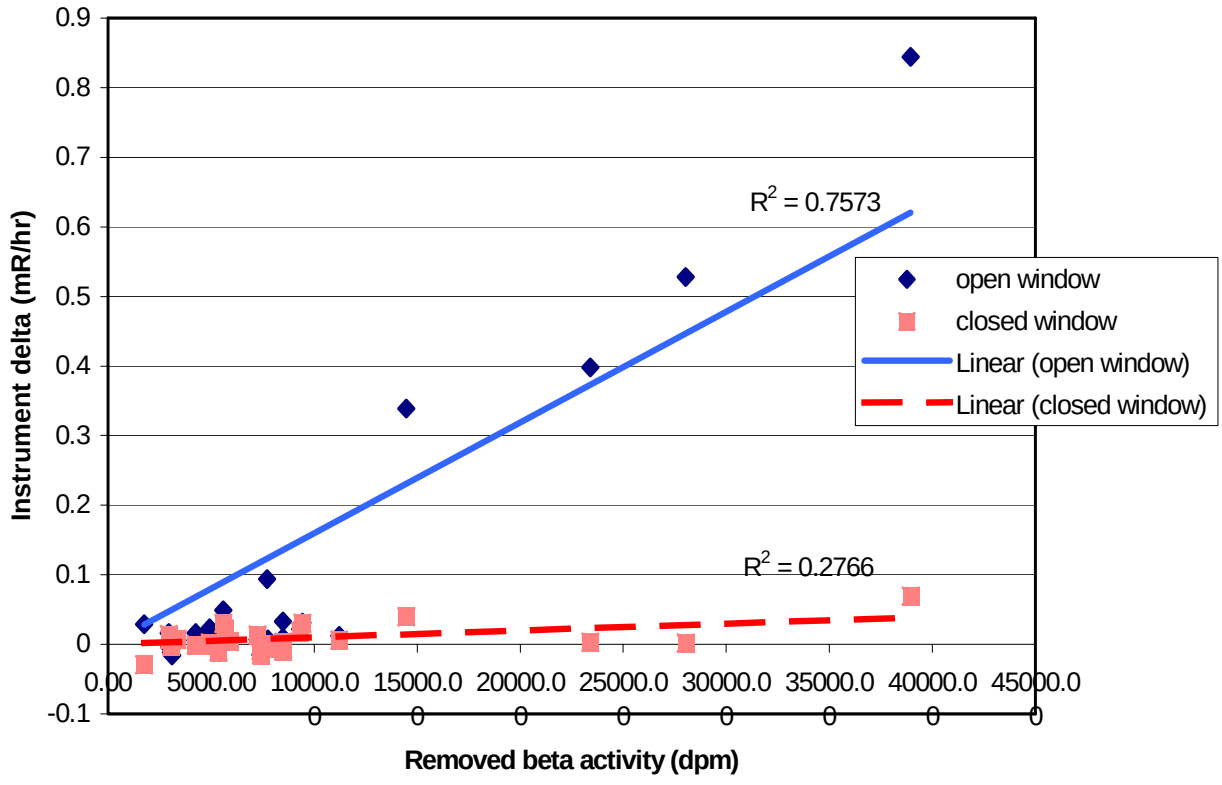

Figure 5.24. Relationship Between AN/PDR-77 Beta-Gamma End-Window Probe to Gross Beta Removable Wipes

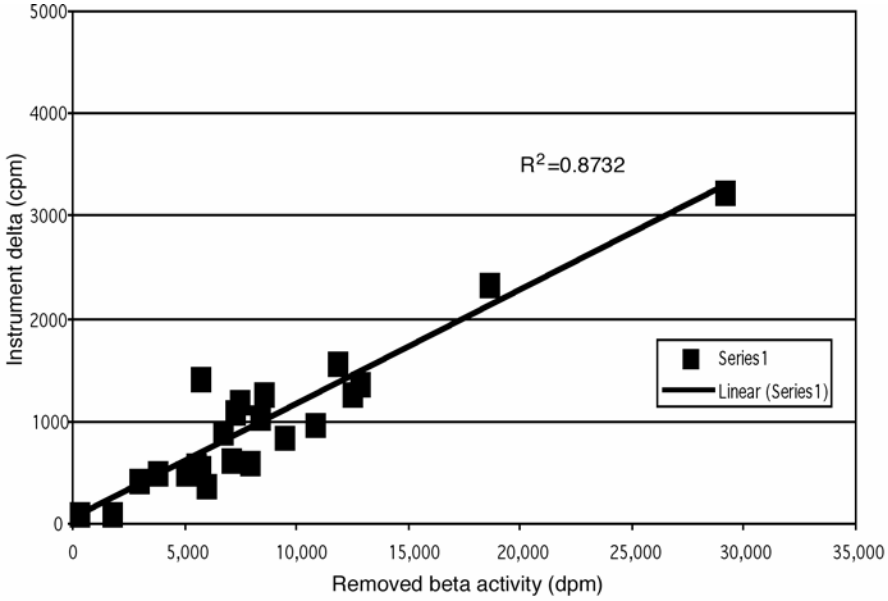

Figure 5.25. Relationship Between AN/PDR-77 Pancake Beta-Gamma Probe to Gross Beta Removable Wipes

5.4 Aerosol Data During Recovery Activities

Recovery activities were conducted beginning several hours after each shot (or double shot). The aerosol suspended during recovery activities included residual airborne material from the shot and deposited material resuspended by the actions of recovery personnel. During shots PI-6 and PI-7, the loader's array was used to monitor the aerosol concentrations prior to and during recovery activities. Results of this analysis are provided in Section 5.4.1. In addition to the samplers inside the vehicle, two recovery personnel were outfitted with two personal air monitors—an IOM and a closed-face Marple CI. A discussion of these results is provided in Section 5.4.2. An estimate of the deposited material potentially available for hand-to-mouth ingestion by those entering the vehicle during personnel and equipment recovery was evaluated by analyzing cotton gloves worn by selected recovery personnel during several of the shots. These results are presented in Section 5.4.3.

5.4.1 IOM Filter and CI Array Samplers

Resuspension of aerosols due to personnel performing post shot and sample recovery operations were measured at the loader's sampling position following the PI-6 and PI-7 shots (Table 5.21). Resuspension baseline sampling began about 2.5 and 3.5 h, respectively, after impact. The operations included personnel photographing the tank as well as personnel collecting air samplers and taking wipe samples. The loader's hatch was used exclusively to enter and exit the tank. The loader's array IOM filters collected during the recovery operations are shown in Figure 5.26. The uranium concentration during the previous time interval for PI-6 (121 through 129 min post impact) averaged 9.47E+03 µg/m^3. Resuspension by recovery activities during PI-6 is evident in the increase in aerosol present during these activities in which the aerosol concentration of DU increased from a baseline of 2.95E+03 µg/m^3 to a maximum of 2.86E+04 µg/m^3 (Figure 5.27). The resuspension aerosol concentration peaked as the workers exited the tank. After the recovery workers exited, the aerosol began to re-settle. Measured mass

concentrations decreased over the next three sampling intervals to a low of 7.46E+03 µg/m^3 about 30 min after recovery activities ceased.

Table 5.21. DU Aerosol Concentrations During Recovery Activities

Field ID	Collection Interval	U Conc. (µg/m^3)	Recovery Activities
PI-6 (Beginning 2 h and 35 min post shot)			
PI-6I-L1-FS	0 to 20 min	2.95E+03	Baseline
PI-6I-L2-FS	31 to 54 min	4.52E+03	Contamination survey
PI-61-L3-FS	54 to 67 min	3.35E+03	Photography survey
PI-6I-L4-FS	67 to 82 min	5.28E+03	Sampler retrieval
PI-6I-L5-FS	82 to 104 min	4.88E+03	Sampler retrieval, continued
PI-6I-L6-FS	105 to 107 min	2.86E+04	No activity
PI-6I-L7-FS	107 to 111 min	2.10E+04	No activity
PI-6L-L8-FS	111 to 119 min	1.57E+04	No activity
PI-6L-L9-FS	119 to 135 min	7.46E+03	No activity
PI-7 (Beginning 3 h and 21 min post shot)			
PI-7I-L1-FS	0 to 20 min	1.15E+03	Baseline
PI-7I-L2-FS	20 to 40 min	4.30E+02	Overlapping times: photography, wipe
PI-7I-L3-FS	40 to 60 min	Background	surveys, sampler retrieval
PI-7I-L4-FS	60 to 69.7 min	Background	No activity

Figure 5.26. IOM Filters from PI-6 Recovery Activities

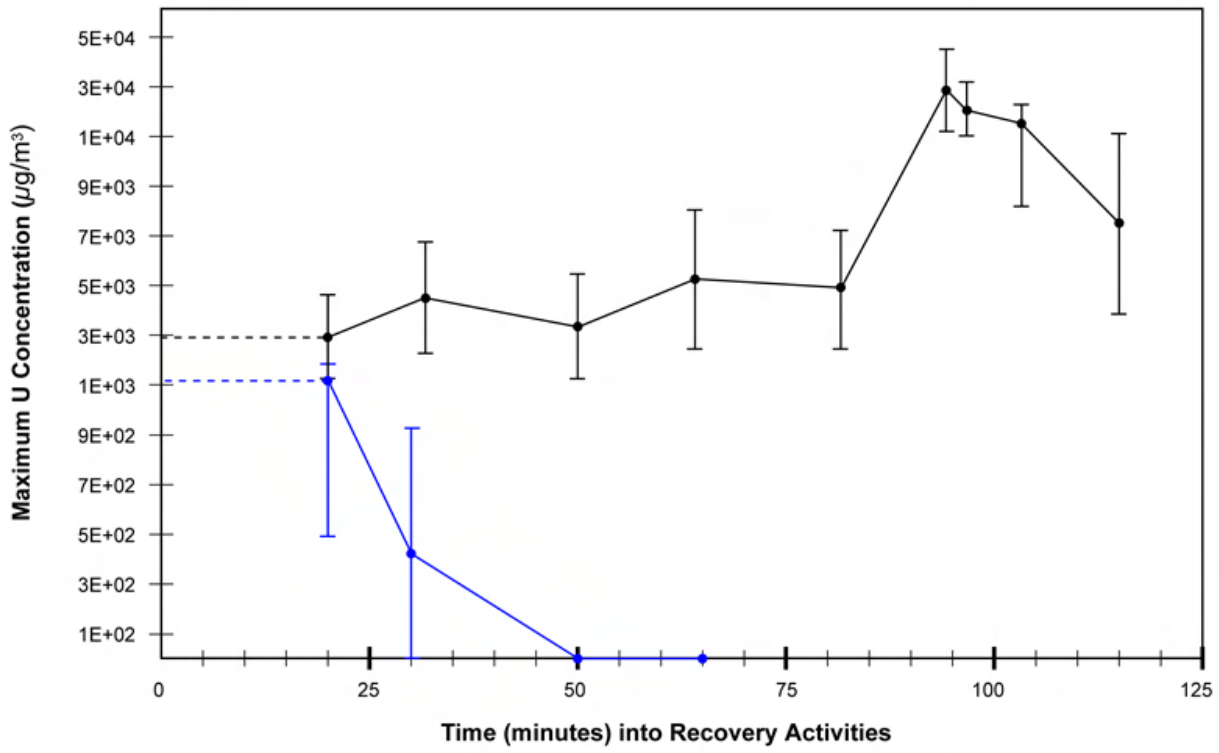

Figure 5.27. Uranium Concentrations during Recovery Activities, PI-6 and PI-7

Only two samples were taken during the recovery activities following the PI-7 shot. The aerosol collected between 121 and 129 min post impact recorded uranium concentrations between 3.96E+04 and 5.09E+04 µg/m^3. By the time the baseline sample for the recovery activities was taken beginning 3.35 h post impact, the uranium concentration in the aerosol had dropped to 1.15E+3 µg/m^3. The first of the three samples taken after the baseline showed a decrease to 4.30E+02 µg/m^3, and the subsequent two samples were at the concentration levels of the field blanks. Based on these very limited data, these activities seem to have resuspended little of the deposited material.

The loader's CIs were analyzed for particle size, and the resulting distributions are presented in Section 5.5.1.

5.4.2 Personal Air Samplers

Recovery personnel entering the perforated vehicles were dressed in anti-contamination clothing and wore respiratory protection because of the occupational requirements of operating within the Superbox. An evaluation of the aerosol to which these staff would have been exposed had they not been wearing respiratory protection was conducted several hours after each shot (or double shot) by equipping each of two of the recovery personnel with an IOM filter cassette and a Marple CI. To minimize the weight carried by each of these workers, the two samplers were connected to a single portable pump, which was operated at 4 Lpm in an attempt to provide a 2 Lpm flow rate to each sampler. It is not known how evenly the flow rate was divided, and this question adds an undetermined level of uncertainty to the

analysis of these samples. The sampling time intervals varied in accordance with the activities being performed.

The uranium aerosol concentrations measured by the IOM samplers are listed in Appendix A, Table A.40, and are summarized in Table 5.22. The samplers operated a total of from 41 to 179 min of the 2-h, post shot sampling phase. The uranium concentrations ranged from about 60 to nearly 1000 µg/m^3. The length of time engaged in recovery activities and the uranium concentrations measured are not necessarily correlated, partly because the actual time in the turret was less than the time the pump operated. The lowest concentrations occurred after the PI-3/4 shots, and the uranium concentrations in the two samples were very consistent at 79 and 86 µg/m^3. The concentration measured by one of the IOM samplers following the PIII-1 shot was actually lower at 59 µg/m^3, while the concentration measured by the second IOM sampler was somewhat higher at 202 µg/m^3. The highest uranium concentration occurred following the PI-5 shot in which the two samplers measured 497 and 968 µg/m^3. These CI samples were not analyzed for particle size distribution but are listed in Appendix A, Table A.41.

Table 5.22. DU Aerosol Concentrations as Measured by Personal IOMs

Field ID	Time (min)	U Mass (µg)	Vol (m^3)	U conc (µg/m^3)	Conc. ± 1σ, (µg U)
PI-1I-P-1-FS	192	154.6	0.386	401	133
PI-1I-P-2-FS	192	239.5	0.386	621	205
PI-2I-P-1-FS	142	64.0	0.284	225	76
PI-2I-P-2-FS	143	104.4	0.286	365	123
PI-3/4I-P-1-FS	179	31.1	0.360	86	22
PI-3/4I-P-2-FS	132	21.0	0.265	79	20
PI-5I-P-1-FS	125	241.9	0.250	968	326
PI-5I-P-2-FS	127	126.3	0.254	497	167
PI-6I-P-1-FS	97	79.2	0.194	408	101
PI-6I-P-2-FS	120	29.0	0.240	121	30
PI-7I-P-1-FS	125	29.7	0.250	119	29
PI-7I-P-2-FS	60	55.0	0.120	458	23[(a)]
PIII-1I-P-1-FS	108	12.7	0.216	59	15
PIII-1I-P-2-FS	41	16.6	0.082	202	51
PIII-2I-P-1-FS	168	37.4	0.336	111	28
PIII-2I-P-2-FS	112	61.8	0.224	276	69
PII-1/2I-P-1-FS	118	84.5	0.236	358	126
PII-1/2I-P-2-FS	107	150.1	0.214	701	248
PII-3I-P-1-FS	84	23.1	0.168	138	46
PII-3I-P-2-FS	84	31.7	0.168	188	64

(a) Based solely on ICP-MS instrument uncertainty of about ± 5%.

5.4.3 Gloves

Inspection gloves (100% cotton, un-hemmed, lightweight, 12-in. long, men's inspection gloves) were used to estimate surface-to-hand transfer of residual DU from vehicle surfaces. Selected individuals wore the cotton gloves over latex gloves while performing specific duties in support of the Capstone DU Aerosol Study. The amount of time required to complete a specific duty was recorded. Table 5.23

depicts the mass of uranium in milligrams (mg) transferred to gloves from contaminated surfaces as derived from gamma spectrometry. The left-hand and right-hand gloves were analyzed separately and usually contained similar uranium masses. The uranium masses on the gloves are related not only to the quantity of aerosol deposited on vehicle surfaces, but also to the activities performed and the time and movement involved. Because both of these parameters varied, the results of the different phases and shots are not directly comparable. For Phases I through III, the gloves used during interior activities ranged from the lowest uranium average of 39 mg for PI-2, to a slightly higher average of 54 mg for PI-1, to the next highest average of 114 mg for PIII-2, and the highest average of 155 mg for PI-5. Gloves from project staff engaged in external wipe surveys contained the least amount of uranium with a combined average of 6 mg for PI-1 and PI-2. The uranium residues collected on gloves by those taking internal wipes and recording activities were intermediate to the others. In Phase IV-4, most of the uranium transferred to the gloves ranged widely from a minimum of 4 mg to a maximum of 118 mg. The highest masses (103 and 118 mg) were received during exterior ammunition removal following the PIV-4 test.

Table 5.23. Mass of DU Collected on Cotton Gloves

Phase/Shot	Glove ID	Mass (mg) of DU Adjusted (± 1σ)	Timeframe (min)	Activities
PI-1	1-L	53 (± 3)	40	Interior sample retrieval
	1-R	52 (± 3)	40	Interior sample retrieval
	2-L	58 (± 3)	60	Sample collection
	2-R	55 (± 3)	60	Sample collection
	3-L	7 (± 0.4)	70	Exterior wipe survey
	3-R	9 (± 1)	70	Exterior wipe survey
	4-L	3 (± 0.2)	70	Exterior wipe survey
	4-R	7 (± 0.4)	70	Exterior wipe survey
PI-2	5-L	64 (± 4)	60	Photography and sample collection
	5-R	61 (± 4)	60	Photography and sample collection
	6-L	10 (± 1)	63	Interior sample retrieval
	6-R	19 (± 1)	63	Interior sample retrieval
	1-7-L	3 (± 0.2)	40	Exterior wipe survey and instrument readings
	1-7-R	6 (± 0.4)	40	Exterior wipe survey and instrument readings
	8-L	23 (± 1)	167	Wipe survey recorder
	8-R	53 (± 3)	167	Wipe survey recorder
	9-L	26 (± 2)	127	Interior wipe survey and instrument readings
	9-R	20 (± 1)	127	Interior wipe survey and instrument readings
PI-5	10-L	120 (± 7)	70	Photography and sample collection
	10-R	151 (± 9)	70	Photography and sample collection
	11-L	162 (± 9)	70	Interior sample retrieval
	11-R	198 (± 11)	70	Interior sample retrieval
	12-L	100 (± 6)	55	Wipe survey and instrument readings
	12-R	87 (± 5)	55	Wipe survey and instrument readings
	13-L	19 (± 1)	55	Wipe survey recorder
	13-R	38 (± 2)	55	Wipe survey recorder
PIII-2	14-L	100 (± 6)	33	Interior wipe survey
	14-R	127 (± 7)	33	Interior wipe survey
PIV Tests (DU Munitions Used only in PIV-4)				
PIV-1	15-L	1 (± 0.1)	12	Exterior wipe survey
	15-R	2 (± 0.2)	12	Exterior wipe survey
	16-L	2 (± 0.2)	34	Interior wipe survey

Phase/Shot	Glove ID	Mass (mg) of DU Adjusted (± 1σ)	Timeframe (min)	Activities
	16-R	3 (± 0.2)	34	Interior wipe survey
	17-L	11 (± 1)	105	Battle damage assessment and repair
	17-R	13 (± 1)	105	Battle damage assessment and repair
PIV-3	18-L	0.5 (± 1)	40	Battle damage assessment and repair
	18-R	1 (± 0.2)	40	Battle damage assessment and repair
	19-L	1 (± 0.1)	40	HEPA vacuum for decontamination
	19-R	3 (± 0.3)	40	HEPA vacuum for decontamination
PIV-4	20-L	33 (± 2)	65	Interior cable removal
	20-R	24 (± 2)	65	Interior cable removal
	21-L	4 (± 1)	65	Interior cable removal
	21-R	5 (± 0.4)	65	Interior cable removal
	22-L	10 (± 1)	65	Interior cable removal
	22-R	5 (± 0.4)	65	Interior cable removal
	23-L	102 (± 6)	60	Interior ammunition removal
	23-R	75 (± 4)	60	Interior ammunition removal
	24-L	45 (± 3	60	Interior ammunition removal
	24-R	34 (± 2)	60	Interior ammunition removal
	25-L	10 (± 1)	60	Exterior ammunition removal
	25-R	26 (± 2)	60	Exterior ammunition removal
	26-L	118 (± 7)	45	Exterior ammunition removal
	26-R	103 (± 6)	45	Exterior ammunition removal
	27-L	5 (± 0.4)	30	Battle damage assessment and repair: HEPA vacuum decontamination
	27-R	5 (± 0.4)	30	Battle damage assessment and repair: HEPA vacuum decontamination
	28-L	9 (± 1)	60	Decontamination
	28-R	5 (± 0.4)	60	Decontamination

5.5 Particle Size Distribution

Particle size distributions of the DU component of aerosols (not the total mass) were evaluated using samples collected by Marple CIs inside the target vehicles and Andersen CIs outside the vehicles. The following description of the method used in determining particle size distributions applies to both the Marple and the Andersen CIs. Sampler-specific results are provided in the following sections.

The analysis of particle size distribution used the uranium concentrations based on radioactivity and the sampled air volume of the individual samples. These values are listed in Appendix A, Tables A.19 through A.32. Particle size distribution data and unimodal AMAD distribution graphs are provided in Appendix B.

Particle size distributions can be analyzed using either radioactivity or uranium mass to determine the relative quantity of uranium collected by the successive CI substrates. In this analysis, radioactivity was first used to evaluate the particle size distributions. After adjusting the data for ingrowth and using the results of substrates analyzed by direct chemical methods, the particle size distributions were re-evaluated using uranium masses.

5.5.1 Cascade Impactors

The example shown in Table 5.24 of the uranium mass by stage is presented for discussion of the procedure used to calculate particle size distribution parameters. This table covers the 5- to 35-sec, post impact time interval for the PI-1 loader's array. It lists the mass of uranium collected on each sample substrate and field blank, the net mass of uranium, and the nominal ECD at 2 Lpm.

Table 5.24. Example of Uranium Mass on CI Stages, First Sampling Interval, PI-1 (Loader's Array)

	Uranium Mass (µg)			
Stage	**Sample**	**Field Blank**	**Net DU (µg)**	**Nominal ECD (µm)**
1	317	144	174	21.3
2	190	5	185	14.8
3	323	2	321	9.8
4	293	0	293	6.0
5	558	1	557	3.5
6	583	8	576[(a)]	1.55
7	276	3	273	0.93
8	600	5	595	0.53
Bottom Filter	859	7	852	0
(a) Difference due to rounding.				

The net mass of uranium for each stage was entered into a software program to determine the AMAD, the geometric standard deviation (GSD), the R^2 value (measures goodness-of-fit), and fraction of the mass in the first peak (for bimodal distributions). The software program used for this was SigmaPlot 2000.[(a)] It used a transformation equation that employed the ECDs for the Marple CIs. A multi-lognormal regression was used to fit the data to unimodal and bimodal distributions.

Except in a few cases where the substrates were analyzed by chemical means, all CI results were based on uranium mass derived from radioactivity measurements. This mass could be compared with the total sample mass to determine the MMAD if positive weights had been consistently obtained for all stages. However, this was not possible because so many of the post impact substrates posted in negative weight changes.

The graph in Figure 5.28 presents the unimodal and bimodal particle size distributions for the sample data shown above. The Y-axis title represents the frequency fraction of mass (or activity) for that particle size. The two regression curves can easily be differentiated. For this set of data, the unimodal regression results calculated that the AMAD was 2.46 µm with a GSD of 6.07 (R^2 = 0.32). The bimodal calculation resulted in an AMAD of the first peak (F) of 0.51 µm, with a GSD of 1.65, and an AMAD of the second peak of 5.68 µm, with a GSD of 2.90 (R^2 = 0.81). The fraction of uranium mass in the first peak was 0.40.

(a) SPSS Inc., Chicago, Illinois.

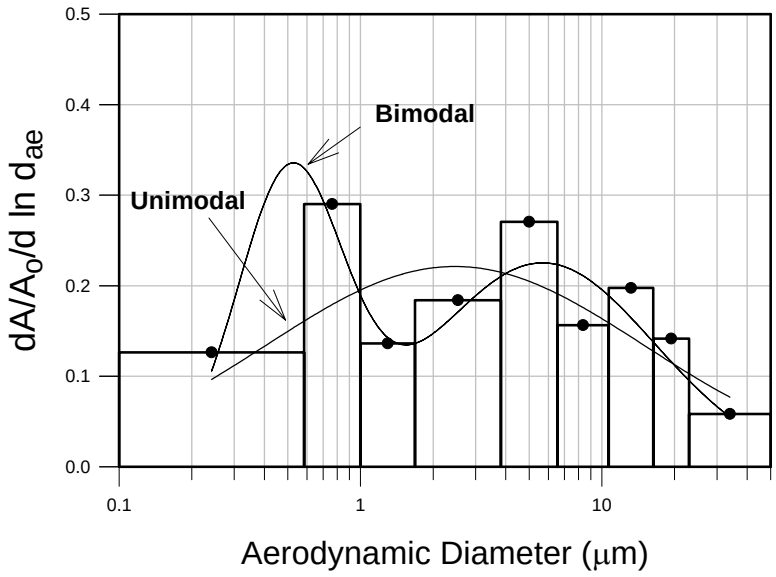

Figure 5.28. Particle Size Distribution for PI-1 (Loader's Array)

In the ideal situation for particles of aerodynamic diameter >0.5 μm, the particle size would be expected to decrease with time because settling velocities increase with increasing particle size. Figures 5.29 and 5.30 show a time-related particle size behavior for samples obtained at one position within one shot (PI-1 loader's position). The post-penetration times displayed are for T = 0.08 min, 1.08 min, 3.125 min, 7.5 min, 16 min, 33 min, 65 min, and 125 min, where these times are midpoints of the sampling interval. Under each graph, the AMAD and GSD for the unimodal distribution and the AMAD, GSD, and fraction of activity in the first peak (F) for the bimodal distribution are listed. The exception to this is the T=3.125 min interval in Figure 5.29, which shows the bimodal curve only. The unimodal would peak at an aerodynamic diameter of 2.3 μm. In general, the aerodynamic diameters for these data decrease with time. The data also show that there can be a large variability in the GSDs and the overall distributions (in terms of the size and shapes of the curves) over the time period that samples were obtained.

The summary data for each CI sample obtained during all phases are listed in Appendix G. Data are listed for each position, for every shot, and for all phases. Included are the AMAD, GSD, R^2 value, and fraction of activity in the first peak (F) for the bimodal distributions. The unimodal AMADs for each shot are graphed in Figures B.1 through B.12 in Appendix B.

T=0.083 min

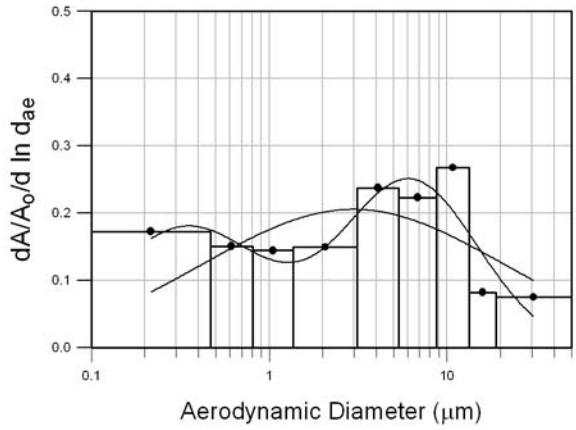

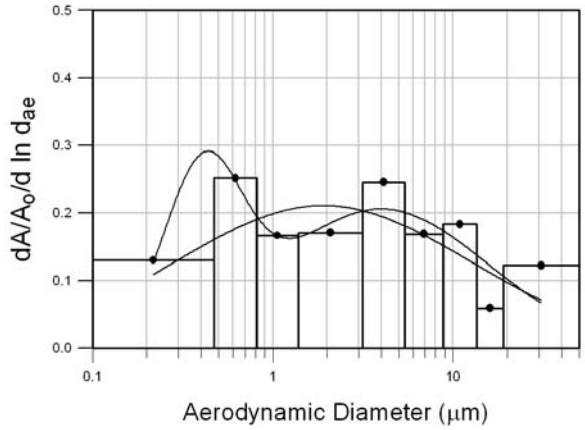

Unimodal: AMAD = 2.97 μm GSD = 6.99
Bimodal: AMAD = 0.34 μm GSD = 2.77 F = 0.40
AMAD = 6.21 μm GSD = 2.40

T=1.083 min

Unimodal: AMAD = 1.90 μm GSD = 6.65
Bimodal: AMAD = 0.41 μm GSD = 1.64 F =0.30
AMAD = 3.98 μm GSD = 3.92

T=3.125 min

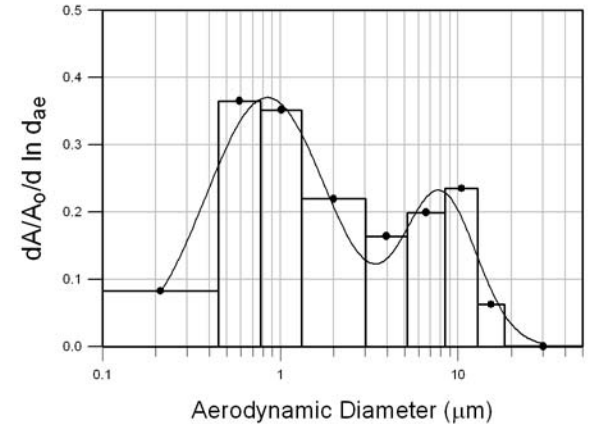

Unimodal: AMAD = 2.3 μm GSD = 4.0
Bimodal: AMAD = 0.84 μm GSD = 2.21 F = 0.73
AMAD = 7.94 μm GSD = 1.60

T=7.5 min

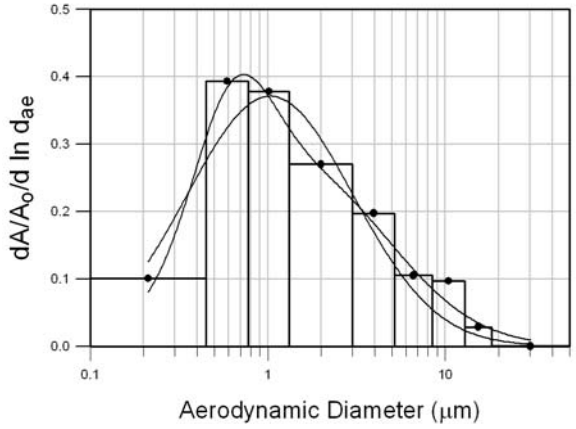

Unimodal: AMAD = 1.03 μm GSD = 2.93
Bimodal: AMAD = 0.63 μm GSD = 1.66 F 0.26
AMAD = 1.52 μm GSD = 3.17

Figure 5.29. Particle Size Histograms for the First Four Time Intervals, PI-1 (Loader's Array)

The GSDs provide a description of how wide the size distribution is around the aerodynamic median diameter—the larger the number, the wider the distribution. A monodispersed particle size distribution (i.e., one diameter only) would have a GSD of 1.0. A GSD of greater than 5 or 6 is considered to be a "broad" peak. A GSD of greater than 20 is considered to be one that is not realistically connected to a "peak." The distribution is so broad that there cannot be much of a peak, just a distribution of activity (or mass) across all of the size intervals. The R^2 value provides a measurement of how well the data fit the particular regression curve. A high number (close to 1.0) would mean that the fit is good. A value less than 0.5 may be considered (by some) to be of lesser value. A value close to zero means that the fit is very poor, and the medians identified may not be "good" data. An example of a situation in which a very low R^2 value occurs is when a unimodal regression is performed on a very bimodal distribution (i.e., where there are clearly two, very identifiable peaks with several micrometers separating them). The unimodal fit would not describe that situation well.

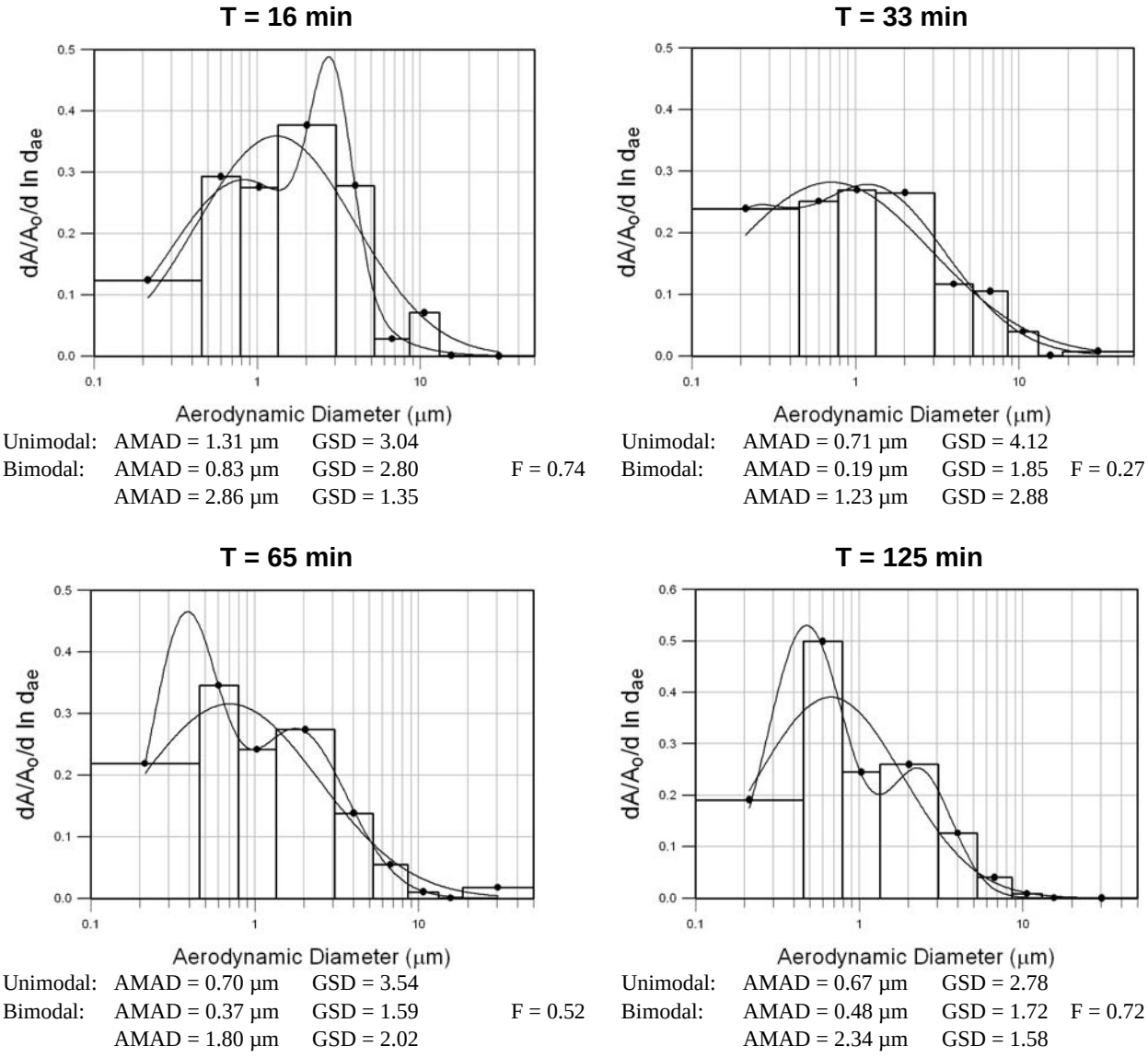

Figure 5.30. Particle Size Histograms for the Last Four Time Intervals, PI-1 (Loader's Array)

The range of aerosol particle sizes as measured by the Marple CIs was between 0.1 and 30 μm, which is adequate for providing good data over most of the respirable particle size range. When the particle sizes occur at the extremes of the range, the fits obtained from regression analyses are not as good. The upper particle size limit is due to the physical characteristics of the first stage and the nominal airflow through the holes in that stage. Particles > 30 μm should be collected on the first stage of the CI, and fine particles (i.e., <0.1 to 0.3 μm) should be collected on the backup filter. Each stage has an ECD associated with it; these diameters change as the flow rate through the CI changes. The ECD is the diameter at which 50% of the particles with that diameter will be deposited on that stage and the remaining 50% will flow past it. Most size distributions measured in this study were clearly bimodal with a small particle size mode in the range of 0.2 to 1.2 μm and a large size mode between 2 and 15 μm. Some particle median diameters were lower and some were higher, but most were in one of those two ranges.

As shown in Figure 5.30, most size distributions measured in the test based on activity had bimodal size distributions with a small particle size mode in the range between 0.1 and 3 μm, and a large size mode between 3 and 30 μm. To describe the particle size distribution, a bimodal lognormal size distribution was used to fit the data:

$$s(x)\frac{f}{\sqrt{2\pi}\ x\ (\ln\sigma_{g1})}\exp\left[-\frac{(\ln x-\ln x_{o1})^2}{2(\ln\sigma_{g1})^2}\right]+\frac{(1-f)}{\sqrt{2\pi}\ x\ (\ln\sigma_{g2})}\exp\left[-\frac{(\ln x-\ln x_{o2})^2}{2(\ln\sigma_{g2})^2}\right]$$

In this relationship, the fit parameter f (in Figures 5.29 and 5.30 as F) is the fraction of the total activity/mass in the first size mode. The AMADs (x_{o1} and x_{o2}), GSDs (σ_{g1} and σ_{g2}), and constant f of the bimodal distribution were obtained by using a non-linear curve-fitting algorithm of SigmaPlot.

Over the period of sample acquisitions, it appears that the fraction of the first (small) size mode increased from about 0.5 to 0.9, indicating that a greater number of larger particles settled. Also the median diameter of the larger size mode decreased with time from about 8 μm to about 4.5 μm. The GSD varied greatly, thus indicating that, in some cases, the particle size distribution was very poly-dispersed. In other cases, the R^2 values indicated that neither unimodal nor bimodal fits were adequate. For cases in which the amount of material collected was small, the GSD tended to be larger, probably influenced by small-sample statistical variability.

To compare changes of particle size over time, the data were also fit with a unimodal lognormal size distribution:

$$s(x)=\frac{1}{\sqrt{\pi}\ x\ \ln\sigma_g}\exp\left[-\frac{(\ln x-\ln x_o)^2}{2(\ln\sigma_g)^2}\right]$$

where x_o is the AMAD, and σ_g is the GSD. Both values were obtained by using non-linear curve-fitting procedures available in SigmaPlot. Particle size parameters for both unimodal and bimodal distributions are listed in tables in Appendix G. The unimodal distribution did not fit the data as well as the bimodal distribution in most cases. This poor fit is indicated by small values of R^2 and the large GSDs; however, the unimodal AMAD parameter does describe the averaged size distribution.

The evolution of the unimodal AMADs as a function of time for each phase and shot are listed in Table 5.25 and are plotted in Appendix B, Figures B.1 through B.12. In general, decreased AMAD would be expected over time due to settling. This phenomenon was observed for many of the distributions. However, in other cases, the measured particle size collected for a particular time interval increased to a larger size or decreased to a smaller size, both results that are inconsistent with the expected trend. The only case for which these results can be rationalized is for the measurements obtained for the loader's position in test PI-6, which represent resuspension data. In that case (as for the activity concentrations), the variable data most likely resulted from personnel activity inside the tank itself.

Table 5.25. Change of Particle Size (Unimodal AMAD, μm) by Stage Over Time

Time Interval	Midpoint (min)	Driver	Commander	Gunner/Right Scout	Loader/Left Scout
PI-1					
0-30 sec	0.25	Did not run	3.07	0.46	2.46
0.5-1.5 min	1.00	1.40	0.90	2.97	3.39
1.5-3.5 min	2.50	1.17	0.69	0.55	1.19
3.5-7.5 min	5.50	1.8	0.95	0.67	1.37
7.5-15.5 min	11.5	1.02	1.8	0.55	1.03
15.5-31.5 min	23.5	0.48	0.96	0.47	1.07
31.5-63.5 min	47.5	0.30	0.50	0.45	0.27
63.6-127.5 min	95.6	0.23	0.43	0.33	0.24
PI-2					
0-15 sec	0.125	7.11	3.48	3.83	1.82
0.5-1 min	0.750	Did not run	1.85	4.39	1.32
1.5-2.5 min	2.00	2.52	1.32	0.98	1.37
3.5-5.5 min	4.50	1.73	1.14	0.79	2.42
7.5-11.5 min	9.50	0.49	1.15	1.07	3.0
15.5-31.5 min	23.5	0.68	0.64	0.73	0.47
31.5-79.5 min	55.5	0.65	0.48	0.78	0.38
79.5-127.5 min	104	0.49	0.31	0.61	0.29
PI-3					
0-10 sec	0.083	0.18	--	0.70	--
3-3.5 min	3.25	3.10	--	1.98	--
9-10 min	9.50	2.50	--	2.0	--
PI-4 (Includes residual aerosol from Shot 3, which was fired 13 min before. The loader's first-stage substrates sustained fragment damage, and their AMAD results may not be reliable.)					
0-10 sec	0.083	5.35	15.8	6.96	4.0
3-3.5 min	3.25	2.56	1.29	1.07	2.11
9-10 min	9.50	2.43	3.70	1.03	6.62
21-23 min	22.0	0.85	0.83	0.68	6.12
45-49 min	47.0	0.88	1.19	0.62	35.70
93-101 min	97.0	--	0.81	--	1.52
PI-5					
0-10 sec	0.083	7.49	3.87	NA	4.60
1-1 min, 10 sec	1.08	5.65	2.85	NA	2.43
3-3 min, 10 sec	3.08	4.56	2.5	NA	2.0
7-7.5 min	7.25	4.00	2.0	NA	2.2
15-16 min	15.5	18.68	1.5	NA	1.38
31-33 min	32.0	9.84	1.6	NA	1.06
61-65 min	62.5	6.92	1.30	NA	1.08
121-129 min	125	1.37	1.02	NA	2.0

144-148 min	146	--	--	NA	1.16
PI-6					
0-10 sec	0.083	2.5	8.46	NA	Resuspension
1-1 min, 10 sec	1.08	2.38	3.22	NA	Resuspension
3-3 min, 10 sec	3.08	1.8	1.5	NA	Resuspension
7-7.5 min	7.25	1.56	1.5	NA	Resuspension
15-16 min	15.5	0.58	1.25	NA	Resuspension
31-33 min	32.0	0.82	2.5	NA	Resuspension
61-65 min	62.5	0.85	8.02	NA	Resuspension
121-129 min	125	0.67	0.56	NA	Resuspension

Table 5.26. (cont'd)

Time Interval	Midpoint (min)	Driver	Commander	Gunner/Right Scout	Loader/Left Scout
PI-7					
0-10 sec	0.083	2.97	4.04	1.64	Resuspension
1-1 min, 10 sec	1.08	1.90	10.94	2.22	Resuspension
3-3 min, 15 sec	3.13	2.3	2.41	2.91	Resuspension
7-8 min	7.50	1.03	3.0	3.60	Resuspension
15-17 min	16.0	1.31	2.0	2.2	Resuspension
31-35 min	33.0	0.71	0.86	0.77	Resuspension
61-69 min	65.0	0.70	0.82	0.51	Resuspension
121-129 min	125	0.67	1.0	0.58	Resuspension
PII-1					
0-10 sec	0.083	1.46	1.71	--	0.58
3-4 min	3.50	1.84	1.52	--	0.81
9-11 min	10.0	1.8	3.65	--	3.07
PII-2 (Includes residual aerosol from Shot 1 fired 14 min before.)					
0-10 sec	0.083	3.57	1.33	1.32	2.79
3-4 min	3.50	0.78	0.99	0.72	1.04
9-11 min	10.0	0.50	0.97	0.86	0.87
21-25 min	23.0	0.55	0.64	0.72	0.51
45-53 min	49.0	0.92	0.93	0.58	0.48
93-109 min	101	0.75	0.64	0.53	0.80
PII-3					
0-10 sec	0.083	2.74	2.84	3.83	21.56
1-1 min, 10 sec	1.08	1.07	2.97	2.41	19.56
3-3 min, 15 sec	3.13	0.46	40.92	2.0	2.5
7-8 min	7.50	0.38	0.56	0.36	1.23
15-17 min	16.0	0.37	0.55	0.81	1.11
31-35 min	33.0	0.59	0.53	0.76	0.95
61-69 min	65.0	0.97	0.59	0.52	1.03
121-129 min	125	0.22	0.57	0.51	1.06
PIII-1					
0-10 sec	0.083	0.82	5.76	7.51	4.80
1-1 min, 10 sec	1.08	0.13	4.55	2.58	4.81
3-3 min, 15 sec	3.13	16.90	5.02	3.0	2.27
7-8 min	7.50	3.0	1.8	1.8	2.0
15-17 min	16.0	2.0	1.48	2.0	2.0
31-35 min	33.0	1.10	3.0	1.8	1.21
61-69 min	65.0	1.24	2.0	0.92	2.0
121-129 min	125	0.82	1.51	0.53	0.93
PIII-2					
0-10 sec	0.083	3.95	6.78	10.65	4.70
1-1 min, 10 sec	1.08	0.63	31.62	14.36	2.33
3-3 min, 15 sec	3.13	3.45	34.22	40.25	2.0
7-8 min	7.50	2.1	2.0	42.01	2.5
15-17 min	16.0	0.82	0.56	42.58	2.5
31-35 min	33.0	0.78	0.55	1.27	1.16
61-69 min	65.0	0.81	0.52	42.10	0.99
121-129 min	125	0.82	10.0	41.57	0.86
PIV					
0-10 sec	0.083	Line severed	NA	NA	Line severed
1-1 min, 10 sec	1.08	0.62	NA	NA	Line severed
5-5 min, 15 sec	5.25	1.28	NA	NA	Line severed
25-27 min	26.0	4.0	NA	NA	Line severed

For the most part, the data were fit to a fairly complex distribution (bimodal lognormal) with relatively few data points (i.e., nine). Almost 400 sets of CI results were analyzed using the models. About a dozen particle size distributions had to be estimated using professional judgment from the graphical representations because regression of the acquired data yielded results that were not logical. An example of a circumstance where professional judgment was applied was when a unimodal fit was attempted with data having a distinctive bimodal distribution (e.g., two clearly separated peaks in the distribution). The resulting estimate achieved through professional judgment would be closer to an arithmetic mean of the two AMADs with the GSD directly associated with the difference between the means.

Example particle size histograms as a function of unimodal AMAD are provided in Figures 5.31 through 5.35. Hyphens denote intervals where no sample was taken within that specific array. "NA" identifies shots were those samplers were not used. The unimodal and bimodal AMADs and GSDs of these examples are listed in Table 5.25.

Particle size distributions during the recovery activities help address resuspension and are provided in Table 5.26.

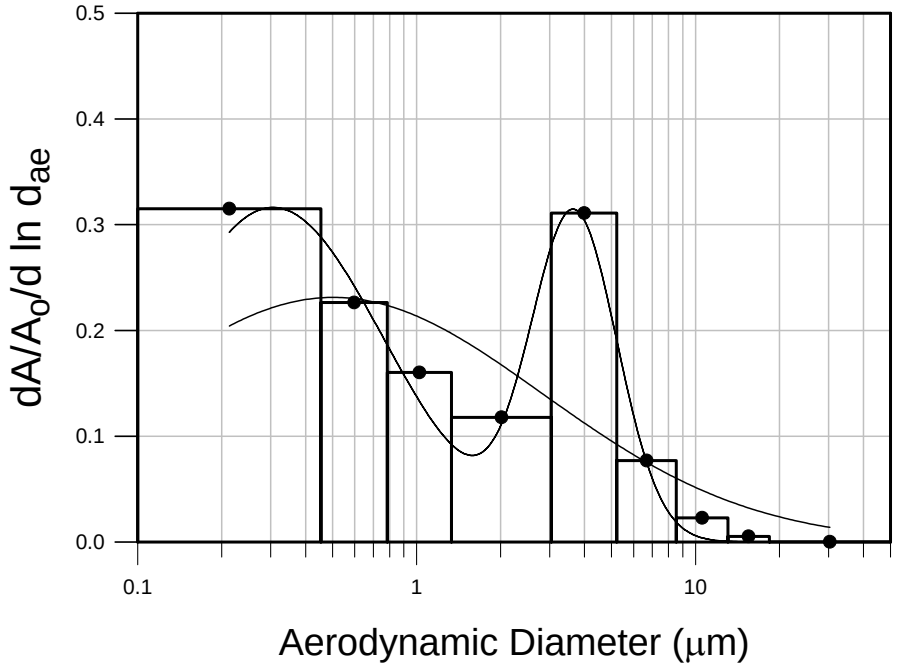

Figure 5.31. Example Histogram with Unimodal AMAD <1 μm (from PI-1-C7)

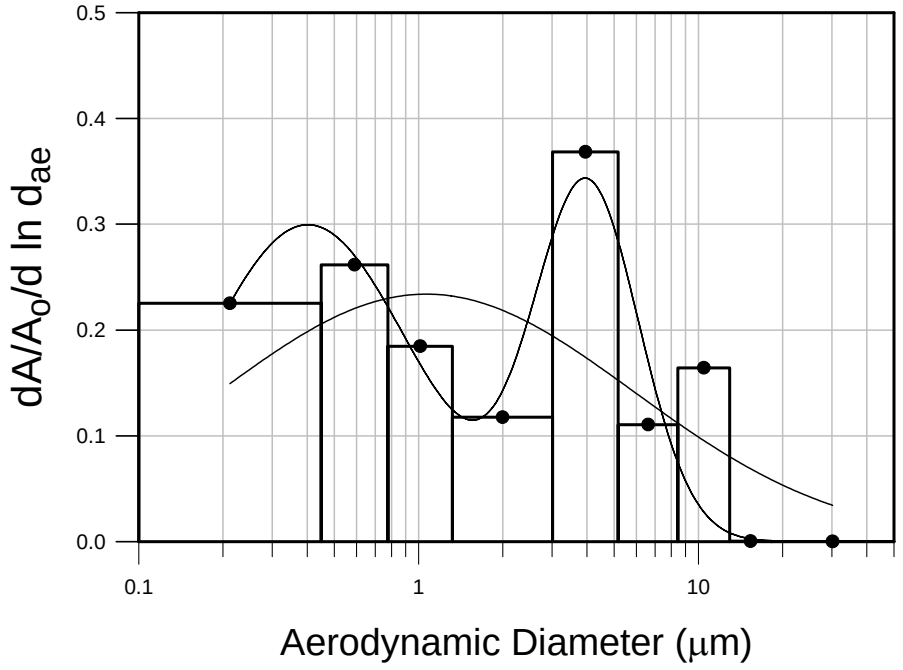

Figure 5.32. Example Histogram with 1 μm < Unimodal AMAD <5 μm (from PI-2-G5)

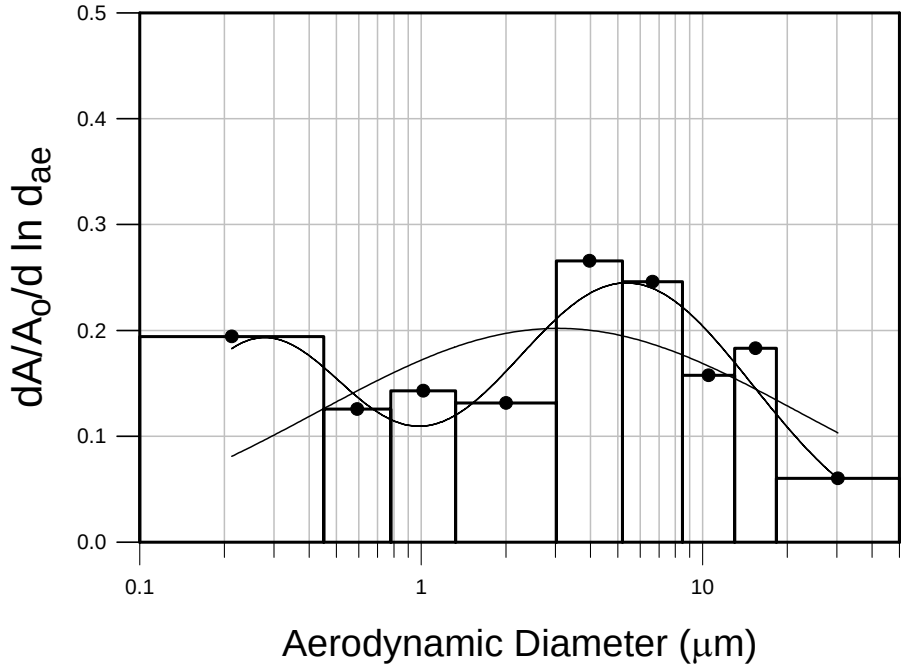

Figure 5.33. Second Example Histogram with 1 μm < Unimodal AMAD <5 μm (from PI-1-C1)

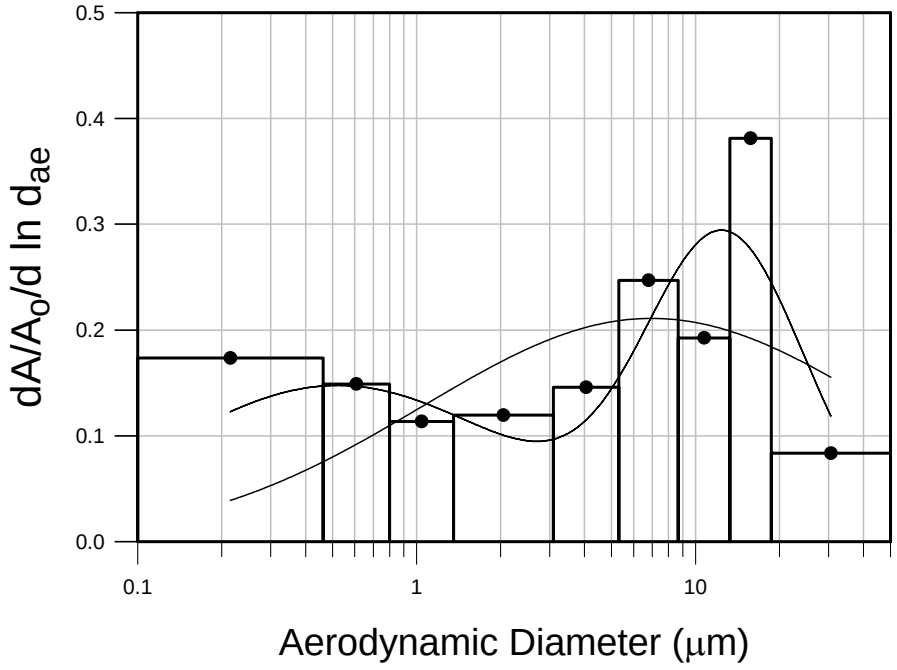

Figure 5.34. Example Histograms with 5 μm < Unimodal AMAD <20 μm (from PI-3-G4)

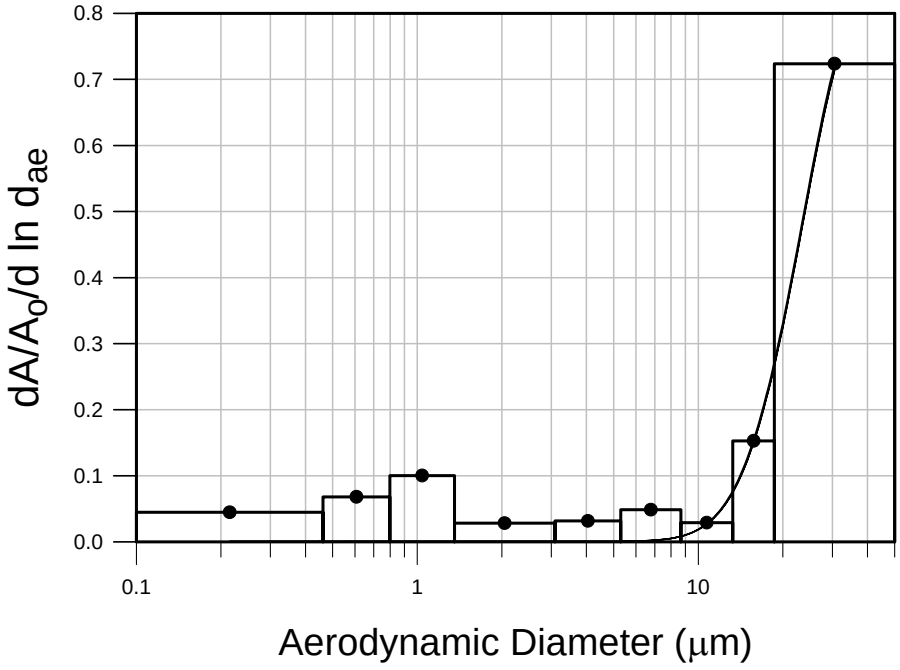

Figure 5.35. Example Histogram with Unimodal AMAD >20 μm (from PI-1-D1)

Table 5.26. List of Unimodal and Bimodal AMADs Used in Figures 5.31 through 5.35

Sample ID (AMAD)	Unimodal Fit			Bimodal Fit			Fraction in First Peak
PI-1-C7 (AMAD<1 μm)	AMAD (μm)	GSD	R^2	AMAD (μm)	GSD	R^2	0.73
	0.50	5.62	0.53	0.31	2.50	0.98	
				3.67	1.43		
PI-2-G5 (1 μm<AMAD<5 μm)	AMAD (μm)	GSD	R^2	AMAD (μm)	GSD	R^2	0.64
	1.07	5.51	0.40	0.40	2.34	0.79	
				3.99	1.54		
PI-1-C1 (1 μm<AMAD<5 μm)	AMAD (μm)	GSD	R^2	AMAD (μm)	GSD	R^2	0.37
	3.07	7.22	0.08	0.27	2.17	0.80	
				5.37	2.80		
PI-3/4-G4 (5 μm<AMAD<20 μm)	AMAD (μm)	GSD	R^2	AMAD (μm)	GSD	R^2	0.54
	6.96	6.63	0	0.52	4.30	0.58	
				12.79	1.92		
PI-1-D1 (AMAD > 20 μm)	AMAD (μm)	GSD	R^2	AMAD (μm)	GSD	R^2	0.03
	38.6	1.64	0.95	>1000	>1000	0.95	
				38.5	1.63		

Table 5.27. Unimodal and Bimodal AMADs during Resuspension Activities

PI-6							
Sample ID (Time +2:35 h)	Unimodal Fit			Bimodal Fits			Fraction in First Peak
L – 1 (0 to 20 min)	AMAD (μm)	GSD	R^2	AMAD (μm)	GSD	R^2	0.31
	0.95	4.88	0.07	0.53	1.17	0.92	
				5.32	6.87		
L – 2 (31 to 54 min)	AMAD (μm)	GSD	R^2	AMAD (μm)	GSD	R^2	0.27
	9.94	9.80	0	0.54	1.63	0.43	
				22.14	3.79		
L – 3 (54 to 67 min)	AMAD (μm)	GSD	R^2	AMAD (μm)	GSD	R^2	0.21
	0.96	4.96	0.25	0.50	1.20	0.74	
				1.95	6.89		
L – 4 (67 to 82 min)	AMAD (μm)	GSD	R^2	AMAD (μm)	GSD	R^2	0.20
	0.80	4.33	0.22	0.69	1.24	0.81	
				2.77	11.45		
L – 5 (82 to 104 min)	AMAD (μm)	GSD	R^2	AMAD (μm)	GSD	R^2	0.68
	11.5	6.74	0.18	2.33	5.01	0.95	
				22.2	1.44		
L – 6 (105 to 107 min)	AMAD (μm)	GSD	R^2	AMAD (μm)	GSD	R^2	0.08
	1.31	6.91	0.03	0.61	1.12	0.76	
				3.55	11.36		
L – 7 (107 to 111 min)	AMAD (μm)	GSD	R^2	AMAD (μm)	GSD	R^2	0.40
	1.34	10.6	0	0.44	1.64	0.36	
				10.1	6.30		
L – 8 (111 to 119 min)	AMAD (μm)	GSD	R^2	AMAD (μm)	GSD	R^2	0.46
	1.65	8.99	0	0.46	1.57	0.74	
				10.2	4.11		
L – 9 (119 to 135 min)	AMAD (μm)	GSD	R^2	AMAD (μm)	GSD	R^2	0.62
	11.5	9.77	0	1.24	4.94	0.85	
				26.9	1.58		

Table 5.27. (cont'd)

PI-7							
Sample ID (Time + 3:21 h)	**Unimodal Fit**			**Bimodal Fits**			**Fraction in First Peak**
L – 1 (0 to 20 min)	AMAD (μm)	GSD	R^2	AMAD (μm)	GSD	R^2	0.42
	0.002 1.59[(a)]	0.22 1.96[(a)]	0	5.47 1.59	9.08 1.96	0.92	
L – 2 (20 to 40 min)	AMAD (μm)	GSD	R^2	AMAD (μm)	GSD	R^2	0
	1.70	4.61	0.35	0.03 1.09	0 7.77	0.21	
L – 3 (40 to 60 min)	AMAD (μm)	GSD	R^2	AMAD (μm)	GSD	R^2	0
	17.26	7.5	0.04	>1000 17.53	>1000 7.84	0.04	
L – 4 (60 to 70 min)	AMAD (μm)	GSD	R^2	AMAD (μm)	GSD	R^2	0.28
	3.70	1.87	0.72	0.30 3.87	1.30 1.66	0.98	
(a) Estimate based on professional judgment used to interpret graphical data representation.							

5.5.2 Exterior Aerosols

The external samples were obtained using Andersen CIs that operated at a higher flow rate than the Marple personal CIs. The uranium masses collected as a function of stage and derived from gamma spectrometry measurements are summarized in Appendix A, Table A.39. Two sets of data were obtained for each test for which they operated. The nominal sample acquisition time was 2 min. Metal fragments severed one line during the PI-5 test. Another sampler (i.e., the first sampler for Phase III-2) was accidentally operated over a 5-h time period because the electrical connections to the power switch were reversed. Much more material was collected with this unit, and the results integrate over that long time period.

Modeled results of the AMADs, GSDs, R^2 values, and fractions of activity in the first peak (for the bimodal distributions) for the external samples obtained in tests PI-5 through PIII-2 are listed in Table 27. These results were obtained using two eight-stage Andersen CIs that were operated at a nominal flow rate of 28.3 Lpm. The samplers identified as PSB-CAE-1 and 2 were from a secondary test in which a C4 explosive was detonated to simulate the concussion to the Superbox similar to a test shot.

The data from PI-5, CI-1 are used to briefly illustrate the modeling results. Particle size distribution calculations applying the unimodal regression model to the PI-5-CI-1 derived-uranium masses resulted in an AMAD of 27.1 μm with a GSD of 3.56 (R^2 = 0.45). Results calculated using the bimodal model were that the AMAD of the first peak equals 1.97 μm with a GSD of 48.3 and the AMAD of the second peak equals 9.32 μm with a GSD of 1.13 (R^2 = 0.92). The fraction of the mass in the first peak is 0.74. An estimate of the unimodal AMAD using professional judgment based on the graphical representation would be 8.0 μm and 2.5 μm, respectively. The types of curves are the same as those obtained using the Marple CIs. Both unimodal and bimodal distributions are present.

Results of the PI-5 to PIII-2 shots show a large range of particle sizes—unimodal AMADs from 0.2 μm to just > 28 μm (before applying professional judgment) with some very large GSDs (except for the 5-h sample). Bimodal AMAD results for the first peak range from 0.16 μm to 1.97 μm; AMAD values for the second peak ranged from 2.93 μm to 30.1 μm. Based on the R^2 goodness-of-fit parameter, the PIII-2, CI-2 results were best described by the unimodal regression. The best bimodal fit was obtained with

Table 5.28. Exterior Cascade Impactor Data

Sample ID (Flow Rate)	Distributions				
	Unimodal		Bimodal		
	AMAD (µm)	GSD/R^2	AMAD (µm)	GSD	Fraction In First Peak/R^2
PI-5E-1 (27.2 Lpm)	27.1 8.0[(a)]	3.54 / 0.45 2.5[(a)]	1.97 9.32	48.28 1.13	0.74/0.92
PI-6E-1 (19.5 Lpm)	0.30 1.0[(a)]	10.3 / 0.20 5.0[(a)]	0.20 2.93	1.70 1.68	0.70/0.96
PI-6E-2 (20.1 Lpm)	0.81 2.0[(a)]	33.4 / 0 16.0[(a)]	0.16 11.57	7.47 1.14	0.91/0.71
PI-7E-1 (23.5 Lpm)	16.2 6.0[(a)]	1.23 / 0.79 5.0[(a)]	0.28 21.34	1.54 6.58	0/0.26
PI-7E-2 (29.4 Lpm)	0.68 1.5[(a)]	34.8 / 0 7.0[(a)]	0.18 11.76	2.15 2.16	0.64/0.83
PII-1/2E-1 (28.1 Lpm)	19.4 9.0[(a)]	2.12 / 0.62 1.5[(a)]	0.25 9.01	1.89 1.11	0.22/0.98
PII-1/2E-2 (28.9 Lpm)	22.1 4.0[(a)]	6.30 / 0.43 5.0[(a)]	1.13 12.73	1.13 2.30	0.47/0.79
PII-3E-1 (27.7 Lpm)	0.19 2.0[(a)]	12.6 / 0.03 5.0[(a)]	0.23 17.57	2.02 2.09	0.57/0.89
PII-3E-2 (28.3 Lpm)	1.29 2.0[(a)]	36.5 / 0 5.0[(a)]	0.34 26.76	1.23 13.59	0.10/0.46
PIII-1E-1 (27.0 Lpm)	17.4 7.0[(a)]	1.86 / 0.92 4.0[(a)]	0.17 23.05	1.52 5.52	0/0.47
PIII-1E-2 (27.3 Lpm)	25.3 3.0[(a)]	3.78 / 0.05 4.0[(a)]	0.42 7.76	1.11 1.10	0.81/0.999
PIII-2E-1 (b) (30.1 Lpm)	0.23 1.5[(a)]	6.89 / 0.84 6.0[(a)]	0.40 30.12	4.26 1.93	0.72/0.89
PIII-2E-2 (28.7 Lpm)	15.0 6.0[(a)]	1.24 / 0.96 5.0[(a)]	0.30 25.05	1.46 6.14	0/0.22
PSB-CAE-1 (28.6 Lpm)	11.8 4.0[(a)]	7.55 / 0.14 2.5[(a)]	0.31 4.26	1.50 5.91	0/0.082
PSB-CAE-2 (25.2 Lpm)	17.2 4.5[(a)]	7.41 / 0.17 5.0[(a)]	0.13 10.72	1.55 6.23	0/0.15

(a) Professional judgment based on graphical representation.
(b) Power switch was reversed and the sample was acquired over a 5-hr period.

PIII-1, CI-2. Neither of the models fit the C4 sample data very well as denoted by their very low R^2 values.

It is difficult to interpret results that varied as widely as these. Relatively small amounts of aerosol were sampled over a short 2-min interval during which time a variety of environmental parameters including air movement around the tank affected the samples. This air movement may have created different flow patterns near the samplers. Only a few large particles on the upper stage or stages of the CIs can create results that show the presence of a large particle size. In general, the unimodal AMADs are associated with larger GSDs, and this result would be expected. However, some of the GSDs for peaks in the bimodal distributions are also unrealistic.

5.6 Chemical Composition of Selected Samples

Samples produced from the field portion of the Capstone DU Aerosol Study were expected to consist predominantly of DU oxides and other metallic particles and oxides in powder form. Samples were

recovered either as a powder on a filter media, in a cyclone grit chamber, on a deposition tray, or on a Defensap wipe. Grit chamber residues were transferred to glass vials for storage and handling. All samples were counted for alpha, beta, and/or gamma levels of radioactivity, and the resulting data provided a means to estimate uranium concentrations in every sample. Selected samples with sufficient mass also underwent a variety of physical and chemical analyses that included:

- uranium mass or concentration as determined by chemical methods (ICP-MS or KPA)
- oxide phases of the uranium oxide particulate materials (XRD)
- physical structure and particle morphology (SEM)
- *in vitro* solubility (in simulated extracellular fluid)
- isotopic composition of U-235 to U-238 to determine whether the uranium in the aerosol samples was from DU or natural uranium (ICP-MS and TIMS)
- limited analysis of other metals in several of the samples (ICP-MS or ICP-AES)
- TRU elemental analysis of a penetrator fragment.

The primary samples selected for extensive characterization were cyclone residues and their backup filters. The cyclones collected the largest sample mass of all samples. They reflect aerosols collected over the 2-h sampling time for each shot and were already size separated. Cost considerations limited the number of cyclone samples characterized to one from each phase. Cyclone sample sets were selected from PI-3/4, PII-1/2, and PIII-2. Additionally, the cyclone from PI-7 was analyzed because it represented the shot that was most representative of the only Abrams turret/hull shot sustained during the Gulf War/ODS. Several other samples also were selected for further analysis either because of specific interest in them or as representative samples for use in comparing uranium-derived data from radioactivity count data versus results from direct chemical analysis.

Uranium masses and concentrations, isotopic results, uranium oxide speciation, TRU analysis, particle structure and morphology, and *in vitro* solubility are discussed in this section.

5.6.1 Uranium Analysis

Results of the uranium analyses of the various sampling types and filter media are discussed in the following sections.

5.6.1.1 Cyclone Samples

The cyclone residues from four shots were analyzed for uranium by ICP-MS, and by KPA initially as a QC check. ICP-AES also was used to detect the presence of non-uranium metals. The ICP-AES analysis automatically included uranium. Although KPA and ICP-MS are generally superior to ICP-AES analysis for uranium, the ICP-AES results (from the same sample dilutions) were very similar to the KPA results and were included in the uranium data analysis. The backup filters were analyzed using all three methods. However, because the ICP-MS analysis was run on a “per filter” basis, rather than on a “per gram sample” basis, only the KPA and ICP-AES results are reported for these few samples. Results of the uranium mass percentages of total mass in the cyclone residues and backup filters are listed in Table5.29. The undigested mass refers to the residue remaining after sample preparation with HNO_3 and HCl (discussed in Section 3.9.2.1) for samples analyzed using KPA and ICP-AES.

Table 5.29. Uranium Mass Percentages in Cyclone Residues

Phase/Shot	Stage	%U by ICP-MS	%U by KPA	%U by ICP-AES	% Mass Undigested
PI-3/4	1	72.0 ± 3.60	62.3 ± 2.49	63.2 ± 9.48	5
	2	57.4 ± 2.87	58.8 ± 2.35	58.8 ± 8.82	17
	3	62.7 ± 3.14	56.2 ± 2.25	52.7 ± 7.91	13
	4	54.8 ± 2.74	55.4 ± 2.22	56.3 ± 8.45	11
	5	52.7 ± 2.64	47.8 ± 1.91	48.5 ± 7.28	13
	Backup Filter	(a)	43.4 ± 1.74	44.3 ± 6.65	13
PI-7	1	54.1 ± 2.71	50.3 ± 2.01	50.5 ± 7.58	18
	2	51.3 ± 2.57	47.7 ± 1.91	48.9 ± 7.34	17
	3	50.0 ± 2.50	45.3 ± 1.81	46.2 ± 6.93	13
	4	49.2 ± 2.46	42.4 ± 1.70	43.4 ± 6.51	11
	5	49.5 ± 2.48	41.3 ± 1.65	40.3 ± 6.05	12
	Backup Filter	(a)	38.3 ± 1.53	39.7 ± 5.96	23
PII-1/2	1	22.3 ± 1.12	18.4 ± 0.74	19.0 ± 2.85	41
	2	25.9 ± 1.30	23.6 ± 0.94	23.9 ± 3.59	38
	3	28.5 ± 1.43	23.3 ± 0.93	23.0 ± 3.45	35
	4	27.7 ± 1.39	24.7 ± 0.99	25.1 ± 3.77	37
	5	27.7 ±1.39	21.7 ± 0.87	23.3 ± 3.50	35
	Backup Filter	(a)	25.9 ± 1.04	27.0 ± 4.05	32
PIII-2	1	65.4 ± 3.27	59.7 ± 2.39	63.1 ± 9.47	5
	2	(b)	(b)	(b)	(b)
	3	(b)	(b)	(b)	(b)
	4	63.6 ± 3.18	64.0 ± 2.56	69.9 ± 10.5	4
	5	62.9 ±3.15	68.2 ± 2.73	71.5 ± 10.7	4
	Backup Filter	(a)	62.0 ± 2.48	65.2 ± 9.78	3

(a) Analyzed on "per filter" basis rather than weight basis.
(b) Insufficient sample for analysis.

Uranium concentrations as detected by ICP-MS, on average, were 9% higher than the uranium concentrations detected by KPA and ICP-AES. Although this difference is within the statistical variation of the data, it suggests nonetheless a bias that is probably due to the presence of varying amounts of uranium in undigested sample, which ranged from 3 to 41% (discussed in Section 3.9.2.1). It is likely that some but not much uranium is tied up in this insoluble matrix. The variability in instrument response with the ICP-MS was less than ± 5%. A 1-sigma standard deviation for KPA analysis was ± 4%. The ICP-AES results were reported as being within ± 15%, though its results correlated very well with the KPA results, and the 15% is probably conservative for the mass of uranium in the samples. These numbers suggest that the results between the ICP-MS and the KPA should be comparable at these concentration levels and that the ICP-AES results also should be similar but may have more variability. However, it does not address the differences created by the two distinctly different digestion processes. Samples analyzed by ICP-MS were digested using hydrofluoric acid (HF), and these samples would be expected to include any uranium tied up in the fraction otherwise undigestable by other acids. The samples analyzed by KPA and ICP-AES were digested in a standard acid mix (nitric and hydrochloric acids) that would not have extracted uranium in the undigested fraction.

Using the ICP-MS values (except for the backup filters) listed in Table 5.29 as the basis for further discussion, the uranium in the PI-3/4 cyclone stages declined slightly though somewhat inconsistently as a function of stage from a high of 72% on Stage 1 to a low of about 53% on Stage 5. From the KPA analysis, it appears that the uranium content in the backup filter was slightly less than the uranium in Stage 5. The uranium in PI-7 remained relatively steady, declining only slightly by stage from a high of 54% to a low of 49%.

The undigested mass of these samples ranged from a low of 5% in Stage 1 of Shot 3/4 to a high of 18% in Stage 1 of Shot 7. The bottom filter contained the highest undigested mass in Phase I of 23%.

The aerosol collected during PII-1/2 contained much lower percentages of uranium that varied from 22% in Stage 1 to about 28% in Stages 3 through 5. The KPA results suggest that the uranium mass fraction in the backup filter remained at about the same level. The undigested fraction was considerably higher in all samples collected from this shot, varying from 32 to 41%.

The aerosols collected from PIII-2 contained very little material in the Stage 1 and 2 cyclone grit chambers in the initial sample collection and in Stages 2 and 3 after the cyclone residues were resuspended. The reason for this anomaly is not known. Comparing cyclone Stages 2 and 3 with CI Stages 5 and 6, which had roughly similar cutoff points, did not substantiate this pattern. The uranium numbers from the stages analyzed and the backup filter show little variation, ranging from 63 to 65% with 62% in the backup filter. The undigested masses ranged from 3 to 5%, which is significantly less than in samples collected from Phases I and II.

The PFDB was used in PI-1 to collect and separate the ultrafine particles that passed through the final cyclone stage. Because the flow rate could not be confirmed and a leak was suspected, the actual percentage of material that would qualify as ultrafine is not known but is believed to be small. Approximately 40% of the coarsest PFDB filter sample was analyzed by KPA and ICP-AES and found to contain about 1.29 mg of uranium. This represented about 59% of the metal ions present in the sample. The remainder of this sample was subjected to *in vitro* solubility analysis. Four PFDB samples were examined by SEM (Appendix D, Section D.2.1).

5.6.1.2 Filter Cassette Samples

The driver's position IOM samples from PI-1 were analyzed by ICP-MS for uranium mass and concentration. The results (not adjusted for the uranium mass of 142 μg collected on the field blank) are presented in Table 5.30.

5.6.1.3 CI Substrates

Several CI substrates were selected for uranium analysis using ICP-MS solely for comparison with the radioactivity counts. These samples were selected to represent low, medium, and high radioactivity levels and to include each impactor stage. The results were used in the verification and ingrowth analysis discussed in Appendix A.3. The samples selected were not in any sequence and are not summarized here. In comparing the direct chemistry results of radioactivity-derived uranium, the higher result was reported in Appendix A, Tables A.19 through A.32.

Table 5.30. PI-1 Driver's Position IOM Uranium Content

Sample ID	Time Interval	Sampling Time	Volume (m^3)	U/filter (µg)	U Conc. (µg/m^3)
PI-1I-D-1	0-30 sec	30 sec	0.00115	3320	2.89E+6
PI-1I-D-2	0.5-1.5 min	1 min	0.0025	2360	9.44E+5
PI-1I-D-3	1.5-3.5 min	2 min	0.0050	3470	6.94E+5
PI-1I-D-4	3.5-7.5 min	4 min	0.010	2850	2.85E+5
PI-1I-D-5	7.5-15.5 min	8 min	0.018	1550	8.61E+4
PI-1I-D-6	15.5-31.5 min	16 min	0.039	1980	5.08E+4
PI-1I-D-7	31.5-63.5 min	32 min	0.076	2660	3.50E+4
PI-1I-D-8	63.6-127.5 min	64 min	0.138	4220	3.05E+4
PI-1I-D-9	Field Blank	NA	NA	142	NA

5.6.1.4 MVF Samples

Three MVF segments, one from each phase, were sent to PNNL for analysis. Unfortunately, so little sample remained on the Phase II sample, that the sample was evaluated using SEM only. The Phase-I and Phase-III MVF samples were analyzed using KPA. Essentially all material in these samples dissolved in the nitric/hydrochloric acid solution. The PI-1 sample that covered the first 5 sec post impact contained 14.3% uranium by mass as measured by KPA. When analyzed by ICP-AES for other metals in a sample scan of the PI-1sample, the mass of uranium was estimated to be 16% of the total sample. The PIII-2 sample taken during the first 3 sec contained 48.3% uranium by mass as measured by KPA and 50.6% as measured by ICP-AES.

5.6.1.5 DU Cone Sample Analysis

The pile of powder collected from an inside ledge of the vehicle after the PI-5 shot was a sample of nearly pure DU oxide. Analysis of its content showed that it contained 83.6 ± 3.34 (1-sigma) percent uranium by weight.

5.6.2 Isotopic Analysis

The USACHPPM chemistry laboratory analyzed the U-235 to U-238 uranium atom ratios on several cyclone residues using ICP-MS. Results of the ratio analyses at the 1-sigma level are listed in Table 5.31. The atom ratios, in which the U-235/U-238 atom ratio is about 0.2%, indicate that the uranium collected in the aerosols is consistent with military DU source material.

In addition to the ICP-MS procedure for running isotopic uranium, the DU oxide cone and the recovered fragment sample (22.5 g) were analyzed at PNNL using thermal ionization mass spectrometry (TIMS). The TIMS procedure provides higher accuracy of the uranium isotopic composition and a wider range of uranium isotopes. The results of this procedure are listed in Table 5.32. The isotopic analysis shows that both samples are DU. The U-238 and U-235 percentages of 99.79 and 0.21%, respectively, are within the normal range defined as DU. The presence of U-234 from the decay of U-238 also is within the expected range. The presence of U-236 suggests that a very small amount of contamination is present in the DU from reprocessed fuel introduced during the process in which DU was separated from enriched uranium.

Table 5.31. Isotopic Analysis of U-235 to U-238 Atom Ratio Percentages in Cyclone Residues

Phase/Shot	Stage	U235/U238 atom ratio	U ratio (± 1σ)
PI-3/4	1	0.205	0.003
	3	0.208	0.001
	5	0.208	0.002
PI-7	1	0.207	0.002
	3	0.211	0.001
	5	0.207	0.001
PII-1/2	1	0.207	0.001
	3	0.206	0.002
	5	0.209	0.001
PIII-2	1	0.208	0.002
	4	0.205	0.002
	5	0.212	0.001

Table 5.32. Uranium Isotopic Composition of Fragment and DU Oxide Cone (TIMS Analysis)

Sample	U Isotope	Atom Percent of Total Uranium (± 1σ)
DU Oxide Cone Sample	234	0.00077 ± 0.00019
	235	0.206 ± 0.004
	236	0.0010 ± 0.0005
	238	99.79 ± 0.004
DU Metallic Fragment	234	0.0022 ± 0.0006
	235	0.207 ± 0.003
	236	0.0027 ± 0.0003
	238	99.79 ± 0.003

5.6.3 Non-DU Metals

Selected samples, primarily material recovered from cyclone grit chambers, were analyzed for other metals besides uranium. Most of the samples were analyzed at the USACHPPM chemistry laboratory by ICP-MS using the samples prepared for uranium analysis. USACHPPM established an instrument variability of <± 5%. PNNL analyzed many of the same samples (as a QC check) and a few different ones using ICP-AES with the same sample solutions prepared for KPA uranium analysis. The uncertainty for many metals is greater with ICP-AES (± 15%), but unlike ICP-MS, ICP-AES provides superior discrimination of elements like iron and zinc. Because of the difference in digestion methods, (USACHPPM used HF in their process), the ICP-MS results were expected to yield higher concentrations than the ICP-AES of most metals.

The concentrations of two major aerosol components (aluminum and iron) and three lesser components (titanium, zinc, and copper) are listed in Table 5.32 for the two analytical processes conducted. Ratios of the ICP-MS results averaged higher for aluminum than the PNNL results. Except for sample PI-3/4, Stage 1, the ratios by test phase are reasonably consistent. The next highest difference between the analytical methods is the ratio of 1.59 for zinc. The difference between the results is substantially less for

the other elements at 1.37 for iron, 1.08 for titanium, and 0.99 for copper. The obvious explanation for the differences noted is that USACHPPM's HF digestion dissolved the samples completely whereas the PNNL samples digested in HNO_3 and HCl contained undissolved residue.

As reported in the section on SEM/EDS compositions, other metals were present in the aerosols to a lesser extent. Titanium, alloyed to DU in the penetrator, was consistently identified in the samples. Additionally, trace levels (within 10 times the detection limit with errors likely to exceed 15%) of chromium, manganese, nickel, cadmium, barium, magnesium, lead, tin, and strontium were detected in some or all the samples.

Table 5.33. Comparison of Concentrations of Aluminum, Iron, and Titanium in Aerosols

Sample ID	Aluminum mg/g		Iron mg/g		Titanium mg/g	
	ICP-MS	ICP-AES	ICP-MS	ICP-AES	ICP-MS	ICP-AES
PI-3/4						
Stage 1	102.2	15.1	11.4	45.2	22.2	6.2
Stage 2	78.0	36.9	103.6	54.7	11.2	6.6
Stage 3	86.6	36.0	73.2	40.9	10.2	5.4
Stage 4	89.2	44.4	49.1	38.4	8.0	5.3
Stage 5	120.0	50.6	57.5	32.1	6.3	4.1
Backup Filter	--	47.9	--	25.2	--	3.6
PI-7						
Stage 1	106.5	40.1	63.9	47.0	12.3	6.4
Stage 2	119.5	57.1	54.9	37.4	9.5	5.5
Stage 3	129.3	77.2	72.5	34.0	7.0	4.7
Stage 4	145.2	89.4	58.9	32.0	6.4	4.0
Stage 5	162.5	82.5	58.3	30.3	5.3	3.3
Backup Filter	--	62.9	--	27.7	--	2.9
PII-1/2						
Stage 1	177.5	54.6	49.6	28.8	13.1	3.9
Stage 2	198.1	62.2	42.2	18.5	13.1	4.1
Stage 3	237.6	61.5	13.7	13.7	10.6	3.7
Stage 4	230.6	76.6	28.4	12.2	7.6	3.3
Stage 5	236.2	72.5	30.0	11.2	5.0	2.3
Backup Filter	--	124.	--	19.1	--	2.3
PIII-2						
Stage 1	--	16.1	--	69.3	--	5.8
Stage 4	--	21.1	--	49.1	--	5.5
Stage 5	--	22.0	--	42.3	--	5.5
Backup Filter	--	26.1	--	33.8	--	4.8

5.6.4 Presence of Transuranic Elements

TRU elements such as plutonium (Pu), neptunium (Np), and americium (Am) are commonly found at a trace levels in DU penetrators due to process equipment contamination. A 22.5-g fragment found inside the turret after PI-5 was dissolved, and a 2-mL aliquot containing about 0.18 g of solution was analyzed for the presence of Pu, Np, and Am. It was also analyzed for thorium (Th-228, a progeny of natural thorium; Th-230, a progeny of U-234; and Th-232, naturally occurring thorium). No detectable quantities of Pu, Np, or Am were found in this sample within the detection limits specified in Table 5.33. The probable reason that these elements were not found is that the amount of material in the sample was small

compared to the amount of material in a full penetrator, and the quantities of these trace elements were too low for detection. A small amount of Th-228 and Th-230 was detected. Am-241 is often detected in association with the Th-228, but further alpha discrimination between the two radioisotopes revealed only the Th-228.

Table 5.34. Analysis of Transuranic Trace Elements in the DU Fragment

Element	pCi/g	Bq/g
Th-228 + Am-241	0.998 ± 11%	0.0369 ± 11%
Th-230	4.74 ± 5%	0.176 ± 5%
Th-232	<0.1 pCi/g	<0.0037
Np-237	<0.5 pCi/g	<0.0185
Pu-238	<0.2 pCi/g	<0.0074
Pu-239+240	<0.1 pCi/g	<0.0037

5.6.5 Uranium Oxide Composition

X-ray diffraction patterns for selected aerosol samples were compared to x-ray patterns in the Inorganic Crystal Structure Database (ICSD) database library of standard materials to identify the crystalline uranium oxide phases and to provide a semi-quantitative analysis of their relative proportion in each sample. The XRD patterns for the aerosol samples can be generally characterized as containing numerous sharp peaks. Typically, several of the peaks exhibited some peak broadening, undoubtedly due to the overlap with diffraction peaks from other solids. Some of the XRD patterns (e.g., PII-1/2-CY-5) contained a broad diffraction profile (or hump) from approximately 20 to 40° 2θ. This broad diffraction profile is indicative of samples containing amorphous (non-crystalline) materials, which cannot be identified by XRD. This amorphous material probably contains oxide phases of target metals as characterized by SEM/EDS (Appendix D) and may contain also some amorphous uranium oxides.

Identification of uranium-containing phases was based on a comparison of the measured XRD patterns to the ICSD diffraction patterns for U, UO_2, U_4O_9, U_3O_8, UO_3, $UO_3 \cdot 2H_2O$ (schoepite), and intermediate stoichiometric forms. The identification routines consistently selected several phases of U_3O_8 and UO_3 as the predominant phases present. Peaks consistent with U_3O_8 are clearly present in all samples and are believed to be the primary, and perhaps the only, phase present in these samples. However, although several attempts were made to distinguish between UO_3 and U_3O_8 patterns, the similarity in the major peaks in their XRD patterns confounded the analysis, and there was insufficient evidence to rule out the presence of UO_3. Additionally, the possible presence of one or more phases similar to UO_3 and U_3O_8 made resolution of these lines impossible from these data. The observed shift in *d* spacings of peaks from sample to sample, in spite of calibration with the corundum (α-Al_2O_3) internal standard, suggested that one or more phases present had not been previously characterized relative to the XRD patterns listed in the ICSD database.

A significant fraction of the remaining oxide detected was the U_4O_9 phase, which fit the database pattern very well, though $U_4O_{9.2}$ was often a slightly better fit to the data than U_4O_9. Schoepite was also identified in several of the samples at a much smaller fraction. Based on the XRD pattern for uranium metal (Card 11-628), there was no evidence of crystalline uranium metal in these samples. Additionally, although the presence of UO_2 cannot be ruled out because of the overlap in the XRD patterns for UO_2 and U_4O_9, it was not specifically detected.

The XRD patterns for several samples contained one or more diffraction peaks that could not be matched to any patterns in the ICSD database for solids containing only uranium, oxygen, and/or hydrogen. These samples included residues from Phase I-3/4, Stage 1; PII-1/2, Stages 1 and 3; and the PI-7 backup filter. Phases responsible for these peaks were not identified, but were likely one or more of the oxide phases of the non-DU metals discussed in Section 5.6.3.

Examples of the XRD patterns are presented in Figures 5.36 and 5.37. All of the measured XRD patterns are shown in Appendix C. Figure 5.36 is the diffraction pattern for the PI-3/4-CY Stage-1 residue. For contrast, Figure 5.37 shows the background-subtracted pattern of PII-1/2-CY Stage 5. In this figure, the XRD patterns from the ICSD database used to identify the peaks in the measured XRD pattern are plotted schematically below the XRD pattern for the residue from PII-1/2-CY Stage 5. Within any database pattern, the height of each line represents the relative intensity of an XRD peak for that phase at that d-spacing/2θ value (i.e., the longest line signifies the XRD peak with the greatest intensity [100% I/I_o], and so on). The measured XRD patterns of the other samples are provided in Appendix C. The overlap in the UO_3 and U_3O_8 phases is visible in these patterns. The small peak at about 12° 2θ is characteristic of a distinctive schoepite peak.

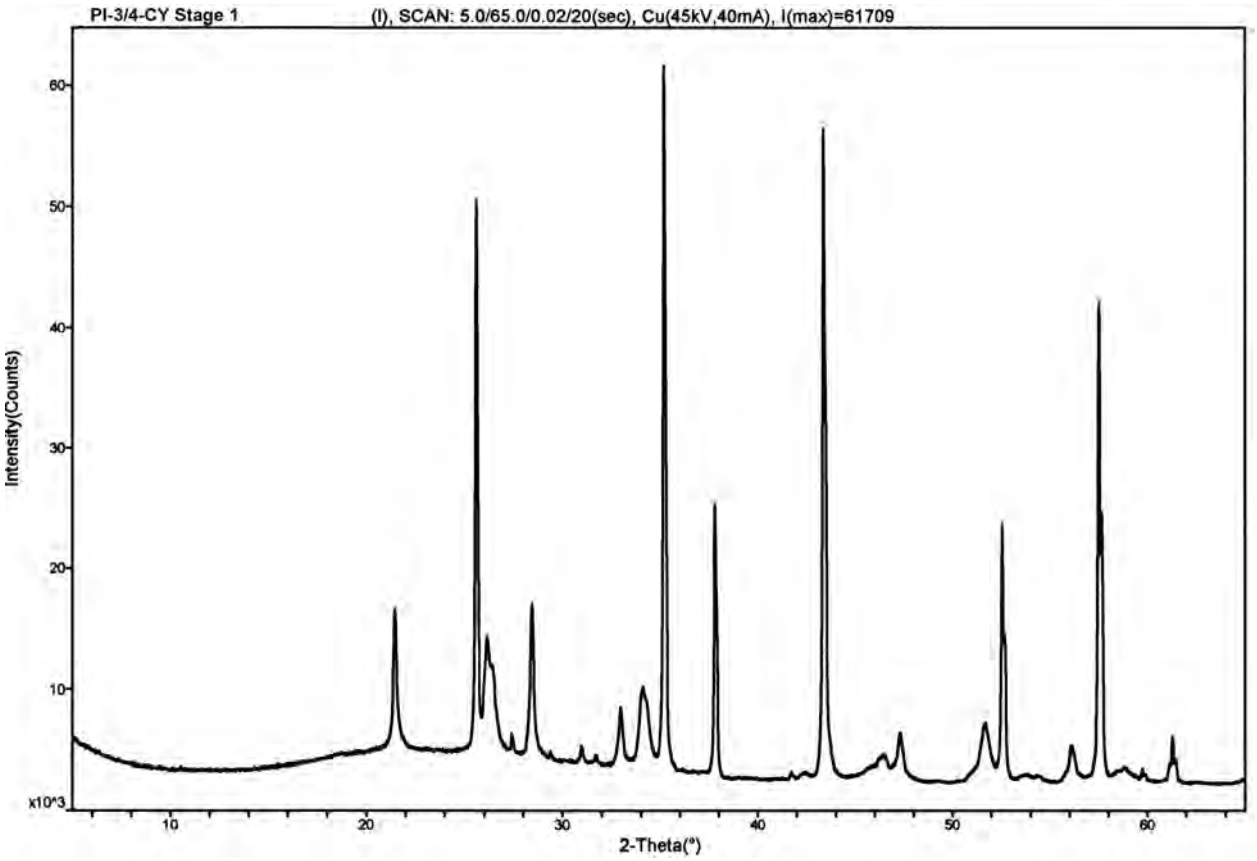

Figure 5.36. XRD Pattern of the Residue from PI-3/4-CY Stage 1

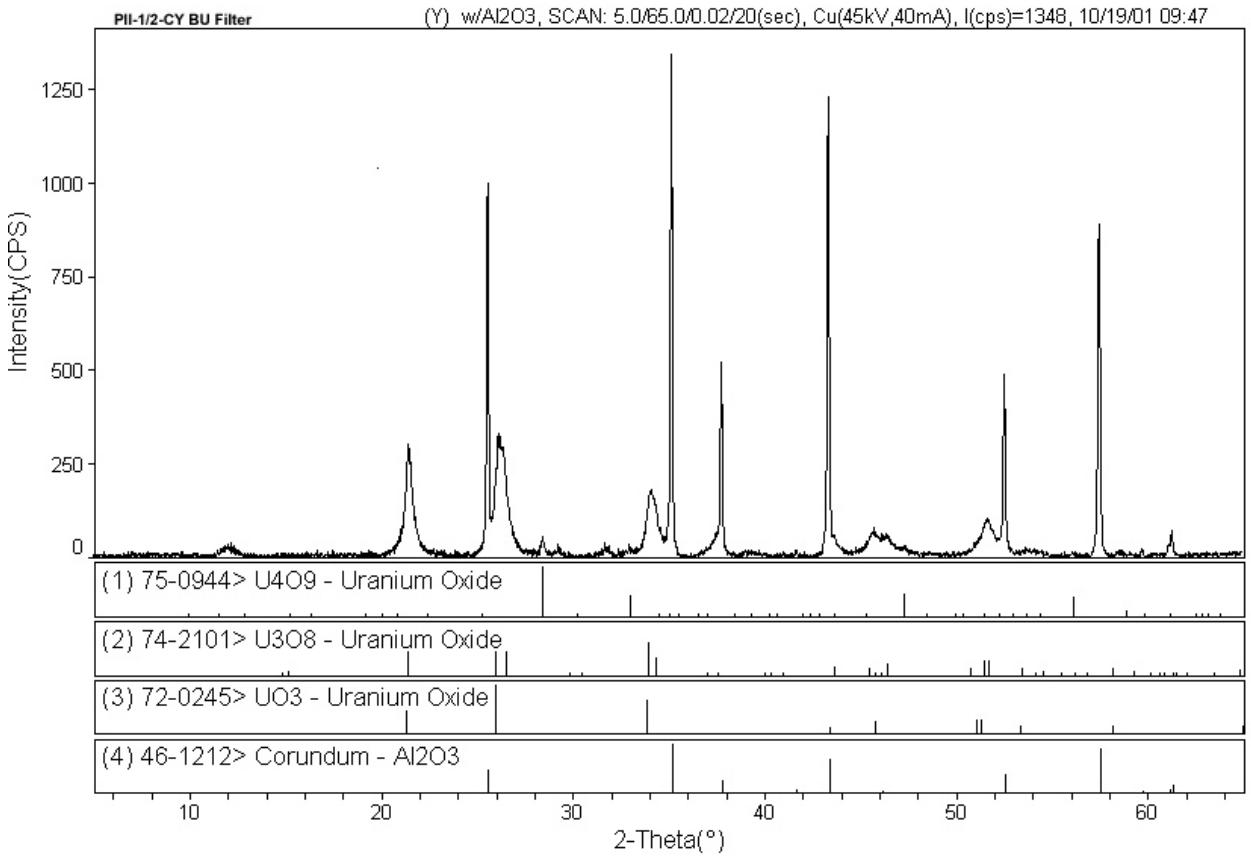

Figure 5.37. XRD Profile-Fitted Pattern of the Residue from PII-1/2-CY Stage 5

Approximate percentages of the major uranium oxide species present are listed in Table 5.35. These weight percentages are based on areas of peaks for identified phases. This calculation refers only to the crystalline phases and does not account for the small fraction of unknown uranium phases or the amorphous species that may be present. As noted previously, the presence of U_3O_8 and/or UO_3 cannot be distinguished due to the overlap in their XRD patterns. Therefore, the U_3O_8/UO_3 column in Table 5.36 represents a combination of UO_3 and/or U_3O_8 that, for practical purposes, cannot be separated by XRD.

Table 5.35. Approximate Percentages of Crystalline Uranium Oxide Species as Determined by XRD

Sample ID	U_4O_9	U_3O_8/UO_3	$UO_3 \cdot 2H_20$ (schoepite)
PI-1 MVF Segment 1	56.6	33.5	10.0
PII-1/2 Stage 5 residue	7.0	89.0	4.0
PIII-2 Stage 1 residue	35.1	63.2	1.7
PIII-2 Stage 5 residue	5.8	88.7	5.6
PI-3/4 Backup filter	2.7	94.3	3.1
PI-7 Backup filter	2.1	95.2	2.7
PII-3 Backup filter A	1.8	92.0	6.2
PII-3 Backup filter B	0.0	92.7	7.3
PIII-2 Backup filter	1.6	94.4	4.0

Table 5.36. Ratio of U_4O_9 to U_3O_8/UO_3 as Determined by Peak Area Analysis from XRD Patterns

Cyclone Stage	PI-3/4	PI-7	PII-1/2	PIII-2
1	1.07	0.95	1.79	1.34
2	1.02	0.72	1.32	--
3	0.73	0.46	0.99	--
4	0.31	0.23	0.45	0.89
5	0.13	0.12	0.20	0.15
Backup Filter	0.07	0.06	0.05	0.05
BU Filter (dup)	0.07	NA	0.05	NA

The PII samples were the only ones placed under a nitrogen atmosphere within a few days of the shot. The rest of the samples were put under nitrogen weeks to months later. The potential for change in oxidation of the uranium in the aerosol samples was greatest for Phase I, less for Phase III, and least for Phase II. The MVF sample was not put under a nitrogen atmosphere. Sample analysis took place six months to a year after sample generation. The consequences with regard to uranium oxidation in these samples relative to the elapsed time between sample generation and placement under a nitrogen atmosphere are unclear but appear to be minimal for this data set. The backup filter samples from PI-7, PII-3, and PIII-2 are very similar in oxide composition, thereby suggesting that little change occurred in the PI and PIII filters as a result of exposure to air. The PI-3/4 sample contained a slightly lower U_3O_8/UO_3 content and a higher percentage in the "unknown" category. The PIII-2 Stages 1 (cutoff point about 10 µm) and 5 (cutoff point about 1.2 µm) contained different quantities of the oxide phases probably related to differences in particles collected by these extreme stages. The MVF segment is the oldest sample of this group and, as stated above, was not stored under nitrogen. It contained the lowest percentage of U_3O_8/UO_3 and the largest percentages of both U_4O_9 and schoepite.

Most samples analyzed were not conducive to breakdown by actual percentage of the uranium compounds present. For these, as well as the samples listed in Table 5.35, ratios were calculated for U_4O_9 content compared with U_3O_8/UO_3 using a least squares profile of major peaks and the area of these peaks. These results are presented by phase in Table 5.36. The backup filter results presented in both tables are similar but not identical, and the differences between them are attributed to the different techniques used to calculate them. PII-1/2-CY Stages 3 and 4 contained other (unknown) phases with ratios compared with U_3O_8/UO_3 of 0.12 and 0.10, respectively.

The data (Table 5.36) demonstrate the decrease of U_4O_9 concentration compared with U_3O_8/UO_3 as particle size decreases. Another apparent trend is the increase in the ratio of U_4O_9 to U_3O_8/UO_3 for the PII-1/2 samples when compared with the PI samples at each cyclone stage. The PIII-2 results lie between the PI and PII results for Stages 1 and 5 and are higher than either at Stage 4. The ratios on the backup filters are similar for the three test phases.

5.6.6 SEM/EDS Particle Morphology and Composition

Aerosols formed inside the turret (and the passenger compartment in the Bradley vehicle) following perforation by the DU penetrator consisted of a variety of shapes and particle aggregates. The SEM/EDS evaluation of these aerosols determined that uranium was present in almost every particle interrogated by EDS. Most of the uranium present appeared to contain sufficient oxygen to qualify as uranium oxide. However, there were some samples that apparently contained a low concentration of oxygen, which

indicates the potential presence of some metallic particles or domains. Appendix D contains descriptions of the samples analyzed and SEM micrographs of typical and atypical particles evaluated.

The shapes varied from highly spherical single particles to aggregates of uranium and other particles. The spheres ranged in size from <1 μm to about 12 μm. Fractures or similar particles were present in some samples and were dominant in the DU cone sample. Both crystalline and amorphous materials were present. Though not typical, some uranium spheres contained dendritic or fine-grained structures (Figure D.7, views e and f).

The majority of particles in the cyclone sample residues contained uranium. The SEM images indicated the presence of particles exhibiting crystalline-like faces or well-defined external surfaces, as well as particles with amorphous-like, indeterminate surface forms. Samples from Phase II contained a much higher aluminum content as expected because of the composition of the Bradley vehicle armor that was penetrated. Iron also was present in many of the samples. The basic chemical makeup of most of the samples can be characterized by the presence of oxides of uranium, aluminum, and iron. EDS analysis also identified lesser amounts of other elements such as copper, zinc, titanium, silicon, calcium, and magnesium.

As the two views show in Figure 5.38, cyclone aerosols were heterogeneous in particle size and shape. Extensive agglomeration, or perhaps better described as coagulation (the adherence of small-sized particles to make larger ones, or small-sized particles onto larger ones), was clearly present in these samples, and little physical size differentiation was visible between cyclone stages. Although the cyclone samples from the three phases were similar, there were some noteworthy differences. For example, the Phase-II cyclone residues contained higher quantities of aluminum and displayed some unique star-shaped morphologies in Stage 5 (Figure D.9 views c and d). At least one particle believed to be a fiber from the spall liner was captured in a micrograph. The fiber is long, hollow, and lacey and appeared to have uranium spheres adhering to its surface.

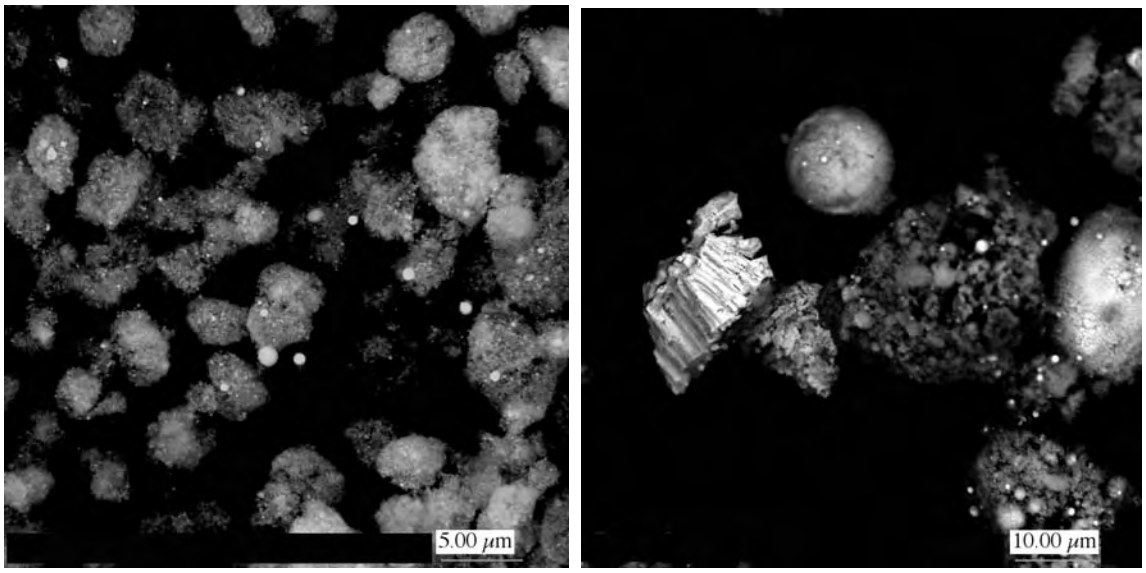

Figure 5.38. Heterogeneity in Particles as Exhibited in a Cyclone Aerosol Sample, Shown in Backscatter Electron (bse) Mode

5.6.7 *In Vitro* Solubility

In general the majority of the dissolution rates obtained from the *in vitro* solubility study showed moderate solubility. These rates resembled most closely the default Type-M absorption behavior as defined in the International Commission on Radiological Protection (ICRP) 66 Human Respiratory Tract Model (HRTM), which resembles, but is not identical with Class-W clearance from ICRP 30 (ICRP 1979 and 1994). Some samples, such as the PI-3/4 cyclone backup filter and DU cone sample (not size separated) samples, were relatively insoluble and more resembled Type-S behavior, which is the least soluble category of the HRTM. None showed the most rapid Type-F behavior. This latter observation suggests that the conditions of aerosol formation were not conducive to formation of large amounts of highly oxidized forms of uranium oxides such as UO_3 or UO_4. However, this does not preclude the possibility that subsequent additional oxidation could occur as a function of time after impact, which could result in a shift to more soluble forms as a result of environmental weathering. Thus the results of this study should be constrained to apply directly to exposures that occur relatively soon after a DU impact event (minutes to weeks); correspondingly, the time frame for potential changes in solubility would probably be extensive—that is, months to years depending on environmental conditions.

Despite the preponderance of Type-M behavior, there were significant differences seen among the various samples. The most significant differences noted were in the fraction of DU that dissolved rapidly, usually within one day. This ranged from about 4% to as much as 30%. There also appeared to be a correlation between the initial rate of dissolution and the subsequent dissolution rate—the higher the rate of dissolution during the first day, the faster the long-term dissolution proceeded. This behavior is exemplified reasonably well in Figure 5.39. The dissolution behavior of the various aerosol samples tested is most likely to be influenced by the particle shapes and sizes, which affect the specific surface area; the chemical form of the uranium within the particles; and the degree of heterogeneity of the various elements comprising the particles.

The categorization of the *in vitro* results in terms of solubility depends on which model is selected (i.e., the ICRP 30 model or the ICRP 66 model). There is a general equivalence between the absorption Types (F, M, S) and the clearance Classes (D, W, Y), respectively, but the numerical values that define the appropriate category for a given set of data are different. Because Type F represents absorption that is significantly more rapid than for Class D, and Type S is significantly slower than Class Y, the consequence is that more results end up classified as Type M. Notwithstanding these differences, the *in vitro* results can be used to assign proportionate amounts of DU to the default clearance Classes D, W, and Y according to the following criteria: the fraction of dissolved DU associated with half-times ($T_{1/2}$) < 10 d are assigned to Class D; fractions associated with 10 d # $T_{1/2}$ # 100 d are Class W; and fractions associated with $T_{1/2}$ > 100 d are Class Y. Accordingly, Table 5.36 summarizes the D, W, and Y classification for the 27 *in vitro* samples analyzed in this study. Note that, when possible, the results of the three-component exponential fits were used. In all cases, more than 50% of the DU aerosol sample was assigned to Class-Y clearance. In some cases, the Class-Y fraction was >90%. From 1% to about 30% of the DU aerosols dissolved rapidly enough to be considered Class D. Seven of the samples had amounts ranging from 4 to 25% assigned to Class W. It thus appears that there was significant variability among the various samples analyzed in terms of their assignments to the default clearance classes. This variability was certainly highlighted by the fitted curves and is reinforced here.

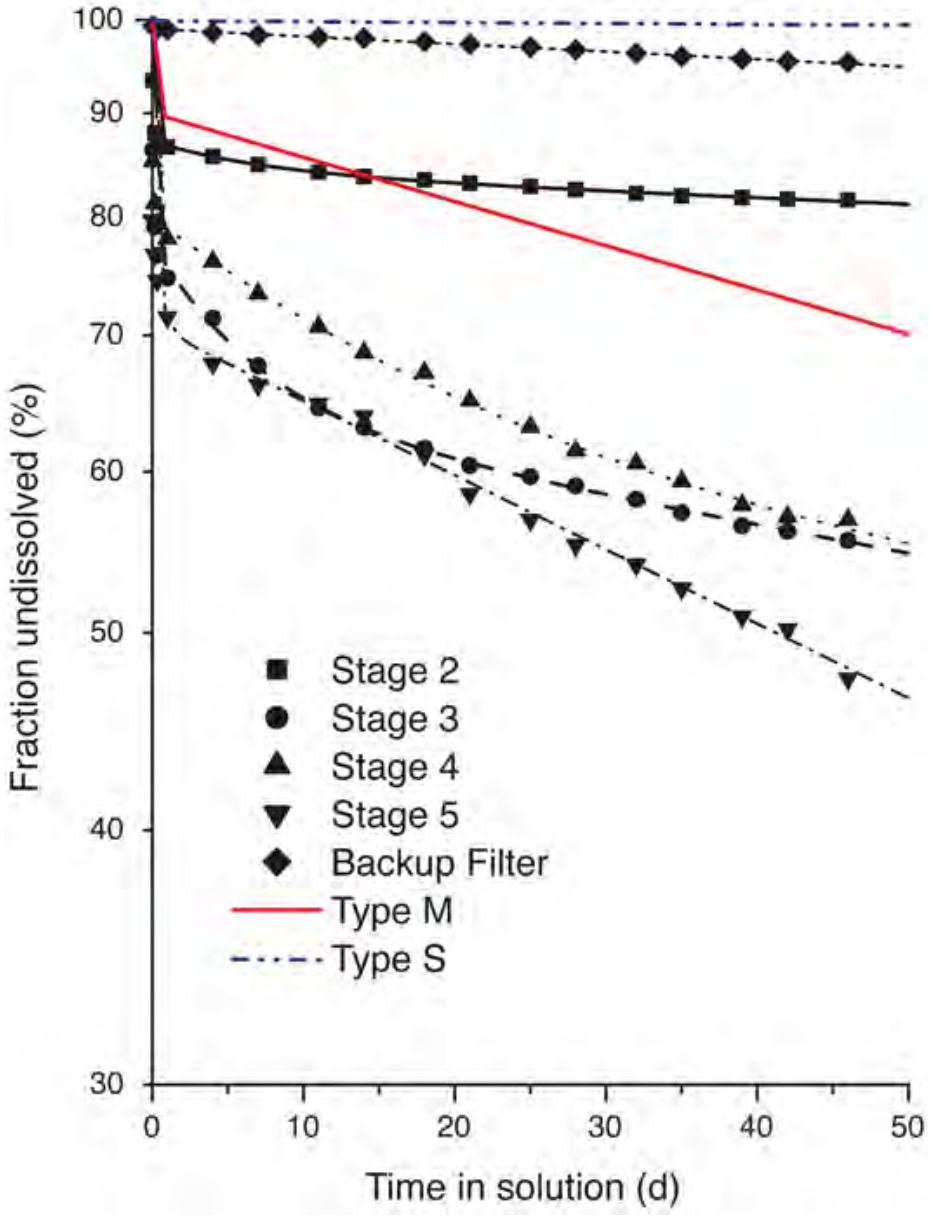

Figure 5.39. *In Vitro* Dissolution of Uranium from Cyclone Stages, PI-3/4

Table 5.37. Assignment of ICRP-30 Clearance Class Based on *In Vitro* Solubility Measurements

Sample ID	D	W	Y
PI-2			
PI-2I-D-1-FS	9.4	--	90.4
PI-2I-D-3-FS	16.8	--	83.2
PI-2I-D-4-FS	22.4	--	77.6
PI-2I-D-6-FS	17.0	--	83.0
PI-2I-D-7-FS	11.4	--	88.6
PI-3/4			
PI-3/4-CY-2	15.8	--	84.2
PI-3/4-CY-3	35.8	--	64.2
PI-3/4-CY-4	20.0	21.3	58.7
PI-3/4-CY-5	29.3	--	70.7
PI-3/4-CY-BU	1.0	--	99
PI-7			
PI-7I-CY-1	35.1	--	64.9
PI-7I-CY-2	15.2	--	84.8
PI-7I-CY-3	31.0	--	69.0
PI-7I-CY-4	31.0	--	69.0
PI-7I-CY-5	31.5	--	68.5
PI-7I-CY-BU	13.2	--	86.8
PII-1/2			
PII-1/2I-CY-2	22.1	--	77.9
PII-1/2I-CY-3	20.8	--	89.2
PII-1/2I-CY-4	25.6	16.8	57.6
PII-1/2I-CY-5	26.0	11.2	62.8
PII-1/2I-CY-BU	14.0	8.8	77.2
PIII-2			
PIII-2I-CY-4	2.7	7.5	89.8
PIII-2I-CY-5	4.6		95.4
PIII-2I-CY-BU	9.8	4.5	84.7
Miscellaneous			
PFDB-DiffBat7	3.1	24.6	72.3
DU cone (unsep)	1.4	--	98.6
DU cone (size separated)	7.0	--	93.0

6.0 Aerosol Data Analysis

Aerosol generation, dispersion and settling, particle size, and composition characteristics are related to the mechanics of the impact and the composition of the target. These mechanics varied with target and shot line in the Capstone DU Aerosol Study. They also varied with hatch openings and other aspects unique to each shot. This chapter summarizes the following aspects by test phase: 1) shot lines and other attributes of each shot that may have influenced the generation of aerosol, 2) interior aerosol concentrations and settling rates, 3) particle size distributions of interior aerosols as defined by AMAD values, 4) particle size distributions as measured by external AMADs beginning with PI-5, and 5) the uranium concentration and oxide composition and *in vitro* solubility of the aerosols. These aspects are organized in Section 6.1 by phase and shot.

The shot lines were specifically designed to support certain retrospective and prospective exposure scenarios. Results are listed by shot in Section 6.1 and are summarized by scenario in Section 6.2. The composition of the aerosols, including the presence of non-DU metals, is presented in Section 6.3. A discussion of deposited particulate matter appears in Section 6.4, and a brief comment about the results of the ventilation tests on the target vehicles and functional vehicles is presented in Section 6.5.

6.1 Interior Aerosol Characteristics by Phase and Shot

Shot attributes and aerosol characteristics are discussed in Sections 6.1.1 to 6.1.3. The shot lines (illustrated in Sections 4.1 through 4.3) and the hatch openings varied, and are listed in Section 6.1 and compared in Section 6.3. Venting through hatches or other vehicle openings, which occurred in each shot except PII-1/2, was not part of the test design but proved difficult to eliminate and contributed to the systematic variability between shots.

Sampling intervals varied as the project progressed based on observed behavior of the test setup and aerosol production by varying shot conditions. Heavy loading of the first sampling set mandated shorter sampling times in subsequent sampling to minimize filter loading while collecting sufficient sample for analysis. The analyses of uranium concentrations and particle settling as a function of time were conducted by plotting the time midpoint of each sample collected (summarized in Table 5.5). Differences in sampling durations as well as start times prevent direct comparison of DU aerosol concentration at specific time periods for all shots, although there were some data sets with identical sampling times. Sampling arrays that were not used and samplers that did not operate are indicated with two hyphens (--) in the tables. To facilitate comparison of results from the various shots, the data were subjected to a curve-fitting routine.

Graphs of the curve-fit data are based on the average of the aerosol concentrations at each crew position for which there were corresponding samples. Mean IOM uranium concentrations were used to calculate a best-fit curve to describe the time course of concentration change. For tests with a single shot, the uranium concentration can be expressed in the following equation:

$$C\ (\mu g/m^3) = ae^{-bt} + ce^{-dt} + ee^{-ft} + ge^{-ht}$$

where constants a through h were obtained by using the curve-fitting procedure of SigmaPlot. The coefficient of determination, R^2 was >0.99 for all fitted curves (as would be expected when using eight variables). In the case of PI-2, the results were expressed by the following equation with three exponential decay terms (constant g=0). In the case of PI-5, a simple single exponential term was the best fit:

$$C\ (\mu g/m^3) = y_o + ae^{-bt}$$

Constants y_o and a, b, c, d, e, f, g for all tests consisting of a single shot are listed in Table 6.1.

Table 6.1. Fitted Constants for Tests with Single Shots

Shot	y_o	a	b	c	d	e	f	g	h
PI-1	--	1.372E+07	2.765E+00	2.684E+06	3.527E-01	7.691E+05	1.522E-01	2.947E+04	1.892E-03
PI-2	--	3.309E+06	1.411E+00	2.355E+05	2.590E-01	2.844E+06	2.590E-01	4.702E+04	1.244E-04
PI-5	2.523E+04	1.658E+07	9.035E-01	--	--	--	--	--	--
PI-6	--	7.963E+06	3.555E+00	6.785E+06	1.803E+00	6.428E+06	6.205E-01	2.507E+04	5.274E-03
PI-7	--	6.758E+06	7.574E+00	4.213E+06	5.538E-01	3.876E+06	2.117E-01	6.352E+04	2.437E-03
PII-3	--	6.816E+05	3.265E+00	5.677E+05	1.492E+00	9.887E+04	1.303E+00	6.988E+04	9.093E-03
PIII-1	--	8.125E+06	1.520E+01	2.207E+06	1.799E-01	1.623E+05	5.400E-02	3.761E+03	8.179E-10
PIII-2	--	1.045E+07	3.429E+00	7.715E+06	8.007E-01	2.353E+06	3.697E-01	3.769E+04	6.175E-03

For tests with double shots, the curve fit was obtained from data of the two separate shots:

$$C\ (\mu g/m^3) = y_o + ae^{-bt}, \text{ when } t < T_1$$

$$C\ (\mu g/m^3) = c\cdot\exp[-d\ (t- T_1)] + e\cdot\exp[-f\ (t- T_1)] + g\cdot\exp[-h\ (t- T_1)], \text{ when } t \geq T_1 \quad (3)$$

where T_1 is the time interval between the two shots. T_1 values were 13 and 13.68 min for PI-3/4 and PII-1/2 shots, respectively. The constants are listed in Table 6.2.

Table 6.2. Fitted Constants for Tests with Double Shots

Shot	y_o	a	b	c	d	e	f	g	h
PI-3/4	3.833E+05	1.372E+07	2.765E+00	1.354E+07	3.962E+00	6.104E+06	2.044E-01	1.533E+05	8.029E-03
PII-1/2	3.248E+05	3.147E+06	5.154E-01	3.250E+06	7.693E-01	1.545E+06	9.366E-02	6.801E+04	6.360E-03

The upper and lower boundary lines in the figures presented represent the actual (not curve-fit) upper and lower values obtained at each sampling increment. More detailed data on which of these numbers are based and the related uncertainty of each uranium concentration are presented in Appendix A, Tables A.9 through A.18.

The sampling intervals used to measure DU aerosol concentrations also were used to evaluate particle size distributions. Parameters listed include both the unimodal and bimodal AMADs. In most but not all cases, the bimodal model provided a better fit of the data. The complete tabulation of these results, including the GSD and R^2 values, is provided in Appendix B, Table B.1. Some of the results in this table are unrealistic (e.g., where the AMAD is given as >1000 μm), and in these cases, professional judgment

was used to estimate a more reasonable value from the graphical presentation of the data. Unimodal AMADs, GSDs, and the range of AMAD values are presented by phase and shot for each time interval at each position for which samplers operated. The bimodal AMADs are listed for each time interval at each active position, and the average of the AMADs is shown for both peaks. Beginning with PI-7, in which there were consistently three or four operating samples, standard deviations (at the ±1-sigma level) are also listed.

The chemical characterization of the aerosols is summarized using parameters of uranium concentration, uranium oxide phase, and *in vitro* solubility. The cyclone residues were the primary samples evaluated for these characteristics. All cyclone residues were analyzed by gamma spectrometry, and uranium mass concentrations were derived from these analyses. Uranium analyses using three chemical methods were conducted on the cyclone residues and backup filters from four of the shots, and these results also are provided. Uranium mass percentages as derived from gamma spectrometry analyses are listed along with results of chemical ICP-MS analysis, when available. For those samples evaluated using ICP-AES and KPA rather than ICP-MS, the results presented are based on the higher values obtained from the two analyses. Results of the chemical analyses are discussed in Section 6.1.

The uranium oxidation products present in the aerosols were evaluated using XRD and consisted primarily of U_3O_8 and U_4O_9. A small quantity of schoepite ($UO_3 \cdot 2.xH_2O$) was present in several samples, and the presence of UO_3 is suspected but could not be separated from U_3O_8. Therefore, when U_3O_8 is listed, the sample may also contain UO_3. Semi-quantitative results of samples analyzed are discussed in Section 6.4.3.

Two models were used to categorize the dissolution rates in lung fluid—the ICRP 66 HRTM (ICRP 1994), which uses absorption Types F (fast), M (moderate), and S (slow), and the ICRP 30 model (ICRP 1979), which uses clearance Classes D (days), W (weeks), and Y (years). Dissolution rates using both models are listed in Section 5.6.7 and are discussed in greater detail in Appendix E.

6.1.1 Phase I—Abrams Tank with Standard Armor

The Phase-I shots consisted of crossing shots through the turret, with and without impact with the breech, and a crossing shot through the hull. The aerosol sampling intervals varied from shot-to-shot; the longest intervals occurred following Shot 1. Uranium concentrations of the two to four arrays operating during the sampling intervals are listed along with the average of the concentrations at the sampling positions for which data were collected.

6.1.1.1 Shot 1 (PI-1)

Information concerning the general configuration of the vehicle, sampler shielding used, and unique aspects about Shot 1 are listed in this section. Additionally, this section includes a table listing the uranium aerosol concentrations as a function of time, a figure plotting this function, particle size distributions, and uranium chemistry and solubility.

Attributes and Unique Aspects of Shot

- Turret-crossing shot line (from the loader's side to the commander's side).
- The turret was in the travel position.

- Louvered shields covered the commander's, gunner's, and loader's arrays.
- The driver's hatch cover (metal plate tack-welded closed) detached at one corner.
- Aerosol escaped from the antenna opening.
- IOM filters at C and G positions were lost.
- Sample acquisition was longest of all shots; some samples may have overloaded.

Interior Uranium Aerosol Concentrations with Time

The uranium concentrations are listed in Table 6.3 for each position for which there was an operating IOM sampler and the average concentrations. Sample collection began 5 sec after impact. The IOM filters in the commander's and gunner's arrays were damaged, and concentrations for these samples are not reported. These data are plotted in Figure 6.1.

Table 6.3. Summary of DU Aerosol Concentrations with Time, PI-1 Turret-Crossing Shot

Sampling Interval (+5 sec)	DU Concentration (μg/m^3)				
	Commander	Driver	Gunner	Loader	Average
0-30 sec	--	3.31E+06	--	1.69E+07	1.01E+07
0.5-1.5 min	--	9.93E+05	--	5.89E+06	3.44E+06
1.5-3.5 min	--	6.89E+05	--	2.67E+06	1.68E+06
3.5-7.5 min	--	2.65E+05	--	1.23E+06	7.48E+05
7.5-15.5 min	--	7.97E+04	--	3.39E+05	2.09E+05
15.5-31.5 min	--	4.57E+04	--	5.51E+04	5.04E+04
31.5-63.5 min	--	3.26E+04	--	2.23E+04	2.75E+04
63.5-127.5 min	--	2.92E+04	--	1.99E+04	2.46E+04

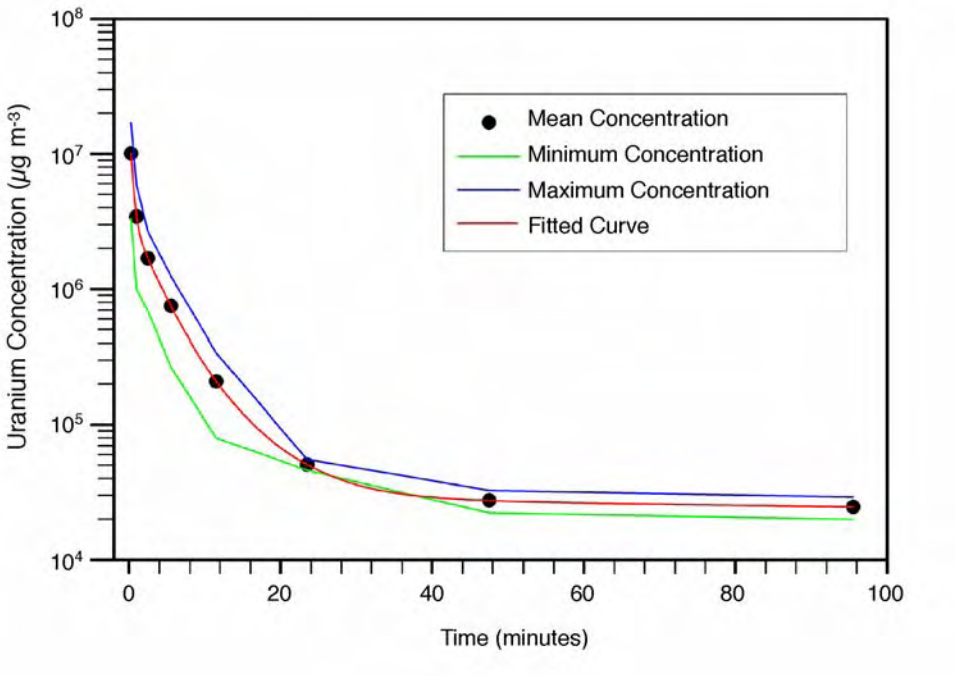

Figure 6.1. Summary of DU Aerosol Concentrations with Time, PI-1 Turret-Crossing Shot

Uranium Chemistry and Solubility

MVF sampler uranium concentrations ($\mu g/m^3$; approximate results on a per second basis beginning with impact):

- First 5 sec 2.3E+06
- 5 to 15 sec (midpoint) 7.8E+05
- 25 to 35 sec (midpoint) 5.8E+05
- 35 to 55 sec 2.1E+05

Particle Size Distribution

Unimodal AMADs: Fitting the particle size data using the unimodal model resulted in the AMAD values and the corresponding GSDs listed in Table 6.4. These parameters and the R^2 goodness-of-fit for each CI distribution are presented in Appendix B. The shaded numbers in the table identify those samples for which professional judgment was applied to provide more realistic values.

Table 6.4. Summary of Unimodal AMADs, PI-1 Turret-Crossing Shot

Sampling Interval (+5 sec)	Unimodal AMAD (μm)								
	Commander		Driver		Gunner		Loader		AMAD Range
	AMAD	GSD	AMAD	GSD	AMAD	GSD	AMAD	GSD	
0-30 sec	3.07	7.22	--	--	0.46	6.06	2.46	6.07	0.46 to 3.07
0.5-1.5 min	0.90	5.71	1.40	8.89	2.97	6.27	3.39	5.89	0.90 to 3.39
1.5-3.5 min	0.69	2.68	1.17	4.77	0.55	2.29	1.19	5.27	0.55 to 1.19
3.5-7.5 min	0.95	4.78	1.8	4.5	0.67	2.29	1.37	4.20	0.67 to 1.8
7.5-15.5 min	1.8	4	1.02	4.43	0.55	2.58	1.03	2.99	0.55 to 1.8
15.5-31.5 min	0.96	3.18	0.48	5.12	0.47	2.93	1.07	4.71	0.47 to 1.07
31.5-63.5 min	0.50	5.62	0.30	3.63	0.45	2.85	0.27	3.69	0.27 to 0.50
63.5-127.5 min	0.43	5.05	0.23	4.43	0.33	0.89	0.24	2.96	0.23 to 0.43

Bimodal AMADs: Fitting the particle size data using the bimodal model resulted in the AMAD values listed in Table 6.5 for each of the two peaks listed (labeled #1 and #2). These values and the GSD, the R^2 goodness-of-fit parameter, and the fraction in the first peak are presented in Appendix B for each CI distribution.

Uranium Chemistry and Solubility

- Mass percent of uranium in aerosol: Cyclone stages—53 to 60% (derived from gamma spectrometry)
- Uranium oxide phases:
  – MVF segment 1 (first time interval)—33.5% U_3O_8, 56.6% U_4O_9, 10% $UO_3 \cdot 2H_2$ 0
- *In vitro* solubility:
  – HRTM Model: IOM samplers—Type-M behavior
  – ICRP 30 Model:
  – IOM samplers—78 to 90% Y, 9 to 22% D
  – Diffusion battery coarsest filter—72% Y, 25% W, 3% D

Table 6.5. Summary of Bimodal AMADs, PI-1 Turret-Crossing Shot

Sampling Interval (+5 sec)	Bimodal AMAD (μm)									
	Commander		Driver		Gunner		Loader		Average	
	#1	#2	#1	#2	#1	#2	#1	#2	#1	#2
0-30 sec	0.27	5.37	--	--	0.35	3.97	0.51	5.68	0.38	5.0
0.5-1.5 min	0.43	4.79	0.38	7.70	0.39	6.42	0.39	5.87	0.40	6.2
1.5-3.5 min	0.60	4.07	0.53	5.11	0.50	4.17	0.63	10.3	0.57	5.9
3.5-7.5 min	0.49	3.84	0.69	4.15	0.61	3.92	0.64	5.07	0.61	4.2
7.5-15.5 min	0.68	4.55	0.57	5.47	0.49	3.89	0.76	4.39	0.63	4.6
15.5-31.5 min	0.60	3.98	0.32	3.53	0.43	4.01	0.50	4.61	0.46	4.0
31.5-63.5 min	0.31	3.67	0.29	4.46	0.43	3.17	0.28	4.74	0.33	4.0
63.5-127.5 min	0.32	4.24	0.24	1.65	0.36	3.56	0.26	0.41	0.30	2.5

6.1.1.2 Shot 2 (PI-2)

Information concerning the general configuration of the vehicle, sampler shielding used, and unique aspects about Shot 2 are listed in this section. Additionally, this section includes a table listing the uranium aerosol concentrations as a function of time, a figure plotting this function, particle size distributions, and uranium chemistry and solubility.

Attributes and Unique Aspects

- Turret-crossing shot line (from the loader's side to the commander's side).
- The turret was in the travel position.
- Louvered shields covered the commander's, gunner's, and loader's arrays; a hinged plate on the gunner's louver was tripped to detach shortly after the shot was fired.
- The loader's hatch blew three-fourths open.
- Most of the C- and G- position and some of the L-position IOM filters were lost.

Interior Uranium Aerosol Concentrations with Time

The uranium concentrations are listed in Table 6.6 for each position for which there was an operating IOM sampler and the average concentrations. Sample collection began 5 sec after impact. The IOM filters in most of the gunner's array and in some of the commander's and loader's arrays were damaged or did not run. These data are plotted in Figure 6.2.

Table 6.6. Summary of DU Aerosol Concentrations with Time, PI-2

Sampling Interval (+5 sec)	DU Concentration (µg/m^3)				
	Commander	**Driver**	**Gunner**	**Loader**	**Average**
0-15 sec	5.60E+06	6.00E+06	--	--	5.80E+06
0.5-1 min	--	2.63E+06	--	4.85E+06	3.74E+06
1.5-2.5 min	2.39E+06	1.22E+06	--	2.56E+06	2.06E+06
3.5-5.5 min	1.30E+06	7.82E+05	--	--	1.04E+06
7.5-11.5 min	3.48E+05	2.28E+05	--	2.71E+05	2.82E+05
15.5-31.5 min	--	8.65E+04	--	7.52E+04	8.09E+04
31.5-79.5 min	1.32E+04	4.32E+04	1.86E+04	2.81E+04	2.58E+04
79.5-127.5 min	Did not run	5.32E+04		--	5.32E+04

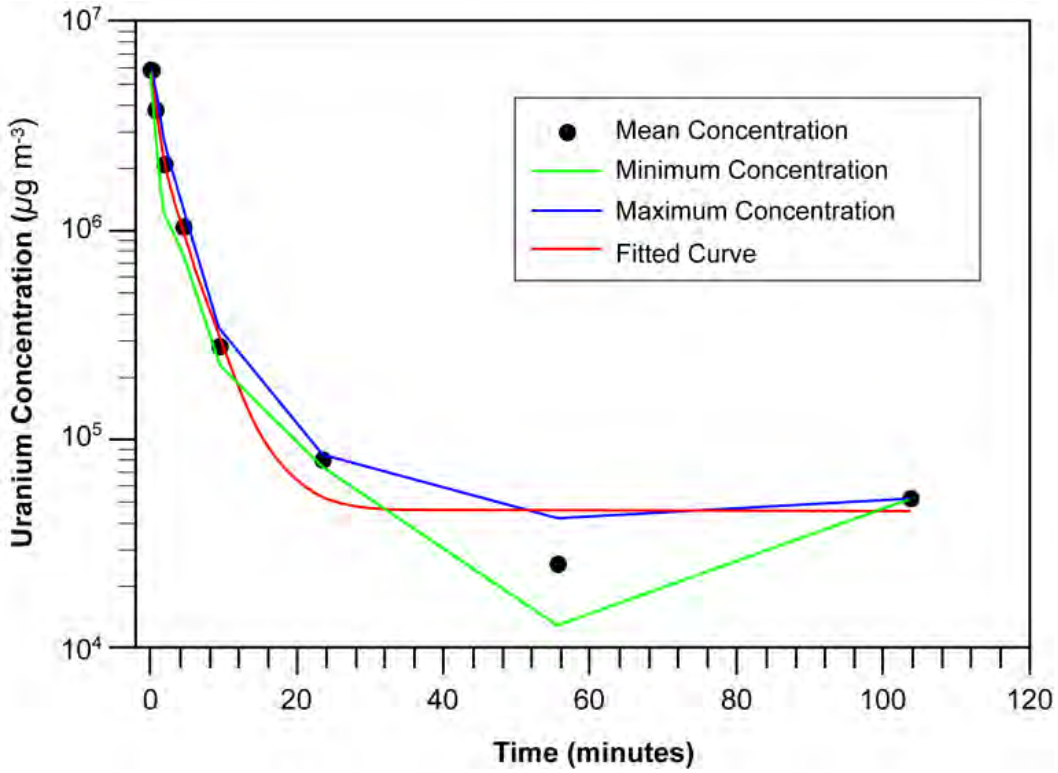

Figure 6.2. Summary of DU Aerosol Concentrations with Time, PI-2 Turret-Crossing Shot

Particle Size Distribution

Unimodal AMADs: Fitting the particle size data using the unimodal model resulted in the AMAD and the corresponding GSD values listed in Table 6.7. These parameters and the R^2 goodness-of-fit for each CI distribution are presented in Appendix B. Shaded values in the table identify those samples for which professional judgment was used to provide more realistic values.

Table 6.7. Summary of Unimodal AMADs, PI-2 Turret-Crossing Shot

Sampling Interval (+5 sec)	Unimodal AMAD (μm)								
	Commander		Driver		Gunner		Loader		Average
	AMAD	GSD	AMAD	GSD	AMAD	GSD	AMAD	GSD	AMAD Range
0-15 sec	3.48	11.1	7.11	5.19	3.83	5.82	1.82	8.87	1.82 to 7.11
0.5-1 min	1.85	7.22	--	--	4.39	7.07	1.32	11.4	1.32 to 4.39
1.5-2.5 min	1.32	6.94	2.52	4.60	0.98	5.78	1.37	4.89	0.98 to 2.52
3.5-5.5 min	1.14	4.56	1.73	4.98	0.79	5.41	2.4	3.4	0.79 to 2.4
7.5-11.5 min	1.15	5.40	0.49	1.40	1.07	5.51	3.0	4.5	0.49 to 3.0
15.5-31.5 min	0.64	4.05	0.68	3.68	0.73	5.77	0.47	4.63	0.47 to 0.73
31.5-79.5 min	0.48	5.27	0.65	5.30	0.78	4.13	0.38	4.35	0.38 to 0.78
79.5-127.5 min	0.31	4.52	0.49	3.73	0.61	6.45	0.29	4.21	0.29 to 0.61

Bimodal AMADs: Fitting the particle size data using the bimodal model resulted in the AMAD values listed in Table 6.8 for each of the two peaks (labeled #1 and #2). These values and the GSD, the R^2 goodness-of-fit parameter, and the fraction in the first peak are presented in Appendix B for each CI distribution. The driver's CI did not run during the second sampling interval.

Table 6.8. Summary of Bimodal AMADs, PI-2 Turret-Crossing Shot

Sampling Interval (+5 sec)	Bimodal AMAD (μm)									
	Commander		Driver		Gunner		Loader		Average	
	#1	#2	#1	#2	#1	#2	#1	#2	#1	#2
0-15 sec	0.31	8.01	0.35	8.08	0.41	5.10	0.51	11.24	0.40	8.1
0.5-1 min	0.31	4.53	--	--	0.43	9.88	0.26	6.65	0.33	7.0
1.5-2.5 min	0.41	6.24	0.51	2.40	0.44	4.92	0.56	5.41	0.48	4.7
3.5-5.5 min	0.60	4.61	0.55	5.90	0.44	5.02	0.24	2.42	0.46	4.5
7.5-11.5 min	0.65	4.12	0.53	2.79	0.40	3.99	1.23	4.04	0.70	3.7
15.5-31.5 min	0.45	3.80	0.47	4.63	0.39	4.27	0.38	5.08	0.42	4.4
31.5-79.5 min	0.33	4.31	0.39	3.68	0.50	4.31	0.34	4.43	0.39	4.2
79.5-127.5 min	0.26	4.00	0.40	2.95	0.37	4.71	0.22	0.45	0.31	3.0

Uranium Chemistry and Solubility

- Mass percent of uranium in aerosol: cyclone stages—48 to 56% (derived from gamma spectrometry)
- Uranium oxide phase: No XRD data for this shot
- *In vitro* solubility: No solubility data for this shot

6.1.1.3 Shots 3/4 (PI-3/4)

Information concerning the general configuration of the vehicle, sampler shielding used, and unique aspects about Shots 3/4 are listed in this section. Additionally, this section includes a table listing the uranium aerosol concentrations as a function of time, a figure plotting this function, particle size distributions, and uranium chemistry and solubility.

Attributes and Unique Aspects

- Two turret-crossing shots were fired 13 min apart (from the commander's side to the loader's side).
- The turret was in the combat position.
- A louvered shield covered the gunner's array; solid armor shields covered the commander's and loader's arrays; the loader's shield tripped prematurely and some samplers were damaged by fragments.
- Shot 3: The loader's hatch raised twice and lowered, resting just above the opening and leaving a crescent-shaped opening.
- Shot 4: The loader's hatch raised again and lowered; some aerosol vented from the GPS slot.
- Many of the L-position IOM filters were damaged because of premature release of the armor shield.

Interior Uranium Aerosol Concentrations with Time

The uranium concentrations are listed in Table 6.9 for each position for which there was an operating IOM sampler and the average concentrations. These data are plotted in Figure 6.3. Samples were not taken during Shot 3 at the commander's and loader's positions. Some of the IOM filters in the loader's array were damaged because a shield opened prematurely. Sample collection began 5 sec after impact.

Table 6.9. Summary of DU Aerosol Concentrations with Time, PI-3/4 Turret-Crossing Shots

Sampling Interval (+5 sec)	DU Concentration ($\mu g/m^3$)				
	Commander	**Driver**	**Gunner**	**Loader**	**Average**
Shot 3: 0-10 sec	--	7.05E+06	3.50E+06	--	5.28E+06
3-3.5 min	--	2.98E+06	1.91E+06	--	2.45E+06
9-10 min	--	8.80E+05	6.39E+05	--	7.60E+05
Shot 4: 0-10 sec	2.26E+07	9.21E+06	Did not run	--	1.59E+07
3-3.5 min	4.42E+06	2.28E+06	3.17E+06	--	3.29E+06
9-10 min	1.09E+06	1.04E+06	1.14E+06	8.19E+05	1.02E+06
21-23 min	1.46E+05	~Bkgd	3.41E+05	--	1.62E+05
45-49 min	8.06E+04	9.16E+04	1.41E+05	1.80E+05	1.23E+05
93-101 min	4.96E+04	Field Blank	Field Blank	7.52E+04	6.24E+04

Particle Size Distribution

Unimodal AMADs: Fitting the particle size data using the unimodal model resulted in the AMAD and the corresponding GSD values listed in Table 6.10. These parameters and the R^2 goodness-of-fit for each CI distribution are presented in Appendix B. Shaded numbers identify those samples for which professional judgment was used to provide more realistic values. Some of the CIs in the loader's array were damaged because a shield opened prematurely. The AMADs were calculated, but because of the CI damage and the possibility that these samplers experienced a drop in collection efficiency, only the first sample (Shot 4, 0 to 10 sec), which is believed to have been unaffected, is included in the range of AMAD values. The remaining sampler results, which were not used in averaging, are shown in bold italics.

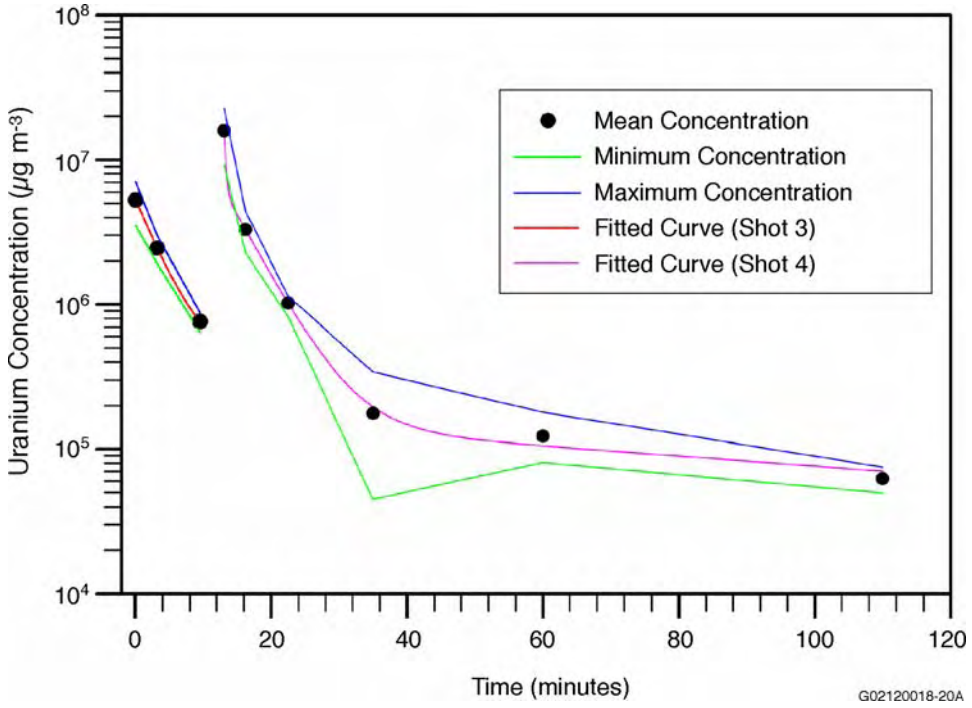

Figure 6.3. Summary of DU Aerosol Concentrations with Time, PI-3/4 Turret-Crossing Shots

Table 6.10. Summary of Unimodal AMADs, PI-3/4 Turret-Crossing Shots

Sampling Interval (+5 sec)	Unimodal AMAD (μm)								
	Commander		Driver		Gunner		Loader		
	AMAD	GSD	AMAD	GSD	AMAD	GSD	AMAD	GSD	AMAD Range
Shot 3: 0-10 sec	--	--	0.18	2.64	0.70	6.73	--	--	0.18 to 0.70
3-3.5 min	--	--	3.1	3.0	1.98	4.18	--	--	1.98 to 3.1
9-10 min	--	--	2.5	4.0	2.0	4.0	--	--	2.0 to 2.5
Shot 4: 0-10 sec	15.8	7.56	5.35	6.10	6.96	6.63	4.0	5.09	4.0 to 15.8
3-3.5 min	1.29	4.97	2.56	4.36	1.07	6.29	***2.11***	***5.15***	1.07 to 2.56
9-10 min	3.70	4.70	2.43	4.39	1.03	3.76	***6.62***	***3.36***	1.03 to 3.70
21-23 min	0.83	2.95	0.85	2.94	0.68	2.52	***6.12***	***3.45***	0.68 to 0.85
45-49 min	1.19	4.55	0.88	3.31	0.62	3.42	***35.7***	***2.14***	0.62 to 1.19
93-101 min	0.81	2.56	FB	FB	FB	FB	***1.52***	***6.83***	0.81 to 1.52

Bimodal AMADs: Fitting the particle size data using the bimodal model resulted in AMAD values listed in Table 6.11 for each of the two peaks (labeled #1 and #2). These values and the GSD, the R^2 goodness-of-fit parameter, and the fraction in the first peak are presented in Appendix B for each CI distribution. Several samples taken at the driver's position had abnormally high values, which are listed as "greater than" numbers. These numbers were not used in averaging. The loader's first CI sample (Shot 4, 0 to 10 sec), which is believed to have been unaffected by fragment damage, is included in the range of AMAD values. The remaining sampler results, which were not used in averaging, are shown in bold italics.

Table 6.11. Summary of Bimodal AMADs, PI-3/4 Turret-Crossing Shots

Sampling Interval (+5 sec)	Bimodal AMAD (μm)									
	Commander		Driver		Gunner		Loader		Average	
	#1	#2	#1	#2	#1	#2	#1	#2	#1	#2
Shot 3: 0-10 sec	--	--	0.20	1.26	0.31	3.74	--	--	0.26	2.5
3-3.5 min	--	--	***>1000***	3.10	0.63	4.88	--	--	0.63	4.0
9-10 min	--	--	1.36	4.81	0.67	4.12	--	--	1.02	4.5
Shot 4: 0-10 sec	0.46	18.7	0.34	9.03	0.52	12.8	0.44	17.3	0.44	14.5
3-3.5 min	0.99	14.7	2.56	***>1000***	0.58	10.2	***0.57***	***5.84***	1.18	10.2
9-10 min	0.56	5.57	2.43	***>100***	0.74	6.37	***0.82***	***8.81***	1.14	6.9
21-23 min	0.53	1.99	0.59	4.00	0.54	3.38	***0.81***	***7.63***	0.62	4.3
45-49 min	0.72	7.84	0.62	4.68	0.49	4.20	***31.3***	***32.3***	8.28	12.3
93-101 min	0.77	1.69	FB	FB	FB	FB	***0.44***	***5.44***	0.61	3.1

Uranium Chemistry and Solubility

- Mass percent of uranium in aerosol:
  - Cyclone stages: 42 to 55% (derived from gamma spectrometry), 58 to 74% (from ICP-MS)
  - Backup filter: 44% (ICP-AES)
  - Moving filter ($\mu g/m^3$):

    Peak concentration at 13 sec (midpoint of ~3-sec interval)—4.55E+06
    30 sec 4.8E+06
    56 sec 1.1E+06

- Uranium oxide phase:
  - Cyclone (weight percent ratios of U_4O_9 to U_3O_8)

    Stage 1—1.07
    Stage 2—1.02
    Stage 3—0.73 (also 0.02 ratio of schoepite to U_3O_8)
    Stage 4—0.31
    Stage 5—0.13
    Backup filter—94% U_3O_8; 3% schoepite; 3% U_4O_9; ratio of U_4O_9 to U_3O_8—0.03 to 0.07 (evaluated using two separate XRD methods)

- *In vitro* solubility:
  - HRTM Model: Type M behavior for cyclone stages, Type S for backup filter
  - ICRP 30 Model:

    Cyclone stages 58 to 84%Y, 21% W (Stage 4), 16 to 36% D
    Backup filter 99% Y, 1% D

6.1.1.4 Shot 5 (PI-5)

Information concerning the general configuration of the vehicle, sampler shielding used, and unique aspects about Shot 5 are listed in this section. Additionally, this section includes a table listing the uranium aerosol concentrations as a function of time, a figure plotting this function, particle size distributions, and uranium chemistry and solubility.

Attributes and Unique Aspects

- Turret-crossing shot into breech (from the commander's side to the loader's side).
- The turret was in the combat position.
- Solid armor shields covered the commander's and loader's arrays; the gunner's array was not used because of the position's proximity to the shot line.
- The commander's hatch blew open and stayed open.
- The loader's hatch blew open but fell back, leaving crescent-shaped opening.

Interior Uranium Aerosol Concentrations with Time

The uranium concentrations are listed in Table 6.12 for each position for which there was an operating IOM sampler and the average concentrations. These data are plotted in Figure 6.4. Sample collection began 5 sec after impact. The gunner's array was not used for sample collection during this shot.

Table 6.12. Summary of DU Aerosol Concentrations with Time, PI-5 Breech Shot

Sampling Interval (+5 sec)	DU Concentration (μg/m^3)				
	Commander	Driver	Gunner	Loader	Average
0-10 sec	2.52E+07	1.47E+07	--	6.29E+06	1.54E+07
1-1 min 10 sec	6.81E+06	7.25E+06	--	4.78E+06	6.28E+06
3-3 min 10 sec	1.40E+06	7.13E+05	--	8.94E+05	1.00E+06
7-7.5 min	8.07E+04	3.18E+04	--	1.10E+05	7.42E+04
15-16 min	~Background	1.60E+04	--	6.68E+04	2.76E+04
31-33 min	2.78E+04	2.12E+04	--	2.05E+04	2.32E+04
61-65 min	2.06E+04	3.72E+04	--	3.35E+04	3.04E+04
121-129 min	2.01E+04	2.58E+04	--	2.62E+04	2.40E+04
144-148 min	Field blank	Field blank	--	2.70E+04	2.70E+04

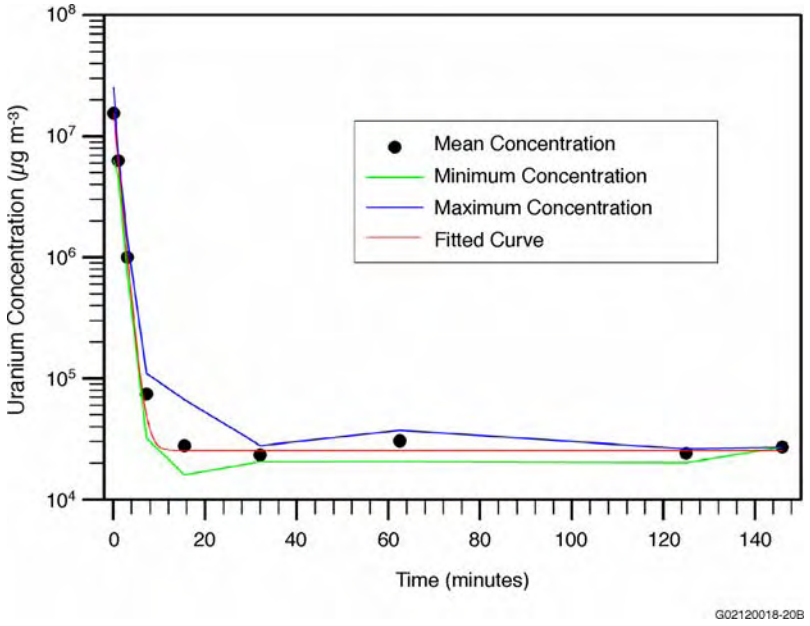

Figure 6.4. Summary of DU Aerosol Concentrations with Time, PI-5 Breech Shot

Particle Size Distribution

Unimodal AMADs: Fitting the particle size data using the unimodal model resulted in the AMAD values and the corresponding GSDs listed in Table 6.13. These parameters and the R^2 goodness-of-fit for each CI distribution are presented in Appendix B. Shaded data in the table identify those samples for which professional judgment was used to provide more realistic values. The gunner's array was not used for sample collection during this shot. The field blank is abbreviated "FB."

Table 6.13. Summary of Unimodal AMADs, PI-5 Breech Shot

Sampling Interval (+5 sec)	Unimodal AMAD (μm)								
	Commander		Driver		Gunner		Loader		AMAD Range
	AMAD	GSD	AMAD	GSD	AMAD	GSD	AMAD	GSD	
0-10 sec	3.87	8.22	7.49	4.07	--	--	4.60	7.38	3.87 to 7.49
1-1 min 10 sec	2.85	5.31	5.65	3.35	--	--	2.43	4.53	2.43 to 5.65
3-3 min 10 sec	2.5	4.0	4.6	2.2	--	--	2.0	5.0	2.0 to 5.0
7-7.5 min	2.0	4.0	4.0	1.8	--	--	2.2	4.5	1.8 to 4.5
15-16 min	1.5	4.0	18.7	9.75	--	--	1.38	4.09	1.38 to 18.7
31-33 min	1.6	4.0	9.84	8.11	--	--	1.06	3.57	1.06 to 9.84
61-65 min	1.30	4.11	6.92	7.70	--	--	1.08	4.18	1.08 to 6.92
121-129 min	1.02	3.21	1.37	4.16	--	--	2.0	3.5	1.02 to 2.0
144-148 min	FB	FB	FB	FB	--	--	1.16	7.63	1.16

Bimodal AMADs: Fitting the particle size data using the bimodal model resulted in the AMAD values listed in Table 6.14 for each of the two peaks (labeled #1 and #2). These values and the GSD, the R^2 goodness-of-fit parameter, and the fraction in the first peak are presented in Appendix B for each CI distribution. Results greater than 100 were not used to calculate averages. The gunner's array was not used for sample collection during this shot.

Table 6.14. Summary of Bimodal AMADs, PI-5 Breech Shot

Sampling Interval (+5 sec)	Bimodal AMAD (μm)									
	Commander		Driver		Gunner		Loader		Average	
	#1	#2	#1	#2	#1	#2	#1	#2	#1	#2
0-10 sec	0.50	11.02	0.41	9.05	--	--	0.53	11.2	0.48	10.4
1-1 min 10 sec	0.67	8.49	0.50	5.71	--	--	0.68	7.50	0.62	7.2
3-3 min 10 sec	0.82	4.77	0.004	4.56	--	--	0.76	4.61	0.53	4.6
7-7.5 min	0.97	5.75	0.56	4.00	--	--	0.95	5.49	0.83	5.1
15-16 min	0.71	2.19	0.13	6.54	--	--	0.57	4.10	0.47	4.3
31-33 min	0.59	3.74	>1000	9.86	--	--	0.67	4.35	0.63	6.0
61-65 min	0.54	4.48	0.26	5.76	--	--	0.52	3.90	0.44	4.7
121-129 min	0.71	4.69	0.49	3.31	--	--	0.70	4.08	0.63	4.0
144-148 min	--	--	--	--	--	--	0.71	9.20	0.71	9.2

Uranium Chemistry and Solubility

- Mass percent of uranium in aerosol: Cyclone did not run, uranium concentration was not measured.
- Uranium oxide phase: No XRD data were obtained for these samples.
- *In vitro* solubility: No solubility data were obtained for these samples.

6.1.1.5 Shot 6 (PI-6)

Information concerning the general configuration of the vehicle, sampler shielding used, and unique aspects about Shot 6 are listed in this section. Additionally, this section includes a table listing the uranium aerosol concentrations as a function of time, a figure plotting this function, particle size distributions, and uranium chemistry and solubility.

Attributes and Unique Aspects

- Turret-crossing shot into breech (from the loader's side to the commander's side).
- The turret was in the combat position.
- Solid armor shields covered the commander's and loader's arrays; a louvered shield covered the driver's array; the gunner's array was not used because of the position's proximity to shot line.
- The commander's hatch blew open and stayed open.
- The loader's hatch blew open but fell back, leaving a crescent-shaped opening.
- The loader's array was used for resuspension evaluation.

Interior Uranium Aerosol Concentrations with Time

The uranium concentrations are listed in Table 6.15 for each position for which there was an operating IOM sampler and the average concentrations. These data are plotted in Figure 6.5. Sample collection began 5 sec after impact. The gunner's array was not used for sample collection during this shot. The loader's array collected aerosols during recovery operations, and these results are reported in Section 6.2.1.4.

Table 6.15. Summary of DU Aerosol Concentrations with Time, PI-6 Breech Shot

Sampling Interval (+5 sec)	DU Concentration ($\mu g/m^3$)				
	Commander	Driver	Gunner	Loader	Average
0-10 sec	2.25E+07	1.33E+07	--	--	1.79E+07
1-1 min 10 sec	5.71E+06	3.16E+06	--	--	4.44E+06
3-3 min 10 sec	7.86E+05	1.22E+06	--	--	1.00E+06
7-7.5 min	5.20E+03	1.86E+05	--	--	9.56E+04
15-16 min	~Bkgd	5.29E+04	--	--	2.65E+04
31-33 min	~Bkgd	2.38E+04	--	--	1.19E+04
61-65 min	3.13E+04	2.40E+04	--	--	2.77E+04
121-129 min	1.81E+04	8.30E+02	--	--	9.47E+03

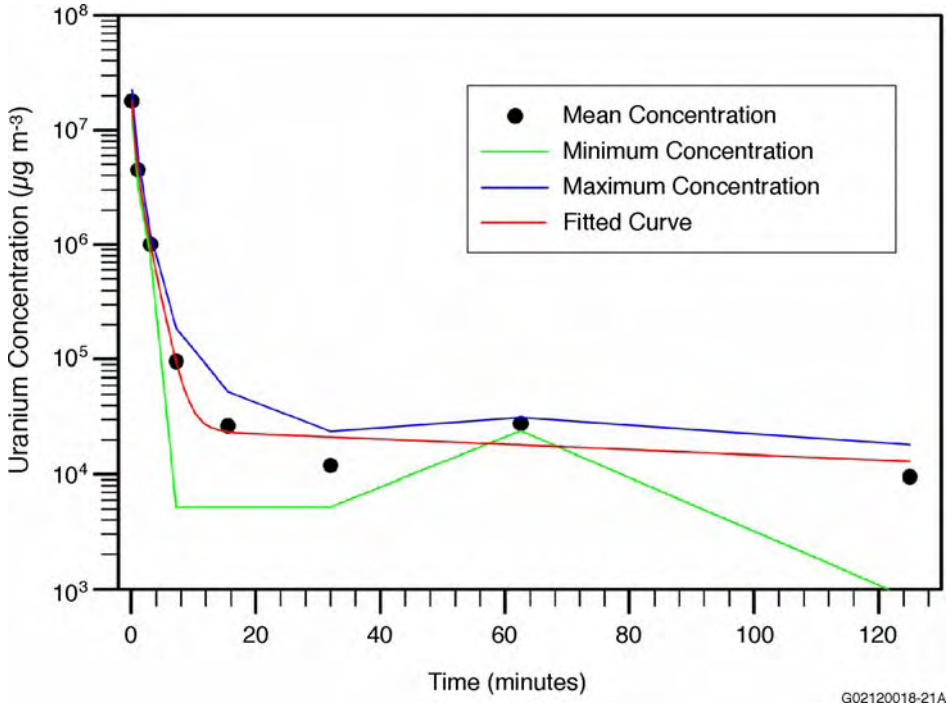

Figure 6.5. Summary of DU Aerosol Concentrations with Time, PI-6 Breech Shot

Particle Size Distribution

Unimodal AMADs: Fitting the particle size data using the unimodal model resulted in the AMAD and the corresponding GSD values in Table 6.16. These parameters and the R^2 goodness-of-fit for each CI distribution are presented in Appendix B. Shaded data shown in the table identify those samples for which professional judgment was used to provide more realistic values. The gunner's array was not used for sample collection during this shot. The loader's array was used to monitor aerosols during recovery activities, and these results are presented in Section 6.2.2.

Table 6.16. Summary of Unimodal AMADs, PI-6 Breech Shot

Sampling Interval (+5 sec)	Unimodal AMAD (μm)								
	Commander		Driver		Gunner		Loader		
	AMAD	GSD	AMAD	GSD	AMAD	GSD	AMAD	GSD	AMAD Range
0-10 sec	8.46	7.11	2.5	3.5	--	--	--	--	2.5 to 8.46
1-1 min 10 sec	3.22	4.41	2.38	4.62	--	--	--	--	2.38 to 3.22
3-3 min 10 sec	1.5	4.0	1.8	4.0	--	--	--	--	1.5 to 1.8
7-7.5 min	1.5	5.0	1.56	5.06	--	--	--	--	1.5 to 1.56
15-16 min	1.25	2.92	0.58	2.84	--	--	--	--	0.58 to 1.25
31-33 min	2.5	8.0	0.82	2.78	--	--	--	--	0.82 to 2.5
61-65 min	8.02	21.5	0.85	3.65	--	--	--	--	0.85 to 8.02
121-129 min	0.56	4.41	0.67	2.39	--	--	--	--	0.56 to 0.67

Bimodal AMADs: Fitting the particle size data using the bimodal model resulted in the AMAD values listed in Table 6.17 for each of the two peaks (labeled #1 and #2). These values and the GSD, the R^2 goodness-of-fit parameter, and the fraction in the first peak are presented in Appendix B for each CI distribution. Results presented as "greater than" are not used in averaging. The gunner's array was not used for sample collection during this shot. The loader's array was used to monitor aerosols during recovery activities, and data from this array are presented in Section 6.2.2.

Table 6.17. Summary of Bimodal AMADs, PI-6 Breech Shot

Sampling Interval (+5 sec)	Bimodal AMAD (μm)									
	Commander		Driver		Gunner		Loader		Average	
	#1	#2	#1	#2	#1	#2	#1	#2	#1	#2
0-10 sec	0.40	10.83	0.55	1.55	--	--	--	--	0.48	6.2
1-1 min 10 sec	0.74	6.29	0.75	7.97	--	--	--	--	0.75	7.1
3-3 min 10 sec	0.62	3.92	0.58	3.96	--	--	--	--	0.60	3.9
7-7.5 min	1.03	4.92	1.62	>1000	--	--	--	--	1.33	4.9
15-16 min	0.66	3.12	0.48	3.80	--	--	--	--	0.57	3.5
31-33 min	0.42	38.3	0.58	1.06	--	--	--	--	0.50	19.7
61-65 min	0.56	16.6	0.52	3.77	--	--	--	--	0.54	10.2
121-129 min	0.45	4.39	0.60	3.81	--	--	--	--	0.53	4.1

Uranium Chemistry and Solubility

- Mass percent of uranium in aerosol: Cyclone stages—62 to 81% (derived from gamma spectrometry)
- Uranium oxide phase: No XRD data for these samples
- *In vitro* solubility: No solubility data for these samples

6.1.1.6 Shot 7 (PI-7)

Information concerning the general configuration of the vehicle, sampler shielding used, and unique aspects about Shot 7 are listed in this section. Additionally, this section includes a table listing the uranium aerosol concentrations as a function of time, a figure plotting this function, particle size distributions, and uranium chemistry and solubility.

Attributes and Unique Aspects

- Hull-crossing shot through turret basket (from the loaders side to the commander's side).
- The turret was in the combat position.
- Solid armor shields covered the commander's, gunner's, and loader's arrays; a louvered shield covered the driver's array.
- The aluminum witness plate (in front of catch plate) shattered when struck by the penetrator, spreading aluminum debris over the fragmentation shield area and severing sampler pressure-drop (flow-rate) feedback lines.
- The commander's hatch released, and the hatch opened about an inch.
- The loader's position array used to evaluate resuspension.

Interior Uranium Aerosol Concentrations with Time

The uranium concentrations are listed in Table 6.18 for each position for which there was an operating IOM sampler and the average concentrations. Standard deviations at the 1-sigma uncertainty (Unc. ± 1σ) level of these three or four points are also provided. These data are plotted in Figure 6.6. Sample collection began 5 sec after impact. The loader's array collected aerosols during recovery operations, and these results are reported in Section 6.2.1.4.

Table 6.18. Summary of DU Aerosol Concentrations with Time, PI-7 Hull Shot

Sampling Interval (+5 sec)	DU Concentration (μg/m^3)					
	Commander	Driver	Gunner	Loader	Average	Unc. ± 1σ
0-10 sec	1.43E+07	8.56E+06	1.17E+07	--	1.15E+07	2.87E+06
1-1 min 10 sec	4.74E+06	5.56E+06	6.07E+06	--	5.46E+06	6.71E+05
3-3 min 15 sec	2.59E+06	2.81E+06	3.02E+06	--	2.81E+06	2.15E+05
7-8 min	8.28E+05	8.74E+05	1.06E+06	--	9.21E+05	1.23E+05
15-17 min	1.86E+05	Did not run	1.99E+05	--	1.93E+05	9.19E+03
31-35 min	7.08E+04	5.27E+04	5.77E+04	--	6.04E+04	9.35E+03
61-69 min	6.26E+04	5.55E+04	5.26E+04	--	5.69E+04	5.14E+03
121-129 min	4.69E+04	5.09E+04	3.96E+04	--	4.58E+04	5.73E+03

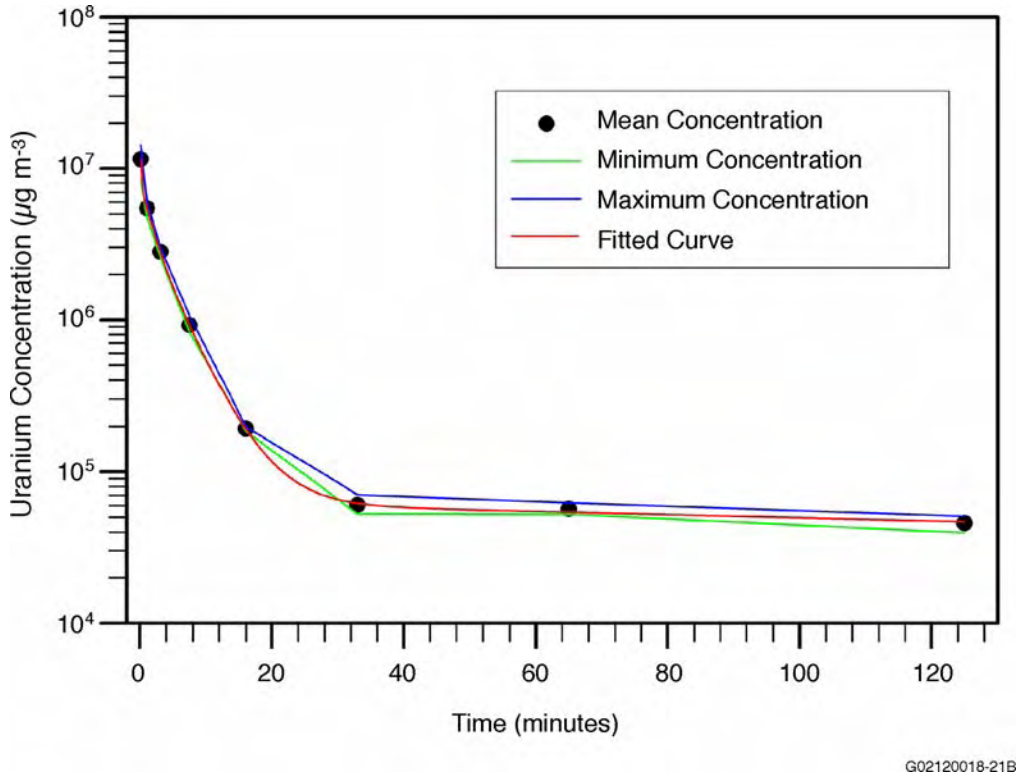

Figure 6.6. Summary of DU Aerosol Concentrations with Time, PI-7 Hull Shot

Particle Size Distribution

Unimodal AMADs: Fitting the particle size data using the unimodal model resulted in the AMAD values and the corresponding GSDs listed in Table 6.19. These parameters and the R^2 goodness-of-fit for each CI distribution are presented in Appendix B. Shaded data in the table identify those samples for which professional judgment was used to provide more realistic values. The loader's array collected aerosols during recovery operations, and these results are reported in Section 6.2.1.4.

Table 6.19. Summary of Unimodal AMADs, PI-7 Hull Shot

Sampling Interval (+5 sec)	Unimodal AMAD (μm)								
	Commander		Driver		Gunner		Loader		AMAD Range
	AMAD	GSD	AMAD	GSD	AMAD	GSD	AMAD	GSD	
0-10 sec	4.04	8.63	2.97	6.99	1.64	8.32	--	--	1.64 to 4.04
1-1 min 10 sec	10.9	1.31	1.90	6.65	2.2	3.6	--	--	1.90 to 10.9
3-3 min 15 sec	2.4	4.1	2.3	4.0	2.9	4.8	--	--	2.3 to 2.9
7-8 min	3.0	4.5	1.03	2.93	3.6	3.4	--	--	1.03 to 3.0
15-17 min	2.0	5.0	1.31	3.04	2.2	4.5	--	--	1.31 to 2.2
31-35 min	0.86	2.76	0.71	4.12	0.77	3.51	--	--	0.71 to 0.86
61-69 min	0.82	3.99	0.70	3.54	0.51	1.74	--	--	0.51 to 0.82
121-129 min	1.0	3.46	0.67	2.78	0.58	1.90	--	--	0.58 to 1.0

Bimodal AMADs: Fitting the particle size data using the bimodal model resulted in the AMAD values listed in Table 6.20 for each of the two peaks (labeled #1 and #2). These values and the GSD, the R^2 goodness-of-fit parameter, and the fraction in the first peak are presented in Appendix B for each CI distribution. "Greater than" values are not used in the calculation of AMAD averages. The loader's array collected aerosols during recovery operations, and these results are reported in Section 6.2.1.4.

Table 6.20. Summary of Bimodal AMADs, PI-7 Turret Shot

Sampling Interval (+5 sec)	Bimodal AMAD (μm)									
	Commander		Driver		Gunner		Loader		Average	
	#1	#2	#1	#2	#1	#2	#1	#2	#1	#2
0-10 sec	0.34	7.64	0.34	6.21	0.45	7.79	--	--	0.38	7.2
1-1 min 10 sec	0.11	>1000	0.41	3.98	0.75	2.22	--	--	0.42	3.1
3-3 min 10 sec	0.61	2.41	0.84	7.94	0.60	2.91	--	--	0.68	4.4
7-7.5 min	1.03	9.27	0.63	1.52	>1000	3.60	--	--	0.83	4.8
15-16 min	0.76	4.48	0.83	2.86	0.79	4.78	--	--	0.79	4.0
31-33 min	0.61	3.34	0.19	1.23	0.50	4.11	--	--	0.43	2.9
61-65 min	0.49	3.90	0.37	1.80	0.54	3.91	--	--	0.47	3.2
121-129 min	0.67	4.01	0.48	2.34	0.58	3.60	--	--	0.58	3.3

Uranium Chemistry and Solubility

- Mass percent of uranium in aerosol:
  - Cyclone stages—52 to 65% (derived from gamma spectrometry), 49 to 54% (ICP-MS)
  - Backup filter—40% (ICP-AES)

- Uranium oxide phase:
  - Cyclone (weight percent ratios of U_4O_9 to U_3O_8)
    Stage 1—0.95
    Stage 2—0.72
    Stage 3—0.46
    Stage 4—0.23
    Stage 5—0.12 (95% U_3O_8; 3% schoepite; 2% U_4O_9
    Backup filter—95% U_3O_8; 3% schoepite; 2% U_4O_9; ratio of U_4O_9 to U_3O_8—0.02 to 0.06 (evaluated using two separate XRD methods)

- *In vitro* solubility:
  - HRTM Model: Cyclone stages and backup filter—Type-M behavior
  - ICRP 30 Model:
    Cyclone stages—65 to 87% Y, 15 to 35% D
    Backup filter—87% Y, 13% D

6.1.2 Bradley Fighting Vehicle

The Phase-II shots consisted of two shots fired in quick succession crossing through the passenger compartment and a shot fired into the turret that subsequently passed into the thick metal of the gun feeder. Uranium concentrations for the various sample collection intervals at each position are listed, and the averages of these data are provided. Because three or more samplers were operating for the Phase-II shots, standard deviations at the 1-sigma level were calculated for these results.

6.1.2.1 Shots 1/2 (PII-1/2)

Information concerning the general configuration of the vehicle, sampler shielding used, and unique aspects about Shots 1/2 are listed in this section. Additionally, this section includes a table listing the uranium aerosol concentrations as a function of time, a figure plotting this function, particle size distributions, and uranium chemistry and solubility.

Attributes and Unique Aspects

- Two passenger-compartment-crossing shots (from left scout side to right scout side) were fired at a 14-min interval and several inches apart.
- The turret was in the combat position.
- Solid armor shields covered the commander's and right scout's arrays; louvered shields covered the driver's and loader's arrays; the commander's shield was left open to collect aerosol from both shots; the right scout's shield blew open for second shot only.
- The turret sliding door was blown into the passenger compartment.
- The hatches remained closed.
- Abundant fiber-like material was released from the perforated Kevlar spall liner.

Interior Uranium Aerosol Concentrations with Time

The uranium concentrations are listed in Table 6.21 for each position for which there was an operating IOM sampler and the average concentrations. These data are plotted in Figure 6.7. Standard deviations at the 1-sigma uncertainty level of these three or four points also are provided. Sample collection began 5 sec after impact. Samplers in the right scout's array were not activated until Shot 2.

Table 6.21. Summary of DU Aerosol Concentrations with Time, PII-1/2 Crossing Shots

Sampling Interval (+5 sec)	DU Concentration (μg/m^3)					
	Commander	Driver	Right Scout	Left Scout	Average	Unc. ± 1σ
Shot 1: 0-10 sec	4.15E+06	1.87E+06	--	4.00E+06	3.34E+06	1.28E+06
3-4 min	1.49E+06	4.08E+05	--	6.32E+05	8.43E+05	5.71E+05
9-11 min	6.31E+05	1.04E+05	--	2.95E+05	3.43E+05	2.67E+05
Shot 2: 0-10 sec	4.23E+06	4.37E+06	4.43E+06	5.56E+06	4.65E+06	6.14E+05
3-4 min	1.50E+06	1.34E+06	1.28E+06	1.46E+06	1.40E+06	1.02E+05
9-11 min	6.72E+05	6.63E+05	6.40E+05	7.08E+05	6.71E+05	2.83E+04
21-25 min	2.40E+05	2.50E+05	2.37E+05	2.26E+05	2.38E+05	9.88E+03
45-53 min	6.13E+04	7.12E+04	6.08E+04	6.87E+04	6.55E+04	5.24E+03
93-109 min	3.82E+04	3.35E+04	3.30E+04	3.90E+04	3.59E+04	3.11E+03

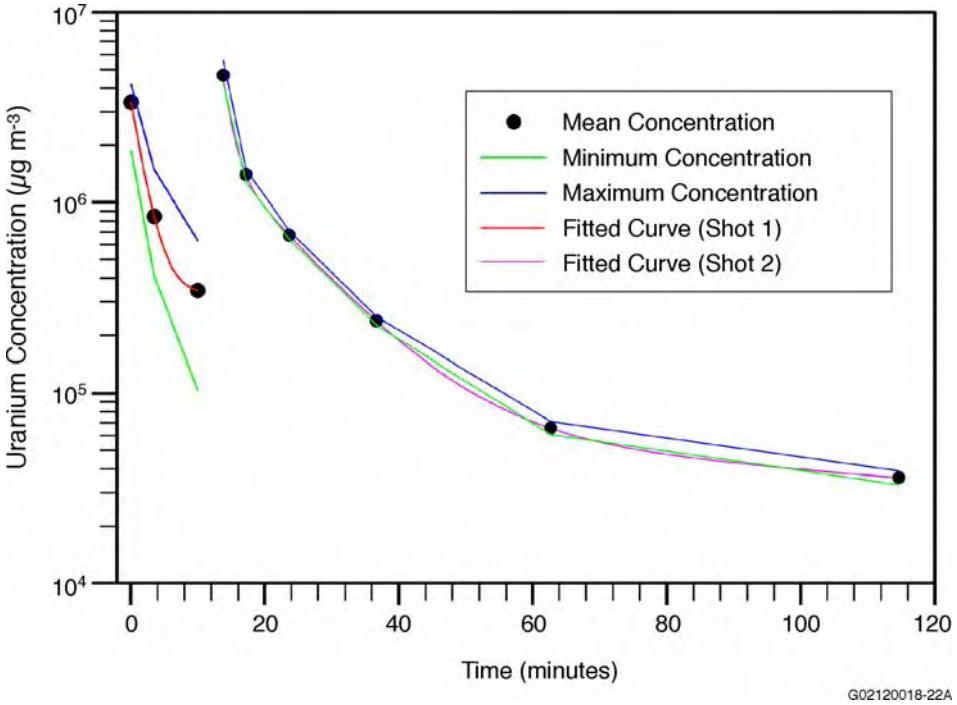

Figure 6.7. Summary of DU Aerosol Concentrations with Time, PII-1/2 Crossing Shots

Particle Size Distribution

Unimodal AMADs: Fitting the particle size data using the unimodal model resulted in the AMAD values and the corresponding GSDs listed in Table 6.22. These parameters and the R^2 goodness-of-fit for each CI distribution are presented in Appendix B. Shaded data in the table identify those samples for which professional judgment was used to provide more realistic values. Sample collection by the sampler array at the right scout's position began with Shot 2.

Table 6.22. Summary of Unimodal AMADs, PII-1/2 Crossing Shots

Sampling Interval (+5 sec)	Unimodal AMAD (μm)								
	Commander		Driver		Right Scout		Left Scout		AMAD Range
	AMAD	GSD	AMAD	GSD	AMAD	GSD	AMAD	GSD	
Shot 1: 0-10 sec	1.71	4.68	1.46	4.74	--	--	0.58	7.52	0.58 to 1.71
3-4 min	1.52	3.96	1.84	4.41	--	--	0.81	8.14	0.81 to 1.84
9-11 min	3.65	3.96	1.8	5.0	--	--	3.07	4.45	1.8 to 3.65
Shot 2: 0-10 sec	1.33	4.21	3.57	5.33	1.32	11.3	2.79	9.76	1.32 to 3.57
3-4 min	0.99	2.86	0.78	3.05	0.72	5.45	1.04	4.15	0.72 to 1.04
9-11 min	0.97	3.09	0.50	1.73	0.86	3.41	0.87	4.30	0.50 to 0.95
21-25 min	0.64	2.42	0.55	1.91	0.72	3.44	0.51	5.61	0.51 to 0.72
45-53 min	0.93	3.70	0.92	3.16	0.58	4.17	0.48	6.36	0.48 to 0.93
93-109 min	0.64	4.79	0.75	3.86	0.53	4.03	0.80	4.44	0.53 to 0.80

Bimodal AMADs: Fitting the particle size data using the bimodal model resulted in the AMAD values listed in Table 6.23 for each of the two peaks (labeled #1 and #2). These values and the GSD, the R2 goodness-of-fit parameter, and the fraction in the first peak are presented in Appendix B for each CI distribution. "Greater than" numbers were not used in the calculation of average AMADs. Sample collection by the sampler array at the right scout's position began with Shot 2.

Table 6.23. Summary of Bimodal AMADs, PII-1/2 Crossing Shots

Sampling Interval (+5 sec)	Bimodal AMAD (μm)									
	Commander		Driver		Right Scout		Left Scout		Average	
	#1	#2	#1	#2	#1	#2	#1	#2	#1	#2
Shot 1: 0-10 sec	0.35	2.35	1.01	3.35	--	--	0.45	19.83	0.60	8.5
3-4 min	0.45	2.97	0.41	3.40	--	--	0.34	3.41	0.40	3.3
9-11 min	3.91	3.97	0.83	5.33	--	--	>1000	3.05	2.37	4.1
Shot 2: 0-10 sec	0.65	4.46	0.41	5.21	0.31	8.09	0.37	8.05	0.44	6.5
3-4 min	0.58	1.78	0.50	3.00	0.47	5.74	0.61	4.73	0.54	3.8
9-11 min	0.63	4.11	0.53	4.12	0.59	4.74	0.63	6.55	0.60	4.9
21-25 min	0.52	2.68	0.54	3.99	0.59	4.60	0.34	3.98	0.50	3.8
45-53 min	0.70	1.46	0.62	4.14	0.44	4.46	0.33	4.40	0.52	3.6
93-109 min	0.36	2.10	0.46	3.25	0.43	4.12	0.58	6.68	0.42	3.2

Uranium Chemistry and Solubility

- Mass percent of uranium in aerosol:
  - Cyclone stages—17 to 37% (derived from gamma spectrometry), 22 to 29% (ICP-MS)
  - Backup filter—27% (ICP-AES)

- Uranium oxide phase:
  - Cyclone (weight percent ratios of U_4O_9 to U_3O_8)
    Stage 1—1.79
    Stage 2—1.32
    Stage 3—0.99 (also 0.04 ratio of schoepite to U_3O_8)
    Stage 4—0.45

Stage 5—0.20 (also 89% U_3O_8, 4% schoepite, 7% U_4O_9)
Backup filter—92% U_3O_8; 7% schoepite; 1% U_4O_9; ratio of U_4O_9 to U_3O_8—0.05

- *In vitro* solubility:
  - HRTM Model: Cyclone stages and backup filter—Type-M behavior
  - ICRP 30 Model:
    Cyclone stages 58 to 89% Y; 11 to 17% W; 21 to 26% D
    Backup filter 77% Y, 9% W, 14% D

6.1.2.2 Shot 3 (PII-3)

Information concerning the general configuration of the vehicle, sampler shielding used, and unique aspects about Shot 3 are listed in this section. Additionally, this section includes a table listing the uranium aerosol concentrations as a function of time, a figure plotting this function, particle size distributions, and uranium chemistry and solubility.

Attributes and Unique Aspects

- The shot was fired into the turret gun feeder and exited through the turret front.
- The turret was turned to right at about a 90° angle.
- Solid armor shields covered the commander's and right scout's arrays; louvered shields covered the driver's and loader's arrays.
- The TOW missile-loading hatch opened at time of impact.
- The armor shield at the right scout's position dropped open only an inch.

Interior Uranium Aerosol Concentrations with Time

The uranium concentrations are listed in Table 6.24 for each position for which there was an operating IOM sampler and the average concentrations. Standard deviations at the 1-sigma uncertainty level of these three or four points are also provided. These data are plotted in Figure 6.8. The lower line is based on the commander's CI samples. These results do not track well with the mean and upper lines, and the reason is most likely because the solid shield did not fully open, leaving the samplers poorly exposed to interior vehicle aerosols. Sample collection began 5 sec after impact.

Table 6.24. Summary of DU Aerosol Concentrations with Time, PII-3 Turret Shot

Sampling Interval (+5 sec)	DU Concentration ($\mu g/m^3$)					
	Commander	Driver	Right Scout	Left Scout	Average	Unc. ± 1σ
0-10 sec	2.05E+06	1.50E+06	5.14E+05	6.75E+05	1.18E+06	7.21E+05
1-1 min 10 sec	2.94E+03	4.05E+05	2.77E+05	2.21E+05	2.26E+05	1.68E+05
3-3 min 15 sec	~Bkgd	1.24E+05	1.32E+05	4.38E+04	7.50E+04	4.88E+04
7-8 min	2.92E+04	8.06E+04	7.22E+04	7.62E+04	6.46E+04	2.38E+04
15-17 min	3.89E+04	6.53E+04	5.43E+04	7.30E+04	5.79E+04	1.48E+04
31-35 min	5.25E+04	5.99E+04	4.93E+04	7.11E+04	5.82E+04	9.68E+03
61-69 min	4.19E+04	4.79E+04	4.63E+02	4.95E+04	3.49E+04	2.32E+04
121-129 min	2.69E+04	3.07E+04	1.18E+03	3.30E+04	2.29E+04	1.47E+04

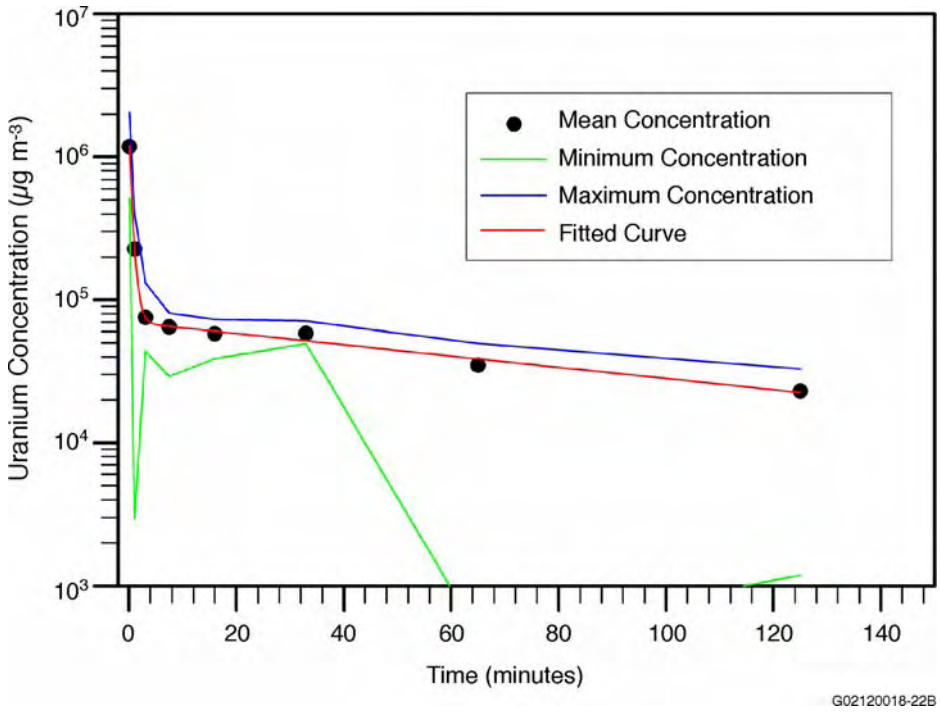

Figure 6.8. Summary of DU Aerosol Concentrations with Time, PII-3 Turret Shot

Particle Size Distribution

Unimodal AMADs: Fitting the particle size data using the unimodal model resulted in the AMAD values and the corresponding GSDs listed in Table 6.25. These parameters and the R^2 goodness-of-fit for each CI distribution are presented in Appendix B. Shaded data in the table identify those samples for which professional judgment was used to provide more realistic values.

Table 6.25. Summary of Unimodal AMADs, PII-3 Turret Shot

Sampling Interval (+5 sec)	Unimodal AMAD (μm)								
	Commander		Driver		Right Scout		Left Scout		AMAD Range
	AMAD	GSD	AMAD	GSD	AMAD	GSD	AMAD	GSD	
0-10 sec	2.84	13.3	2.74	14.3	3.83	3.46	21.6	2.07	2.74 to 21.6
1-1 min 10 sec	2.97	2.44	1.07	12.8	2.41	6.15	19.6	4.43	1.07 to 19.6
3-3 min 15 sec	40.9	1.42	0.46	1.65	2.0	6.0	2.5	4.5	0.46 to 40.9
7-8 min	0.56	2.84	0.38	2.77	0.36	5.25	1.23	6.08	0.36 to 1.23
15-17 min	0.55	2.88	0.37	2.17	0.81	3.51	1.11	9.23	0.37 to 1.11
31-35 min	0.53	4.89	0.59	2.47	0.76	2.73	0.95	7.03	0.53 to 0.95
61-69 min	0.59	4.78	0.97	3.69	0.52	2.02	1.03	4.23	0.52 to 1.03
121-129 min	0.57	3.40	0.22	2.61	0.51	1.08	1.06	4.86	0.22 to 1.06

Bimodal AMADs: Fitting the particle size data using the bimodal model resulted in the AMAD values listed in Table 6.26 for each of the two peaks (labeled #1 and #2). These values and the GSD, the R^2 goodness-of-fit parameter, and the fraction in the first peak are presented in Appendix B for each CI distribution. "Greater than" numbers were not used in calculating average AMADs.

Table 6.26. Summary of Bimodal AMADs, PII-3 Turret Shot

Sampling Interval (+5 sec)	Bimodal AMAD (μm)									
	Commander		Driver		Right Scout		Left Scout		Average	
	#1	#2	#1	#2	#1	#2	#1	#2	#1	#2
0-10 sec	0.35	11.9	0.42	13.5	3.76	>100	>1000	20.9	1.51	12.7
1-1 min 10 sec	1.16	4.28	0.48	19.4	0.33	3.95	0.91	19.1	0.72	11.7
3-3 min 15 sec	0.32	19.6	0.46	>1000	1.07	5.38	0.64	11.1	0.62	12.0
7-8 min	0.46	2.73	0.39	2.72	0.27	3.11	0.38	0.67	0.38	2.3
15-17 min	0.47	3.27	0.37	1.41	0.53	3.04	0.33	4.05	0.43	2.9
31-35 min	0.33	2.07	0.50	2.56	0.52	2.80	0.36	3.59	0.43	2.8
61-69 min	0.36	2.97	0.50	3.20	0.54	5.65	0.45	3.36	0.46	3.8
121-129 min	0.41	2.14	0.25	2.94	0.73	12.4	0.45	3.57	0.46	5.3

Uranium Chemistry and Solubility

- Mass percent of uranium in aerosol:
  - Cyclone—8 to 15% (derived from gamma spectrometry)
  - Moving filter ($\mu g/m^3$):

    Peak concentration 1 7 sec 1.07E+6
    1.4 sec 1.5E+05
    10 sec 7.0E+05
    16 sec 5.0E+05 (closest point to 10 sec + 5 sec post impact)
    30 sec 3.6E+05
    1 min 2.6E+05 (avg. of 2 segments)
    2 min 1.3E+05 (avg. of 2 segments)
    7.5 min 7.9E+04 (avg. of 3 segments)
    61 min 6.8E+04 (avg. of 11 segments)
    121 min 3.4E+4 (avg. of 11 segments)

- Uranium oxide phase:
  - Cyclone (Weight percent ratios)

    Backup filter: 92% U_3O_8; 7% schoepite; 1% U_4O_9; ratio of U_4O_9 to U_3O_8—0.01

- *In vitro* solubility: No solubility data for these samples.

6.1.3 Phase III—Abrams Tank with DU Armor

The Phase-III shots consisted of two separate events during which shots perforated DU armor. The aerosol sampling intervals were identical for these two shots. Uranium concentrations for the various sample collection intervals are listed, and the averages of these data are provided. Because three or more samplers were operating for the Phase-III shots, standard deviations at the 1-sigma level were calculated for these results.

6.1.3.1 Shot 1 (PIII-1)

Information concerning the general configuration of the vehicle, sampler shielding used, and unique aspects about Shot 1 are listed in this section. Additionally, this section includes a table listing the

uranium aerosol concentrations as a function of time, a figure plotting this function, particle size distributions, and uranium chemistry and solubility.

Attributes and Unique Aspects

- The shot was fired through DU armor package into breech.
- The turret was in the combat position, angled so the penetrator would impact the left front panel.
- Solid armor shields covered the commander's, gunner's, and loader's arrays; a louvered shield covered the driver's array.
- Flames from burning of residual hydraulic fluid erupted for about 4 sec.
- Smoke/aerosol vented from the perimeter of the loader's hatch and the GPS position.
- Thin oily residue coated the interior of the turret.

Interior Uranium Aerosol Concentrations with Time

The uranium concentrations are listed in Table 6.27 for each position for which there was an operating IOM sampler and the average concentrations. Standard deviations at the 1-sigma uncertainty level of these three or four points are also provided. These data are plotted in Figure 6.9. Sample collection began 5 sec after impact.

Table 6.27. Summary of DU Aerosol Concentrations with Time, PIII-1 DU Armor Shot

Sampling Interval (+5 sec)	DU Concentration ($\mu g/m^3$)					
	Commander	Driver	Gunner	Loader	Average	Unc. ± 1σ
0-10 sec	4.89E+06	2.59E+06	7.67E+06	3.42E+06	4.64E+06	2.23E+06
1-1 min 10 sec	1.97E+06	2.72E+06	2.32E+06	8.45E+05	1.96E+06	8.06E+05
3-3 min 15 sec	1.37E+06	1.42E+06	1.56E+06	1.35E+06	1.43E+06	9.47E+04
7-8 min	7.15E+05	6.96E+05	5.97E+05	6.08E+05	6.54E+05	6.01E+04
15-17 min	1.93E+05	2.27E+05	2.42E+05	1.92E+05	2.14E+05	2.50E+04
31-35 min	3.43E+04	4.02E+04	1.06E+04	3.74E+04	3.06E+04	1.36E+04
61-69 min	6.48E+03	7.94E+03	8.44E+03	8.12E+03	7.75E+03	8.68E+02
121-129 min	4.60E+03	8.07E+03	5.04E+03	5.53E+03	5.81E+03	1.55E+03

Particle Size Distribution

Unimodal AMADs: Fitting the particle size data using the unimodal model resulted in the AMAD values and the corresponding GSDs listed in Table 6.28. These parameters and the R^2 goodness-of-fit for each CI distribution are presented in Appendix B. Shaded data shown in the table identify those samples for which professional judgment was used to provide more realistic values.

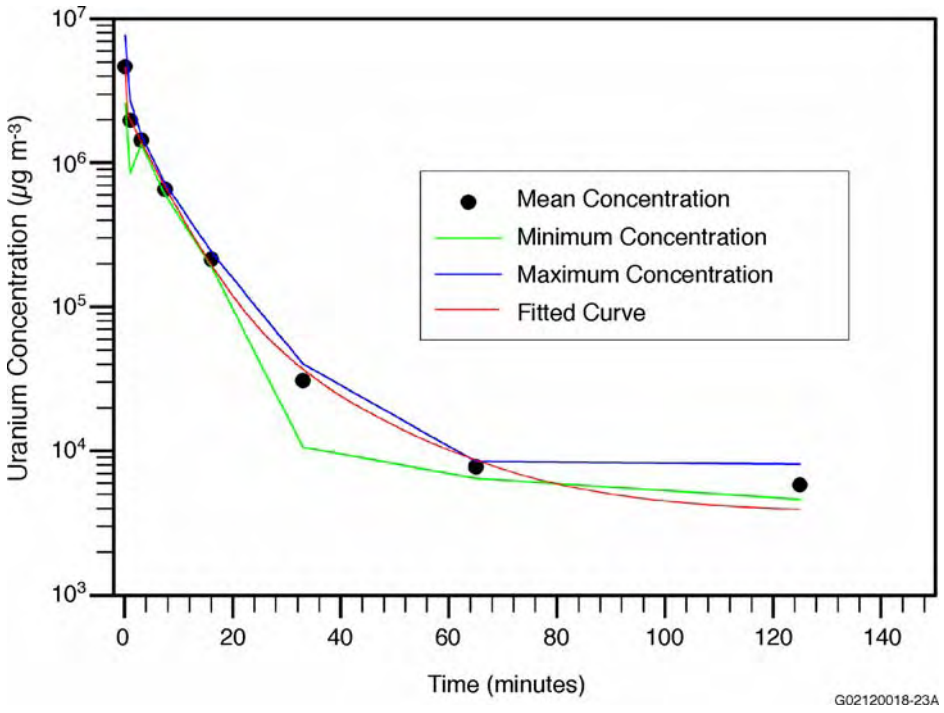

Figure 6.9. Summary of DU Aerosol Concentrations with Time, PIII-1 DU Armor Shot

Table 6.28. Summary of Unimodal AMADs, PIII-1 DU Armor Shot

Sampling Interval (+5 sec)	Unimodal AMAD (μm)								
	Commander		Driver		Gunner		Loader		AMAD Range
	AMAD	GSD	AMAD	GSD	AMAD	GSD	AMAD	GSD	
0-10 sec	5.76	3.69	0.82	4.02	7.51	4.56	4.80	4.34	0.82 to 7.51
1-1 min 10 sec	4.55	3.70	0.13	2.14	2.6	3.2	4.81	2.85	0.13 to 4.81
3-3 min 15 sec	5.02	7.65	16.9	7.63	3.0	4.0	2.3	3.3	2.3 to 16.9
7-8 min	1.8	4.0	3.0	4.5	1.8	4.0	2.0	5.0	1.8 to 3.0
15-17 min	1.48	4.01	2.0	5.0	2.0	4.0	2.0	5.5	1.48 to 2.0
31-35 min	3.0	4.5	1.10	2.92	1.8	4.0	1.21	2.49	1.10 to 3.0
61-69 min	2.0	3.5	1.24	2.28	0.92	2.07	2.0	4.0	0.92 to 2.0
121-129 min	1.51	7.56	0.82	2.14	0.53	1.23	0.93	3.59	0.53 to 1.51

Bimodal AMADs: Fitting the particle size data using the bimodal model resulted in the AMAD values listed in Table 6.29 for each of the two peaks (labeled #1 and #2). These values and the GSD, the R^2 goodness-of-fit parameter, and the fraction in the first peak are presented in Appendix B for each CI distribution. "Greater than" numbers were not used in calculating average AMADs.

Table 6.29. Summary of Bimodal AMADs, PIII-2 DU Armor Shot

Sampling Interval (+5 sec)	Bimodal AMAD (μm)									
	Commander		Driver		Gunner		Loader		Average	
	#1	#2	#1	#2	#1	#2	#1	#2	#1	#2
0-10 sec	0.60	7.12	0.50	4.13	0.73	8.49	2.94	14.5	1.19	8.6
1-1 min 10 sec	0.39	4.85	0.22	40.4	>1000	**2.6**	0.003	1.58	0.20	12.4
3-3 min 15 sec	1.06	5.88	0.98	19.1	0.93	4.95	>1000	2.27	0.99	8.1
7-8 min	0.64	4.15	0.71	4.08	0.71	4.05	0.64	4.28	0.68	4.1
15-17 min	0.51	2.36	0.76	6.03	0.74	3.90	0.67	3.79	0.67	4.0
31-35 min	0.73	2.94	0.73	3.90	0.79	3.45	0.81	3.16	0.77	3.4
61-69 min	0.64	2.88	0.81	2.88	0.74	2.38	0.46	2.45	0.66	2.6
121-129 min	0.37	2.51	0.77	1.33	0.55	>100	0.49	3.09	0.55	2.3

Uranium Chemistry and Solubility

- Mass percent of uranium in aerosol:
  - Cyclones 30 to 75+% (Derived from gamma spectrometry; Stages 2 and 3 overestimated U content)
  - Moving filter ($\mu g/m^3$):

    Peak concentration at 7 sec (midpoint of ~3 sec interval) 8.2E+06
    1.4 sec 1.5E+06
    10 sec 3.8E+06
    16 sec 2.6E+06 (closest point to 10 sec + 5 sec post impact)
    30 sec 2.5E+06
    60 sec 2.9E+06 (average of 2 segments)
    120 sec 2.1E+06 (average of 2 segments)
    7.4 min 1.1E+06
    16 min 5.2E+5
    61 min 5.3E+04 (average of 11 segments)
    121 min 4.8E+4 (average of 4 segments

- Uranium oxide phase: No XRD data for these samples
- *In vitro* solubility: No solubility data for these samples.

6.1.3.2 Shot 2 (PIII-2)

Information concerning the general configuration of the vehicle, sampler shielding used, and unique aspects about Shot 2 are listed in this section. Additionally, this section includes a table listing the uranium aerosol concentrations as a function of time, a figure plotting this function, particle size distributions, and uranium chemistry and solubility.

Attributes and Unique Aspects

- The shot was fired through DU armor package (several inches from PIII-1 shot) into breech.
- The turret was in the combat position, angled so the penetrator would impact the left front panel.

- Solid armor shields covered the commander's, gunner's, and loader's arrays; a louvered shield covered the driver's array.
- The loader's hatch opened several inches upon impact; a chimney effect was apparent.
- The cyclone connection between Stages 2 and 3 was loose; the sample was resuspended at LRRI.

Interior Uranium Aerosol Concentrations with Time

The uranium concentrations are listed in Table 6.30 for each position for which there was an operating IOM sampler and the average concentrations. Standard deviations at the 1-sigma uncertainty level of these three or four points are also provided. These data are plotted in Figure 6.10. Sample collection began 5 sec after impact.

Table 6.30. Summary of DU Aerosol Concentrations with Time, PIII-2 DU Armor Shot

Sampling Interval (+5 sec)	DU Concentration (μg/m^3)					
	Commander	Driver	Gunner	Loader	Average	Unc. ± 1σ
0-10 sec	1.38E+07	8.49E+06	3.62E+07	1.13E+07	1.74E+07	1.27E+07
1-1 min 10 sec	3.75E+06	5.32E+06	9.20E+06	2.15E+06	5.11E+06	3.02E+06
3-3 min 15 sec	1.30E+06	1.53E+06	5.36E+06	1.41E+06	2.40E+06	1.98E+06
7-8 min	1.91E+05	1.63E+05	3.56E+05	9.65E+04	2.02E+05	1.10E+05
15-17 min	9.29E+03	8.29E+03	1.04E+05	--	4.05E+04	5.50E+04
31-35 min	1.89E+04	1.95E+04	7.04E+04	2.38E+04	3.32E+04	2.49E+04
61-69 min	6.10E+03	1.89E+04	4.04E+04	1.74E+04	2.07E+04	1.43E+04
121-129 min	1.05E+04	1.88E+04	3.53E+04	1.40E+04	1.97E+04	1.10E+04

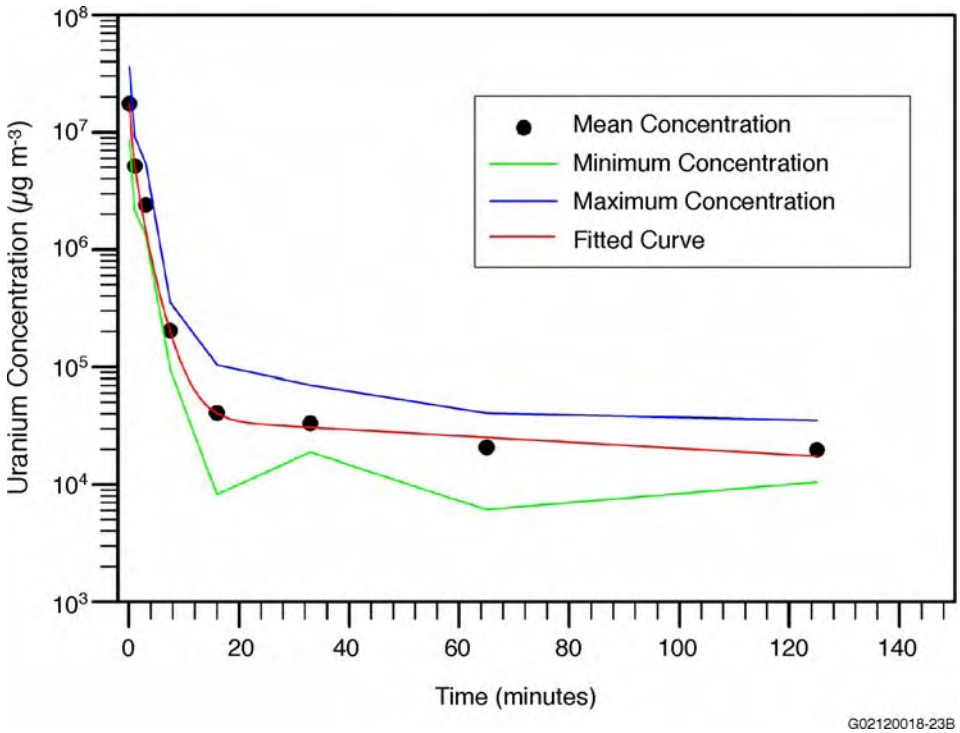

Figure 6.10. Summary of DU Aerosol Concentrations with Time, PIII-2 DU Armor Shot

Particle Size Distribution

Unimodal AMADs: Fitting the particle size data using the unimodal model resulted in the AMAD values and the corresponding GSDs listed in Table 6.31. These parameters and the R^2 goodness-of-fit for each CI distribution are presented in Appendix B. Shaded data in the table identify those samples for which professional judgment was used to provide more realistic values.

Table 6.31. Summary of Unimodal AMADs, PIII-2 DU Armor Shot

Sampling Interval (+5 sec)	Unimodal AMAD (μm)								
	Commander		Driver		Gunner		Loader		AMAD Range
	AMAD	GSD	AMAD	GSD	AMAD	GSD	AMAD	GSD	
0-10 sec	6.78	3.86	3.95	7.68	10.7	4.66	4.70	5.56	3.95 to 10.7
1-1 min 10 sec	31.6	1.91	0.63	2.60	14.4	8.00	2.33	4.45	0.63 to 31.6
3-3 min 15 sec	34.2	2.29	3.45	3.71	40.3	1.50	2.0	4.0	1.5 to 40.3
7-8 min	2.0	4.0	2.1	4.0	42.0	1.46	2.5	4.0	2.0 to 42.0
15-17 min	0.56	1.22	0.82	3.94	42.6	1.34	2.5	4.5	0.56 to 42.6
31-35 min	0.55	1.24	0.78	3.45	1.27	4.35	1.16	4.64	0.55 to 1.27
61-69 min	0.52	1.20	0.81	3.92	42.1	1.32	0.99	3.71	0.52 to 3.92
121-129 min	10	4.5	0.82	3.29	41.6	1.44	0.86	2.98	0.882 to 41.6

Bimodal AMADs: Fitting the particle size data using the bimodal model resulted in the AMAD values listed in Table 6.32 for each of the two peaks (labeled #1 and #2). These values and the GSD, the R^2 goodness-of-fit parameter, and the fraction in the first peak are presented in Appendix B for each CI distribution.

Table 6.32. Summary of Bimodal AMADs, PIII-2 DU Armor Shot

Sampling Interval (+5 sec)	Bimodal AMAD (μm)									
	Commander		Driver		Gunner		Loader		Average	
	#1	#2	#1	#2	#1	#2	#1	#2	#1	#2
0-10 sec	0.43	7.56	0.29	7.71	0.46	11.4	0.48	7.05	0.42	8.4
1-1 min 10 sec	0.40	31.6	0.66	16.2	0.52	**21.9**	1.22	***0.006***	0.70	**17.4**
3-3 min 15 sec	0.65	30.7	3.45	>1000	>1000	39.9	0.82	5.35	1.64	25.3
7-8 min	0.72	13.5	0.80	3.88	1.38	37.0	1.37	4.27	1.07	14.7
15-17 min	0.57	>100	0.54	3.56	13.3	40.7	0.76	5.03	3.79	16.4
31-35 min	0.56	>100	0.52	3.21	0.41	3.08	0.72	4.92	0.55	3.7
61-69 min	0.54	>100	0.69	1.98	0.59	70.1	0.54	3.56	0.59	25.2
121-129 min	0.58	39.1	0.71	9.83	1.19	40.9	0.78	1.18	0.82	22.8

Uranium Chemistry and Solubility

- Mass percent of uranium in aerosol:
  - Cyclone stages: stage separation problem—results may not be representative
    Stage 1—65% (ICP-MS)
    Stage 2—no sample
    Stage 3—no sample
    Stage 4—64% (ICP-MS)
    Stage 5—63% (ICP-MS)
    Backup filter—65% (ICP-AES)
  - Moving filter ($\mu g/m^3$):
    Peak concentration at 1.4 sec (midpoint of ~3 sec interval) 9.1E+06
    1.4 sec 9.1E+06
    10 sec 6.3E+06
    16 sec 5.2E+06 (closest point to 10 sec + 5 sec post impact)
    30 sec 3.9E+06
    1 min 3.4E+06 (average of 2 segments)
    2 min 2.1E+06 (average of 2 segments)
    7.5 min 1.6E+05
    16 min 3.0E+04
    61 min 1.9E+04 (average of 11 segments)
    121 min 1.7E+04 (average of 10 segments

- Uranium oxide phase:
  - Cyclone (weight percent ratios of U_4O_9 to U_3O_8)
    Stage 1—1.34 (also 63% U_3O_8; 2% schoepite; 35% U_4O_9)
    Stage 2—no sample
    Stage 3—no sample
    Stage 4—0.39
    Stage 5—0.15 (also 89% U_3O_8; 6% schoepite; 6% U_4O_9)
    Backup filter—94% U_3O_8; 4% schoepite; 2% U_4O_9; ratio of U_4O_9 to U_3O_8—0.02 to 0.05 (evaluated using two XRD methods)

- *In vitro* solubility:
  - HRTM Model: Cyclones and backup filter—Type-M behavior
  - ICRP 30 Model:
    Cyclone Stages 4 and 5 only 90 to 95% Y, 7.5% W (Stage 4), 3 to 5% D
    Backup filter 85% Y, 4.5% W, 10% D

6.1.4 Phase IV—Abrams with DU Armor, Operating Vehicle

Phase IV consisted of a series of shots, three for which CI samplers operated and four for which wipe samples were collected. These four shots included the following:

- PIV-1: a non-DU cartridge that did not perforate tank armor
- PIV-2: a DU munition that did not perforate the tank armor
- PIV-3: a non-DU munition that perforated the tank armor
- PIV-4: a DU munition that perforated the tank armor.

Attributes and Unique Aspects

Because the Phase-IV shots were part of another test and the Capstone team was only minimally involved, little information was provided about any attributes or unique aspects of the tests. Little room for samplers was available, and no shielding was provided for the CI samplers used. The MVF and cyclone were minimally shielded.

Interior Uranium Aerosol Concentrations with Time

The only samplers used in the tests were the CIs, MVF, and cyclone. The IOMs, used for the analysis of concentration in Phases I through III, were not used in this test because of space limitations. Uranium concentrations from the CIs are listed in Table 6.33 for PIV-4 shot only. (The CI results were not corrected for wall loss or sampling efficiency.) Sample collection began 5 sec after impact.

Table 6.33. Summary of DU Aerosol Concentrations with Time, Phase IV, Driver's CIs

	Uranium Mass Concentration (μg/m^3)			
CI Stage	**CI-1 (0 to 10 sec)**	**CI-2 (1 min to 1 min, 10 sec)**	**CI-4 (5 min to 5 min, 15 sec)**	**CI-5 (25 to 27 min)**
Stage 1	3.12E+04	6.85E+03	1.60E+03	4.14E+02
Stage 2	4.80E+03	~Background	1.60E+03	4.14E+02
Stage 3	~Background	2.28E+03	~ Background	1.65E+03
Stage 4	~Background	4.57E+03	3.19E+02	1.65E+03
Stage 5	~Background	~Background	~ Background	3.52E+03
Stage 6	4.80E+03	3.42E+04	2.72E+04	1.65E+03
Stage 7	2.40E+03	5.48E+04	1.60E+03	1.45E+03
Stage 8	~Background	1.03E+05	1.44E+04	2.07E+02
Backup Filter	3.60E+04	2.74E+04	3.19E+02	2.07E+02
Total	**7.92E+04**	**2.33E+05**	**4.70E+04**	**1.12E+04**

Particle Size Distribution

PIV-4 was the only shot in the Phase IV test series for which uranium aerosols were generally above background readings. Fragments severed the loader's CI lines. Samples from the second through fourth CIs at the driver's position that collected aerosol were evaluated for particle size. Unimodal AMAD results are shown in Table 6.34 with their GSD and R^2 values of goodness-of-fit. Shaded data in the table identify those samples for which professional judgment was applied to provide more realistic values. The bimodal AMADs include these parameters and the fraction in the first peak.

Table 6.34. Unimodal and Bimodal AMADs for PIV-4

Sampling Interval (+5 sec)	Unimodal Fit			Bimodal Fit			
	AMAD (μm)	GSD	R^2	AMAD (μm)	GSD	R^2	Fraction in First Peak
0 to 10 sec	Not evaluated						
1 to 1 min, 10 sec	0.62	1.67	0.97	0.53	1.16	1.00	0.17
				0.76	1.94		
5 to 5 min, 15 sec	1.28	2.38	0.42	0.50	1.17	0.99	0.48
				1.84	1.29		
25 to 27 min	>1000; 4.0	0; 4.0	0	0.03	0	0	0.37
				0.91	2.06		

Uranium Chemistry and Solubility

The MVF and cyclone vacuum lines were severed by DU fragments and collected only minimal material. Consequently, insufficient sample material was available for chemical analysis.

6.2 Interior Aerosol Properties by Scenario

Capstone Phases I through III involved 12 shots on BHTs. The test shots were designed to simulate, to the extent possible, conditions that would have resulted in the generation of aerosols when armored vehicles were hit during the Gulf War/ODS and to evaluate the aerosols formed by perforations of DU armor. The test shots most resembling vehicle perforations experienced during the Gulf War/ODS (retrospective scenarios) are PI-7 and PII-1/2. Test shot PII-3 was designed to be an upper bound of the Gulf War/ODS incidents involving Bradley vehicles. Test shots designed to simulate incidents in future (prospective) combat scenarios include the turret-crossing shots of the Abrams tank as simulated in test shots PI-1 through PI-4. The PI-5 and PI-6 shots added the element of striking the breech and further eroding the penetrator. The PIII-1 and PIII-2 shots incorporated perforation of the DU armor, and PIV-4 challenged DU armor on an operational vehicle.

In a separate organization of data from Section 6.1, the aerosol properties are grouped by scenario and are discussed in terms of their general similarity and their distinctiveness. The following sections describe DU aerosol concentrations and settling times by shot lines and particle size distributions as a function of time.

6.2.1 DU Aerosol Concentrations

The DU aerosol concentrations are divided into three main time increments between the time of impact, 1 h post impact, and during recovery activities. The data presented in these tables are listed by phase and shot in Section 6.2.1. The full concentration data set is summarized in Table 5.5. These data are also presented in Appendix A, Tables A.9 through A.18 along with the propagated uncertainty for each concentration.

6.2.1.1 DU Aerosol Concentrations Within the First 5 Seconds

Viewing of the video taken inside the turret suggests that the aerosol created by vehicle perforation disperses instantly and that mixing continues by turbulence in the aerosol cloud. The MVF was the only air monitoring instrumentation that collected aerosol samples during the first 5 sec after impact. Except for Shot PI-1, which alternated sample collection between stationary and moving positions, the filter media collected samples as it moved continually for the first 3 min. Peak uranium concentrations within the first few seconds and the simple average (not weighted) concentration over the first minute are listed below in Table 6.35. Peak concentrations ranged from 1.1E+06 to 9.1E+06 μg/m^3, about an order of magnitude difference, and occurred at a minimum of 1.4 sec and a maximum of 13 sec post shot. The shot through the Bradley (PII-3) provided the lowest DU aerosol concentration, and the shots through the DU armor (PIII-1 and 2) had the highest peak DU aerosol concentrations. The MVF did not operate during the shots through the non-DU armor into the breech (PI-5 and 6).

Table 6.35. Uranium Concentrations as Measured by the MVF Sampler

Shot Description	Peak Concentration/Time (μg/m^3)	Average U Concentration over First Minute (μg/m^3)
Retrospective Scenarios		
• Bradley—turret shot (PII-3)	1.1E+06 at 7.2 sec	4.36E+05
Prospective Scenarios		
• Abrams—crossing turret (PI-1)	2.3E+06 avg. over first 5 sec	--
• Abrams—crossing turret (PI-3)	6.0E+06 at 13 sec	4.55E+06
• Abrams—into DU armor (PIII-1)	8.2E+06 at 7.2 sec	2.99E+06
• Abrams—into DU armor (PIII-2)	9.1E+06 at 1.4 sec	4.53E+06

6.2.1.2 DU Aerosol Concentration—Within the First Few Minutes

The IOM filter cassettes provided the primary samples used to measure aerosol concentrations after the first 5 sec. These samplers ran for a minimum of 10 to 30 sec for the first time interval up to a maximum of 64 min (PI-1) for the final sampling interval. Although these sample durations are very short and the shielding varied between louvered and solid shields, the team believes that aerosol mixing was nearly instantaneous and that sample collection was likely to have been representative of existing aerosol conditions. The pressure drop data suggests that the nominal flow rates were reached within 1 sec of operation. As with the MVF data, the DU aerosol concentration as measured by the IOMs was highest during the first sampling interval. Table 6.36 provides the lowest and highest concentrations measured within the operating crew positions (maximum of four). It includes the length of sampling time for the first interval and the midpoint for the second interval. For scenarios simulated by two separate shots, the lowest and highest concentrations for the combined results are presented. The double shots are presented individually, but the concentrations during the second shot include the aerosol still suspended from the first shot.

The concentrations for the first time interval range from a low of 5.41E+05 μg/m^3 in the Bradley vehicle turret shot (PII-3) to a high of 3.62E+07 μg/m^3 in the DU armor shot (PIII-2). Surprisingly, the DU aerosol concentrations reached during the hull shot (PI-7), in which the penetrator traversed the thinnest armor of the Abrams tank shots, were similar to the turret shots. For this shot (PI-7), the DU aerosol concentration ranged from a low of 8.56E+06 μg/m^3 at the driver's position to 1.17E+07 μg/m^3 at the

gunner's position and 1.43E+07 µg/m^3 at the commander's position, which is only slightly below the levels reached in the PIII-2 shot into DU armor. These three concentrations were quite similar and suggest that relatively uniform aerosol dispersion was achieved quickly. An even closer spread in concentrations was achieved with Shot PI-2, in which the concentrations at the driver's and loader's positions were 5.60E+06 and 6.00E+06 µg/m^3, respectively. The second Bradley vehicle shot also had a tight grouping with DU aerosol concentrations of 4.23E+06 and 5.56E+06 µg/m^3. The concentrations from the other shots were within a factor of 1.6 to 5.1, with the least agreement between results from samples taken at the driver's and loader's positions in Shot PI-1.

Table 6.36. Uranium Concentration Ranges within a Few Minutes Post Impact

Shot Description	First Time Interval (beginning 5 sec after Impact, µg/m^3)	Second Time Interval (midpoint, µg/m^3)
Retrospective Scenarios		
• Abrams—crossing hull (through turret) (PI-7)	8.56E+06 to 1.43E+07 (10 sec)	4.74E+06 to 6.07E+06 (1.1 min)
• Bradley—passenger compartment—double shot (PII-1/2)	1st: 1.87E+06 to 4.15E+06 (10 sec) 2nd: 4.23E+06 to 5.56E+06 (10 sec)	4.08E+05 to 1.49E+06 (3.5 min) 1.28E+06 to 1.50E+06 (3.5 min)
• Bradley—turret shot (PII-3)	5.41E+05 to 2.05E+06 (10 sec)	2.94E+03 to 4.05 E+05 (1.1 min)
Prospective Scenarios		
• Abrams—crossing turret (PI-1, PI-2)	3.31E+06 to 1.69E+07 (30 sec) 5.60E+06 to 6.00E+06 (15 sec)	2.63E+06 to 4.85E+06 (0.75 min) 9.93E+05 to 5.89E+06 (1 min)
• Abrams—crossing turret—double shot (PI-3/4)	1st: 3.50E+06 to 7.05E+06 (10 sec 2nd: 9.21E+06 to 2.26E+07 (10 sec)	1.91E+06 to 2.98E+06 (3.25 min) 2.28E+06 to 4.42E+06 (3.25 min)
• Abrams—turret into breech (PI-5, PI-6)	6.29E+06 to 2.52E+07 (10 sec)	3.16E+06 to 7.25E+06 (1.1 min)
• Abrams—into DU armor (PIII-1, PIII-2)	2.59E+06 to 3.62E+07 (10 sec)	8.45E+05 to 9.20E+06 (1.1 min)

The timing of the second collection interval varied from a midpoint of 0.75 min to 3.25 min, so comparing these results is less useful. However, some generalizations can be made about these data including the drop in concentration from the first interval, which was typically a factor of 2 to 5 less than during the first interval. As with the first time interval, the PII-3 shot into the Bradley vehicle turret yielded the lowest DU aerosol concentration, and was lower at 1 min than the concentrations generated by the PII-1/2 shot at 3.5 min from both the first and the second shots.

6.2.1.3 DU Aerosol Concentrations—30 to 60 min after Impact

DU aerosol concentrations declined rapidly over time and were usually about two orders of magnitude lower 22 to 33 min post shot, although sometimes the concentrations were 3 orders of magnitude lower (Table 6.37). By 49 to 65 min post shot, the concentrations again were reduced by about a factor of 2. The exception was Shot PI-5, which was fired into the Abrams tank breech. In this case, the concentration at the driver's and loader's positions increased slightly while it decreased at the commander's position. The replicate shot (PI-6) showed almost identical aerosol concentrations at these two time intervals at the driver's position, which was the only position for which samples were available at both intervals.

Table 6.37. Uranium Concentration Ranges within an Hour Post Impact

Shot Description	Closest Interval to 30 min Post Impact (midpoint, μg/m^3)	Closest Interval to 60 min Post Impact (midpoint, μg/m^3)
Retrospective Scenarios		
• Abrams—crossing hull (through turret) (PI-7)	5.27E+04 to 7.08E+04 (33 min)	5.26E+04 to 6.26E+04 (65 min)
• Bradley—passenger compartment—double shot (PII-1/2)	2.37E+05 to 2.50E+05 (23 min after second shot; 37 min after first shot)	6.08E+04 to 7.12E+04 (49 min after second shot; 63 min after first shot)
• Bradley—turret shot (PII-3)	4.93E+04 to 5.99E+04 (33 min)	4.19E+04 to 4.95E+04 (65 min)
Prospective Scenarios		
• Abrams—crossing turret (PI-1, PI-2)	4.57E+04 to 8.65E+04 (23 min)	2.23E+04 to 3.26E+04 (48 min) 1.32E+04 to 4.32E+04 (56 min)
• Abrams—crossing turret—double shot (PI-3/4)	1.46E+05 to 3.41E+05 (22 min after second shot; 36 min after first shot)	8.06E+04 to 1.80E+05 (47 min after second shot; 60 min after first shot)
• Abrams—turret into breech (PI-5, PI-6)	2.05E+04 to 2.78E+04 (32 min)	2.06E+04 to 3.72E+04 (63 min)
• Abrams—into DU armor (PIII-1, PIII-2	1.06E+04 to 7.04E+04 (33 min)	6.10E+03 to 4.04E+04 (65 min)

6.2.1.4 Summary of Curve Fits

The curve fits of the mean concentrations over time for several shots were combined in Figures 6.11 through 6.13. Figure 6.11 plots each of the Abrams tank Phase-I single shots (PI-1, PI-2, PI-5, PI-6, and PI-7) and also includes the Bradley vehicle Phase-II single shot (PII-3) on a single graph to illustrate the spread in the concentration mean values. These lines show that the samplers for breech shots (PI-5 and PI-6) did register the highest concentrations during the first sampling interval but that the hull shot (PI-7) was consistently higher than the rest beginning with the third sampling interval, and remaining higher by a larger margin through the 2-h sampling period. The Bradley vehicle turret shot (PII-3) initially produced an aerosol concentration about an order of magnitude lower than the Abrams tank shots and continued this trend over the short term, but the aerosol concentration leveled off quickly, decreasing only slightly after the third sampling interval.

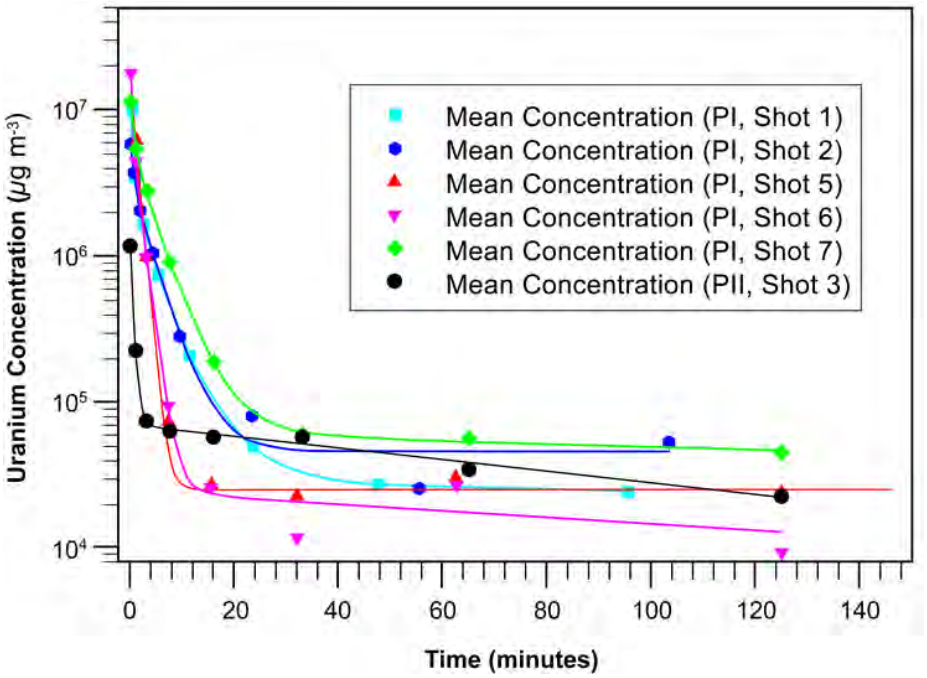

Figure 6.11. Summary of Single Shot Mean Concentrations from Phase I and Phase II

Figure 6.12 shows the mean concentration curves of the Abrams tank double shot (PI-3/4) and the Bradley vehicle double shot (PII-1/2). The shape of these curves is quite similar. The initial aerosol concentrations from the Abrams tank shots are higher and remain higher except for the samples taken between 35 and 40 min post impact.

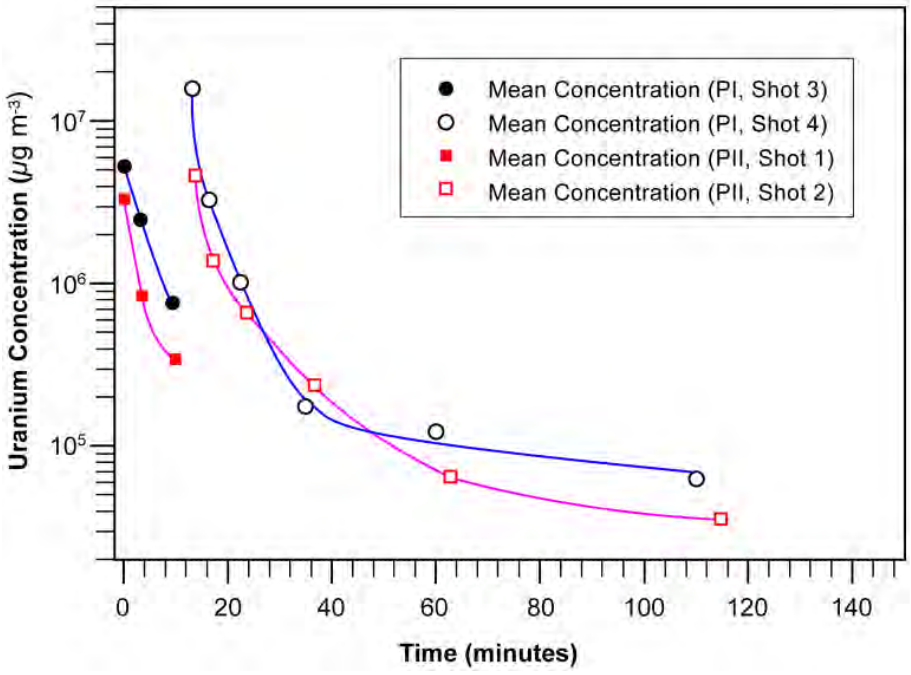

Figure 6.12. Summary of Double Shots from Phase I and Phase II

Figure 6.13 is a graph of the two single shots from the Abrams tank Phase-III tests (PIII-1 and PIII-2). Initial aerosol concentrations and the shapes of the curves vary visibly. Hydraulic fluid, which caught fire in PIII-1, may be partially responsible for these differences. The team speculates that residue of this fluid deposited on the interior of the vehicle, thus creating an oily surface that aerosol particles would stick to instead of bouncing off and remaining airborne. The shape of the PIII-2 curve resembles those of the breech shots (PI-5 and PI-6).

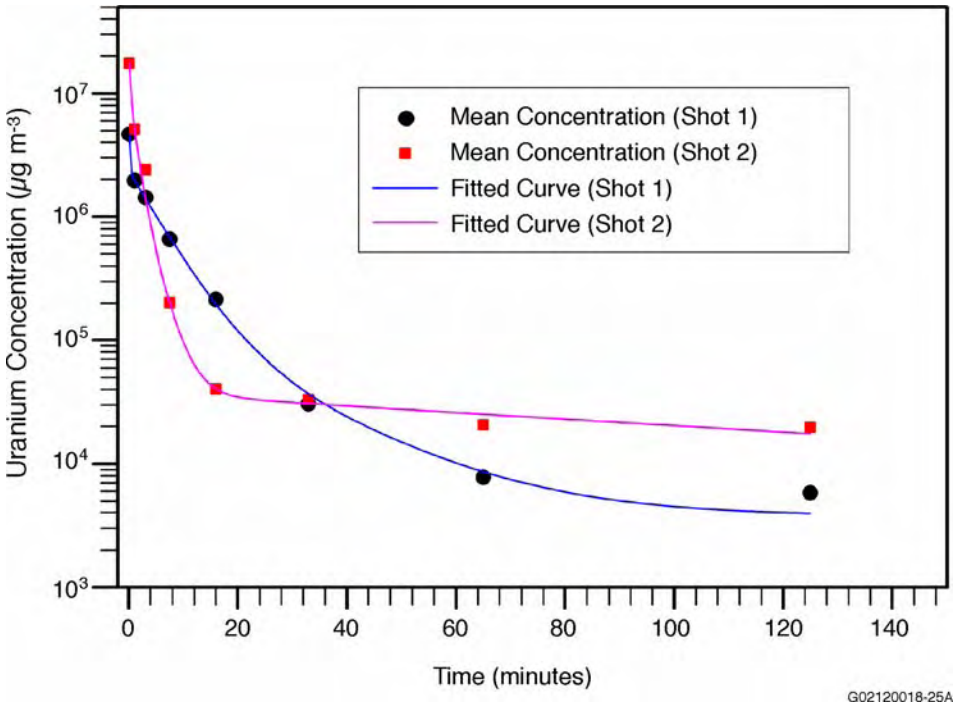

Figure 6.13. Curves from the Abrams Phase-III Tests

6.2.1.5 Summary of Means and Medians of Phases I Through III

The DU concentration data were standardized for time intervals from 10 sec to 2 h (beginning 5 sec post shot) so that means and medians could be calculated by phase and for sets of data with similar shot lines. DU concentrations at midpoint sample collection times were linearly interpolated using MATLAB routines[(a)] to estimate concentrations at the end of the standard intervals. No extrapolation was applied to the calculations, which were truncated at the midpoint of the last collected sample. Results of these calculations and mean standard deviations are listed in Table 6.38. The mean and median concentrations were quite similar. The means were generally higher than the medians for Phase-I and -III results and lower for Phase-II results.

[(a)] MATLAB software is available from The MathWorks, Inc., Natick, Massachusetts

Table 6.38. Comparison of Mean and Median DU Concentrations by Phase and Similar Shots

Time (min)	Mean Concentration ($\mu g/m^3$)	Median Concentration ($\mu g/m^3$)
Phase I – All Shots (1-7)		
0.17	1.17E+07 ± 7.69E+06	1.01E+07
0.5	9.33E+06 ± 5.88E+06	8.68E+06
1	5.96E+06 ± 3.82E+06	5.81E+06
30	1.03E+05 ± 1.17E+05	6.56E+04
60	4.87E+04 ± 3.65E+04	3.59E+04
120	2.95E+04 ± 1.81E+04	2.67E+04
Phase I – Crossing Turret (Shots 1, 2, 3, and 4)		
0.17	8.81E+06 ± 6.64E+06	6.36E+06
0.5	7.88E+06 ± 6.26E+06	5.74E+06
1	5.69E+06 ± 4.85E+06	4.39E+06
30	1.48E+05 ± 1.44E+05	7.77E+04
60	6.38E+04 ± 4.65E+04	4.41E+04
120	NA	NA
Phase I – Crossing Turret Through Breech (Shots 5 and 6)		
0.17	1.55E+07 ± 7.01E+06	1.41E+07
0.5	1.19E+07 ± 4.79E+06	1.16E+07
1	6.44E+06 ± 1.90E+06	7.10E+06
30	1.97E+04 ± 1.13E+04	2.44E+04
60	2.84E+04 ± 6.00E+03	2.87E+04
120	1.91E+04 ± 9.84E+03	2.01E+04
Phase I – Crossing Hull (Shot 7)		
0.17	1.10E+07 ± 2.60E+06	1.12E+07
0.5	8.99E+06 ± 1.53E+06	9.35E+06
1	5.96E+06 ± 5.19E+05	5.81E+06
30	1.08E+05 ± 3.63E+04	9.11E+04
60	5.74E+04 ± 5.63E+03	5.51E+04
120	4.67E+04 ± 5.45E+03	4.82E+04
Phase II – Crossing Passenger Compartment (Shots 1 and 2)		
0.17	2.96E+06 ± 1.73E+06	3.92E+06
0.5	2.66E+06 ± 1.69E+06	3.59E+06
1	2.21E+06 ± 1.67E+06	3.10E+06
30	1.25E+05 ± 8.38E+04	1.28E+05
60	4.89E+04 ± 2.72E+04	5.39E+04
120	2.39E+04± 1.47E+04	3.01E+04
Phase III – Firing Through Turret, DU Armor (Shots 1 and 2)		
0.17	1.04E+07 ± 1.02E+07	7.72E+06
0.5	7.91E+06 ± 7.33E+06	6.30E+06
1	4.16E+06 ± 3.26E+06	2.84E+06
30	4.94E+04 ± 2.40E+04	5.69E+04
60	1.70E+04 ±1.20E+04	1.28E+04
120	1.29E+04 ± 1.04E+04	9.10E+03
Phase IV – Firing into Turret, DU Armor, Operating Ventilation (Shot 4)		
0.17	9.21E+04	NA
0.5	1.43E+05	NA
1	2.20E+05	NA
30[(a)]	1.12E+04	NA

(a) Based on sampling to midpoint of 26 min.

6.2.1.6 DU Concentration During Recovery Activities

During two of the shots (PI-6 and PI-7), aerosols were collected using the loader's sampler array beginning several hours after impact. Following these baseline samples, aerosols were measured during the recovery activities (Section 5.4). Although the data are limited, these results provide another data point in the evaluation of DU aerosol concentration as a function of time (Table 6.39). The PI-6 test simulated the prospective scenario (i.e., Abrams tank—shot penetrating the turret into breech). The DU (baseline) aerosol concentration measured at 2 h and 35 min post shot was 3.0E+03 µg/m^3. The DU aerosol concentrations measured during recovery ranged from 3.3E+03 to a high of 2.9E+04 µg/m^3, which occurred immediately after recovery activities ceased.

The PI-7 test simulated the retrospective scenario (Abrams tank—crossing hull shot through the turret). The DU aerosol (baseline) concentration measured at 3 h and 21 min post shot was 1.2E+03 µg/m^3. Of the two samples taken during recovery activities, one was 4.3E+02 µg/m^3 and the second was at background levels. This suggests that either the baseline reading was high or that the samples measured were low; therefore, no conclusion can be reached on the basis of these minimal data.

Table 6.39. Uranium Concentrations During Recovery Activities

Activity	Collection Interval (post–impact)	U Conc. (µg/m^3)
PI-6 (Beginning 2 h and 35 min post shot)		
Baseline	0 to 20 min	2.95E+03
Recovery Activities	31 to 104 min	3.35E+03 to 5.28E+03
No activity	105 to 107 min	2.86E+04
No activity	107 to 111 min	2.10E+04
No activity	111 to 119 min	1.57E+04
No activity	119 to 135 min	7.46E+03
PI-7 (Beginning 3 h and 21 min post shot)		
Baseline	0 to 20 min	1.15E+03
Recovery Activities	20 to 60 min	4.30E+02
No activity	60 to 69.7 min	Background

DU aerosol concentrations collected by personnel air samplers during recovery activities ranged from 60 to nearly 1000 µg/m^3 (assuming a 2 Lpm flow rate). Recovery activities lasted between about 40 and 180 min (based on pump operation time, not actual time inside the vehicle). Because the recovery personnel were engaged in different tasks and were inside the vehicle for different lengths of time that were not recorded, no further analysis was attempted with these data.

6.2.2 Particle Size Distributions

Particle size analysis of aerosols collected inside the target vehicles was evaluated using data from the Marple CIs, which collected sample material during the same eight time intervals as the IOMs. Uranium masses from the CI substrates were analyzed using unimodal and bimodal AMAD models and are summarized by scenario in Sections 6.2.2.1 and 6.2.2.2. The unimodal AMAD values were seldom adequate to describe the particle size distributions. Bimodal AMAD values appeared to better model most, but not all, of the samples. However, with both models, there were numerous cases where the

AMAD values were much higher or lower than was reasonable. Several situations contributed to these unreasonable results. The most common was where a large sample was collected on Stage 1 and very little aerosol was collected on the remaining stages. This situation artificially raised the AMAD value and may not adequately represent the particle size distribution below the cutoff diameter on the first stage (nominally 21 μm). The second example occurred when the mass collected on each stage (or most of them) was similar, thus resulting in a flat, amodal distribution.

During the test shots, DU aerosols and other residues were formed in a transient pressurized environment. This could have deposited a coating of particulates on Stage 1 (ECD of ~21 μm) of unshielded (or louvered shielded) CIs not covered with solid shields that would not occur during sampling under more typical conditions. Although one or more field blanks were subtracted from the samples, any non-uniformity that caused more to be deposited on the sample than on the field blank would inflate the mass on the first stage, thereby disproportionately increasing the AMAD value. On the other hand, if creation of artifacts on the various sampler stages were random, then the blanks would represent the status of artifacts on the individual collected samples.

Particle size analysis of exterior aerosols (outside the vehicles but inside the Superbox) was conducted using data from the Andersen CIs. These data also were evaluated using unimodal and bimodal AMAD models. Their results are summarized by scenario in Section 6.2.2.3.

6.2.2.1 Interior Aerosol Unimodal Distributions

The particle size distributions for the retrospective and prospective scenarios as described by the unimodal AMAD are summarized in Table 6.40. A more extensive summary is provided in Table 5.25, and the data on which these AMAD estimates are based, along with their respective GSD and R^2 values, are graphed and listed in Appendix G. The AMAD values that are much larger or smaller than the rest are considered suspect and are shown in parentheses following the AMAD. Within the retrospective scenarios, the peak AMAD value was reached within the first minute following the Abrams tank hull shot (PI-7) and the Bradley vehicle turret shot (PII-3). For the Bradley vehicle passenger compartment shot (PII-1/2), the highest AMAD value occurred in the 10-min sample, and the highest AMAD range of 2.74 to 3.85 μm occurred with the Bradley vehicle turret shot (PII-3). For each scenario and all positions, the AMAD values declined over time and were generally at their lowest value at the last time period measured. This finding is consistent with the known mechanisms of particle settling, particularly within closed volumes.

The unimodal AMAD data associated with the prospective scenarios appear to be less consistent than the data obtained for the retrospective scenarios, and many of the values in the upper-end AMAD range are higher than those seen in the retrospective scenarios. Data from the lower end of the AMAD range for the Abrams tank turret-crossing shots (PI-1 and 2) are similar to data resulting from the Abrams tank hull-crossing shot (PI-7), but the AMAD values from the breech shots (PI-5 and 6) and the DU armor shots (PIII-1 and 2) are generally higher than for the other shots. These also display more samples for which the upper end of the range is unusually and perhaps unrealistically high.

Table 6.40. Interior Particle Size Distributions—Unimodal AMADs

Shot Description	Time Increment	AMAD (μm)
Retrospective Scenarios		
• Abrams—crossing hull (through turret)	First 10 sec 1.1 min 7.5 min 16 min 65 min	1.64 to 4.04 1.90 to 2.22 (10.9) 1.03 to 3.6 1.31 to 2.2 0.51 to 0.82
• Bradley—passenger compartment—double shot	Shot 1: First 10 sec 3.5 min 10 min Shot 2: First 10 sec 3.5 min 10 min 49 min	0.58 to 1.71 0.81 to 1.84 1.80 to 3.65 1.32 to 3.57 0.72 to 1.04 0.50 to 0.97 0.48 to 0.93
• Bradley—turret shot	First 10 sec 1.1 min 7.5 min 16 min 65 min	2.74 to 3.83 (21.6) 1.07 to 2.97 (19.6) 0.36 to 1.23 0.37 to 1.11 0.52 to 1.03
Prospective Scenarios		
• Abrams—crossing turret	First 15 sec First 30 sec 0.75 min 1 min 4.5 min 5.5 min 9.5 min 11.5 min 47.5 min 55.5 min	1.82 to 7.11 0.46 to 3.07 1.32 to 4.39 0.90 to 3.39 0.79 to 2.42 0.67 to 1.8 0.49 to 3.0 0.55 to 1.8 0.27 to 0.50 0.38 to 0.78
• Abrams—crossing turret—double shot	Shot 1: First 10 sec 3.25 min 9.5 min Shot 2: First 10 sec 3.25 min 9.5 min 47 min	0.18 to 0.70 1.98 to 3.10 2.0 to 2.5 4.0 to 6.96 (15.8) 1.07 to 2.56 1.03 to 6.62 0.62 to 1.19 (35.7)
• Abrams—turret into breech	First 10 sec 1.1 min 7.3 min 15.5 min 63 min	2.5 to 8.46 2.38 to 5.65 1.5 to 4.0 0.58 to 1.5 (18.7) 0.85 to 1.30 (6.92, 8.02)
• Abrams—into DU armor	First 10 sec 1.1 min 7.5 min 16 min 65 min	0.82 to 7.51 (10.7) 0.13 to 4.81 (14.4, 31.6) 1.8 to 3.0 (42.0) 0.56 to 2.5 (42.6) 0.52 to 2.0 (42.1)

6.2.2.2 Interior Aerosol Bimodal Distributions

The particle size distributions for the retrospective and prospective scenarios as described by the bimodal AMAD are summarized in Table 6.41. A more extensive summary, along with their respective GSD and R^2 values, is listed in Appendix G. The AMADs that are much larger or smaller than the rest are considered suspect and are shown in parentheses following the AMAD.

Table 6.41. Interior Particle Size Distributions—Bimodal AMADs

Shot Description	Time Increment	AMAD, μm	
		First Peak	Second Peak
Retrospective Scenarios			
• Abrams—crossing hull (through turret)	First 10 sec	0.34 to 0.45	6.21 to 7.79
	1.1 min	0.11 to 0.75	2.22 to 3.98
	7.5 min	0.63 to 1.03	1.52 to 9.27
	16 min	0.76 to 0.83	2.86 to 4.78
	65 min	0.37 to 0.54	1.80 to 3.91
• Bradley—passenger compartment—double shot	Shot 1: First 10 sec	0.35 to 1.01	2.35 to 19.8
	3.5 min	0.34 to 0.41	2.97 to 3.41
	10 min	0.59 to 3.91	3.05 to 5.33
	Shot 2: First 10 sec	0.31 to 0.65	4.46 to 8.09
	3.5 min	0.47 to 0.61	1.78 to 5.74
	10 min	0.53 to 0.63	4.11 to 6.55
	49 min	0.33 to 0.62	1.46 to 4.46
• Bradley—turret shot	First 10 sec	0.35 to 3.76	11.9 to 20.9
	1.1 min	0.33 to 1.16	3.95 to 19.4
	7.5 min	0.27 to 0.46	0.67 to 3.11
	16 min	0.33 to 0.53	1.41 to 4.05
	65 min	0.36 to 0.54	2.97 to 5.65
Prospective Scenarios			
• Abrams—crossing turret	First 15 sec	0.31 to 0.51	5.10 to 11.24
	First 30 sec	0.27 to 0.51	3.97 to 5.68
	0.75 min	0.26 to 0.43	4.53 to 9.88
	1 min	0.38 to 0.43	4.79 to 7.70
	4.5 min	0.24 to 0.60	2.42 to 5.90
	5.5 min	0.49 to 0.64	3.84 to 5.07
	9.5 min	0.40 to 0.65	2.79 to 4.12
	11.5 min	0.49 to 0.76	3.89 to 5.47
	47.5 min	0.28 to 0.43	3.17 to 4.74
	55.5 min	0.33 to 0.50	3.68 to 4.43
• Abrams—crossing turret—double shot	Shot 1: First 10 sec	0.20 to 0.31	1.26 to 3.74
	3.25 min	0.63 (G)	3.10 to 4.88
	9.5 min	0.67 to 1.36	4.12 to 4.81
	Shot 2: First 10 sec	0.34 to 0.52	9.03 to 18.7
	3.25 min	0.58 to 2.56	10.18 to 14.7
	9.5 min	0.56 to 2.43	5.57 to 6.37
	47 min	0.49 to 0.72	4.20 to 7.84
• Abrams—turret into breech	First 10 sec	0.40 to 0.55	1.55 to 11.2
	1.1 min	0.50 to 0.75	5.71 to 8.49
	7.3 min	0.56 to 1.62	4.00 to 5.75
	15.5 min	0.13 to 0.71	2.19 to 6.54
	63 min	0.26 to 0.56	3.77 to 5.76 (16.6)
• Abrams—into DU armor	First 10 sec	0.29 to 2.94	4.13 to 14.5
	1.1 min	0.01 to 1.22	(0.006 to 40.4)
	7.5 min	0.64 to 1.38	3.88 to 4.28 (13.5, 37.0)
	16 min	0.51 to 0.76 (13.3)	2.36 to 6.03 (40.7)
	65 min	0.46 to 0.81	1.98 to 2.88 (70.1)

These data are rather inconsistent. With the exception of the Abrams tank double shot through the turret (PI-3/4), which has an erratic size pattern, the upper end of the second peak range decreases with time. However, the range in the first peak is rather stable, remaining essentially constant through the full sampling time. As with the unimodal AMADs, the second peak for the Abrams tank DU armor shot did not accurately represent the particle size distribution.

Aerosols collected during recovery activities, which began several hours post impact, included those still suspended from the perforating event and previously deposited material resuspended by the mechanical turbulence of entering, exiting, and performing recovery tasks within the turret (PI-6 and PI-7). In addition to the samplers inside the vehicle, two recovery personnel were outfitted with a closed-face Marple CI. Concentration results of these are provided in Appendix A, Table A.41, but these data were not analyzed for particle size distribution. The unimodal AMADs provided poor fits of the data for each sample collected. The bimodal provided better fits and are summarized in Table 6.42.

Table 6.42. Recovery Activities Particle Size Distribution—Bimodal AMADs

Activity	Time Increment	AMAD (µm)	
		First Peak	Second Peak
PI-6 (Beginning 2 h and 35 min post shot)			
Baseline	0 to 20 min	0.53	5.32
Recovery Activities	20 to 92 min	0.50 to 2.33	1.95 to 22.2
No activity	92 to 94 min	0.61	3.55
No activity	94 to 98 min	0.44	10.1
No activity	98 to 106 min	0.46	10.2
No activity	106 to 122 min	1.24	26.9
PI-7 (Beginning 3 h and 21 min post shot)			
Baseline	0 to 20 min	1.59	5.47
Recovery Activities	20 to 60 min	0.03 to >1000	1.09 to 17.5
No activity	60 to 69.7 min	0.30	3.87

The bimodal AMAD of the initial PI-6 sample was a reasonable fit with an R^2 of 0.92. Though better than the unimodal fits, the fits of the bimodal AMADs of the remaining PI-6 recovery samples including those collected after activities had ceased were inconsistent and showed no discernible pattern. Most of the second peaks were large (10 to 27 µm).

The bimodal AMADs of the PI-7 recovery samples collected before entry and after activities had ceased were reasonably good fits (R^2 of 0.92 and 0.98, respectively). The two samples collected during entry had very poor fits (R^2 of 0.21 and 0.04).

6.2.2.3 External Aerosol Unimodal and Bimodal Distributions

Aerosols outside the target vehicles but within the Superbox were collected on Andersen CI substrates for shots beginning with PI-5. The samplers ran for 2 min (with the exception of PIII-2, Sampler 2), and the aerosols were evaluated for particle size distribution. Unimodal and bimodal AMAD values are listed in Appendix B and by scenario in Table 6.43. The unimodal results range from 1.0 to 9.0 µm, and the PII-1/2 had the highest minimum and maximum values. In the bimodal data, the lower value in the first peak was very consistent, ranging from 0.16 to 0.25 µm. The upper end was less consistent with results ranging from 0.28 to 1.97 µm. The AMAD values in the second peak were high, ranging from a low of 2.93 µm to a high of 30.1 µm.

Table 6.43. Exterior Aerosol Particle Size Distributions by Scenario

Shot Description	Unimodal AMAD (μm)	Bimodal AMAD (μm)	
		First Peak	Second Peak
Retrospective Scenarios			
• Abrams—crossing hull (through turret)	1.5 to 6.0	0.18 to 0.28	11.8 to 21.4
• Bradley—passenger compartment—double shot	4.0 to 9.0	0.25 to 1.13	9.01 to 12.7
• Bradley—turret shot	~2.0	0.23 to 0.34	17.6 to 26.8
Prospective Scenarios			
• Abrams—turret into breech	1.0 to 8.0	0.16 to 1.97	2.93 to 11.6
• Abrams—into DU armor	1.5 to 7.0	0.17 to 0.42	7.76 to 30.1

6.3 Deposited Particulate Matter

Deposited particulate matter was collected inside and outside the target vehicles using wipe surveys and deposition trays. The deposition trays were limited to four inside, two on the vehicles' exterior horizontal surfaces, and two on the floor on either side of the vehicle. Additionally, selected members of the recovery crew wore cotton gloves during sample recovery operations, and the uranium adhering to the gloves was measured to estimate the potential surface-to-hand transfer that could lead to hand-to-mouth transfer. The data from each type of sample collected are presented for both the retrospective and prospective scenarios.

6.3.1 Wipe-Test Surveys

Wipe-test surveys to determine removable contamination were collected before and after each shot (or double shot). The wipe tests from PI-2, PI-5, and PI-6 were cross-contaminated and were not analyzed. Average removable uranium masses (with the background count subtracted) of the remaining shots are summarized in Table 6.44. These masses are listed for the interior surfaces and the exterior surfaces and are rounded to two significant figures.

Table 6.44. Removable Uranium Mass from Vehicle Surfaces

Shot Description	U Mass (μg/100 cm^2)	
	Interior Surfaces	Exterior Surfaces
Retrospective Scenarios		
• Abrams—crossing hull (through turret)	2500	1400
• Bradley—passenger compartment—double shot	1400	1100
• Bradley—turret shot	530	3100
Prospective Scenarios		
• Abrams—crossing turret	3000	1100
• Abrams—crossing turret—double shot	7000	3800
• Abrams—turret into breech	--	1800
• Abrams—into DU armor (PIII)	8600	1700
• Abrams—into DU armor (PIV)	1200	350

6.3.2 Deposition Trays

Deposition trays were positioned inside the vehicles (four trays), on their exterior horizontal surfaces (two trays), and on the floor on either side of the vehicles (two trays). These trays consisted of 100 cm^2 of flat surface area and approximately 60 cm^2 of 45° beveled surface area. Ranges of masses for these positions, which are limited particularly for exterior samples, are summarized by scenario in Table 6.45. Deposition was not uniform, and the pattern most likely depends on the shot line and the dispersion of random fragments. As expected, the largest mass of uranium collected inside the target resulted from the shots into the breech (PI-5 and PI-6) and the shots through DU armor (PIII-1 and PIII-2). However, it should be noted that the mass collected on the four deposition trays for each of these shots was notably non-uniform.

Table 6.45. Uranium Mass Collected on Deposition Trays

Shot Description	U Mass (mg/deposition tray)		
	In Crew Compartments	On Vehicle Surface	On Floor Nearby
Retrospective Scenarios			
• Abrams—crossing hull (through turret)	79 to 258	1.95 to 62.5	16.6 to 32
• Bradley—passenger compartment—double shot	10.8 to 45.1	8.07 to 18.1	30.4 to 234
• Bradley—turret shot	4.26 to 14.3	17.5 to 34.9	19.3 to 45.3
Prospective Scenarios			
• Abrams—crossing turret	29.7 to 442	9.16 to 28.0	9.05 to 79
• Abrams—crossing turret—double shot	18.8 to 648	45.4 to 50.8	50.8 to 93.4
• Abrams—turret into breech	15.1 to 853	3.9 to 29.0	11 to 65.4
• Abrams—into DU armor	3.83 to 3460	3.77 to 28.8	6.45 to 534

6.3.3 Gloves

The extent of DU surface contamination from vehicle to hands depends on the deposited material present, the activities being conducted, and the exposure durations. The use of cotton gloves and their subsequent analysis for uranium provide data for evaluating surface-to-hand transfer or hand-to-mouth transfer. The range of uranium masses collected on gloves for Phases I, III, and IV is presented in Table 6.46 by shot line. No gloves were analyzed from the Bradley vehicle shots. The final entry in the table (Abrams tank—shot fired into DU armor) includes gloves from tests PIII-2 and PIV-4. The uranium mass on the gloves is related not only to the quantity of aerosol deposited on vehicle surfaces, but also to the activities performed and the length of time and movement involved in those activities. As a consequence, the results of the different phases and shots are not directly comparable.

Table 6.46. Uranium Mass Collected on Cotton Gloves

Prospective Scenarios	Range of U Mass (mg)
• Abrams—crossing turret	3 to 64
• Abrams—turret into breech	19 to 198
• Abrams—into DU armor	4 to 127

6.4 Aerosol Composition

Aerosols were evaluated for their uranium content, the other predominant metals present, uranium oxide phases, particle morphology, and *in vitro* dissolution. An explanation of the data is provided below. For all but the particle morphology section, the data are presented for both the retrospective and prospective scenarios in other sections within this chapter.

The composition of the aerosols was evaluated almost exclusively using the cyclone residue samples and the backup filters. This approach ensured sufficient sample material for various analyses. Because the cyclones operated for the 2-h interval post shot, the residues are an integrated sample for that period of time. (An analysis of changes in the concentrations of other metals over time is outside the scope of this report.) The cyclone samples analyzed were from the following shots: PI-3/4, PI-7, PII-1/2, and PIII-2.

6.4.1 Uranium Content

The uranium content was analyzed using radiological counting and the chemical methods ICP-MS, KPA, and ICP-AES. Agreement among the chemical analyses was good with a relative standard deviation of 9%. Cyclone residue samples prepared for ICP-MS analysis were digested in a solution of HNO_3/HF that dissolved all or almost all the mass of each sample. Cyclone residue and backup filter samples prepared for KPA and ICP-AES analysis were digested in a solution of HNO_3/HCl that apparently dissolved nearly all the uranium, but did not completely dissolve the total sample mass.

The ICP-MS results were used to adjust gamma spectrometry results as discussed in Section 5.6.1. The results from the chemical analyses, where available, were used preferentially in data analysis because they are believed to be more accurate.

Table 6.47 lists the minimum and maximum uranium mass percentages of each total sample mass for the cyclone residues by scenario and by stage based on the three separate chemical analyses. The backup filter results are based on the average of the KPA and ICP-AES analyses.

As expected, the percentage of uranium in the total aerosol mass generated by the Abrams tank shots was larger than in the Bradley vehicle shots. Although there were some differences in the results both by chemical process and by stage, the uranium values for each scenario are relatively constant. They appear to decline slightly by stage in the Abrams tank (non-DU armor) shots and increase slightly in the Bradley vehicle shots. The aerosols from the Abrams tank DU-armor shot contained the most uranium.

For comparison with the cyclone residues, the uranium composition of the DU cone sample was 82%, and it contained no undissolved residue following HNO_3/HCl digestion.

Table 6.47. Uranium Mass Percentages in Cyclone Aerosols by Scenario

Scenario	Stage	Uranium Mass Percentage	
		Minimum	Maximum
Retrospective			
• Abrams—crossing hull (through turret)	1	50.3	54.1
	2	47.7	51.3
	3	45.3	50.0
	4	42.4	49.2
	5	40.3	49.5
	Backup Filter	38.3	39.7
• Bradley—passenger compartment—double shot	1	18.4	22.3
	2	23.6	25.9
	3	23.0	28.5
	4	24.7	27.7
	5	21.7	27.7
	Backup Filter	25.9	27.0
Prospective			
• Abrams—crossing turret—double shot	1	62.3	72.0
	2	57.4	58.8
	3	52.7	62.7
	4	54.8	56.3
	5	47.8	52.7
	Backup Filter	43.4	44.3
• Abrams—into DU armor	1	59.7	65.4
	4	63.6	69.9
	5	62.9	71.5
	Backup Filter	62.0	65.2

6.4.2 Other Metals Content

The composition of the aerosol mass that did not consist of uranium was composed mostly of other metals and oxygen in the form of metal oxides. Next to uranium, the primary metals present in the aerosols were aluminum and iron. Titanium (alloyed to the DU in the penetrator), zinc, and copper were next highest in concentration. Very small or trace levels of chromium, manganese, nickel, barium, cadmium, magnesium, lead, tin, and strontium were present in some or most of the samples, and silicon was a frequent contaminant. Percentages of aluminum, iron, and titanium in the cyclone residues are presented in Table 6.48 based on analysis of ICP-MS (HNO_3/HCl/HF digestion) and ICP-AES (HNO_3/HCl digestion). Because different techniques were used, the measured concentrations numbers were not identical, and in fact, the differences are large, presumably due primarily to the residue of undissolved aerosol that occurred in the absence of HF digestion. The lower and higher of the two results are shown as a range for aluminum, iron, and titanium. The data are presented by scenario and are rounded to two significant figures.

The sums of the masses of uranium and of the metals shown in Tables 6.47 and 6.48 is less than 100% for each stage. The residue difference in total mass is attributed to the presence of oxygen because most of these materials contained oxides (as determined by SEM/EDS) rather than pure metals. (With PII-1/2, the spall liner fibers made of carbon, hydrogen, oxygen, and nitrogen contributed to the overall mass, although few fibers were observed in samples examined by SEM). For comparison, the DU cone sample contained 82% uranium, <0.03% aluminum, 0.28% iron, and 0.29% titanium. Pure U_3O_8 is approximately 85% uranium and 15% oxygen.

Table 6.48. Mass Percentages of Non-DU Metals in Cyclone Aerosols by Scenario

Scenario	Stage	Aluminum, Mass %	Iron, Mass %	Titanium, Mass %
Retrospective Scenarios				
• Abrams—crossing hull (through turret)	1	4.0 to 11	4.7 to 6.4	0.64 to 1.2
	2	5.7 to 12	3.7 to 5.5	0.55 to 0.95
	3	7.7 to 13	3.4 to 7.3	0.47 to 0.70
	4	8.9 to 15	3.2 to 5.9	0.40 to 0.64
	5	8.3 to 16	3.0 to 5.8	0.33 to 0.53
	Backup Filter	6.3	2.8	0.29
• Bradley—passenger compartment—double shot	1	5.5 to 18	2.9 to 5.0	0.39 to 1.3
	2	6.2 to 20	1.9 to 4.2	0.41 to 1.3
	3	6.2 to 24	1.4 to 1.7	0.37 to 1.1
	4	7.7 to 23	1.2 to 2.8	0.33 to 0.76
	5	7.3 to 24	1.1 to 3.0	0.23 to 0.50
	Backup Filter	12	1.9	0.23
Prospective Scenarios				
• Abrams—crossing turret—double shot	1	1.5 to 10	1.1 to 4.5	0.62 to 2.2
	2	3.7 to 7.8	5.5 to 10	0.66 to 1.1
	3	3.6 to 8.7	4.1 to 7.3	0.54 to 1.1
	4	4.4 to 8.9	3.8 to 4.9	0.53 to 1.1
	5	5.1 to 12	3.2 to 5.8	0.41 to 0.63
	Backup Filter	3.8	2.5	0.36
• Abrams—into DU armor	1	1.6	6.9	0.58
	4	2.1	4.9	0.55
	5	2.2	4.2	0.55
	Backup Filter	2.6	3.4	0.48

6.4.3 Uranium Oxide Characterization

Uranium oxidation at high temperature (and with no water or at low water vapor) progresses according to the following sequence of progressively oxidized products (Levin et al. 1975; Taylor et al. 1993):

$$\text{U metal} \Rightarrow UO_2 \Rightarrow U_4O_9 \Rightarrow U_3O_8 \Rightarrow UO_3.$$

Other stoichiometric forms exist in the form of $UO_{2.x}$. Uranium in UO_2 is in the +4 valence state, and its rate of aqueous dissolution is slow in *in vitro* dissolution studies relative to other uranium oxides. On the opposite (heavily oxidized) end, uranium in UO_3 is in the +6 valence state and is relatively more soluble than UO_2 in biological fluids. The intermediate stoichiometric oxides contain uranium in a combination of these two valence states and show increasing solubility as their oxygen-to-uranium content increases. With prolonged exposure to certain natural environments, UO_3 may react to form schoepite. Schoepite (commonly $UO_3 \cdot 2H_2O$ or $UO_3 \cdot 2.25H_2O$) forms at ambient temperatures and in the presence of liquid water and/or water vapor. UO_3 is more stable at high partial pressures of oxygen and lower partial pressures of water relative to U_3O_8 and schoepite. Schoepite, a very stable form at ambient temperatures, becomes less stable and loses water with increasing temperature.

The aerosol samples created from the Capstone tests were formed at high temperature. The XRD analysis of the aerosol samples established that these uranium aerosols contained a complicated collection of uranium oxidation products. The oxidation products identified appear to be reasonable relative to those that should have formed in the high temperature environment of these impacts. Predominantly U_3O_8/UO_3, there also was a significant concentration of U_4O_9, an intermediate uranium oxidation product between UO_2 and U_3O_8 in the aerosols. A small amount of schoepite was detected in cyclone backup filter samples and in several cyclone residues, with the largest concentration found in the MVF sample. The length of storage time (7 to 9 months) is believed to have had only a minor impact on the oxidation phases of these samples, in part because they were maintained under an inert atmosphere for ultimate storage. No uranium metal or UO_2 was detected by the XRD analysis.

A high incidence of overlap in the major peaks of UO_3 and U_3O_8 prevented XRD pattern discrimination of these two phases. Additionally, small amounts of other phases were present but could not be identified by match searches using the ICSD XRD database.

The U_4O_9:U_3O_8 ratio varied with phase and particle size. For each shot phase, the weight percentage of U_4O_9 decreased with stage as the percentage of U_3O_8 increased. The initial U_4O_9:U_3O_8 ratio (Stages 1 and 2) was highest for Phase II, intermediate in Phase III (for the Stage 1 sample only, the amount of sample from Stage 2 was insufficient for analysis), and lowest in Phase I. In Phases II and III, the U_4O_9 concentration was higher than the U_3O_8. The ratios of the backup filters showed that almost all of the uranium oxide collected in these samples was U_3O_8 (or a combination of U_3O_8 and UO_3). The DU cone sample contained about 96% U_3O_8/UO_3 based on XRD analysis, and the rest was U_4O_9. These various oxide phases probably resulted from differences in temperature histories of the particles.

6.4.4 Uranium Morphology and Formation

Although an assessment of the mechanisms of aerosol particle formation is outside the scope of this report, some speculation may be useful. Based on the observed morphology and composition of aerosol particles collected in the various shots, it appears that there are several mechanisms that affected the formation of the particles as well as their ultimate appearance when collected. Because the initial aerosol cloud was created under highly energetic conditions and at very high mass concentrations, there was ample opportunity for initially formed particles to coagulate as they came in contact with other similar or dissimilar particles in the cloud. The heterogeneous structure of particles seen in the electron micrographs supports this hypothesis.

The question of aerosol vaporization/condensation versus liquid aerosol droplet formation is complicated because of the variety of elements contributing to the composition of the aerosol particles. The spherical uranium particles observed microscopically, particularly those in the submicrometer size range, appear to have formed by liquid droplet aerosolization. On the other hand, the presence of low-density, branched-chain, aggregate aerosols indicates that vaporization/condensation also was occurring, probably simultaneously with liquid droplet formation, as evidenced by the presence of aerosols consisting of both types of particles (Appendix D, Figure D.13, view b). There were a few particles that appear to have melted components that cooled slowly enough to support formation of crystal grains. In other particles, grains appeared without appearing to have been melted. Generally, the different shapes also seem to indicate that the samples cooled at different rates, thereby forming a variety of shapes and combinations of elements.

The observations described above indicate the importance of temperature history in the formation of aerosol particles. This study collected no temperature data relevant to the site of aerosol formation (i.e., the penetrator-metal interface), so the actual temperatures involved were not characterized. In any case, however, it is reasonable to assume that the time during which high temperatures applied to the forming aerosol particles was probably brief (i.e., on the order of seconds). Consider that the melting points of aluminum, iron, and uranium metals are 660°C, 1538°C, and 1135°C, respectively, and that the EDS analysis of the aerosol particles indicates that all three metals were found associated with droplet-type or melt particles. This suggests that the penetrator-metal temperature was greater than 1500°C, though the melting points of mixtures of metals may be lower than the melting points of the pure metals. On the other hand, the boiling points of aluminum, iron, and uranium are 2519°C, 2861°C, and about 4131°C, respectively (CRC 2001). Because there was no clear evidence in the many SEM micrographs analyzed that the DU had vaporized, one can surmise that the maximum DU-metal temperature was less than 4000°C. Additionally, metallic droplet dispersion by energetic impact from a projectile could result from much lower temperatures, approximately 1200 to 1400°C (above the melting temperature of uranium) rather than the nearly 3000°C needed to melt UO_2. However, the temperature potentially was in the range of 3000°C because a significant amount of aluminum is believed to have vaporized, along with some iron, although the latter is more difficult to quantify.

Additional SEM/EDS analysis may help to further elucidate the temperatures reached and the mechanisms responsible for particle formation. Ultramicrotomy sectioning of particles may allow SEM/EDS analysis of whether some of the particles observed actually consisted of metallic cores with a surface coating of oxide.

From the perspective of the future needs of the dose/risk assessor, knowledge of how the DU aerosols were formed is useful. For example, the lack of vaporization/condensation aerosols is important in modeling the deposition and dissolution/retention of the inhaled DU-containing aerosols, because this particle size range need not be considered. Second, the extreme heterogeneity of the aerosol particles also presents a difficulty in interpreting the particle-size-specific data, particularly the relationship between particle size and solubility. In this case, the two parameters are likely to be only weakly related, which is not the case with more uniform particles.

6.4.5 Uranium *In Vitro* Dissolution

General trends were identified in the *in vitro* dissolution data (e.g., increasing dissolution with decreasing particle size), although the results also demonstrated distinct variability that is likely due to the heterogeneity of the aerosol particles. The solubility functions of the samples most closely resembled the Type-M absorption behavior except for the backup filter in PI-3/4-CY, which resembled Type-S behavior. Categorization based on the Class D, W, and Y clearance model showed more variance. Although more than half of each sample fit the Class-Y category, the percentages of Classes D and W varied significantly. The ICRP clearance classes are summarized by scenario to two significant figures in Table 6.49. (Rounding error accounts for >100% in some samples.)

Table 6.49. Clearance Classes in Cyclone Aerosols by Scenario

Shot Description	Stage	ICRP-30 Clearance Class, %		
		D	W	Y
Retrospective Scenarios				
• Abrams—crossing hull (through turret)	1	35	--	65
	2	15	--	85
	3	31	--	69
	4	31	--	69
	5	32	--	69
	Backup Filter	13	--	87
• Bradley—passenger compartment—double shot	2	22	--	78
	3	21	--	89
	4	26	17	58
	5	26	11	63
	Backup Filter	14	9	77
Prospective Scenarios				
• Abrams—crossing turret—double shot	2	16	--	84
	3	36	--	64
	4	20	21	59
	5	29	--	71
	Backup Filter	1.0	--	99
• Abrams—into DU armor	4	3	7	90
	5	5	--	95
	Backup Filter	10	5	85

For comparison, the size-separated (respirable fraction) of the DU cone sample contained 7% of Class-D material and 93% of Class-Y material. The DU cone sample that was not size-separated to eliminate non-respirable large particles exhibited Type-S behavior and contained 98.6% Class-Y material and 1.4% Class-D material. The team speculates that this cone sample is more characteristic of DU that oxidizes in a fire rather than from impact.

In terms of particle size effects on solubility, few consistent trends were noted. Although some cyclone stages with smaller particles showed greater solubility with decreasing size, particularly in the short term (e.g., Stages 2 and 3 [PI-3/4, PI-7], Stages 3 and 4 [PII-1/2]), a grouping of results into more or less soluble classes (e.g., PI-3/4, PI-7, PII-1/2) was more common. Of interest was the finding that some of the cyclone backup filters that contained the smallest particles had the least solubility. This was particularly the case for the backup filters (PI-3/4, PI-7, PII-1/2).

This observation is reminiscent of a similar observation by co-author, R. A. Guilmette, whereby the smaller size particles of plutonium-239 dioxide ($^{239}PuO_2$) particles, another actinide aerosol, were sometimes less soluble than larger sizes, which is the inverse of what is expected based on considering specific surface area as the principal determinant of dissolution rate (all other factors [i.e., the chemical form, particle shape and density] being equal). This was attributed to the manner in which the $^{239}PuO_2$ was produced (i.e., by "flash oxidation" as $Pu(OH)_4$ colloidal droplets passed through a 1100°C tube furnace [about 1 m long] in less than 30 sec). This temperature treatment, being surmised to be too brief

to establish equilibrium temperature conditions within the aerosol droplet, resulted in different temperature histories in particles of different sizes, with smaller particles receiving a "better" heat treatment. Kanapilly and Diel (1980) noted comparable less-than-expected solubility behavior when they measured the solubility and biokinetics of an ultrafine aerosol of $^{239}PuO_2$. This mechanism may be relevant to the DU aerosol formation associated with DU-armor interactions. In this case, nonequilibrium temperatures were also likely to be the case, and the temperature history may also have been related to the size/mass of the nebulized droplet. Thus the particle-size-related results in this study appear to be credible.

In comparing aerosols obtained as a result of different DU-target interactions, the most significant difference seen was the smaller solubility of the aerosol resulting from DU-DU interaction in PIII-2 (Figure E.37) than occurred as a result of DU interaction with conventional Abrams tank (PI) or Bradley vehicle (PII) armor. For the PI and PII cases, no consistent differences were seen when comparing the same cyclone stage (equivalent aerodynamic particle size). For example, Stage 2 data from PII showed lower solubility than PI results, but for Stage 3 the solubility was greater. This difference may be related to the relative fraction of non-DU materials collected on the respective stages, recognizing that the DU fractions for PII samples were much lower than for PI or PIII samples.

In general, most of the samples analyzed showed at least biphasic dissolution patterns, with the first or fastest component having dissolution half-times <1 day and the second component (or third depending on whether 2 or 3 components were fitted) with half-times on the order of hundreds of days. The relative amounts associated with the different phases are a significant source of uncertainty given that there did not appear to be many unifying principles that could explain the differences. It is clear that convolution of the particle-size-specific results to obtain overall behavior of the inhaled aerosols will be an important part of a sensitivity analysis that is recommended to be performed as a part of follow-on during human health risk assessment.

6.5 Ventilation Rates

The results of the studies in which ventilation rates of intact vehicles were measured are difficult to understand, especially with the results measured from post-perforation artifacts in the Abrams BHT during the various DU impact studies. Nevertheless, these data may be useful to the exposure/dose assessors as long as they recognize that the conditions under which the DU tests were conducted were conservative (i.e., decreased amount of interior surface area, absence of ventilation and/or fire suppression). These differences will need to be taken into account in scaling the results of these studies to more realistic exposure scenarios for the crew members of Abrams tanks and Bradley vehicles.

7.0 Conclusions

The Capstone DU Aerosol Study was designed to develop a source of aerosol information specific to DU aerosols created by the perforation of armored combat vehicles by DU munitions. This study focused on the collection and analyses of aerosols and particles inside and, to a lesser extent, outside selected vehicles struck by large-caliber (LC), kinetic-energy DU penetrators. The firing tests used to generate aerosol replicated, as closely as circumstances permitted, retrospective scenarios from firing incidences in the Gulf War/ODS and probable prospective scenarios that could occur in future actions. An extensive database of aerosol concentrations, particle size distributions, and surface contamination has been generated over the course of the Capstone tests. These data were analyzed, and their results were grouped by scenario for use as input to exposure assessments. Scientists and engineers will use this information to assess human health risk associated with probable or projected exposure levels to U.S. DoD personnel potentially exposed to DU particulate matter during combat or recovery activities.

The information resulting from the study will be used to determine if health risks to personnel are high enough to warrant changes in the medical policy, medical treatment and monitoring practices, and in personnel protective measures for DoD personnel potentially exposed to DU 1) in, on, or near an armored vehicle, at the time the crew compartment is perforated by DU munitions; 2) by entering (without protective clothing) a perforated armored vehicle immediately after the perforation; or 3) by entering (without protective clothing) an armored vehicle well after the vehicle is perforated by DU munitions.

7.1 Field Testing, Equipment, and Observations

The field portion of the study was conducted in four phases at the Army's Superbox facility at the Aberdeen Test Center (ATC). Vehicle configurations and shot lines were varied in the four phases, which included:

- Phase I (PI) in which seven shots were fired at an Abrams tank ballistic hull and turret (BHT) equipped with conventional, non-DU armor. **No ventilation systems were present in the BHTs**.

- Phase II (PII) in which three shots were fired at a Bradley vehicle BHT. **No ventilation systems were present in the BHTs**.

- Phase III (PIII) in which two shots were fired directly into the DU-armor package of an Abrams BHT. **No ventilation systems were present in the BHTs.**

- Phase IV in which four shots were fired at an operational M1A2 Abrams Main Battle Tank. The Phase-IV samples were collected as part another study known as the Abrams Live-Fire tests. The scope of the Live-Fire tests was different from that of the Capstone study, and space restrictions allowed only a minimum of aerosol sampling. A second and very important difference with the Phase-IV series was that the target tank's environmental control/nuclear, biological, chemical (EC/NBC) **ventilation system was operating during and after the shots.**

Generalizations of results from the field portion of the four test phases include the following:

During the Phase-I through -III field tests, LC-DU munitions were successfully fired at an Abrams BHT (through conventional and DU armor) and at a Bradley BHT, and DU aerosols were generated. These BHTs were not equipped with ventilation systems. Test conditions were imposed to simulate Gulf War/ODS incidents in which armored vehicles were perforated. Shots also were fired to simulate possible future incidents in which higher aerosol concentrations in crew compartments would be expected.

- During the Phase-IV Live-Fire tests, a LC-DU cartridge was successfully fired at a fully operational Abrams tank, in which its ventilation system was operating. The LC-DU cartridge was loaded to perforate the vehicle's DU armor. This test simulates a possible future incident in which aerosols may be generated from the DU munition and from the DU armor.

- Instrumentation selected to collect aerosols inside the target vehicles was essentially off-the-shelf equipment chosen for its sensitivity, ruggedness, and availability. Sampling arrays that paired filter cassettes with cascade impactors (CIs) for eight separate sampling times were an effective means of containing and operating the samplers. Quick-disconnect stems facilitated sampler insertion and removal. The cyclone collected aerosols over a longer time period in sufficient quantities for physical and chemical characterization and for qualitative size partitioning. In general, the samplers performed well under the adverse conditions in the tests.

- The sampling strategy, particularly regarding sampling duration, evolved over the course of the shots. Sampling durations and the starting and stopping times were evaluated after each shot and were changed as appropriate to collect sufficient samples without overloading the filters. Initially, one set of samplers was operating during the entire 2-h, post shot sampling period. For later shots, the sampler starting times relative to the shot time were similar, but the samplers ran for shorter durations.

- The moving filter (MVF) successfully collected aerosols immediately after impact on several of the shots before the other samplers could be operated. Use of the MVF provided a way of estimating the initial aerosol concentration immediately after impact and provided sufficient sample material for physical and chemical characterization for the shots during which it operated successfully. Various difficulties were encountered with using the MVF, including inadequate shielding of the sampler intake, that precluded obtaining samples for all shots.

- Sampler shielding evolved during the course of the program and generally was successful in protecting samplers from the violence and after-effects of each shot. A change in IOM filter cassette medium from Supor to Zefluor in the filter cassettes improved filter survivability.

- The use of the LabVIEW software package to program sampling times and monitor the air sampler pressure drops provided real-time indications of sampler operation and second-to-second flow rates (after establishing the correlation between pressure drop and flow rate).

- The Army's Superbox facility allowed target vehicles to be configured for aerosol sampling and sample recovery, so the facility was well suited for this type of test.

- Visual observation of the interior of the turret via high-speed videotape consistently showed that, immediately after perforation, the interior was illuminated by "fireflies" as the uranium particulate

matter created by erosion of the DU penetrator underwent spontaneous oxidation (burning). This phenomenon lasted about 1 sec. The atmosphere inside the vehicle was visually very dusty and cleared gradually.

- Recorded instantaneous pressure peaks inside the turret reached a maximum of 22 psig and lasted for milliseconds. This pressure pulse caused one or more secured vehicle hatches to open during all but one test shot. Open hatches and other smaller vehicle openings allowed aerosols to vent, thereby dispersing the turret aerosol to the atmosphere outside the vehicle.

- Ventilation measurements of the BHTs and operational vehicles under several conditions will enable risk assessors to scale the results to exposures scenarios.

7.2 Analysis of Samples

Uranium sample masses were derived from radioactivity measurements of the collected samples. Many samples underwent further chemical and physical characterization. Generalizations about sample analyses are provided below.

- All samples conducive to proportional counting were analyzed for alpha and beta activity by this technique. These samples included IOM filters, media and bottom filters from the CI samplers, MVF tape, diffusion battery filters, and wipe test samples. Samples that were too large or unwieldy for proportional counting were evaluated using gamma spectrometry. Sample types analyzed by gamma spectrometry included the cyclone residues, external Andersen CIs, gloves, and deposition tray debris. The radioanalytical data were used to determine the uranium content of the samples.

- Beta activity and gamma spectrometry measurements detect radiations from immediate short-lived progeny of uranium. An underlying assumption in these analyses is that uranium is in equilibrium with its immediate short-lived progeny. This assumption was tested and found to be incorrect for most sample types and particle sizes. Therefore, to ensure that the uranium in these aerosols was not underestimated, an analysis was undertaken to identify appropriate adjustment factors to relate the radioactivity measurements to the uranium mass. Samples that were analyzed by both radiological and chemical analytical techniques were used in the analysis to determine appropriate adjustment factors. The adjustment factors were then applied to the data sets.

- The particle size distributions from CI samples of interior and exterior aerosols were evaluated using SigmaPlot software and unimodal and bimodal activity median aerodynamic diameter (AMAD) models to characterize the distributions and variability.

- The residues from one cyclone for each scenario were characterized using physical and chemical methods. These analyses quantified its uranium content, its oxide composition, and *in vitro* solubility; examined the aerosol particle morphology; and provided a semi-quantitative evaluation of the non-DU metal composition.

Data for the parameters most critical to human health risk assessment were collected and analyzed as a part of this study. Additional data that may be useful to risk assessors were collected and reported.

7.3 Test Results

Aerosol concentrations, deposition, and particle size distributions for Phases I through IV were characterized and compared. Aerosol residues were analyzed for metals composition, oxidation phase, *in vitro* dissolution, and particle morphology.

7.3.1 DU Aerosol Concentrations

Aerosol concentrations inside the vehicles as a function of time were analyzed using samples collected immediately after perforation and at time intervals varying up to 2 h post shot. DU concentrations varied with shot and with crew position within the vehicle. Deposition occurred as particles settled on vehicle surfaces and some dispersed through open hatches or other structures. These mechanisms served to reduce the vehicle's internal aerosol concentration as demonstrated by the graphs of concentration versus time (presented in Section 5.1). A summary of the mean DU concentrations (time-standardized) as measured by the IOM filter cassettes (in grams per cubic meter [g/m^3]) by scenario are listed to two significant figures in Table 7.1. The IOM filter cassettes measured aerosol concentrations beginning 5 sec post shot and sampled periodically, typically in eight sequential time intervals.

Table 7.1. Mean DU Aerosol Concentrations Over Time

Shot Description	Mean DU Concentration (g/m^3)					
	10 sec	**30 sec**	**1 min**	**30 min**	**1 h**	**2 h**
Retrospective						
Abrams—crossing hull (through turret) (PI-7; no ventilation)	11	9.0	6.0	0.11	0.057	0.047
Bradley—turret and passenger comp't (PII-1, 2, and 3; no ventilation)	3.0	2.7	2.2	0.13	0.049	0.024
Prospective						
Abrams—crossing turret (PI-1, 2, 3, and 4; no ventilation)	8.8	7.9	5.7	0.15	0.064	--[(a)]
Abrams—crossing turret into breech (PI-5 and 6; no ventilation)	16	12	6.4	0.020[(b)]	0.029	0.019
Abrams—into DU armor (PIII-1 and 2; no ventilation)	10	7.9	4.2	0.049	0.017	0.013
Abrams—into DU armor (PIV-4; with ventilation)	0.092	0.14	0.22	0.011	--[(a)]	--[(a)]

(a) Averages not extrapolated past last sample.
(b) Samplers for both shots showed similar pattern in large reduction from 1 min; most 30 min DU concentrations were lower than at 1 h.

Some generalizations about the mean DU aerosol concentrations include the following:

- The highest DU aerosol concentrations occurred in the BHTs during the first sampling interval, which ranged from 10 to 30 sec. The highest mean concentrations representative of the retrospective scenarios were 11 g/m^3 for the Abrams BHT hull shot and 3.0 g/m^3 for the Bradley BHT shot. The Abrams level dropped by a factor of nearly 2 within 1 min, and the Bradley level dropped by a factor

of about 1.4 in 1 min. Within 30 min, these aerosol concentrations were reduced to 0.11 and 0.13 g/m^3, respectively. These relatively rapid initial drops in concentration reflect the high settling velocities corresponding to the large initial particles sizes present in the interior atmospheres of the Bradley and Abrams vehicles.

- Of the prospective scenarios, all of which involved Abrams BHTs, the highest mean DU aerosol concentration during the first sampling interval was 16 g/m^3, resulting from perforation of the Abrams through non-DU armor and through the breech. Within 1 min, the aerosol concentration had dropped by a factor of 2.5, and at 30 min, this aerosol concentration was reduced to <0.1 g/m^3. The other unventilated Abrams BHTs followed a similar pattern.

- The ventilated Abrams tank showed a different pattern in which there was an increase from 0.092 to 0.22 g/m^3 in concentration between the 10 sec sample and the 1 min sample, which then fell to about 0.011 g/m^3 within 30 min. The cause of this difference in behavior is probably due to a slower dispersion of aerosol into the driver's position where the surviving samplers were located.

- Sampling in conjunction with sample recovery activities was conducted after shots PI-6 (Abrams/breech) and PI-7 (Abrams/hull). The baseline DU aerosol concentration measured in the PI-6 at 2.5 h post shot before recovery activities began was 0.0030 g/m^3. The maximum concentration measured during recovery activities was 0.029 g/m^3. The baseline from PI-7 was 1.2E+03 g/m^3. Data from the two samples taken during recovery activities were lower than the baseline concentration for reasons that were not determined.

The MVF sampler measured aerosol during the first five seconds post shot and covered the time gap before the other samplers began operating. The sampler ran during PI-1, PI-3, PII-3, PIII-1, and PIII-2. A summary of the peak DU concentrations collected on the MVF within the first 10 sec is listed in Table 7.2. The similarity in the measured DU masses between the MVF and the filter cassette results suggests that the results in Table 7.1 for the first sampling interval are reasonable.

Table 7.2. MVF Peak DU Concentrations

Shot Description	MVP Peak U Concentration (g/m^3)
• Bradley—turret shot (PII-3)	1.1 at 7 sec
• Abrams—crossing turret (PI-1)	2.3 (total over 1st 5 sec)
• Abrams—crossing turret (PI-3)	6.0 at 13 sec
• Abrams—into DU armor (PIII-1)	8.2 at 7 sec
• Abrams—into DU armor (PIII-2)	9.1 at 1.4 sec

The highest uranium concentration measured by the MVF in the perforated Bradley BHT was 1.1 g/m^3 (1.1E+06 µg/ m^3), which occurred 7 sec post shot. The highest concentrations in a perforated Abrams BHT ranged from 2.3 to 6.0 g/m^3 in a vehicle without DU armor and 8.2 to 9.1 g/m^3 in a vehicle with DU armor. In each case for which MVF data were collected, the peak occurred within the first 13 sec post shot. Of the samples collected, the Bradley (PII-3) BHT shot had the lowest peak DU aerosol concentration, and the shots that perforated the Abrams with DU armor had the highest peak DU aerosol

concentration. The highest concentration measured in a Bradley BHT was a factor of eight lower than the highest concentration measured in an Abrams BHT with DU armor.

7.3.2 Particle Size Distributions

Interior and external particle size distributions were evaluated from aerosols collected using CIs. Aerosols inside the vehicle and their change over time beginning 5 sec post shot were collected using Marple CIs, and the resulting data were evaluated using unimodal and bimodal AMAD models. Particle size distributions varied with shot and with crew position within the vehicle. Andersen CI data were used to model aerosols collected outside the vehicle. Some generalizations about particle size distributions are provided below.

- As the larger particles deposited mostly by settling on vehicle surfaces, the AMAD values decreased with time. This is the expected behavior of aerosols for which a significant mass fraction is present initially as particles >10 μm AD. Some data were somewhat inconsistent, making generalizations difficult. More intensive data analysis is needed, although the results may simply reflect the complex physics and chemistry of the aerosols created. It is recommended that this analysis be performed during the updated human health risk assessment project. The data are summarized in Tables 5.4 and 5.5.

- Unimodal AMAD values were seldom adequate to describe the particle size distributions. Most often, the bimodal AMAD model appeared to better fit the data. However, there were other cases for which neither model provided adequate fits, mainly because most of the sample mass was measured within the largest size fraction, and very little mass was in the smaller particle fractions. In other cases, the particle size distribution was uniform (i.e., without mode).

- Exterior aerosols were collected beginning with PI-5 (Abrams/breech shot), and these samples were also evaluated using unimodal and bimodal AMAD models (Table 5.6). The unimodal AMAD values ranged from 1 to 9 μm. The bimodal first peak AMAD values ranged from 0.16 to 1.97 μm, and the second peak values ranged from 2.9 to 30 μm. Time-related changes in concentration and particle size could not be conducted because of equipment limitations. However, because the measured concentrations were substantially less than those measured within the armored vehicles, the data obtained should be amenable to conventional atmospheric dispersion modeling, so that exposures to DoD personnel outside the vehicles can be estimated.

- Particle size distributions were calculated from three PIV-4 CIs, and good fits from both the unimodal and bimodal models were obtained for the sample collected 1 min post shot. The unimodal AMAD was 0.62 μm, and the bimodal AMAD peaks occurred at 0.53 μm and 0.76 μm, suggesting that the aerosol particle size at the point was relatively small. The bimodal distribution for the 5-min time interval was a good fit, and the bimodal AMADs were 0.50 μm and 1.84 μm, respectively. Neither model fit the 25-min size distribution.

7.3.3 Surface-Deposited Material

Wipe surveys and deposition trays were used to evaluate removable contamination and deposited material, and cotton gloves worn over protective clothing by sampler recovery personnel were used to

develop a database that could be used in the evaluation of the levels of DU potentially available for hand-to-mouth transfer. The uranium collected on these media were quantified and summarized by phase and similar shot lines. Some generalizations about the data are the following:

- Wipes from the interior surfaces averaged by shot or similar shots ranged from a low of 0.53 mg/100 cm^2 for the Bradley BHT turret shot to a high of 8.6 mg/100 cm^2 for the Abrams BHT (with no ventilation) perforated through DU armor.

- Wipes from the exterior surfaces averaged by shot or similar shots ranged from a low of 0.35 mg/100 cm^2 in the Abrams tank (with ventilation) perforated through DU armor to 3.8 mg/100 cm^2.

- Deposition trays placed in the Bradley BHT collected between 4.3 and 45 mg/tray for the single and double shots. Trays placed in the Abrams BHT ranged from 3.8 to 3460 mg/tray and showed little uniformity.

- The uranium mass collected on the gloves (analyzed for the Abrams BHT/tank shots only) ranged from 3 to 198 mg and are believed to relate not only to the aerosol deposited on vehicle surfaces, but also to the activities performed and the length of time and movement involved in those activities.

7.3.4 Aerosol Composition and Characteristics

Cyclone residues were analyzed for their uranium content, content of other metals, uranium oxide phases, particle morphology and structure, and *in vitro* dissolution. Generalizations about these characteristics follow:

- The percentages of uranium mass in the total mass of collected aerosol present in the cyclone samples (based on the combined results of three separate chemical analyses) varied as follows:

  - 38 to 54% in the PI-7 shot (Abrams BHT/hull, conventional armor)
  - 43 to 72% in the PI-3/4 shot (Abrams BHT/turret shots, conventional armor)
  - 60 to 72% in the PIII-2 shot (Abrams BHT/turret shot, DU armor)
  - 18 to 29% in the PII-1/2 shot (Bradley BHT/passenger compartment shots).

- The percentages of uranium mass in the total cyclone mass varied by stage, but this variation was not consistent. It is not clear whether the reductions in uranium percentages are due to decreasing relative amounts of DU or increasing amounts of the other metals. The percentages present may be related to the mechanisms of aerosol formation. General results were the following (based on the combined chemical results):

  - With the Abrams BHT/non-DU armor shots (PI-3/4), the uranium mass generally decreased with stage from a high of 72% on Stage 1 to a low of 48% on Stage 5. The uranium mass in the backup filter was about 44%.

  - With the Abrams BHT/hull shot (PI-7), the uranium mass ranged from a maximum of 54% on Stage 1 to a minimum of 40% on Stage 5. The backup-filter mass was about 39%.

- With the Bradley BHT/double shot (PII-1/2), the uranium mass was the lowest on Stage 1 (18%) and remained relatively constant for Stage 2 through 5 (from 22 to 29%) and the backup filter.

- With the Abrams BHT/DU armor shot, in which insufficient material was collected on Stages 2 and 3 for analysis, the uranium masses on the stages and backup filter ranged from 60 to 72%.

- The other metals present in the aerosol consisted primarily of aluminum and iron. Aluminum varied the most by phase and was highest in Phase-II samples and lowest in Phase-III samples. Other major constituents included iron, titanium (alloyed to DU in the penetrator), zinc, and copper.

- Several oxidation phases were found in the uranium aerosol residues. The predominant phase consisted of U_3O_8/UO_3, believed to be primarily hyperstoichometric forms of U_3O_8. Its presence increased as particle size decreased while the percentage of U_4O_9, which was highest with the large particles, decreased as particle size decreased. A small amount of schoepite was detected in several cyclone stages and in backup filter samples.

- The particles obtained from the cyclone residues have a complex, heterogeneous structure. The uranium particles displayed many different shapes from spherical to granular and fractured structures.

- The *in vitro* dissolution rates of the cyclone residues tended to increase with decreasing particle size, but there was variability in the results, believed to be caused by the particle heterogeneity. The samples had dissolution rates that most closely resembled Type-M absorption behavior with the exception of one backup filter, which resembled Type-S behavior. More than half of each sample (about 58 to 99%) fit the Class-Y clearance category of ICRP 30. In most cases, the remaining percentage fit the Class-D category, but Class-W behavior was present in the range of 9 to 17% for three Phase-II samples, 5 to 7% in two Phase-III samples, and 21% in one Phase-I sample. In any case, the evidence indicates that variable fractions (up to 40%) of the inhalable DU particles were relatively soluble.

Studying the mechanisms of DU particle formation was not part of the Capstone project scope. However, electron micrographs may provide useful information about how they were formed, which may assist health risk assessors in modeling the deposition, dissolution, and clearance of DU-containing aerosols.

7.4 Capstone Study Evaluation

The Capstone DU Aerosol Study was designed to generate data to fill knowledge gaps about aerosols created by impact and perforation of armored vehicles. Data sets useful for both retrospective and prospective scenarios were intended. A list of test evaluation priorities (Table 2.1) identified 11 types of data collection efforts and analyses that were the bases of this project. Review of the actual information collected reveals the extent to which the priorities were addressed.

- **Interior DU source term:** The numerous IOM filter cassette samplers collected mass that was used to derive uranium concentrations within the target vehicles at sequential time intervals. Sample collection was conducted at a minimum of two points (and up to five counting the MVF sampler) for each time increment sampled over the first 2 h post shot. These data were graphed and are available for use in dose and risk assessments to address retrospective and prospective situations. This database is extensive and satisfies this priority.

  The primary limitations in the data are that the BHT target vehicles have greater interior volume than fully loaded operating vehicles (a potentially diluting effect counteracted to some extent by the loss of aerosol through greater deposition) and there was no ventilation system present and operating that would filter the air and more quickly remove aerosols. Therefore, the measured concentration levels are probably much higher than would actually occur with most operating vehicles. This expectation is supported by the limited results from the PIV-4 shot at an operating vehicle.

- **Interior DU concentration by particle size distribution over time**: Particle size distributions were measured using the equally numerous 8-stage CIs that operated during the same sequential time intervals over the first 2 h post shot. AMADs were calculated using unimodal and bimodal fits of the data. The resulting database is extensive although the fits were not always satisfactory. The primary limitation is that the selection of AMADs in risk assessments will require careful decisions to avoid biasing the quantity available for inhalation.

- **Lung fluid solubility and dissolution rates by particle size**: The following samples were analyzed for dissolution *in vitro*: three sets of 5-stage cyclone samples (PI-3/4, PI-7, and PII-1/2) and their backup filters (and a partial set [PIII-2]), one set of IOM filters, a PFDB filter, and the DU cone sample. This variety of samples helps bracket the range of dissolution rates in these heterogeneous DU aerosols over a series of particle sizes. The *in vitro* samples were analyzed for uranium only. It would be desirable to also evaluate the dissolution rates of the other metals present in the aerosols.

- **Chemical forms by particle size over time**: The same cyclone samples identified above were analyzed for uranium oxide compositions along with the first segment from a MVF tape. These results help establish the trends of oxides present and their approximate ratios in DU aerosols of various particle sizes created in this manner. However, the cyclone samples were collected during a 2-h period and represent an integration of this time period rather than discrete time periods. As a result, the importance of and change in oxide composition over this short timeframe was not evaluated.

- **Particle shape and morphology by particle size over time**: Samples evaluated by SEM included the same samples as those used for the chemical form analysis above, with the addition of several PFDB filters, the DU cone sample, three MVF segments, and several CI Stage-3 substrates. The SEM micrographs of the aerosol particles show a large variation in particle structures and combinations, probably related to several different mechanisms of formation. Again, this data set analyzes the aerosol collected over the 2-h sampling period, but it does not address any differences in shape and morphology over time except for samples collected within the first 5 sec.

- **Effect of Ventilation Systems (HVAC and EC/NBC) on interior DU concentration by particle size over time**: Use of the BHT vehicles and the intent to maximize DU aerosols precluded the use of operating ventilation systems following vehicle perforation. To compensate for this, air exchange

rates in similar vehicles were evaluated with their systems off and on so that factors could be used to estimate aerosol concentrations under a variety of ventilation conditions. Though such rates were measured, they were quite variable and their usefulness in scaling from the BHT air exchange to operating vehicles will have to be further analyzed.

- **Total elemental concentration and composition by particle size**: The primary non-DU metal constituents were evaluated for the cyclone and backup filter samples and for the DU cone sample. Trace metals in these samples were also identified. The cyclones/backup filters provided size separation so that the results represent composition by particle size.

- **Resuspension rates from interior and exterior surfaces**: Resuspension rates from interior surfaces were studied during recovery activities. A limited number of samples were collected to assess interior resuspension rates, but the data provide some trends for aerosols that were deposited on a vehicles interior surface. Sample collection to determine vehicle exterior resuspension rates was not feasible given the various constraints of the tests. However, many wipe test samples were collected from the vehicles exterior surface, and the data obtained from analysis of these samples may be used as input to exterior resuspension modeling. Likewise, data obtained from analysis of the wipe test samples taken from the vehicle interiors may be used as input to interior resuspension modeling.

- **Transferable DU from interior and exterior surface contamination to hands**: Entering personnel wore cotton gloves over their protective gloves during the sample recovery activities from several shots, and these cotton gloves were analyzed for DU content. These results have been associated with the activities and length of time during which these activities were performed. This information provides a useful starting point for estimating the transfer of surface contamination to hands when evaluating the hand-to-mouth pathway as part of human health risk assessments.

- **Exterior source term including particle size distribution**: Samples were collected to determine exterior particle size distributions exterior to the vehicle from seven of the shots. Uranium concentrations have also been calculated for these samples. Deposition trays and wipe test samples were collected to assess external surface contamination. Use of data from any of these samples for vehicle exterior estimates will provide an estimate greater than similar measurements performed in an open environment, because sampling was done within the confines of the Superbox, which precluded dispersion due to environmental conditions. This data must be used with care because estimates from them will be greater than an upper bound on similar data in an open environment and how much greater than an upper bound cannot be quantified.

- **Isotopic uranium concentration by particle size**: The uranium-235 to uranium-238 atom ratios were evaluated by particle size by analyzing samples from Stages 1, 3, and 5 of three cyclones and Stages 1, 4, and 5 of a fourth cyclone. The atom ratios for uranium-235 to uranium-238 were consistent, ranging from 0.205 to 0.212, and no obvious pattern was identified. These results are consistent with previous analyses of DU used by the U.S. military.

7.5 Lessons Learned and Recommendations

During the course of firing DU munitions at the target vehicles and analyzing the aerosols collected, several lessons were learned, and implementing some of the lesson-based recommendations would improve future testing. These lessons (with and without recommendations) are described below.

- The system monitoring the aerosol arrays was an essential part of the sample collection design that provided remote control and second-by-second data on the pressure drops for each sampler. This system was extremely useful and is recommended for future testing.

- The sampler arrays require protection from the fragments produced during perforation. The types of sample filters also have a bearing on filter survival during the initial temperature/pressure pulse for samplers not fully covered with an armored shield. Survival of Zefluor was greater than Supor filters. Likewise, MCE substrates in the CIs were satisfactory for analysis of radioactivity but were not satisfactory for gravimetric analysis.

- The DU in the aerosols was not in secular equilibrium with its immediate short-lived progeny when analyzed, and the extent of disequilibrium varied. If sample analysis depends on detection of immediate short-lived progeny of DU, then samples should be held an appropriate amount of time prior to analysis. If holding samples prior to analysis is not feasible, then methodology must be applied to determine the amount of disequilibrium and apply appropriate correction factors.

- The DU aerosols showed significant heterogeneity in morphology and chemical composition, suggesting several mechanisms of formation. This heterogeneity led to greater than expected variation in solubility.

- Particle size distribution data were successfully developed, but the use of these data is problematic. The particle size distributions vary widely, and no single model described all data well. Although the bimodal AMADs fit the majority of samples best, some samples were better characterized with a unimodal model, and other samples clearly were not well characterized by either. A possible approach to applying this data set is to develop a mechanism that uses the full set rather than one or two parameters.

- Because models for internal exposure from inhalation depend strongly on applying appropriate dissolution factors, the use of these data would benefit from more study of the particle variation between samples and the extent that other metals present in the aerosols contribute to the dissolution rates.

The Capstone DU Aerosol Study resulted in this independent, peer-reviewed report that contains a robust and scientifically valid data set describing many parameters of the DU aerosols formed when an LC, kinetic-energy, DU penetrator perforates an armored vehicle BHT and, to a lesser extent, a functional Abrams tank. This data set is applicable for assessing the human health risks associated with various DU exposure scenarios for DoD personnel and may be used to update the human health risk assessments associated with plausible DU exposure scenarios for DoD personnel involved in such incidents.

8.0 References

This list includes references cited in the main text or in the appendixes.

Bish DL and RC Reynolds, Jr. 1989. "Sample Preparation for X-Ray Diffraction." In *Reviews in Mineralogy. Volume 20. Modern Powder Diffraction,* eds. DL Bish and JE Post, pp. 74-99, The Mineralogical Society of America, Washington, DC.

Brina R and AG Miller. 1992. "Direct Detection of Trace Levels of Uranium by Laser-Induced Kinetic Phosphorimetry." *Analytical Chemistry* 64:1413-1418.

(CRC) The Chemical Rubber Company. 1970. *CRC Handbook of Applied Engineering Science.* RE Bolz and GL Tuve, Contributing Editors. CRC Press, Cleveland, Ohio.

(CRC) The Chemical Rubber Company. 2001. *CRC Handbook of Chemistry and Physics*, 82nd Edition, 2001-2002. DR Lide, Editor-in-Chief. CRC Press, Boca Raton, Florida.

Cullity BD. 1967. *Elements of X-Ray Diffraction*. Addison-Wesley Publishing Company, Inc., Reading, Massachusetts.

Eidson AF and WC Griffith, Jr. 1984. "Techniques for Yellowcake Dissolution Studies In Vitro and Their Use in Bioassay Interpretation." *Health Physics* 46:151-173.

Eidson AF and JA Mewhinney. 1980. "In Vitro Solubility of Yellowcake Samples from Four Uranium Mills and the Implications for Bioassay Interpretation." *Health Physics* 39:893-902.

Fliszar RW, EF Wilsey, and EW Bloore. 1989. *Radiological Contamination from Impacted Abrams Heavy Armor*. Technical Report BRL-TR-3068, Aberdeen Proving Ground, Ballistic Research Laboratory, Aberdeen, Maryland.

Gamble JL. 1967. *Chemical Anatomy, Physiology and Pathology of Extracellular Fluid.* Eighth Edition, Harvard University Press, Boston, Massachusetts.

Guilmette RA, MA Parkhurst, G Miller, FF Hahn, LE Roszell, EG Daxon, TT Little, JJ Whicker, YS Cheng, RJ Traub, GM Lodde, F Szrom, DE Bihl, KL Creek, and CB McKee. 2004. Human Health Risk Assessment of Capstone Depleted Uranium Aerosols. Prepared for the US Army by Battelle under Chemical and Biological Defense Information Analysis Center Task 241, DO 0189, Aberdeen, Maryland.

International Commission on Radiological Protection (ICRP). 1979. *Limits for Intakes of Radionuclides by Workers.* Publication 30, Ann. 2, Nos. 3/4, Pergamon Press, Oxford.

International Commission on Radiological Protection (ICRP). 1994. *Human Respiratory Tract Model for Radiological Protection*. Publication 66, Ann. 24, Nos. 1-3, Pergamon Press, Oxford.

Jenkins R. 1989. "Instrumentation." In *Reviews in Mineralogy. Volume 20. Modern Powder Diffractio.* Eds. DL Bish and JE Post, pp.19-45, The Mineralogical Society of America, Washington, DC.

Kanapilly GM and JH Diel. 1980. "Ultrafine $^{239}PuO_2$ Aerosol Generation, Characterization and Short-term Inhalation Study in the Rat." *Health Physics* 39:505-519.

Kanapilly GM and CHT Goh. 1973. "Some Factors Affecting the In Vitro Rates of Dissolution of Respirable Particles of Relatively Low Solubility." *Health Physics* 25:225-237.

Levin EM, HF McMurdie, and MK Reser (eds.). 1975. *Phase Diagrams for Ceramists. 1975 Supplement.* American Ceramic Society, Columbus, Ohio.

Mercer TT 1967. "On the Role of Particle Size in the Dissolution of Lung Burdens." *Health Physics* 13:1211-1221.

Office of the Special Assistant to the Deputy Secretary of Defense for Gulf War Illnesses (OSAGWI). 1998. *Exposure Investigation Report, Depleted Uranium in the Gulf.* Online report available at URL: www.gulflink.osd.mikl in the Environmental Exposure Reports Section.

Office of the Special Assistant for Gulf War Illnesses, Medical Readiness and Military Deployments (OSAGWI). 2000. *Depleted Uranium in the Gulf, Environmental Interim Exposure Report, July 13, 1998.* Accessed at <www.gulflink.osd.mil> in the Environmental Exposure Reports Section, Follow-Up DU Exposure Report – December 13, 2000.

Phalen RF, WC Hinds, W John, PJ Lioy, M Lippmann, MA McCawley, OG Raabe, SC Soderholm, and BO Stuart. 1986. "Rationale and Recommendations for Particle Size-Selective Sampling in the Workplace." *Applied Industrial Hygiene*, (1):3-14.

Taylor P, RJ Lemire, and DD Wood. 1993. "The Influence of Moisture on Air Oxidation of UO_2: Calculations and Observations." *Nuclear Technology* (104):164-170.

US Army Center for Health Protection and Preventive Medicine (USACHPPM). 2000. *Statement of Data Quality Objectives for Testing to Support Human Health Risk Assessments of Potential Depleted Uranium Exposures During the 1991 Gulf War*." Memorandum, July 2000.

Appendix A

Capstone Data Summaries

Appendix A

Capstone Data Summaries

The main objective of the Capstone DU Aerosol Study was to establish concentrations and particle size distributions over time of depleted uranium (DU) aerosol inside Abrams tanks and Bradley Fighting Vehicles perforated by DU munitions. The DU concentrations were measured using aerosol samplers placed inside the Abrams turret, the Bradley turret and crew compartment, and outside the vehicles. Samples of the particulate material created by the shots were collected on various media and in cyclone grit chambers and were analyzed to determine DU mass. The aerosol concentrations were calculated using DU mass, data documenting the quantity of air pulled through the samplers, and the length of sampling times. This appendix contains tables of DU mass concentrations of the major sampler types and descriptions of the parameters used to calculate these concentrations.

Table A.1 briefly summarizes important aspects of the testing program by phase and shot including 1) the shot trajectories, 2) information identifying hatches and other structures that opened or otherwise vented aerosol because of the blast pressure, and 3) comments regarding sample survival and other pertinent observations.

Table A.1. Overview of Capstone Test Shots

Shot	Shot Type	Vehicle Venting	General Comments
Phase I			
PI-1	Turret crossing	Driver's (tack-welded cover)	Commander's and gunner's IOMs damaged Longest sample collection duration
PI-2	Turret crossing	Loader's hatch	One or more IOM filters damaged at each array
PI-3/4	Turret crossing	Loader's hatch rose and fell	Loader's shield opened prematurely, samplers damaged
PI-5	Through breech	Commander's, loader's open a crack	All IOM filters survived
PI-6	Through breech	Commander's, loader's open a crack	All IOM filters survived; loader's array used for resuspension
PI-7	Through hull	Commander's hatch raised an inch	Aluminum plate shattered, severed a driver's IOM line
Phase II			
PII-1/2	Scout compartment	Hatches intact, small venting losses	Spall liner fibers visible during recovery operations
PII-3	Through feeder tube	TOW missile loading hatch	Right scout's shield opened only partially
Phase III			
PIII-1	Turret/DU armor	Loader's hatch perimeter, GPS unit	Hydraulic fluid burst into flames, left oily residue on surfaces
PIII-2	Turret/DU armor	Loader's hatch opened briefly, GPS	Nothing noteworthy

GPS = gunner's primary site
IOM = Institute of Occupational Medicine (used as an abbreviation for filter cassettes)

The samplers used to collect aerosols immediately after each shot included

- IOM filter cassettes (abbreviated as IOMs or FSs [for filter samplers])
- Marple cascade impactors (CIs)
- a five-stage cyclone (CY) connected to a backup filter (CF) or a parallel-flow diffusion battery (PFDB)
- a moving filter (MVF)
- Andersen cascade impactors (E-CIs)
- Staplex high volume air samplers (HV, or referred to as Hi-Vols)
- deposition trays (DT).

Additionally, staff performing recovery activities wore personal samplers including an IOM (P-FS) and a Marple CI (P-CI) or 37-mm closed face cassette (LA) samplers to collect aerosols within the vehicle to evaluate uranium concentrations from residual aerosols and from mechanical activities that resuspended previously deposited material. Some staff also wore cotton gloves during sampler recovery activities to provide information on the quantity of DU that might be transferred from contaminated surfaces to hands.

All samples were analyzed radioanalytically, chemically, or by both techniques. Samples analyzed shortly (within a few days to 75 days) after the shot by beta proportional counting techniques were adjusted to account for disequilibrium of immediate short-lived beta progeny. The approaches used to calculate uranium in the samples are discussed in Sections A.1 through A.3. Section A.1 contains a discussion of how sample flow rates were determined and subsequent volumes calculated. Section A.2 contains a description of the approach used to convert radioactivity measurements to uranium masses. Section A.3 contains tables of Capstone samples evaluated radioanalytically. These tables contain total sample mass, uranium mass derived from radioanalytical measurements, uranium concentrations, and propagated uranium concentration uncertainties.

A.1 Flow and Volume Data

Samplers operating within the vehicles were controlled by the LabVIEW[(a)] software, which logged the pressure drop of each sampler on a second-by-second basis. Flow calibrations made it possible to correlate the pressure drop readings with sampler flow rates. The pressure drop at each of 72 positions (36 IOM FS samples, 36 CIs) was measured prior to each event, and flow rates were derived from the pressure drops established by calibration.

Flow rates for the IOM filters and the CIs are discussed in Section A.1.2. Cyclone and MVF average flow rates and volumes are discussed in Sections A.1.3 and A.1.4, respectively. A discussion of exterior samplers and their flow and volume measurements are presented in Section A.1.5. Personal air samplers are briefly discussed in Section A.1.6.

A.1.1 Flow Calibrations

An initial flow calibration was performed on 10 critical orifices used in sampling positions within the vehicle. A BIOS DC-1 Flow Calibrator[(b)] was used to measure the flow through each orifice. The

(a) National Instruments, Inc., Austin, Texas.
(b) BIOS International, Pompton Plains, New Jersey.

pressure drop (Δp) was varied from 0.5 to about 5 psig locally at each position and was measured using a 0 to 15 psig magnahelic gauge.[(a)] The measured flow rates were plotted against the Δp as indicated on the computer control panel. Calibrated Omega PX-605 pressure transducers[(b)] were used to measure the Δp electronically and display the value on the computer control panel.

The equation used to relate flow rate to pressure drop (Δp) from fitting the curves described above follows:

$$Q(Lpm) = Q_o(Lpm) + b * \Delta p \quad (A.1)$$

where Q_o is the flow rate at zero pressure drop and b is the slope of the flow rate/pressure drop calibration curve. The value of Q_o was 2.6970 ± 0.0661 with a range of 2.58 to 2.95. The slope of the plot, b was -0.18797 ± 0.004567 (standard deviation [SD]) with a range of -0.181 to -0.204. A single fitted equation did not adequately describe the flow-pressure drop relationship, but it is reasonable to assume that for each critical orifice, a linear equation similar to Equation A.2 could be used to determine the flow. For the later shots, the constant slope -0.18797 was used for each equation, but Q_o was determined for each orifice before each test.

$$Q(Lpm) = Q_o(Lpm) - 0.18797 * \Delta p \quad (A.2)$$

This procedure provided simple, accurate information about the flow rate.

A.1.1.1 Verification of the Calibration Procedure

The flow rate with zero pressure drop is obtained from a single point flow calibration for each sample location prior to the test using the following equation:

$$Q_o(Lpm) = Q(Lpm) + 0.18797 * \Delta p \quad (A.3)$$

where Q and Δp are the flow rate and pressure drop from the single point measurement.

Table A.2 shows an example of the calibration data using samplers from PI-1. This table lists the measured flow rates for the 10 critical orifices during the detailed calibration. Also listed in the table are calculated flow rates based on Equation A.2, where Q_o for each orifice was determined by a single point measurement before Phase I, Shot 2 (PI-2) at a Δp near 2.5 psig. The percent difference of the calculated and measured flow rate was 0.93% with a maximum error of 3.0%. Therefore we concluded that this procedure is accurate within 3% of error for the determination of the flow rate.

(a) Dwyer Instruments Inc., Michigan City, Indiana.
(b) Omega Engineering, Inc., Stamford, Connecticut.

Table A.2. Example of Measured and Calculated Flow Comparisons Using PI-1

Sampler ID	Pressure (psig)	Measured Flow (Qm)	Calculated Flow (Qc)	% Difference (Qc-Qm)/Qm
FS1 (L)	0.50	2.65	2.68	1.29
	1.07	2.54	2.58	1.63
	2.02	2.35	2.40	2.05
	2.98	2.17	2.22	2.25
	4.03	1.97	2.02	2.58
	5.15	1.76	1.81	3.03
FS3 (L)	0.71	2.54	2.56	1.02
	1.17	2.44	2.47	1.22
	2.14	2.27	2.29	1.01
	3.09	2.09	2.11	1.00
	4.11	1.91	1.92	0.80
	5.29	1.69	1.70	0.62
FS5 (L)	0.73	2.49	2.53	1.58
	1.21	2.40	2.44	1.72
	2.19	2.22	2.25	1.62
	3.18	2.04	2.07	1.16
	4.17	1.87	1.88	0.78
	5.18	1.68	1.69	0.65
FS7 (L)	0.78	2.56	2.57	0.26
	1.16	2.48	2.50	0.79
	2.16	2.29	2.31	0.97
	3.03	2.13	2.14	0.76
	4.00	1.95	1.96	0.79
	5.21	1.72	1.73	0.97
IMP1 (L)	0.82	2.63	2.58	-1.69
	1.31	2.52	2.49	-1.21
	2.18	2.35	2.33	-1.19
	3.17	2.16	2.14	-1.03
	4.29	1.95	1.93	-1.19
	5.22	1.77	1.75	-1.12
IMP3 (L)	0.78	2.60	2.58	-0.52
	1.12	2.52	2.52	0.08
	2.12	2.33	2.33	0.12
	3.10	2.15	2.15	-0.05
	4.06	1.96	1.97	0.27
	5.10	1.77	1.77	0.07
IMP5 (L)	0.64	2.58	2.58	0.12
	1.10	2.49	2.50	0.20
	2.03	2.32	2.32	-0.07
	3.01	2.14	2.14	0.12
	3.96	1.96	1.96	-0.01
	5.09	1.75	1.75	-0.01
IMP7 (L)	0.26	2.54	2.57	0.91
	0.74	2.43	2.48	2.05
	1.65	2.28	2.31	0.99
	2.60	2.11	2.13	1.00
	3.55	1.93	1.95	1.02
	4.60	1.74	1.75	0.80

Table A.2. (contd)

Sampler ID	Pressure (psig)	Measured Flow (Qm)	Calculated Flow (Qc)	% Difference (Qc-Qm)/Qm
FS1 (G)	0.51	2.67	2.66	-0.26
	0.98	2.57	2.57	0.15
	1.99	2.38	2.38	0.31
	2.91	2.20	2.21	0.72
	3.92	2.00	2.02	0.90
	4.94	1.81	1.83	1.24
IMP1 (G)	0.74	2.80	2.77	-1.17
	1.31	2.68	2.66	-0.75
	2.31	2.48	2.47	-0.39
	3.26	2.29	2.29	0.29
	4.22	2.09	2.11	0.96
	5.23	1.88	1.92	2.19

A.1.1.2 Total Sampling Volume and Average Sampling Flow

Because the Δp changes as the sampler collects and accumulates particles on its substrates, an averaged flow rate and the total volume through the sampler were calculated. The Δp was recorded each second. From the procedure described in the previous sections, the instantaneous flow rate was calculated from the Δp. These values were then integrated using the following equation to determine the total sample volume.

$$\text{Total Volume} = \Delta t(1/2\ Q_1 + Q_2 + Q_{3\ldots} + 1/2\ Q_n) \qquad \text{(A.4)}$$

The average flow rate was calculated as the total sample volume divided by the sampling time.

A.1.2 IOM Filter Samples and Cascade Impactors

The sheer quantity of data collected on flow data precludes its presentation here on a second-by-second basis. Rather, a summary of the data is given for each shot for which aerosol samples were collected. This summary includes a list of the time interval of sampler operation **beginning 5 sec post-shot**, the average flow rates, and the total volume of air passing through each IOM filter and CI sampler in each array (Tables A.9 through A.32, beginning on Page A.31). Comments are provided noting the damage to filters, vacuum or electrical lines, or discussion of other anomalies for which explanations are known. The number of decimal places does not necessarily confer significance but rather was imported from spreadsheets that maintained extra decimals to minimize rounding error.

As itemized by shot, the following IOM filters were damaged by the shot or the vacuum or electrical lines were cut. Data from these samplers were omitted from aerosol analysis.

Phase I:

- Shot 1: All gunner and all commander filters.
- Shot 2:
  - Loader 1, 4, 5, and 9
  - Commander 2, 6, 7, 8
  - Gunner 1, 2, 3, 4, 6, 7, 9
  - Driver 9.
- Shot 3/4:
  - Loader 1, 2, 4, 7, 9
  - Gunner 5 (Sample head fell or broke off).
- Shot 6: Samplers intact.
- Shot 7: Driver 5 electrical line was apparently cut.

Phase II: Samplers intact.

Phase III:

- Shot 1: Samplers intact
- Shot 2: Loader 5 was bent, tilting out of holder upon recovery; its filter had collected somewhat less sample than other FS samples operating in the same time interval.

General comments about the various samplers in Phase I are noted in the following text. With the exception stated above, all samplers operated and filters survived undamaged during Phases II and III. All CI substrates survived, though several of the loader's samplers sustained damaged from the PI-3/4 shots.

PI-1: The flow rate data for FS and CI samples were collected without a problem. However, all the gunner's and commander's FS filters were damaged and should not be used in the analysis. The cyclone/ parallel-flow diffusion battery (PFDB) and MVF were operated by another pump, and it appeared that a leak developed that made post-test flow rates unreliable. The cyclone and PFDB appeared to have collected aerosols normally, but the cut-points are uncertain.

PI-2: Most of the gunner's and commander's FS filters were damaged, and loss also occurred at the loader and driver FS positions. Because of the apparent leakage with the use of the PFDB, a backup filter (four filters collected in parallel) replaced the PFDB unit and was attached to the outlet of the cyclone. The MVF was not used. The field blank for the gunner was changed to Sampler 2 rather than Sampler 9 because of the better flow properties of Sampler 9.

PI-3/4: The gunner's and driver's samples ran during Shot 3. No damage to these samplers was attributed to this shot except that the gunner's FS5 IOM head had separated from the stem. As a result of the apparent premature release of the drop door on the solid shield protecting the loader's array, fragments from Shot 4 (and possibly Shot 3) damaged most of the loader's IOM filters. The samplers may have been exposed to "field blank" levels from the Shot 3 as well as collecting Shot 4 aerosol. Several of the loader's CI sampler bodies sustained damage by fragments, though the substrates appeared to be unaffected. The cyclone sampled normally. The MVF ran during Shot 3 but did not operate during Shot 4.

PI-5: Several driver's samplers (but not filters) were damaged by fragments. Additionally, fragments cut the vacuum lines of the cyclone and the MVF, thereby preventing sample collection.

PI-6: A fragment entered the inlet of the MVF sample, and no sample was obtained during or after this shot.

PI-7: Extensive aluminum fragmentation of the witness plate severed the electrical lines to the Δp feed-back lines. As a result, post-test measurements were made to determine the change in Δp levels. The sampling volume was based on the average of the pre- and post-test flow rate (Δp) measurements. The driver's position FS5 and MVF sampler lines were cut by aluminum fragments.

A.1.3 Cyclone Flow Data Summary

The flow rate and total volume data for the cyclone samplers are summarized in Table A.3. The post-test flow rate data from PI-1 is suspect because it is believed that there was a leak in the PFDB test apparatus to which the cyclone was attached. Therefore, the volume collected is not specified, but is probably less than the 4019 Lpm derived from multiplying the sample time by the average flow rate.

Table A.3. Cyclone Flow Rates and Volumes

Phase/Shot	Sample Time (min)	Flow Rate (Lpm)	Volume (L)
PI-1	128	31.4	Uncertain
PI-2	128	9.9	1256.9
PI-3/4	114	12.7	1447.8
PI-5	Line cut, sampler did not operate		
PI-6	129	9.0	1170.0
PI-7	129	11.5	1483.5
PII-1/2	120	13.4	1603.2
PII-3	129	10.0	1283.6
PIII-1	129	10.9	1400.9
PIII-2	129	12.8	1646.0

A.1.4 Moving Filter Flow Rates

The MVF was operated during only five of the tests. For those during which it ran, sampling was conducted at various times beginning just before the shot was fired to collect aerosol during the first few seconds. PI-1 is the only shot in which the MVF was stationary during alternating sampling intervals. Flow rates and volumes over the course of each MVF sample slice are recorded in Table A.4.

Table A.4. Moving Filter Flow Rates and Volumes

Phase/Shot	Flow Rate (Lpm)	Volume (L)
PI-1	18.8	Not Meaningful
PI-3/4	30.0	1.4384
PII-3	18.95	0.9086
PIII-1	25.81	1.2375
PIII-2	32.97	1.5808

A.1.5 Exterior Samplers

The test emphasized vehicle interior sampling. Concern about the relevance of sampling exterior to the vehicle, but inside the Superbox fragmentation shield, was expressed because of the confounding aspects of airflow in the Superbox structure. However, to the extent that sampling could be conducted exterior to the vehicle, limited sampling was conducted. The caveat, and it is a major one, is that in an actual outdoor environment, more mixing, more diffusion, and more dilution would occur. Therefore, the sample collection exterior to the vehicle provides an overestimate of the upper bound for a DU concentration source term exterior to the vehicle in an outdoor environment.

Two types of external aerosol samplers were used in this analysis—high-volume Staplex samplers (Hi-Vols) and Andersen CIs, which were not available until the PI-5 shot. These samplers operated at about 560 Lpm (20 cfm) and collected total mass onto a single 10-cm (4-in.) Whatman-41 filter. Following the first two tests, four Hi-Vols were positioned at various points within the fragmentation shield and away from the direct line of fire. Three were used in the PI-3/4 event. Beginning with PI-5, the Hi-Vols were only used for background measurements of aerosolized particulate matter.

Exterior sampler flow rates were checked before and after sampling and were occasionally problematic when a post-sampling flow rate proved difficult to measure.

A.1.5.1 Andersen CI Samplers

Beginning with PI-5, two Andersen CIs collected external vehicle aerosols so that particle size distributions could be evaluated. Though relatively well shielded, a fragment damaged one of the vacuum lines, so only one sampler functioned during PI-5. For the remainder of the shots, both samplers operated. Sampler 1 for PIII-2 ran for 5 h (300 min) rather than the intended 2 min because of an electrical connection miswiring. Use of data from this sampler needs to be considered carefully because the large volume would dilute the calculated concentration. Sample flows and volumes are listed in Table A.39.

A.1.5.2 Hi-Vol Samplers

Hi-Vol samplers were used to collect aerosols before each test and as the sole post-impact external sampler through PI-3/4, after which time, the Andersen CI was used to collect post-impact samples. Alpha and beta proportional counting techniques were used to analyze samples collected in the Hi-Vol filters, and inductively coupled plasma-mass spectrometry (ICP-MS) was used to analyze three of the samples. There was no correlation in uranium mass between the few samples analyzed chemically and those measured by alpha/beta counting. Because there was no way to determine whether one or more of

these samples had been misidentified when converted to random numbers, and because these results were not critical to the project, they were eliminated from further consideration and are not presented here.

A.1.6 Personal Air Samplers

Sample recovery personnel entering the vehicle post-shot wore an IOM filter cassette P-FS and a Marple CI (P-CI) or a 37-mm, closed-face-cassette (LA) sampler. To minimize the weight carried by the workers that wore both the P-FS and P-CI samplers, the two samplers were connected to a single portable pump, which was operated at 4-Lpm in an attempt to provide 2-Lpm flow rate to each sampler. It is not known how evenly the flow rate was divided, and this division adds an undetermined about of uncertainty to the analysis of these samples.

A.2 Uranium Mass Calculated from Radioactivity

Establishing the uranium mass concentration or activity concentration is necessary for subsequent estimates of dose and associated health risk. All filters, filter substrates, and cyclones that collected aerosol during the Capstone DU Aerosol Study were analyzed by radioactivity counting techniques. Select samples also were analyzed using chemical methods to enable the derivation of uranium mass from the radioactivity counting data. Beta and gamma activity measurements were used as surrogate measurements of uranium mass for the majority of the samples. The sample types that were analyzed by proportional counting included the backup filters to the cyclone train (CF), the Marple CIs—eight stages with a backup filter (stage 1 = CI-1 through stage 8 = CI-8, backup filter = CI-9), the PFDB (DB) samples, the IOM field samplers (FSs), the high volume air samplers (HV), the personal samplers including IOM (P-FS), Marple CI (P-CI) and 37-mm closed face cassette (LA) samplers, the moving filter segments (MV [rather than MVF]), and the wipe test samples (W).

All sample types that lent themselves to proportional counting, were counted by this technique at the U.S. Army Aberdeen Test Center (ATC) Health Physics Laboratory. Approximately 10% of these samples were selected and sent to the U.S. Army Center for Health Promotion and Preventive Medicine (USACHPPM) Radiological Laboratory for verification analyses by proportional counting. Approximately 20% of the verification samples were also analyzed for uranium using ICP-MS. All samples submitted to laboratories other than ATC were submitted blind. A random number, between 1 and 8000, was assigned to all samples by the ATC laboratory prior to sending the samples to the other laboratories.

Sample types that could not easily be analyzed by proportional counting were analyzed by gamma spectrometry and a subset of these samples was also analyzed by ICP-MS. Cyclone residues, deposition tray debris, Andersen CI substrates, and the cotton gloves used in certain recovery activities were analyzed using gamma spectroscopy because the sample geometry could not be readily analyzed by proportional counting. Additionally, filter and substrate samples selected for destructive chemical analysis (ICP-MS) were first analyzed by gamma spectrometry, prior to destroying the sample matrix.

Procedures used to count the samples are briefly described in Section 3.9.1. The uranium mass concentrations derived from the counting data for IOM, CI, and MVF samples are listed by sample types in Tables A.9 through A.37. The wipe data are listed in Appendix F.

A.2.1 Uranium Derived from Beta Radioactivity

All sample types that readily lent themselves to proportional counting were analyzed for alpha and beta activity by this technique at the ATC Health Physics Laboratory. Sample analysis began in November 2000, the day following shot PI-1. During the course of alpha and beta activity data review, a problem was identified with the setup of one of two proportional counters used for analysis. After the counter was serviced and operating within manufacturer specifications, the samples that had been analyzed on that counter were reanalyzed. This reanalysis was completed in June 2001. Sample analyses at the USACHPPM laboratory were performed between September 2001 and January 2002.

Verification samples that were analyzed at USACHPPM were selected based on the ATC alpha activity, the ATC beta activity, and the ATC beta/alpha activity ratio. Uranium that consists of 99.8% by mass uranium-238 (also referred to as U-238 or ^{238}U) and 0.2% by mass uranium-235 (also referred to as U-235 or 235U) in equilibrium with its immediate beta-emitting short-lived progeny would produce approximately 2 disintegrations per minute (dpm) from beta for each dpm from alpha, assuming "weightless" samples. Alpha particles are usually more readily absorbed within the sample than beta particles as sample mass increases. Therefore the beta/alpha activity ratio for samples that are not "weightless" would be expected to be greater than 2.

The ATC beta/alpha activity ratio for samples analyzed within a week or two of sample collection appeared to be "lower" than the beta/alpha ratio for samples counted 88 days or more after collection. This phenomenon appeared to occur for smaller aerodynamic diameters samples (such as Stages 6 through 8 and the backup filter of the Marple CIs). Some of the lower ratios were on the order of 0.5 or less for samples with significant activity suggesting that, contrary to expectations, much more alpha activity was being detected than beta activity. A plausible explanation for this phenomenon was that the interaction between the penetrator and the target had disrupted the secular equilibrium between the penetrator's uranium isotopes and their immediate beta-emitting short-lived progeny. Immediately after this disruption, the radioactive decay processes begins again, and equilibrium will be re-established after a sufficient number of progeny half-lives. Over time (about 100 days), this equilibrium was reestablished. The process during which the activity of the progeny comes into equilibrium with the uranium parent is typically referred to as ingrowth or more precisely radioactive ingrowth of progeny.

Analysis of the counting data indicated the need to assess and adjust for ingrowth of beta-emitting, short-lived progeny. To accomplish this, the following four analyses were required: 1) comparison of the ATC-USACHPPM alpha/beta activity results, 2) prediction of ICP-MS micrograms of uranium (μg U) from USACHPPM beta activity, 3) prediction of ICP-MS (μg U) from ATC beta activity, and 4) development of ingrowth correction factors. Data analyses were performed using SPSS for Windows Version 10.1 software. The statistical analyses performed in support of these comparisons, predictions, and ingrowth correction factor developments are extensive. A summary of the process used is presented in the next sections.

A.2.1.1 Regression Model Selection

Weighted regressions through the origin were used in the data analyses. Conventions used throughout the data analysis included displaying the predicted value on the y-axis as the dependent variable. When comparing a measured value with an estimated value, the estimated value was placed on the y-axis.

The zero-intercept model was selected on a theoretical basis, because both analytical laboratories had corrected for instrument and media background prior to reporting results. Regression analyses were also performed that did not force the intercept through zero. The results of these unforced regressions supported the theoretical basis because the 95% confidence interval for the intercept usually included zero.

The analytical laboratories reported counting uncertainties for the results derived from radioactivity measurements. When a radioactivity-derived measurement was the dependent variable, the regression was weighted by the variance of the reported counting uncertainty. Unweighted regressions were initially performed; however, the weighted regressions produced a higher R^2 statistic and a lower standard error of the regression coefficient for most regressions performed. Therefore, weighted regressions were performed when the dependent variable was a radioactivity measurement.

The analytical laboratory did not report analytical uncertainties for the ICP-MS uranium mass results. Therefore, when the ICP-MS results were to be predicted, an iterative regression technique was employed. First an unweighted regression was performed and the regression coefficient derived was used to estimate the predicted value. A weighted regression was then performed using the predicted value as the weighting factor. The iteratively weighted regressions produced a higher R^2 statistic and a lower standard error of the regression coefficient for most regressions performed. Therefore, iterative weighted regressions were performed when the dependent variable was ICP-MS uranium mass data.

A.2.1.2 ATC/USACHPPM Laboratory Comparison

USACHPPM analyzed 735 samples previously analyzed by ATC for alpha and beta activity verification. Because beta progeny ingrowth may account for differences in beta activity between "early" ATC counts and "late" USACHPPM counts, the data set was limited to ATC counts with a count date 75 days or later than the sample collection date. Selection of this value was based on inspection of the data set and the fact that, if the thorium-234 (Th-234; 24.1 day half-life) activity were completely separated from the U-238 activity, the Th-234 activity would be 88% of the U-238 activity 75 days later. Therefore, the Th-234/protactinium-234m (Pa-234m; 1.2 min half-life) activity would be approximately 90% of the U-238 activity if completely separated at the time of the shot.

After the verification samples were counted and the activities of the samples were determined, regression analyses were performed on the ATC-USACHPPM beta activity and the ATC-USACHPPM alpha activity. The regression (weighted through zero regression model) equations derived from the data were:

$$CHPPM\,\beta_{eq} = (0.977 \pm 0.007) * ATC\,\beta_{eq} \quad \text{(A.5)}$$

and

$$CHPPM\,\alpha = (0.736 \pm 0.019) * ATC\,\alpha \quad \text{(A.6)}$$

where $\beta_{eq} \equiv$ beta activity (dpm) at equilibrium ($\geq$ 75 days between collection and count).

The regression coefficients were expected to be close to 1, and the beta activity coefficient was close to 1 (0.977). However, the alpha coefficient was considerably less at 0.736. The difference in the ATC and USACHPPM alpha activity results is believed to be due to differences in the geometries of the alpha

efficiency standards used by the two laboratories. The difference has not been thoroughly investigated partly because it was intended that the beta activity results rather than the alpha activity results would be used in subsequent analyses.

The data set was then analyzed by sample type, and scatter plots and correlation and regression analyses were performed by sample type. Each stage of the Marple CIs was treated as a different sample type due to the different deposition geometries and, therefore, potentially different biases between the sample deposition geometry and the beta efficiency standard geometry. Both laboratories used plated, large-area (5-cm; 2 in.) sources to determine the beta efficiencies for all sample types. All subsequent analyses were evaluated by sample type. Scatter plots of the comparison of the two laboratories' alpha and beta data by sample type are shown in Figures A.1 and A.2, respectively.

For the sample types whose correlation (ATC beta activity/USACHPPM beta activity) was significant at the 0.05 level or greater, the beta activity regression coefficient was entered into the data set. These coefficients enabled USACHPPM beta activity (at equilibrium) to be calculated from ATC beta activity (at equilibrium). The dependent and independent variables were switched, and the regressions were performed again. The sample types with correlation significant at the 0.05 level or greater included: CF, CI-1, CI-2, CI-3, CI-4, CI-5, CI-6, CI-7, CI-8, CI-9, FS, MV, and W. Two sample-types—HV and LA—with only 3 samples each in the data set did not have correlations that were significant.

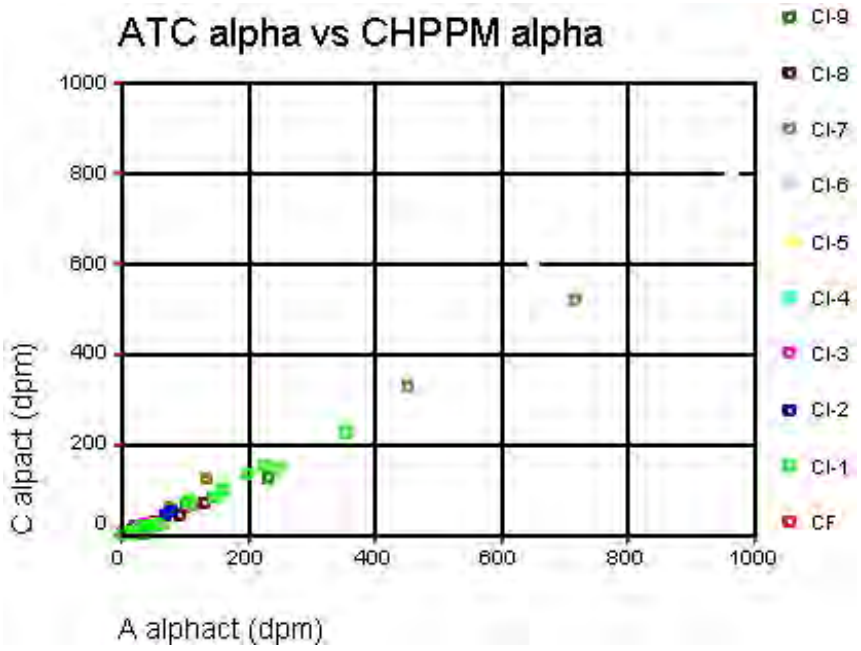

Figure A.1. Scatter Plot Comparison of Alpha Activity by CI Stage

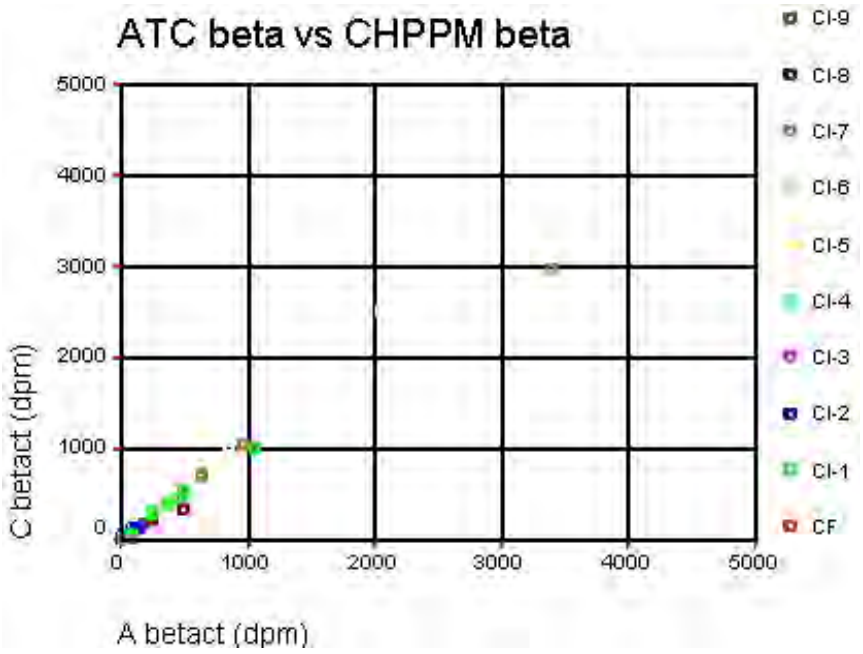

Figure A.2. Scatter Plot Comparison of Beta Activity by CI Stage

The sample type beta regression equations (weighted regression through zero) derived from the data and used to predict USACHPPM beta activity at equilibrium are presented in Equation A.7 array below:

$$\begin{aligned}
CF \quad & CHPPMB_{eq} = (1.231 \pm 0.014) * ATC\beta_{eq} \\
CI-1 \quad & CHPPM\beta_{eq} = (0.994 \pm 0.012) * ATC\beta_{eq} \\
CI-2 \quad & CHPPM\beta_{eq} = (1.012 \pm 0.016) * ATC\beta_{eq} \\
CI-3 \quad & CHPPM\beta_{eq} = (1.054 \pm 0.044) * ATC\beta_{eq} \\
CI-4 \quad & CHPPM\beta_{eq} = (0.981 \pm 0.094) * ATC\beta_{eq} \\
CI-5 \quad & CHPPM\beta_{eq} = (1.017 \pm 0.045) * ATC\beta_{eq} \\
CI-6 \quad & CHPPM\beta_{eq} = (0.784 \pm 0.068) * ATC\beta_{eq} \\
CI-7 \quad & CHPPM\beta_{eq} = (1.073 \pm 0.017) * ATC\beta_{eq} \\
CI-8 \quad & CHPPM\beta_{eq} = (0.748 \pm 0.028) * ATC\beta_{eq} \\
CI-9 \quad & CHPPM\beta_{eq} = (1.015 \pm 0.008) * ATC\beta_{eq}
\end{aligned} \tag{A.7}$$

The sample type beta regression equations (weighted regression through zero) derived from the data and used to predict ATC beta activity at equilibrium are presented in Equation A.8 array below:

$$\begin{aligned}
CF \quad & ATC\beta_{eq} = (0.814 \pm 0.007) * CHPPM\beta_{eq} \\
CI-1 \quad & ATC\beta_{eq} = (1.014 \pm 0.010) * CHPPM\beta_{eq} \\
CI-2 \quad & ATC\beta_{eq} = (0.987 \pm 0.021) * CHPPM\beta_{eq} \\
CI-3 \quad & ATC\beta_{eq} = (0.943 \pm 0.043) * CHPPM\beta_{eq}
\end{aligned} \tag{A.8}$$

$$
\begin{aligned}
CI-4 \quad ATC\beta_{eq} &= (1.003 \pm 0.123) * CHPPM\beta_{eq} \\
CI-5 \quad ATC\beta_{eq} &= (0.982 \pm 0.049) * CHPPM\beta_{eq} \\
CI-6 \quad ATC\beta_{eq} &= (1.274 \pm 0.110) * CHPPM\beta_{eq} \\
CI-7 \quad ATC\beta_{eq} &= (0.930 \pm 0.016) * CHPPM\beta_{eq} \\
CI-8 \quad ATC\beta_{eq} &= (1.336 \pm 0.045) * CHPPM\beta_{eq} \\
CI-9 \quad ATC\beta_{eq} &= (0.986 \pm 0.006) * CHPPM\beta_{eq} \\
FS \quad ATC\beta_{eq} &= (1.132 \pm 0.011) * CHPPM\beta_{eq} \\
MV \quad ATC\beta_{eq} &= (1.053 \pm 0.000) * CHPPM\beta_{eq} \\
W \quad ATC\beta_{eq} &= (0.859 \pm 0.004) * CHPPM\beta_{eq}
\end{aligned}
$$

A.2.1.3 Comparison of USACHPPM Beta to ICP-MS (μg U)

To demonstrate that beta activity at equilibrium can be used to predict uranium mass, samples that were analyzed for beta activity (at USACHPPM 75 days or more after sample collection), and uranium mass by ICP-MS were evaluated. An assumption was made that minimal sample loss occurred between the USACHPPM beta activity count and the USACHPPM uranium analysis. The data set as a whole was examined, and then the data set was split and analyzed by sample type.

The USACHPPM beta activity/USACHPPM uranium mass correlation was significant at the 0.01 level (0.980) for the data set of 162 samples. The USACHPPM beta activity/uranium mass regression equation (unweighted regression through zero) derived from the data is presented below:

$$CHPPM\mu g\,U = (1.224 \pm 0.019) * CHPPM\beta_{eq} \qquad \text{(A.9)}$$

where $\beta_{eq} \equiv$ beta activity (dpm) at equilibrium (≥ 75 days between collection and count), and μg U ≡ ICP-MS uranium results in microgram per sample.

The theoretical regression coefficient for a "weightless" sample of the uranium that consists of 99.8% by mass U-238 and 0.2% by mass U-235 in equilibrium with its immediate short-lived progeny would be approximately 1.5. The theoretical regression coefficient for a weightless sample with a 100-mg/cm^2 absorber between the sample and the detector is approximately 0.7. The ranges of beta particles from Th-234 and Th-231 are less than 100 mg/cm^2; therefore, the Th-234 and Th-231 beta particles would be stopped in the absorber and would not reach the detector.

The sample types with correlation (USACHPPM beta activity/USACHPPM uranium mass) significant at the 0.05 level or greater included CI-1, CI-2, CI-3, CI-4, CI-5, CI-6, CI-7, CI-8, CI-9, DB, FS, MV, and W. Three sample-types—CF, HV and LA—whose correlations were not significant all had only three samples each in the data set. The calculated regression coefficients for these sample types are all within the range of theoretical regression coefficients between a "weightless" sample (1.5) and a sample with a 100-mg/cm^2 absorber between the sample and the detector (0.7).

The sample type USACHPPM beta activity – USACHPPM uranium mass regression equations (iterative weighted through zero) derived from the data are presented in Equation A.10 array that follows:

$$
\begin{aligned}
CI-1 \quad CHPPM\mu g\ U &= (0.985 \pm 0.008) * CHPPM\beta_{eq} \\
CI-2 \quad CHPPM\mu g\ U &= (0.889 \pm 0.032) * CHPPM\beta_{eq} \\
CI-3 \quad CHPPM\mu g\ U &= (0.983 \pm 0.036) * CHPPM\beta_{eq} \\
CI-4 \quad CHPPM\mu g\ U &= (0.941 \pm 0.018) * CHPPM\beta_{eq} \\
CI-5 \quad CHPPM\mu g\ U &= (0.806 \pm 0.016) * CHPPM\beta_{eq} \\
CI-6 \quad CHPPM\mu g\ U &= (1.075 \pm 0.049) * CHPPM\beta_{eq} \\
CI-7 \quad CHPPM\mu g\ U &= (1.105 \pm 0.034) * CHPPM\beta_{eq} \\
CI-8 \quad CHPPM\mu g\ U &= (0.708 \pm 0.056) * CHPPM\beta_{eq} \\
CI-9 \quad CHPPM\mu g\ U &= (0.894 \pm 0.021) * CHPPM\beta_{eq} \\
DB \quad CHPPM\mu g\ U &= (0.853 \pm 0.007) * CHPPM\beta_{eq} \\
FS \quad CHPPM\mu g\ U &= (1.328 \pm 0.077) * CHPPM\beta_{eq} \\
MV \quad CHPPM\mu g\ U &= (1.141 \pm 0.019) * CHPPM\beta_{eq} \\
W \quad CHPPM\mu g\ U &= (1.316 \pm 0.070) * CHPPM\beta_{eq}
\end{aligned}
\tag{A.10}
$$

A.2.1.4 Comparison of ATC Beta to ICP-MS (μg U)

The ultimate goal was to predict the uranium mass from an ATC beta activity count, because the majority of the Capstone samples were only analyzed by proportional counting at ATC. However varying degrees of sample handling and processing occurred between the ATC count and the USACHPPM ICP-MS uranium analyses that may have resulted in sample loss.

To demonstrate "no sample loss" between the ATC activity count and the USACHPPM ICP-MS analyses, an estimate of USACHPPM beta activity was calculated from the ATC beta activity, and the ratio of the estimated USACHPPM beta activity to the measured USACHPPM beta activity was calculated. If this ratio was between 0.7 and 1.3, then the sample was considered not to have significant sample loss between the ATC beta activity count and the USACHPPM beta activity count. Therefore, the data set used to derive the ATC beta activity at equilibrium to uranium mass conversion factors were samples analyzed for beta activity at ATC 75 days or more after sample collection with no demonstrated sample loss. These samples were analyzed for uranium mass by ICP-MS at USACHPPM.

The data set as a whole was examined; then the data set was split, and scatter plots were generated by sample type. Of the 90 samples analyzed at ATC 75 days or more after sample collection and that also had no observable sample loss, 59 were analyzed for uranium mass by ICP-MS at USACHPPM. A scatter plot (Figure A.3.), as well as, correlation and regression analyses for the ATC beta activity/ USACHPPM uranium mass data set (58 samples) were performed.

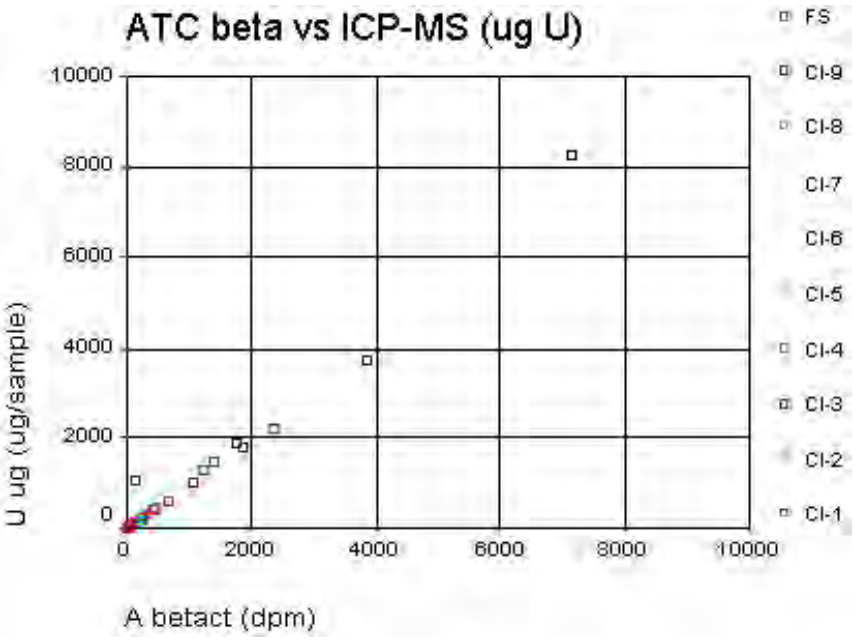

Figure A.3. Comparison of the Beta-Derived and Chemically Analyzed Uranium Concentrations

The ATC beta activity/uranium mass regression equation (unweighted regression) derived for the data set is presented below:

$$CHPPM\mu g\,U \quad = \quad (1.084 \pm 0.003) * ATC\beta_{eq} \tag{A.11}$$

where $\beta_{eq} \equiv$ beta activity (dpm) at equilibrium (≥ 75 days between collection and count), and μg U ≡ ICP-MS uranium results in microgram per sample.

The sample types with correlations (ATC beta activity/USACHPPM uranium mass) significant at the 0.01 level included CI-1, CI-2, CI-3, CI-4, CI-5, CI-6, CI-7, CI-8, CI-9, and FS. The wipe sample type had only three samples in the data set.

The sample type ATC beta activity/USACHPPM uranium mass regression (iterative weighted regression through zero) equations derived from the data are presented in Equation A.12 array below:

$$\begin{aligned}
CI-1 \quad CHPPM\mu g\ U &= (1.014 \pm 0.012) * ATC\beta_{eq} \\
CI-2 \quad CHPPM\mu g\ U &= (0.938 \pm 0.074) * ATC\beta_{eq} \\
CI-3 \quad CHPPM\mu g\ U &= (0.793 \pm 0.022) * ATC\beta_{eq} \\
CI-4 \quad CHPPM\mu g\ U &= (0.962 \pm 0.018) * ATC\beta_{eq} \\
CI-5 \quad CHPPM\mu g\ U &= (1.039 \pm 0.046) * ATC\beta_{eq} \\
CI-6 \quad CHPPM\mu g\ U &= (0.903 \pm 0.025) * ATC\beta_{eq} \\
CI-7 \quad CHPPM\mu g\ U &= (1.197 \pm 0.054) * ATC\beta_{eq}
\end{aligned} \tag{A.12}$$

$$CI-8 \quad CHPPM\mu g\ U = (1.044 \pm 0.035) * ATC\beta_{eq}$$
$$CI-9 \quad CHPPM\mu g\ U = (0.961 \pm 0.045) * ATC\beta_{eq}$$
$$FS \quad CHPPM\mu g\ U = (0.965 \pm 0.027) * ATC\beta_{eq}$$
$$W \quad CHPPM\mu g\ U = (1.132 \pm 0.046) * ATC\beta_{eq}$$

The calculated regression coefficients for the sample types listed above are all within the range of theoretical regression coefficients between a "weightless" sample (1.5) and a sample with a 100-mg/cm^2 absorber between the sample and the detector (0.7). (Calculations assume that the uranium in the sample consists of 99.8% by mass U-238 and 0.2% by mass U-235 and is in equilibrium with its immediate short-lived progeny.)

A.2.1.5 Ingrowth

Uranium isotopes with immediate short-lived progeny that undergo beta emission include U-238 and U-235. The beta-emitting immediate short-lived progeny of U-238 include Th-234 ($t_{1/2}$ = 24.10 days) and Pa-234m ($t_{1/2}$ = 1.17 min). The beta-emitting immediate short-lived progeny of U-235 include Th-231 ($t_{1/2}$ = 25.5 hours). For a weightless sample of uranium that consists of 99.8% by mass U-238 and 0.2% by mass U-235 in equilibrium with its immediate short-lived progeny over 99% of the beta particle activity would come from the U-238 progeny. Furthermore, because the Pa-234m half-life is much shorter than Th-234, approximately 6 to 7 minutes are required for equilibrium to be established between the Th-234 and Pa-234m activity in the sample. Therefore, for the ingrowth analyses only the Th-234 rate of ingrowth had to be considered.

From calculations of "earlier count" beta/alpha activity ratios and "later count" beta/alpha activity ratios, it was apparent that some fraction of the beta progeny activity was not in equilibrium with its "parent" uranium activity. The fraction of beta progeny not in equilibrium immediately after the shot grows in according to the equation $1 - e^{-\lambda t}$, where λ is the Th-234 decay constant and "t" is the time between the shot and sample analysis. Therefore, the observed beta activity at time t_1 after the shot may be represented algebraically by Equation A.13.

$$\beta_{t1} = f\beta_{eq} + (1-f) * \beta_{eq} * (1-e^{-\lambda t}) \qquad \text{(A.13)}$$

where:

β_{t1} ≡ observed beta activity at time t_1
β_{eq} ≡ total beta activity at equilibrium
f ≡ fraction of total beta equilibrium activity that is in equilibrium at t_0
1-f ≡ fraction of total beta equilibrium activity that is not in equilibrium at t_0
λ ≡ Th-234 decay constant, ln 2 / 24.10 days
t ≡ time between t_1 (analysis date) and t_0 (shot date), in days.

There may be beta activity (Th/Pa) in the sample at time t_1 whose associated uranium activity is not in the sample. This activity, if *f* in the above equation equals 1, would decay according to the decay equation, $e^{-\lambda t}$. If this were the case, then the total beta activity at equilibrium (β_{eq}) will be overestimated because

some of the observed activity (β_{t1}) may be due to Th/Pa activity without the associated uranium activity. The beta activity (Th/Pa) in the sample at time t_1 whose associated uranium activity is not in the sample has been assumed to be zero to avoid the introduction of a second unknown into Equation A.13. Therefore, if *f* equals 1, the total beta activity at equilibrium (β_{eq}) calculated from a beta activity count shortly after the shot with the above equation may be overestimated.

Equation A.13 is solved for *f* and presented in Equation A.14:

$$f = \frac{\beta_{t1} - \beta_{eq}(1 - e^{-\lambda t})}{\beta_{eq} - \beta_{eq}(1 - e^{-\lambda t})} \qquad \text{A.14}$$

To calculate *f* for a sample, two beta activity analyses are required: one shortly after the shot and one much longer after the shot, as well as the dates of the activity analyses and the shot date. Short counts were selected based on a count date less than 75 days after the shot date, and long counts were selected based on a count date greater than or equal to 75 days after the shot date. The value of 75 days was selected by inspection of the data set and by the fact that if the Th-234 (24.1-day half-life) activity were completely separated from U-238 activity, 75 days later the Th-234 activity would be 88% of the U-238 activity. The data set selected included samples that were counted at ATC less than 75 days after the shot and at USACHPPM more than or equal to 75 days after the shot. The data set was further limited to samples for which the ATC beta activity was greater than 5 dpm and the USACHPPM beta activity was greater than its associated MDA. Initially, only samples with no significant sample loss as the result of sample handling were to be used in the analyses. However, for sample types that included CI stages 5 (CI-5) through 8 (CI-8) and the backup filter (CI-9), there were only four or fewer samples meeting these criteria. Therefore, another strategy had to be employed in selecting the samples for which to calculate individual *f* values.

The USACHPPM beta activity results (assumed to be at equilibrium since $\triangle t \geq 75$ days) were used to estimate the ATC beta activity results at equilibrium. The USACHPPM to ATC beta activity at equilibrium regression coefficients previously derived (Section A.2.1.2) were used. The ATC beta activity at equilibrium (derived from the USACHPPM beta activity analysis) was divided by the ATC initial beta activity. This calculated ratio was then categorized into three groups. Ratios less than 0.70 were categorized as 0.70, ratios between 0.70 and 1.30 inclusive were categorized as 1.0, and ratios greater than 1.30 were categorized as 1.30. Ratio category 2.00 was assigned to sample types DB, HV, and LA because they did not have estimates of the ATC beta activity. Sample loss between the ATC beta activity count and the USACHPPM beta activity count could explain ratios less than 0.7. Ingrowth could explain ratios greater than 1.3. And ratios between 0.7 and 1.3, category 1.0, are in a “gray area” where ingrowth is not occurring or ingrowth occurred which was offset by sample loss between the two analyses.

Individual *f* values were calculated using Equation A.14 for the 193 samples in categories 1.0 and 1.3. In order to apply the *f* values calculated, Equation A.13 was solved for the total beta activity at equilibrium (β_{eq}), and this relationship is presented below in Equation A.15.

$$\beta_{eq} = \frac{\beta_{t1}}{f + (1 - f) * (1 - e^{-\lambda t})} \qquad \text{A.15}$$

From Equation A.15, the total beta activity at equilibrium can now be predicted with an *f* value, one beta activity analysis, the date of the shot, and the date of the activity analysis. This ATC beta activity at equilibrium value can then be used to estimate the uranium mass. Regression coefficients to convert ATC beta activity at equilibrium to ICP-MS μg U results had been derived previously.

The question then becomes how to assign *f* values to a class of sample types. The decision rule simply assigned the median *f* value by sample type. If the median *f* value was greater than 1.0, it was set to 1.0 because the fraction of the beta activity at equilibrium at t_0 should not be greater than 100%. The median value was selected rather than the mean because it is usually a more robust measure of central tendency. The median value is not as sensitive as the mean value when outliers are in a data set or the data set distribution is skewed.

A summary of the sample type *f* value assigned is presented in Table A.5.

Table A.5. Total Beta Equilibrium Activity in Equilibrium at t_0

***f* Value Assigned**	
Sample Type	***f* value**
CF	0.163
CI-1	1.000
CI-2	0.839
CI-3	1.000
CI-4	1.000
CI-5	0.657
CI-6	0.299
CI-7	0.414
CI-8	0.156
CI-9	0.262
FS	0.395
MV	0.577
W	1.000

Sixty-eight samples that had been analyzed at ATC less than 75 days after the shot and were also analyzed for total uranium by ICP-MS at USACHPPM were used to verify the efficacy of the approach described above. The correlation for the measured uranium values versus estimated uranium values for all 68 samples was significant at the 0.01 level (0.958). The regression coefficient for the 68-sample data set was close to 1 (0.962). Samples in which the estimated uranium value is much greater than the USACHPPM-measured uranium value could be explained by sample loss between the two analyses, application of an ingrowth correction when beta progeny separation had not occurred, or the presence of Th/Pa progeny activity "unsupported" by U activity (if *f* value is 1). The presented data do not account for any of these situations if in fact they occurred.

Another technique to demonstrate the need for adjusting beta activity for ingrowth of short-lived progeny was employed. The ATC beta activity measured for samples counted at ATC ≤ 75 days after the shot was converted to uranium mass based on the ATC beta activity/uranium mass regression coefficients previously derived (Section A.2.1.2). Correlation and regression analyses were performed on the

"unadjusted beta activity" mass, and the uranium mass of these samples was measured by ICP-MS. For most, but not all, sample types, the correlation was significant at the 0.05 level or greater. However, the regression coefficients, which should be close to 1, ranged from 0.322 to 1.70.

A.2.1.6 FS, CI, and W Data Sets

The goal for the proportional counter data analysis was to predict the uranium mass in a sample based on a single ATC beta activity count at a known time after the shot. In order to accomplish this, several steps in the process must be completed including the ability to 1) predict USACHPPM beta activity from ATC beta activity, 2) predict ATC beta activity from USACHPPM beta activity, 3) predict uranium mass from ATC beta at equilibrium value, and 4) estimate the fraction of a sample type at equilibrium at the time of a shot. If one or more of these steps was unable to be completed, the ultimate goal could not be accomplished. Sample types FS, CI-1 through CI-9, and W had all the requisite steps completed. However, for sample types CF, HV, LA and MV one or more steps in the process were unable to be completed, usually due to an insufficient number of samples meeting the selection criteria. Therefore, only portions of the data analyses were performed on these sample types. An alternate approach, with additional ATC recount data has been developed for the MV sample type and is described in Section A.2.1.8).

A database of pertinent analytical data had been collated for all samples. A spreadsheet application was used to implement the database. The database contained the beta activity, the beta activity counting uncertainty, the shot date, and the beta activity analysis date. The calculated *f* medians were entered into the spreadsheet along with the regression coefficients for the ATC beta equilibrium to ICP-MS U mass values calculated in Section A.2.1.5 above for sample types FS, CI-1 through CI-9 (subsequently referred to as CI) and W. Equation A.15 was implemented in the spreadsheet to calculate the beta activity equilibrium value for the FS, CI, and W samples, using the beta activity, the shot date, the count date and the *f* median value. The beta activity equilibrium values were calculated using Equation A.15 and then the mass of uranium was calculated using Equation A.16.

$$\mu gU = ICP\_\mathrm{Re}g * \beta_{eq} \tag{A.16}$$

where *ICP_Reg* is the ATC beta activity at equilibrium to uranium mass regression coefficients derived in Section A.2.1.4.

A.2.1.7 Uncertainty Propagation

One-sigma uncertainties were propagated for the calculated values based on the counting uncertainties and derived values. Substituting Equation A.15 into A.16 results in Equation A.17. For simplicity in nomenclature Equation A.18 is substituted into Equation A.17 resulting in 3 terms to propagate into the uncertainty, which is propagated by Equation A.19. Mathematically rearranging Equation A.18 results in Equation A.20. Because the shot date, the count date, and the half-life of Th-234 are well known, the uncertainty in the fraction of Th-234 that ingrows in that time ($1 - e^{-\lambda t}$) is assumed to be zero. Substituting Equations A.18 and A.21 into Equation A.19 results in Equation A.22. Solving Equation A.22 for the 1-sigma uncertainty in the uranium mass estimate results in Equation A.23.

$$\mu gU = ICP\_\mathrm{Re}g * \frac{\beta_{t1}}{f + (1 - f)(1 - e^{-\lambda t})} \tag{A.17}$$

$$ING = f + (1 - f)\,(1 - e^{-\lambda t}) \tag{A.18}$$

$$\left(\frac{\sigma_{\mu g\,U}}{\mu g\,U}\right)^2 = \left(\frac{\sigma_{ICP\_Reg}}{ICP\_Reg}\right)^2 + \left(\frac{\sigma_{\beta t1}}{\beta_{t1}}\right)^2 + \left(\frac{\sigma_{ING}}{ING}\right)^2 \tag{A.19}$$

$$ING = f - f\,(1 - e^{-\lambda t}) + (1 - e^{-\lambda t}) \tag{A.20}$$

$$\sigma_{ING}^2 = \sigma_f^2 + (1 - e^{-\lambda t})^2\,\sigma_f^2 \tag{A.21}$$

$$\left(\frac{\sigma_{\mu g\,U}}{\mu g\,U}\right)^2 = \left(\frac{\sigma_{ICP\_Reg}}{ICP\_Reg}\right)^2 + \left(\frac{\sigma_{\beta t1}}{\beta_{t1}}\right)^2 + \left(\frac{\sigma_f^2 + (1 - e^{-\lambda t})^2\,\sigma_f^2}{\left[f + (1 - f)\,(1 - e^{-\lambda t})\right]^2}\right) \tag{A.22}$$

$$\sigma_{\mu g\,U} = \left|\mu g\,U\right| \sqrt{\left(\frac{\sigma_{ICP\_Reg}}{ICP\_Reg}\right)^2 + \left(\frac{\sigma_{\beta t1}}{\beta_{t1}}\right)^2 + \left(\frac{\sigma_f^2 + (1 - e^{-\lambda t})^2\,\sigma_f^2}{\left[f + (1 - f)\,(1 - e^{-\lambda t})\right]^2}\right)} \tag{A.23}$$

To implement Equation A.23 the uncertainties in the regression coefficients (σ_{ICP_Reg}), the beta activity count ($\sigma_{\beta t1}$) and the *f* median values (σ_f) are needed. The standard errors of the regression coefficients calculated in Section A.2.1.4 were used as estimates of σ_{ICP_Reg}. The 1-sigma beta counting uncertainties were used as estimates of $\sigma_{\beta t1}$. The average deviations from the f median values were used as estimates of σ_f.

A.2.1.8 MVF Data Set

Only one sample met the criteria for performing the regression that enabled ATC beta activity at equilibrium to be converted to uranium mass. Therefore an alternate approach was taken for the MVF (MV) sample type. Twenty-four MV segments were analyzed by proportional counting techniques at USACHPPM. Twelve of the 24 samples were then analyzed for uranium mass by ICP-MS. Two of the 24 samples were sent to PNNL for additional analyses. Ten samples remained and were reanalyzed by proportional counting at ATC. In the data analyses that follow this reanalysis at ATC is referred to as "ATC2 beta" or "A2 beta act."

ATC Beta to ICP-MS (μg U)

Graphs and correlations analyses for the USACHPPM beta activities and ATC2 beta activities were produced for all samples and then for only the samples that were analyzed 75 days or more after the shots. Nine of the 10 remaining samples were analyzed 75 days or more after the shots at USACHPPM and ATC2. Regression analyses were also performed. The beta regression equation (weighted regression through zero) derived from the 9 data points and used to predict ATC beta activity at equilibrium is presented below.

$$MV\ ATC\beta_{eq} = (0.917 \pm 0.001) * CHPPM\beta_{eq} \quad \text{A.24}$$

The above equation was used to predict the ATC beta at equilibrium value for the samples that had been analyzed by ICP-MS. Correlation and regression analyses were then performed on the predicted ATC values and the ICP-MS μg U results for samples analyzed at USACHPPM 75 days or more after the shot. For the 10 samples meeting this criterion, the ATC beta activity/USACHPPM uranium mass regression (iterative weighted regression through zero) equation derived from the data is presented below:

$$MV\ CHPPM\ \mu g\ U = (1.244 \pm 0.021) * ATC\beta_{eq} \quad \text{A.25}$$

MVF Ingrowth

Equation A.14 was used to calculate *f* values for the MV samples. For this calculation two beta activity analyses are required: one shortly after the shot and one much longer after the shot, as well as the dates of the activity analyses and the shot date. Short counts were selected based on an ATC count date less than 75 days after the shot date, and long counts were selected based on an ATC2 count date greater than or equal to 75 days after the shot date. The median *f* value for the MV sample type is 0.701, and the average deviation from the median is 0.234.

As described in Section A.2.1.4 and as shown in Equation A.15, the total beta activity at equilibrium is predicted with the median *f* value, one beta activity analysis, and the date of the shot and the date of the activity analysis. This ATC beta activity at equilibrium value is then used to estimate the uranium mass. The regression coefficient to convert ATC beta activity at equilibrium to ICP-MS μg U results had been derived in Section A.2.1.4.

Eleven samples that had been analyzed at ATC less than 75 days after the shot and were also analyzed for total uranium by ICP-MS at USACHPPM were used to verify the efficacy of the approach described above. The correlation between ICP-MS measured uranium values versus the estimated U values from the ATC beta activities using the above approach is significant at the 0.01 level (0.970). The regression coefficient for the 11-sample data set is close to 1 (1.255).

MVF Data Set Application

The database described in Section A.2.1.6 also contained pertinent analytical information for the MV sample type. A spreadsheet application was used to implement the database. The database contained the beta activity, the beta activity counting uncertainty, the shot date, and the beta activity analysis date. The *f* median value calculated above (MVF ingrowth) was entered into the spreadsheet along with the regression coefficient for the ATC beta equilibrium to ICP-MS U mass values calculated above (coefficient in Equation A.23) for the MV sample type. Equation A.15 was implemented in the spreadsheet to calculate the beta activity equilibrium value for the MV samples, using the beta activity, the shot date, the count date, and the *f* median value. The beta activity equilibrium values were calculated using Equation A.15, and then the mass of uranium was calculated using Equation A.16.

MVF Uncertainty Propagation

The 1-sigma uncertainty in the uranium mass estimate was propagated as previously described in Section A.2.1.7.

A.2.2 Uranium Mass Derived from Gamma Radioactivity

All samples selected for destructive analyses (ICP-MS or other chemical analysis technique) were analyzed by gamma spectrometry before the sample matrix was destroyed. Gamma spectrometry was performed at the USACHPPM laboratory on all sample types that were not analyzed by proportional counting, including media from the Andersen CIs (E-CI), the gloves (GL), the cyclone residues (CY), and the deposition tray debris (DT).

The USACHPPM laboratory analyzed 144 E-CI, 56 GL, 52 CY, and 93 DT samples by gamma spectrometry. Selected samples were then analyzed by ICP-MS, including 12 E-CI, 23 CY and 10 GL samples. The gamma analyses were usually performed well after the samples were collected. Therefore, gamma-emitting, immediate short-lived progeny disequilibrium was not an issue. SPSS was used to derive equations to predict the ICP-MS uranium mass from the gamma spectrometry results.

A.2.2.1 Gamma-Ray Energies and Abundances

The USACHPPM laboratory's gamma spectrometry nuclide library was updated for the U-238 short-lived gamma-emitting progeny (Th-234 and Pa-234m) and for U-235 and its short-lived gamma-emitting progeny, Th-231. Information presented in Table A.6 was obtained from Brookhaven National Laboratory's National Nuclear Data Center (http://www.nndc.bnl.gov/) and was used to update the gamma spectrometry nuclide library. The gamma spectrometry system's energy resolution is 0.75 keV per channel. Therefore, the system cannot resolve gamma energies of 92.38 and 92.80 keV (rec# 2.1 and 2.2) separately. These two gamma energies were treated as a single gamma line with an energy of 92.59 keV (average of 92.38 and 92.80) and an abundance of 5.58% (sum of 2.81% and 2.77%) in the nuclide library.

Table A.6. Uranium Gamma-Ray Energies and Abundances

Record #	Nuclide Name	Half-life	Energy (keV)	Abundance (%)
1	Th-234	24.10 d	63.29[(a)]	4.8
2.1	Th-234	24.10 d	92.38	2.81
2.2	Th-234	24.10 d	92.80	2.77
3	Pa-234m	1.17 m	766.36	0.294
4	Pa-234m	1.17 m	1001.03[(a)]	0.837
5	U-235	7.038E8 y	143.76[(a)]	10.96
6	U-235	7.038E8 y	163.33	5.08
7	U-235	7.038E8 y	185.715	57.2
8	U-235	7.038E8 y	205.311	5.01
9	Th-231	25.52 h	84.214[(a)]	6.6
10	Th-231	25.52 h	25.64	14.5

Notes: Th-234 energies and abundances are based on NNDC/BNL DATA (3/20/2000).
Pa-234m energies and abundances are based on NNDC/BNL DATA (2/8/00).
U-235 and Th-231 energies and abundances are based on NNDC/BNL DATA (8/5/99).
[a] Indicates gamma key-line.

A.2.2.2 Gamma Activity to Uranium Mass Conversions

The laboratory routinely reports only the activity, 95% counting uncertainty, and the MDA for the key-line of a gamma-emitting nuclide. To obtain the activity, counting uncertainty, and MDA for all gamma energy lines in the nuclide library, a custom report format was developed. However, this custom report format was not available electronically, so the gamma information for all lines in the nuclide library was manually transcribed into spreadsheets to expedite the subsequent data analyses. A second individual checked the spreadsheet entries for transcription accuracy.

Weighted means and weighted uncertainties were calculated for each nuclide in the nuclide library. The following formulas were implemented in the spreadsheets to calculate the weighted mean (Equation A.26) and weighted uncertainty (Equation A.27) for Th-234:

$$wt\_Th\_act = \frac{\frac{act\_63}{(unc_{95}\_63)^2} + \frac{act\_92}{(unc_{95}\_92)^2}}{\frac{1}{(unc_{95}\_63)^2} + \frac{1}{(unc_{95}\_92)^2}} \quad \text{A.26}$$

$$wt\_Th\_unc = \sqrt{\frac{1}{\frac{1}{(unc_{95}\_63)^2} + \frac{1}{(unc_{95}\_92)^2}}} \quad \text{A.27}$$

where:

wt_Th_act = weighted Th-234 mean activity
wt_Th_unc = weighted Th-234 counting uncertainty (95%)
act_63 = Th-234 gamma activity based on 63-keV gamma line
act_92 = Th-234 gamma activity based on 92-keV gamma line(s)
unc95_63 = 95% gamma counting uncertainty based on 63-keV line
unc95_92 = 95% gamma counting uncertainty based on 92keV line(s).

The specific activity of U-238 was then used to calculate the mass of U-238 in the samples based on the Th-234 and Pa-234m gamma activities and weighted mean activities. The results of the ICP-MS uranium mass analyses were merged into the spreadsheets.

The only samples analyzed by ICP-MS that did not consume the entire sample were the CY residues. A measured mass of the CY residues was analyzed. The gamma spectrometry analyses were performed on the entire samples as received. Therefore, the gamma spectrometry results and the ICP-MS results should be directly comparable for all samples except for the CY residues. The ICP-MS CY residue results were reported as μg U per gram of residue. The mass of CY residue collected and subsequently analyzed by

gamma spectrometry had been recorded and was then used to normalize the ICP-MS uranium mass concentrations to uranium mass per sample in order to compare these results to the gamma spectrometry results.

Various gamma lines were reviewed in the data analyses. The gamma spectrometry nuclide identification algorithm identified Th-234, if the peak search routine had identified peaks at 63 keV and 92 keV in the gamma ray spectrum. In some spectra only the 63 keV or 92 keV peak had been identified, and therefore, the nuclide identification algorithm did not identify the presence of Th-234. However, because these samples are known to contain uranium, these peaks when identified individually were also evaluated. The data were then examined using SPSS. Correlation analyses were performed on the ICP-MS results (µg_U) and the gamma spectrometry results converted to mass for the 63 keV, 92 keV, and the Th-234 weighted mean activities. The 63 keV (id_63µg) or the 92 keV (id_92µg) activities converted to mass were used when the peak search algorithm identified a peak at 63 keV or 92 keV, respectively, regardless of whether the other peak had been identified. The Th-234 weighted mean activity converted to mass (y_Th_µg) was used in the subsequent data analyses when the nuclide identification algorithm had identified Th-234 (both peaks identified by the peak search algorithm). For most sample types and all of the sample types of focus (E-CI, GL, and CY), the correlation of ICP-MS uranium results to the gamma spectrometry results converted to mass (id_63µg, id_92µg, and y_Th_µg) was significant at the 0.01 level. (See correlation analyses below.)

Regression analyses were performed with the ICP-MS results (µg_U) as the dependent variable, and the gamma spectrometry activity results converted to mass (id_63µg, id_92µg, and y_Th_µg) as the independent variable. First, unweighted regressions that were not forced through the origin were performed to demonstrate that the data supported forced regressions through the origin. Both the ICP-MS and gamma spectrometry analyses "subtracted" a background, so the regression model was expected to pass through the origin. Then unweighted regressions through the origin were performed. If the ICP-MS results and the gamma spectrometry results agreed, the regression coefficients were expected to be close to 1. The regression coefficients are summarized in Table A.7 and it is apparent that they are not close to 1. Because the regression coefficients were less than 1, the gamma spectrometry results predicted more uranium in the sample than were measured by ICP-MS.

The difference in the gamma spectrometry results versus the ICP-MS results varies from a factor of 4.95 (1/0.202) to 1.28 (1/0.781). It is hypothesized that sample geometry and efficiency calibration energy line differences in the gamma spectrometry analyses are the cause of the apparent differences. Both USACHPPM (ICP-MS) and PNNL (KPA, ICP-AES) analyzed several of the CY residues for uranium mass and the two laboratories' results agree. Several of the samples analyzed at USACHPPM by ICP-MS were also analyzed for U-235/U-238 atom ratios. The results of the ICP-MS atom ratios analyses are in very good agreement with the expected atom ratios for U.S. Army DU. The ICP-MS atom ratios were converted to U235/U238 activity ratios and compared with the U235/U238 activity ratios based on gamma spectrometry results. The two ratios were not in agreement. Therefore, it is believed that the gamma spectrometry results overestimated the true uranium content of the samples. A methodology was developed to "adjust" the gamma spectrometry results to "gold standard" ICP-MS results.

An iterative regression technique was applied to the gamma spectrometry results. The weighted regression coefficients were then used to predict the ICP-MS uranium mass values from the gamma spectrometry activity results converted to mass (id_63_µg, id_92µg, or y_Th_µg) dependent on which

Table A.7. Unweighted, Forced Regression Coefficients Summary

Sample Type	Regression Coefficients ± Standard Error		
	id_63μg	id_92μg	y_Th_μg
CF	0.425 ± 0.013	0.410 ± 0.013	0.418 ± 0.013
CI-1	0.338 ± 0.015	0.328 ± 0.020	0.338 ± 0.015
CI-2	0.202 ± 0.022	0.268 ± 0.036	0.235 ± 0.026
CI-3	0.203 ± 0.018	0.225 ± 0.025	0.226 ± 0.011
CI-4	0.259 ± 0.026	0.289 ± 0.025	0.278 ± 0.024
CI-5	0.286 ± 0.017	0.287 ± 0.021	0.288 ± 0.018
CI-6	0.269 ± 0.016	0.237 ± 0.024	0.262 ± 0.015
CI-7	0.251 ± 0.032	0.431 ± 0.058	0.319 ± 0.040
CI-8	0.343 ± 0.024	0.327 ± 0.019	0.343 ± 0.020
CI-9	0.331 ± 0.028	0.274 ± 0.026	0.301 ± 0.027
CY	0.556 ± 0.027	0.476 ± 0.022	0.515 ± 0.024
DB	0.270 ± 0.024	0.222 ± 0.018	0.243 ± 0.017
E-CI	0.616 ± 0.016	0.507 ± 0.011	0.562 ± 0.012
FS	0.456 ± 0.027	0.377 ± 0.018	0.414 ± 0.022
GL	0.781 ± 0.051	0.702 ± 0.038	0.739 ± 0.043
MV	0.395 ± 0.006	0.339 ± 0.007	0.363 ± 0.006
W	0.560 ± 0.049	0.455 ± 0.035	0.498 ± 0.040

Table A.8. Iterative Weighted, Forced Regression Coefficients Summary

Sample Type	Regression Coefficients ± Standard Error		
	id_63μg	id_92μg	y_Th_μg
CY	0.572 ± 0.026	0.478 ± 0.022	0.518 ± 0.024
E-CI	0.625 ± 0.012	0.511 ± 0.005	0.569 ± 0.006
GL	0.748 ± 0.047	0.679 ± 0.035	0.712 ± 0.040

The above regression coefficients were applied to the E-CI, GL, and CY data sets. One-sigma uncertainties were also propagated, similar to the uncertainties propagated for the beta activity analyses. No DT debris samples were analyzed by ICP-MS, but because the CY residues and the DT debris samples were both placed in vials for storage and gamma spectrometry analyses (i.e., their geometries were similar), the CY residue sample was a reasonable surrogate for adjusting the DT debris sample results.

A.3 Data Tables of Uranium Masses and Concentrations Derived from Beta and Gamma Counting

The flow and volume data discussed in Section A.1 and the uranium masses discussed in Section A.2 were used to calculate uranium aerosol concentrations listed in a series of tables at the end of Appendix A. These tables include total mass (where available), calculated uranium mass and uncertainty, flow rates, total volume, and the uranium concentration and its propagated uncertainty. Results of the uranium masses collected on the deposition trays and gloves are listed in the main text (Sections 5.3 and 5.4.3, respectively) and are not repeated here.

Data tables include the following:

- Tables A.9 through A.18 list IOM filter cassette sample data (beginning 5 sec post-shot) used to evaluate uranium aerosol concentration as a function of time. The entries are listed by crew position and time sequence.

- Tables A.19 through A.32 list the Marple CI sample data (beginning 5 sec post-shot) used to calculate uranium particle size distributions. The entries are listed by crew position and time sequence.

- Tables A.33 through A.37 list the radioactivity measurements of the MVF samples from the shots in which samples were successfully collected. The samples are numbered by 2.54-cm (1-in.) segments from the beginning at the time of perforation.

- Table A.38 lists the cyclone residues collected over the 2-h, post-shot interval.

- Table A.39 lists the Andersen CI sample uranium masses and aerosol concentrations collected exterior to the vehicle beginning with the PI-5 shot. Sample collection was initiated 10 sec post-shot.

- Table A.40 lists the personal IOM filter cassette sample masses and concentrations for samplers operated during sample recovery activities.

- Table A.41 lists the personal Marple CI sampler masses and concentration for samplers operated during sample recovery activities.

The data were imported from spreadsheet files, sometimes without regard to significance of the number of decimals carried in. As such, although round-off error is reduced in consequent calculations, it suggests a higher degree of significance than is intended. Most data summarized in the main text are reported to three significant figures. Hyphens in the columns instead of numerical data indicate the field blanks samples and filters that were damaged or did not run (intentionally or otherwise). MVF segments listed in the time column as “transition” indicate those sample segments between sampling intervals during which time no vacuum was pulled through the MVF.

Sample identification and data parameters listed in the tables are briefly discussed below. Flow and volume data, uranium mass, and propagation of uncertainty are discussed in Sections A.1 and A.2.

A.3.1 Sample Identification

The identification strategy included a series of alternating alpha and numeric components separated by hyphens. Each sample had a unique identifier. The sampling designators for all samples (including those presented in the main text and not repeated here) were as follows:

- Phases 1 through 4: represented as Roman numerals I, II, III, and IV

- Shots: numbered 1 through 7; double shots (those performed within a few minutes of each other) were noted as 1/2

- Sample location relative to vehicle: E=external, I-internal

- Position within vehicle: C=commander, L=loader, G=gunner, D=driver; for Phase-II tests on the Bradley vehicle, the pre-stamped G identifiers were used to indicate the right scout and the L identifiers were used for the left scout

- Position (programmed time interval) within array: 1 through 9

- Sampler type: FS=IOM filter cassettes, CI=Marple cascade impactor, CY=cyclone, DB=diffusion battery, MV=moving filter, CF=cyclone backup filter, DT=deposition tray, HV=Hi-Vol, E (when used in addition to E for external)=Andersen CI; P=samplers clipped to recovery team during resuspension tests

- Stage number (for CIs and CYs): 1 through x, where x represents the bottom or lowest stage (CIs have eight stages and the backup filter, which is designated as Stage 9; the CY has five stages).

For example, applying the sample identification system to the driver's IOM at position 3 from Phase I, Shot 2 (PI-2), yields the following sample number: PI-2I-D3-FS. The Stage-4 CI from the same array and operating at the same time interval is identified as PI-2I-D3-CI-4. In cases where there is little opportunity for confusion, shorter sample designations based on phase and shot are used in this report. For example, PI-1 is the shorthand for Phase I, Shot 1.

A.3.2 Sample Collection Intervals and Sampling Durations (Elapsed Time)

The second and third columns in the data tables list the sample collection interval and elapsed sample time (sample duration) for the each of the sampling types. The sampling times also are listed separately by phase and shot in Chapter 4. Except where indicated otherwise, the sample intervals for IOM and CI sampler arrays are based on time beginning 5 sec post-shot.

A.3.3 Total Mass

Tables A.9 through A.32 provide each net weight of the total mass (Column 4) of sample collected on each filter or substrate as discussed in Sections 5.1.2.1 and 5.1.3.1. With a few exceptions, all IOM filter weights of filters that were not damaged by the shot were positive and could be used in conjunction with the net DU mass (Column 7) to estimate the percent of uranium in the sample. However, many of the CI substrate weights were negative (discussed in Section 5.1.3.1), and these data should not be used. The Andersen CI substrates were not weighed, and consequently, no mass measurements are listed for these samples.

A.3.4 Calculated Uranium Mass

Column 5 provides the derived uranium mass based on the beta radioactivity measurements of each sample before subtracting the field blank, if appropriate. The calculations were adjusted for radioactivity (progeny) ingrowth for those samples counted shortly after the aerosol was generated. The field blanks

(samplers that were in the array but did not pull a vacuum) are noted in the data set for each crew position. For the IOMs, the field blank was usually, but not always, the ninth IOM in each array. Some field blanks were destroyed or collected an unusually high amount of uranium. In those circumstances, a field blank from another array was used instead. The field blank for each eight-stage CI was usually the ninth CI in the array. With the CI samples, the uranium mass on the corresponding stage was subtracted from the total mass to calculate net mass. For samples that were analyzed by ICP-MS, the listed results are from the chemical analysis rather than derived the radioactivity (unless the beta-derived mass was greater), and an "NA" appears in the uncertainty column.

A.3.5 DU Mass Uncertainty

The DU mass uncertainty at the 1-sigma level was calculated for each radioactivity measurement of calculated uranium mass (Column 4). These uncertainties are based on statistical counting. For a discussion of the calculation of these uncertainties, see Section A.2. For samples that were chemically analyzed, an "NA" appears in the uncertainty column.

A.3.6 Net DU Mass

The net DU mass was calculated by subtracting the appropriate field blank from the calculated uranium listed in Column 5. In the samples that also were analyzed using chemical analysis, the higher of the two values appears in this column. Samples that collected less radioactivity than the field blank are shown as negative in these tables.

A.3.7 Flow Rate

Column 8 contains the average flow rates (Lpm) measured from and calibrated against pressure drops through the filters. The flow data are discussed in Section A.1.

A.3.8 Volume

The total sample volume in liters collected is listed in Column 9. The volume data are discussed in Section A.1.

A.3.9 DU Concentration

The DU mass concentration represented by the net mass (Column 7) divided by the volume is listed in Column 10. These numbers are based on volumes expressed in micrograms per cubic meter. For samples in which the field blank was higher than the sample blank, the calculations were carried through, and the numbers listed are negative. In summary tables in the text, negative numbers are shown as being approximately at background levels.

A.3.10 DU Concentration Uncertainty

Propagation of uncertainties based on the DU mass uncertainty and the uncertainties associated with the volume measurement are listed in Column 11. The calculations on which uncertainties related to radio-activity are based are discussed in Section A.2. For those samplers controlled by LabView, a value of 3%

was used in calculating volume-related uncertainty. A factor of 10%, not measured but believed to be reasonable, was applied to the remaining samplers. Volume uncertainties applied were the following:

- IOM filter cassette samplers—3%
- Marple CI samplers—3%
- Moving filter sampler—3%
- Cyclone—3%
- Andersen CI samplers—10%
- Personal filter cassette samplers—10%
- Personal CI samplers—10%

For samples that were chemically analyzed, an "NA" appears in the uncertainty column, and these were not propagated because the laboratory did not report analytical uncertainties.

For further explanation of the net DU mass uncertainty and the DU concentration mass uncertainty, refer to Section A.2.1.7.

Table A.9. PI-1 IOM Filters—Mass, Volume, and Concentration

Sample ID	Collection Interval	Elapsed Time	Total Mass (mg)	Calculated U (μg)	DU Mass ± 1σ (μg)	Net DU Mass (μg)	Flow Rate (Lpm)	Volume (L)	DU Conc. (μg/m^3)	DU Conc. ± 1σ (μg/m^3)
PI-1I-C1-FS	0-30 sec	30 sec	1.899	(a)	--	--	--	--	--	--
PI-1I-C2-FS	0.5-1.5 min	1 min	1.123	(a)	--	--	--	--	--	--
PI-1I-C3-FS	1.5-3.5 min	2 min	17.333	(a)	--	--	--	--	--	--
PI-1I-C4-FS	3.5-7.5 min	4 min	13.144	(a)	--	--	--	--	--	--
PI-1I-C5-FS	7.5-15.5 min	8 min	0.972	(a)	--	--	--	--	--	--
PI-1I-C6-FS	15.5-31.5 min	16 min	2.249	(a)	--	--	--	--	--	--
PI-1I-C7-FS	31.5-63.5 min	32 min	1.08	(a)	--	--	--	--	--	--
PI-1I-C8-FS	63.6-127.5 min	64 min	1.677	(a)	--	--	--	--	--	--
PI-1I-C9-FS	Field Blank	--	1.115	(a)	--	--	--	--	--	--
PI-1I-D1-FS	0-30 sec	30 sec	5.316	3987	1256	3802	2.294	1.15	3.31E+06	1.10E+06
PI-1I-D2-FS	0.5-1.5 min	1 min	3.853	2677	845	2491	2.509	2.51	9.93E+05	3.39E+05
PI-1I-D3-FS	1.5-3.5 min	2 min	6.253	3611	1139	3425	2.485	4.97	6.89E+05	2.30E+05
PI-1I-D4-FS	3.5-7.5 min	4 min	4.676	2850	NA[(b)]	2664	2.518	10.1	2.65E+05	NA[(b)]
PI-1I-D5-FS	7.5-15.5 min	8 min	2.95	1646	522	1460	2.291	18.3	7.97E+04	2.88E+04
PI-1I-D6-FS	15.5-31.5 min	16 min	3.926	1980	NA[(b)]	1794	2.452	39.2	4.57E+04	NA[(b)]
PI-1I-D7-FS	31.5-63.5 min	32 min	4.809	2660	NA[(b)]	2474	2.375	76.0	3.26E+04	NA[(b)]
PI-1I-D8-FS	63.6-127.5 min	64 min	8.585	4220	NA[(b)]	4034	2.161	138	2.92E+04	NA[(b)]
PI-1I-D9-FS	Field Blank	--	0.29	186	59	--	--	--	--	--
PI-1I-G1-FS	0-30 sec	30 sec	1.578	(a)	--	--	--	--	--	--
PI-1I-G2-FS	0.5-1.5 min	1 min	0.52	(a)	--	--	--	--	--	--
PI-1I-G3-FS	1.5-3.5 min	2 min	-0.415	(a)	--	--	--	--	--	--
PI-1I-G4-FS	3.5-7.5 min	4 min	0.532	(a)	--	--	--	--	--	--
PI-1I-G5-FS	7.5-15.5 min	8 min	-0.252	(a)	--	--	--	--	--	--
PI-1I-G6-FS	15.5-31.5 min	16 min	1.244	(a)	--	--	--	--	--	--
PI-1I-G7-FS	31.5-63.5 min	32 min	-1.371	(a)	--	--	--	--	--	--
PI-1I-G8-FS	63.6-127.5 min	64 min	0.621	(a)	--	--	--	--	--	--
PI-1I-G9-FS	Field Blank	--	0.808	(a)	--	--	--	--	--	--
PI-1I-L1-FS	0-30 sec	30 sec	23.21	17491	5492	17426	2.064	1.03	1.69E+07	5.35E+06
PI-1I-L2-FS	0.5-1.5 min	1 min	18.771	12402	3896	12337	2.093	2.09	5.89E+06	1.87E+06
PI-1I-L3-FS	1.5-3.5 min	2 min	18.277	11141	3500	11075	2.077	4.15	2.67E+06	8.46E+05
PI-1I-L4-FS	3.5-7.5 min	4 min	19.451	10313	3241	10248	2.088	8.35	1.23E+06	3.90E+05
PI-1I-L5-FS	7.5-15.5 min	8 min	11.368	5767	1814	5701	2.101	16.8	3.39E+05	1.08E+05
PI-1I-L6-FS	15.5-31.5 min	16 min	4.647	2115	669	2050	2.327	37.2	5.51E+04	1.81E+04
PI-1I-L7-FS	31.5-63.5 min	32 min	5.091	1693	536	1627	2.281	73.0	2.23E+04	7.38E+03
PI-1I-L8-FS	63.6-127.5 min	64 min	7.957	2864	904	2799	2.194	140	1.99E+04	6.47E+03
PI-1I-L9-FS	Field Blank	--	0.143	65	22	--	--	--	--	--

(a) Filter damaged.
(b) DU mass based on ICP-MS results; no analytical uncertainty was reported.

Table A.10. PI-2 IOM Filters—Mass, Volume, and Concentration

Sample ID	Collection Interval	Elapsed Time	Total Mass (mg)	Calculated U (μg)	DU Mass ± 1σ (μg)	Net DU Mass (μg)	Flow Rate (Lpm)	Volume (L)	DU Conc. (μg/m^3)	DU Conc. ± 1σ (μg/m^3)
PI-2I-C-1-FS	0-15 sec	15 sec	8.782	3797	862	3669	2.622	0.655	5.60E+06	1.33E+06
PI-2I-C-2-FS	0.5-1 min	30 sec	0.868	(a)	--	--	2.669	--	--	--
PI-2I-C-3-FS	1.5-2.5 min	1 min	12.13	5708	1295	5579	2.336	2.336	2.39E+06	5.59E+05
PI-2I-C-4-FS	3.5-5.5 min	2 min	12.309	5881	1336	5753	2.208	4.417	1.30E+06	3.05E+05
PI-2I-C-5-FS	7.5-11.5 min	4 min	6.697	3319	754	3191	2.292	9.169	3.48E+05	8.29E+04
PI-2I-C-6-FS	Did not run	--	-4.957	--	--	--	n/a[(c)]	--	--	--
PI-2I-C-7-FS	Did not run	--	0.919	--	--	--	n/a[(c)]	--	--	--
PI-2I-C-8-FS	15.5-31.5 min	16 min	0.979	(a)	--	--	2.74	--	--	--
PI-2I-C-9-FS	31.5-79.5 min	48 min	4.144	1744	396	1615	2.551	122.5	1.32E+04	3.27E+03
PI-2I-D-1-FS	0-15 sec	15 sec	7.108	3643	827	3514	2.344	0.586	6.00E+06	1.42E+06
PI-2I-D-2-FS	0.5-1 min	30 sec	6.587	3345	760	3217	2.445	1.223	2.63E+06	6.27E+05
PI-2I-D-3-FS	1.5-2.5 min	1 min	6.184	3239	736	3111	2.551	2.551	1.22E+06	2.91E+05
PI-2I-D-4-FS	3.5-5.5 min	2 min	7.794	3947	896	3818	2.44	4.88	7.82E+05	1.85E+05
PI-2I-D-5-FS	7.5-11.5 min	4 min	4.49	2269	516	2141	2.343	9.374	2.28E+05	5.56E+04
PI-2I-D-6-FS	15.5-31.5 min	16 min	7.785	3551	806	3422	2.472	39.56	8.65E+04	2.06E+04
PI-2I-D-7-FS	31.5-79.5 min	48 min	12.55	5096	1157	4968	2.395	115.0	4.32E+04	1.01E+04
PI-2I-D-8-FS	79.5-127.5 min	48 min	14.064	5549	1260	5421	2.125	102.0	5.32E+04	1.25E+04
PI-2I-D-9-FS	Field Blank[(c)]	--	0.334	128[c]	30	--	--	--	--	--
PI-2I-G-1-FS	0-15 sec	15 sec	1.58	(a)	--	--	--	--	--	--
PI-2I-G-2-FS	Field Blank	--	0.988	(a)	--	--	--	--	--	--
PI-2I-G-3-FS	0.5-1 min	30 sec	1.772	(a)	--	--	--	--	--	--
PI-2I-G-4-FS	1.5-2.5 min	1 min	-0.282	(a)	--	--	--	--	--	--
PI-2I-G-5-FS	3.5-5.5 min	2 min	-0.31	(a)	--	--	--	--	--	--
PI-2I-G-6-FS	7.5-11.5 min	4 min	1.022	(a)	--	--	--	--	--	--
PI-2I-G-7-FS	15.5-31.5 min	16 min	4.434	(a)	--	--	--	--	--	--
PI-2I-G-8-FS	31.5-79.5 min	48 min	2.76	1422	324	826	2.774	44.38	1.86E+04	7.93E+03
PI-2I-G-9-FS	79.5-127.5 min	48 min	0.383	(a)	--	--	--	--	--	--
PI-2I-L-1-FS	0-15 sec	15 sec	0.707	(a)	62.5	--	2.722	--	--	--
PI-2I-L-2-FS	0.5-1 min	30 sec	11.77	5655	1284	5527	2.279	1.14	4.85E+06	1.14E+06
PI-2I-L-3-FS	1.5-2.5 min	1 min	11.708	5771	1310	5643	2.206	2.206	2.56E+06	5.99E+05
PI-2I-L-4-FS	3.5-5.5 min	2 min	0.34	(a)	--	--	--	--	--	--
PI-2I-L-5-FS	Did not run	--	0.121	--	--	--		--	--	--
PI-2I-L-6-FS	7.5-11.5 min	4 min	4.502	2200	500	2072	2.412	7.639	2.71E+05	6.61E+04
PI-2I-L-7-FS	15.5-31.5 min	16 min	6.932	2946	669	2817	2.341	37.45	7.52E+04	1.80E+04
PI-2I-L-8-FS	31.5-79.5 min	48 min	4.788	3345	759	3216	2.382	114.3	2.81E+04	6.70E+03
PI-2I-L-9-FS	79.5-127.5 min	48 min	-0.183	(a)	--	--	--	--	--	--

(a) Filter damaged.
(b) Field blank filter damaged but U concentration used for FS8 as most representative of gunner samples.
(c) Field blank from driver's sample.

Table A.11. PI-3/4 IOM Filters—Mass, Volume, and Concentration

Sample ID	Collection Interval	Elapsed Time	Total Mass (mg)	Calculated U (μg)	DU Mass ± 1σ (μg)	Net DU Mass (μg)	Flow Rate (Lpm)	Volume (L)	DU Conc. (μg/m^3)	DU Conc. ± 1σ (μg/m^3)
PI-3/4I-C-1-FS	Shot 4: 0-10 sec	10 sec	9.288	8652	2781	8326	2.209	0.368	2.26E+07	7.59E+06
PI-3/4I-C-2-FS	3-3.5 min	30 sec	7.615	5501	1770	5175	2.339	1.17	4.42E+06	1.52E+06
PI-3/4I-C-3-FS	9-10 min	1 min	4.958	2834	914	2509	2.309	2.309	1.09E+06	3.98E+05
PI-3/4I-C-4-FS	21-23 min	2 min	2.297	1035	335	710	2.429	4.858	1.46E+05	7.03E+04
PI-3/4I-C-5-FS	45-49 min	4 min	2.745	1067	345	742	2.304	9.214	8.06E+04	3.81E+04
PI-3/4I-C-6-FS	93-101 min	8 min	3.949	1262	408	937	2.359	18.876	4.96E+04	2.19E+04
PI-3/4I-C-7-FS	Field Blank	--	0.32	204	66.8	--	--	--	--	--
PI-3/4I-C-8-FS	Field Blank	--	0.682	413	133	--	--	--	--	--
PI-3/4I-C-9-FS	Field Blank	--	0.593	358	116	--	--	--	--	--
PI-3/4I-D-1-FS	Shot 3: 0-10 sec	10 sec	4.006	3251	1046	2574	2.193	0.365	7.05E+06	2.93E+06
PI-3/4I-D-2-FS	3-3.5 min	30 sec	6.001	4266	1372	3588	2.407	1.203	2.98E+06	1.16E+06
PI-3/4I-D-3-FS	9-10 min	1 min	4.645	2865	922	2188	2.487	2.487	8.80E+05	3.82E+05
PI-3/4I-D-4-FS	Shot 4: 0-10 sec	10 sec	4.941	4553	1464	3876	2.524	0.421	9.21E+06	3.53E+06
PI-3/4I-D-5-FS	3-3.5 min	30 sec	4.676	3303	1063	2626	2.3	1.15	2.28E+06	9.46E+05
PI-3/4I-D-6-FS	9-10 min	1 min	5.273	3249	1047	2572	2.477	2.477	1.04E+06	4.33E+05
PI-3/4I-D-7-FS	21-23 min	2 min	0.482	232	75.5	-445	2.652	5.304	-8.39E+04	4.36E+04
PI-3/4I-D-8-FS	45-49 min	4 min	3.238	1563	504	886	2.418	9.673	9.16E+04	5.68E+04
PI-3/4I-D-9-FS	Field Blank	--	0.711	677	218	--	--	--	--	--
PI-3/4I-G-1-FS	Shot 3: 0-10 sec	10 sec	2.444	2068	666	1391[(b)]	2.38	0.397	3.50E+06	1.77E+06
PI-3/4I-G-2-FS	Field Blank	--	77.787	15945[)b)]	5120	--	--	--	--	--
PI-3/4I-G-3-FS	3-3.5 min	30 sec	3.369	2891	929	2214	2.316	1.158	1.91E+06	8.26E+05
PI-3/4I-G-4-FS	9-10 min	1 min	3.005	2226	717	1549	2.425	2.425	6.39E+05	3.10E+05
PI-3/4I-G-5-FS	Shot 4: 0-10 sec	10 sec	1.008	(a)	--	--	--	--	--	--
PI-3/4I-G-6-FS	3-3.5 min	30 sec	6.192	4573	1471	3895	2.522	1.229	3.17E+06	1.21E+06
PI-3/4I-G-7-FS	9-10 min	1 min	5.308	3360	1082	2683	2.457	2.36	1.14E+06	4.69E+05
PI-3/4I-G-8-FS	21-23 min	2 min	3.86	2414	778	1736	2.36	5.097	3.41E+05	1.59E+05
PI-3/4I-G-9-FS	45-49 min	4 min	3.613	2058	661	1381	2.549	9.782	1.41E+05	7.13E+04
PI-3/4I-L-1-FS	Shot 4: 0-10 sec	10 sec	-1.236	(c)	473	--	2.628	--	--	--
PI-3/4I-L-2-FS	3-3.5 min	30 sec	-9.203	(c)	1045	--	2.58	--	--	--
PI-3/4I-L-3-FS	9-10 min	1 min	4.328	4772	1533	2081[(d)]	2.54	2.54	8.19E+05	6.94E+05
PI-3/4I-L-4-FS	21-23 min	2 min	-4.063	(c)	388	--	2.63	--	--	--
PI-3/4I-L-5-FS	45-49 min	4 min	6.719	4412	1417	1721	2.394	9.578	1.80E+05	1.73E+05
PI-3/4I-L-6-FS	93-101 min	8 min	7.293	4158	1337	1468	2.439	19.513	7.52E+04	8.16E+04
PI-3/4I-L-7-FS	Field Blank	--	-12.032	(c)	146	--	--	--	--	--
PI-3/4I-L-8-FS	Field Blank	--	2.718	2690	864	--	--	--	--	--
PI-3/4I-L-9-FS	Field Blank	--	2.58	(c)	871	--	--	--	--	--

(a) IOM sampling head separated from stem.
(b) Driver's field blank replaced gunner's field blank, which had collected a large DU particle.
(c) Filter damaged.
(d) Used Loader 8 as field blank—may not be very meaningful.

Table A.12. PI-5 IOM Filters—Mass, Volume, and Concentration

Sample ID	Collection Interval	Elapsed Time	Total Mass (mg)	Calculated U (μg)	DU Mass ± 1σ (μg)	Net DU Mass (μg)	Flow Rate (Lpm)	Volume (L)	DU Conc. (μg/m^3)	DU Conc. ± 1σ (μg/m^3)
PI-5I-C1-FS	0-10 sec	10 sec	10.509	10330	3852	10042	2.393	0.399	2.52E+07	9.69E+06
PI-5I-C2-FS	1-1 min 10 sec	10 sec	3.222	2850	1064	2562	2.504	0.376	6.81E+06	2.85E+06
PI-5I-C3-FS	3-3 min 10 sec	10 sec	1.179	886	332	598	2.565	0.427	1.40E+06	8.19E+05
PI-5I-C4-FS	7-7.5 min	30 sec	0.593	389	147	101	2.504	1.252	8.07E+04	1.45E+05
PI-5I-C5-FS	15-16 min	1 min	0.451	276	105	-12.4	2.506	2.506	-4.77E+03	5.78E+04
PI-5I-C6-FS	31-33 min	2 min	0.608	436	164	148	2.665	5.33	2.78E+04	3.69E+04
PI-5I-C7-FS	61-65 min	4 min	0.93	517	195	229	2.779	11.116	2.06E+04	2.00E+04
PI-5I-C8-FS	121-129 min	8 min	1.405	720	271	432	2.69	21.524	2.01E+04	1.36E+04
PI-5I-C9-FS	Field Blank	--	0.366	288	108	--	--	--	--	--
PI-5I-D1-FS	0-10 sec	10 sec	6.362	6519	2431	6106	2.493	0.415	1.47E+07	5.89E+06
PI-5I-D2-FS	1-1 min 10 sec	10 sec	3.661	3174	1185	2762	2.538	0.381	7.25E+06	3.14E+06
PI-5I-D3-FS	3-3 min 10 sec	10 sec	0.889	727	273	314	2.641	0.44	7.13E+05	7.13E+05
PI-5I-D4-FS	7-7.5 min	30 sec	0.511	455	170	41.7	2.624	1.312	3.18E+04	1.77E+05
PI-5I-D5-FS	15-16 min	1 min	0.394	454	170	41.5	2.601	2.601	1.60E+04	8.73E+04
PI-5I-D6-FS	31-33 min	2 min	0.664	525	197	112	2.634	5.267	2.12E+04	4.77E+04
PI-5I-D7-FS	61-65 min	4 min	1.075	793	296	380	2.554	10.217	3.72E+04	3.27E+04
PI-5I-D8-FS	121-129 min	8 min	1.486	913	343	500	2.424	19.395	2.58E+04	1.94E+04
PI-5I-D9-FS	Field Blank	--	0.403	413	154	--	--	--	--	--
PI-5I-L1-FS	0-10 sec	10 sec	3.229	3016	1126	2728[(a)]	2.602	0.434	6.29E+06	2.61E+06
PI-5I-L2-FS	1-1 min 10 sec	10 sec	2.523	2103	786	1815	2.532	0.38	4.78E+06	2.09E+06
PI-5I-L3-FS	3-3 min 10 sec	10 sec	0.884	663	249	375	2.515	0.419	8.94E+05	6.49E+05
PI-5I-L4-FS	7-7.5 min	30 sec	0.031	432	163	144	2.62	1.31	1.10E+05	1.49E+05
PI-5I-L5-FS	15-16 min	1 min	0.591	458	172	170	2.537	2.537	6.68E+04	8.02E+04
PI-5I-L6-FS	31-33 min	2 min	0.581	395	149	107	2.605	5.209	2.05E+04	3.54E+04
PI-5I-L7-FS	61-65 min	4 min	0.995	631	237	343	2.564	10.256	3.35E+04	2.54E+04
PI-5I-L8-FS	121-129 min	8 min	1.409	788	296	500	2.388	19.103	2.62E+04	1.65E+04
PI-5I-L9-FS	144-148 min	4 min	0.79	554	208	267	2.469	9.877	2.70E+04	2.36E+04

(a) Commander's field blank used to substitute for a loader's field blank. Gunner position array was not used.

Table A.13. PI-6 IOM Filters—Mass, Volume, and Concentration

Sample ID	Collection Interval	Elapsed Time	Total Mass (mg)	Calculated U (μg)	DU Mass ± 1σ (μg)	Net DU Mass (μg)	Flow Rate (Lpm)	Volume (L)	DU Conc. (μg/m^3)	DU Conc. ± 1σ (μg/m^3)
PI-6I-C1-FS	0-10 sec	10 sec	12.825	8550	2264.9	8090.82	2.159	0.36	2.25E+07	6.35E+06
PI-6I-C2-FS	1-1 min 10 sec	10 sec	3.07	2766	1032.7	2306.61	2.426	0.404	5.71E+06	2.60E+06
PI-6I-C3-FS	3-3 min 10 sec	10 sec	0.959	779	291.4	318.92	2.434	0.406	7.86E+05	8.35E+05
PI-6I-C4-FS	7-7.5 min	30 sec	0.63	466	174.6	6.08	2.341	1.17	5.20E+03	2.21E+05
PI-6I-C5-FS	15-16 min	1 min	0.529	444	166.4	-15.2	2.49	2.49	-6.26E+03	9.84E+04
PI-6I-C6-FS	31-33 min	2 min	0.478	372	139.3	-88.05	2.51	5.02	-1.74E+04	4.38E+04
PI-6I-C7-FS	61-65 min	4 min	1.033	810	303	350.5	2.801	11.204	3.13E+04	3.11E+04
PI-6I-C8-FS	121-129 min	8 min	1.472	850	318.2	390.5	2.694	21.553	1.81E+04	1.68E+04
PI-6I-C9-FS	Field Blank	--	0.418	460	171.6	--	--	--	--	--
PI-6I-D1-FS	0-10 sec	10 sec	5.688	5702	2126.4	5599.08	2.524	0.421	1.33E+07	5.07E+06
PI-6I-D2-FS	1-1 min 10 sec	10 sec	1.813	1428	533.9	1325.45	2.518	0.42	3.16E+06	1.28E+06
PI-6I-D3-FS	3-3 min 10 sec	10 sec	0.978	647	242.8	544.35	2.685	0.448	1.22E+06	5.50E+05
PI-6I-D4-FS	7-7.5 min	30 sec	0.564	368	138.5	265.53	2.849	1.425	1.86E+05	1.01E+05
PI-6I-D5-FS	15-16 min	1 min	0.527	234	88	131.22	2.48	2.48	5.29E+04	3.88E+04
PI-6I-D6-FS	31-33 min	2 min	0.467	238	89.6	134.92	2.838	5.677	2.38E+04	1.73E+04
PI-6I-D7-FS	61-65 min	4 min	0.809	342	129	239.19	2.489	9.954	2.40E+04	1.36E+04
PI-6I-D8-FS	121-129 min	8 min	0.208	119	44.9	16.68	2.514	20.112	8.30E+02	2.87E+03
PI-6I-D9-FS	Field Blank	--	0.217	103	38.7	--	--	--	--	--
PI-6I-L1-FS	0-20 min[(a)]	20 min	0.214	228	85.7	149.7	2.54	50.807	2.95E+03	1.70E+03
PI-6I-L2-FS	31-54 min	~23 min	0.366	340	127.8	261.7	2.554	57.849	4.52E+03	2.22E+03
PI-6I-L3-FS	54-67 min	~13 min	0.2	193	72.5	114.4	2.567	34.142	3.35E+03	2.14E+03
PI-6I-L4-FS	67-82 min	~15 min	0.282	278	104.6	199.2	2.562	37.747	5.28E+03	2.79E+03
PI-6I-L5-FS	82-104 min	~22 min	0.348	343	128.3	264.5	2.498	54.172	4.88E+03	2.38E+03
PI-6I-L6-FS	105-107 min	2 min	0.257	226	85.3	147.2	2.573	5.147	2.86E+04	1.67E+04
PI-6I-L7-FS	107-111 min	4 min	0.301	293	109.8	214.7	2.554	10.218	2.10E+04	1.08E+04
PI-6I-L8-FS	111-119 min	8 min	0.357	380	142.6	301.3	2.397	19.176	1.57E+04	7.46E+03
PI-6I-L9-FS	119-135 min	16 min	0.339	372	139.7	293.6	2.458	39.327	7.46E+03	3.57E+03

(a) Loader's position sampling began at 2 h and 35 min (represented as zero) post shot for resuspension evaluation. Gunner position array was not used. Field blank average from PI-7 loader was applied.

Table A.14. PI-7 IOM Filters—Mass, Volume, and Concentration

Sample ID	Collection Interval	Elapsed Time	Total Mass (mg)	Calculated U (μg)	DU Mass ± 1σ (μg)	Net DU Mass (μg)	Flow Rate (Lpm)	Volume (L)	DU Conc. (μg/m^3)	DU Conc. ± 1σ (μg/m^3)
PI-7I-C1-FS	0-10 sec	10 sec	11.64	5917	1346.9	5802.97	2.445	0.407	1.43E+07	3.34E+06
PI-7I-C2-FS	1-1 min 10 sec	10 sec	4.796	2051	467.5	1936.9	2.452	0.409	4.74E+06	1.15E+06
PI-7I-C3-FS	3-3 min 15 sec	15 sec	3.687	1704	388.6	1589.94	2.455	0.614	2.59E+06	6.39E+05
PI-7I-C4-FS	7-8 min	1 min	5.177	2097	478.1	1982.88	2.395	2.395	8.28E+05	2.01E+05
PI-7I-C5-FS	15-17 min	2 min	2.149	1026	234.2	911.87	2.448	4.895	1.86E+05	4.85E+04
PI-7I-C6-FS	31-35 min	4 min	1.88	856	195.5	741.07	2.618	10.472	7.08E+04	1.90E+04
PI-7I-C7-FS	61-69 min	8 min	3.106	1482	338.1	1367.97	2.732	21.856	6.26E+04	1.56E+04
PI-7I-C8-FS	121-129 min	8 min	2.386	1092	249.3	977.23	2.606	20.848	4.69E+04	1.21E+04
PI-7I-C9-FS	Field Blank	--	0.207	114	26.6	--	--	--	--	--
PI-7I-D1-FS	0-10 sec	10 sec	6.309	3303	752.2	3227.46	2.264	0.377	8.56E+06	2.01E+06
PI-7I-D2-FS	1-1 min 10 sec	10 sec	4.781	2471	561.7	2396.07	2.586	0.431	5.56E+06	1.31E+06
PI-7I-D3-FS	3-3 min 15 sec	15 sec	3.88	1947	444.1	1872	2.665	0.666	2.81E+06	6.73E+05
PI-7I-D4-FS	7-8 min	1 min	4.637	2356	535.6	2281.15	2.61	2.61	8.74E+05	2.07E+05
PI-7I-D5-FS	Did not run	2 min	0.158	(a)	18.2	--	2.346	--	--	--
PI-7I-D6-FS	31-35 min	4 min	1.557	624	142.7	548.82	2.603	10.411	5.27E+04	1.39E+04
PI-7I-D7-FS	61-69 min	8 min	2.617	1178	268.9	1103.23	2.485	19.884	5.55E+04	1.37E+04
PI-7I-D8-FS	121-129 min	8 min	2.399	1081	246.5	1005.42	2.471	19.771	5.09E+04	1.26E+04
PI-7I-D9-FS	Field Blank	--	0.165	75	17.7	--	--	--	--	--
PI-7I-G1-FS	0-10 sec	10 sec	10.548	4864	1107.7	4724.58	2.429	0.405	1.17E+07	2.76E+06
PI-7I-G2-FS	Field Blank	--	0.277	139	32.1	--	--	--	--	--
PI-7I-G3-FS	1-1 min 10 sec	10 sec	5.08	2674	609.8	2535.47	2.508	0.418	6.07E+06	1.47E+06
PI-7I-G4-FS	3-3 min 15 sec	15 sec	4.2	2069	471.7	1930.19	2.557	0.639	3.02E+06	7.45E+05
PI-7I-G5-FS	7-8 min	1 min	5.391	2688	612.9	2548.96	2.407	2.407	1.06E+06	2.57E+05
PI-7I-G6-FS	15-17 min	2 min	2.264	1169	267	1030.42	2.587	5.174	1.99E+05	5.23E+04
PI-7I-G7-FS	31-35 min	4 min	1.618	729	166.7	590.41	2.558	10.231	5.77E+04	1.67E+04
PI-7I-G8-FS	61-69 min	8 min	2.904	1257	286.9	1118.14	2.658	21.26	5.26E+04	1.37E+04
PI-7I-G9-FS	121-129 min	8 min	2.381	938	214.3	798.89	2.521	20.164	3.96E+04	1.08E+04
PI-7I-L1-FS	0-20 min[(a)]	20 min	0.281	135	31.2	56.62	2.461	49.229	1.15E+03	6.60E+02
PI-7I-L2-FS	20-40 min	20 min	0.222	100	23.6	21.83	2.541	50.825	4.30E+02	4.95E+02
PI-7I-L3-FS	40-60 min	20 min	0.116	56	13.6	-22.52	2.483	49.654	-4.54E+02	3.25E+02
PI-7I-L4-FS	60-69 m 40 sec	9 min 40 sec	0.16	64	15.3	-14.31	2.658	26.581	-5.38E+02	6.61E+02
PI-7I-L5-FS	Field Blank	--	0.177	80	18.9	--	--	--	--	--
PI-7I-L6-FS	Field Blank	--	0.134	86	20.1	--	--	--	--	--
PI-7I-L7-FS	Field Blank	--	0.216	100	23.5	--	--	--	--	--
PI-7I-L8-FS	Field Blank	--	0.201	93	22	--	--	--	--	--
PI-7I-L9-FS	Field Blank	--	0.109	34	8.4	--	--	--	--	--

(a) Loader's position sampling began at 3 h and 21 min post shot for resuspension evaluation.

Table A.15. PII-1/2 IOM Filters—Mass, Volume, and Concentration

Sample ID	Collection Interval	Elapsed Time	Total Mass (mg)	Calculated U (μg)	DU Mass ± 1σ (μg)	Net DU Mass (μg)	Flow Rate (Lpm)	Volume (L)	DU Conc. (μg/m^3)	DU Conc. ± 1σ (μg/m^3)
PII-1/2I-C1-FS	Shot 1: 0-10 sec	10 sec	4.273	1638	555	1637.5	2.369	0.395	4.15E+06	1.41E+06
PII-1/2I-C2-FS	3-4 min	1 min	10.333	3447	1167.8	3447.36	2.32	2.32	1.49E+06	5.05E+05
PII-1/2I-C3-FS	9-11 min	2 min	10.605	3028	1025.8	3027.9	2.398	4.797	6.31E+05	2.15E+05
PII-1/2I-C4-FS	Shot 2: 0-10 sec	10 sec	4.288	1740	589.8	1740.23	2.465	0.411	4.23E+06	1.44E+06
PII-1/2I-C5-FS	3-4 min	1 min	9.963	3599	1219	3598.89	2.406	2.406	1.50E+06	5.09E+05
PII-1/2I-C6-FS	9-11 min	2 min	11.298	3401	1151.9	3401.3	2.533	5.065	6.72E+05	2.28E+05
PII-1/2I-C7-FS	21-25 min	4 min	9.068	2613	886.7	2613.26	2.717	10.866	2.40E+05	8.19E+04
PII-1/2I-C8-FS	45-53 min	8 min	4.161	1257	429.1	1257.48	2.563	20.507	6.13E+04	2.10E+04
PII-1/2I-C9-FS	93-109 min	16 min	4.113	1446	494.4	1446.07	2.364	37.82	3.82E+04	1.31E+04
PII-1/2I-D1-FS	Shot 1: 0-10 sec	10 sec	2.007	762	258.3	761.57	2.44	0.407	1.87E+06	6.37E+05
PII-1/2I-D2-FS	3-4 min	1 min	3.299	1012	343.1	1012.09	2.482	2.482	4.08E+05	1.39E+05
PII-1/2I-D3-FS	9-11 min	2 min	1.636	511	174	511.19	2.45	4.901	1.04E+05	3.56E+04
PII-1/2I-D4-FS	Shot 2: 0-10 sec	10 sec	4.364	1937	656.1	1936.52	2.66	0.443	4.37E+06	1.49E+06
PII-1/2I-D5-FS	3-4 min	1 min	8.76	3200	1084.2	3200.21	2.381	2.381	1.34E+06	4.57E+05
PII-1/2I-D6-FS	9-11 min	2 min	11.745	3198	1083.8	3197.89	2.411	4.822	6.63E+05	2.26E+05
PII-1/2I-D7-FS	21-25 min	4 min	8.5	2395	813.2	2394.95	2.396	9.582	2.50E+05	8.52E+04
PII-1/2I-D8-FS	45-53 min	8 min	4.453	1316	449.4	1316.35	2.31	18.48	7.12E+04	2.44E+04
PII-1/2I-D9-FS	93-109 min	16 min	3.962	1342	459.4	1342.21	2.503	40.044	3.35E+04	1.15E+04
PII-1/2I-G1-FS	Shot 2: 0-10 sec	10 sec	5.003	1873	634.6	1772.11[(a)]	2.397	0.4	4.43E+06	1.59E+06
PII-1/2I-G2-FS	Field Blank	--	0.155	102	35.2	--	--	--	--	--
PII-1/2I-G3-FS	3-4 min	1 min	8.74	3255	1102.8	3154	2.462	2.462	1.28E+06	4.50E+05
PII-1/2I-G4-FS	9-11 min	2 min	10.364	3290	1114.8	3188.96	2.49	4.981	6.40E+05	2.25E+05
PII-1/2I-G5-FS	21-25 min	4 min	7.62	2262	768	2161.06	2.278	9.113	2.37E+05	8.46E+04
PII-1/2I-G6-FS	45-53 min	8 min	4.222	1271	433.6	1169.82	2.406	19.251	6.08E+04	2.26E+04
PII-1/2I-G7-FS	93-109 min	16 min	3.762	1346	460.9	1244.83	2.355	37.678	3.30E+04	1.23E+04
PII-1/2I-G8-FS	Field Blank	--	0.231	86	30	--	--	--	--	--
PII-1/2I-G9-FS	Field Blank	--	0.267	114	39.2	--	--	--	--	--
PII-1/2I-L1-FS	Shot 1: 0-10 sec	10 sec	3.844	1683	570.3	1682.89	2.527	0.421	4.00E+06	1.36E+06
PII-1/2I-L2-FS	3-4 min	1 min	4.475	1489	504.3	1488.7	2.356	2.356	6.32E+05	2.15E+05
PII-1/2I-L3-FS	9-11 min	2 min	3.904	1382	468.5	1382.16	2.343	4.686	2.95E+05	1.00E+05
PII-1/2I-L4-FS	Shot 2: 0-10 sec	10 sec	5.236	2353	797	2352.74	2.539	0.423	5.56E+06	1.89E+06
PII-1/2I-L5-FS	3-4 min	1 min	9.327	3419	1158.3	3418.85	2.344	2.344	1.46E+06	4.96E+05
PII-1/2I-L6-FS	9-11 min	2 min	10.814	3406	1154.3	3406.41	2.405	4.81	7.08E+05	2.41E+05
PII-1/2I-L7-FS	21-25 min	4 min	8.529	2143	727.9	2143.42	2.376	9.502	2.26E+05	7.69E+04
PII-1/2I-L8-FS	45-53 min	8 min	4.692	1289	439.8	1289.22	2.346	18.772	6.87E+04	2.35E+04
PII-1/2I-L9-FS	93-109 min	16 min	4.15	1467	501	1466.7	2.35	37.605	3.90E+04	1.34E+04

(a) Average of gunner field blanks subtracted from calculated uranium mass.

Table A.16. PII-3 IOM Filters—Mass, Volume, and Concentration

Sample ID	Collection Interval	Elapsed Time	Total Mass (mg)	Calculated U (μg)	DU Mass ± 1σ (μg)	Net DU Mass (μg)	Flow Rate (Lpm)	Volume (L)	DU Conc. (μg/m^3)	DU Conc. ± 1σ (μg/m^3)
PII-3I-C1-FS	Field Blank	--	1.12	247	72.6	--	--	--	--	--
PII-3I-C2-FS	0-10 sec	10 sec	7.898	1107	323	859.62	2.514	0.419	2.05E+06	7.93E+05
PII-3I-C3-FS	1-1 min 10 sec	10 sec	1.2	249	73.3	1.24	2.52	0.42	2.94E+03	3.29E+05
PII-3I-C4-FS	3-3 min 15 sec	15 sec	0.529	196	58	-50.9	2.475	0.619	-8.29E+04	1.51E+05
PII-3I-C5-FS	7-8 min	1 min	1.075	318	94.1	71.14	2.435	2.435	2.92E+04	4.85E+04
PII-3I-C6-FS	15-17 min	2 min	1.338	439	128.7	191.8	2.463	4.926	3.89E+04	3.00E+04
PII-3I-C7-FS	31-35 min	4 min	1.804	822	241.8	575.13	2.74	10.961	5.25E+04	2.31E+04
PII-3I-C8-FS	61-69 min	8 min	2.535	1111	326.8	863.51	2.577	20.613	4.19E+04	1.63E+04
PII-3I-C9-FS	121-129 min	8 min	1.726	773	227.6	525.77	2.443	19.54	2.69E+04	1.23E+04
PII-3I-D1-FS	0-10 sec	10 sec	5.07	653	190.9	606.63	2.431	0.405	1.50E+06	4.75E+05
PII-3I-D2-FS	1-1 min 10 sec	10 sec	1.328	223	65.9	177.2	2.625	0.437	4.05E+05	1.54E+05
PII-3I-D3-FS	3-3 min 15 sec	15 sec	0.73	127	37.6	80.94	2.61	0.652	1.24E+05	6.16E+04
PII-3I-D4-FS	7-8 min	1 min	0.887	263	78	216.41	2.684	2.684	8.06E+04	2.97E+04
PII-3I-D5-FS	15-17 min	2 min	0.965	371	109.9	325.14	2.49	4.98	6.53E+04	2.23E+04
PII-3I-D6-FS	31-35 min	4 min	1.478	688	202.8	642.05	2.678	10.713	5.99E+04	1.91E+04
PII-3I-D7-FS	61-69 min	8 min	2.16	1001	294.7	955.11	2.493	19.946	4.79E+04	1.49E+04
PII-3I-D8-FS	121-129 min	8 min	1.518	635	187.7	588.46	2.398	19.183	3.07E+04	9.86E+03
PII-3I-D9-FS	Field Blank	--	0.178	46	14	--	--	--	--	--
PII-3I-G1-FS	0-10 sec	10 sec	1.099	239	70.6	227.09	2.649	0.442	5.14E+05	1.61E+05
PII-3I-G2-FS	Field Blank	--	0.032	12	4	--	--	--	--	--
PII-3I-G3-FS	1-1 min 10 sec	10 sec	0.485	131	39.1	118.93	2.575	0.429	2.77E+05	9.19E+04
PII-3I-G4-FS	3-3 min 15 sec	15 sec	0.258	99	29.9	87.25	2.653	0.663	1.32E+05	4.55E+04
PII-3I-G5-FS	7-8 min	1 min	0.562	194	58.1	182.1	2.522	2.522	7.22E+04	2.32E+04
PII-3I-G6-FS	15-17 min	2 min	0.786	290	85.1	277.63	2.557	5.115	5.43E+04	1.67E+04
PII-3I-G7-FS	31-35 min	4 min	1.215	526	155.5	513.5	2.605	10.418	4.93E+04	1.50E+04
PII-3I-G8-FS	61-69 min	8 min	0.034	23	7.4	10.8	2.914	23.308	4.63E+02	3.62E+02
PII-3I-G9-FS	121-129 min	8 min	0.048	38	11.6	26.02	2.754	22.03	1.18E+03	5.54E+02
PII-3I-L1-FS	0-10 sec	10 sec	2.41	386	113.1	290.93	2.586	0.431	6.75E+05	2.72E+05
PII-3I-L2-FS	1-1 min 10 sec	10 sec	0.847	185	54.4	90.63	2.468	0.411	2.21E+05	1.49E+05
PII-3I-L3-FS	3-3 min 15 sec	15 sec	0.391	122	36.5	27.75	2.531	0.633	4.38E+04	7.19E+04
PII-3I-L4-FS	7-8 min	1 min	0.897	293	86.7	198.6	2.605	2.605	7.62E+04	3.50E+04
PII-3I-L5-FS	15-17 min	2 min	1.124	462	136.3	367.47	2.518	5.035	7.30E+04	2.77E+04
PII-3I-L6-FS	31-35 min	4 min	1.643	830	243.7	735.39	2.587	10.347	7.11E+04	2.38E+04
PII-3I-L7-FS	61-69 min	8 min	2.346	1100	323.1	1005.21	2.538	20.304	4.95E+04	1.60E+04
PII-3I-L8-FS	121-129 min	8 min	1.786	763	224.6	667.88	2.528	20.223	3.30E+04	1.12E+04
PII-3I-L9-FS	Field Blank	--	0.372	95	28.2	--	--	--	--	--

Table A.17. PIII-1 IOM Filters—Mass, Volume, and Concentration

Sample ID	Collection Interval	Elapsed Time	Total Mass (mg)	Calculated U (μg)	DU Mass ± 1σ (μg)	Net DU Mass (μg)	Flow Rate (Lpm)	Volume (L)	DU Conc. (μg/m^3)	DU Conc. ± 1σ (μg/m^3)
PIII-1I-C1-FS	0-10 sec	10 sec	4.299	2036	463.2	1985.12	2.438	0.406	4.89E+06	1.15E+06
PIII-1I-C2-FS	1-1 min 10 sec	10 sec	1.947	866	197.4	814.51	2.486	0.414	1.97E+06	4.82E+05
PIII-1I-C3-FS	3-3 min 15 sec	15 sec	2.066	888	202.5	836.97	2.438	0.609	1.37E+06	3.36E+05
PIII-1I-C4-FS	7-8 min	1 min	4.057	1762	401.3	1711.25	2.394	2.394	7.15E+05	1.69E+05
PIII-1I-C5-FS	15-17 min	2 min	2.505	989	225.6	938.23	2.429	4.858	1.93E+05	4.69E+04
PIII-1I-C6-FS	31-35 min	4 min	0.975	407	93.1	355.91	2.591	10.364	3.43E+04	9.12E+03
PIII-1I-C7-FS	61-69 min	8 min	0.59	194	44.6	143.03	2.757	22.059	6.48E+03	2.10E+03
PIII-1I-C8-FS	121-129 min	8 min	0.419	143	32.8	91.6	2.49	19.923	4.60E+03	1.77E+03
PIII-1I-C9-FS	Field Blank	--	0.101	51	12	--	--	--	--	--
PIII-1I-D1-FS	0-10 sec	10 sec	2.378	1110	252.7	1039.62	2.406	0.401	2.59E+06	6.36E+05
PIII-1I-D2-FS	1-1 min 10 sec	10 sec	2.77	1211	275.8	1140.44	2.52	0.42	2.72E+06	6.63E+05
PIII-1I-D3-FS	3-3 min 15 sec	15 sec	3.832	994	226.5	922.91	2.608	0.652	1.42E+06	3.51E+05
PIII-1I-D4-FS	7-8 min	1 min	4.768	1899	432.1	1828.09	2.627	2.627	6.96E+05	1.66E+05
PIII-1I-D5-FS	15-17 min	2 min	2.725	1162	264.8	1090.96	2.399	4.798	2.27E+05	5.57E+04
PIII-1I-D6-FS	31-35 min	4 min	1.169	500	114.3	429.02	2.666	10.663	4.02E+04	1.09E+04
PIII-1I-D7-FS	61-69 min	8 min	0.642	230	52.8	158.79	2.5	20.003	7.94E+03	2.78E+03
PIII-1I-D8-FS	121-129 min	8 min	0.62	232	53.1	160.86	2.49	19.923	8.07E+03	2.81E+03
PIII-1I-D9-FS	Field Blank	--	0.251	71	16.4	--	--	--	--	--
PIII-1I-G1-FS	0-10 sec	10 sec	6.746	3155	717.8	3120.07	2.441	0.407	7.67E+06	1.78E+06
PIII-1I-G2-FS	Field Blank	--	0.12	35	8.4	--	--	--	--	--
PIII-1I-G3-FS	1-1 min 10 sec	10 sec	2.418	1019	232.3	984.3	2.552	0.425	2.32E+06	5.51E+05
PIII-1I-G4-FS	3-3 min 15 sec	15 sec	2.202	1021	232.9	986.46	2.532	0.633	1.56E+06	3.71E+05
PIII-1I-G5-FS	7-8 min	1 min	4.561	1465	333.6	1430.04	2.397	2.397	5.97E+05	1.40E+05
PIII-1I-G6-FS	15-17 min	2 min	2.972	1303	297.1	1268.39	2.621	5.241	2.42E+05	5.72E+04
PIII-1I-G7-FS	31-35 min	4 min	0.407	148	34.3	113.28	2.66	10.64	1.06E+04	3.33E+03
PIII-1I-G8-FS	61-69 min	8 min	0.602	212	NA[(a)]	177.02	2.623	20.984	8.44E+03	NA[(a)]
PIII-1I-G9-FS	121-129 min	8 min	0.504	137	31.4	101.57	2.521	20.164	5.04E+03	1.63E+03
PIII-1I-L1-FS	0-10 sec	10 sec	3.09	1410	321.2	1394.09	2.448	0.408	3.42E+06	7.94E+05
PIII-1I-L2-FS	1-1 min 10 sec	10 sec	1.029	374	85.4	357.34	2.539	0.423	8.45E+05	2.04E+05
PIII-1I-L3-FS	3-3 min 15 sec	15 sec	2.913	840	191.5	823.88	2.444	0.611	1.35E+06	3.16E+05
PIII-1I-L4-FS	7-8 min	1 min	3.404	1496	340.8	1479.55	2.433	2.433	6.08E+05	1.41E+05
PIII-1I-L5-FS	15-17 min	2 min	2.366	949	216.3	933.06	2.425	4.849	1.92E+05	4.50E+04
PIII-1I-L6-FS	31-35 min	4 min	0.982	396	90.6	379.64	2.536	10.143	3.74E+04	9.01E+03
PIII-1I-L7-FS	61-69 min	8 min	0.523	173	39.7	156.42	2.409	19.274	8.12E+03	2.09E+03
PIII-1I-L8-FS	121-129 min	8 min	0.424	122	28.2	105.89	2.393	19.142	5.53E+03	1.50E+03
PIII-1I-L9-FS	Field Blank	--	0.05	16	4.1	--	--	--	--	--

(a) DU mass based on ICP-MS results; no analytical uncertainty was reported.

Table A.18. PIII-2 IOM Filters—Mass, Volume, and Concentration

Sample ID	Collection Interval	Elapsed Time	Total Mass (mg)	Calculated U (μg)	DU Mass ± 1σ (μg)	Net DU Mass (μg)	Flow Rate (Lpm)	Volume (L)	DU Conc. (μg/m^3)	DU Conc. ± 1σ (μg/m^3)
PIII-2I-C1-FS	0-10 sec	10 sec	8.174	6283	1933.8	5741.09	2.497	0.416	1.38E+07	4.68E+06
PIII-2I-C2-FS	1-1 min 10 sec	10 sec	3.061	2198	677.2	1655.71	2.655	0.442	3.75E+06	1.58E+06
PIII-2I-C3-FS	3-3 min 15 sec	15 sec	2.007	1402	432.2	859.9	2.637	0.659	1.30E+06	7.04E+05
PIII-2I-C3-FS	7-8 min	1 min	1.507	1024	316.1	482.09	2.526	2.526	1.91E+05	1.42E+05
PIII-2I-C5-FS	15-17 min	2 min	0.941	589	182.4	47.03	2.531	5.061	9.29E+03	4.87E+04
PIII-2I-C6-FS	31-35 min	4 min	1.189	739	227.8	196.41	2.594	10.374	1.89E+04	2.73E+04
PIII-2I-C7-FS	61-69 min	8 min	1.348	675	208.6	132.32	2.711	21.69	6.10E+03	1.24E+04
PIII-2I-C8-FS	121-129 min	8 min	1.401	768	237.4	226.1	2.692	21.539	1.05E+04	1.35E+04
PIII-2I-C9-FS	Field Blank	--	0.753	542	167.7	--	--	--	--	--
PIII-2I-D1-FS	0-10 sec	10 sec	5.164	3735	1150.1	3446.09	2.433	0.406	8.49E+06	2.85E+06
PIII-2I-D2-FS	1-1 min 10 sec	10 sec	3.83	2553	786.7	2264.53	2.555	0.426	5.32E+06	1.87E+06
PIII-2I-D3-FS	3-3 min 15 sec	15 sec	2.096	1282	395.6	993.48	2.592	0.648	1.53E+06	6.27E+05
PIII-2I-D4-FS	7-8 min	1 min	1.458	728	225.5	439.01	2.686	2.686	1.63E+05	9.04E+04
PIII-2I-D5-FS	15-17 min	2 min	0.652	330	101.9	40.77	2.46	4.921	8.29E+03	2.78E+04
PIII-2I-D6-FS	31-35 min	4 min	0.879	497	153.8	207.96	2.662	10.646	1.95E+04	1.67E+04
PIII-2I-D7-FS	61-69 min	8 min	1.394	664	205.3	375.27	2.482	19.86	1.89E+04	1.13E+04
PIII-2I-D8-FS	121-129 min	8 min	1.662	654	202.1	365.33	2.434	19.472	1.88E+04	1.14E+04
PIII-2I-D9-FS	Field Blank	--	0.54	289	89.1	--	--	--	--	--
PIII-2I-G1-FS	0-10 sec	10 sec	12.231	15600	NA[(b)]	15079.93	2.503	0.417	3.62E+07	NA[(b)]
PIII-2I-G2-FS	Field Blank	--	1.326	520	163.5	--	--	--	--	--
PIII-2I-G3-FS	1-1 min 10 sec	10 sec	6.039	4198	1319.5	3678.42	2.403	0.4	9.20E+06	3.33E+06
PIII-2I-G4-FS	3-3 min 15 sec	15 sec	5.594	3945	1239.1	3424.78	2.555	0.639	5.36E+06	1.96E+06
PIII-2I-G5-FS	7-8 min	1 min	3.181	1389	437.2	868.71	2.438	2.438	3.56E+05	1.92E+05
PIII-2I-G6-FS	15-17 min	2 min	1.961	1051	330.3	530.72	2.557	5.114	1.04E+05	7.22E+04
PIII-2I-G7-FS	31-35 min	4 min	1.642	1251	393.5	731.19	2.596	10.383	7.04E+04	4.11E+04
PIII-2I-G8-FS	61-69 min	8 min	2.127	1364	428.8	843.84	2.611	20.886	4.04E+04	2.20E+04
PIII-2I-G9-FS	121-129 min	8 min	3.173	1247	392.3	726.99	2.575	20.602	3.53E+04	2.07E+04
PIII-2I-L1-FS	0-10 sec	10 sec	5.783	4654	1462.8	4568.61	2.431	0.405	1.13E+07	3.63E+06
PIII-2I-L2-FS	1-1 min 10 sec	10 sec	1.424	988	311.2	902.09	2.518	0.42	2.15E+06	7.47E+05
PIII-2I-L3-FS	3-3 min 15 sec	15 sec	1.524	965	304.3	878.87	2.489	0.622	1.41E+06	4.93E+05
PIII-2I-L4-FS	7-8 min	1 min	0.661	337	104.6	250.81	2.6	2.6	9.65E+04	4.17E+04
PIII-2I-L5-FS	15-17 min	2 min	0.439	(a)	--	--	2.585	--	--	--
PIII-2I-L6-FS	31-35 min	4 min	0.643	321	99.9	235.32	2.473	9.893	2.38E+04	1.05E+04
PIII-2I-L7-FS	61-69 min	8 min	1	425	132.3	338.8	2.436	19.49	1.74E+04	6.96E+03
PIII-2I-L8-FS	121-129 min	8 min	0.878	357	111.1	270.82	2.412	19.293	1.40E+04	5.95E+03
PIII-2I-L9-FS	Field Blank	--	0.131	86	26.9	--	--	--	--	--

(a) Filter bent over.
(b) DU mass based on ICP-MS results; no analytical uncertainty was reported.

Table A.19. PI-1 Cascade Impactor Substrates—Mass, Volume, and Concentration

Sample ID	Collection Interval	Elapsed Time	Total Mass (mg)	Calculated U (μg)	DU Mass ± 1σ (μg)	Net DU Mass (μg)	Flow Rate (Lpm)	Volume (L)	DU Conc. (μg/m^3)	DU Conc. ± 1σ (μg/m^3)
PI-1I-C-1-CI-1	0-30 sec	30 sec	0.831	1182	159.5	290	2.662	1.331	2.18E+05	1.50E+05
PI-1I-C-1-CI-2	0-30 sec	30 sec	0.944	322	126.5	299	2.662	1.331	2.25E+05	9.55E+04
PI-1I-C-1-CI-3	0-30 sec	30 sec	1.19	325	60.1	321	2.662	1.331	2.41E+05	4.57E+04
PI-1I-C-1-CI-4	0-30 sec	30 sec	1.564	582	153.3	579	2.662	1.331	4.35E+05	1.16E+05
PI-1I-C-1-CI-5	0-30 sec	30 sec	1.447	691	261.1	687	2.662	1.331	5.16E+05	1.97E+05
PI-1I-C-1-CI-6	0-30 sec	30 sec	1.159	522	200.1	518	2.662	1.331	3.89E+05	1.51E+05
PI-1I-C-1-CI-7	0-30 sec	30 sec	1.158	367	80.9	363	2.662	1.331	2.73E+05	6.14E+04
PI-1I-C-1-CI-8	0-30 sec	30 sec	1.131	335	68.4	330	2.662	1.331	2.48E+05	5.20E+04
PI-1I-C-1-CI-9	0-30 sec	30 sec	3.803	1413	409	1398	2.662	1.331	1.05E+06	3.09E+05
PI-1I-C-2-CI-1	05-1.5 min	1 min	2.001	722	97.6	-170	2.606	2.606	-6.52E+04	5.96E+04
PI-1I-C-2-CI-2	05-1.5 min	1 min	-0.98	236	92.6	213	2.606	2.606	8.17E+04	3.58E+04
PI-1I-C-2-CI-3	05-1.5 min	1 min	1.163	134	25.1	130	2.606	2.606	4.99E+04	9.76E+03
PI-1I-C-2-CI-4	05-1.5 min	1 min	1.729	487	128.5	484	2.606	2.606	1.86E+05	4.96E+04
PI-1I-C-2-CI-5	05-1.5 min	1 min	1.564	520	196.7	516	2.606	2.606	1.98E+05	7.57E+04
PI-1I-C-2-CI-6	05-1.5 min	1 min	1.446	508	194.7	504	2.606	2.606	1.93E+05	7.49E+04
PI-1I-C-2-CI-7	05-1.5 min	1 min	0.54	445	97.6	441	2.606	2.606	1.69E+05	3.78E+04
PI-1I-C-2-CI-8	05-1.5 min	1 min	0.917	901	175.8	896	2.606	2.606	3.44E+05	6.83E+04
PI-1I-C-2-CI-9	05-1.5 min	1 min	4.354	1551	448.4	1536	2.606	2.606	5.89E+05	1.73E+05
PI-1I-C-3-CI-1	1.5-3.5 min	2 min	2.139	497	67.4	-395	2.553	5.105	-7.74E+04	2.72E+04
PI-1I-C-3-CI-2	1.5-3.5 min	2 min	0.167	96	37.8	73	2.553	5.105	1.43E+04	7.64E+03
PI-1I-C-3-CI-3	1.5-3.5 min	2 min	-1.16	78	14.8	74	2.553	5.105	1.45E+04	2.94E+03
PI-1I-C-3-CI-4	1.5-3.5 min	2 min	0.627	58	15.8	55	2.553	5.105	1.08E+04	3.12E+03
PI-1I-C-3-CI-5	1.5-3.5 min	2 min	1.584	416	157.6	412	2.553	5.105	8.07E+04	3.10E+04
PI-1I-C-3-CI-6	1.5-3.5 min	2 min	1.551	326	NA[(a)]	322	2.553	5.105	6.31E+04	NA[(a)]
PI-1I-C-3-CI-7	1.5-3.5 min	2 min	1.657	623	135.4	619	2.553	5.105	1.21E+05	2.68E+04
PI-1I-C-3-CI-8	1.5-3.5 min	2 min	2.425	867	168.9	862	2.553	5.105	1.69E+05	3.35E+04
PI-1I-C-3-CI-9	1.5-3.5 min	2 min	2.417	878	255.3	863	2.553	5.105	1.69E+05	5.03E+04
PI-1I-C-4-CI-1	3.5-7.5 min	4 min	-0.835	116	16.4	-776	2.373	9.493	-8.17E+04	1.31E+04
PI-1I-C-4-CI-2	3.5-7.5 min	4 min	-1.138	73	28.9	50	2.373	9.493	5.27E+03	3.20E+03
PI-1I-C-4-CI-3	3.5-7.5 min	4 min	-0.476	291	54	287	2.373	9.493	3.02E+04	5.76E+03
PI-1I-C-4-CI-4	3.5-7.5 min	4 min	0.887	102	27.4	99	2.373	9.493	1.04E+04	2.91E+03
PI-1I-C-4-CI-5	3.5-7.5 min	4 min	2.126	704	266.4	700	2.373	9.493	7.37E+04	2.82E+04
PI-1I-C-4-CI-6	3.5-7.5 min	4 min	-1.831	341	131.3	337	2.373	9.493	3.55E+04	1.39E+04
PI-1I-C-4-CI-7	3.5-7.5 min	4 min	0.37	429	94.4	425	2.373	9.493	4.48E+04	1.00E+04
PI-1I-C-4-CI-8	3.5-7.5 min	4 min	2.357	821	160.5	816	2.373	9.493	8.60E+04	1.71E+04
PI-1I-C-4-CI-9	3.5-7.5 min	4 min	1.472	1170	338	1155	2.373	9.493	1.22E+05	3.58E+04
PI-1I-C-5-CI-1	7.5-15.5 min	8 min	0.625	125	17.4	-767	2.44	19.519	-3.93E+04	6.36E+03
PI-1I-C-5-CI-2	7.5-15.5 min	8 min	0.346	24	9.8	1	2.44	19.519	5.12E+01	6.92E+02
PI-1I-C-5-CI-3	7.5-15.5 min	8 min	1.394	170	31.9	166	2.44	19.519	8.50E+03	1.66E+03
PI-1I-C-5-CI-4	7.5-15.5 min	8 min	0.85	141	37.7	138	2.44	19.519	7.07E+03	1.94E+03
PI-1I-C-5-CI-5	7.5-15.5 min	8 min	2.252	404	153.4	400	2.44	19.519	2.05E+04	7.88E+03
PI-1I-C-5-CI-6	7.5-15.5 min	8 min	0.867	209	81	205	2.44	19.519	1.05E+04	4.16E+03
PI-1I-C-5-CI-7	7.5-15.5 min	8 min	1.42	435	95.2	431	2.44	19.519	2.21E+04	4.92E+03

Table A.19 (cont'd). Phase I, Shot 1, Commander

Sample ID	Collection Interval	Elapsed Time	Total Mass (mg)	Calculated U (μg)	DU Mass ± 1σ (μg)	Net DU Mass (μg)	Flow Rate (Lpm)	Volume (L)	DU Conc. (μg/m^3)	DU Conc. ± 1σ (μg/m^3)
PI-1I-C-5-CI-8	7.5-15.5 min	8 min	1.4	606	118.1	601	2.44	19.519	3.08E+04	6.12E+03
PI-1I-C-5-CI-9	7.5-15.5 min	8 min	0.861	297	87.6	282	2.44	19.519	1.44E+04	4.52E+03
PI-1I-C-6-CI-1	15.5-31.5 min	16 min	0.992	212	29.2	-680	2.446	39.136	-1.74E+04	3.22E+03
PI-1I-C-6-CI-2	15.5-31.5 min	16 min	0.828	7	3.4	-16	2.446	39.136	-4.09E+02	2.53E+02
PI-1I-C-6-CI-3	15.5-31.5 min	16 min	0.848	18	3.8	14	2.446	39.136	3.58E+02	1.02E+02
PI-1I-C-6-CI-4	15.5-31.5 min	16 min	0.749	95	25.6	92	2.446	39.136	2.35E+03	6.59E+02
PI-1I-C-6-CI-5	15.5-31.5 min	16 min	1.278	223	84.3	219	2.446	39.136	5.60E+03	2.16E+03
PI-1I-C-6-CI-6	15.5-31.5 min	16 min	1.249	166	62.7	162	2.446	39.136	4.14E+03	1.61E+03
PI-1I-C-6-CI-7	15.5-31.5 min	16 min	1.291	204	44.7	200	2.446	39.136	5.11E+03	1.15E+03
PI-1I-C-6-CI-8	15.5-31.5 min	16 min	0.775	365	68.8	360	2.446	39.136	9.20E+03	1.78E+03
PI-1I-C-6-CI-9	15.5-31.5 min	16 min	1.122	244	70.5	229	2.446	39.136	5.85E+03	1.81E+03
PI-1I-C-7-CI-1	31.5-63.5 min	32 min	1.041	338	46.3	-554	2.63	84.175	-6.58E+03	1.55E+03
PI-1I-C-7-CI-2	31.5-63.5 min	32 min	1.218	26	10.5	3	2.63	84.175	3.56E+01	1.67E+02
PI-1I-C-7-CI-3	31.5-63.5 min	32 min	0.698	18	3.9	14	2.63	84.175	1.66E+02	4.87E+01
PI-1I-C-7-CI-4	31.5-63.5 min	32 min	0.503	61	16.4	58	2.63	84.175	6.89E+02	1.97E+02
PI-1I-C-7-CI-5	31.5-63.5 min	32 min	0.003	260	97.9	256	2.63	84.175	3.04E+03	1.17E+03
PI-1I-C-7-CI-6	31.5-63.5 min	32 min	0.868	152	57.4	148	2.63	84.175	1.76E+03	6.84E+02
PI-1I-C-7-CI-7	31.5-63.5 min	32 min	1.599	133	30.1	129	2.63	84.175	1.53E+03	3.62E+02
PI-1I-C-7-CI-8	31.5-63.5 min	32 min	0.884	194	38.5	189	2.63	84.175	2.25E+03	4.64E+02
PI-1I-C-7-CI-9	31.5-63.5 min	32 min	2.877	740	209.2	725	2.63	84.175	8.61E+03	2.50E+03
PI-1I-C-8-CI-1	63.5-127.5 min	64 min	1.188	466	63.5	-426	2.496	159.725	-2.67E+03	8.58E+02
PI-1I-C-8-CI-2	63.5-127.5 min	64 min	0.051	26	10.6	3	2.496	159.725	1.88E+01	8.83E+01
PI-1I-C-8-CI-3	63.5-127.5 min	64 min	2.846	16	3.7	12	2.496	159.725	7.51E+01	2.45E+01
PI-1I-C-8-CI-4	63.5-127.5 min	64 min	-1.37	98	26.3	95	2.496	159.725	5.95E+02	1.66E+02
PI-1I-C-8-CI-5	63.5-127.5 min	64 min	2.347	261	98.4	257	2.496	159.725	1.61E+03	6.18E+02
PI-1I-C-8-CI-6	63.5-127.5 min	64 min	1.443	147	55.5	143	2.496	159.725	8.95E+02	3.49E+02
PI-1I-C-8-CI-7	63.5-127.5 min	64 min	0.683	192	42.4	188	2.496	159.725	1.18E+03	2.68E+02
PI-1I-C-8-CI-8	63.5-127.5 min	64 min	0.962	260	50.8	255	2.496	159.725	1.60E+03	3.22E+02
PI-1I-C-8-CI-9	63.5-127.5 min	64 min	3.592	992	279.1	977	2.496	159.725	6.12E+03	1.76E+03
PI-1I-C-9-CI-1	Field Blank	--	2.938	892	120.8	--	--	--	--	--
PI-1I-C-9-CI-2	Field Blank	--	0.421	23	9.3	--	--	--	--	--
PI-1I-C-9-CI-3	Field Blank	--	0.875	4	1.2	--	--	--	--	--
PI-1I-C-9-CI-4	Field Blank	--	0.821	3	1.4	--	--	--	--	--
PI-1I-C-9-CI-5	Field Blank	--	0.264	4	1.9	--	--	--	--	--
PI-1I-C-9-CI-6	Field Blank	--	0.182	4	2.2	--	--	--	--	--
PI-1I-C-9-CI-7	Field Blank	--	0.072	4	2.5	--	--	--	--	--
PI-1I-C-9-CI-8	Field Blank	--	-0.385	5	3.3	--	--	--	--	--
PI-1I-C-9-CI-9	Field Blank	--	-0.014	15	5.1	--	--	--	--	--

(a) DU mass based on ICP-MS results; no analytical uncertainty was reported.

Table A.20 (cont'd). Phase I, Shot 1, Driver

Sample ID	Collection Interval	Elapsed Time	Total Mass (mg)	Calculated U (μg)	DU Mass ± 1σ (μg)	Net DU Mass (μg)	Flow Rate (Lpm)	Volume (L)	DU Conc. (μg/m^3)	DU Conc. ± 1σ (μg/m^3)
PI-1I-D-1-CI-1	0-30 sec	30 sec	2.462	574	106.6	161	2.551	1.275	1.26E+05	1.03E+05
PI-1I-D-1-CI-2	0-30 sec	30 sec	-0.956	26	12.5	12	2.551	1.275	9.41E+03	1.12E+04
PI-1I-D-1-CI-3	0-30 sec	30 sec	0.520	6	2.2	3	2.551	1.275	2.35E+03	1.97E+03
PI-1I-D-1-CI-4	0-30 sec	30 sec	-0.137	21	7.8	6	2.551	1.275	4.71E+03	7.58E+03
PI-1I-D-1-CI-5	0-30 sec	30 sec	0.322	24	9.4	4	2.551	1.275	3.14E+03	9.58E+03
PI-1I-D-1-CI-6	0-30 sec	30 sec	-0.192	21	5.3	5	2.551	1.275	3.92E+03	5.31E+03
PI-1I-D-1-CI-7	0-30 sec	30 sec	-0.468	19	3.9	12	2.551	1.275	9.41E+03	3.38E+03
PI-1I-D-1-CI-8	0-30 sec	30 sec	0.163	15	2.2	8	2.551	1.275	6.27E+03	2.05E+03
PI-1I-D-1-CI-9	0-30 sec	30 sec	0.001	18	3.2	16	2.551	1.275	1.25E+04	2.66E+03
PI-1I-D-2-CI-1	05-1.5 min	1 min	1.171	485	90.2	72	2.376	2.376	3.03E+04	4.99E+04
PI-1I-D-2-CI-2	05-1.5 min	1 min	0.098	75	35.2	61	2.376	2.376	2.57E+04	1.51E+04
PI-1I-D-2-CI-3	05-1.5 min	1 min	1.172	115	29.3	112	2.376	2.376	4.71E+04	1.24E+04
PI-1I-D-2-CI-4	05-1.5 min	1 min	0.314	203	73.9	188	2.376	2.376	7.91E+04	3.13E+04
PI-1I-D-2-CI-5	05-1.5 min	1 min	1.068	129	49.5	109	2.376	2.376	4.59E+04	2.11E+04
PI-1I-D-2-CI-6	05-1.5 min	1 min	0.185	200	47.6	184	2.376	2.376	7.74E+04	2.02E+04
PI-1I-D-2-CI-7	05-1.5 min	1 min	1.328	127	21.6	120	2.376	2.376	5.05E+04	9.25E+03
PI-1I-D-2-CI-8	05-1.5 min	1 min	0.345	190	18.6	183	2.376	2.376	7.70E+04	8.18E+03
PI-1I-D-2-CI-9	05-1.5 min	1 min	1.063	551	93.6	549	2.376	2.376	2.31E+05	4.00E+04
PI-1I-D-3-CI-1	1.5-3.5 min	2 min	2.408	574	106.8	161	2.643	5.286	3.05E+04	2.49E+04
PI-1I-D-3-CI-2	1.5-3.5 min	2 min	-0.713	67	31.7	53	2.643	5.286	1.00E+04	6.15E+03
PI-1I-D-3-CI-3	1.5-3.5 min	2 min	0.249	149	37.9	146	2.643	5.286	2.76E+04	7.22E+03
PI-1I-D-3-CI-4	1.5-3.5 min	2 min	1.171	135	49.0	120	2.643	5.286	2.27E+04	9.36E+03
PI-1I-D-3-CI-5	1.5-3.5 min	2 min	-0.610	321	122.2	301	2.643	5.286	5.69E+04	2.32E+04
PI-1I-D-3-CI-6	1.5-3.5 min	2 min	0.312	148	35.4	132	2.643	5.286	2.50E+04	6.79E+03
PI-1I-D-3-CI-7	1.5-3.5 min	2 min	0.470	226	37.4	219	2.643	5.286	4.14E+04	7.19E+03
PI-1I-D-3-CI-8	1.5-3.5 min	2 min	0.991	509	48.0	502	2.643	5.286	9.50E+04	9.52E+03
PI-1I-D-3-CI-9	1.5-3.5 min	2 min	0.457	266	45.7	264	2.643	5.286	4.99E+04	8.78E+03
PI-1I-D-4-CI-1	3.5-7.5 min	4 min	3.514	317	59.1	-96	2.667	10.666	-9.00E+03	9.09E+03
PI-1I-D-4-CI-2	3.5-7.5 min	4 min	-0.152	24	11.8	10	2.667	10.666	9.38E+02	1.29E+03
PI-1I-D-4-CI-3	3.5-7.5 min	4 min	2.129	94	24.1	91	2.667	10.666	8.53E+03	2.28E+03
PI-1I-D-4-CI-4	3.5-7.5 min	4 min	0.050	127	46.4	112	2.667	10.666	1.05E+04	4.39E+03
PI-1I-D-4-CI-5	3.5-7.5 min	4 min	0.335	293	111.5	273	2.667	10.666	2.56E+04	1.05E+04
PI-1I-D-4-CI-6	3.5-7.5 min	4 min	0.011	186	44.2	170	2.667	10.666	1.59E+04	4.19E+03
PI-1I-D-4-CI-7	3.5-7.5 min	4 min	0.271	219	36.2	212	2.667	10.666	1.99E+04	3.45E+03
PI-1I-D-4-CI-8	3.5-7.5 min	4 min	0.535	274	26.1	267	2.667	10.666	2.50E+04	2.56E+03
PI-1I-D-4-CI-9	3.5-7.5 min	4 min	0.108	107	18.4	105	2.667	10.666	9.84E+03	1.75E+03
PI-1I-D-5-CI-1	7.5-15.5 min	8 min	2.355	271	50.5	-142	2.563	20.503	-6.93E+03	4.49E+03
PI-1I-D-5-CI-2	7.5-15.5 min	8 min	0.503	16	7.9	2	2.563	20.503	9.75E+01	5.15E+02
PI-1I-D-5-CI-3	7.5-15.5 min	8 min	-0.145	63	16.4	60	2.563	20.503	2.93E+03	8.07E+02
PI-1I-D-5-CI-4	7.5-15.5 min	8 min	-0.091	83	30.3	68	2.563	20.503	3.32E+03	1.51E+03
PI-1I-D-5-CI-5	7.5-15.5 min	8 min	-0.252	119	45.5	99	2.563	20.503	4.83E+03	2.26E+03
PI-1I-D-5-CI-6	7.5-15.5 min	8 min	-0.482	102	24.5	86	2.563	20.503	4.19E+03	1.22E+03
PI-1I-D-5-CI-7	7.5-15.5 min	8 min	0.075	124	21.1	117	2.563	20.503	5.71E+03	1.05E+03

Table A.20 (cont'd). Phase I, Shot 1, Driver

Sample ID	Collection Interval	Elapsed Time	Total Mass (mg)	Calculated U (μg)	DU Mass ± 1σ (μg)	Net DU Mass (μg)	Flow Rate (Lpm)	Volume (L)	DU Conc. (μg/m^3)	DU Conc. ± 1σ (μg/m^3)
PI-1I-D-5-CI-8	7.5-15.5 min	8 min	-0.005	164	16.1	157	2.563	20.503	7.66E+03	8.21E+02
PI-1I-D-5-CI-9	7.5-15.5 min	8 min	0.243	207	35.3	205	2.563	20.503	1.00E+04	1.75E+03
PI-1I-D-6-CI-1	15.5-31.5 min	16 min	2.020	357	66.5	-56	2.631	42.095	-1.33E+03	2.41E+03
PI-1I-D-6-CI-2	15.5-31.5 min	16 min	0.528	6	3.5	-8	2.631	42.095	-1.90E+02	1.86E+02
PI-1I-D-6-CI-3	15.5-31.5 min	16 min	0.536	41	10.7	38	2.631	42.095	9.03E+02	2.57E+02
PI-1I-D-6-CI-4	15.5-31.5 min	16 min	-0.944	48	17.6	33	2.631	42.095	7.84E+02	4.40E+02
PI-1I-D-6-CI-5	15.5-31.5 min	16 min	1.074	119	45.5	99	2.631	42.095	2.35E+03	1.10E+03
PI-1I-D-6-CI-6	15.5-31.5 min	16 min	-0.972	119	28.5	103	2.631	42.095	2.45E+03	6.88E+02
PI-1I-D-6-CI-7	15.5-31.5 min	16 min	-0.317	102	17.2	95	2.631	42.095	2.26E+03	4.16E+02
PI-1I-D-6-CI-8	15.5-31.5 min	16 min	0.376	130	13.1	123	2.631	42.095	2.92E+03	3.25E+02
PI-1I-D-6-CI-9	15.5-31.5 min	16 min	1.096	422	71.3	420	2.631	42.095	9.98E+03	1.72E+03
PI-1I-D-7-CI-1	31.5-63.5 min	32 min	1.067	356	66.5	-57	2.564	82.050	-6.95E+02	1.24E+03
PI-1I-D-7-CI-2	31.5-63.5 min	32 min	0.613	9	4.5	-5	2.564	82.050	-6.09E+01	1.01E+02
PI-1I-D-7-CI-3	31.5-63.5 min	32 min	0.010	25	6.7	22	2.564	82.050	2.68E+02	8.33E+01
PI-1I-D-7-CI-4	31.5-63.5 min	32 min	-0.035	36	13.3	21	2.564	82.050	2.56E+02	1.77E+02
PI-1I-D-7-CI-5	31.5-63.5 min	32 min	0.378	137	52.3	117	2.564	82.050	1.43E+03	6.46E+02
PI-1I-D-7-CI-6	31.5-63.5 min	32 min	-0.256	76	18.3	60	2.564	82.050	7.31E+02	2.30E+02
PI-1I-D-7-CI-7	31.5-63.5 min	32 min	-0.229	128	21.6	121	2.564	82.050	1.47E+03	2.68E+02
PI-1I-D-7-CI-8	31.5-63.5 min	32 min	0.493	160	15.8	153	2.564	82.050	1.86E+03	2.01E+02
PI-1I-D-7-CI-9	31.5-63.5 min	32 min	0.731	661	111.6	659	2.564	82.050	8.03E+03	1.38E+03
PI-1I-D-8-CI-1	63.5-127.5 min	64 min	1.448	645	120.1	232	2.640	168.989	1.37E+03	8.45E+02
PI-1I-D-8-CI-2	63.5-127.5 min	64 min	0.096	53	25.1	39	2.640	168.989	2.31E+02	1.54E+02
PI-1I-D-8-CI-3	63.5-127.5 min	64 min	-2.398	27	7.3	24	2.640	168.989	1.42E+02	4.40E+01
PI-1I-D-8-CI-4	63.5-127.5 min	64 min	-0.562	67	24.4	52	2.640	168.989	3.08E+02	1.49E+02
PI-1I-D-8-CI-5	63.5-127.5 min	64 min	-0.595	210	80.2	190	2.640	168.989	1.12E+03	4.78E+02
PI-1I-D-8-CI-6	63.5-127.5 min	64 min	0.517	146	34.9	130	2.640	168.989	7.69E+02	2.09E+02
PI-1I-D-8-CI-7	63.5-127.5 min	64 min	0.240	179	29.8	172	2.640	168.989	1.02E+03	1.79E+02
PI-1I-D-8-CI-8	63.5-127.5 min	64 min	0.332	238	23.1	231	2.640	168.989	1.37E+03	1.43E+02
PI-1I-D-8-CI-9	63.5-127.5 min	64 min	2.745	1198	201.7	1196	2.640	168.989	7.08E+03	1.21E+03
PI-1I-D-9-CI-1	Field Blank	--	1.687	413	76.8	--	--	--	--	--
PI-1I-D-9-CI-2	Field Blank	--	0.641	14	7.0	--	--	--	--	--
PI-1I-D-9-CI-3	Field Blank	--	0.023	3	1.2	--	--	--	--	--
PI-1I-D-9-CI-4	Field Blank	--	0.398	15	5.7	--	--	--	--	--
PI-1I-D-9-CI-5	Field Blank	--	-0.892	20	7.8	--	--	--	--	--
PI-1I-D-9-CI-6	Field Blank	--	-1.552	16	4.2	--	--	--	--	--
PI-1I-D-9-CI-7	Field Blank	--	-0.982	7	1.8	--	--	--	--	--
PI-1I-D-9-CI-8	Field Blank	--	-0.218	7	1.4	--	--	--	--	--
PI-1I-D-9-CI-9	Field Blank	--	0.719	2	1.0	--	--	--	--	--

Table A.20 (cont'd). Phase I, Shot 1, Gunner

Sample ID	Collection Interval	Elapsed Time	Total Mass (mg)	Calculated U (μg)	DU Mass ± 1σ (μg)	Net DU Mass (μg)	Flow Rate (Lpm)	Volume (L)	DU Conc. (μg/m^3)	DU Conc. ± 1σ (μg/m^3)
PI-1I-G-1-CI-1	0-30 sec	30 sec	1.470	847	115.0	151	2.611	1.305	1.16E+05	1.14E+05
PI-1I-G-1-CI-2	0-30 sec	30 sec	0.514	151	59.6	126	2.611	1.305	9.66E+04	4.64E+04
PI-1I-G-1-CI-3	0-30 sec	30 sec	0.004	199	37.1	194	2.611	1.305	1.49E+05	2.88E+04
PI-1I-G-1-CI-4	0-30 sec	30 sec	1.016	375	99.5	372	2.611	1.305	2.85E+05	7.67E+04
PI-1I-G-1-CI-5	0-30 sec	30 sec	1.684	459	172.7	457	2.611	1.305	3.50E+05	1.33E+05
PI-1I-G-1-CI-6	0-30 sec	30 sec	0.602	527	195.9	525	2.611	1.305	4.02E+05	1.51E+05
PI-1I-G-1-CI-7	0-30 sec	30 sec	0.335	327	70.8	326	2.611	1.305	2.50E+05	5.48E+04
PI-1I-G-1-CI-8	0-30 sec	30 sec	1.910	884	164.6	883	2.611	1.305	6.77E+05	1.28E+05
PI-1I-G-1-CI-9	0-30 sec	30 sec	4.235	2450	NA[(a)]	2441	2.611	1.305	1.87E+06	NA[(a)]
PI-1I-G-2-CI-1	05-1.5 min	1 min	0.972	516	70.2	-180	2.460	2.460	-7.32E+04	4.79E+04
PI-1I-G-2-CI-2	05-1.5 min	1 min	1.283	328	128.8	303	2.460	2.460	1.23E+05	5.26E+04
PI-1I-G-2-CI-3	05-1.5 min	1 min	0.897	398	73.9	393	2.460	2.460	1.60E+05	3.04E+04
PI-1I-G-2-CI-4	05-1.5 min	1 min	0.588	437	115.8	434	2.460	2.460	1.76E+05	4.74E+04
PI-1I-G-2-CI-5	05-1.5 min	1 min	1.129	580	218.1	578	2.460	2.460	2.35E+05	8.89E+04
PI-1I-G-2-CI-6	05-1.5 min	1 min	0.621	492	183.3	490	2.460	2.460	1.99E+05	7.48E+04
PI-1I-G-2-CI-7	05-1.5 min	1 min	0.200	313	68.4	312	2.460	2.460	1.27E+05	2.81E+04
PI-1I-G-2-CI-8	05-1.5 min	1 min	0.744	418	80.5	417	2.460	2.460	1.70E+05	3.31E+04
PI-1I-G-2-CI-9	05-1.5 min	1 min	2.554	1139	318.7	1130	2.460	2.460	4.59E+05	1.30E+05
PI-1I-G-3-CI-1	1.5-3.5 min	2 min	1.057	675	91.7	-21	2.558	5.117	-4.10E+03	2.57E+04
PI-1I-G-3-CI-2	1.5-3.5 min	2 min	0.417	195	76.7	170	2.558	5.117	3.32E+04	1.52E+04
PI-1I-G-3-CI-3	1.5-3.5 min	2 min	0.015	136	25.5	131	2.558	5.117	2.56E+04	5.05E+03
PI-1I-G-3-CI-4	1.5-3.5 min	2 min	0.474	89	23.9	86	2.558	5.117	1.68E+04	4.71E+03
PI-1I-G-3-CI-5	1.5-3.5 min	2 min	-0.121	206	77.9	204	2.558	5.117	3.99E+04	1.53E+04
PI-1I-G-3-CI-6	1.5-3.5 min	2 min	0.444	389	145.5	387	2.558	5.117	7.56E+04	2.85E+04
PI-1I-G-3-CI-7	1.5-3.5 min	2 min	0.539	449	96.9	448	2.558	5.117	8.76E+04	1.91E+04
PI-1I-G-3-CI-8	1.5-3.5 min	2 min	1.878	987	182.6	986	2.558	5.117	1.93E+05	3.62E+04
PI-1I-G-3-CI-9	1.5-3.5 min	2 min	2.207	952	266.7	943	2.558	5.117	1.84E+05	5.24E+04
PI-1I-G-4-CI-1	3.5-7.5 min	4 min	1.287	435	59.2	-261	2.565	10.261	-2.54E+04	1.09E+04
PI-1I-G-4-CI-2	3.5-7.5 min	4 min	0.688	113	44.6	88	2.565	10.261	8.58E+03	4.46E+03
PI-1I-G-4-CI-3	3.5-7.5 min	4 min	0.912	58	11.1	53	2.565	10.261	5.17E+03	1.10E+03
PI-1I-G-4-CI-4	3.5-7.5 min	4 min	0.633	81	21.8	78	2.565	10.261	7.60E+03	2.14E+03
PI-1I-G-4-CI-5	3.5-7.5 min	4 min	1.375	292	110.3	290	2.565	10.261	2.83E+04	1.08E+04
PI-1I-G-4-CI-6	3.5-7.5 min	4 min	0.704	280	104.8	278	2.565	10.261	2.71E+04	1.02E+04
PI-1I-G-4-CI-7	3.5-7.5 min	4 min	2.048	535	115.1	534	2.565	10.261	5.20E+04	1.13E+04
PI-1I-G-4-CI-8	3.5-7.5 min	4 min	2.305	783	145.3	782	2.565	10.261	7.62E+04	1.43E+04
PI-1I-G-4-CI-9	3.5-7.5 min	4 min	1.215	573	161.5	564	2.565	10.261	5.50E+04	1.58E+04
PI-1I-G-5-CI-1	7.5-15.5 min	8 min	0.579	103	14.7	-593	2.642	21.138	-2.81E+04	4.60E+03
PI-1I-G-5-CI-2	7.5-15.5 min	8 min	0.039	17	7.2	-8	2.642	21.138	-3.78E+02	5.87E+02
PI-1I-G-5-CI-3	7.5-15.5 min	8 min	-0.115	94	17.9	89	2.642	21.138	4.21E+03	8.59E+02
PI-1I-G-5-CI-4	7.5-15.5 min	8 min	0.214	78	21.1	75	2.642	21.138	3.55E+03	1.01E+03
PI-1I-G-5-CI-5	7.5-15.5 min	8 min	0.446	205	77.8	203	2.642	21.138	9.60E+03	3.69E+03
PI-1I-G-5-CI-6	7.5-15.5 min	8 min	0.238	214	80.5	212	2.642	21.138	1.00E+04	3.82E+03
PI-1I-G-5-CI-7	7.5-15.5 min	8 min	0.027	314	68.4	313	2.642	21.138	1.48E+04	3.27E+03

Table A.20 (cont'd). Phase I, Shot 1, Gunner

Sample ID	Collection Interval	Elapsed Time	Total Mass (mg)	Calculated U (μg)	DU Mass ± 1σ (μg)	Net DU Mass (μg)	Flow Rate (Lpm)	Volume (L)	DU Conc. (μg/m^3)	DU Conc. ± 1σ (μg/m^3)
PI-1I-G-5-CI-8	7.5-15.5 min	8 min	0.751	624	116.5	623	2.642	21.138	2.95E+04	5.58E+03
PI-1I-G-5-CI-9	7.5-15.5 min	8 min	1.730	739	207.4	730	2.642	21.138	3.45E+04	9.87E+03
PI-1I-G-6-CI-1	15.5-31.5 min	16 min	0.553	112	15.9	-584	2.654	42.457	-1.38E+04	2.29E+03
PI-1I-G-6-CI-2	15.5-31.5 min	16 min	-0.286	12	5.2	-13	2.654	42.457	-3.06E+02	2.68E+02
PI-1I-G-6-CI-3	15.5-31.5 min	16 min	0.589	35	6.9	30	2.654	42.457	7.07E+02	1.67E+02
PI-1I-G-6-CI-4	15.5-31.5 min	16 min	-0.112	56	15.1	53	2.654	42.457	1.25E+03	3.59E+02
PI-1I-G-6-CI-5	15.5-31.5 min	16 min	0.132	85	32.3	83	2.654	42.457	1.95E+03	7.64E+02
PI-1I-G-6-CI-6	15.5-31.5 min	16 min	0.062	107	41.2	105	2.654	42.457	2.47E+03	9.74E+02
PI-1I-G-6-CI-7	15.5-31.5 min	16 min	-0.125	142	32.1	141	2.654	42.457	3.32E+03	7.63E+02
PI-1I-G-6-CI-8	15.5-31.5 min	16 min	0.463	287	54.3	286	2.654	42.457	6.74E+03	1.30E+03
PI-1I-G-6-CI-9	15.5-31.5 min	16 min	1.544	499	141.8	490	2.654	42.457	1.15E+04	3.36E+03
PI-1I-G-7-CI-1	31.5-63.5 min	32 min	2.577	777	105.3	81	2.366	75.726	1.07E+03	1.87E+03
PI-1I-G-7-CI-2	31.5-63.5 min	32 min	0.749	18	7.3	-7	2.366	75.726	-9.24E+01	1.65E+02
PI-1I-G-7-CI-3	31.5-63.5 min	32 min	1.435	16	3.4	11	2.366	75.726	1.45E+02	4.88E+01
PI-1I-G-7-CI-4	31.5-63.5 min	32 min	0.196	35	9.6	32	2.366	75.726	4.23E+02	1.29E+02
PI-1I-G-7-CI-5	31.5-63.5 min	32 min	-0.082	77	29.6	75	2.366	75.726	9.90E+02	3.93E+02
PI-1I-G-7-CI-6	31.5-63.5 min	32 min	-0.082	104	39.5	102	2.366	75.726	1.35E+03	5.24E+02
PI-1I-G-7-CI-7	31.5-63.5 min	32 min	0.098	95	22.5	94	2.366	75.726	1.24E+03	3.00E+02
PI-1I-G-7-CI-8	31.5-63.5 min	32 min	0.626	284	55.1	283	2.366	75.726	3.74E+03	7.38E+02
PI-1I-G-7-CI-9	31.5-63.5 min	32 min	1.251	478	135.7	469	2.366	75.726	6.19E+03	1.80E+03
PI-1I-G-8-CI-1	63.5-127.5 min	64 min	1.493	602	81.8	-94	2.524	161.556	-5.82E+02	7.73E+02
PI-1I-G-8-CI-2	63.5-127.5 min	64 min	0.272	26	10.4	1	2.524	161.556	6.19E+00	8.97E+01
PI-1I-G-8-CI-3	63.5-127.5 min	64 min	-0.939	19	3.9	14	2.524	161.556	8.67E+01	2.58E+01
PI-1I-G-8-CI-4	63.5-127.5 min	64 min	0.004	49	13.4	46	2.524	161.556	2.85E+02	8.38E+01
PI-1I-G-8-CI-5	63.5-127.5 min	64 min	0.262	121	45.9	119	2.524	161.556	7.37E+02	2.85E+02
PI-1I-G-8-CI-6	63.5-127.5 min	64 min	0.002	133	50.4	131	2.524	161.556	8.11E+02	3.13E+02
PI-1I-G-8-CI-7	63.5-127.5 min	64 min	-0.216	142	32.0	141	2.524	161.556	8.73E+02	2.00E+02
PI-1I-G-8-CI-8	63.5-127.5 min	64 min	0.813	349	67.5	348	2.524	161.556	2.15E+03	4.23E+02
PI-1I-G-8-CI-9	63.5-127.5 min	64 min	2.543	976	273.6	967	2.524	161.556	5.99E+03	1.70E+03
PI-1I-G-9-CI-1	Field Blank	--	1.892	696	94.4	--	--	--	--	--
PI-1I-G-9-CI-2	Field Blank	--	-1.245	25	10.1	--	--	--	--	--
PI-1I-G-9-CI-3	Field Blank	--	-0.207	5	1.4	--	--	--	--	--
PI-1I-G-9-CI-4	Field Blank	--	0.127	3	1.4	--	--	--	--	--
PI-1I-G-9-CI-5	Field Blank	--	-0.124	2	1.7	--	--	--	--	--
PI-1I-G-9-CI-6	Field Blank	--	0.769	2	1.6	--	--	--	--	--
PI-1I-G-9-CI-7	Field Blank	--	-1.112	1	1.1	--	--	--	--	--
PI-1I-G-9-CI-8	Field Blank	--	-1.168	1	3.4	--	--	--	--	--
PI-1I-G-9-CI-9	Field Blank	--	-0.170	9	3.4	--	--	--	--	--

(a) DU mass based on ICP-MS results; no analytical uncertainty was reported.

Table A.20 (cont'd). Phase I, Shot 1, Loader

Sample ID	Collection Interval	Elapsed Time	Total Mass (mg)	Calculated U (μg)	DU Mass ± 1σ (μg)	Net DU Mass (μg)	Flow Rate (Lpm)	Volume (L)	DU Conc. (μg/m^3)	DU Conc. ± 1σ (μg/m^3)
PI-1I-L-1-CI-1	0-30 sec	30 sec	1.405	317	43.7	173	1.688	0.844	2.05E+05	5.73E+04
PI-1I-L-1-CI-2	0-30 sec	30 sec	0.988	190	74.8	185	1.688	0.844	2.19E+05	8.89E+04
PI-1I-L-1-CI-3	0-30 sec	30 sec	2.187	323	60.3	321	1.688	0.844	3.80E+05	7.24E+04
PI-1I-L-1-CI-4	0-30 sec	30 sec	1.598	293	78.2	293	1.688	0.844	3.47E+05	9.32E+04
PI-1I-L-1-CI-5	0-30 sec	30 sec	0.857	558	208.5	557	1.688	0.844	6.60E+05	2.48E+05
PI-1I-L-1-CI-6	0-30 sec	30 sec	1.065	583	210.8	575	1.688	0.844	6.81E+05	2.51E+05
PI-1I-L-1-CI-7	0-30 sec	30 sec	0.665	276	58.7	273	1.688	0.844	3.23E+05	7.03E+04
PI-1I-L-1-CI-8	0-30 sec	30 sec	1.296	600	107.2	595	1.688	0.844	7.05E+05	1.29E+05
PI-1I-L-1-CI-9	0-30 sec	30 sec	2.343	859	233.9	852	1.688	0.844	1.01E+06	2.79E+05
PI-1I-L-2-CI-1	05-1.5 min	1 min	1.184	275	38.0	131	2.458	2.458	5.33E+04	1.76E+04
PI-1I-L-2-CI-2	05-1.5 min	1 min	1.034	373	146.6	368	2.458	2.458	1.50E+05	5.98E+04
PI-1I-L-2-CI-3	05-1.5 min	1 min	0.593	459	85.5	457	2.458	2.458	1.86E+05	3.52E+04
PI-1I-L-2-CI-4	05-1.5 min	1 min	1.376	693	184.2	693	2.458	2.458	2.82E+05	7.54E+04
PI-1I-L-2-CI-5	05-1.5 min	1 min	1.627	937	350.2	936	2.458	2.458	3.81E+05	1.43E+05
PI-1I-L-2-CI-6	05-1.5 min	1 min	0.351	530	NA[(a)]	522	2.458	2.458	2.12E+05	NA
PI-1I-L-2-CI-7	05-1.5 min	1 min	0.478	337	71.8	334	2.458	2.458	1.36E+05	2.95E+04
PI-1I-L-2-CI-8	05-1.5 min	1 min	1.021	595	106.1	590	2.458	2.458	2.40E+05	4.38E+04
PI-1I-L-2-CI-9	05-1.5 min	1 min	3.445	1442	390.1	1435	2.458	2.458	5.84E+05	1.60E+05
PI-1I-L-3-CI-1	1.5-3.5 min	2 min	1.120	153	21.4	9	2.229	4.459	2.02E+03	6.58E+03
PI-1I-L-3-CI-2	1.5-3.5 min	2 min	0.350	211	83.0	206	2.229	4.459	4.62E+04	1.87E+04
PI-1I-L-3-CI-3	1.5-3.5 min	2 min	1.661	375	69.9	373	2.229	4.459	8.37E+04	1.59E+04
PI-1I-L-3-CI-4	1.5-3.5 min	2 min	0.858	280	74.6	280	2.229	4.459	6.28E+04	1.68E+04
PI-1I-L-3-CI-5	1.5-3.5 min	2 min	1.393	220	82.8	219	2.229	4.459	4.91E+04	1.86E+04
PI-1I-L-3-CI-6	1.5-3.5 min	2 min	0.786	76	28.1	68	2.229	4.459	1.53E+04	6.36E+03
PI-1I-L-3-CI-7	1.5-3.5 min	2 min	0.875	351	74.6	348	2.229	4.459	7.80E+04	1.69E+04
PI-1I-L-3-CI-8	1.5-3.5 min	2 min	1.418	977	172.4	972	2.229	4.459	2.18E+05	3.92E+04
PI-1I-L-3-CI-9	1.5-3.5 min	2 min	0.858	421	115.7	414	2.229	4.459	9.28E+04	2.61E+04
PI-1I-L-4-CI-1	3.5-7.5 min	4 min	0.769	77	11.2	-67	2.480	9.919	-6.75E+03	2.33E+03
PI-1I-L-4-CI-2	3.5-7.5 min	4 min	-0.589	80	31.7	75	2.480	9.919	7.56E+03	3.21E+03
PI-1I-L-4-CI-3	3.5-7.5 min	4 min	-0.732	381	71.1	379	2.480	9.919	3.82E+04	7.26E+03
PI-1I-L-4-CI-4	3.5-7.5 min	4 min	-0.430	135	36.2	135	2.480	9.919	1.36E+04	3.67E+03
PI-1I-L-4-CI-5	3.5-7.5 min	4 min	1.249	530	198.7	529	2.480	9.919	5.33E+04	2.01E+04
PI-1I-L-4-CI-6	3.5-7.5 min	4 min	0.791	494	178.8	486	2.480	9.919	4.90E+04	1.81E+04
PI-1I-L-4-CI-7	3.5-7.5 min	4 min	-0.092	569	119.7	566	2.480	9.919	5.71E+04	1.22E+04
PI-1I-L-4-CI-8	3.5-7.5 min	4 min	-0.853	652	116.7	647	2.480	9.919	6.52E+04	1.19E+04
PI-1I-L-4-CI-9	3.5-7.5 min	4 min	0.100	615	168.1	608	2.480	9.919	6.13E+04	1.70E+04
PI-1I-L-5-CI-1	7.5-15.5 min	8 min	0.547	49	7.5	-95	2.529	20.234	-4.70E+03	1.07E+03
PI-1I-L-5-CI-2	7.5-15.5 min	8 min	-0.684	27	11.1	22	2.529	20.234	1.09E+03	5.63E+02
PI-1I-L-5-CI-3	7.5-15.5 min	8 min	-1.239	87	16.5	85	2.529	20.234	4.20E+03	8.26E+02
PI-1I-L-5-CI-4	7.5-15.5 min	8 min	-1.864	106	28.7	106	2.529	20.234	5.24E+03	1.43E+03
PI-1I-L-5-CI-5	7.5-15.5 min	8 min	-2.484	351	131.8	350	2.529	20.234	1.73E+04	6.53E+03
PI-1I-L-5-CI-6	7.5-15.5 min	8 min	-2.429	314	114.2	306	2.529	20.234	1.51E+04	5.66E+03
PI-1I-L-5-CI-7	7.5-15.5 min	8 min	-0.435	506	106.6	503	2.529	20.234	2.49E+04	5.32E+03

Table A.20 (cont'd). Phase I, Shot 1, Loader

Sample ID	Collection Interval	Elapsed Time	Total Mass (mg)	Calculated U (μg)	DU Mass ± 1σ (μg)	Net DU Mass (μg)	Flow Rate (Lpm)	Volume (L)	DU Conc. (μg/m^3)	DU Conc. ± 1σ (μg/m^3)
PI-1I-L-5-CI-8	7.5-15.5 min	8 min	-0.848	511	91.9	506	2.529	20.234	2.50E+04	4.60E+03
PI-1I-L-5-CI-9	7.5-15.5 min	8 min	0.665	375	103.6	368	2.529	20.234	1.82E+04	5.15E+03
PI-1I-L-6-CI-1	15.5-31.5 min	16 min	0.621	42	6.2	-102	2.527	40.437	-2.52E+03	5.26E+02
PI-1I-L-6-CI-2	15.5-31.5 min	16 min	0.363	4	2.3	-1	2.527	40.437	-2.47E+01	8.40E+01
PI-1I-L-6-CI-3	15.5-31.5 min	16 min	0.151	27	5.5	25	2.527	40.437	6.18E+02	1.38E+02
PI-1I-L-6-CI-4	15.5-31.5 min	16 min	0.400	148	39.8	148	2.527	40.437	3.66E+03	9.90E+02
PI-1I-L-6-CI-5	15.5-31.5 min	16 min	0.444	296	111.1	295	2.527	40.437	7.30E+03	2.76E+03
PI-1I-L-6-CI-6	15.5-31.5 min	16 min	0.302	120	44.4	112	2.527	40.437	2.77E+03	1.10E+03
PI-1I-L-6-CI-7	15.5-31.5 min	16 min	0.675	178	38.8	175	2.527	40.437	4.33E+03	9.70E+02
PI-1I-L-6-CI-8	15.5-31.5 min	16 min	0.716	264	48.4	259	2.527	40.437	6.41E+03	1.21E+03
PI-1I-L-6-CI-9	15.5-31.5 min	16 min	1.254	459	126.5	452	2.527	40.437	1.12E+04	3.15E+03
PI-1I-L-7-CI-1	31.5-63.5 min	32 min	0.236	168	23.1	24	2.436	77.964	3.08E+02	3.93E+02
PI-1I-L-7-CI-2	31.5-63.5 min	32 min	1.750	9	3.8	4	2.436	77.964	5.13E+01	5.84E+01
PI-1I-L-7-CI-3	31.5-63.5 min	32 min	0.993	23	4.8	21	2.436	77.964	2.69E+02	6.27E+01
PI-1I-L-7-CI-4	31.5-63.5 min	32 min	0.886	44	12.1	44	2.436	77.964	5.64E+02	1.56E+02
PI-1I-L-7-CI-5	31.5-63.5 min	32 min	0.649	72	27.5	71	2.436	77.964	9.11E+02	3.54E+02
PI-1I-L-7-CI-6	31.5-63.5 min	32 min	-0.978	67	25.0	59	2.436	77.964	7.57E+02	3.24E+02
PI-1I-L-7-CI-7	31.5-63.5 min	32 min	2.106	105	23.8	102	2.436	77.964	1.31E+03	3.09E+02
PI-1I-L-7-CI-8	31.5-63.5 min	32 min	0.903	131	26.4	126	2.436	77.964	1.62E+03	3.43E+02
PI-1I-L-7-CI-9	31.5-63.5 min	32 min	1.764	621	170.2	614	2.436	77.964	7.88E+03	2.20E+03
PI-1I-L-8-CI-1	63.5-127.5 min	64 min	1.620	189	26.1	45	2.498	159.882	2.81E+02	2.06E+02
PI-1I-L-8-CI-2	63.5-127.5 min	64 min	0.218	8	3.8	3	2.498	159.882	1.88E+01	2.85E+01
PI-1I-L-8-CI-3	63.5-127.5 min	64 min	0.628	11	2.7	9	2.498	159.882	5.63E+01	1.75E+01
PI-1I-L-8-CI-4	63.5-127.5 min	64 min	0.745	50	13.8	50	2.498	159.882	3.13E+02	8.69E+01
PI-1I-L-8-CI-5	63.5-127.5 min	64 min	0.601	42	16.3	41	2.498	159.882	2.56E+02	1.02E+02
PI-1I-L-8-CI-6	63.5-127.5 min	64 min	0.610	159	57.1	151	2.498	159.882	9.44E+02	3.59E+02
PI-1I-L-8-CI-7	63.5-127.5 min	64 min	0.673	144	31.8	141	2.498	159.882	8.82E+02	2.01E+02
PI-1I-L-8-CI-8	63.5-127.5 min	64 min	0.537	211	39.7	206	2.498	159.882	1.29E+03	2.52E+02
PI-1I-L-8-CI-9	63.5-127.5 min	64 min	3.723	1114	293.4	1107	2.498	159.882	6.92E+03	1.85E+03
PI-1I-L-9-CI-1	Field Blank	--	0.882	144	20.1	--	--	--	--	--
PI-1I-L-9-CI-2	Field Blank	--	0.762	5	2.5	--	--	--	--	--
PI-1I-L-9-CI-3	Field Blank	--	0.676	2	0.7	--	--	--	--	--
PI-1I-L-9-CI-4	Field Blank	--	0.762	0	0.6	--	--	--	--	--
PI-1I-L-9-CI-5	Field Blank	--	0.071	1	0.6	--	--	--	--	--
PI-1I-L-9-CI-6	Field Blank	--	1.397	8	3.1	--	--	--	--	--
PI-1I-L-9-CI-7	Field Blank	--	0.832	3	2.2	--	--	--	--	--
PI-1I-L-9-CI-8	Field Blank	--	0.559	5	1.7	--	--	--	--	--
PI-1I-L-9-CI-9	Field Blank	--	1.237	7	2.4	--	--	--	--	--

(a) DU mass based on ICP-MS results; no analytical uncertainty was reported.

Table A.21. PI-2 Cascade Impactor Substrates—Mass, Volume, and Concentration

Sample ID	Collection Interval	Elapsed Time	Total Mass (mg)	Calculated U (µg)	DU Mass ± 1σ (µg)	Net DU Mass (µg)	Flow Rate (Lpm)	Volume (L)	DU Conc. (µg/m^3)	DU Conc. ± 1σ (µg/m^3)
PI-2I-C-1-CI-1	0-15 sec	15 sec	1.808	703	130.6	314	2.663	0.666	4.71E+05	2.25E+05
PI-2I-C-1-CI-2	0-15 sec	15 sec	-0.364	190	NA[(a)]	155	2.663	0.666	2.33E+05	NA[(a)]
PI-2I-C-1-CI-3	0-15 sec	15 sec	0.813	182	46.1	164	2.663	0.666	2.46E+05	7.00E+04
PI-2I-C-1-CI-4	0-15 sec	15 sec	0.880	311	113.3	303	2.663	0.666	4.55E+05	1.71E+05
PI-2I-C-1-CI-5	0-15 sec	15 sec	0.522	261	99.4	256	2.663	0.666	3.84E+05	1.50E+05
PI-2I-C-1-CI-6	0-15 sec	15 sec	-0.155	158	37.6	155	2.663	0.666	2.33E+05	5.69E+04
PI-2I-C-1-CI-7	0-15 sec	15 sec	0.173	122	20.5	117	2.663	0.666	1.76E+05	3.13E+04
PI-2I-C-1-CI-8	0-15 sec	15 sec	0.677	231	22.0	224	2.663	0.666	3.36E+05	3.46E+04
PI-2I-C-1-CI-9	0-15 sec	15 sec	1.194	846	142.9	828	2.663	0.666	1.24E+06	2.18E+05
PI-2I-C-2-CI-1	0.5-1 min	30 sec	0.847	266	49.7	-123	2.647	1.324	-9.29E+04	6.63E+04
PI-2I-C-2-CI-2	0.5-1 min	30 sec	0.626	277	130.3	242	2.647	1.324	1.83E+05	9.94E+04
PI-2I-C-2-CI-3	0.5-1 min	30 sec	-1.379	143	36.5	125	2.647	1.324	9.44E+04	2.79E+04
PI-2I-C-2-CI-4	0.5-1 min	30 sec	0.124	202	73.6	194	2.647	1.324	1.47E+05	5.58E+04
PI-2I-C-2-CI-5	0.5-1 min	30 sec	0.031	580	220.5	575	2.647	1.324	4.34E+05	1.67E+05
PI-2I-C-2-CI-6	0.5-1 min	30 sec	1.278	285	67.5	282	2.647	1.324	2.13E+05	5.14E+04
PI-2I-C-2-CI-7	0.5-1 min	30 sec	-0.767	228	37.7	223	2.647	1.324	1.68E+05	2.89E+04
PI-2I-C-2-CI-8	0.5-1 min	30 sec	0.033	299	28.5	292	2.647	1.324	2.21E+05	2.25E+04
PI-2I-C-2-CI-9	0.5-1 min	30 sec	1.668	1023	172.4	1005	2.647	1.324	7.59E+05	1.32E+05
PI-2I-C-3-CI-1	1.5-2.5 min	1 min	1.385	169	31.7	-220	2.629	2.629	-8.37E+04	3.01E+04
PI-2I-C-3-CI-2	1.5-2.5 min	1 min	0.515	70	33.3	35	2.629	2.629	1.33E+04	1.42E+04
PI-2I-C-3-CI-3	1.5-2.5 min	1 min	0.958	236	60.0	218	2.629	2.629	8.29E+04	2.30E+04
PI-2I-C-3-CI-4	1.5-2.5 min	1 min	-0.634	144	52.5	136	2.629	2.629	5.17E+04	2.01E+04
PI-2I-C-3-CI-5	1.5-2.5 min	1 min	-0.598	247	94.1	242	2.629	2.629	9.21E+04	3.59E+04
PI-2I-C-3-CI-6	1.5-2.5 min	1 min	-0.321	147	35.0	144	2.629	2.629	5.48E+04	1.34E+04
PI-2I-C-3-CI-7	1.5-2.5 min	1 min	-0.503	176	29.0	171	2.629	2.629	6.50E+04	1.12E+04
PI-2I-C-3-CI-8	1.5-2.5 min	1 min	1.163	263	25.2	256	2.629	2.629	9.74E+04	1.00E+04
PI-2I-C-3-CI-9	1.5-2.5 min	1 min	0.642	622	105.2	604	2.629	2.629	2.30E+05	4.06E+04
PI-2I-C-4-CI-1	3.5-5.5 min	2 min	1.574	266	49.5	-123	2.465	4.929	-2.50E+04	1.78E+04
PI-2I-C-4-CI-2	3.5-5.5 min	2 min	-0.378	37	17.9	2	2.465	4.929	4.06E+02	4.97E+03
PI-2I-C-4-CI-3	3.5-5.5 min	2 min	-0.178	60	15.4	42	2.465	4.929	8.52E+03	3.28E+03
PI-2I-C-4-CI-4	3.5-5.5 min	2 min	-0.933	102	37.0	94	2.465	4.929	1.91E+04	7.56E+03
PI-2I-C-4-CI-5	3.5-5.5 min	2 min	-0.549	408	155.1	403	2.465	4.929	8.18E+04	3.16E+04
PI-2I-C-4-CI-6	3.5-5.5 min	2 min	-0.302	197	46.7	194	2.465	4.929	3.94E+04	9.55E+03
PI-2I-C-4-CI-7	3.5-5.5 min	2 min	-0.652	302	49.3	297	2.465	4.929	6.03E+04	1.02E+04
PI-2I-C-4-CI-8	3.5-5.5 min	2 min	-1.443	200	19.3	193	2.465	4.929	3.92E+04	4.09E+03
PI-2I-C-4-CI-9	3.5-5.5 min	2 min	1.643	646	109.3	628	2.465	4.929	1.27E+05	2.25E+04
PI-2I-C-5-CI-1	7.5-11.5 min	4 min	0.691	246	45.8	-143	2.469	9.876	-1.45E+04	8.68E+03
PI-2I-C-5-CI-2	7.5-11.5 min	4 min	-0.125	34.8	16.6	-0.2	2.469	9.876	-2.03E+01	2.38E+03
PI-2I-C-5-CI-3	7.5-11.5 min	4 min	-2.871	72	18.4	54	2.469	9.876	5.47E+03	1.93E+03
PI-2I-C-5-CI-4	7.5-11.5 min	4 min	-0.317	46	17.1	38	2.469	9.876	3.85E+03	1.77E+03
PI-2I-C-5-CI-5	7.5-11.5 min	4 min	-0.395	166	63.2	161	2.469	9.876	1.63E+04	6.42E+03
PI-2I-C-5-CI-6	7.5-11.5 min	4 min	0.340	106	25.2	103	2.469	9.876	1.04E+04	2.57E+03

Table A.21 (cont'd). Phase I, Shot 2, Commander

Sample ID	Collection Interval	Elapsed Time	Total Mass (mg)	Calculated U (μg)	DU Mass ± 1σ (μg)	Net DU Mass (μg)	Flow Rate (Lpm)	Volume (L)	DU Conc. (μg/m^3)	DU Conc. ± 1σ (μg/m^3)
PI-2I-C-5-CI-7	7.5-11.5 min	4 min	-0.744	97	16.2	92	2.469	9.876	9.32E+03	1.67E+03
PI-2I-C-5-CI-8	7.5-11.5 min	4 min	0.615	102	10.1	95	2.469	9.876	9.62E+03	1.07E+03
PI-2I-C-5-CI-9	7.5-11.5 min	4 min	1.022	302	51.4	284	2.469	9.876	2.88E+04	5.29E+03
PI-2I-C-6-CI-1	15.5-31.5 min	16 min	2.445	321	59.8	-68	2.436	38.972	-1.74E+03	2.41E+03
PI-2I-C-6-CI-2	15.5-31.5 min	16 min	0.858	27	12.9	-8	2.436	38.972	-2.05E+02	5.42E+02
PI-2I-C-6-CI-3	15.5-31.5 min	16 min	0.429	40	10.4	22	2.436	38.972	5.65E+02	2.94E+02
PI-2I-C-6-CI-4	15.5-31.5 min	16 min	0.905	56	20.7	48	2.436	38.972	1.23E+03	5.39E+02
PI-2I-C-6-CI-5	15.5-31.5 min	16 min	0.392	269	102.4	264	2.436	38.972	6.77E+03	2.64E+03
PI-2I-C-6-CI-6	15.5-31.5 min	16 min	-0.137	118	28.2	115	2.436	38.972	2.95E+03	7.30E+02
PI-2I-C-6-CI-7	15.5-31.5 min	16 min	-1.449	144	24.1	139	2.436	38.972	3.57E+03	6.29E+02
PI-2I-C-6-CI-8	15.5-31.5 min	16 min	1.459	358	33.8	351	2.436	38.972	9.01E+03	9.09E+02
PI-2I-C-6-CI-9	15.5-31.5 min	16 min	1.111	568	96.4	550	2.436	38.972	1.41E+04	2.51E+03
PI-2I-C-7-CI-1	31.5-79.5 min	48 min	0.623	276	51.7	-113	2.612	125.361	-9.01E+02	7.10E+02
PI-2I-C-7-CI-2	31.5-79.5 min	48 min	0.312	36	17.3	1	2.612	125.361	7.98E+00	1.92E+02
PI-2I-C-7-CI-3	31.5-79.5 min	48 min	1.547	78	20.0	60	2.612	125.361	4.79E+02	1.65E+02
PI-2I-C-7-CI-4	31.5-79.5 min	48 min	-0.359	191	69.4	183	2.612	125.361	1.46E+03	5.56E+02
PI-2I-C-7-CI-5	31.5-79.5 min	48 min	0.584	361	137.3	356	2.612	125.361	2.84E+03	1.10E+03
PI-2I-C-7-CI-6	31.5-79.5 min	48 min	0.129	256	60.6	253	2.612	125.361	2.02E+03	4.87E+02
PI-2I-C-7-CI-7	31.5-79.5 min	48 min	0.059	296	48.5	291	2.612	125.361	2.32E+03	3.93E+02
PI-2I-C-7-CI-8	31.5-79.5 min	48 min	0.320	412	39.1	405	2.612	125.361	3.23E+03	3.27E+02
PI-2I-C-7-CI-9	31.5-79.5 min	48 min	2.574	1401	236.2	1383	2.612	125.361	1.10E+04	1.91E+03
PI-2I-C-8-CI-1	79.5-127.5 min	48 min	1.453	266	49.8	-123	2.521	121.029	-1.02E+03	7.26E+02
PI-2I-C-8-CI-2	79.5-127.5 min	48 min	1.100	44	20.8	9	2.521	121.029	7.44E+01	2.20E+02
PI-2I-C-8-CI-3	79.5-127.5 min	48 min	0.652	35	9.2	17	2.521	121.029	1.40E+02	8.58E+01
PI-2I-C-8-CI-4	79.5-127.5 min	48 min	-0.014	60	22.1	52	2.521	121.029	4.30E+02	1.85E+02
PI-2I-C-8-CI-5	79.5-127.5 min	48 min	-0.089	259	98.8	254	2.521	121.029	2.10E+03	8.19E+02
PI-2I-C-8-CI-6	79.5-127.5 min	48 min	0.174	135	32.1	132	2.521	121.029	1.09E+03	2.67E+02
PI-2I-C-8-CI-7	79.5-127.5 min	48 min	-0.148	235	38.8	230	2.521	121.029	1.90E+03	3.26E+02
PI-2I-C-8-CI-8	79.5-127.5 min	48 min	0.240	216	21.0	209	2.521	121.029	1.73E+03	1.81E+02
PI-2I-C-8-CI-9	79.5-127.5 min	48 min	3.369	1253	211.2	1235	2.521	121.029	1.02E+04	1.77E+03
PI-2I-C-9-CI-1	Field Blank	--	-2.870	389	72.3	--	--	--	--	--
PI-2I-C-9-CI-2	Field Blank	--	-0.358	35	16.7	--	--	--	--	--
PI-2I-C-9-CI-3	Field Blank	--	-0.982	18	4.8	--	--	--	--	--
PI-2I-C-9-CI-4	Field Blank	--	-0.660	8	3.2	--	--	--	--	--
PI-2I-C-9-CI-5	Field Blank	--	-1.158	5	2.2	--	--	--	--	--
PI-2I-C-9-CI-6	Field Blank	--	0.338	3	1.2	--	--	--	--	--
PI-2I-C-9-CI-7	Field Blank	--	0.032	5	1.4	--	--	--	--	--
PI-2I-C-9-CI-8	Field Blank	--	0.562	7	1.1	--	--	--	--	--
PI-2I-C-9-CI-9	Field Blank	--	0.537	18	3.5	--	--	--	--	--

(a) DU mass based on ICP-MS results; no analytical uncertainty was reported.

Table A.21 (cont'd). Phase I, Shot 2, Driver

Sample ID	Collection Interval	Elapsed Time	Total Mass (mg)	Calculated U (μg)	DU Mass ± 1σ (μg)	Net DU Mass (μg)	Flow Rate (Lpm)	Volume (L)	DU Conc. (μg/m^3)	DU Conc. ± 1σ (μg/m^3)
PI-2I-D-1-CI-1	0-15 sec	15 sec	1.087	492	65.5	215	2.576	0.644	3.34E+05	1.17E+05
PI-2I-D-1-CI-2	0-15 sec	16 sec	0.641	327	129.3	322	2.576	0.644	5.00E+05	2.01E+05
PI-2I-D-1-CI-3	0-15 sec	17 sec	0.940	141	25.9	137	2.576	0.644	2.13E+05	4.08E+04
PI-2I-D-1-CI-4	0-15 sec	18 sec	0.711	333	86.4	332	2.576	0.644	5.16E+05	1.35E+05
PI-2I-D-1-CI-5	0-15 sec	19 sec	1.322	362	142.8	355	2.576	0.644	5.51E+05	2.22E+05
PI-2I-D-1-CI-6	0-15 sec	20 sec	0.341	255	119.8	246	2.576	0.644	3.82E+05	1.87E+05
PI-2I-D-1-CI-7	0-15 sec	21 sec	-0.665	99	26.8	72	2.576	0.644	1.12E+05	4.35E+04
PI-2I-D-1-CI-8	0-15 sec	22 sec	0.372	207	62.4	207	2.576	0.644	3.21E+05	9.80E+04
PI-2I-D-1-CI-9	0-15 sec	23 sec	0.039	651	239.0	563	2.576	0.644	8.74E+05	3.76E+05
PI-2I-D-2-CI-1	Did not run	--	--	--	--	--	--	--	--	--
PI-2I-D-2-CI-2	Did not run	--	--	--	--	--	--	--	--	--
PI-2I-D-2-CI-3	Did not run	--	--	--	--	--	--	--	--	--
PI-2I-D-2-CI-4	Did not run	--	--	--	--	--	--	--	--	--
PI-2I-D-2-CI-5	Did not run	--	--	--	--	--	--	--	--	--
PI-2I-D-2-CI-6	Did not run	--	--	--	--	--	--	--	--	--
PI-2I-D-2-CI-7	Did not run	--	--	--	--	--	--	--	--	--
PI-2I-D-2-CI-8	Did not run	--	--	--	--	--	--	--	--	--
PI-2I-D-2-CI-9	Did not run	--	--	--	--	--	--	--	--	--
PI-2I-D-3-CI-1	1.5-2.5 min	1 min	0.422	190	25.5	-87	2.687	2.687	-3.24E+04	1.68E+04
PI-2I-D-3-CI-2	1.5-2.5 min	2 min	0.540	56	22.4	51	2.687	2.687	1.90E+04	8.42E+03
PI-2I-D-3-CI-3	1.5-2.5 min	3 min	0.354	171	31.3	167	2.687	2.687	6.22E+04	1.18E+04
PI-2I-D-3-CI-4	1.5-2.5 min	4 min	0.363	149	39.0	148	2.687	2.687	5.51E+04	1.46E+04
PI-2I-D-3-CI-5	1.5-2.5 min	5 min	0.747	262	104.1	255	2.687	2.687	9.49E+04	3.89E+04
PI-2I-D-3-CI-6	1.5-2.5 min	6 min	-0.069	153	73.1	144	2.687	2.687	5.36E+04	2.74E+04
PI-2I-D-3-CI-7	1.5-2.5 min	7 min	-0.932	127	33.6	100	2.687	2.687	3.72E+04	1.29E+04
PI-2I-D-3-CI-8	1.5-2.5 min	8 min	0.519	285	83.2	285	2.687	2.687	1.06E+05	3.12E+04
PI-2I-D-3-CI-9	1.5-2.5 min	9 min	-0.409	229	87.1	141	2.687	2.687	5.25E+04	3.48E+04
PI-2I-D-4-CI-1	3.5-5.5 min	2 min	0.976	133	18.1	-144	2.669	5.339	-2.70E+04	7.81E+03
PI-2I-D-4-CI-2	3.5-5.5 min	3 min	1.002	14	6.2	9	2.669	5.339	1.69E+03	1.27E+03
PI-2I-D-4-CI-3	3.5-5.5 min	4 min	3.063	116	21.4	112	2.669	5.339	2.10E+04	4.07E+03
PI-2I-D-4-CI-4	3.5-5.5 min	5 min	-1.443	68	17.9	67	2.669	5.339	1.25E+04	3.39E+03
PI-2I-D-4-CI-5	3.5-5.5 min	6 min	-1.182	112	45.2	105	2.669	5.339	1.97E+04	8.53E+03
PI-2I-D-4-CI-6	3.5-5.5 min	7 min	-1.208	95	46.5	86	2.669	5.339	1.61E+04	8.85E+03
PI-2I-D-4-CI-7	3.5-5.5 min	8 min	-1.550	109	29.6	82	2.669	5.339	1.54E+04	5.75E+03
PI-2I-D-4-CI-8	3.5-5.5 min	9 min	-1.283	166	51.0	166	2.669	5.339	3.11E+04	9.69E+03
PI-2I-D-4-CI-9	3.5-5.5 min	10 min	-0.716	196	73.8	108	2.669	5.339	2.02E+04	1.52E+04
PI-2I-D-5-CI-1	7.5-11.5 min	4 min	0.862	269	36.0	-8	2.621	10.484	-7.63E+02	4.94E+03
PI-2I-D-5-CI-2	7.5-11.5 min	5 min	1.990	41	16.5	36	2.621	10.484	3.43E+03	1.60E+03
PI-2I-D-5-CI-3	7.5-11.5 min	6 min	-0.376	19	4.0	15	2.621	10.484	1.43E+03	4.17E+02
PI-2I-D-5-CI-4	7.5-11.5 min	7 min	-2.000	24	6.7	23	2.621	10.484	2.19E+03	6.65E+02
PI-2I-D-5-CI-5	7.5-11.5 min	8 min	-0.639	67	27.0	60	2.621	10.484	5.72E+03	2.62E+03
PI-2I-D-5-CI-6	7.5-11.5 min	9 min	-0.902	111	53.4	102	2.621	10.484	9.73E+03	5.16E+03
PI-2I-D-5-CI-7	7.5-11.5 min	10 min	-0.731	62	19.5	35	2.621	10.484	3.34E+03	2.01E+03

Table A.21 (cont'd). Phase I, Shot 2, Driver

Sample ID	Collection Interval	Elapsed Time	Total Mass (mg)	Calculated U (μg)	DU Mass ± 1σ (μg)	Net DU Mass (μg)	Flow Rate (Lpm)	Volume (L)	DU Conc. (μg/m^3)	DU Conc. ± 1σ (μg/m^3)
PI-2I-D-5-CI-8	7.5-11.5 min	11 min	0.182	310	88.4	310	2.621	10.484	2.96E+04	8.50E+03
PI-2I-D-5-CI-9	7.5-11.5 min	12 min	0.047	75	31.5	-13	2.621	10.484	-1.24E+03	4.41E+03
PI-2I-D-6-CI-1	15.5-31.5 min	16 min	1.765	265	35.3	-12	2.630	42.079	-2.85E+02	1.22E+03
PI-2I-D-6-CI-2	15.5-31.5 min	17 min	1.763	0	0.9	-5	2.630	42.079	-1.19E+02	6.77E+01
PI-2I-D-6-CI-3	15.5-31.5 min	18 min	-2.340	58	10.9	54	2.630	42.079	1.28E+03	2.65E+02
PI-2I-D-6-CI-4	15.5-31.5 min	19 min	-0.733	105	27.4	104	2.630	42.079	2.47E+03	6.57E+02
PI-2I-D-6-CI-5	15.5-31.5 min	20 min	-1.234	101	40.6	94	2.630	42.079	2.23E+03	9.74E+02
PI-2I-D-6-CI-6	15.5-31.5 min	21 min	-0.445	131	62.3	122	2.630	42.079	2.90E+03	1.50E+03
PI-2I-D-6-CI-7	15.5-31.5 min	22 min	-0.247	112	30.4	85	2.630	42.079	2.02E+03	7.48E+02
PI-2I-D-6-CI-8	15.5-31.5 min	23 min	0.549	323	93.3	323	2.630	42.079	7.68E+03	2.24E+03
PI-2I-D-6-CI-9	15.5-31.5 min	24 min	0.927	364	136.4	276	2.630	42.079	6.56E+03	3.35E+03
PI-2I-D-7-CI-1	31.5-79.5 min	48 min	0.734	263	35.3	-14	2.523	121.116	-1.16E+02	4.24E+02
PI-2I-D-7-CI-2	31.5-79.5 min	49 min	3.067	12	5.2	7	2.523	121.116	5.78E+01	4.84E+01
PI-2I-D-7-CI-3	31.5-79.5 min	50 min	0.246	99	18.5	95	2.523	121.116	7.84E+02	1.55E+02
PI-2I-D-7-CI-4	31.5-79.5 min	51 min	-0.485	78	20.6	77	2.523	121.116	6.36E+02	1.72E+02
PI-2I-D-7-CI-5	31.5-79.5 min	52 min	0.131	478	186.8	471	2.523	121.116	3.89E+03	1.55E+03
PI-2I-D-7-CI-6	31.5-79.5 min	53 min	-0.952	235	105.9	226	2.523	121.116	1.87E+03	8.79E+02
PI-2I-D-7-CI-7	31.5-79.5 min	54 min	0.449	228	56.5	201	2.523	121.116	1.66E+03	4.74E+02
PI-2I-D-7-CI-8	31.5-79.5 min	55 min	-0.210	450	117.6	450	2.523	121.116	3.72E+03	9.79E+02
PI-2I-D-7-CI-9	31.5-79.5 min	56 min	2.788	1129	388.6	1041	2.523	121.116	8.60E+03	3.23E+03
PI-2I-D-8-CI-1	79.5-127.5 min	48 min	0.960	177	24.0	-100	2.640	126.730	-7.89E+02	3.51E+02
PI-2I-D-8-CI-2	79.5-127.5 min	49 min	-0.577	8	3.8	3	2.640	126.730	2.37E+01	3.68E+01
PI-2I-D-8-CI-3	79.5-127.5 min	50 min	0.132	23	5.0	19	2.640	126.730	1.50E+02	4.19E+01
PI-2I-D-8-CI-4	79.5-127.5 min	51 min	-0.288	35	9.6	34	2.640	126.730	2.68E+02	7.75E+01
PI-2I-D-8-CI-5	79.5-127.5 min	52 min	-1.163	119	47.1	112	2.640	126.730	8.84E+02	3.75E+02
PI-2I-D-8-CI-6	79.5-127.5 min	53 min	0.073	171	77.6	162	2.640	126.730	1.28E+03	6.17E+02
PI-2I-D-8-CI-7	79.5-127.5 min	54 min	-0.266	138	36.3	111	2.640	126.730	8.76E+02	2.94E+02
PI-2I-D-8-CI-8	79.5-127.5 min	55 min	0.187	255	69.4	255	2.640	126.730	2.01E+03	5.54E+02
PI-2I-D-8-CI-9	79.5-127.5 min	56 min	1.503	594	208.2	506	2.640	126.730	3.99E+03	1.67E+03
PI-2I-D-9-CI-1	Field Blank	--	-0.962	277	37.3	--	--	--	--	--
PI-2I-D-9-CI-2	Field Blank	--	3.161	5	2.7	--	--	--	--	--
PI-2I-D-9-CI-3	Field Blank	--	-0.950	4	1.7	--	--	--	--	--
PI-2I-D-9-CI-4	Field Blank	--	-0.710	1	1.8	--	--	--	--	--
PI-2I-D-9-CI-5	Field Blank	--	-0.030	7	4.8	--	--	--	--	--
PI-2I-D-9-CI-6	Field Blank	--	-0.368	9	8.0	--	--	--	--	--
PI-2I-D-9-CI-7	Field Blank	--	-0.623	27	7.8	--	--	--	--	--
PI-2I-D-9-CI-8	Field Blank	--	-0.129	-2	7.0	--	--	--	--	--
PI-2I-D-9-CI-9	Field Blank	--	-1.638	88	33.8	--	--	--	--	--

Table A.21 (cont'd). Phase I, Shot 2, Gunner

Sample ID	Collection Interval	Elapsed Time	Total Mass (mg)	Calculated U (μg)	DU Mass ± 1σ (μg)	Net DU Mass (μg)	Flow Rate (Lpm)	Volume (L)	DU Conc. (μg/m^3)	DU Conc. ± 1σ (μg/m^3)
PI-2I-G-1-CI-1	0-15 sec	15 sec	1.06	350	47.3	90	2.681	0.670	1.34E+05	8.81E+04
PI-2I-G-1-CI-2	0-15 sec	15 sec	0.509	332	130.2	318	2.681	0.670	4.74E+05	1.95E+05
PI-2I-G-1-CI-3	0-15 sec	15 sec	0.462	216	39.8	215	2.681	0.670	3.21E+05	6.02E+04
PI-2I-G-1-CI-4	0-15 sec	15 sec	0.085	489	128	489	2.681	0.670	7.30E+05	1.92E+05
PI-2I-G-1-CI-5	0-15 sec	15 sec	0.554	551	211.2	551	2.681	0.670	8.22E+05	3.16E+05
PI-2I-G-1-CI-6	0-15 sec	15 sec	0.25	162	67.5	156	2.681	0.670	2.33E+05	1.01E+05
PI-2I-G-1-CI-7	0-15 sec	15 sec	0.198	152	36.5	133	2.681	0.670	1.98E+05	5.54E+04
PI-2I-G-1-CI-8	0-15 sec	15 sec	0.966	488	109.6	488	2.681	0.670	7.28E+05	1.65E+05
PI-2I-G-1-CI-9	0-15 sec	15 sec	0.46	770	243.4	765	2.681	0.670	1.14E+06	3.65E+05
PI-2I-G-2-CI-1	0.5-1 min	30 sec	1.753	370	50.1	110	2.507	1.254	8.77E+04	4.89E+04
PI-2I-G-2-CI-2	0.5-1 min	30 sec	-0.561	318	124.9	304	2.507	1.254	2.42E+05	1.00E+05
PI-2I-G-2-CI-3	0.5-1 min	30 sec	0.04	313	57.4	312	2.507	1.254	2.49E+05	4.64E+04
PI-2I-G-2-CI-4	0.5-1 min	30 sec	-0.455	86	22.9	86	2.507	1.254	6.86E+04	1.84E+04
PI-2I-G-2-CI-5	0.5-1 min	30 sec	0.79	397	152.3	397	2.507	1.254	3.17E+05	1.22E+05
PI-2I-G-2-CI-6	0.5-1 min	30 sec	-0.311	164	68.7	158	2.507	1.254	1.26E+05	5.50E+04
PI-2I-G-2-CI-7	0.5-1 min	30 sec	-0.743	155	37.7	136	2.507	1.254	1.08E+05	3.06E+04
PI-2I-G-2-CI-8	0.5-1 min	30 sec	-1.654	345	78.9	345	2.507	1.254	2.75E+05	6.37E+04
PI-2I-G-2-CI-9	0.5-1 min	30 sec	0.756	647	205.3	642	2.507	1.254	5.12E+05	1.64E+05
PI-2I-G-3-CI-1	1.5-2.5 min	30 sec	0.674	366	49.5	106	2.673	2.673	3.97E+04	2.28E+04
PI-2I-G-3-CI-2	1.5-2.5 min	30 sec	0.022	167	65.7	153	2.673	2.673	5.72E+04	2.47E+04
PI-2I-G-3-CI-3	1.5-2.5 min	30 sec	-0.188	133	24.7	132	2.673	2.673	4.94E+04	9.37E+03
PI-2I-G-3-CI-4	1.5-2.5 min	30 sec	-0.407	114	30.2	114	2.673	2.673	4.26E+04	1.14E+04
PI-2I-G-3-CI-5	1.5-2.5 min	30 sec	-1.026	284	109.6	284	2.673	2.673	1.06E+05	4.11E+04
PI-2I-G-3-CI-6	1.5-2.5 min	30 sec	-0.105	276	114.1	270	2.673	2.673	1.01E+05	4.28E+04
PI-2I-G-3-CI-7	1.5-2.5 min	30 sec	-2.28	257	59.8	238	2.673	2.673	8.90E+04	2.26E+04
PI-2I-G-3-CI-8	1.5-2.5 min	30 sec	-0.844	504	111.9	504	2.673	2.673	1.89E+05	4.23E+04
PI-2I-G-3-CI-9	1.5-2.5 min	30 sec	0.166	641	201.9	636	2.673	2.673	2.38E+05	7.59E+04
PI-2I-G-4-CI-1	3.5-5.5 min	2 min	2.231	339	45.9	79	2.623	5.246	1.51E+04	1.10E+04
PI-2I-G-4-CI-2	3.5-5.5 min	2 min	-1.541	50	20.2	36	2.623	5.246	6.86E+03	4.01E+03
PI-2I-G-4-CI-3	3.5-5.5 min	2 min	-0.931	143	26.6	142	2.623	5.246	2.71E+04	5.14E+03
PI-2I-G-4-CI-4	3.5-5.5 min	2 min	-0.692	86	23	86	2.623	5.246	1.64E+04	4.42E+03
PI-2I-G-4-CI-5	3.5-5.5 min	2 min	-3.309	171	66.3	171	2.623	5.246	3.26E+04	1.27E+04
PI-2I-G-4-CI-6	3.5-5.5 min	2 min	-0.38	175	72.9	169	2.623	5.246	3.22E+04	1.39E+04
PI-2I-G-4-CI-7	3.5-5.5 min	2 min	-0.595	182	43.5	163	2.623	5.246	3.11E+04	8.41E+03
PI-2I-G-4-CI-8	3.5-5.5 min	2 min	-1.063	367	85.2	367	2.623	5.246	7.00E+04	1.64E+04
PI-2I-G-4-CI-9	3.5-5.5 min	2 min	0.821	495	157.1	490	2.623	5.246	9.34E+04	3.01E+04
PI-2I-G-5-CI-1	7.5-11.5 min	4 min	0.362	122	16.9	-138	2.681	10.724	-1.29E+04	3.66E+03
PI-2I-G-5-CI-2	7.5-11.5 min	4 min	-0.26	9	4.2	-5	2.681	10.724	-4.66E+02	6.60E+02
PI-2I-G-5-CI-3	7.5-11.5 min	4 min	-0.322	72	13.7	71	2.681	10.724	6.62E+03	1.30E+03
PI-2I-G-5-CI-4	7.5-11.5 min	4 min	-0.202	63	17.1	63	2.681	10.724	5.87E+03	1.61E+03
PI-2I-G-5-CI-5	7.5-11.5 min	4 min	0.151	200	77.7	200	2.681	10.724	1.86E+04	7.27E+03
PI-2I-G-5-CI-6	7.5-11.5 min	4 min	-0.733	103	44.1	97	2.681	10.724	9.05E+03	4.13E+03
PI-2I-G-5-CI-7	7.5-11.5 min	4 min	-0.899	118	29.6	99	2.681	10.724	9.23E+03	2.82E+03

Table A.21 (cont'd). Phase I, Shot 2, Gunner

Sample ID	Collection Interval	Elapsed Time	Total Mass (mg)	Calculated U (μg)	DU Mass ± 1σ (μg)	Net DU Mass (μg)	Flow Rate (Lpm)	Volume (L)	DU Conc. (μg/m^3)	DU Conc. ± 1σ (μg/m^3)
PI-2I-G-5-CI-8	7.5-11.5 min	4 min	-0.05	145	35.1	145	2.681	10.724	1.35E+04	3.35E+03
PI-2I-G-5-CI-9	7.5-11.5 min	4 min	0.896	346	110.9	341	2.681	10.724	3.18E+04	1.04E+04
PI-2I-G-6-CI-1	15.5-31.5 min	16 min	0.925	199	27.2	-61	2.656	42.499	-1.44E+03	1.05E+03
PI-2I-G-6-CI-2	15.5-31.5 min	16 min	-0.896	13	5.6	-1	2.656	42.499	-2.35E+01	1.88E+02
PI-2I-G-6-CI-3	15.5-31.5 min	16 min	-0.434	56	10.7	55	2.656	42.499	1.29E+03	2.56E+02
PI-2I-G-6-CI-4	15.5-31.5 min	16 min	-0.06	144	38.1	144	2.656	42.499	3.39E+03	9.03E+02
PI-2I-G-6-CI-5	15.5-31.5 min	16 min	-0.318	301	115.9	301	2.656	42.499	7.08E+03	2.74E+03
PI-2I-G-6-CI-6	15.5-31.5 min	16 min	-0.103	110	46.5	104	2.656	42.499	2.45E+03	1.10E+03
PI-2I-G-6-CI-7	15.5-31.5 min	16 min	-0.352	158	38.3	139	2.656	42.499	3.27E+03	9.16E+02
PI-2I-G-6-CI-8	15.5-31.5 min	16 min	0.175	288	66.3	288	2.656	42.499	6.78E+03	1.58E+03
PI-2I-G-6-CI-9	15.5-31.5 min	16 min	0.552	664	210.4	659	2.656	42.499	1.55E+04	4.97E+03
PI-2I-G-7-CI-1	31.5-79.5 min	48 min	0.518	359	48.5	99	2.05	98.409	1.01E+03	6.10E+02
PI-2I-G-7-CI-2	31.5-79.5 min	48 min	-2.781	25	10	11	2.05	98.409	1.12E+02	1.17E+02
PI-2I-G-7-CI-3	31.5-79.5 min	48 min	1.046	40	8	39	2.05	98.409	3.96E+02	8.28E+01
PI-2I-G-7-CI-4	31.5-79.5 min	48 min	-0.606	158	41.7	158	2.05	98.409	1.61E+03	4.27E+02
PI-2I-G-7-CI-5	31.5-79.5 min	48 min	-0.817	199	76.8	199	2.05	98.409	2.02E+03	7.83E+02
PI-2I-G-7-CI-6	31.5-79.5 min	48 min	-0.789	235	97.5	229	2.05	98.409	2.33E+03	9.94E+02
PI-2I-G-7-CI-7	31.5-79.5 min	48 min	-1.18	178	42.7	159	2.05	98.409	1.62E+03	4.40E+02
PI-2I-G-7-CI-8	31.5-79.5 min	48 min	0.991	479	107.1	479	2.05	98.409	4.87E+03	1.10E+03
PI-2I-G-7-CI-9	31.5-79.5 min	48 min	0.317	557	177.9	552	2.05	98.409	5.61E+03	1.82E+03
PI-2I-G-8-CI-1	79.5-127.5 min	48 min	0.906	416	56.1	156	2.546	122.206	1.28E+03	5.43E+02
PI-2I-G-8-CI-2	79.5-127.5 min	48 min	-1.328	31	12.6	17	2.546	122.206	1.39E+02	1.13E+02
PI-2I-G-8-CI-3	79.5-127.5 min	48 min	-1.151	27	5.7	26	2.546	122.206	2.13E+02	4.78E+01
PI-2I-G-8-CI-4	79.5-127.5 min	48 min	-0.086	188	49.7	188	2.546	122.206	1.54E+03	4.10E+02
PI-2I-G-8-CI-5	79.5-127.5 min	48 min	-0.273	253	97.4	253	2.546	122.206	2.07E+03	8.00E+02
PI-2I-G-8-CI-6	79.5-127.5 min	48 min	-0.403	146	61.6	140	2.546	122.206	1.15E+03	5.06E+02
PI-2I-G-8-CI-7	79.5-127.5 min	48 min	-0.045	172	41.3	153	2.546	122.206	1.25E+03	3.43E+02
PI-2I-G-8-CI-8	79.5-127.5 min	48 min	0.569	325	73.7	325	2.546	122.206	2.66E+03	6.10E+02
PI-2I-G-8-CI-9	79.5-127.5 min	48 min	3.357	795	250.2	790	2.546	122.206	6.46E+03	2.06E+03
PI-2I-G-9-CI-1	Field Blank	--	0.762	260	35.2	--	--	--	--	--
PI-2I-G-9-CI-2	Field Blank	--	-0.256	14	5.7	--	--	--	--	--
PI-2I-G-9-CI-3	Field Blank	--	-1.102	1	1	--	--	--	--	--
PI-2I-G-9-CI-4	Field Blank	--	-0.325	-4	1.7	--	--	--	--	--
PI-2I-G-9-CI-5	Field Blank	--	0.03	-2	1.8	--	--	--	--	--
PI-2I-G-9-CI-6	Field Blank	--	-0.497	6	3.6	--	--	--	--	--
PI-2I-G-9-CI-7	Field Blank	--	-0.013	19	5.6	--	--	--	--	--
PI-2I-G-9-CI-8	Field Blank	--	-0.003	-11	6.2	--	--	--	--	--
PI-2I-G-9-CI-9	Field Blank	--	-1.556	5	4	--	--	--	--	--

Table A.21 (cont'd). Phase I, Shot 2, Loader

Sample ID	Collection Interval	Elapsed Time	Total Mass (mg)	Calculated U (μg)	DU Mass ± 1σ (μg)	Net DU Mass (μg)	Flow Rate (Lpm)	Volume (L)	DU Conc. (μg/m^3)	DU Conc. ± 1σ (μg/m^3)
PI-2I-L-1-CI-1	0-15 sec	15 sec	1.258	389	72.4	282	2.396	0.599	4.71E+05	1.26E+05
PI-2I-L-1-CI-2	0-15 sec	15 sec	0.466	168	79.3	156	2.396	0.599	2.60E+05	1.33E+05
PI-2I-L-1-CI-3	0-15 sec	15 sec	-0.480	282	71.5	276	2.396	0.599	4.61E+05	1.20E+05
PI-2I-L-1-CI-4	0-15 sec	15 sec	-0.462	141	51.5	138	2.396	0.599	2.30E+05	8.63E+04
PI-2I-L-1-CI-5	0-15 sec	15 sec	0.122	233	88.6	228	2.396	0.599	3.81E+05	1.48E+05
PI-2I-L-1-CI-6	0-15 sec	15 sec	-0.408	304	72.0	299	2.396	0.599	4.99E+05	1.21E+05
PI-2I-L-1-CI-7	0-15 sec	15 sec	-0.227	248	40.8	242	2.396	0.599	4.04E+05	6.92E+04
PI-2I-L-1-CI-8	0-15 sec	15 sec	-3.102	409	38.7	406	2.396	0.599	6.78E+05	6.78E+04
PI-2I-L-1-CI-9	0-15 sec	15 sec	1.388	751	127.0	735	2.396	0.599	1.23E+06	2.15E+05
PI-2I-L-2-CI-1	0.5-1 min	30 sec	1.411	251	46.7	144	2.496	1.248	1.15E+05	4.09E+04
PI-2I-L-2-CI-2	0.5-1 min	30 sec	0.161	137	64.6	125	2.496	1.248	1.00E+05	5.21E+04
PI-2I-L-2-CI-3	0.5-1 min	30 sec	0.953	170	43.2	164	2.496	1.248	1.31E+05	3.49E+04
PI-2I-L-2-CI-4	0.5-1 min	30 sec	-1.156	259	94.2	256	2.496	1.248	2.05E+05	7.57E+04
PI-2I-L-2-CI-5	0.5-1 min	30 sec	-0.213	220	83.6	215	2.496	1.248	1.72E+05	6.72E+04
PI-2I-L-2-CI-6	0.5-1 min	30 sec	-0.686	224	53.1	219	2.496	1.248	1.75E+05	4.29E+04
PI-2I-L-2-CI-7	0.5-1 min	30 sec	0.026	178	29.4	172	2.496	1.248	1.38E+05	2.40E+04
PI-2I-L-2-CI-8	0.5-1 min	30 sec	-0.363	214	20.6	211	2.496	1.248	1.69E+05	1.73E+04
PI-2I-L-2-CI-9	0.5-1 min	30 sec	0.166	1069	180.3	1053	2.496	1.248	8.44E+05	1.47E+05
PI-2I-L-3-CI-1	1.5-2.5 min	30 sec	0.596	153	28.8	46	2.405	2.405	1.91E+04	1.47E+04
PI-2I-L-3-CI-2	1.5-2.5 min	30 sec	-0.435	98	46.0	86	2.405	2.405	3.58E+04	1.93E+04
PI-2I-L-3-CI-3	1.5-2.5 min	30 sec	0.051	90	23.0	84	2.405	2.405	3.49E+04	9.65E+03
PI-2I-L-3-CI-4	1.5-2.5 min	30 sec	0.247	150	54.8	147	2.405	2.405	6.11E+04	2.29E+04
PI-2I-L-3-CI-5	1.5-2.5 min	30 sec	-0.312	238	90.5	233	2.405	2.405	9.69E+04	3.78E+04
PI-2I-L-3-CI-6	1.5-2.5 min	30 sec	-1.048	169	40.1	164	2.405	2.405	6.82E+04	1.68E+04
PI-2I-L-3-CI-7	1.5-2.5 min	30 sec	-0.920	226	37.2	220	2.405	2.405	9.15E+04	1.57E+04
PI-2I-L-3-CI-8	1.5-2.5 min	30 sec	0.546	347	32.7	344	2.405	2.405	1.43E+05	1.43E+04
PI-2I-L-3-CI-9	1.5-2.5 min	30 sec	0.796	328	56.0	312	2.405	2.405	1.30E+05	2.36E+04
PI-2I-L-4-CI-1	3.5-5.5 min	2 min	0.414	97	18.3	-10	2.542	5.085	-1.97E+03	5.38E+03
PI-2I-L-4-CI-2	3.5-5.5 min	2 min	-0.856	31	14.9	19	2.542	5.085	3.74E+03	3.14E+03
PI-2I-L-4-CI-3	3.5-5.5 min	2 min	-0.867	145	36.8	139	2.542	5.085	2.73E+04	7.29E+03
PI-2I-L-4-CI-4	3.5-5.5 min	2 min	-0.928	182	66.4	179	2.542	5.085	3.52E+04	1.31E+04
PI-2I-L-4-CI-5	3.5-5.5 min	2 min	0.060	329	125.1	324	2.542	5.085	6.37E+04	2.47E+04
PI-2I-L-4-CI-6	3.5-5.5 min	2 min	-3.238	198	46.9	193	2.542	5.085	3.80E+04	9.30E+03
PI-2I-L-4-CI-7	3.5-5.5 min	2 min	-0.366	288	47.3	282	2.542	5.085	5.55E+04	9.45E+03
PI-2I-L-4-CI-8	3.5-5.5 min	2 min	0.454	105	10.6	102	2.542	5.085	2.01E+04	2.18E+03
PI-2I-L-4-CI-9	3.5-5.5 min	2 min	-0.286	267	45.6	251	2.542	5.085	4.94E+04	9.11E+03
PI-2I-L-5-CI-1	7.5-11.5 min	4 min	0.543	66	12.8	-41	2.560	10.242	-4.00E+03	2.35E+03
PI-2I-L-5-CI-2	7.5-11.5 min	4 min	0.265	21	10.1	9	2.560	10.242	8.79E+02	1.13E+03
PI-2I-L-5-CI-3	7.5-11.5 min	4 min	-0.427	98	25.0	92	2.560	10.242	8.98E+03	2.46E+03
PI-2I-L-5-CI-4	7.5-11.5 min	4 min	-0.174	70	25.6	67	2.560	10.242	6.54E+03	2.51E+03
PI-2I-L-5-CI-5	7.5-11.5 min	4 min	-1.643	259	98.4	254	2.560	10.242	2.48E+04	9.64E+03
PI-2I-L-5-CI-6	7.5-11.5 min	4 min	0.315	118	28.1	113	2.560	10.242	1.10E+04	2.77E+03
PI-2I-L-5-CI-7	7.5-11.5 min	4 min	-0.400	173	28.7	167	2.560	10.242	1.63E+04	2.85E+03

Table A.21 (cont'd). Phase I, Shot 2, Loader

Sample ID	Collection Interval	Elapsed Time	Total Mass (mg)	Calculated U (μg)	DU Mass ± 1σ (μg))	Net DU Mass (μg)	Flow Rate (Lpm)	Volume (L)	DU Conc. (μg/m^3)	DU Conc. ± 1σ (μg/m^3)
PI-2I-L-5-CI-8	7.5-11.5 min	4 min	-0.229	136	13.3	133	2.560	10.242	1.30E+04	1.36E+03
PI-2I-L-5-CI-9	7.5-11.5 min	4 min	0.478	212	36.2	196	2.560	10.242	1.91E+04	3.59E+03
PI-2I-L-6-CI-1	15.5-31.5 min	16 min	0.362	82	15.7	-25	2.525	40.407	-6.19E+02	6.35E+02
PI-2I-L-6-CI-2	15.5-31.5 min	16 min	0.122	13	6.1	1	2.525	40.407	2.47E+01	2.07E+02
PI-2I-L-6-CI-3	15.5-31.5 min	16 min	-0.663	39	10.2	33	2.525	40.407	8.17E+02	2.58E+02
PI-2I-L-6-CI-4	15.5-31.5 min	16 min	-0.028	113	41.2	110	2.525	40.407	2.72E+03	1.02E+03
PI-2I-L-6-CI-5	15.5-31.5 min	16 min	-0.208	157	59.9	152	2.525	40.407	3.76E+03	1.49E+03
PI-2I-L-6-CI-6	15.5-31.5 min	16 min	-0.084	139	33.2	134	2.525	40.407	3.32E+03	8.28E+02
PI-2I-L-6-CI-7	15.5-31.5 min	16 min	0.067	197	32.6	191	2.525	40.407	4.73E+03	8.20E+02
PI-2I-L-6-CI-8	15.5-31.5 min	16 min	0.768	254	24.3	251	2.525	40.407	6.21E+03	6.30E+02
PI-2I-L-6-CI-9	15.5-31.5 min	16 min	0.674	775	131.1	759	2.525	40.407	1.88E+04	3.29E+03
PI-2I-L-7-CI-1	31.5-79.5 min	48 min	1.601	103	19.4	-4	2.381	114.266	-3.50E+01	2.46E+02
PI-2I-L-7-CI-2	31.5-79.5 min	48 min	0.744	23	10.9	11	2.381	114.266	9.63E+01	1.08E+02
PI-2I-L-7-CI-3	31.5-79.5 min	48 min	-0.114	69	17.6	63	2.381	114.266	5.51E+02	1.56E+02
PI-2I-L-7-CI-4	31.5-79.5 min	48 min	0.298	144	52.3	141	2.381	114.266	1.23E+03	4.59E+02
PI-2I-L-7-CI-5	31.5-79.5 min	48 min	0.818	327	124.4	322	2.381	114.266	2.82E+03	1.09E+03
PI-2I-L-7-CI-6	31.5-79.5 min	48 min	0.348	268	63.5	263	2.381	114.266	2.30E+03	5.60E+02
PI-2I-L-7-CI-7	31.5-79.5 min	48 min	-0.308	359	NA[(a)]	353	2.381	114.266	3.09E+03	NA[(a)]
PI-2I-L-7-CI-8	31.5-79.5 min	48 min	0.898	496	NA[(a)]	493	2.381	114.266	4.31E+03	NA[(a)]
PI-2I-L-7-CI-9	31.5-79.5 min	48 min	3.525	1800	303.3	1784	2.381	114.266	1.56E+04	2.70E+03
PI-2I-L-8-CI-1	79.5-127.5 min	48 min	1.258	249	46.6	142	2.428	116.560	1.22E+03	4.38E+02
PI-2I-L-8-CI-2	79.5-127.5 min	48 min	-0.126	24	11.4	12	2.428	116.560	1.03E+02	1.09E+02
PI-2I-L-8-CI-3	79.5-127.5 min	48 min	-0.402	32	8.5	26	2.428	116.560	2.23E+02	7.48E+01
PI-2I-L-8-CI-4	79.5-127.5 min	48 min	-0.064	95	34.8	92	2.428	116.560	7.89E+02	3.00E+02
PI-2I-L-8-CI-5	79.5-127.5 min	48 min	-0.656	192	73.2	187	2.428	116.560	1.60E+03	6.30E+02
PI-2I-L-8-CI-6	79.5-127.5 min	48 min	0.135	191	45.3	186	2.428	116.560	1.60E+03	3.92E+02
PI-2I-L-8-CI-7	79.5-127.5 min	48 min	0.637	288	47.2	282	2.428	116.560	2.42E+03	4.12E+02
PI-2I-L-8-CI-8	79.5-127.5 min	48 min	0.941	289	27.6	286	2.428	116.560	2.45E+03	2.48E+02
PI-2I-L-8-CI-9	79.5-127.5 min	48 min	2.672	1502	253.2	1486	2.428	116.560	1.27E+04	2.21E+03
PI-2I-L-9-CI-1	Field Blank	--	0.843	107	20.3	--	--	--	--	--
PI-2I-L-9-CI-2	Field Blank	--	0.154	12	5.7	--	--	--	--	--
PI-2I-L-9-CI-3	Field Blank	--	0.063	6	1.8	--	--	--	--	--
PI-2I-L-9-CI-4	Field Blank	--	0.326	3	1.4	--	--	--	--	--
PI-2I-L-9-CI-5	Field Blank	--	-0.393	5	2.3	--	--	--	--	--
PI-2I-L-9-CI-6	Field Blank	--	-0.177	5	1.5	--	--	--	--	--
PI-2I-L-9-CI-7	Field Blank	--	-1.090	6	1.6	--	--	--	--	--
PI-2I-L-9-CI-8	Field Blank	--	-0.247	3	1.1	--	--	--	--	--
PI-2I-L-9-CI-9	Field Blank	--	0.281	16	2.9	--	--	--	--	--

(a) DU mass based on ICP-MS results; no analytical uncertainty was reported.

Table A.22. PI-3/4 Cascade Impactor Substrates—Mass, Volume, and Concentration

Sample ID	Collection Interval	Elapsed Time	Total Mass (mg)	Calculated U (μg)	DU Mass ± 1σ (μg)	Net DU Mass (μg)	Flow Rate (Lpm)	Volume (L)	DU Conc. (μg/m^3)	DU Conc. ± 1σ (μg/m^3)
PI-3/4I-C-1-CI-1	Shot 4: 0-10 sec	10 sec	2.814	471	63	366	2.631	0.439	8.34E+05	1.47E+05
PI-3/4I-C-1-CI-2	Shot 4: 0-10 sec	10 sec	0.772	409	160.7	406	2.631	0.439	9.25E+05	3.67E+05
PI-3/4I-C-1-CI-3	Shot 4: 0-10 sec	10 sec	0.807	102	18.8	101	2.631	0.439	2.31E+05	4.34E+04
PI-3/4I-C-1-CI-4	Shot 4: 0-10 sec	10 sec	2.314	60	15.9	58	2.631	0.439	1.32E+05	3.65E+04
PI-3/4I-C-1-CI-5	Shot 4: 0-10 sec	10 sec	0.838	204	79.1	202	2.631	0.439	4.60E+05	1.81E+05
PI-3/4I-C-1-CI-6	Shot 4: 0-10 sec	10 sec	0.952	184	79.2	179	2.631	0.439	4.08E+05	1.81E+05
PI-3/4I-C-1-CI-7	Shot 4: 0-10 sec	10 sec	1.409	107	27	104	2.631	0.439	2.36E+05	6.20E+04
PI-3/4I-C-1-CI-8	Shot 4: 0-10 sec	10 sec	5.1	109	30.6	99	2.631	0.439	2.26E+05	7.04E+04
PI-3/4I-C-1-CI-9	Shot 4: 0-10 sec	10 sec	2.654	863	283.4	839	2.631	0.439	1.91E+06	6.48E+05
PI-3/4I-C-2-CI-1	3-3.5 min	30 sec	0.261	109	15.1	4	2.589	1.294	3.09E+03	1.38E+04
PI-3/4I-C-2-CI-2	3-3.5 min	30 sec	-0.333	112	44.2	109	2.589	1.294	8.42E+04	3.43E+04
PI-3/4I-C-2-CI-3	3-3.5 min	30 sec	0.897	40	7.8	39	2.589	1.294	3.04E+04	6.11E+03
PI-3/4I-C-2-CI-4	3-3.5 min	30 sec	0.019	49	13.2	47	2.589	1.294	3.63E+04	1.03E+04
PI-3/4I-C-2-CI-5	3-3.5 min	30 sec	0.319	129	50.6	127	2.589	1.294	9.81E+04	3.92E+04
PI-3/4I-C-2-CI-6	3-3.5 min	30 sec	0.091	179	77.2	174	2.589	1.294	1.34E+05	5.98E+04
PI-3/4I-C-2-CI-7	3-3.5 min	30 sec	0.533	171	40.9	168	2.589	1.294	1.30E+05	3.19E+04
PI-3/4I-C-2-CI-8	3-3.5 min	30 sec	0.226	193	47.5	183	2.589	1.294	1.41E+05	3.70E+04
PI-3/4I-C-2-CI-9	3-3.5 min	30 sec	1.4	257	85.8	233	2.589	1.294	1.80E+05	6.67E+04
PI-3/4I-C-3-CI-1	9-10 min	1 min	1.234	184	24.9	79	2.602	2.602	3.04E+04	1.03E+04
PI-3/4I-C-3-CI-2	9-10 min	1 min	-0.126	43	17.3	40	2.602	2.602	1.54E+04	6.68E+03
PI-3/4I-C-3-CI-3	9-10 min	1 min	0.331	43	8.5	42	2.602	2.602	1.63E+04	3.31E+03
PI-3/4I-C-3-CI-4	9-10 min	1 min	0.384	94	25.1	92	2.602	2.602	3.54E+04	9.71E+03
PI-3/4I-C-3-CI-5	9-10 min	1 min	0.401	121	47.6	119	2.602	2.602	4.57E+04	1.84E+04
PI-3/4I-C-3-CI-6	9-10 min	1 min	0.238	70	31.5	65	2.602	2.602	2.50E+04	1.22E+04
PI-3/4I-C-3-CI-7	9-10 min	1 min	-0.404	74	19.2	71	2.602	2.602	2.72E+04	7.45E+03
PI-3/4I-C-3-CI-8	9-10 min	1 min	0.144	82	23.7	72	2.602	2.602	2.77E+04	9.22E+03
PI-3/4I-C-3-CI-9	9-10 min	1 min	0.135	82	29.2	58	2.602	2.602	2.22E+04	1.14E+04
PI-3/4I-C-4-CI-1	21-23 min	2 min	0.216	116	15.8	11	2.369	4.738	2.32E+03	3.89E+03
PI-3/4I-C-4-CI-2	21-23 min	2 min	-0.023	5	2.7	2	2.369	4.738	4.22E+02	6.21E+02
PI-3/4I-C-4-CI-3	21-23 min	2 min	-0.405	16	3.5	15	2.369	4.738	3.24E+03	7.53E+02
PI-3/4I-C-4-CI-4	21-23 min	2 min	0.011	38	10.5	36	2.369	4.738	7.60E+03	2.23E+03
PI-3/4I-C-4-CI-5	21-23 min	2 min	0.649	27	11	25	2.369	4.738	5.28E+03	2.34E+03
PI-3/4I-C-4-CI-6	21-23 min	2 min	0.112	86	37.4	81	2.369	4.738	1.71E+04	7.92E+03
PI-3/4I-C-4-CI-7	21-23 min	2 min	-0.131	71	18.7	68	2.369	4.738	1.43E+04	3.99E+03
PI-3/4I-C-4-CI-8	21-23 min	2 min	-0.08	126	32.4	116	2.369	4.738	2.45E+04	6.91E+03
PI-3/4I-C-4-CI-9	21-23 min	2 min	2.402	108	37.5	84	2.369	4.738	1.77E+04	8.02E+03
PI-3/4I-C-5-CI-1	45-49 min	4 min	0.416	101	14	-4	2.453	9.812	-4.08E+02	1.73E+03
PI-3/4I-C-5-CI-2	45-49 min	4 min	-0.402	56	22.2	53	2.453	9.812	5.40E+03	2.27E+03
PI-3/4I-C-5-CI-3	45-49 min	4 min	0.142	11	2.5	10	2.453	9.812	1.05E+03	2.62E+02
PI-3/4I-C-5-CI-4	45-49 min	4 min	-0.115	28	7.7	26	2.453	9.812	2.65E+03	7.92E+02
PI-3/4I-C-5-CI-5	45-49 min	4 min	-0.185	46	18.4	44	2.453	9.812	4.48E+03	1.88E+03
PI-3/4I-C-5-CI-6	45-49 min	4 min	0.013	42	19.7	37	2.453	9.812	3.77E+03	2.02E+03
PI-3/4I-C-5-CI-7	45-49 min	4 min	-2.501	50	14.3	47	2.453	9.812	4.76E+03	1.47E+03

Table A.22 (cont'd). Phase I, Shot 3/4, Commander

Sample ID	Collection Interval	Elapsed Time	Total Mass (mg)	Calculated U (μg)	DU Mass ± 1σ (μg)	Net DU Mass (μg)	Flow Rate (Lpm)	Volume (L)	DU Conc. (μg/m^3)	DU Conc. ± 1σ (μg/m^3)
PI-3/4I-C-5-CI-8	45-49 min	4 min	0.653	129	33.6	119	2.453	9.812	1.21E+04	3.46E+03
PI-3/4I-C-5-CI-9	45-49 min	4 min	0.784	69	25	45	2.453	9.812	4.55E+03	2.61E+03
PI-3/4I-C-6-CI-1	93-101 min	8 min	1.208	137	18.7	32	2.432	19.452	1.65E+03	1.08E+03
PI-3/4I-C-6-CI-2	93-101 min	8 min	-2.571	7	3.4	4	2.432	19.452	2.06E+02	1.85E+02
PI-3/4I-C-6-CI-3	93-101 min	8 min	0.693	5	1.8	4	2.432	19.452	2.23E+02	9.66E+01
PI-3/4I-C-6-CI-4	93-101 min	8 min	-0.839	20	5.6	18	2.432	19.452	9.25E+02	2.91E+02
PI-3/4I-C-6-CI-5	93-101 min	8 min	-2.113	56	22.6	54	2.432	19.452	2.78E+03	1.17E+03
PI-3/4I-C-6-CI-6	93-101 min	8 min	0.536	40	17.7	35	2.432	19.452	1.80E+03	9.18E+02
PI-3/4I-C-6-CI-7	93-101 min	8 min	-1.005	81	20.1	78	2.432	19.452	3.99E+03	1.04E+03
PI-3/4I-C-6-CI-8	93-101 min	8 min	-1.019	117	29.8	107	2.432	19.452	5.50E+03	1.55E+03
PI-3/4I-C-6-CI-9	93-101 min	8 min	-1.967	73	25.1	49	2.432	19.452	2.50E+03	1.32E+03
PI-3/4I-C-7-CI-1	Field Blank	--	0.097	38	5.5	--	--	--	--	--
PI-3/4I-C-7-CI-2	Field Blank	--	0.159	4	2	--	--	--	--	--
PI-3/4I-C-7-CI-3	Field Blank	--	0.293	-1	0.7	--	--	--	--	--
PI-3/4I-C-7-CI-4	Field Blank	--	-0.179	5	1.7	--	--	--	--	--
PI-3/4I-C-7-CI-5	Field Blank	--	-0.748	-1	1.6	--	--	--	--	--
PI-3/4I-C-7-CI-6	Field Blank	--	-0.007	6	3.4	--	--	--	--	--
PI-3/4I-C-7-CI-7	Field Blank	--	0.48	-4	2.3	--	--	--	--	--
PI-3/4I-C-7-CI-8	Field Blank	--	-0.137	13	5.4	--	--	--	--	--
PI-3/4I-C-7-CI-9	Field Blank	--	-1.678	37	12.5	--	--	--	--	--
PI-3/4I-C-8-CI-1	Field Blank	--	0.281	96	13.3	--	--	--	--	--
PI-3/4I-C-8-CI-2	Field Blank	--	0.22	1	1.6	--	--	--	--	--
PI-3/4I-C-8-CI-3	Field Blank	--	-0.154	3	1	--	--	--	--	--
PI-3/4I-C-8-CI-4	Field Blank	--	-0.937	1	0.8	--	--	--	--	--
PI-3/4I-C-8-CI-5	Field Blank	--	0.15	2	2	--	--	--	--	--
PI-3/4I-C-8-CI-6	Field Blank	--	-0.447	0	2.7	--	--	--	--	--
PI-3/4I-C-8-CI-7	Field Blank	--	-0.597	9	3.5	--	--	--	--	--
PI-3/4I-C-8-CI-8	Field Blank	--	0.653	10	4.8	--	--	--	--	--
PI-3/4I-C-8-CI-9	Field Blank	--	-0.766	12	5.7	--	--	--	--	--
PI-3/4I-C-9-CI-1	Field Blank	--	1.287	181	24.7	--	--	--	--	--
PI-3/4I-C-9-CI-2	Field Blank	--	0.611	4	2.4	--	--	--	--	--
PI-3/4I-C-9-CI-3	Field Blank	--	0.4	0	1	--	--	--	--	--
PI-3/4I-C-9-CI-4	Field Blank	--	0.084	0	0.9	--	--	--	--	--
PI-3/4I-C-9-CI-5	Field Blank	--	0.123	5	2.5	--	--	--	--	--
PI-3/4I-C-9-CI-6	Field Blank	--	-0.036	9	4.3	--	--	--	--	--
PI-3/4I-C-9-CI-7	Field Blank	--	0.797	5	2.8	--	--	--	--	--
PI-3/4I-C-9-CI-8	Field Blank	--	-0.299	7	5.1	--	--	--	--	--
PI-3/4I-C-9-CI-9	Field Blank	--	-0.644	24	8.8	--	--	--	--	--

Table A.22 (cont'd). Phase I, Shots 3/4, Driver

Sample ID	Collection Interval	Elapsed Time	Total Mass (mg)	Calculated U (μg)	DU Mass ± 1σ (μg)	Net DU Mass (μg)	Flow Rate (Lpm)	Volume (L)	DU Conc. (μg/m^3)	DU Conc. ± 1σ (μg/m^3)
PI-3/4I-D-1-CI-1	Shot 3: 0-10 sec	10 sec	2.797	509	94.7	69	2.444	0.407	1.70E+05	3.08E+05
PI-3/4I-D-1-CI-2	Shot 3: 0-10 sec	10 sec	0.425	34	16.0	20	2.444	0.407	4.91E+04	4.27E+04
PI-3/4I-D-1-CI-3	Shot 3: 0-10 sec	10 sec	0.436	32	8.5	27	2.444	0.407	6.63E+04	2.13E+04
PI-3/4I-D-1-CI-4	Shot 3: 0-10 sec	10 sec	0.502	39	14.5	34	2.444	0.407	8.35E+04	3.61E+04
PI-3/4I-D-1-CI-5	Shot 3: 0-10 sec	10 sec	1.921	106	40.7	106	2.444	0.407	2.60E+05	1.00E+05
PI-3/4I-D-1-CI-6	Shot 3: 0-10 sec	10 sec	0.742	73	17.6	73	2.444	0.407	1.79E+05	4.36E+04
PI-3/4I-D-1-CI-7	Shot 3: 0-10 sec	10 sec	0.745	87	14.9	87	2.444	0.407	2.14E+05	3.73E+04
PI-3/4I-D-1-CI-8	Shot 3: 0-10 sec	10 sec	1.061	116	11.9	114	2.444	0.407	2.80E+05	3.05E+04
PI-3/4I-D-1-CI-9	Shot 3: 0-10 sec	10 sec	2.361	1020	NA[(a)]	1015	2.444	0.407	2.49E+06	NA[(a)]
PI-3/4I-D-2-CI-1	3-3.5 min	30 sec	0.594	237	44.5	-203	2.390	1.195	-1.70E+05	7.82E+04
PI-3/4I-D-2-CI-2	3-3.5 min	30 sec	0.570	48	23.0	34	2.390	1.195	2.85E+04	2.01E+04
PI-3/4I-D-2-CI-3	3-3.5 min	30 sec	0.962	73	19.0	68	2.390	1.195	5.69E+04	1.60E+04
PI-3/4I-D-2-CI-4	3-3.5 min	30 sec	0.681	314	114.4	309	2.390	1.195	2.59E+05	9.61E+04
PI-3/4I-D-2-CI-5	3-3.5 min	30 sec	0.851	337	128.1	337	2.390	1.195	2.82E+05	1.08E+05
PI-3/4I-D-2-CI-6	3-3.5 min	30 sec	1.053	237	56.1	237	2.390	1.195	1.98E+05	4.73E+04
PI-3/4I-D-2-CI-7	3-3.5 min	30 sec	2.095	267	43.8	267	2.390	1.195	2.23E+05	3.73E+04
PI-3/4I-D-2-CI-8	3-3.5 min	30 sec	0.880	80	8.5	78	2.390	1.195	6.53E+04	7.42E+03
PI-3/4I-D-2-CI-9	3-3.5 min	30 sec	1.645	339	57.6	334	2.390	1.195	2.79E+05	4.89E+04
PI-3/4I-D-3-CI-1	9-10 min	1 min	1.177	260	48.6	-180	2.592	2.592	-6.94E+04	3.68E+04
PI-3/4I-D-3-CI-2	9-10 min	1 min	0.605	42	20.0	28	2.592	2.592	1.08E+04	8.16E+03
PI-3/4I-D-3-CI-3	9-10 min	1 min	0.833	65	16.9	60	2.592	2.592	2.31E+04	6.59E+03
PI-3/4I-D-3-CI-4	9-10 min	1 min	1.125	169	61.7	164	2.592	2.592	6.33E+04	2.39E+04
PI-3/4I-D-3-CI-5	9-10 min	1 min	0.912	306	116.4	306	2.592	2.592	1.18E+05	4.50E+04
PI-3/4I-D-3-CI-6	9-10 min	1 min	0.710	166	NA[(a)]	166	2.592	2.592	6.40E+04	NA[(a)]
PI-3/4I-D-3-CI-7	9-10 min	1 min	0.727	181	29.8	181	2.592	2.592	6.98E+04	1.17E+04
PI-3/4I-D-3-CI-8	9-10 min	1 min	1.241	124	12.3	122	2.592	2.592	4.71E+04	4.97E+03
PI-3/4I-D-3-CI-9	9-10 min	1 min	2.254	202	34.5	197	2.592	2.592	7.60E+04	1.35E+04
PI-3/4I-D-4-CI-1	Shot 4: 0-10 sec	10 sec	0.869	341	63.6	-99	2.602	0.434	-2.28E+05	2.39E+05
PI-3/4I-D-4-CI-2	Shot 4: 0-10 sec	10 sec	1.107	143	67.5	129	2.602	0.434	2.97E+05	1.57E+05
PI-3/4I-D-4-CI-3	Shot 4: 0-10 sec	10 sec	4.503	122	31.2	117	2.602	0.434	2.70E+05	7.24E+04
PI-3/4I-D-4-CI-4	Shot 4: 0-10 sec	10 sec	0.878	105	38.4	100	2.602	0.434	2.30E+05	8.89E+04
PI-3/4I-D-4-CI-5	Shot 4: 0-10 sec	10 sec	0.618	143	54.5	143	2.602	0.434	3.29E+05	1.26E+05
PI-3/4I-D-4-CI-6	Shot 4: 0-10 sec	10 sec	1.158	59	14.4	59	2.602	0.434	1.36E+05	3.35E+04
PI-3/4I-D-4-CI-7	Shot 4: 0-10 sec	10 sec	0.250	53	9.2	53	2.602	0.434	1.22E+05	2.17E+04
PI-3/4I-D-4-CI-8	Shot 4: 0-10 sec	10 sec	0.762	99	10.1	97	2.602	0.434	2.24E+05	2.43E+04
PI-3/4I-D-4-CI-9	Shot 4: 0-10 sec	10 sec	3.245	336	57.0	331	2.602	0.434	7.63E+05	1.33E+05
PI-3/4I-D-5-CI-1	3-3.5 min	30 sec	1.320	222	41.6	-218	2.509	1.254	-1.74E+05	7.34E+04
PI-3/4I-D-5-CI-2	3-3.5 min	30 sec	6.053	39	18.6	25	2.509	1.254	1.99E+04	1.58E+04
PI-3/4I-D-5-CI-3	3-3.5 min	30 sec	0.609	98	25.2	93	2.509	1.254	7.42E+04	2.03E+04
PI-3/4I-D-5-CI-4	3-3.5 min	30 sec	0.134	77	28.4	72	2.509	1.254	5.74E+04	2.28E+04
PI-3/4I-D-5-CI-5	3-3.5 min	30 sec	-0.854	150	57.1	150	2.509	1.254	1.20E+05	4.57E+04
PI-3/4I-D-5-CI-6	3-3.5 min	30 sec	-0.746	120	28.7	120	2.509	1.254	9.57E+04	2.31E+04
PI-3/4I-D-5-CI-7	3-3.5 min	30 sec	-0.184	83	14.2	83	2.509	1.254	6.62E+04	1.15E+04

Table A.22 (cont'd). Phase I, Shots 3/4, Driver

Sample ID	Collection Interval	Elapsed Time	Total Mass (mg)	Calculated U (μg)	DU Mass ± 1σ (μg)	Net DU Mass (μg)	Flow Rate (Lpm)	Volume (L)	DU Conc. (μg/m^3)	DU Conc. ± 1σ (μg/m^3)
PI-3/4I-D-5-CI-8	3-3.5 min	30 sec	0.788	105	NA[(a)]	103	2.509	1.254	8.21E+04	NA[(a)]
PI-3/4I-D-5-CI-9	3-3.5 min	30 sec	1.506	141	24.3	136	2.509	1.254	1.08E+05	1.97E+04
PI-3/4I-D-6-CI-1	9-10 min	1 min	1.108	501	93.2	61	2.583	2.583	2.36E+04	4.80E+04
PI-3/4I-D-6-CI-2	9-10 min	1 min	4.019	29	13.9	15	2.583	2.583	5.81E+03	5.99E+03
PI-3/4I-D-6-CI-3	9-10 min	1 min	0.973	26	6.8	21	2.583	2.583	8.13E+03	2.72E+03
PI-3/4I-D-6-CI-4	9-10 min	1 min	-2.848	77	28.1	72	2.583	2.583	2.79E+04	1.09E+04
PI-3/4I-D-6-CI-5	9-10 min	1 min	-2.906	110	42.1	110	2.583	2.583	4.26E+04	1.64E+04
PI-3/4I-D-6-CI-6	9-10 min	1 min	0.636	64	15.4	64	2.583	2.583	2.48E+04	6.01E+03
PI-3/4I-D-6-CI-7	9-10 min	1 min	0.346	73	12.6	73	2.583	2.583	2.83E+04	4.97E+03
PI-3/4I-D-6-CI-8	9-10 min	1 min	1.419	63	6.9	61	2.583	2.583	2.36E+04	2.79E+03
PI-3/4I-D-6-CI-9	9-10 min	1 min	1.753	74	13.0	69	2.583	2.583	2.67E+04	5.12E+03
PI-3/4I-D-7-CI-1	21-23 min	2 min	2.700	362	67.6	-78	2.550	5.100	-1.53E+04	2.08E+04
PI-3/4I-D-7-CI-2	21-23 min	2 min	4.716	15	7.2	1	2.550	5.100	1.96E+02	1.94E+03
PI-3/4I-D-7-CI-3	21-23 min	2 min	0.933	15	4.2	10	2.550	5.100	1.96E+03	8.83E+02
PI-3/4I-D-7-CI-4	21-23 min	2 min	1.038	26	9.8	21	2.550	5.100	4.12E+03	1.97E+03
PI-3/4I-D-7-CI-5	21-23 min	2 min	0.419	41	15.8	41	2.550	5.100	8.04E+03	3.11E+03
PI-3/4I-D-7-CI-6	21-23 min	2 min	0.629	37	9.0	37	2.550	5.100	7.25E+03	1.78E+03
PI-3/4I-D-7-CI-7	21-23 min	2 min	0.379	46	8.3	46	2.550	5.100	9.02E+03	1.66E+03
PI-3/4I-D-7-CI-8	21-23 min	2 min	0.256	92	9.3	90	2.550	5.100	1.76E+04	1.91E+03
PI-3/4I-D-7-CI-9	21-23 min	2 min	1.761	51	9.2	46	2.550	5.100	9.02E+03	1.84E+03
PI-3/4I-D-8-CI-1	45-49 min	4 min	2.772	230	42.9	-210	2.587	10.349	-2.03E+04	8.95E+03
PI-3/4I-D-8-CI-2	45-49 min	4 min	2.257	8	4.0	-6	2.587	10.349	-5.80E+02	7.63E+02
PI-3/4I-D-8-CI-3	45-49 min	4 min	2.582	11	3.1	6	2.587	10.349	5.80E+02	3.38E+02
PI-3/4I-D-8-CI-4	45-49 min	4 min	1.565	26	9.8	21	2.587	10.349	2.03E+03	9.68E+02
PI-3/4I-D-8-CI-5	45-49 min	4 min	1.135	63	24.1	63	2.587	10.349	6.09E+03	2.34E+03
PI-3/4I-D-8-CI-6	45-49 min	4 min	0.483	22	5.5	22	2.587	10.349	2.13E+03	5.38E+02
PI-3/4I-D-8-CI-7	45-49 min	4 min	0.294	69	11.9	69	2.587	10.349	6.67E+03	1.17E+03
PI-3/4I-D-8-CI-8	45-49 min	4 min	0.499	83	8.6	81	2.587	10.349	7.83E+03	8.69E+02
PI-3/4I-D-8-CI-9	45-49 min	4 min	0.950	88	15.3	83	2.587	10.349	8.02E+03	1.50E+03
PI-3/4I-D-9-CI-1	Field Blank	--	3.091	440	81.9	--	--	--	--	--
PI-3/4I-D-9-CI-2	Field Blank	--	3.929	14	6.8	--	--	--	--	--
PI-3/4I-D-9-CI-3	Field Blank	--	3.581	5	1.6	--	--	--	--	--
PI-3/4I-D-9-CI-4	Field Blank	--	-0.847	5	2.0	--	--	--	--	--
PI-3/4I-D-9-CI-5	Field Blank	--	0.836	-1	0.9	--	--	--	--	--
PI-3/4I-D-9-CI-6	Field Blank	--	0.965	0	0.6	--	--	--	--	--
PI-3/4I-D-9-CI-7	Field Blank	--	0.127	0	1.1	--	--	--	--	--
PI-3/4I-D-9-CI-8	Field Blank	--	-0.129	2	1.0	--	--	--	--	--
PI-3/4I-D-9-CI-9	Field Blank	--	1.825	5	1.3	--	--	--	--	--

(a) DU mass based on ICP-MS results; no analytical uncertainty was reported.

Table A.22 (cont'd). Phase I, Shots 3/4, Gunner

Sample ID	Collection Interval	Elapsed Time	Total Mass (mg)	Calculated U (μg)	DU Mass ± 1σ (μg)	Net DU Mass (μg)	Flow Rate (Lpm)	Volume (L)	DU Conc. (μg/m^3)	DU Conc. ± 1σ (μg/m^3)
PI-3/4I-G-1-CI-1	Shot 3: 0-10 sec	10 sec	0.481	639	85.9	105	2.527	0.421	2.49E+05	2.67E+05
PI-3/4I-G-1-CI-2	Shot 3: 0-10 sec	10 sec	0.450	108	42.6	83	2.527	0.421	1.97E+05	1.04E+05
PI-3/4I-G-1-CI-3	Shot 3: 0-10 sec	10 sec	-0.512	70	13.3	59	2.527	0.421	1.40E+05	3.23E+04
PI-3/4I-G-1-CI-4	Shot 3: 0-10 sec	10 sec	0.232	110	29.1	105	2.527	0.421	2.49E+05	6.96E+04
PI-3/4I-G-1-CI-5	Shot 3: 0-10 sec	10 sec	-1.305	533	204.2	522	2.527	0.421	1.24E+06	4.87E+05
PI-3/4I-G-1-CI-6	Shot 3: 0-10 sec	10 sec	-0.147	330	135.3	327	2.527	0.421	7.77E+05	3.22E+05
PI-3/4I-G-1-CI-7	Shot 3: 0-10 sec	10 sec	-0.839	250	57.6	247	2.527	0.421	5.87E+05	1.38E+05
PI-3/4I-G-1-CI-8	Shot 3: 0-10 sec	10 sec	-1.048	384	86.1	364	2.527	0.421	8.65E+05	2.07E+05
PI-3/4I-G-1-CI-9	Shot 3: 0-10 sec	10 sec	2.664	1275	398.5	1265	2.527	0.421	3.00E+06	9.51E+05
PI-3/4I-G-2-CI-1	3-3.5 min	30 sec	0.677	444	60.0	-90	2.510	1.255	-7.17E+04	7.48E+04
PI-3/4I-G-2-CI-2	3-3.5 min	30 sec	0.035	82	32.4	57	2.510	1.255	4.54E+04	2.71E+04
PI-3/4I-G-2-CI-3	3-3.5 min	30 sec	-3.552	110	20.7	99	2.510	1.255	7.89E+04	1.68E+04
PI-3/4I-G-2-CI-4	3-3.5 min	30 sec	0.137	259	68.2	254	2.510	1.255	2.02E+05	5.47E+04
PI-3/4I-G-2-CI-5	3-3.5 min	30 sec	-0.647	406	155.9	395	2.510	1.255	3.15E+05	1.25E+05
PI-3/4I-G-2-CI-6	3-3.5 min	30 sec	-0.923	293	120.8	290	2.510	1.255	2.31E+05	9.65E+04
PI-3/4I-G-2-CI-7	3-3.5 min	30 sec	0.577	277	63.7	274	2.510	1.255	2.18E+05	5.12E+04
PI-3/4I-G-2-CI-8	3-3.5 min	30 sec	0.055	289	65.6	269	2.510	1.255	2.14E+05	5.29E+04
PI-3/4I-G-2-CI-9	3-3.5 min	30 sec	1.623	422	133.2	412	2.510	1.255	3.28E+05	1.07E+05
PI-3/4I-G-3-CI-1	9-10 min	1 min	0.847	497	67.1	-37	2.652	2.652	-1.40E+04	3.72E+04
PI-3/4I-G-3-CI-2	9-10 min	1 min	-1.644	46	18.4	21	2.652	2.652	7.92E+03	7.92E+03
PI-3/4I-G-3-CI-3	9-10 min	1 min	-0.681	49	9.5	38	2.652	2.652	1.43E+04	3.71E+03
PI-3/4I-G-3-CI-4	9-10 min	1 min	-0.455	110	29.6	105	2.652	2.652	3.96E+04	1.12E+04
PI-3/4I-G-3-CI-5	9-10 min	1 min	-0.438	285	109.6	274	2.652	2.652	1.03E+05	4.15E+04
PI-3/4I-G-3-CI-6	9-10 min	1 min	-1.004	187	77.6	184	2.652	2.652	6.94E+04	2.93E+04
PI-3/4I-G-3-CI-7	9-10 min	1 min	-1.416	203	47.4	200	2.652	2.652	7.54E+04	1.80E+04
PI-3/4I-G-3-CI-8	9-10 min	1 min	-1.613	246	56.0	226	2.652	2.652	8.52E+04	2.14E+04
PI-3/4I-G-3-CI-9	9-10 min	1 min	-0.833	214	68.5	204	2.652	2.652	7.69E+04	2.60E+04
PI-3/4I-G-4-CI-1	Shot 4: 0-10 sec	10 sec	1.233	731	98.1	197	2.545	0.424	4.65E+05	2.88E+05
PI-3/4I-G-4-CI-2	Shot 4: 0-10 sec	10 sec	-1.148	336	132.1	311	2.545	0.424	7.33E+05	3.13E+05
PI-3/4I-G-4-CI-3	Shot 4: 0-10 sec	10 sec	-0.615	207	NA[(a)]	196	2.545	0.424	4.62E+05	NA[(a)]
PI-3/4I-G-4-CI-4	Shot 4: 0-10 sec	10 sec	-1.081	295	77.3	290	2.545	0.424	6.84E+05	1.84E+05
PI-3/4I-G-4-CI-5	Shot 4: 0-10 sec	10 sec	-1.490	199	76.5	188	2.545	0.424	4.43E+05	1.81E+05
PI-3/4I-G-4-CI-6	Shot 4: 0-10 sec	10 sec	-1.229	239	98.4	236	2.545	0.424	5.57E+05	2.33E+05
PI-3/4I-G-4-CI-7	Shot 4: 0-10 sec	10 sec	-0.499	147	35.1	144	2.545	0.424	3.40E+05	8.35E+04
PI-3/4I-G-4-CI-8	Shot 4: 0-10 sec	10 sec	-1.102	215	50.2	195	2.545	0.424	4.60E+05	1.20E+05
PI-3/4I-G-4-CI-9	Shot 4: 0-10 sec	10 sec	0.498	646	204.0	636	2.545	0.424	1.50E+06	4.83E+05
PI-3/4I-G-5-CI-1	3-3.5 min	30 sec	0.576	352	47.7	-182	2.617	1.308	-1.39E+05	6.63E+04
PI-3/4I-G-5-CI-2	3-3.5 min	30 sec	-1.544	67	26.7	42	2.617	1.308	3.21E+04	2.18E+04
PI-3/4I-G-5-CI-3	3-3.5 min	30 sec	-2.486	76	14.3	65	2.617	1.308	4.97E+04	1.12E+04
PI-3/4I-G-5-CI-4	3-3.5 min	30 sec	-1.220	64	17.2	59	2.617	1.308	4.51E+04	1.33E+04
PI-3/4I-G-5-CI-5	3-3.5 min	30 sec	-1.254	68	26.4	57	2.617	1.308	4.36E+04	2.05E+04
PI-3/4I-G-5-CI-6	3-3.5 min	30 sec	0.264	106	44.8	103	2.617	1.308	7.87E+04	3.44E+04
PI-3/4I-G-5-CI-7	3-3.5 min	30 sec	-0.270	99	24.7	96	2.617	1.308	7.34E+04	1.90E+04

Table A.22 (cont'd). Phase I, Shots 3/4, Gunner

Sample ID	Collection Interval	Elapsed Time	Total Mass (mg)	Calculated U (μg)	DU Mass ± 1σ (μg)	Adj'd Net DU Mass (μg)	Flow Rate (Lpm)	Volume (L)	DU Conc. (μg/m^3)	DU Conc. ± 1σ (μg/m^3)
PI-3/4I-G-5-CI-8	3-3.5 min	30 sec	-1.224	144	35.3	124	2.617	1.308	9.48E+04	2.75E+04
PI-3/4I-G-5-CI-9	3-3.5 min	30 sec	-1.564	261	83.3	251	2.617	1.308	1.92E+05	6.40E+04
PI-3/4I-G-6-CI-1	9-10 min	1 min	1.035	310	42.1	-224	2.650	2.650	-8.45E+04	3.16E+04
PI-3/4I-G-6-CI-2	9-10 min	1 min	-0.875	29	11.6	4	2.650	2.650	1.51E+03	5.80E+03
PI-3/4I-G-6-CI-3	9-10 min	1 min	0.400	47	9.2	36	2.650	2.650	1.36E+04	3.60E+03
PI-3/4I-G-6-CI-4	9-10 min	1 min	-0.829	70	18.7	65	2.650	2.650	2.45E+04	7.12E+03
PI-3/4I-G-6-CI-5	9-10 min	1 min	-2.373	78	30.5	67	2.650	2.650	2.53E+04	1.16E+04
PI-3/4I-G-6-CI-6	9-10 min	1 min	1.115	114	47.6	111	2.650	2.650	4.19E+04	1.80E+04
PI-3/4I-G-6-CI-7	9-10 min	1 min	-1.003	132	32.4	129	2.650	2.650	4.87E+04	1.23E+04
PI-3/4I-G-6-CI-8	9-10 min	1 min	-0.864	147	35.5	127	2.650	2.650	4.79E+04	1.37E+04
PI-3/4I-G-6-CI-9	9-10 min	1 min	1.631	169	54.4	159	2.650	2.650	6.00E+04	2.07E+04
PI-3/4I-G-7-CI-1	21-23 min	2 min	0.642	259	35.2	-275	2.370	4.739	-5.80E+04	1.70E+04
PI-3/4I-G-7-CI-2	21-23 min	2 min	-0.616	21	8.5	-4	2.370	4.739	-8.44E+02	2.79E+03
PI-3/4I-G-7-CI-3	21-23 min	2 min	3.527	12	2.7	1	2.370	4.739	2.11E+02	7.48E+02
PI-3/4I-G-7-CI-4	21-23 min	2 min	-0.258	34	9.3	29	2.370	4.739	6.12E+03	2.00E+03
PI-3/4I-G-7-CI-5	21-23 min	2 min	-0.687	35	14.4	24	2.370	4.739	5.06E+03	3.17E+03
PI-3/4I-G-7-CI-6	21-23 min	2 min	-0.932	57	24.2	54	2.370	4.739	1.14E+04	5.13E+03
PI-3/4I-G-7-CI-7	21-23 min	2 min	1.851	56	15.2	53	2.370	4.739	1.12E+04	3.23E+03
PI-3/4I-G-7-CI-8	21-23 min	2 min	0.107	124	29.7	104	2.370	4.739	2.19E+04	6.43E+03
PI-3/4I-G-7-CI-9	21-23 min	2 min	1.237	99	33.0	89	2.370	4.739	1.88E+04	7.03E+03
PI-3/4I-G-8-CI-1	45-49 min	4 min	0.433	332	44.9	-202	2.481	9.926	-2.04E+04	8.59E+03
PI-3/4I-G-8-CI-2	45-49 min	4 min	-0.060	22	9.1	-3	2.481	9.926	-3.02E+02	1.37E+03
PI-3/4I-G-8-CI-3	45-49 min	4 min	-0.737	9	2.1	-2	2.481	9.926	-2.01E+02	3.14E+02
PI-3/4I-G-8-CI-4	45-49 min	4 min	1.920	30	8.2	25	2.481	9.926	2.52E+03	8.45E+02
PI-3/4I-G-8-CI-5	45-49 min	4 min	-0.014	69	26.9	58	2.481	9.926	5.84E+03	2.75E+03
PI-3/4I-G-8-CI-6	45-49 min	4 min	-0.663	34	14.7	31	2.481	9.926	3.12E+03	1.50E+03
PI-3/4I-G-8-CI-7	45-49 min	4 min	-0.612	53	14.2	50	2.481	9.926	5.04E+03	1.44E+03
PI-3/4I-G-8-CI-8	45-49 min	4 min	-0.109	127	29.4	107	2.481	9.926	1.08E+04	3.04E+03
PI-3/4I-G-8-CI-9	45-49 min	4 min	-0.100	154	46.6	144	2.481	9.926	1.45E+04	4.73E+03
PI-3/4I-G-9-CI-1	Field Blank	--	0.700	534	72.2	--	--	--	--	--
PI-3/4I-G-9-CI-2	Field Blank	--	-0.088	25	10.1	--	--	--	--	--
PI-3/4I-G-9-CI-3	Field Blank	--	0.147	11	2.3	--	--	--	--	--
PI-3/4I-G-9-CI-4	Field Blank	--	-0.052	5	1.6	--	--	--	--	--
PI-3/4I-G-9-CI-5	Field Blank	--	-0.612	11	4.3	--	--	--	--	--
PI-3/4I-G-9-CI-6	Field Blank	--	-0.221	3	1.9	--	--	--	--	--
PI-3/4I-G-9-CI-7	Field Blank	--	-0.864	3	1.2	--	--	--	--	--
PI-3/4I-G-9-CI-8	Field Blank	--	-0.798	20	6.0	--	--	--	--	--
PI-3/4I-G-9-CI-9	Field Blank	--	-1.439	10	3.7	--	--	--	--	--

(a) DU mass based on ICP-MS results; no analytical uncertainty was reported.

Table A.22 (cont'd). Phase I, Shots 3/4, Loader

Sample ID	Collection Interval	Elapsed Time	Total Mass (mg)	Calculated U (μg)	DU Mass ± 1σ (μg)	Net DU Mass (μg)	Flow Rate (Lpm)	Volume (L)	DU Conc. (μg/m^3)	DU Conc. ± 1σ (μg/m^3)
PI-3/4I-L-1-CI-1	Shot 4: 0-10 sec	10 sec	2.206	1408	261.5	395	2.329	0.388	1.02E+06	7.33E+05
PI-3/4I-L-1-CI-2	Shot 4: 0-10 sec	10 sec	-0.275	238	112.2	163	2.329	0.388	4.20E+05	2.94E+05
PI-3/4I-L-1-CI-3	Shot 4: 0-10 sec	10 sec	-1.109	272	69.1	246	2.329	0.388	6.34E+05	1.79E+05
PI-3/4I-L-1-CI-4	Shot 4: 0-10 sec	10 sec	0.079	106	38.8	82	2.329	0.388	2.11E+05	1.01E+05
PI-3/4I-L-1-CI-5	Shot 4: 0-10 sec	10 sec	-1.583	115	44.1	83	2.329	0.388	2.14E+05	1.16E+05
PI-3/4I-L-1-CI-6	Shot 4: 0-10 sec	10 sec	-0.772	112	26.7	96	2.329	0.388	2.47E+05	6.95E+04
PI-3/4I-L-1-CI-7	Shot 4: 0-10 sec	10 sec	-0.429	90	15.5	64	2.329	0.388	1.66E+05	4.10E+04
PI-3/4I-L-1-CI-8	Shot 4: 0-10 sec	10 sec	-0.025	223	21.7	187	2.329	0.388	4.83E+05	5.81E+04
PI-3/4I-L-1-CI-9	Shot 4: 0-10 sec	10 sec	0.785	467	79.1	376	2.329	0.388	9.69E+05	2.07E+05
PI-3/4I-L-2-CI-1	3-3.5 min	30 sec	1.31	927	172.3	-86	2.442	1.221	-7.02E+04	1.68E+05
PI-3/4I-L-2-CI-2	3-3.5 min	30 sec	0.576	104	49.1	29	2.442	1.221	2.38E+04	4.38E+04
PI-3/4I-L-2-CI-3	3-3.5 min	30 sec	0.283	90	23.1	64	2.442	1.221	5.24E+04	1.93E+04
PI-3/4I-L-2-CI-4	3-3.5 min	30 sec	-0.331	114	41.5	90	2.442	1.221	7.37E+04	3.43E+04
PI-3/4I-L-2-CI-5	3-3.5 min	30 sec	0.014	171	65.4	139	2.442	1.221	1.14E+05	5.41E+04
PI-3/4I-L-2-CI-6	3-3.5 min	30 sec	-1.727	109	26.1	93	2.442	1.221	7.62E+04	2.16E+04
PI-3/4I-L-2-CI-7	3-3.5 min	30 sec	-0.409	133	22.2	107	2.442	1.221	8.79E+04	1.85E+04
PI-3/4I-L-2-CI-8	3-3.5 min	30 sec	-0.122	116	11.8	80	2.442	1.221	6.58E+04	1.01E+04
PI-3/4I-L-2-CI-9	3-3.5 min	30 sec	0.298	305	51.9	214	2.442	1.221	1.75E+05	4.35E+04
PI-3/4I-L-3-CI-1	9-10 min	1 min	-2.752	1062	197.1	49	2.336	2.336	2.11E+04	9.68E+04
PI-3/4I-L-3-CI-2	9-10 min	1 min	-0.746	138	65.0	63	2.336	2.336	2.70E+04	2.93E+04
PI-3/4I-L-3-CI-3	9-10 min	1 min	-0.314	188	47.6	162	2.336	2.336	6.93E+04	2.06E+04
PI-3/4I-L-3-CI-4	9-10 min	1 min	-1.579	138	50.3	114	2.336	2.336	4.88E+04	2.17E+04
PI-3/4I-L-3-CI-5	9-10 min	1 min	-1.094	169	64.5	137	2.336	2.336	5.86E+04	2.79E+04
PI-3/4I-L-3-CI-6	9-10 min	1 min	-0.555	79	19.0	63	2.336	2.336	2.70E+04	8.24E+03
PI-3/4I-L-3-CI-7	9-10 min	1 min	-1.044	109	18.5	83	2.336	2.336	3.57E+04	8.09E+03
PI-3/4I-L-3-CI-8	9-10 min	1 min	-0.307	106	10.6	70	2.336	2.336	3.01E+04	4.75E+03
PI-3/4I-L-3-CI-9	9-10 min	1 min	-0.335	167	28.8	76	2.336	2.336	3.25E+04	1.30E+04
PI-3/4I-L-4-CI-1	21-23 min	2 min	-4.281	1015	188.4	2	2.428	4.855	4.81E+02	4.50E+04
PI-3/4I-L-4-CI-2	21-23 min	2 min	0.232	176	83.1	101	2.428	4.855	2.08E+04	1.77E+04
PI-3/4I-L-4-CI-3	21-23 min	2 min	-0.021	75	19.4	49	2.428	4.855	1.01E+04	4.09E+03
PI-3/4I-L-4-CI-4	21-23 min	2 min	-0.096	110	40.0	86	2.428	4.855	1.77E+04	8.33E+03
PI-3/4I-L-4-CI-5	21-23 min	2 min	-0.991	165	63.0	133	2.428	4.855	2.74E+04	1.31E+04
PI-3/4I-L-4-CI-6	21-23 min	2 min	-1.359	58	14.0	42	2.428	4.855	8.65E+03	2.94E+03
PI-3/4I-L-4-CI-7	21-23 min	2 min	-0.061	86	14.5	60	2.428	4.855	1.24E+04	3.07E+03
PI-3/4I-L-4-CI-8	21-23 min	2 min	-0.567	90	9.3	54	2.428	4.855	1.12E+04	2.01E+03
PI-3/4I-L-4-CI-9	21-23 min	2 min	-0.458	163	28.0	72	2.428	4.855	1.48E+04	6.09E+03
PI-3/4I-L-5-CI-1	45-49 min	4 min	-4.157	1575	292.3	562	2.468	9.874	5.70E+04	3.17E+04
PI-3/4I-L-5-CI-2	45-49 min	4 min	-0.709	180	84.8	105	2.468	9.874	1.06E+04	8.85E+03
PI-3/4I-L-5-CI-3	45-49 min	4 min	-0.502	86	22.1	60	2.468	9.874	6.08E+03	2.28E+03

Table A.22 (cont'd). Phase I, Shots 3/4, Loader

Sample ID	Collection Interval	Elapsed Time	Total Mass (mg)	Calculated U (μg)	DU Mass ± 1σ (μg)	Net DU Mass (μg)	Flow Rate (Lpm)	Volume (L)	DU Conc. (μg/m^3)	DU Conc. ± 1σ (μg/m^3)
PI-3/4I-L-5-CI-4	45-49 min	4 min	-1.191	76	27.7	52	2.468	9.874	5.27E+03	2.86E+03
PI-3/4I-L-5-CI-5	45-49 min	4 min	-0.382	106	40.5	74	2.468	9.874	7.49E+03	4.20E+03
PI-3/4I-L-5-CI-6	45-49 min	4 min	-0.21	43	10.4	27	2.468	9.874	2.73E+03	1.08E+03
PI-3/4I-L-5-CI-7	45-49 min	4 min	-1.134	71	12.2	45	2.468	9.874	4.59E+03	1.28E+03
PI-3/4I-L-5-CI-8	45-49 min	4 min	2.803	87	9.2	51	2.468	9.874	5.20E+03	9.78E+02
PI-3/4I-L-5-CI-9	45-49 min	4 min	0.858	192	33.1	101	2.468	9.874	1.02E+04	3.49E+03
PI-3/4I-L-6-CI-1	93-101 min	8 min	1.15	1038	192.9	25	2.475	19.804	1.28E+03	1.12E+04
PI-3/4I-L-6-CI-2	93-101 min	8 min	-0.138	124	58.4	49	2.475	19.804	2.47E+03	3.14E+03
PI-3/4I-L-6-CI-3	93-101 min	8 min	-0.893	31	8.0	5	2.475	19.804	2.52E+02	4.53E+02
PI-3/4I-L-6-CI-4	93-101 min	8 min	-0.055	53	19.6	29	2.475	19.804	1.46E+03	1.03E+03
PI-3/4I-L-6-CI-5	93-101 min	8 min	-0.7	101	38.6	69	2.475	19.804	3.48E+03	2.00E+03
PI-3/4I-L-6-CI-6	93-101 min	8 min	-0.04	65	15.7	49	2.475	19.804	2.47E+03	8.06E+02
PI-3/4I-L-6-CI-7	93-101 min	8 min	-0.671	85	14.3	59	2.475	19.804	3.00E+03	7.43E+02
PI-3/4I-L-6-CI-8	93-101 min	8 min	-1.124	100	10.1	64	2.475	19.804	3.25E+03	5.34E+02
PI-3/4I-L-6-CI-9	93-101 min	8 min	-0.085	223	38.0	132	2.475	19.804	6.67E+03	1.98E+03
PI-3/4I-L-7-CI-1	Field Blank	--	2.052	755	140.4	--	--	--	--	--
PI-3/4I-L-7-CI-2	Field Blank	--	0.494	71	33.7	--	--	--	--	--
PI-3/4I-L-7-CI-3	Field Blank	--	-0.274	30	7.8	--	--	--	--	--
PI-3/4I-L-7-CI-4	Field Blank	--	0.886	20	7.7	--	--	--	--	--
PI-3/4I-L-7-CI-5	Field Blank	--	0.191	13	5.3	--	--	--	--	--
PI-3/4I-L-7-CI-6	Field Blank	--	-0.215	17	4.4	--	--	--	--	--
PI-3/4I-L-7-CI-7	Field Blank	--	-1.727	30	5.4	--	--	--	--	--
PI-3/4I-L-7-CI-8	Field Blank	--	-0.448	38	4.4	--	--	--	--	--
PI-3/4I-L-7-CI-9	Field Blank	--	1.589	77	13.4	--	--	--	--	--
PI-3/4I-L-8-CI-1	Field Blank	--	1.482	1036	192.4	--	--	--	--	--
PI-3/4I-L-8-CI-2	Field Blank	--	0.048	56	26.5	--	--	--	--	--
PI-3/4I-L-8-CI-3	Field Blank	--	-0.278	30	8.0	--	--	--	--	--
PI-3/4I-L-8-CI-4	Field Blank	--	-1.137	25	9.4	--	--	--	--	--
PI-3/4I-L-8-CI-5	Field Blank	--	-0.862	63	24.2	--	--	--	--	--
PI-3/4I-L-8-CI-6	Field Blank	--	-1.408	14	3.9	--	--	--	--	--
PI-3/4I-L-8-CI-7	Field Blank	--	-0.587	35	6.3	--	--	--	--	--
PI-3/4I-L-8-CI-8	Field Blank	--	-1.007	35	4.3	--	--	--	--	--
PI-3/4I-L-8-CI-9	Field Blank	--	-0.612	83	14.4	--	--	--	--	--
PI-3/4I-L-9-CI-1	Field Blank	--	3.095	1247	231.5	--	--	--	--	--
PI-3/4I-L-9-CI-2	Field Blank	--	0.825	98	46.4	--	--	--	--	--
PI-3/4I-L-9-CI-3	Field Blank	--	0.36	18	4.8	--	--	--	--	--
PI-3/4I-L-9-CI-4	Field Blank	--	1.337	27	10.0	--	--	--	--	--
PI-3/4I-L-9-CI-5	Field Blank	--	0.301	20	7.9	--	--	--	--	--
PI-3/4I-L-9-CI-6	Field Blank	--	-0.024	17	4.3	--	--	--	--	--

Table A.22 (cont'd). Phase I, Shots 3/4, Loader

Sample ID	Collection Interval	Elapsed Time	Total Mass (mg)	Calculated U (μg)	DU Mass ± 1σ (μg)	Adj'd Net DU Mass (μg)	Flow Rate (Lpm)	Volume (L)	DU Conc. (μg/m^3)	DU Conc. ± 1σ (μg/m^3)
PI-3/4I-L-9-CI-7	Field Blank	--	-0.691	12	3.0	--	--	--	--	--
PI-3/4I-L-9-CI-8	Field Blank	--	0.052	34	4.3	--	--	--	--	--
PI-3/4I-L-9-CI-9	Field Blank	--	1.038	113	19.5	--	--	--	--	--

Table A.23. PI-5 Cascade Impactor Substrates—Mass, Volume, and Concentration

Sample ID	Collection Interval	Elapsed Time	Total Mass (mg)	Calculated U (μg)	DU Mass ± 1σ (μg)	Net DU Mass (μg)	Flow Rate (Lpm)	Volume (L)	DU Conc. (μg/m^3)	DU Conc. ± 1σ (μg/m^3)
PI-5I-C-1-CI-1	0-10 sec	10 sec	1.741	293	54.5	228	2.701	0.450	5.07E+05	1.25E+05
PI-5I-C-1-CI-2	0-10 sec	10 sec	1.689	220	103.1	210	2.701	0.450	4.67E+05	2.30E+05
PI-5I-C-1-CI-3	0-10 sec	10 sec	-1.160	231	58.4	229	2.701	0.450	5.09E+05	1.31E+05
PI-5I-C-1-CI-4	0-10 sec	10 sec	-1.912	266	96.4	264	2.701	0.450	5.87E+05	2.15E+05
PI-5I-C-1-CI-5	0-10 sec	10 sec	-0.236	199	75.8	195	2.701	0.450	4.33E+05	1.69E+05
PI-5I-C-1-CI-6	0-10 sec	10 sec	-2.126	179	42.5	177	2.701	0.450	3.93E+05	9.52E+04
PI-5I-C-1-CI-7	0-10 sec	10 sec	-1.843	281	46.1	279	2.701	0.450	6.20E+05	1.04E+05
PI-5I-C-1-CI-8	0-10 sec	10 sec	-2.388	183	18.0	181	2.701	0.450	4.02E+05	4.18E+04
PI-5I-C-1-CI-9	0-10 sec	10 sec	1.100	660	111.7	651	2.701	0.450	1.45E+06	2.52E+05
PI-5I-C-2-CI-1	1-1 min 10 sec	10 sec	1.237	71	13.4	6	2.640	0.396	1.52E+04	4.61E+04
PI-5I-C-2-CI-2	1-1 min 10 sec	10 sec	-3.377	61	29.0	51	2.640	0.396	1.29E+05	7.45E+04
PI-5I-C-2-CI-3	1-1 min 10 sec	10 sec	-1.401	105	26.7	103	2.640	0.396	2.60E+05	6.79E+04
PI-5I-C-2-CI-4	1-1 min 10 sec	10 sec	-1.101	116	42.1	114	2.640	0.396	2.88E+05	1.07E+05
PI-5I-C-2-CI-5	1-1 min 10 sec	10 sec	-5.179	75	28.5	71	2.640	0.396	1.79E+05	7.23E+04
PI-5I-C-2-CI-6	1-1 min 10 sec	10 sec	-1.926	81	19.4	79	2.640	0.396	1.99E+05	4.94E+04
PI-5I-C-2-CI-7	1-1 min 10 sec	10 sec	-1.453	100	17.1	98	2.640	0.396	2.47E+05	4.39E+04
PI-5I-C-2-CI-8	1-1 min 10 sec	10 sec	-0.065	115	11.4	113	2.640	0.396	2.85E+05	3.01E+04
PI-5I-C-2-CI-9	1-1 min 10 sec	10 sec	0.944	144	NA[(a)]	135	2.640	0.396	3.41E+05	NA[(a)]
PI-5I-C-3-CI-1	3-3 min 10 sec	10 sec	0.927	82	15.5	17	2.645	0.441	3.85E+04	4.50E+04
PI-5I-C-3-CI-2	3-3 min 10 sec	10 sec	-0.371	12	5.8	2	2.645	0.441	4.54E+03	1.77E+04
PI-5I-C-3-CI-3	3-3 min 10 sec	10 sec	-1.139	31	8.1	29	2.645	0.441	6.58E+04	1.86E+04
PI-5I-C-3-CI-4	3-3 min 10 sec	10 sec	0.244	64	23.3	62	2.645	0.441	1.41E+05	5.31E+04
PI-5I-C-3-CI-5	3-3 min 10 sec	10 sec	-3.141	89	33.9	85	2.645	0.441	1.93E+05	7.72E+04
PI-5I-C-3-CI-6	3-3 min 10 sec	10 sec	-1.991	42	10.2	40	2.645	0.441	9.07E+04	2.34E+04
PI-5I-C-3-CI-7	3-3 min 10 sec	10 sec	-2.831	63	10.8	61	2.645	0.441	1.38E+05	2.49E+04
PI-5I-C-3-CI-8	3-3 min 10 sec	10 sec	0.732	50	5.7	48	2.645	0.441	1.09E+05	1.34E+04
PI-5I-C-3-CI-9	3-3 min 10 sec	10 sec	1.275	19	3.8	10	2.645	0.441	2.27E+04	9.56E+03
PI-5I-C-4-CI-1	7-7.5 min	30 sec	1.477	22	4.1	-43	2.477	1.239	-3.47E+04	1.06E+04
PI-5I-C-4-CI-2	7-7.5 min	30 sec	-0.974	11	5.4	1	2.477	1.239	8.07E+02	6.05E+03
PI-5I-C-4-CI-3	7-7.5 min	30 sec	-0.137	10	2.7	8	2.477	1.239	6.46E+03	2.31E+03
PI-5I-C-4-CI-4	7-7.5 min	30 sec	-0.903	17	6.3	15	2.477	1.239	1.21E+04	5.17E+03
PI-5I-C-4-CI-5	7-7.5 min	30 sec	-3.397	19	7.5	15	2.477	1.239	1.21E+04	6.20E+03
PI-5I-C-4-CI-6	7-7.5 min	30 sec	0.232	20	5.2	18	2.477	1.239	1.45E+04	4.27E+03
PI-5I-C-4-CI-7	7-7.5 min	30 sec	-3.432	30	5.5	28	2.477	1.239	2.26E+04	4.56E+03
PI-5I-C-4-CI-8	7-7.5 min	30 sec	-1.344	21	2.8	19	2.477	1.239	1.53E+04	2.37E+03
PI-5I-C-4-CI-9	7-7.5 min	30 sec	0.176	10	2.2	1	2.477	1.239	8.07E+02	2.29E+03
PI-5I-C-5-CI-1	15-16 min	1 min	1.964	66	12.6	1	2.462	2.462	4.06E+02	7.18E+03
PI-5I-C-5-CI-2	15-16 min	1 min	0.674	11	5.4	1	2.462	2.462	4.06E+02	3.04E+03
PI-5I-C-5-CI-3	15-16 min	1 min	-2.794	7	2.2	5	2.462	2.462	2.03E+03	9.67E+02
PI-5I-C-5-CI-4	15-16 min	1 min	-0.108	6	2.5	4	2.462	2.462	1.62E+03	1.11E+03
PI-5I-C-5-CI-5	15-16 min	1 min	-3.780	16	6.4	12	2.462	2.462	4.87E+03	2.68E+03
PI-5I-C-5-CI-6	15-16 min	1 min	-2.234	22	5.5	20	2.462	2.462	8.12E+03	2.27E+03
PI-5I-C-5-CI-7	15-16 min	1 min	-3.775	16	3.3	14	2.462	2.462	5.69E+03	1.41E+03

Table A.23 (cont'd). Phase I, Shot 5, Commander

Sample ID	Collection Interval	Elapsed Time	Total Mass (mg)	Calculated U (μg)	DU Mass ± 1σ (μg)	Net DU Mass (μg)	Flow Rate (Lpm)	Volume (L)	DU Conc. (μg/m^3)	DU Conc. ± 1σ (μg/m^3)
PI-5I-C-5-CI-8	15-16 min	1 min	-0.105	25	3.2	23	2.462	2.462	9.34E+03	1.36E+03
PI-5I-C-5-CI-9	15-16 min	1 min	1.129	13	2.7	4	2.462	2.462	1.62E+03	1.32E+03
PI-5I-C-6-CI-1	31-33 min	2 min	2.091	66	12.5	1	2.478	4.957	2.02E+02	3.55E+03
PI-5I-C-6-CI-2	31-33 min	2 min	-0.821	5	2.7	-5	2.478	4.957	-1.01E+03	1.18E+03
PI-5I-C-6-CI-3	31-33 min	2 min	-2.397	5	1.6	3	2.478	4.957	6.05E+02	3.71E+02
PI-5I-C-6-CI-4	31-33 min	2 min	-0.749	14	5.3	12	2.478	4.957	2.42E+03	1.09E+03
PI-5I-C-6-CI-5	31-33 min	2 min	-0.694	37	14.2	33	2.478	4.957	6.66E+03	2.89E+03
PI-5I-C-6-CI-6	31-33 min	2 min	-0.033	27	6.7	25	2.478	4.957	5.04E+03	1.37E+03
PI-5I-C-6-CI-7	31-33 min	2 min	-5.338	15	3.2	13	2.478	4.957	2.62E+03	6.81E+02
PI-5I-C-6-CI-8	31-33 min	2 min	-1.217	40	4.7	38	2.478	4.957	7.67E+03	9.86E+02
PI-5I-C-6-CI-9	31-33 min	2 min	0.916	23	4.4	14	2.478	4.957	2.82E+03	9.63E+02
PI-5I-C-7-CI-1	61-65 min	4 min	1.037	42	8.4	-23	2.640	10.561	-2.18E+03	1.42E+03
PI-5I-C-7-CI-2	61-65 min	4 min	-3.023	9	4.6	-1	2.640	10.561	-9.47E+01	6.57E+02
PI-5I-C-7-CI-3	61-65 min	4 min	-4.196	8	2.3	6	2.640	10.561	5.68E+02	2.34E+02
PI-5I-C-7-CI-4	61-65 min	4 min	-4.989	27	10.2	25	2.640	10.561	2.37E+03	9.74E+02
PI-5I-C-7-CI-5	61-65 min	4 min	-5.269	38	14.5	34	2.640	10.561	3.22E+03	1.38E+03
PI-5I-C-7-CI-6	61-65 min	4 min	-2.006	28	7.1	26	2.640	10.561	2.46E+03	6.81E+02
PI-5I-C-7-CI-7	61-65 min	4 min	-4.253	25	4.9	23	2.640	10.561	2.18E+03	4.78E+02
PI-5I-C-7-CI-8	61-65 min	4 min	-1.898	44	4.9	42	2.640	10.561	3.98E+03	4.84E+02
PI-5I-C-7-CI-9	61-65 min	4 min	-0.994	48	8.5	39	2.640	10.561	3.69E+03	8.30E+02
PI-5I-C-8-CI-1	121-129 min	8 min	1.383	27	5.6	-38	2.553	20.427	-1.86E+03	6.68E+02
PI-5I-C-8-CI-2	121-129 min	8 min	-2.955	9	4.3	-1	2.553	20.427	-4.90E+01	3.30E+02
PI-5I-C-8-CI-3	121-129 min	8 min	-0.977	5	1.4	3	2.553	20.427	1.47E+02	8.16E+01
PI-5I-C-8-CI-4	121-129 min	8 min	0.175	18	6.9	16	2.553	20.427	7.83E+02	3.43E+02
PI-5I-C-8-CI-5	121-129 min	8 min	-0.713	60	23.1	56	2.553	20.427	2.74E+03	1.14E+03
PI-5I-C-8-CI-6	121-129 min	8 min	-1.918	34	8.4	32	2.553	20.427	1.57E+03	4.16E+02
PI-5I-C-8-CI-7	121-129 min	8 min	-4.542	66	11.3	64	2.553	20.427	3.13E+03	5.63E+02
PI-5I-C-8-CI-8	121-129 min	8 min	-3.554	63	6.9	61	2.553	20.427	2.99E+03	3.51E+02
PI-5I-C-8-CI-9	121-129 min	8 min	0.522	73	12.8	64	2.553	20.427	3.13E+03	6.40E+02
PI-5I-C-9-CI-1	Field Blank	--	1.398	65	12.4	--	--	--	--	--
PI-5I-C-9-CI-2	Field Blank	--	-0.549	10	5.2	--	--	--	--	--
PI-5I-C-9-CI-3	Field Blank	--	-1.752	2	0.9	--	--	--	--	--
PI-5I-C-9-CI-4	Field Blank	--	-0.002	2	1.1	--	--	--	--	--
PI-5I-C-9-CI-5	Field Blank	--	0.162	4	1.6	--	--	--	--	--
PI-5I-C-9-CI-6	Field Blank	--	-0.218	2	0.8	--	--	--	--	--
PI-5I-C-9-CI-7	Field Blank	--	-0.740	2	1.0	--	--	--	--	--
PI-5I-C-9-CI-8	Field Blank	--	-2.264	2	0.7	--	--	--	--	--
PI-5I-C-9-CI-9	Field Blank	--	1.163	9	1.8	--	--	--	--	--

(a) DU mass based on ICP-MS results; no analytical uncertainty was reported.

Table A.23 (cont'd). Phase I, Shot 5, Driver

Sample ID	Collection Interval	Elapsed Time	Total Mass (mg)	Calculated U (μg)	DU Mass ± 1σ (μg)	Net DU Mass (μg)	Flow Rate (Lpm)	Volume (L)	DU Conc. (μg/m^3)	DU Conc. ± 1σ (μg/m^3)
PI-5I-D-1-CI-1	0-10 sec	10 sec	0.706	393	52.4	207	2.430	0.405	5.11E+05	1.44E+05
PI-5I-D-1-CI-2	0-10 sec	10 sec	0.391	252	99.8	249	2.430	0.405	6.15E+05	2.47E+05
PI-5I-D-1-CI-3	0-10 sec	10 sec	-0.039	337	61.3	336	2.430	0.405	8.30E+05	1.53E+05
PI-5I-D-1-CI-4	0-10 sec	10 sec	-0.994	222	57.5	220	2.430	0.405	5.43E+05	1.43E+05
PI-5I-D-1-CI-5	0-10 sec	10 sec	0.179	366	146.2	366	2.430	0.405	9.04E+05	3.62E+05
PI-5I-D-1-CI-6	0-10 sec	10 sec	-0.126	287	141.5	285	2.430	0.405	7.04E+05	3.50E+05
PI-5I-D-1-CI-7	0-10 sec	10 sec	-0.708	120	33.6	120	2.430	0.405	2.96E+05	8.37E+04
PI-5I-D-1-CI-8	0-10 sec	10 sec	-0.994	147	50.2	122	2.430	0.405	3.01E+05	1.26E+05
PI-5I-D-1-CI-9	0-10 sec	10 sec	0.984	419	166.4	401	2.430	0.405	9.90E+05	4.12E+05
PI-5I-D-2-CI-1	1-1 min 10 sec	10 sec	0.508	343	45.8	157	2.744	0.412	3.81E+05	1.27E+05
PI-5I-D-2-CI-2	1-1 min 10 sec	10 sec	-0.690	53	21.2	50	2.744	0.412	1.21E+05	5.18E+04
PI-5I-D-2-CI-3	1-1 min 10 sec	10 sec	0.057	115	21.2	114	2.744	0.412	2.77E+05	5.22E+04
PI-5I-D-2-CI-4	1-1 min 10 sec	10 sec	0.673	135	35.3	133	2.744	0.412	3.23E+05	8.63E+04
PI-5I-D-2-CI-5	1-1 min 10 sec	10 sec	-0.013	243	97.0	243	2.744	0.412	5.90E+05	2.36E+05
PI-5I-D-2-CI-6	1-1 min 10 sec	10 sec	-1.472	23	13.3	21	2.744	0.412	5.10E+04	3.27E+04
PI-5I-D-2-CI-7	1-1 min 10 sec	10 sec	-0.003	49	16.8	49	2.744	0.412	1.19E+05	4.14E+04
PI-5I-D-2-CI-8	1-1 min 10 sec	10 sec	-0.149	130	46.1	105	2.744	0.412	2.55E+05	1.14E+05
PI-5I-D-2-CI-9	1-1 min 10 sec	10 sec	0.129	62	27.5	44	2.744	0.412	1.07E+05	6.93E+04
PI-5I-D-3-CI-1	3-3 min 10 sec	10 sec	0.768	208	27.8	22	2.620	0.437	5.03E+04	8.57E+04
PI-5I-D-3-CI-2	3-3 min 10 sec	10 sec	-1.098	7	3.4	4	2.620	0.437	9.15E+03	8.92E+03
PI-5I-D-3-CI-3	3-3 min 10 sec	10 sec	-0.216	28	5.5	27	2.620	0.437	6.18E+04	1.31E+04
PI-5I-D-3-CI-4	3-3 min 10 sec	10 sec	-1.099	54	14.4	52	2.620	0.437	1.19E+05	3.32E+04
PI-5I-D-3-CI-5	3-3 min 10 sec	10 sec	-0.931	62	25.6	62	2.620	0.437	1.42E+05	5.89E+04
PI-5I-D-3-CI-6	3-3 min 10 sec	10 sec	-0.858	28	16.0	26	2.620	0.437	5.95E+04	3.69E+04
PI-5I-D-3-CI-7	3-3 min 10 sec	10 sec	0.218	21	9.3	21	2.620	0.437	4.81E+04	2.21E+04
PI-5I-D-3-CI-8	3-3 min 10 sec	10 sec	-2.132	41	17.3	16	2.620	0.437	3.66E+04	4.47E+04
PI-5I-D-3-CI-9	3-3 min 10 sec	10 sec	-0.028	-4	4.5	-22	2.620	0.437	-5.03E+04	2.01E+04
PI-5I-D-4-CI-1	7-7.5 min	30 sec	0.408	187	25.1	1	2.564	1.282	7.80E+02	2.77E+04
PI-5I-D-4-CI-2	7-7.5 min	30 sec	-0.318	5	2.3	2	2.564	1.282	1.56E+03	2.33E+03
PI-5I-D-4-CI-3	7-7.5 min	30 sec	0.993	9	2.0	8	2.564	1.282	6.24E+03	1.91E+03
PI-5I-D-4-CI-4	7-7.5 min	30 sec	0.204	16	4.6	14	2.564	1.282	1.09E+04	3.70E+03
PI-5I-D-4-CI-5	7-7.5 min	30 sec	-0.901	31	13.3	31	2.564	1.282	2.42E+04	1.05E+04
PI-5I-D-4-CI-6	7-7.5 min	30 sec	0.819	23	13.6	21	2.564	1.282	1.64E+04	1.07E+04
PI-5I-D-4-CI-7	7-7.5 min	30 sec	0.115	2	4.8	2	2.564	1.282	1.56E+03	4.26E+03
PI-5I-D-4-CI-8	7-7.5 min	30 sec	-0.070	32	14.7	7	2.564	1.282	5.46E+03	1.35E+04
PI-5I-D-4-CI-9	7-7.5 min	30 sec	0.560	11	6.2	-7	2.564	1.282	-5.46E+03	7.59E+03
PI-5I-D-5-CI-1	15-16 min	1 min	0.447	274	36.5	88	2.558	2.558	3.44E+04	1.73E+04
PI-5I-D-5-CI-2	15-16 min	1 min	-0.173	4	2.0	1	2.558	2.558	3.91E+02	1.08E+03
PI-5I-D-5-CI-3	15-16 min	1 min	-0.575	6	1.4	5	2.558	2.558	1.95E+03	7.76E+02
PI-5I-D-5-CI-4	15-16 min	1 min	-0.662	11	3.3	9	2.558	2.558	3.52E+03	1.36E+03
PI-5I-D-5-CI-5	15-16 min	1 min	-0.545	20	8.9	20	2.558	2.558	7.82E+03	3.55E+03
PI-5I-D-5-CI-6	15-16 min	1 min	-0.824	39	20.2	37	2.558	2.558	1.45E+04	7.95E+03
PI-5I-D-5-CI-7	15-16 min	1 min	0.007	13	NA[(a)]	13	2.558	2.558	5.08E+03	NA[(a)]

Table A.23 (cont'd). Phase I, Shot 5, Driver

Sample ID	Collection Interval	Elapsed Time	Total Mass (mg)	Calculated U (μg)	DU Mass ± 1σ (μg)	Net DU Mass (μg)	Flow Rate (Lpm)	Volume (L)	DU Conc. (μg/m^3)	DU Conc. ± 1σ (μg/m^3)
PI-5I-D-5-CI-8	15-16 min	1 min	-1.182	26	13.5	1	2.558	2.558	3.91E+02	6.36E+03
PI-5I-D-5-CI-9	15-16 min	1 min	-0.314	34	15.4	16	2.558	2.558	6.25E+03	6.70E+03
PI-5I-D-6-CI-1	31-33 min	2 min	0.468	281	37.5	95	2.579	5.158	1.84E+04	8.77E+03
PI-5I-D-6-CI-2	31-33 min	2 min	-0.182	13	5.6	10	2.579	5.158	1.94E+03	1.15E+03
PI-5I-D-6-CI-3	31-33 min	2 min	-0.361	7	1.9	6	2.579	5.158	1.16E+03	4.59E+02
PI-5I-D-6-CI-4	31-33 min	2 min	0.740	21	5.9	19	2.579	5.158	3.68E+03	1.17E+03
PI-5I-D-6-CI-5	31-33 min	2 min	-0.177	35	14.3	35	2.579	5.158	6.79E+03	2.80E+03
PI-5I-D-6-CI-6	31-33 min	2 min	-2.653	34	18.0	32	2.579	5.158	6.20E+03	3.52E+03
PI-5I-D-6-CI-7	31-33 min	2 min	-2.234	19	7.0	19	2.579	5.158	3.68E+03	1.45E+03
PI-5I-D-6-CI-8	31-33 min	2 min	-0.162	42	NA[(a)]	17	2.579	5.158	3.30E+03	NA[(a)]
PI-5I-D-6-CI-9	31-33 min	2 min	0.410	23	11.7	5	2.579	5.158	9.69E+02	2.69E+03
PI-5I-D-7-CI-1	61-65 min	4 min	0.568	265	35.5	79	2.544	10.176	7.76E+03	4.28E+03
PI-5I-D-7-CI-2	61-65 min	4 min	1.323	7	3.2	4	2.544	10.176	3.93E+02	3.66E+02
PI-5I-D-7-CI-3	61-65 min	4 min	-0.127	4	1.3	3	2.544	10.176	2.95E+02	1.88E+02
PI-5I-D-7-CI-4	61-65 min	4 min	-0.093	20	5.5	18	2.544	10.176	1.77E+03	5.54E+02
PI-5I-D-7-CI-5	61-65 min	4 min	-0.328	59	23.9	59	2.544	10.176	5.80E+03	2.36E+03
PI-5I-D-7-CI-6	61-65 min	4 min	-0.063	15	8.6	13	2.544	10.176	1.28E+03	8.69E+02
PI-5I-D-7-CI-7	61-65 min	4 min	0.395	14	6.8	14	2.544	10.176	1.38E+03	7.17E+02
PI-5I-D-7-CI-8	61-65 min	4 min	-0.691	38	17.7	13	2.544	10.176	1.28E+03	1.96E+03
PI-5I-D-7-CI-9	61-65 min	4 min	-0.012	41	17.9	23	2.544	10.176	2.26E+03	1.91E+03
PI-5I-D-8-CI-1	121-129 min	8 min	0.578	227	30.3	41	2.547	20.378	2.01E+03	1.93E+03
PI-5I-D-8-CI-2	121-129 min	8 min	0.173	1	1.4	-2	2.547	20.378	-9.81E+01	1.16E+02
PI-5I-D-8-CI-3	121-129 min	8 min	0.033	2	1.1	1	2.547	20.378	4.91E+01	8.74E+01
PI-5I-D-8-CI-4	121-129 min	8 min	0.210	17	4.8	15	2.547	20.378	7.36E+02	2.43E+02
PI-5I-D-8-CI-5	121-129 min	8 min	0.210	62	25.1	62	2.547	20.378	3.04E+03	1.24E+03
PI-5I-D-8-CI-6	121-129 min	8 min	0.059	61	30.1	59	2.547	20.378	2.90E+03	1.48E+03
PI-5I-D-8-CI-7	121-129 min	8 min	-0.282	26	9.7	26	2.547	20.378	1.28E+03	4.94E+02
PI-5I-D-8-CI-8	121-129 min	8 min	-0.074	79	25.9	54	2.547	20.378	2.65E+03	1.35E+03
PI-5I-D-8-CI-9	121-129 min	8 min	-0.732	65	25.2	47	2.547	20.378	2.31E+03	1.29E+03
PI-5I-D-9-CI-1	Field Blank	--	0.524	186	25.1	--	--	--	--	--
PI-5I-D-9-CI-2	Field Blank	--	-0.146	3	1.9	--	--	--	--	--
PI-5I-D-9-CI-3	Field Blank	--	0.327	1	1.4	--	--	--	--	--
PI-5I-D-9-CI-4	Field Blank	--	-0.337	2	1.1	--	--	--	--	--
PI-5I-D-9-CI-5	Field Blank	--	-0.249	-3	1.7	--	--	--	--	--
PI-5I-D-9-CI-6	Field Blank	--	-0.389	2	2.0	--	--	--	--	--
PI-5I-D-9-CI-7	Field Blank	--	0.008	-6	2.6	--	--	--	--	--
PI-5I-D-9-CI-8	Field Blank	--	0.040	25	9.1	--	--	--	--	--
PI-5I-D-9-CI-9	Field Blank	--	0.284	18	7.5	--	--	--	--	--

(a) DU mass based on ICP-MS results; no analytical uncertainty was reported.

Table A.23 (cont'd). Phase I, Shot 5, Loader

Sample ID	Collection Interval	Elapsed Time	Total Mass (mg)	Calculated U (μg)	DU Mass ± 1σ (μg)	Net DU Mass (μg)	Flow Rate (Lpm)	Volume (L)	DU Conc. (μg/m^3)	DU Conc. ± 1σ (μg/m^3)
PI-5I-L-1-CI-1	0-10 sec	10 sec	2.508	456	NA[(a)]	391	2.482	0.414	9.44E+05	NA[(a)]
PI-5I-L-1-CI-2	0-10 sec	10 sec	-1.753	179	84.1	169	2.482	0.414	4.08E+05	2.04E+05
PI-5I-L-1-CI-3	0-10 sec	10 sec	1.167	371	93.6	369	2.482	0.414	8.91E+05	2.28E+05
PI-5I-L-1-CI-4	0-10 sec	10 sec	-1.332	153	55.4	151	2.482	0.414	3.65E+05	1.34E+05
PI-5I-L-1-CI-5	0-10 sec	10 sec	-1.386	280	106.5	276	2.482	0.414	6.67E+05	2.58E+05
PI-5I-L-1-CI-6	0-10 sec	10 sec	-0.774	132	31.3	130	2.482	0.414	3.14E+05	7.62E+04
PI-5I-L-1-CI-7	0-10 sec	10 sec	-0.775	190	31.5	188	2.482	0.414	4.54E+05	7.73E+04
PI-5I-L-1-CI-8	0-10 sec	10 sec	-1.322	435	41.1	433	2.482	0.414	1.05E+06	1.04E+05
PI-5I-L-1-CI-9	0-10 sec	10 sec	0.191	356	60.8	347	2.482	0.414	8.38E+05	1.49E+05
PI-5I-L-2-CI-1	1-1 min 10 sec	10 sec	0.422	31	6.1	-34	2.510	0.376	-9.04E+04	3.69E+04
PI-5I-L-2-CI-2	1-1 min 10 sec	10 sec	-1.532	28	NA[(a)]	18	2.510	0.376	4.79E+04	NA[(a)]
PI-5I-L-2-CI-3	1-1 min 10 sec	10 sec	-1.174	79	20.2	77	2.510	0.376	2.05E+05	5.41E+04
PI-5I-L-2-CI-4	1-1 min 10 sec	10 sec	-2.232	106	38.6	104	2.510	0.376	2.77E+05	1.03E+05
PI-5I-L-2-CI-5	1-1 min 10 sec	10 sec	-3.746	63	24.1	59	2.510	0.376	1.57E+05	6.44E+04
PI-5I-L-2-CI-6	1-1 min 10 sec	10 sec	-1.755	48	11.6	46	2.510	0.376	1.22E+05	3.11E+04
PI-5I-L-2-CI-7	1-1 min 10 sec	10 sec	-4.718	82	13.9	80	2.510	0.376	2.13E+05	3.76E+04
PI-5I-L-2-CI-8	1-1 min 10 sec	10 sec	-4.894	112	11.1	110	2.510	0.376	2.93E+05	3.09E+04
PI-5I-L-2-CI-9	1-1 min 10 sec	10 sec	0.100	75	13.2	66	2.510	0.376	1.76E+05	3.58E+04
PI-5I-L-3-CI-1	3-3 min 10 sec	10 sec	1.435	80	15.2	15	2.584	0.431	3.48E+04	4.55E+04
PI-5I-L-3-CI-2	3-3 min 10 sec	10 sec	-0.968	11	5.5	1	2.584	0.431	2.32E+03	1.76E+04
PI-5I-L-3-CI-3	3-3 min 10 sec	10 sec	-2.331	20	5.3	18	2.584	0.431	4.18E+04	1.25E+04
PI-5I-L-3-CI-4	3-3 min 10 sec	10 sec	-0.677	31	11.5	29	2.584	0.431	6.73E+04	2.69E+04
PI-5I-L-3-CI-5	3-3 min 10 sec	10 sec	-1.781	54	20.9	50	2.584	0.431	1.16E+05	4.88E+04
PI-5I-L-3-CI-6	3-3 min 10 sec	10 sec	-3.008	44	10.6	42	2.584	0.431	9.74E+04	2.48E+04
PI-5I-L-3-CI-7	3-3 min 10 sec	10 sec	-0.279	47	8.4	45	2.584	0.431	1.04E+05	1.99E+04
PI-5I-L-3-CI-8	3-3 min 10 sec	10 sec	-3.091	44	5.0	42	2.584	0.431	9.74E+04	1.21E+04
PI-5I-L-3-CI-9	3-3 min 10 sec	10 sec	1.388	29	5.3	20	2.584	0.431	4.64E+04	1.31E+04
PI-5I-L-4-CI-1	7-7.5 min	30 sec	2.158	58	11.2	-7	2.556	1.278	-5.48E+03	1.31E+04
PI-5I-L-4-CI-2	7-7.5 min	30 sec	-4.462	9	4.7	-1	2.556	1.278	-7.82E+02	5.48E+03
PI-5I-L-4-CI-3	7-7.5 min	30 sec	-3.961	5	1.8	3	2.556	1.278	2.35E+03	1.58E+03
PI-5I-L-4-CI-4	7-7.5 min	30 sec	-2.020	20	7.6	18	2.556	1.278	1.41E+04	6.02E+03
PI-5I-L-4-CI-5	7-7.5 min	30 sec	-6.048	24	9.5	20	2.556	1.278	1.56E+04	7.55E+03
PI-5I-L-4-CI-6	7-7.5 min	30 sec	-1.075	33	8.2	31	2.556	1.278	2.43E+04	6.49E+03
PI-5I-L-4-CI-7	7-7.5 min	30 sec	-2.349	25	5.1	23	2.556	1.278	1.80E+04	4.10E+03
PI-5I-L-4-CI-8	7-7.5 min	30 sec	-2.800	29	3.5	27	2.556	1.278	2.11E+04	2.86E+03
PI-5I-L-4-CI-9	7-7.5 min	30 sec	0.402	18	3.4	9	2.556	1.278	7.04E+03	3.02E+03
PI-5I-L-5-CI-1	15-16 min	1 min	0.703	50	9.7	-15	2.579	2.579	-5.82E+03	6.11E+03
PI-5I-L-5-CI-2	15-16 min	1 min	-5.745	15	7.3	5	2.579	2.579	1.94E+03	3.48E+03
PI-5I-L-5-CI-3	15-16 min	1 min	-2.077	9	2.6	7	2.579	2.579	2.71E+03	1.07E+03
PI-5I-L-5-CI-4	15-16 min	1 min	-0.653	14	5.6	12	2.579	2.579	4.65E+03	2.22E+03
PI-5I-L-5-CI-5	15-16 min	1 min	-2.718	18	7.1	14	2.579	2.579	5.43E+03	2.83E+03
PI-5I-L-5-CI-6	15-16 min	1 min	-3.613	26	6.5	24	2.579	2.579	9.31E+03	2.55E+03

Table A.23 (cont'd). Phase I, Shot 5, Loader

Sample ID	Collection Interval	Elapsed Time	Total Mass (mg)	Calculated U (μg)	DU Mass ± 1σ (μg)	Net DU Mass (μg)	Flow Rate (Lpm)	Volume (L)	DU Conc. (μg/m^3)	DU Conc. ± 1σ (μg/m^3)
PI-5I-L-5-CI-7	15-16 min	1 min	-4.146	19	3.8	17	2.579	2.579	6.59E+03	1.54E+03
PI-5I-L-5-CI-8	15-16 min	1 min	-4.255	27	3.4	25	2.579	2.579	9.69E+03	1.38E+03
PI-5I-L-5-CI-9	15-16 min	1 min	-0.516	26	4.9	17	2.579	2.579	6.59E+03	2.03E+03
PI-5I-L-6-CI-1	31-33 min	2 min	1.472	17	3.7	-48	2.539	5.079	-9.45E+03	2.56E+03
PI-5I-L-6-CI-2	31-33 min	2 min	-2.152	6	3.1	-4	2.539	5.079	-7.88E+02	1.19E+03
PI-5I-L-6-CI-3	31-33 min	2 min	-0.135	4	1.6	2	2.539	5.079	3.94E+02	3.62E+02
PI-5I-L-6-CI-4	31-33 min	2 min	-2.559	15	5.7	13	2.539	5.079	2.56E+03	1.15E+03
PI-5I-L-6-CI-5	31-33 min	2 min	-1.701	29	11.2	25	2.539	5.079	4.92E+03	2.23E+03
PI-5I-L-6-CI-6	31-33 min	2 min	-2.427	33	8.0	31	2.539	5.079	6.10E+03	1.59E+03
PI-5I-L-6-CI-7	31-33 min	2 min	-3.781	29	5.1	27	2.539	5.079	5.32E+03	1.04E+03
PI-5I-L-6-CI-8	31-33 min	2 min	-1.325	34	4.2	32	2.539	5.079	6.30E+03	8.59E+02
PI-5I-L-6-CI-9	31-33 min	2 min	0.608	48	8.5	39	2.539	5.079	7.68E+03	1.73E+03
PI-5I-L-7-CI-1	61-65 min	4 min	0.706	86	16.1	21	2.402	9.610	2.19E+03	2.12E+03
PI-5I-L-7-CI-2	61-65 min	4 min	-2.059	11	5.4	1	2.402	9.610	1.04E+02	7.80E+02
PI-5I-L-7-CI-3	61-65 min	4 min	-6.054	5	1.7	3	2.402	9.610	3.12E+02	2.00E+02
PI-5I-L-7-CI-4	61-65 min	4 min	-2.433	22	8.2	20	2.402	9.610	2.08E+03	8.63E+02
PI-5I-L-7-CI-5	61-65 min	4 min	-5.616	52	19.8	48	2.402	9.610	4.99E+03	2.07E+03
PI-5I-L-7-CI-6	61-65 min	4 min	-1.694	39	9.5	37	2.402	9.610	3.85E+03	9.99E+02
PI-5I-L-7-CI-7	61-65 min	4 min	-5.815	31	5.8	29	2.402	9.610	3.02E+03	6.19E+02
PI-5I-L-7-CI-8	61-65 min	4 min	-1.986	63	6.7	61	2.402	9.610	6.35E+03	7.26E+02
PI-5I-L-7-CI-9	61-65 min	4 min	-0.182	64	11.4	55	2.402	9.610	5.72E+03	1.21E+03
PI-5I-L-8-CI-1	121-129 min	8 min	0.660	71	13.4	6	2.545	20.364	2.95E+02	8.97E+02
PI-5I-L-8-CI-2	121-129 min	8 min	-5.242	8	3.9	-2	2.545	20.364	-9.82E+01	3.19E+02
PI-5I-L-8-CI-3	121-129 min	8 min	-1.626	7	2.1	5	2.545	20.364	2.46E+02	1.12E+02
PI-5I-L-8-CI-4	121-129 min	8 min	-2.979	11	4.5	9	2.545	20.364	4.42E+02	2.28E+02
PI-5I-L-8-CI-5	121-129 min	8 min	-7.907	83	31.5	79	2.545	20.364	3.88E+03	1.55E+03
PI-5I-L-8-CI-6	121-129 min	8 min	-3.252	46	11.1	44	2.545	20.364	2.16E+03	5.50E+02
PI-5I-L-8-CI-7	121-129 min	8 min	-5.230	61	10.6	59	2.545	20.364	2.90E+03	5.30E+02
PI-5I-L-8-CI-8	121-129 min	8 min	-3.741	73	7.6	71	2.545	20.364	3.49E+03	3.89E+02
PI-5I-L-8-CI-9	121-129 min	8 min	0.890	65	11.7	56	2.545	20.364	2.75E+03	5.87E+02
PI-5I-L-9-CI-1	144-148 min	4 min	1.600	114	21.5	49	2.510	10.040	4.88E+03	2.48E+03
PI-5I-L-9-CI-2	144-148 min	4 min	-1.494	12	6.0	2	2.510	10.040	1.99E+02	7.91E+02
PI-5I-L-9-CI-3	144-148 min	4 min	-0.279	6	1.7	4	2.510	10.040	3.98E+02	1.92E+02
PI-5I-L-9-CI-4	144-148 min	4 min	-4.491	6	2.7	4	2.510	10.040	3.98E+02	2.91E+02
PI-5I-L-9-CI-5	144-148 min	4 min	0.511	20	8.1	16	2.510	10.040	1.59E+03	8.24E+02
PI-5I-L-9-CI-6	144-148 min	4 min	-2.016	25	6.3	23	2.510	10.040	2.29E+03	6.36E+02
PI-5I-L-9-CI-7	144-148 min	4 min	-1.638	18	3.7	16	2.510	10.040	1.59E+03	3.85E+02
PI-5I-L-9-CI-8	144-148 min	4 min	-2.670	34	4.1	32	2.510	10.040	3.19E+03	4.25E+02
PI-5I-L-9-CI-9	144-148 min	4 min	1.343	27	4.9	18	2.510	10.040	1.79E+03	5.23E+02

(a) DU mass based on ICP-MS results; no analytical uncertainty was reported.

Table A.24. PI-6 Cascade Impactor Substrates—Mass, Volume, and Concentration

Sample ID	Collection Interval	Elapsed Time	Total Mass (mg)	Calculated U (μg)	DU Mass ± 1σ (μg)	Net DU Mass (μg)	Flow Rate (Lpm)	Volume (L)	DU Conc. (μg/m^3)	DU Conc. ± 1σ (μg/m^3)
PI-6I-C-1-CI-1	0-10 sec	10 sec	2.386	1068	142.4	755	2.660	0.443	1.70E+06	3.39E+05
PI-6I-C-1-CI-2	0-10 sec	10 sec	-0.355	210	82.9	179	2.660	0.443	4.04E+05	1.90E+05
PI-6I-C-1-CI-3	0-10 sec	10 sec	0.213	229	42.0	219	2.660	0.443	4.94E+05	9.61E+04
PI-6I-C-1-CI-4	0-10 sec	10 sec	0.564	380	99.1	373	2.660	0.443	8.42E+05	2.25E+05
PI-6I-C-1-CI-5	0-10 sec	10 sec	0.119	385	149.0	369	2.660	0.443	8.33E+05	3.38E+05
PI-6I-C-1-CI-6	0-10 sec	10 sec	-0.128	207	89.1	195	2.660	0.443	4.40E+05	2.02E+05
PI-6I-C-1-CI-7	0-10 sec	10 sec	0.199	174	42.4	162	2.660	0.443	3.66E+05	9.66E+04
PI-6I-C-1-CI-8	0-10 sec	10 sec	-0.099	284	70.6	263	2.660	0.443	5.94E+05	1.61E+05
PI-6I-C-1-CI-9	0-10 sec	10 sec	1.184	486	161.1	463	2.660	0.443	1.05E+06	3.65E+05
PI-6I-C-2-CI-1	1-1 min 10 sec	10 sec	0.994	236	31.8	-77	2.628	0.438	-1.76E+05	1.20E+05
PI-6I-C-2-CI-2	1-1 min 10 sec	10 sec	-1.681	93	36.8	62	2.628	0.438	1.42E+05	8.87E+04
PI-6I-C-2-CI-3	1-1 min 10 sec	10 sec	-0.221	124	22.9	114	2.628	0.438	2.60E+05	5.31E+04
PI-6I-C-2-CI-4	1-1 min 10 sec	10 sec	-0.216	82	21.6	75	2.628	0.438	1.71E+05	4.98E+04
PI-6I-C-2-CI-5	1-1 min 10 sec	10 sec	-0.271	176	68.2	160	2.628	0.438	3.65E+05	1.57E+05
PI-6I-C-2-CI-6	1-1 min 10 sec	10 sec	-0.260	84	37.4	72	2.628	0.438	1.64E+05	8.64E+04
PI-6I-C-2-CI-7	1-1 min 10 sec	10 sec	-0.797	112	27.7	100	2.628	0.438	2.28E+05	6.41E+04
PI-6I-C-2-CI-8	1-1 min 10 sec	10 sec	0.011	162	41.8	141	2.628	0.438	3.22E+05	9.69E+04
PI-6I-C-2-CI-9	1-1 min 10 sec	10 sec	0.040	83	29.3	60	2.628	0.438	1.37E+05	6.93E+04
PI-6I-C-3-CI-1	3-3 min 10 sec	10 sec	0.806	55	7.8	-258	2.620	0.437	-5.90E+05	9.91E+04
PI-6I-C-3-CI-2	3-3 min 10 sec	10 sec	-1.703	11	4.4	-20	2.620	0.437	-4.58E+04	2.99E+04
PI-6I-C-3-CI-3	3-3 min 10 sec	10 sec	-0.458	29	5.7	19	2.620	0.437	4.35E+04	1.40E+04
PI-6I-C-3-CI-4	3-3 min 10 sec	10 sec	0.303	53	14.2	46	2.620	0.437	1.05E+05	3.30E+04
PI-6I-C-3-CI-5	3-3 min 10 sec	10 sec	-2.238	89	34.8	73	2.620	0.437	1.67E+05	8.11E+04
PI-6I-C-3-CI-6	3-3 min 10 sec	10 sec	-0.926	77	33.8	65	2.620	0.437	1.49E+05	7.84E+04
PI-6I-C-3-CI-7	3-3 min 10 sec	10 sec	-1.135	54	14.9	42	2.620	0.437	9.61E+04	3.51E+04
PI-6I-C-3-CI-8	3-3 min 10 sec	10 sec	0.273	122	31.1	101	2.620	0.437	2.31E+05	7.28E+04
PI-6I-C-3-CI-9	3-3 min 10 sec	10 sec	0.494	46	16.0	23	2.620	0.437	5.26E+04	4.08E+04
PI-6I-C-4-CI-1	7-7.5 min	30 sec	0.829	86	11.9	-227	2.452	1.226	-1.85E+05	3.60E+04
PI-6I-C-4-CI-2	7-7.5 min	30 sec	0.159	9	4.0	-22	2.452	1.226	-1.79E+04	1.06E+04
PI-6I-C-4-CI-3	7-7.5 min	30 sec	-2.255	9.7	2.3	-0.3	2.452	1.226	-2.45E+02	2.60E+03
PI-6I-C-4-CI-4	7-7.5 min	30 sec	-0.141	19	5.4	12	2.452	1.226	9.79E+03	4.74E+03
PI-6I-C-4-CI-5	7-7.5 min	30 sec	-1.756	64	25.0	48	2.452	1.226	3.92E+04	2.11E+04
PI-6I-C-4-CI-6	7-7.5 min	30 sec	-0.595	54	23.9	42	2.452	1.226	3.43E+04	2.00E+04
PI-6I-C-4-CI-7	7-7.5 min	30 sec	-0.825	65	16.2	53	2.452	1.226	4.32E+04	1.36E+04
PI-6I-C-4-CI-8	7-7.5 min	30 sec	-0.316	58	17.2	37	2.452	1.226	3.02E+04	1.49E+04
PI-6I-C-4-CI-9	7-7.5 min	30 sec	0.544	44	15.4	21	2.452	1.226	1.71E+04	1.41E+04
PI-6I-C-5-CI-1	15-16 min	1 min	0.748	143	19.4	-170	2.441	2.441	-6.96E+04	1.90E+04
PI-6I-C-5-CI-2	15-16 min	1 min	-1.498	20	8.2	-11	2.441	2.441	-4.51E+03	6.06E+03
PI-6I-C-5-CI-3	15-16 min	1 min	-1.041	8	1.8	-2	2.441	2.441	-8.19E+02	1.16E+03
PI-6I-C-5-CI-4	15-16 min	1 min	-1.153	12	3.5	5	2.441	2.441	2.05E+03	1.67E+03
PI-6I-C-5-CI-5	15-16 min	1 min	-0.576	38	15.1	22	2.441	2.441	9.01E+03	6.71E+03
PI-6I-C-5-CI-6	15-16 min	1 min	-1.413	40	17.8	28	2.441	2.441	1.15E+04	7.62E+03
PI-6I-C-5-CI-7	15-16 min	1 min	-0.644	20	6.3	8	2.441	2.441	3.28E+03	2.93E+03

Table A.24 (cont'd). Phase I, Shot 6, Commander

Sample ID	Collection Interval	Elapsed Time	Total Mass (mg)	Calculated U (μg)	DU Mass ± 1σ (μg)	Net DU Mass (μg)	Flow Rate (Lpm)	Volume (L)	DU Conc. (μg/m^3)	DU Conc. ± 1σ (μg/m^3)
PI-6I-C-5-CI-8	15-16 min	1 min	0.127	59	15.6	38	2.441	2.441	1.56E+04	6.85E+03
PI-6I-C-5-CI-9	15-16 min	1 min	0.144	22	8.2	-1	2.441	2.441	-4.10E+02	4.64E+03
PI-6I-C-6-CI-1	31-33 min	2 min	0.309	368	49.3	55	2.421	4.843	1.14E+04	1.34E+04
PI-6I-C-6-CI-2	31-33 min	2 min	-0.668	9	3.9	-22	2.421	4.843	-4.54E+03	2.67E+03
PI-6I-C-6-CI-3	31-33 min	2 min	-0.058	8	1.8	-2	2.421	4.843	-4.13E+02	5.87E+02
PI-6I-C-6-CI-4	31-33 min	2 min	-0.129	14	3.9	7	2.421	4.843	1.45E+03	9.16E+02
PI-6I-C-6-CI-5	31-33 min	2 min	-0.472	11	4.4	-5	2.421	4.843	-1.03E+03	1.59E+03
PI-6I-C-6-CI-6	31-33 min	2 min	0.015	16	7.2	4	2.421	4.843	8.26E+02	1.85E+03
PI-6I-C-6-CI-7	31-33 min	2 min	0.060	40	10.6	28	2.421	4.843	5.78E+03	2.31E+03
PI-6I-C-6-CI-8	31-33 min	2 min	0.161	31	8.5	10	2.421	4.843	2.06E+03	2.14E+03
PI-6I-C-6-CI-9	31-33 min	2 min	0.134	82	27.3	59	2.421	4.843	1.22E+04	5.87E+03
PI-6I-C-7-CI-1	61-65 min	4 min	1.214	460	61.3	147	2.602	10.409	1.41E+04	7.15E+03
PI-6I-C-7-CI-2	61-65 min	4 min	-0.437	14	5.9	-17	2.602	10.409	-1.63E+03	1.31E+03
PI-6I-C-7-CI-3	61-65 min	4 min	0.078	4	1.3	-6	2.602	10.409	-5.76E+02	2.46E+02
PI-6I-C-7-CI-4	61-65 min	4 min	-0.030	13	3.9	6	2.602	10.409	5.76E+02	4.26E+02
PI-6I-C-7-CI-5	61-65 min	4 min	-0.155	46	18.0	30	2.602	10.409	2.88E+03	1.83E+03
PI-6I-C-7-CI-6	61-65 min	4 min	-0.214	67	29.9	55	2.602	10.409	5.28E+03	2.92E+03
PI-6I-C-7-CI-7	61-65 min	4 min	-0.734	23	7.1	11	2.602	10.409	1.06E+03	7.57E+02
PI-6I-C-7-CI-8	61-65 min	4 min	0.285	55	16.4	34	2.602	10.409	3.27E+03	1.68E+03
PI-6I-C-7-CI-9	61-65 min	4 min	0.320	73	26.5	50	2.602	10.409	4.80E+03	2.66E+03
PI-6I-C-8-CI-1	121-129 min	8 min	0.822	409	54.6	96	2.497	19.973	4.81E+03	3.45E+03
PI-6I-C-8-CI-2	121-129 min	8 min	-0.712	16	6.5	-15	2.497	19.973	-7.51E+02	6.97E+02
PI-6I-C-8-CI-3	121-129 min	8 min	-0.139	4	1.1	-6	2.497	19.973	-3.00E+02	1.23E+02
PI-6I-C-8-CI-4	121-129 min	8 min	-0.296	13	3.8	6	2.497	19.973	3.00E+02	2.18E+02
PI-6I-C-8-CI-5	121-129 min	8 min	-0.448	46	18.2	30	2.497	19.973	1.50E+03	9.65E+02
PI-6I-C-8-CI-6	121-129 min	8 min	0.054	65	28.8	53	2.497	19.973	2.65E+03	1.47E+03
PI-6I-C-8-CI-7	121-129 min	8 min	-0.478	30	9.2	18	2.497	19.973	9.01E+02	4.92E+02
PI-6I-C-8-CI-8	121-129 min	8 min	-0.110	115	29.6	94	2.497	19.973	4.71E+03	1.52E+03
PI-6I-C-8-CI-9	121-129 min	8 min	0.912	102	35.9	79	2.497	19.973	3.96E+03	1.84E+03
PI-6I-C-9-CI-1	Field Blank	--	0.751	313	41.9	--	--	--	--	--
PI-6I-C-9-CI-2	Field Blank	--	-0.499	31	12.3	--	--	--	--	--
PI-6I-C-9-CI-3	Field Blank	--	-0.583	10	2.2	--	--	--	--	--
PI-6I-C-9-CI-4	Field Blank	--	0.059	7	2.1	--	--	--	--	--
PI-6I-C-9-CI-5	Field Blank	--	-0.504	16	6.3	--	--	--	--	--
PI-6I-C-9-CI-6	Field Blank	--	-0.521	12	5.3	--	--	--	--	--
PI-6I-C-9-CI-7	Field Blank	--	-0.065	12	3.4	--	--	--	--	--
PI-6I-C-9-CI-8	Field Blank	--	-0.419	21	5.9	--	--	--	--	--
PI-6I-C-9-CI-9	Field Blank	--	0.821	23	7.8	--	--	--	--	--

Table A.24 (cont'd). Phase I, Shot 6, Driver

Sample ID	Collection Interval	Elapsed Time	Total Mass (mg)	Calculated U (μg)	DU Mass ± 1σ (μg)	Net DU Mass (μg)	Flow Rate (Lpm)	Volume (L)	DU Conc. (μg/m^3)	DU Conc. ± 1σ (μg/m^3)
PI-6I-D-1-CI-1	0-10 sec	10 sec	1.578	37	7.3	-13	2.710	0.452	-2.88E+04	2.69E+04
PI-6I-D-1-CI-2	0-10 sec	10 sec	-1.344	5	2.7	3	2.710	0.452	6.64E+03	7.06E+03
PI-6I-D-1-CI-3	0-10 sec	10 sec	-0.409	3.9	1.4	-0.1	2.710	0.452	-2.21E+02	4.38E+03
PI-6I-D-1-CI-4	0-10 sec	10 sec	-1.250	21	NA[(a)]	16	2.710	0.452	3.54E+04	NA[(a)]
PI-6I-D-1-CI-5	0-10 sec	10 sec	-0.200	4	2.2	2	2.710	0.452	4.42E+03	5.77E+03
PI-6I-D-1-CI-6	0-10 sec	10 sec	-0.521	3	1.4	-1	2.710	0.452	-2.21E+03	4.54E+03
PI-6I-D-1-CI-7	0-10 sec	10 sec	-1.035	4	1.6	2	2.710	0.452	4.42E+03	5.33E+03
PI-6I-D-1-CI-8	0-10 sec	10 sec	-0.042	11	1.9	8	2.710	0.452	1.77E+04	5.12E+03
PI-6I-D-1-CI-9	0-10 sec	10 sec	0.192	4	1.5	-4	2.710	0.452	-8.85E+03	5.54E+03
PI-6I-D-2-CI-1	1-1 min 10 sec	10 sec	1.019	21	4.6	-29	2.452	0.409	-7.09E+04	2.63E+04
PI-6I-D-2-CI-2	1-1 min 10 sec	10 sec	-0.482	21	10.1	19	2.452	0.409	4.65E+04	2.51E+04
PI-6I-D-2-CI-3	1-1 min 10 sec	10 sec	-0.330	84	21.4	80	2.452	0.409	1.96E+05	5.28E+04
PI-6I-D-2-CI-4	1-1 min 10 sec	10 sec	-0.100	75	27.5	70	2.452	0.409	1.71E+05	6.77E+04
PI-6I-D-2-CI-5	1-1 min 10 sec	10 sec	0.101	66	25.2	64	2.452	0.409	1.56E+05	6.19E+04
PI-6I-D-2-CI-6	1-1 min 10 sec	10 sec	-0.512	75	18.3	71	2.452	0.409	1.74E+05	4.52E+04
PI-6I-D-2-CI-7	1-1 min 10 sec	10 sec	-0.852	73	12.8	71	2.452	0.409	1.74E+05	3.20E+04
PI-6I-D-2-CI-8	1-1 min 10 sec	10 sec	-0.815	99	10.3	96	2.452	0.409	2.35E+05	2.63E+04
PI-6I-D-2-CI-9	1-1 min 10 sec	10 sec	-0.511	80	14.2	72	2.452	0.409	1.76E+05	3.55E+04
PI-6I-D-3-CI-1	3-3 min 10 sec	10 sec	1.315	68	13.1	18	2.678	0.446	4.04E+04	3.66E+04
PI-6I-D-3-CI-2	3-3 min 10 sec	10 sec	-1.274	8	4.3	6	2.678	0.446	1.35E+04	1.04E+04
PI-6I-D-3-CI-3	3-3 min 10 sec	10 sec	-1.168	26	7.0	22	2.678	0.446	4.93E+04	1.61E+04
PI-6I-D-3-CI-4	3-3 min 10 sec	10 sec	-0.917	41	15.1	36	2.678	0.446	8.07E+04	3.44E+04
PI-6I-D-3-CI-5	3-3 min 10 sec	10 sec	-1.047	115	NA[(a)]	113	2.678	0.446	2.53E+05	NA[(a)]
PI-6I-D-3-CI-6	3-3 min 10 sec	10 sec	-1.469	35	8.6	31	2.678	0.446	6.95E+04	1.97E+04
PI-6I-D-3-CI-7	3-3 min 10 sec	10 sec	-1.629	27	5.3	25	2.678	0.446	5.61E+04	1.27E+04
PI-6I-D-3-CI-8	3-3 min 10 sec	10 sec	-1.168	64	6.7	61	2.678	0.446	1.37E+05	1.58E+04
PI-6I-D-3-CI-9	3-3 min 10 sec	10 sec	-1.111	16	3.4	8	2.678	0.446	1.79E+04	8.86E+03
PI-6I-D-4-CI-1	7-7.5 min	30 sec	1.223	15	3.4	-35	2.862	1.431	-2.45E+04	7.22E+03
PI-6I-D-4-CI-2	7-7.5 min	30 sec	-3.761	13	6.4	11	2.862	1.431	7.69E+03	4.63E+03
PI-6I-D-4-CI-3	7-7.5 min	30 sec	-1.164	6	1.9	2	2.862	1.431	1.40E+03	1.65E+03
PI-6I-D-4-CI-4	7-7.5 min	30 sec	-0.872	8	3.4	3	2.862	1.431	2.10E+03	2.91E+03
PI-6I-D-4-CI-5	7-7.5 min	30 sec	-2.171	11	4.5	9	2.862	1.431	6.29E+03	3.30E+03
PI-6I-D-4-CI-6	7-7.5 min	30 sec	-0.313	13	3.6	9	2.862	1.431	6.29E+03	2.73E+03
PI-6I-D-4-CI-7	7-7.5 min	30 sec	-1.540	17	3.8	15	2.862	1.431	1.05E+04	2.96E+03
PI-6I-D-4-CI-8	7-7.5 min	30 sec	-1.284	13	2.6	10	2.862	1.431	6.99E+03	2.04E+03
PI-6I-D-4-CI-9	7-7.5 min	30 sec	-0.523	19	3.9	11	2.862	1.431	7.69E+03	3.07E+03
PI-6I-D-5-CI-1	15-16 min	1 min	0.727	9	2.5	-41	2.627	2.627	-1.56E+04	3.84E+03
PI-6I-D-5-CI-2	15-16 min	1 min	-0.383	7	3.8	5	2.627	2.627	1.90E+03	1.59E+03
PI-6I-D-5-CI-3	15-16 min	1 min	-0.772	5	1.9	1	2.627	2.627	3.81E+02	8.98E+02
PI-6I-D-5-CI-4	15-16 min	1 min	-0.297	8	3.3	3	2.627	2.627	1.14E+03	1.55E+03
PI-6I-D-5-CI-5	15-16 min	1 min	-1.387	10	4.6	8	2.627	2.627	3.05E+03	1.83E+03
PI-6I-D-5-CI-6	15-16 min	1 min	-0.678	11	3.2	7	2.627	2.627	2.66E+03	1.35E+03
PI-6I-D-5-CI-7	15-16 min	1 min	-0.570	13	3.1	11	2.627	2.627	4.19E+03	1.37E+03

Table A.24 (cont'd). Phase I, Shot 6, Driver

Sample ID	Collection Interval	Elapsed Time	Total Mass (mg)	Calculated U (μg)	DU Mass ± 1σ (μg)	Net DU Mass (μg)	Flow Rate (Lpm)	Volume (L)	DU Conc. (μg/m^3)	DU Conc. ± 1σ (μg/m^3)
PI-6I-D-5-CI-8	15-16 min	1 min	-1.030	25	3.4	22	2.627	2.627	8.37E+03	1.41E+03
PI-6I-D-5-CI-9	15-16 min	1 min	-1.001	33	6.3	25	2.627	2.627	9.52E+03	2.53E+03
PI-6I-D-6-CI-1	31-33 min	2 min	0.031	47	9.0	-3	2.583	5.165	-5.81E+02	2.56E+03
PI-6I-D-6-CI-2	31-33 min	2 min	-1.637	3	2.0	1	2.583	5.165	1.94E+02	5.08E+02
PI-6I-D-6-CI-3	31-33 min	2 min	-0.185	3	1.3	-1	2.583	5.165	-1.94E+02	3.70E+02
PI-6I-D-6-CI-4	31-33 min	2 min	-1.102	6	2.7	1	2.583	5.165	1.94E+02	6.99E+02
PI-6I-D-6-CI-5	31-33 min	2 min	0.153	15	6.2	13	2.583	5.165	2.52E+03	1.23E+03
PI-6I-D-6-CI-6	31-33 min	2 min	-0.953	19	5.1	15	2.583	5.165	2.90E+03	1.03E+03
PI-6I-D-6-CI-7	31-33 min	2 min	-2.936	27	5.0	25	2.583	5.165	4.84E+03	1.04E+03
PI-6I-D-6-CI-8	31-33 min	2 min	-1.040	24	3.6	21	2.583	5.165	4.07E+03	7.51E+02
PI-6I-D-6-CI-9	31-33 min	2 min	0.940	38	7.3	30	2.583	5.165	5.81E+03	1.48E+03
PI-6I-D-7-CI-1	61-65 min	4 min	0.537	55	10.8	5	2.477	9.907	5.05E+02	1.47E+03
PI-6I-D-7-CI-2	61-65 min	4 min	0.131	2.1	1.8	0.1	2.477	9.907	1.01E+01	2.50E+02
PI-6I-D-7-CI-3	61-65 min	4 min	0.642	6	2.0	2	2.477	9.907	2.02E+02	2.46E+02
PI-6I-D-7-CI-4	61-65 min	4 min	0.142	14	5.6	9	2.477	9.907	9.08E+02	6.16E+02
PI-6I-D-7-CI-5	61-65 min	4 min	-0.709	33	13.0	31	2.477	9.907	3.13E+03	1.32E+03
PI-6I-D-7-CI-6	61-65 min	4 min	0.455	23	5.9	19	2.477	9.907	1.92E+03	6.17E+02
PI-6I-D-7-CI-7	61-65 min	4 min	0.095	22	5.0	20	2.477	9.907	2.02E+03	5.40E+02
PI-6I-D-7-CI-8	61-65 min	4 min	0.131	50	5.9	47	2.477	9.907	4.74E+03	6.26E+02
PI-6I-D-7-CI-9	61-65 min	4 min	1.248	51	9.5	43	2.477	9.907	4.34E+03	9.89E+02
PI-6I-D-8-CI-1	121-129 min	8 min	0.631	53	10.3	3	2.705	21.642	1.39E+02	6.54E+02
PI-6I-D-8-CI-2	121-129 min	8 min	-0.626	7	3.6	5	2.705	21.642	2.31E+02	1.84E+02
PI-6I-D-8-CI-3	121-129 min	8 min	0.224	3	1.6	-1	2.705	21.642	-4.62E+01	9.82E+01
PI-6I-D-8-CI-4	121-129 min	8 min	-0.866	14	5.2	9	2.705	21.642	4.16E+02	2.65E+02
PI-6I-D-8-CI-5	121-129 min	8 min	-0.366	34	13.4	32	2.705	21.642	1.48E+03	6.24E+02
PI-6I-D-8-CI-6	121-129 min	8 min	-0.102	38	9.4	34	2.705	21.642	1.57E+03	4.42E+02
PI-6I-D-8-CI-7	121-129 min	8 min	-1.030	61	10.7	59	2.705	21.642	2.73E+03	5.08E+02
PI-6I-D-8-CI-8	121-129 min	8 min	0.234	87	9.1	84	2.705	21.642	3.88E+03	4.40E+02
PI-6I-D-8-CI-9	121-129 min	8 min	0.620	77	13.8	69	2.705	21.642	3.19E+03	6.51E+02
PI-6I-D-9-CI-1	Field Blank	--	0.656	50	9.7	--	--	--	--	--
PI-6I-D-9-CI-2	Field Blank	--	-0.026	2	1.7	--	--	--	--	--
PI-6I-D-9-CI-3	Field Blank	--	1.956	4	1.4	--	--	--	--	--
PI-6I-D-9-CI-4	Field Blank	--	0.706	5	2.4	--	--	--	--	--
PI-6I-D-9-CI-5	Field Blank	--	0.017	2	1.4	--	--	--	--	--
PI-6I-D-9-CI-6	Field Blank	--	0.326	4	1.5	--	--	--	--	--
PI-6I-D-9-CI-7	Field Blank	--	0.376	2	1.8	--	--	--	--	--
PI-6I-D-9-CI-8	Field Blank	--	0.281	3	1.3	--	--	--	--	--
PI-6I-D-9-CI-9	Field Blank	--	0.631	8	2.0	--	--	--	--	--

(a) DU mass based on ICP-MS results; no analytical uncertainty was reported.

Table A.24 (cont'd). Phase I, Shot 6, Loader

Sample ID	Collection Interval	Elapsed Time	Total Mass (mg)	Calculated U (μg)	DU Mass ± 1σ (μg)	Net DU Mass (μg)[(b)]	Flow Rate (Lpm)	Volume (L)	DU Conc. (μg/m^3)	DU Conc. ± 1σ (μg/m^3)
PI-6I-L-1-CI-1	0-20 min[(a)]	20 min	0.475	64	9.1	-16	2.451	49.017	-3.26E+02	2.16E+02
PI-6I-L-1-CI-2	0-20 min	20 min	-0.152	16	6.3	-1	2.451	49.017	-2.86E+01	1.58E+02
PI-6I-L-1-CI-3	0-20 min	20 min	0.055	17	3.4	13	2.451	49.017	2.61E+02	7.11E+01
PI-6I-L-1-CI-4	0-20 min	20 min	0.242	17	4.9	13	2.451	49.017	2.73E+02	1.01E+02
PI-6I-L-1-CI-5	0-20 min	20 min	0.117	41	16.7	33	2.451	49.017	6.65E+02	3.43E+02
PI-6I-L-1-CI-6	0-20 min	20 min	-0.244	44	22.5	36	2.451	49.017	7.34E+02	4.62E+02
PI-6I-L-1-CI-7	0-20 min	20 min	-0.064	21	6.9	18	2.451	49.017	3.59E+02	1.43E+02
PI-6I-L-1-CI-8	0-20 min	20 min	0.030	117	38.3	106	2.451	49.017	2.17E+03	7.86E+02
PI-6I-L-1-CI-9	0-20 min	20 min	0.019	38	16.9	27	2.451	49.017	5.51E+02	3.48E+02
PI-6I-L-2-CI-1	31-54 min	~23 min	0.732	131	17.8	51	2.497	56.561	9.02E+02	3.30E+02
PI-6I-L-2-CI-2	31-54 min	~23 min	0.077	23	9.4	6	2.497	56.561	9.90E+01	1.84E+02
PI-6I-L-2-CI-3	31-54 min	~23 min	0.655	22	4.4	18	2.497	56.561	3.15E+02	7.92E+01
PI-6I-L-2-CI-4	31-54 min	~23 min	0.170	31	8.3	27	2.497	56.561	4.84E+02	1.48E+02
PI-6I-L-2-CI-5	31-54 min	~23 min	-0.028	34	13.8	26	2.497	56.561	4.53E+02	2.46E+02
PI-6I-L-2-CI-6	31-54 min	~23 min	0.250	37	18.6	29	2.497	56.561	5.13E+02	3.32E+02
PI-6I-L-2-CI-7	31-54 min	~23 min	-0.097	21	7.0	18	2.497	56.561	3.11E+02	1.26E+02
PI-6I-L-2-CI-8	31-54 min	~23 min	0.197	53	20.1	42	2.497	56.561	7.50E+02	3.59E+02
PI-6I-L-2-CI-9	31-54 min	~23 min	0.534	42	17.4	31	2.497	56.561	5.48E+02	3.11E+02
PI-6I-L-3-CI-1	54-67 min	~13 min	0.357	72	10.0	-8	2.583	34.360	-2.33E+02	3.30E+02
PI-6I-L-3-CI-2	54-67 min	~13 min	-0.048	21	8.6	4	2.583	34.360	1.05E+02	2.82E+02
PI-6I-L-3-CI-3	54-67 min	~13 min	0.048	12	2.7	8	2.583	34.360	2.27E+02	8.12E+01
PI-6I-L-3-CI-4	54-67 min	~13 min	-0.088	19	5.1	15	2.583	34.360	4.48E+02	1.50E+02
PI-6I-L-3-CI-5	54-67 min	~13 min	-0.014	36	14.7	28	2.583	34.360	8.03E+02	4.32E+02
PI-6I-L-3-CI-6	54-67 min	~13 min	0.005	102	50.2	94	2.583	34.360	2.74E+03	1.47E+03
PI-6I-L-3-CI-7	54-67 min	~13 min	-1.047	36	10.2	33	2.583	34.360	9.49E+02	3.00E+02
PI-6I-L-3-CI-8	54-67 min	~13 min	0.026	110	35.3	99	2.583	34.360	2.89E+03	1.03E+03
PI-6I-L-3-CI-9	54-67 min	~13 min	0.094	74	29.1	63	2.583	34.360	1.83E+03	8.51E+02
PI-6I-L-4-CI-1	67-82 min	~15 min	0.229	77	10.7	-3	2.483	36.587	-8.20E+01	3.27E+02
PI-6I-L-4-CI-2	67-82 min	~15 min	-0.085	11	4.7	-6	2.483	36.587	-1.75E+02	1.78E+02
PI-6I-L-4-CI-3	67-82 min	~15 min	-0.268	11	2.3	7	2.483	36.587	1.86E+02	6.56E+01
PI-6I-L-4-CI-4	67-82 min	~15 min	-0.050	14	4.0	10	2.483	36.587	2.84E+02	1.11E+02
PI-6I-L-4-CI-5	67-82 min	~15 min	0.434	34	13.8	26	2.483	36.587	7.00E+02	3.81E+02
PI-6I-L-4-CI-6	67-82 min	~15 min	0.042	56	27.6	48	2.483	36.587	1.31E+03	7.58E+02
PI-6I-L-4-CI-7	67-82 min	~15 min	-0.061	38	10.4	35	2.483	36.587	9.46E+02	2.87E+02
PI-6I-L-4-CI-8	67-82 min	~15 min	0.061	100	31.3	89	2.483	36.587	2.44E+03	8.61E+02
PI-6I-L-4-CI-9	67-82 min	~15 min	1.054	62	24.5	51	2.483	36.587	1.39E+03	6.74E+02
PI-6I-L-5-CI-1	82-104 min	~22 min	0.316	90	12.4	10	2.538	55.035	1.82E+02	2.46E+02
PI-6I-L-5-CI-2	82-104 min	~22 min	-0.155	34	13.6	17	2.538	55.035	3.02E+02	2.60E+02
PI-6I-L-5-CI-3	82-104 min	~22 min	-0.377	21	4.2	17	2.538	55.035	3.05E+02	7.78E+01
PI-6I-L-5-CI-4	82-104 min	~22 min	0.158	23	6.2	19	2.538	55.035	3.53E+02	1.14E+02
PI-6I-L-5-CI-5	82-104 min	~22 min	-0.320	29	12.1	21	2.538	55.035	3.74E+02	2.23E+02
PI-6I-L-5-CI-6	82-104 min	~22 min	-0.377	43	21.4	35	2.538	55.035	6.36E+02	3.92E+02
PI-6I-L-5-CI-7	82-104 min	~22 min	0.241	21	6.4	18	2.538	55.035	3.20E+02	1.19E+02

Table A.24 (cont'd). Phase I, Shot 6, Loader

Sample ID	Collection Interval	Elapsed Time	Total Mass (mg)	Calculated U (μg)	DU Mass ± 1σ (μg)	Net DU Mass (μg)	Flow Rate (Lpm)	Volume (L)	DU Conc. (μg/m^3)	DU Conc. ± 1σ (μg/m^3)
PI-6I-L-5-CI-8	82-104 min	~22 min	-0.141	28	10.1	17	2.538	55.035	3.16E+02	1.89E+02
PI-6I-L-5-CI-9	82-104 min	~22 min	0.218	28	12.0	17	2.538	55.035	3.09E+02	2.22E+02
PI-6I-L-6-CI-1	105-107 min	2 min	0.302	48	6.7	-32	2.515	5.030	-6.36E+03	1.72E+03
PI-6I-L-6-CI-2	105-107 min	2 min	-0.085	6	2.6	-11	2.515	5.030	-2.27E+03	1.03E+03
PI-6I-L-6-CI-3	105-107 min	2 min	0.145	10	2.3	6	2.515	5.030	1.15E+03	4.77E+02
PI-6I-L-6-CI-4	105-107 min	2 min	1.062	16	4.3	12	2.515	5.030	2.47E+03	8.70E+02
PI-6I-L-6-CI-5	105-107 min	2 min	-0.256	22	9.0	14	2.515	5.030	2.70E+03	1.83E+03
PI-6I-L-6-CI-6	105-107 min	2 min	0.269	37	18.3	29	2.515	5.030	5.77E+03	3.68E+03
PI-6I-L-6-CI-7	105-107 min	2 min	0.004	17	5.4	14	2.515	5.030	2.70E+03	1.10E+03
PI-6I-L-6-CI-8	105-107 min	2 min	-0.034	50	17.2	39	2.515	5.030	7.83E+03	3.46E+03
PI-6I-L-6-CI-9	105-107 min	2 min	0.084	34	14.8	23	2.515	5.030	4.57E+03	2.98E+03
PI-6I-L-7-CI-1	107-111 min	4 min	0.426	59	8.2	-21	2.330	9.320	-2.25E+03	1.05E+03
PI-6I-L-7-CI-2	107-111 min	4 min	-0.145	8	3.3	-9	2.330	9.320	-1.01E+03	5.98E+02
PI-6I-L-7-CI-3	107-111 min	4 min	-0.403	8	2.0	4	2.330	9.320	4.08E+02	2.26E+02
PI-6I-L-7-CI-4	107-111 min	4 min	0.247	11	3.1	7	2.330	9.320	7.94E+02	3.42E+02
PI-6I-L-7-CI-5	107-111 min	4 min	0.287	30	12.3	22	2.330	9.320	2.32E+03	1.34E+03
PI-6I-L-7-CI-6	107-111 min	4 min	0.455	23	11.2	15	2.330	9.320	1.61E+03	1.23E+03
PI-6I-L-7-CI-7	107-111 min	4 min	-0.891	17	5.3	14	2.330	9.320	1.46E+03	5.84E+02
PI-6I-L-7-CI-8	107-111 min	4 min	0.015	44	14.1	33	2.330	9.320	3.58E+03	1.54E+03
PI-6I-L-7-CI-9	107-111 min	4 min	0.290	64	23.7	53	2.330	9.320	5.69E+03	2.56E+03
PI-6I-L-8-CI-1	111-119 min	8 min	1.734	50	7.2	-30	2.505	20.042	-1.50E+03	4.50E+02
PI-6I-L-8-CI-2	111-119 min	8 min	0.028	19	7.5	2	2.505	20.042	7.98E+01	4.36E+02
PI-6I-L-8-CI-3	111-119 min	8 min	0.411	16	3.2	12	2.505	20.042	5.89E+02	1.64E+02
PI-6I-L-8-CI-4	111-119 min	8 min	0.095	14	3.9	10	2.505	20.042	5.19E+02	1.98E+02
PI-6I-L-8-CI-5	111-119 min	8 min	0.057	29	12.0	21	2.505	20.042	1.03E+03	6.06E+02
PI-6I-L-8-CI-6	111-119 min	8 min	0.127	27	13.2	19	2.505	20.042	9.48E+02	6.71E+02
PI-6I-L-8-CI-7	111-119 min	8 min	0.138	17	5.3	14	2.505	20.042	6.79E+02	2.71E+02
PI-6I-L-8-CI-8	111-119 min	8 min	0.124	60	18.4	49	2.505	20.042	2.46E+03	9.29E+02
PI-6I-L-8-CI-9	111-119 min	8 min	0.957	61	22.5	50	2.505	20.042	2.49E+03	1.13E+03
PI-6I-L-9-CI-1	119-135 min	16 min	0.828	135	18.5	55	2.467	39.466	1.39E+03	4.90E+02
PI-6I-L-9-CI-2	119-135 min	16 min	0.010	29	11.7	12	2.467	39.466	2.94E+02	3.18E+02
PI-6I-L-9-CI-3	119-135 min	16 min	-0.686	23	4.5	19	2.467	39.466	4.76E+02	1.16E+02
PI-6I-L-9-CI-4	119-135 min	16 min	-0.223	16	4.5	12	2.467	39.466	3.14E+02	1.16E+02
PI-6I-L-9-CI-5	119-135 min	16 min	1.206	31	12.4	23	2.467	39.466	5.73E+02	3.18E+02
PI-6I-L-9-CI-6	119-135 min	16 min	-0.171	49	23.3	41	2.467	39.466	1.04E+03	5.95E+02
PI-6I-L-9-CI-7	119-135 min	16 min	-0.512	22	6.7	19	2.467	39.466	4.71E+02	1.73E+02
PI-6I-L-9-CI-8	119-135 min	16 min	0.439	46	15.4	35	2.467	39.466	8.97E+02	3.96E+02
PI-6I-L-9-CI-9	119-135 min	16 min	0.594	52	19.7	41	2.467	39.466	1.04E+03	5.03E+02

(a) Loader's position sampling began at 2 h and 35 min (represented in column as zero) post-shot for resuspension evaluation.
(b) Field blanks from PI-7 Loader were subtracted from PI-6 Loader data.

Table A.25. PI-7 Cascade Impactor Substrates—Mass, Volume, and Concentration

Sample ID	Collection Interval	Elapsed Time	Total Mass (mg)	Calculated U (μg)	DU Mass ± 1σ (μg)	Net DU Mass (μg)	Flow Rate (Lpm)	Volume (L)	DU Conc. (μg/m^3)	DU Conc. ± 1σ (μg/m^3)
PI-7I-C-1-CI-1	0-10 sec	10 sec	2.250	978	130.3	517	2.671	0.445	1.16E+06	3.26E+05
PI-7I-C-1-CI-2	0-10 sec	10 sec	-0.560	274	107.7	227	2.671	0.445	5.10E+05	2.46E+05
PI-7I-C-1-CI-3	0-10 sec	10 sec	-2.306	363	66.2	355	2.671	0.445	7.98E+05	1.51E+05
PI-7I-C-1-CI-4	0-10 sec	10 sec	-1.001	263	68.6	258	2.671	0.445	5.80E+05	1.55E+05
PI-7I-C-1-CI-5	0-10 sec	10 sec	-0.553	424	164.0	417	2.671	0.445	9.37E+05	3.70E+05
PI-7I-C-1-CI-6	0-10 sec	10 sec	-0.346	430	183.2	418	2.671	0.445	9.39E+05	4.13E+05
PI-7I-C-1-CI-7	0-10 sec	10 sec	-0.005	282	66.7	270	2.671	0.445	6.07E+05	1.51E+05
PI-7I-C-1-CI-8	0-10 sec	10 sec	1.640	322	78.5	309	2.671	0.445	6.94E+05	1.78E+05
PI-7I-C-1-CI-9	0-10 sec	10 sec	3.038	853	280.3	839	2.671	0.445	1.89E+06	6.33E+05
PI-7I-C-2-CI-1	1-1 min 10 sec	10 sec	0.926	440	58.8	-21	2.626	0.438	-4.79E+04	1.95E+05
PI-7I-C-2-CI-2	1-1 min 10 sec	10 sec	-0.224	78	30.7	31	2.626	0.438	7.08E+04	8.22E+04
PI-7I-C-2-CI-3	1-1 min 10 sec	10 sec	-0.667	105	19.4	97	2.626	0.438	2.21E+05	4.49E+04
PI-7I-C-2-CI-4	1-1 min 10 sec	10 sec	0.538	16	4.5	11	2.626	0.438	2.51E+04	1.11E+04
PI-7I-C-2-CI-5	1-1 min 10 sec	10 sec	-4.130	18	7.2	11	2.626	0.438	2.51E+04	1.79E+04
PI-7I-C-2-CI-6	1-1 min 10 sec	10 sec	-3.752	11	5.9	-1	2.626	0.438	-2.28E+03	1.86E+04
PI-7I-C-2-CI-7	1-1 min 10 sec	10 sec	-1.642	11	3.7	-1	2.626	0.438	-2.28E+03	1.19E+04
PI-7I-C-2-CI-8	1-1 min 10 sec	10 sec	-1.338	29	10.2	16	2.626	0.438	3.65E+04	2.57E+04
PI-7I-C-2-CI-9	1-1 min 10 sec	10 sec	-2.016	19	6.4	5	2.626	0.438	1.14E+04	1.91E+04
PI-7I-C-3-CI-1	3-3 min 15 sec	15 sec	0.961	269	36.2	-192	2.638	0.659	-2.91E+05	1.09E+05
PI-7I-C-3-CI-2	3-3 min 15 sec	15 sec	-0.496	46	18.3	-1	2.638	0.659	-1.52E+03	3.98E+04
PI-7I-C-3-CI-3	3-3 min 15 sec	15 sec	-0.570	160	29.5	152	2.638	0.659	2.31E+05	4.54E+04
PI-7I-C-3-CI-4	3-3 min 15 sec	15 sec	-0.767	38	10.2	33	2.638	0.659	5.01E+04	1.58E+04
PI-7I-C-3-CI-5	3-3 min 15 sec	15 sec	-1.462	144	56.1	137	2.638	0.659	2.08E+05	8.55E+04
PI-7I-C-3-CI-6	3-3 min 15 sec	15 sec	-1.254	66	29.4	54	2.638	0.659	8.19E+04	4.55E+04
PI-7I-C-3-CI-7	3-3 min 15 sec	15 sec	-0.329	117	29.3	105	2.638	0.659	1.59E+05	4.51E+04
PI-7I-C-3-CI-8	3-3 min 15 sec	15 sec	-0.989	146	36.5	133	2.638	0.659	2.02E+05	5.62E+04
PI-7I-C-3-CI-9	3-3 min 15 sec	15 sec	0.528	50	17.7	36	2.638	0.659	5.46E+04	2.81E+04
PI-7I-C-4-CI-1	7-8 min	1 min	1.116	306	41.1	-155	2.459	2.459	-6.30E+04	3.03E+04
PI-7I-C-4-CI-2	7-8 min	1 min	0.799	46	18.5	-1	2.459	2.459	-4.07E+02	1.07E+04
PI-7I-C-4-CI-3	7-8 min	1 min	-4.171	107	20.1	99	2.459	2.459	4.03E+04	8.29E+03
PI-7I-C-4-CI-4	7-8 min	1 min	-0.756	70	18.7	65	2.459	2.459	2.64E+04	7.68E+03
PI-7I-C-4-CI-5	7-8 min	1 min	-0.745	62	24.7	55	2.459	2.459	2.24E+04	1.01E+04
PI-7I-C-4-CI-6	7-8 min	1 min	-1.327	103	45.0	91	2.459	2.459	3.70E+04	1.85E+04
PI-7I-C-4-CI-7	7-8 min	1 min	-1.878	102	25.6	90	2.459	2.459	3.66E+04	1.06E+04
PI-7I-C-4-CI-8	7-8 min	1 min	-2.127	120	31.0	107	2.459	2.459	4.35E+04	1.28E+04
PI-7I-C-4-CI-9	7-8 min	1 min	1.050	36	14.2	22	2.459	2.459	8.95E+03	6.18E+03
PI-7I-C-5-CI-1	15-17 min	2 min	1.586	374	50.0	-87	2.526	5.051	-1.72E+04	1.58E+04
PI-7I-C-5-CI-2	15-17 min	2 min	-1.159	72	28.5	25	2.526	5.051	4.95E+03	6.76E+03
PI-7I-C-5-CI-3	15-17 min	2 min	-1.634	19	3.9	11	2.526	5.051	2.18E+03	8.37E+02
PI-7I-C-5-CI-4	15-17 min	2 min	-1.658	34	9.3	29	2.526	5.051	5.74E+03	1.88E+03
PI-7I-C-5-CI-5	15-17 min	2 min	-1.621	62	24.5	55	2.526	5.051	1.09E+04	4.90E+03
PI-7I-C-5-CI-6	15-17 min	2 min	-0.368	52	23.3	40	2.526	5.051	7.92E+03	4.75E+03
PI-7I-C-5-CI-7	15-17 min	2 min	-0.699	59	15.5	47	2.526	5.051	9.31E+03	3.17E+03

Table A.25 (cont'd). Phase I, Shot 7, Commander

Sample ID	Collection Interval	Elapsed Time	Total Mass (mg)	Calculated U (μg)	DU Mass ± 1σ (μg)	Net DU Mass (μg)	Flow Rate (Lpm)	Volume (L)	DU Conc. (μg/m^3)	DU Conc. ± 1σ (μg/m^3)
PI-7I-C-5-CI-8	15-17 min	2 min	0.047	71	19.8	58	2.526	5.051	1.15E+04	4.04E+03
PI-7I-C-5-CI-9	15-17 min	2 min	-0.491	29	9.8	15	2.526	5.051	2.97E+03	2.22E+03
PI-7I-C-6-CI-1	31-35 min	4 min	1.202	296	39.7	-165	2.473	9.892	-1.67E+04	7.45E+03
PI-7I-C-6-CI-2	31-35 min	4 min	-0.187	6	2.8	-41	2.473	9.892	-4.14E+03	1.93E+03
PI-7I-C-6-CI-3	31-35 min	4 min	-0.607	10	2.2	2	2.473	9.892	2.02E+02	2.75E+02
PI-7I-C-6-CI-4	31-35 min	4 min	-0.785	19	5.4	14	2.473	9.892	1.42E+03	5.77E+02
PI-7I-C-6-CI-5	31-35 min	4 min	-0.943	73	28.6	66	2.473	9.892	6.67E+03	2.92E+03
PI-7I-C-6-CI-6	31-35 min	4 min	-1.661	70	30.7	58	2.473	9.892	5.86E+03	3.16E+03
PI-7I-C-6-CI-7	31-35 min	4 min	-0.695	48	12.7	36	2.473	9.892	3.64E+03	1.34E+03
PI-7I-C-6-CI-8	31-35 min	4 min	0.202	143	35.0	130	2.473	9.892	1.31E+04	3.59E+03
PI-7I-C-6-CI-9	31-35 min	4 min	1.486	49	18.5	35	2.473	9.892	3.54E+03	1.95E+03
PI-7I-C-7-CI-1	61-69 min	8 min	1.291	244	33.0	-217	2.654	21.229	-1.02E+04	3.32E+03
PI-7I-C-7-CI-2	61-69 min	8 min	-0.540	22	9.0	-25	2.654	21.229	-1.18E+03	9.82E+02
PI-7I-C-7-CI-3	61-69 min	8 min	-2.154	16	3.3	8	2.654	21.229	3.77E+02	1.73E+02
PI-7I-C-7-CI-4	61-69 min	8 min	0.484	38	10.2	33	2.654	21.229	1.55E+03	4.90E+02
PI-7I-C-7-CI-5	61-69 min	8 min	-1.444	65	25.5	58	2.654	21.229	2.73E+03	1.21E+03
PI-7I-C-7-CI-6	61-69 min	8 min	-0.784	69	29.1	57	2.654	21.229	2.69E+03	1.40E+03
PI-7I-C-7-CI-7	61-69 min	8 min	-0.727	66	17.0	54	2.654	21.229	2.54E+03	8.23E+02
PI-7I-C-7-CI-8	61-69 min	8 min	0.113	106	27.3	93	2.654	21.229	4.38E+03	1.31E+03
PI-7I-C-7-CI-9	61-69 min	8 min	0.496	138	46.5	124	2.654	21.229	5.84E+03	2.21E+03
PI-7I-C-8-CI-1	121-129 min	8 min	0.665	238	32.1	-223	2.501	20.007	-1.11E+04	3.50E+03
PI-7I-C-8-CI-2	121-129 min	8 min	-0.871	16	6.6	-31	2.501	20.007	-1.55E+03	9.97E+02
PI-7I-C-8-CI-3	121-129 min	8 min	-1.955	12	2.5	4	2.501	20.007	2.00E+02	1.48E+02
PI-7I-C-8-CI-4	121-129 min	8 min	-3.137	23	6.2	18	2.501	20.007	9.00E+02	3.24E+02
PI-7I-C-8-CI-5	121-129 min	8 min	-0.862	80	31.3	73	2.501	20.007	3.65E+03	1.58E+03
PI-7I-C-8-CI-6	121-129 min	8 min	-0.477	81	34.0	69	2.501	20.007	3.45E+03	1.73E+03
PI-7I-C-8-CI-7	121-129 min	8 min	-2.421	83	20.8	71	2.501	20.007	3.55E+03	1.06E+03
PI-7I-C-8-CI-8	121-129 min	8 min	-1.897	97	24.3	84	2.501	20.007	4.20E+03	1.24E+03
PI-7I-C-8-CI-9	121-129 min	8 min	1.434	123	40.1	109	2.501	20.007	5.45E+03	2.03E+03
PI-7I-C-9-CI-1	Field Blank	--	0.917	461	61.9	--	--	--	--	--
PI-7I-C-9-CI-2	Field Blank	--	0.644	47	18.8	--	--	--	--	--
PI-7I-C-9-CI-3	Field Blank	--	-1.596	8	1.6	--	--	--	--	--
PI-7I-C-9-CI-4	Field Blank	--	-0.660	5	1.8	--	--	--	--	--
PI-7I-C-9-CI-5	Field Blank	--	-1.602	7	3.1	--	--	--	--	--
PI-7I-C-9-CI-6	Field Blank	--	-1.445	12	5.6	--	--	--	--	--
PI-7I-C-9-CI-7	Field Blank	--	-0.593	12	3.7	--	--	--	--	--
PI-7I-C-9-CI-8	Field Blank	--	-1.307	13	4.7	--	--	--	--	--
PI-7I-C-9-CI-9	Field Blank	--	0.203	14	5.4	--	--	--	--	--

Table A.25 (cont'd). Phase I, Shot 7, Driver

Sample ID	Collection Interval	Elapsed Time	Total Mass (mg)	Calculated U (μg)	DU Mass ± 1σ (μg)	Net DU Mass (μg)	Flow Rate (Lpm)	Volume (L)	DU Conc. (μg/m^3)	DU Conc. ± 1σ (μg/m^3)
PI-7I-D-1-CI-1	0-10 sec	10 sec	0.183	354	47.9	191	2.511	0.419	4.56E+05	1.27E+05
PI-7I-D-1-CI-2	0-10 sec	10 sec	0.206	91	36.0	73	2.511	0.419	1.74E+05	8.79E+04
PI-7I-D-1-CI-3	0-10 sec	10 sec	-1.002	302	55.7	298	2.511	0.419	7.11E+05	1.35E+05
PI-7I-D-1-CI-4	0-10 sec	10 sec	0.603	291	76.4	287	2.511	0.419	6.85E+05	1.84E+05
PI-7I-D-1-CI-5	0-10 sec	10 sec	-0.652	339	128.9	336	2.511	0.419	8.02E+05	3.09E+05
PI-7I-D-1-CI-6	0-10 sec	10 sec	-0.083	322	127.4	322	2.511	0.419	7.68E+05	3.05E+05
PI-7I-D-1-CI-7	0-10 sec	10 sec	0.897	205	46.5	200	2.511	0.419	4.77E+05	1.12E+05
PI-7I-D-1-CI-8	0-10 sec	10 sec	-0.086	216	48.1	216	2.511	0.419	5.16E+05	1.16E+05
PI-7I-D-1-CI-9	0-10 sec	10 sec	2.057	703	211.8	695	2.511	0.419	1.66E+06	5.08E+05
PI-7I-D-2-CI-1	1-1 min 10 sec	10 sec	0.575	394	53.3	231	2.461	0.410	5.63E+05	1.42E+05
PI-7I-D-2-CI-2	1-1 min 10 sec	10 sec	0.009	57	22.7	39	2.461	0.410	9.51E+04	5.83E+04
PI-7I-D-2-CI-3	1-1 min 10 sec	10 sec	-0.468	157	29.0	153	2.461	0.410	3.73E+05	7.17E+04
PI-7I-D-2-CI-4	1-1 min 10 sec	10 sec	-0.192	166	43.8	162	2.461	0.410	3.95E+05	1.08E+05
PI-7I-D-2-CI-5	1-1 min 10 sec	10 sec	0.513	263	100.3	260	2.461	0.410	6.34E+05	2.45E+05
PI-7I-D-2-CI-6	1-1 min 10 sec	10 sec	0.613	275	109.0	275	2.461	0.410	6.71E+05	2.67E+05
PI-7I-D-2-CI-7	1-1 min 10 sec	10 sec	0.856	177	40.5	172	2.461	0.410	4.20E+05	9.99E+04
PI-7I-D-2-CI-8	1-1 min 10 sec	10 sec	-1.789	269	58.3	269	2.461	0.410	6.56E+05	1.44E+05
PI-7I-D-2-CI-9	1-1 min 10 sec	10 sec	0.982	403	121.8	395	2.461	0.410	9.63E+05	2.99E+05
PI-7I-D-3-CI-1	3-3 min 15 sec	15 sec	1.122	129	17.8	-34	2.682	0.670	-5.07E+04	4.25E+04
PI-7I-D-3-CI-2	3-3 min 15 sec	15 sec	-1.090	40	15.9	22	2.682	0.670	3.28E+04	2.62E+04
PI-7I-D-3-CI-3	3-3 min 15 sec	15 sec	3.018	106	19.9	102	2.682	0.670	1.52E+05	3.01E+04
PI-7I-D-3-CI-4	3-3 min 15 sec	15 sec	0.613	104	27.5	100	2.682	0.670	1.49E+05	4.13E+04
PI-7I-D-3-CI-5	3-3 min 15 sec	15 sec	-1.033	94	36.2	91	2.682	0.670	1.36E+05	5.43E+04
PI-7I-D-3-CI-6	3-3 min 15 sec	15 sec	-0.515	185	73.7	185	2.682	0.670	2.76E+05	1.10E+05
PI-7I-D-3-CI-7	3-3 min 15 sec	15 sec	1.396	195	44.4	190	2.682	0.670	2.84E+05	6.70E+04
PI-7I-D-3-CI-8	3-3 min 15 sec	15 sec	1.142	205	44.7	205	2.682	0.670	3.06E+05	6.76E+04
PI-7I-D-3-CI-9	3-3 min 15 sec	15 sec	1.471	134	41.6	126	2.682	0.670	1.88E+05	6.26E+04
PI-7I-D-4-CI-1	7-8 min	1 min	0.695	79	11.1	-84	2.687	2.687	-3.13E+04	9.28E+03
PI-7I-D-4-CI-2	7-8 min	1 min	3.205	28	11.3	10	2.687	2.687	3.72E+03	5.03E+03
PI-7I-D-4-CI-3	7-8 min	1 min	4.558	45	8.9	41	2.687	2.687	1.53E+04	3.38E+03
PI-7I-D-4-CI-4	7-8 min	1 min	-1.620	55	15.2	51	2.687	2.687	1.90E+04	5.71E+03
PI-7I-D-4-CI-5	7-8 min	1 min	0.081	110	42.6	107	2.687	2.687	3.98E+04	1.59E+04
PI-7I-D-4-CI-6	7-8 min	1 min	-0.310	223	88.8	223	2.687	2.687	8.30E+04	3.32E+04
PI-7I-D-4-CI-7	7-8 min	1 min	1.310	206	46.9	201	2.687	2.687	7.48E+04	1.76E+04
PI-7I-D-4-CI-8	7-8 min	1 min	1.995	216	47.1	216	2.687	2.687	8.04E+04	1.77E+04
PI-7I-D-4-CI-9	7-8 min	1 min	0.377	159	49.9	151	2.687	2.687	5.62E+04	1.87E+04
PI-7I-D-5-CI-1	15-17 min	2 min	2.596	101	14.0	-62	2.610	5.220	-1.19E+04	5.04E+03
PI-7I-D-5-CI-2	15-17 min	2 min	3.079	3	2.1	-15	2.610	5.220	-2.87E+03	1.48E+03
PI-7I-D-5-CI-3	15-17 min	2 min	0.191	17	3.7	13	2.610	5.220	2.49E+03	7.62E+02
PI-7I-D-5-CI-4	15-17 min	2 min	0.199	10	3.2	6	2.610	5.220	1.15E+03	6.70E+02
PI-7I-D-5-CI-5	15-17 min	2 min	-0.401	71	27.9	68	2.610	5.220	1.30E+04	5.37E+03
PI-7I-D-5-CI-6	15-17 min	2 min	-1.433	141	56.6	141	2.610	5.220	2.70E+04	1.09E+04
PI-7I-D-5-CI-7	15-17 min	2 min	0.126	71	18.2	66	2.610	5.220	1.26E+04	3.56E+03

Table A.25 (cont'd). Phase I, Shot 7, Driver

Sample ID	Collection Interval	Elapsed Time	Total Mass (mg)	Calculated U (μg)	DU Mass ± 1σ (μg)	Net DU Mass (μg)	Flow Rate (Lpm)	Volume (L)	DU Conc. (μg/m^3)	DU Conc. ± 1σ (μg/m^3)
PI-7I-D-5-CI-8	15-17 min	2 min	0.144	73	18.8	73	2.610	5.220	1.40E+04	3.69E+03
PI-7I-D-5-CI-9	15-17 min	2 min	0.828	93	30.6	85	2.610	5.220	1.63E+04	5.93E+03
PI-7I-D-6-CI-1	31-35 min	4 min	-0.087	166	22.6	3	2.633	10.531	2.85E+02	3.01E+03
PI-7I-D-6-CI-2	31-35 min	4 min	-1.382	7	3.3	-11	2.633	10.531	-1.04E+03	7.70E+02
PI-7I-D-6-CI-3	31-35 min	4 min	-0.737	11	2.5	7	2.633	10.531	6.65E+02	2.73E+02
PI-7I-D-6-CI-4	31-35 min	4 min	-2.686	26	7.1	22	2.633	10.531	2.09E+03	6.90E+02
PI-7I-D-6-CI-5	31-35 min	4 min	-0.099	30	12.0	27	2.633	10.531	2.56E+03	1.16E+03
PI-7I-D-6-CI-6	31-35 min	4 min	-3.478	94	37.7	94	2.633	10.531	8.93E+03	3.60E+03
PI-7I-D-6-CI-7	31-35 min	4 min	-2.011	66	16.3	61	2.633	10.531	5.79E+03	1.59E+03
PI-7I-D-6-CI-8	31-35 min	4 min	3.139	59	17.0	59	2.633	10.531	5.60E+03	1.66E+03
PI-7I-D-6-CI-9	31-35 min	4 min	2.295	163	51.8	155	2.633	10.531	1.47E+04	4.95E+03
PI-7I-D-7-CI-1	61-69 min	8 min	0.660	176	24.0	13	2.580	20.641	6.30E+02	1.58E+03
PI-7I-D-7-CI-2	61-69 min	8 min	3.171	6	3.0	-12	2.580	20.641	-5.81E+02	3.87E+02
PI-7I-D-7-CI-3	61-69 min	8 min	0.217	7	2.0	3	2.580	20.641	1.45E+02	1.18E+02
PI-7I-D-7-CI-4	61-69 min	8 min	-0.152	24	6.7	20	2.580	20.641	9.69E+02	3.33E+02
PI-7I-D-7-CI-5	61-69 min	8 min	0.120	58	22.8	55	2.580	20.641	2.66E+03	1.11E+03
PI-7I-D-7-CI-6	61-69 min	8 min	0.195	167	66.3	167	2.580	20.641	8.09E+03	3.22E+03
PI-7I-D-7-CI-7	61-69 min	8 min	0.781	99	23.5	94	2.580	20.641	4.55E+03	1.16E+03
PI-7I-D-7-CI-8	61-69 min	8 min	0.368	140	31.8	140	2.580	20.641	6.78E+03	1.56E+03
PI-7I-D-7-CI-9	61-69 min	8 min	1.158	254	78.8	246	2.580	20.641	1.19E+04	3.84E+03
PI-7I-D-8-CI-1	121-129 min	8 min	0.885	135	18.5	-28	2.607	20.856	-1.34E+03	1.39E+03
PI-7I-D-8-CI-2	121-129 min	8 min	-1.316	7	3.2	-11	2.607	20.856	-5.27E+02	3.87E+02
PI-7I-D-8-CI-3	121-129 min	8 min	2.441	6	1.8	2	2.607	20.856	9.59E+01	1.09E+02
PI-7I-D-8-CI-4	121-129 min	8 min	-0.416	13	4.1	9	2.607	20.856	4.32E+02	2.08E+02
PI-7I-D-8-CI-5	121-129 min	8 min	0.017	35	14.0	32	2.607	20.856	1.53E+03	6.80E+02
PI-7I-D-8-CI-6	121-129 min	8 min	1.327	100	40.5	100	2.607	20.856	4.79E+03	1.95E+03
PI-7I-D-8-CI-7	121-129 min	8 min	0.549	65	16.7	60	2.607	20.856	2.88E+03	8.19E+02
PI-7I-D-8-CI-8	121-129 min	8 min	0.611	128	28.8	128	2.607	20.856	6.14E+03	1.40E+03
PI-7I-D-8-CI-9	121-129 min	8 min	1.442	144	45.5	136	2.607	20.856	6.52E+03	2.20E+03
PI-7I-D-9-CI-1	Field Blank	--	1.531	163	22.2	--	--	--	--	--
PI-7I-D-9-CI-2	Field Blank	--	2.026	18	7.4	--	--	--	--	--
PI-7I-D-9-CI-3	Field Blank	--	0.261	4	1.4	--	--	--	--	--
PI-7I-D-9-CI-4	Field Blank	--	0.202	4	1.4	--	--	--	--	--
PI-7I-D-9-CI-5	Field Blank	--	1.384	3	2.0	--	--	--	--	--
PI-7I-D-9-CI-6	Field Blank	--	0.401	-2	2.8	--	--	--	--	--
PI-7I-D-9-CI-7	Field Blank	--	-0.522	5	3.1	--	--	--	--	--
PI-7I-D-9-CI-8	Field Blank	--	-1.238	-4	3.7	--	--	--	--	--
PI-7I-D-9-CI-9	Field Blank	--	0.743	8	4.0	--	--	--	--	--

Table A.25 (cont'd). Phase I, Shot 7, Gunner

Sample ID	Collection Interval	Elapsed Time	Total Mass (mg)	Calculated U (μg)	DU Mass ± 1σ (μg)	Net DU Mass (μg)	Flow Rate (Lpm)	Volume (L)	DU Conc. (μg/m^3)	DU Conc. ± 1σ (μg/m^3)
PI-7I-G-1-CI-1	0-10 sec	10 sec	1.425	403	74.5	297	2.691	0.448	6.63E+05	1.73E+05
PI-7I-G-1-CI-2	0-10 sec	10 sec	0.130	154	72.1	141	2.691	0.448	3.15E+05	1.62E+05
PI-7I-G-1-CI-3	0-10 sec	10 sec	0.185	178	44.9	176	2.691	0.448	3.93E+05	1.01E+05
PI-7I-G-1-CI-4	0-10 sec	10 sec	-0.109	189	68.1	188	2.691	0.448	4.20E+05	1.53E+05
PI-7I-G-1-CI-5	0-10 sec	10 sec	0.383	261	99.1	258	2.691	0.448	5.76E+05	2.22E+05
PI-7I-G-1-CI-6	0-10 sec	10 sec	0.394	202	48.0	200	2.691	0.448	4.46E+05	1.08E+05
PI-7I-G-1-CI-7	0-10 sec	10 sec	-0.223	218	36.0	215	2.691	0.448	4.80E+05	8.17E+04
PI-7I-G-1-CI-8	0-10 sec	10 sec	1.045	448	42.5	442	2.691	0.448	9.87E+05	9.94E+04
PI-7I-G-1-CI-9	0-10 sec	10 sec	2.018	573	97.4	552	2.691	0.448	1.23E+06	2.21E+05
PI-7I-G-2-CI-1	Field Blank	--	1.732	106	19.9	--	--	--	--	--
PI-7I-G-2-CI-2	Field Blank	--	0.678	13	6.5	--	--	--	--	--
PI-7I-G-2-CI-3	Field Blank	--	0.016	2	1.2	--	--	--	--	--
PI-7I-G-2-CI-4	Field Blank	--	0.683	1	1.1	--	--	--	--	--
PI-7I-G-2-CI-5	Field Blank	--	-0.881	3	1.9	--	--	--	--	--
PI-7I-G-2-CI-6	Field Blank	--	0.254	2	1.2	--	--	--	--	--
PI-7I-G-2-CI-7	Field Blank	--	-0.105	3	1.4	--	--	--	--	--
PI-7I-G-2-CI-8	Field Blank	--	0.365	6	1.5	--	--	--	--	--
PI-7I-G-2-CI-9	Field Blank	--	0.220	21	4.1	--	--	--	--	--
PI-7I-G-3-CI-1	1-1 min 10 sec	10 sec	0.424	88	16.7	-18	2.677	0.446	-4.04E+04	5.83E+04
PI-7I-G-3-CI-2	1-1 min 10 sec	10 sec	0.919	55	25.8	42	2.677	0.446	9.42E+04	5.97E+04
PI-7I-G-3-CI-3	1-1 min 10 sec	10 sec	0.587	99	25.0	97	2.677	0.446	2.17E+05	5.65E+04
PI-7I-G-3-CI-4	1-1 min 10 sec	10 sec	-0.431	121	43.9	120	2.677	0.446	2.69E+05	9.88E+04
PI-7I-G-3-CI-5	1-1 min 10 sec	10 sec	0.823	239	90.7	236	2.677	0.446	5.29E+05	2.04E+05
PI-7I-G-3-CI-6	1-1 min 10 sec	10 sec	0.643	79	19.1	77	2.677	0.446	1.73E+05	4.32E+04
PI-7I-G-3-CI-7	1-1 min 10 sec	10 sec	0.253	151	25.1	148	2.677	0.446	3.32E+05	5.72E+04
PI-7I-G-3-CI-8	1-1 min 10 sec	10 sec	-0.468	215	20.8	209	2.677	0.446	4.69E+05	4.88E+04
PI-7I-G-3-CI-9	1-1 min 10 sec	10 sec	1.321	76	13.4	55	2.677	0.446	1.23E+05	3.16E+04
PI-7I-G-4-CI-1	3-3 min 15 sec	15 sec	0.463	34	6.8	-72	2.651	0.663	-1.09E+05	3.19E+04
PI-7I-G-4-CI-2	3-3 min 15 sec	15 sec	-0.460	32	15.3	19	2.651	0.663	2.87E+04	2.51E+04
PI-7I-G-4-CI-3	3-3 min 15 sec	15 sec	0.591	93	23.6	91	2.651	0.663	1.37E+05	3.59E+04
PI-7I-G-4-CI-4	3-3 min 15 sec	15 sec	0.188	123	44.4	122	2.651	0.663	1.84E+05	6.72E+04
PI-7I-G-4-CI-5	3-3 min 15 sec	15 sec	-0.180	190	72.4	187	2.651	0.663	2.82E+05	1.10E+05
PI-7I-G-4-CI-6	3-3 min 15 sec	15 sec	0.862	66	16.1	64	2.651	0.663	9.65E+04	2.45E+04
PI-7I-G-4-CI-7	3-3 min 15 sec	15 sec	-1.559	129	21.5	126	2.651	0.663	1.90E+05	3.30E+04
PI-7I-G-4-CI-8	3-3 min 15 sec	15 sec	0.142	126	12.6	120	2.651	0.663	1.81E+05	1.99E+04
PI-7I-G-4-CI-9	3-3 min 15 sec	15 sec	0.281	67	11.7	46	2.651	0.663	6.94E+04	1.88E+04
PI-7I-G-5-CI-1	7-8 min	1 min	1.088	94	17.8	-12	2.693	2.693	-4.46E+03	9.92E+03
PI-7I-G-5-CI-2	7-8 min	1 min	-0.710	37	17.4	24	2.693	2.693	8.91E+03	6.90E+03
PI-7I-G-5-CI-3	7-8 min	1 min	0.575	172	43.3	170	2.693	2.693	6.31E+04	1.62E+04
PI-7I-G-5-CI-4	7-8 min	1 min	0.316	183	66.0	182	2.693	2.693	6.76E+04	2.46E+04
PI-7I-G-5-CI-5	7-8 min	1 min	0.122	184	69.8	181	2.693	2.693	6.72E+04	2.60E+04
PI-7I-G-5-CI-6	7-8 min	1 min	0.491	133	31.8	131	2.693	2.693	4.86E+04	1.19E+04
PI-7I-G-5-CI-7	7-8 min	1 min	0.127	176	29.1	173	2.693	2.693	6.42E+04	1.10E+04

Table A.25 (cont'd). Phase I, Shot 7, Gunner

Sample ID	Collection Interval	Elapsed Time	Total Mass (mg)	Calculated U (μg)	DU Mass ± 1σ (μg)	Net DU Mass (μg)	Flow Rate (Lpm)	Volume (L)	DU Conc. (μg/m^3)	DU Conc. ± 1σ (μg/m^3)
PI-7I-G-5-CI-8	7-8 min	1 min	-0.328	97	10.0	91	2.693	2.693	3.38E+04	3.89E+03
PI-7I-G-5-CI-9	7-8 min	1 min	1.903	86	15.1	65	2.693	2.693	2.41E+04	5.86E+03
PI-7I-G-6-CI-1	15-17 min	2 min	0.791	63	11.9	-43	2.727	5.454	-7.88E+03	4.26E+03
PI-7I-G-6-CI-2	15-17 min	2 min	0.235	10	5.0	-3	2.727	5.454	-5.50E+02	1.50E+03
PI-7I-G-6-CI-3	15-17 min	2 min	0.047	32	8.3	30	2.727	5.454	5.50E+03	1.55E+03
PI-7I-G-6-CI-4	15-17 min	2 min	-0.431	60	21.9	59	2.727	5.454	1.08E+04	4.03E+03
PI-7I-G-6-CI-5	15-17 min	2 min	-0.092	82	31.3	79	2.727	5.454	1.45E+04	5.77E+03
PI-7I-G-6-CI-6	15-17 min	2 min	0.369	50	12.1	48	2.727	5.454	8.80E+03	2.25E+03
PI-7I-G-6-CI-7	15-17 min	2 min	0.005	68	11.9	65	2.727	5.454	1.19E+04	2.23E+03
PI-7I-G-6-CI-8	15-17 min	2 min	-0.040	66	7.0	60	2.727	5.454	1.10E+04	1.35E+03
PI-7I-G-6-CI-9	15-17 min	2 min	1.157	44	8.1	23	2.727	5.454	4.22E+03	1.67E+03
PI-7I-G-7-CI-1	31-35 min	4 min	1.162	44	8.5	-62	2.419	9.676	-6.41E+03	2.24E+03
PI-7I-G-7-CI-2	31-35 min	4 min	-0.275	7	3.4	-6	2.419	9.676	-6.20E+02	7.58E+02
PI-7I-G-7-CI-3	31-35 min	4 min	1.834	8	NA[(a)]	6	2.419	9.676	6.20E+02	NA[(a)]
PI-7I-G-7-CI-4	31-35 min	4 min	0.075	25	9.4	24	2.419	9.676	2.48E+03	9.81E+02
PI-7I-G-7-CI-5	31-35 min	4 min	-1.021	49	18.7	46	2.419	9.676	4.75E+03	1.95E+03
PI-7I-G-7-CI-6	31-35 min	4 min	0.030	35	8.5	33	2.419	9.676	3.41E+03	8.93E+02
PI-7I-G-7-CI-7	31-35 min	4 min	0.314	24	4.8	21	2.419	9.676	2.17E+03	5.21E+02
PI-7I-G-7-CI-8	31-35 min	4 min	-0.320	104	10.6	98	2.419	9.676	1.01E+04	1.15E+03
PI-7I-G-7-CI-9	31-35 min	4 min	3.281	91	16.0	70	2.419	9.676	7.23E+03	1.72E+03
PI-7I-G-8-CI-1	61-69 min	8 min	0.314	62	11.7	-44	2.440	19.518	-2.25E+03	1.18E+03
PI-7I-G-8-CI-2	61-69 min	8 min	-0.002	5	3.0	-8	2.440	19.518	-4.10E+02	3.67E+02
PI-7I-G-8-CI-3	61-69 min	8 min	-0.316	9	2.8	7	2.440	19.518	3.59E+02	1.56E+02
PI-7I-G-8-CI-4	61-69 min	8 min	0.083	37	13.7	36	2.440	19.518	1.84E+03	7.06E+02
PI-7I-G-8-CI-5	61-69 min	8 min	0.160	70	26.6	67	2.440	19.518	3.43E+03	1.37E+03
PI-7I-G-8-CI-6	61-69 min	8 min	0.081	62	15.1	60	2.440	19.518	3.07E+03	7.82E+02
PI-7I-G-8-CI-7	61-69 min	8 min	-0.142	68	11.8	65	2.440	19.518	3.33E+03	6.17E+02
PI-7I-G-8-CI-8	61-69 min	8 min	0.203	197	19.1	191	2.440	19.518	9.79E+03	1.02E+03
PI-7I-G-8-CI-9	61-69 min	8 min	0.997	137	23.8	116	2.440	19.518	5.94E+03	1.25E+03
PI-7I-G-9-CI-1	121-129 min	8 min	2.630	69	13.1	-37	2.425	19.401	-1.91E+03	1.23E+03
PI-7I-G-9-CI-2	121-129 min	8 min	-0.869	8	4.1	-5	2.425	19.401	-2.58E+02	3.96E+02
PI-7I-G-9-CI-3	121-129 min	8 min	-0.428	5	1.7	3	2.425	19.401	1.55E+02	1.07E+02
PI-7I-G-9-CI-4	121-129 min	8 min	0.515	19	7.2	18	2.425	19.401	9.28E+02	3.76E+02
PI-7I-G-9-CI-5	121-129 min	8 min	-1.383	45	17.3	42	2.425	19.401	2.16E+03	8.99E+02
PI-7I-G-9-CI-6	121-129 min	8 min	0.021	47	11.5	45	2.425	19.401	2.32E+03	6.00E+02
PI-7I-G-9-CI-7	121-129 min	8 min	-0.188	58	10.3	55	2.425	19.401	2.83E+03	5.42E+02
PI-7I-G-9-CI-8	121-129 min	8 min	0.689	132	13.0	126	2.425	19.401	6.49E+03	7.02E+02
PI-7I-G-9-CI-9	121-129 min	8 min	0.400	92	16.2	71	2.425	19.401	3.66E+03	8.68E+02

(a) DU mass based on ICP-MS results; no analytical uncertainty was reported.

Table A.25 (cont'd). Phase I, Shot 7, Loader

Sample ID	Collection Interval	Elapsed Time	Total Mass (mg)	Calculated U (μg)	DU Mass ± 1σ (μg)	Net DU Mass (μg)	Flow Rate (Lpm)	Volume (L)	DU Conc. (μg/m^3)	DU Conc. ± 1σ (μg/m^3)
PI-7I-L-1-CI-1	0-20 min	20 min	0.813	108	14.8	28	2.464	49.275	5.68E+02	3.20E+02
PI-7I-L-1-CI-2	0-20 min	20 min	-0.223	11	4.9	-6	2.464	49.275	-1.30E+02	1.35E+02
PI-7I-L-1-CI-3	0-20 min	20 min	-0.385	14	2.9	10	2.464	49.275	1.99E+02	6.06E+01
PI-7I-L-1-CI-4	0-20 min	20 min	-0.464	20	5.5	16	2.464	49.275	3.33E+02	1.13E+02
PI-7I-L-1-CI-5	0-20 min	20 min	-0.135	36	14.4	28	2.464	49.275	5.60E+02	2.95E+02
PI-7I-L-1-CI-6	0-20 min	20 min	1.077	87	38.7	79	2.464	49.275	1.60E+03	7.89E+02
PI-7I-L-1-CI-7	0-20 min	20 min	-2.481	53	13.7	50	2.464	49.275	1.01E+03	2.81E+02
PI-7I-L-1-CI-8	0-20 min	20 min	-0.606	33	11.5	22	2.464	49.275	4.55E+02	2.39E+02
PI-7I-L-1-CI-9	0-20 min	20 min	0.432	32	12.2	21	2.464	49.275	4.26E+02	2.52E+02
PI-7I-L-2-CI-1	20-40 min	20 min	1.871	201	27.1	121	2.512	50.233	2.41E+03	5.55E+02
PI-7I-L-2-CI-2	20-40 min	20 min	-0.276	10	4.8	-7	2.512	50.233	-1.47E+02	1.31E+02
PI-7I-L-2-CI-3	20-40 min	20 min	0.230	13	2.7	9	2.512	50.233	1.75E+02	5.56E+01
PI-7I-L-2-CI-4	20-40 min	20 min	-1.789	174	45.5	170	2.512	50.233	3.39E+03	9.12E+02
PI-7I-L-2-CI-5	20-40 min	20 min	-0.462	166	65.0	158	2.512	50.233	3.14E+03	1.30E+03
PI-7I-L-2-CI-6	20-40 min	20 min	-1.980	131	59.3	123	2.512	50.233	2.45E+03	1.18E+03
PI-7I-L-2-CI-7	20-40 min	20 min	-3.015	125	32.1	122	2.512	50.233	2.42E+03	6.44E+02
PI-7I-L-2-CI-8	20-40 min	20 min	-1.500	181	48.7	170	2.512	50.233	3.39E+03	9.76E+02
PI-7I-L-2-CI-9	20-40 min	20 min	0.526	154	54.2	143	2.512	50.233	2.85E+03	1.08E+03
PI-7I-L-3-CI-1	40-60 min	20 min	-0.917	116	15.8	36	2.595	51.901	6.94E+02	3.22E+02
PI-7I-L-3-CI-2	40-60 min	20 min	-1.929	5	2.4	-12	2.595	51.901	-2.39E+02	9.83E+01
PI-7I-L-3-CI-3	40-60 min	20 min	-0.417	10	2.2	6	2.595	51.901	1.12E+02	4.44E+01
PI-7I-L-3-CI-4	40-60 min	20 min	-0.882	9	2.6	5	2.595	51.901	1.04E+02	5.20E+01
PI-7I-L-3-CI-5	40-60 min	20 min	-0.530	15	6.5	7	2.595	51.901	1.27E+02	1.30E+02
PI-7I-L-3-CI-6	40-60 min	20 min	-0.328	9	4.9	1	2.595	51.901	1.93E+01	1.06E+02
PI-7I-L-3-CI-7	40-60 min	20 min	-2.162	19	5.3	16	2.595	51.901	3.01E+02	1.05E+02
PI-7I-L-3-CI-8	40-60 min	20 min	-1.745	12	5.9	1	2.595	51.901	2.70E+01	1.23E+02
PI-7I-L-3-CI-9	40-60 min	20 min	0.945	13	6.3	2	2.595	51.901	3.85E+01	1.29E+02
PI-7I-L-4-CI-1	60-69m 40 sec	9 m 40 sec	1.904	52	7.4	-28	2.519	25.192	-1.11E+03	3.65E+02
PI-7I-L-4-CI-2	60-69m 40 sec	9 m 40 sec	-0.116	7	3.3	-10	2.519	25.192	-4.13E+02	2.21E+02
PI-7I-L-4-CI-3	60-69m 40 sec	9 m 40 sec	-0.581	3	1.2	-1	2.519	25.192	-4.76E+01	5.43E+01
PI-7I-L-4-CI-4	60-69m 40 sec	9 m 40 sec	-0.428	6	2.0	2	2.519	25.192	9.53E+01	8.43E+01
PI-7I-L-4-CI-5	60-69m 40 sec	9 m 40 sec	-0.085	13	5.4	5	2.519	25.192	1.83E+02	2.26E+02
PI-7I-L-4-CI-6	60-69m 40 sec	9 m 40 sec	-0.874	12	5.9	4	2.519	25.192	1.59E+02	2.54E+02
PI-7I-L-4-CI-7	60-69m 40 sec	9 m 40 sec	-1.488	4	3.2	1	2.519	25.192	2.38E+01	1.35E+02
PI-7I-L-4-CI-8	60-69m 40 sec	9 m 40 sec	-1.844	5	5.1	-6	2.519	25.192	-2.22E+02	2.24E+02
PI-7I-L-4-CI-9	60-69m 40 sec	9 m 40 sec	-0.447	16	6.4	5	2.519	25.192	1.98E+02	2.70E+02
PI-7I-L-5-CI-1	Field Blank	--	1.518	55	7.8	--	--	--	--	--
PI-7I-L-5-CI-2	Field Blank	--	1.058	51	20.4	--	--	--	--	--
PI-7I-L-5-CI-3	Field Blank	--	-1.032	0	1.0	--	--	--	--	--
PI-7I-L-5-CI-4	Field Blank	--	-0.296	2	1.2	--	--	--	--	--
PI-7I-L-5-CI-5	Field Blank	--	-1.168	3	2.3	--	--	--	--	--
PI-7I-L-5-CI-6	Field Blank	--	0.024	0	3.2	--	--	--	--	--
PI-7I-L-5-CI-7	Field Blank	--	-1.303	-4	2.2	--	--	--	--	--

Table A.25 (cont'd). Phase I, Shot 7, Loader

Sample ID	Collection Interval	Elapsed Time	Total Mass (mg)	Calculated U (μg)	DU Mass ± 1σ (μg)	Net DU Mass (μg)	Flow Rate (Lpm)	Volume (L)	DU Conc. (μg/m^3)	DU Conc. ± 1σ (μg/m^3)
PI-7I-L-5-CI-8	Field Blank	--	-0.705	8	4.8	--	--	--	--	--
PI-7I-L-5-CI-9	Field Blank	--	0.210	9	5.1	--	--	--	--	--
PI-7I-L-6-CI-1	Field Blank	--	0.804	64	9.1	--	--	--	--	--
PI-7I-L-6-CI-2	Field Blank	--	-2.007	4	2.0	--	--	--	--	--
PI-7I-L-6-CI-3	Field Blank	--	-0.716	1	0.8	--	--	--	--	--
PI-7I-L-6-CI-4	Field Blank	--	-0.601	2	1.1	--	--	--	--	--
PI-7I-L-6-CI-5	Field Blank	--	-1.765	9	3.9	--	--	--	--	--
PI-7I-L-6-CI-6	Field Blank	--	0.997	18	8.6	--	--	--	--	--
PI-7I-L-6-CI-7	Field Blank	--	-0.500	9	3.1	--	--	--	--	--
PI-7I-L-6-CI-8	Field Blank	--	-0.492	17	6.6	--	--	--	--	--
PI-7I-L-6-CI-9	Field Blank	--	0.363	13	5.2	--	--	--	--	--
PI-7I-L-7-CI-1	Field Blank	--	0.110	46	6.7	--	--	--	--	--
PI-7I-L-7-CI-2	Field Blank	--	-1.465	5	2.5	--	--	--	--	--
PI-7I-L-7-CI-3	Field Blank	--	-0.387	3	1.1	--	--	--	--	--
PI-7I-L-7-CI-4	Field Blank	--	-0.887	1	1.1	--	--	--	--	--
PI-7I-L-7-CI-5	Field Blank	--	-0.285	10	4.6	--	--	--	--	--
PI-7I-L-7-CI-6	Field Blank	--	-0.662	6	3.4	--	--	--	--	--
PI-7I-L-7-CI-7	Field Blank	--	-0.526	2	2.1	--	--	--	--	--
PI-7I-L-7-CI-8	Field Blank	--	-0.406	8	3.7	--	--	--	--	--
PI-7I-L-7-CI-9	Field Blank	--	0.876	13	5.6	--	--	--	--	--
PI-7I-L-8-CI-1	Field Blank	--	0.385	103	14.2	--	--	--	--	--
PI-7I-L-8-CI-2	Field Blank	--	-0.191	7	3.1	--	--	--	--	--
PI-7I-L-8-CI-3	Field Blank	--	1.530	5	1.3	--	--	--	--	--
PI-7I-L-8-CI-4	Field Blank	--	0.047	4	1.4	--	--	--	--	--
PI-7I-L-8-CI-5	Field Blank	--	-0.861	7	3.4	--	--	--	--	--
PI-7I-L-8-CI-6	Field Blank	--	-2.180	1	2.8	--	--	--	--	--
PI-7I-L-8-CI-7	Field Blank	--	-0.351	4	2.5	--	--	--	--	--
PI-7I-L-8-CI-8	Field Blank	--	-2.246	9	5.3	--	--	--	--	--
PI-7I-L-8-CI-9	Field Blank	--	0.113	9	4.9	--	--	--	--	--
PI-7I-L-9-CI-1	Field Blank	--	0.789	132	18.2	--	--	--	--	--
PI-7I-L-9-CI-2	Field Blank	--	0.061	20	8.2	--	--	--	--	--
PI-7I-L-9-CI-3	Field Blank	--	-0.928	12	2.5	--	--	--	--	--
PI-7I-L-9-CI-4	Field Blank	--	1.286	9	2.6	--	--	--	--	--
PI-7I-L-9-CI-5	Field Blank	--	-0.443	13	5.3	--	--	--	--	--
PI-7I-L-9-CI-6	Field Blank	--	-0.478	15	7.3	--	--	--	--	--
PI-7I-L-9-CI-7	Field Blank	--	0.752	6	2.8	--	--	--	--	--
PI-7I-L-9-CI-8	Field Blank	--	-1.283	11	6.0	--	--	--	--	--
PI-7I-L-9-CI-9	Field Blank	--	0.802	11	4.5	--	--	--	--	--

Table A.26. PII-1/2 Cascade Impactor Substrates—Mass, Volume, and Concentration

Sample ID	Collection Interval	Elapsed Time	Total Mass (mg)	Calculated U (μg)	DU Mass ± 1σ (μg)	Net DU Mass (μg)	Flow Rate (Lpm)	Volume (L)	DU Conc. (μg/m^3)	DU Conc. ± 1σ (μg/m^3)
PII-1/2I-C-1-CI-1	Shot 1: 0-10 sec	10 sec	1.389	103	14.1	103	2.696	0.449	2.29E+05	3.21E+04
PII-1/2I-C-1-CI-2	Shot 1: 0-10 sec	10 sec	0.825	27	10.8	27	2.696	0.449	6.01E+04	2.41E+04
PII-1/2I-C-1-CI-3	Shot 1: 0-10 sec	10 sec	-0.858	21	4.2	21	2.696	0.449	4.68E+04	9.46E+03
PII-1/2I-C-1-CI-4	Shot 1: 0-10 sec	10 sec	-1.267	44	11.6	44	2.696	0.449	9.80E+04	2.60E+04
PII-1/2I-C-1-CI-5	Shot 1: 0-10 sec	10 sec	-0.387	163	64.2	163	2.696	0.449	3.63E+05	1.43E+05
PII-1/2I-C-1-CI-6	Shot 1: 0-10 sec	10 sec	0.389	168	78.5	168	2.696	0.449	3.74E+05	1.75E+05
PII-1/2I-C-1-CI-7	Shot 1: 0-10 sec	10 sec	-0.853	100	25.3	100	2.696	0.449	2.23E+05	5.67E+04
PII-1/2I-C-1-CI-8	Shot 1: 0-10 sec	10 sec	0.579	93	29.2	93	2.696	0.449	2.07E+05	6.53E+04
PII-1/2I-C-1-CI-9	Shot 1: 0-10 sec	10 sec	-0.097	146	57.0	146	2.696	0.449	3.25E+05	1.27E+05
PII-1/2I-C-2-CI-1	3-4 min	1 min	1.245	68	9.6	68	2.554	2.554	2.66E+04	3.84E+03
PII-1/2I-C-2-CI-2	3-4 min	1 min	0.445	29	11.8	29	2.554	2.554	1.14E+04	4.63E+03
PII-1/2I-C-2-CI-3	3-4 min	1 min	0.096	45	8.5	45	2.554	2.554	1.76E+04	3.37E+03
PII-1/2I-C-2-CI-4	3-4 min	1 min	0.556	196	50.9	196	2.554	2.554	7.67E+04	2.01E+04
PII-1/2I-C-2-CI-5	3-4 min	1 min	0.510	263	103.7	263	2.554	2.554	1.03E+05	4.07E+04
PII-1/2I-C-2-CI-6	3-4 min	1 min	-0.047	434	202.0	434	2.554	2.554	1.70E+05	7.93E+04
PII-1/2I-C-2-CI-7	3-4 min	1 min	0.196	187	46.8	187	2.554	2.554	7.32E+04	1.85E+04
PII-1/2I-C-2-CI-8	3-4 min	1 min	-0.179	327	93.2	327	2.554	2.554	1.28E+05	3.67E+04
PII-1/2I-C-2-CI-9	3-4 min	1 min	1.539	292	108.8	292	2.554	2.554	1.14E+05	4.27E+04
PII-1/2I-C-3-CI-1	9-11 min	2 min	2.041	125	17.0	125	2.648	5.297	2.36E+04	3.29E+03
PII-1/2I-C-3-CI-2	9-11 min	2 min	0.366	31	12.3	31	2.648	5.297	5.85E+03	2.33E+03
PII-1/2I-C-3-CI-3	9-11 min	2 min	0.485	63	11.7	63	2.648	5.297	1.19E+04	2.24E+03
PII-1/2I-C-3-CI-4	9-11 min	2 min	0.638	71	18.5	71	2.648	5.297	1.34E+04	3.52E+03
PII-1/2I-C-3-CI-5	9-11 min	2 min	-0.356	253	NA[(a)]	253	2.648	5.297	4.78E+04	NA[(a)]
PII-1/2I-C-3-CI-6	9-11 min	2 min	1.403	80	38.1	80	2.648	5.297	1.51E+04	7.21E+03
PII-1/2I-C-3-CI-7	9-11 min	2 min	1.425	68	17.9	68	2.648	5.297	1.28E+04	3.40E+03
PII-1/2I-C-3-CI-8	9-11 min	2 min	-0.008	67	22.5	67	2.648	5.297	1.26E+04	4.26E+03
PII-1/2I-C-3-CI-9	9-11 min	2 min	1.051	110	45.5	110	2.648	5.297	2.08E+04	8.61E+03
PII-1/2I-C-4-CI-1	Shot 2: 0-10 sec	10 sec	1.396	65	9.4	65	2.481	0.414	1.57E+05	2.32E+04
PII-1/2I-C-4-CI-2	Shot 2: 0-10 sec	10 sec	-0.310	26	10.8	26	2.481	0.414	6.28E+04	2.62E+04
PII-1/2I-C-4-CI-3	Shot 2: 0-10 sec	10 sec	-2.862	64	12.0	64	2.481	0.414	1.55E+05	2.94E+04
PII-1/2I-C-4-CI-4	Shot 2: 0-10 sec	10 sec	-2.392	171	44.6	171	2.481	0.414	4.13E+05	1.08E+05
PII-1/2I-C-4-CI-5	Shot 2: 0-10 sec	10 sec	-0.678	350	138.0	350	2.481	0.414	8.45E+05	3.34E+05
PII-1/2I-C-4-CI-6	Shot 2: 0-10 sec	10 sec	-0.585	351	163.8	351	2.481	0.414	8.48E+05	3.96E+05
PII-1/2I-C-4-CI-7	Shot 2: 0-10 sec	10 sec	-1.138	300	74.1	300	2.481	0.414	7.25E+05	1.80E+05
PII-1/2I-C-4-CI-8	Shot 2: 0-10 sec	10 sec	-0.649	324	91.6	324	2.481	0.414	7.83E+05	2.22E+05
PII-1/2I-C-4-CI-9	Shot 2: 0-10 sec	10 sec	-0.960	481	174.6	481	2.481	0.414	1.16E+06	4.23E+05
PII-1/2I-C-5-CI-1	3-4 min	1 min	1.698	101	13.9	101	2.322	2.322	4.35E+04	6.13E+03
PII-1/2I-C-5-CI-2	3-4 min	1 min	-1.421	13	5.5	13	2.322	2.322	5.60E+03	2.37E+03
PII-1/2I-C-5-CI-3	3-4 min	1 min	-0.091	32	6.1	32	2.322	2.322	1.38E+04	2.66E+03
PII-1/2I-C-5-CI-4	3-4 min	1 min	-3.391	31	8.3	31	2.322	2.322	1.34E+04	3.60E+03
PII-1/2I-C-5-CI-5	3-4 min	1 min	0.478	114	45.2	114	2.322	2.322	4.91E+04	1.95E+04
PII-1/2I-C-5-CI-6	3-4 min	1 min	-0.958	206	96.4	206	2.322	2.322	8.87E+04	4.16E+04
PII-1/2I-C-5-CI-7	3-4 min	1 min	-0.454	136	34.8	136	2.322	2.322	5.86E+04	1.51E+04

Table A.26 (cont'd). Phase II, Shot 1/2, Commander

Sample ID	Collection Interval	Elapsed Time	Total Mass (mg)	Calculated U (μg)	DU Mass ± 1σ (μg)	Net DU Mass (μg)	Flow Rate (Lpm)	Volume (L)	DU Conc. (μg/m^3)	DU Conc. ± 1σ (μg/m^3)
PII-1/2I-C-5-CI-8	3-4 min	1 min	0.791	283	80.4	283	2.322	2.322	1.22E+05	3.48E+04
PII-1/2I-C-5-CI-9	3-4 min	1 min	-1.352	58	25.0	58	2.322	2.322	2.50E+04	1.08E+04
PII-1/2I-C-6-CI-1	9-11 min	2 min	0.843	73	10.4	73	2.461	4.922	1.48E+04	2.16E+03
PII-1/2I-C-6-CI-2	9-11 min	2 min	-2.599	16	6.9	16	2.461	4.922	3.25E+03	1.41E+03
PII-1/2I-C-6-CI-3	9-11 min	2 min	-0.889	51	9.8	51	2.461	4.922	1.04E+04	2.02E+03
PII-1/2I-C-6-CI-4	9-11 min	2 min	0.736	80	21.2	80	2.461	4.922	1.63E+04	4.33E+03
PII-1/2I-C-6-CI-5	9-11 min	2 min	-0.575	181	72.0	181	2.461	4.922	3.68E+04	1.47E+04
PII-1/2I-C-6-CI-6	9-11 min	2 min	-0.523	157	73.9	157	2.461	4.922	3.19E+04	1.50E+04
PII-1/2I-C-6-CI-7	9-11 min	2 min	0.058	220	55.0	220	2.461	4.922	4.47E+04	1.13E+04
PII-1/2I-C-6-CI-8	9-11 min	2 min	1.155	357	99.9	357	2.461	4.922	7.25E+04	2.04E+04
PII-1/2I-C-6-CI-9	9-11 min	2 min	2.241	149	56.3	149	2.461	4.922	3.03E+04	1.15E+04
PII-1/2I-C-7-CI-1	21-25 min	4 min	1.877	68	9.8	68	2.651	10.602	6.41E+03	9.44E+02
PII-1/2I-C-7-CI-2	21-25 min	4 min	-0.184	10	4.6	10	2.651	10.602	9.43E+02	4.35E+02
PII-1/2I-C-7-CI-3	21-25 min	4 min	0.445	28	5.6	28	2.651	10.602	2.64E+03	5.34E+02
PII-1/2I-C-7-CI-4	21-25 min	4 min	0.998	43	11.6	43	2.651	10.602	4.06E+03	1.10E+03
PII-1/2I-C-7-CI-5	21-25 min	4 min	-0.378	87	34.9	87	2.651	10.602	8.21E+03	3.30E+03
PII-1/2I-C-7-CI-6	21-25 min	4 min	-1.532	123	58.5	123	2.651	10.602	1.16E+04	5.53E+03
PII-1/2I-C-7-CI-7	21-25 min	4 min	-1.296	169	43.4	169	2.651	10.602	1.59E+04	4.12E+03
PII-1/2I-C-7-CI-8	21-25 min	4 min	-0.068	304	86.3	304	2.651	10.602	2.87E+04	8.19E+03
PII-1/2I-C-7-CI-9	21-25 min	4 min	0.395	214	80.0	214	2.651	10.602	2.02E+04	7.57E+03
PII-1/2I-C-8-CI-1	45-53 min	8 min	2.318	75	10.6	75	2.561	20.491	3.66E+03	5.29E+02
PII-1/2I-C-8-CI-2	45-53 min	8 min	0.081	4	2.5	4	2.561	20.491	1.95E+02	1.22E+02
PII-1/2I-C-8-CI-3	45-53 min	8 min	0.136	4	1.6	4	2.561	20.491	1.95E+02	7.83E+01
PII-1/2I-C-8-CI-4	45-53 min	8 min	0.886	44	12.1	44	2.561	20.491	2.15E+03	5.94E+02
PII-1/2I-C-8-CI-5	45-53 min	8 min	-0.067	53	21.5	53	2.561	20.491	2.59E+03	1.05E+03
PII-1/2I-C-8-CI-6	45-53 min	8 min	-0.352	77	37.0	77	2.561	20.491	3.76E+03	1.81E+03
PII-1/2I-C-8-CI-7	45-53 min	8 min	-0.750	79	21.2	79	2.561	20.491	3.86E+03	1.04E+03
PII-1/2I-C-8-CI-8	45-53 min	8 min	0.708	120	35.1	120	2.561	20.491	5.86E+03	1.72E+03
PII-1/2I-C-8-CI-9	45-53 min	8 min	1.098	83	32.6	83	2.561	20.491	4.05E+03	1.60E+03
PII-1/2I-C-9-CI-1	93-109 min	16 min	2.133	37	5.7	37	2.499	39.983	9.25E+02	1.45E+02
PII-1/2I-C-9-CI-2	93-109 min	16 min	-0.048	8	3.9	8	2.499	39.983	2.00E+02	9.77E+01
PII-1/2I-C-9-CI-3	93-109 min	16 min	-0.519	7	2.0	7	2.499	39.983	1.75E+02	5.03E+01
PII-1/2I-C-9-CI-4	93-109 min	16 min	0.127	42	11.3	42	2.499	39.983	1.05E+03	2.84E+02
PII-1/2I-C-9-CI-5	93-109 min	16 min	0.504	74	29.2	74	2.499	39.983	1.85E+03	7.32E+02
PII-1/2I-C-9-CI-6	93-109 min	16 min	0.247	153	68.9	153	2.499	39.983	3.83E+03	1.73E+03
PII-1/2I-C-9-CI-7	93-109 min	16 min	-0.416	78	21.7	78	2.499	39.983	1.95E+03	5.46E+02
PII-1/2I-C-9-CI-8	93-109 min	16 min	-0.117	136	38.3	136	2.499	39.983	3.40E+03	9.63E+02
PII-1/2I-C-9-CI-9	93-109 min	16 min	1.758	303	107.4	303	2.499	39.983	7.58E+03	2.70E+03

(a) DU mass based on ICP-MS results; no analytical uncertainty was reported.

Table A.26 (cont'd). Phase II, Shots 1/ 2, Driver

Sample ID	Collection Interval	Elapsed Time	Total Mass (mg)	Calculated U (μg)	DU Mass ± 1σ (μg)	Net DU Mass (μg)	Flow Rate (Lpm)	Volume (L)	DU Conc. (μg/m^3)	DU Conc. ± 1σ (μg/m^3)
PII-1/2I-D-1-CI-1	Shot 1: 0-10 sec	10 sec	0.958	79	11.1	79.0	2.558	0.426	1.85E+05	2.66E+04
PII-1/2I-D-1-CI-2	Shot 1: 0-10 sec	10 sec	-1.462	19	7.6	19.0	2.558	0.426	4.46E+04	1.79E+04
PII-1/2I-D-1-CI-3	Shot 1: 0-10 sec	10 sec	-2.166	27	5.3	27.0	2.558	0.426	6.34E+04	1.26E+04
PII-1/2I-D-1-CI-4	Shot 1: 0-10 sec	10 sec	-0.669	38	10.1	38.0	2.558	0.426	8.92E+04	2.39E+04
PII-1/2I-D-1-CI-5	Shot 1: 0-10 sec	10 sec	0.035	168	67.0	168.0	2.558	0.426	3.94E+05	1.58E+05
PII-1/2I-D-1-CI-6	Shot 1: 0-10 sec	10 sec	-1.922	174	85.6	174.0	2.558	0.426	4.08E+05	2.01E+05
PII-1/2I-D-1-CI-7	Shot 1: 0-10 sec	10 sec	-2.747	94	24.7	94.0	2.558	0.426	2.21E+05	5.84E+04
PII-1/2I-D-1-CI-8	Shot 1: 0-10 sec	10 sec	-1.427	117	39.0	117.0	2.558	0.426	2.75E+05	9.19E+04
PII-1/2I-D-1-CI-9	Shot 1: 0-10 sec	10 sec	2.196	189	78.9	189.0	2.558	0.426	4.44E+05	1.86E+05
PII-1/2I-D-2-CI-1	3-4 min	1 min	1.659	85	11.8	85.0	2.459	2.459	3.46E+04	4.91E+03
PII-1/2I-D-2-CI-2	3-4 min	1 min	-1.463	18	7.4	18.0	2.459	2.459	7.32E+03	3.02E+03
PII-1/2I-D-2-CI-3	3-4 min	1 min	-2.535	38	7.3	38.0	2.459	2.459	1.55E+04	3.00E+03
PII-1/2I-D-2-CI-4	3-4 min	1 min	-2.230	182	47.3	182.0	2.459	2.459	7.40E+04	1.94E+04
PII-1/2I-D-2-CI-5	3-4 min	1 min	-0.352	291	116.0	291.0	2.459	2.459	1.18E+05	4.73E+04
PII-1/2I-D-2-CI-6	3-4 min	1 min	-1.950	366	179.7	366.0	2.459	2.459	1.49E+05	7.32E+04
PII-1/2I-D-2-CI-7	3-4 min	1 min	-2.455	115	30.2	115.0	2.459	2.459	4.68E+04	1.24E+04
PII-1/2I-D-2-CI-8	3-4 min	1 min	-1.231	213	67.8	213.0	2.459	2.459	8.66E+04	2.77E+04
PII-1/2I-D-2-CI-9	3-4 min	1 min	3.996	345	136.0	345.0	2.459	2.459	1.40E+05	5.55E+04
PII-1/2I-D-3-CI-1	9-11 min	2 min	1.179	43	6.4	43.0	2.659	5.317	8.09E+03	1.23E+03
PII-1/2I-D-3-CI-2	9-11 min	2 min	0.275	17	6.9	17.0	2.659	5.317	3.20E+03	1.30E+03
PII-1/2I-D-3-CI-3	9-11 min	2 min	-2.956	57	10.9	57.0	2.659	5.317	1.07E+04	2.08E+03
PII-1/2I-D-3-CI-4	9-11 min	2 min	1.079	181	47.2	181.0	2.659	5.317	3.40E+04	8.94E+03
PII-1/2I-D-3-CI-5	9-11 min	2 min	0.418	221	88.2	221.0	2.659	5.317	4.16E+04	1.66E+04
PII-1/2I-D-3-CI-6	9-11 min	2 min	0.695	307	151.1	307.0	2.659	5.317	5.77E+04	2.85E+04
PII-1/2I-D-3-CI-7	9-11 min	2 min	0.585	289	73.8	289.0	2.659	5.317	5.44E+04	1.40E+04
PII-1/2I-D-3-CI-8	9-11 min	2 min	-1.439	285	90.2	285.0	2.659	5.317	5.36E+04	1.70E+04
PII-1/2I-D-3-CI-9	9-11 min	2 min	1.964	229	90.5	229.0	2.659	5.317	4.31E+04	1.71E+04
PII-1/2I-D-4-CI-1	Shot 2: 0-10 sec	10 sec	3.081	64	9.0	64.0	2.695	0.449	1.43E+05	2.05E+04
PII-1/2I-D-4-CI-2	Shot 2: 0-10 sec	10 sec	-0.867	58	23.0	58.0	2.695	0.449	1.29E+05	5.14E+04
PII-1/2I-D-4-CI-3	Shot 2: 0-10 sec	10 sec	1.121	49	9.1	49.0	2.695	0.449	1.09E+05	2.05E+04
PII-1/2I-D-4-CI-4	Shot 2: 0-10 sec	10 sec	-1.094	85	22.3	85.0	2.695	0.449	1.89E+05	5.00E+04
PII-1/2I-D-4-CI-5	Shot 2: 0-10 sec	10 sec	-1.862	125	50.2	125.0	2.695	0.449	2.78E+05	1.12E+05
PII-1/2I-D-4-CI-6	Shot 2: 0-10 sec	10 sec	-2.165	97	48.5	97.0	2.695	0.449	2.16E+05	1.08E+05
PII-1/2I-D-4-CI-7	Shot 2: 0-10 sec	10 sec	-0.287	55	15.4	55.0	2.695	0.449	1.22E+05	3.45E+04
PII-1/2I-D-4-CI-8	Shot 2: 0-10 sec	10 sec	0.279	82	29.9	82.0	2.695	0.449	1.83E+05	6.68E+04
PII-1/2I-D-4-CI-9	Shot 2: 0-10 sec	10 sec	1.427	113	47.4	113.0	2.695	0.449	2.52E+05	1.06E+05
PII-1/2I-D-5-CI-1	3-4 min	1 min	2.016	32	5.0	32.0	2.612	2.612	1.23E+04	1.95E+03
PII-1/2I-D-5-CI-2	3-4 min	1 min	-5.561	15	6.2	15.0	2.612	2.612	5.74E+03	2.38E+03
PII-1/2I-D-5-CI-3	3-4 min	1 min	-3.429	41	7.7	41.0	2.612	2.612	1.57E+04	2.99E+03
PII-1/2I-D-5-CI-4	3-4 min	1 min	-1.271	32	8.5	32.0	2.612	2.612	1.23E+04	3.27E+03
PII-1/2I-D-5-CI-5	3-4 min	1 min	-0.383	140	56.1	140.0	2.612	2.612	5.36E+04	2.15E+04
PII-1/2I-D-5-CI-6	3-4 min	1 min	-1.571	188	92.8	188.0	2.612	2.612	7.20E+04	3.56E+04
PII-1/2I-D-5-CI-7	3-4 min	1 min	-1.193	132	35.2	132.0	2.612	2.612	5.05E+04	1.36E+04

Table A.26 (cont'd). Phase II, Shots 1/ 2, Driver

Sample ID	Collection Interval	Elapsed Time	Total Mass (mg)	Calculated U (μg)	DU Mass ± 1σ (μg)	Net DU Mass (μg)	Flow Rate (Lpm)	Volume (L)	DU Conc. (μg/m^3)	DU Conc. ± 1σ (μg/m^3)
PII-1/2I-D-5-CI-8	3-4 min	1 min	-0.971	337	105.5	337.0	2.612	2.612	1.29E+05	4.06E+04
PII-1/2I-D-5-CI-9	3-4 min	1 min	2.924	208	83.1	208.0	2.612	2.612	7.96E+04	3.19E+04
PII-1/2I-D-6-CI-1	9-11 min	2 min	1.698	43	6.2	43.0	2.620	5.241	8.20E+03	1.21E+03
PII-1/2I-D-6-CI-2	9-11 min	2 min	-0.733	9	4.1	9.0	2.620	5.241	1.72E+03	7.84E+02
PII-1/2I-D-6-CI-3	9-11 min	2 min	0.273	27	5.3	27.0	2.620	5.241	5.15E+03	1.02E+03
PII-1/2I-D-6-CI-4	9-11 min	2 min	-0.221	101	26.3	101.0	2.620	5.241	1.93E+04	5.05E+03
PII-1/2I-D-6-CI-5	9-11 min	2 min	-0.840	141	56.8	141.0	2.620	5.241	2.69E+04	1.09E+04
PII-1/2I-D-6-CI-6	9-11 min	2 min	-1.995	132	65.8	132.0	2.620	5.241	2.52E+04	1.26E+04
PII-1/2I-D-6-CI-7	9-11 min	2 min	-2.376	183	47.6	183.0	2.620	5.241	3.49E+04	9.14E+03
PII-1/2I-D-6-CI-8	9-11 min	2 min	-2.137	509	157.2	509.0	2.620	5.241	9.71E+04	3.01E+04
PII-1/2I-D-6-CI-9	9-11 min	2 min	1.980	285	111.6	285.0	2.620	5.241	5.44E+04	2.14E+04
PII-1/2I-D-7-CI-1	21-25 min	4 min	2.073	27	4.2	27.0	2.588	10.353	2.61E+03	4.13E+02
PII-1/2I-D-7-CI-2	21-25 min	4 min	1.336	10	4.5	10.0	2.588	10.353	9.66E+02	4.36E+02
PII-1/2I-D-7-CI-3	21-25 min	4 min	-0.825	30	6.3	30.0	2.588	10.353	2.90E+03	6.15E+02
PII-1/2I-D-7-CI-4	21-25 min	4 min	-1.886	56	14.9	56.0	2.588	10.353	5.41E+03	1.45E+03
PII-1/2I-D-7-CI-5	21-25 min	4 min	-4.331	67	27.6	67.0	2.588	10.353	6.47E+03	2.67E+03
PII-1/2I-D-7-CI-6	21-25 min	4 min	-0.730	101	50.6	101.0	2.588	10.353	9.76E+03	4.90E+03
PII-1/2I-D-7-CI-7	21-25 min	4 min	-0.869	146	38.7	146.0	2.588	10.353	1.41E+04	3.76E+03
PII-1/2I-D-7-CI-8	21-25 min	4 min	-0.865	319	99.7	319.0	2.588	10.353	3.08E+04	9.67E+03
PII-1/2I-D-7-CI-9	21-25 min	4 min	0.863	186	74.6	186.0	2.588	10.353	1.80E+04	7.23E+03
PII-1/2I-D-8-CI-1	45-53 min	8 min	3.478	37	5.4	37.0	2.692	21.538	1.72E+03	2.56E+02
PII-1/2I-D-8-CI-2	45-53 min	8 min	0.468	4	2.4	4.0	2.692	21.538	1.86E+02	1.12E+02
PII-1/2I-D-8-CI-3	45-53 min	8 min	-2.442	5	1.9	5.0	2.692	21.538	2.32E+02	8.85E+01
PII-1/2I-D-8-CI-4	45-53 min	8 min	-1.833	41	11.2	41.0	2.692	21.538	1.90E+03	5.23E+02
PII-1/2I-D-8-CI-5	45-53 min	8 min	0.244	96	38.8	96.0	2.692	21.538	4.46E+03	1.81E+03
PII-1/2I-D-8-CI-6	45-53 min	8 min	-0.699	56	27.9	56.0	2.692	21.538	2.60E+03	1.30E+03
PII-1/2I-D-8-CI-7	45-53 min	8 min	-1.111	107	28.7	107.0	2.692	21.538	4.97E+03	1.34E+03
PII-1/2I-D-8-CI-8	45-53 min	8 min	-1.551	155	47.3	155.0	2.692	21.538	7.20E+03	2.21E+03
PII-1/2I-D-8-CI-9	45-53 min	8 min	1.037	85	35.1	85.0	2.692	21.538	3.95E+03	1.63E+03
PII-1/2I-D-9-CI-1	93-109 min	16 min	2.790	28	4.4	28.0	2.489	39.825	7.03E+02	1.12E+02
PII-1/2I-D-9-CI-2	93-109 min	16 min	0.540	4	2.3	4.0	2.489	39.825	1.00E+02	5.78E+01
PII-1/2I-D-9-CI-3	93-109 min	16 min	-0.300	5	1.7	5.0	2.489	39.825	1.26E+02	4.29E+01
PII-1/2I-D-9-CI-4	93-109 min	16 min	0.387	35	9.3	35.0	2.489	39.825	8.79E+02	2.35E+02
PII-1/2I-D-9-CI-5	93-109 min	16 min	0.314	116	46.1	116.0	2.489	39.825	2.91E+03	1.16E+03
PII-1/2I-D-9-CI-6	93-109 min	16 min	0.070	136	64.1	136.0	2.489	39.825	3.41E+03	1.61E+03
PII-1/2I-D-9-CI-7	93-109 min	16 min	-0.128	80	22.1	80.0	2.489	39.825	2.01E+03	5.58E+02
PII-1/2I-D-9-CI-8	93-109 min	16 min	-1.368	201	60.4	201.0	2.489	39.825	5.05E+03	1.52E+03
PII-1/2I-D-9-CI-9	93-109 min	16 min	0.466	251	94.8	251.0	2.489	39.825	6.30E+03	2.39E+03

Table A.26 (cont'd). Phase II, Shots 1/2, Gunner

Sample ID	Collection Interval	Elapsed Time	Total Mass (mg)	Calculated U (μg)	DU Mass ± 1σ (μg)	Net DU Mass (μg)	Flow Rate (Lpm)	Volume (L)	DU Conc. (μg/m^3)	DU Conc. ± 1σ (μg/m^3)
PII-1/2I-G-1-CI-1	Shot 2: 0-10 sec	10 sec	2.054	81	15.0	56	2.730	0.455	1.24E+05	3.38E+04
PII-1/2I-G-1-CI-2	Shot 2: 0-10 sec	10 sec	-1.958	46	21.5	38	2.730	0.455	8.28E+04	4.78E+04
PII-1/2I-G-1-CI-3	Shot 2: 0-10 sec	10 sec	-2.216	38	9.6	33	2.730	0.455	7.25E+04	2.14E+04
PII-1/2I-G-1-CI-4	Shot 2: 0-10 sec	10 sec	-1.030	48	17.1	44	2.730	0.455	9.60E+04	3.78E+04
PII-1/2I-G-1-CI-5	Shot 2: 0-10 sec	10 sec	-0.555	58	22.1	56	2.730	0.455	1.23E+05	4.88E+04
PII-1/2I-G-1-CI-6	Shot 2: 0-10 sec	10 sec	1.431	42	10.6	39	2.730	0.455	8.64E+04	2.35E+04
PII-1/2I-G-1-CI-7	Shot 2: 0-10 sec	10 sec	-1.127	52	9.5	49	2.730	0.455	1.07E+05	2.12E+04
PII-1/2I-G-1-CI-8	Shot 2: 0-10 sec	10 sec	-0.239	68	7.4	61	2.730	0.455	1.35E+05	1.69E+04
PII-1/2I-G-1-CI-9	Shot 2: 0-10 sec	10 sec	1.712	219	38.7	219	2.730	0.455	4.81E+05	8.63E+04
PII-1/2I-G-2-CI-1	Field Blank	--	0.935	19	3.9	--	--	--	--	--
PII-1/2I-G-2-CI-2	Field Blank	--	-1.361	3	1.8	--	--	--	--	--
PII-1/2I-G-2-CI-3	Field Blank	--	-2.728	1	1.1	--	--	--	--	--
PII-1/2I-G-2-CI-4	Field Blank	--	-2.374	4	1.9	--	--	--	--	--
PII-1/2I-G-2-CI-5	Field Blank	--	-3.915	-1	1.5	--	--	--	--	--
PII-1/2I-G-2-CI-6	Field Blank	--	-1.746	3	1.4	--	--	--	--	--
PII-1/2I-G-2-CI-7	Field Blank	--	-2.397	5	1.9	--	--	--	--	--
PII-1/2I-G-2-CI-8	Field Blank	--	-2.566	5	1.7	--	--	--	--	--
PII-1/2I-G-2-CI-9	Field Blank	--	1.830	-4	2.8	--	--	--	--	--
PII-1/2I-G-3-CI-1	3-4 min	1 min	1.827	11	NA[(a)]	-14	2.616	2.616	-5.22E+03	NA[(a)]
PII-1/2I-G-3-CI-2	3-4 min	1 min	-2.763	14	6.7	6	2.616	2.616	2.17E+03	2.81E+03
PII-1/2I-G-3-CI-3	3-4 min	1 min	-1.944	34	8.6	29	2.616	2.616	1.11E+04	3.34E+03
PII-1/2I-G-3-CI-4	3-4 min	1 min	-2.761	42	14.8	38	2.616	2.616	1.44E+04	5.70E+03
PII-1/2I-G-3-CI-5	3-4 min	1 min	-0.682	68	26.1	66	2.616	2.616	2.52E+04	1.00E+04
PII-1/2I-G-3-CI-6	3-4 min	1 min	-2.098	61	15.0	58	2.616	2.616	2.23E+04	5.78E+03
PII-1/2I-G-3-CI-7	3-4 min	1 min	-3.057	102	17.5	99	2.616	2.616	3.77E+04	6.80E+03
PII-1/2I-G-3-CI-8	3-4 min	1 min	-0.932	63	7.5	56	2.616	2.616	2.15E+04	2.97E+03
PII-1/2I-G-3-CI-9	3-4 min	1 min	2.229	244	42.8	244	2.616	2.616	9.33E+04	1.66E+04
PII-1/2I-G-4-CI-1	9-11 min	2 min	2.134	35	6.9	10	2.618	5.236	1.97E+03	1.43E+03
PII-1/2I-G-4-CI-2	9-11 min	2 min	-1.693	5	3.1	-3	2.618	5.236	-6.37E+02	8.31E+02
PII-1/2I-G-4-CI-3	9-11 min	2 min	-0.763	30	7.8	25	2.618	5.236	4.77E+03	1.51E+03
PII-1/2I-G-4-CI-4	9-11 min	2 min	-4.011	100	35.3	96	2.618	5.236	1.83E+04	6.77E+03
PII-1/2I-G-4-CI-5	9-11 min	2 min	-1.020	156	59.0	154	2.618	5.236	2.94E+04	1.13E+04
PII-1/2I-G-4-CI-6	9-11 min	2 min	-3.994	74	18.1	71	2.618	5.236	1.36E+04	3.48E+03
PII-1/2I-G-4-CI-7	9-11 min	2 min	-2.815	180	30.2	177	2.618	5.236	3.37E+04	5.86E+03
PII-1/2I-G-4-CI-8	9-11 min	2 min	-2.497	275	26.8	268	2.618	5.236	5.12E+04	5.35E+03
PII-1/2I-G-4-CI-9	9-11 min	2 min	2.501	216	38.2	216	2.618	5.236	4.13E+04	7.41E+03
PII-1/2I-G-5-CI-1	21-25 min	4 min	1.795	38	7.3	13	2.656	10.626	1.25E+03	7.39E+02
PII-1/2I-G-5-CI-2	21-25 min	4 min	-2.660	13	6.1	5	2.656	10.626	4.39E+02	6.42E+02
PII-1/2I-G-5-CI-3	21-25 min	4 min	-3.899	31	7.9	26	2.656	10.626	2.45E+03	7.56E+02
PII-1/2I-G-5-CI-4	21-25 min	4 min	-1.628	36	12.8	32	2.656	10.626	2.98E+03	1.21E+03
PII-1/2I-G-5-CI-5	21-25 min	4 min	-0.872	89	33.9	87	2.656	10.626	8.19E+03	3.20E+03
PII-1/2I-G-5-CI-6	21-25 min	4 min	-2.871	67	16.6	64	2.656	10.626	6.05E+03	1.57E+03
PII-1/2I-G-5-CI-7	21-25 min	4 min	-1.018	159	26.8	156	2.656	10.626	1.46E+04	2.56E+03

Table A.26 (cont'd). Phase II, Shots 1/2, Gunner

Sample ID	Collection Interval	Elapsed Time	Total Mass (mg)	Calculated U (μg)	DU Mass ± 1σ (μg)	Net DU Mass (μg)	Flow Rate (Lpm)	Volume (L)	DU Conc. (μg/m^3)	DU Conc. ± 1σ (μg/m^3)
PII-1/2I-G-5-CI-8	21-25 min	4 min	-3.012	149	15.3	142	2.656	10.626	1.34E+04	1.50E+03
PII-1/2I-G-5-CI-9	21-25 min	4 min	3.245	242	42.5	242	2.656	10.626	2.28E+04	4.06E+03
PII-1/2I-G-6-CI-1	45-53 min	8 min	1.619	23	4.7	-2	2.699	21.594	-7.72E+01	2.55E+02
PII-1/2I-G-6-CI-2	45-53 min	8 min	-1.814	25	11.7	17	2.699	21.594	7.72E+02	5.60E+02
PII-1/2I-G-6-CI-3	45-53 min	8 min	-3.883	8	2.7	3	2.699	21.594	1.39E+02	1.37E+02
PII-1/2I-G-6-CI-4	45-53 min	8 min	-2.251	27	9.7	23	2.699	21.594	1.05E+03	4.54E+02
PII-1/2I-G-6-CI-5	45-53 min	8 min	-2.642	102	38.5	100	2.699	21.594	4.63E+03	1.79E+03
PII-1/2I-G-6-CI-6	45-53 min	8 min	0.203	63	15.4	60	2.699	21.594	2.79E+03	7.19E+02
PII-1/2I-G-6-CI-7	45-53 min	8 min	-4.976	101	17.6	98	2.699	21.594	4.52E+03	8.28E+02
PII-1/2I-G-6-CI-8	45-53 min	8 min	-2.670	134	13.9	127	2.699	21.594	5.90E+03	6.70E+02
PII-1/2I-G-6-CI-9	45-53 min	8 min	2.469	285	50.1	285	2.699	21.594	1.32E+04	2.35E+03
PII-1/2I-G-7-CI-1	93-109 min	16 min	1.827	20	4.0	-5	2.447	39.146	-1.19E+02	1.26E+02
PII-1/2I-G-7-CI-2	93-109 min	16 min	-1.575	10	5.0	2	2.447	39.146	4.26E+01	1.50E+02
PII-1/2I-G-7-CI-3	93-109 min	16 min	-0.205	10	2.7	5	2.447	39.146	1.28E+02	7.56E+01
PII-1/2I-G-7-CI-4	93-109 min	16 min	-1.839	29	10.6	25	2.447	39.146	6.30E+02	2.73E+02
PII-1/2I-G-7-CI-5	93-109 min	16 min	-2.182	145	54.9	143	2.447	39.146	3.65E+03	1.41E+03
PII-1/2I-G-7-CI-6	93-109 min	16 min	-4.026	68	16.8	65	2.447	39.146	1.67E+03	4.33E+02
PII-1/2I-G-7-CI-7	93-109 min	16 min	-1.489	112	19.3	109	2.447	39.146	2.78E+03	5.01E+02
PII-1/2I-G-7-CI-8	93-109 min	16 min	-1.713	190	19.1	183	2.447	39.146	4.68E+03	5.09E+02
PII-1/2I-G-7-CI-9	93-109 min	16 min	2.186	418	72.8	418	2.447	39.146	1.07E+04	1.89E+03
PII-1/2I-G-8-CI-1	Field Blank	--	1.301	24	4.8	--	--	--	--	--
PII-1/2I-G-8-CI-2	Field Blank	--	-0.418	4	2.2	--	--	--	--	--
PII-1/2I-G-8-CI-3	Field Blank	--	-0.604	12	3.3	--	--	--	--	--
PII-1/2I-G-8-CI-4	Field Blank	--	-0.934	8	3.2	--	--	--	--	--
PII-1/2I-G-8-CI-5	Field Blank	--	-3.183	8	3.2	--	--	--	--	--
PII-1/2I-G-8-CI-6	Field Blank	--	-1.392	4	1.7	--	--	--	--	--
PII-1/2I-G-8-CI-7	Field Blank	--	-0.590	5	1.9	--	--	--	--	--
PII-1/2I-G-8-CI-8	Field Blank	--	-0.392	7	2.1	--	--	--	--	--
PII-1/2I-G-8-CI-9	Field Blank	--	1.320	3	2.6	--	--	--	--	--
PII-1/2I-G-9-CI-1	Field Blank	--	1.330	31	6.0	--	--	--	--	--
PII-1/2I-G-9-CI-2	Field Blank	--	-1.633	18	8.7	--	--	--	--	--
PII-1/2I-G-9-CI-3	Field Blank	--	-4.341	2	1.0	--	--	--	--	--
PII-1/2I-G-9-CI-4	Field Blank	--	-2.076	1	1.1	--	--	--	--	--
PII-1/2I-G-9-CI-5	Field Blank	--	-1.721	-1	1.1	--	--	--	--	--
PII-1/2I-G-9-CI-6	Field Blank	--	-2.106	1	1.0	--	--	--	--	--
PII-1/2I-G-9-CI-7	Field Blank	--	-2.120	0	1.3	--	--	--	--	--
PII-1/2I-G-9-CI-8	Field Blank	--	-0.160	8	1.9	--	--	--	--	--
PII-1/2I-G-9-CI-9	Field Blank	--	0.691	-3	2.5	--	--	--	--	--

(a) DU mass based on ICP-MS results; no analytical uncertainty was reported.

Table A.26 (cont'd). Phase II, Shots 1/2 Loader

Sample ID	Collection Interval	Elapsed Time	Total Mass (mg)	Calculated U (μg)	DU Mass ± 1σ (μg)	Net DU Mass (μg)	Flow Rate (Lpm)	Volume (L)	DU Conc. (μg/m^3)	DU Conc. ± 1σ (μg/m^3)
PII-1/2I-L-1-CI-1	Shot 1: 0-10 sec	10 sec	2.410	108	19.8	108	2.443	0.407	2.65E+05	4.93E+04
PII-1/2I-L-1-CI-2	Shot 1: 0-10 sec	10 sec	0.108	18	8.7	18	2.443	0.407	4.42E+04	2.14E+04
PII-1/2I-L-1-CI-3	Shot 1: 0-10 sec	10 sec	-1.402	15	4.0	15	2.443	0.407	3.69E+04	9.89E+03
PII-1/2I-L-1-CI-4	Shot 1: 0-10 sec	10 sec	-0.825	18	6.8	18	2.443	0.407	4.42E+04	1.68E+04
PII-1/2I-L-1-CI-5	Shot 1: 0-10 sec	10 sec	-0.124	38	14.7	38	2.443	0.407	9.34E+04	3.62E+04
PII-1/2I-L-1-CI-6	Shot 1: 0-10 sec	10 sec	-0.452	36	9.1	36	2.443	0.407	8.85E+04	2.25E+04
PII-1/2I-L-1-CI-7	Shot 1: 0-10 sec	10 sec	0.346	39	7.3	39	2.443	0.407	9.58E+04	1.82E+04
PII-1/2I-L-1-CI-8	Shot 1: 0-10 sec	10 sec	-1.857	104	10.8	104	2.443	0.407	2.56E+05	2.76E+04
PII-1/2I-L-1-CI-9	Shot 1: 0-10 sec	10 sec	0.946	162	28.3	162	2.443	0.407	3.98E+05	7.06E+04
PII-1/2I-L-2-CI-1	3-4 min	1 min	0.587	52	9.8	52	2.419	2.419	2.15E+04	4.10E+03
PII-1/2I-L-2-CI-2	3-4 min	1 min	0.284	28	13.0	28	2.419	2.419	1.16E+04	5.39E+03
PII-1/2I-L-2-CI-3	3-4 min	1 min	-2.141	29	7.5	29	2.419	2.419	1.20E+04	3.12E+03
PII-1/2I-L-2-CI-4	3-4 min	1 min	-0.140	97	34.5	97	2.419	2.419	4.01E+04	1.43E+04
PII-1/2I-L-2-CI-5	3-4 min	1 min	-0.666	144	54.2	144	2.419	2.419	5.95E+04	2.25E+04
PII-1/2I-L-2-CI-6	3-4 min	1 min	-2.597	138	33.3	138	2.419	2.419	5.70E+04	1.39E+04
PII-1/2I-L-2-CI-7	3-4 min	1 min	-1.993	80	13.7	80	2.419	2.419	3.31E+04	5.75E+03
PII-1/2I-L-2-CI-8	3-4 min	1 min	0.600	114	11.6	114	2.419	2.419	4.71E+04	5.00E+03
PII-1/2I-L-2-CI-9	3-4 min	1 min	1.890	478	82.3	478	2.419	2.419	1.98E+05	3.45E+04
PII-1/2I-L-3-CI-1	9-11 min	2 min	2.036	105	19.2	105	2.571	5.142	2.04E+04	3.78E+03
PII-1/2I-L-3-CI-2	9-11 min	2 min	-0.882	32	14.9	32	2.571	5.142	6.22E+03	2.90E+03
PII-1/2I-L-3-CI-3	9-11 min	2 min	-3.620	55	13.9	55	2.571	5.142	1.07E+04	2.72E+03
PII-1/2I-L-3-CI-4	9-11 min	2 min	0.174	226	79.8	226	2.571	5.142	4.40E+04	1.56E+04
PII-1/2I-L-3-CI-5	9-11 min	2 min	1.884	215	81.2	215	2.571	5.142	4.18E+04	1.58E+04
PII-1/2I-L-3-CI-6	9-11 min	2 min	1.069	137	32.9	137	2.571	5.142	2.66E+04	6.45E+03
PII-1/2I-L-3-CI-7	9-11 min	2 min	2.273	116	19.6	116	2.571	5.142	2.26E+04	3.87E+03
PII-1/2I-L-3-CI-8	9-11 min	2 min	-0.594	118	12.3	118	2.571	5.142	2.29E+04	2.49E+03
PII-1/2I-L-3-CI-9	9-11 min	2 min	1.208	208	36.2	208	2.571	5.142	4.05E+04	7.14E+03
PII-1/2I-L-4-CI-1	Shot 2: 0-10 sec	10 sec	1.110	105	19.3	105	2.560	0.427	2.46E+05	4.58E+04
PII-1/2I-L-4-CI-2	Shot 2: 0-10 sec	10 sec	0.319	31	14.6	31	2.560	0.427	7.26E+04	3.43E+04
PII-1/2I-L-4-CI-3	Shot 2: 0-10 sec	10 sec	-1.362	46	11.6	46	2.560	0.427	1.08E+05	2.74E+04
PII-1/2I-L-4-CI-4	Shot 2: 0-10 sec	10 sec	-0.162	68	24.1	68	2.560	0.427	1.59E+05	5.66E+04
PII-1/2I-L-4-CI-5	Shot 2: 0-10 sec	10 sec	-2.826	76	29.0	76	2.560	0.427	1.78E+05	6.81E+04
PII-1/2I-L-4-CI-6	Shot 2: 0-10 sec	10 sec	-1.460	44	10.9	44	2.560	0.427	1.03E+05	2.57E+04
PII-1/2I-L-4-CI-7	Shot 2: 0-10 sec	10 sec	-0.513	66	11.2	66	2.560	0.427	1.55E+05	2.66E+04
PII-1/2I-L-4-CI-8	Shot 2: 0-10 sec	10 sec	-0.146	66	7.2	66	2.560	0.427	1.55E+05	1.75E+04
PII-1/2I-L-4-CI-9	Shot 2: 0-10 sec	10 sec	0.849	177	31.0	177	2.560	0.427	4.15E+05	7.37E+04
PII-1/2I-L-5-CI-1	3-4 min	1 min	1.770	54	10.1	54	2.560	2.560	2.11E+04	4.00E+03
PII-1/2I-L-5-CI-2	3-4 min	1 min	-0.087	22	10.3	22	2.560	2.560	8.59E+03	4.03E+03
PII-1/2I-L-5-CI-3	3-4 min	1 min	0.889	37	9.2	37	2.560	2.560	1.45E+04	3.62E+03
PII-1/2I-L-5-CI-4	3-4 min	1 min	0.730	52	18.4	52	2.560	2.560	2.03E+04	7.21E+03
PII-1/2I-L-5-CI-5	3-4 min	1 min	1.056	95	36.1	95	2.560	2.560	3.71E+04	1.41E+04
PII-1/2I-L-5-CI-6	3-4 min	1 min	0.902	100	24.2	100	2.560	2.560	3.91E+04	9.53E+03

Table A.26 (cont'd). Phase II, Shots 1/2 Loader

Sample ID	Collection Interval	Elapsed Time	Total Mass (mg)	Calculated U (μg)	DU Mass ± 1σ (μg)	Net DU Mass (μg)	Flow Rate (Lpm)	Volume (L)	DU Conc. (μg/m^3)	DU Conc. ± 1σ (μg/m^3)
PII-1/2I-L-5-CI-7	3-4 min	1 min	-0.422	152	25.5	152	2.560	2.560	5.94E+04	1.01E+04
PII-1/2I-L-5-CI-8	3-4 min	1 min	1.197	145	14.7	145	2.560	2.560	5.66E+04	5.99E+03
PII-1/2I-L-5-CI-9	3-4 min	1 min	1.331	174	30.3	174	2.560	2.560	6.80E+04	1.20E+04
PII-1/2I-L-6-CI-1	9-11 min	2 min	1.604	48	9.2	48	2.523	5.046	9.51E+03	1.85E+03
PII-1/2I-L-6-CI-2	9-11 min	2 min	-0.397	27	12.8	27	2.523	5.046	5.35E+03	2.54E+03
PII-1/2I-L-6-CI-3	9-11 min	2 min	-0.609	23	5.9	23	2.523	5.046	4.56E+03	1.18E+03
PII-1/2I-L-6-CI-4	9-11 min	2 min	1.043	102	36.1	102	2.523	5.046	2.02E+04	7.18E+03
PII-1/2I-L-6-CI-5	9-11 min	2 min	-0.843	60	22.9	60	2.523	5.046	1.19E+04	4.55E+03
PII-1/2I-L-6-CI-6	9-11 min	2 min	-0.293	79	19.1	79	2.523	5.046	1.57E+04	3.81E+03
PII-1/2I-L-6-CI-7	9-11 min	2 min	0.432	166	27.4	166	2.523	5.046	3.29E+04	5.52E+03
PII-1/2I-L-6-CI-8	9-11 min	2 min	-0.793	170	16.8	170	2.523	5.046	3.37E+04	3.48E+03
PII-1/2I-L-6-CI-9	9-11 min	2 min	1.266	229	39.9	229	2.523	5.046	4.54E+04	8.02E+03
PII-1/2I-L-7-CI-1	21-25 min	4 min	1.962	63	11.7	63	2.464	9.858	6.39E+03	1.20E+03
PII-1/2I-L-7-CI-2	21-25 min	4 min	-0.683	12	5.6	12	2.464	9.858	1.22E+03	5.69E+02
PII-1/2I-L-7-CI-3	21-25 min	4 min	-0.767	13	3.6	13	2.464	9.858	1.32E+03	3.67E+02
PII-1/2I-L-7-CI-4	21-25 min	4 min	0.881	54	19.2	54	2.464	9.858	5.48E+03	1.95E+03
PII-1/2I-L-7-CI-5	21-25 min	4 min	-1.001	55	20.8	55	2.464	9.858	5.58E+03	2.12E+03
PII-1/2I-L-7-CI-6	21-25 min	4 min	0.058	49	12.1	49	2.464	9.858	4.97E+03	1.24E+03
PII-1/2I-L-7-CI-7	21-25 min	4 min	0.923	115	19.3	115	2.464	9.858	1.17E+04	1.99E+03
PII-1/2I-L-7-CI-8	21-25 min	4 min	-2.490	87	9.1	87	2.464	9.858	8.83E+03	9.60E+02
PII-1/2I-L-7-CI-9	21-25 min	4 min	1.694	321	55.5	321	2.464	9.858	3.26E+04	5.71E+03
PII-1/2I-L-8-CI-1	45-53 min	8 min	0.634	110	20.2	110	2.510	20.077	5.48E+03	1.02E+03
PII-1/2I-L-8-CI-2	45-53 min	8 min	-1.039	9	4.4	9	2.510	20.077	4.48E+02	2.20E+02
PII-1/2I-L-8-CI-3	45-53 min	8 min	0.605	17	4.3	17	2.510	20.077	8.47E+02	2.16E+02
PII-1/2I-L-8-CI-4	45-53 min	8 min	-0.926	28	10.1	28	2.510	20.077	1.39E+03	5.05E+02
PII-1/2I-L-8-CI-5	45-53 min	8 min	-0.281	72	27.4	72	2.510	20.077	3.59E+03	1.37E+03
PII-1/2I-L-8-CI-6	45-53 min	8 min	-1.385	67	16.4	67	2.510	20.077	3.34E+03	8.23E+02
PII-1/2I-L-8-CI-7	45-53 min	8 min	-1.937	92	15.8	92	2.510	20.077	4.58E+03	7.99E+02
PII-1/2I-L-8-CI-8	45-53 min	8 min	-1.902	95	10.0	95	2.510	20.077	4.73E+03	5.18E+02
PII-1/2I-L-8-CI-9	45-53 min	8 min	0.678	316	54.7	316	2.510	20.077	1.57E+04	2.77E+03
PII-1/2I-L-9-CI-1	93-109 min	16 min	1.738	78	14.4	78	2.525	40.396	1.93E+03	3.61E+02
PII-1/2I-L-9-CI-2	93-109 min	16 min	0.376	22	10.5	22	2.525	40.396	5.45E+02	2.60E+02
PII-1/2I-L-9-CI-3	93-109 min	16 min	-1.257	12	3.1	12	2.525	40.396	2.97E+02	7.73E+01
PII-1/2I-L-9-CI-4	93-109 min	16 min	-2.254	27	9.9	27	2.525	40.396	6.68E+02	2.46E+02
PII-1/2I-L-9-CI-5	93-109 min	16 min	-1.205	67	25.5	67	2.525	40.396	1.66E+03	6.33E+02
PII-1/2I-L-9-CI-6	93-109 min	16 min	0.450	65	15.9	65	2.525	40.396	1.61E+03	3.97E+02
PII-1/2I-L-9-CI-7	93-109 min	16 min	-3.023	109	18.2	109	2.525	40.396	2.70E+03	4.58E+02
PII-1/2I-L-9-CI-8	93-109 min	16 min	0.218	115	11.9	115	2.525	40.396	2.85E+03	3.07E+02
PII-1/2I-L-9-CI-9	93-109 min	16 min	-0.028	168	29.2	168	2.525	40.396	4.16E+03	7.34E+02

Table A.27. PII-3 Cascade Impactor Substrates—Mass, Volume, and Concentration

Sample ID	Collection Interval	Elapsed Time	Total Mass (mg)	Calculated U (μg)	DU Mass ± 1σ (μg)	Net DU Mass (μg)	Flow Rate (Lpm)	Volume (L)	DU Conc. (μg/m^3)	DU Conc. ± 1σ (μg/m^3)
PII-3I-C-1-CI-1	Field Blank	--	0.490	19	4.1	--	--	--	--	--
PII-3I-C-1-CI-2	Field Blank	--	0.800	12	5.7	--	--	--	--	--
PII-3I-C-1-CI-3	Field Blank	--	-0.480	8	2.3	--	--	--	--	--
PII-3I-C-1-CI-4	Field Blank	--	-0.264	5	2.1	--	--	--	--	--
PII-3I-C-1-CI-5	Field Blank	--	-0.262	5	2.1	--	--	--	--	--
PII-3I-C-1-CI-6	Field Blank	--	-2.822	6	1.7	--	--	--	--	--
PII-3I-C-1-CI-7	Field Blank	--	-0.519	6	1.5	--	--	--	--	--
PII-3I-C-1-CI-8	Field Blank	--	-0.986	8	1.8	--	--	--	--	--
PII-3I-C-1-CI-9	Field Blank	--	-0.943	16	3.3	--	--	--	--	--
PII-3I-C-2-CI-1	0-10 sec	10 sec	1.407	56	10.6	37	2.566	0.428	8.64E+04	2.67E+04
PII-3I-C-2-CI-2	0-10 sec	10 sec	-0.194	26	12.0	14	2.566	0.428	3.27E+04	3.11E+04
PII-3I-C-2-CI-3	0-10 sec	10 sec	-0.754	23	6.0	15	2.566	0.428	3.50E+04	1.51E+04
PII-3I-C-2-CI-4	0-10 sec	10 sec	-0.613	18	6.7	13	2.566	0.428	3.04E+04	1.64E+04
PII-3I-C-2-CI-5	0-10 sec	10 sec	-0.195	28	10.8	23	2.566	0.428	5.37E+04	2.58E+04
PII-3I-C-2-CI-6	0-10 sec	10 sec	-0.705	17	4.6	11	2.566	0.428	2.57E+04	1.15E+04
PII-3I-C-2-CI-7	0-10 sec	10 sec	0.271	18	3.8	12	2.566	0.428	2.80E+04	9.58E+03
PII-3I-C-2-CI-8	0-10 sec	10 sec	-0.077	33	4.0	25	2.566	0.428	5.84E+04	1.04E+04
PII-3I-C-2-CI-9	0-10 sec	10 sec	-1.074	86	15.7	70	2.566	0.428	1.64E+05	3.78E+04
PII-3I-C-3-CI-1	1-1 min 10 sec	10 sec	0.002	25	4.6	6	2.628	0.438	1.37E+04	1.41E+04
PII-3I-C-3-CI-2	1-1 min 10 sec	10 sec	-0.125	7	3.4	-5	2.628	0.438	-1.14E+04	1.52E+04
PII-3I-C-3-CI-3	1-1 min 10 sec	10 sec	-0.303	9	2.6	1	2.628	0.438	2.28E+03	7.93E+03
PII-3I-C-3-CI-4	1-1 min 10 sec	10 sec	0.060	8	3.3	3	2.628	0.438	6.85E+03	8.93E+03
PII-3I-C-3-CI-5	1-1 min 10 sec	10 sec	-0.309	19	7.7	14	2.628	0.438	3.20E+04	1.82E+04
PII-3I-C-3-CI-6	1-1 min 10 sec	10 sec	-0.071	10	2.8	4	2.628	0.438	9.13E+03	7.48E+03
PII-3I-C-3-CI-7	1-1 min 10 sec	10 sec	-1.402	12	2.8	6	2.628	0.438	1.37E+04	7.26E+03
PII-3I-C-3-CI-8	1-1 min 10 sec	10 sec	-0.778	7	2.0	-1	2.628	0.438	-2.28E+03	6.14E+03
PII-3I-C-3-CI-9	1-1 min 10 sec	10 sec	-0.008	24	4.9	8	2.628	0.438	1.83E+04	1.35E+04
PII-3I-C-4-CI-1	3-3 min 15 sec	15 sec	1.284	28	5.6	9	2.451	0.613	1.47E+04	1.13E+04
PII-3I-C-4-CI-2	3-3 min 15 sec	15 sec	-0.959	2	1.4	-10	2.451	0.613	-1.63E+04	9.59E+03
PII-3I-C-4-CI-3	3-3 min 15 sec	15 sec	-0.630	3	1.1	-5	2.451	0.613	-8.16E+03	4.17E+03
PII-3I-C-4-CI-4	3-3 min 15 sec	15 sec	-1.746	6	2.5	1	2.451	0.613	1.63E+03	5.33E+03
PII-3I-C-4-CI-5	3-3 min 15 sec	15 sec	-0.481	4.9	2.3	-0.1	2.451	0.613	-1.63E+02	5.08E+03
PII-3I-C-4-CI-6	3-3 min 15 sec	15 sec	-0.487	4	1.7	-2	2.451	0.613	-3.26E+03	3.92E+03
PII-3I-C-4-CI-7	3-3 min 15 sec	15 sec	-0.800	3	1.4	-3	2.451	0.613	-4.89E+03	3.35E+03
PII-3I-C-4-CI-8	3-3 min 15 sec	15 sec	-0.704	6	1.9	-2	2.451	0.613	-3.26E+03	4.27E+03
PII-3I-C-4-CI-9	3-3 min 15 sec	15 sec	-0.962	16.5	3.8	1	2.451	0.613	8.16E+02	8.21E+03
PII-3I-C-5-CI-1	7-8 min	1 min	-0.020	42	8.0	23	2.438	2.438	9.43E+03	3.70E+03
PII-3I-C-5-CI-2	7-8 min	1 min	0.764	10	4.8	-2	2.438	2.438	-8.20E+02	3.06E+03
PII-3I-C-5-CI-3	7-8 min	1 min	-2.103	7	2.2	-1	2.438	2.438	-4.10E+02	1.31E+03
PII-3I-C-5-CI-4	7-8 min	1 min	-1.961	6	2.7	1	2.438	2.438	4.10E+02	1.40E+03
PII-3I-C-5-CI-5	7-8 min	1 min	-0.275	20	7.7	15	2.438	2.438	6.15E+03	3.28E+03
PII-3I-C-5-CI-6	7-8 min	1 min	-4.764	16	4.5	10	2.438	2.438	4.10E+03	1.98E+03
PII-3I-C-5-CI-7	7-8 min	1 min	-2.473	14	3.3	8	2.438	2.438	3.28E+03	1.49E+03

Table A.27 (cont'd). Phase II, Shot 3, Commander

Sample ID	Collection Interval	Elapsed Time	Total Mass (mg)	Calculated U (μg)	DU Mass ± 1σ (μg)	Net DU Mass (μg)	Flow Rate (Lpm)	Volume (L)	DU Conc. (μg/m^3)	DU Conc. ± 1σ (μg/m^3)
PII-3I-C-5-CI-8	7-8 min	1 min	-0.642	45	5.6	37	2.438	2.438	1.52E+04	2.46E+03
PII-3I-C-5-CI-9	7-8 min	1 min	-1.812	45	8.6	29	2.438	2.438	1.19E+04	3.80E+03
PII-3I-C-6-CI-1	15-17 min	2 min	1.151	27	5.2	8	2.461	4.922	1.63E+03	1.35E+03
PII-3I-C-6-CI-2	15-17 min	2 min	-2.763	18	8.4	6	2.461	4.922	1.22E+03	2.06E+03
PII-3I-C-6-CI-3	15-17 min	2 min	-2.600	2	1.0	-6	2.461	4.922	-1.22E+03	5.11E+02
PII-3I-C-6-CI-4	15-17 min	2 min	-1.657	10	3.9	5	2.461	4.922	1.02E+03	9.00E+02
PII-3I-C-6-CI-5	15-17 min	2 min	-1.641	29	11.2	24	2.461	4.922	4.88E+03	2.32E+03
PII-3I-C-6-CI-6	15-17 min	2 min	0.147	32	8.1	26	2.461	4.922	5.28E+03	1.69E+03
PII-3I-C-6-CI-7	15-17 min	2 min	-0.487	29	5.6	23	2.461	4.922	4.67E+03	1.19E+03
PII-3I-C-6-CI-8	15-17 min	2 min	-0.510	73	8.1	65	2.461	4.922	1.32E+04	1.73E+03
PII-3I-C-6-CI-9	15-17 min	2 min	-0.793	94	17.0	78	2.461	4.922	1.58E+04	3.55E+03
PII-3I-C-7-CI-1	31-35 min	4 min	1.503	26	5.2	7	2.598	10.391	6.74E+02	6.38E+02
PII-3I-C-7-CI-2	31-35 min	4 min	-2.654	10	4.8	-2	2.598	10.391	-1.92E+02	7.17E+02
PII-3I-C-7-CI-3	31-35 min	4 min	-1.118	11	2.9	3	2.598	10.391	2.89E+02	3.56E+02
PII-3I-C-7-CI-4	31-35 min	4 min	-0.316	27	9.7	22	2.598	10.391	2.12E+03	9.57E+02
PII-3I-C-7-CI-5	31-35 min	4 min	-1.291	47	18.0	42	2.598	10.391	4.04E+03	1.75E+03
PII-3I-C-7-CI-6	31-35 min	4 min	-0.460	83	20.5	77	2.598	10.391	7.41E+03	1.99E+03
PII-3I-C-7-CI-7	31-35 min	4 min	-0.896	47	8.6	41	2.598	10.391	3.95E+03	8.48E+02
PII-3I-C-7-CI-8	31-35 min	4 min	-1.916	70	8.1	62	2.598	10.391	5.97E+03	8.18E+02
PII-3I-C-7-CI-9	31-35 min	4 min	-0.365	210	37.1	194	2.598	10.391	1.87E+04	3.63E+03
PII-3I-C-8-CI-1	61-69 min	8 min	0.707	23	4.7	4	2.487	19.900	2.01E+02	3.13E+02
PII-3I-C-8-CI-2	61-69 min	8 min	-0.783	5	2.7	-7	2.487	19.900	-3.52E+02	3.17E+02
PII-3I-C-8-CI-3	61-69 min	8 min	-2.571	9	2.5	1	2.487	19.900	5.03E+01	1.71E+02
PII-3I-C-8-CI-4	61-69 min	8 min	-0.957	22	8.1	17	2.487	19.900	8.54E+02	4.21E+02
PII-3I-C-8-CI-5	61-69 min	8 min	-0.816	71	27.1	66	2.487	19.900	3.32E+03	1.37E+03
PII-3I-C-8-CI-6	61-69 min	8 min	-0.931	114	27.8	108	2.487	19.900	5.43E+03	1.41E+03
PII-3I-C-8-CI-7	61-69 min	8 min	-1.230	50	9.1	44	2.487	19.900	2.21E+03	4.68E+02
PII-3I-C-8-CI-8	61-69 min	8 min	-0.546	91	10.1	83	2.487	19.900	4.17E+03	5.31E+02
PII-3I-C-8-CI-9	61-69 min	8 min	-1.244	249	43.9	233	2.487	19.900	1.17E+04	2.24E+03
PII-3I-C-9-CI-1	121-129 min	8 min	1.325	30	5.8	11	2.459	19.673	5.59E+02	3.61E+02
PII-3I-C-9-CI-2	121-129 min	8 min	-1.940	16	7.6	4	2.459	19.673	2.03E+02	4.83E+02
PII-3I-C-9-CI-3	121-129 min	8 min	-0.982	1	1.2	-7	2.459	19.673	-3.56E+02	1.32E+02
PII-3I-C-9-CI-4	121-129 min	8 min	-1.866	9	3.9	4	2.459	19.673	2.03E+02	2.25E+02
PII-3I-C-9-CI-5	121-129 min	8 min	-1.111	30	11.6	25	2.459	19.673	1.27E+03	6.00E+02
PII-3I-C-9-CI-6	121-129 min	8 min	-1.001	73	17.9	67	2.459	19.673	3.41E+03	9.20E+02
PII-3I-C-9-CI-7	121-129 min	8 min	-3.419	45	8.5	39	2.459	19.673	1.98E+03	4.43E+02
PII-3I-C-9-CI-8	121-129 min	8 min	-0.001	87	9.6	79	2.459	19.673	4.02E+03	5.11E+02
PII-3I-C-9-CI-9	121-129 min	8 min	-1.246	154	27.2	138	2.459	19.673	7.01E+03	1.41E+03

Table A.27 (cont'd). Phase II, Shot 3, Driver

Sample ID	Collection Interval	Elapsed Time	Total Mass (mg)	Calculated U (μg)	DU Mass ± 1σ (μg)	Net DU Mass (μg)	Flow Rate (Lpm)	Volume (L)	DU Conc. (μg/m^3)	DU Conc. ± 1σ (μg/m^3)
PII-3I-D-1-CI-1	0-10 sec	10 sec	1.808	34	6.5	17	2.519	0.420	4.05E+04	1.76E+04
PII-3I-D-1-CI-2	0-10 sec	10 sec	0.419	13	6.4	11	2.519	0.420	2.62E+04	1.57E+04
PII-3I-D-1-CI-3	0-10 sec	10 sec	0.259	24	6.1	19	2.519	0.420	4.52E+04	1.51E+04
PII-3I-D-1-CI-4	0-10 sec	10 sec	0.099	22	8.1	8	2.519	0.420	1.90E+04	2.29E+04
PII-3I-D-1-CI-5	0-10 sec	10 sec	-0.260	19.1	7.5	0.1	2.519	0.420	2.38E+02	2.48E+04
PII-3I-D-1-CI-6	0-10 sec	10 sec	1.052	18.2	4.8	0.2	2.519	0.420	4.76E+02	1.58E+04
PII-3I-D-1-CI-7	0-10 sec	10 sec	0.008	17	3.6	13	2.519	0.420	3.10E+04	9.43E+03
PII-3I-D-1-CI-8	0-10 sec	10 sec	1.612	26	3.3	21	2.519	0.420	5.00E+04	8.58E+03
PII-3I-D-1-CI-9	0-10 sec	10 sec	0.378	46	8.6	46	2.519	0.420	1.10E+05	2.09E+04
PII-3I-D-2-CI-1	1-1 min 10 sec	10 sec	0.388	25	5.1	8	2.514	0.419	1.91E+04	1.48E+04
PII-3I-D-2-CI-2	1-1 min 10 sec	10 sec	-0.158	4	2.5	2	2.514	0.419	4.77E+03	6.96E+03
PII-3I-D-2-CI-3	1-1 min 10 sec	10 sec	0.476	9	2.6	4	2.514	0.419	9.55E+03	7.29E+03
PII-3I-D-2-CI-4	1-1 min 10 sec	10 sec	0.632	11	4.1	-3	2.514	0.419	-7.16E+03	1.58E+04
PII-3I-D-2-CI-5	1-1 min 10 sec	10 sec	-0.540	11	4.4	-8	2.514	0.419	-1.91E+04	2.01E+04
PII-3I-D-2-CI-6	1-1 min 10 sec	10 sec	0.577	15	4.1	-3	2.514	0.419	-7.16E+03	1.47E+04
PII-3I-D-2-CI-7	1-1 min 10 sec	10 sec	-0.125	10	2.3	6	2.514	0.419	1.43E+04	6.70E+03
PII-3I-D-2-CI-8	1-1 min 10 sec	10 sec	0.305	11	1.9	6	2.514	0.419	1.43E+04	5.51E+03
PII-3I-D-2-CI-9	1-1 min 10 sec	10 sec	0.608	14	3.0	14	2.514	0.419	3.34E+04	7.69E+03
PII-3I-D-3-CI-1	3-3 min 15 sec	15 sec	2.041	10	2.4	-7	2.696	0.674	-1.04E+04	6.30E+03
PII-3I-D-3-CI-2	3-3 min 15 sec	15 sec	-0.762	1	1.1	-1	2.696	0.674	-1.48E+03	2.76E+03
PII-3I-D-3-CI-3	3-3 min 15 sec	15 sec	-1.066	5.3	1.7	0.3	2.696	0.674	4.45E+02	3.46E+03
PII-3I-D-3-CI-4	3-3 min 15 sec	15 sec	-0.636	10	3.6	-4	2.696	0.674	-5.93E+03	9.39E+03
PII-3I-D-3-CI-5	3-3 min 15 sec	15 sec	-0.685	16	6.4	-3	2.696	0.674	-4.45E+03	1.43E+04
PII-3I-D-3-CI-6	3-3 min 15 sec	15 sec	-1.562	6	1.9	-12	2.696	0.674	-1.78E+04	7.40E+03
PII-3I-D-3-CI-7	3-3 min 15 sec	15 sec	0.199	8	2.4	4	2.696	0.674	5.93E+03	4.28E+03
PII-3I-D-3-CI-8	3-3 min 15 sec	15 sec	-0.160	17	2.5	12	2.696	0.674	1.78E+04	4.21E+03
PII-3I-D-3-CI-9	3-3 min 15 sec	15 sec	0.823	12	2.8	12	2.696	0.674	1.78E+04	4.50E+03
PII-3I-D-4-CI-1	7-8 min	1 min	1.309	13	2.7	-4	2.685	2.685	-1.49E+03	1.65E+03
PII-3I-D-4-CI-2	7-8 min	1 min	0.182	1.8	1.2	-0.2	2.685	2.685	-7.45E+01	7.15E+02
PII-3I-D-4-CI-3	7-8 min	1 min	-0.924	6	1.9	1	2.685	2.685	3.72E+02	9.25E+02
PII-3I-D-4-CI-4	7-8 min	1 min	2.879	11	4.1	-3	2.685	2.685	-1.12E+03	2.47E+03
PII-3I-D-4-CI-5	7-8 min	1 min	2.131	24	9.3	5	2.685	2.685	1.86E+03	4.38E+03
PII-3I-D-4-CI-6	7-8 min	1 min	0.240	30	7.5	12	2.685	2.685	4.47E+03	3.28E+03
PII-3I-D-4-CI-7	7-8 min	1 min	-0.548	11	2.9	7	2.685	2.685	2.61E+03	1.24E+03
PII-3I-D-4-CI-8	7-8 min	1 min	0.367	27	3.8	22	2.685	2.685	8.19E+03	1.52E+03
PII-3I-D-4-CI-9	7-8 min	1 min	-0.891	44	8.2	44	2.685	2.685	1.64E+04	3.12E+03
PII-3I-D-5-CI-1	15-17 min	2 min	1.391	12	2.8	-5	2.625	5.250	-9.52E+02	8.54E+02
PII-3I-D-5-CI-2	15-17 min	2 min	1.471	4	2.1	2	2.625	5.250	3.81E+02	4.92E+02
PII-3I-D-5-CI-3	15-17 min	2 min	0.858	2	1.0	-3	2.625	5.250	-5.71E+02	3.60E+02
PII-3I-D-5-CI-4	15-17 min	2 min	0.492	15	5.7	1	2.625	5.250	1.90E+02	1.47E+03
PII-3I-D-5-CI-5	15-17 min	2 min	0.655	19.5	7.5	0.5	2.625	5.250	9.52E+01	1.98E+03
PII-3I-D-5-CI-6	15-17 min	2 min	0.461	30	7.7	12	2.625	5.250	2.29E+03	1.71E+03

Table A.27 (cont'd). Phase II, Shot 3, Driver

Sample ID	Collection Interval	Elapsed Time	Total Mass (mg)	Calculated U (μg)	DU Mass ± 1σ (μg)	Net DU Mass (μg)	Flow Rate (Lpm)	Volume (L)	DU Conc. (μg/m^3)	DU Conc. ± 1σ (μg/m^3)
PII-3I-D-5-CI-7	15-17 min	2 min	0.735	18	3.9	14	2.625	5.250	2.67E+03	8.07E+02
PII-3I-D-5-CI-8	15-17 min	2 min	0.585	44	5.3	39	2.625	5.250	7.43E+03	1.06E+03
PII-3I-D-5-CI-9	15-17 min	2 min	-0.626	92	NA[(a)]	92	2.625	5.250	1.75E+04	NA (a)
PII-3I-D-6-CI-1	31-35 min	4 min	0.595	23	4.7	6	2.655	10.621	5.65E+02	5.52E+02
PII-3I-D-6-CI-2	31-35 min	4 min	0.145	2.4	1.5	0.4	2.655	10.621	3.77E+01	2.00E+02
PII-3I-D-6-CI-3	31-35 min	4 min	-0.076	6	1.9	1	2.655	10.621	9.42E+01	2.34E+02
PII-3I-D-6-CI-4	31-35 min	4 min	-0.669	16	5.8	2	2.655	10.621	1.88E+02	7.33E+02
PII-3I-D-6-CI-5	31-35 min	4 min	-0.993	36	14.1	17	2.655	10.621	1.60E+03	1.49E+03
PII-3I-D-6-CI-6	31-35 min	4 min	1.150	69	17.0	51	2.655	10.621	4.80E+03	1.66E+03
PII-3I-D-6-CI-7	31-35 min	4 min	1.581	47	8.5	43	2.655	10.621	4.05E+03	8.23E+02
PII-3I-D-6-CI-8	31-35 min	4 min	3.019	91	9.7	86	2.655	10.621	8.10E+03	9.53E+02
PII-3I-D-6-CI-9	31-35 min	4 min	0.535	92	16.5	92	2.655	10.621	8.66E+03	1.58E+03
PII-3I-D-7-CI-1	61-69 min	8 min	1.774	20	4.0	3	2.590	20.718	1.45E+02	2.57E+02
PII-3I-D-7-CI-2	61-69 min	8 min	2.058	3	NA[(a)]	1	2.590	20.718	4.83E+01	NA[(a)]
PII-3I-D-7-CI-3	61-69 min	8 min	0.569	4	1.5	-1	2.590	20.718	-4.83E+01	1.06E+02
PII-3I-D-7-CI-4	61-69 min	8 min	-0.464	24	8.9	10	2.590	20.718	4.83E+02	4.98E+02
PII-3I-D-7-CI-5	61-69 min	8 min	0.234	107	40.6	88	2.590	20.718	4.25E+03	1.99E+03
PII-3I-D-7-CI-6	61-69 min	8 min	-1.140	102	24.9	84	2.590	20.718	4.05E+03	1.23E+03
PII-3I-D-7-CI-7	61-69 min	8 min	-0.392	54	9.7	50	2.590	20.718	2.41E+03	4.80E+02
PII-3I-D-7-CI-8	61-69 min	8 min	-1.037	99	10.4	94	2.590	20.718	4.54E+03	5.24E+02
PII-3I-D-7-CI-9	61-69 min	8 min	0.221	117	20.8	117	2.590	20.718	5.65E+03	1.02E+03
PII-3I-D-8-CI-1	121-129 min	8 min	0.389	29	5.8	12	2.688	21.504	5.58E+02	3.15E+02
PII-3I-D-8-CI-2	121-129 min	8 min	-0.710	6	2.8	4	2.688	21.504	1.86E+02	1.48E+02
PII-3I-D-8-CI-3	121-129 min	8 min	-0.480	4	1.5	-1	2.688	21.504	-4.65E+01	1.02E+02
PII-3I-D-8-CI-4	121-129 min	8 min	-0.393	10	4.0	-4	2.688	21.504	-1.86E+02	3.05E+02
PII-3I-D-8-CI-5	121-129 min	8 min	-0.860	66	25.2	47	2.688	21.504	2.19E+03	1.22E+03
PII-3I-D-8-CI-6	121-129 min	8 min	-0.161	72	17.7	54	2.688	21.504	2.51E+03	8.54E+02
PII-3I-D-8-CI-7	121-129 min	8 min	-0.142	36	6.8	32	2.688	21.504	1.49E+03	3.28E+02
PII-3I-D-8-CI-8	121-129 min	8 min	-0.474	95	10.0	90	2.688	21.504	4.19E+03	4.85E+02
PII-3I-D-8-CI-9	121-129 min	8 min	-1.626	449	NA[(a)]	449	2.688	21.504	2.09E+04	NA[(a)]
PII-3I-D-9-CI-1	Field Blank	--	1.249	17	3.5	--	--	--	--	--
PII-3I-D-9-CI-2	Field Blank	--	0.547	2	1.5	--	--	--	--	--
PII-3I-D-9-CI-3	Field Blank	--	-0.143	5	1.6	--	--	--	--	--
PII-3I-D-9-CI-4	Field Blank	--	0.014	14	5.2	--	--	--	--	--
PII-3I-D-9-CI-5	Field Blank	--	0.440	19	7.2	--	--	--	--	--
PII-3I-D-9-CI-6	Field Blank	--	0.144	18	4.6	--	--	--	--	--
PII-3I-D-9-CI-7	Field Blank	--	0.520	4	1.6	--	--	--	--	--
PII-3I-D-9-CI-8	Field Blank	--	-0.652	5	1.3	--	--	--	--	--
PII-3I-D-9-CI-9	Field Blank	--	-0.519	0	1.1	--	--	--	--	--

(a) DU mass based on ICP-MS results; no analytical uncertainty was reported.

Table A.27 (cont'd). Phase II, Shot 3, Right Scout

Sample ID	Collection Interval	Elapsed Time	Total Mass (mg)	Calculated U (μg)	DU Mass ± 1σ (μg)	Net DU Mass (μg)	Flow Rate (Lpm)	Volume (L)	DU Conc. (μg/m^3)	DU Conc. ± 1σ (μg/m^3)
PII-3I-G-1-CI-1	0-10 sec	10 sec	2.393	18	2.8	3	2.723	0.454	6.61E+03	8.27E+03
PII-3I-G-1-CI-2	0-10 sec	10 sec	-2.507	7	3.2	3	2.723	0.454	6.61E+03	8.56E+03
PII-3I-G-1-CI-3	0-10 sec	10 sec	-0.449	17	3.5	17	2.723	0.454	3.74E+04	7.99E+03
PII-3I-G-1-CI-4	0-10 sec	10 sec	-0.722	22	6.0	22	2.723	0.454	4.85E+04	1.36E+04
PII-3I-G-1-CI-5	0-10 sec	10 sec	-0.512	25	10.2	25	2.723	0.454	5.51E+04	2.28E+04
PII-3I-G-1-CI-6	0-10 sec	10 sec	-0.067	23	10.3	19	2.723	0.454	4.19E+04	2.37E+04
PII-3I-G-1-CI-7	0-10 sec	10 sec	-1.635	8	4.8	8	2.723	0.454	1.76E+04	1.18E+04
PII-3I-G-1-CI-8	0-10 sec	10 sec	-0.126	16	7.6	15	2.723	0.454	3.30E+04	1.87E+04
PII-3I-G-1-CI-9	0-10 sec	10 sec	1.248	21	9.3	21	2.723	0.454	4.63E+04	2.13E+04
PII-3I-G-2-CI-1	Field Blank	--	2.556	15	2.5	--	--	--	--	
PII-3I-G-2-CI-2	Field Blank	--	1.021	4	2.2	--	--	--	--	
PII-3I-G-2-CI-3	Field Blank	--	-0.394	-1	0.8	--	--	--	--	
PII-3I-G-2-CI-4	Field Blank	--	2.425	-2	1.2	--	--	--	--	
PII-3I-G-2-CI-5	Field Blank	--	1.542	-2	1.6	--	--	--	--	
PII-3I-G-2-CI-6	Field Blank	--	1.865	4	3.1	--	--	--	--	
PII-3I-G-2-CI-7	Field Blank	--	-0.319	-3	2.4	--	--	--	--	
PII-3I-G-2-CI-8	Field Blank	--	0.419	1	3.8	--	--	--	--	
PII-3I-G-2-CI-9	Field Blank	--	1.317	0	2.5	--	--	--	--	
PII-3I-G-3-CI-1	1-1 min 10 sec	10 sec	2.930	10	2.0	-5	2.679	0.447	-1.12E+04	7.17E+03
PII-3I-G-3-CI-2	1-1 min 10 sec	10 sec	0.594	-1	1.3	-5	2.679	0.447	-1.12E+04	5.73E+03
PII-3I-G-3-CI-3	1-1 min 10 sec	10 sec	1.739	6	1.6	6	2.679	0.447	1.34E+04	4.02E+03
PII-3I-G-3-CI-4	1-1 min 10 sec	10 sec	1.551	5	2.0	5	2.679	0.447	1.12E+04	5.23E+03
PII-3I-G-3-CI-5	1-1 min 10 sec	10 sec	2.067	19	7.8	19	2.679	0.447	4.25E+04	1.79E+04
PII-3I-G-3-CI-6	1-1 min 10 sec	10 sec	2.621	8	4.8	4	2.679	0.447	8.95E+03	1.28E+04
PII-3I-G-3-CI-7	1-1 min 10 sec	10 sec	0.504	0.4	2.9	0.4	2.679	0.447	8.95E+02	8.42E+03
PII-3I-G-3-CI-8	1-1 min 10 sec	10 sec	1.725	6	6.3	5	2.679	0.447	1.12E+04	1.65E+04
PII-3I-G-3-CI-9	1-1 min 10 sec	10 sec	1.019	24	9.3	24	2.679	0.447	5.37E+04	2.16E+04
PII-3I-G-4-CI-1	3-3 min 15 sec	15 sec	3.341	18	2.8	3	2.685	0.671	4.47E+03	5.60E+03
PII-3I-G-4-CI-2	3-3 min 15 sec	15 sec	2.444	3	1.9	-1	2.685	0.671	-1.49E+03	4.33E+03
PII-3I-G-4-CI-3	3-3 min 15 sec	15 sec	0.549	1	1.0	1	2.685	0.671	1.49E+03	1.91E+03
PII-3I-G-4-CI-4	3-3 min 15 sec	15 sec	-1.210	10	3.0	10	2.685	0.671	1.49E+04	4.84E+03
PII-3I-G-4-CI-5	3-3 min 15 sec	15 sec	0.787	10	4.5	10	2.685	0.671	1.49E+04	7.13E+03
PII-3I-G-4-CI-6	3-3 min 15 sec	15 sec	0.360	19	8.5	15	2.685	0.671	2.24E+04	1.35E+04
PII-3I-G-4-CI-7	3-3 min 15 sec	15 sec	2.522	13	4.5	13	2.685	0.671	1.94E+04	7.62E+03
PII-3I-G-4-CI-8	3-3 min 15 sec	15 sec	0.241	11	7.0	10	2.685	0.671	1.49E+04	1.19E+04
PII-3I-G-4-CI-9	3-3 min 15 sec	15 sec	0.886	5	4.6	5	2.685	0.671	7.45E+03	7.81E+03
PII-3I-G-5-CI-1	7-8 min	1 min	0.979	10	2.0	-5	2.720	2.720	-1.84E+03	1.18E+03
PII-3I-G-5-CI-2	7-8 min	1 min	-0.352	-1	1.2	-5	2.720	2.720	-1.84E+03	9.23E+02
PII-3I-G-5-CI-3	7-8 min	1 min	1.114	-0.1	0.7	-0.1	2.720	2.720	-3.68E+01	3.91E+02
PII-3I-G-5-CI-4	7-8 min	1 min	0.343	4	1.7	4	2.720	2.720	1.47E+03	7.66E+02
PII-3I-G-5-CI-5	7-8 min	1 min	-0.415	22	9.1	22	2.720	2.720	8.09E+03	3.41E+03
PII-3I-G-5-CI-6	7-8 min	1 min	0.403	26	12.2	22	2.720	2.720	8.09E+03	4.63E+03
PII-3I-G-5-CI-7	7-8 min	1 min	-2.518	9	5.2	9	2.720	2.720	3.31E+03	2.11E+03

Table A.27 (cont'd). Phase II, Shot 3, Right Scout

Sample ID	Collection Interval	Elapsed Time	Total Mass (mg)	Calculated U (μg)	DU Mass ± 1σ (μg)	Net DU Mass (μg)	Flow Rate (Lpm)	Volume (L)	DU Conc. (μg/m^3)	DU Conc. ± 1σ (μg/m^3)
PII-3I-G-5-CI-8	7-8 min	1 min	0.918	21	10.7	20	2.720	2.720	7.35E+03	4.18E+03
PII-3I-G-5-CI-9	7-8 min	1 min	0.142	84	28.1	84	2.720	2.720	3.09E+04	1.04E+04
PII-3I-G-6-CI-1	15-17 min	2 min	2.578	9	2.1	-6	2.708	5.416	-1.11E+03	6.04E+02
PII-3I-G-6-CI-2	15-17 min	2 min	0.025	-1	1.4	-5	2.708	5.416	-9.23E+02	4.82E+02
PII-3I-G-6-CI-3	15-17 min	2 min	0.578	2	1.2	2	2.708	5.416	3.69E+02	2.67E+02
PII-3I-G-6-CI-4	15-17 min	2 min	0.865	9	2.7	9	2.708	5.416	1.66E+03	5.48E+02
PII-3I-G-6-CI-5	15-17 min	2 min	2.951	43	16.8	43	2.708	5.416	7.94E+03	3.13E+03
PII-3I-G-6-CI-6	15-17 min	2 min	0.721	77	32.1	73	2.708	5.416	1.35E+04	5.97E+03
PII-3I-G-6-CI-7	15-17 min	2 min	-0.869	49	12.7	49	2.708	5.416	9.05E+03	2.40E+03
PII-3I-G-6-CI-8	15-17 min	2 min	-0.418	66	18.2	65	2.708	5.416	1.20E+04	3.45E+03
PII-3I-G-6-CI-9	15-17 min	2 min	2.133	104	34.9	104	2.708	5.416	1.92E+04	6.49E+03
PII-3I-G-7-CI-1	31-35 min	4 min	1.408	10	2.1	-5	2.480	9.919	-5.04E+02	3.30E+02
PII-3I-G-7-CI-2	31-35 min	4 min	-2.076	12	5.0	8	2.480	9.919	8.07E+02	5.51E+02
PII-3I-G-7-CI-3	31-35 min	4 min	2.577	11	2.5	11	2.480	9.919	1.11E+03	2.67E+02
PII-3I-G-7-CI-4	31-35 min	4 min	1.826	25	7.1	25	2.480	9.919	2.52E+03	7.30E+02
PII-3I-G-7-CI-5	31-35 min	4 min	1.322	50	19.6	50	2.480	9.919	5.04E+03	1.99E+03
PII-3I-G-7-CI-6	31-35 min	4 min	0.894	96	40.3	92	2.480	9.919	9.28E+03	4.08E+03
PII-3I-G-7-CI-7	31-35 min	4 min	-0.007	53	14.1	53	2.480	9.919	5.34E+03	1.45E+03
PII-3I-G-7-CI-8	31-35 min	4 min	-0.289	160	38.1	159	2.480	9.919	1.60E+04	3.89E+03
PII-3I-G-7-CI-9	31-35 min	4 min	-0.007	80	28.7	80	2.480	9.919	8.07E+03	2.91E+03
PII-3I-G-8-CI-1	61-69 min	8 min	0.669	17	2.9	2	2.792	22.338	8.95E+01	1.71E+02
PII-3I-G-8-CI-2	61-69 min	8 min	0.074	2	1.5	-2	2.792	22.338	-8.95E+01	1.19E+02
PII-3I-G-8-CI-3	61-69 min	8 min	-0.791	5	1.4	5	2.792	22.338	2.24E+02	7.25E+01
PII-3I-G-8-CI-4	61-69 min	8 min	0.367	3	1.5	3	2.792	22.338	1.34E+02	8.61E+01
PII-3I-G-8-CI-5	61-69 min	8 min	0.335	8	3.6	8	2.792	22.338	3.58E+02	1.77E+02
PII-3I-G-8-CI-6	61-69 min	8 min	0.719	5	3.4	1	2.792	22.338	4.48E+01	2.06E+02
PII-3I-G-8-CI-7	61-69 min	8 min	-0.374	17	5.0	17	2.792	22.338	7.61E+02	2.49E+02
PII-3I-G-8-CI-8	61-69 min	8 min	1.195	25	7.2	24	2.792	22.338	1.07E+03	3.66E+02
PII-3I-G-8-CI-9	61-69 min	8 min	-0.193	25	8.2	25	2.792	22.338	1.12E+03	3.85E+02
PII-3I-G-9-CI-1	121-129 min	8 min	1.207	16	2.8	1	2.775	22.196	4.51E+01	1.69E+02
PII-3I-G-9-CI-2	121-129 min	8 min	1.312	13	5.2	9	2.775	22.196	4.05E+02	2.55E+02
PII-3I-G-9-CI-3	121-129 min	8 min	0.671	-0.3	0.8	-0.3	2.775	22.196	-1.35E+01	5.10E+01
PII-3I-G-9-CI-4	121-129 min	8 min	-1.038	-2	1.1	-2	2.775	22.196	-9.01E+01	7.34E+01
PII-3I-G-9-CI-5	121-129 min	8 min	0.622	-5	2.3	-5	2.775	22.196	-2.25E+02	1.26E+02
PII-3I-G-9-CI-6	121-129 min	8 min	-2.824	-1	2.1	-5	2.775	22.196	-2.25E+02	1.69E+02
PII-3I-G-9-CI-7	121-129 min	8 min	-2.454	-7	2.9	-7	2.775	22.196	-3.15E+02	1.70E+02
PII-3I-G-9-CI-8	121-129 min	8 min	0.917	30	7.3	29	2.775	22.196	1.31E+03	3.73E+02
PII-3I-G-9-CI-9	121-129 min	8 min	-0.493	1	2.5	1	2.775	22.196	4.51E+01	1.59E+02

Table A.27 (cont'd). Phase II, Shot 3, Left Scout

Sample ID	Collection Interval	Elapsed Time	Total Mass (mg)	Calculated U (μg)	DU Mass ± 1σ (μg)	Net DU Mass (μg)[(a)]	Flow Rate (Lpm)	Volume (L)	DU Conc. (μg/m^3)	DU Conc. ± 1σ (μg/m^3)
PII-3I-L-1-CI-1	0-10 sec	10 sec	1.806	90	12.7	73	2.438	0.406	1.80E+05	3.21E+04
PII-3I-L-1-CI-2	0-10 sec	10 sec	0.634	25	10.1	19	2.438	0.406	4.68E+04	2.54E+04
PII-3I-L-1-CI-3	0-10 sec	10 sec	-0.332	26	5.2	22	2.438	0.406	5.42E+04	1.31E+04
PII-3I-L-1-CI-4	0-10 sec	10 sec	1.041	19	5.5	13	2.438	0.406	3.28E+04	1.44E+04
PII-3I-L-1-CI-5	0-10 sec	10 sec	0.821	32	12.1	25	2.438	0.406	6.08E+04	3.05E+04
PII-3I-L-1-CI-6	0-10 sec	10 sec	-0.554	18	7.2	9	2.438	0.406	2.13E+04	1.84E+04
PII-3I-L-1-CI-7	0-10 sec	10 sec	1.016	12.7	3.9	10.4	2.438	0.406	2.55E+04	1.00E+04
PII-3I-L-1-CI-8	0-10 sec	10 sec	0.809	32	7.2	27	2.438	0.406	6.73E+04	1.82E+04
PII-3I-L-1-CI-9	0-10 sec	10 sec	-1.456	19	6.6	14	2.438	0.406	3.37E+04	1.67E+04
PII-3I-L-2-CI-1	1-1 min 10 sec	10 sec	1.655	44	6.6	27	2.518	0.420	6.43E+04	1.65E+04
PII-3I-L-2-CI-2	1-1 min 10 sec	10 sec	0.617	4.5	2.2	-1.5	2.518	0.420	2.38E+02	7.24E+03
PII-3I-L-2-CI-3	1-1 min 10 sec	10 sec	-0.183	14	2.9	10	2.518	0.420	2.38E+04	7.32E+03
PII-3I-L-2-CI-4	1-1 min 10 sec	10 sec	-0.014	10	3.2	4	2.518	0.420	1.03E+04	8.88E+03
PII-3I-L-2-CI-5	1-1 min 10 sec	10 sec	-0.014	13	5.2	6	2.518	0.420	1.35E+04	1.38E+04
PII-3I-L-2-CI-6	1-1 min 10 sec	10 sec	-0.180	18	7.0	9	2.518	0.420	2.06E+04	1.73E+04
PII-3I-L-2-CI-7	1-1 min 10 sec	10 sec	-0.046	20	5.7	18	2.518	0.420	4.21E+04	1.39E+04
PII-3I-L-2-CI-8	1-1 min 10 sec	10 sec	0.252	19	5.8	14	2.518	0.420	3.41E+04	1.43E+04
PII-3I-L-2-CI-9	1-1 min 10 sec	10 sec	-0.777	22.4	6.9	17.1	2.518	0.420	4.06E+04	1.68E+04
PII-3I-L-3-CI-1	3-3 min 15 sec	15 sec	1.207	24	3.7	7	2.572	0.643	1.09E+04	6.54E+03
PII-3I-L-3-CI-2	3-3 min 15 sec	15 sec	0.512	5	2.2	-1	2.572	0.643	1.56E+02	4.73E+03
PII-3I-L-3-CI-3	3-3 min 15 sec	15 sec	1.004	9	1.9	5	2.572	0.643	7.78E+03	3.33E+03
PII-3I-L-3-CI-4	3-3 min 15 sec	15 sec	0.289	8	2.7	2	2.572	0.643	3.63E+03	5.15E+03
PII-3I-L-3-CI-5	3-3 min 15 sec	15 sec	0.364	30	11.3	23	2.572	0.643	3.53E+04	1.80E+04
PII-3I-L-3-CI-6	3-3 min 15 sec	15 sec	0.146	22	8.4	13	2.572	0.643	1.97E+04	1.34E+04
PII-3I-L-3-CI-7	3-3 min 15 sec	15 sec	0.162	18	4.6	16	2.572	0.643	2.44E+04	7.39E+03
PII-3I-L-3-CI-8	3-3 min 15 sec	15 sec	0.496	28	7.3	23	2.572	0.643	3.63E+04	1.16E+04
PII-3I-L-3-CI-9	3-3 min 15 sec	15 sec	0.076	21	7.4	16	2.572	0.643	2.44E+04	1.17E+04
PII-3I-L-4-CI-1	7-8 min	1 min	1.175	25	4.0	8	2.549	2.549	3.14E+03	1.75E+03
PII-3I-L-4-CI-2	7-8 min	1 min	0.926	9	3.9	3	2.549	2.549	1.18E+03	1.74E+03
PII-3I-L-4-CI-3	7-8 min	1 min	0.496	9	2.2	5	2.549	2.549	1.96E+03	9.45E+02
PII-3I-L-4-CI-4	7-8 min	1 min	0.515	19	5.3	13	2.549	2.549	5.23E+03	2.22E+03
PII-3I-L-4-CI-5	7-8 min	1 min	0.276	38	14.5	31	2.549	2.549	1.20E+04	5.79E+03
PII-3I-L-4-CI-6	7-8 min	1 min	0.729	23	9.2	14	2.549	2.549	5.36E+03	3.69E+03
PII-3I-L-4-CI-7	7-8 min	1 min	0.199	14	4.9	12	2.549	2.549	4.58E+03	1.97E+03
PII-3I-L-4-CI-8	7-8 min	1 min	0.049	38	9.2	33	2.549	2.549	1.31E+04	3.68E+03
PII-3I-L-4-CI-9	7-8 min	1 min	0.715	40	12.4	35	2.549	2.549	1.36E+04	4.91E+03
PII-3I-L-5-CI-1	15-17 min	2 min	1.992	21	3.5	4	2.572	5.144	7.78E+02	7.82E+02
PII-3I-L-5-CI-2	15-17 min	2 min	0.657	5	2.4	-1	2.572	5.144	1.94E+01	6.20E+02
PII-3I-L-5-CI-3	15-17 min	2 min	-0.293	9	2.2	5	2.572	5.144	9.72E+02	4.68E+02
PII-3I-L-5-CI-4	15-17 min	2 min	0.495	24	6.9	18	2.572	5.144	3.56E+03	1.40E+03
PII-3I-L-5-CI-5	15-17 min	2 min	0.090	60	22.5	53	2.572	5.144	1.02E+04	4.41E+03
PII-3I-L-5-CI-6	15-17 min	2 min	0.967	39	14.9	30	2.572	5.144	5.77E+03	2.93E+03
PII-3I-L-5-CI-7	15-17 min	2 min	0.487	12.9	4.6	10.6	2.572	5.144	2.05E+03	9.21E+02

Table A.27 (cont'd). Phase II, Shot 3, Left Scout

Sample ID	Collection Interval	Elapsed Time	Total Mass (mg)	Calculated U (μg)	DU Mass ± 1σ (μg)	Net DU Mass (μg)	Flow Rate (Lpm)	Volume (L)	DU Conc. (μg/m^3)	DU Conc. ± 1σ (μg/m^3)
PII-3I-L-5-CI-8	15-17 min	2 min	1.396	27	8.9	22	2.572	5.144	4.34E+03	1.76E+03
PII-3I-L-5-CI-9	15-17 min	2 min	-0.081	82	23.5	77	2.572	5.144	1.49E+04	4.60E+03
PII-3I-L-6-CI-1	31-35 min	4 min	0.739	24	3.8	7	2.539	10.154	6.89E+02	4.23E+02
PII-3I-L-6-CI-2	31-35 min	4 min	-0.327	6	2.6	0	2.539	10.154	0.00E+00	#DIV/0!
PII-3I-L-6-CI-3	31-35 min	4 min	0.206	19	4.0	15	2.539	10.154	1.48E+03	4.08E+02
PII-3I-L-6-CI-4	31-35 min	4 min	1.004	34	9.4	28	2.539	10.154	2.79E+03	9.48E+02
PII-3I-L-6-CI-5	31-35 min	4 min	1.479	87	32.6	80	2.539	10.154	7.85E+03	3.23E+03
PII-3I-L-6-CI-6	31-35 min	4 min	0.466	84	30.4	75	2.539	10.154	7.35E+03	3.01E+03
PII-3I-L-6-CI-7	31-35 min	4 min	0.959	19	6.5	17	2.539	10.154	1.64E+03	6.51E+02
PII-3I-L-6-CI-8	31-35 min	4 min	0.914	60	14.6	55	2.539	10.154	5.45E+03	1.45E+03
PII-3I-L-6-CI-9	31-35 min	4 min	0.357	149	41.7	144	2.539	10.154	1.41E+04	4.13E+03
PII-3I-L-7-CI-1	61-69 min	8 min	2.173	34	5.1	17	2.478	19.827	8.57E+02	2.77E+02
PII-3I-L-7-CI-2	61-69 min	8 min	0.917	2	1.5	-4	2.478	19.827	-2.02E+02	1.30E+02
PII-3I-L-7-CI-3	61-69 min	8 min	-0.476	8	2.1	4	2.478	19.827	2.02E+02	1.17E+02
PII-3I-L-7-CI-4	61-69 min	8 min	1.343	30	8.6	24	2.478	19.827	1.23E+03	4.46E+02
PII-3I-L-7-CI-5	61-69 min	8 min	0.621	151	56.5	144	2.478	19.827	7.25E+03	2.86E+03
PII-3I-L-7-CI-6	61-69 min	8 min	0.623	123	44.4	114	2.478	19.827	5.73E+03	2.25E+03
PII-3I-L-7-CI-7	61-69 min	8 min	0.248	46	11.4	44	2.478	19.827	2.20E+03	5.81E+02
PII-3I-L-7-CI-8	61-69 min	8 min	0.489	133	24.8	128	2.478	19.827	6.47E+03	1.27E+03
PII-3I-L-7-CI-9	61-69 min	8 min	-0.472	174	47.2	169	2.478	19.827	8.51E+03	2.40E+03
PII-3I-L-8-CI-1	121-129 min	8 min	2.964	51	7.4	34	2.548	20.382	1.67E+03	3.79E+02
PII-3I-L-8-CI-2	121-129 min	8 min	0.004	6	2.6	0	2.548	20.382	0.00E+00	#DIV/0!
PII-3I-L-8-CI-3	121-129 min	8 min	1.298	2	1.1	-2	2.548	20.382	-9.81E+01	7.21E+01
PII-3I-L-8-CI-4	121-129 min	8 min	0.221	13	3.9	7	2.548	20.382	3.60E+02	2.13E+02
PII-3I-L-8-CI-5	121-129 min	8 min	1.029	118	44.0	111	2.548	20.382	5.43E+03	2.17E+03
PII-3I-L-8-CI-6	121-129 min	8 min	0.236	42	15.9	33	2.548	20.382	1.60E+03	7.87E+02
PII-3I-L-8-CI-7	121-129 min	8 min	-0.612	30	8.5	28	2.548	20.382	1.36E+03	4.22E+02
PII-3I-L-8-CI-8	121-129 min	8 min	2.015	76	16.6	71	2.548	20.382	3.50E+03	8.24E+02
PII-3I-L-8-CI-9	121-129 min	8 min	0.063	96	26.6	91	2.548	20.382	4.45E+03	1.31E+03
PII-3I-L-9-CI-1	Field Blank	--	2.177	32	5.1	--	--	--	--	--
PII-3I-L-9-CI-2	Field Blank	--	-0.031	4	1.9	--	--	--	--	--
PII-3I-L-9-CI-3	Field Blank	--	-0.087	3	1.1	--	--	--	--	--
PII-3I-L-9-CI-4	Field Blank	--	0.315	14	4.0	--	--	--	--	--
PII-3I-L-9-CI-5	Field Blank	--	0.483	26	9.9	--	--	--	--	--
PII-3I-L-9-CI-6	Field Blank	--	0.070	32	11.2	--	--	--	--	--
PII-3I-L-9-CI-7	Field Blank	--	2.044	13	3.5	--	--	--	--	--
PII-3I-L-9-CI-8	Field Blank	--	1.254	16	4.9	--	--	--	--	--
PII-3I-L-9-CI-9	Field Blank	--	-0.515	22	6.0	--	--	--	--	--

(a) The field blanks for the commander, driver, and gunner were averaged and substituted for the nonrepresentative loader's field blanks.

Table A.28. PIII-1 Cascade Impactor Substrates—Mass, Volume, and Concentration

Sample ID	Collection Interval	Elapsed Time	Total Mass (mg)	Calculated U (μg)	DU Mass ± 1σ (μg)	Net DU Mass (μg)	Flow Rate (Lpm)	Volume (L)	DU Conc. (μg/m^3)	DU Conc. ± 1σ (μg/m^3)
PIII-1I-C-1-CI-1	0-10 sec	10 sec	0.396	189	25.9	116	2.714	0.452	2.57E+05	6.21E+04
PIII-1I-C-1-CI-2	0-10 sec	10 sec	-0.512	105	41.3	86	2.714	0.452	1.90E+05	9.32E+04
PIII-1I-C-1-CI-3	0-10 sec	10 sec	1.416	184	34.1	180	2.714	0.452	3.98E+05	7.64E+04
PIII-1I-C-1-CI-4	0-10 sec	10 sec	1.501	164	43.4	159	2.714	0.452	3.52E+05	9.67E+04
PIII-1I-C-1-CI-5	0-10 sec	10 sec	-0.799	179	68.4	173	2.714	0.452	3.83E+05	1.52E+05
PIII-1I-C-1-CI-6	0-10 sec	10 sec	0.051	161	64.1	157	2.714	0.452	3.47E+05	1.42E+05
PIII-1I-C-1-CI-7	0-10 sec	10 sec	-0.236	93	21.8	78	2.714	0.452	1.73E+05	4.92E+04
PIII-1I-C-1-CI-8	0-10 sec	10 sec	-0.976	127	28.1	106	2.714	0.452	2.35E+05	6.36E+04
PIII-1I-C-1-CI-9	0-10 sec	10 sec	-0.065	70	22.7	57	2.714	0.452	1.26E+05	5.13E+04
PIII-1I-C-2-CI-1	1-1 min 10 sec	10 sec	0.689	157	21.5	84	2.651	0.442	1.90E+05	5.41E+04
PIII-1I-C-2-CI-2	1-1 min 10 sec	10 sec	0.103	53	21.1	34	2.651	0.442	7.69E+04	5.09E+04
PIII-1I-C-2-CI-3	1-1 min 10 sec	10 sec	-0.661	76	14.4	72	2.651	0.442	1.63E+05	3.30E+04
PIII-1I-C-2-CI-4	1-1 min 10 sec	10 sec	-2.117	86	22.8	81	2.651	0.442	1.83E+05	5.20E+04
PIII-1I-C-2-CI-5	1-1 min 10 sec	10 sec	0.253	166	63.4	160	2.651	0.442	3.62E+05	1.44E+05
PIII-1I-C-2-CI-6	1-1 min 10 sec	10 sec	-2.438	107	43.0	103	2.651	0.442	2.33E+05	9.77E+04
PIII-1I-C-2-CI-7	1-1 min 10 sec	10 sec	-0.906	39	10.2	24	2.651	0.442	5.43E+04	2.47E+04
PIII-1I-C-2-CI-8	1-1 min 10 sec	10 sec	-1.986	79	20.7	58	2.651	0.442	1.31E+05	4.84E+04
PIII-1I-C-2-CI-9	1-1 min 10 sec	10 sec	1.618	87	27.6	74	2.651	0.442	1.67E+05	6.35E+04
PIII-1I-C-3-CI-1	3-3 min 15 sec	15 sec	1.656	347	47.0	274	2.657	0.664	4.13E+05	7.35E+04
PIII-1I-C-3-CI-2	3-3 min 15 sec	15 sec	-0.665	35	14.2	16	2.657	0.664	2.41E+04	2.44E+04
PIII-1I-C-3-CI-3	3-3 min 15 sec	15 sec	-0.738	55	10.5	51	2.657	0.664	7.68E+04	1.61E+04
PIII-1I-C-3-CI-4	3-3 min 15 sec	15 sec	0.084	82	21.8	77	2.657	0.664	1.16E+05	3.31E+04
PIII-1I-C-3-CI-5	3-3 min 15 sec	15 sec	0.349	125	48.1	119	2.657	0.664	1.79E+05	7.28E+04
PIII-1I-C-3-CI-6	3-3 min 15 sec	15 sec	0.311	152	60.7	148	2.657	0.664	2.23E+05	9.18E+04
PIII-1I-C-3-CI-7	3-3 min 15 sec	15 sec	0.653	91	21.4	76	2.657	0.664	1.14E+05	3.29E+04
PIII-1I-C-3-CI-8	3-3 min 15 sec	15 sec	0.914	88	21.6	67	2.657	0.664	1.01E+05	3.36E+04
PIII-1I-C-3-CI-9	3-3 min 15 sec	15 sec	2.592	53	17.2	40	2.657	0.664	6.02E+04	2.68E+04
PIII-1I-C-4-CI-1	7-8 min	1 min	0.584	103	14.1	30	2.502	2.502	1.20E+04	6.96E+03
PIII-1I-C-4-CI-2	7-8 min	1 min	-0.445	26	10.4	7	2.502	2.502	2.80E+03	5.20E+03
PIII-1I-C-4-CI-3	7-8 min	1 min	0.725	25	5.1	21	2.502	2.502	8.39E+03	2.10E+03
PIII-1I-C-4-CI-4	7-8 min	1 min	1.353	119	31.5	114	2.502	2.502	4.56E+04	1.27E+04
PIII-1I-C-4-CI-5	7-8 min	1 min	0.698	214	82.0	208	2.502	2.502	8.31E+04	3.29E+04
PIII-1I-C-4-CI-6	7-8 min	1 min	0.601	126	50.6	122	2.502	2.502	4.88E+04	2.03E+04
PIII-1I-C-4-CI-7	7-8 min	1 min	0.006	118	28.1	103	2.502	2.502	4.12E+04	1.14E+04
PIII-1I-C-4-CI-8	7-8 min	1 min	0.501	229	48.6	208	2.502	2.502	8.31E+04	1.97E+04
PIII-1I-C-4-CI-9	7-8 min	1 min	3.419	56	18.4	43	2.502	2.502	1.72E+04	7.59E+03
PIII-1I-C-5-CI-1	15-17 min	2 min	1.865	138	19.0	65	2.499	4.997	1.30E+04	4.33E+03
PIII-1I-C-5-CI-2	15-17 min	2 min	-0.821	33	13.2	14	2.499	4.997	2.80E+03	3.07E+03
PIII-1I-C-5-CI-3	15-17 min	2 min	-2.064	16	3.4	12	2.499	4.997	2.40E+03	7.19E+02
PIII-1I-C-5-CI-4	15-17 min	2 min	-0.417	35	9.7	30	2.499	4.997	6.00E+03	1.98E+03
PIII-1I-C-5-CI-5	15-17 min	2 min	-0.376	78	30.3	72	2.499	4.997	1.44E+04	6.10E+03
PIII-1I-C-5-CI-6	15-17 min	2 min	-2.043	98	39.5	94	2.499	4.997	1.88E+04	7.94E+03
PIII-1I-C-5-CI-7	15-17 min	2 min	0.705	64	16.0	49	2.499	4.997	9.81E+03	3.30E+03

Table A.28 (cont'd). Phase III, Shot 1, Commander

Sample ID	Collection Interval	Elapsed Time	Total Mass (mg)	Calculated U (μg)	DU Mass ± 1σ (μg)	Net DU Mass (μg)	Flow Rate (Lpm)	Volume (L)	DU Conc. (μg/m^3)	DU Conc. ± 1σ (μg/m^3)
PIII-1I-C-5-CI-8	15-17 min	2 min	-0.206	122	27.0	101	2.499	4.997	2.02E+04	5.54E+03
PIII-1I-C-5-CI-9	15-17 min	2 min	1.615	36	11.8	23	2.499	4.997	4.60E+03	2.53E+03
PIII-1I-C-6-CI-1	31-35 min	4 min	1.305	116	16.0	43	2.494	9.978	4.31E+03	1.91E+03
PIII-1I-C-6-CI-2	31-35 min	4 min	-0.376	9	3.8	-10	2.494	9.978	-1.00E+03	8.70E+02
PIII-1I-C-6-CI-3	31-35 min	4 min	-1.127	3	1.1	-1	2.494	9.978	-1.00E+02	1.56E+02
PIII-1I-C-6-CI-4	31-35 min	4 min	-0.051	6	2.1	1	2.494	9.978	1.00E+02	2.65E+02
PIII-1I-C-6-CI-5	31-35 min	4 min	-1.335	54	20.9	48	2.494	9.978	4.81E+03	2.12E+03
PIII-1I-C-6-CI-6	31-35 min	4 min	-2.114	68	27.5	64	2.494	9.978	6.41E+03	2.78E+03
PIII-1I-C-6-CI-7	31-35 min	4 min	-2.292	47	13.1	32	2.494	9.978	3.21E+03	1.37E+03
PIII-1I-C-6-CI-8	31-35 min	4 min	0.716	71	17.7	50	2.494	9.978	5.01E+03	1.85E+03
PIII-1I-C-6-CI-9	31-35 min	4 min	0.311	10	4.9	-3	2.494	9.978	-3.01E+02	6.67E+02
PIII-1I-C-7-CI-1	61-69 min	8 min	1.259	61	8.6	-12	2.669	21.350	-5.62E+02	6.25E+02
PIII-1I-C-7-CI-2	61-69 min	8 min	-0.515	4	2.0	-15	2.669	21.350	-7.03E+02	3.78E+02
PIII-1I-C-7-CI-3	61-69 min	8 min	0.426	5	1.2	1	2.669	21.350	4.68E+01	7.63E+01
PIII-1I-C-7-CI-4	61-69 min	8 min	-0.054	8	2.6	3	2.669	21.350	1.41E+02	1.43E+02
PIII-1I-C-7-CI-5	61-69 min	8 min	-0.775	36	14.3	30	2.669	21.350	1.41E+03	6.83E+02
PIII-1I-C-7-CI-6	61-69 min	8 min	-2.255	46	19.0	42	2.669	21.350	1.97E+03	9.01E+02
PIII-1I-C-7-CI-7	61-69 min	8 min	-1.830	28	8.2	13	2.669	21.350	6.09E+02	4.24E+02
PIII-1I-C-7-CI-8	61-69 min	8 min	-0.297	46	13.2	25	2.669	21.350	1.17E+03	6.65E+02
PIII-1I-C-7-CI-9	61-69 min	8 min	3.042	17	7.2	4	2.669	21.350	1.87E+02	3.98E+02
PIII-1I-C-8-CI-1	121-129 min	8 min	0.519	88	12.2	15	2.553	20.422	7.35E+02	7.79E+02
PIII-1I-C-8-CI-2	121-129 min	8 min	-1.312	3	1.8	-16	2.553	20.422	-7.83E+02	3.93E+02
PIII-1I-C-8-CI-3	121-129 min	8 min	-0.399	5	1.2	1	2.553	20.422	4.90E+01	7.97E+01
PIII-1I-C-8-CI-4	121-129 min	8 min	-1.912	7	2.2	2	2.553	20.422	9.79E+01	1.33E+02
PIII-1I-C-8-CI-5	121-129 min	8 min	0.110	14	5.9	8	2.553	20.422	3.92E+02	3.18E+02
PIII-1I-C-8-CI-6	121-129 min	8 min	0.106	31	13.2	27	2.553	20.422	1.32E+03	6.62E+02
PIII-1I-C-8-CI-7	121-129 min	8 min	0.472	14	4.8	-1	2.553	20.422	-4.90E+01	3.00E+02
PIII-1I-C-8-CI-8	121-129 min	8 min	0.492	27	NA[(a)]	6	2.553	20.422	2.94E+02	NA[(a)]
PIII-1I-C-8-CI-9	121-129 min	8 min	0.433	25	9.0	12	2.553	20.422	5.88E+02	4.93E+02
PIII-1I-C-9-CI-1	Field Blank	--	1.880	73	10.2	--	--	--	--	--
PIII-1I-C-9-CI-2	Field Blank	--	-0.292	19	7.8	--	--	--	--	--
PIII-1I-C-9-CI-3	Field Blank	--	-0.228	4	1.1	--	--	--	--	--
PIII-1I-C-9-CI-4	Field Blank	--	0.329	5	1.6	--	--	--	--	--
PIII-1I-C-9-CI-5	Field Blank	--	-1.917	6	2.7	--	--	--	--	--
PIII-1I-C-9-CI-6	Field Blank	--	-1.007	4	2.8	--	--	--	--	--
PIII-1I-C-9-CI-7	Field Blank	--	0.339	15	3.8	--	--	--	--	--
PIII-1I-C-9-CI-8	Field Blank	--	-0.252	21	5.2	--	--	--	--	--
PIII-1I-C-9-CI-9	Field Blank	--	3.360	13	4.5	--	--	--	--	--

(a) DU mass based on ICP-MS results; no analytical uncertainty was reported.

Table A.28 (cont'd). Phase III, Shot 1, Driver

Sample ID	Collection Interval	Elapsed Time	Total Mass (mg)	Calculated U (μg)	DU Mass ± 1σ (μg)	Net DU Mass (μg)	Flow Rate (Lpm)	Volume (L)	DU Conc. (μg/m^3)	DU Conc. ± 1σ (μg/m^3)
PIII-1I-D-1-CI-1	0-10 sec	10 sec	1.392	303	55.9	209	2.535	0.422	4.95E+05	1.40E+05
PIII-1I-D-1-CI-2	0-10 sec	10 sec	-3.720	33	15.5	15	2.535	0.422	3.55E+04	4.21E+04
PIII-1I-D-1-CI-3	0-10 sec	10 sec	-3.418	58	15.0	55	2.535	0.422	1.30E+05	3.59E+04
PIII-1I-D-1-CI-4	0-10 sec	10 sec	-2.413	50	18.3	46	2.535	0.422	1.09E+05	4.37E+04
PIII-1I-D-1-CI-5	0-10 sec	10 sec	-1.159	96	36.8	96	2.535	0.422	2.27E+05	8.75E+04
PIII-1I-D-1-CI-6	0-10 sec	10 sec	-4.726	44	11.0	41	2.535	0.422	9.72E+04	2.64E+04
PIII-1I-D-1-CI-7	0-10 sec	10 sec	-4.805	43	7.6	43	2.535	0.422	1.02E+05	1.85E+04
PIII-1I-D-1-CI-8	0-10 sec	10 sec	-4.306	58	6.5	49	2.535	0.422	1.16E+05	1.64E+04
PIII-1I-D-1-CI-9	0-10 sec	10 sec	-1.475	1060	NA[(a)]	1048	2.535	0.422	2.48E+06	NA[(a)]
PIII-1I-D-2-CI-1	1-1 min 10 sec	10 sec	0.981	470	86.5	376	2.492	0.415	9.06E+05	2.14E+05
PIII-1I-D-2-CI-2	1-1 min 10 sec	10 sec	-4.148	26	12.4	8	2.492	0.415	1.93E+04	3.65E+04
PIII-1I-D-2-CI-3	1-1 min 10 sec	10 sec	-1.188	56	14.5	53	2.492	0.415	1.28E+05	3.53E+04
PIII-1I-D-2-CI-4	1-1 min 10 sec	10 sec	-4.496	94	34.1	90	2.492	0.415	2.17E+05	8.25E+04
PIII-1I-D-2-CI-5	1-1 min 10 sec	10 sec	-0.777	102	38.9	102	2.492	0.415	2.46E+05	9.41E+04
PIII-1I-D-2-CI-6	1-1 min 10 sec	10 sec	-2.248	78	18.9	75	2.492	0.415	1.81E+05	4.60E+04
PIII-1I-D-2-CI-7	1-1 min 10 sec	10 sec	-2.122	49	8.8	49	2.492	0.415	1.18E+05	2.17E+04
PIII-1I-D-2-CI-8	1-1 min 10 sec	10 sec	-0.603	62	7.0	53	2.492	0.415	1.28E+05	1.79E+04
PIII-1I-D-2-CI-9	1-1 min 10 sec	10 sec	0.040	95	16.8	83	2.492	0.415	2.00E+05	4.16E+04
PIII-1I-D-3-CI-1	3-3 min 15 sec	15 sec	1.119	70	13.3	-24	2.700	0.675	-3.56E+04	3.27E+04
PIII-1I-D-3-CI-2	3-3 min 15 sec	15 sec	-4.370	17	8.1	-1	2.700	0.675	-1.48E+03	1.76E+04
PIII-1I-D-3-CI-3	3-3 min 15 sec	15 sec	-2.725	43	11.3	40	2.700	0.675	5.93E+04	1.70E+04
PIII-1I-D-3-CI-4	3-3 min 15 sec	15 sec	-3.993	73	26.4	69	2.700	0.675	1.02E+05	3.93E+04
PIII-1I-D-3-CI-5	3-3 min 15 sec	15 sec	-2.354	164	62.5	164	2.700	0.675	2.43E+05	9.29E+04
PIII-1I-D-3-CI-6	3-3 min 15 sec	15 sec	-2.094	74	18.0	71	2.700	0.675	1.05E+05	2.69E+04
PIII-1I-D-3-CI-7	3-3 min 15 sec	15 sec	-3.030	46	8.5	46	2.700	0.675	6.81E+04	1.29E+04
PIII-1I-D-3-CI-8	3-3 min 15 sec	15 sec	-1.793	59	6.9	50	2.700	0.675	7.41E+04	1.08E+04
PIII-1I-D-3-CI-9	3-3 min 15 sec	15 sec	-0.616	37	7.0	25	2.700	0.675	3.70E+04	1.14E+04
PIII-1I-D-4-CI-1	7-8 min	1 min	0.430	97	18.0	3	2.686	2.686	1.12E+03	9.37E+03
PIII-1I-D-4-CI-2	7-8 min	1 min	-2.253	9	4.2	-9	2.686	2.686	-3.35E+03	3.60E+03
PIII-1I-D-4-CI-3	7-8 min	1 min	-1.727	68	NA[(a)]	65	2.686	2.686	2.42E+04	NA[(a)]
PIII-1I-D-4-CI-4	7-8 min	1 min	-3.321	86	31.4	82	2.686	2.686	3.05E+04	1.17E+04
PIII-1I-D-4-CI-5	7-8 min	1 min	-1.007	82	31.4	82	2.686	2.686	3.05E+04	1.17E+04
PIII-1I-D-4-CI-6	7-8 min	1 min	-1.220	104	25.1	101	2.686	2.686	3.76E+04	9.42E+03
PIII-1I-D-4-CI-7	7-8 min	1 min	-1.294	121	20.4	121	2.686	2.686	4.50E+04	7.73E+03
PIII-1I-D-4-CI-8	7-8 min	1 min	-2.774	152	15.2	143	2.686	2.686	5.32E+04	5.92E+03
PIII-1I-D-4-CI-9	7-8 min	1 min	-1.926	71	12.9	59	2.686	2.686	2.20E+04	4.98E+03
PIII-1I-D-5-CI-1	15-17 min	2 min	0.527	27	5.2	-67	2.617	5.235	-1.28E+04	3.53E+03
PIII-1I-D-5-CI-2	15-17 min	2 min	-1.551	12	5.7	-6	2.617	5.235	-1.15E+03	1.99E+03
PIII-1I-D-5-CI-3	15-17 min	2 min	-1.686	19	5.0	16	2.617	5.235	3.06E+03	9.96E+02
PIII-1I-D-5-CI-4	15-17 min	2 min	-2.715	28	10.2	24	2.617	5.235	4.58E+03	1.98E+03
PIII-1I-D-5-CI-5	15-17 min	2 min	-1.488	103	NA[(a)]	103	2.617	5.235	1.97E+04	NA[(a)]
PIII-1I-D-5-CI-6	15-17 min	2 min	-1.841	61	14.9	58	2.617	5.235	1.11E+04	2.87E+03
PIII-1I-D-5-CI-7	15-17 min	2 min	-1.619	106	18.0	106	2.617	5.235	2.02E+04	3.50E+03

Table A.28 (cont'd). Phase III, Shot 1, Driver

Sample ID	Collection Interval	Elapsed Time	Total Mass (mg)	Calculated U (μg)	DU Mass ± 1σ (μg)	Net DU Mass (μg)	Flow Rate (Lpm)	Volume (L)	DU Conc. (μg/m^3)	DU Conc. ± 1σ (μg/m^3)
PIII-1I-D-5-CI-8	15-17 min	2 min	-3.727	136	13.6	127	2.617	5.235	2.43E+04	2.72E+03
PIII-1I-D-5-CI-9	15-17 min	2 min	-0.719	57	10.4	45	2.617	5.235	8.60E+03	2.09E+03
PIII-1I-D-6-CI-1	31-35 min	4 min	0.445	16	3.4	-78	2.660	10.639	-7.33E+03	1.70E+03
PIII-1I-D-6-CI-2	31-35 min	4 min	-2.011	19	9.0	1	2.660	10.639	9.40E+01	1.18E+03
PIII-1I-D-6-CI-3	31-35 min	4 min	-0.925	4	1.5	1	2.660	10.639	9.40E+01	1.93E+02
PIII-1I-D-6-CI-4	31-35 min	4 min	-0.515	7	2.7	3	2.660	10.639	2.82E+02	3.05E+02
PIII-1I-D-6-CI-5	31-35 min	4 min	-2.152	48	18.6	48	2.660	10.639	4.51E+03	1.76E+03
PIII-1I-D-6-CI-6	31-35 min	4 min	-0.868	66	16.1	63	2.660	10.639	5.92E+03	1.53E+03
PIII-1I-D-6-CI-7	31-35 min	4 min	-1.643	78	13.5	78	2.660	10.639	7.33E+03	1.29E+03
PIII-1I-D-6-CI-8	31-35 min	4 min	-0.530	55	6.2	46	2.660	10.639	4.32E+03	6.23E+02
PIII-1I-D-6-CI-9	31-35 min	4 min	-2.255	25	4.9	13	2.660	10.639	1.22E+03	5.46E+02
PIII-1I-D-7-CI-1	61-69 min	8 min	0.227	48	NA[(a)]	-46	2.589	20.712	-2.22E+03	NA[(a)]
PIII-1I-D-7-CI-2	61-69 min	8 min	-1.542	15	7.2	-3	2.589	20.712	-1.45E+02	5.45E+02
PIII-1I-D-7-CI-3	61-69 min	8 min	-2.313	3.3	1.2	0.3	2.589	20.712	1.45E+01	8.90E+01
PIII-1I-D-7-CI-4	61-69 min	8 min	-3.304	6	2.5	2	2.589	20.712	9.66E+01	1.49E+02
PIII-1I-D-7-CI-5	61-69 min	8 min	-2.693	15	6.0	15	2.589	20.712	7.24E+02	2.96E+02
PIII-1I-D-7-CI-6	61-69 min	8 min	-4.153	20	5.3	17	2.589	20.712	8.21E+02	2.64E+02
PIII-1I-D-7-CI-7	61-69 min	8 min	-0.084	31	5.9	31	2.589	20.712	1.50E+03	2.93E+02
PIII-1I-D-7-CI-8	61-69 min	8 min	-0.146	42	4.8	33	2.589	20.712	1.59E+03	2.54E+02
PIII-1I-D-7-CI-9	61-69 min	8 min	-1.976	27	5.2	15	2.589	20.712	7.24E+02	2.93E+02
PIII-1I-D-8-CI-1	121-129 min	8 min	2.451	80	15.4	-14	2.669	21.354	-6.56E+02	1.10E+03
PIII-1I-D-8-CI-2	121-129 min	8 min	0.319	10	4.8	-8	2.669	21.354	-3.75E+02	4.65E+02
PIII-1I-D-8-CI-3	121-129 min	8 min	-2.141	11	3.1	8	2.669	21.354	3.75E+02	1.60E+02
PIII-1I-D-8-CI-4	121-129 min	8 min	-0.939	13	4.9	9	2.669	21.354	4.21E+02	2.45E+02
PIII-1I-D-8-CI-5	121-129 min	8 min	-2.113	19	7.3	19	2.669	21.354	8.90E+02	3.47E+02
PIII-1I-D-8-CI-6	121-129 min	8 min	-1.665	21	5.5	18	2.669	21.354	8.43E+02	2.65E+02
PIII-1I-D-8-CI-7	121-129 min	8 min	-2.345	20	4.1	20	2.669	21.354	9.37E+02	2.01E+02
PIII-1I-D-8-CI-8	121-129 min	8 min	-0.748	42	5.0	33	2.669	21.354	1.55E+03	2.55E+02
PIII-1I-D-8-CI-9	121-129 min	8 min	-2.454	53	9.5	41	2.669	21.354	1.92E+03	4.71E+02
PIII-1I-D-9-CI-1	Field Blank	--	0.912	94	17.6	--	--	--	--	--
PIII-1I-D-9-CI-2	Field Blank	--	-1.556	18	8.7	--	--	--	--	--
PIII-1I-D-9-CI-3	Field Blank	--	-0.930	3	1.4	--	--	--	--	--
PIII-1I-D-9-CI-4	Field Blank	--	-1.052	4	1.8	--	--	--	--	--
PIII-1I-D-9-CI-5	Field Blank	--	-1.512	0	1.2	--	--	--	--	--
PIII-1I-D-9-CI-6	Field Blank	--	-1.013	3	1.2	--	--	--	--	--
PIII-1I-D-9-CI-7	Field Blank	--	-1.975	0	1.1	--	--	--	--	--
PIII-1I-D-9-CI-8	Field Blank	--	-1.460	9	1.9	--	--	--	--	--
PIII-1I-D-9-CI-9	Field Blank	--	-2.749	12	3.1	--	--	--	--	--

(a) DU mass based on ICP-MS results; no analytical uncertainty was reported.

Table A.28 (cont'd). Phase III, Shot 1, Gunner

Sample ID	Collection Interval	Elapsed Time	Total Mass (mg)	Calculated U (μg)	DU Mass ± 1σ (μg)	Net DU Mass (μg)	Flow Rate (Lpm)	Volume (L)	DU Conc. (μg/m^3)	DU Conc. ± 1σ (μg/m^3)
PIII-1I-G-1-CI-1	0-10 sec	10 sec	2.743	464	62.4	375	2.783	0.464	8.08E+05	1.39E+05
PIII-1I-G-1-CI-2	0-10 sec	10 sec	-3.955	148	58.4	130	2.783	0.464	2.80E+05	1.27E+05
PIII-1I-G-1-CI-3	0-10 sec	10 sec	-2.346	235	43.2	234	2.783	0.464	5.04E+05	9.44E+04
PIII-1I-G-1-CI-4	0-10 sec	10 sec	-1.495	171	44.9	168	2.783	0.464	3.62E+05	9.74E+04
PIII-1I-G-1-CI-5	0-10 sec	10 sec	-0.262	245	94.9	238	2.783	0.464	5.13E+05	2.05E+05
PIII-1I-G-1-CI-6	0-10 sec	10 sec	1.140	251	107.6	239	2.783	0.464	5.15E+05	2.33E+05
PIII-1I-G-1-CI-7	0-10 sec	10 sec	-1.246	124	30.7	121	2.783	0.464	2.61E+05	6.70E+04
PIII-1I-G-1-CI-8	0-10 sec	10 sec	1.917	117	31.0	102	2.783	0.464	2.20E+05	6.88E+04
PIII-1I-G-1-CI-9	0-10 sec	10 sec	-0.302	89	30.6	53	2.783	0.464	1.14E+05	7.15E+04
PIII-1I-G-2-CI-1	Field Blank	--	0.871	89	12.5	--	--	--	--	--
PIII-1I-G-2-CI-2	Field Blank	--	0.270	18	7.4	--	--	--	--	--
PIII-1I-G-2-CI-3	Field Blank	--	-0.170	1	1.3	--	--	--	--	--
PIII-1I-G-2-CI-4	Field Blank	--	-1.033	3	1.6	--	--	--	--	--
PIII-1I-G-2-CI-5	Field Blank	--	-1.499	7	3.6	--	--	--	--	--
PIII-1I-G-2-CI-6	Field Blank	--	-0.750	12	6.2	--	--	--	--	--
PIII-1I-G-2-CI-7	Field Blank	--	0.509	3	3.2	--	--	--	--	--
PIII-1I-G-2-CI-8	Field Blank	--	-0.650	15	7.0	--	--	--	--	--
PIII-1I-G-2-CI-9	Field Blank	--	0.686	36	12.7	--	--	--	--	--
PIII-1I-G-3-CI-1	1-1 min 10 sec	10 sec	0.890	58	8.6	-31	2.700	0.450	-6.89E+04	3.38E+04
PIII-1I-G-3-CI-2	1-1 min 10 sec	10 sec	0.579	64	25.5	46	2.700	0.450	1.02E+05	5.91E+04
PIII-1I-G-3-CI-3	1-1 min 10 sec	10 sec	-1.422	50	9.5	49	2.700	0.450	1.09E+05	2.16E+04
PIII-1I-G-3-CI-4	1-1 min 10 sec	10 sec	-0.285	112	29.6	109	2.700	0.450	2.42E+05	6.63E+04
PIII-1I-G-3-CI-5	1-1 min 10 sec	10 sec	-1.070	189	73.5	182	2.700	0.450	4.04E+05	1.64E+05
PIII-1I-G-3-CI-6	1-1 min 10 sec	10 sec	-1.185	164	70.8	152	2.700	0.450	3.38E+05	1.58E+05
PIII-1I-G-3-CI-7	1-1 min 10 sec	10 sec	-0.065	143	34.8	140	2.700	0.450	3.11E+05	7.82E+04
PIII-1I-G-3-CI-8	1-1 min 10 sec	10 sec	-0.018	111	29.9	96	2.700	0.450	2.13E+05	6.85E+04
PIII-1I-G-3-CI-9	1-1 min 10 sec	10 sec	1.345	59	20.4	23	2.700	0.450	5.11E+04	5.34E+04
PIII-1I-G-4-CI-1	3-3 min 15 sec	15 sec	-0.032	51	7.3	-38	2.711	0.678	-5.60E+04	2.14E+04
PIII-1I-G-4-CI-2	3-3 min 15 sec	15 sec	-0.020	16	6.6	-2	2.711	0.678	-2.95E+03	1.46E+04
PIII-1I-G-4-CI-3	3-3 min 15 sec	15 sec	0.100	56	10.6	55	2.711	0.678	8.11E+04	1.59E+04
PIII-1I-G-4-CI-4	3-3 min 15 sec	15 sec	-1.448	89	23.6	86	2.711	0.678	1.27E+05	3.51E+04
PIII-1I-G-4-CI-5	3-3 min 15 sec	15 sec	-1.523	117	45.5	110	2.711	0.678	1.62E+05	6.75E+04
PIII-1I-G-4-CI-6	3-3 min 15 sec	15 sec	-0.135	107	46.5	95	2.711	0.678	1.40E+05	6.93E+04
PIII-1I-G-4-CI-7	3-3 min 15 sec	15 sec	-2.327	71	18.4	68	2.711	0.678	1.00E+05	2.77E+04
PIII-1I-G-4-CI-8	3-3 min 15 sec	15 sec	-1.910	67	22.2	52	2.711	0.678	7.67E+04	3.44E+04
PIII-1I-G-4-CI-9	3-3 min 15 sec	15 sec	0.626	28	11.4	-8	2.711	0.678	-1.18E+04	2.52E+04
PIII-1I-G-5-CI-1	7-8 min	1 min	2.247	29	4.4	-60	2.733	2.733	-2.20E+04	4.89E+03
PIII-1I-G-5-CI-2	7-8 min	1 min	-3.223	35	14.0	17	2.733	2.733	6.22E+03	5.80E+03
PIII-1I-G-5-CI-3	7-8 min	1 min	-1.123	36	7.1	35	2.733	2.733	1.28E+04	2.67E+03
PIII-1I-G-5-CI-4	7-8 min	1 min	-1.981	71	18.8	68	2.733	2.733	2.49E+04	6.94E+03
PIII-1I-G-5-CI-5	7-8 min	1 min	-3.338	157	61.2	150	2.733	2.733	5.49E+04	2.25E+04
PIII-1I-G-5-CI-6	7-8 min	1 min	-0.757	88	38.6	76	2.733	2.733	2.78E+04	1.43E+04
PIII-1I-G-5-CI-7	7-8 min	1 min	0.575	103	26.4	100	2.733	2.733	3.66E+04	9.79E+03

Table A.28 (cont'd). Phase III, Shot 1, Gunner

Sample ID	Collection Interval	Elapsed Time	Total Mass (mg)	Calculated U (μg)	DU Mass ± 1σ (μg)	Net DU Mass (μg)	Flow Rate (Lpm)	Volume (L)	DU Conc. (μg/m^3)	DU Conc. ± 1σ (μg/m^3)
PIII-1I-G-5-CI-8	7-8 min	1 min	0.944	197	50.1	182	2.733	2.733	6.66E+04	1.86E+04
PIII-1I-G-5-CI-9	7-8 min	1 min	0.882	34	13.9	-2	2.733	2.733	-7.32E+02	6.89E+03
PIII-1I-G-6-CI-1	15-17 min	2 min	1.853	20	3.6	-69	2.778	5.556	-1.24E+04	2.37E+03
PIII-1I-G-6-CI-2	15-17 min	2 min	0.337	1	1.8	-17	2.778	5.556	-3.06E+03	1.37E+03
PIII-1I-G-6-CI-3	15-17 min	2 min	0.926	11	2.6	10	2.778	5.556	1.80E+03	5.26E+02
PIII-1I-G-6-CI-4	15-17 min	2 min	-1.712	60	16.0	57	2.778	5.556	1.03E+04	2.91E+03
PIII-1I-G-6-CI-5	15-17 min	2 min	0.141	139	54.1	132	2.778	5.556	2.38E+04	9.78E+03
PIII-1I-G-6-CI-6	15-17 min	2 min	-0.593	67	29.0	55	2.778	5.556	9.90E+03	5.35E+03
PIII-1I-G-6-CI-7	15-17 min	2 min	-0.736	111	27.0	108	2.778	5.556	1.94E+04	4.93E+03
PIII-1I-G-6-CI-8	15-17 min	2 min	0.377	144	34.5	129	2.778	5.556	2.32E+04	6.37E+03
PIII-1I-G-6-CI-9	15-17 min	2 min	1.324	41	15.3	5	2.778	5.556	9.00E+02	3.58E+03
PIII-1I-G-7-CI-1	31-35 min	4 min	1.279	34	5.1	-55	2.449	9.798	-5.61E+03	1.39E+03
PIII-1I-G-7-CI-2	31-35 min	4 min	-0.302	1	1.7	-17	2.449	9.798	-1.74E+03	7.77E+02
PIII-1I-G-7-CI-3	31-35 min	4 min	0.176	4	1.5	3	2.449	9.798	3.06E+02	2.03E+02
PIII-1I-G-7-CI-4	31-35 min	4 min	-0.050	5	2.3	2	2.449	9.798	2.04E+02	2.86E+02
PIII-1I-G-7-CI-5	31-35 min	4 min	-0.042	24	10.3	17	2.449	9.798	1.74E+03	1.11E+03
PIII-1I-G-7-CI-6	31-35 min	4 min	1.155	23	11.1	11	2.449	9.798	1.12E+03	1.30E+03
PIII-1I-G-7-CI-7	31-35 min	4 min	0.373	41	12.4	38	2.449	9.798	3.88E+03	1.31E+03
PIII-1I-G-7-CI-8	31-35 min	4 min	1.594	62	17.1	47	2.449	9.798	4.80E+03	1.89E+03
PIII-1I-G-7-CI-9	31-35 min	4 min	0.921	4	5.3	-32	2.449	9.798	-3.27E+03	1.41E+03
PIII-1I-G-8-CI-1	61-69 min	8 min	1.169	33	5.1	-56	2.525	20.198	-2.77E+03	6.74E+02
PIII-1I-G-8-CI-2	61-69 min	8 min	-1.246	3	1.8	-15	2.525	20.198	-7.43E+02	3.78E+02
PIII-1I-G-8-CI-3	61-69 min	8 min	0.379	-1	1.1	-2	2.525	20.198	-9.90E+01	8.44E+01
PIII-1I-G-8-CI-4	61-69 min	8 min	-0.148	3	NA[(a)]	0	2.525	20.198	0.00E+00	NA[(a)]
PIII-1I-G-8-CI-5	61-69 min	8 min	1.423	13	5.9	6	2.525	20.198	2.97E+02	3.42E+02
PIII-1I-G-8-CI-6	61-69 min	8 min	0.129	28	13.1	16	2.525	20.198	7.92E+02	7.18E+02
PIII-1I-G-8-CI-7	61-69 min	8 min	0.442	17	NA[(a)]	14	2.525	20.198	6.93E+02	NA[(a)]
PIII-1I-G-8-CI-8	61-69 min	8 min	-0.753	35	11.7	20	2.525	20.198	9.90E+02	6.76E+02
PIII-1I-G-8-CI-9	61-69 min	8 min	-0.260	6	4.5	-30	2.525	20.198	-1.49E+03	6.69E+02
PIII-1I-G-9-CI-1	121-129 min	8 min	1.463	61	8.5	-28	2.425	19.401	-1.44E+03	7.80E+02
PIII-1I-G-9-CI-2	121-129 min	8 min	0.358	1	1.7	-17	2.425	19.401	-8.76E+02	3.92E+02
PIII-1I-G-9-CI-3	121-129 min	8 min	-0.363	0	1.1	-1	2.425	19.401	-5.15E+01	8.78E+01
PIII-1I-G-9-CI-4	121-129 min	8 min	0.297	1	1.5	-2	2.425	19.401	-1.03E+02	1.13E+02
PIII-1I-G-9-CI-5	121-129 min	8 min	0.293	4	3.0	-3	2.425	19.401	-1.55E+02	2.42E+02
PIII-1I-G-9-CI-6	121-129 min	8 min	0.447	21	9.8	9	2.425	19.401	4.64E+02	5.98E+02
PIII-1I-G-9-CI-7	121-129 min	8 min	-2.463	-3	4.1	-6	2.425	19.401	-3.09E+02	2.68E+02
PIII-1I-G-9-CI-8	121-129 min	8 min	-1.111	52	14.7	37	2.425	19.401	1.91E+03	8.41E+02
PIII-1I-G-9-CI-9	121-129 min	8 min	0.598	8	5.0	-28	2.425	19.401	-1.44E+03	7.05E+02

(a) DU mass based on ICP-MS results; no analytical uncertainty was reported.

Table A.28 (cont'd). Phase III, Shot 1, Loader

Sample ID	Collection Interval	Elapsed Time	Total Mass (mg)	Calculated U (μg)	DU Mass ± 1σ (μg)	Net DU Mass (μg)	Flow Rate (Lpm)	Volume (L)	DU Conc. (μg/m^3)	DU Conc. ± 1σ (μg/m^3)
PIII-1I-L-1-CI-1	0-10 sec	10 sec	0.406	98	13.7	44	2.464	0.411	1.07E+05	3.83E+04
PIII-1I-L-1-CI-2	0-10 sec	10 sec	-4.949	103	40.7	101	2.464	0.411	2.46E+05	9.94E+04
PIII-1I-L-1-CI-3	0-10 sec	10 sec	-2.351	80	14.9	79	2.464	0.411	1.92E+05	3.68E+04
PIII-1I-L-1-CI-4	0-10 sec	10 sec	-2.493	76	20.3	76	2.464	0.411	1.85E+05	4.97E+04
PIII-1I-L-1-CI-5	0-10 sec	10 sec	-2.654	122	47.1	121	2.464	0.411	2.94E+05	1.15E+05
PIII-1I-L-1-CI-6	0-10 sec	10 sec	-2.143	173	71.4	173	2.464	0.411	4.21E+05	1.74E+05
PIII-1I-L-1-CI-7	0-10 sec	10 sec	-3.240	70	18.0	66	2.464	0.411	1.61E+05	4.44E+04
PIII-1I-L-1-CI-8	0-10 sec	10 sec	-5.666	78	21.0	67	2.464	0.411	1.63E+05	5.29E+04
PIII-1I-L-1-CI-9	0-10 sec	10 sec	2.289	74	24.7	67	2.464	0.411	1.63E+05	6.10E+04
PIII-1I-L-2-CI-1	1-1 min 10 sec	10 sec	0.692	36	5.4	-18	2.510	0.418	-4.31E+04	2.23E+04
PIII-1I-L-2-CI-2	1-1 min 10 sec	10 sec	-4.753	37	14.9	35	2.510	0.418	8.37E+04	3.60E+04
PIII-1I-L-2-CI-3	1-1 min 10 sec	10 sec	-3.029	57	10.8	56	2.510	0.418	1.34E+05	2.62E+04
PIII-1I-L-2-CI-4	1-1 min 10 sec	10 sec	-5.127	87	23.1	87	2.510	0.418	2.08E+05	5.56E+04
PIII-1I-L-2-CI-5	1-1 min 10 sec	10 sec	-5.835	96	37.1	95	2.510	0.418	2.27E+05	8.91E+04
PIII-1I-L-2-CI-6	1-1 min 10 sec	10 sec	-3.343	92	38.3	92	2.510	0.418	2.20E+05	9.19E+04
PIII-1I-L-2-CI-7	1-1 min 10 sec	10 sec	-2.971	23	8.0	19	2.510	0.418	4.55E+04	1.99E+04
PIII-1I-L-2-CI-8	1-1 min 10 sec	10 sec	-1.283	55	16.8	44	2.510	0.418	1.05E+05	4.22E+04
PIII-1I-L-2-CI-9	1-1 min 10 sec	10 sec	1.674	51	17.7	44	2.510	0.418	1.05E+05	4.35E+04
PIII-1I-L-3-CI-1	3-3 min 15 sec	15 sec	3.471	22	3.6	-32	2.553	0.638	-5.02E+04	1.33E+04
PIII-1I-L-3-CI-2	3-3 min 15 sec	15 sec	-4.139	26	10.4	24	2.553	0.638	3.76E+04	1.66E+04
PIII-1I-L-3-CI-3	3-3 min 15 sec	15 sec	-3.286	51	9.6	50	2.553	0.638	7.84E+04	1.53E+04
PIII-1I-L-3-CI-4	3-3 min 15 sec	15 sec	-3.777	53	14.2	53	2.553	0.638	8.31E+04	2.24E+04
PIII-1I-L-3-CI-5	3-3 min 15 sec	15 sec	-6.742	114	44.2	113	2.553	0.638	1.77E+05	6.95E+04
PIII-1I-L-3-CI-6	3-3 min 15 sec	15 sec	-6.964	145	60.3	145	2.553	0.638	2.27E+05	9.48E+04
PIII-1I-L-3-CI-7	3-3 min 15 sec	15 sec	-3.974	103	24.9	99	2.553	0.638	1.55E+05	3.95E+04
PIII-1I-L-3-CI-8	3-3 min 15 sec	15 sec	-7.382	77	21.2	66	2.553	0.638	1.03E+05	3.44E+04
PIII-1I-L-3-CI-9	3-3 min 15 sec	15 sec	2.173	53	17.9	46	2.553	0.638	7.21E+04	2.88E+04
PIII-1I-L-4-CI-1	7-8 min	1 min	2.108	19	3.2	-35	2.519	2.519	-1.39E+04	3.30E+03
PIII-1I-L-4-CI-2	7-8 min	1 min	-6.499	19	7.8	17	2.519	2.519	6.75E+03	3.18E+03
PIII-1I-L-4-CI-3	7-8 min	1 min	-5.733	29	5.9	28	2.519	2.519	1.11E+04	2.39E+03
PIII-1I-L-4-CI-4	7-8 min	1 min	-1.708	107	28.4	107	2.519	2.519	4.25E+04	1.14E+04
PIII-1I-L-4-CI-5	7-8 min	1 min	-3.450	96	37.3	95	2.519	2.519	3.77E+04	1.49E+04
PIII-1I-L-4-CI-6	7-8 min	1 min	-4.017	126	52.7	126	2.519	2.519	5.00E+04	2.10E+04
PIII-1I-L-4-CI-7	7-8 min	1 min	-4.107	90	23.0	86	2.519	2.519	3.41E+04	9.23E+03
PIII-1I-L-4-CI-8	7-8 min	1 min	-2.895	153	36.4	142	2.519	2.519	5.64E+04	1.47E+04
PIII-1I-L-4-CI-9	7-8 min	1 min	3.076	48	17.7	41	2.519	2.519	1.63E+04	7.21E+03
PIII-1I-L-5-CI-1	15-17 min	2 min	-0.119	21	3.5	-33	2.510	5.020	-6.57E+03	1.68E+03
PIII-1I-L-5-CI-2	15-17 min	2 min	-2.815	38	15.2	36	2.510	5.020	7.17E+03	3.06E+03
PIII-1I-L-5-CI-3	15-17 min	2 min	-7.803	7	1.7	6	2.510	5.020	1.20E+03	3.76E+02
PIII-1I-L-5-CI-4	15-17 min	2 min	-5.795	47	12.9	47	2.510	5.020	9.36E+03	2.59E+03
PIII-1I-L-5-CI-5	15-17 min	2 min	-5.876	110	42.8	109	2.510	5.020	2.17E+04	8.56E+03
PIII-1I-L-5-CI-6	15-17 min	2 min	-4.353	93	39.2	93	2.510	5.020	1.85E+04	7.84E+03
PIII-1I-L-5-CI-7	15-17 min	2 min	-5.746	80	20.5	76	2.510	5.020	1.51E+04	4.13E+03

Table A.28 (cont'd). Phase III, Shot 1, Loader

Sample ID	Collection Interval	Elapsed Time	Total Mass (mg)	Calculated U (μg)	DU Mass ± 1σ (μg)	Net DU Mass (μg)	Flow Rate (Lpm)	Volume (L)	DU Conc. (μg/m^3)	DU Conc. ± 1σ (μg/m^3)
PIII-1I-L-5-CI-8	15-17 min	2 min	-2.857	117	29.3	106	2.510	5.020	2.11E+04	5.96E+03
PIII-1I-L-5-CI-9	15-17 min	2 min	2.136	38	13.3	31	2.510	5.020	6.18E+03	2.77E+03
PIII-1I-L-6-CI-1	31-35 min	4 min	0.855	25	3.8	-29	2.515	10.061	-2.88E+03	8.49E+02
PIII-1I-L-6-CI-2	31-35 min	4 min	-4.476	5	2.6	3	2.515	10.061	2.98E+02	3.14E+02
PIII-1I-L-6-CI-3	31-35 min	4 min	-1.977	1.5	1.0	0.5	2.515	10.061	4.97E+01	1.27E+02
PIII-1I-L-6-CI-4	31-35 min	4 min	-2.507	10	3.0	10	2.515	10.061	9.94E+02	3.10E+02
PIII-1I-L-6-CI-5	31-35 min	4 min	-4.702	29	12.1	28	2.515	10.061	2.78E+03	1.21E+03
PIII-1I-L-6-CI-6	31-35 min	4 min	-6.650	39	17.2	39	2.515	10.061	3.88E+03	1.72E+03
PIII-1I-L-6-CI-7	31-35 min	4 min	-1.678	47	13.5	43	2.515	10.061	4.27E+03	1.37E+03
PIII-1I-L-6-CI-8	31-35 min	4 min	-5.162	50	15.8	39	2.515	10.061	3.88E+03	1.66E+03
PIII-1I-L-6-CI-9	31-35 min	4 min	1.408	12	6.5	5	2.515	10.061	4.97E+02	7.54E+02
PIII-1I-L-7-CI-1	61-69 min	8 min	1.530	33	4.8	-21	2.459	19.670	-1.07E+03	4.58E+02
PIII-1I-L-7-CI-2	61-69 min	8 min	-2.837	4	2.2	2	2.459	19.670	1.02E+02	1.45E+02
PIII-1I-L-7-CI-3	61-69 min	8 min	-3.722	5	1.4	4	2.459	19.670	2.03E+02	8.22E+01
PIII-1I-L-7-CI-4	61-69 min	8 min	-2.413	2	1.2	2	2.459	19.670	1.02E+02	7.34E+01
PIII-1I-L-7-CI-5	61-69 min	8 min	-5.376	14	6.0	13	2.459	19.670	6.61E+02	3.14E+02
PIII-1I-L-7-CI-6	61-69 min	8 min	-3.887	45	19.3	45	2.459	19.670	2.29E+03	9.87E+02
PIII-1I-L-7-CI-7	61-69 min	8 min	-3.239	9	5.5	5	2.459	19.670	2.54E+02	3.01E+02
PIII-1I-L-7-CI-8	61-69 min	8 min	-2.015	28	9.7	17	2.459	19.670	8.64E+02	5.60E+02
PIII-1I-L-7-CI-9	61-69 min	8 min	1.465	16	7.2	9	2.459	19.670	4.58E+02	4.17E+02
PIII-1I-L-8-CI-1	121-129 min	8 min	2.596	13	2.4	-41	2.524	20.193	-2.03E+03	3.99E+02
PIII-1I-L-8-CI-2	121-129 min	8 min	-2.281	4	2.2	2	2.524	20.193	9.90E+01	1.41E+02
PIII-1I-L-8-CI-3	121-129 min	8 min	-2.343	2	0.8	1	2.524	20.193	4.95E+01	5.60E+01
PIII-1I-L-8-CI-4	121-129 min	8 min	-2.749	1	1.2	1	2.524	20.193	4.95E+01	7.14E+01
PIII-1I-L-8-CI-5	121-129 min	8 min	-2.732	13	5.7	12	2.524	20.193	5.94E+02	2.91E+02
PIII-1I-L-8-CI-6	121-129 min	8 min	-4.266	12	6.7	12	2.524	20.193	5.94E+02	3.42E+02
PIII-1I-L-8-CI-7	121-129 min	8 min	-2.864	7	4.6	3	2.524	20.193	1.49E+02	2.53E+02
PIII-1I-L-8-CI-8	121-129 min	8 min	-2.213	28	11.3	17	2.524	20.193	8.42E+02	6.17E+02
PIII-1I-L-8-CI-9	121-129 min	8 min	1.153	20	8.9	13	2.524	20.193	6.44E+02	4.82E+02
PIII-1I-L-9-CI-1	Field Blank	--	0.408	54	7.6	--	--	--	--	--
PIII-1I-L-9-CI-2	Field Blank	--	-4.892	2	1.8	--	--	--	--	--
PIII-1I-L-9-CI-3	Field Blank	--	-1.252	1	0.8	--	--	--	--	--
PIII-1I-L-9-CI-4	Field Blank	--	-5.786	-1	0.8	--	--	--	--	--
PIII-1I-L-9-CI-5	Field Blank	--	-2.462	1	1.4	--	--	--	--	--
PIII-1I-L-9-CI-6	Field Blank	--	-2.402	0	1.6	--	--	--	--	--
PIII-1I-L-9-CI-7	Field Blank	--	-2.641	4	2.2	--	--	--	--	--
PIII-1I-L-9-CI-8	Field Blank	--	-1.856	11	5.2	--	--	--	--	--
PIII-1I-L-9-CI-9	Field Blank	--	0.853	7	3.9	--	--	--	--	--

Table A.29. PIII-2 Cascade Impactor Substrates—Mass, Volume, and Concentration

Sample ID	Collection Interval	Elapsed Time	Total Mass (mg)	Calculated U (μg)	DU Mass ± 1σ (μg)	Net DU Mass (μg)[(s)]	Flow Rate (Lpm)	Volume (L)	DU Conc. (μg/m^3)	DU Conc. ± 1σ (μg/m^3)
PIII-2I-C-1-CI-1	0-10 sec	10 sec	1.011	548	74.5	227	2.740	0.457	4.97E+05	1.81E+05
PIII-2I-C-1-CI-2	0-10 sec	10 sec	-1.802	210	82.7	197	2.740	0.457	4.32E+05	1.82E+05
PIII-2I-C-1-CI-3	0-10 sec	10 sec	0.489	255	47.4	250	2.740	0.457	5.47E+05	1.05E+05
PIII-2I-C-1-CI-4	0-10 sec	10 sec	0.428	409	108.0	398	2.740	0.457	8.70E+05	2.38E+05
PIII-2I-C-1-CI-5	0-10 sec	10 sec	-0.955	390	147.5	383	2.740	0.457	8.39E+05	3.24E+05
PIII-2I-C-1-CI-6	0-10 sec	10 sec	0.289	277	106.5	264	2.740	0.457	5.77E+05	2.34E+05
PIII-2I-C-1-CI-7	0-10 sec	10 sec	-2.023	156	35.9	148	2.740	0.457	3.25E+05	7.93E+04
PIII-2I-C-1-CI-8	0-10 sec	10 sec	-0.533	256	53.1	243	2.740	0.457	5.32E+05	1.17E+05
PIII-2I-C-1-CI-9	0-10 sec	10 sec	0.780	355	105.1	342	2.740	0.457	7.48E+05	2.31E+05
PIII-2I-C-2-CI-1	1-1 min 10 sec	10 sec	1.376	1078	145.7	757	2.686	0.448	1.69E+06	3.38E+05
PIII-2I-C-2-CI-2	1-1 min 10 sec	10 sec	-0.032	150	58.9	137	2.686	0.448	3.07E+05	1.32E+05
PIII-2I-C-2-CI-3	1-1 min 10 sec	10 sec	-0.697	87	16.4	82	2.686	0.448	1.83E+05	3.71E+04
PIII-2I-C-2-CI-4	1-1 min 10 sec	10 sec	-1.688	79	21.1	68	2.686	0.448	1.51E+05	4.77E+04
PIII-2I-C-2-CI-5	1-1 min 10 sec	10 sec	-0.452	106	40.4	99	2.686	0.448	2.22E+05	9.05E+04
PIII-2I-C-2-CI-6	1-1 min 10 sec	10 sec	-1.169	85	33.1	72	2.686	0.448	1.60E+05	7.44E+04
PIII-2I-C-2-CI-7	1-1 min 10 sec	10 sec	-1.840	79	18.8	71	2.686	0.448	1.59E+05	4.24E+04
PIII-2I-C-2-CI-8	1-1 min 10 sec	10 sec	-0.478	143	31.2	130	2.686	0.448	2.91E+05	7.03E+04
PIII-2I-C-2-CI-9	1-1 min 10 sec	10 sec	0.777	129	39.2	116	2.686	0.448	2.59E+05	8.80E+04
PIII-2I-C-3-CI-1	3-3 min 15 sec	15 sec	1.044	704	95.2	383	2.702	0.675	5.68E+05	1.51E+05
PIII-2I-C-3-CI-2	3-3 min 15 sec	15 sec	-1.876	58	23.1	45	2.702	0.675	6.72E+04	3.47E+04
PIII-2I-C-3-CI-3	3-3 min 15 sec	15 sec	-1.916	90	17.0	85	2.702	0.675	1.26E+05	2.55E+04
PIII-2I-C-3-CI-4	3-3 min 15 sec	15 sec	-0.874	79	21.3	68	2.702	0.675	1.00E+05	3.19E+04
PIII-2I-C-3-CI-5	3-3 min 15 sec	15 sec	-0.440	123	46.9	116	2.702	0.675	1.72E+05	6.97E+04
PIII-2I-C-3-CI-6	3-3 min 15 sec	15 sec	-0.702	90	35.6	77	2.702	0.675	1.14E+05	5.31E+04
PIII-2I-C-3-CI-7	3-3 min 15 sec	15 sec	-0.869	86	21.0	78	2.702	0.675	1.16E+05	3.14E+04
PIII-2I-C-3-CI-8	3-3 min 15 sec	15 sec	-1.857	136	29.3	123	2.702	0.675	1.83E+05	4.39E+04
PIII-2I-C-3-CI-9	3-3 min 15 sec	15 sec	0.567	48	15.5	35	2.702	0.675	5.19E+04	2.33E+04
PIII-2I-C-4-CI-1	7-8 min	1 min	0.548	131	18.0	-190	2.511	2.511	-7.55E+04	1.58E+04
PIII-2I-C-4-CI-2	7-8 min	1 min	-1.104	31	12.2	18	2.511	2.511	7.30E+03	5.08E+03
PIII-2I-C-4-CI-3	7-8 min	1 min	-0.377	17	3.7	12	2.511	2.511	4.78E+03	1.52E+03
PIII-2I-C-4-CI-4	7-8 min	1 min	-1.267	30	8.5	19	2.511	2.511	7.43E+03	3.55E+03
PIII-2I-C-4-CI-5	7-8 min	1 min	-1.984	75	28.8	68	2.511	2.511	2.72E+04	1.15E+04
PIII-2I-C-4-CI-6	7-8 min	1 min	-0.588	71	28.5	58	2.511	2.511	2.30E+04	1.14E+04
PIII-2I-C-4-CI-7	7-8 min	1 min	-0.138	76	18.6	68	2.511	2.511	2.72E+04	7.49E+03
PIII-2I-C-4-CI-8	7-8 min	1 min	-0.401	72	16.9	59	2.511	2.511	2.36E+04	6.82E+03
PIII-2I-C-4-CI-9	7-8 min	1 min	-0.022	20	7.4	7	2.511	2.511	2.79E+03	3.13E+03
PIII-2I-C-5-CI-1	15-17 min	2 min	0.237	171	23.5	-150	2.514	5.029	-2.98E+04	8.40E+03
PIII-2I-C-5-CI-2	15-17 min	2 min	-2.860	13	5.5	0	2.514	5.029	6.63E+01	1.32E+03
PIII-2I-C-5-CI-3	15-17 min	2 min	-1.639	9.9	2.4	4.9	2.514	5.029	9.74E+02	5.09E+02
PIII-2I-C-5-CI-4	15-17 min	2 min	-1.329	16	4.8	5	2.514	5.029	9.28E+02	1.09E+03
PIII-2I-C-5-CI-5	15-17 min	2 min	-1.535	45	17.6	38	2.514	5.029	7.62E+03	3.53E+03
PIII-2I-C-5-CI-6	15-17 min	2 min	-0.766	43	17.4	30	2.514	5.029	5.90E+03	3.52E+03

Table A.29 (cont'd). Phase III, Shot 2, Commander

Sample ID	Collection Interval	Elapsed Time	Total Mass (mg)	Calculated U (μg)	DU Mass ± 1σ (μg)	Net DU Mass (μg)	Flow Rate (Lpm)	Volume (L)	DU Conc. (μg/m^3)	DU Conc. ± 1σ (μg/m^3)
PIII-2I-C-5-CI-7	15-17 min	2 min	-0.972	16	6.2	8	2.514	5.029	1.66E+03	1.28E+03
PIII-2I-C-5-CI-8	15-17 min	2 min	-2.408	61	14.8	48	2.514	5.029	9.61E+03	2.99E+03
PIII-2I-C-5-CI-9	15-17 min	2 min	-0.011	18	6.6	5	2.514	5.029	9.94E+02	1.41E+03
PIII-2I-C-6-CI-1	31-35 min	4 min	0.767	260	35.4	-61	2.518	10.070	-6.02E+03	4.94E+03
PIII-2I-C-6-CI-2	31-35 min	4 min	0.380	20	8.3	7	2.518	10.070	7.28E+02	9.03E+02
PIII-2I-C-6-CI-3	31-35 min	4 min	-0.736	7	1.9	2	2.518	10.070	1.99E+02	2.08E+02
PIII-2I-C-6-CI-4	31-35 min	4 min	-1.070	24	6.8	13	2.518	10.070	1.26E+03	7.25E+02
PIII-2I-C-6-CI-5	31-35 min	4 min	-1.044	52	20.3	45	2.518	10.070	4.50E+03	2.03E+03
PIII-2I-C-6-CI-6	31-35 min	4 min	-0.511	35	14.6	22	2.518	10.070	2.15E+03	1.49E+03
PIII-2I-C-6-CI-7	31-35 min	4 min	-1.171	18	6.2	10	2.518	10.070	1.03E+03	6.41E+02
PIII-2I-C-6-CI-8	31-35 min	4 min	-1.479	51	14.4	38	2.518	10.070	3.81E+03	1.45E+03
PIII-2I-C-6-CI-9	31-35 min	4 min	0.360	25	8.7	12	2.518	10.070	1.19E+03	9.03E+02
PIII-2I-C-7-CI-1	61-69 min	8 min	0.486	199	27.1	-122	2.714	21.709	-5.60E+03	2.04E+03
PIII-2I-C-7-CI-2	61-69 min	8 min	-0.928	8	3.8	-5	2.714	21.709	-2.15E+02	2.45E+02
PIII-2I-C-7-CI-3	61-69 min	8 min	-0.830	7	1.8	2	2.714	21.709	9.21E+01	9.22E+01
PIII-2I-C-7-CI-4	61-69 min	8 min	-0.354	27	7.7	16	2.714	21.709	7.22E+02	3.76E+02
PIII-2I-C-7-CI-5	61-69 min	8 min	-0.837	79	30.4	72	2.714	21.709	3.33E+03	1.41E+03
PIII-2I-C-7-CI-6	61-69 min	8 min	-1.221	51	20.7	38	2.714	21.709	1.74E+03	9.66E+02
PIII-2I-C-7-CI-7	61-69 min	8 min	-2.722	33	10.0	25	2.714	21.709	1.17E+03	4.69E+02
PIII-2I-C-7-CI-8	61-69 min	8 min	-2.939	86	20.2	73	2.714	21.709	3.38E+03	9.41E+02
PIII-2I-C-7-CI-9	61-69 min	8 min	0.163	34	13.4	21	2.714	21.709	9.67E+02	6.30E+02
PIII-2I-C-8-CI-1	121-129 min	8 min	1.129	608	82.1	287	2.575	20.602	1.39E+04	4.35E+03
PIII-2I-C-8-CI-2	121-129 min	8 min	-2.254	11	4.8	-2	2.575	20.602	-8.09E+01	2.95E+02
PIII-2I-C-8-CI-3	121-129 min	8 min	-2.812	9	2.0	4	2.575	20.602	1.94E+02	1.06E+02
PIII-2I-C-8-CI-4	121-129 min	8 min	-4.072	12	3.6	1	2.575	20.602	3.24E+01	2.17E+02
PIII-2I-C-8-CI-5	121-129 min	8 min	-0.683	50	19.6	43	2.575	20.602	2.10E+03	9.59E+02
PIII-2I-C-8-CI-6	121-129 min	8 min	-2.452	73	28.7	60	2.575	20.602	2.90E+03	1.40E+03
PIII-2I-C-8-CI-7	121-129 min	8 min	-0.903	43	11.4	35	2.575	20.602	1.72E+03	5.62E+02
PIII-2I-C-8-CI-8	121-129 min	8 min	0.447	90	20.7	77	2.575	20.602	3.75E+03	1.02E+03
PIII-2I-C-8-CI-9	121-129 min	8 min	0.100	44	14.6	31	2.575	20.602	1.50E+03	7.22E+02
PIII-2I-C-9-CI-1	Field Blank	--	0.922	334	45.4	--	--	--	--	--
PIII-2I-C-9-CI-2	Field Blank	--	-0.413	23	9.3	--	--	--	--	--
PIII-2I-C-9-CI-3	Field Blank	--	-0.795	10	2.1	--	--	--	--	--
PIII-2I-C-9-CI-4	Field Blank	--	-1.293	45	12.1	--	--	--	--	--
PIII-2I-C-9-CI-5	Field Blank	--	-1.396	99	37.4	--	--	--	--	--
PIII-2I-C-9-CI-6	Field Blank	--	-1.804	127	48.6	--	--	--	--	--
PIII-2I-C-9-CI-7	Field Blank	--	-3.434	65	14.6	--	--	--	--	--
PIII-2I-C-9-CI-8	Field Blank	--	-5.206	43	10.4	--	--	--	--	--
PIII-2I-C-9-CI-9	Field Blank	--	0.334	57	16.8	--	--	--	--	--

(a) Field blanks from the driver, gunner, and loader were averaged and substituted for the nonrepresentative commander's field blanks.

Table A.29 (cont'd). Phase III, Shot 2, Driver

Sample ID	Collection Interval	Elapsed Time	Total Mass (mg)	Calculated U (μg)	DU Mass ± 1σ (μg)	Net DU Mass (μg)	Flow Rate (Lpm)	Volume (L)	DU Conc. (μg/m^3)	DU Conc. ± 1σ (μg/m^3)
PIII-2I-D-1-CI-1	0-10 sec	10 sec	1.787	151	27.9	-16	2.514	0.419	-3.82E+04	9.95E+04
PIII-2I-D-1-CI-2	0-10 sec	10 sec	4.818	103	47.9	100	2.514	0.419	2.39E+05	1.15E+05
PIII-2I-D-1-CI-3	0-10 sec	10 sec	0.404	193	48.1	191	2.514	0.419	4.56E+05	1.16E+05
PIII-2I-D-1-CI-4	0-10 sec	10 sec	-1.472	146	52.3	129	2.514	0.419	3.08E+05	1.26E+05
PIII-2I-D-1-CI-5	0-10 sec	10 sec	0.379	220	83.6	209	2.514	0.419	4.99E+05	2.00E+05
PIII-2I-D-1-CI-6	0-10 sec	10 sec	0.208	67	16.3	48	2.514	0.419	1.15E+05	4.06E+04
PIII-2I-D-1-CI-7	0-10 sec	10 sec	-0.053	74	12.8	68	2.514	0.419	1.62E+05	3.13E+04
PIII-2I-D-1-CI-8	0-10 sec	10 sec	-0.537	112	11.6	104	2.514	0.419	2.48E+05	2.88E+04
PIII-2I-D-1-CI-9	0-10 sec	10 sec	0.851	537	91.8	531	2.514	0.419	1.27E+06	2.22E+05
PIII-2I-D-2-CI-1	1-1 min 10 sec	10 sec	0.858	223	41.2	56	2.489	0.415	1.35E+05	1.24E+05
PIII-2I-D-2-CI-2	1-1 min 10 sec	10 sec	2.353	32	15.2	29	2.489	0.415	6.99E+04	3.69E+04
PIII-2I-D-2-CI-3	1-1 min 10 sec	10 sec	-0.010	37	9.5	35	2.489	0.415	8.43E+04	2.32E+04
PIII-2I-D-2-CI-4	1-1 min 10 sec	10 sec	-0.546	31	11.4	14	2.489	0.415	3.37E+04	3.14E+04
PIII-2I-D-2-CI-5	1-1 min 10 sec	10 sec	-0.563	22	8.6	11	2.489	0.415	2.65E+04	2.34E+04
PIII-2I-D-2-CI-6	1-1 min 10 sec	10 sec	-0.383	59	14.4	40	2.489	0.415	9.64E+04	3.65E+04
PIII-2I-D-2-CI-7	1-1 min 10 sec	10 sec	0.155	99	16.9	93	2.489	0.415	2.24E+05	4.15E+04
PIII-2I-D-2-CI-8	1-1 min 10 sec	10 sec	-1.669	119	12.4	111	2.489	0.415	2.67E+05	3.11E+04
PIII-2I-D-2-CI-9	1-1 min 10 sec	10 sec	0.940	112	19.6	106	2.489	0.415	2.55E+05	4.80E+04
PIII-2I-D-3-CI-1	3-3 min 15 sec	15 sec	0.689	280	51.6	113	2.654	0.663	1.70E+05	9.09E+04
PIII-2I-D-3-CI-2	3-3 min 15 sec	15 sec	-0.873	15	7.2	12	2.654	0.663	1.81E+04	1.12E+04
PIII-2I-D-3-CI-3	3-3 min 15 sec	15 sec	-0.005	68	17.3	66	2.654	0.663	9.95E+04	2.63E+04
PIII-2I-D-3-CI-4	3-3 min 15 sec	15 sec	-0.734	131	46.8	114	2.654	0.663	1.72E+05	7.14E+04
PIII-2I-D-3-CI-5	3-3 min 15 sec	15 sec	0.076	201	76.4	190	2.654	0.663	2.87E+05	1.16E+05
PIII-2I-D-3-CI-6	3-3 min 15 sec	15 sec	0.828	73	17.8	54	2.654	0.663	8.14E+04	2.78E+04
PIII-2I-D-3-CI-7	3-3 min 15 sec	15 sec	-0.843	97	16.5	91	2.654	0.663	1.37E+05	2.54E+04
PIII-2I-D-3-CI-8	3-3 min 15 sec	15 sec	1.688	98	10.0	90	2.654	0.663	1.36E+05	1.57E+04
PIII-2I-D-3-CI-9	3-3 min 15 sec	15 sec	1.983	30	5.5	24	2.654	0.663	3.62E+04	8.75E+03
PIII-2I-D-4-CI-1	7-8 min	1 min	0.445	121	22.6	-46	2.679	2.679	-1.72E+04	1.43E+04
PIII-2I-D-4-CI-2	7-8 min	1 min	-0.005	6	3.0	3	2.679	2.679	1.12E+03	1.29E+03
PIII-2I-D-4-CI-3	7-8 min	1 min	4.296	15	4.3	13	2.679	2.679	4.85E+03	1.65E+03
PIII-2I-D-4-CI-4	7-8 min	1 min	-0.344	59	21.5	42	2.679	2.679	1.57E+04	8.38E+03
PIII-2I-D-4-CI-5	7-8 min	1 min	-1.325	103	39.4	92	2.679	2.679	3.43E+04	1.48E+04
PIII-2I-D-4-CI-6	7-8 min	1 min	0.342	72	17.5	53	2.679	2.679	1.98E+04	6.78E+03
PIII-2I-D-4-CI-7	7-8 min	1 min	-0.524	128	21.7	122	2.679	2.679	4.55E+04	8.25E+03
PIII-2I-D-4-CI-8	7-8 min	1 min	-0.476	90	9.2	82	2.679	2.679	3.06E+04	3.59E+03
PIII-2I-D-4-CI-9	7-8 min	1 min	0.110	25	4.7	19	2.679	2.679	7.09E+03	1.88E+03
PIII-2I-D-5-CI-1	15-17 min	2 min	0.320	49	9.4	-118	2.594	5.188	-2.27E+04	6.28E+03
PIII-2I-D-5-CI-2	15-17 min	2 min	0.422	3	1.9	0.1	2.594	5.188	1.93E+01	4.91E+02
PIII-2I-D-5-CI-3	15-17 min	2 min	1.344	2	1.0	0.1	2.594	5.188	1.93E+01	2.73E+02
PIII-2I-D-5-CI-4	15-17 min	2 min	1.096	10	3.8	-7	2.594	5.188	-1.35E+03	1.42E+03
PIII-2I-D-5-CI-5	15-17 min	2 min	-0.136	29	11.3	18	2.594	5.188	3.47E+03	2.35E+03
PIII-2I-D-5-CI-6	15-17 min	2 min	0.220	27	6.9	8	2.594	5.188	1.54E+03	1.60E+03
PIII-2I-D-5-CI-7	15-17 min	2 min	-0.454	19	3.9	13	2.594	5.188	2.51E+03	8.40E+02

Table A.29 (cont'd). Phase III, Shot 2, Driver

Sample ID	Collection Interval	Elapsed Time	Total Mass (mg)	Calculated U (μg)	DU Mass ± 1σ (μg)	Net DU Mass (μg)	Flow Rate (Lpm)	Volume (L)	DU Conc. (μg/m^3)	DU Conc. ± 1σ (μg/m^3)
PIII-2I-D-5-CI-8	15-17 min	2 min	-2.678	21	3.1	13	2.594	5.188	2.51E+03	6.52E+02
PIII-2I-D-5-CI-9	15-17 min	2 min	0.790	34	6.4	28	2.594	5.188	5.40E+03	1.29E+03
PIII-2I-D-6-CI-1	31-35 min	4 min	0.563	64	12.2	-103	2.654	10.616	-9.70E+03	3.15E+03
PIII-2I-D-6-CI-2	31-35 min	4 min	1.345	3	1.7	0.2	2.654	10.616	1.88E+01	2.26E+02
PIII-2I-D-6-CI-3	31-35 min	4 min	-1.053	8	2.4	6	2.654	10.616	5.65E+02	2.45E+02
PIII-2I-D-6-CI-4	31-35 min	4 min	-0.002	18	6.7	1	2.654	10.616	9.42E+01	8.66E+02
PIII-2I-D-6-CI-5	31-35 min	4 min	-0.136	40	15.6	29	2.654	10.616	2.73E+03	1.53E+03
PIII-2I-D-6-CI-6	31-35 min	4 min	0.003	42	10.4	23	2.654	10.616	2.17E+03	1.07E+03
PIII-2I-D-6-CI-7	31-35 min	4 min	0.522	30	5.5	24	2.654	10.616	2.26E+03	5.52E+02
PIII-2I-D-6-CI-8	31-35 min	4 min	5.012	50	5.6	42	2.654	10.616	3.96E+03	5.54E+02
PIII-2I-D-6-CI-9	31-35 min	4 min	0.526	55	9.8	49	2.654	10.616	4.62E+03	9.47E+02
PIII-2I-D-7-CI-1	61-69 min	8 min	1.728	248	45.6	81	2.615	20.920	3.87E+03	2.64E+03
PIII-2I-D-7-CI-2	61-69 min	8 min	-1.232	5	2.6	2	2.615	20.920	9.56E+01	1.49E+02
PIII-2I-D-7-CI-3	61-69 min	8 min	-0.547	4	1.5	2	2.615	20.920	9.56E+01	8.62E+01
PIII-2I-D-7-CI-4	61-69 min	8 min	0.290	24	8.8	7	2.615	20.920	3.35E+02	5.17E+02
PIII-2I-D-7-CI-5	61-69 min	8 min	-0.552	78	29.8	67	2.615	20.920	3.20E+03	1.44E+03
PIII-2I-D-7-CI-6	61-69 min	8 min	0.124	43	10.7	24	2.615	20.920	1.15E+03	5.58E+02
PIII-2I-D-7-CI-7	61-69 min	8 min	-0.576	52	9.4	46	2.615	20.920	2.20E+03	4.63E+02
PIII-2I-D-7-CI-8	61-69 min	8 min	-0.223	103	10.5	95	2.615	20.920	4.54E+03	5.24E+02
PIII-2I-D-7-CI-9	61-69 min	8 min	0.831	64	11.5	58	2.615	20.920	2.77E+03	5.62E+02
PIII-2I-D-8-CI-1	121-129 min	8 min	1.573	249	45.9	82	2.675	21.399	3.83E+03	2.59E+03
PIII-2I-D-8-CI-2	121-129 min	8 min	1.848	12	5.7	9	2.675	21.399	4.21E+02	2.78E+02
PIII-2I-D-8-CI-3	121-129 min	8 min	0.461	3	1.3	1	2.675	21.399	4.67E+01	7.67E+01
PIII-2I-D-8-CI-4	121-129 min	8 min	2.803	17	6.5	0.1	2.675	21.399	4.67E+00	4.23E+02
PIII-2I-D-8-CI-5	121-129 min	8 min	0.661	54	20.8	43	2.675	21.399	2.01E+03	9.96E+02
PIII-2I-D-8-CI-6	121-129 min	8 min	-1.187	44	10.9	25	2.675	21.399	1.17E+03	5.54E+02
PIII-2I-D-8-CI-7	121-129 min	8 min	0.226	53	9.4	47	2.675	21.399	2.20E+03	4.53E+02
PIII-2I-D-8-CI-8	121-129 min	8 min	-0.707	84	8.7	76	2.675	21.399	3.55E+03	4.25E+02
PIII-2I-D-8-CI-9	121-129 min	8 min	0.284	30	5.8	24	2.675	21.399	1.12E+03	2.84E+02
PIII-2I-D-9-CI-1	Field Blank	--	2.963	167	31.0	--	--	--	--	--
PIII-2I-D-9-CI-2	Field Blank	--	-0.281	3	1.7	--	--	--	--	--
PIII-2I-D-9-CI-3	Field Blank	--	1.660	2	1.0	--	--	--	--	--
PIII-2I-D-9-CI-4	Field Blank	--	0.029	17	6.3	--	--	--	--	--
PIII-2I-D-9-CI-5	Field Blank	--	1.340	11	4.5	--	--	--	--	--
PIII-2I-D-9-CI-6	Field Blank	--	-0.193	19	4.6	--	--	--	--	--
PIII-2I-D-9-CI-7	Field Blank	--	-0.125	6	1.9	--	--	--	--	--
PIII-2I-D-9-CI-8	Field Blank	--	-0.376	8	1.3	--	--	--	--	--
PIII-2I-D-9-CI-9	Field Blank	--	0.167	6	1.7	--	--	--	--	--

Table A.29 (cont'd). Phase III, Shot 2, Gunner

Sample ID	Collection Interval	Elapsed Time	Total Mass (mg)	Calculated U (μg)	DU Mass ± 1σ (μg)	Net DU Mass (μg)	Flow Rate (Lpm)	Volume (L)	DU Conc. (μg/m^3)	DU Conc. ± 1σ (μg/m^3)
PIII-2I-G-1-CI-1	0-10 sec	10 sec	2.989	1615	215.9	874	2.722	0.454	1.93E+06	5.27E+05
PIII-2I-G-1-CI-2	0-10 sec	10 sec	-1.134	426	167.2	405	2.722	0.454	8.92E+05	3.70E+05
PIII-2I-G-1-CI-3	0-10 sec	10 sec	0.857	583	106.8	573	2.722	0.454	1.26E+06	2.38E+05
PIII-2I-G-1-CI-4	0-10 sec	10 sec	0.381	479	125.4	462	2.722	0.454	1.02E+06	2.78E+05
PIII-2I-G-1-CI-5	0-10 sec	10 sec	0.267	435	166.8	426	2.722	0.454	9.38E+05	3.69E+05
PIII-2I-G-1-CI-6	0-10 sec	10 sec	0.370	335	138.0	315	2.722	0.454	6.94E+05	3.05E+05
PIII-2I-G-1-CI-7	0-10 sec	10 sec	-0.125	127	31.4	111	2.722	0.454	2.44E+05	7.03E+04
PIII-2I-G-1-CI-8	0-10 sec	10 sec	0.869	534	119.6	516	2.722	0.454	1.14E+06	2.66E+05
PIII-2I-G-1-CI-9	0-10 sec	10 sec	1.008	442	140.7	422	2.722	0.454	9.30E+05	3.12E+05
PIII-2I-G-2-CI-1	Field Blank	--	2.154	741	99.3	--	--	--	--	
PIII-2I-G-2-CI-2	Field Blank	--	-0.739	21	8.5	--	--	--	--	
PIII-2I-G-2-CI-3	Field Blank	--	-1.120	10	2.1	--	--	--	--	
PIII-2I-G-2-CI-4	Field Blank	--	0.827	17	4.7	--	--	--	--	
PIII-2I-G-2-CI-5	Field Blank	--	-1.320	9	3.9	--	--	--	--	
PIII-2I-G-2-CI-6	Field Blank	--	-0.095	20	8.4	--	--	--	--	
PIII-2I-G-2-CI-7	Field Blank	--	-0.410	16	4.8	--	--	--	--	
PIII-2I-G-2-CI-8	Field Blank	--	-0.158	18	6.0	--	--	--	--	
PIII-2I-G-2-CI-9	Field Blank	--	0.305	20	7.2	--	--	--	--	
PIII-2I-G-3-CI-1	1-1 min 10 sec	10 sec	3.012	1718	229.2	977	2.671	0.445	2.20E+06	5.65E+05
PIII-2I-G-3-CI-2	1-1 min 10 sec	10 sec	-0.076	110	43.3	89	2.671	0.445	2.00E+05	9.93E+04
PIII-2I-G-3-CI-3	1-1 min 10 sec	10 sec	-1.521	162	30.0	152	2.671	0.445	3.42E+05	6.84E+04
PIII-2I-G-3-CI-4	1-1 min 10 sec	10 sec	-0.290	133	35.0	116	2.671	0.445	2.61E+05	7.97E+04
PIII-2I-G-3-CI-5	1-1 min 10 sec	10 sec	-1.332	374	143.4	365	2.671	0.445	8.20E+05	3.23E+05
PIII-2I-G-3-CI-6	1-1 min 10 sec	10 sec	-0.388	150	62.8	130	2.671	0.445	2.92E+05	1.43E+05
PIII-2I-G-3-CI-7	1-1 min 10 sec	10 sec	-0.707	138	34.0	122	2.671	0.445	2.74E+05	7.76E+04
PIII-2I-G-3-CI-8	1-1 min 10 sec	10 sec	-2.400	279	63.4	261	2.671	0.445	5.87E+05	1.44E+05
PIII-2I-G-3-CI-9	1-1 min 10 sec	10 sec	0.086	139	45.4	119	2.671	0.445	2.67E+05	1.04E+05
PIII-2I-G-4-CI-1	3-3 min 15 sec	15 sec	6.374	3206	427.6	2465	2.645	0.661	3.73E+06	6.73E+05
PIII-2I-G-4-CI-2	3-3 min 15 sec	15 sec	0.415	81	31.8	60	2.645	0.661	9.08E+04	4.99E+04
PIII-2I-G-4-CI-3	3-3 min 15 sec	15 sec	-1.364	68	12.9	58	2.645	0.661	8.77E+04	1.99E+04
PIII-2I-G-4-CI-4	3-3 min 15 sec	15 sec	-0.303	138	36.5	121	2.645	0.661	1.83E+05	5.59E+04
PIII-2I-G-4-CI-5	3-3 min 15 sec	15 sec	-0.561	80	31.3	71	2.645	0.661	1.07E+05	4.78E+04
PIII-2I-G-4-CI-6	3-3 min 15 sec	15 sec	-0.295	70	30.0	50	2.645	0.661	7.56E+04	4.72E+04
PIII-2I-G-4-CI-7	3-3 min 15 sec	15 sec	-1.402	124	30.7	108	2.645	0.661	1.63E+05	4.73E+04
PIII-2I-G-4-CI-8	3-3 min 15 sec	15 sec	-0.433	234	53.1	216	2.645	0.661	3.27E+05	8.14E+04
PIII-2I-G-4-CI-9	3-3 min 15 sec	15 sec	-0.079	63	21.3	43	2.645	0.661	6.51E+04	3.41E+04
PIII-2I-G-5-CI-1	7-8 min	1 min	3.443	2228	297.3	1487	2.707	2.707	5.49E+05	1.17E+05
PIII-2I-G-5-CI-2	7-8 min	1 min	-0.294	39	15.6	18	2.707	2.707	6.65E+03	6.57E+03
PIII-2I-G-5-CI-3	7-8 min	1 min	-0.003	31	5.9	21	2.707	2.707	7.76E+03	2.33E+03
PIII-2I-G-5-CI-4	7-8 min	1 min	-0.449	40	11.1	23	2.707	2.707	8.50E+03	4.46E+03
PIII-2I-G-5-CI-5	7-8 min	1 min	-0.549	130	50.6	121	2.707	2.707	4.47E+04	1.88E+04
PIII-2I-G-5-CI-6	7-8 min	1 min	-3.926	138	57.7	118	2.707	2.707	4.36E+04	2.16E+04
PIII-2I-G-5-CI-7	7-8 min	1 min	0.094	131	32.0	115	2.707	2.707	4.25E+04	1.20E+04

Table A.29 (cont'd). Phase III, Shot 2, Gunner

Sample ID	Collection Interval	Elapsed Time	Total Mass (mg)	Calculated U (μg)	DU Mass ± 1σ (μg)	Net DU Mass (μg)	Flow Rate (Lpm)	Volume (L)	DU Conc. (μg/m^3)	DU Conc. ± 1σ (μg/m^3)
PIII-2I-G-5-CI-8	7-8 min	1 min	-2.375	130	31.3	112	2.707	2.707	4.14E+04	1.18E+04
PIII-2I-G-5-CI-9	7-8 min	1 min	-0.112	49	16.6	29	2.707	2.707	1.07E+04	6.69E+03
PIII-2I-G-6-CI-1	15-17 min	2 min	4.039	1155	154.3	414	2.717	5.433	7.62E+04	3.39E+04
PIII-2I-G-6-CI-2	15-17 min	2 min	0.061	19	NA[(a)]	-2	2.717	5.433	-3.68E+02	NA[(a)]
PIII-2I-G-6-CI-3	15-17 min	2 min	-1.192	16	3.1	6	2.717	5.433	1.10E+03	6.90E+02
PIII-2I-G-6-CI-4	15-17 min	2 min	-1.856	14	4.0	-3	2.717	5.433	-5.52E+02	1.14E+03
PIII-2I-G-6-CI-5	15-17 min	2 min	-0.231	52	20.3	43	2.717	5.433	7.91E+03	3.81E+03
PIII-2I-G-6-CI-6	15-17 min	2 min	-2.797	98	40.8	78	2.717	5.433	1.44E+04	7.68E+03
PIII-2I-G-6-CI-7	15-17 min	2 min	-0.209	21	7.5	5	2.717	5.433	9.20E+02	1.64E+03
PIII-2I-G-6-CI-8	15-17 min	2 min	-0.797	63	16.8	45	2.717	5.433	8.28E+03	3.29E+03
PIII-2I-G-6-CI-9	15-17 min	2 min	0.376	35	13.1	15	2.717	5.433	2.76E+03	2.75E+03
PIII-2I-G-7-CI-1	31-35 min	4 min	2.882	617	82.5	-124	2.427	9.708	-1.28E+04	1.33E+04
PIII-2I-G-7-CI-2	31-35 min	4 min	0.722	23	9.2	2	2.427	9.708	2.06E+02	1.29E+03
PIII-2I-G-7-CI-3	31-35 min	4 min	1.082	6	1.6	-4	2.427	9.708	-4.12E+02	2.72E+02
PIII-2I-G-7-CI-4	31-35 min	4 min	-0.114	16	4.6	-1	2.427	9.708	-1.03E+02	6.77E+02
PIII-2I-G-7-CI-5	31-35 min	4 min	-0.825	67	26.2	58	2.427	9.708	5.97E+03	2.73E+03
PIII-2I-G-7-CI-6	31-35 min	4 min	-0.854	87	36.6	67	2.427	9.708	6.90E+03	3.87E+03
PIII-2I-G-7-CI-7	31-35 min	4 min	-0.718	16	6.0	0.3	2.427	9.708	3.09E+01	7.91E+02
PIII-2I-G-7-CI-8	31-35 min	4 min	-0.505	58	15.9	40	2.427	9.708	4.12E+03	1.75E+03
PIII-2I-G-7-CI-9	31-35 min	4 min	0.319	87	27.6	67	2.427	9.708	6.90E+03	2.95E+03
PIII-2I-G-8-CI-1	61-69 min	8 min	3.073	1702	227.1	961	2.467	19.735	4.87E+04	1.26E+04
PIII-2I-G-8-CI-2	61-69 min	8 min	1.320	20	8.3	-1	2.467	19.735	-5.07E+01	6.02E+02
PIII-2I-G-8-CI-3	61-69 min	8 min	-0.351	22	4.3	12	2.467	19.735	6.08E+02	2.43E+02
PIII-2I-G-8-CI-4	61-69 min	8 min	-0.157	20	5.6	3	2.467	19.735	1.52E+02	3.70E+02
PIII-2I-G-8-CI-5	61-69 min	8 min	0.585	76	29.9	67	2.467	19.735	3.39E+03	1.53E+03
PIII-2I-G-8-CI-6	61-69 min	8 min	0.406	83	35.0	63	2.467	19.735	3.19E+03	1.83E+03
PIII-2I-G-8-CI-7	61-69 min	8 min	0.177	54	14.1	38	2.467	19.735	1.93E+03	7.57E+02
PIII-2I-G-8-CI-8	61-69 min	8 min	-0.323	131	31.5	113	2.467	19.735	5.73E+03	1.63E+03
PIII-2I-G-8-CI-9	61-69 min	8 min	0.583	59	20.2	39	2.467	19.735	1.98E+03	1.09E+03
PIII-2I-G-9-CI-1	121-129 min	8 min	3.406	1504	200.7	763	2.453	19.628	3.89E+04	1.15E+04
PIII-2I-G-9-CI-2	121-129 min	8 min	-0.015	33	13.1	12	2.453	19.628	6.11E+02	7.96E+02
PIII-2I-G-9-CI-3	121-129 min	8 min	-0.496	12	2.4	2	2.453	19.628	1.02E+02	1.63E+02
PIII-2I-G-9-CI-4	121-129 min	8 min	-0.829	16	4.4	-1	2.453	19.628	-5.09E+01	3.28E+02
PIII-2I-G-9-CI-5	121-129 min	8 min	-0.421	47	18.2	38	2.453	19.628	1.94E+03	9.50E+02
PIII-2I-G-9-CI-6	121-129 min	8 min	1.973	73	30.5	53	2.453	19.628	2.70E+03	1.61E+03
PIII-2I-G-9-CI-7	121-129 min	8 min	0.503	47	13.0	31	2.453	19.628	1.58E+03	7.08E+02
PIII-2I-G-9-CI-8	121-129 min	8 min	-0.025	94	25.0	76	2.453	19.628	3.87E+03	1.31E+03
PIII-2I-G-9-CI-9	121-129 min	8 min	0.359	52	18.1	32	2.453	19.628	1.63E+03	9.94E+02

(a) DU mass based on ICP-MS results; no analytical uncertainty was reported.

Table A.29 (cont'd). Phase III, Shot 2, Loader

Sample ID	Collection Interval	Elapsed Time	Total Mass (mg)	Calculated U (μg)	DU Mass ± 1σ (μg)	Net DU Mass (μg)	Flow Rate (Lpm)	Volume (L)	DU Conc. (μg/m^3)	DU Conc. ± 1σ (μg/m^3)
PIII-2I-L-1-CI-1	0-10 sec	10 sec	0.626	252	46.5	198	2.489	0.415	4.77E+05	1.16E+05
PIII-2I-L-1-CI-2	0-10 sec	10 sec	1.331	76	35.4	62	2.489	0.415	1.49E+05	8.71E+04
PIII-2I-L-1-CI-3	0-10 sec	10 sec	0.410	178	NA[(a)]	175	2.489	0.415	4.22E+05	NA[(a)]
PIII-2I-L-1-CI-4	0-10 sec	10 sec	-0.297	192	NA[(a)]	192	2.489	0.415	4.63E+05	NA[(a)]
PIII-2I-L-1-CI-5	0-10 sec	10 sec	0.526	206	NA[(a)]	206	2.489	0.415	4.96E+05	NA[(a)]
PIII-2I-L-1-CI-6	0-10 sec	10 sec	0.522	117	28.1	116	2.489	0.415	2.80E+05	6.83E+04
PIII-2I-L-1-CI-7	0-10 sec	10 sec	-0.014	80	14.0	79	2.489	0.415	1.90E+05	3.43E+04
PIII-2I-L-1-CI-8	0-10 sec	10 sec	0.091	221	21.9	209	2.489	0.415	5.04E+05	5.51E+04
PIII-2I-L-1-CI-9	0-10 sec	10 sec	1.149	176	30.9	163	2.489	0.415	3.93E+05	7.57E+04
PIII-2I-L-2-CI-1	1-1 min 10 sec	10 sec	0.399	73	13.8	19	2.528	0.421	4.51E+04	4.09E+04
PIII-2I-L-2-CI-2	1-1 min 10 sec	10 sec	2.959	15	7.1	1	2.528	0.421	2.38E+03	2.37E+04
PIII-2I-L-2-CI-3	1-1 min 10 sec	10 sec	-0.338	45	11.5	42	2.528	0.421	9.98E+04	2.76E+04
PIII-2I-L-2-CI-4	1-1 min 10 sec	10 sec	0.896	66	23.9	66	2.528	0.421	1.57E+05	5.70E+04
PIII-2I-L-2-CI-5	1-1 min 10 sec	10 sec	-0.373	65	25.0	65	2.528	0.421	1.54E+05	5.96E+04
PIII-2I-L-2-CI-6	1-1 min 10 sec	10 sec	0.790	65	16.0	64	2.528	0.421	1.52E+05	3.84E+04
PIII-2I-L-2-CI-7	1-1 min 10 sec	10 sec	-0.360	46	8.6	45	2.528	0.421	1.07E+05	2.09E+04
PIII-2I-L-2-CI-8	1-1 min 10 sec	10 sec	-0.526	76	8.6	64	2.528	0.421	1.52E+05	2.14E+04
PIII-2I-L-2-CI-9	1-1 min 10 sec	10 sec	1.714	75	13.5	62	2.528	0.421	1.47E+05	3.30E+04
PIII-2I-L-3-CI-1	3-3 min 15 sec	15 sec	0.138	50	9.6	-4	2.616	0.654	-6.12E+03	2.15E+04
PIII-2I-L-3-CI-2	3-3 min 15 sec	15 sec	3.623	11	5.4	-3	2.616	0.654	-4.59E+03	1.35E+04
PIII-2I-L-3-CI-3	3-3 min 15 sec	15 sec	0.156	43	11.2	40	2.616	0.654	6.12E+04	1.73E+04
PIII-2I-L-3-CI-4	3-3 min 15 sec	15 sec	0.416	81	29.5	81	2.616	0.654	1.24E+05	4.53E+04
PIII-2I-L-3-CI-5	3-3 min 15 sec	15 sec	0.162	85	32.6	85	2.616	0.654	1.30E+05	5.00E+04
PIII-2I-L-3-CI-6	3-3 min 15 sec	15 sec	-0.715	72	17.6	71	2.616	0.654	1.09E+05	2.72E+04
PIII-2I-L-3-CI-7	3-3 min 15 sec	15 sec	-0.051	91	15.8	90	2.616	0.654	1.38E+05	2.46E+04
PIII-2I-L-3-CI-8	3-3 min 15 sec	15 sec	-0.369	103	10.6	91	2.616	0.654	1.39E+05	1.70E+04
PIII-2I-L-3-CI-9	3-3 min 15 sec	15 sec	1.036	25	5.0	12	2.616	0.654	1.83E+04	8.78E+03
PIII-2I-L-4-CI-1	7-8 min	1 min	0.646	54	10.3	0.2	2.608	2.608	7.67E+01	5.59E+03
PIII-2I-L-4-CI-2	7-8 min	1 min	2.262	6	3.1	-8	2.608	2.608	-3.07E+03	2.94E+03
PIII-2I-L-4-CI-3	7-8 min	1 min	-1.474	6	1.9	3	2.608	2.608	1.15E+03	8.62E+02
PIII-2I-L-4-CI-4	7-8 min	1 min	-1.103	22	8.2	22	2.608	2.608	8.44E+03	3.17E+03
PIII-2I-L-4-CI-5	7-8 min	1 min	-0.570	50	19.3	50	2.608	2.608	1.92E+04	7.44E+03
PIII-2I-L-4-CI-6	7-8 min	1 min	-2.104	67	16.3	66	2.608	2.608	2.53E+04	6.31E+03
PIII-2I-L-4-CI-7	7-8 min	1 min	-0.964	40	7.4	39	2.608	2.608	1.50E+04	2.91E+03
PIII-2I-L-4-CI-8	7-8 min	1 min	-1.493	28	4.0	16	2.608	2.608	6.13E+03	1.69E+03
PIII-2I-L-4-CI-9	7-8 min	1 min	1.102	20	3.9	7	2.608	2.608	2.68E+03	1.84E+03
PIII-2I-L-5-CI-1	15-17 min	2 min	0.046	43	8.1	-11	2.612	5.224	-2.11E+03	2.51E+03
PIII-2I-L-5-CI-2	15-17 min	2 min	0.521	9	4.7	-5	2.612	5.224	-9.57E+02	1.61E+03
PIII-2I-L-5-CI-3	15-17 min	2 min	-0.111	12	3.4	9	2.612	5.224	1.72E+03	6.92E+02
PIII-2I-L-5-CI-4	15-17 min	2 min	-0.481	21	7.8	21	2.612	5.224	4.02E+03	1.51E+03
PIII-2I-L-5-CI-5	15-17 min	2 min	-2.020	28	11.0	28	2.612	5.224	5.36E+03	2.12E+03
PIII-2I-L-5-CI-6	15-17 min	2 min	-1.627	23	6.0	22	2.612	5.224	4.21E+03	1.17E+03
PIII-2I-L-5-CI-7	15-17 min	2 min	-0.213	18	3.5	17	2.612	5.224	3.25E+03	7.15E+02

Table A.29 (cont'd). Phase III, Shot 2, Loader

Sample ID	Collection Interval	Elapsed Time	Total Mass (mg)	Calculated U (μg)	DU Mass ± 1σ (μg)	Net DU Mass (μg)	Flow Rate (Lpm)	Volume (L)	DU Conc. (μg/m^3)	DU Conc. ± 1σ (μg/m^3)
PIII-2I-L-5-CI-8	15-17 min	2 min	-0.014	28	3.7	16	2.612	5.224	3.06E+03	7.93E+02
PIII-2I-L-5-CI-9	15-17 min	2 min	0.509	36	6.7	23	2.612	5.224	4.40E+03	1.40E+03
PIII-2I-L-6-CI-1	31-35 min	4 min	0.261	56	10.5	2	2.543	10.170	1.97E+02	1.45E+03
PIII-2I-L-6-CI-2	31-35 min	4 min	0.543	19	8.9	5	2.543	10.170	4.92E+02	1.11E+03
PIII-2I-L-6-CI-3	31-35 min	4 min	-0.643	6	1.9	3	2.543	10.170	2.95E+02	2.21E+02
PIII-2I-L-6-CI-4	31-35 min	4 min	-0.384	20	7.4	20	2.543	10.170	1.97E+03	7.35E+02
PIII-2I-L-6-CI-5	31-35 min	4 min	-0.396	36	14.2	36	2.543	10.170	3.54E+03	1.41E+03
PIII-2I-L-6-CI-6	31-35 min	4 min	-1.228	36	8.8	35	2.543	10.170	3.44E+03	8.77E+02
PIII-2I-L-6-CI-7	31-35 min	4 min	-1.613	31	5.8	30	2.543	10.170	2.95E+03	5.89E+02
PIII-2I-L-6-CI-8	31-35 min	4 min	-0.562	43	5.4	31	2.543	10.170	3.05E+03	5.67E+02
PIII-2I-L-6-CI-9	31-35 min	4 min	1.301	79	14.3	66	2.543	10.170	6.49E+03	1.45E+03
PIII-2I-L-7-CI-1	61-69 min	8 min	0.532	69	NA[(a)]	15	2.511	20.086	7.47E+02	NA[(a)]
PIII-2I-L-7-CI-2	61-69 min	8 min	0.805	14	6.7	-0.2	2.511	20.086	-9.96E+00	4.82E+02
PIII-2I-L-7-CI-3	61-69 min	8 min	0.518	5	1.7	2	2.511	20.086	9.96E+01	1.04E+02
PIII-2I-L-7-CI-4	61-69 min	8 min	-1.423	20	7.5	20	2.511	20.086	9.96E+02	3.77E+02
PIII-2I-L-7-CI-5	61-69 min	8 min	-0.555	70	26.7	70	2.511	20.086	3.49E+03	1.33E+03
PIII-2I-L-7-CI-6	61-69 min	8 min	-0.627	65	15.8	64	2.511	20.086	3.19E+03	7.94E+02
PIII-2I-L-7-CI-7	61-69 min	8 min	-1.562	53	9.3	52	2.511	20.086	2.59E+03	4.73E+02
PIII-2I-L-7-CI-8	61-69 min	8 min	-0.422	97	10.0	85	2.511	20.086	4.23E+03	5.22E+02
PIII-2I-L-7-CI-9	61-69 min	8 min	1.670	107	19.0	94	2.511	20.086	4.68E+03	9.66E+02
PIII-2I-L-8-CI-1	121-129 min	8 min	0.462	89	16.5	35	2.569	20.550	1.70E+03	9.48E+02
PIII-2I-L-8-CI-2	121-129 min	8 min	-1.155	10	5.0	-4	2.569	20.550	-1.95E+02	4.19E+02
PIII-2I-L-8-CI-3	121-129 min	8 min	-0.458	5	1.7	2	2.569	20.550	9.73E+01	1.01E+02
PIII-2I-L-8-CI-4	121-129 min	8 min	-1.501	12	4.7	12	2.569	20.550	5.84E+02	2.34E+02
PIII-2I-L-8-CI-5	121-129 min	8 min	-0.724	38	14.7	38	2.569	20.550	1.85E+03	7.20E+02
PIII-2I-L-8-CI-6	121-129 min	8 min	-1.262	34	8.6	33	2.569	20.550	1.61E+03	4.24E+02
PIII-2I-L-8-CI-7	121-129 min	8 min	-0.895	60	10.6	59	2.569	20.550	2.87E+03	5.26E+02
PIII-2I-L-8-CI-8	121-129 min	8 min	-0.214	77	8.4	65	2.569	20.550	3.16E+03	4.29E+02
PIII-2I-L-8-CI-9	121-129 min	8 min	0.932	62	11.1	49	2.569	20.550	2.38E+03	5.62E+02
PIII-2I-L-9-CI-1	Field Blank	--	0.398	54	10.3	--	--	--	--	--
PIII-2I-L-9-CI-2	Field Blank	--	5.892	14	7.0	--	--	--	--	--
PIII-2I-L-9-CI-3	Field Blank	--	-0.748	3	1.2	--	--	--	--	--
PIII-2I-L-9-CI-4	Field Blank	--	-0.551	0	0.9	--	--	--	--	--
PIII-2I-L-9-CI-5	Field Blank	--	-1.502	0	1.2	--	--	--	--	--
PIII-2I-L-9-CI-6	Field Blank	--	-1.371	1	1.0	--	--	--	--	--
PIII-2I-L-9-CI-7	Field Blank	--	-1.124	1	1.2	--	--	--	--	--
PIII-2I-L-9-CI-8	Field Blank	--	-2.390	12	1.8	--	--	--	--	--
PIII-2I-L-9-CI-9	Field Blank	--	2.039	13	2.8	--	--	--	--	--

(a) DU mass based on ICP-MS results; no analytical uncertainty was reported.

Table A.30. PIV-1 Cascade Impactor Substrates—Mass, Volume, and Concentration

Sample ID	Collection Interval	Elapsed Time	Total Mass (mg)	Calculated U (μg)	DU Mass ± 1σ (μg)	Net DU Mass (μg)	Flow Rate (Lpm)	Volume (L)	DU Conc. (μg/m^3)	DU Conc. ± 1σ (μg/m^3)
PIV-1I-D-6-CI-1	0-1 min	1 min	0.432	2.0	0.7	2	2.254	2.254	8.87E+02	3.12E+02
PIV-1I-D-6-CI-2	0-1 min	1 min	-0.601	1.0	1.1	1	2.254	2.254	4.44E+02	4.88E+02
PIV-1I-D-6-CI-3	0-1 min	1 min	-0.115	-1.0	0.6	-1	2.254	2.254	-4.44E+02	2.67E+02
PIV-1I-D-6-CI-4	0-1 min	1 min	-0.003	0.3	0.7	0.3	2.254	2.254	1.33E+02	3.11E+02
PIV-1I-D-6-CI-5	0-1 min	1 min	-0.647	1.0	1.3	1	2.254	2.254	4.44E+02	5.77E+02
PIV-1I-D-6-CI-6	0-1 min	1 min	-0.943	1.0	1.7	1	2.254	2.254	4.44E+02	7.54E+02
PIV-1I-D-6-CI-7	0-1 min	1 min	-0.652	2.0	1.7	2	2.254	2.254	8.87E+02	7.55E+02
PIV-1I-D-6-CI-8	0-1 min	1 min	-0.709	1.0	2.5	1	2.254	2.254	4.44E+02	1.11E+03
PIV-1I-D-6-CI-9	0-1 min	1 min	-1.388	4.0	2.3	4	2.254	2.254	1.77E+03	1.02E+03
PIV-1I-D-7-CI-1	1-3 min	2 min	0.778	-0.5	0.7	-0.5	2.252	4.504	-1.11E+02	1.55E+02
PIV-1I-D-7-CI-2	1-3 min	2 min	0.629	-0.3	0.7	-0.3	2.252	4.504	-6.66E+01	1.55E+02
PIV-1I-D-7-CI-3	1-3 min	2 min	-3.122	0.04	0.4	0.04	2.252	4.504	8.88E+00	8.88E+01
PIV-1I-D-7-CI-4	1-3 min	2 min	0.182	3.0	1	3	2.252	4.504	6.66E+02	2.23E+02
PIV-1I-D-7-CI-5	1-3 min	2 min	0.003	1.0	1.2	1	2.252	4.504	2.22E+02	2.67E+02
PIV-1I-D-7-CI-6	1-3 min	2 min	-0.972	-1.0	1.7	-1	2.252	4.504	-2.22E+02	3.78E+02
PIV-1I-D-7-CI-7	1-3 min	2 min	0.755	1.0	1.7	1	2.252	4.504	2.22E+02	3.78E+02
PIV-1I-D-7-CI-8	1-3 min	2 min	1.519	-0.5	1.7	-0.5	2.252	4.504	-1.11E+02	3.77E+02
PIV-1I-D-7-CI-9	1-3 min	2 min	-1.974	-1.0	2	-1	2.252	4.504	-2.22E+02	4.44E+02
PIV-1I-D-8-CI-1	5-9 min	4 min	0.385	0.1	0.7	0.1	2.516	10.063	9.94E+00	6.96E+01
PIV-1I-D-8-CI-2	5-9 min	4 min	0.273	4.0	1.6	4	2.516	10.063	3.97E+02	1.59E+02
PIV-1I-D-8-CI-3	5-9 min	4 min	-0.097	2.0	0.8	2	2.516	10.063	1.99E+02	7.97E+01
PIV-1I-D-8-CI-4	5-9 min	4 min	-3.660	-0.1	0.7	-0.1	2.516	10.063	-9.94E+00	6.96E+01
PIV-1I-D-8-CI-5	5-9 min	4 min	-0.852	2.0	1.2	2	2.516	10.063	1.99E+02	1.19E+02
PIV-1I-D-8-CI-6	5-9 min	4 min	0.580	-1.0	1.3	-1	2.516	10.063	-9.94E+01	1.29E+02
PIV-1I-D-8-CI-7	5-9 min	4 min	2.839	6.0	3	6	2.516	10.063	5.96E+02	2.99E+02
PIV-1I-D-8-CI-8	5-9 min	4 min	0.651	1.0	2.1	1	2.516	10.063	9.94E+01	2.09E+02
PIV-1I-D-8-CI-9	5-9 min	4 min	-0.538	-3.0	1.7	-3	2.516	10.063	-2.98E+02	1.69E+02
PIV-1I-D-9-CI-1	25-33 min	8 min	1.335	1.0	0.9	1	2.433	19.467	5.14E+01	4.63E+01
PIV-1I-D-9-CI-2	25-33 min	8 min	1.356	5.0	2.2	5	2.433	19.467	2.57E+02	1.13E+02
PIV-1I-D-9-CI-3	25-33 min	8 min	-0.506	0.1	0.5	0.1	2.433	19.467	5.14E+00	2.57E+01
PIV-1I-D-9-CI-4	25-33 min	8 min	0.557	0.2	0.5	0.2	2.433	19.467	1.03E+01	2.57E+01
PIV-1I-D-9-CI-5	25-33 min	8 min	-0.605	-1.0	1.1	-1	2.433	19.467	-5.14E+01	5.65E+01
PIV-1I-D-9-CI-6	25-33 min	8 min	-3.946	1.0	2	1	2.433	19.467	5.14E+01	1.03E+02
PIV-1I-D-9-CI-7	25-33 min	8 min	-1.022	3.0	1.6	3	2.433	19.467	1.54E+02	8.23E+01
PIV-1I-D-9-CI-8	25-33 min	8 min	-1.413	-3.0	1.7	-3	2.433	19.467	-1.54E+02	8.74E+01
PIV-1I-D-9-CI-9	25-33 min	8 min	0.444	-2.0	1.5	-2	2.433	19.467	-1.03E+02	7.71E+01

Table A.30 (cont'd). Phase IV, Shot 1, Loader

Sample ID	Collection Interval	Elapsed Time	Total Mass (mg)	Calculated U (μg)	DU Mass ± 1σ (μg)	Net DU Mass (μg)	Flow Rate (Lpm)	Volume (L)	DU Conc. (μg/m^3)	DU Conc. ± 1σ (μg/m^3)
PIV-1I-L-1-CI-1	0-1 min	1 min	0.686	11	1.9	11	2.430	2.430	4.53E+03	8.94E+02
PIV-1I-L-1-CI-2	0-1 min	1 min	-0.695	3	1.7	-3	2.430	2.430	-1.23E+03	1.31E+03
PIV-1I-L-1-CI-3	0-1 min	1 min	-1.263	5	1.1	-1	2.430	2.430	-4.12E+02	7.66E+02
PIV-1I-L-1-CI-4	0-1 min	1 min	-3.013	1	0.7	-8	2.430	2.430	-3.29E+03	1.07E+03
PIV-1I-L-1-CI-5	0-1 min	1 min	-1.519	1.1	1.0	0.1	2.430	2.430	4.12E+01	6.12E+02
PIV-1I-L-1-CI-6	0-1 min	1 min	0.582	4	1.9	2	2.430	2.430	8.23E+02	9.25E+02
PIV-1I-L-1-CI-7	0-1 min	1 min	-1.220	2	1.5	2	2.430	2.430	8.23E+02	8.45E+02
PIV-1I-L-1-CI-8	0-1 min	1 min	-1.147	5	3.3	-6	2.430	2.430	-2.47E+03	1.81E+03
PIV-1I-L-1-CI-9	0-1 min	1 min	-1.166	7	3.1	1	2.430	2.430	4.12E+02	1.64E+03
PIV-1I-L-2-CI-1	1-3 min	2 min	1.520	2	0.8	2	2.574	5.148	3.89E+02	2.49E+02
PIV-1I-L-2-CI-2	1-3 min	3 min	0.683	0	0.8	-6	2.574	5.148	-1.17E+03	5.48E+02
PIV-1I-L-2-CI-3	1-3 min	4 min	-1.469	1	0.6	-5	2.574	5.148	-9.71E+02	3.15E+02
PIV-1I-L-2-CI-4	1-3 min	5 min	-0.063	1	0.8	-8	2.574	5.148	-1.55E+03	5.12E+02
PIV-1I-L-2-CI-5	1-3 min	6 min	1.330	2	1.3	1	2.574	5.148	1.94E+02	3.31E+02
PIV-1I-L-2-CI-6	1-3 min	7 min	-1.614	1	1.8	-1	2.574	5.148	-1.94E+02	4.20E+02
PIV-1I-L-2-CI-7	1-3 min	8 min	-1.595	5	2.6	5	2.574	5.148	9.71E+02	5.74E+02
PIV-1I-L-2-CI-8	1-3 min	9 min	0.057	11.3	3.6	0.3	2.574	5.148	5.83E+01	8.98E+02
PIV-1I-L-2-CI-9	1-3 min	10 min	-1.330	9	3.2	3	2.574	5.148	5.83E+02	7.89E+02
PIV-1I-L-3-CI-1	5-9 min	4 min	0.204	0.3	0.8	0.3	2.664	10.658	2.81E+01	1.20E+02
PIV-1I-L-3-CI-2	5-9 min	4 min	0.759	3	1.4	-3	2.664	10.658	-2.81E+02	2.85E+02
PIV-1I-L-3-CI-3	5-9 min	4 min	-0.173	3	0.9	-3	2.664	10.658	-2.81E+02	1.64E+02
PIV-1I-L-3-CI-4	5-9 min	4 min	-0.471	0	--	-9	2.664	10.658	-8.44E+02	--
PIV-1I-L-3-CI-5	5-9 min	4 min	0.222	15	5.9	14	2.664	10.658	1.31E+03	5.64E+02
PIV-1I-L-3-CI-6	5-9 min	4 min	-0.400	8	3.5	6	2.664	10.658	5.63E+02	3.48E+02
PIV-1I-L-3-CI-7	5-9 min	4 min	0.959	13	3.6	13	2.664	10.658	1.22E+03	3.64E+02
PIV-1I-L-3-CI-8	5-9 min	4 min	-1.000	3	2.6	-8	2.664	10.658	-7.51E+02	3.66E+02
PIV-1I-L-3-CI-9	5-9 min	4 min	-0.766	7	3.4	1	2.664	10.658	9.38E+01	3.96E+02
PIV-1I-L-4-CI-1	25-33 min	8 min	0.721	5	1.0	5	2.696	21.566	2.32E+02	6.59E+01
PIV-1I-L-4-CI-2	25-33 min	8 min	-0.523	2	1.0	-4	2.696	21.566	-1.85E+02	1.34E+02
PIV-1I-L-4-CI-3	25-33 min	8 min	-0.562	0	0.5	-6	2.696	21.566	-2.78E+02	7.38E+01
PIV-1I-L-4-CI-4	25-33 min	8 min	-0.621	-1	0.8	-10	2.696	21.566	-4.64E+02	1.23E+02
PIV-1I-L-4-CI-5	25-33 min	8 min	0.429	0	1.1	-1	2.696	21.566	-4.64E+01	7.21E+01
PIV-1I-L-4-CI-6	25-33 min	8 min	-0.438	-2	1.7	-4	2.696	21.566	-1.85E+02	9.66E+01
PIV-1I-L-4-CI-7	25-33 min	8 min	-0.394	-3	1.7	-3	2.696	21.566	-1.39E+02	1.02E+02
PIV-1I-L-4-CI-8	25-33 min	8 min	0.155	-1	1.9	-12	2.696	21.566	-5.56E+02	1.62E+02
PIV-1I-L-4-CI-9	25-33 min	8 min	0.085	4	2.0	-2	2.696	21.566	-9.27E+01	1.48E+02
PIV-1I-L-5-CI-1	Field Blank	--	1.050	0	1.0	--	--	--	--	
PIV-1I-L-5-CI-2	Field Blank	--	0.004	6	2.7	--	--	--	--	
PIV-1I-L-5-CI-3	Field Blank	--	0.341	6	1.5	--	--	--	--	
PIV-1I-L-5-CI-4	Field Blank	--	0.098	9	2.5	--	--	--	--	
PIV-1I-L-5-CI-5	Field Blank	--	-1.599	1	1.1	--	--	--	--	
PIV-1I-L-5-CI-6	Field Blank	--	-0.285	2	1.2	--	--	--	--	

Table A.30 (cont'd). Phase IV, Shot 1, Loader

Sample ID	Collection Interval	Elapsed Time	Total Mass (mg)	Calculated U (μg)	DU Mass ± 1σ (μg)	Net DU Mass (μg)	Flow Rate (Lpm)	Volume (L)	DU Conc. (μg/m^3)	DU Conc. ± 1σ (μg/m^3)
PIV-1I-L-5-CI-7	Field Blank	--	-0.546	-2	1.4	--	--	--	--	
PIV-1I-L-5-CI-8	Field Blank	--	2.602	11	2.9	--	--	--	--	
PIV-1I-L-5-CI-9	Field Blank	--	1.665	6	2.5	--	--	--	--	
-- = Original count activity = 0.00, therefore no uncertainty propagated for mass or concentration results.										

Table A.31. PIV-3 Cascade Impactor Substrates—Mass, Volume, and Concentration

Sample ID	Collection Interval	Elapsed Time	Total Mass (mg)	Calculated U (μg)	DU Mass ± 1σ (μg)	Net DU Mass (μg)	Flow Rate (Lpm)	Volume (L)	DU Conc. (μg/m^3)	DU Conc. ± 1σ (μg/m^3)
PIV-3I-D-1-CI-1	0-10 sec	10 sec	1.444	2	0.9	-1	2.232	0.372	-2.69E+03	3.42E+03
PIV-3I-D-1-CI-2	0-10 sec	10 sec	-3.462	-2	1.2	-10	2.232	0.372	-2.69E+04	9.73E+03
PIV-3I-D-1-CI-3	0-10 sec	10 sec	-0.859	0	0.6	-2	2.232	0.372	-5.38E+03	3.14E+03
PIV-3I-D-1-CI-4	0-10 sec	10 sec	-1.268	0	0.8	-1	2.232	0.372	-2.69E+03	3.04E+03
PIV-3I-D-1-CI-5	0-10 sec	10 sec	1.806	1	1.2	1	2.232	0.372	2.69E+03	4.96E+03
PIV-3I-D-1-CI-6	0-10 sec	10 sec	-0.425	10	5.5	5	2.232	0.372	1.34E+04	1.71E+04
PIV-3I-D-1-CI-7	0-10 sec	10 sec	-0.958	11	3.9	5	2.232	0.372	1.34E+04	1.26E+04
PIV-3I-D-1-CI-8	0-10 sec	10 sec	0.475	2	4.4	2	2.232	0.372	5.38E+03	1.79E+04
PIV-3I-D-1-CI-9	0-10 sec	10 sec	-1.362	-2	2.8	-4	2.232	0.372	-1.08E+04	9.75E+03
PIV-3I-D-2-CI-1	1-1 min, 10 sec	10 sec	1.279	3.4	1.0	0.4	2.658	0.443	9.03E+02	3.04E+03
PIV-3I-D-2-CI-2	1-1 min, 10 sec	10 sec	-1.852	0	0.8	-8	2.658	0.443	-1.81E+04	7.90E+03
PIV-3I-D-2-CI-3	1-1 min, 10 sec	10 sec	-0.036	-1	0.9	-3	2.658	0.443	-6.77E+03	3.04E+03
PIV-3I-D-2-CI-4	1-1 min, 10 sec	10 sec	-0.572	-1	0.8	-2	2.658	0.443	-4.51E+03	2.56E+03
PIV-3I-D-2-CI-5	1-1 min, 10 sec	10 sec	-2.041	-3	1.6	-3	2.658	0.443	-6.77E+03	4.80E+03
PIV-3I-D-2-CI-6	1-1 min, 10 sec	10 sec	-2.948	-5	3.0	-10	2.658	0.443	-2.26E+04	9.92E+03
PIV-3I-D-2-CI-7	1-1 min, 10 sec	10 sec	-2.113	2	2.7	-4	2.658	0.443	-9.03E+03	8.47E+03
PIV-3I-D-2-CI-8	1-1 min, 10 sec	10 sec	-3.671	-3	4.2	-3	2.658	0.443	-6.77E+03	1.47E+04
PIV-3I-D-2-CI-9	1-1 min, 10 sec	10 sec	0.230	-2	2.7	-4	2.658	0.443	-9.03E+03	8.01E+03
PIV-3I-D-3-CI-1	5-5 min, 15 sec	15 sec	0.279	6	1.4	3	2.544	0.636	4.72E+03	2.62E+03
PIV-3I-D-3-CI-2	5-5 min, 15 sec	15 sec	-0.963	-1	0.8	-9	2.544	0.636	-1.42E+04	5.51E+03
PIV-3I-D-3-CI-3	5-5 min, 15 sec	15 sec	-0.881	-1	0.7	-3	2.544	0.636	-4.72E+03	1.92E+03
PIV-3I-D-3-CI-4	5-5 min, 15 sec	15 sec	-2.454	-1	0.9	-2	2.544	0.636	-3.14E+03	1.90E+03
PIV-3I-D-3-CI-5	5-5 min, 15 sec	15 sec	-2.675	-2	1.7	-2	2.544	0.636	-3.14E+03	3.46E+03
PIV-3I-D-3-CI-6	5-5 min, 15 sec	15 sec	-3.792	-1	2.1	-6	2.544	0.636	-9.43E+03	6.02E+03
PIV-3I-D-3-CI-7	5-5 min, 15 sec	15 sec	-1.850	4	3.4	-2	2.544	0.636	-3.14E+03	6.73E+03
PIV-3I-D-3-CI-8	5-5 min, 15 sec	15 sec	-1.902	-2	4.4	-2	2.544	0.636	-3.14E+03	1.05E+04
PIV-3I-D-3-CI-9	5-5 min, 15 sec	15 sec	-2.143	-6	3.3	-8	2.544	0.636	-1.26E+04	6.34E+03
PIV-3I-D-4-CI-1	25-27 min	2 min	0.401	0	0.7	-3	2.439	4.878	-6.15E+02	2.34E+02
PIV-3I-D-4-CI-2	25-27 min	2 min	-1.511	0	0.7	-8	2.439	4.878	-1.64E+03	7.13E+02
PIV-3I-D-4-CI-3	25-27 min	2 min	-0.762	-1	0.6	-3	2.439	4.878	-6.15E+02	2.40E+02
PIV-3I-D-4-CI-4	25-27 min	2 min	-0.996	-1	0.9	-2	2.439	4.878	-4.10E+02	2.47E+02
PIV-3I-D-4-CI-5	25-27 min	2 min	-2.666	-0.3	0.9	-0.3	2.439	4.878	2.05E+01	3.41E+02
PIV-3I-D-4-CI-6	25-27 min	2 min	0.325	-3	2.1	-8	2.439	4.878	-1.64E+03	7.86E+02
PIV-3I-D-4-CI-7	25-27 min	2 min	-1.728	-2	1.7	-8	2.439	4.878	-1.64E+03	6.39E+02
PIV-3I-D-4-CI-8	25-27 min	2 min	-1.897	25	9.0	25	2.439	4.878	5.13E+03	2.12E+03
PIV-3I-D-4-CI-9	25-27 min	2 min	-1.511	7	3.8	5	2.439	4.878	1.03E+03	9.11E+02
PIV-3I-D-5-CI-1	Field Blank	--	0.115	3	0.9	--	--	--	--	--
PIV-3I-D-5-CI-2	Field Blank	--	-0.002	8	3.4	--	--	--	--	--
PIV-3I-D-5-CI-3	Field Blank	--	0.115	2	1.0	--	--	--	--	--
PIV-3I-D-5-CI-4	Field Blank	--	-0.209	1	0.8	--	--	--	--	--
PIV-3I-D-5-CI-5	Field Blank	--	0.076	-2	1.4	--	--	--	--	--
PIV-3I-D-5-CI-6	Field Blank	--	-0.170	5	3.2	--	--	--	--	--

Table A.31 (cont'd). Phase IV, Shot 3, Driver

Sample ID	Collection Interval	Elapsed Time	Total Mass (mg)	Calculated U (μg)	DU Mass ± 1σ (μg)	Net DU Mass (μg)	Flow Rate (Lpm)	Volume (L)	DU Conc. (μg/m^3)	DU Conc. ± 1σ (μg/m^3)
PIV-3I-D-5-CI-7	Field Blank	--	-0.416	6	2.6	--	--	--	--	--
PIV-3I-D-5-CI-8	Field Blank	--	0.061	-5	5.0	--	--	--	--	--
PIV-3I-D-5-CI-9	Field Blank	--	0.109	2	2.3	--	--	--	--	--

Table A.31 (cont'd). Phase IV, Shot 3, Loader

Sample ID	Collection Interval	Elapsed Time	Total Mass (mg)	Calculated U (μg)	DU Mass ± 1σ (μg)	Net DU Mass (μg)	Flow Rate (Lpm)	Volume (L)	DU Conc. (μg/m^3)	DU Conc. ± 1σ (μg/m^3)
PIV-3I-L-1-CI-1	0-10 sec	10 sec	0.584	3	1.2	3	2.524	0.421	7.13E+03	3.87E+03
PIV-3I-L-1-CI-2	0-10 sec	10 sec	0.850	-4	1.8	-5	2.524	0.421	-1.19E+04	5.29E+03
PIV-3I-L-1-CI-3	0-10 sec	10 sec	0.274	-1	0.8	-1	2.524	0.421	-2.38E+03	2.69E+03
PIV-3I-L-1-CI-4	0-10 sec	10 sec	-0.216	-2	1.0	-2	2.524	0.421	-4.75E+03	3.90E+03
PIV-3I-L-1-CI-5	0-10 sec	10 sec	1.232	0.2	1.8	0.2	2.524	0.421	4.75E+02	6.39E+03
PIV-3I-L-1-CI-6	0-10 sec	10 sec	1.376	3	3.7	3	2.524	0.421	7.13E+03	1.19E+04
PIV-3I-L-1-CI-7	0-10 sec	10 sec	2.550	-1	2.7	-1	2.524	0.421	-2.38E+03	9.77E+03
PIV-3I-L-1-CI-8	0-10 sec	10 sec	-0.038	-22	7.7	-22	2.524	0.421	-5.23E+04	2.20E+04
PIV-3I-L-1-CI-9	0-10 sec	10 sec	-1.954	-8	4.1	-8	2.524	0.421	-1.90E+04	1.46E+04
PIV-3I-L-2-CI-1	1-1 min, 10 sec	10 sec	0.470	-0.3	1.0	-0.3	2.604	0.434	2.30E+02	3.43E+03
PIV-3I-L-2-CI-2	1-1 min, 10 sec	10 sec	-1.299	-3	1.6	-4	2.604	0.434	-9.22E+03	4.76E+03
PIV-3I-L-2-CI-3	1-1 min, 10 sec	10 sec	-1.368	1	1.0	1	2.604	0.434	2.30E+03	2.95E+03
PIV-3I-L-2-CI-4	1-1 min, 10 sec	10 sec	-0.392	-2	1.0	-2	2.604	0.434	-4.61E+03	3.78E+03
PIV-3I-L-2-CI-5	1-1 min, 10 sec	10 sec	-0.818	-4	2.4	-4	2.604	0.434	-9.22E+03	7.20E+03
PIV-3I-L-2-CI-6	1-1 min, 10 sec	10 sec	-0.897	-5	3.6	-5	2.604	0.434	-1.15E+04	1.14E+04
PIV-3I-L-2-CI-7	1-1 min, 10 sec	10 sec	1.538	-8	3.1	-8	2.604	0.434	-1.84E+04	1.01E+04
PIV-3I-L-2-CI-8	1-1 min, 10 sec	10 sec	-0.063	-8	4.5	-8	2.604	0.434	-1.84E+04	1.57E+04
PIV-3I-L-2-CI-9	1-1 min, 10 sec	10 sec	-1.580	-10	4.8	-10	2.604	0.434	-2.30E+04	1.53E+04
PIV-3I-L-3-CI-1	5-5 min, 15 sec	15 sec	0.527	-3	1.3	-3	2.682	0.670	-4.48E+03	2.55E+03
PIV-3I-L-3-CI-2	5-5 min, 15 sec	15 sec	-2.664	-3	1.7	-4	2.682	0.670	-5.97E+03	3.20E+03
PIV-3I-L-3-CI-3	5-5 min, 15 sec	15 sec	0.313	-1	0.7	-1	2.682	0.670	-1.49E+03	1.59E+03
PIV-3I-L-3-CI-4	5-5 min, 15 sec	15 sec	-0.885	-3	1.3	-3	2.682	0.670	-4.48E+03	2.75E+03
PIV-3I-L-3-CI-5	5-5 min, 15 sec	15 sec	-1.079	-5	2.6	-5	2.682	0.670	-7.46E+03	4.90E+03
PIV-3I-L-3-CI-6	5-5 min, 15 sec	15 sec	-2.151	4	4.2	4	2.682	0.670	5.97E+03	8.07E+03
PIV-3I-L-3-CI-7	5-5 min, 15 sec	15 sec	1.162	-8	3.3	-8	2.682	0.670	-1.19E+04	6.77E+03
PIV-3I-L-3-CI-8	5-5 min, 15 sec	15 sec	-0.774	-18	6.1	-18	2.682	0.670	-2.69E+04	1.19E+04
PIV-3I-L-3-CI-9	5-5 min, 15 sec	15 sec	-1.509	-6	3.5	-6	2.682	0.670	-8.96E+03	8.63E+03
PIV-3I-L-4-CI-1	25-27 min	2 min	0.726	-3	1.4	-3	2.756	5.511	-5.44E+02	3.23E+02
PIV-3I-L-4-CI-2	25-27 min	2 min	-1.360	-3	1.6	-4	2.756	5.511	-7.26E+02	3.75E+02
PIV-3I-L-4-CI-3	25-27 min	2 min	-1.427	-1	0.8	-1	2.756	5.511	-1.81E+02	2.05E+02
PIV-3I-L-4-CI-4	25-27 min	2 min	-2.845	-2	1.0	-2	2.756	5.511	-3.63E+02	2.98E+02
PIV-3I-L-4-CI-5	25-27 min	2 min	0.168	-5	2.5	-5	2.756	5.511	-9.07E+02	5.82E+02
PIV-3I-L-4-CI-6	25-27 min	2 min	-1.539	-6	3.5	-6	2.756	5.511	-1.09E+03	8.86E+02
PIV-3I-L-4-CI-7	25-27 min	2 min	-3.307	-6	3.3	-6	2.756	5.511	-1.09E+03	8.22E+02
PIV-3I-L-4-CI-8	25-27 min	2 min	-0.476	-16	6.1	-16	2.756	5.511	-2.90E+03	1.45E+03
PIV-3I-L-4-CI-9	25-27 min	2 min	-1.042	-3	3.2	-3	2.756	5.511	-5.44E+02	1.02E+03
PIV-3I-L-5-CI-1	Field Blank	--	0.699	-1	1.1	--	--	--	--	--
PIV-3I-L-5-CI-2	Field Blank	--	0.245	1	1.3	--	--	--	--	--
PIV-3I-L-5-CI-3	Field Blank	--	1.657	-3	0.8	--	--	--	--	--
PIV-3I-L-5-CI-4	Field Blank	--	0.060	-3	1.3	--	--	--	--	--
PIV-3I-L-5-CI-5	Field Blank	--	0.249	-2	2.0	--	--	--	--	--
PIV-3I-L-5-CI-6	Field Blank	--	2.498	-5	3.4	--	--	--	--	--

Table A.31 (cont'd). Phase IV, Shot 3, Loader

Sample ID	Collection Interval	Elapsed Time	Total Mass (mg)	Calculated U (μg)	DU Mass ± 1σ (μg)	Net DU Mass (μg)	Flow Rate (Lpm)	Volume (L)	DU Conc. (μg/m^3)	DU Conc. ± 1σ (μg/m^3)
PIV-3I-L-5-CI-7	Field Blank	--	-0.273	-8	3.1	--	--	--	--	--
PIV-3I-L-5-CI-8	Field Blank	--	1.568	-8	5.1	--	--	--	--	--
PIV-3I-L-5-CI-9	Field Blank	--	-2.769	-10	4.6	--	--	--	--	--

Table A.32. PIV-4 Cascade Impactor Substrates—Mass, Volume, and Concentration

Sample ID	Collection Interval	Elapsed Time	Total Mass (mg)	Calculated U (μg)	DU Mass ± 1σ (μg)	Net DU Mass (μg)	Flow Rate (Lpm)	Volume (L)	DU Conc. (μg/m^3)	DU Conc. ± 1σ (μg/m^3)
PIV-4I-D-1-CI-1	0-10 sec	10 sec	0.302	13	2.3	13	2.499	0.417	3.12E+04	6.09E+03
PIV-4I-D-1-CI-2	0-10 sec	10 sec	0.045	2	1.5	2	2.499	0.417	4.80E+03	4.33E+03
PIV-4I-D-1-CI-3	0-10 sec	10 sec	-1.080	-0.1	0.9	-0.1	2.499	0.417	-2.40E+02	2.89E+03
PIV-4I-D-1-CI-4	0-10 sec	10 sec	0.479	-0.1	1.0	-0.1	2.499	0.417	-2.40E+02	3.23E+03
PIV-4I-D-1-CI-5	0-10 sec	10 sec	-0.565	1	1.7	-1	2.499	0.417	-2.40E+03	5.94E+03
PIV-4I-D-1-CI-6	0-10 sec	10 sec	-0.405	2	2.3	2	2.499	0.417	4.80E+03	8.33E+03
PIV-4I-D-1-CI-7	0-10 sec	10 sec	-0.699	1	2.7	1	2.499	0.417	2.40E+03	8.66E+03
PIV-4I-D-1-CI-8	0-10 sec	10 sec	-0.261	-1	3.2	-1	2.499	0.417	-2.40E+03	1.17E+04
PIV-4I-D-1-CI-9	0-10 sec	10 sec	-0.364	15	5.7	15	2.499	0.417	3.60E+04	1.47E+04
PIV-4I-D-2-CI-1	1-1 min, 10 sec	10 sec	0.916	3	1.2	3	2.627	0.438	6.85E+03	3.57E+03
PIV-4I-D-2-CI-2	1-1 min, 10 sec	10 sec	0.192	-2	1.3	-2	2.627	0.438	-4.57E+03	3.75E+03
PIV-4I-D-2-CI-3	1-1 min, 10 sec	10 sec	-0.267	1	0.9	1	2.627	0.438	2.28E+03	2.75E+03
PIV-4I-D-2-CI-4	1-1 min, 10 sec	10 sec	0.035	2	1.4	2	2.627	0.438	4.57E+03	3.80E+03
PIV-4I-D-2-CI-5	1-1 min, 10 sec	10 sec	0.503	1	1.4	-1	2.627	0.438	-2.28E+03	5.21E+03
PIV-4I-D-2-CI-6	1-1 min, 10 sec	10 sec	0.026	15	6.9	15	2.627	0.438	3.42E+04	1.69E+04
PIV-4I-D-2-CI-7	1-1 min, 10 sec	10 sec	-0.608	24	7.6	24	2.627	0.438	5.48E+04	1.83E+04
PIV-4I-D-2-CI-8	1-1 min, 10 sec	10 sec	0.196	45	11.4	45	2.627	0.438	1.03E+05	2.75E+04
PIV-4I-D-2-CI-9	1-1 min, 10 sec	10 sec	-2.902	12	4.9	12	2.627	0.438	2.74E+04	1.23E+04
PIV-4I-D-3-CI-1	5-5 min, 15 sec	15 sec	0.142	1	1.3	1	2.504	0.626	1.60E+03	2.62E+03
PIV-4I-D-3-CI-2	5-5 min, 15 sec	15 sec	-0.477	1	1.2	1	2.504	0.626	1.60E+03	2.50E+03
PIV-4I-D-3-CI-3	5-5 min, 15 sec	15 sec	-0.226	-1	0.8	-1	2.504	0.626	-1.60E+03	1.81E+03
PIV-4I-D-3-CI-4	5-5 min, 15 sec	15 sec	0.492	0.2	0.9	0.2	2.504	0.626	3.19E+02	2.03E+03
PIV-4I-D-3-CI-5	5-5 min, 15 sec	15 sec	-0.769	-2	1.6	-2	2.504	0.626	-3.19E-03	3.85E+03
PIV-4I-D-3-CI-6	5-5 min, 15 sec	15 sec	-0.299	17	7.1	17	2.504	0.626	2.72E+04	1.21E+04
PIV-4I-D-3-CI-7	5-5 min, 15 sec	15 sec	0.386	1	2.6	1	2.504	0.626	1.60E+03	5.65E+03
PIV-4I-D-3-CI-8	5-5 min, 15 sec	15 sec	-0.118	9	3.6	9	2.504	0.626	1.44E+04	8.26E+03
PIV-4I-D-3-CI-9	5-5 min, 15 sec	15 sec	-2.006	0.2	2.4	0.2	2.504	0.626	3.19E+02	5.20E+03
PIV-4I-D-4-CI-1	25-27 min	2 min	0.326	2	1.2	2	2.418	4.836	4.14E+02	3.23E+02
PIV-4I-D-4-CI-2	25-27 min	2 min	0.261	2	1.2	2	2.418	4.836	4.14E+02	3.23E+02
PIV-4I-D-4-CI-3	25-27 min	2 min	-1.178	8	1.8	8	2.418	4.836	1.65E+03	4.10E+02
PIV-4I-D-4-CI-4	25-27 min	2 min	-2.764	8	2.5	8	2.418	4.836	1.65E+03	5.52E+02
PIV-4I-D-4-CI-5	25-27 min	2 min	-2.349	19	7.5	19	2.418	4.836	3.93E+03	1.60E+03
PIV-4I-D-4-CI-6	25-27 min	2 min	-0.568	8	3.8	8	2.418	4.836	1.65E+03	9.53E+02
PIV-4I-D-4-CI-7	25-27 min	2 min	-1.375	7	2.8	7	2.418	4.836	1.45E+03	7.64E+02
PIV-4I-D-4-CI-8	25-27 min	2 min	-2.305	1	2.7	1	2.418	4.836	2.07E+02	9.47E+02
PIV-4I-D-4-CI-9	25-27 min	2 min	-2.351	1	2.1	1	2.418	4.836	2.07E+02	6.29E+02
PIV-4I-D-5-CI-1	Field Blank	--	0.319	0	1.0	--	--	--	--	--
PIV-4I-D-5-CI-2	Field Blank	--	0.346	0	1.0	--	--	--	--	--
PIV-4I-D-5-CI-3	Field Blank	--	-0.245	-2	0.8	--	--	--	--	--
PIV-4I-D-5-CI-4	Field Blank	--	-0.387	-1	0.9	--	--	--	--	--
PIV-4I-D-5-CI-5	Field Blank	--	-0.001	2	1.8	--	--	--	--	--
PIV-4I-D-5-CI-6	Field Blank	--	-0.057	-5	2.6	--	--	--	--	--

Table A.32 (cont'd). Phase IV, Shot 4, Driver

Sample ID	Collection Interval	Elapsed Time	Total Mass (mg)	Calculated U (μg)	DU Mass ± 1σ (μg)	Net DU Mass (μg)	Flow Rate (Lpm)	Volume (L)	DU Conc. (μg/m^3)	DU Conc. ± 1σ (μg/m^3)
PIV-4I-D-5-CI-7	Field Blank	--	-0.456	-6	2.4	--	--	--	--	--
PIV-4I-D-5-CI-8	Field Blank	--	-0.751	-4	3.7	--	--	--	--	--
PIV-4I-D-5-CI-9	Field Blank	--	-0.612	-3	2.2	--	--	--	--	--

Table A.32 (cont'd). Phase IV, Shot 4, Loader

Sample ID	Collection Interval	Elapsed Time	Total Mass (mg)	Calculated U (μg)	DU Mass ± 1σ (μg)	Net DU Mass (μg)	Flow Rate (Lpm)	Volume (L)	DU Conc. (μg/m^3)	DU Conc. ± 1σ (μg/m^3)
PIV-4I-L-1-CI-1	0-10 sec	Lines	1.194	28	NA[(b)]	-65	2.547	--	--	--
PIV-4I-L-1-CI-2	0-10 sec	Severed	-1.115	1	1.7	-4	2.547	--	--	--
PIV-4I-L-1-CI-3	0-10 sec	--	-1.048	74	NA[(b)]	70	2.547	--	--	--
PIV-4I-L-1-CI-4	0-10 sec	--	-0.311	2	1.6	2	2.547	--	--	--
PIV-4I-L-1-CI-5	0-10 sec	--	-1.426	-3	2.5	-3	2.547	--	--	--
PIV-4I-L-1-CI-6	0-10 sec	--	-2.53	-6	3.6	-11	2.547	--	--	--
PIV-4I-L-1-CI-7	0-10 sec	--	-4.112	9	4	9	2.547	--	--	--
PIV-4I-L-1-CI-8	0-10 sec	--	-2.922	7	4.6	7	2.547	--	--	--
PIV-4I-L-1-CI-9	0-10 sec	--	-3.88	-2	3.1	-5	2.547	--	--	--
PIV-4I-L-2-CI-1	1-1 min 10 sec	(a)	0.227	52	7.5	-41	2.709	--	--	--
PIV-4I-L-2-CI-2	1-1 min 10 sec	--	-0.201	2	1.9	-3	2.709	--	--	--
PIV-4I-L-2-CI-3	1-1 min 10 sec	--	0.152	2	1.3	-2	2.709	--	--	--
PIV-4I-L-2-CI-4	1-1 min 10 sec	--	-2.508	0.3	1.4	0.3	2.709	--	--	--
PIV-4I-L-2-CI-5	1-1 min 10 sec	--	-0.782	0.1	1.8	0.1	2.709	--	--	--
PIV-4I-L-2-CI-6	1-1 min 10 sec	--	-2.582	-4	3.3	-9	2.709	--	--	--
PIV-4I-L-2-CI-7	1-1 min 10 sec	--	-0.09	2	3.2	2	2.709	--	--	--
PIV-4I-L-2-CI-8	1-1 min 10 sec	--	-0.886	0.4	4.6	0.4	2.709	--	--	--
PIV-4I-L-2-CI-9	1-1 min 10 sec	--	-2.84	-1	3.5	-4	2.709	--	--	--
PIV-4I-L-3-CI-1	5-5min 15 sec	(b)	1.146	72	10.5	-21	2.749	--	--	--
PIV-4I-L-3-CI-2	5-5min 15 sec	(b)	-0.794	2	2	-3	2.749	--	--	--
PIV-4I-L-3-CI-3	5-5min 15 sec	(c)	1.629	3	1.2	-1	2.749	--	--	--
PIV-4I-L-3-CI-4	5-5min 15 sec	--	-1.242	-1	1.1	-1	2.749	--	--	--
PIV-4I-L-3-CI-5	5-5min 15 sec	--	0.551	5	2.9	5	2.749	--	--	--
PIV-4I-L-3-CI-6	5-5min 15 sec	--	-0.21	0	2.5	-5	2.749	--	--	--
PIV-4I-L-3-CI-7	5-5min 15 sec	--	0.441	15	4.6	15	2.749	--	--	--
PIV-4I-L-3-CI-8	5-5min 15 sec	--	-1.77	4	4.4	4	2.749	--	--	--
PIV-4I-L-3-CI-9	5-5min 15 sec	--	-0.219	-1	4	-4	2.749	--	--	--
PIV-4I-L-4-CI-1	25-27 min	(d)	0.452	39	5.8	-54	2.764	--	--	--
PIV-4I-L-4-CI-2	25-27 min	--	0.607	0	1.8	-5	2.764	--	--	--
PIV-4I-L-4-CI-3	25-27 min	(e)	-0.326	0	1.1	-4	2.764	--	--	--
PIV-4I-L-4-CI-4	25-27 min	(f)	-0.283	4	1.9	4	2.764	--	--	--
PIV-4I-L-4-CI-5	25-27 min	--	-2.211	-5	2.8	-5	2.764	--	--	--
PIV-4I-L-4-CI-6	25-27 min	--	-0.595	-6	3.6	-11	2.764	--	--	--
PIV-4I-L-4-CI-7	25-27 min	--	-1.643	-2	3.1	-2	2.764	--	--	--
PIV-4I-L-4-CI-8	25-27 min	--	-1.241	-4	4	-4	2.764	--	--	--
PIV-4I-L-4-CI-9	25-27 min	--	-1.642	1	3.1	-2	2.764	--	--	--
PIV-4I-L-5-CI-1	Field Blank	--	0.565	93	13	--	--	--	--	--
PIV-4I-L-5-CI-2	Field Blank	(g)	0.01	5	2.9	--	--	--	--	--
PIV-4I-L-5-CI-3	Field Blank	(h)	-1.509	4	1.4	--	--	--	--	--
PIV-4I-L-5-CI-4	Field Blank	(i)	-1.312	0	1.4	--	--	--	--	--
PIV-4I-L-5-CI-5	Field Blank	--	-1.219	-3	2.3	--	--	--	--	--
PIV-4I-L-5-CI-6	Field Blank	--	-0.277	5	3.1	--	--	--	--	--

Table A.32 (cont'd). Phase IV, Shot 4, Loader

Sample ID	Collection Interval	Elapsed Time	Total Mass (mg)	Calculated U (μg)	DU Mass ± 1σ (μg)	Net DU Mass (μg)	Flow Rate (Lpm)	Volume (L)	DU Conc. (μg/m^3)	DU Conc. ± 1σ (μg/m^3)
PIV-4I-L-5-CI-7	Field Blank	--	-1.106	-6	3.1	--	--	--	--	--
PIV-4I-L-5-CI-8	Field Blank	--	-2.708	-5	4.3	--	--	--	--	--
PIV-4I-L-5-CI-9	Field Blank	--	-1.139	3	3.2	--	--	--	--	--

(a) Burn mark on substrate.
(b) Burn hole in substrate.
(c) Burn hole in substrate.
(d) Three burn holes in substrate.
(e) An 8.5 mg fragment recovered on substrate.
(f) A 3.0 mg fragment recovered on substrate.
(g) A 24.6 mg fragment recovered on substrate.
(h) A 0.88 mg fragment recovered on substrate.
(i) Two fragments weighing a total of 1.77 mg were recovered on substrate.

Table A.33. PI-1 Moving Filter Segments—Mass, Volume, and Concentration

Sample ID	Collection Interval	Elapsed Time	Calculated U (μg)	DU Mass ± 1σ (μg)	Net DU Mass (μg)	Flow Rate (Lpm)	Volume (L)	DU Conc. (μg/m^3)	DU Conc. ± 1σ (μg/m^3)
PI-1F-1-MV-1	0-5 sec	5 sec (stationary)	18234	5635.9	18234	18.8	Uncertain	Not calc'd	Not calc'd
PI-1F-1-MV-2	5-15 sec	10 sec (moving)	6316	1952.2	6316	18.8	Uncertain	Not calc'd	Not calc'd
PI-1F-1-MV-3	15-30 sec	10 sec (stationary)	7202	2225.9	7202	18.8	Uncertain	Not calc'd	Not calc'd
PI-1F-1-MV-4	30-50 sec	20 sec (moving)	4531	1400.5	4531	18.8	Uncertain	Not calc'd	Not calc'd
PI-1F-1-MV-5	50-70 sec	20 sec (stationary)	3964	1225.5	3964	18.8	Uncertain	Not calc'd	Not calc'd
PI-1F-1-MV-6	1.17-1.5 min	20 sec (moving)	2372	733.2	2372	18.8	Uncertain	Not calc'd	Not calc'd
PI-1F-1-MV-7	1.5-2.17 min	40 sec (stationary)	24102	7449.4	24102	18.8	Uncertain	Not calc'd	Not calc'd
PI-1F-1-MV-8	2.17-2.83 min	40 sec (moving)	9167	2833.6	9167	18.8	Uncertain	Not calc'd	Not calc'd
PI-1F-1-MV-9	2.83-3.5 min	40 sec (stationary)	26802	8284.1	26802	18.8	Uncertain	Not calc'd	Not calc'd
PI-1F-1-MV-10	3.5-4.83 min	1 min, 20 sec (smeared)	1196	369.8	1196	18.8	Uncertain	Not calc'd	Not calc'd
PI-1F-1-MV-11	4.83-6.17 min	1 min, 20 sec (smeared-uncertain)	755	233.7	755	18.8	Uncertain	Not calc'd	Not calc'd
PI-1F-1-MV-12	6.17-7.5 min	1 min, 20 sec (smeared-uncertain)	534	165.1	534	18.8	Uncertain	Not calc'd	Not calc'd
PI-1F-1-MV-13	7.5-10.17 min	2 min, 40 sec (smeared-uncertain)	560	173.2	560	18.8	Uncertain	Not calc'd	Not calc'd
PI-1F-1-MV-14	10.17-12.83 min	2 min, 40 sec (smeared-uncertain)	17629	5448.9	17629	18.8	Uncertain	Not calc'd	Not calc'd
PI-1F-1-MV-15	12.83-15.5 min	2 min, 40 sec (stationary, stuck)	506	157.0	506	18.8	Uncertain	Not calc'd	Not calc'd

Table A.34. PI-3/4 Moving Filter Segments—Mass, Volume, and Concentration

Sample ID	Sampling Midpoint (min)	Elapsed Time (sec)	Calc'd U (µg)	DU Mass ± 1σ (µg)	Net DU Mass (µg)	Flow Rate (Lpm)	Volume (liters)	DU Conc. (µg, m^3)	DU Conc. ± 1σ (µg/m^3)
PI-3/4I-F-1-MV-001	0.024	1.4	2561	808.7	2561	30.0	1.4384	1.78E+06	5.65E+05
PI-3/4I-F-1-MV-002	0.0719	4.3	7139	2254.1	7139	30.0	1.4384	4.96E+06	1.57E+06
PI-3/4I-F-1-MV-003	0.1199	7.2	6973	2202.0	6973	30.0	1.4384	4.85E+06	1.54E+06
PI-3/4I-F-1-MV-004	0.1678	10.1	6692	2113.3	6692	30.0	1.4384	4.65E+06	1.48E+06
PI-3/4I-F-1-MV-005	0.2158	12.9	8660	2734.4	8660	30.0	1.4384	6.02E+06	1.91E+06
PI-3/4I-F-1-MV-006	0.2637	15.8	8295	2619.3	8295	30.0	1.4384	5.77E+06	1.83E+06
PI-3/4I-F-1-MV-007	0.3116	18.7	7891	2492.2	7891	30.0	1.4384	5.49E+06	1.74E+06
PI-3/4I-F-1-MV-008	0.3596	21.6	8417	2658.2	8417	30.0	1.4384	5.85E+06	1.86E+06
PI-3/4I-F-1-MV-009	0.4075	24.5	7335	2316.7	7335	30.0	1.4384	5.10E+06	1.62E+06
PI-3/4I-F-1-MV-010	0.4555	27.3	6203	1959.1	6203	30.0	1.4384	4.31E+06	1.37E+06
PI-3/4I-F-1-MV-011	0.5034	30.2	6837	2159.5	6837	30.0	1.4384	4.75E+06	1.51E+06
PI-3/4I-F-1-MV-012	0.5514	33.1	6552	2068.8	6552	30.0	1.4384	4.56E+06	1.44E+06
PI-3/4I-F-1-MV-013	0.5993	36	6367	2011.0	6367	30.0	1.4384	4.43E+06	1.40E+06
PI-3/4I-F-1-MV-014	0.6473	38.8	5764	1820.7	5764	30.0	1.4384	4.01E+06	1.27E+06
PI-3/4I-F-1-MV-015	0.6952	41.7	5098	1609.9	5098	30.0	1.4384	3.54E+06	1.12E+06
PI-3/4I-F-1-MV-016	0.7432	44.6	5284	1668.8	5284	30.0	1.4384	3.67E+06	1.17E+06
PI-3/4I-F-1-MV-017	0.7911	47.5	6095	1925.2	6095	30.0	1.4384	4.24E+06	1.34E+06
PI-3/4I-F-1-MV-018	0.839	50.3	5525	1745.3	5525	30.0	1.4384	3.84E+06	1.22E+06
PI-3/4I-F-1-MV-019	0.887	53.2	1511	478.2	1511	30.0	1.4384	1.05E+06	3.34E+05
PI-3/4I-F-1-MV-020	0.9349	56.1	1601	506.6	1601	30.0	1.4384	1.11E+06	3.54E+05

Table A.35. PII-3 Moving Filter Segments—Mass, Volume, and Concentration

Sample ID	Sampling Midpoint (min)	Sampling Midpoint (sec)	Calc'd U (μg)	DU Mass ± 1σ (μg)	Net DU Mass (μg)	Flow Rate (Lpm)	Volume (liters)	DU Conc. (μg/m^3)	DU Conc. ± 1σ (μg/m^3)
PII-3F-1-MV-001	0.024	1.4	137	43.9	137	18.95	0.9086	1.51E+05	4.85E+04
PII-3F-1-MV-002	0.0719	4.3	738	233.7	738	18.95	0.9086	8.12E+05	2.58E+05
PII-3F-1-MV-003	0.1199	7.2	971	307.1	971	18.95	0.9086	1.07E+06	3.40E+05
PII-3F-1-MV-004	0.1678	10.1	632	200.2	632	18.95	0.9086	6.96E+05	2.21E+05
PII-3F-1-MV-005	0.2158	12.9	597	189.1	597	18.95	0.9086	6.57E+05	2.09E+05
PII-3F-1-MV-006	0.2637	15.8	457	145.0	457	18.95	0.9086	5.03E+05	1.60E+05
PII-3F-1-MV-007	0.3116	18.7	494	156.7	494	18.95	0.9086	5.44E+05	1.73E+05
PII-3F-1-MV-008	0.3596	21.6	410	130.0	410	18.95	0.9086	4.51E+05	1.44E+05
PII-3F-1-MV-009	0.4075	24.5	377	119.8	377	18.95	0.9086	4.15E+05	1.32E+05
PII-3F-1-MV-010	0.4555	27.3	330	104.9	330	18.95	0.9086	3.63E+05	1.16E+05
PII-3F-1-MV-011	0.5034	30.2	325	103.3	325	18.95	0.9086	3.58E+05	1.14E+05
PII-3F-1-MV-012	0.5514	33.1	319	101.4	319	18.95	0.9086	3.51E+05	1.12E+05
PII-3F-1-MV-013	0.5993	36	359	114.0	359	18.95	0.9086	3.95E+05	1.26E+05
PII-3F-1-MV-014	0.6473	38.8	369	117.3	369	18.95	0.9086	4.06E+05	1.30E+05
PII-3F-1-MV-015	0.6952	41.7	268	85.5	268	18.95	0.9086	2.95E+05	9.45E+04
PII-3F-1-MV-016	0.7432	44.6	312	99.3	312	18.95	0.9086	3.43E+05	1.10E+05
PII-3F-1-MV-017	0.7911	47.5	229	72.9	229	18.95	0.9086	2.52E+05	8.06E+04
PII-3F-1-MV-018	0.839	50.3	272	86.7	272	18.95	0.9086	2.99E+05	9.58E+04
PII-3F-1-MV-019	0.887	53.2	234	74.7	234	18.95	0.9086	2.58E+05	8.26E+04
PII-3F-1-MV-020	0.9349	56.1	243	77.7	243	18.95	0.9086	2.67E+05	8.59E+04
PII-3F-1-MV-021	0.9829	59	253	80.6	253	18.95	0.9086	2.78E+05	8.91E+04
PII-3F-1-MV-022	1.0308	61.8	213	68.1	213	18.95	0.9086	2.34E+05	7.53E+04
PII-3F-1-MV-023	1.0788	64.7	213	68.1	213	18.95	0.9086	2.34E+05	7.53E+04
PII-3F-1-MV-024	1.1267	67.6	226	72.0	226	18.95	0.9086	2.49E+05	7.96E+04
PII-3F-1-MV-025	1.1747	70.5	237	75.6	237	18.95	0.9086	2.61E+05	8.36E+04
PII-3F-1-MV-026	1.2226	73.4	198	63.4	198	18.95	0.9086	2.18E+05	7.01E+04
PII-3F-1-MV-027	1.2705	76.2	196	62.7	196	18.95	0.9086	2.16E+05	6.93E+04
PII-3F-1-MV-028	1.3185	79.1	182	58.6	182	18.95	0.9086	2.00E+05	6.48E+04
PII-3F-1-MV-029	1.3664	82	192	61.5	192	18.95	0.9086	2.11E+05	6.80E+04
PII-3F-1-MV-030	1.4144	84.9	206	65.7	206	18.95	0.9086	2.27E+05	7.26E+04
PII-3F-1-MV-031	1.4623	87.7	176	56.7	176	18.95	0.9086	1.94E+05	6.27E+04
PII-3F-1-MV-032	1.5103	90.6	165	53.2	165	18.95	0.9086	1.82E+05	5.88E+04
PII-3F-1-MV-033	1.5582	93.5	153	49.3	153	18.95	0.9086	1.68E+05	5.45E+04
PII-3F-1-MV-034	1.6062	96.4	141	45.5	141	18.95	0.9086	1.55E+05	5.03E+04
PII-3F-1-MV-035	1.6541	99.2	137	44.1	137	18.95	0.9086	1.51E+05	4.87E+04
PII-3F-1-MV-036	1.7021	102.1	147	47.3	147	18.95	0.9086	1.62E+05	5.23E+04
PII-3F-1-MV-037	1.75	105	134	43.5	134	18.95	0.9086	1.47E+05	4.81E+04
PII-3F-1-MV-038	1.7979	107.9	145	46.8	145	18.95	0.9086	1.60E+05	5.17E+04

Table A.35 (cont'd). PII-3 Moving Filter Segments

Sample ID	Sampling Midpoint (min)	Sampling Midpoint (sec)	Calc'd U (μg)	DU Mass ± 1σ (μg)	Net DU Mass (μg)	Flow Rate (Lpm)	Volume (liters)	DU Conc. (μg/m^3)	DU Conc. ± 1σ (μg/m^3)
PII-3F-1-MV-039	1.8459	110.8	134	43.2	134	18.95	0.9086	1.47E+05	4.78E+04
PII-3F-1-MV-040	1.8938	113.6	126	40.8	126	18.95	0.9086	1.39E+05	4.51E+04
PII-3F-1-MV-041	1.9418	116.5	128	41.3	128	18.95	0.9086	1.41E+05	4.57E+04
PII-3F-1-MV-042	1.9897	119.4	113	37.0	113	18.95	0.9086	1.24E+05	4.09E+04
PII-3F-1-MV-043	2.0377	122.3	128	41.4	128	18.95	0.9086	1.41E+05	4.58E+04
PII-3F-1-MV-044	2.0856	125.1	108	35.2	108	18.95	0.9086	1.19E+05	3.89E+04
PII-3F-1-MV-045	2.1336	128	122	39.4	122	18.95	0.9086	1.34E+05	4.36E+04
PII-3F-1-MV-046	2.1815	130.9	111	35.9	111	18.95	0.9086	1.22E+05	3.97E+04
PII-3F-1-MV-047	2.2295	133.8	114	36.6	114	18.95	0.9086	1.25E+05	4.05E+04
PII-3F-1-MV-048	2.2774	136.6	121	39.0	121	18.95	0.9086	1.33E+05	4.31E+04
PII-3F-1-MV-049	2.3253	139.5	115	36.9	115	18.95	0.9086	1.27E+05	4.08E+04
PII-3F-1-MV-050	2.3733	142.4	105	34.0	105	18.95	0.9086	1.16E+05	3.76E+04
PII-3F-1-MV-051	2.4212	145.3	100	32.5	100	18.95	0.9086	1.10E+05	3.59E+04
PII-3F-1-MV-052	2.4692	148.2	88	29.0	88	18.95	0.9086	9.69E+04	3.20E+04
PII-3F-1-MV-053	2.5171	151	102	33.0	102	18.95	0.9086	1.12E+05	3.65E+04
PII-3F-1-MV-054	2.5651	153.9	93	30.3	93	18.95	0.9086	1.02E+05	3.35E+04
PII-3F-1-MV-055	2.613	156.8	117	37.5	117	18.95	0.9086	1.29E+05	4.15E+04
PII-3F-1-MV-056	2.661	159.7	93	30.3	93	18.95	0.9086	1.02E+05	3.35E+04
PII-3F-1-MV-057	2.7089	162.5	84	27.5	84	18.95	0.9086	9.24E+04	3.04E+04
PII-3F-1-MV-058	2.7568	165.4	82	NA[(a)]	82	18.95	0.9086	9.02E+04	NA[(a)]
PII-3F-1-MV-059	2.8048	168.3	94	30.3	94	18.95	0.9086	1.03E+05	3.35E+04
PII-3F-1-MV-060	2.8527	171.2	82	27.0	82	18.95	0.9086	9.02E+04	2.98E+04
PII-3F-1-MV-061	2.9007	174	87	28.3	87	18.95	0.9086	9.58E+04	3.13E+04
PII-3F-1-MV-062	2.9486	176.9	79	26.2	79	18.95	0.9086	8.69E+04	2.90E+04
PII-3F-1-MV-063	2.9966	179.8	101	32.5	101	18.95	0.9086	1.11E+05	3.59E+04
PII-3F-1-MV-064	3.0445	182.7	75	24.9	75	18.95	0.9086	8.25E+04	2.75E+04
PII-3F-1-MV-065	3.0925	185.5	94	30.3	94	18.95	0.9086	1.03E+05	3.35E+04
PII-3F-1-MV-066	3.1404	188.4	74	24.4	74	18.95	0.9086	8.14E+04	2.70E+04
PII-3F-1-MV-067	3.1884	191.3	90	29.4	90	18.95	0.9086	9.91E+04	3.25E+04
PII-3F-1-MV-068	3.2363	194.2	69	22.8	69	18.95	0.9086	7.59E+04	2.52E+04
PII-3F-1-MV-069	3.2842	197.1	69	22.8	69	18.95	0.9086	7.59E+04	2.52E+04
PII-3F-1-MV-070	3.3322	199.9	76	24.9	76	18.95	0.9086	8.36E+04	2.75E+04
PII-3F-1-MV-071	3.3801	202.8	84	27.5	84	18.95	0.9086	9.24E+04	3.04E+04
PII-3F-1-MV-072	3.4281	205.7	71	23.3	71	18.95	0.9086	7.81E+04	2.58E+04
PII-3F-1-MV-073	3.476	208.6	70	23.0	70	18.95	0.9086	7.70E+04	2.54E+04
PII-3I-F-1-MV-074	--	Transition	90	30.1	90	18.95	0.909	9.90E+04	3.33E+04
PII-3I-F-1-MV-075	--	Transition	82	27.6	82	18.95	0.909	9.02E+04	3.04E+04
PII-3I-F-1-MV-076	7.024	421.4	84	28.2	84	18.95	0.909	9.24E+04	3.12E+04

Table A.35 (cont'd). PII-3 Moving Filter Segments

Sample ID	Sampling Midpoint (min)	Sampling Midpoint (sec)	Calc'd U (μg)	DU Mass ± 1σ (μg)	Net DU Mass (μg)	Flow Rate (Lpm)	Volume (liters)	DU Conc. (μg/m^3)	DU Conc. ± 1σ (μg/m^3)
PII-3I-F-1-MV-077	7.0719	424.3	87	29.3	87	18.95	0.909	9.57E+04	3.23E+04
PII-3I-F-1-MV-078	7.1199	427.2	83	28.0	83	18.95	0.909	9.13E+04	3.09E+04
PII-3I-F-1-MV-079	7.1678	430.1	87	29.3	87	18.95	0.909	9.57E+04	3.24E+04
PII-3I-F-1-MV-080	7.2158	432.9	93	31.2	93	18.95	0.909	1.02E+05	3.45E+04
PII-3I-F-1-MV-081	7.2637	435.8	92	31.0	92	18.95	0.909	1.01E+05	3.42E+04
PII-3I-F-1-MV-082	7.3116	438.7	82	27.7	82	18.95	0.909	9.02E+04	3.06E+04
PII-3I-F-1-MV-083	7.3596	441.6	90	30.4	90	18.95	0.909	9.90E+04	3.35E+04
PII-3I-F-1-MV-084	7.4075	444.5	75	25.5	75	18.95	0.909	8.25E+04	2.82E+04
PII-3I-F-1-MV-085	7.4555	447.3	76	25.6	76	18.95	0.909	8.36E+04	2.83E+04
PII-3I-F-1-MV-086	7.5034	450.2	37	12.9	37	18.95	0.909	4.07E+04	1.43E+04
PII-3I-F-1-MV-087	--	Transition	67	22.8	67	18.95	0.909	7.37E+04	2.51E+04
PII-3I-F-1-MV-088	--	Transition	91	30.5	91	18.95	0.909	1.00E+05	3.36E+04
PII-3I-F-1-MV-089	15.024	901.4	67	22.9	67	18.95	0.909	7.37E+04	2.53E+04
PII-3I-F-1-MV-090	15.0719	904.3	81	27.1	81	18.95	0.909	8.91E+04	2.99E+04
PII-3I-F-1-MV-091	15.1199	907.2	80	27.0	80	18.95	0.909	8.80E+04	2.98E+04
PII-3I-F-1-MV-092	15.1678	910.1	76	25.5	76	18.95	0.909	8.36E+04	2.82E+04
PII-3I-F-1-MV-093	15.2158	912.9	79	26.5	79	18.95	0.909	8.69E+04	2.93E+04
PII-3I-F-1-MV-094	15.2637	915.8	73	24.7	73	18.95	0.909	8.03E+04	2.73E+04
PII-3I-F-1-MV-095	15.3116	918.7	83	28.1	83	18.95	0.909	9.13E+04	3.10E+04
PII-3I-F-1-MV-096	15.3596	921.6	76	25.6	76	18.95	0.909	8.36E+04	2.83E+04
PII-3I-F-1-MV-097	15.4075	924.5	77	26.0	77	18.95	0.909	8.47E+04	2.87E+04
PII-3I-F-1-MV-098	15.4555	927.3	78	26.3	78	18.95	0.909	8.58E+04	2.91E+04
PII-3I-F-1-MV-099	15.5034	930.2	66	22.3	66	18.95	0.909	7.26E+04	2.47E+04
PII-3I-F-1-MV-100	--	Transition	69	23.2	69	18.95	0.909	7.59E+04	2.56E+04
PII-3I-F-1-MV-101	--	Transition	66	22.3	66	18.95	0.909	7.26E+04	2.46E+04
PII-3I-F-1-MV-102	31.024	1861.4	58	19.5	58	18.95	0.909	6.38E+04	2.16E+04
PII-3I-F-1-MV-103	31.0719	1864.3	61	20.6	61	18.95	0.909	6.71E+04	2.28E+04
PII-3I-F-1-MV-104	31.1199	1867.2	67	22.6	67	18.95	0.909	7.37E+04	2.49E+04
PII-3I-F-1-MV-105	31.1678	1870.1	61	20.7	61	18.95	0.909	6.71E+04	2.28E+04
PII-3I-F-1-MV-106	31.2158	1872.9	62	21.1	62	18.95	0.909	6.82E+04	2.33E+04
PII-3I-F-1-MV-107	31.2637	1875.8	84	28.2	84	18.95	0.909	9.24E+04	3.11E+04
PII-3I-F-1-MV-108	31.3116	1878.7	66	22.3	66	18.95	0.909	7.26E+04	2.46E+04
PII-3I-F-1-MV-109	31.3596	1881.6	72	24.4	72	18.95	0.909	7.92E+04	2.70E+04
PII-3I-F-1-MV-110	31.4075	1884.5	60	20.4	60	18.95	0.909	6.60E+04	2.25E+04
PII-3I-F-1-MV-111	31.4555	1887.3	68	23.0	68	18.95	0.909	7.48E+04	2.54E+04
PII-3I-F-1-MV-112	31.5034	1890.2	52	17.9	52	18.95	0.909	5.72E+04	1.97E+04
PII-3I-F-1-MV-113	--	Transition	9	3.4	9	18.95	0.909	9.90E+03	3.78E+03
PII-3I-F-1-MV-114	--	Transition	25	8.6	25	18.95	0.909	2.75E+04	9.51E+03

Table A.35 (cont'd). PII-3 Moving Filter Segments

Sample ID	Sampling Midpoint (min)	Sampling Midpoint (sec)	Calc'd U (μg)	DU Mass ± 1σ (μg)	Net DU Mass (μg)	Flow Rate (Lpm)	Volume (liters)	DU Conc. (μg/m^3)	DU Conc. ± 1σ (μg/m^3)
PII-3I-F-1-MV-115	61.024	3661.4	58	19.8	58	18.95	0.909	6.38E+04	2.19E+04
PII-3I-F-1-MV-116	61.0719	3664.3	68	22.8	68	18.95	0.909	7.48E+04	2.52E+04
PII-3I-F-1-MV-117	61.1199	3667.2	64	21.8	64	18.95	0.909	7.04E+04	2.40E+04
PII-3I-F-1-MV-118	61.1678	3670.1	51	17.4	51	18.95	0.909	5.61E+04	1.92E+04
PII-3I-F-1-MV-119	61.2158	3672.9	57	19.3	57	18.95	0.909	6.27E+04	2.13E+04
PII-3I-F-1-MV-120	61.2637	3675.8	62	21.1	62	18.95	0.909	6.82E+04	2.33E+04
PII-3I-F-1-MV-121	61.3116	3678.7	66	22.5	66	18.95	0.909	7.26E+04	2.49E+04
PII-3I-F-1-MV-122	61.3596	3681.6	62	20.9	62	18.95	0.909	6.82E+04	2.31E+04
PII-3I-F-1-MV-123	61.4075	3684.5	57	19.3	57	18.95	0.909	6.27E+04	2.13E+04
PII-3I-F-1-MV-124	61.4555	3687.3	71	24.1	71	18.95	0.909	7.81E+04	2.66E+04
PII-3I-F-1-MV-125	61.5034	3690.2	62	20.9	62	18.95	0.909	6.82E+04	2.31E+04
PII-3I-F-1-MV-126	--	Transition	59	20.0	59	18.95	0.909	6.49E+04	2.21E+04
PII-3I-F-1-MV-127	--	Transition	49	16.5	49	18.95	0.909	5.39E+04	1.82E+04
PII-3I-F-1-MV-128	--	Transition	10	3.7	10	18.95	0.909	1.10E+04	4.13E+03
PII-3I-F-1-MV-129	121.024	7261.4	32	11.0	32	18.95	0.909	3.52E+04	1.22E+04
PII-3I-F-1-MV-130	121.0719	7264.3	42	14.3	42	18.95	0.909	4.62E+04	1.57E+04
PII-3I-F-1-MV-131	121.1199	7267.2	45	15.3	45	18.95	0.909	4.95E+04	1.69E+04
PII-3I-F-1-MV-132	121.1678	7270.1	49	16.8	49	18.95	0.909	5.39E+04	1.86E+04
PII-3I-F-1-MV-133	121.2158	7272.9	32	11.0	32	18.95	0.909	3.52E+04	1.22E+04
PII-3I-F-1-MV-134	121.2637	7275.8	20	7.1	20	18.95	0.909	2.20E+04	7.84E+03
PII-3I-F-1-MV-135	121.3116	7278.7	24	8.2	24	18.95	0.909	2.64E+04	9.10E+03
PII-3I-F-1-MV-136	121.3596	7281.6	24	8.5	24	18.95	0.909	2.64E+04	9.39E+03
PII-3I-F-1-MV-137	121.4075	7284.5	18	6.4	18	18.95	0.909	1.98E+04	7.07E+03
PII-3I-F-1-MV-138	121.4555	7287.3	31	10.7	31	18.95	0.909	3.41E+04	1.18E+04
PII-3I-F-1-MV-139	121.5034	7290.2	18	6.6	18	18.95	0.909	1.98E+04	7.23E+03

Table A.36. PIII-1 Moving Filter Segments—Mass, Volume, and Concentration

Sample ID	Sampling Midpoint (min)	Sampling Midpoint (sec)	Calc'd U (μg)	DU Mass ± 1σ (μg)	Net DU Mass (μg)	Flow Rate (Lpm)	Volume (liters)	DU Conc. (μg/m^3)	DU Conc. ± 1σ (μg/m^3)
PIII-1F-1-MV-001	Pre-shot	--	9	3.5	9	--	--	--	--
PIII-1F-1-MV-002	Pre-shot	--	27	8.6	27	--	--	--	--
PIII-1F-1-MV-003	Pre-shot	--	23	7.6	23	--	--	--	--
PIII-1F-1-MV-004	Pre-shot	--	17	5.8	17	--	--	--	--
PIII-1F-1-MV-005	Pre-shot	--	10	3.7	10	--	--	--	--
PIII-1F-1-MV-006	Pre-shot	--	8	3.1	8	--	--	--	--
PIII-1F-1-MV-007	Pre-shot	--	18	6.2	18	--	--	--	--
PIII-1F-1-MV-008	Pre-shot	--	40	12.6	40	--	--	--	--
PIII-1F-1-MV-009	Pre-shot	--	27	9.0	27	--	--	--	--
PIII-1F-1-MV-010	Pre-shot	--	9	3.7	9	--	--	--	--
PIII-1F-1-MV-011	Pre-shot	--	10	3.6	10	--	--	--	--
PIII-1F-1-MV-012	Pre-shot	--	24	7.7	24	--	--	--	--
PIII-1F-1-MV-013	Pre-shot	--	13	4.6	13	--	--	--	--
PIII-1F-1-MV-014	Pre-shot	--	31	10.2	31	--	--	--	--
PIII-1F-1-MV-015	Pre-shot	--	12	4.6	12	--	--	--	--
PIII-1F-1-MV-016	Pre-shot	--	43	13.9	43	--	--	--	--
PIII-1F-1-MV-017	Pre-shot	--	20	6.8	20	--	--	--	--
PIII-1F-1-MV-018	Pre-shot	--	12	4.4	12	--	--	--	--
PIII-1F-1-MV-019	Pre-shot	--	16	5.7	16	--	--	--	--
PIII-1F-1-MV-020	Pre-shot	--	23	7.8	23	--	--	--	--
PIII-1F-1-MV-021	Pre-shot	--	29	9.6	29	--	--	--	--
PIII-1F-1-MV-022	Pre-shot	--	25	8.4	25	--	--	--	--
PIII-1F-1-MV-023	Pre-shot	--	14	5.0	14	--	--	--	--
PIII-1F-1-MV-024	Pre-shot	--	22	7.4	22	--	--	--	--
PIII-1F-1-MV-025	Pre-shot	--	117	36.8	117	--	--	--	--
PIII-1F-1-MV-026	Pre-shot	--	235	73.7	235	--	--	--	--
PIII-1F-1-MV-027	Pre-shot	--	347	108.9	347	--	--	--	--
PIII-1F-1-MV-028	0.024	1.4	1877	589.6	1877	25.81	1.2375	1.52E+06	4.79E+05
PIII-1F-1-MV-029	0.0719	4.3	8095	2544.5	8095	25.81	1.2375	6.54E+06	2.07E+06
PIII-1F-1-MV-030	0.1199	7.2	10105	3175.5	10105	25.81	1.2375	8.17E+06	2.58E+06
PIII-1F-1-MV-031	0.1678	10.1	4721	1484.4	4721	25.81	1.2375	3.81E+06	1.20E+06
PIII-1F-1-MV-032	0.2158	12.9	4046	1272.2	4046	25.81	1.2375	3.27E+06	1.03E+06
PIII-1F-1-MV-033	0.2637	15.8	3240	1018.4	3240	25.81	1.2375	2.62E+06	8.27E+05
PIII-1F-1-MV-034	0.3116	18.7	3237	1018.1	3237	25.81	1.2375	2.62E+06	8.26E+05
PIII-1F-1-MV-035	0.3596	21.6	3156	992.3	3156	25.81	1.2375	2.55E+06	8.06E+05
PIII-1F-1-MV-036	0.4075	24.5	2613	821.9	2613	25.81	1.2375	2.11E+06	6.67E+05
PIII-1F-1-MV-037	0.4555	27.3	2828	889.6	2828	25.81	1.2375	2.29E+06	7.22E+05
PIII-1F-1-MV-038	0.5034	30.2	3063	963.3	3063	25.81	1.2375	2.48E+06	7.82E+05

Table A.36 (cont'd). PIII-1 Moving Filter Segments

Sample ID	Sampling Midpoint (min)	Sampling Midpoint (sec)	Calc'd U (μg)	DU Mass ± 1σ (μg)	Net DU Mass (μg)	Flow Rate (Lpm)	Volume (liters)	DU Conc. (μg/m^3)	DU Conc. ± 1σ (μg/m^3)
PIII-1F-1-MV-039	0.5514	33.1	2898	911.1	2898	25.81	1.2375	2.34E+06	7.40E+05
PIII-1F-1-MV-040	0.5993	36	2595	816.4	2595	25.81	1.2375	2.10E+06	6.63E+05
PIII-1F-1-MV-041	0.6473	38.8	2585	812.9	2585	25.81	1.2375	2.09E+06	6.60E+05
PIII-1F-1-MV-042	0.6952	41.7	2639	830.2	2639	25.81	1.2375	2.13E+06	6.74E+05
PIII-1F-1-MV-043	0.7432	44.6	2902	912.7	2902	25.81	1.2375	2.35E+06	7.41E+05
PIII-1F-1-MV-044	0.7911	47.5	2805	882.3	2805	25.81	1.2375	2.27E+06	7.16E+05
PIII-1F-1-MV-045	0.839	50.3	3471	1091.8	3471	25.81	1.2375	2.80E+06	8.86E+05
PIII-1F-1-MV-046	0.887	53.2	3707	1165.6	3707	25.81	1.2375	3.00E+06	9.46E+05
PIII-1F-1-MV-047	0.9349	56.1	3719	1169.9	3719	25.81	1.2375	3.01E+06	9.50E+05
PIII-1F-1-MV-048	0.9829	59	3437	1080.9	3437	25.81	1.2375	2.78E+06	8.77E+05
PIII-1F-1-MV-049	1.0308	61.8	3752	1179.9	3752	25.81	1.2375	3.03E+06	9.58E+05
PIII-1F-1-MV-050	1.0788	64.7	3814	1199.6	3814	25.81	1.2375	3.08E+06	9.74E+05
PIII-1F-1-MV-051	1.1267	67.6	4086	1285.5	4086	25.81	1.2375	3.30E+06	1.04E+06
PIII-1F-1-MV-052	1.1747	70.5	3721	1170.5	3721	25.81	1.2375	3.01E+06	9.50E+05
PIII-1F-1-MV-053	1.2226	73.4	4651	1463.1	4651	25.81	1.2375	3.76E+06	1.19E+06
PIII-1F-1-MV-054	1.2705	76.2	3684	1159.0	3684	25.81	1.2375	2.98E+06	9.41E+05
PIII-1F-1-MV-055	1.3185	79.1	3837	1207.1	3837	25.81	1.2375	3.10E+06	9.80E+05
PIII-1F-1-MV-056	1.3664	82	3284	1033.2	3284	25.81	1.2375	2.65E+06	8.39E+05
PIII-1F-1-MV-057	1.4144	84.9	3840	1207.8	3840	25.81	1.2375	3.10E+06	9.80E+05
PIII-1F-1-MV-058	1.4623	87.7	3429	1078.9	3429	25.81	1.2375	2.77E+06	8.76E+05
PIII-1F-1-MV-059	1.5103	90.6	3055	961.1	3055	25.81	1.2375	2.47E+06	7.80E+05
PIII-1F-1-MV-060	1.5582	93.5	3160	994.1	3160	25.81	1.2375	2.55E+06	8.07E+05
PIII-1F-1-MV-061	1.6062	96.4	3102	976.1	3102	25.81	1.2375	2.51E+06	7.92E+05
PIII-1F-1-MV-062	1.6541	99.2	3038	955.7	3038	25.81	1.2375	2.45E+06	7.76E+05
PIII-1F-1-MV-063	1.7021	102.1	3227	1015.5	3227	25.81	1.2375	2.61E+06	8.24E+05
PIII-1F-1-MV-064	1.75	105	3077	968.0	3077	25.81	1.2375	2.49E+06	7.86E+05
PIII-1F-1-MV-065	1.7979	107.9	2790	877.8	2790	25.81	1.2375	2.25E+06	7.13E+05
PIII-1F-1-MV-066	1.8459	110.8	3108	977.8	3108	25.81	1.2375	2.51E+06	7.94E+05
PIII-1F-1-MV-067	1.8938	113.6	2846	895.4	2846	25.81	1.2375	2.30E+06	7.27E+05
PIII-1F-1-MV-068	1.9418	116.5	2791	878.3	2791	25.81	1.2375	2.26E+06	7.13E+05
PIII-1F-1-MV-069	1.9897	119.4	2831	890.8	2831	25.81	1.2375	2.29E+06	7.23E+05
PIII-1F-1-MV-070	2.0377	122.3	2357	741.9	2357	25.81	1.2375	1.90E+06	6.02E+05
PIII-1F-1-MV-071	2.0856	125.1	2607	820.3	2607	25.81	1.2375	2.11E+06	6.66E+05
PIII-1F-1-MV-072	2.1336	128	2570	808.7	2570	25.81	1.2375	2.08E+06	6.56E+05
PIII-1F-1-MV-073	2.1815	130.9	2303	724.7	2303	25.81	1.2375	1.86E+06	5.88E+05
PIII-1F-1-MV-074	2.2295	133.8	2045	643.8	2045	25.81	1.2375	1.65E+06	5.23E+05
PIII-1F-1-MV-075	2.2774	136.6	2530	796.3	2530	25.81	1.2375	2.04E+06	6.46E+05
PIII-1F-1-MV-076	2.3253	139.5	2420	761.6	2420	25.81	1.2375	1.96E+06	6.18E+05

Table A.36 (cont'd). PIII-1 Moving Filter Segments

Sample ID	Sampling Midpoint (min)	Sampling Midpoint (sec)	Calc'd U (μg)	DU Mass ± 1σ (μg)	Net DU Mass (μg)	Flow Rate (Lpm)	Volume (liters)	DU Conc. (μg/m^3)	DU Conc. ± 1σ (μg/m^3)
PIII-1F-1-MV-077	2.3733	142.4	2115	665.7	2115	25.81	1.2375	1.71E+06	5.40E+05
PIII-1F-1-MV-078	2.4212	145.3	2264	712.8	2264	25.81	1.2375	1.83E+06	5.79E+05
PIII-1F-1-MV-079	2.4692	148.2	2341	737.0	2341	25.81	1.2375	1.89E+06	5.98E+05
PIII-1F-1-MV-080	2.5171	151	2105	662.8	2105	25.81	1.2375	1.70E+06	5.38E+05
PIII-1F-1-MV-081	2.5651	153.9	2101	661.4	2101	25.81	1.2375	1.70E+06	5.37E+05
PIII-1F-1-MV-082	2.613	156.8	2091	658.1	2091	25.81	1.2375	1.69E+06	5.34E+05
PIII-1F-1-MV-083	2.661	159.7	2149	676.6	2149	25.81	1.2375	1.74E+06	5.49E+05
PIII-1F-1-MV-084	2.7089	162.5	2009	632.5	2009	25.81	1.2375	1.62E+06	5.13E+05
PIII-1F-1-MV-085	2.7568	165.4	1974	621.5	1974	25.81	1.2375	1.60E+06	5.04E+05
PIII-1F-1-MV-086	2.8048	168.3	1950	614.2	1950	25.81	1.2375	1.58E+06	4.99E+05
PIII-1F-1-MV-087	2.8527	171.2	1822	573.8	1822	25.81	1.2375	1.47E+06	4.66E+05
PIII-1F-1-MV-088	2.9007	174	1825	574.8	1825	25.81	1.2375	1.47E+06	4.67E+05
PIII-1F-1-MV-089	2.9486	176.9	1839	579.3	1839	25.81	1.2375	1.49E+06	4.70E+05
PIII-1F-1-MV-090	2.9966	179.8	1938	610.3	1938	25.81	1.2375	1.57E+06	4.95E+05
PIII-1F-1-MV-091	3.0445	182.7	1872	589.3	1872	25.81	1.2375	1.51E+06	4.78E+05
PIII-1F-1-MV-092	3.0925	185.5	1897	597.5	1897	25.81	1.2375	1.53E+06	4.85E+05
PIII-1F-1-MV-093	3.1404	188.4	1503	473.4	1503	25.81	1.2375	1.21E+06	3.84E+05
PIII-1F-1-MV-094	3.1884	191.3	1769	557.1	1769	25.81	1.2375	1.43E+06	4.52E+05
PIII-1F-1-MV-095	3.2363	194.2	1877	591.4	1877	25.81	1.2375	1.52E+06	4.80E+05
PIII-1F-1-MV-096	3.2842	197.1	1682	529.7	1682	25.81	1.2375	1.36E+06	4.30E+05
PIII-1F-1-MV-097	3.3322	199.9	1751	551.6	1751	25.81	1.2375	1.41E+06	4.48E+05
PIII-1F-1-MV-098	3.3801	202.8	1813	570.9	1813	25.81	1.2375	1.47E+06	4.63E+05
PIII-1F-1-MV-099	3.4281	205.7	1582	498.4	1582	25.81	1.2375	1.28E+06	4.05E+05
PIII-1F-1-MV-100	3.476	208.6	11000	NA[(a)]	11000	25.81	1.2375	8.89E+06	NA[(a)]
PIII-1F-1-MV-101	3.524	211.4	1546	484.9	1546	25.81	1.2375	1.25E+06	3.94E+05
PIII-1F-1-MV-102	--	Transition	2006	629.2	2006	25.81	1.2375	1.62E+06	5.11E+05
PIII-1F-1-MV-103	--	Transition	1707	535.4	1707	25.81	1.2375	1.38E+06	4.35E+05
PIII-1F-1-MV-104	7.024	421.4	1378	432.3	1378	25.81	1.2375	1.11E+06	3.51E+05
PIII-1F-1-MV-105	7.0719	424.3	1415	444.1	1415	25.81	1.2375	1.14E+06	3.61E+05
PIII-1F-1-MV-106	7.1199	427.2	1572	493.2	1572	25.81	1.2375	1.27E+06	4.00E+05
PIII-1F-1-MV-107	7.1678	430.1	1429	448.3	1429	25.81	1.2375	1.15E+06	3.64E+05
PIII-1F-1-MV-108	7.2158	432.9	1480	464.6	1480	25.81	1.2375	1.20E+06	3.77E+05
PIII-1F-1-MV-109	7.2637	435.8	1478	463.8	1478	25.81	1.2375	1.19E+06	3.76E+05
PIII-1F-1-MV-110	7.3116	438.7	1429	448.4	1429	25.81	1.2375	1.15E+06	3.64E+05
PIII-1F-1-MV-111	7.3596	441.6	1371	430.2	1371	25.81	1.2375	1.11E+06	3.49E+05
PIII-1F-1-MV-112	7.4075	444.5	1313	411.9	1313	25.81	1.2375	1.06E+06	3.34E+05
PIII-1F-1-MV-113	7.4555	447.3	1493	468.7	1493	25.81	1.2375	1.21E+06	3.80E+05
PIII-1F-1-MV-114	--	Transition	979	307.7	979	25.81	1.2375	7.91E+05	2.50E+05

Table A.36 (cont'd). PIII-1 Moving Filter Segments

Sample ID	Sampling Midpoint (min)	Sampling Midpoint (sec)	Calc'd U (μg)	DU Mass ± 1σ (μg)	Net DU Mass (μg)	Flow Rate (Lpm)	Volume (liters)	DU Conc. (μg/m^3)	DU Conc. ± 1σ (μg/m^3)
PIII-1F-1-MV-115	15.024	901.4	650	204.6	650	25.81	1.2375	5.25E+05	1.66E+05
PIII-1F-1-MV-116	15.0719	904.3	586	184.5	586	25.81	1.2375	4.74E+05	1.50E+05
PIII-1F-1-MV-117	15.1199	907.2	650	204.7	650	25.81	1.2375	5.25E+05	1.66E+05
PIII-1F-1-MV-118	15.1678	910.1	664	208.8	664	25.81	1.2375	5.37E+05	1.69E+05
PIII-1F-1-MV-119	15.2158	912.9	666	209.7	666	25.81	1.2375	5.38E+05	1.70E+05
PIII-1F-1-MV-120	15.2637	915.8	680	214.0	680	25.81	1.2375	5.49E+05	1.74E+05
PIII-1F-1-MV-121	15.3116	918.7	738	232.1	738	25.81	1.2375	5.96E+05	1.88E+05
PIII-1F-1-MV-122	15.3596	921.6	639	200.9	639	25.81	1.2375	5.16E+05	1.63E+05
PIII-1F-1-MV-123	15.4075	924.5	612	192.9	612	25.81	1.2375	4.95E+05	1.57E+05
PIII-1F-1-MV-124	15.4555	927.3	564	177.9	564	25.81	1.2375	4.56E+05	1.44E+05
PIII-1F-1-MV-125	15.5034	930.2	575	181.2	575	25.81	1.2375	4.65E+05	1.47E+05
PIII-1F-1-MV-126	15.5514	933.1	644	203.3	644	25.81	1.2375	5.20E+05	1.65E+05
PIII-1F-1-MV-127	--	Transition	429	135.5	429	25.81	1.2375	3.47E+05	1.10E+05
PIII-1F-1-MV-128	--	Transition	101	32.3	101	25.81	1.2375	8.16E+04	2.62E+04
PIII-1F-1-MV-129	31.024	1861.4	232	73.6	232	25.81	1.2375	1.87E+05	5.97E+04
PIII-1F-1-MV-130	31.0719	1864.3	266	84.3	266	25.81	1.2375	2.15E+05	6.84E+04
PIII-1F-1-MV-131	31.1199	1867.2	227	72.1	227	25.81	1.2375	1.83E+05	5.85E+04
PIII-1F-1-MV-132	31.1678	1870.1	261	82.8	261	25.81	1.2375	2.11E+05	6.72E+04
PIII-1F-1-MV-133	31.2158	1872.9	264	83.4	264	25.81	1.2375	2.13E+05	6.77E+04
PIII-1F-1-MV-134	31.2637	1875.8	208	66.3	208	25.81	1.2375	1.68E+05	5.38E+04
PIII-1F-1-MV-135	31.3116	1878.7	251	79.9	251	25.81	1.2375	2.03E+05	6.49E+04
PIII-1F-1-MV-136	31.3596	1881.6	257	81.5	257	25.81	1.2375	2.08E+05	6.62E+04
PIII-1F-1-MV-137	31.4075	1884.5	222	70.6	222	25.81	1.2375	1.79E+05	5.73E+04
PIII-1F-1-MV-138	31.4555	1887.3	233	74.3	233	25.81	1.2375	1.88E+05	6.03E+04
PIII-1F-1-MV-139	31.5034	1890.2	185	59.3	185	25.81	1.2375	1.49E+05	4.81E+04
PIII-1F-1-MV-140	--	Transition	196	62.7	196	25.81	1.2375	1.58E+05	5.09E+04
PIII-1F-1-MV-141	--	Transition	198	63.1	198	25.81	1.2375	1.60E+05	5.12E+04
PIII-1F-1-MV-142	--	Transition	196	62.4	196	25.81	1.2375	1.58E+05	5.06E+04
PIII-1F-1-MV-143	61.024	3661.4	63	20.3	63	25.81	1.2375	5.09E+04	1.65E+04
PIII-1F-1-MV-144	61.0719	3664.3	53	17.2	53	25.81	1.2375	4.28E+04	1.40E+04
PIII-1F-1-MV-145	61.1199	3667.2	68	22.1	68	25.81	1.2375	5.49E+04	1.79E+04
PIII-1F-1-MV-146	61.1678	3670.1	74	25.0	74	25.81	1.2375	5.98E+04	2.03E+04
PIII-1F-1-MV-147	61.2158	3672.9	61	20.7	61	25.81	1.2375	4.93E+04	1.68E+04
PIII-1F-1-MV-148	61.2637	3675.8	67	22.5	67	25.81	1.2375	5.41E+04	1.83E+04
PIII-1F-1-MV-149	61.3116	3678.7	68	22.8	68	25.81	1.2375	5.49E+04	1.85E+04
PIII-1F-1-MV-150	61.3596	3681.6	71	24.0	71	25.81	1.2375	5.74E+04	1.95E+04
PIII-1F-1-MV-151	61.4075	3684.5	67	22.6	67	25.81	1.2375	5.41E+04	1.83E+04
PIII-1F-1-MV-152	61.4555	3687.3	58	19.6	58	25.81	1.2375	4.69E+04	1.59E+04

Table A.36 (cont'd). PIII-1 Moving Filter Segments

Sample ID	Sampling Midpoint (min)	Sampling Midpoint (sec)	Calc'd U (µg)	DU Mass ± 1σ (µg)	Net DU Mass (µg)	Flow Rate (Lpm)	Volume (liters)	DUConc. (µg/m^3)	DU Conc. ± 1σ (µg/m^3)
PIII-1F-1-MV-153	61.5034	3690.2	70	23.4	70	25.81	1.2375	5.66E+04	1.90E+04
PIII-1F-1-MV-154	121.024	7261.4	56	18.9	56	25.81	1.2375	4.53E+04	1.53E+04
PIII-1F-1-MV-155	121.0719	7264.3	64	21.7	64	25.81	1.2375	5.17E+04	1.76E+04
PIII-1F-1-MV-156	121.1199	7267.2	56	19.0	56	25.81	1.2375	4.53E+04	1.54E+04
PIII-1F-1-MV-157	121.1678	7270.1	60	20.2	60	25.81	1.2375	4.85E+04	1.64E+04
PIII-1F-1-MV-158	121.2158	7272.9	26	9.2	26	25.81	1.2375	2.10E+04	7.46E+03
PIII-1F-1-MV-159	121.2637	7275.8	22	7.6	22	25.81	1.2375	1.78E+04	6.16E+03
PIII-1F-1-MV-160	121.3116	7278.7	22	7.6	22	25.81	1.2375	1.78E+04	6.16E+03

(a) DU mass based on ICP-MS results; no analytical uncertainty was reported.

Table A.37. Phase III-2 Moving Filter Segments—Mass, Volume, and Concentration

Sample ID	Sampling Midpoint (min)	Sampling Midpoint (sec)	Calc'd U (μg)	DU Mass ± 1σ (μg)	Net DU Mass (μg)	Flow Rate (Lpm)	Volume (liters)	DU Conc. (μg/m^3)	DU Conc. ± 1σ (μg/m^3)
PIII-2F-1-MV-001	0.024	1.4	14384	4463.0	14384	32.97	1.5808	9.10E+06	2.84E+06
PIII-2F-1-MV-002	0.0719	4.3	12689	3937.3	12689	32.97	1.5808	8.03E+06	2.50E+06
PIII-2F-1-MV-003	0.1199	7.2	11020	3420.0	11020	32.97	1.5808	6.97E+06	2.17E+06
PIII-2F-1-MV-004	0.1678	10.1	9917	3078.4	9917	32.97	1.5808	6.27E+06	1.96E+06
PIII-2F-1-MV-005	0.2158	12.9	8442	2620.4	8442	32.97	1.5808	5.34E+06	1.67E+06
PIII-2F-1-MV-006	0.2637	15.8	8196	2544.6	8196	32.97	1.5808	5.18E+06	1.62E+06
PIII-2F-1-MV-007	0.3116	18.7	6993	2171.1	6993	32.97	1.5808	4.42E+06	1.38E+06
PIII-2F-1-MV-008	0.3596	21.6	6753	2097.2	6753	32.97	1.5808	4.27E+06	1.33E+06
PIII-2F-1-MV-009	0.4075	24.5	6156	1911.7	6156	32.97	1.5808	3.89E+06	1.21E+06
PIII-2F-1-MV-010	0.4555	27.3	5786	1796.7	5786	32.97	1.5808	3.66E+06	1.14E+06
PIII-2F-1-MV-011	0.5034	30.2	6151	1910.8	6151	32.97	1.5808	3.89E+06	1.21E+06
PIII-2F-1-MV-012	0.5514	33.1	6171	1916.6	6171	32.97	1.5808	3.90E+06	1.22E+06
PIII-2F-1-MV-013	0.5993	36	6500	2018.6	6500	32.97	1.5808	4.11E+06	1.28E+06
PIII-2F-1-MV-014	0.6473	38.8	5372	1668.6	5372	32.97	1.5808	3.40E+06	1.06E+06
PIII-2F-1-MV-015	0.6952	41.7	5268	1636.0	5268	32.97	1.5808	3.33E+06	1.04E+06
PIII-2F-1-MV-016	0.7432	44.6	5181	1609.1	5181	32.97	1.5808	3.28E+06	1.02E+06
PIII-2F-1-MV-017	0.7911	47.5	4713	1463.7	4713	32.97	1.5808	2.98E+06	9.30E+05
PIII-2F-1-MV-018	0.839	50.3	5194	1613.3	5194	32.97	1.5808	3.29E+06	1.03E+06
PIII-2F-1-MV-019	0.887	53.2	4817	1496.2	4817	32.97	1.5808	3.05E+06	9.51E+05
PIII-2F-1-MV-020	0.9349	56.1	5089	1581.0	5089	32.97	1.5808	3.22E+06	1.00E+06
PIII-2F-1-MV-021	0.9829	59	5737	1781.8	5737	32.97	1.5808	3.63E+06	1.13E+06
PIII-2F-1-MV-022	1.0308	61.8	4874	1514.2	4874	32.97	1.5808	3.08E+06	9.62E+05
PIII-2F-1-MV-023	1.0788	64.7	5102	1585.2	5102	32.97	1.5808	3.23E+06	1.01E+06
PIII-2F-1-MV-024	1.1267	67.6	4142	1286.9	4142	32.97	1.5808	2.62E+06	8.18E+05
PIII-2F-1-MV-025	1.1747	70.5	4664	1449.3	4664	32.97	1.5808	2.95E+06	9.21E+05
PIII-2F-1-MV-026	1.2226	73.4	4628	1438.2	4628	32.97	1.5808	2.93E+06	9.14E+05
PIII-2F-1-MV-027	1.2705	76.2	4618	1434.6	4618	32.97	1.5808	2.92E+06	9.12E+05
PIII-2F-1-MV-028	1.3185	79.1	4465	1387.1	4465	32.97	1.5808	2.82E+06	8.82E+05
PIII-2F-1-MV-029	1.3664	82	4281	1330.1	4281	32.97	1.5808	2.71E+06	8.45E+05
PIII-2F-1-MV-030	1.4144	84.9	4239	1317.1	4239	32.97	1.5808	2.68E+06	8.37E+05
PIII-2F-1-MV-031	1.4623	87.7	3668	1139.7	3668	32.97	1.5808	2.32E+06	7.24E+05
PIII-2F-1-MV-032	1.5103	90.6	3793	1178.7	3793	32.97	1.5808	2.40E+06	7.49E+05
PIII-2F-1-MV-033	1.5582	93.5	3999	1242.8	3999	32.97	1.5808	2.53E+06	7.90E+05
PIII-2F-1-MV-034	1.6062	96.4	3891	1209.0	3891	32.97	1.5808	2.46E+06	7.68E+05

Table A.37 (cont'd). Phase III-2 Moving Filter Segments

Sample ID	Sampling Midpoint (min)	Sampling Midpoint (sec)	Calc'd U (μg)	DU Mass ± 1σ (μg)	Net DU Mass (μg)	Flow Rate (Lpm)	Volume (liters)	DU Conc. (μg/m^3)	DU Conc. ± 1σ (g/m^3)
PIII-2F-1-MV-035	1.6541	99.2	3578	1112.1	3578	32.97	1.5808	2.26E+06	7.07E+05
PIII-2F-1-MV-036	1.7021	102.1	3183	989.5	3183	32.97	1.5808	2.01E+06	6.29E+05
PIII-2F-1-MV-037	1.75	105	3436	1067.9	3436	32.97	1.5808	2.17E+06	6.79E+05
PIII-2F-1-MV-038	1.7979	107.9	3172	985.7	3172	32.97	1.5808	2.01E+06	6.26E+05
PIII-2F-1-MV-039	1.8459	110.8	3506	1089.6	3506	32.97	1.5808	2.22E+06	6.92E+05
PIII-2F-1-MV-040	1.8938	113.6	3541	1100.5	3541	32.97	1.5808	2.24E+06	6.99E+05
PIII-2F-1-MV-041	1.9418	116.5	2977	925.3	2977	32.97	1.5808	1.88E+06	5.88E+05
PIII-2F-1-MV-042	1.9897	119.4	3025	940.1	3025	32.97	1.5808	1.91E+06	5.97E+05
PIII-2F-1-MV-043	2.0377	122.3	3493	1085.6	3493	32.97	1.5808	2.21E+06	6.90E+05
PIII-2F-1-MV-044	2.0856	125.1	3137	975.0	3137	32.97	1.5808	1.98E+06	6.20E+05
PIII-2F-1-MV-045	2.1336	128	2597	807.2	2597	32.97	1.5808	1.64E+06	5.13E+05
PIII-2F-1-MV-046	2.1815	130.9	2903	902.3	2903	32.97	1.5808	1.84E+06	5.73E+05
PIII-2F-1-MV-047	2.2295	133.8	2795	868.8	2795	32.97	1.5808	1.77E+06	5.52E+05
PIII-2F-1-MV-048	2.2774	136.6	2693	837.2	2693	32.97	1.5808	1.70E+06	5.32E+05
PIII-2F-1-MV-049	2.3253	139.5	2499	776.8	2499	32.97	1.5808	1.58E+06	4.94E+05
PIII-2F-1-MV-050	2.3733	142.4	2364	734.6	2364	32.97	1.5808	1.50E+06	4.67E+05
PIII-2F-1-MV-051	2.4212	145.3	2435	756.8	2435	32.97	1.5808	1.54E+06	4.81E+05
PIII-2F-1-MV-052	2.4692	148.2	2303	715.8	2303	32.97	1.5808	1.46E+06	4.55E+05
PIII-2F-1-MV-053	2.5171	151	2139	664.9	2139	32.97	1.5808	1.35E+06	4.23E+05
PIII-2F-1-MV-054	2.5651	153.9	2162	672.1	2162	32.97	1.5808	1.37E+06	4.27E+05
PIII-2F-1-MV-055	2.613	156.8	2198	683.3	2198	32.97	1.5808	1.39E+06	4.34E+05
PIII-2F-1-MV-056	2.661	159.7	1939	602.8	1939	32.97	1.5808	1.23E+06	3.83E+05
PIII-2F-1-MV-057	2.7089	162.5	1862	579.2	1862	32.97	1.5808	1.18E+06	3.68E+05
PIII-2F-1-MV-058	2.7568	165.4	1943	604.2	1943	32.97	1.5808	1.23E+06	3.84E+05
PIII-2F-1-MV-059	2.8048	168.3	1813	563.5	1813	32.97	1.5808	1.15E+06	3.58E+05
PIII-2F-1-MV-060	2.8527	171.2	1825	567.4	1825	32.97	1.5808	1.15E+06	3.61E+05
PIII-2F-1-MV-061	2.9007	174	1582	492.3	1582	32.97	1.5808	1.00E+06	3.13E+05
PIII-2F-1-MV-062	2.9486	176.9	1598	496.9	1598	32.97	1.5808	1.01E+06	3.16E+05
PIII-2F-1-MV-063	2.9966	179.8	1572	488.8	1572	32.97	1.5808	9.94E+05	3.11E+05
PIII-2F-1-MV-064	3.0445	182.7	1384	430.6	1384	32.97	1.5808	8.76E+05	2.74E+05
PIII-2F-1-MV-065	3.0925	185.5	1503	467.4	1503	32.97	1.5808	9.51E+05	2.97E+05
PIII-2F-1-MV-066	3.1404	188.4	1494	464.9	1494	32.97	1.5808	9.45E+05	2.95E+05
PIII-2F-1-MV-067	3.1884	191.3	1500	466.7	1500	32.97	1.5808	9.49E+05	2.97E+05
PIII-2F-1-MV-068	3.2363	194.2	1390	432.5	1390	32.97	1.5808	8.79E+05	2.75E+05

Table A.37 (cont'd). Phase III-2 Moving Filter Segments

Sample ID	Sampling Midpoint (min)	Sampling Midpoint (sec)	Calc'd U (μg)	DU Mass ± 1σ (μg)	Net DU Mass (μg)	Flow Rate (Lpm)	Volume (liters)	DU Conc. μg/m^3)	DU Conc. ± 1σ (g/m^3)
PIII-2F-1-MV-069	3.2842	197.1	1402	436.3	1402	32.97	1.5808	8.87E+05	2.77E+05
PIII-2F-1-MV-070	3.3322	199.9	1271	395.8	1271	32.97	1.5808	8.04E+05	2.52E+05
PIII-2F-1-MV-071	3.3801	202.8	1219	379.8	1219	32.97	1.5808	7.71E+05	2.41E+05
PIII-2F-1-MV-072	3.4281	205.7	1285	400.0	1285	32.97	1.5808	8.13E+05	2.54E+05
PIII-2F-1-MV-073	3.476	208.6	1048	326.4	1048	32.97	1.5808	6.63E+05	2.07E+05
PIII-2F-1-MV-074	--	Transition	146	45.6	146	32.97	1.5808	9.24E+04	2.90E+04
PIII-2F-1-MV-075	--	Transition	361	112.9	361	32.97	1.5808	2.28E+05	7.17E+04
PIII-2F-1-MV-076	7.024	421.4	385	120.4	385	32.97	1.5808	2.44E+05	7.65E+04
PIII-2F-1-MV-077	7.0719	424.3	378	118.1	378	32.97	1.5808	2.39E+05	7.51E+04
PIII-2F-1-MV-078	7.1199	427.2	348	108.9	348	32.97	1.5808	2.20E+05	6.92E+04
PIII-2F-1-MV-079	7.1678	430.1	326	102.1	326	32.97	1.5808	2.06E+05	6.49E+04
PIII-2F-1-MV-080	7.2158	432.9	310	97.3	310	32.97	1.5808	1.96E+05	6.18E+04
PIII-2F-1-MV-081	7.2637	435.8	319	100.2	319	32.97	1.5808	2.02E+05	6.37E+04
PIII-2F-1-MV-082	7.3116	438.7	288	90.2	288	32.97	1.5808	1.82E+05	5.73E+04
PIII-2F-1-MV-083	7.3596	441.6	301	94.4	301	32.97	1.5808	1.90E+05	6.00E+04
PIII-2F-1-MV-084	7.4075	444.5	222	70.1	222	32.97	1.5808	1.40E+05	4.45E+04
PIII-2F-1-MV-085	7.4555	447.3	234	73.5	234	32.97	1.5808	1.48E+05	4.67E+04
PIII-2F-1-MV-086	7.5034	450.2	254	80.0	254	32.97	1.5808	1.61E+05	5.08E+04
PIII-2F-1-MV-087	--	Transition	167	52.8	167	32.97	1.5808	1.06E+05	3.36E+04
PIII-2F-1-MV-088	--	Transition	53	17.1	53	32.97	1.5808	3.35E+04	1.09E+04
PIII-2F-1-MV-089	15.024	901.4	54	17.6	54	32.97	1.5808	3.42E+04	1.12E+04
PIII-2F-1-MV-090	15.0719	904.3	46	15.3	46	32.97	1.5808	2.91E+04	9.72E+03
PIII-2F-1-MV-091	15.1199	907.2	47	15.7	47	32.97	1.5808	2.97E+04	9.97E+03
PIII-2F-1-MV-092	15.1678	910.1	52	16.7	52	32.97	1.5808	3.29E+04	1.06E+04
PIII-2F-1-MV-093	15.2158	912.9	55	17.8	55	32.97	1.5808	3.48E+04	1.13E+04
PIII-2F-1-MV-094	15.2637	915.8	45	14.8	45	32.97	1.5808	2.85E+04	9.40E+03
PIII-2F-1-MV-095	15.3116	918.7	50	16.4	50	32.97	1.5808	3.16E+04	1.04E+04
PIII-2F-1-MV-096	15.3596	921.6	71	22.7	71	32.97	1.5808	4.49E+04	1.44E+04
PIII-2F-1-MV-097	15.4075	924.5	68	21.7	68	32.97	1.5808	4.30E+04	1.38E+04
PIII-2F-1-MV-098	15.4555	927.3	47	15.5	47	32.97	1.5808	2.97E+04	9.85E+03
PIII-2F-1-MV-099	15.5034	930.2	47	15.3	47	32.97	1.5808	2.97E+04	9.72E+03
PIII-2F-1-MV-100	--	Transition	47	15.3	47	32.97	1.5808	2.97E+04	9.72E+03
PIII-2F-1-MV-101	--	Transition	37	12.3	37	32.97	1.5808	2.34E+04	7.81E+03
PIII-2F-1-MV-102	31.024	1861.4	36	12.1	36	32.97	1.5808	2.28E+04	7.68E+03

Table A.37 (cont'd). Phase III-2 Moving Filter Segments

Sample ID	Sampling Midpoint (min)	Sampling Midpoint (sec)	Calc'd U (μg)	DU Mass ± 1σ (μg)	Net DU Mass (μg)	Flow Rate (Lpm)	Volume (liters)	DU Conc. (μg/m^3)	DU Conc. ± 1σ (g/m^3)
PIII-2F-1-MV-103	31.0719	1864.3	47	15.3	47	32.97	1.5808	2.97E+04	9.72E+03
PIII-2F-1-MV-104	31.1199	1867.2	43	14.1	43	32.97	1.5808	2.72E+04	8.96E+03
PIII-2F-1-MV-105	31.1678	1870.1	41	13.4	41	32.97	1.5808	2.59E+04	8.51E+03
PIII-2F-1-MV-106	31.2158	1872.9	40	13.3	40	32.97	1.5808	2.53E+04	8.45E+03
PIII-2F-1-MV-107	31.2637	1875.8	48	15.5	48	32.97	1.5808	3.04E+04	9.85E+03
PIII-2F-1-MV-108	31.3116	1878.7	45	14.8	45	32.97	1.5808	2.85E+04	9.40E+03
PIII-2F-1-MV-109	31.3596	1881.6	32	10.7	32	32.97	1.5808	2.02E+04	6.80E+03
PIII-2F-1-MV-110	31.4075	1884.5	31	10.9	31	32.97	1.5808	1.96E+04	6.92E+03
PIII-2F-1-MV-111	31.4555	1887.3	38	12.5	38	32.97	1.5808	2.40E+04	7.94E+03
PIII-2F-1-MV-112	31.5034	1890.2	35	11.8	35	32.97	1.5808	2.21E+04	7.49E+03
PIII-2F-1-MV-113	--	Transition	25	8.8	25	32.97	1.5808	1.58E+04	5.59E+03
PIII-2F-1-MV-114	--	Transition	30	10.0	30	32.97	1.5808	1.90E+04	6.35E+03
PIII-2F-1-MV-115	61.024	3661.4	41	13.5	41	32.97	1.5808	2.59E+04	8.58E+03
PIII-2F-1-MV-116	61.0719	3664.3	35	11.5	35	32.97	1.5808	2.21E+04	7.31E+03
PIII-2F-1-MV-117	61.1199	3667.2	32	11.0	32	32.97	1.5808	2.02E+04	6.98E+03
PIII-2F-1-MV-118	61.1678	3670.1	35	11.8	35	32.97	1.5808	2.21E+04	7.49E+03
PIII-2F-1-MV-119	61.2158	3672.9	32	10.9	32	32.97	1.5808	2.02E+04	6.92E+03
PIII-2F-1-MV-120	61.2637	3675.8	24	8.7	24	32.97	1.5808	1.52E+04	5.52E+03
PIII-2F-1-MV-121	61.3116	3678.7	23	8.0	23	32.97	1.5808	1.45E+04	5.08E+03
PIII-2F-1-MV-122	61.3596	3681.6	31	10.4	31	32.97	1.5808	1.96E+04	6.61E+03
PIII-2F-1-MV-123	61.4075	3684.5	24	8.5	24	32.97	1.5808	1.52E+04	5.40E+03
PIII-2F-1-MV-124	61.4555	3687.3	28	9.5	28	32.97	1.5808	1.77E+04	6.03E+03
PIII-2F-1-MV-125	61.5034	3690.2	20	7.2	20	32.97	1.5808	1.27E+04	4.57E+03
PIII-2F-1-MV-126	--	Transition	20	7.4	20	32.97	1.5808	1.27E+04	4.70E+03
PIII-2F-1-MV-127	--	Transition	69	NA[(a)]	69	32.97	1.5808	4.36E+04	NA[(a)]
PIII-2F-1-MV-128	121.024	7261.4	24	8.4	24	32.97	1.5808	1.52E+04	5.33E+03
PIII-2F-1-MV-129	121.0719	7264.3	25	8.8	25	32.97	1.5808	1.58E+04	5.59E+03
PIII-2F-1-MV-130	121.1199	7267.2	31	10.3	31	32.97	1.5808	1.96E+04	6.54E+03
PIII-2F-1-MV-131	121.1678	7270.1	21	7.9	21	32.97	1.5808	1.33E+04	5.01E+03
PIII-2F-1-MV-132	121.2158	7272.9	31	10.6	31	32.97	1.5808	1.96E+04	6.73E+03
PIII-2F-1-MV-133	121.2637	7275.8	26	8.9	26	32.97	1.5808	1.64E+04	5.65E+03
PIII-2F-1-MV-134	121.3116	7278.7	22	7.8	22	32.97	1.5808	1.39E+04	4.95E+03

Table A.37 (cont'd). Phase III-2 Moving Filter Segments

Sample ID	Sampling Midpoint (min)	Sampling Midpoint (sec)	Calc'd U (µg)	DU Mass ± 1σ (µg)	Net DU Mass (µg)	Flow Rate (Lpm)	Volume (liters)	DU Conc. (µg/m^3)	DU Conc. ± 1σ (g/m^3)
PIII-2F-1-MV-135	121.3596	7281.6	28	9.6	28	32.97	1.5808	1.77E+04	6.10E+03
PIII-2F-1-MV-136	121.4075	7284.5	32	10.7	32	32.97	1.5808	2.02E+04	6.80E+03
PIII-2F-1-MV-137	121.4555	7287.3	29	9.8	29	32.97	1.5808	1.83E+04	6.22E+03

(a) DU mass based on ICP-MS results; no analytical uncertainty was reported.

Table A.38. Cyclone Residues—Mass, Volume, and Concentration

Sample ID	Sampling Time (min)	Footnotes	Total Mass (mg)	Calc'd U Mass (µg)	U Mass ± 1σ (µg)	Net U Mass (µg)	Flow Lpm	Volume (L)	DU Conc. (µg/m^3)	DU Conc. ± 1σ (µg/m^3)
PI-1-CY-1	128	(a)	54.000	2.980E+04	1.425E+03	2.980E+04	31.4	4019	7.413E+03	4.185E+02
PI-1-CY-2	128	(a)	76.000	4.767E+04	2.252E+03	4.767E+04	31.4	4019	1.186E+04	6.638E+02
PI-1-CY-3	128	(a)	58.000	3.305E+04	1.573E+03	3.305E+04	31.4	4019	8.224E+03	4.627E+02
PI-1-CY-4	128	(a)	71.000	3.776E+04	1.800E+03	3.776E+04	31.4	4019	9.396E+03	5.291E+02
PI-1-CY-5	128	(a) (b)	55.000	NA	NA	NA	NA	NA	NA	NA
PI-2-CY-1	128		34.192	1.809E+04	8.806E+02	1.809E+04	9.9	1267	1.428E+04	8.163E+02
PI-2-CY-2	128		62.483	3.281E+04	1.727E+03	3.281E+04	9.9	1267	2.589E+04	1.569E+03
PI-2-CY-3	128		35.077	2.003E+04	9.704E+02	2.003E+04	9.9	1267	1.581E+04	9.007E+02
PI-2-CY-4	128		46.734	2.630E+04	1.401E+03	2.630E+04	9.9	1267	2.075E+04	1.269E+03
PI-2-CY-5	128		76.196	3.683E+04	1.937E+03	3.683E+04	9.9	1267	2.907E+04	1.760E+03
PI-3/4-CY-1	114		46.541	2.351E+04	1.135E+03	2.351E+04	12.7	1448	1.624E+04	9.229E+02
PI-3/4-CY-2	114		276.411	1.325E+05	6.376E+03	1.325E+05	12.7	1448	9.151E+04	5.189E+03
PI-3/4-CY-3	114		109.671	5.314E+04	2.668E+03	5.314E+04	12.7	1448	3.671E+04	2.147E+03
PI-3/4-CY-4	114		165.007	9.138E+04	4.440E+03	9.138E+04	12.7	1448	6.312E+04	3.604E+03
PI-3/4-CY-5	114		105.177	4.411E+04	2.259E+03	4.411E+04	12.7	1448	3.047E+04	1.808E+03
PI-5 (line cut--did not run)	--		--	--	--	--	--	--	--	--
PI-6-CY-1	129		8.532	5.104E+03	2.862E+02	5.104E+03	9.0	1161	4.396E+03	2.795E+02
PI-6-CY-2	129		7.404	5.266E+03	2.966E+02	5.266E+03	9.0	1161	4.536E+03	2.895E+02
PI-6-CY-3	129		11.289	7.013E+03	3.685E+02	7.013E+03	9.0	1161	6.040E+03	3.655E+02
PI-6-CY-4	129		9.567	7.742E+03	4.000E+02	7.742E+03	9.0	1161	6.668E+03	3.984E+02
PI-6-CY-5	129	(b)	3.100	NA	NA	NA	NA	NA	NA	NA
PI-7-CY-1	129		125.129	6.413E+04	3.171E+03	6.413E+04	115.0	14835	4.323E+03	2.500E+02
PI-7-CY-2	129		190.709	1.236E+05	5.933E+03	1.236E+05	115.0	14835	8.330E+03	4.716E+02
PI-7-CY-3	129		131.302	7.472E+04	3.654E+03	7.472E+04	115.0	14835	5.037E+03	2.890E+02
PI-7-CY-4	129		98.119	6.540E+04	3.071E+03	6.540E+04	115.0	14835	4.408E+03	2.456E+02
PI-7-CY-5	129		71.508	4.247E+04	2.008E+03	4.247E+04	115.0	14835	2.863E+03	1.603E+02
PII-1/2-CY-1	120		76.358	2.222E+04	1.073E+03	2.222E+04	13.4	1608	1.382E+04	7.856E+02
PII-1/2-CY-2	120		158.420	5.920E+04	2.785E+03	5.920E+04	13.4	1608	3.682E+04	2.054E+03
PII-1/2-CY-3	120		151.679	2.597E+04	1.291E+03	2.597E+04	13.4	1608	1.615E+04	9.377E+02
PII-1/2-CY-4	120		144.187	4.930E+04	2.327E+03	4.930E+04	13.4	1608	3.066E+04	1.715E+03
PII-1/2-CY-5	120		82.884	2.678E+04	1.285E+03	2.678E+04	13.4	1608	1.665E+04	9.427E+02
PII-3-CY-1	129		48.004	4.375E+02	6.992E+01	4.375E+02	10.0	1290	3.391E+02	5.515E+01
PII-3-CY-2	129		54.384	4.253E+03	2.452E+02	4.253E+03	10.0	1290	3.297E+03	2.142E+02
PII-3-CY-3	129		57.752	7.638E+03	3.967E+02	7.638E+03	10.0	1290	5.921E+03	3.551E+02
PII-3-CY-4	129		57.222	6.632E+03	3.510E+02	6.632E+03	10.0	1290	5.141E+03	3.128E+02
PII-3-CY-5	129		57.502	8.638E+03	4.420E+02	8.638E+03	10.0	1290	6.696E+03	3.972E+02

Table A.38 (cont'd). Cyclone Residues

Sample ID	Sampling Time (min)	Foot-notes	Total Mass (mg)	Calc'd U Mass (µg as U-238)	U Mass µg ± 1σ U-238	Net U Mass (µg)	Flow Lpm	Volume (Liters)	U-238 Conc. (µg/m^3)	U-238 Conc. ± 1σ (µg/m^3)
PIII-1-CY-1	129		29.866	2.233E+04	1.079E+03	2.233E+04	10.9	1406	1.588E+04	9.030E+02
PIII-1-CY-2	129		29.115	4.205E+04	2.140E+03	4.205E+04	10.9	1406	2.991E+04	1.767E+03
PIII-1-CY-3	129		26.122	4.072E+04	2.127E+03	4.072E+04	10.9	1406	2.896E+04	1.745E+03
PIII-1-CY-4	129		75.469	2.249E+04	1.083E+03	2.249E+04	10.9	1406	1.600E+04	9.074E+02
PIII-1-CY-5	129		139.113	5.062E+04	2.386E+03	5.062E+04	10.9	1406	3.600E+04	2.012E+03
PIII-2-CY-1	129	(c)	8.447	1.175E+03	1.098E+02	1.175E+03	12.8	1651	7.114E+02	6.982E+01
PIII-2-CY-2	129	(c)	0.957	1.079E+02	5.673E+01	1.079E+02	12.8	1651	6.534E+01	3.441E+01
PIII-2-CY-3	129	(c)	132.505	1.074E+05	5.015E+03	1.074E+05	12.8	1651	6.506E+04	3.610E+03
PIII-2-CY-4	129	(c)	88.584	6.824E+04	3.203E+03	6.824E+04	12.8	1651	4.133E+04	2.302E+03
PIII-2-CY-5	129	(c)	69.530	5.610E+04	2.639E+03	5.610E+04	12.8	1651	3.398E+04	1.896E+03
PIII-2-CY-1 resuspended	129	(d)	57.8	7.050E+03	3.732E+02	7.050E+03	12.8	1651	4.269E+03	2.594E+02
PIII-2-CY-4-resuspended	129	(d)	72.5	1.611E+04	7.892E+02	1.611E+04	12.8	1651	9.756E+03	5.601E+02
PIII-2-CY-5-resuspended	129	(d)	62.9	1.373E+04	6.775E+02	1.373E+04	12.8	1651	8.317E+03	4.798E+02
PIV-3-CY-1	33		9.472	1.271E+02	4.833E+01	1.271E+02	9.9	325	3.911E+02	1.491E+02
PIV-3-CY-2	33		2.620	8.591E+01	5.647E+01	8.591E+01	9.9	325	2.643E+02	1.739E+02
PIV-3-CY-3	33		4.960	8.584E+01	1.100E+01	8.584E+01	9.9	325	2.641E+02	3.476E+01
PIV-3-CY-4	33		5.277	1.056E+02	5.655E+01	1.056E+02	9.9	325	3.248E+02	1.742E+02
PIV-3-CY-5	33		49.236	1.686E+02	5.855E+01	1.686E+02	9.9	325	5.187E+02	1.808E+02
PIV-4 (line cut--did not run)	--		--	--	--	--	--	--	--	--

(a) Volume uncertain because of possible leak in PFDB test apparatus
(b) Some sample lost when transferring from cyclone grit chamber.
(c) Cyclone train had separated between stages 2 and 3. Therefore stage 1, 2, & 3 material was in stage 3.
(d) Sample was resuspended at LRRI. Results adjusted for entire sample.

Table A.39. Andersen CI External Samplers—Mass, Volume, and Concentration

Sample ID	Sampling Time (min)	Average Flow (Lpm)	Volume (L)	Calculated U Mass (µg)	DU Mass ± 1σ (µg)	DU Conc. (µg/m^3)	DU Conc. ± 1σ (µg/m^3)
PI-5E-E-1-CI-1	2	27.2	54.4	832	159	1.53E+04	3.30E+03
PI-5E-E-1-CI-2	2	27.2	54.4	560	97	1.03E+04	2.06E+03
PI-5E-E-1-CI-3	2	27.2	54.4	82	151	1.50E+03	2.78E+03
PI-5E-E-1-CI-4	2	27.2	54.4	341	103	6.26E+03	2.00E+03
PI-5E-E-1-CI-5	2	27.2	54.4	260	133	4.77E+03	2.48E+03
PI-5E-E-1-CI-6	2	27.2	54.4	199	89	3.67E+03	1.68E+03
PI-5E-E-1-CI-7	2	27.2	54.4	194	82	3.56E+03	1.55E+03
PI-5E-E-1-CI-8	2	27.2	54.4	188	89	3.46E+03	1.68E+03
PI-5E-E-1-CI-9	2	27.2	54.4	207	99	3.80E+03	1.85E+03
PI-5E-E-2-CI-1	line severed	0.0	--	258	54	--	--
PI-5E-E-2-CI-2	line severed	0.0	--	367	60	--	--
PI-5E-E-2-CI-3	line severed	0.0	--	NA	NA	--	--
PI-5E-E-2-CI-4	line severed	0.0	--	160	83	--	--
PI-5E-E-2-CI-5	line severed	0.0	--	11	73	--	--
PI-5E-E-2-CI-6	line severed	0.0	--	65	62	--	--
PI-5E-E-2-CI-7	line severed	0.0	--	NA	NA	--	--
PI-5E-E-2-CI-8	line severed	0.0	--	NA	NA	--	--
PI-5E-E-2-CI-9	line severed	0.0	--	13	83	--	--
PI-6E-E-1-CI-1	2	19.5	39.1	NA	NA	BDL[(a)]	--
PI-6E-E-1-CI-2	2	19.5	39.1	NA	NA	BDL	--
PI-6E-E-1-CI-3	2	19.5	39.1	117	137	2.98E+03	3.52E+03
PI-6E-E-1-CI-4	2	19.5	39.1	146	67	3.74E+03	1.76E+03
PI-6E-E-1-CI-5	2	19.5	39.1	221	60	5.64E+03	1.63E+03
PI-6E-E-1-CI-6	2	19.5	39.1	186	66	4.77E+03	1.75E+03
PI-6E-E-1-CI-7	2	19.5	39.1	NA	NA	BDL	--
PI-6E-E-1-CI-8	2	19.5	39.1	63	86	1.60E+03	2.21E+03
PI-6E-E-1-CI-9	2	19.5	39.1	333	69	8.52E+03	1.96E+03
PI-6E-E-2-CI-1	2	20.1	40.1	591	66	1.47E+04	2.21E+03
PI-6E-E-2-CI-2	2	20.1	40.1	111	43	2.77E+03	1.11E+03
PI-6E-E-2-CI-3	2	20.1	40.1	117	73	2.92E+03	1.84E+03
PI-6E-E-2-CI-4	2	20.1	40.1	266	82	6.62E+03	2.15E+03
PI-6E-E-2-CI-5	2	20.1	40.1	62	59	1.55E+03	1.47E+03
PI-6E-E-2-CI-6	2	20.1	40.1	224	68	5.57E+03	1.78E+03
PI-6E-E-2-CI-7	2	20.1	40.1	174	61	4.32E+03	1.57E+03
PI-6E-E-2-CI-8	2	20.1	40.1	215	102	5.35E+03	2.60E+03
PI-6E-E-2-CI-9	2	20.1	40.1	538	140	1.34E+04	3.73E+03
PI-7E-E-1-CI-1	1	23.5	23.5	447	66	1.91E+04	4.00E+03
PI-7E-E-1-CI-2	1	23.5	23.5	NA	NA	BDL	--
PI-7E-E-1-CI-3	1	23.5	23.5	116	105	4.95E+03	4.52E+03
PI-7E-E-1-CI-4	1	23.5	23.5	53	61	2.28E+03	2.63E+03
PI-7E-E-1-CI-5	1	23.5	23.5	NA	NA	BDL	--
PI-7E-E-1-CI-6	1	23.5	23.5	144	105	6.14E+03	4.51E+03

Table A.39 (cont'd). Andersen CI External Samplers

Sample ID	Sampling Time (min)	Average Flow (Lpm)	Volume (L)	Calculated U Mass (µg)	DU Mass ± 1σ (µg)	DU Conc. (µg/m^3)	DU Conc. ± 1σ (µg/m^3)
PI-7E-E-1-CI-7	1	23.5	23.5	NA	NA	BDL	--
PI-7E-E-1-CI-8	1	23.5	23.5	NA	NA	BDL	--
PI-7E-E-1-CI-9	1	23.5	23.5	NA	NA	BDL	--
PI-7E-E-2-CI-1	1	29.4	29.4	294	56	1.00E+04	2.16E+03
PI-7E-E-2-CI-2	1	29.4	29.4	287	59	9.77E+03	2.25E+03
PI-7E-E-2-CI-3	1	29.4	29.4	74	114	2.52E+03	3.91E+03
PI-7E-E-2-CI-4	1	29.4	29.4	184	58	6.27E+03	2.07E+03
PI-7E-E-2-CI-5	1	29.4	29.4	NA	NA	BDL	--
PI-7E-E-2-CI-6	1	29.4	29.4	94	109	3.19E+03	3.74E+03
PI-7E-E-2-CI-7	1	29.4	29.4	80	95	2.72E+03	3.26E+03
PI-7E-E-2-CI-8	1	29.4	29.4	180	79	6.14E+03	2.77E+03
PI-7E-E-2-CI-9	1	29.4	29.4	431	171	1.47E+04	6.01E+03
PII-1/2E-E-1-CI-1	2	28.1	56.2	483	65	8.59E+03	1.45E+03
PII-1/2E-E-1-CI-2	2	28.1	56.2	517	71	9.20E+03	1.56E+03
PII-1/2E-E-1-CI-3	2	28.1	56.2	NA	NA	BDL	--
PII-1/2E-E-1-CI-4	2	28.1	56.2	NA	NA	BDL	--
PII-1/2E-E-1-CI-5	2	28.1	56.2	63	112	1.11E+03	1.99E+03
PII-1/2E-E-1-CI-6	2	28.1	56.2	NA	NA	BDL	--
PII-1/2E-E-1-CI-7	2	28.1	56.2	NA	NA	BDL	--
PII-1/2E-E-1-CI-8	2	28.1	56.2	124	111	2.21E+03	1.99E+03
PII-1/2E-E-1-CI-9	2	28.1	56.2	181	93	3.22E+03	1.69E+03
PII-1/2E-E-2-CI-1	2	28.9	57.8	477	143	8.26E+03	2.61E+03
PII-1/2E-E-2-CI-2	2	28.9	57.8	436	96	7.55E+03	1.82E+03
PII-1/2E-E-2-CI-3	2	28.9	57.8	119	70	2.05E+03	1.23E+03
PII-1/2E-E-2-CI-4	2	28.9	57.8	351	113	6.08E+03	2.05E+03
PII-1/2E-E-2-CI-5	2	28.9	57.8	NA	NA	BDL	--
PII-1/2E-E-2-CI-6	2	28.9	57.8	238	87	4.12E+03	1.57E+03
PII-1/2E-E-2-CI-7	2	28.9	57.8	318	101	5.50E+03	1.84E+03
PII-1/2E-E-2-CI-8	2	28.9	57.8	NA	NA	BDL	--
PII-1/2E-E-2-CI-9	2	28.9	57.8	NA	NA	BDL	--
PII-3E-E-1-CI-1	2	27.7	55.3	1261	143	2.28E+04	3.44E+03
PII-3E-E-1-CI-2	2	27.7	55.3	597	104	1.08E+04	2.17E+03
PII-3E-E-1-CI-3	2	27.7	55.3	192	133	3.48E+03	2.42E+03
PII-3E-E-1-CI-4	2	27.7	55.3	362	137	6.54E+03	2.56E+03
PII-3E-E-1-CI-5	2	27.7	55.3	389	108	7.04E+03	2.08E+03
PII-3E-E-1-CI-6	2	27.7	55.3	181	108	3.27E+03	1.98E+03
PII-3E-E-1-CI-7	2	27.7	55.3	440	105	7.96E+03	2.06E+03
PII-3E-E-1-CI-8	2	27.7	55.3	779	120	1.41E+04	2.59E+03
PII-3E-E-1-CI-9	2	27.7	55.3	1820	177	3.29E+04	4.58E+03
PII-3E-E-2-CI-1	2	28.3	56.5	1516	160	2.68E+04	3.90E+03
PII-3E-E-2-CI-2	2	28.3	56.5	431	100	7.62E+03	1.93E+03
PII-3E-E-2-CI-3	2	28.3	56.5	350	110	6.19E+03	2.04E+03

Table A.39 (cont'd). Andersen CI External Samplers

PII-3E-E-2-CI-4	2	28.3	56.5	763	133	1.35E+04	2.71E+03
PII-3E-E-2-CI-5	2	28.3	56.5	467	78	8.27E+03	1.61E+03
PII-3E-E-2-CI-6	2	28.3	56.5	750	103	1.33E+04	2.26E+03
PII-3E-E-2-CI-7	2	28.3	56.5	547	127	9.68E+03	2.45E+03
PII-3E-E-2-CI-8	2	28.3	56.5	444	120	7.86E+03	2.26E+03
PII-3E-E-2-CI-9	2	28.3	56.5	1455	173	2.57E+04	3.99E+03
PIII-1E-E-1-CI-1	2	27.0	53.9	716	120	1.33E+04	2.59E+03
PIII-1E-E-1-CI-2	2	27.0	53.9	453	86	8.41E+03	1.81E+03
PIII-1E-E-1-CI-3	2	27.0	53.9	81	89	1.51E+03	1.65E+03
PIII-1E-E-1-CI-4	2	27.0	53.9	NA	NA	BDL	--
PIII-1E-E-1-CI-5	2	27.0	53.9	77	68	1.43E+03	1.26E+03
PIII-1E-E-1-CI-6	2	27.0	53.9	147	66	2.72E+03	1.25E+03
PIII-1E-E-1-CI-7	2	27.0	53.9	NA	NA	BDL	--
PIII-1E-E-1-CI-8	2	27.0	53.9	NA	NA	BDL	--
PIII-1E-E-1-CI-9	2	27.0	53.9	NA	NA	BDL	--
PIII-1E-E-2-CI-1	2	27.3	54.6	NA	NA	BDL	--
PIII-1E-E-2-CI-2	2	27.3	54.6	341	77	6.24E+03	1.53E+03
PIII-1E-E-2-CI-3	2	27.3	54.6	NA	NA	BDL	--
PIII-1E-E-2-CI-4	2	27.3	54.6	NA	NA	BDL	--
PIII-1E-E-2-CI-5	2	27.3	54.6	NA	NA	BDL	--
PIII-1E-E-2-CI-6	2	27.3	54.6	NA	NA	BDL	--
PIII-1E-E-2-CI-7	2	27.3	54.6	NA	NA	BDL	--
PIII-1E-E-2-CI-8	2	27.3	54.6	107	78	1.97E+03	1.44E+03
PIII-1E-E-2-CI-9	2	27.3	54.6	38	68	6.90E+02	1.24E+03
PIII-2E-E-1-CI-1	300	30.1	9027	4011	296	4.44E+02	5.52E+01
PIII-2E-E-1-CI-2	300	30.1	9027	3575	305	3.96E+02	5.21E+01
PIII-2E-E-1-CI-3	300	30.1	9027	2144	248	2.38E+02	3.63E+01
PIII-2E-E-1-CI-4	300	30.1	9027	2669	275	2.96E+02	4.25E+01
PIII-2E-E-1-CI-5	300	30.1	9027	5481	338	6.07E+02	7.13E+01
PIII-2E-E-1-CI-6	300	30.1	9027	9558	474	1.06E+03	1.18E+02
PIII-2E-E-1-CI-7	300	30.1	9027	12216	522	1.35E+03	1.47E+02
PIII-2E-E-1-CI-8	300	30.1	9027	9460	495	1.05E+03	1.18E+02
PIII-2E-E-1-CI-9	300	30.1	9027	13669	595	1.51E+03	1.65E+02
PIII-2E-E-2-CI-1	2	28.7	57.3	2687	226	4.69E+04	6.13E+03
PIII-2E-E-2-CI-2	2	28.7	57.3	NA	NA	BDL	--
PIII-2E-E-2-CI-3	2	28.7	57.3	NA	NA	BDL	--
PIII-2E-E-2-CI-4	2	28.7	57.3	256	61	4.47E+03	1.16E+03
PIII-2E-E-2-CI-5	2	28.7	57.3	295	158	5.15E+03	2.81E+03
PIII-2E-E-2-CI-6	2	28.7	57.3	264	128	4.61E+03	2.28E+03
PIII-2E-E-2-CI-7	2	28.7	57.3	NA	NA	BDL	--
PIII-2E-E-2-CI-8	2	28.7	57.3	NA	NA	BDL	--
PIII-2E-E-2-CI-9	2	28.7	57.3	199	297	3.47E+03	5.20E+03
PSB-C4E-1-CI-1	2	28.6	57.2	NA	NA	BDL	--
PSB-C4E-1-CI-2	2	28.6	57.2	NA	NA	BDL	--

Table A.39 (cont'd). Andersen CI External Samplers

Sample ID	Sampling Time (min)	Average Flow (Lpm)	Volume (L)	Calculated U Mass (µg)	DU Mass ± 1σ (µg)	DU Conc. (µg/m^3)	DU Conc. ± 1σ (µg/m^3)
PSB-C4E-1-CI-3	2	28.6	57.2	143	105	2.49E+03	1.86E+03
PSB-C4E-1-CI-4	2	28.6	57.2	46	67	7.98E+02	1.18E+03
PSB-C4E-1-CI-5	2	28.6	57.2	104	86	1.81E+03	1.51E+03
PSB-C4E-1-CI-6	2	28.6	57.2	NA	NA	BDL	
PSB-C4E-1-CI-7	2	28.6	57.2	NA	NA	BDL	--
PSB-C4E-1-CI-8	2	28.6	57.2	NA	NA	BDL	--
PSB-C4E-1-CI-9	2	28.6	57.2	NA	NA	BDL	--
PSB-C4E-2-CI-1	2	25.2	50.4	NA	NA	BDL	--
PSB-C4E-2-CI-2	2	25.2	50.4	451	75	8.96E+03	1.74E+03
PSB-C4E-2-CI-3	2	25.2	50.4	64	63	1.26E+03	1.26E+03
PSB-C4E-2-CI-4	2	25.2	50.4	27	74	5.30E+02	1.47E+03
PSB-C4E-2-CI-5	2	25.2	50.4	207	83	4.11E+03	1.70E+03
PSB-C4E-2-CI-6	2	25.2	50.4	148	59	2.93E+03	1.20E+03
PSB-C4E-2-CI-7	2	25.2	50.4	18	85	3.53E+02	1.69E+03
PSB-C4E-2-CI-8	2	25.2	50.4	NA	NA	BDL	--
PSB-C4E-2-CI-9	2	25.2	50.4	NA	NA	BDL	--

(a) BDL=below detection level

Table A.40. Personal Filter Cassette Samples – Mass, Volume, and Concentration

Sample ID	Sampling Time (min)	Total Mass (mg)	Calculated U (μg)	DU Mass ± 1σ (μg)	Flow Rate (Lpm)	Volume (L)	DU Conc. (μg/m^3)	DU Conc. ± 1σ (μg/m^3)
PI-1I-P-1-FS	192	0.310	155	49	2.01	386	401	133
PI-1I-P-2-FS	192	0.421	240	75	2.01	386	621	205
PI-2I-P-1-FS	142	-0.017	64	21	2	284	225	76
PI-2I-P-2-FS	143	0.186	104	34	2	286	365	123
PI-3/4I-P-1-FS	179	0.160	31	7	2.01	360	86	22
PI-3/4I-P-2-FS	132	0.203	21	5	2.01	265	79	20
PI-5I-P-1-FS	125	0.253	242	78	2	250	968	326
PI-5I-P-2-FS	127	0.252	126	41	2	254	497	167
PI-6I-P-1-FS	97	0.227	79	18	2	194	408	101
PI-6I-P-2-FS	120	0.413	29	7	2	240	121	30
PI-7I-P-1-FS	125	0.161	30	7	2	250	119	29
PI-7I-P-2-FS	60	0.235	55	NA (b)	2	120	458	NA [(a)]
PIII-1I-P-1-FS	108	0.045	13	3	2	216	59	15
PIII-1I-P-2-FS	41	0.045	17	4	2	82	202	51
PIII-2I-P-1-FS	168	0.131	37	9	2	336	111	28
PIII-2I-P-2-FS	112	0.387	62	14	2	224	276	69
PII-1/2I-P-1-FS	118	0.249	85	29	2	236	358	126
PII-1/2I-P-2-FS	107	0.376	150	51	2	214	701	248
PII-3I-P-1-FS	84	0.171	23	7	2	168	138	46
PII-3I-P-2-FS	84	0.239	32	10	2	168	189	64

(a) DU mass based on ICP-MS results; no analytical uncertainty was reported.

Table A.41. Personal CI Samples – Mass, Volume, and Concentration

Field ID	Sampling Time (min)	Calculated U Mass (µg)	DU Mass ± 1σ (µg)	Flow Rate (Lpm)	Volume (L)	DU Conc. (µg)	DU Conc. ± 1σ (µg/m^3)
PI-1I-P-1-CI-1	190	59.8	8.7	2	385.9	1.55E+02	2.73E+01
PI-1I-P-1-CI-2	190	25.1	10.1	2	385.9	6.51E+01	2.71E+01
PI-1I-P-1-CI-3	190	25.4	4.9	2	385.9	6.59E+01	1.44E+01
PI-1I-P-1-CI-4	190	17.6	4.9	2	385.9	4.55E+01	1.35E+01
PI-1I-P-1-CI-5	190	10.0	4.1	2	385.9	2.59E+01	1.09E+01
PI-1I-P-1-CI-6	190	4.6	2.5	2	385.9	1.19E+01	6.68E+00
PI-1I-P-1-CI-7	190	6.1	2.7	2	385.9	1.58E+01	7.11E+00
PI-1I-P-1-CI-8	190	6.0	2.9	2	385.9	1.56E+01	7.75E+00
PI-1I-P-1-CI-9	190	8.6	3.5	2	385.9	2.24E+01	9.22E+00
PI-1I-P-2-CI-1	192	47.5	6.8	2	385.9	1.23E+02	2.15E+01
PI-1I-P-2-CI-2	192	18.2	7.4	2	385.9	4.73E+01	1.97E+01
PI-1I-P-2-CI-3	192	17.2	3.6	2	385.9	4.45E+01	1.03E+01
PI-1I-P-2-CI-4	192	11.2	3.4	2	385.9	2.91E+01	9.31E+00
PI-1I-P-2-CI-5	192	10.5	4.3	2	385.9	2.73E+01	1.15E+01
PI-1I-P-2-CI-6	192	9.2	4.1	2	385.9	2.38E+01	1.09E+01
PI-1I-P-2-CI-7	192	7.8	2.5	2	385.9	2.03E+01	6.88E+00
PI-1I-P-2-CI-8	192	6.5	3.8	2	385.9	1.67E+01	9.92E+00
PI-1I-P-2-CI-9	192	15.9	5.6	2	385.9	4.13E+01	1.51E+01
PI-2I-P-1-CI-1	142	1.2	0.9	2	284.0	4.34E+00	3.12E+00
PI-2I-P-1-CI-2	142	2.9	1.9	2	284.0	1.02E+01	6.60E+00
PI-2I-P-1-CI-3	142	5.1	1.5	2	284.0	1.78E+01	5.41E+00
PI-2I-P-1-CI-4	142	11.2	3.3	2	284.0	3.95E+01	1.21E+01
PI-2I-P-1-CI-5	142	9.7	3.9	2	284.0	3.41E+01	1.41E+01
PI-2I-P-1-CI-6	142	121.3	50.0	2	284.0	4.27E+02	1.81E+02
PI-2I-P-1-CI-7	142	1.9	2.6	2	284.0	6.63E+00	9.16E+00
PI-2I-P-1-CI-8	142	-1.3	2.9	2	284.0	-4.45E+00	1.01E+01
PI-2I-P-1-CI-9	142	-2.9	1.7	2	284.0	-1.02E+01	6.03E+00
PI-2I-P-2-CI-1	143	131.1	18.1	2	286.0	4.58E+02	7.82E+01
PI-2I-P-2-CI-2	143	28.0	11.0	2	286.0	9.80E+01	3.97E+01
PI-2I-P-2-CI-3	143	18.6	3.5	2	286.0	6.52E+01	1.38E+01
PI-2I-P-2-CI-4	143	21.9	6.0	2	286.0	7.64E+01	2.22E+01
PI-2I-P-2-CI-5	143	14.9	6.4	2	286.0	5.19E+01	2.29E+01
PI-2I-P-2-CI-6	143	14.6	6.4	2	286.0	5.11E+01	2.29E+01
PI-2I-P-2-CI-7	143	3.9	2.4	2	286.0	1.35E+01	8.65E+00
PI-2I-P-2-CI-8	143	1.1	3.2	2	286.0	3.92E+00	1.12E+01
PI-2I-P-2-CI-9	143	6.6	2.6	2	286.0	2.32E+01	9.22E+00
PI-3/4I-P-1-CI-1	179	21.0	4.4	2	359.8	5.83E+01	1.36E+01
PI-3/4I-P-1-CI-2	179	2.1	1.4	2	359.8	5.71E+00	4.01E+00
PI-3/4I-P-1-CI-3	179	3.9	1.5	2	359.8	1.08E+01	4.42E+00
PI-3/4I-P-1-CI-4	179	1.8	1.6	2	359.8	5.09E+00	4.45E+00
PI-3/4I-P-1-CI-5	179	0.1	1.0	2	359.8	3.82E-01	2.89E+00
PI-3/4I-P-1-CI-6	179	7.4	2.3	2	359.8	2.05E+01	6.60E+00

Table A.41 (contd). Personal CI Samples – Mass, Volume, and Concentration

Field ID	Sampling Time (min)	Calculated U Mass (µg)	DU Mass ± 1σ (µg)	Flow Rate (Lpm)	Volume (L)	DU Conc. (µg)	DU Conc. ± 1σ (µg/m^3)
PI-3/4I-P-1-CI-7	179	5.8	1.9	2	359.8	1.62E+01	5.54E+00
PI-3/4I-P-1-CI-8	179	2.2	1.5	2	359.8	6.06E+00	4.10E+00
PI-3/4I-P-1-CI-9	179	3.9	1.3	2	359.8	1.10E+01	3.87E+00
PI-3/4I-P-2-CI-1	132	53.6	10.0	2	265.3	2.02E+02	4.28E+01
PI-3/4I-P-2-CI-2	132	12.5	6.2	2	265.3	4.73E+01	2.38E+01
PI-3/4I-P-2-CI-3	132	5.6	1.9	2	265.3	2.10E+01	7.32E+00
PI-3/4I-P-2-CI-4	132	10.2	4.1	2	265.3	3.85E+01	1.59E+01
PI-3/4I-P-2-CI-5	132	4.9	2.2	2	265.3	1.86E+01	8.60E+00
PI-3/4I-P-2-CI-6	132	6.0	1.9	2	265.3	2.27E+01	7.48E+00
PI-3/4I-P-2-CI-7	132	0.2	1.4	2	265.3	7.01E-01	5.27E+00
PI-3/4I-P-2-CI-8	132	0.7	1.1	2	265.3	2.71E+00	4.13E+00
PI-3/4I-P-2-CI-9	132	5.1	1.7	2	265.3	1.94E+01	6.56E+00
PI-5I-P-1-CI-1	125	44.7	6.5	2	250.0	1.79E+02	3.14E+01
PI-5I-P-1-CI-2	125	9.1	3.8	2	250.0	3.62E+01	1.55E+01
PI-5I-P-1-CI-3	125	9.1	2.2	2	250.0	3.63E+01	9.51E+00
PI-5I-P-1-CI-4	125	13.9	4.2	2	250.0	5.56E+01	1.76E+01
PI-5I-P-1-CI-5	125	10.3	4.5	2	250.0	4.13E+01	1.84E+01
PI-5I-P-1-CI-6	125	9.4	4.8	2	250.0	3.76E+01	1.96E+01
PI-5I-P-1-CI-7	125	1.4	2.3	2	250.0	5.50E+00	9.26E+00
PI-5I-P-1-CI-8	125	4.0	2.8	2	250.0	1.58E+01	1.13E+01
PI-5I-P-1-CI-9	125	8.5	3.3	2	250.0	3.41E+01	1.35E+01
PI-5I-P-2-CI-1	127	27.4	4.3	2	254.0	1.08E+02	2.02E+01
PI-5I-P-2-CI-2	127	10.4	4.4	2	254.0	4.10E+01	1.79E+01
PI-5I-P-2-CI-3	127	10.0	2.3	2	254.0	3.95E+01	9.77E+00
PI-5I-P-2-CI-4	127	14.7	4.3	2	254.0	5.81E+01	1.81E+01
PI-5I-P-2-CI-5	127	12.5	5.2	2	254.0	4.93E+01	2.10E+01
PI-5I-P-2-CI-6	127	6.6	3.9	2	254.0	2.62E+01	1.57E+01
PI-5I-P-2-CI-7	127	2.0	2.1	2	254.0	8.01E+00	8.38E+00
PI-5I-P-2-CI-8	127	3.9	3.6	2	254.0	1.53E+01	1.42E+01
PI-5I-P-2-CI-9	127	8.9	3.4	2	254.0	3.50E+01	1.39E+01
PI-6I-P-1-CI-1	97	14.0	NA	2	194.0	8.14E+01	NA[(a)]
PI-6I-P-1-CI-2	97	3.0	1.8	2	194.0	1.53E+01	9.48E+00
PI-6I-P-1-CI-3	97	7.7	2.5	2	194.0	3.97E+01	1.33E+01
PI-6I-P-1-CI-4	97	5.1	2.4	2	194.0	2.63E+01	1.25E+01
PI-6I-P-1-CI-5	97	4.5	2.2	2	194.0	2.30E+01	1.15E+01
PI-6I-P-1-CI-6	97	2.8	1.2	2	194.0	1.46E+01	6.48E+00
PI-6I-P-1-CI-7	97	-1.3	1.6	2	194.0	-6.89E+00	8.27E+00
PI-6I-P-1-CI-8	97	0.8	1.2	2	194.0	4.11E+00	5.94E+00
PI-6I-P-1-CI-9	97	5.7	1.3	2	194.0	2.95E+01	7.36E+00
PI-6I-P-2-CI-1	120	33.3	6.6	2	240.0	1.39E+02	3.10E+01
PI-6I-P-2-CI-2	120	9.5	4.6	2	240.0	3.97E+01	1.96E+01
PI-6I-P-2-CI-3	120	10.3	3.1	2	240.0	4.31E+01	1.35E+01

Table A.41 (contd). Personal CI Samples – Mass, Volume, and Concentration

Field ID	Sampling Time (min)	Calculated U Mass (µg)	DU Mass ± 1σ (µg)	Flow Rate (Lpm)	Volume (L)	DU Conc. (µg)	DU Conc. ± 1σ (µg/m^3)
PI-6I-P-2-CI-4	120	8.0	3.3	2	240.0	3.33E+01	1.42E+01
PI-6I-P-2-CI-5	120	3.0	1.8	2	240.0	1.23E+01	7.59E+00
PI-6I-P-2-CI-6	120	2.9	1.5	2	240.0	1.20E+01	6.19E+00
PI-6I-P-2-CI-7	120	0.5	1.5	2	240.0	2.12E+00	6.07E+00
PI-6I-P-2-CI-8	120	-0.5	1.0	2	240.0	-2.05E+00	3.99E+00
PI-6I-P-2-CI-9	120	6.0	1.5	2	240.0	2.49E+01	6.72E+00
PI-7I-P-1-CI-1	125	14.3	3.2	2	250.0	5.73E+01	1.41E+01
PI-7I-P-1-CI-2	125	-0.4	1.1	2	250.0	-1.58E+00	4.44E+00
PI-7I-P-1-CI-3	125	2.5	1.3	2	250.0	9.83E+00	5.11E+00
PI-7I-P-1-CI-4	125	0.6	1.2	2	250.0	2.47E+00	4.99E+00
PI-7I-P-1-CI-5	125	-1.4	1.3	2	250.0	-5.73E+00	5.21E+00
PI-7I-P-1-CI-6	125	2.3	1.1	2	250.0	9.14E+00	4.47E+00
PI-7I-P-1-CI-7	125	0.7	1.4	2	250.0	3.00E+00	5.47E+00
PI-7I-P-1-CI-8	125	0.0	1.2	2	250.0	9.67E-02	4.77E+00
PI-7I-P-1-CI-9	125	3.7	0.9	2	250.0	1.49E+01	3.97E+00
PI-7I-P-2-CI-1	60	14.4	3.1	2	120.0	1.20E+02	2.83E+01
PI-7I-P-2-CI-2	60	1.5	1.4	2	120.0	1.25E+01	1.19E+01
PI-7I-P-2-CI-3	60	1.9	1.0	2	120.0	1.56E+01	8.77E+00
PI-7I-P-2-CI-4	60	1.8	1.2	2	120.0	1.52E+01	1.01E+01
PI-7I-P-2-CI-5	60	1.0	0.9	2	120.0	8.09E+00	7.62E+00
PI-7I-P-2-CI-6	60	1.3	1.1	2	120.0	1.05E+01	9.26E+00
PI-7I-P-2-CI-7	60	-1.6	1.3	2	120.0	-1.29E+01	1.08E+01
PI-7I-P-2-CI-8	60	1.3	1.0	2	120.0	1.06E+01	8.51E+00
PI-7I-P-2-CI-9	60	3.7	1.0	2	120.0	3.07E+01	8.67E+00
PIII-1I-P-1-CI-1	108	20.0	4.1	2	216.0	9.24E+01	2.10E+01
PIII-1I-P-1-CI-2	108	5.8	2.9	2	216.0	2.67E+01	1.35E+01
PIII-1I-P-1-CI-3	108	4.7	1.4	2	216.0	2.18E+01	7.01E+00
PIII-1I-P-1-CI-4	108	1.1	0.9	2	216.0	5.22E+00	4.04E+00
PIII-1I-P-1-CI-5	108	2.1	1.1	2	216.0	9.54E+00	5.37E+00
PIII-1I-P-1-CI-6	108	6.2	1.7	2	216.0	2.89E+01	8.44E+00
PIII-1I-P-1-CI-7	108	4.3	1.2	2	216.0	2.00E+01	5.87E+00
PIII-1I-P-1-CI-8	108	6.6	1.6	2	216.0	3.04E+01	7.83E+00
PIII-1I-P-1-CI-9	108	7.5	1.8	2	216.0	3.49E+01	9.12E+00
PIII-1I-P-2-CI-1	41	7.3	1.7	2	82.0	8.92E+01	2.20E+01
PIII-1I-P-2-CI-2	41	4.1	2.1	2	82.0	5.05E+01	2.56E+01
PIII-1I-P-2-CI-3	41	3.8	1.1	2	82.0	4.68E+01	1.42E+01
PIII-1I-P-2-CI-4	41	3.4	1.3	2	82.0	4.10E+01	1.69E+01
PIII-1I-P-2-CI-5	41	3.0	1.3	2	82.0	3.64E+01	1.67E+01
PIII-1I-P-2-CI-6	41	4.1	1.5	2	82.0	4.95E+01	1.94E+01
PIII-1I-P-2-CI-7	41	3.4	1.3	2	82.0	4.12E+01	1.67E+01
PIII-1I-P-2-CI-8	41	1.6	0.7	2	82.0	1.89E+01	9.09E+00
PIII-1I-P-2-CI-9	41	6.1	1.6	2	82.0	7.45E+01	2.04E+01

Table A.41 (contd). Personal CI Samples – Mass, Volume, and Concentration

Field ID	Sampling Time (min)	Calculated U Mass (µg)	DU Mass ± 1σ (µg)	Flow Rate (Lpm)	Volume (L)	DU Conc. (µg)	DU Conc. ± 1σ (µg/m^3)
PIII-2I-P-1-CI-1	168	37.9	7.4	2	336.0	1.13E+02	2.47E+01
PIII-2I-P-1-CI-2	168	6.8	3.4	2	336.0	2.01E+01	1.02E+01
PIII-2I-P-1-CI-3	168	6.4	1.9	2	336.0	1.89E+01	6.00E+00
PIII-2I-P-1-CI-4	168	5.6	2.5	2	336.0	1.67E+01	7.54E+00
PIII-2I-P-1-CI-5	168	14.7	5.8	2	336.0	4.38E+01	1.79E+01
PIII-2I-P-1-CI-6	168	7.2	1.9	2	336.0	2.15E+01	6.18E+00
PIII-2I-P-1-CI-7	168	11.8	2.6	2	336.0	3.52E+01	8.52E+00
PIII-2I-P-1-CI-8	168	9.7	1.7	2	336.0	2.89E+01	5.84E+00
PIII-2I-P-1-CI-9	168	8.8	1.9	2	336.0	2.61E+01	6.13E+00
PIII-2I-P-2-CI-1	112	7.1	2.0	2	224.0	3.17E+01	9.49E+00
PIII-2I-P-2-CI-2	112	5.9	3.0	2	224.0	2.62E+01	1.34E+01
PIII-2I-P-2-CI-3	112	5.2	1.6	2	224.0	2.33E+01	7.63E+00
PIII-2I-P-2-CI-4	112	2.2	1.2	2	224.0	9.69E+00	5.59E+00
PIII-2I-P-2-CI-5	112	3.0	1.5	2	224.0	1.34E+01	7.02E+00
PIII-2I-P-2-CI-6	112	0.6	1.0	2	224.0	2.56E+00	4.34E+00
PIII-2I-P-2-CI-7	112	1.9	1.1	2	224.0	8.68E+00	4.92E+00
PIII-2I-P-2-CI-8	112	39.6	4.5	2	224.0	1.77E+02	2.68E+01
PIII-2I-P-2-CI-9	112	3.2	1.3	2	224.0	1.45E+01	5.97E+00
PII-1/2I-P-1-CI-1	118	19.6	3.3	2	236.0	8.32E+01	1.63E+01
PII-1/2I-P-1-CI-2	118	8.4	3.6	2	236.0	3.55E+01	1.57E+01
PII-1/2I-P-1-CI-3	118	6.9	1.7	2	236.0	2.91E+01	7.88E+00
PII-1/2I-P-1-CI-4	118	5.9	2.0	2	236.0	2.48E+01	8.83E+00
PII-1/2I-P-1-CI-5	118	13.1	5.4	2	236.0	5.54E+01	2.33E+01
PII-1/2I-P-1-CI-6	118	11.5	5.7	2	236.0	4.89E+01	2.45E+01
PII-1/2I-P-1-CI-7	118	9.9	3.7	2	236.0	4.19E+01	1.63E+01
PII-1/2I-P-1-CI-8	118	21.2	6.8	2	236.0	8.98E+01	3.01E+01
PII-1/2I-P-1-CI-9	118	11.8	4.4	2	236.0	4.99E+01	1.94E+01
PII-1/2I-P-2-CI-1	107	23.7	3.9	2	214.0	1.11E+02	2.11E+01
PII-1/2I-P-2-CI-2	107	9.3	4.0	2	214.0	4.35E+01	1.91E+01
PII-1/2I-P-2-CI-3	107	17.7	3.6	2	214.0	8.29E+01	1.86E+01
PII-1/2I-P-2-CI-4	107	13.7	3.8	2	214.0	6.41E+01	1.91E+01
PII-1/2I-P-2-CI-5	107	8.3	3.6	2	214.0	3.87E+01	1.71E+01
PII-1/2I-P-2-CI-6	107	12.4	5.6	2	214.0	5.77E+01	2.70E+01
PII-1/2I-P-2-CI-7	107	10.1	3.9	2	214.0	4.70E+01	1.90E+01
PII-1/2I-P-2-CI-8	107	20.0	6.4	2	214.0	9.35E+01	3.12E+01
PII-1/2I-P-2-CI-9	107	6.0	3.0	2	214.0	2.78E+01	1.41E+01
PII-3I-P-1-CI-1	84	7.0	1.3	2	168.0	4.16E+01	9.01E+00
PII-3I-P-1-CI-2	84	3.5	1.6	2	168.0	2.09E+01	9.88E+00
PII-3I-P-1-CI-3	84	1.6	0.7	2	168.0	9.50E+00	4.47E+00
PII-3I-P-1-CI-4	84	2.3	0.8	2	168.0	1.39E+01	4.91E+00
PII-3I-P-1-CI-5	84	2.8	1.4	2	168.0	1.67E+01	8.74E+00
PII-3I-P-1-CI-6	84	-0.8	1.3	2	168.0	-5.01E+00	7.83E+00

Table A.41 (cont'd). Personal CI Samples

Field ID	Sampling Time (min)	Calculated U Mass (µg)	DU Mass ± 1σ (µg)	Flow Rate (Lpm)	Volume (L)	DU Conc. (µg)	DU Conc. ± 1σ (µg/m^3)
PII-3I-P-1-CI-7	84	-1.8	1.4	2	168.0	-1.09E+01	8.62E+00
PII-3I-P-1-CI-8	84	-2.3	2.5	2	168.0	-1.37E+01	1.51E+01
PII-3I-P-1-CI-9	84	-0.7	1.8	2	168.0	-4.14E+00	1.07E+01
PII-3I-P-2-CI-1	84	6.5	1.4	2	168.0	3.87E+01	9.02E+00
PII-3I-P-2-CI-2	84	3.3	1.5	2	168.0	1.99E+01	9.34E+00
PII-3I-P-2-CI-3	84	2.0	0.7	2	168.0	1.18E+01	4.26E+00
PII-3I-P-2-CI-4	84	0.1	0.9	2	168.0	7.66E-01	5.44E+00
PII-3I-P-2-CI-5	84	1.8	1.4	2	168.0	1.05E+01	8.38E+00
PII-3I-P-2-CI-6	84	-1.3	1.4	2	168.0	-7.52E+00	8.16E+00
PII-3I-P-2-CI-7	84	1.3	1.6	2	168.0	7.56E+00	9.36E+00
PII-3I-P-2-CI-8	84	-1.0	2.5	2	168.0	-5.76E+00	1.48E+01
PII-3I-P-2-CI-9	84	-0.4	1.3	2	168.0	-2.24E+00	7.54E+00
PIV-1I-P-1-CI-1	121	1.3	1.0	2	242.0	5.56E+00	4.28E+00
PIV-1I-P-1-CI-2	121	-0.4	1.2	2	242.0	-1.55E+00	4.80E+00
PIV-1I-P-1-CI-3	121	7.2	1.6	2	242.0	2.97E+01	7.42E+00
PIV-1I-P-1-CI-4	121	3.4	1.4	2	242.0	1.41E+01	6.12E+00
PIV-1I-P-1-CI-5	121	-1.6	1.4	2	242.0	-6.71E+00	5.77E+00
PIV-1I-P-1-CI-6	121	1.4	1.8	2	242.0	5.90E+00	7.56E+00
PIV-1I-P-1-CI-7	121	13.5	3.5	2	242.0	5.57E+01	1.55E+01
PIV-1I-P-1-CI-8	121	24.2	5.7	2	242.0	9.99E+01	2.55E+01
PIV-1I-P-1-CI-9	121	2.9	2.5	2	242.0	1.20E+01	1.02E+01
PIV-1I-P-2-CI-1	122	2.8	1.2	2	244.0	1.16E+01	5.06E+00
PIV-1I-P-2-CI-2	122	1.1	1.3	2	244.0	4.33E+00	5.20E+00
PIV-1I-P-2-CI-3	122	1.9	1.0	2	244.0	7.98E+00	4.36E+00
PIV-1I-P-2-CI-4	122	4.9	1.8	2	244.0	1.99E+01	7.48E+00
PIV-1I-P-2-CI-5	122	-0.4	1.4	2	244.0	-1.76E+00	5.94E+00
PIV-1I-P-2-CI-6	122	-2.3	2.3	2	244.0	-9.37E+00	9.44E+00
PIV-1I-P-2-CI-7	122	-5.6	2.5	2	244.0	-2.31E+01	1.03E+01
PIV-1I-P-2-CI-8	122	-1.7	2.6	2	244.0	-6.89E+00	1.06E+01
PIV-1I-P-2-CI-9	122	-2.6	2.2	2	244.0	-1.07E+01	9.00E+00
PIV-3I-P-2-CI-1	100	1.6	0.6	2	200.0	8.07E+00	3.24E+00
PIV-3I-P-2-CI-2	100	1.0	0.6	2	200.0	5.09E+00	3.19E+00
PIV-3I-P-2-CI-3	100	2.0	0.4	2	200.0	9.76E+00	2.06E+00
PIV-3I-P-2-CI-4	100	0.4	0.4	2	200.0	1.86E+00	2.23E+00
PIV-3I-P-2-CI-5	100	0.0	0.0	2	200.0	0.00E+00	--
PIV-3I-P-2-CI-6	100	3.2	1.5	2	200.0	1.59E+01	7.55E+00
PIV-3I-P-2-CI-7	100	-0.2	0.8	2	200.0	-1.01E+00	3.94E+00
PIV-3I-P-2-CI-8	100	2.7	1.1	2	200.0	1.36E+01	5.47E+00
PIV-3I-P-2-CI-9	100	3.3	1.8	2	200.0	1.64E+01	8.92E+00
PIV-3I-P-1-CI-1	93	1.6	1.2	2	186.0	8.40E+00	6.63E+00
PIV-3I-P-1-CI-2	93	0.9	1.2	2	186.0	4.71E+00	6.58E+00
PIV-3I-P-1-CI-3	93	0.3	0.9	2	186.0	1.65E+00	4.73E+00

Table A.41 (cont'd). Personal CI Samples

Field ID	Sampling Time (min)	Calculated U Mass (µg)	DU Mass ± 1σ (µg)	Flow Rate (Lpm)	Volume (L)	DU Conc. (µg)	DU Conc. ± 1σ (µg/m^3)
PIV-3I-P-1-CI-4	93	8.3	2.5	2	186.0	4.48E+01	1.40E+01
PIV-3I-P-1-CI-5	93	0.2	1.2	2	186.0	1.24E+00	6.65E+00
PIV-3I-P-1-CI-6	93	4.6	3.5	2	186.0	2.48E+01	1.91E+01
PIV-3I-P-1-CI-7	93	-0.3	2.8	2	186.0	-1.41E+00	1.48E+01
PIV-3I-P-1-CI-8	93	3.9	4.8	2	186.0	2.10E+01	2.61E+01
PIV-3I-P-1-CI-9	93	5.8	4.0	2	186.0	3.12E+01	2.17E+01
PIV-4I-P-2-CI-1	49	2.9	1.4	2	98.0	3.00E+01	1.44E+01
PIV-4I-P-2-CI-2	49	-0.8	1.0	2	98.0	-8.43E+00	1.07E+01
PIV-4I-P-2-CI-3	49	0.2	0.8	2	98.0	2.08E+00	7.87E+00
PIV-4I-P-2-CI-4	49	-1.0	0.8	2	98.0	-1.01E+01	8.47E+00
PIV-4I-P-2-CI-5	49	-0.2	1.2	2	98.0	-1.88E+00	1.19E+01
PIV-4I-P-2-CI-6	49	-1.2	1.9	2	98.0	-1.22E+01	1.98E+01
PIV-4I-P-2-CI-7	49	-3.2	2.8	2	98.0	-3.27E+01	2.83E+01
PIV-4I-P-2-CI-8	49	-3.6	3.0	2	98.0	-3.64E+01	3.08E+01
PIV-4I-P-2-CI-9	49	-1.1	2.3	2	98.0	-1.09E+01	2.33E+01
PIV-4I-P-3-CI-1	75	2.7	1.0	2	150.0	1.78E+01	6.91E+00
PIV-4I-P-3-CI-2	75	-1.2	1.1	2	150.0	-8.08E+00	7.37E+00
PIV-4I-P-3-CI-3	75	0.5	0.7	2	150.0	3.53E+00	4.93E+00
PIV-4I-P-3-CI-4	75	-0.2	0.9	2	150.0	-1.47E+00	5.92E+00
PIV-4I-P-3-CI-5	75	1.1	1.2	2	150.0	7.31E+00	8.25E+00
PIV-4I-P-3-CI-6	75	-3.4	2.3	2	150.0	-2.26E+01	1.54E+01
PIV-4I-P-3-CI-7	75	3.2	2.5	2	150.0	2.11E+01	1.67E+01
PIV-4I-P-3-CI-8	75	-5.5	2.8	2	150.0	-3.68E+01	1.89E+01
PIV-4I-P-3-CI-9	75	-2.2	2.2	2	150.0	-1.47E+01	1.49E+01
PIV-4I-P-1-CI-1	88	1.1	0.8	2	176.0	6.49E+00	4.81E+00
PIV-4I-P-1-CI-2	88	-1.0	1.1	2	176.0	-5.81E+00	6.12E+00
PIV-4I-P-1-CI-3	88	-0.1	0.6	2	176.0	-5.80E-01	3.66E+00
PIV-4I-P-1-CI-4	88	0.0	--	2	176.0	0.00E+00	--
PIV-4I-P-1-CI-5	88	-1.4	1.4	2	176.0	-7.77E+00	8.15E+00
PIV-4I-P-1-CI-6	88	6.3	3.2	2	176.0	3.60E+01	1.84E+01
PIV-4I-P-1-CI-7	88	1.2	2.0	2	176.0	7.03E+00	1.15E+01
PIV-4I-P-1-CI-8	88	10.3	3.6	2	176.0	5.84E+01	2.12E+01
PIV-4I-P-1-CI-9	88	-0.6	2.2	2	176.0	-3.17E+00	1.27E+01
PIV-4I-P-4-CI-1	30	4.6	1.0	2	60.0	7.70E+01	1.85E+01
PIV-4I-P-4-CI-2	30	2.6	1.2	2	60.0	4.28E+01	1.98E+01
PIV-4I-P-4-CI-3	30	1.9	0.7	2	60.0	3.13E+01	1.23E+01
PIV-4I-P-4-CI-4	30	3.6	1.1	2	60.0	5.99E+01	1.86E+01
PIV-4I-P-4-CI-5	30	2.9	1.7	2	60.0	4.91E+01	2.80E+01
PIV-4I-P-4-CI-6	30	8.8	4.2	2	60.0	1.46E+02	7.18E+01
PIV-4I-P-4-CI-7	30	4.2	1.9	2	60.0	6.93E+01	3.32E+01
PIV-4I-P-4-CI-8	30	28.6	7.8	2	60.0	4.77E+02	1.38E+02

Table A.41 (cont'd). Personal CI Samples

Field ID	Sampling Time (min)	Calculated U Mass (µg)	DU Mass ± 1σ (µg)	Flow Rate (Lpm)	Volume (L)	DU Conc. (µg)	DU Conc. ± 1σ (µg/m^3)
PIV-4I-P-4-CI-9	30	8.3	3.2	2	60.0	1.38E+02	5.43E+01
PIV-4I-P-5-CI-1	33	10.7	1.9	2	66.0	1.62E+02	3.26E+01
PIV-4I-P-5-CI-2	33	3.5	1.5	2	66.0	5.24E+01	2.30E+01
PIV-4I-P-5-CI-3	33	4.5	1.1	2	66.0	6.86E+01	1.75E+01
PIV-4I-P-5-CI-4	33	3.4	1.0	2	66.0	5.09E+01	1.66E+01
PIV-4I-P-5-CI-5	33	2.1	1.4	2	66.0	3.25E+01	2.14E+01
PIV-4I-P-5-CI-6	33	4.9	2.6	2	66.0	7.46E+01	4.07E+01
PIV-4I-P-5-CI-7	33	5.2	2.3	2	66.0	7.89E+01	3.55E+01
PIV-4I-P-5-CI-8	33	14.4	5.6	2	66.0	2.19E+02	8.71E+01
PIV-4I-P-5-CI-9	33	8.7	4.0	2	66.0	1.32E+02	6.21E+01

(a) DU mass based on ICP-MS results; no analytical uncertainty was reported.
-- = Original count activity was 0.00; therefore no uncertainty propagated for mass or concentration results.

Appendix B

Particle Size Distributions – Cascade Impactor Summary Data

Appendix B

Particle Size Distributions – Cascade Impactor Summary Data

The Marple cascade impactors (CIs) were used to collect aerosols inside the target vehicles. Particle size distributions of Marple CI data were modeled using unimodal and bimodal distributions to derive the activity median aerodynamic diameters (AMADs) as discussed in Section 5.5.1. No corrections for wall loss were applied. In most, but not all cases, the bimodal distributions provided the better fit. Several example histograms of the particle size distributions illustrating the unimodal and bimodal curve fits are shown in Figures 5.28 through 5.35. A simpler presentation of the AMADs using only the unimodal model is shown in Figures B.1 through B.12. These figures provide curves for each array position for which a sampler operated over the total sampling period for Phases I through IV.

Table B.1 lists the AMAD values, the geometric standard deviations (GSDs), and the correlation coefficient (R^2) for the unimodal and bimodal models. The GSD is a parameter of data spread and goodness of fit. The table includes these columns: sample identification, unimodal fit for AMAD, GSD, and R^2 for a unimodal fit, AMAD, GSD, R^2, and fraction in the first peak for a bimodal fit. Except where indicated, the ninth sampler in each array was the field blank. In several cases noted in the table, the AMAD and GSD results did not make sense, and professional judgment based on graphical presentation of the data was applied, denoted as (a), to provide better estimates of these parameters.

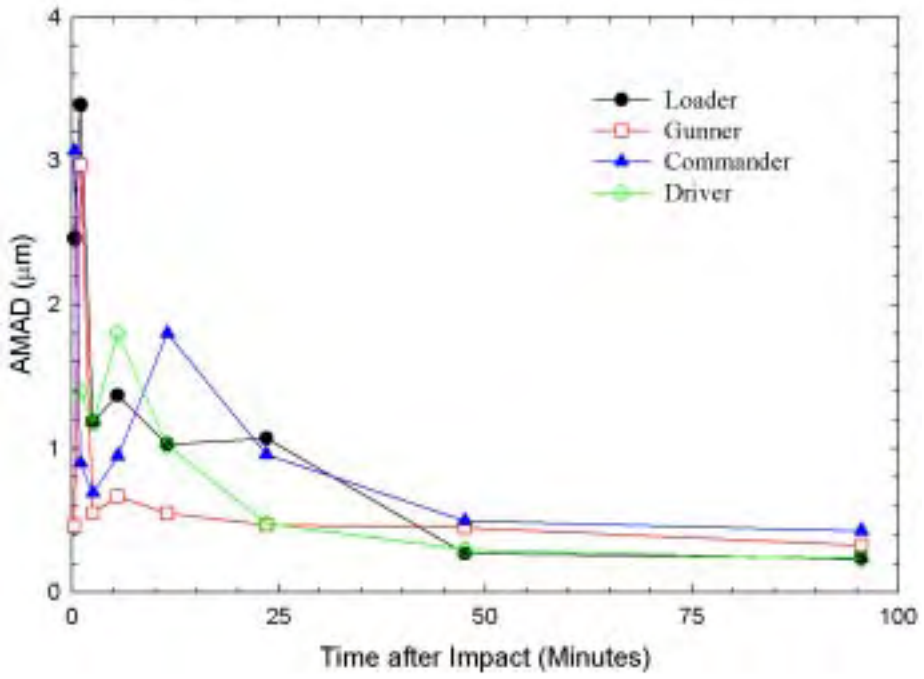

Figure B.1. AMAD Values as a Function of Time, PI-1

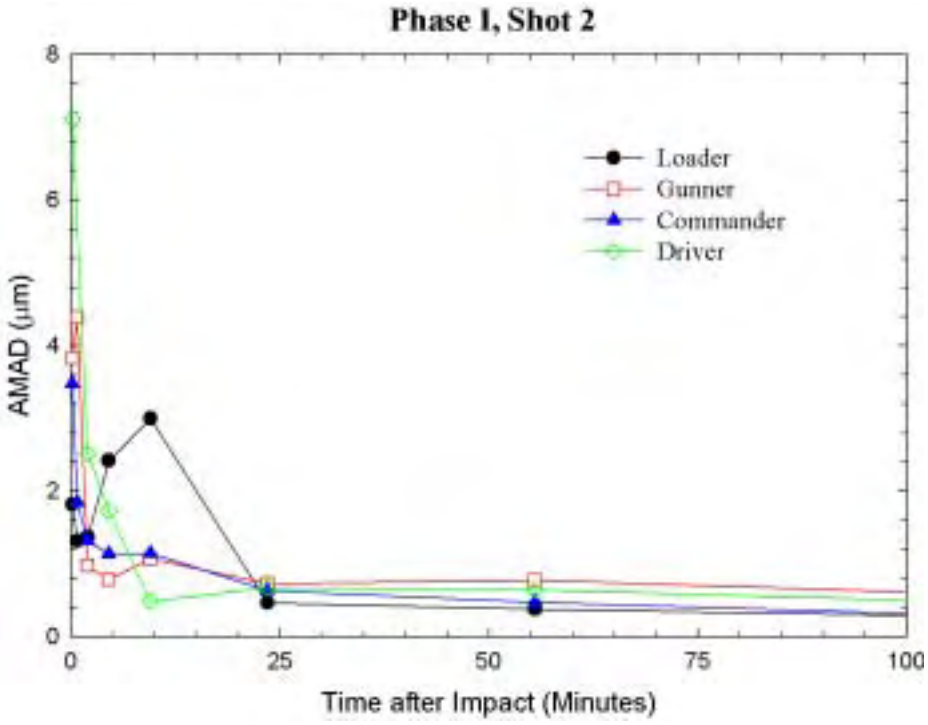

Figure B.2. AMAD Values as a Function of Time, P1-2

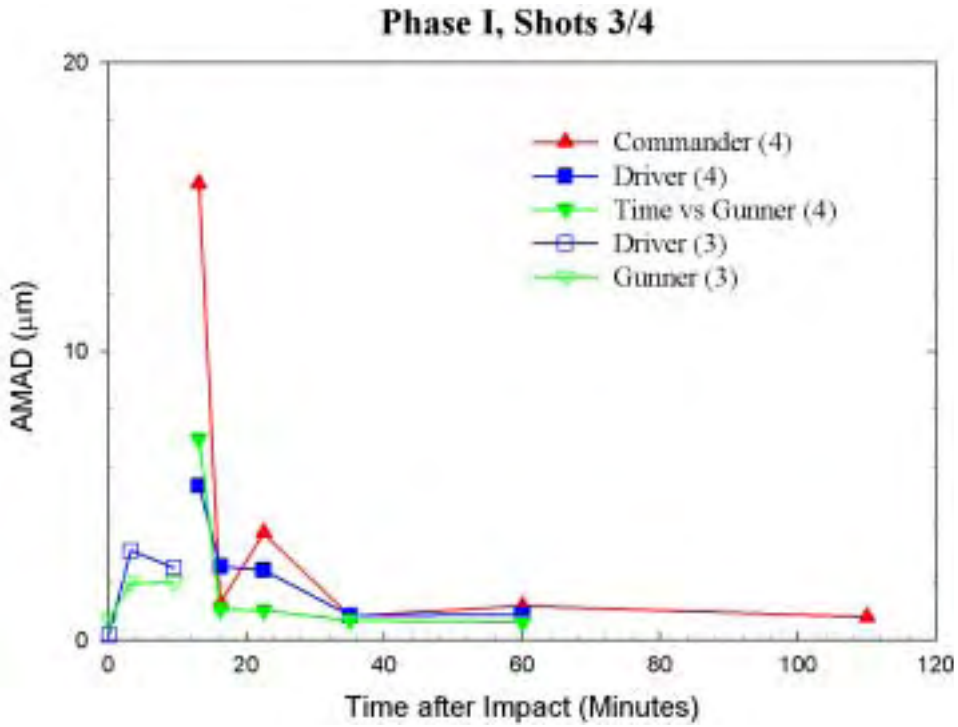

Figure B.3. AMAD Values as a Function of Time, PI-3/4

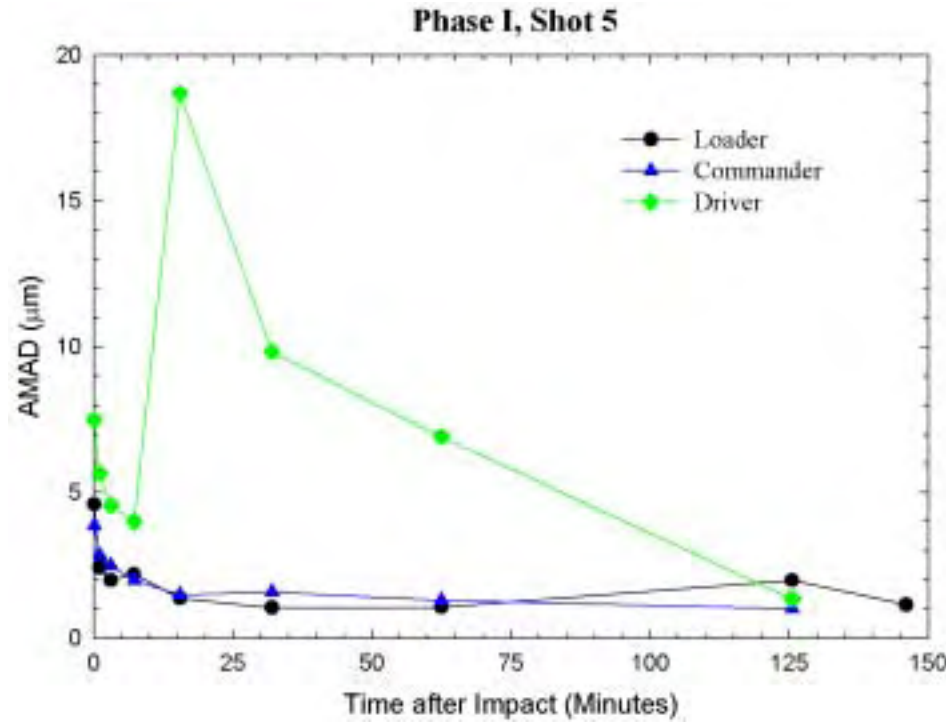

Figure B.4. AMAD Values as a Function of Time, PI-5

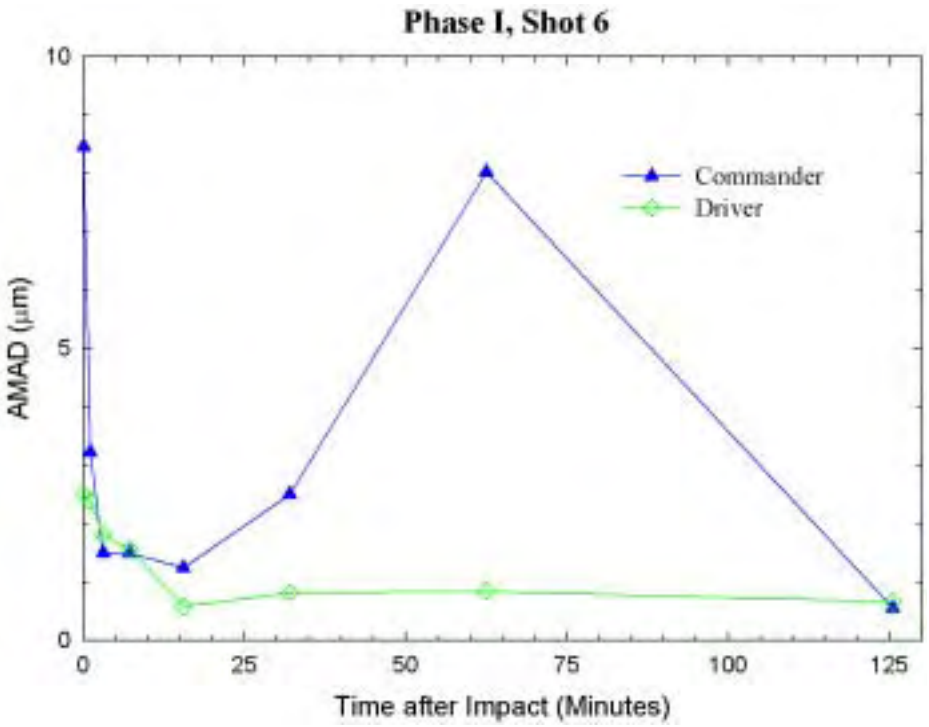

Figure B.5. AMAD Values as a Function of Time, PI-6

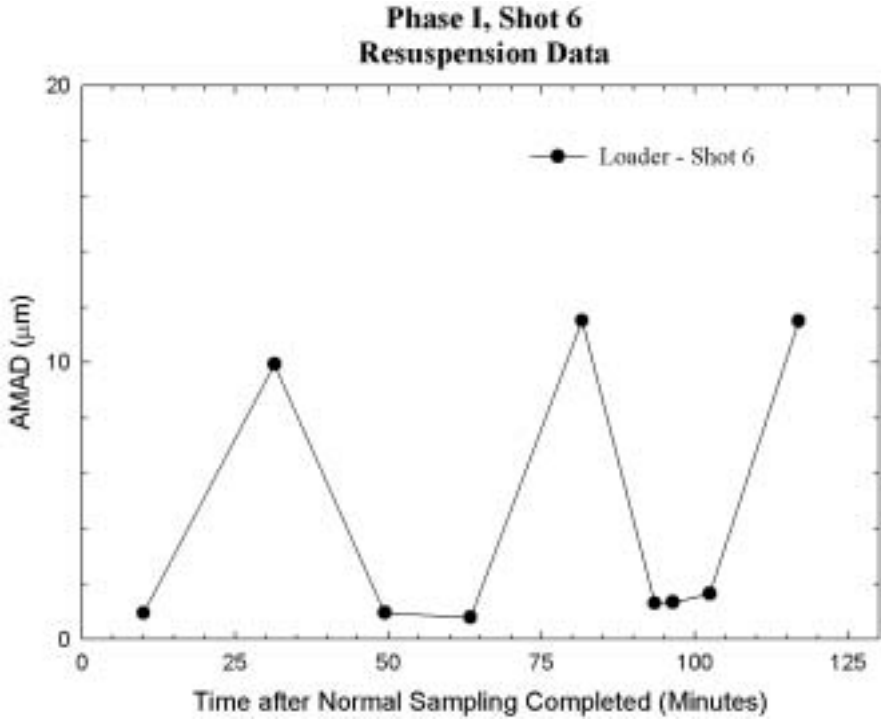

Figure B.6. AMAD Values as a Function of Time, PI-6

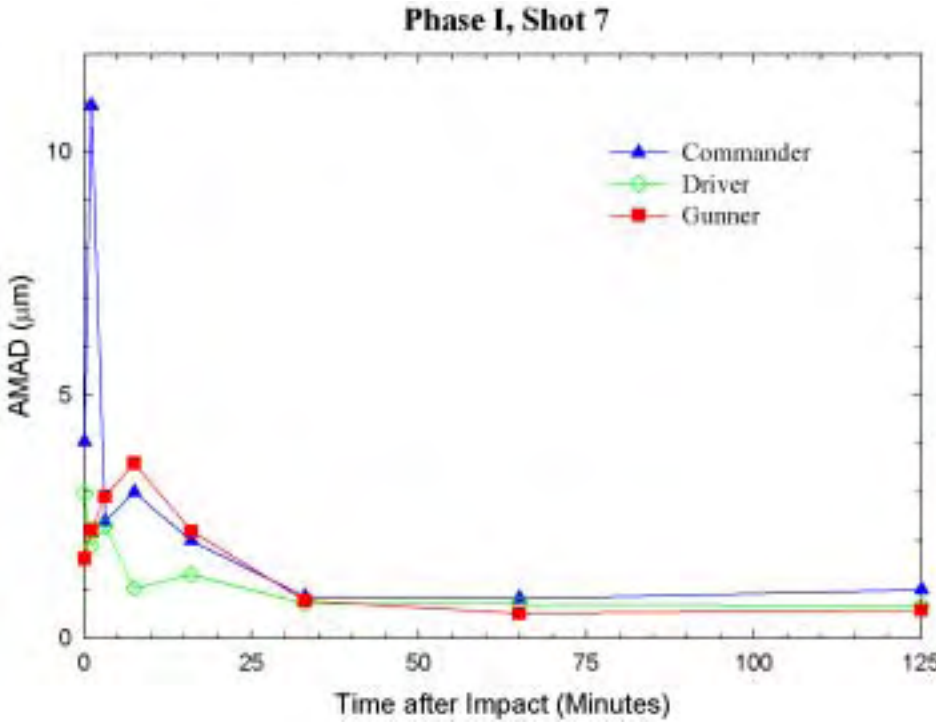

Figure B.7. AMAD Values as a Function of Time, PI-7

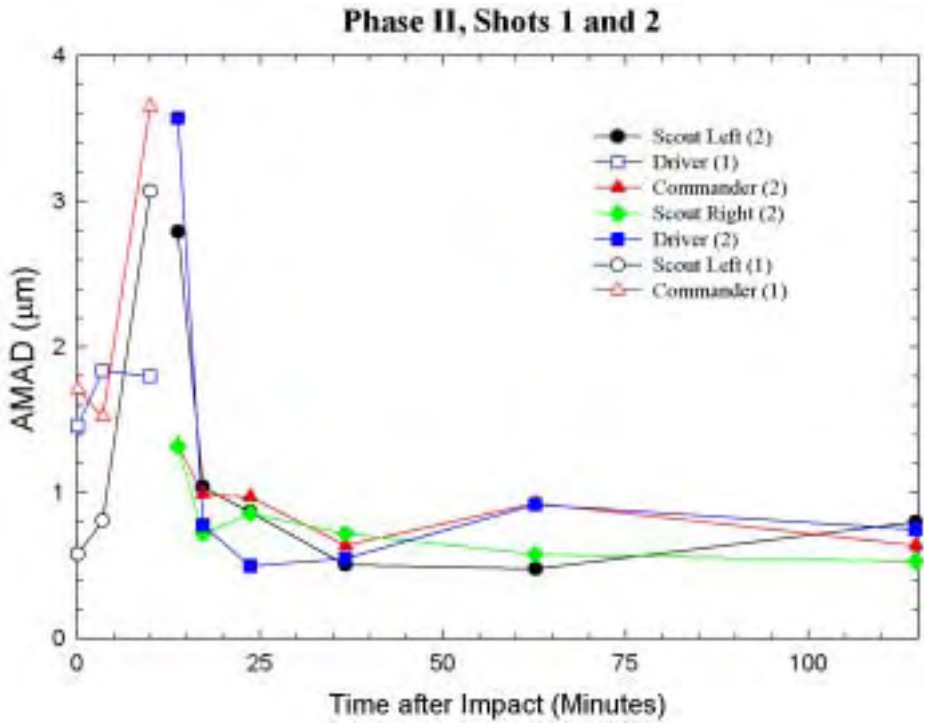

Figure B.8. AMAD Values as a Function of Time, PII-1 and 2

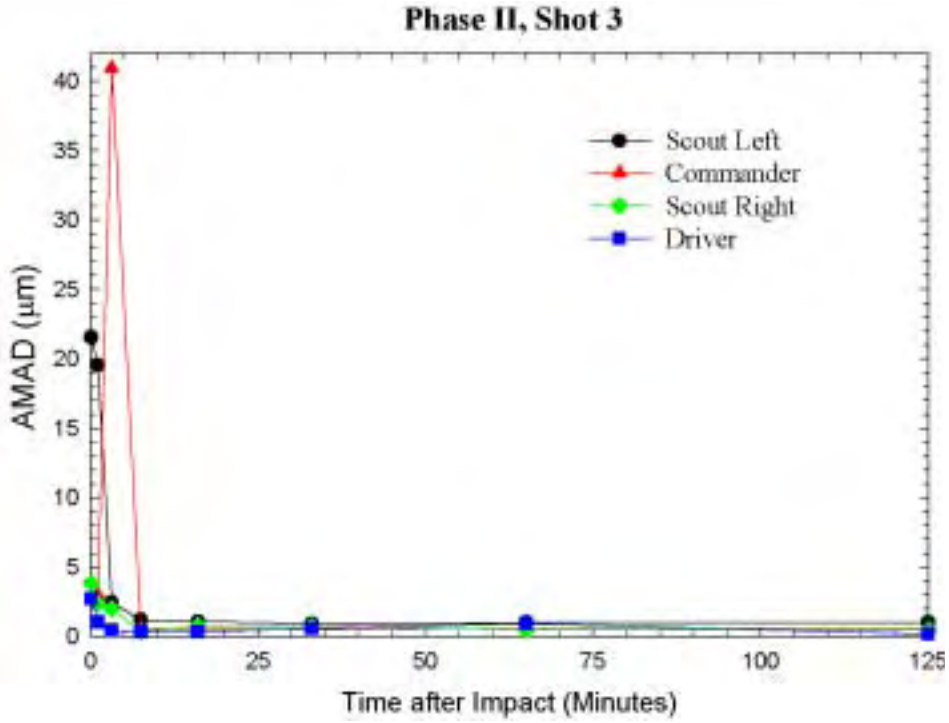

Figure B.9. AMAD Values as a Function of Time, PII-3

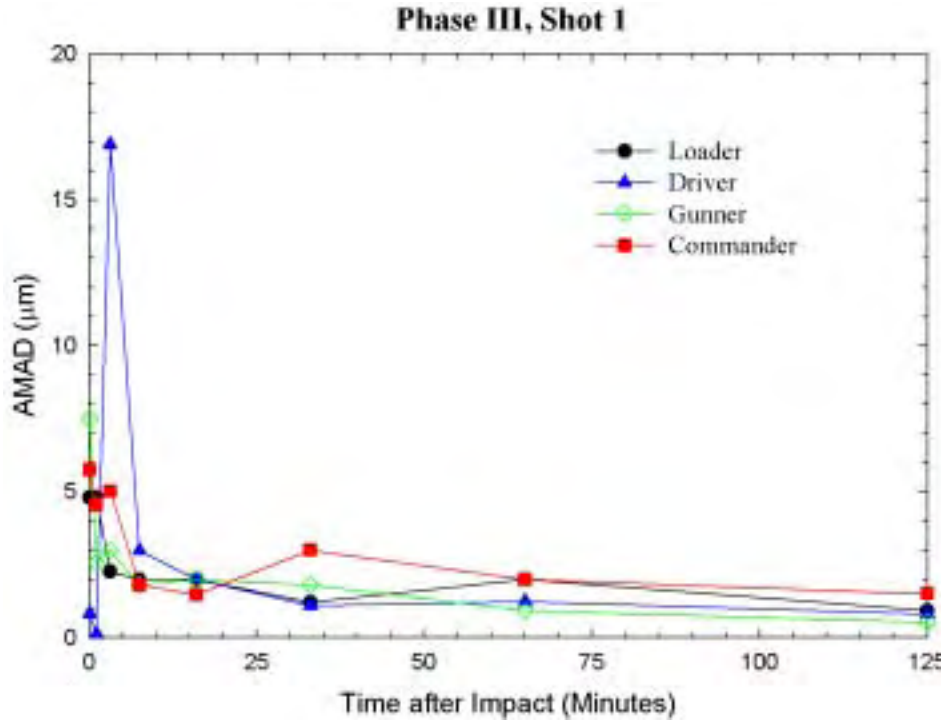

Figure B.10. AMAD Values as a Function of Time, PIII-1

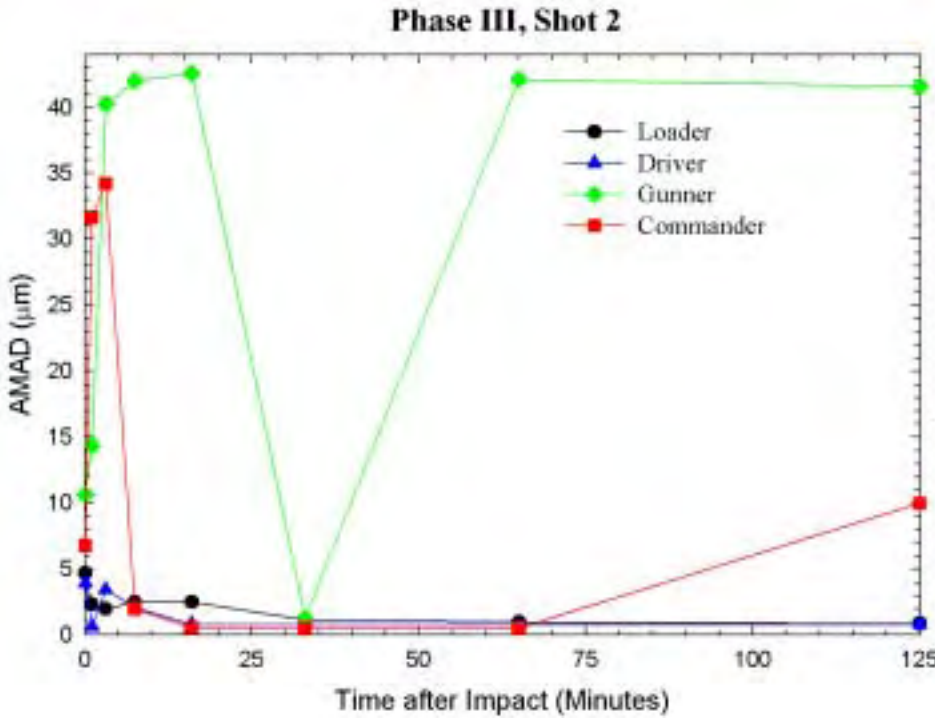

Figure B.11. AMAD Values as a Function of Time, PIII-2

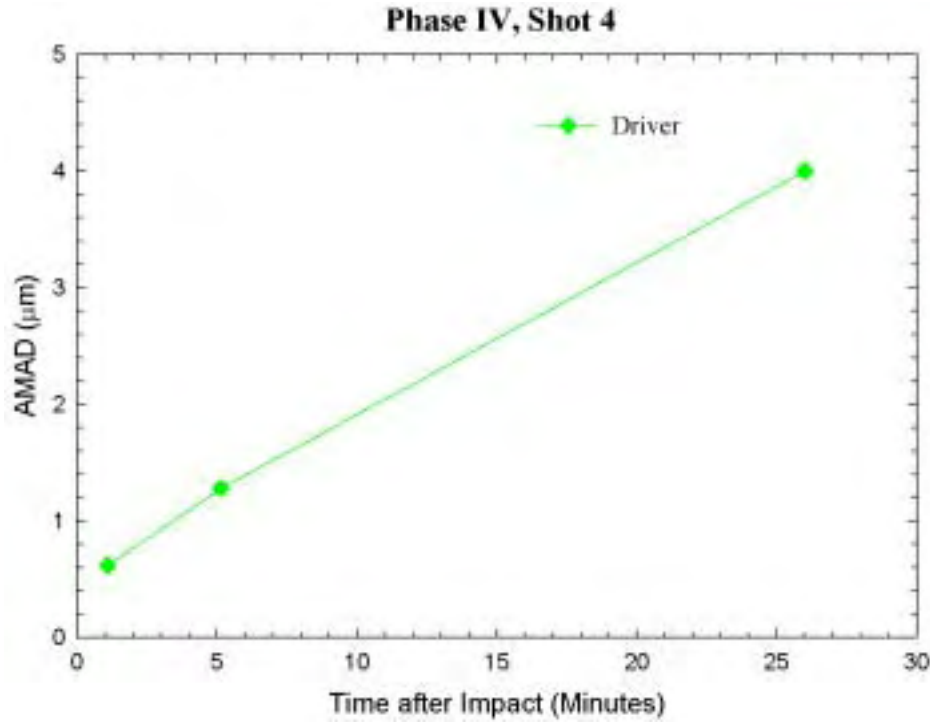

Figure B.12. AMAD Values as a Function of Time, PIV-4

Table B.1. Unimodal and Bimodal AMADs

Phase I, Shot 1, Commander							
Sample ID (Time)	**Unimodal Fit**			**Bimodal Fit**			**Fraction in First Peak**
C – 1 (0.25 min)	AMAD (μm)	GSD	R^2	AMAD (μm)	GSD	R^2	0.37
	3.07	7.22	0.08	0.27	2.17	0.80	
				5.37	2.80		
C – 2 (1.0 min)	AMAD (μm)	GSD	R^2	AMAD (μm)	GSD	R^2	0.60
	0.90	5.71	0.45	0.43	1.85	0.89	
				4.79	2.24		
C – 3 (2.5 min)	AMAD (μm)	GSD	R^2	AMAD (μm)	GSD	R^2	0.86
	0.69	2.68	0.78	0.60	2.04	0.97	
				4.07	1.30		
C – 4 (5.5 min)	AMAD (μm)	GSD	R^2	AMAD (μm)	GSD	R^2	0.70
	0.95	4.78	0.43	0.49	1.94	0.77	
				3.84	1.41		
C – 5 (11.5 min)	AMAD (μm)	GSD	R^2	AMAD (μm)	GSD	R^2	0.63
	0.42 1.8[(a)]	1.34 4[(a)]	0	0.68	1.65	0.90	
				4.55	1.70		
C – 6 (23.5 min)	AMAD (μm)	GSD	R^2	AMAD (μm)	GSD	R^2	0.67
	0.96	3.18	0.63	0.60	1.71	0.99	
				3.98	1.54		
C – 7 (47.5 min)	AMAD (μm)	GSD	R^2	AMAD (μm)	GSD	R^2	0.73
	0.50	5.62	0.53	0.31	2.50	0.98	
				3.67	1.43		
C – 8 (95.5 min)	AMAD (μm)	GSD	R^2	AMAD (μm)	GSD	R^2	0.79
	0.43	5.05	0.65	0.32	2.63	0.98	
				4.24	1.43		
C – 9 Field Blank	AMAD (μm)	GSD	R^2	AMAD (μm)	GSD	R^2	-----
	-----	-----	-----	-----	-----	-----	
				-----	-----		
Phase I, Shot 1, Gunner							
G – 1 (0.25 min)	AMAD (μm)	GSD	R^2	AMAD (μm)	GSD	R^2	0.60
	0.46	6.06	0.54	0.35	1.64	0.995	
				3.97	2.87		
G – 2 (1.0 min)	AMAD (μm)	GSD	R^2	AMAD (μm)	GSD	R^2	0.42
	2.97	6.27	0.17	0.39	2.22	0.77	
				6.42	2.45		
G – 3 (2.5 min)	AMAD (μm)	GSD	R^2	AMAD (μm)	GSD	R^2	0.93
	0.55	2.29	0.69	0.50	1.70	0.69	
				4.17	3.55		
G – 4 (5.5 min)	AMAD (μm)	GSD	R^2	AMAD (μm)	GSD	R^2	0.82
	0.67	2.29	0.80	0.61	1.86	0.95	
				3.92	1.45		
G – 5 (11.5 min)	AMAD (μm)	GSD	R^2	AMAD (μm)	GSD	R^2	0.78
	0.55	2.58	0.78	0.49	1.81	0.97	
				3.89	1.90		

Table B.1. (cont'd)

Phase I, Shot 1, Gunner							
Sample ID (Time)	**Unimodal Fit**			**Bimodal Fit**			**Fraction in First Peak**
G – 6 (23.5 min)	AMAD (μm)	GSD	R^2	AMAD (μm)	GSD	R^2	0.80
	0.47	2.93	0.84	0.43	1.93	0.996	
				4.01	1.93		
G – 7 (47.50 min)	AMAD (μm)	GSD	R^2	AMAD (μm)	GSD	R^2	0.78
	0.45	2.85	0.76	0.43	1.68	0.96	
				3.17	1.96		
G – 8 (95.50 min)	AMAD (μm)	GSD	R^2	AMAD (μm)	GSD	R^2	0.83
	0.33	2.88	0.89	0.36	1.99	0.999	
				3.56	1.68		
G – 9 Field Blank	AMAD (μm)	GSD	R^2	AMAD (μm)	GSD	R^2	-----
	-----	-----	-----	-----	-----	-----	
				-----	-----		
Phase I, Shot 1, Driver							
D – 1 (0.25 min)	AMAD (μm)	GSD	R^2	AMAD (μm)	GSD	R^2	--
	Did not run	--	--	--	--	--	
				--	--		
D – 2 (1.0 min)	AMAD (μm)	GSD	R^2	AMAD (μm)	GSD	R^2	0.64
	1.40	8.89	0.06	0.38	2.96	0.85	
				7.70	2.04		
D – 3 (2.5 min)	AMAD (μm)	GSD	R^2	AMAD (μm)	GSD	R^2	0.56
	1.17	4.77	0.22	0.53	1.59	0.86	
				5.11	2.30		
D – 4 (5.5 min)	AMAD (μm)	GSD	R^2	AMAD (μm)	GSD	R^2	0.50
	0.46 1.8[(a)]	0 4.5[(a)]	0	0.69	1.62	0.92	
				4.15	1.75		
D – 5 (11.5 min)	AMAD (μm)	GSD	R^2	AMAD (μm)	GSD	R^2	0.67
	1.02	4.43	0.61	0.57	2.10	0.93	
				5.47	1.82		
D – 6 (23.5 min)	AMAD (μm)	GSD	R^2	AMAD (μm)	GSD	R^2	0.71
	0.48	5.12	0.76	0.32	2.38	0.93	
				3.53	2.04		
D – 7 (47.5 min)	AMAD (μm)	GSD	R^2	AMAD (μm)	GSD	R^2	0.90
	0.30	3.63	0.77	0.29	2.73	0.96	
				4.46	1.23		
D – 8 (95.5 min)	AMAD (μm)	GSD	R^2	AMAD (μm)	GSD	R^2	0.45
	0.23	4.43	0.57	0.24	1.88	0.84	
				1.65	9.52		
D – 9 Field Blank	AMAD (μm)	GSD	R^2	AMAD (μm)	GSD	R^2	-----
	-----	-----	-----	-----	-----	-----	
				-----	-----		

Table B.1. (Cont'd)

Phase 1, Shot 1, Loader							
Sample ID (Time)	**Unimodal Fit**			**Bimodal Fit**			**Fraction in First Peak**
L – 1 (0.25 min)	AMAD (μm)	GSD	R^2	AMAD (μm)	GSD	R^2	0.40
	2.46	6.07	0.32	0.51	1.65	0.81	
				5.68	2.90		
L – 2 (1.0 min)	AMAD (μm)	GSD	R^2	AMAD (μm)	GSD	R^2	0.39
	3.39	5.89	0.18	0.39	1.85	0.86	
				5.87	2.32		
L – 3 (2.5 min)	AMAD (μm)	GSD	R^2	AMAD (μm)	GSD	R^2	0.62
	1.19	5.27	0.02	0.63	1.50	0.96	
				10.25	1.73		
L – 4 (5.5 min)	AMAD (μm)	GSD	R^2	AMAD (μm)	GSD	R^2	0.56
	1.37	4.20	0.51	0.64	1.95	0.70	
				5.07	2.36		
L – 5 (11.5 min)	AMAD (μm)	GSD	R^2	AMAD (μm)	GSD	R^2	0.79
	1.03	2.99	0.76	0.76	2.03	0.96	
				4.39	1.37		
L – 6 (23.5 min)	AMAD (μm)	GSD	R^2	AMAD (μm)	GSD	R^2	0.66
	1.07	4.71	0.46	0.50	2.21	0.996	
				4.61	1.42		
L – 7 (47.5 min)	AMAD (μm)	GSD	R^2	AMAD (μm)	GSD	R^2	0.84
	0.27	3.69	0.79	0.28	2.57	0.96	
				4.74	1.77		
L – 8 (95.5 min)	AMAD (μm)	GSD	R^2	AMAD (μm)	GSD	R^2	0.31
	0.24	2.96	0.92	0.26	1.59	0.99	
				0.41	4.86		
L – 9 Field Blank	AMAD (μm)	GSD	R^2	AMAD (μm)	GSD	R^2	-----
	-----	-----	-----	-----	-----	-----	
				-----	-----		

Phase I, Shot 2, Driver							
Sample ID (Time)	**Unimodal Fit**			**Bimodal Fit**			**Fraction in First Peak**
D – 1 (0.125 min)	AMAD (μm)	GSD	R^2	AMAD (μm)	GSD	R^2	0.28
	7.11	5.19	0.14	0.35	1.65	0.47	
				8.08	2.89		
D – 2 (0.75 min)	AMAD (μm)	GSD	R^2	AMAD (μm)	GSD	R^2	----
	Did not run---	---	---	---	---	---	
				---	---		
D – 3 (2.0 min)	AMAD (μm)	GSD	R^2	AMAD (μm)	GSD	R^2	0.50
	2.52	4.60	0.25	0.51	1.60	0	
				2.40	1.08		
D – 4 (4.5 min)	AMAD (μm)	GSD	R^2	AMAD (μm)	GSD	R^2	0.50
	1.73	4.98	0.24	0.55	1.67	0.73	
				5.90	2.08		

Table B.1. (cont'd)

Phase I, Shot 2, Driver							
Sample ID (Time)	**Unimodal Fit**			**Bimodal Fit**			**Fraction in First Peak**
D – 5 (9.5 min)	AMAD (μm)	GSD	R^2	AMAD (μm)	GSD	R^2	0.44
	0.49	1.40	0.82	0.53	1.13	0.97	
				2.79	3.40		
D – 6 (23.5 min)	AMAD (μm)	GSD	R^2	AMAD (μm)	GSD	R^2	0.69
	0.68	3.68	0.44	0.47	1.58	0.96	
				4.63	1.94		
D – 7 (55.5 min)	AMAD (μm)	GSD	R^2	AMAD (μm)	GSD	R^2	0.69
	0.65	5.30	0.47	0.39	2.03	0.95	
				3.68	1.41		
D – 8 (103.5 min)	AMAD (μm)	GSD	R^2	AMAD (μm)	GSD	R^2	0.72
	0.49	3.73	0.83	0.40	1.81	0.995	
				2.95	1.80		
D – 9 Field Blank	AMAD (μm)	GSD	R^2	AMAD (μm)	GSD	R^2	-----
	-----	-----	-----	-----	-----	-----	
				-----	-----		
Phase I, Shot 2, Commander							
C – 1 (0.125 min)	AMAD (μm)	GSD	R^2	AMAD (μm)	GSD	R^2	0.40
	3.48	11.14	0	0.31	1.87	0.78	
				8.01	3.11		
C – 2 (0.75 min)	AMAD (μm)	GSD	R^2	AMAD (μm)	GSD	R^2	0.41
	1.85	7.22	0.07	0.31	1.89	0.40	
				4.53	2.67		
C – 3 (2.0 min)	AMAD (μm)	GSD	R^2	AMAD (μm)	GSD	R^2	0.58
	1.32	6.94	0.19	0.41	2.23	0.70	
				6.24	2.03		
C – 4 (4.5 min)	AMAD (μm)	GSD	R^2	AMAD (μm)	GSD	R^2	0.81
	1.14	4.56	0.48	0.60	3.75	0.91	
				4.61	1.23		
C – 5 (9.5 min)	AMAD (μm)	GSD	R^2	AMAD (μm)	GSD	R^2	0.92
	1.15	5.40	0.46	0.65	5.77	0.87	
				4.12	1.15		
C – 6 (23.5 min)	AMAD (μm)	GSD	R^2	AMAD (μm)	GSD	R^2	0.72
	0.64	4.05	0.54	0.45	1.81	0.99	
				3.80	1.39		
C – 7 (55.5 min)	AMAD (μm)	GSD	R^2	AMAD (μm)	GSD	R^2	0.77
	0.48	5.27	0.67	0.33	2.57	0.98	
				4.31	1.57		
C – 8 (103.5 min)	AMAD (μm)	GSD	R^2	AMAD (μm)	GSD	R^2	0.85
	0.31	4.52	0.65	0.26	2.74	0.91	
				4.00	1.35		
C – 9 Field Blank	AMAD (μm)	GSD	R^2	AMAD (μm)	GSD	R^2	-----
	-----	-----	-----	-----	-----	-----	
				-----	-----		

Table B.1. (cont'd)

Phase I, Shot 2, Gunner							
Sample ID (Time)	**Unimodal Fit**			**Bimodal Fit**			**Fraction in First Peak**
G – 1 (0.125 min)	AMAD (μm)	GSD	R^2	AMAD (μm)	GSD	R^2	0.47
	3.83	5.82	0.01	0.41	1.73	0	
				5.10	1.16		
G – 2 (0.75 min)	AMAD (μm)	GSD	R^2	AMAD (μm)	GSD	R^2	0.42
	4.39	7.07	0	0.43	1.80	0.34	
				9.88	2.45		
G – 3 (2.0 min)	AMAD (μm)	GSD	R^2	AMAD (μm)	GSD	R^2	0.51
	0.98	5.78	0.26	0.44	1.70	0.79	
				4.92	3.48		
G – 4 (4.5 min)	AMAD (μm)	GSD	R^2	AMAD (μm)	GSD	R^2	0.58
	0.79	5.41	0.38	0.44	1.72	0.87	
				5.02	2.88		
G – 5 (9.5 min)	AMAD (μm)	GSD	R^2	AMAD (μm)	GSD	R^2	0.64
	1.07	5.51	0.40	0.40	2.34	0.79	
				3.99	1.54		
G – 6 (23.5 min)	AMAD (μm)	GSD	R^2	AMAD (μm)	GSD	R^2	0.66
	0.73	5.77	0.41	0.39	2.02	0.98	
				4.27	1.52		
G – 7 (55.5 min)	AMAD (μm)	GSD	R^2	AMAD (μm)	GSD	R^2	0.68
	0.78	4.13	0.53	0.50	1.66	0.97	
				4.31	1.91		
G – 8 (103.5 min)	AMAD (μm)	GSD	R^2	AMAD (μm)	GSD	R^2	0.72
	0.61	6.45	0.41	0.37	2.31	0.90	
				4.71	1.58		
G – 9 Field Blank	AMAD (μm)	GSD	R^2	AMAD (μm)	GSD	R^2	-----
	-----	-----	-----	-----	-----	-----	
				-----	-----		
Phase I, Shot 2, Loader							
L – 1 (0.125 min)	AMAD (μm)	GSD	R^2	AMAD (μm)	GSD	R^2	0.56
	1.82	8.87	0	0.51	2.39	0.63	
				11.24	2.63		
L – 2 (0.75 min)	AMAD (μm)	GSD	R^2	AMAD (μm)	GSD	R^2	0.53
	1.32	11.35	0	0.26	2.24	0.92	
				6.65	2.79		
L – 3 (2.0 min)	AMAD (μm)	GSD	R^2	AMAD (μm)	GSD	R^2	0.54
	1.37	4.89	0.40	0.56	1.78	0.89	
				5.41	2.35		
L – 4 (4.5 min)	AMAD (μm)	GSD	R^2	AMAD (μm)	GSD	R^2	0
	0.98 2.42[(a)]	0 3.4[(a)]	0	0.24	3.43	0.56	
				2.42	3.40		
L – 5 (9.5 min)	AMAD (μm)	GSD	R^2	AMAD (μm)	GSD	R^2	0.93
	0.27 3.0[(a)]	0 4.5[(a)]	0	1.23	4.88	0.81	
				4.04	1.12		

Table B.1. (cont'd)

Phase I, Shot 2, Loader							
Sample ID (Time)	**Unimodal Fit**			**Bimodal Fit**			**Fraction in First Peak**
L – 6 (23.5 min)	AMAD (μm)	GSD	R^2	AMAD (μm)	GSD	R^2	0.82
	0.47	4.63	0.78	0.38	2.71	0.99	
				5.08	1.54		
L – 7 (55.5 min)	AMAD (μm)	GSD	R^2	AMAD (μm)	GSD	R^2	0.83
	0.38	4.35	0.80	0.34	2.62	0.98	
				4.43	1.56		
L – 8 (103.5 min)	AMAD (μm)	GSD	R^2	AMAD (μm)	GSD	R^2	0.12
	0.29	4.21	0.78	0.22	1.32	0.93	
				0.45	6.08		
L – 9 Field Blank	AMAD (μm)	GSD	R^2	AMAD (μm)	GSD	R^2	-----
	-----	-----	-----	-----	-----	-----	
				-----	-----		

Phase I, Shot 3/4, Driver							
Sample ID (Time)	**Unimodal Fit**			**Bimodal Fit**			**Fraction in First Peak**
D – 1 (0.083 min)	AMAD (μm)	GSD	R^2	AMAD (μm)	GSD	R^2	0.52
	0.18	2.64	0.77	0.20	1.77	0.96	
				1.26	8.45		
D – 2 (3.25 min)	AMAD (μm)	GSD	R^2	AMAD (μm)	GSD	R^2	0.08
	2.71 3.10[(a)]	0.99 2.97[(a)]	0	>1000	>1000	0.56	
				3.10	2.97		
D – 3 (9.5 min)	AMAD (μm)	GSD	R^2	AMAD (μm)	GSD	R^2	0.76
	2.50[(a)]	0 4.0[(a)]	0	1.36	4.06	0.94	
				4.81	1.28		
D – 4 (13.083 min)	AMAD (μm)	GSD	R^2	AMAD (μm)	GSD	R^2	0.41
	5.35	6.10	0	0.34	2.01	0.60	
				9.03	2.23		
D – 5 (16.25 min)	AMAD (μm)	GSD	R^2	AMAD (μm)	GSD	R^2	1.0
	2.56	4.36	0.52	2.56	4.36	0.52	
				>1000	>1000		
D – 6 (22.5 min)	AMAD (μm)	GSD	R^2	AMAD (μm)	GSD	R^2	1.0
	2.43	4.39	0.47	2.43	4.39	0.47	
				>100	<1		
D – 7 (35.0 min)	AMAD (μm)	GSD	R^2	AMAD (μm)	GSD	R^2	0.67
	0.85	2.94	0.62	0.59	1.63	0.99	
				4.00	1.74		
D – 8 (60.0 min)	AMAD (μm)	GSD	R^2	AMAD (μm)	GSD	R^2	0.77
	0.88	3.31	0.61	0.62	1.99	0.98	
				4.68	1.27		
D – 9 Field Blank	AMAD (μm)	GSD	R^2	AMAD (μm)	GSD	R^2	-----
	-----	-----	-----	-----	-----	-----	
				-----	-----		

Table B.1. (cont'd)

Phase I, Shot 3/4, Gunner							
Sample ID (Time)	**Unimodal Fit**			**Bimodal Fit**			**Fraction in First Peak**
G – 1 (0.083 min)	AMAD (μm)	GSD	R^2	AMAD (μm)	GSD	R^2	0.73
	0.70	6.73	0.40	0.31	2.93	0.89	
				3.74	1.42		
G – 2 (3.25 min)	AMAD (μm)	GSD	R^2	AMAD (μm)	GSD	R^2	0.55
	1.98	4.18	0.64	0.63	2.38	0.94	
				4.88	1.73		
G – 3 (9.5 min)	AMAD (μm)	GSD	R^2	AMAD (μm)	GSD	R^2	0.62
	0.16 2.0[(a)]	0 4.0[(a)]	0	0.67	2.09	0.97	
				4.12	1.49		
G – 4 (13.083 min)	AMAD (μm)	GSD	R^2	AMAD (μm)	GSD	R^2	0.54
	6.96	6.63	0	0.52	4.30	0.58	
				12.79	1.92		
G – 5 (16.25 min)	AMAD (μm)	GSD	R^2	AMAD (μm)	GSD	R^2	0.76
	1.07	6.29	0.38	0.58	3.13	0.94	
				10.18	1.69		
G – 6 (22.5 min)	AMAD (μm)	GSD	R^2	AMAD (μm)	GSD	R^2	0.79
	1.03	3.76	0.82	0.74	2.47	0.99	
				6.37	1.59		
G – 7 (35.0 min)	AMAD (μm)	GSD	R^2	AMAD (μm)	GSD	R^2	0.73
	0.68	2.52	0.79	0.54	1.72	0.96	
				3.38	1.99		
G – 8 (60.0 min)	AMAD (μm)	GSD	R^2	AMAD (μm)	GSD	R^2	0.76
	0.62	3.42	0.64	0.49	1.84	0.99	
				4.20	1.46		
G – 9 Field Blank	AMAD (μm)	GSD	R^2	AMAD (μm)	GSD	R^2	-----
	-----	-----	-----	-----	-----	-----	
				-----	-----		
Phase I, Shot 4, Commander							
C – 1 (13.083 min)	AMAD (μm)	GSD	R^2	AMAD (μm)	GSD	R^2	0.59
	15.8	7.56	0	0.46	6.65	0.83	
				18.67	1.32		
C – 2 (16.25 min)	AMAD (μm)	GSD	R^2	AMAD (μm)	GSD	R^2	0.89
	1.29	4.97	0.30	0.99	3.50	0.91	
				14.65	1.16		
C – 3 (22.5 min)	AMAD (μm)	GSD	R^2	AMAD (μm)	GSD	R^2	0.28
	3.70	4.70	0.46	0.56	1.77	0.68	
				5.57	2.71		
C – 4 (35.0 min)	AMAD (μm)	GSD	R^2	AMAD (μm)	GSD	R^2	0.45
	0.83	2.95	0.75	0.53	1.61	0.95	
				1.99	3.31		
C – 5 (60.0 min)	AMAD (μm)	GSD	R^2	AMAD (μm)	GSD	R^2	0.39
	1.19	4.55	0.04	0.72	1.27	0.64	
				7.84	3.47		

Table B.1. (cont'd)

Phase I, Shot 4, Commander							
Sample ID (Time)	**Unimodal Fit**			**Bimodal Fit**			**Fraction in First Peak**
C – 6 (110.0 min)	AMAD (μm)	GSD	R^2	AMAD (μm)	GSD	R^2	0.33
	0.81	2.56	0.66	0.77	1.28	0.89	
				1.69	4.61		
C – 7 Field Blank	AMAD (μm)	GSD	R^2	AMAD (μm)	GSD	R^2	-----
	-----	-----	-----	-----	-----	-----	
				-----	-----		
C – 8 Field Blank	AMAD (μm)	GSD	R^2	AMAD (μm)	GSD	R^2	-----
	-----	-----	-----	-----	-----	-----	
				-----	-----		
C – 9 Field Blank	AMAD (μm)	GSD	R^2	AMAD (μm)	GSD	R^2	-----
	-----	-----	-----	-----	-----	-----	
				-----	-----		
Phase I, Shot 4, Loader (minor to moderate damage to 1st substrate in L2 through L6)							
L – 1 (13.083 min)	AMAD (μm)	GSD	R^2	AMAD (μm)	GSD	R^2	0.39
	20.94 4.0[(a)]	5.09	0.03	0.44	2.03	0.83	
				17.29	2.15		
L – 2 (16.25 min)	AMAD (μm)	GSD	R^2	AMAD (μm)	GSD	R^2	0.57
	2.11	5.15	0.49	0.57	2.96	0.81	
				5.84	1.95		
L – 3 (22.5 min)	AMAD (μm)	GSD	R^2	AMAD (μm)	GSD	R^2	0.33
	6.62	3.36	0.49	0.82	2.15	0.81	
				8.81	1.97		
L – 4 (35.0 min)	AMAD (μm)	GSD	R^2	AMAD (μm)	GSD	R^2	0.16
	6.12	3.45	0.30	0.81	1.30	0.44	
				7.63	2.54		
L – 5 (60.0 min)	AMAD (μm)	GSD	R^2	AMAD (μm)	GSD	R^2	0.02
	35.70	2.14	0.82	31.32	1.02	0.88	
				32.27	6.54		
L – 6 (110.0 min)	AMAD (μm)	GSD	R^2	AMAD (μm)	GSD	R^2	0.41
	1.52	6.83	0.04	0.44	2.15	0.18	
				5.44	4.08		
L – 7 Field Blank	AMAD (μm)	GSD	R^2	AMAD (μm)	GSD	R^2	-----
	-----	----	-----	-----	-----	-----	
				-----	-----		
L – 8 Field Blank	AMAD (μm)	GSD	R^2	AMAD (μm)	GSD	R^2	-----
	-----	-----	-----	-----	-----	-----	
				-----	-----		
L – 9 Field Blank	AMAD (μm)	GSD	R^2	AMAD (μm)	GSD	R^2	-----
	-----	-----	-----	-----	-----	-----	
				-----	-----		

Table B.1. (cont'd)

Sample ID (Time)	Unimodal Fit			Bimodal Fit			Fraction in First Peak
Phase I, Shot 5, Driver							
D – 1 (0.083 min)	AMAD (μm)	GSD	R^2	AMAD (μm)	GSD	R^2	0.29
	7.49	4.07	0.55	0.41	3.36	0.72	
				9.05	2.53		
D – 2 (1.083 min)	AMAD (μm)	GSD	R^2	AMAD (μm)	GSD	R^2	0.25
	5.65	3.35	0.40	0.50	1.56	0.65	
				5.71	2.11		
D – 3 (3.083 min)	AMAD (μm)	GSD	R^2	AMAD (μm)	GSD	R^2	0.07
	>1000 4.56[(a)]	0 2.21[(a)]	0	0.004	<1	0.77	
				4.56	2.21		
D – 4 (7.25 min)	AMAD (μm)	GSD	R^2	AMAD (μm)	GSD	R^2	0.10
	>1000 4.00[(a)]	0 1.77[(a)]	0	0.56	1.32	0.96	
				4.00	1.77		
D – 5 (15.5 min)	AMAD (μm)	GSD	R^2	AMAD (μm)	GSD	R^2	0
	18.68	9.75	0.08	0.13	1.15	0.02	
				6.54	8.99		
D – 6 (32 min)	AMAD (μm)	GSD	R^2	AMAD (μm)	GSD	R^2	0
	9.84	8.11	0.11	>1000	>1000	0.11	
				9.86	8.14		
D – 7 (62.5 min)	AMAD (μm)	GSD	R^2	AMAD (μm)	GSD	R^2	0
	6.92	7.70	0.06	0.26	1.47	0.06	
				5.76	7.41		
D – 8 (125 min)	AMAD (μm)	GSD	R^2	AMAD (μm)	GSD	R^2	0.53
	1.37	4.16	0.43	0.49	1.76	0.85	
				3.31	1.54		
D – 9 Field Blank	AMAD (μm)	GSD	R^2	AMAD (μm)	GSD	R^2	-----
	-----	-----	-----	-----	-----	-----	
				-----	-----		
Phase I, Shot 5, Commander							
C – 1 (0.083 min)	AMAD (μm)	GSD	R^2	AMAD (μm)	GSD	R^2	0.56
	3.87	8.22	0	0.50	3.39	0.65	
				11.02	2.07		
C – 2 (1.083 min)	AMAD (μm)	GSD	R^2	AMAD (μm)	GSD	R^2	0.54
	2.85	5.31	0.12	0.67	2.27	0.99	
				8.49	1.73		
C – 3 (3.083 min)	AMAD (μm)	GSD	R^2	AMAD (μm)	GSD	R^2	0.35
	0.15 2.5[(a)]	0 4.0[(a)]	0	0.82	1.44	0.97	
				4.77	1.74		
C – 4 (7.25 min)	AMAD (μm)	GSD	R^2	AMAD (μm)	GSD	R^2	0.60
	0.62 2.0[(a)]	0 4.0[(a)]	0	0.97	1.60	0.99	
				5.75	1.68		
C – 5 (15.5 min)	AMAD (μm)	GSD	R^2	AMAD (μm)	GSD	R^2	0.27
	0.03 1.5[(a)]	0.59 4.0[(a)]	0	0.71	1.27	0.95	
				2.19	2.87		

Table B.1. (cont'd)

Phase I, Shot 5, Commander							
Sample ID (Time)	**Unimodal Fit**			**Bimodal Fit**			**Fraction in First Peak**
C – 6 (32 min)	AMAD (μm)	GSD	R^2	AMAD (μm)	GSD	R^2	0.50
	0.10 1.6[(a)]	0 4.0[(a)]	0	0.59 3.74	1.50 1.57	0.99	
C – 7 (62.5 min)	AMAD (μm)	GSD	R^2	AMAD (μm)	GSD	R^2	0.58
	1.30	4.11	0.54	0.54 4.48	1.83 1.66	0.99	
C – 8 (125 min)	AMAD (μm)	GSD	R^2	AMAD (μm)	GSD	R^2	0.77
	1.02	3.21	0.68	0.71 4.69	2.10 1.25	0.98	
C – 9 Field Blank	AMAD (μm)	GSD	R^2	AMAD (μm)	GSD	R^2	-----
	-----	-----	-----	----- -----	----- -----	-----	
Phase I, Shot 5, Loader							
L – 1 (0.083 min)	AMAD (μm)	GSD	R^2	AMAD (μm)	GSD	R^2	0.41
	4.60	7.38	0	0.53 11.19	1.67 2.53	0.66	
L – 2 (1.083 min)	AMAD (μm)	GSD	R^2	AMAD (μm)	GSD	R^2	0.54
	2.43	4.53	0.18	0.68 7.50	1.85 1.59	0.98	
L – 3 (3.083 min)	AMAD (μm)	GSD	R^2	AMAD (μm)	GSD	R^2	0.52
	0.97 2.0[(a)]	0 5.0[(a)]	0	0.76 4.61	1.83 1.78	0.92	
L – 4 (7.25 min)	AMAD (μm)	GSD	R^2	AMAD (μm)	GSD	R^2	0.74
	0.20 2.2[(a)]	0 4.5[(a)]	0	0.95 5.49	2.18 1.39	0.96	
L – 5 (15.5 min)	AMAD (μm)	GSD	R^2	AMAD (μm)	GSD	R^2	0.47
	1.38	4.09	0.67	0.57 4.10	1.75 2.61	0.96	
L – 6 (32 min)	AMAD (μm)	GSD	R^2	AMAD (μm)	GSD	R^2	0.74
	1.06	3.57	0.85	0.67 4.35	2.37 1.55	0.997	
L – 7 (62.5 min)	AMAD (μm)	GSD	R^2	AMAD (μm)	GSD	R^2	0.62
	1.08	4.18	0.52	0.52 3.90	1.76 1.60	0.95	
L – 8 (125 min)	AMAD (μm)	GSD	R^2	AMAD (μm)	GSD	R^2	0.74
	0.07 2.0[(a)]	1.83 3.5[(a)]	0	0.70 4.08	2.10 1.29	0.99	
L – 9 (146 min)	AMAD (μm)	GSD	R^2	AMAD (μm)	GSD	R^2	0.20
	1.16	7.63	0	0.71	1.28	0.39	
L – 8 (125 min)				9.20	13.09		

Table B.1. (cont'd)

Phase I, Shot 6, Driver							
Sample ID (Time)	**Unimodal Fit**			**Bimodal Fit**			**Fraction in First Peak**
D – 1 (0.083 min)	AMAD (μm)	GSD	R^2	AMAD (μm)	GSD	R^2	0.35
	>1000 2.5[(a)]	0 3.5[(a)]	0	0.55 1.55	1.79 0	0	
D – 2 (1.083 min)	AMAD (μm)	GSD	R^2	AMAD (μm)	GSD	R^2	0.57
	2.38	4.62	0.30	0.75 7.97	2.15 1.72	0.87	
D – 3 (3.083 min)	AMAD (μm)	GSD	R^2	AMAD (μm)	GSD	R^2	0.38
	>1000 1.8[(a)]	0 4.0[(a)]	0	0.58 3.96	1.54 1.47	0.92	
D – 4 (7.25 min)	AMAD (μm)	GSD	R^2	AMAD (μm)	GSD	R^2	1.0
	1.56	5.06	0.06	1.62 >1000	5.12 >1000	0.06	
D – 5 (15.5 min)	AMAD (μm)	GSD	R^2	AMAD (μm)	GSD	R^2	0.68
	0.58	2.84	0.61	0.48 3.80	1.76 3.06	0.84	
D – 6 (32 min)	AMAD (μm)	GSD	R^2	AMAD (μm)	GSD	R^2	0.33
	0.82	2.78	0.88	0.58 1.06	2.19 2.91	0.88	
D – 7 (62.5 min)	AMAD (μm)	GSD	R^2	AMAD (μm)	GSD	R^2	0.68
	0.85	3.65	0.54	0.52 3.77	1.72 1.48	0.99	
D – 8 (125 min)	AMAD (μm)	GSD	R^2	AMAD (μm)	GSD	R^2	0.84
	0.67	2.39	0.85	0.60 3.81	1.94 1.40	0.99	
D – 9 Field Blank	AMAD (μm)	GSD	R^2	AMAD (μm)	GSD	R^2	-----
	-----	-----	-----	----- -----	----- -----	-----	
Phase I, Shot 6, Commander							
C – 1 (0.083 min)	AMAD (μm)	GSD	R^2	AMAD (μm)	GSD	R^2	0.22
	8.46	7.11	0.13	0.40 10.83	1.72 4.10	0.50	
C – 2 (1.083 min)	AMAD (μm)	GSD	R^2	AMAD (μm)	GSD	R^2	0.29
	3.22	4.41	0.24	0.74 6.29	1.30 2.40	0.72	
C – 3 (3.083 min)	AMAD (μm)	GSD	R^2	AMAD (μm)	GSD	R^2	0.43
	0.32 1.5[(a)]	0 4.0[(a)]	0	0.62 3.92	1.42 1.86	0.99	
C – 4 (7.25 min)	AMAD (μm)	GSD	R^2	AMAD (μm)	GSD	R^2	0.73
	0.17 1.5[(a)]	0 5.0[(a)]	0	1.03 4.92	1.91 1.21	0.99	
C – 5 (15.5 min)	AMAD (μm)	GSD	R^2	AMAD (μm)	GSD	R^2	0.44
	1.25	2.92	0.46	0.66 3.12	1.28 1.58	0.999	

Table B.1. (cont'd)

Phase I, Shot 6, Commander							
Sample ID (Time)	**Unimodal Fit**			**Bimodal Fit**			**Fraction in First Peak**
C – 6 (32 min)	AMAD (μm)	GSD	R^2	AMAD (μm)	GSD	R^2	0.69
	0.30 2.5[(a)]	8.72 8.0[(a)]	0	0.42 38.30	3.45 1.24	0.71	
C – 7 (62.5 min)	AMAD (μm)	GSD	R^2	AMAD (μm)	GSD	R^2	0
	8.02	21.5	0	0.56 16.60	1.16 18.95	0	
C – 8 (125 min)	AMAD (μm)	GSD	R^2	AMAD (μm)	GSD	R^2	0.48
	0.56	4.41	0.19	0.45 4.39	1.45 10.23	0.59	
C – 9 Field Blank	AMAD (μm)	GSD	R^2	AMAD (μm)	GSD	R^2	-----
	-----	-----	-----	----- -----	----- -----	-----	
Phase I, Shot 6, Loader (Resuspension Data)							
L – 1 (10.05 min)[(a)]	AMAD (μm)	GSD	R^2	AMAD (μm)	GSD	R^2	0.31
	0.95	4.88	0.07	0.53 5.32	1.17 6.87	0.92	
L – 2 (31.425 min)[(a)]	AMAD (μm)	GSD	R^2	AMAD (μm)	GSD	R^2	0.27
	9.94	9.80	0	0.54 22.14	1.63 3.79	0.43	
L – 3 (49.39 min)[(a)]	AMAD (μm)	GSD	R^2	AMAD (μm)	GSD	R^2	0.21
	0.96	4.96	0.25	0.50 1.95	1.20 6.89	0.74	
L – 4 (63.39 min)[(a)]	AMAD (μm)	GSD	R^2	AMAD (μm)	GSD	R^2	0.20
	0.80	4.33	0.22	0.69 2.77	1.24 11.45	0.81	
L – 5 (81.585 min)[(a)]	AMAD (μm)	GSD	R^2	AMAD (μm)	GSD	R^2	0.68
	11.52	6.74	0.18	2.33 22.16	5.01 1.44	0.95	
L – 6 (93.42 min)[(a)]	AMAD (μm)	GSD	R^2	AMAD (μm)	GSD	R^2	0.08
	1.31	6.91	0.03	0.61 3.55	1.12 11.36	0.76	
L – 7 (96.42 min)[(a)]	AMAD (μm)	GSD	R^2	AMAD (μm)	GSD	R^2	0.40
	1.34	10.61	0	0.44 10.13	1.64 6.30	0.36	
L – 8 (102.42 min)[(a)]	AMAD (μm)	GSD	R^2	AMAD (μm)	GSD	R^2	0.46
	1.65	8.99	0	0.46 10.24	1.57 4.11	0.74	
L – 9 (116.92 min)[(a)]	AMAD (μm)	GSD	R^2	AMAD (μm)	GSD	R^2	0.62
	11.50	9.77	0	1.24 26.86	4.94 1.58	0.85	

(a) Sample times based on preliminary information. Actual sampling times beginning began 2 h and 35 min post shot. Sampler L1 collected residual aerosols for 20 min, followed by the next 8 samplers than ran for 23, 13, 15, 22, 2, 4, 8, and 16 min, respectively. Section 4.1.5.3 provides more information about this sampling sequence.

Table B.1. (cont'd)

Phase I, Shot 7, Gunner							
Sample ID (Time)	**Unimodal Fit**			**Bimodal Fit**			**Fraction in First Peak**
G – 1 (0.083 min)	AMAD (μm)	GSD	R^2	AMAD (μm)	GSD	R^2	0.46
	1.64	8.32	0	0.45 7.79	1.74 3.37	0.90	
G – 2 Field Blank	AMAD (μm)	GSD	R^2	AMAD (μm)	GSD	R^2	-----
	-----	-----	-----	----- -----	----- -----	-----	
G – 3 (1.083 min)	AMAD (μm)	GSD	R^2	AMAD (μm)	GSD	R^2	0.04
	2.02 2.22[(a)]	0 3.59[(a)]	0	0.75 2.22	0 3.59	0.31	
G – 4 (3.125 min)	AMAD (μm)	GSD	R^2	AMAD (μm)	GSD	R^2	0.16
	>1000 2.91[(a)]	0 4.80[(a)]	0	0.60 2.91	0 4.80	0.19	
G – 5 (7.5 min)	AMAD (μm)	GSD	R^2	AMAD (μm)	GSD	R^2	0
	>1000 3.60[(a)]	0 3.37[(a)]	0	>1000 3.60	0.0001 3.37	0.52	
G – 6 (16 min)	AMAD (μm)	GSD	R^2	AMAD (μm)	GSD	R^2	0.44
	1.50 2.2[(a)]	0 4.5[(a)]	0	0.79 4.78	1.61 1.71	0.97	
G – 7 (33 min)	AMAD (μm)	GSD	R^2	AMAD (μm)	GSD	R^2	0.69
	0.77	3.51	0.42	0.50 4.11	1.52 1.62	0.97	
G – 8 (65 min)	AMAD (μm)	GSD	R^2	AMAD (μm)	GSD	R^2	0.73
	0.51	1.74	0.70	0.54 3.91	1.57 1.65	0.98	
G – 9 (125 min)	AMAD (μm)	GSD	R^2	AMAD (μm)	GSD	R^2	0.75
	0.58	1.90	0.77	0.58 3.60	1.61 1.62	0.98	
Phase I, Shot 7, Driver							
D – 1 (0.083 min)	AMAD (μm)	GSD	R^2	AMAD (μm)	GSD	R^2	0.46
	2.97	6.99	0.17	0.34 6.21	2.77 2.40	0.73	
D – 2 (1.083 min)	AMAD (μm)	GSD	R^2	AMAD (μm)	GSD	R^2	0.30
	1.90	6.65	0.34	0.41 3.98	1.64 3.92	0.65	
D – 3 (3.125 min)	AMAD (μm)	GSD	R^2	AMAD (μm)	GSD	R^2	0.73
	0.05 2.3[(a)]	0.77 4.0[(a)]	0	0.84 7.94	2.21 1.60	0.96	
D – 4 (7.5 min)	AMAD (μm)	GSD	R^2	AMAD (μm)	GSD	R^2	0.26
	1.03	2.93	0.93	0.63 1.52	1.66 3.17	0.99	
D – 5 (16 min)	AMAD (μm)	GSD	R^2	AMAD (μm)	GSD	R^2	0.74
	1.31	3.04	0.87	0.83 2.86	2.80 1.35	0.98	

Table B.1. (cont'd)

Phase I, Shot 7, Driver							
Sample ID (Time)	**Unimodal Fit**			**Bimodal Fit**			**Fraction in First Peak**
D – 6 (33 min)	AMAD (μm)	GSD	R^2	AMAD (μm)	GSD	R^2	0.27
	0.71	4.12	0.93	0.19	1.85	0.98	
				1.23	2.88		
D – 7 (65 min)	AMAD (μm)	GSD	R^2	AMAD (μm)	GSD	R^2	0.52
	0.70	3.54	0.94	0.37	1.59	0.997	
				1.80	2.02		
D – 8 (125 min)	AMAD (μm)	GSD	R^2	AMAD (μm)	GSD	R^2	0.72
	0.67	2.78	0.87	0.48	1.72	0.99	
				2.34	1.58		
D – 9 Field Blank	AMAD (μm)	GSD	R^2	AMAD (μm)	GSD	R^2	-----
	-----	-----	-----	-----	-----	-----	
				-----	-----		
Phase I, Shot 7, Loader (Resuspension Data)							
L – 1 (10 min)	AMAD (μm)	GSD	R^2	AMAD (μm)	GSD	R^2	0.42
	0.002 1.59[(a)]	0.22 1.96[(a)]	0	1.59	1.96	0.92	
				5.47	9.08		
L – 2 (25 min)	AMAD (μm)	GSD	R^2	AMAD (μm)	GSD	R^2	0
	1.70	4.61	0.35	0.03	0	0.21	
				1.09	7.77		
L – 3 (50 min)	AMAD (μm)	GSD	R^2	AMAD (μm)	GSD	R^2	0
	17.26	7.5	0.04	>1000	>1000	0.04	
				17.53	7.84		
L – 4 (64.83 min)	AMAD (μm)	GSD	R^2	AMAD (μm)	GSD	R^2	0.28
	3.70	1.87	0.72	0.30	1.30	0.98	
				3.87	1.66		
L – 5 Field Blank	AMAD (μm)	GSD	R^2	AMAD (μm)	GSD	R^2	-----
	-----	-----	-----	-----	-----	-----	
				-----	-----		
L – 6 Field Blank	AMAD (μm)	GSD	R^2	AMAD (μm)	GSD	R^2	-----
	-----	-----	-----	-----	-----	-----	
				-----	-----		
L – 7 Field Blank	AMAD (μm)	GSD	R^2	AMAD (μm)	GSD	R^2	-----
	-----	-----	-----	-----	-----	-----	
				-----	-----		
L – 8 Field Blank	AMAD (μm)	GSD	R^2	AMAD (μm)	GSD	R^2	------
	-----	-----	-----	-----	-----	-----	
				-----	-----		
L – 9 Field Blank	AMAD (μm)	GSD	R^2	AMAD (μm)	GSD	R^2	-----
	-----	-----	-----	-----	-----	-----	
				-----	-----		

Table B.1. (cont'd)

Phase I, Shot 7, Commander							
Sample ID (Time)	**Unimodal Fit**			**Bimodal Fit**			**Fraction in First Peak**
C – 1 (0.083 min)	AMAD (μm)	GSD	R^2	AMAD (μm)	GSD	R^2	0.29
	4.04	8.63	0	0.34	2.11	0.33	
				7.64	4.11		
C – 2 (1.083 min)	AMAD (μm)	GSD	R^2	AMAD (μm)	GSD	R^2	<0.01
	10.94	1.31	0.94	0.11	<0.1	0	
				>1000	0		
C – 3 (3.125 min)	AMAD (μm)	GSD	R^2	AMAD (μm)	GSD	R^2	0
	0.42 2.41[(a)]	0 4.10[(a)]	0	0.61	0.999	0.16	
				2.41	4.10		
C – 4 (7.5 min)	AMAD (μm)	GSD	R^2	AMAD (μm)	GSD	R^2	0.70
	1.84 3.0[(a)]	0 4.5[(a)]	0	1.03	2.36	0.89	
				9.27	1.23		
C – 5 (16 min)	AMAD (μm)	GSD	R^2	AMAD (μm)	GSD	R^2	0.31
	1.51 2.0[(a)]	0 5.0[(a)]	0	0.76	1.29	0.74	
				4.48	2.67		
C – 6 (33 min)	AMAD (μm)	GSD	R^2	AMAD (μm)	GSD	R^2	0.60
	0.86	2.76	0.49	0.61	1.41	0.99	
				3.34	1.49		
C – 7 (65 min)	AMAD (μm)	GSD	R^2	AMAD (μm)	GSD	R^2	0.67
	0.82	3.99	0.73	0.49	1.94	0.997	
				3.90	1.69		
C – 8 (125 min)	AMAD (μm)	GSD	R^2	AMAD (μm)	GSD	R^2	0.78
	1.0	3.46	0.80	0.67	2.41	0.997	
				4.01	1.38		
C – 9 Field Blank	AMAD (μm)	GSD	R^2	AMAD (μm)	GSD	R^2	-----
	-----	-----	-----	-----	-----	-----	
				-----	-----		
Phase II, Shot 1/2, Scout Left							
SL – 1 (0.083 min)	AMAD (μm)	GSD	R^2	AMAD (μm)	GSD	R^2	0.55
	0.58	7.52	0	0.45	1.77	0.75	
				19.83	4.42		
SL – 2 (3.5 min)	AMAD (μm)	GSD	R^2	AMAD (μm)	GSD	R^2	0.48
	0.81	8.14	0.39	0.34	1.45	0.88	
				3.41	2.75		
SL – 3 (10.0 min)	AMAD (μm)	GSD	R^2	AMAD (μm)	GSD	R^2	<0.01
	3.07	4.45	0.39	>1000	>1000	0.39	
				3.05	4.47		
SL – 4 (13.77 min)	AMAD (μm)	GSD	R^2	AMAD (μm)	GSD	R^2	0.38
	2.79	9.76	0	0.37	2.18	0.17	
				8.05	3.87		
SL – 5 (17.18 min)	AMAD (μm)	GSD	R^2	AMAD (μm)	GSD	R^2	0.58
	1.04	4.15	0.70	0.61	2.10	0.89	
				4.73	3.08		

Table B.1. (cont'd)

Phase II, Shot 1/2, Scout Left							
Sample ID (Time)	**Unimodal Fit**			**Bimodal Fit**			**Fraction in First Peak**
SL – 6 (23.68 min)	AMAD (μm)	GSD	R^2	AMAD (μm)	GSD	R^2	0.79
	0.87	4.30	0.52	0.63	2.30	0.87	
				6.55	1.48		
SL – 7 (36.68 min)	AMAD (μm)	GSD	R^2	AMAD (μm)	GSD	R^2	0.63
	0.51	5.61	0.58	0.34	2.75	0.69	
				3.98	4.71		
SL – 8 (62.68 min)	AMAD (μm)	GSD	R^2	AMAD (μm)	GSD	R^2	0.56
	0.48	6.36	0.51	0.33	2.76	0.66	
				4.40	7.55		
SL – 9 (114.68 min)	AMAD (μm)	GSD	R^2	AMAD (μm)	GSD	R^2	0.57
	0.80	4.44	0.57	0.58	2.23	0.79	
				6.68	5.83		
Phase II, Shot 1/2, Commander							
C – 1 (0.083 min)	AMAD (μm)	GSD	R^2	AMAD (μm)	GSD	R^2	0.25
	1.71	4.68	0.52	0.35	1.37	0.56	
				2.35	2.88		
C – 2 (3.5 min)	AMAD (μm)	GSD	R^2	AMAD (μm)	GSD	R^2	0.39
	1.52	3.96	0.76	0.45	1.58	0.96	
				2.97	2.26		
C – 3 (10.0 min)	AMAD (μm)	GSD	R^2	AMAD (μm)	GSD	R^2	0.87
	3.65	3.96	0.29	3.91	9.11	0.96	
				3.97	1.14		
C – 4 (13.77 min)	AMAD (μm)	GSD	R^2	AMAD (μm)	GSD	R^2	0.69
	1.33	4.21	0.80	0.65	2.62	0.97	
				4.46	1.64		
C – 5 (17.18 min)	AMAD (μm)	GSD	R^2	AMAD (μm)	GSD	R^2	0.27
	0.99	2.86	0.62	0.58	1.32	0.93	
				1.78	3.08		
C – 6 (23.68 min)	AMAD (μm)	GSD	R^2	AMAD (μm)	GSD	R^2	0.65
	0.97	3.09	0.60	0.63	1.67	0.96	
				4.11	1.84		
C – 7 (36.68 min)	AMAD (μm)	GSD	R^2	AMAD (μm)	GSD	R^2	0.63
	0.64	2.42	0.77	0.52	1.68	0.98	
				2.68	3.02		
C – 8 (62.68 min)	AMAD (μm)	GSD	R^2	AMAD (μm)	GSD	R^2	0.19
	0.93	3.70	0.58	0.70	1.30	0.82	
				1.46	5.86		
C – 9 (114.68 min)	AMAD (μm)	GSD	R^2	AMAD (μm)	GSD	R^2	0.51
	0.64	4.79	0.85	0.36	1.50	0.97	
				2.10	2.46		

Table B.1. (cont'd)

Phase II, Shot 1/2, Scout Right							
Sample ID (Time)	**Unimodal Fit**			**Bimodal Fit**			**Fraction in First Peak**
SR – 1 (13.77 min)	AMAD (μm)	GSD	R^2	AMAD (μm)	GSD	R^2	0.50
	1.32	11.32	0	0.31	2.18	0.71	
				8.09	3.41		
SR – 2 Field Blank	AMAD (μm)	GSD	R^2	AMAD (μm)	GSD	R^2	-----
	-----	-----	-----	-----	-----	-----	
				-----	-----		
SR – 3 (17.18 min)	AMAD (μm)	GSD	R^2	AMAD (μm)	GSD	R^2	0.83
	0.72	5.45	0.63	0.47	3.65	0.73	
				5.74	1.70		
SR – 4 (23.68 min)	AMAD (μm)	GSD	R^2	AMAD (μm)	GSD	R^2	0.72
	0.86	3.41	0.57	0.59	1.84	0.99	
				4.74	1.46		
SR – 5 (36.68 min)	AMAD (μm)	GSD	R^2	AMAD (μm)	GSD	R^2	0.86
	0.72	3.44	0.78	0.59	2.45	0.90	
				4.60	1.32		
SR – 6 (62.68 min)	AMAD (μm)	GSD	R^2	AMAD (μm)	GSD	R^2	0.85
	0.58	4.17	0.71	0.44	2.66	0.96	
				4.46	1.24		
SR – 7 (114.68 min)	AMAD (μm)	GSD	R^2	AMAD (μm)	GSD	R^2	0.81
	0.53	4.03	0.68	0.43	2.30	0.999	
				4.12	1.33		
SR – 8 Field Blank	AMAD (μm)	GSD	R^2	AMAD (μm)	GSD	R^2	-----
	-----	-----	-----	-----	-----	-----	
				-----	-----		
SR – 9 Field Blank	AMAD (μm)	GSD	R^2	AMAD (μm)	GSD	R^2	-----
	-----	-----	-----	-----	-----	-----	
				-----	-----		
Phase II, Shot 1/2, Driver							
D – 1 (0.083 min)	AMAD (μm)	GSD	R^2	AMAD (μm)	GSD	R^2	0.84
	1.46	4.74	0.57	1.01	4.93	0.91	
				3.35	1.27		
D – 2 (3.5 min)	AMAD (μm)	GSD	R^2	AMAD (μm)	GSD	R^2	0.39
	1.84	4.41	0.58	0.41	1.61	0.96	
				3.40	2.00		
D – 3 (10.0 min)	AMAD (μm)	GSD	R^2	AMAD (μm)	GSD	R^2	0.72
	0.003 1.8[(a)]	0.61 5.0[(a)]	0	0.83	2.32	0.99	
				5.33	1.61		
D – 4 (13.77 min)	AMAD (μm)	GSD	R^2	AMAD (μm)	GSD	R^2	0.26
	3.57	5.33	0.40	0.41	1.67	0.69	
				5.21	3.12		
D – 5 (17.18 min)	AMAD (μm)	GSD	R^2	AMAD (μm)	GSD	R^2	0.66
	0.78	3.05	0.62	0.50	1.59	0.96	
				3.00	1.78		

Table B.1. (cont'd)

Phase II, Shot 1/2, Driver							
Sample ID (Time)	**Unimodal Fit**			**Bimodal Fit**			**Fraction in First Peak**
D – 6 (23.68 min)	AMAD (μm)	GSD	R^2	AMAD (μm)	GSD	R^2	0.75
	0.50	1.73	0.74	0.53	1.58	0.99	
				4.12	1.76		
D – 7 (36.68 min)	AMAD (μm)	GSD	R^2	AMAD (μm)	GSD	R^2	0.74
	0.55	1.91	0.79	0.54	1.63	0.99	
				3.99	2.26		
D – 8 (62.68 min)	AMAD (μm)	GSD	R^2	AMAD	GSD	R^2	0.71
	0.92	3.16	0.60	0.62	1.81	0.98	
				4.14	1.46		
D – 9 (114.68 min)	AMAD (μm)	GSD	R^2	AMAD (μm)	GSD	R^2	0.67
	0.75	3.86	0.68	0.46	1.73	0.99	
				3.25	1.61		
Phase II, Shot 3, Scout Left							
SL – 1 (0.083 min)	AMAD (μm)	GSD	R^2	AMAD (μm)	GSD	R^2	0.06
	21.56	2.07	0.82	>1000	0	0.82	
				20.86	1.98		
SL – 2 (1.083 min)	AMAD (μm)	GSD	R^2	AMAD (μm)	GSD	R^2	0
	19.56	4.43	0.03	0.91	2.07	0.01	
				19.07	6.47		
SL – 3 (3.125 min)	AMAD (μm)	GSD	R^2	AMAD (μm)	GSD	R^2	0.77
	0.01 2.5[(a)]	0.62 4.5[(a)]	0	0.64	1.46	0.93	
				11.05	1.19		
SL – 4 (7.50 min)	AMAD (μm)	GSD	R^2	AMAD (μm)	GSD	R^2	1.0
	1.23	6.08	0	0.38	1.55	0.01	
				0.67	0		
SL – 5 (16.0 min)	AMAD (μm)	GSD	R^2	AMAD (μm)	GSD	R^2	0.57
	1.11	9.23	0.07	0.33	1.43	0.95	
				4.05	1.45		
SL – 6 (33.0 min)	AMAD (μm)	GSD	R^2	AMAD (μm)	GSD	R^2	0.55
	0.95	7.03	0.29	0.36	1.53	0.94	
				3.59	1.73		
SL – 7 (65.0 min)	AMAD (μm)	GSD	R^2	AMAD (μm)	GSD	R^2	0.58
	1.03	4.23	0.44	0.45	1.67	0.99	
				3.36	1.41		
SL – 8 (125.0 min)	AMAD (μm)	GSD	R^2	AMAD (μm)	GSD	R^2	0.60
	1.06	4.86	0.16	0.45	1.67	0.98	
				3.57	1.24		
SL – 9 Field Blank	AMAD (μm)	GSD	R^2	AMAD (μm)	GSD	R^2	-----
	-----	-----	-----	-----	-----	-----	
				-----	-----		

Table B.1. (cont'd)

Phase II, Shot 3, Commander							
Sample ID (Time)	**Unimodal Fit**			**Bimodal Fit**			**Fraction in First Peak**
C – 1 Field Blank	AMAD (μm)	GSD	R^2	AMAD (μm)	GSD	R^2	-----
	-----	-----	-----	-----	----	-----	
				-----	-----		
C – 2 (0.083 min)	AMAD (μm)	GSD	R^2	AMAD (μm)	GSD	R^2	0.40
	2.84	13.3	0	0.35	1.81	0.59	
				11.85	3.99		
C – 3 (1.083 min)	AMAD (μm)	GSD	R^2	AMAD (μm)	GSD	R^2	0.73
	2.97	2.44	0.29	1.16	8.86	0.83	
				4.28	1.21		
C – 4 (3.125 min)	AMAD (μm)	GSD	R^2	AMAD (μm)	GSD	R^2	0
	40.92	1.42	0.90	0.32	1.19	0.13	
				19.57	9.87		
C – 5 (7.50 min)	AMAD (μm)	GSD	R^2	AMAD (μm)	GSD	R^2	0.62
	0.56	2.84	0.40	0.46	1.48	0.77	
				2.73	4.39		
C – 6 (16.0 min)	AMAD (μm)	GSD	R^2	AMAD (μm)	GSD	R^2	0.78
	0.55	2.88	0.69	0.47	1.72	0.96	
				3.27	1.52		
C – 7 (33.0 min)	AMAD (μm)	GSD	R^2	AMAD (μm)	GSD	R^2	0.52
	0.53	4.89	0.84	0.33	1.49	0.99	
				2.07	2.34		
C – 8 (65.0 min)	AMAD (μm)	GSD	R^2	AMAD (μm)	GSD	R^2	0.66
	0.59	4.78	0.75	0.36	2.16	0.999	
				2.97	1.62		
C – 9 (125.0 min)	AMAD (μm)	GSD	R^2	AMAD (μm)	GSD	R^2	0.66
	0.57	3.40	0.89	0.41	1.67	0.99	
				2.14	1.83		
Phase II, Shot 3, Scout Right							
SR – 1 (0.083 min)	AMAD (μm)	GSD	R^2	AMAD (μm)	GSD	R^2	0.93
	3.83	3.46	0.53	3.76	3.29	0.54	
				>100	>1000		
SR – 2 Field Blank	AMAD (μm)	GSD	R^2	AMAD (μm)	GSD	R^2	-----
	-----	-----	-----	-----	-----	-----	
				-----	-----		
SR – 3 (1.083 min)	AMAD (μm)	GSD	R^2	AMAD (μm)	GSD	R^2	0.51
	2.41	6.15	0.08	0.33	1.41	0.84	
				3.95	1.42		
SR – 4 (3.125 min)	AMAD (μm)	GSD	R^2	AMAD (μm)	GSD	R^2	0.74
	0.45 2.0[(a)]	0 6.0[(a)]	0	1.07	2.20	0.99	
				5.38	1.31		
SR – 5 (7.50 min)	AMAD (μm)	GSD	R^2	AMAD (μm)	GSD	R^2	0.71
	0.36	5.25	0.58	0.27	2.16	0.999	
				3.11	1.47		

Table B.1. (cont'd)

Phase II, Shot 3, Scout Right							
Sample ID (Time)	**Unimodal Fit**			**Bimodal Fit**			**Fraction in First Peak**
SR – 6 (16.0 min)	AMAD (μm)	GSD	R^2	AMAD (μm)	GSD	R^2	0.74
	0.81	3.51	0.91	0.53	2.37	0.999	
				3.04	1.52		
SR – 7 (33.0 min)	AMAD (μm)	GSD	R^2	AMAD (μm)	GSD	R^2	0.61
	0.76	2.73	0.62	0.52	1.49	0.98	
				2.80	2.05		
SR – 8 (65.0 min)	AMAD (μm)	GSD	R^2	AMAD (μm)	GSD	R^2	0.82
	0.52	2.02	0.76	0.54	1.84	0.91	
				5.65	1.69		
SR – 9 (125.0 min)	AMAD (μm)	GSD	R^2	AMAD (μm)	GSD	R^2	1.0
	0.51	1.08	0.78	0.73	1.66	0.29	
				12.44	96.11		
Phase II, Shot 3, Driver							
D-1 (0.083 min)	AMAD (μm)	GSD	R^2	AMAD (μm)	GSD	R^2	0.59
	2.74	14.26	0	0.42	2.07	0.93	
				13.45	1.72		
D-2 (1.083 min)	AMAD (μm)	GSD	R^2	AMAD (μm)	GSD	R^2	0.63
	1.07	12.82	0	0.48	2.27	0.76	
				19.39	1.82		
D-3 (3.125 min)	AMAD (μm)	GSD	R^2	AMAD (μm)	GSD	R^2	1.0
	0.46	1.65	0.99	0.46	1.65	0.99	
				>1000	>1000		
D-4 (7.5 min)	AMAD (μm)	GSD	R^2	AMAD (μm)	GSD	R^2	0.81
	0.38	2.77	0.86	0.39	1.78	0.995	
				2.72	1.32		
D-5 (16.5 min)	AMAD (μm)	GSD	R^2	AMAD (μm)	GSD	R^2	0.86
	0.37	2.17	0.96	0.37	1.59	0.99	
				1.41	1.59		
D-6 (33.0 min)	AMAD (μm)	GSD	R^2	AMAD (μm)	GSD	R^2	0.81
	0.59	2.47	0.91	0.50	1.81	0.997	
				2.56	1.44		
D-7 (65.0 min)	AMAD (μm)	GSD	R^2	AMAD (μm)	GSD	R^2	0.62
	0.97	3.69	0.65	0.50	1.88	0.997	
				3.20	1.41		
D-8 (125.0 min)	AMAD (μm)	GSD	R^2	AMAD (μm)	GSD	R^2	0.85
	0.22	2.61	0.87	0.25	2.13	0.996	
				2.94	1.32		
D-9 Field Blank	AMAD (μm)	GSD	R^2	AMAD (μm)	GSD	R^2	-----
	-----	-----	-----	-----	-----	-----	
				-----	-----		

Table B.1. (cont'd)

Phase III, Shot 1, Loader							
Sample ID (Time)	**Unimodal Fit**			**Bimodal Fit**			**Fraction in First Peak**
L – 1 (0.083 min)	AMAD (μm)	GSD	R^2	AMAD (μm)	GSD	R^2	0.87
	4.80	4.34	0.48	2.94	3.75	0.96	
				14.52	1.18		
L – 2 (1.083 min)	AMAD (μm)	GSD	R^2	AMAD (μm)	GSD	R^2	0.54
	4.81	2.85	0.81	0.003	0	0	
				1.58	1.30		
L – 3 (3.125 min)	AMAD (μm)	GSD	R^2	AMAD (μm)	GSD	R^2	0
	1.98 2.27[(a)]	0 3.30[(a)]	0	>1000	>1000	0.89	
				2.27	3.30		
L – 4 (7.5 min)	AMAD (μm)	GSD	R^2	AMAD (μm)	GSD	R^2	0.41
	0.91 2.0[(a)]	0 5.0[(a)]	0	0.64	1.53	0.92	
				4.28	2.08		
L – 5 (16.0 min)	AMAD (μm)	GSD	R^2	AMAD (μm)	GSD	R^2	0.48
	0.93 2.0[(a)]	0 5.5[(a)]	0	0.67	1.63	0.77	
				3.79	1.72		
L – 6 (33.0 min)	AMAD (μm)	GSD	R^2	AMAD (μm)	GSD	R^2	0.55
	1.21	2.49	0.85	0.81	1.48	0.99	
				3.16	1.67		
L – 7 (65.0 min)	AMAD (μm)	GSD	R^2	AMAD (μm)	GSD	R^2	0.40
	0.32 2.0[(a)]	0 4.0[(a)]	0	0.46	1.46	0.95	
				2.45	1.47		
L – 8 (125.0 min)	AMAD (μm)	GSD	R^2	AMAD (μm)	GSD	R^2	0.60
	0.93	3.59	0.44	0.49	1.51	0.97	
				3.09	1.38		
L – 9 Field Blank	AMAD (μm)	GSD	R^2	AMAD (μm)	GSD	R^2	-----
	-----	-----	-----	-----	-----	-----	
				-----	-----		
Phase III, Shot 1, Commander							
C – 1 (0.083 min)	AMAD (μm)	GSD	R^2	AMAD (μm)	GSD	R^2	0.21
	5.76	3.69	0.71	0.60	1.74	0.91	
				7.12	2.54		
C – 2 (1.083 min)	AMAD (μm)	GSD	R^2	AMAD (μm)	GSD	R^2	0.23
	4.55	3.70	0.58	0.39	1.44	0.76	
				4.85	2.46		
C – 3 (3.125 min)	AMAD (μm)	GSD	R^2	AMAD (μm)	GSD	R^2	0
	5.02	7.65	0.14	1.06	1.85	0.14	
				5.88	8.01		
C – 4 (7.5 min)	AMAD (μm)	GSD	R^2	AMAD (μm)	GSD	R^2	0.46
	0.76 1.8[(a)]	0 4.0[(a)]	0	0.64	1.51	0.99	
				4.15	1.62		
C – 5 (16.0 min)	AMAD (μm)	GSD	R^2	AMAD (μm)	GSD	R^2	0.20
	1.48	4.01	0.45	0.51	1.21	0.80	
				2.36	3.60		

Table B.1. (cont'd)

Phase III, Shot 1, Commander							
Sample ID (Time)	**Unimodal Fit**			**Bimodal Fit**			**Fraction in First Peak**
C – 6 (33.0 min)	AMAD (μm)	GSD	R^2	AMAD (μm)	GSD	R^2	0.39
	0.02 3.0[(a)]	0.47 4.5[(a)]	0	0.73 2.94	1.44 1.25	0.85	
C – 7 (65.0 min)	AMAD (μm)	GSD	R^2	AMAD (μm)	GSD	R^2	0.38
	0.02 2.0[(a)]	0 3.5[(a)]	0	0.64 2.88	1.46 1.45	0.998	
C – 8 (125.0 min)	AMAD (μm)	GSD	R^2	AMAD (μm)	GSD	R^2	0.54
	1.51	7.56	0.08	0.37 2.51	1.32 1.41	0.70	
C – 9 Field Blank	AMAD (μm)	GSD	R^2	AMAD (μm)	GSD	R^2	-----
	-----	-----	-----	----- -----	----- -----	-----	
Phase III, Shot 1, Driver							
D – 1 (0.083 min)	AMAD (μm)	GSD	R^2	AMAD (μm)	GSD	R^2	0.66
	0.82	4.02	0.69	0.50 4.13	1.89 1.91	0.96	
D – 2 (1.083 min)	AMAD (μm)	GSD	R^2	AMAD (μm)	GSD	R^2	0.27
	0.13	2.14	0.65	0.22 40.40	1.31 30.75	0.93	
D – 3 (3.125 min)	AMAD (μm)	GSD	R^2	AMAD (μm)	GSD	R^2	0
	16.90	7.63	0.13	0.98 19.09	2.08 8.32	0.12	
D – 4 (7.5 min)	AMAD (μm)	GSD	R^2	AMAD (μm)	GSD	R^2	0.26
	>1000 3.0[(a)]	0 4.5[(a)]	0	0.71 4.08	1.62 1.61	0.93	
D – 5 (16.0 min)	AMAD (μm)	GSD	R^2	AMAD (μm)	GSD	R^2	0.63
	0.33 2.0[(a)]	0 5.0[(a)]	0	0.76 6.03	1.89 1.70	0.93	
D – 6 (33.0 min)	AMAD (μm)	GSD	R^2	AMAD (μm)	GSD	R^2	0.68
	1.10	2.92	0.62	0.73 3.90	1.72 1.39	0.98	
D – 7 (65.0 min)	AMAD (μm)	GSD	R^2	AMAD (μm)	GSD	R^2	0.54
	1.24	2.28	0.85	0.81 2.88	1.23 1.39	0.996	
D – 8 (125.0 min)	AMAD (μm)	GSD	R^2	AMAD (μm)	GSD	R^2	0.35
	0.82	2.14	0.88	0.77 1.33	1.30 2.98	0.92	
D – 9 Field Blank	AMAD (μm)	GSD	R^2	AMAD (μm)	GSD	R^2	-----
	-----	-----	-----	----- -----	----- -----	-----	

Table B.1. (cont'd)

Phase III, Shot 1, Gunner							
Sample ID (Time)	**Unimodal Fit**			**Bimodal Fit**			**Fraction in First Peak**
G – 1 (0.083 min)	AMAD (μm)	GSD	R^2	AMAD (μm)	GSD	R^2	0.06
	7.51	4.56	0.78	0.73 8.49	1.31 3.98	0.83	
G – 2 (Field Blank)	AMAD (μm)	GSD	R^2	AMAD (μm)	GSD	R^2	-----
	-----	-----	-----	----- -----	----- -----	-----	
G – 3 (1.083 min)	AMAD (μm)	GSD	R^2	AMAD (μm)	GSD	R^2	0
	>1000 2.58[(a)]	0 3.21[(a)]	0	>1000 2.58[(a)]	1.81 3.21	0.74	
G – 4 (3.125 min)	AMAD (μm)	GSD	R^2	AMAD (μm)	GSD	R^2	0.35
	>1000 3.0[(a)]	0 4.0[(a)]	0	0.93 4.95	1.71 1.74	0.94	
G – 5 (7.5 min)	AMAD (μm)	GSD	R^2	AMAD (μm)	GSD	R^2	0.45
	0.50 1.8[(a)]	0 4.0[(a)]	0	0.71 4.05	1.29 1.71	0.96	
G – 6 (16.0 min)	AMAD (μm)	GSD	R^2	AMAD (μm)	GSD	R^2	0.49
	0.02 2.0[(a)]	0 4.0[(a)]	0	0.74 3.90	1.31 1.53	0.999	
G – 7 (33.0 min)	AMAD (μm)	GSD	R^2	AMAD (μm)	GSD	R^2	0.73
	0.76 1.8[(a)]	1.69 4.0[(a)]	0	0.79 3.45	1.31 1.43	0.99	
G – 8 (65.0 min)	AMAD (μm)	GSD	R^2	AMAD (μm)	GSD	R^2	0.58
	0.92	2.07	0.89	0.74 2.38	1.36 1.58	0.9999	
G – 9 (125.0 min)	AMAD (μm)	GSD	R^2	AMAD (μm)	GSD	R^2	0.98
	0.53	1.23	0.97	0.55 >100	1.27 >1000	0.97	
Phase III, Shot 2, Commander							
C – 1 (0.083 min)	AMAD (μm)	GSD	R^2	AMAD (μm)	GSD	R^2	0.28
	6.78	3.86	0.48	0.43 7.56	1.71 2.32	0.96	
C – 2 (1.083 min)	AMAD (μm)	GSD	R^2	AMAD (μm)	GSD	R^2	0
	31.62	1.91	0.92	0.40 31.61	0.97 1.91	0.92	
C – 3 (3.125 min)	AMAD (μm)	GSD	R^2	AMAD (μm)	GSD	R^2	0.15
	34.22	2.29	0.56	0.65 30.74	1.24 2.07	0.80	
C – 4 (7.5 min)	AMAD (μm)	GSD	R^2	AMAD (μm)	GSD	R^2	0.72
	0.59 2.0[(a)]	1.50 4.0[(a)]	0.70	0.72 13.47	1.28 1.21	0.999	
C – 5 (16.0 min)	AMAD (μm)	GSD	R^2	AMAD (μm)	GSD	R^2	0.999
	0.56	1.22	0.999	0.57 >100	1.24 >1000	0.999	

Table B.1. (cont'd)

Phase III, Shot 2, Commander							
Sample ID (Time)	**Unimodal Fit**			**Bimodal Fit**			**Fraction in First Peak**
C – 6 (33.0 min)	AMAD (μm)	GSD	R^2	AMAD (μm)	GSD	R^2	0.997
	0.55	1.24	0.999	0.56	1.25	0.999	
				>100	>1000		
C – 7 (65.0 min)	AMAD (μm)	GSD	R^2	AMAD (μm)	GSD	R^2	0.995
	0.52	1.20	0.999	0.54	1.22	0.999	
				>100	>1000		
C – 8 (125.0 min)	AMAD (μm)	GSD	R^2	AMAD (μm)	GSD	R^2	0.12
	40.47 10.0[(a)]	1.31 4.5[(a)]	0.89	0.58	1.18	0.999	
				39.07	1.27		
C – 9 Field Blank	AMAD (μm)	GSD	R^2	AMAD (μm)	GSD	R^2	-----
	-----	-----	-----	-----	-----	-----	
				-----	-----		
Phase III, Shot 2, Driver							
Sample ID (Time)	**Unimodal Fit**			**Bimodal Fit**			**Fraction in First Peak**
D – 1 (0.083 min)	AMAD (μm)	GSD	R^2	AMAD (μm)	GSD	R^2	0.45
	3.95	7.68	0	0.29	2.01	0.74	
				7.71	2.14		
D – 2 (1.083 min)	AMAD (μm)	GSD	R^2	AMAD (μm)	GSD	R^2	0.73
	0.63	2.60	0.34	0.66	2.01	0.98	
				16.19	1.81		
D – 3 (3.125 min)	AMAD (μm)	GSD	R^2	AMAD (μm)	GSD	R^2	1.0
	3.45	3.71	0.40	3.45	3.73	0.40	
				>1000	>1000		
D – 4 (7.5 min)	AMAD (μm)	GSD	R^2	AMAD (μm)	GSD	R^2	0.52
	2.1[(a)]	0 4.0[(a)]	0	0.80	1.24	0.99	
				3.88	1.63		
D – 5 (16.0 min)	AMAD (μm)	GSD	R^2	AMAD (μm)	GSD	R^2	0.82
	0.82	3.94	0.55	0.54	2.68	0.99	
				3.56	1.13		
D – 6 (33.0 min)	AMAD (μm)	GSD	R^2	AMAD (μm)	GSD	R^2	0.72
	0.78	3.45	0.67	0.52	1.90	0.96	
				3.21	1.34		
D – 7 (65.0 min)	AMAD (μm)	GSD	R^2	AMAD (μm)	GSD	R^2	0.24
	0.81	3.92	0.26	0.69	1.26	0.56	
				1.98	9.84		
D – 8 (125.0 min)	AMAD (μm)	GSD	R^2	AMAD (μm)	GSD	R^2	0.33
	0.82	3.29	0.21	0.71	1.31	0.61	
				9.83	10.73		
D – 9 Field Blank	AMAD (μm)	GSD	R^2	AMAD (μm)	GSD	R^2	-----
	-----	-----	-----	-----	-----	-----	
				-----	-----		

Table B.1. (cont'd)

Phase III, Shot 2, Gunner (first substrate in G-3 had a small hole)							
Sample ID (Time)	**Unimodal Fit**			**Bimodal Fit**			**Fraction in First Peak**
G – 1 (0.083 min)	AMAD (μm)	GSD	R^2	AMAD (μm)	GSD	R^2	0.26
	10.65	4.66	0.37	0.46	1.51	0.94	
				11.37	2.69		
G – 2 (Field Blank)	AMAD (μm)	GSD	R^2	AMAD (μm)	GSD	R^2	-----
	-----	-----	-----	-----	-----	-----	
				-----	-----		
G – 3 (1.083 min)	AMAD (μm)	GSD	R^2	AMAD (μm)	GSD	R^2	0.08
	14.36	8.00	0.06	0.52	1.13	0.26	
				21.92	5.28		
G – 4 (3.125 min)	AMAD (μm)	GSD	R^2	AMAD (μm)	GSD	R^2	0.03
	40.25	1.50	0.94	>1000	>1000	0.94	
				39.86	1.49		
G – 5 (7.5 min)	AMAD (μm)	GSD	R^2	AMAD (μm)	GSD	R^2	0.31
	42.01	1.46	0.90	1.38	3.14	0.99	
				37.04	1.36		
G – 6 (16.0 min)	AMAD (μm)	GSD	R^2	AMAD (μm)	GSD	R^2	0.17
	42.58	1.34	0.83	13.34	>1000	0.85	
				40.74	1.34		
G – 7 (33.0 min)	AMAD (μm)	GSD	R^2	AMAD (μm)	GSD	R^2	0.47
	1.27	4.35	0.30	0.41	1.54	0.98	
				3.08	1.37		
G – 8 (65.0 min)	AMAD (μm)	GSD	R^2	AMAD (μm)	GSD	R^2	0
	42.10	1.32	0.91	0.59	4.91	0.27	
				70.13	3.92		
G – 9 (125.0 min)	AMAD (μm)	GSD	R^2	AMAD (μm)	GSD	R^2	0.05
	41.57	1.44	0.94	1.19	>1000	0.94	
				40.93	1.43		
Phase III, Shot 2, Loader							
Sample ID (Time)	**Unimodal Fit**			**Bimodal Fit**			**Fraction in First Peak**
L – 1 (0.083 min)	AMAD (μm)	GSD	R^2	AMAD (μm)	GSD	R^2	0.34
	4.70	5.56	0.17	0.48	1.59	0.82	
				7.05	2.50		
L – 2 (1.083 min)	AMAD (μm)	GSD	R^2	AMAD (μm)	GSD	R^2	1.0
	2.33	4.45	0.50	1.22	2.39	0	
				0.006	8.74		
L – 3 (3.125 min)	AMAD (μm)	GSD	R^2	AMAD (μm)	GSD	R^2	0.51
	1.34 2.0[(a)]	0 4.0[(a)]	0	0.82	1.69	0.97	
				5.35	1.68		
L – 4 (7.5 min)	AMAD (μm)	GSD	R^2	AMAD (μm)	GSD	R^2	0.997
	1.15 2.5[(a)]	0 4.0[(a)]	0	1.37	1.80	0.61	
				4.27	1.50		

Table B.1. (cont'd)

Phase III, Shot 2, Loader							
Sample ID (Time)	**Unimodal Fit**			**Bimodal Fit**			**Fraction in First Peak**
L – 5 (16.0 min)	AMAD (μm)	GSD	R^2	AMAD (μm)	GSD	R^2	0.56
	0.34 2.5[(a)]	0 4.5[(a)]	0	0.76 5.03	2.72 1.64	0.98	
L – 6 (33.0 min)	AMAD (μm)	GSD	R^2	AMAD (μm)	GSD	R^2	0.85
	1.16	4.64	0.73	0.72 4.92	3.89 1.27	0.98	
L – 7 (65.0 min)	AMAD (μm)	GSD	R^2	AMAD (μm)	GSD	R^2	0.65
	0.99	3.71	0.70	0.54 3.56	1.94 1.52	0.99	
L – 8 (125.0 min)	AMAD (μm)	GSD	R^2	AMAD (μm)	GSD	R^2	0.25
	0.86	2.98	0.72	0.78 1.18	1.24 4.82	0.84	
L – 9 Field Blank	AMAD (μm)	GSD	R^2	AMAD (μm)	GSD	R^2	-----
	-----	-----	-----	----- -----	----- -----	-----	
Phase IV, Shot 4, Driver							
Sample ID (Time)	**Unimodal Fit**			**Bimodal Fit**			**Fraction in First Peak**
D – 1	AMAD (μm)	GSD	R^2	AMAD (μm)	GSD	R^2	----
	----	----	----	---- ----	---- ----	----	
D – 2 (1.083 min)	AMAD (μm)	GSD	R^2	AMAD (μm)	GSD	R^2	0.17
	0.62	1.67	0.97	0.53 0.76	1.16 1.94	1.00	
D – 3 (5.125 min)	AMAD (μm)	GSD	R^2	AMAD (μm)	GSD	R^2	0.48
	1.28	2.38	0.42	0.50 1.84	1.17 1.29	0.99	
D – 4 (26.0 min)	AMAD (μm)	GSD	R^2	AMAD (μm)	GSD	R^2	0.37
	>1000 4.0[(a)]	0 4.0[(a)]	0	0.03 0.91	0 2.06	0	
D – 5 Field Blank	AMAD (μm)	GSD	R^2	AMAD (μm)	GSD	R^2	----
	----	----	----	---- ----	---- ----	----	
(a) Professional judgment based on graphical representation.							

Appendix C

X-Ray Diffraction Patterns of Uranium Aerosols

Appendix C

X-Ray Diffraction Patterns of Uranium Aerosols

The x-ray diffraction (XRD) patterns were evaluated for selected uranium aerosol samples to identify the crystalline uranium oxide phases present and to provide a semi-quantitative analysis of their relative proportion in each sample. Knowledge of these phases provides insight into particle formation and may be instrumental in estimating the relative solubility of the aerosols in biological fluids. The samples examined were the following:

- all five stages of the cyclone residues from PI-3/4, PI-7, PII-1/2, and PIII-2
- backup filters from the above cyclones including duplicates (two of the four filters collecting fine particles in parallel) for PI-3/4 and PII-1/2
- the first MVF segment from PI-1
- the DU cone sample.

Results of the XRD analysis are presented in Section 5.6.5 and discussed in Section 6.4.3.

C.1 Sample Preparation

The uranium-containing crystalline solids in the aerosol powder formed during impact testing with target materials consisted of a mixture of uranium oxide(s). The crystalline uranium-oxide phases in these samples were identified using standard powder XRD analysis (Jenkins 1989; Cullity 1967) and a Scintag PAD V x-ray diffractometer.[(a)] In preparation for analysis, samples were prepared for XRD by mixing 2 to 10 mg of dry sample powder with 3 to 4 drops of nitrocellulose glue in a small glass vial. Nitrocellulose dissolved in amyl acetate was used as a binder in powder mounts for XRD analysis of limited sized samples (Bish and Reynolds 1989). Corundum powder, a National Institute of Standards and Technology (NIST) standard reference material (SRM 676, α-Al_2O_3) was added to all but the first six samples analyzed when it became apparent that an internal standard was needed to distinguish between UO_2 and U_4O_9. Each sample slurry was then transferred to a glass slide into an area of 1.3 cm by 1.9 cm (0.5 in. by 0.75 in.) and allowed to dry.

C.2 Instrumentation

The diffractometer was operated using copper (Cu) K_α radiation (λ=1.5406 Å), and tube conditions of 45 kilovolts (kV) and 40 milliamperes (mA). Samples were generally examined using 0.02 degrees 2-theta (2θ) step size with counting time varying from 1.2 sec/step (1.0 degree/min) to 20 sec/step. The columinating slits used were 4, 2, 0.5, and 0.2 mm. JADE+5 software, developed by Materials Data Incorporated (MDI's)[(b)], and the Inorganic Crystal Structure Database (ICSD) XRD pattern library

(a) Scintag, 707 Kifer Rd., Sunnyvale, California 94086
(b) Manufactured by Materials Data Incorporated, 1224 Concannon Blvd, Livermore, California 94550

(maintained by Fachsinformationzentrum)[a] were used as the source of standard (known) patterns. This database contains an extensive library of *d*-spacings and their associated Relative Intensity Ratio (RIR) values, and chemical and structural formulas used in semi-quantitative analysis. The JADE+5 routines were used to subtract background, calculate interplanar *d*-spacings, and compare the acquired patterns from the various aerosols to similar patterns in the database. The diffraction angle 2θ is related to the interplanar spacing (*d*-spacing) by Bragg's Law, $n\lambda=2d \sin\theta$, where λ is the wavelength in angstroms of the incident x-ray beam.

C.3 X-Ray Diffraction Patterns

The diffractometer was calibrated with NIST card 1976. Individual runs were calibrated with NIST 676 (alumina/corundum) using the American International Center for Diffraction Data (ICDD) card 46-1212. The ICSD XRD patterns considered for identification of the uranium oxides included the cards for numerous U_3O_8 patterns (72-0246, 72-1078, 72-1257, 74-0562, 74-2101, 74-2103, 74-2104, 76-1850, 77-0144), UO_3 (72-0245), U_4O_9 (72-0125, 75-0944), UO_2 (75-0421), schoepite ($UO_3 \cdot 2H_2O$, 86-1383), and uranium metal (11-628).

Figure C.1 is an example of the XRD pattern for the Stage 5 cyclone residue from the PII-1/2 shot. This figure shows the background-subtracted pattern for this sample. The XRD patterns from the ICSD database used to identify the peaks in the measured XRD pattern are plotted schematically below the pattern. The height of each line represents the relative intensity of an XRD peak for that phase at that d-spacing/2θ value. The XRD patterns (without background subtraction) for the rest of the samples analyzed are presented graphically in Figures C.2 through C.25. The patterns are organized first by phase and then by CI stage and backup filter. Patterns of the PI-1 MVF Segment 1 sample and the DU cone sample follow the CI pattern sets. Each XRD pattern shows the U_3O_8/UO_3 peaks based on Cu K_α radiation (λ=1.5406 Å), and the overlap in these phases is visible in the patterns. Some patterns contain a small peak at about 12 degrees 2θ, which is characteristic of a distinctive schoepite peak.

C.4 Estimation of Percentages

Ratios of the primary oxides U_3O_8/UO_3, U_4O_9, and schoepite were calculated by comparing the major line of each phase to U_3O_8/UO_3. The calculation used a least squares profile of major peaks and the area of these peaks to estimate the ratio of the U_4O_9 and schoepite against U_3O_8/UO_3. These results are presented in Section 4.7.3, Table 4.29.

Those samples most conducive to species separation were further evaluated using MDI's Easy Quant routine to estimate the percentage of oxides in a given phase using the peak area of one of the most intense lines for each phase identified.

Because there was a phase present that could not be identified but is very similar to U_3O_8, it was assumed to be U_3O_8 for purposes of this analysis. In some cases that phase is present in quite significant quantities. The effect, and magnitude on the calculated values, of this assumption cannot be evaluated.

(a) Fachsinformationzentrum,Karlsruhe, Herman-von-Helmholtz-Platz 1, D76344 Eggenstein-Leopoldshafen, Germany.

The basic equation for calculation of percentage composition is as follows:

$$Percent_i = \frac{A_{ij} / I_{ij} / R_i}{\sum_i A_{ij} / I_{ij} / R_i} * 100$$

where A_{ij} is the measured area of the ith component of line j,

I_{ij} is the intensity of the ith component for line j (from the ICSD database), and

R_i is the Relative Intensity ratio of the ith component (from the ICSD database).

The data for schoepite, U_3O_8 and U_4O_9 were available from either experimental data or the ICSD database. Results of the analysis of these samples are provided in Section 4.7.3, Table 4.30.

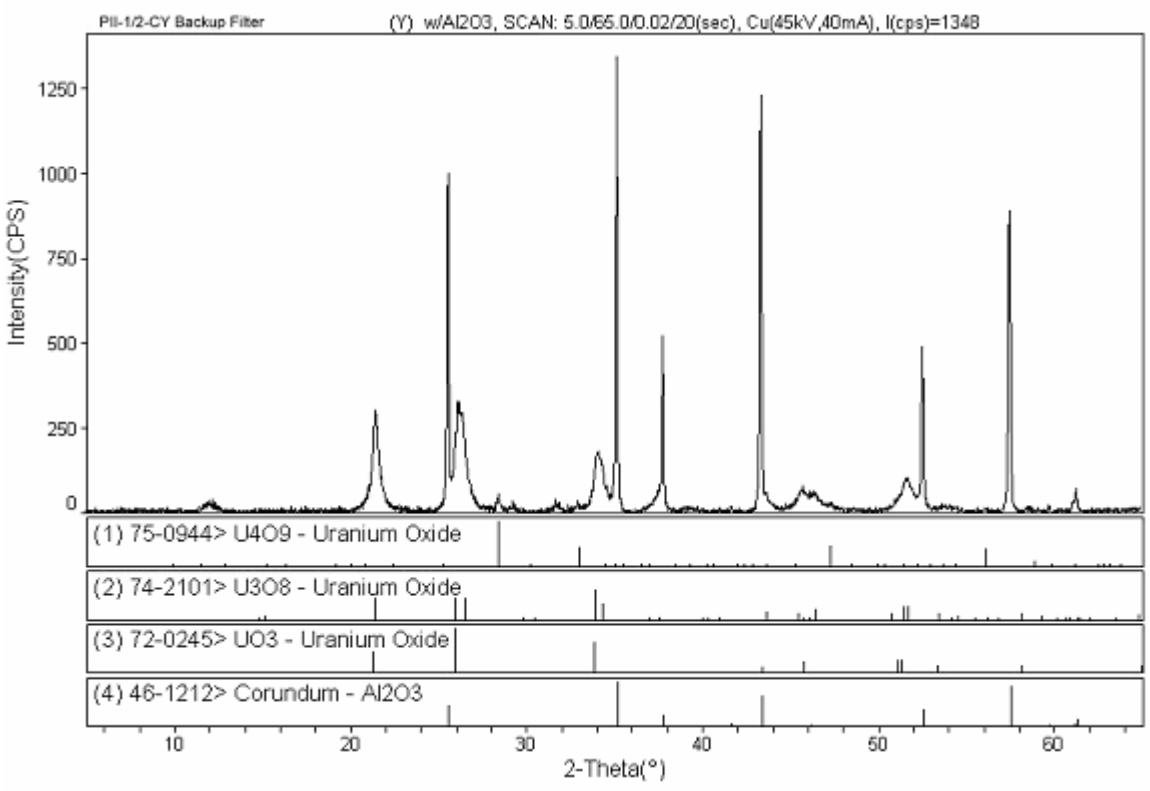

Figure C.1. XRD Profile-Fitted Pattern of the PII-1/2 Cyclone Stage-5 Residue

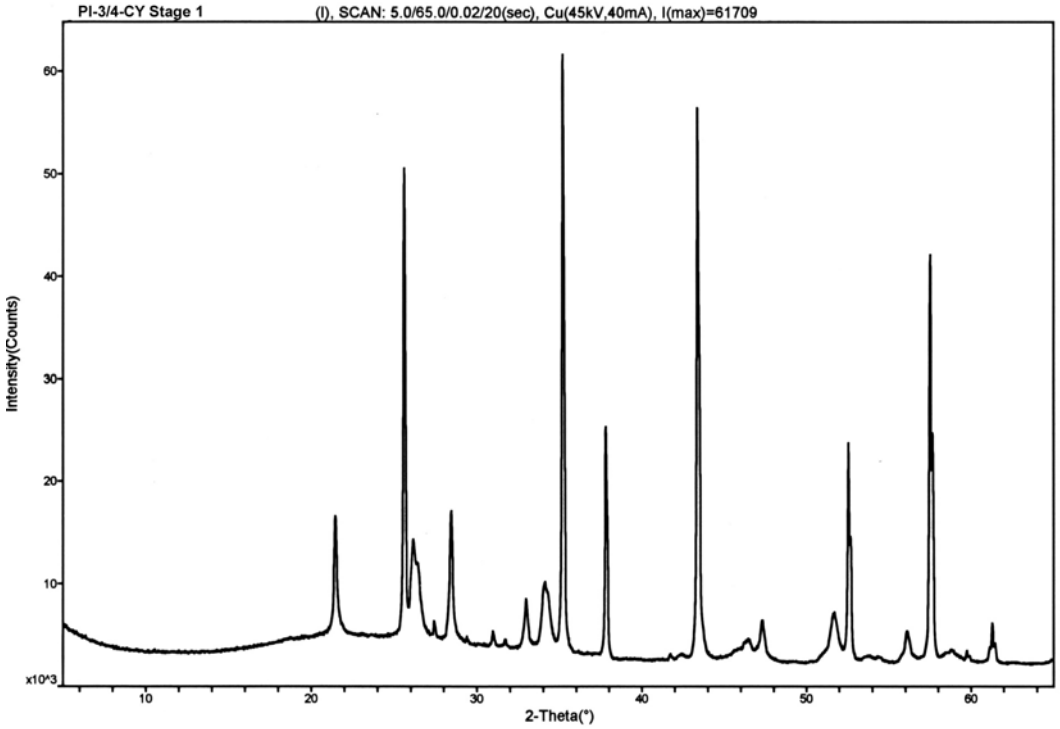

Figure C.2. XRD Pattern of the Residue from PI-3/4-CY Stage 1

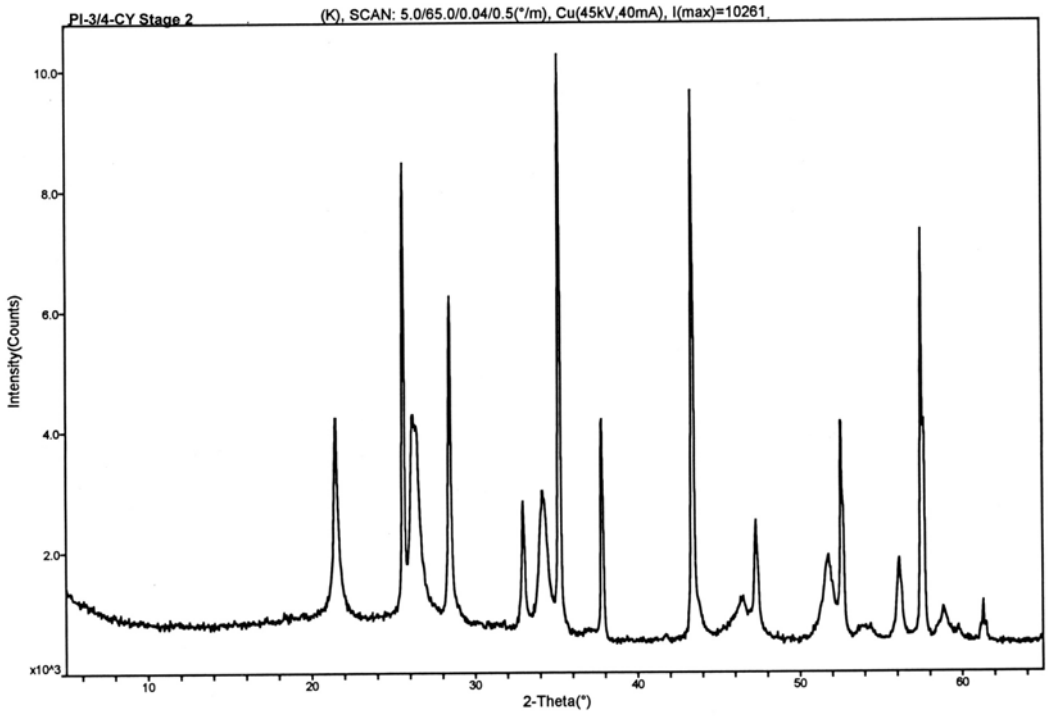

Figure C.3. XRD Pattern of the Residue from PI-3/4-CY Stage 2

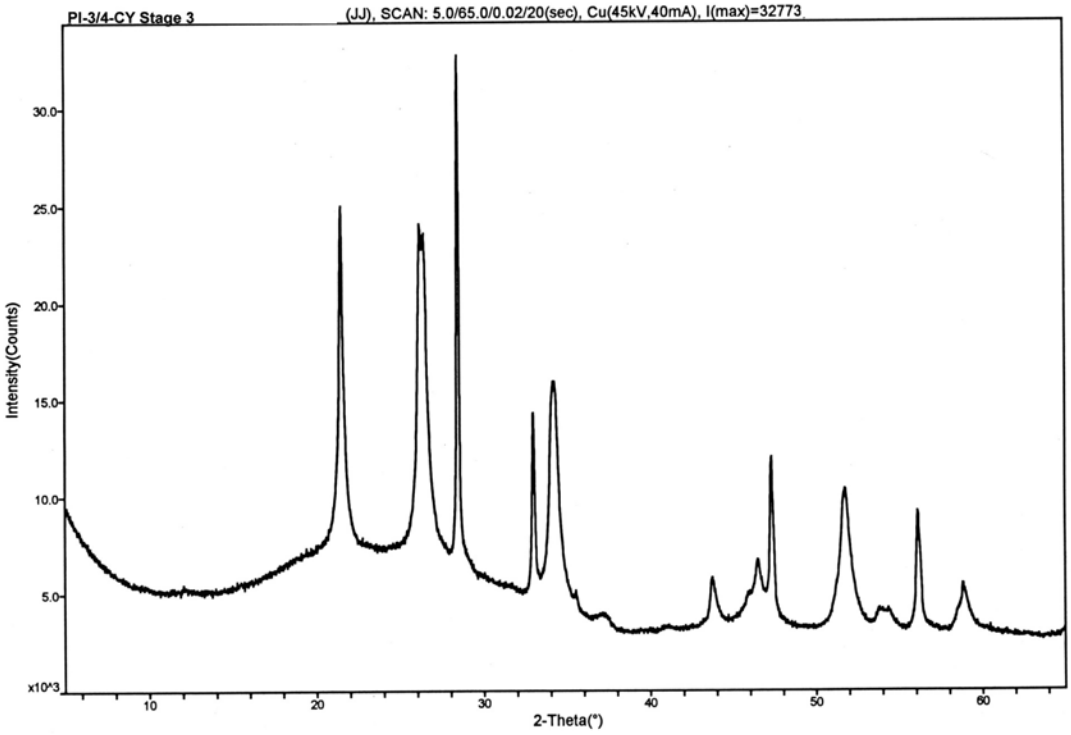

Figure C.4. XRD Pattern of the Residue from PI-3/4-CY Stage 3

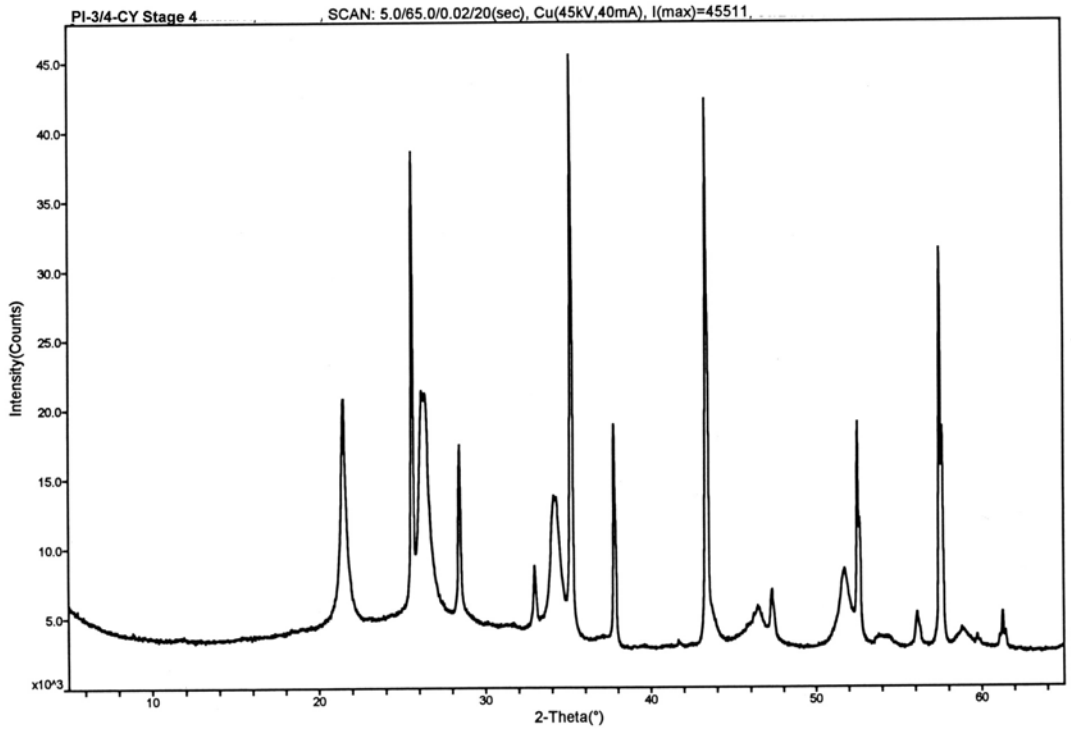

Figure C.5. XRD Pattern of the Residue from PI-3/4-CY Stage 4

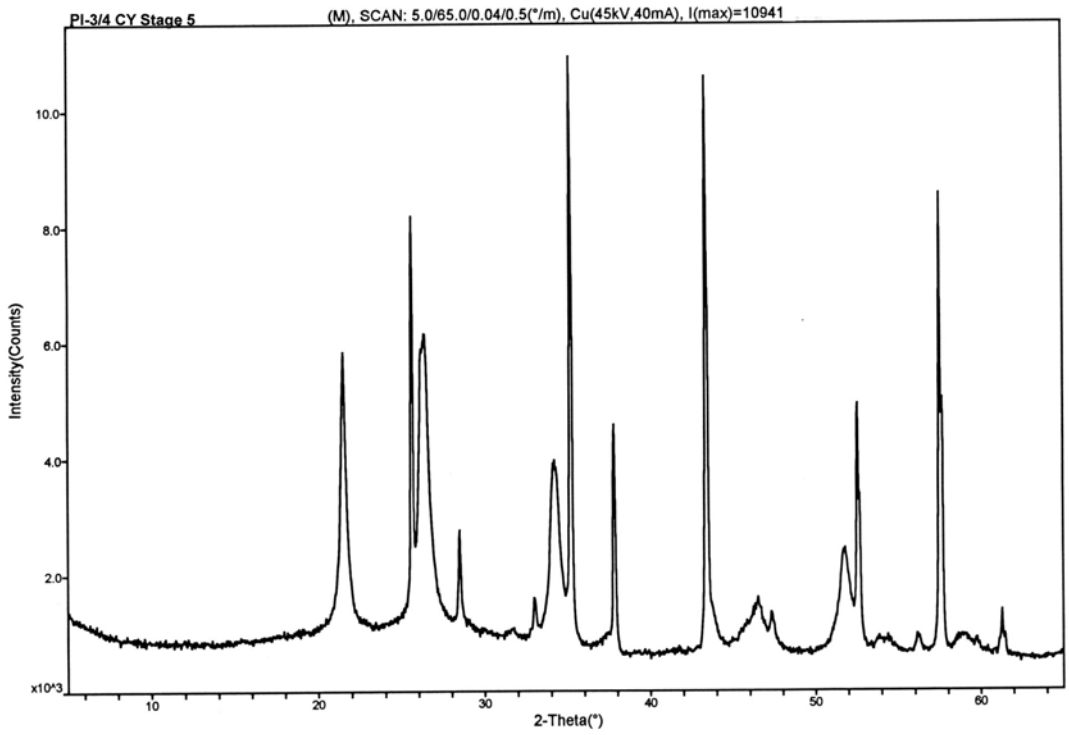

Figure C.6. XRD Pattern of the Residue from PI-3/4-CY Stage 5

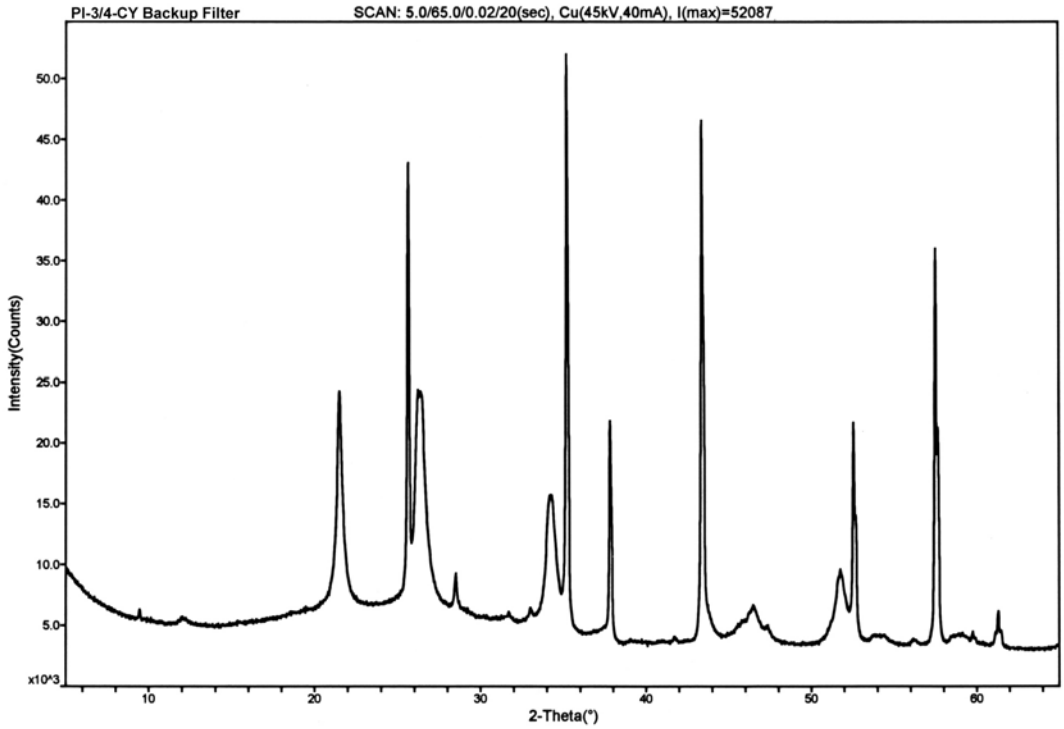

Figure C.7. XRD Pattern of the Residue from PI-3/4-CY Backup Filter

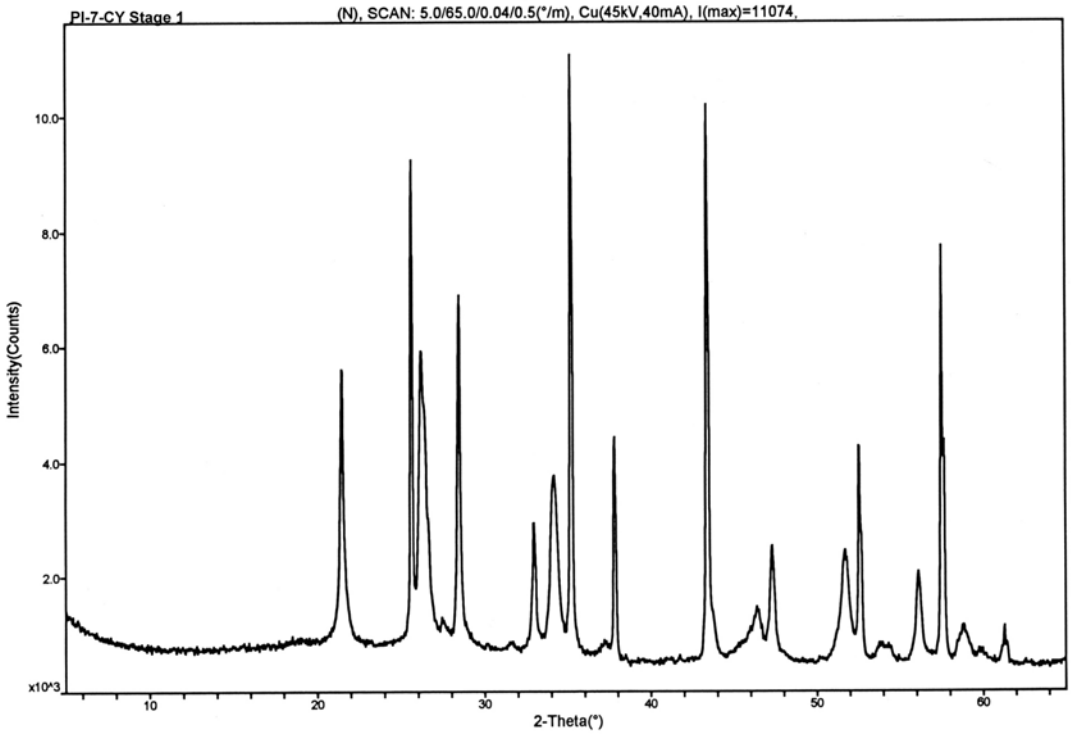

Figure C.8. XRD Pattern of the Residue from PI-7-CY Stage 1

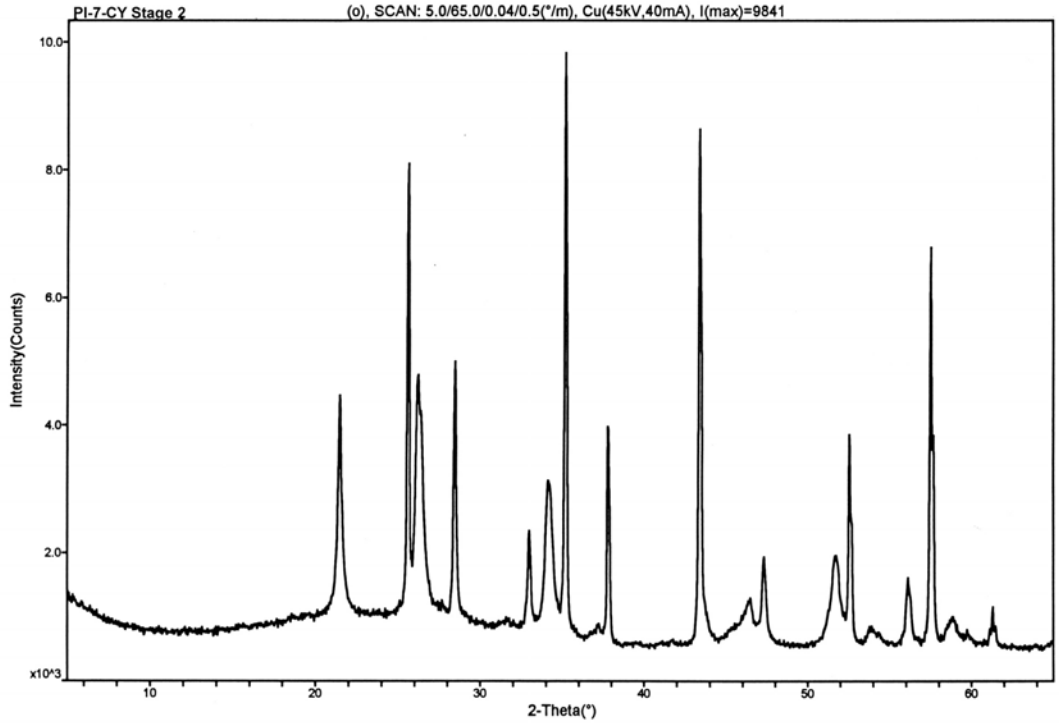

Figure C.9. XRD Pattern of the Residue from PI-7-CY Stage 2

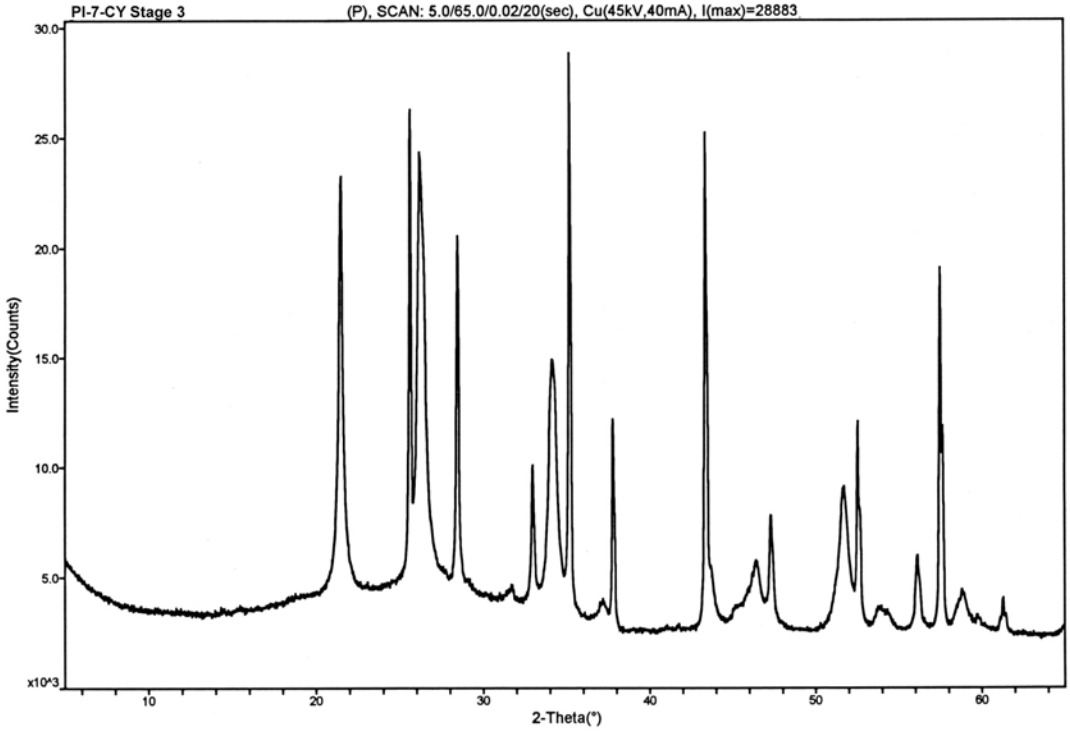

Figure C.10. XRD Pattern of the Residue from PI-7-CY Stage 3

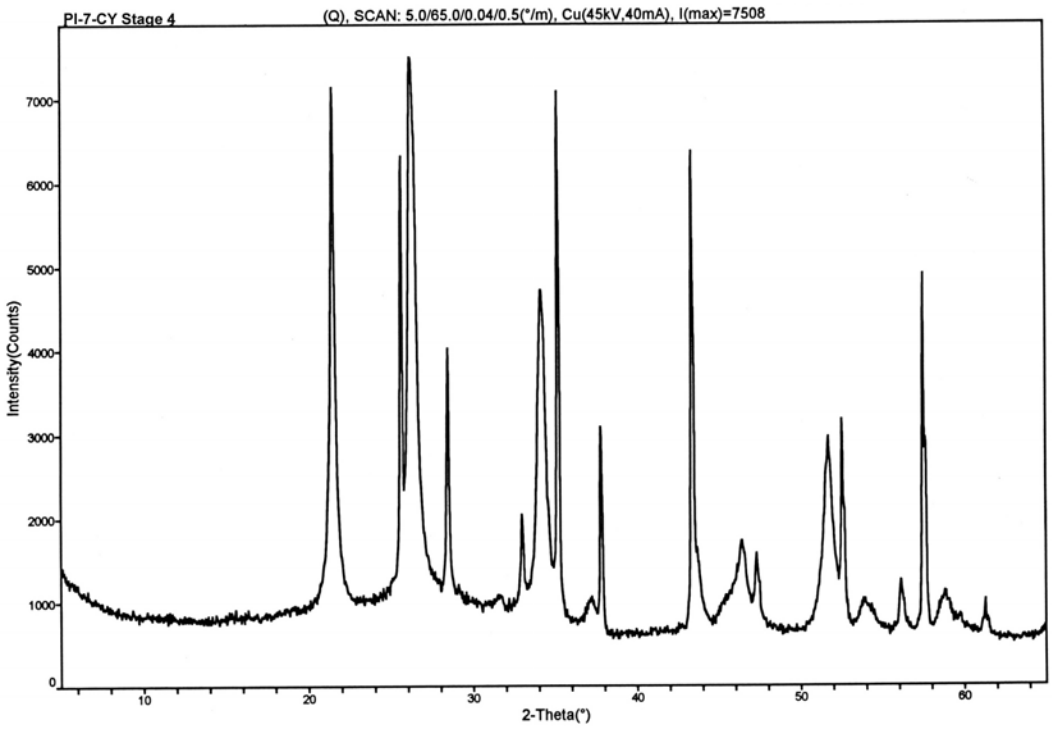

Figure C.11. XRD Pattern of the Residue from PI-7-CY Stage 4

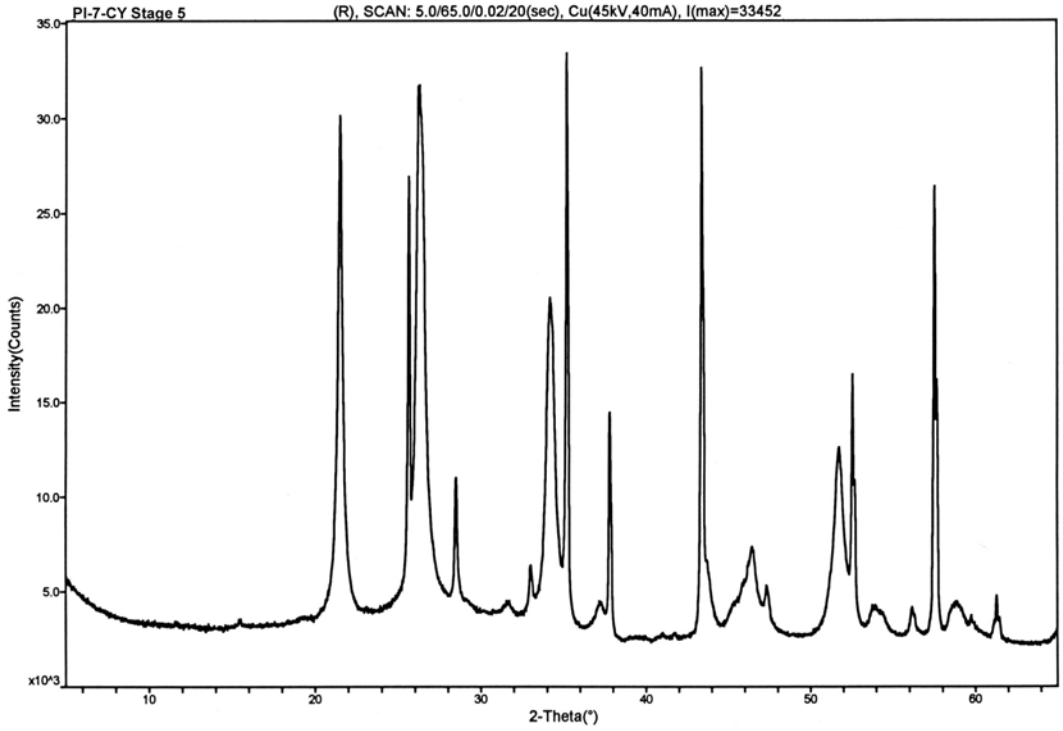

Figure C.12. XRD Pattern of the Residue from PI-7-CY Stage 5

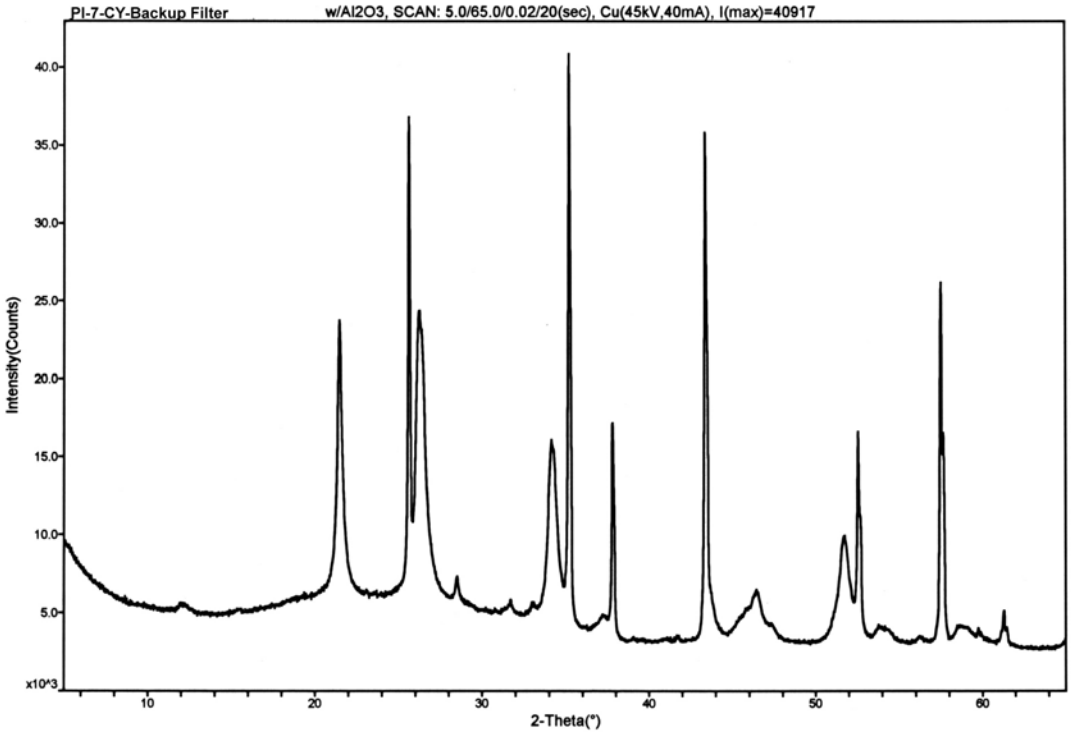

Figure C.13. XRD Pattern of the Residue from PI-7-CY Backup Filter

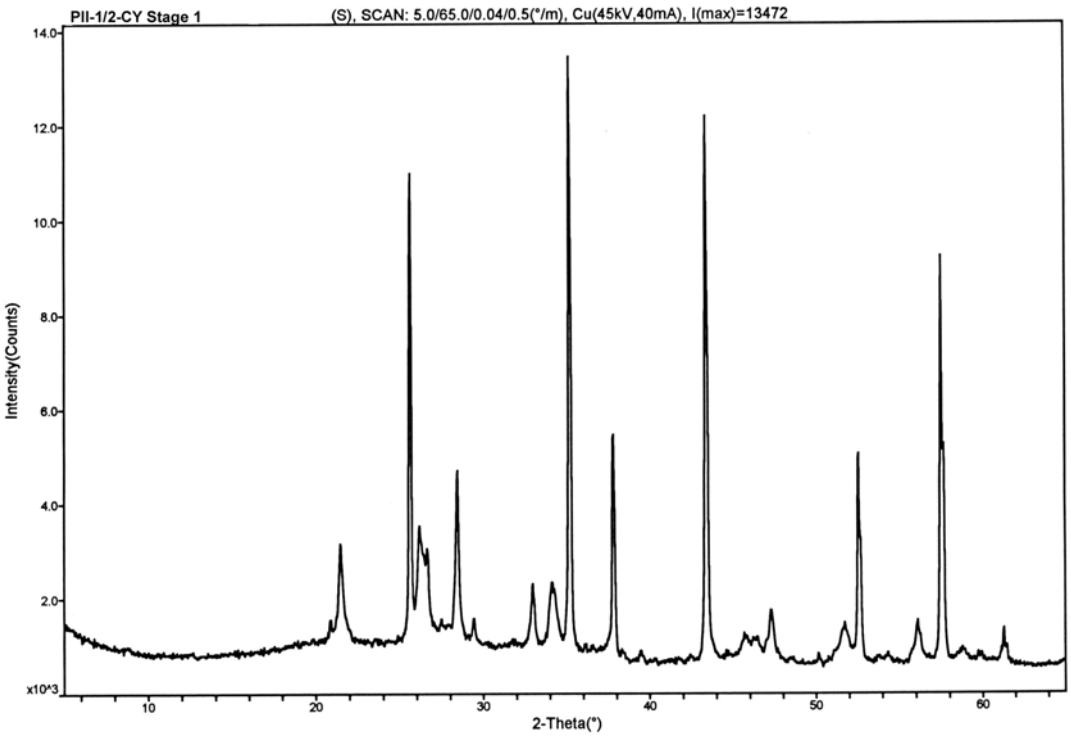

Figure C.14. XRD Pattern of the Residue from PII-1/2-CY Stage 1

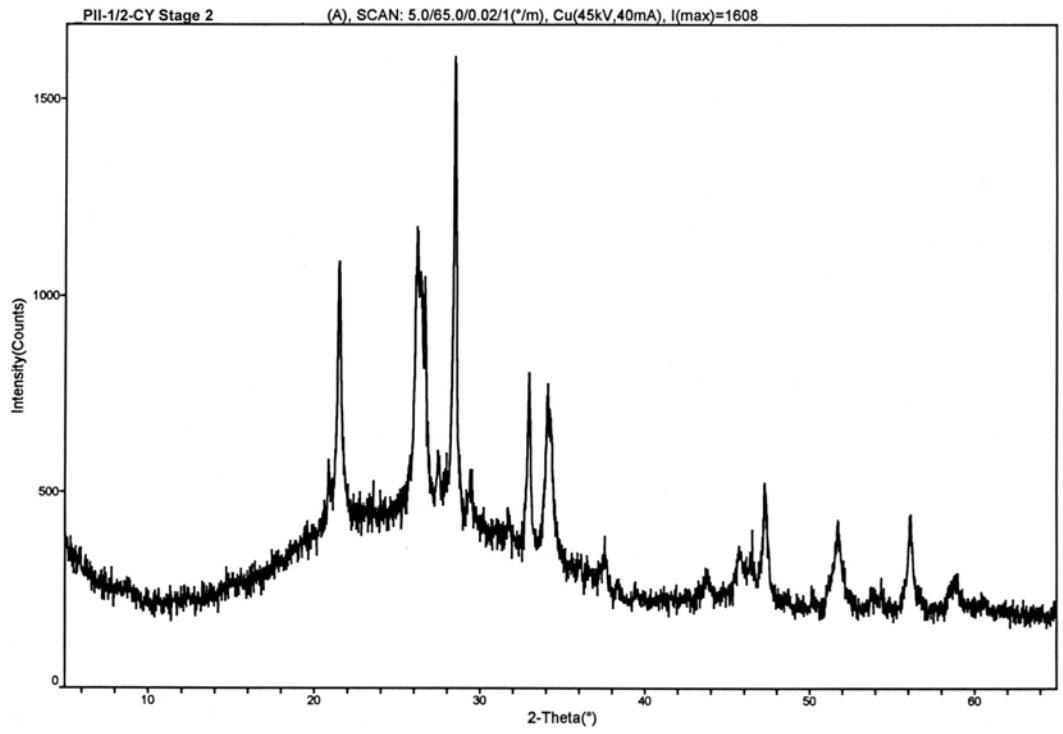

Figure C.15. XRD Pattern of the Residue from PII-1/2-CY Stage 2

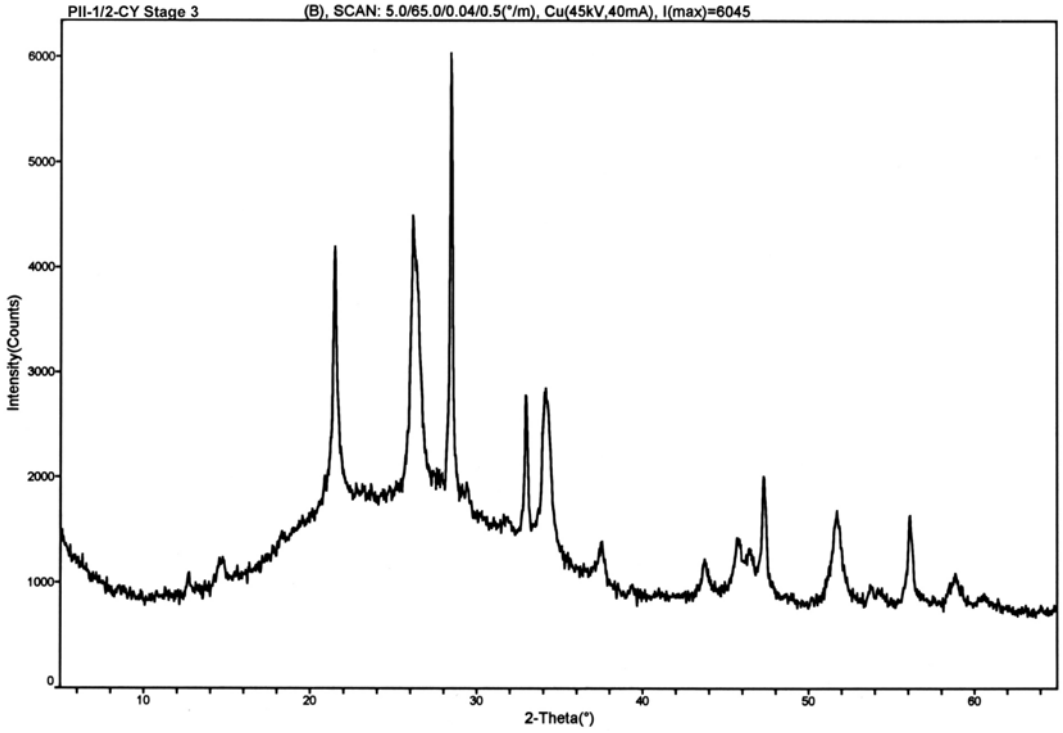

Figure C.16. XRD Pattern of the Residue from PII-1/2-CY Stage 3

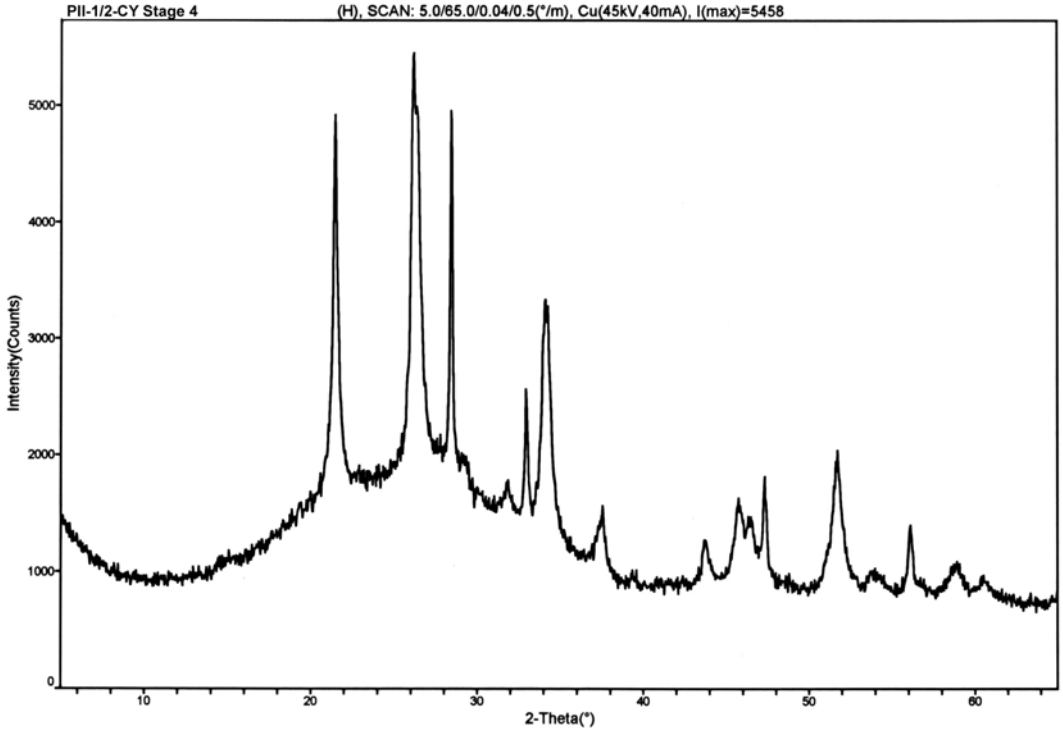

Figure C.17. XRD Pattern of the Residue from PII-1/2-CY Stage 4

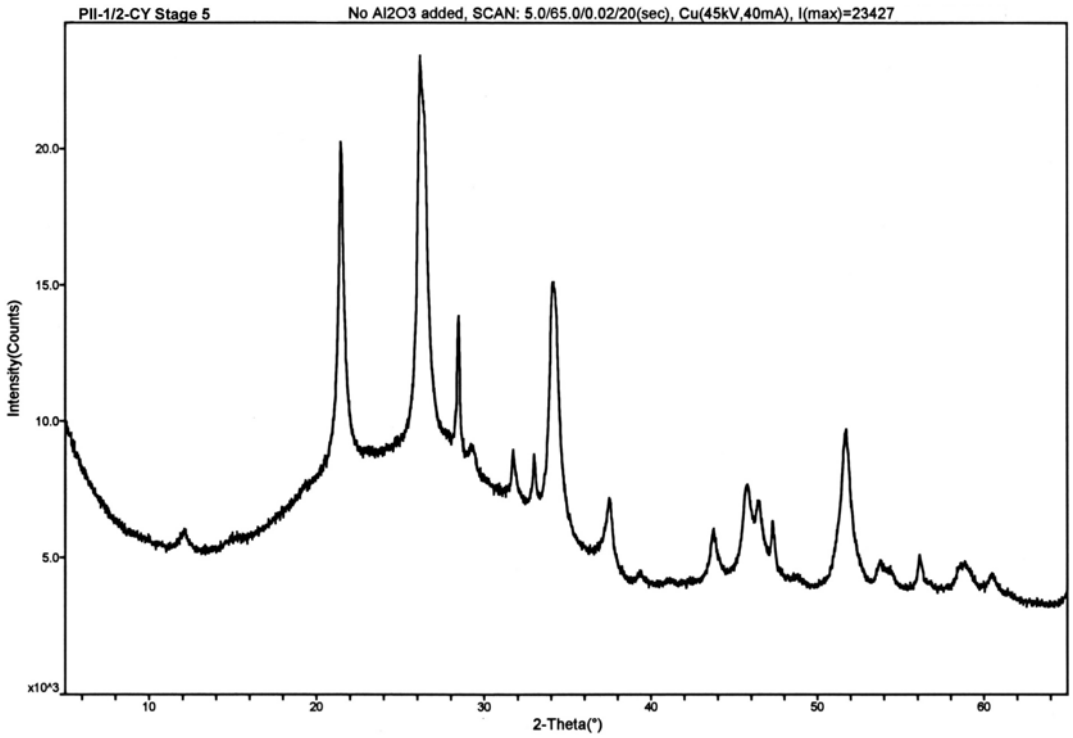

Figure C.18. XRD Pattern of the Residue from PII-1/2-CY Stage 5

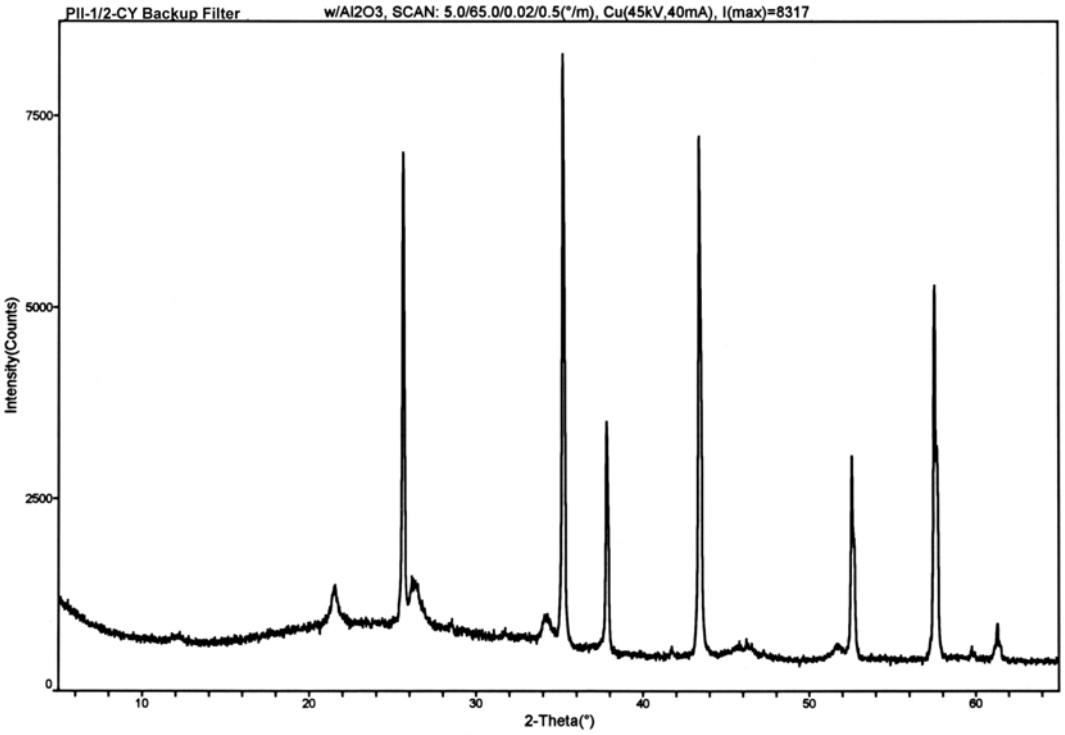

Figure C.19. XRD Pattern of the Residue from PII-1/2-CY Backup Filter

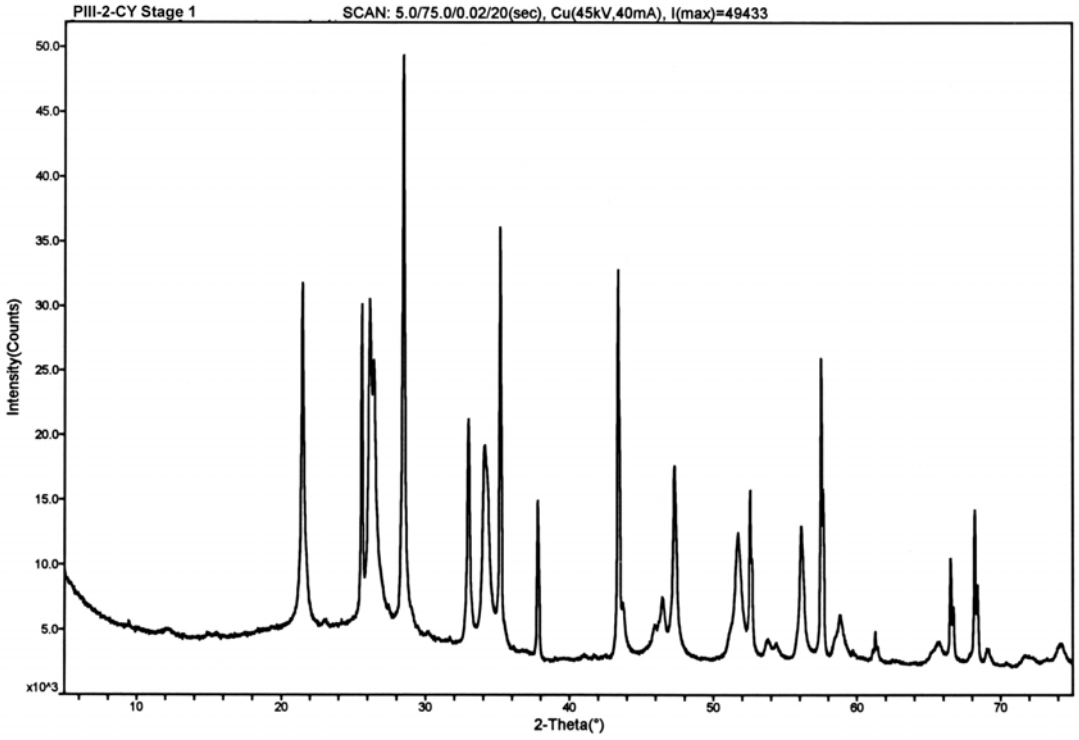

Figure C.20. XRD Pattern of the Residue from PIII-2-CY Stage 1

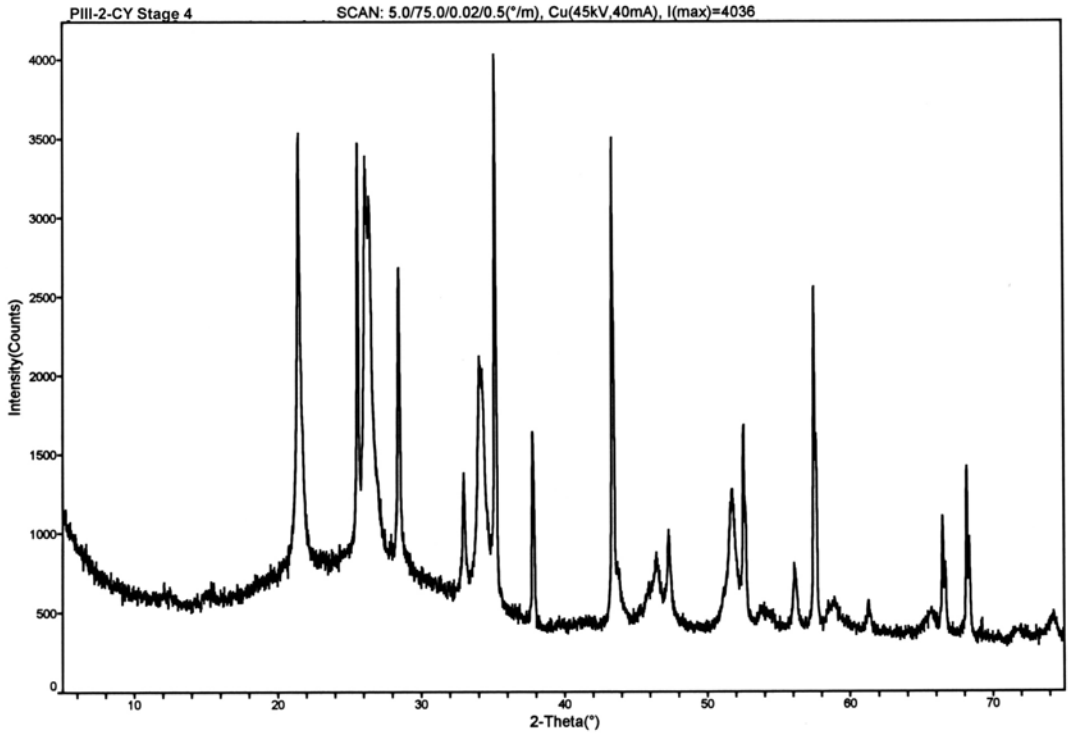

Figure C.21. XRD Pattern of the Residue from PIII-2-CY Stage 4

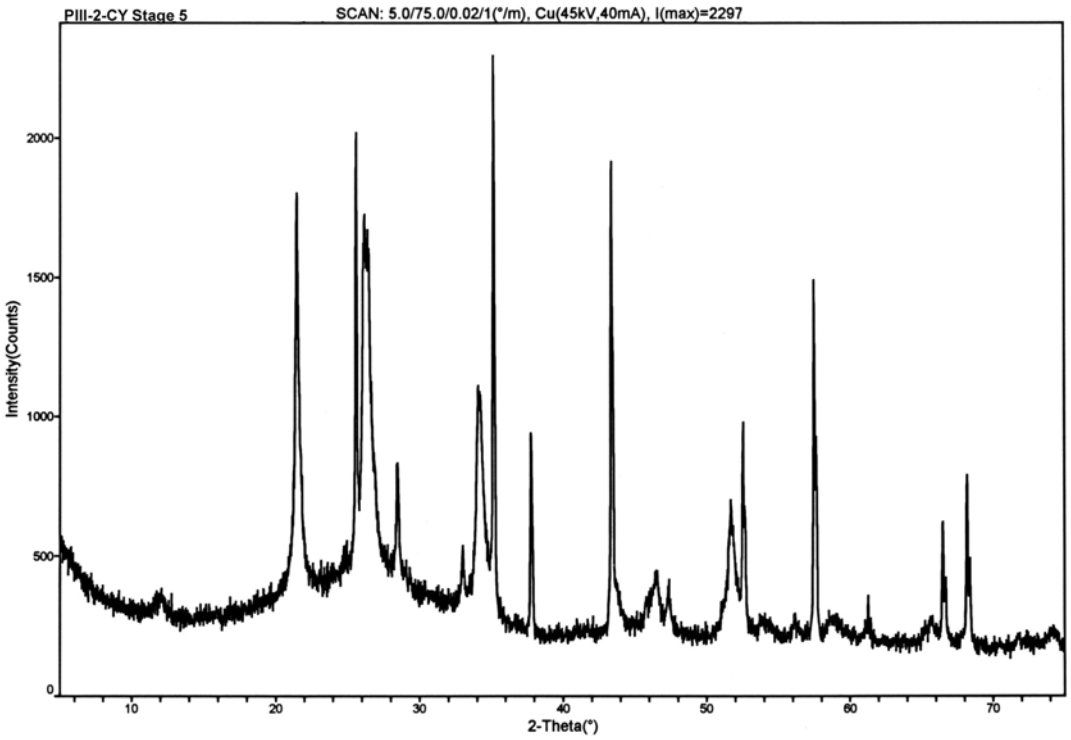

Figure C.22. XRD Pattern of the Residue from PIII-2-CY Stage 5

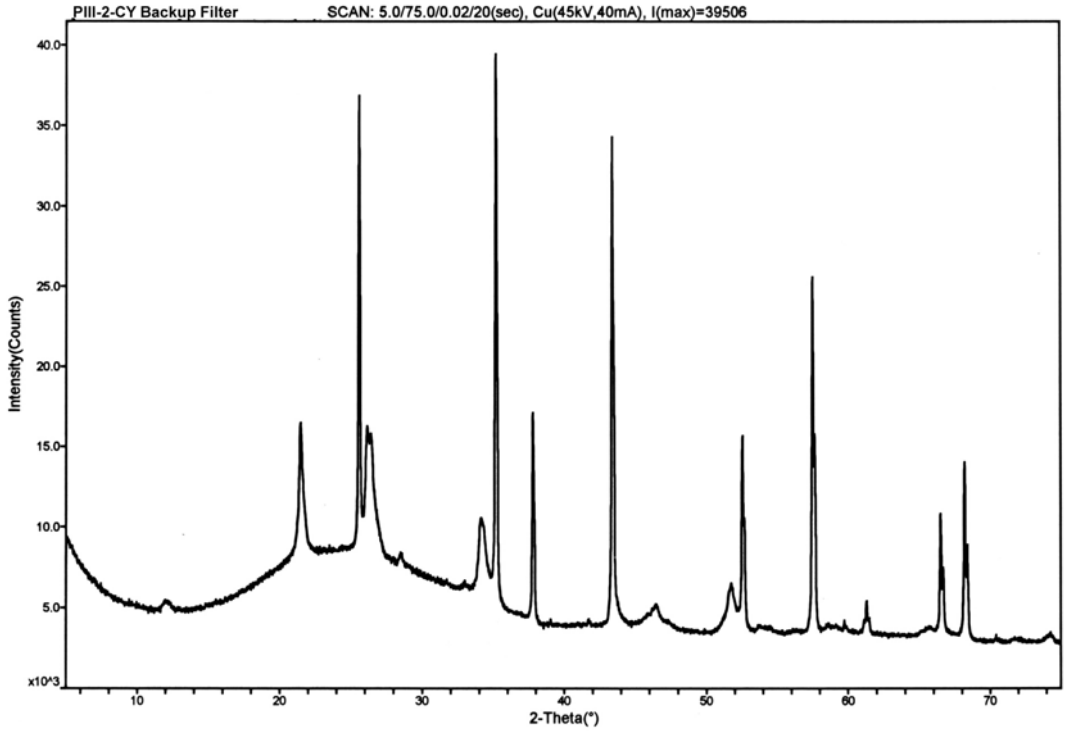

Figure C.23. XRD Pattern of the Residue from PIII-2-CY Backup Filter

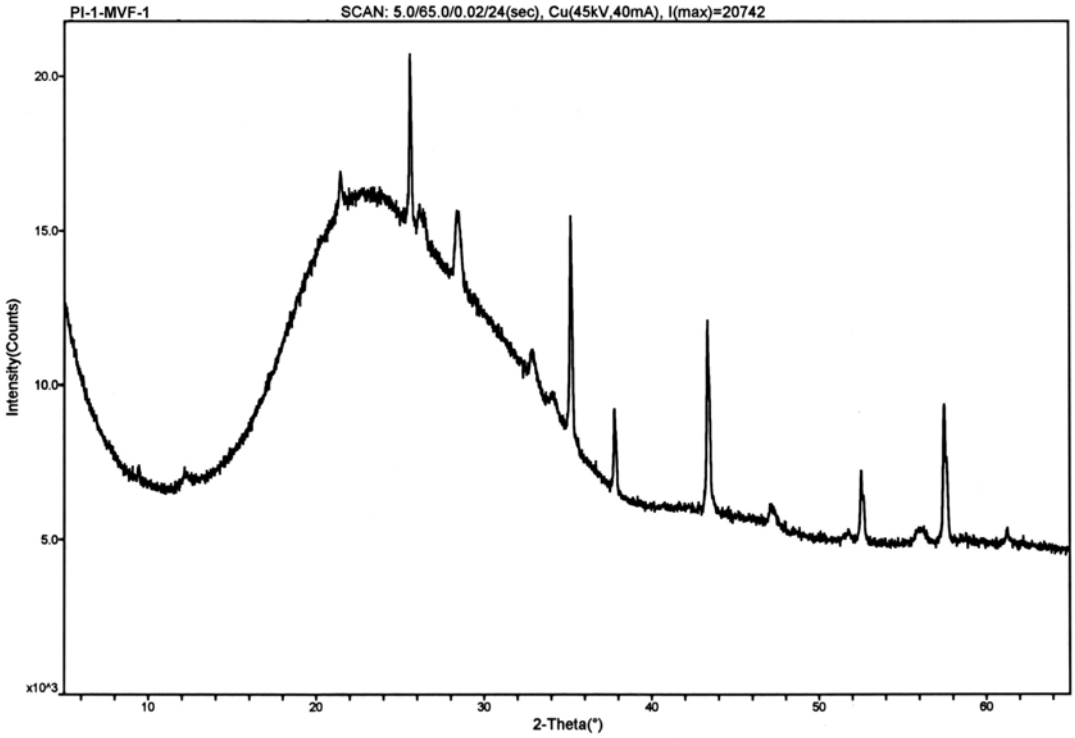

Figure C.24. XRD Pattern of the Residue from PI-1-MVF-1

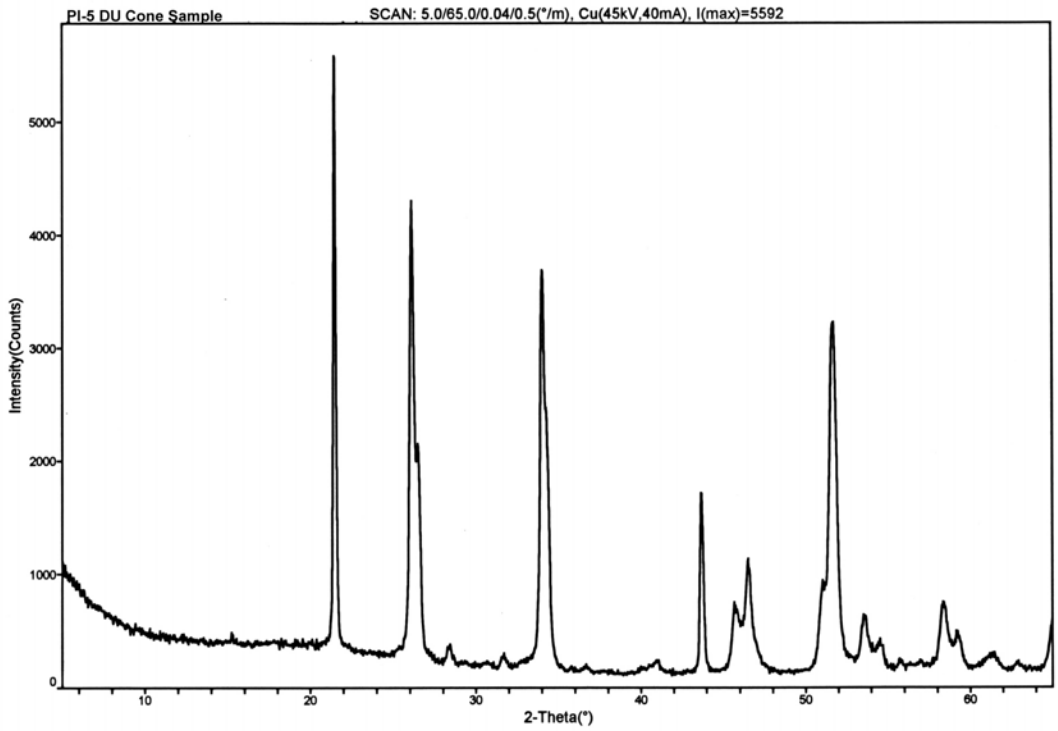

Figure C.25. XRD Pattern from PI-5 DU Cone Residue

Appendix D

Particle Morphology and Composition

Appendix D

Particle Morphology and Composition

Particle morphology and composition of selected depleted uranium (DU) aerosol samples created by vehicle perforations with DU munitions in the Capstone DU Aerosol Study were examined using scanning electron microscopy (SEM) to observe particle structure and shape. Particle compositions of these aerosol samples were evaluated using energy dispersive spectroscopy (EDS) to qualitatively examine particle chemical composition. In addition to providing a means of discerning the diversity in particle shapes, the extent of agglomerization, and the composition of individual particles/agglomerates, these analyses supplemented other analyses relating to chemical composition and particle size distribution data for cascade impactor (CI) and cyclone separators. A brief description of SEM/EDS analysis is provided in Section 3.9.6, and a summary of the results is presented in Section 4.7.4.

The samples that were evaluated included one set of cyclone residues and backup filters from Phase I, Shots 3/4 and Shot 7, from Phase II, Shots 1/2, and from Phase III, Shot 2. Also analyzed were moving filter (MVF) samples from Phase I, Shots 3/4 and from Phases II and III, four parallel-flow diffusion battery filters (PFDBs) that collected ultra-fine particles that were less than 1.2-μm aerodynamic equivalent diameter (AED), and the nearly pure pile of DU oxide from a fragment that completely oxidized (the so-called DU cone sample). Additionally, a qualitative evaluation of sample bounce was conducted determined using three Stage-3 CI substrates.

The analysis of aerosols by SEM was limited to an examination of the relative particle sizes and a determination of the particle elemental components. Analysis of the mechanisms of particle formation was outside the scope of this study, although possible mechanisms are discussed in this report for certain cases. The EDS analysis of chemical composition was performed on selected particles or agglomerates rather than on comprehensive sets of sample material. Although the EDS analysis was useful in identifying the various elements present in certain agglomerates, it was not used to quantify the concentrations or amounts of these elements.

D.1 Instrumentation and Sample Preparation

A JEOL JSM-840 SEM[(a)] was used for high-resolution imaging of micron (μm)/sub-micron-sized particles of solid DU material. The system is equipped with an Oxford Link ISIS 300 EDS[(b)] used for qualitative elemental analysis. The operating voltage for the SEM imaging ranged from 10 to 30 keV; for the EDS analysis, the conditions were changed to either 20 or 30 keV, and spectra were acquired for 100 sec with automatic correction for counting deadtimes between 20 and 30%. The EDS analysis of particles was limited to elements with atomic weights heavier than carbon (atomic number 6). High-resolution secondary electron (SE) and backscattered electron (BSE) images were obtained as digital images and stored in electronic format. All images displayed in this appendix are BSE images.

(a) JEOL USA, Inc., Peabody, Massachusetts
(b) Oxford Instruments, Whitney Oxon, United Kingdom

The sample mounts used for most SEM/EDS analyses consisted of double-sided carbon tape attached to standard aluminum mounting stubs. Sample powders were mounted by gently placing a representative sample from each sample vial onto the carbon tape. The mount was then inverted and tapped on the backside to dislodge excess material. After an initial optical inspection of the sample, the mount was coated with carbon (using a vacuum-sputter coater) to improve the conductivity of the samples and, thus, the quality of the SEM images and the EDS signals.

Analysis of the MVF, PFDB, and CI filter samples was conducted using two different techniques. Most samples were collected using a "touch grid" process to physically transfer material from the residues or the various substrates to the carbon tape. Using this transfer technique, individual particles and possibly loose particles on the sample could be collected and mounted. The second technique involved examining the filter itself by cutting out a representative section and mounting it on an aluminum stub. By taking a representative piece or segment from the filter, a view of the structure and where the individual particles were located within the structure could be observed.

D.2 SEM and EDS Results

Micrographs of particles examined by SEM analysis were reviewed, and some of the most typical and atypical samples are provided in Figures D.1 to D.29 to represent images of the particles collected. Over the course of the analysis, there was one significant change in how the EDS data were evaluated. In some of the samples, the voltage was changed from 20 keV to 30 keV. This voltage increase improved detection of the uranium peaks at 13.5, 16.3, and 17.3 keV and also helped identify some of the minor elements present in the material (e.g., copper and zinc). The disadvantage of using a higher voltage was a loss of image detail at the surfaces due to enhanced beam penetration. At lower voltages, surface structural details were more clearly defined.

EDS analysis was used to qualitatively evaluate the elemental compositions of selected particles. No attempt was made to quantify or even to qualitatively evaluate the chemical constituents in any given sample. Aside from some generalizations, including the typical oxide composition of the samples, only the contents of a single particle or agglomerate were evaluated for composition. When we refer to samples in this report as "amorphous looking," we are not suggesting a quantification of amorphous material, which is outside the capability of the SEM/EDS evaluation. Rather, we are suggesting that those samples lacked any faceted particle shapes characteristic of crystals. Other words used to describe a group of particles in the samples evaluated by SEM include aggregates, conglomerates, and agglomerates. In this context, they have similar or overlapping meaning. "Agglomerates" is the default used most commonly in the following text. "Aggregates" suggests a looser group of particles than agglomerates and is typically defined as a mixture of particles that can be separated mechanically. "Conglomerates" suggests particles that appear to have been cemented together.

General results of the chemical matrices are discussed below.

D.2.1 Cyclone Residues

The residues from 19 cyclone grit chambers, which collected samples throughout the 2-h, post-shot period, were evaluated by SEM/EDS analyses. Cyclone Stages 1, 2, 3, 4, and 5 collected material with particle sizes greater than 10, 4.3, 2.9, 2.0, and 1.2-μm AED, respectively, for cyclone flow rates of about 10 Lpm. For flow rates closer to 14 Lpm, the cutoff points decreased to 7.8, 3.2, 2.3, 1.2, and 0.7 μm,

respectively. Micrographs of these samples were taken at relatively low magnification to provide an overview of particle sizes and morphologies, and at high magnification to view individual particles and small particle groupings. As the particle image contrast in the BSE mode used in most of the micrographs is sensitive to average atomic number of the constituent elements, particles containing heavy elements such as uranium appear very light colored in the SEM images. By contrast, particles composed of light elements such as aluminum appear dark in the BSE images. The various aerosol samples showed significant heterogeneity in particle size and shape. Extensive particle agglomeration is visible in these samples.

There was not as much demarcation as expected between the particle size distributions collected from the various cyclone stages and little apparent correlation between adjacent stages and their associated aerodynamic diameter cut-off points. For example, the micrographs in Figure D.1 (page D-14) show particles from Stages 1 through 5 from Phase I, Shot 3/4. These micrographs were selected because the same scale (i.e., 40 µm) was used in each image. Considerable overlap in particle sizes collected was apparent in these micrographs. Note that the number of particles shown in the micrographs varies considerably and is not related to the total quantity of particles collected in the stages. Also, note that the contrast used in the micrographs varied.

The EDS analysis suggests that all the samples were composed of a basic chemical makeup that included uranium, aluminum, iron, and oxygen (oxide) particles along with lesser amounts of other elements. Quantifying the EDS data was not practical because of the structure of the material and the different particle geometries. Uranium was associated with almost every particle or particle matrix evaluated, either as a pure or nearly pure uranium oxide or as an agglomerate with other metal oxides. Uranium combined with aluminum predominated. Iron and elements typically associated with steel also were present, and titanium from the penetrator uranium alloy consistently was identified as a minor presence.

Uranium particles formed during the course of the tests varied greatly in morphology, ranging from fractured-looking material to small or medium-sized spheres. Representative uranium particles and particle agglomerates are shown in Figure D.2. Views (a) through (f) are from PI-3/4. Micrograph (a) in Figure D.2 includes a large fracture-type uranium particle and small spherical uranium particles above and to the right of the large particle recovered from Stage 1. View (b) from Stage 1 is typical of a fairly dense mixture of uranium spheres and uranium and aluminum oxides. View (c) from Stage 2 shows particle agglomerate made up primarily of uranium and aluminum. Many uranium mixtures similar to those shown in view (b) and view (c) are less dense and have a diffuse or cottony appearance. View (d) from Stage 1 displays several types of common uranium particles including one with a fracture-type appearance at the far left and spheres of assorted sizes. Above and to the left of the agglomerate present in view (e) from Stage 2, which consists mostly of uranium, aluminum, and iron, is a spherical formation consisting of uranium particles and voids. View (f) from Stage 2 of Phase I, Shot 7 contains a particle with a fractured and cratered surface that provides a larger surface area than the particle in shown in View (a).

Generally, there were few distinguishable differences in morphologies among the powder particles examined. The loose particles all had similar amorphous-looking structures that contained spherical uranium particles within the structure. In all the samples examined, uranium was present primarily as an oxide phase, although some samples appeared to contain low-oxygen-content solid particles that are suggestive of metallic structures. The oxygen content of most particles was within the range expected for uranium oxides.

Some of the uranium spheres included either a dendritic or fine-grained structures. A dendritic structure forms when a particle slowly cools as it passes through the liquid state to the solid state. These uranium spheres could be compared with residual particles that form during a gunshot. The residual particles, which originate mostly from the primer composition of the cartridge, are spheroidical in shape. They are formed at high temperature, where the surface tension of the molten residue droplets contracts them into spheroids prior to solidification. These particles are relatively small because they are created under explosive conditions—first under high-pressure conditions inside the firearm and then suddenly under lower atmospheric pressure at which time the particles expand.

A micrographic illustration of particles and agglomerates from each phase and shot follows along with a description the morphology and composition of each cyclone residue stage sample evaluated. The smaller particles collected on the cyclone backup filters and PFDB filters are discussed separately at the end of the section.

D.2.1.1 Phase I, Shots 3/4 (PI-3/4)

The particle size distributions of the residues collected after the PI-3/4 shots are illustrated in Figure D.1. In addition to the particles in Figure D.2, views (a) and (b) above, more particles/agglomerates from the PI-3/4 cyclone stages are shown in Figure D.3, views (a) through (e). View (a) is from Stage 1; view (c) is from Stage 2; view (d) is from Stage 3; and views (b) and (e) are from Stage 5. View (f) provides a micrograph of the particle size distribution recovered from Stage 5 using higher magnification than presented in Figure D.1. Observations of the cyclone residues by stage follow.

- Stage 1: This sample contained large pieces that appeared to be fractured uranium metal and spherical particles containing uranium and oxygen. Some of the spherical particles show a dendritic grain structure. A few particles appeared to contain a material deposited on the surface. Other common elements in this sample were U, Al, O, and Fe.

- Stage 2: This sample contained some large particles, including some that looked like fractured metallic pieces. It also contained some smaller particles that looked amorphous. A spherical particle large enough for imaging and EDS analysis was present in this sample, and the morphology of the particle indicated that it had a dendritic or grainy structure. The most common combinations of elements found in this sample were U, Al, and O and U, Al, O, and Fe.

- Stage 3: The particles in this sample were generally spherical, with particle diameters ranging from 1 to 20 μm. The entire sample had an amorphous appearance, and the larger particles appeared to be a conglomerate of smaller particles. The BSE images revealed very small (1 μm or less in diameter), distinctive particles of uranium oxide. The EDS analysis revealed that the sample was made up of U, Al, Fe, and O, with minor Mg, Cu, and Si.

- Stage 4: This sample appeared to be amorphous and was similar to the material collected on Stage 2. The same geometry and size distribution of particles were evident. Uranium oxide particles 1 μm and smaller were dispersed within the matrix. The particles were a fairly consistent combination of U, Al, Fe, and O.

- Stage 5: The particles in this sample generally had a finer particle distribution (1 to 5 μm) than the particles in other samples. There were a few particles larger than 10 μm and some spherical particles

that were <1 μm in diameter. The particles generally had an amorphous appearance. The common composition of the particles sample was U, Al, O, and Fe.

D.2.1.2 Phase I, Shot 7 (PI-7)

Particle size distributions in the samples for PI-7 are shown by stage in Figure D.4, again using a relatively low magnification that gave a 40 μm per inch scale. The first stage had a high number of spherical particles and less uniform structures with discernable grains—Figure D.5, views (a) through (d). Particles collected in Stage 2 and Stage 4, respectively, appeared to have a slightly melted and fractured metallic appearance and are shown in views (e) and (f). Observations of the morphology and composition of residues in the individual stages follow:

- Stage 1: A variety of different types of particles were associated with agglomerates in this sample from Stage 1. Generally, the particles had an amorphous structure, and some larger particles >40 μm in diameter were observed. Some solid spherical particles also were observed, and the larger particles appeared to consist of a fine grain structure. This solid material contained Fe, Al, Si, Cu, Zn, and Ti, with very little U present. The more typical composition was predominantly U, Al, O, and Fe.

- Stage 2: The particle sizes in this sample ranged from 1 to 40 μm in diameter. The particles generally had an amorphous structure. Some spherical uranium particles and uranium metal shards were also contained within the sample. Typically, the particles consisted of U, Al, O, and Fe, with some containing titanium.

- Stage 3: The particles in this sample were very similar in size, distribution, and chemistry to the particles found in the Stage 2 sample. The main difference was that there were no metal pieces or any other types of material in this sample. All particles viewed consisted of loosely populated to tightly packed aggregates.

- Stage 4: The size distribution of particles in this sample was uniform within the 10 to 20 μm range with some smaller particles observed. The particles appeared to be amorphous, and some uranium spheres were also present. More Al was present in this than in some of the other samples, but the main composition of the particles was U, Al, O, and Fe. Mg, Fe, and Si were also present.

- Stage 5: This sample consisted of fine particles that generally were <10 μm in diameter. Again, the particles were amorphous and contained some spherical particles of uranium that were <1 μm in diameter. The same general chemistry was observed (i.e., U, Al, O, Mg, and Fe were the primary elemental constituents).

D.2.1.3 Phase II, Shots 1/2 (PII-1/2)

The particle size distributions from the samples collected in PII-1/2 are illustrated in Figure D.6. Residues in these samples contained agglomerates of a range of particles that resembled those from Phase I and some particles that were unique to Phase II. Because the shots hit the Bradley spall liner, fibers of this material were suspended inside the vehicle, and a few fibers were collected in the cyclone. Additionally, particles with a three-dimensional star morphology that contained various fractions of uranium and aluminum were collected in the lower stages of the cyclone. Some of the representative and

unique particles from the PII-1/2 shots are shown in Figures D.7 through D.10. Views (a) through (e) in Figure D.7 are from Stage 1. Views (a) and (b) are different magnifications of the same grain structure. Views (c) and (d) are different magnifications of what is believed to be a fiber from the spall liner. Small spheres of uranium appear to be attached to the fiber. View (e) shows a sphere in which aluminum is dominant. In view (f), which is from Stage 2, dendritic structures are visible.

Figure D.8 contains particles similar and dissimilar to previous particles. Views (a) through (d) are from Stage 2. Views (e) and (f) are from Stage 3. Views (a) and (b) in Figure D.9 are from Stage 4. Views (c) through (f) are from Stage 5. The star-shaped particle in view (c) is predominately uranium with aluminum present. View (d) contains uranium and aluminum, but in this case, aluminum is dominant. The six views in Figure D.10 are from Stage 5.

Descriptions of the samples by stage follow:

- Stage 1: Most of the agglomerate-like material in this sample had a structure that mirrored the structure found in previous samples. The spherical particles material contained small grain/dendritic structures. The same elemental constituents were present, although the aluminum concentration may have been higher in this sample than in others. Some differences in the chemistry and shapes were related to the aerosol matrix. In addition to the uranium, the overall sample included elemental groupings of 1) Fe, Si, Al, Ca, Mg, Ti, and O; 2) Al, Si, Ca, and O; and 3) Fe, Al, O, and Si. The shapes tend to be elongated and look like pieces of fragmented material.

- Stage 2. The average agglomerate size in this sample was in the approximate diameter range of 10 to 20 μm with some larger pieces over 40 μm in diameter. The larger agglomerates tended to consist of smaller, tightly packed particles and appeared to be denser than the agglomerates in other samples. The spherical pieces had unique structures; one of the spheres contained a snowflake-like structure and had an elemental composition that included U, Al, and O. Generally, the basic elemental composition of the material found in this sample was the usual U, Al, O, and Fe. However, some of the agglomerates were composed of Si, Al, Mg, Fe, U, and O; Mg, Si, Al, and O; and Si, Al, Mg, K, Fe, Ca, Ti, and O.

- Stage 3. The material in this sample ranged in size from 5 to 40 μm and, for the most part, was similar to that collected in the other cyclone stages during these test shots. The sample had the same type of agglomerate structure, and the composition typically included U, Al, oxides, Fe, and Mg. In a few of the agglomerates, the chemical makeup varied somewhat, but the geometry and morphology did not appear to differ much from that of the other samples. The different chemical compositions involved particulates that contained Si, Al, Ti, and O; Cu, Zn, and O; and one particle that contained lead (Pb) along with the other elements present that typically are present.

- Stage 4. The geometry of the material in this sample was consistent with that in other samples. The same agglomerate-like morphology and chemical makeup (U, Al, Fe, O, Mg, and Si) were found. The material tended to have an average diameter of 10 μm, and no unusual material was observed.

- Stage 5. In this sample, unusually large and odd-shaped agglomerates were present along with the typical round agglomerates. The larger agglomerates, 30 to 50 μm in diameter, were star-shaped and had a glassy appearance. The composition of these agglomerates had a higher peak ratio of

aluminum to uranium than the other material evaluated. Some metallic uranium, copper, and zinc particles were found in this sample.

D.2.1.4 Phase III, Shot 2 (PIII-2)

This shot in which the Abrams tank DU armor was perforated by a DU penetrator contained particle/agglomerates similar to Phase I particles. There were also some morphologies unique to this phase. For some reason, the Stage-2 grit chamber collected only a negligible quantity of material, and the Stage-3 chamber collected much less than was expected. We were concerned that a leak might have caused this lack of sample collection, so we resuspended and recollected the total sample. Again, essentially no material was collected in Stage 2, and only a very small amount of material was collected in Stage 3. Particle sizes distributions from Stages 1, 3, 4, and 5 are shown in Figure D.11. The Stage-1 sample is shown with a scale of 40 μm per inch in the full size micrograph. The scale on remaining micrographs is 20 μm, indicating twice as high a magnification.

Some rather unique particles from Stage 1 are pictured in views (a) through (f) of Figure D.12. Both the nearly square (possibly cubic) particle and the spherical structures in view (a) are uranium oxide, the primary constituent in the material shown in the other views. An overview of particle sizes from Stage 2 is shown in view (a) in Figure D.13. View (b) of that figure shows a loose aggregate of aluminum "cloud" structure with multiple sizes of uranium spheres. View (c) shows a denser aggregate of uranium, aluminum, and iron. A similar structure, though with finer detail, is shown in view (d). View (e) clearly shows a large void in an otherwise spherical grain shape, and view (f) consists of particles with dendritic structures. Figure D.14 provides an overview of the particle sizes in view (a) and various particle agglomerates in views (b) through (e) from Stage 4. View (f) shows the particle sizes from Stage 5.

Sample descriptions by stage are provided in the following text.

- Stage 1: Spherical particles were a predominant feature in this sample. There was some agglomerate structure associated with the sample, along with some solid pieces of material. The general chemical composition included U, Al, Fe, O, and Si. Some of the spherical particles contained Fe, Ni and O; and Ti, Al, and Si. Still other particles contained Si, Mg, Al, and O.

- Stage 2: There was essentially no material collected in this stage.

- Stage 3: The material in this sample had the same general structure as found in Stage 1, but the spheres appeared to be larger than the agglomerated particles. Still, the structure contained fine particles in the 1- to 10-μm range. There were some differences in chemistry in this sample. A few of the spherical particles contained Fe/Ni rich chemistry, but again the general chemical makeup of both the particles and the agglomerate structure was a combination of U, Al, Fe, O, and Si.

- Stage 4: The same general agglomerate structure was found in this material with spherical uranium particles dispersed within the structure. The particle size range was 1 to 10 μm, with some particles >40 μm. No unusual morphology was found in this sample, and the chemical makeup was the typical combination of U, Al, Fe, Si, and O.

- Stage 5: An even distribution of particles in the 5- to 10-μm range was visible in this sample, which had an agglomerate structure with spherical uranium particles and a few pieces of uranium metal

dispersed within the structure. A few particles also contained an iron impurity. Chemically, the material in this sample contained U, Al, O, Fe, Si, and Mg.

D.2.1.5 Backup Filters

In all but the first shot (PI-1), small particles passing through the Stage 5 grit chambers were collected on a set of four parallel (assumed to be identical) backup filters. Samples collected on two separate filters were examined for the Phases I and II shots, and a sample from one filter was examined for the Phase III shot.

D.2.1.6 PI-3/4

The particle size distribution of the material collected on these backup filters is illustrated in Figure D.15, view (a). The morphology of typical particle aggregates is shown in views (b) through (f). The two filter samples were very similar. They contained fine particles and larger particles that appeared to have been formed from small particles "caked" together. The typical elemental composition of these samples included Al, U, O, Fe, Mg, and Si. Some calcium was noted in one of the samples.

D.2.1.7 PI-7

A view of the material on a backup filter surface is shown in Figure D.16 view (a). The morphologies of several particle aggregates are featured in views (b) through (d). The trapezoid structure at the lower edge of the mass in view (b) is especially concentrated with uranium, and its oxygen content was low. This sample was very similar to the backup filters in PI-3/4. It contained fine particles that were <1 or 2 μm in diameter and were joined together to form larger pieces. The particles had no real structure, and dimensionally appeared to be either very thin sections or compacted material consisting of smaller particles forming dense, thick particles. The larger pieces had some unusual shapes. Some of these particles appeared to be very dense, while other particles had a very porous structure. The typical elemental composition (Al, U, O, Fe, Mg, and Si) was apparent in this sample, although it may have contained more aluminum than samples taken from the backup filters described above.

D.2.1.8 PII-1/2

The material collected on the backup filters from this shot closely resembled the material collected for shots PI-3/4 (see Figure D.16, views (e) and (f)). This sample consisted mostly of large pieces, 50 to 100 μm, that appeared to be agglomerates of fine particles <1 μm in diameter. The sample from these filters contained fewer spherical particles than the samples from other filters, and the material contained a higher concentration of aluminum than uranium. Copper and zinc were also present in the matrix. In

addition, a few particles contained a combination of aluminum, sulfur, chlorides, and oxides, with very little uranium. One speculation is that a combination of heat and vapor pressure was involved in the formation of the large particles.

D.2.1.9 PIII-2

Examples of particle morphologies from the backup filters for shot PIII-2 are shown in Figure D.17. Views (a) through (d) show the filter surface at different levels of magnification. Views (e) and (f) are direct views of collected residues that contain a high concentration of uranium particles. For the most part, the particle concentration on this filter was loose and thinly populated; however, in some areas, the particle distribution was tightly packed, and the particles had a dense appearance. The elemental composition of the material in this sample was fairly uniform, with the typical combination of U, Al, Fe, and O, with some Cu, Zn, Ti, and Mg elements present.

D.2.1.10 Diffusion Battery Filters

In the PI-1 test, a parallel flow diffusion battery was used. The PFDB filters collected seven samples of increasingly smaller particle size using a stack of screens to selectively remove smaller and smaller fractions. SEM analysis was conducted on the coarsest fraction (sample 7), which is the only fraction for which a screen is not used, and on samples 2, 4, and 6 for which an increasing number screens were used to exclude all but the smallest particles. The surface of these samples had a brown glazed appearance. Sample 4, which contained the smallest particles, contained some sulfur-rich material, probably originating from the filter. Figure D.18 shows views of the filter surfaces at varying levels of magnification. The material found on the PFDB filters from this test is described below beginning with the coarsest particles and ending with the finest.

Sample 7 (no screens, views a and b): The particles collected in this sample included all sizes <1.2-μm AED. This material displayed a different morphology than the material collected in the cyclones; however, the chemical composition did not differ significantly. The morphology of particles in some areas of the filter appeared to be dense (i.e., tightly packed with particles). In some of the areas of the filter, the collection of particles had a "broken up" appearance similar to that of a clay surface that had dried and cracked. Spherical uranium oxide particles were present in the matrix, and some of the higher magnification images show an amorphous-type structure. The chemical composition of the material in this sample was consistent with the cyclone residues.

Sample 2 (15 screens, view c): This sample was observed both as a transfer of particles onto carbon and by directly examining a section of the filter. The transfer of particles onto carbon included a random mixture of particles with different chemical compositions. The filter appeared to have an even coating of the aerosol particles. Results of the EDS analysis were fairly consistent with elements present in the cyclone samples though some of the elemental proportions differed in some instances.

Sample 4 (25 screens, views d and e): Some of the particles collected on this filter resembled particles found in the cyclone residues. Material in the sample had an amorphous structure that contained a high concentration of uranium particles. A few sulfur particles were observed in the chemical analysis, but

overall the composition was U, Al, Fe, O, Si, Mg, Cu, Zn, and Ti. Observation of the top surface of this filter revealed a few differences in the morphological structure but no differences in chemistry. The particles deposited heavily around the filter pores.

***Sample 6 (35 screens, view f)*:** A few different types of particles appeared during chemical analysis. Again, the particles from this filter appeared to be amorphous with very fine particles (<1 μm) caked together to form a large particle structure. The particle composition was characteristic of salt and consisted of combinations that included sulfur/oxygen, silicon/oxygen, and calcium/potassium/silicon. The filter itself had a glassy appearance. Two adjacent areas with distinctly different appearances were examined and compared. One area, which had a glassy appearance, contained U, Al, Fe, O, and Si; the other area, which may have been in the groove of the filter, appeared to be brighter in BSE mode and contained a high sulfur peak. The sulfur probably originated from the Supor filter.

D.2.2 Cascade Impactor Substrates

The first stage substrate in the CIs was sprayed with silicon to minimize particle bounce from the top stage. (Particle bounce refers to the phenomenon occurring when a particle approaches the collecting surface of an impactor stage and rebounds instead of staying on the surface. Particle bounce could occur if the kinetic energy of the particle exceeds the attraction force between it and the filter surface.) The remaining MCE substrates were untreated. In response to a question regarding whether particle bounce was a concern in the lower stages, three Stage-3 substrates were examined using SEM to observe the particle size consistency and determine if a wide spread of particles was collected along the slot lines. The aerodynamic cutoff diameter for Stage 3 was approximately 10 μm. Several low magnification micrographs were taken to help evaluate the spread of particles and to observe how tightly they were stacked. Two magnifications at a scale of 400 and 100 μm, respectively, are presented in Figure D.19 for each of the three Stage-3 substrates. Views (a) and (b) are from PI-7, views (c) and (d) are from PI-1, and views (e) and (f) are from PIII-2. Although the magnification was slightly too high to observe the full slot lines, from what can be viewed, it does not appear that particle bounce was significant in these samples.

The CIs provide a narrower particle size separation than the cyclone stages, and this effect is visible in the SEM micrographs of these three CIs. The spheres appear to be fairly consistent in size. Although the magnification in these micrographs is not quite low enough to determine the extent of particle bounce that occurred, there is little evidence to suggest that it was significant.

The following observations describe the visual and chemical nature of the individual CI samples.

- ***PI-7 (gunner's position, first time interval—5 to 15 sec post-shot):*** This sample consisted small, 5- to 10-μm diameter spheres often separated by an amorphous-type structure (see Figure D.20, view a). Some of these spheres are shown in views (b) through (f). The ratio of compositions varied in the spheres with some spheres showing a predominance of aluminum, with some uranium and iron present (see view c) and some containing titanium, copper, and zinc. The compositions observed in these samples included U, Al, O, Fe, Mg, and Si; U, Al, Ti, O, Fe, and Cu; and Si, U, Al, Ca, Fe and O.

- ***PI-1 (loader position, second time interval—35 sec to 1 min, 35 sec post-shot)*:** A combination of spheres and irregularly shaped material was observed (see Figure D.21, views a through f). Some of the spheres appeared to be glued or fused together by a combination of materials. The results from the EDS analysis showed the material to be composed of Si, Al, Mg, K, Fe, Ti, and O and Si, Al, Ca, Fe, Mg, and O, with very little U present. The general chemical composition of the spheres was a combination of U, Al, Fe, and O, along with some Mg and Si.

- ***PIII-2 (commander position, second time interval—1 min, 5 sec to 1 min, 15 sec post-shot)*:** This sample consisted of spheres and combinations particles that appeared to be glued or fused together (see Figure D.22, views a through f). The particles/agglomerates ranged from 1- to10-μm. Some of the spheres were composed of a Fe, Cr, O, U, Ti, Fe, Al, and O combination. Several other particles contained high concentrations of Ti, Fe, and Si associated with the other elements present.

D.2.3 Moving Filters

Three moving filter segments, all taken from the first time interval, were evaluated using SEM and EDS. These three samples included the first segments from PI-1 and PIII-2 and the third segment from PII-3. Descriptions of these samples are provided in the following discussion:

- ***PI-1:*** The first segment in the PI-1 moving filter sample collected sample material during the first 5 sec after impact. The filter was stationary during sample collection. Some particulate material was removed from the filter and examined (see Figures D.23 and D.24). No direct observations were made of the filter surface, but it was prepared as a cross-section sample to determine whether any additional useful information might be revealed. The cross section was prepared using a multi-step process that began by cutting a section of the filter and mounting it between two glass slides. The slide assembly then was placed in a standard metallography resin. In preparation for SEM observation, the sample was polished to a 1-μm surface roughness and coated with carbon.

  The SEM analysis revealed a fairly uniform U/Al/Fe/O coating across the filter. The coating thickness was ~30 μm and was relatively uniform over the surface as illustrated in a cross-sectional montage of the width of the filter medium. This analysis helped identify the particle chemistry and the binding material for the uranium particles. Also, the homogeneity of the particles was revealed, thereby identifying the various particles as solids or as having some porosity to the structure. Some solid particles contained an iron base with a uranium phase on the outside (see view c). Of the other particles in which the uranium predominated, a general porous structure was apparent.

- ***PII-3:*** This third filter segment collected aerosol samples in the time interval between about 6 and 9 sec post-shot. The filter moved at a speed of about 0.88 cm/sec (20.9 in./min). SEM observation was conducted on the filter itself, and no particle transfer analysis was performed (see Figure D.25). Film thickness/depositions on the filter looked fairly thin, perhaps in the 10- to 20-μm range, with some spherical and odd shaped pieces imbedded in the matrix. The composition of the bulk material showed a high concentration of Al, Si, U, Fe, and O in the matrix. A few spherical particles were composed of Ca, Al, Si, Fe, and O or Si, Al, Ti, U, Fe, and O. A few of the odd shaped particles that contained iron and oxygen possibly were iron oxide particles.

- ***PIII-2:*** This filter segment covered the initial time interval (0 to 3 sec) with the filter moving at a speed of about 0.88 cm/sec (20.9 in./min). Sample collection occurred during the first three seconds

post-shot. The samples collected on this filter differed from other MVF samples observed in that there appeared to be more spherical particles and odd shaped particles within the matrix in this sample (see Figure D.26). The chemistry of single particles appeared to be very consistent with larger-scale EDS scans within this sample. The major elements present included U, Al, Fe, and O, with Si, Cu, Zn, Ti, and Mg present in minor concentrations.

A montage of cross-sectional segments was also made of this sample and is shown in Figure D.27. The montage was developed to evaluate the general uniformity of uranium deposition and to examine it for changes in the appearance of this deposition with time as the filter moved. The white striation indicates the presence of uranium. Although the segments are presented in order, they are not continuous (i.e., there is some time lapse between each set of two). Because the segment cut from the filter tape was placed in a PetriSlide without an identifying mark noting which end was at the beginning of the tape, it is not known which segment designated “end” was actually the beginning. A closer look at various particles photographed in cross section are shown in views (a) through (f) in Figure D.28.

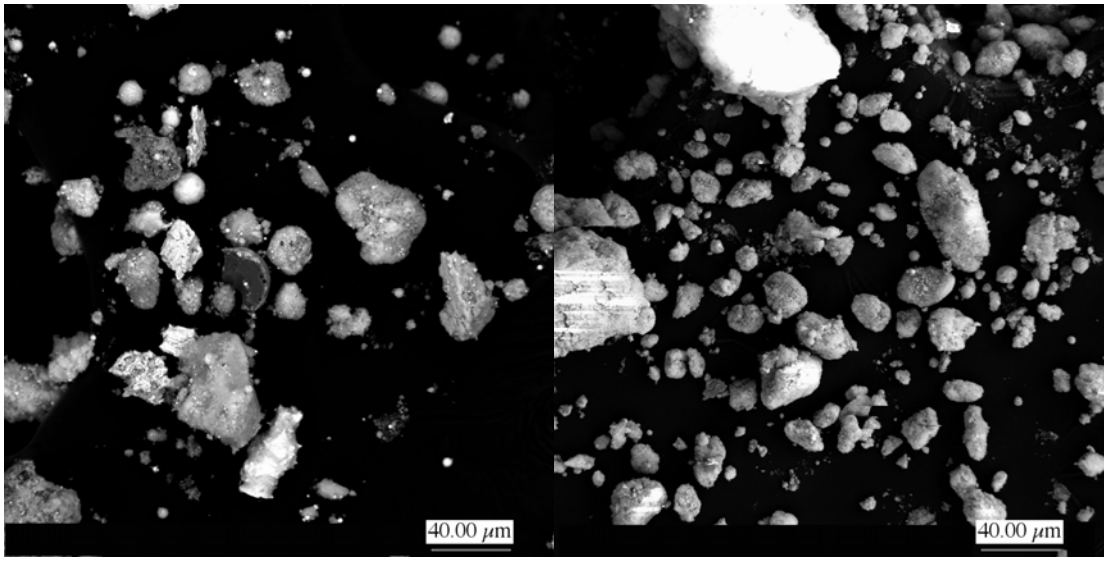

Stage 1 Stage 2

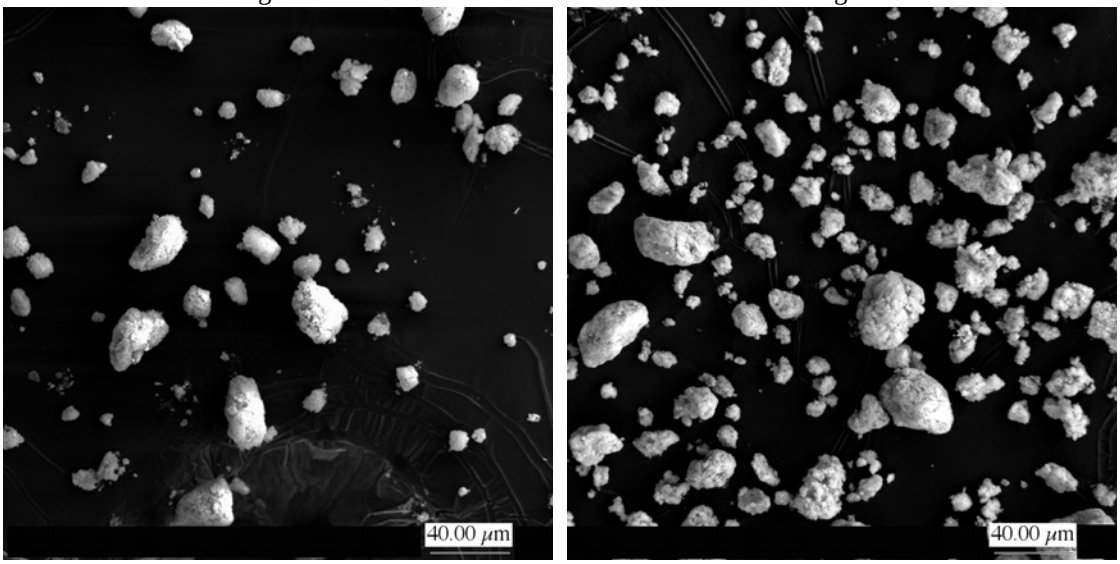

Stage 3 Stage 4

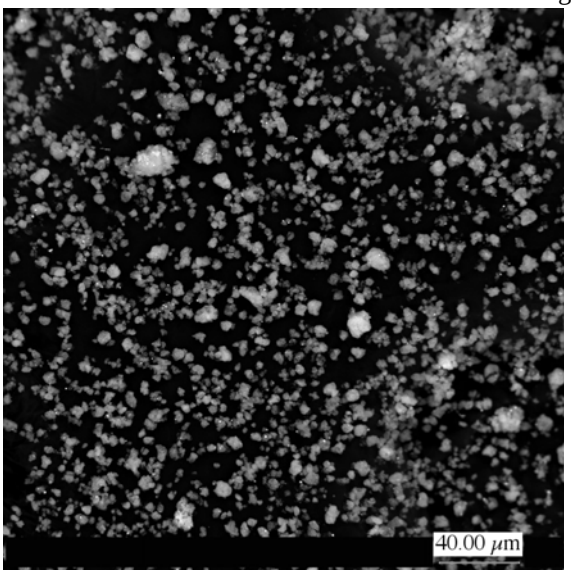

Stage 5

Figure D.1. Low-Magnification Overviews of PI-3/4, Stages 1 to 5, Using Same Scale

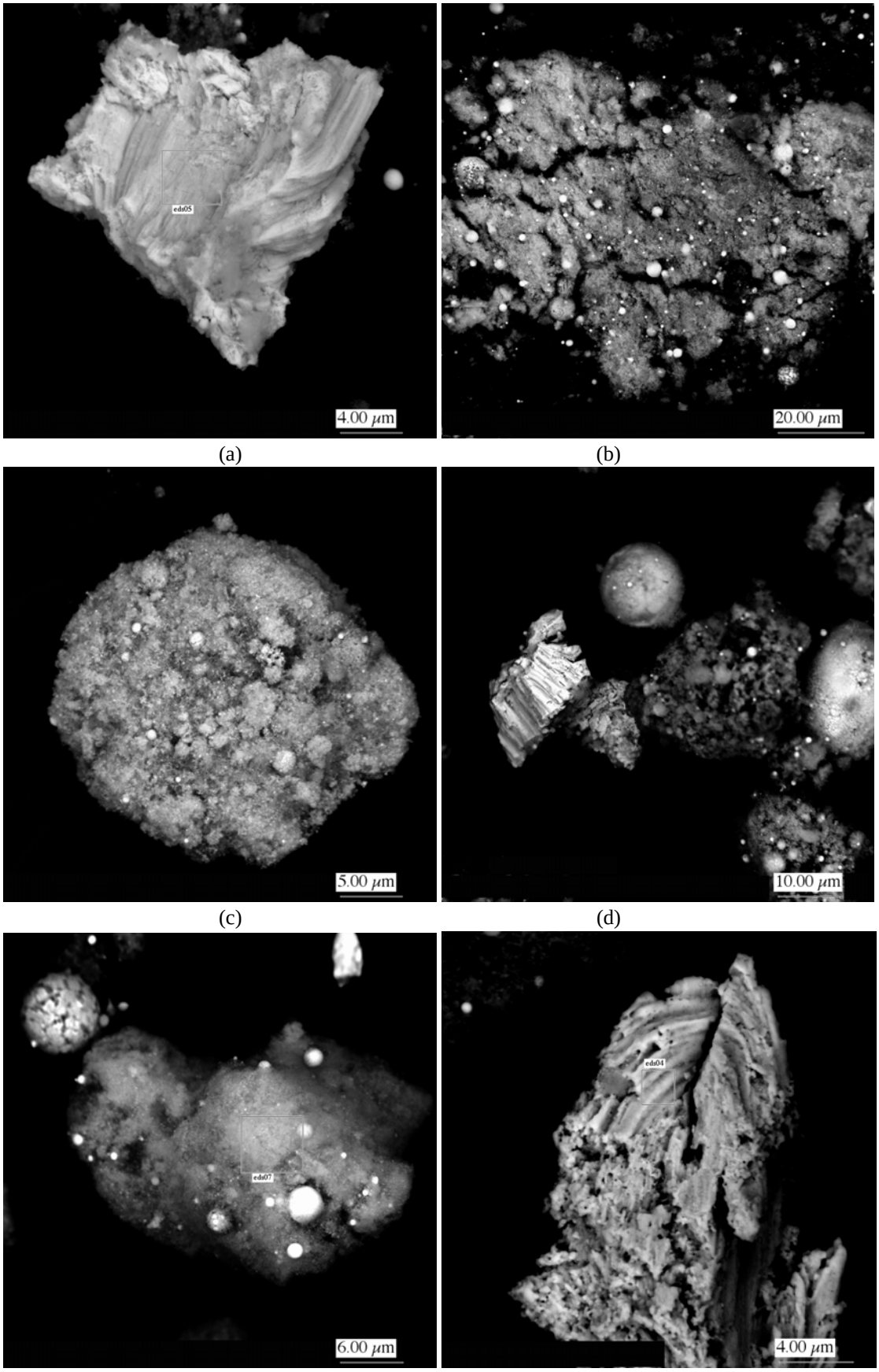

(a) (b)

(c) (d)

(e) (f)

Figure D.2. Typical Uranium Particles from Phase I

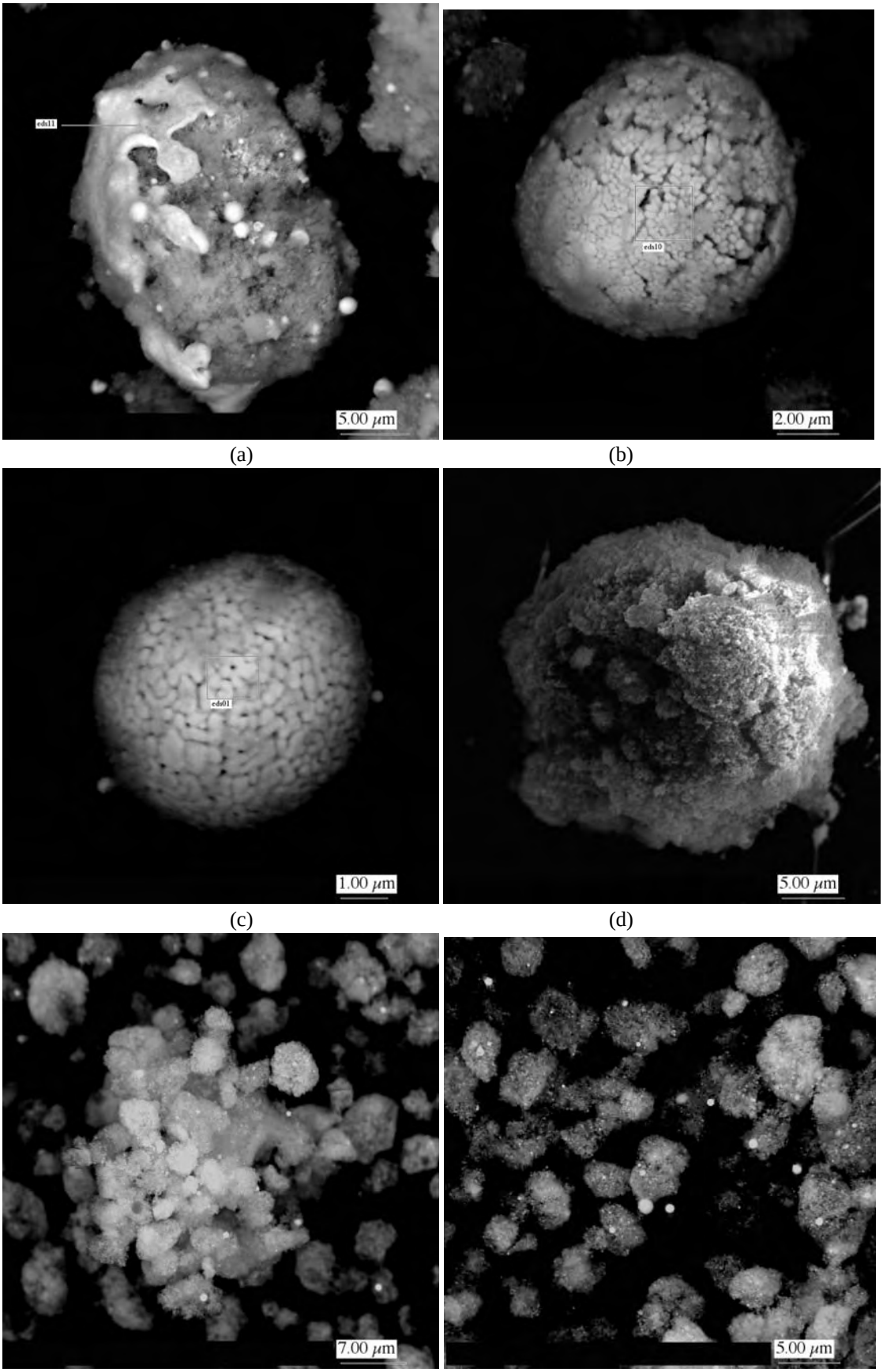

(a) (b)

(c) (d)

(e) (f)

Figure D.3. Additional Phase I Particles

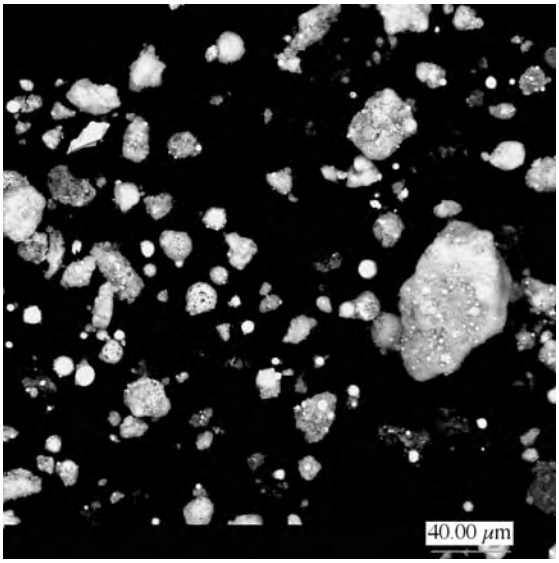

Stage 1

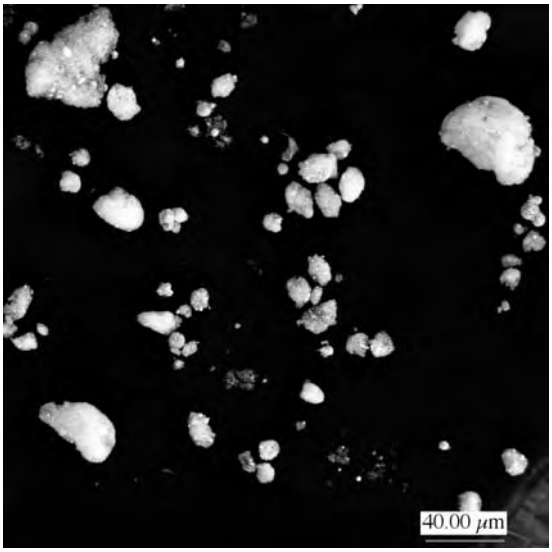

Stage 2

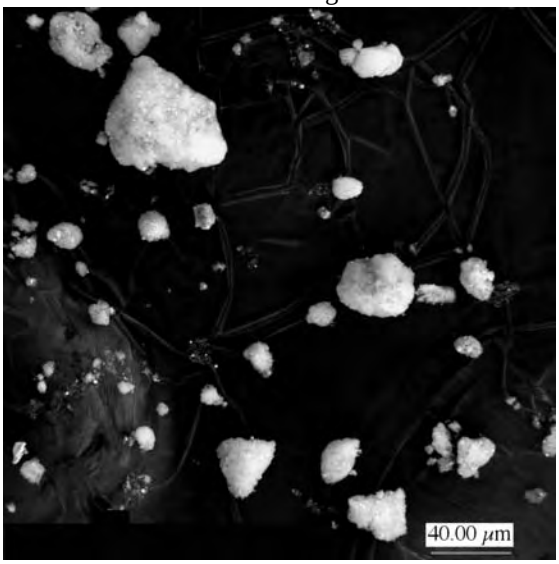

Stage 3

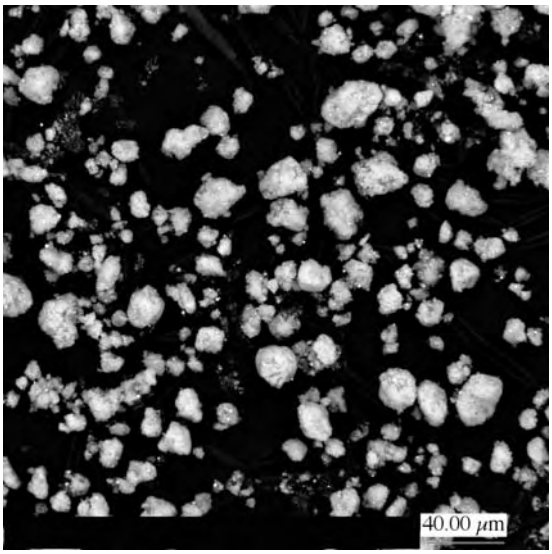

Stage 4

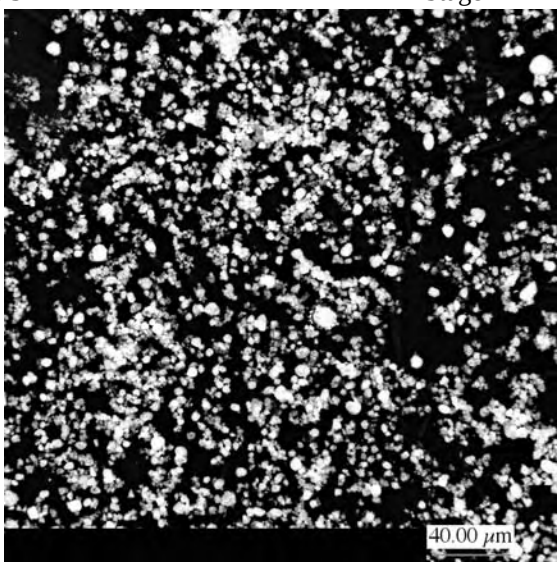

Stage 5

Figure D.4. Low-Magnification Overview of PI-7, Stages 1 to 5, Using Same Scale

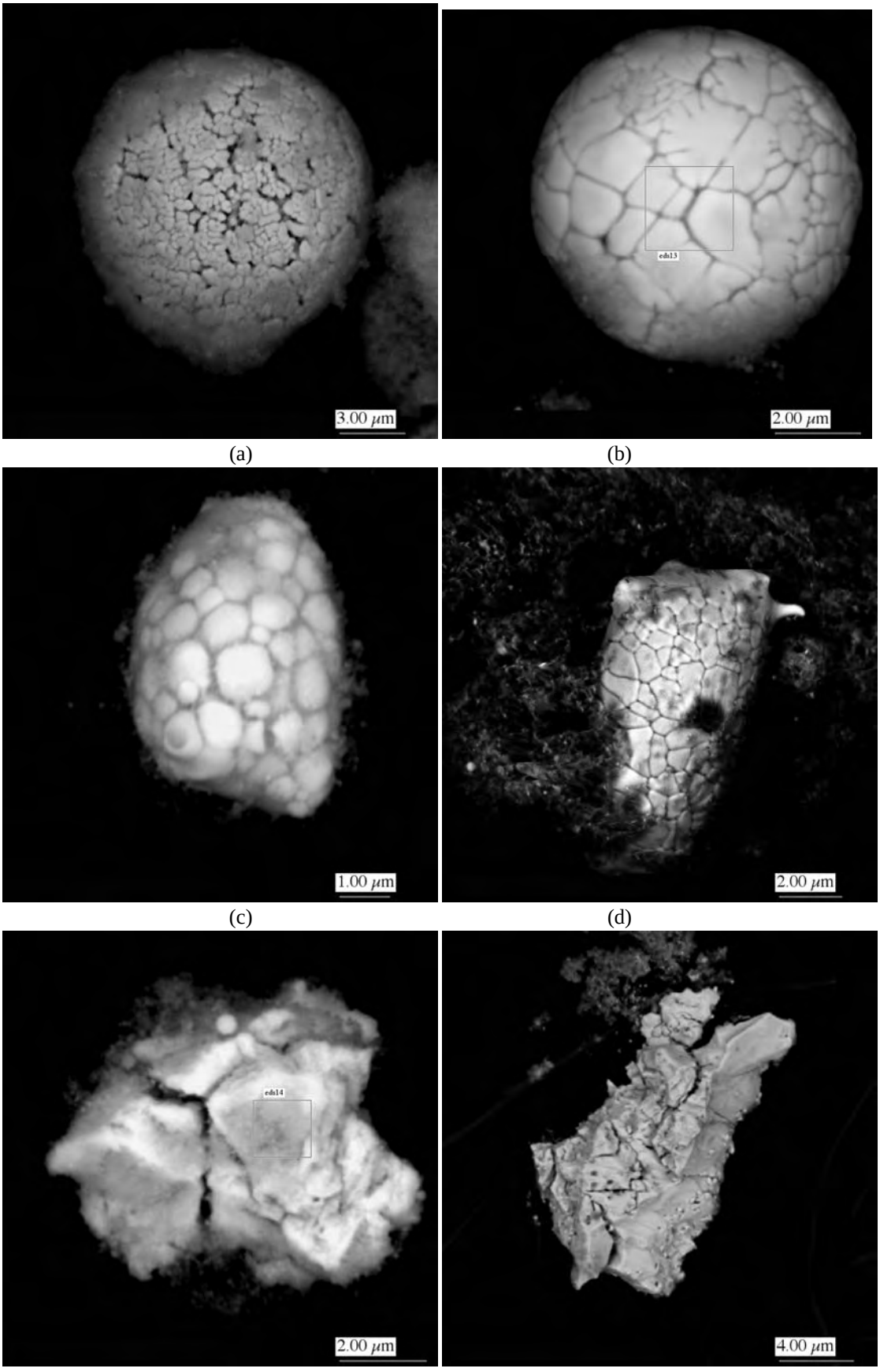

Figure D.5. Grain-Like Particle Formations and Fissures from PI-7

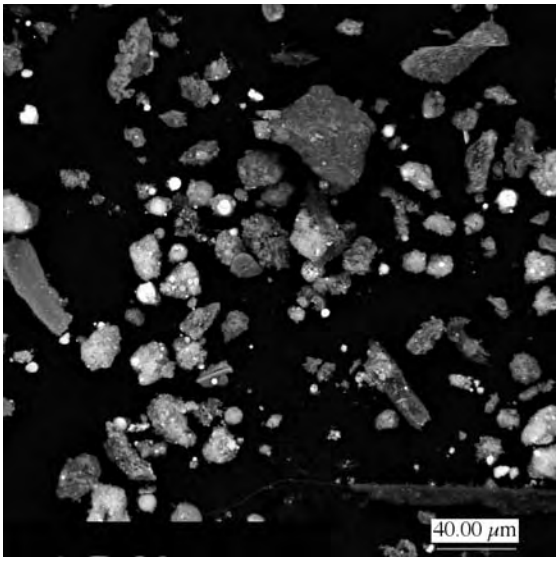

Stage 1

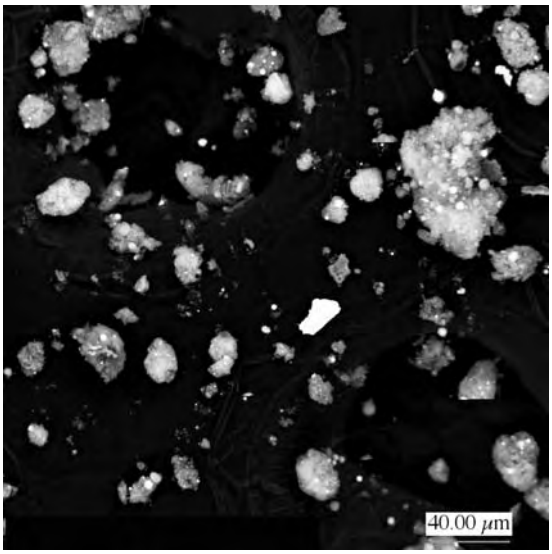

Stage 2

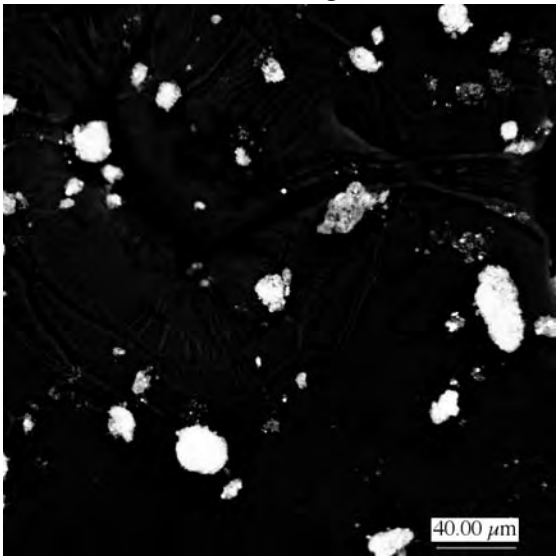

Stage 3

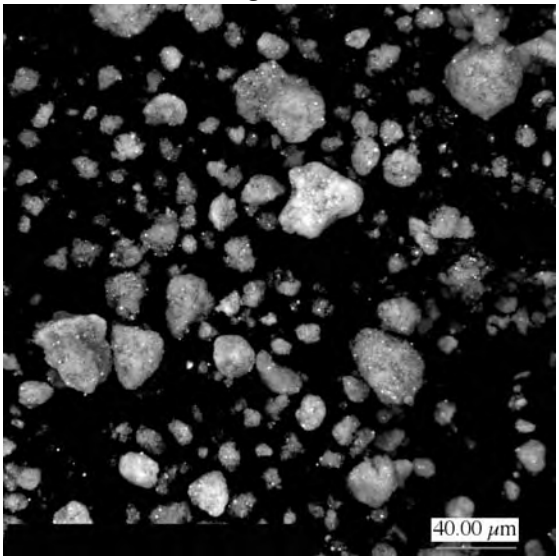

Stage 4

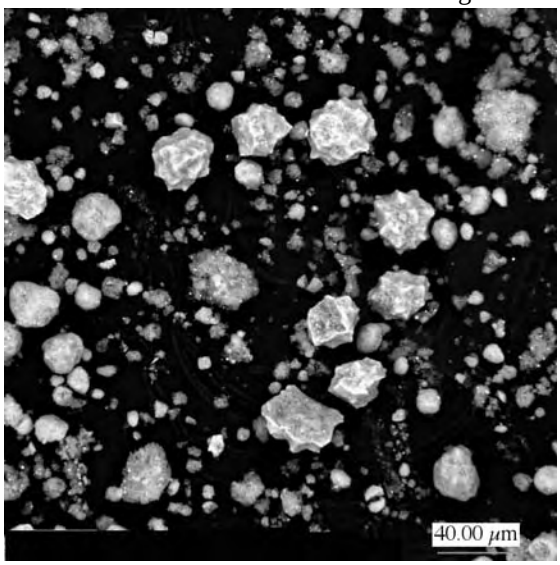

Stage 5

Figure D.6. Low-Magnification Overviews for PII-1/2, Stages 1 to 5, Using Same Scale

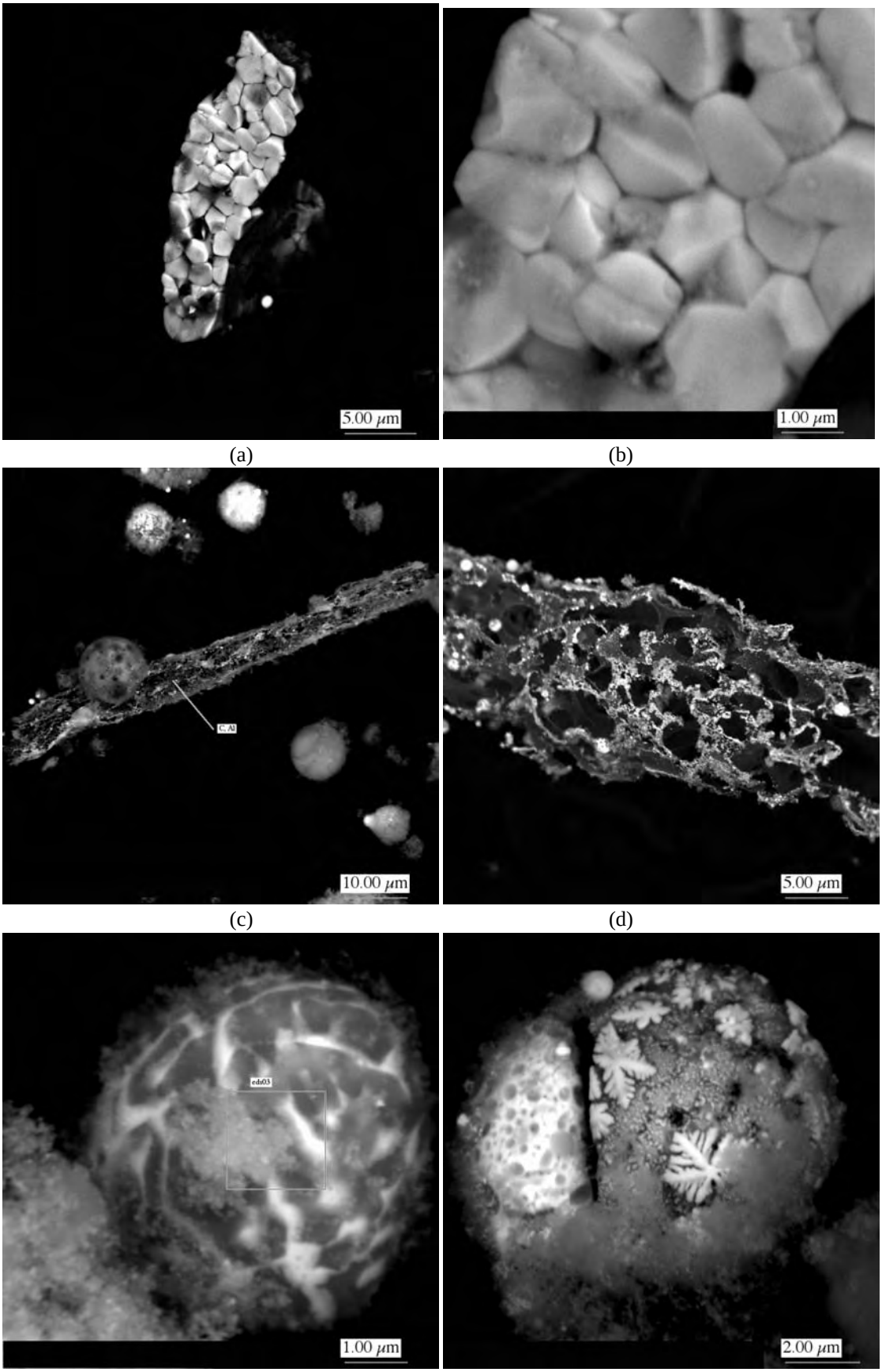

(a) (b)

(c) (d)

(e) (f)

Figure D.7. Interesting Particles from Phase II, First Set

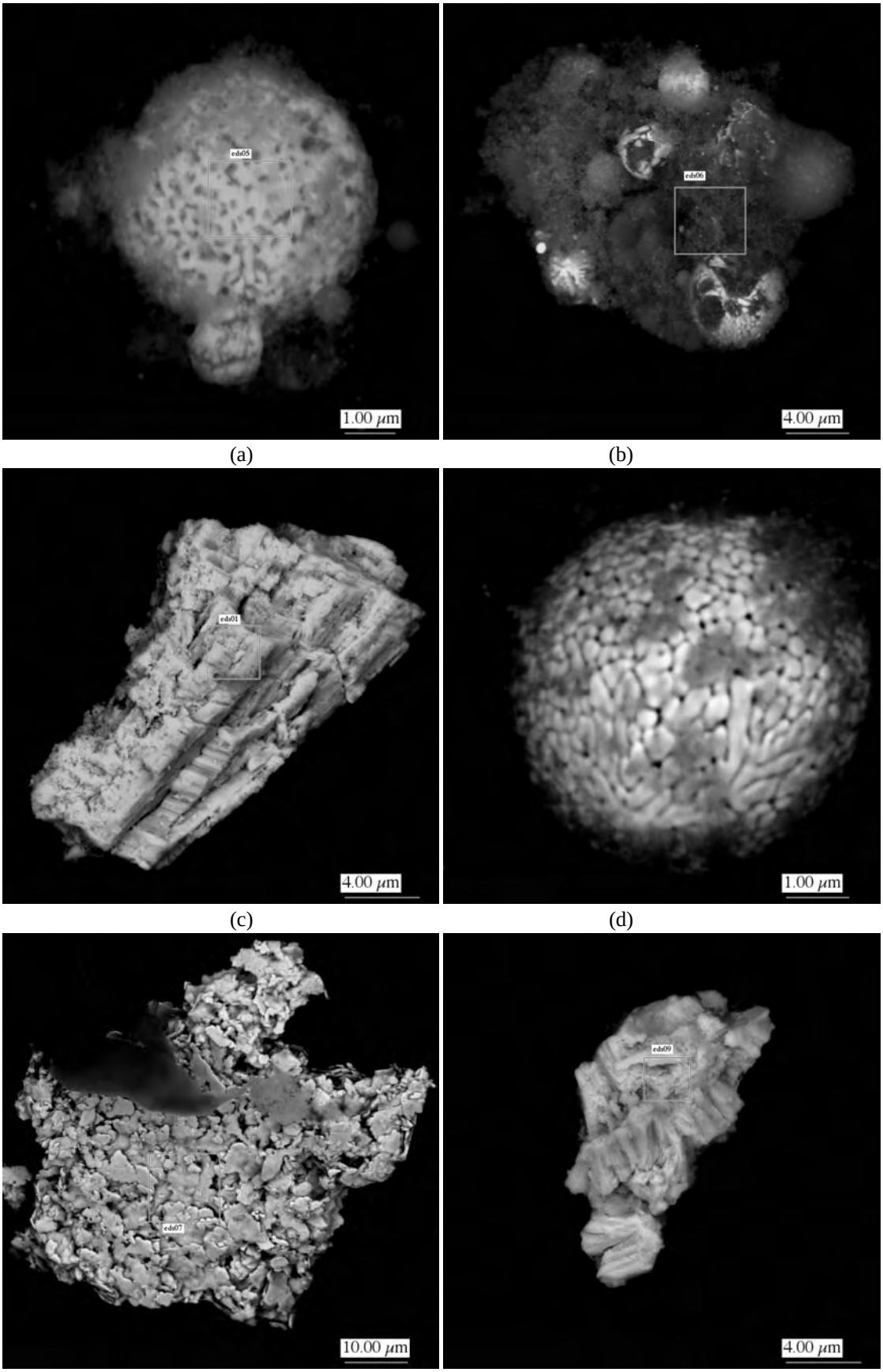

(a) (b)

(c) (d)

(e) (f)

Figure D.8. Interesting Particles from Phase II, Second Set

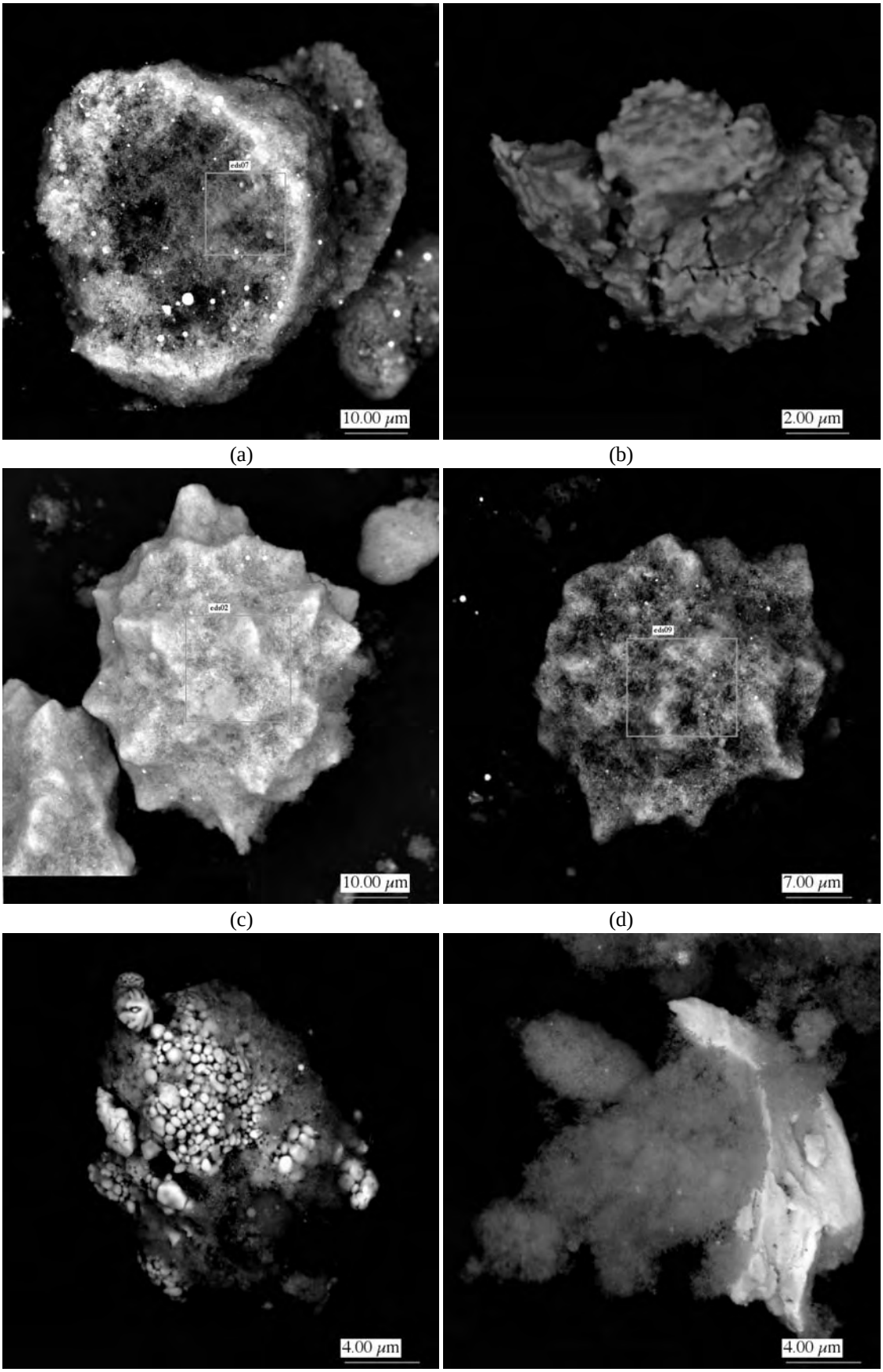

(a) (b)

(c) (d)

(e) (f)

Figure D.9. Interesting Particles from Phase II, Third Set

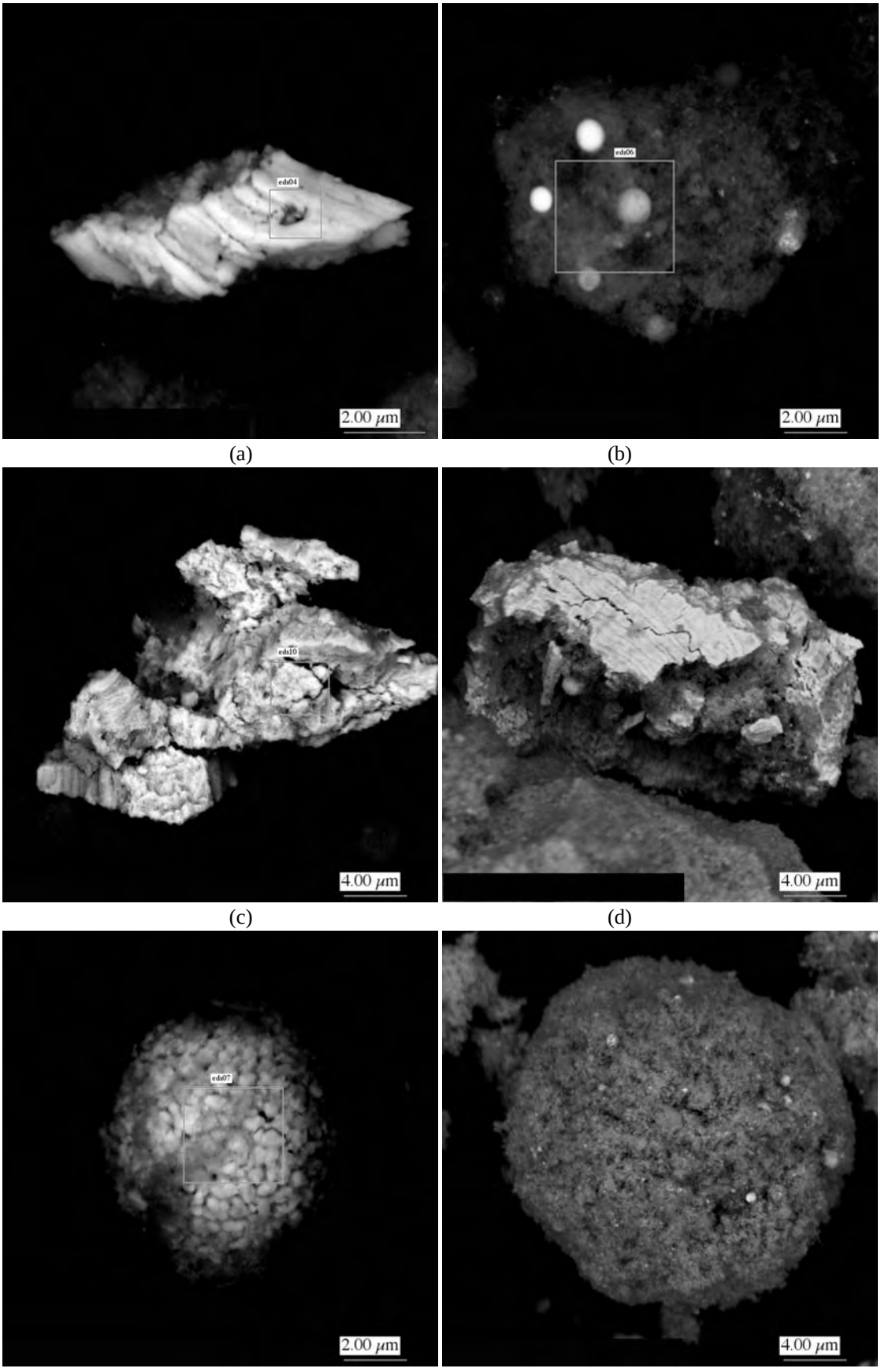

(a) (b)

(c) (d)

(e) (f)

Figure D.10. Interesting Particles from Phase II, Fourth Set

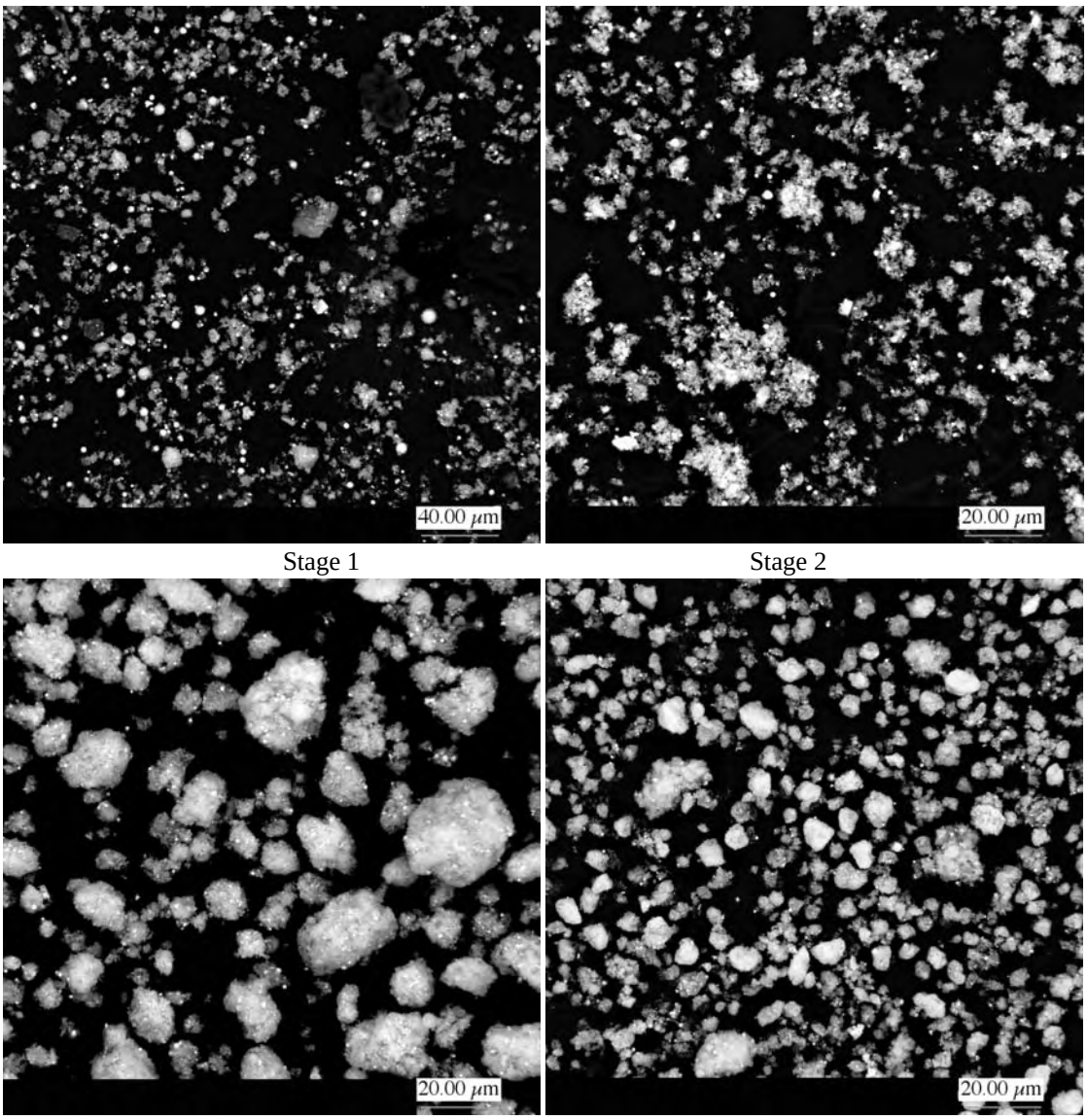

Stage 1 Stage 2

Stage 4 Stage 5

Figure D.11. Low-Magnification Overviews of PIII-2, Stages 1, 2, 4, and 5

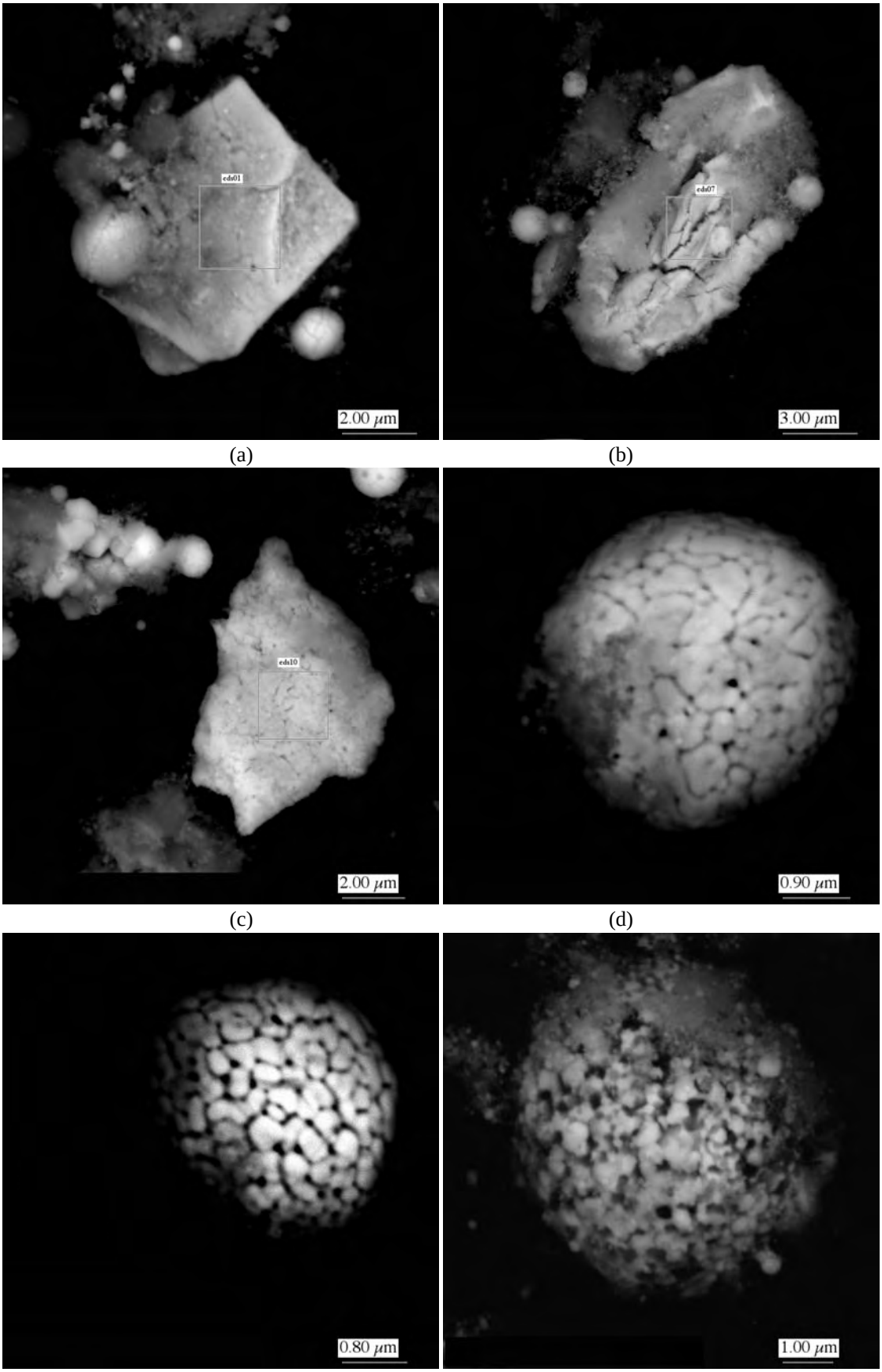

(a) (b)

(c) (d)

(e) (f)

Figure D.12. Interesting Particles from Phase III, First Set (Stage 1)

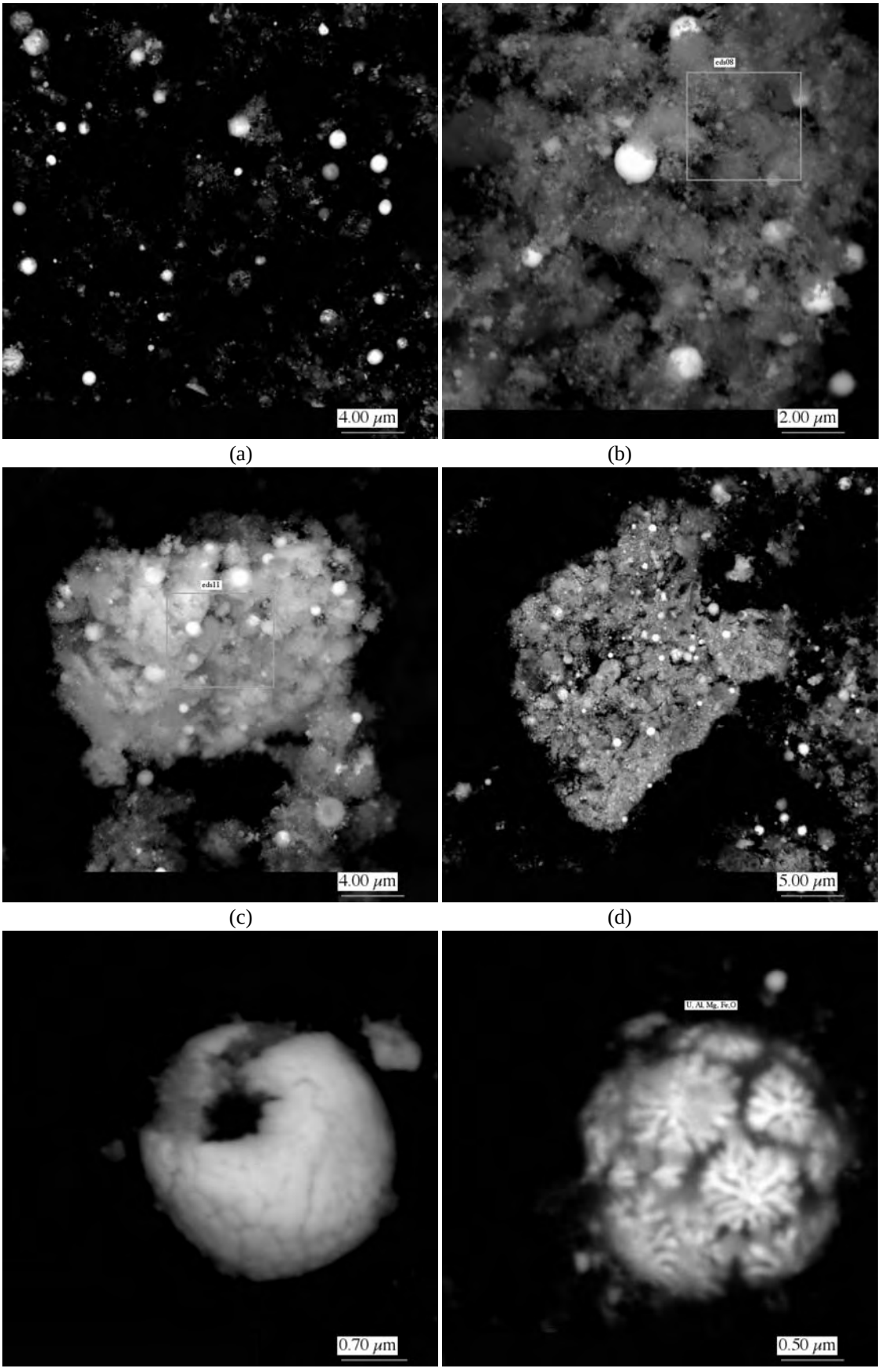

(a) (b)

(c) (d)

(e) (f)

Figure D.13. Interesting Particles from Phase III, Second Set (Stage 3)

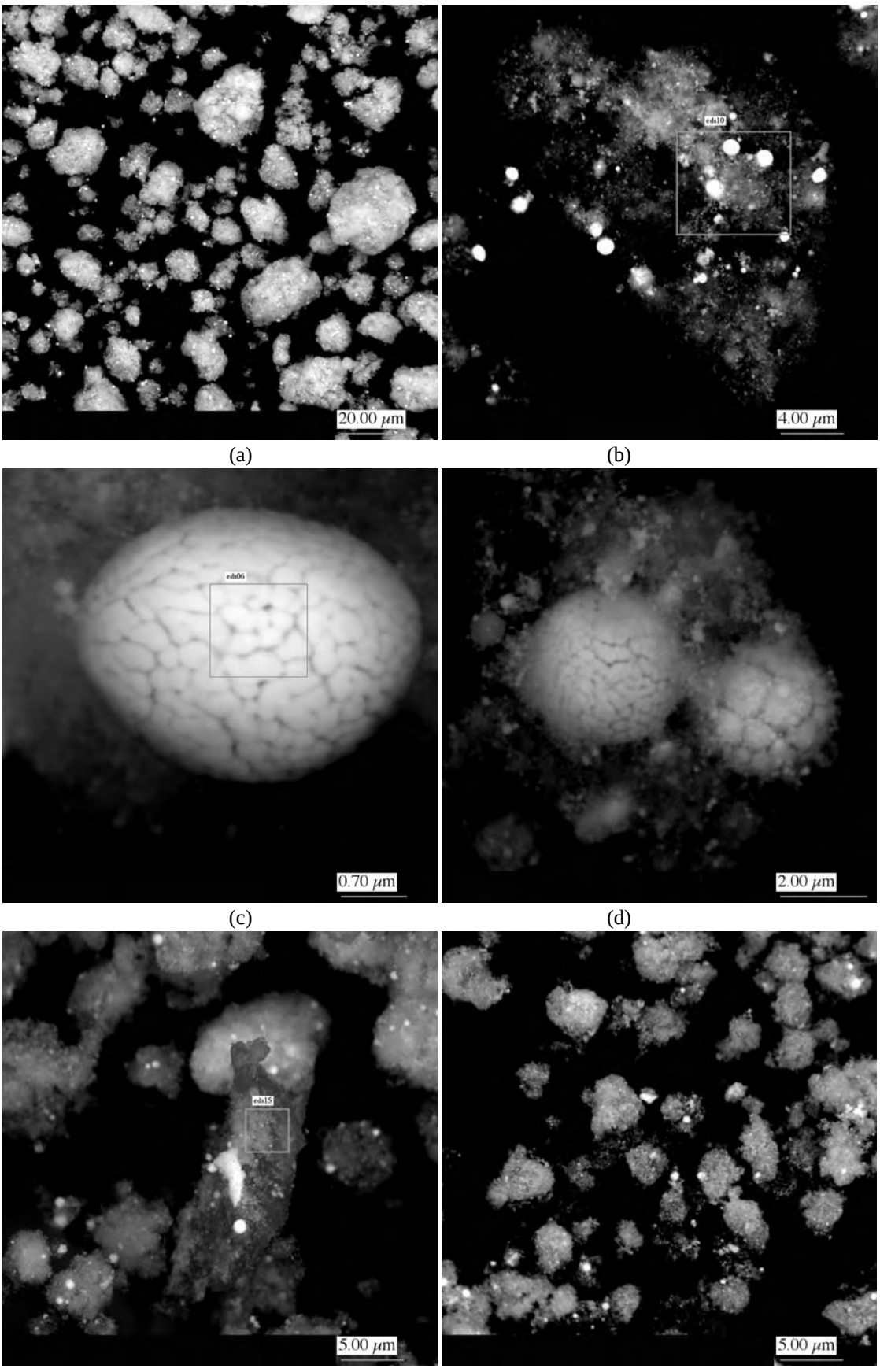

(a) (b)

(c) (d)

(e) (f)

Figure D.14. Interesting Particles for Phase III, Third Set (Stages 4 and 5)

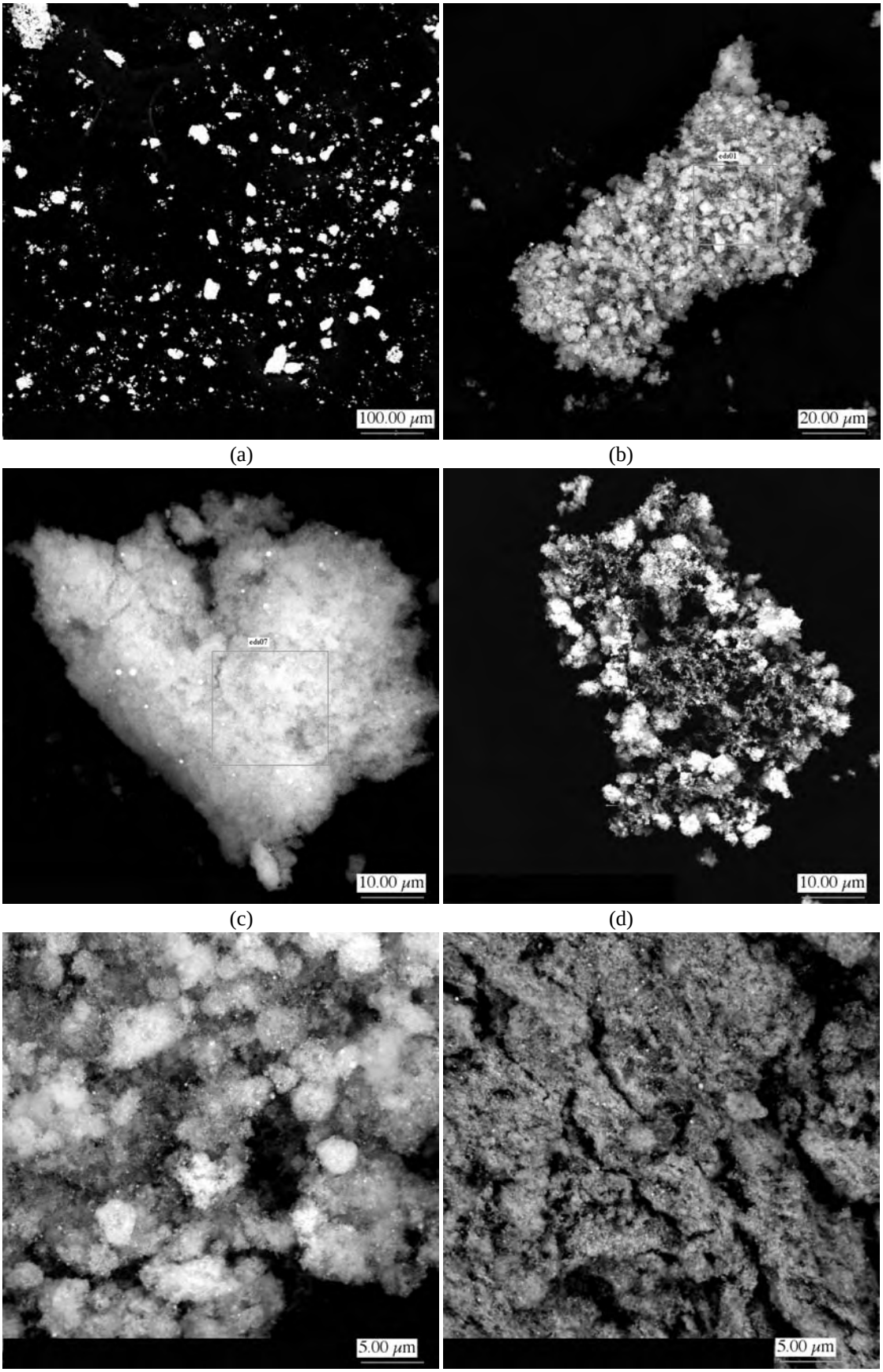

(a) (b)

(c) (d)

(e) (f)

Figure D.15. Backup Filter Particles from PI-3/4

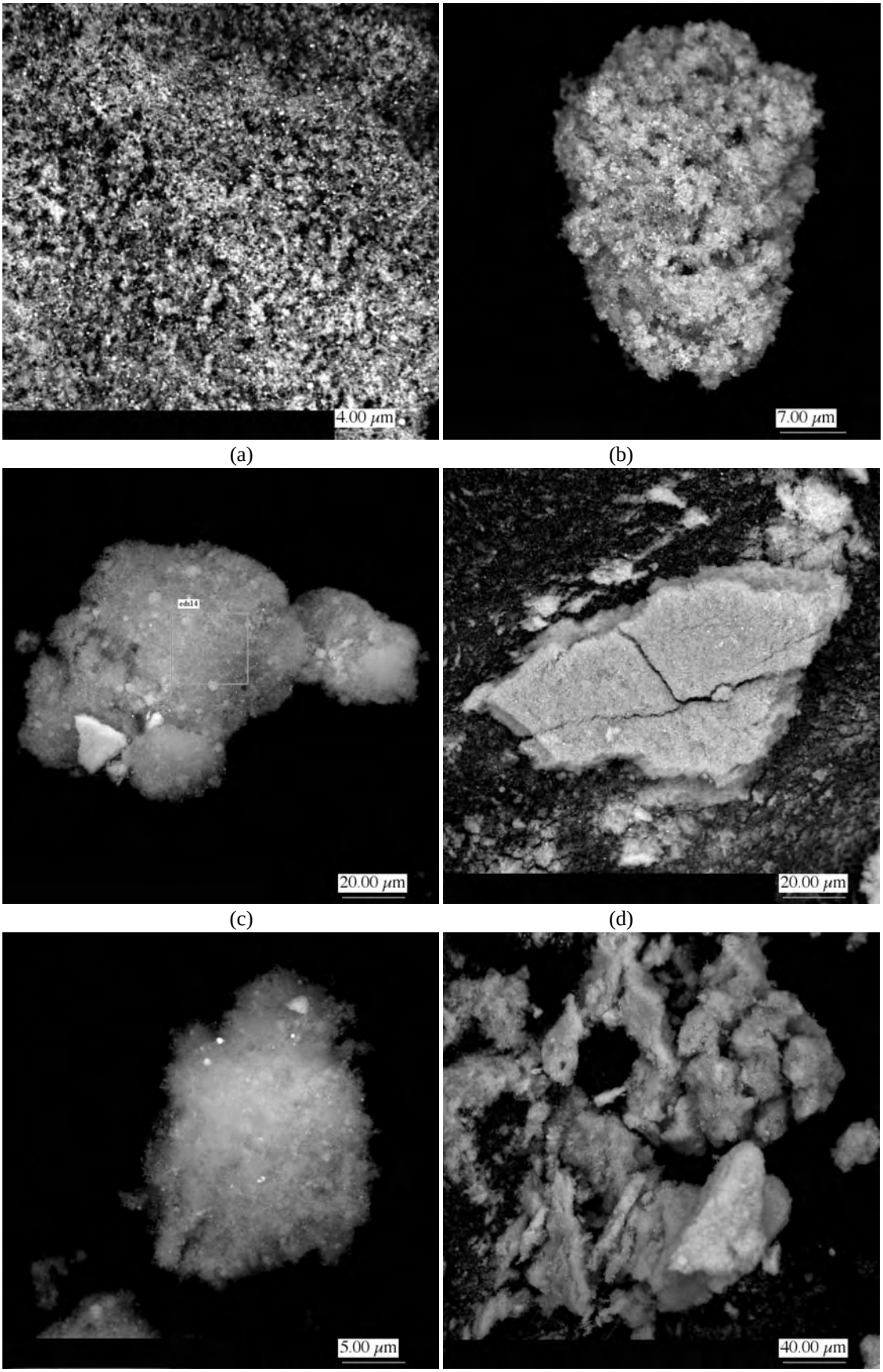

Figure D.16. Backup Filter Particles from PI-7 and PII-1/2

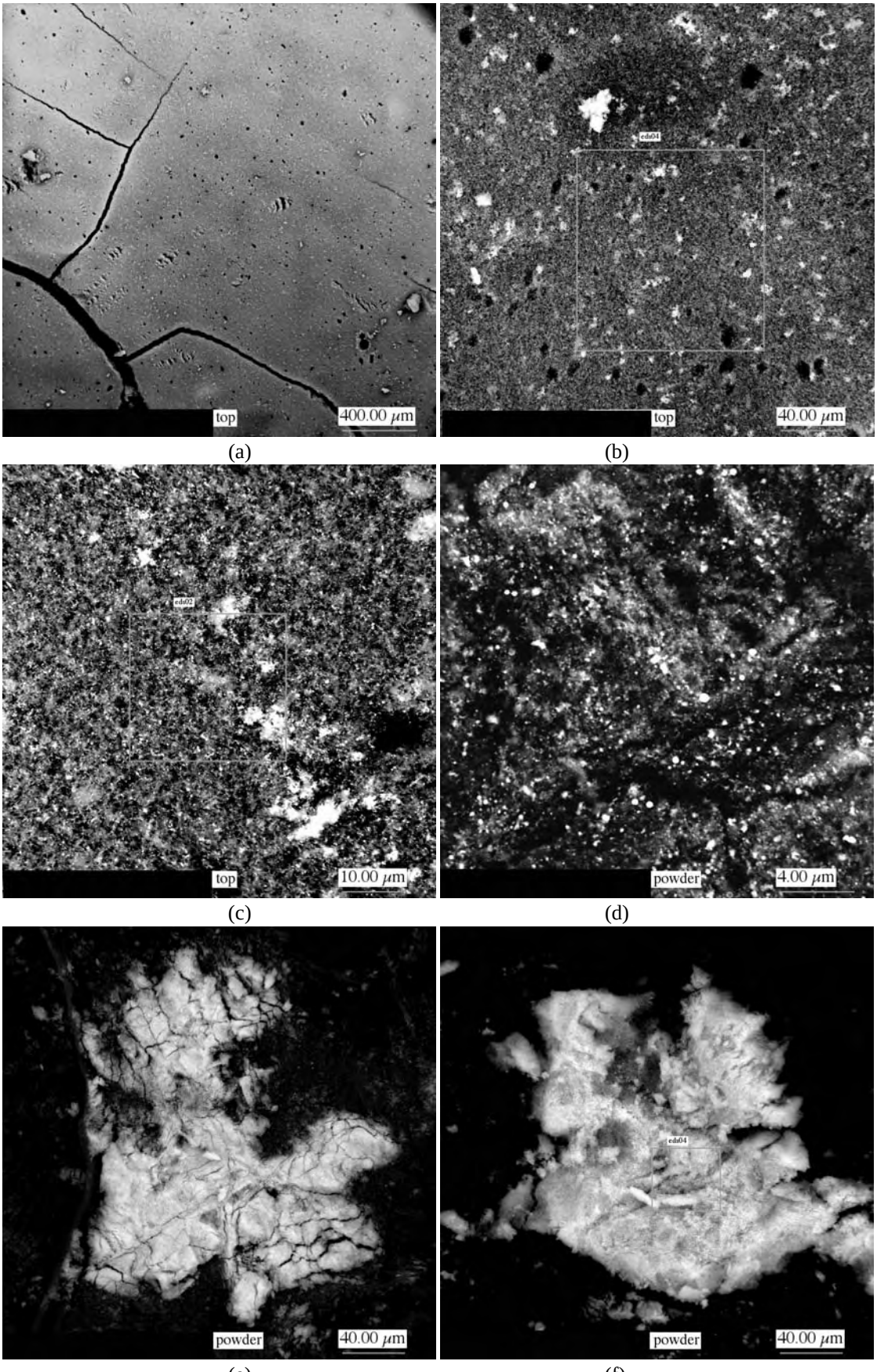

(a) (b)

(c) (d)

(e) (f)

Figure D.17. Phase-III Backup Filter and Particles

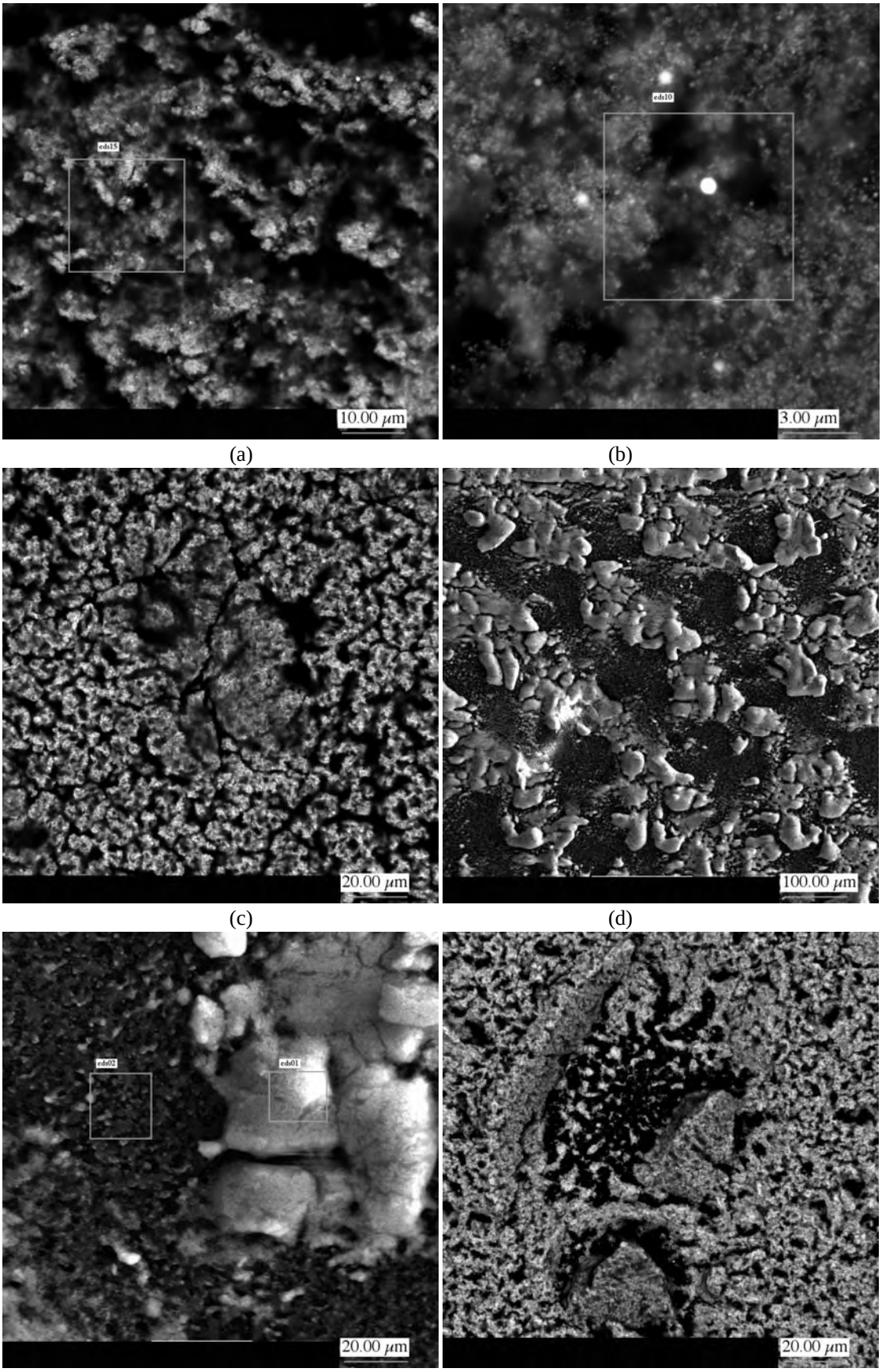

(a) (b)

(c) (d)

(e) (f)

Figure D.18. Diffusion Battery Filters Viewed from Top

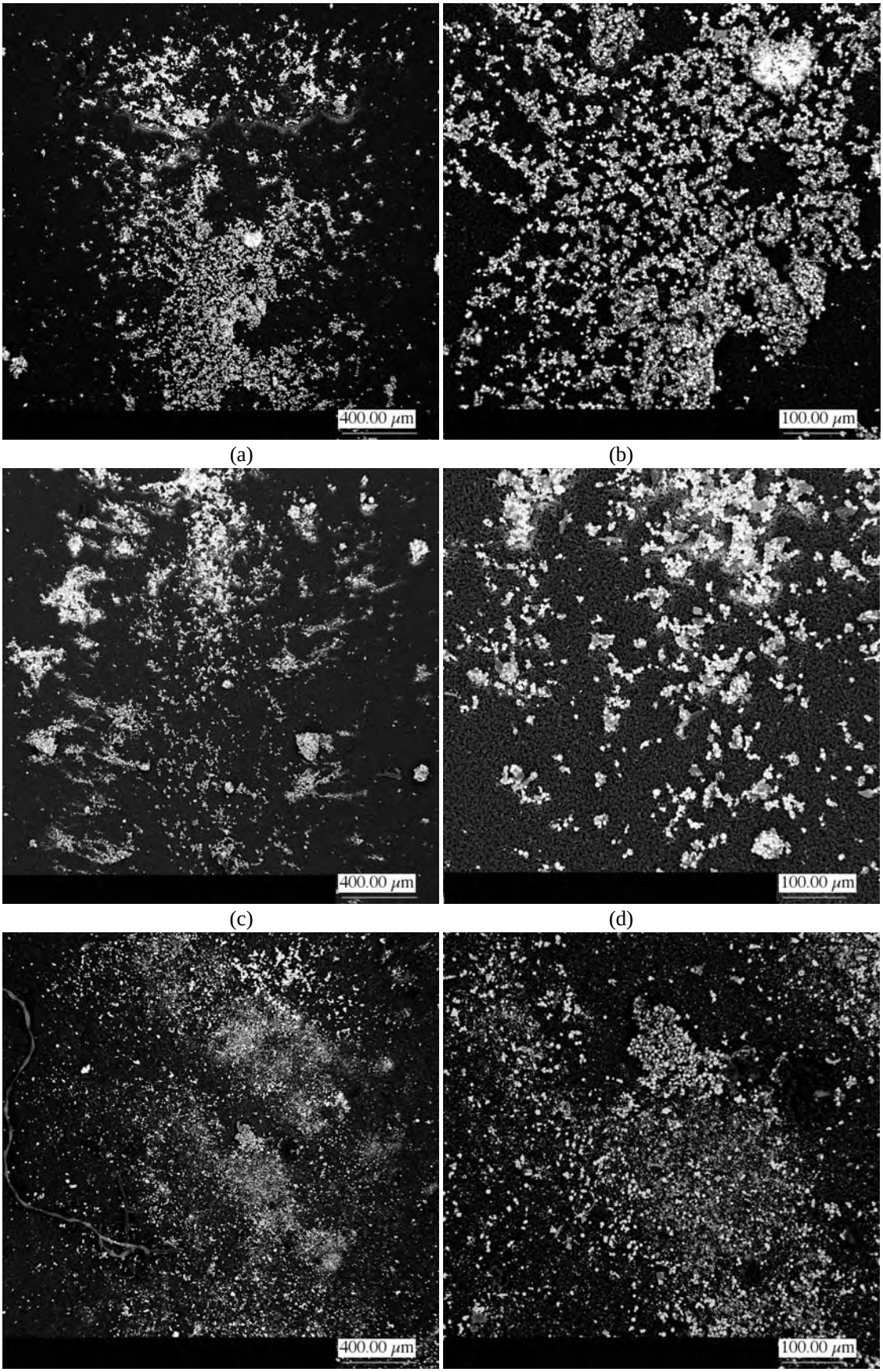

(a) (b)

(c) (d)

(e) (f)

Figure D.19. Cascade Impactor Stage-3 Dispersion Patterns

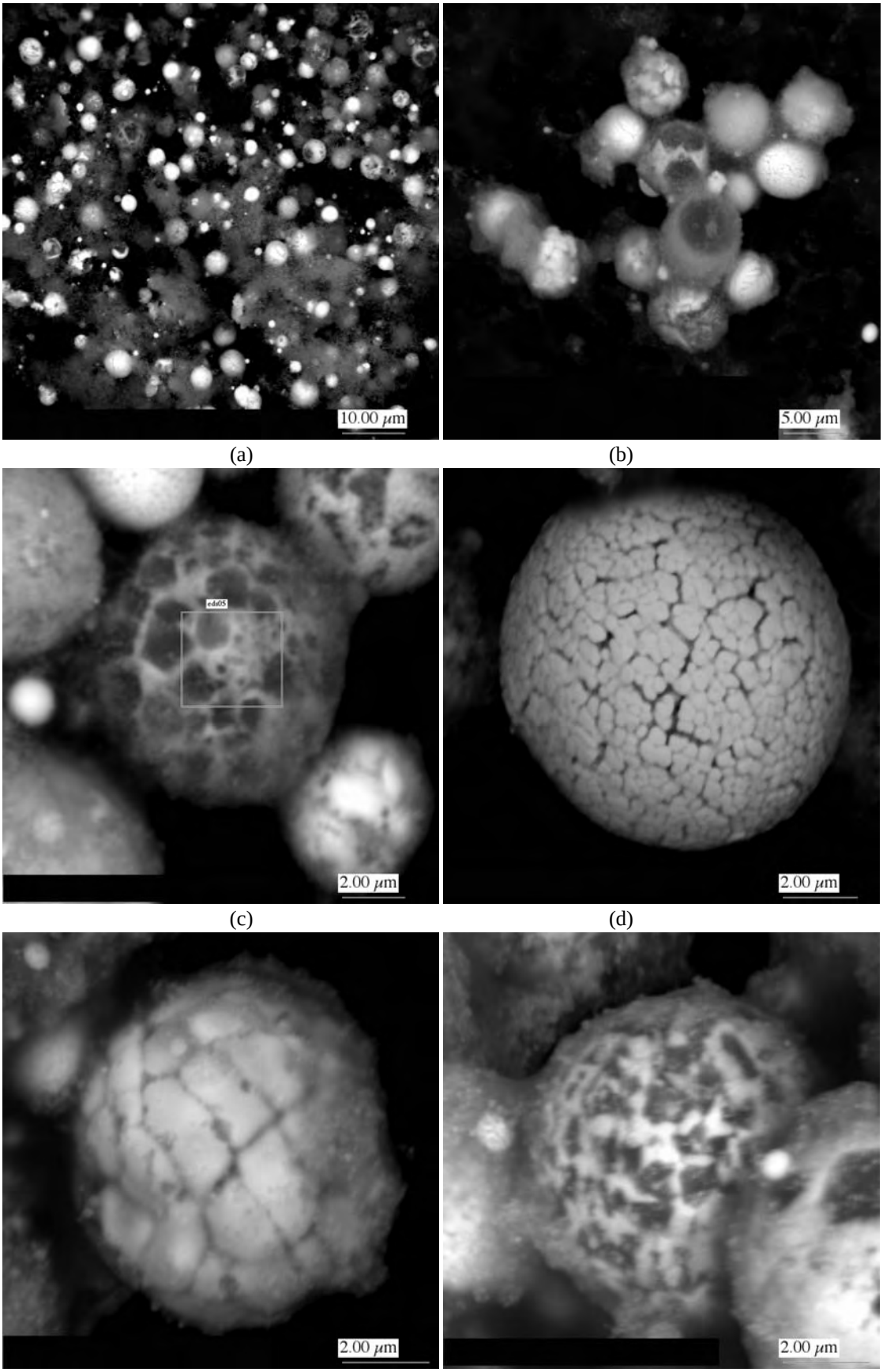

(a) (b)

(c) (d)

(e) (f)

Figure D.20. Particles Collected on Cascade Impactor Stage 3 (PI-7, G-1)

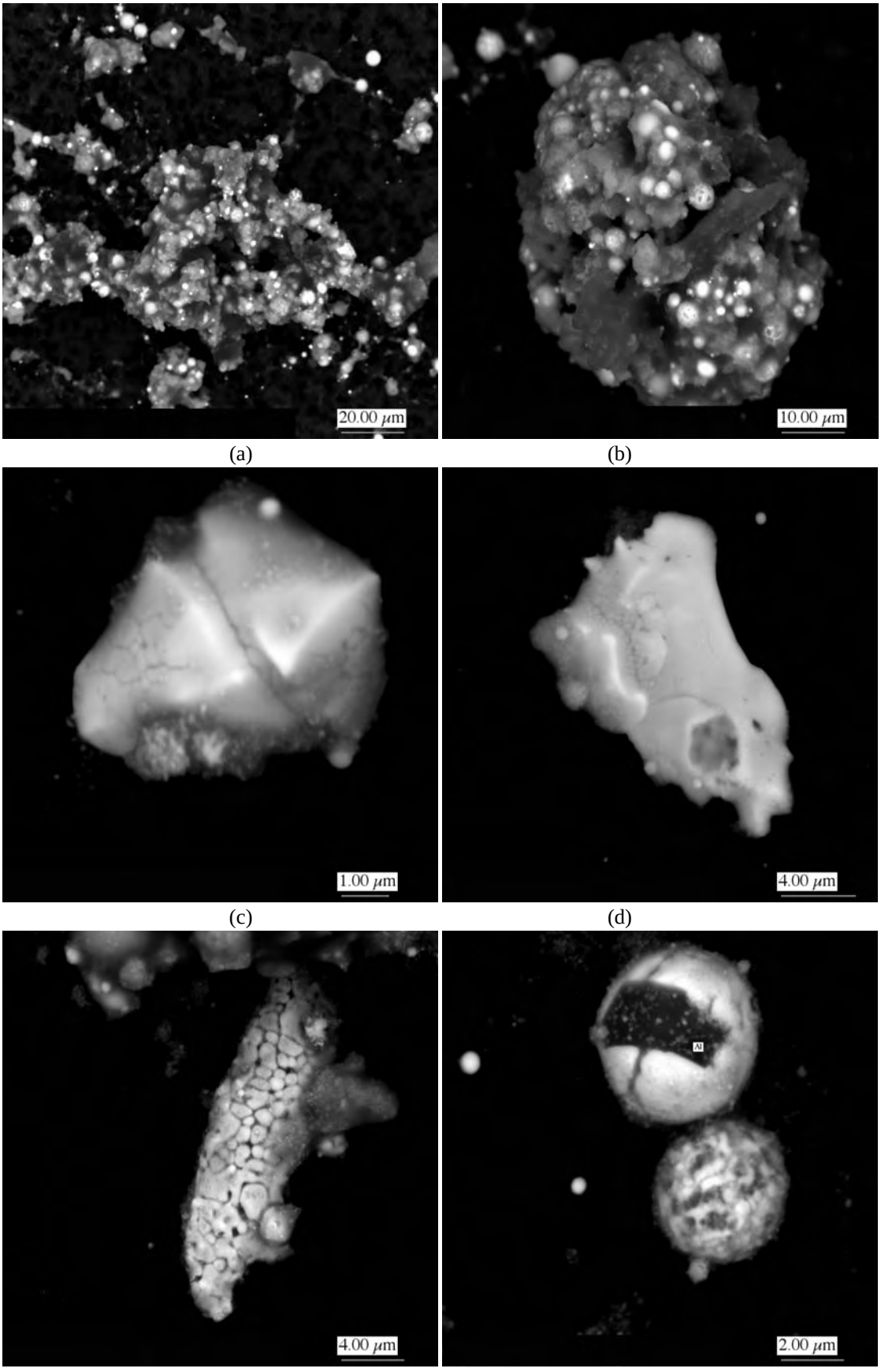

Figure D.21. Particles Collected on Cascade Impactor Stage 3 (PI-1, L-2)

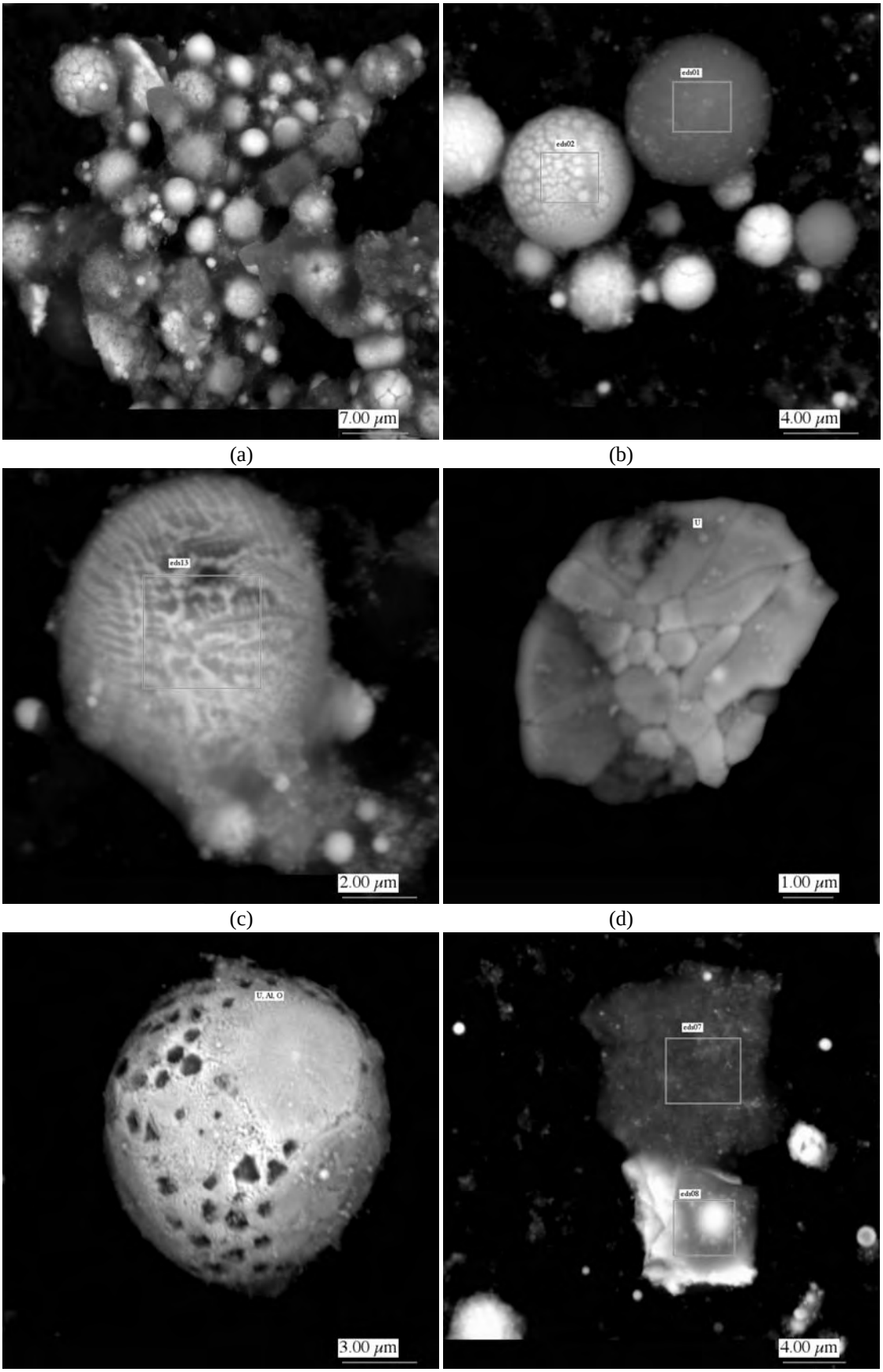

Figure D.22. Particles Collected on Cascade Impactor Stage 3 (PIII-2, C-2

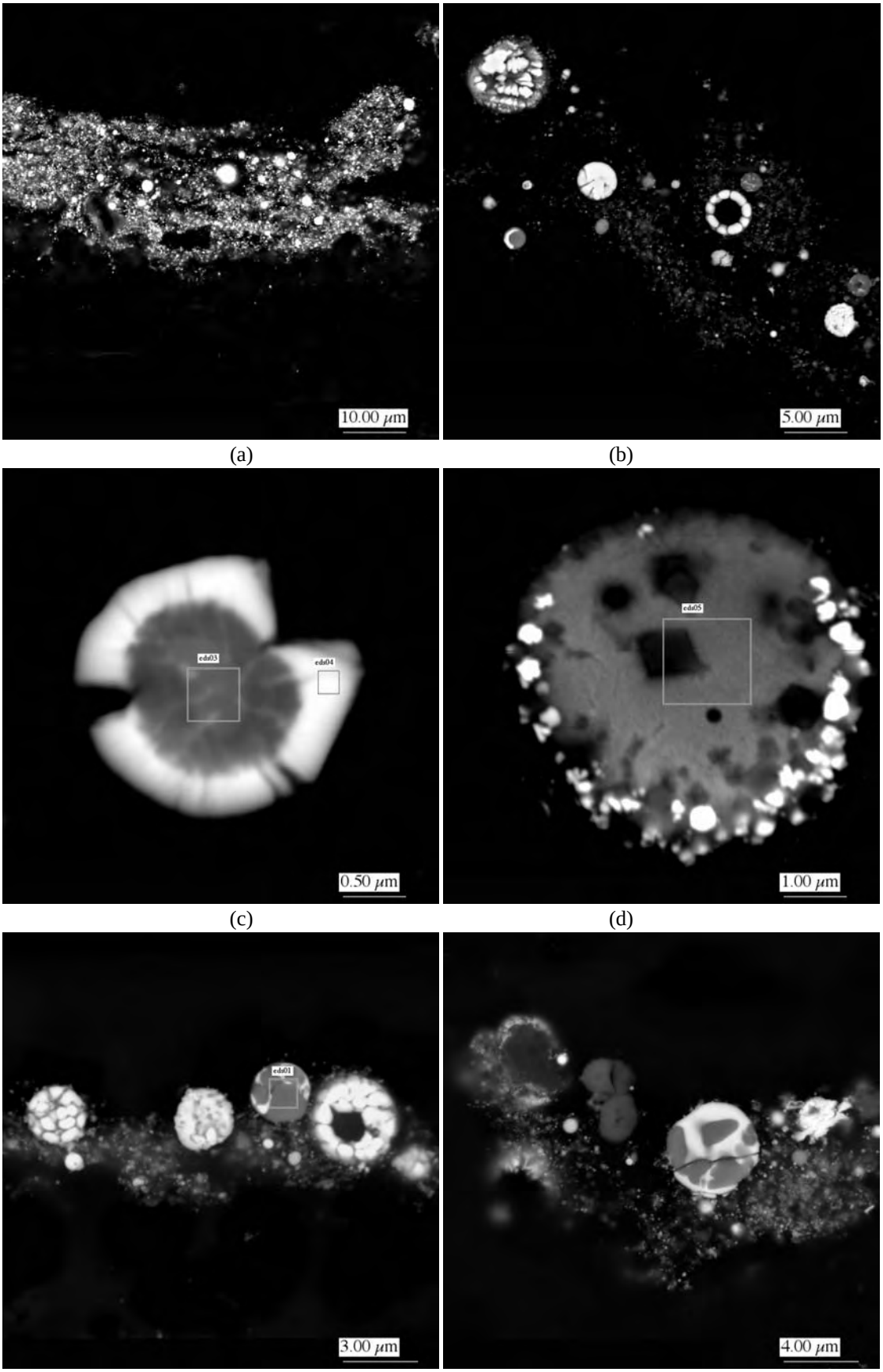

Figure D.23. Moving Filter Particles from PI-1, First Time Interval (Set 1)

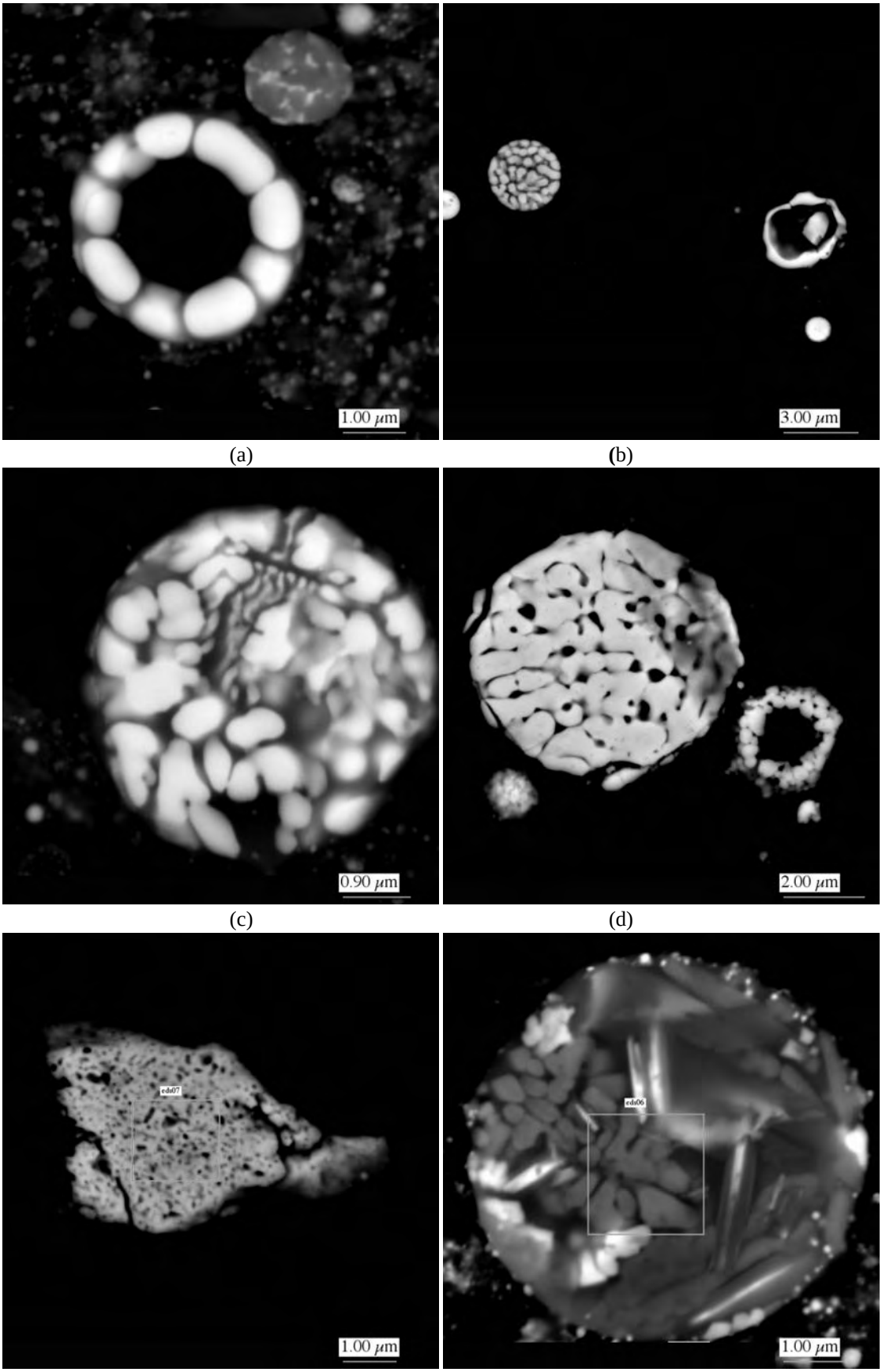

(a) (b)

(c) (d)

(e) (f)

Figure D.24. Moving Filter Particles from PI-1, First Time Interval (Set 2)

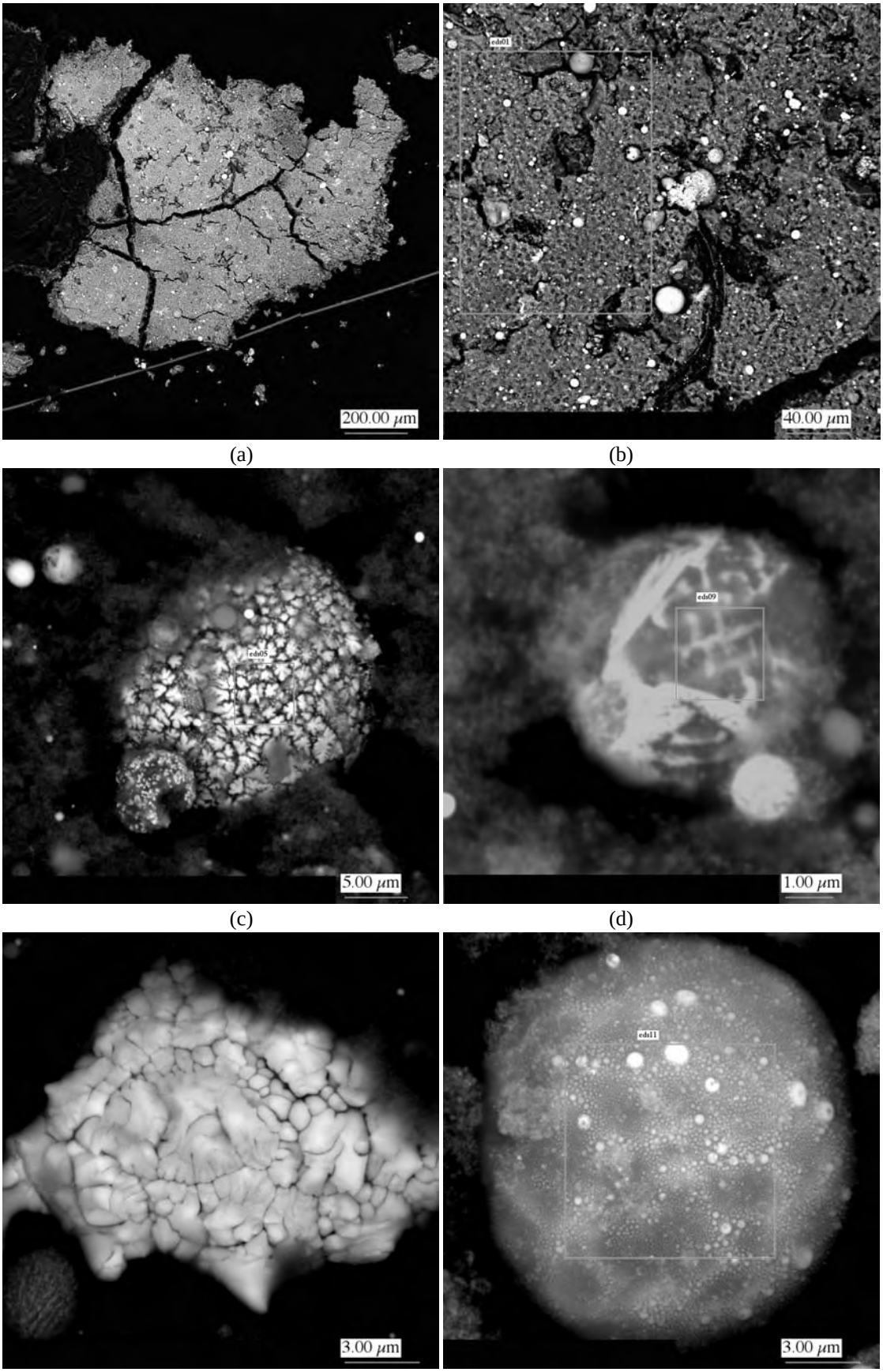

(a) (b)

(c) (d)

(e) (f)

Figure D.25. Moving Filter Particles from PII-3

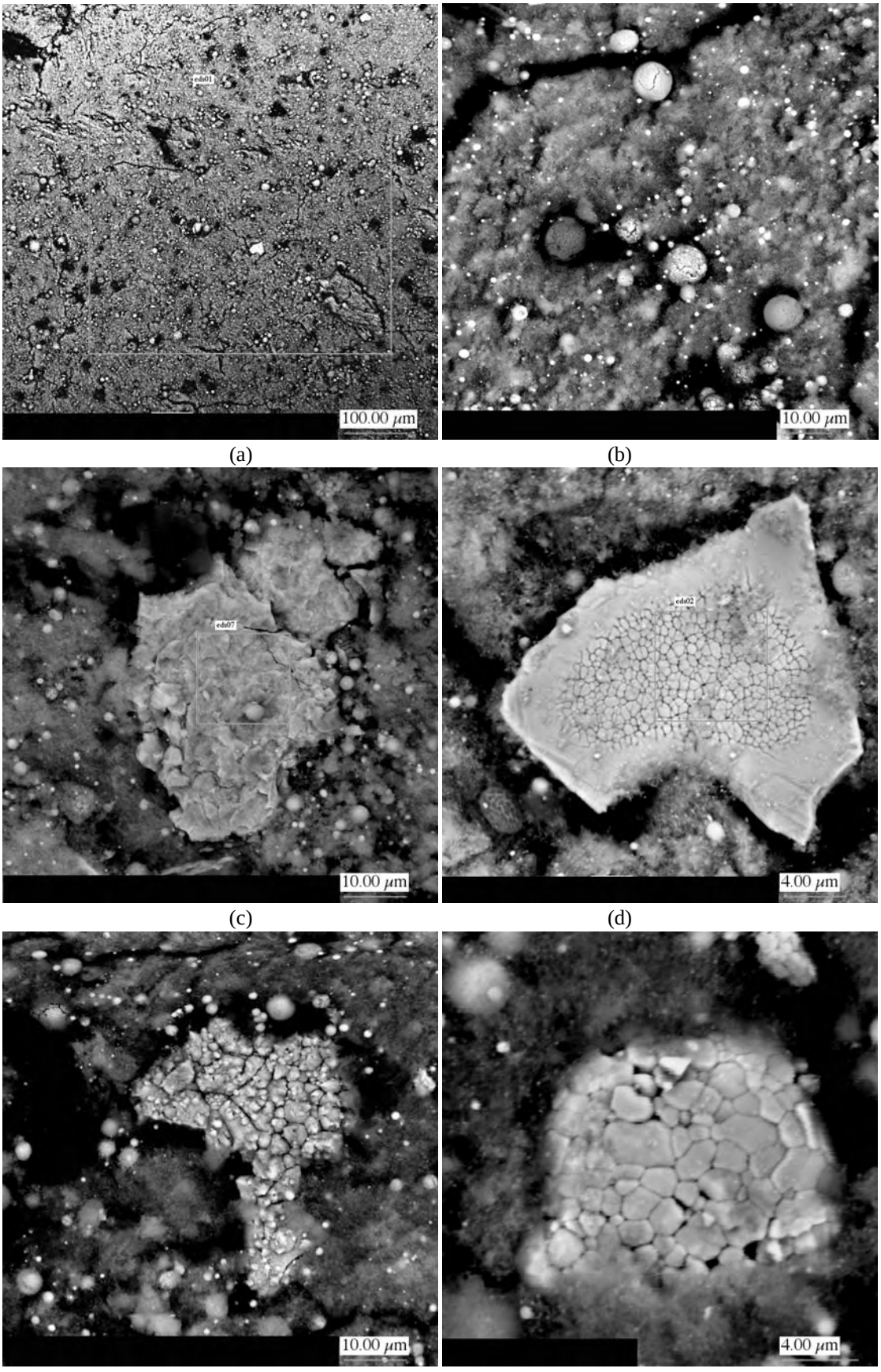

(a) (b)

(c) (d)

(e) (f)

Figure D.26. Moving Filter Particles from PIII-2

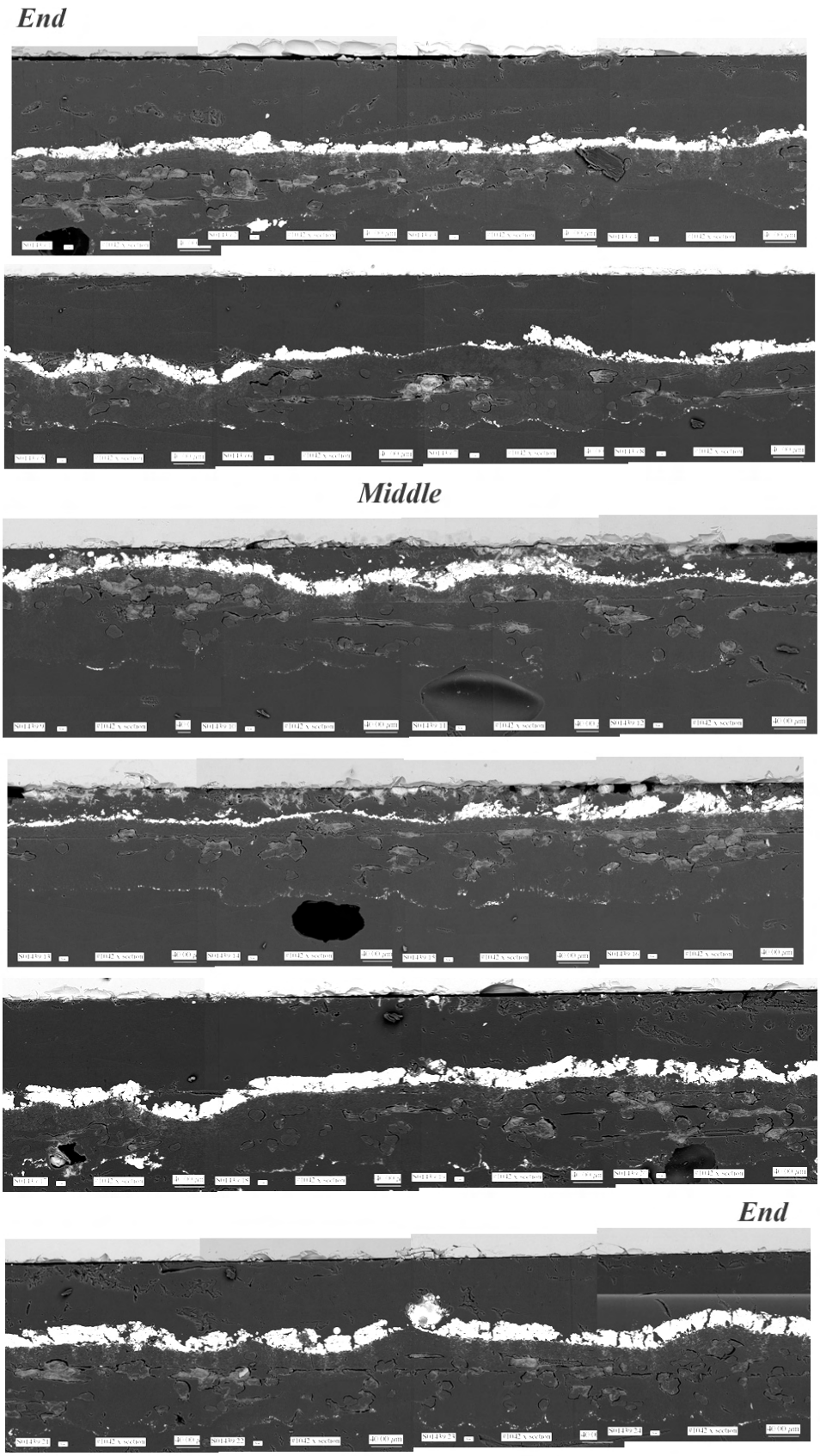

Figure D.27. Cross Section of Phase-III Moving Filter Sample, First Segment

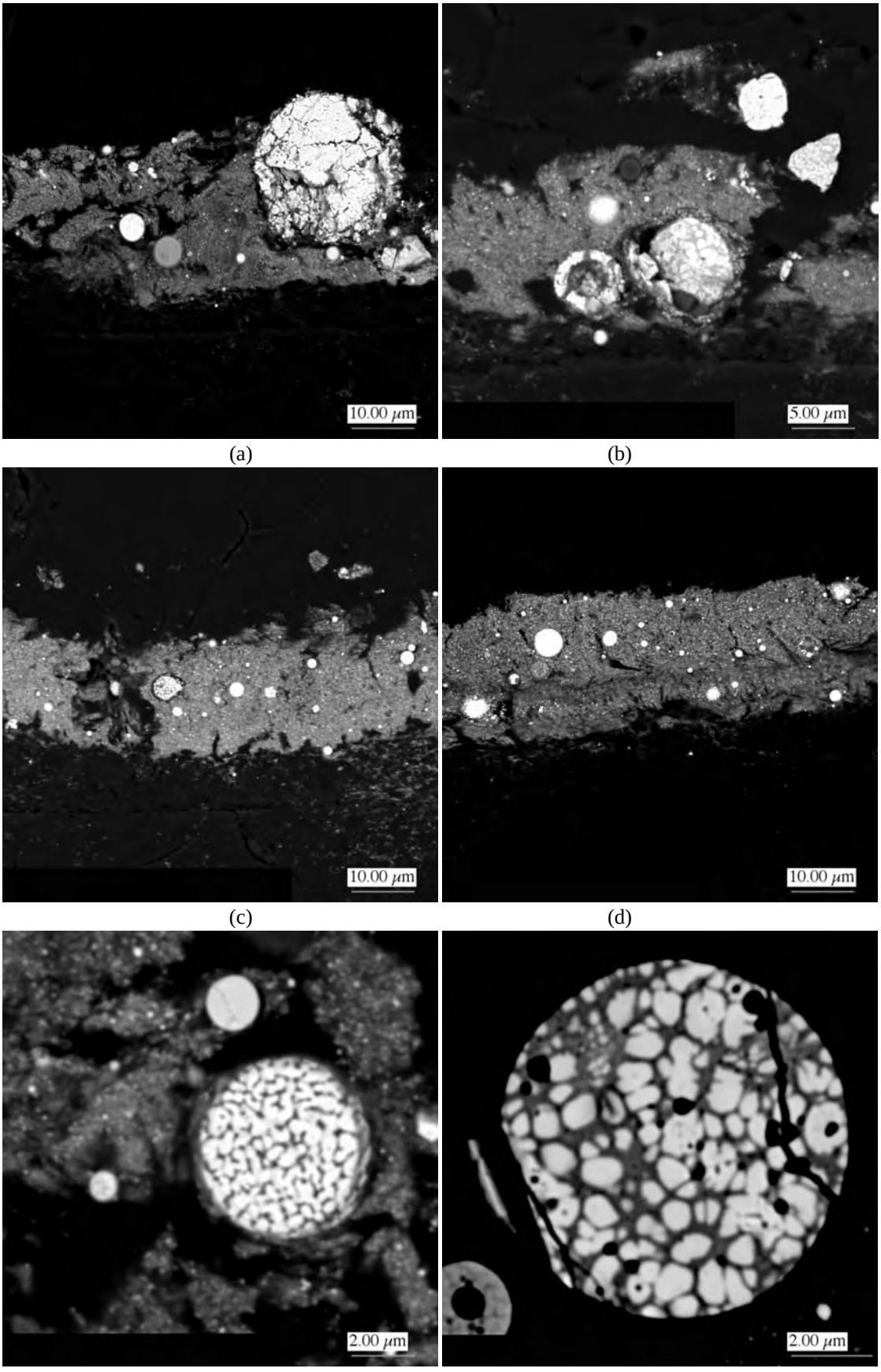

(a) (b)

(c) (d)

(e) (f)

Figure D.28. Moving Filter Particles from Phase III, Cross Section

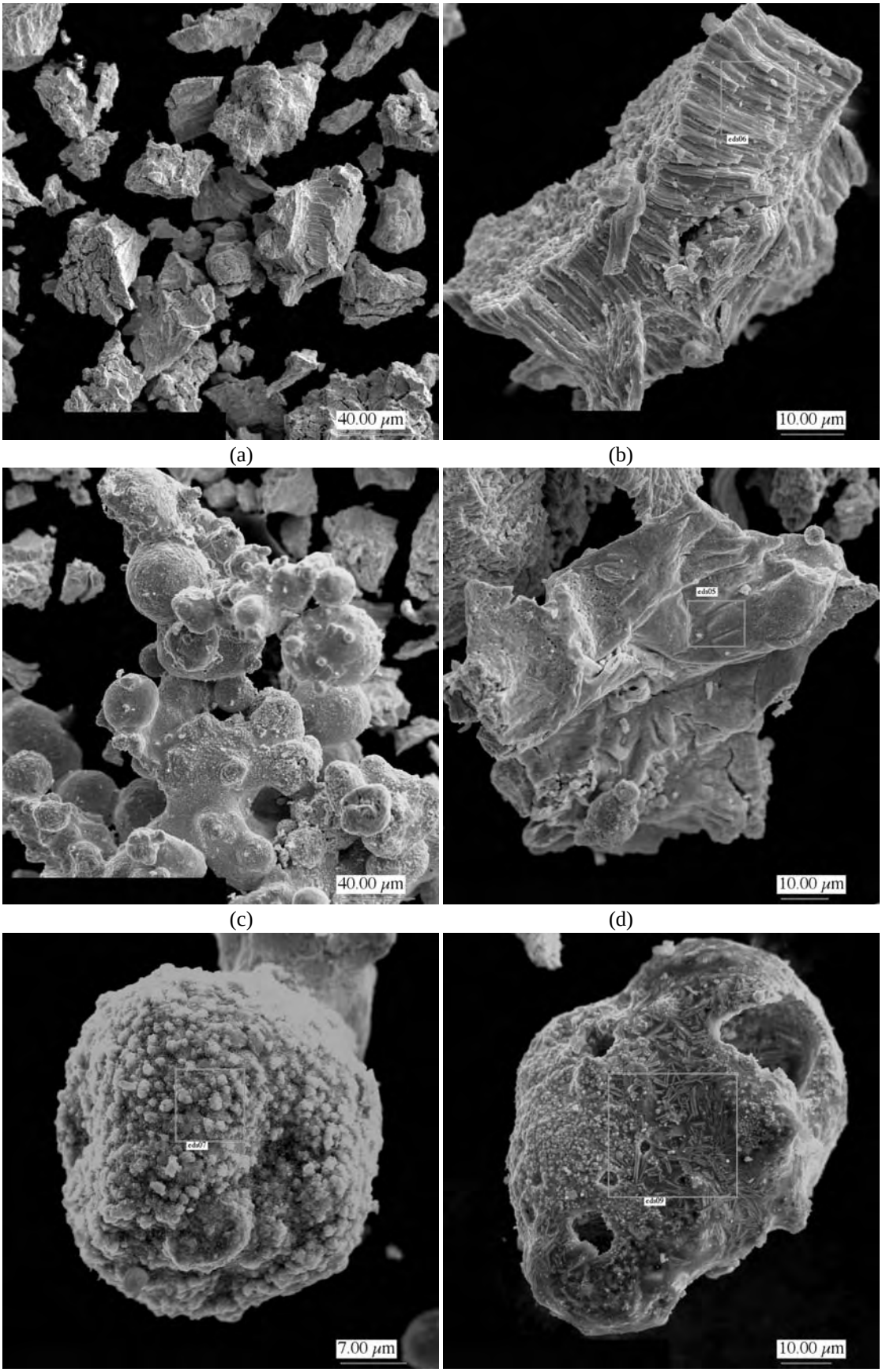

(a) (b)

(c) (d)

(e) (f)

Figure D.29. Particles from DU Cone Sample

Appendix E

In Vitro Solubility of Aerosol Samples

Appendix E

In Vitro Solubility of Aerosol Samples

The solubility and dissolution rates of depleted uranium (DU) aerosols are essential to conducting human health risk assessments from inhalation of DU. Once established, these rates may be used in appropriate lung and biokinetic models to assess radiation dose and chemical toxicity and to interpret post-incident bioassay. The *in vitro* solubility analysis procedure was briefly discussed in Section 3.9.7, the results of the analysis were presented in Section 5.6.4 and interpreted in Section 6.4.5. A more detailed explanation of the analytical procedures, the samples selected for analysis, the *in vitro* dissolution results and a discussion of these results are presented in the following sections.

E.1 Analytical Procedure

As briefly reviewed in Section 3.9.7, the solubility of uranium in simulated lung fluid was evaluated using an *in vitro* process employed at the Lovelace Respiratory Research Institute (LRRI). This procedure used synthetic ultrafiltrate (SUF) as its aqueous solvent. The composition of the SUF is given in Table E.1. Two nonphysiological chemicals were added to SUF: DTPA (see footnote in table below for chemical name) to reduce the adherence of polyvalent cations to the plastic surfaces of the containers and filter assembly, and ABDC (see footnote below for chemical name) as an antibacterial agent (Eidson and Mewhinney 1980).

Table E.1. Chemical Composition of SUF *In* Vitro Solvent Used in This Study

Chemical	Molar Concentration (Moles L^{-1})	Concentration (g L^{-1})
NaCl	0.116	6.779
NH_4Cl	0.010	0.5349
$NaHCO_3$	0.027	2.2628
Glycine	0.005	0.3754
L Cysteine	0.001	0.1756
Na_3Citrate	0.0002	0.0588
$CaCl_2$	0.0002	0.0294
H_2SO_4 (concentrated; 18M)	0.0005	0.03 mL L^{-1}
NaH_2PO_4	0.0012	0.1656
DTPA	0.0002	0.0787
ABDC	50 ppm	0.1 mL L^{-1}
diethylenetriaminepentaacetic acid. alkylbenzyldimethylammonium chloride, (50% by volume).		

Each weighed sample of aerosol powder (0.1 to 1 mg) was placed in a dissolution cell by positioning the sample filter containing the powder between two 47-mm hydrophilic, polysulphone membrane filters[(a)] and clamping them together with a screw-fastened Teflon ring. This assembly holds the Tuffryn filters securely around the test materials and prevents contamination of the solvent with undissolved DU. The assembled cell was then immersed in a volume of 50 mL SUF and maintained at room temperature without stirring. The pH of the solvent was kept at 7.3±0.05 for the duration of the study by maintaining a 5% CO_2 atmosphere in the headspace above the SUF solvent. At selected times (1, 4, and 8 h; 1, 4, 7, 11, 14, 18, 21, 25, 28, 32, 35, 39, 42, and 46 days), the solvent was exchanged with an equal volume of fresh solvent by manually transferring the Teflon assembly to a new container. At the end of the 46-day dissolution study, the dissolution cell containing the undissolved uranium was removed from the solvent, disassembled, and prepared for radiochemical analysis. The filter "sandwich", consisting of the Tuffryn filters, the undissolved DU, and the Teflon filter holder assembly were analyzed as a separate sample. Each of the solvent samples was transferred to a glass beaker, dried in a convection oven at 110°C, and thermally ashed at 550°C for 96 hours. The ash was then treated with concentrated (16M) nitric acid ($HNO_{3)}$ and 30% peroxide (H_2O_2) until a clear solution (mostly colorless unless more than100 µg uranium was present, in which case the solution would be yellow) was obtained. Each sample was then dissolved in a final volume of 60 mL 1M HNO_3.

All uranium samples were analyzed using kinetic phosphorescence (KPA)[(b)] (Brina and Miller 1992). Briefly, this method involves laser excitation of soluble uranium ions that have been complexed with a proprietary ligand. Complexation of the uranium with the ligand increases the time to fluorescence emission so that rapidly fluorescing signals can be electronically eliminated by gating the detector on the laser excitation pulse. This approach permits the measurement of trace concentrations of uranium in complex solutions. The method is designed to detect concentrations of U(VI) down to 0.01 µg/L. LRRI experience with the KPA-11 indicates a practical limit of detection of 0.05 :g/L.

The analysis of each batch of solvent samples was accompanied by a set of 50-mL SUF samples: three samples were spiked with natural uranium (National Institute of Standards and Technolgy derived), and two samples were maintained as process quality control (QC) blanks. These samples were treated along with the experimental samples to provide batch-specific QC data.

To ascertain the extent to which dissolved uranium might have adhered to the solvent plastic containers, a random sample of 30 containers taken from the first 120 samples (which, being the first samples obtained in time, would have contained the largest amounts of dissolved uranium). These containers were dried and combined into three sample sets of 10 samples each. The samples were processed using the standard radiochemical technique used for the solvent and filter samples. The analysis indicated that an average of 0.45 :g uranium or about 0.5% uranium adhered to the plastic container. Therefore, we concluded for this study that uranium did not adhere to an appreciable extent.

The data from the KPA analysis were obtained as total :g U per sample. These data were re-expressed as the fraction of the total recovered uranium by summing the amounts of uranium measured in all of the solvent samples and the undissolved amount measured on the filter at the end of the dissolution study. Although data expressed in this manner are statistically correlated because of the sequential subtraction of

(a) Tuffryn-HT, 0.2 :m pore size, Pall Gelman Laboratory, Ann Arbor, Michigan.
(b) ChemChek Model KPA-11, ChemCheck Instruments, Inc., Richland, Washington.

the time-related dissolved uranium quantities, they are nevertheless in the best form for function fitting, which results directly in dissolution rate constants.

These data were fitted to two- and three-component negative exponential equations using a Levenberg-Marquardt nonlinear least-squares fitting algorithm.[(a)]

E.2 Samples Analyzed

The sample analysis focused on the respirable particle sizes (nominally <10-µm aerodynamic diameter) that were captured by the cyclone stages and backup filter. Only one Stage-1 sample was analyzed. Other samples evaluated included the coarsest fraction recovered by the diffusion battery (PFDB) filters, five IOM cassette filter samples from the driver's position to evaluate the time-dependent solubility behavior of the collected aerosols, and the DU "cone" sample, which was analyzed as a bulk powder and as the size-separated respirable fraction. Twenty-seven samples were submitted for *in vitro* dissolution analysis. Their ID codes and sample descriptions are summarized in Table E.2.

Table E.2. Description of Samples Submitted for *In Vitro* Dissolution Study

Sample ID	Figure	Page #	Sample Description
PI-2I-D-1-FS	E.2	E.16	Phase I, Shot 2, driver IOM filter, sampling period No. 1
PI-2I-D-3-FS	E.3	E.16	Phase I, Shot 2, driver IOM filter, sampling period No. 3
PI-2I-D-4-FS	E.4	E.16	Phase I, Shot 2, driver IOM filter, sampling period No. 4
PI-2I-D-6-FS	E.5	E.16	Phase I, Shot 2, driver IOM filter, sampling period No. 6
PI-2I-D-7-FS	E.6	E.17	Phase I, Shot 2, driver IOM filter, sampling period No. 7
PI-3/4-CY-2	E.7	E.17	Phase I, Shots ¾ (double shot), cyclone stage 2
PI-3/4-CY-3	E.8	E.17	Phase I, Shots ¾ (double shot), cyclone stage 3
PI-3/4-CY-4	E.9	E.17	Phase I, Shots ¾ (double shot), cyclone stage 4
PI-3/4-CY-5	E.10	E.18	Phase I, Shots ¾ (double shot), cyclone stage 5
PI-3/4-CY-BU	E.11	E.18	Phase I, Shots ¾ (double shot), cyclone back-up filter
PI-7I-CY-1	E.12	E.18	Phase I, Shot 7, cyclone stage 1
PI-7I-CY-2	E.13	E.18	Phase I, Shot 7, cyclone stage 2
PI-7I-CY-3	E.14	E.19	Phase I, Shot 7, cyclone stage 3
PI-7I-CY-4	E.15	E.19	Phase I, Shot 7, cyclone stage 4
PI-7I-CY-5	E.16	E.19	Phase I, Shot 7, cyclone stage 5

(a) Origin, v.6.1, OriginLab Corp., Northampton, Massachusetts.

Table E.2. (contd)

Sample ID	Figure	Page #	Sample Description
PI-7I-CY-BU	E.17	E-19	Phase I, Shot 7, cyclone backup filter
PII-1/2I-CY-2	E.18	E-20	Phase II, Shots 1/2 (double shot), cyclone stage 2
PII-1/2I-CY-3	E.19	E-20	Phase II, Shots 1/2 (double shot), cyclone stage 3
PII-1/2I-CY-4	E.20	E-20	Phase II, Shots 1/2 (double shot), cyclone stage 4
PII-1/2I-CY-5	E.21	E-20	Phase II, Shots 1/2 (double shot), cyclone stage 5
PII-1/2I-CY-BU	E.22	E-21	Phase II, Shots 1/2 (double shot), cyclone backup filter
PIII-2I-CY-4	E.23	E-21	Phase III, Shot 2, cyclone stage 4
PIII-2I-CY-5	E.24	E-21	Phase III, Shot 2, cyclone stage 5
PIII-2I-CY-BU	E.25	E-21	Phase III, Shot 2, cyclone backup filter
DiffBat7	E.26	E-22	Phase I, Shot 1, diffusion battery screen assembly 7
DU cone (unsep)	E.27	E-22	Conical powder deposit (Phase I, Shot 5); bulk powder
DU cone U (sep)	E.28	E-22	Conical powder deposit (Phase I, Shot 5); size-separated

E.3 Results

Using the results of the KPA analysis of uranium concentration in the samples, the uranium dissolution was plotted as a function of time for each sample. During this process, a low recovery of the QC spike samples and a data anomaly were discovered. Discussions of these concerns and their resolutions follow along with a discussion of the results obtained in the *in vitro* dissolution analysis.

E.3.1 QC Spike Recovery Analysis

The average recovery (± standard deviation) for all of the batches run during this study was 93% ∀ 43%. Although the average recovery appeared to be reasonable for a tracer-free method, the precision was very large and was inconsistent with past experiences with *in vitro* dissolution studies of uranium at LRRI. Upon investigation, it was discovered that a change in the spiking method was made during the course of the analyses, purportedly to speed up the analytical process. The change corrupted a significant fraction of the batch QC spikes and invalidated their usefulness as process QC samples. Briefly, instead of spiking each QC sample with a uranium standard solution at the beginning of processing each batch, a "master spiking solution" was created by spiking about 2 L SUF with an appropriate level of uranium and storing it in a capped container. Then when a new batch was run, aliquots from the master solution were taken and spiked into the SUF. Unfortunately, this procedure did not account for the time-related changes that occur when SUF is not maintained under a flowing 5% CO_2 atmosphere. In a capped container, CO_2 is created with time from degradation of the bicarbonate present in the SUF. This reaction results in a higher pH in the SUF. For example, within 24 h the original pH of 7.4 would have increased to about 8.0, and in another 24 h, the pH would establish a new equilibrium at about 9 (Eidson and Griffith 1984). The effect of this pH change on the uranium existing as uranyl ion $(UO_2)^{+2}$ is to shift the equilibrium from a

soluble uranyl carbonate to an insoluble phosphate, which forms microprecipitates with time, and, if left unstirred, tends to settle out or stick to the container walls.

To test this theory, a 1-L container of SUF was spiked with uranium as was done with the original master solution, and aliquots were carefully removed at different times from the original container, taking care not to mix the solution/suspension. The results shown in Table E.3 indicate that, over time, there was a settling of the uranium in the container. This stratification of the spike solution undoubtedly contributed to the large error measured in the QC samples since about 80% of the batches were dosed with the master spiking solution. In comparison, a second set of five aerosol samples was introduced into the *in vitro* dissolution study at a later time, and their solvent samples were analyzed separately. By the time these latter analyses were completed, the problem with the spiking method had been identified, and the original spiking method was re-instituted. The average recovery for the analysis of the batch of five samples was 101% ∀ 11%, which is a more reasonable and expected result.

Table E.3. Effect of Time on Unstirred Spiked SUF Not Maintained Under 5% CO_2 Atmosphere

Relative Concentration (% original spike concentration)			
Sampling Depth	**1 Hour**	**1 Week**	**2 Weeks**
Top	97.6	83.7	60.1
Middle	94.5	90.6	81.5
Bottom	96.2	112.6	125.5

The consequence of the above error in technique was to invalidate the majority of the control samples as monitors of the quality of the analytical process. Fortunately, however, the QC values obtained under normal spiking conditions indicate that there were no systematic problems during this study. This finding is consistent with results of *in vitro* studies done over the past 5 years at LRRI involving uranium dissolution. Therefore, the investigators conclude that the analyses were valid.

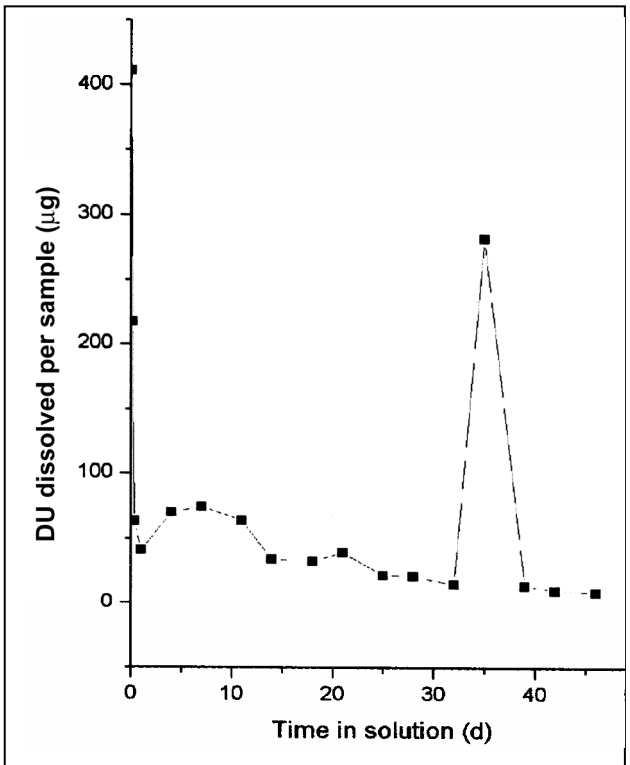

Figure E.1. Example KPA Data Showing Anomalous Day-35 Uranium Value

E.3.2 Data Anomaly

During early data evaluation, the investigators realized that the data associated with samples collected at 35 days were unreasonably high and were inconsistent with the uranium values measured for the samples that were collected before and after the 35-day mark (Figure E.1). Because these data comprised a single batch of analyzed samples, the investigators deduced that a problem had occurred with, and was limited to, this particular batch. To determine whether there had been any systematic bias associated with the KPA instrument for the

samples in this batch, all of the 35-day samples were re-analyzed for U content. The average ratio (∀SD) of the rerun/original U values was 0.94∀0.08, indicating that the KPA was properly calibrated and that the measured uranium values reflected the uranium content of those samples. The possibility that this sample batch could have been mislabeled in terms of the collection data was also ruled out because the sample batches were run sequentially as they were collected. A mistake in date assignment would not have resolved this problem; instead the problem would have appeared at a different time. The only logical conclusion was that several of these samples became contaminated with uranium in some unknown manner. Therefore, the entire measured set of data for day-35 was replaced by interpolated results based on averaging the uranium content in the day-32 and day-39 samples. These averaged data were then inserted into the data set for fitting. This approach is believed to be a prudent solution to resolving the data anomaly and, in some cases, improved the statistical data fits substantially.

E.3.3 *In Vitro* Dissolution

The *in vitro* dissolution data set from each sample was fitted to both two- (Equation E.1) and three-component (E.2) exponential equations:

$$Y = a_1 e^{-b1t} + (100-a_1) e^{-b2t} \quad [E.1]$$

$$Y = a_1 e^{-b1t} + a_2 e^{-b2t} + (100 - a_1 - a_2) e^{-b3t} \quad [E.2]$$

where Y is the fraction (in percent) of undissolved DU in the sample at time t. Note that each individual fit was constrained to equal 100% undissolved at time t = 0. The fits were done using the nonlinear least-squares fitting module of the Origin software (v.6.0), which uses a Levenberg-Marquardt algorithm for optimization. The results of analyzing the adjusted data sets from the *in vitro* dissolution studies are depicted in Figures E.2 through E.28, and the parameters for the two- and three-component negative exponential fits of the respective data sets are summarized in Tables E.4 and E.5 along with the standard errors for the values of the fitted parameters. All of the data could be fit adequately by multi-component negative exponential functions, which is typical for *in vitro* dissolution data. In general, the results indicated that the three-component fits were superior to the two-component fits, sometimes marginally (e.g., PI-2I-D-7-FS), and sometimes significantly (e.g., PI-3/4I-CY-3). This judgment was based on both the value of the correlation coefficients (R^2) and visual inspection. In a few cases (e.g., PI-3/4I-CY-BU and DU cone [unsep]), only two-component fits were obtained.

The consequence of selecting a two- or three-component fit impacts the predicted retention function for the inhaled material. Because the retention of particles in the lung is determined by several clearance mechanisms, including *in vivo* dissolution, it is not immediately obvious how large an impact this choice of functions would have. However, if the dissolution functions are integrated, a measure of the integrated activity at the deposition site (in Bq-d or equivalent units) is obtained. For example, comparing the integrated activities to 50 days after exposure for sample PI-2I-D-7-FS shows that the three-component fit is the same as that for the two-component fit; for sample PI-3/4-CY-3, the three-component fit is 7% greater. Therefore, for short periods after exposure, there are no significant differences. However, if one compares the projected results for a 1000-day period, differences emerge. Using the same samples, the three-component fits for samples PI-2I-D-7-FS and PI-3/4-CY-3 are 16% and 180% greater than those for the two-component fits. This latter example would lead to a different organ dose distribution (because of longer predicted lung retention, and consequently less uptake and dose to the systemic organs), and would also affect the shape of the urine bioassay curve, especially for longer times after exposure. This uncertainty should be investigated in the dose assessment study planned to follow the Capstone study.

Table E.4. Two-Component Fit Parameters for *In Vitro* Dissolution of DU Aerosol Samples

Sample ID	Two-Component Fit								
	a_1 (%)	SE*	b_1 (d^{-1})	SE*	a_2 (%)	SE*	b_2(d^{-1})	SE*	R^2
PI-2I-D-1-FS	7.8	0.4	2.1	0.4	92.2	0.4	0.0014	0.0002	0.9708
PI-2I-D-3-FS	13.8	0.7	2.4	0.5	86.2	0.7	0.0033	0.0003	0.9717
PI-2I-D-4-FS	18.5	0.8	4.1	0.7	81.5	0.8	0.0034	0.0004	0.9674
PI-2I-D-6-FS	13.6	0.7	1.9	0.4	86.4	0.7	0.0028	0.0003	0.9752
PI-2I-D-7-FS	9.2	0.4	3.9	0.6	90.8	0.4	0.0039	0.0002	0.9922
PI-3/4I-CY-2	13.9	0.3	13.7	1.5	86.3	0.3	0.0014	0.0001	0.9706
PI-3/4I-CY-3	27.5	1.2	11.0	2.6	72.5	1.2	0.0069	0.0007	0.9414
PI-3/4I-CY-4	21.6	0.6	26.1	4.7	78.4	0.6	0.0080	0.0004	0.9813
PI-3/4I-CY-5	27.2	0.7	31.7	5.4	72.8	0.7	0.0095	0.0004	0.9786
PI-3/4I-CY-BU	1.0	0.04	25.7	6.7	99	0.04	0.00086	0.0002	0.9987
PI-7I-CY-1	28.2	0.7	4.1	0.4	71.8	0.7	0.0033	0.0004	0.9838
PI-7I-CY-2	11.8	0.4	14.2	2.8	88.2	0.4	0.0018	0.0002	0.9405
PI-7I-CY-3	25.9	1.2	4.5	0.8	74.1	1.2	0.00061	0.0006	0.9524
PI-7I-CY-4	25.7	1.0	8.1	1.6	74.3	1.0	0.0050	0.0006	0.9460
PI-7I-CY-5	21.9	0.7	21.8	4.6	78.1	0.7	0.0059	0.0004	0.9601
PI-7I-CY-BU	10.5	0.6	4.2	0.9	89.5	0.6	0.0019	0.0002	0.9441
PII-1/2I-CY-2	18.9	0.5	6.7	0.8	81.1	0.5	0.0033	0.0002	0.9814
PII-1/2I-CY-3	19.8	0.5	6.6	0.8	81.2	0.5	0.0039	0.0002	0.9834
PII-1/2I-CY-4	27.1	1.1	6.4	1.1	72.9	1.1	0.0068	0.0006	0.9716
PII-1/2I-CY-5	27.6	0.4	10.5	0.9	72.4	0.4	0.0066	0.0002	0.9924
PII-1/2I-CY-BU	15.0	0.3	6.7	0.7	85.0	0.3	0.0029	0.00015	0.9890
PIII-2I-CY-4	4.0	0.3	1.8	0.5	96.0	0.3	0.0013	0.0001	0.9746
PIII-2I-CY-5	4.6	0.4	2.8	1.0	95.4	0.4	0.0024	0.0002	0.9765
PIII-2I-CY-BU	11.0	0.2	3.9	0.3	89.0	0.2	0.0014	0.0001	0.9892
DiffBat7	20.5	7.7	0.084	0.035	79.5	7.7	0.0014	0.0021	0.9802
DU cone (unsep)	1.4	0.1	6.2	1.6	98.6	0.1	0.00041	0.00003	0.9640
DU cone (sepated)	6.3	0.2	16.2	3.4	93.7	0.2	0.0015	0.00009	0.9711
SE* Standard error of the respective fitted parameter									
ND† Standard error not determined by the fitting program									

E.3.4 Effect of Aerodynamic Particle Size on *In Vitro* Solubility

The U *in vitro* dissolution results for the cyclone stages obtained from PI-3/4, PI-7; PII-1/2; and PIII-2 are depicted in Figures E.29 through E.32, respectively. Briefly, the results indicate that there were differences in the *in vitro* solubility characteristics for the various stages, but the differences were not systematic; that is, the dependence of dissolution rate on aerodynamic particle size was not straightforward.

Table E.5. Three-Component Fit Parameters for *In Vitro* Dissolution of DU Aerosol Samples

Sample ID	Three-Component Fit												
	a_1 (%)	SE*	$b_1(d^{-1})$	SE*	a_2 (%)	SE*	$b_2(d^{-1})$	SE*	a_3 (%)	SE*	$b_3(d^{-1})$	SE*	R^2
PI-2I-D-1-FS	4.7	0.4	5.7	1.1	4.7	0.5	0.18	0.04	90.6	0.6	0.00091	0.00014	0.9961
PI-2I-D-3-FS	8.0	0.4	8.2	1.1	8.8	0.5	0.20	0.03	83.2	0.6	0.0022	0.0002	0.9984
PI-2I-D-4-FS	14.9	1.4	6.0	1.3	7.5	2.4	0.14	0.10	77.6	2.8	0.0018	0.0009	0.9857
PI-2I-D-6-FS	8.3	0.5	5.0	0.7	8.7	0.8	0.15	0.03	83.0	0.9	0.0016	0.0003	0.9978
PI-2I-D-7-FS	7.2	0.3	6.2	0.7	4.2	0.6	0.13	0.04	88.6	0.7	0.0032	0.0002	0.9989
PI-3/4I-CY-2	12.8	0.1	17.1	0.4	3.0	0.2	0.14	0.02	84.2	0.2	0.00073	0.00008	0.9992
PI-3/4I-CY-3	22.3	0.4	21.7	1.5	13.5	1.1	0.15	0.02	64.2	1.2	0.0032	0.0005	0.9978
PI-3/4I-CY-4	20.0	0.4	31.5	2.8	21	19	0.043	0.029	58.7	19	0.0021	0.0045	0.9971
PI-3/4I-CY-5	21.1	1.2	63	17	8.2	1.2	1.9	0.6	70.7	1.7	0.0084	0.0002	0.9976
PI-3/4I-CY-BU	--		--		--		--		--		--		--
PI-7I-CY-1	24.9	0.6	5.1	0.3	10.2	3.3	0.084	0.033	64.9	3.2	0.00067	0.0010	0.9977
PI-7I-CY-2	10.2	0.1	21.8	1.3	5.0	0.7	0.11	0.02	84.8	0.7	0.00062	0.00020	0.9974
PI-7I-CY-3	18.1	1.0	11.4	2.0	12.9	1.4	0.21	0.05	69.0	1.7	0.0025	0.0006	0.9920
PI-7I-CY-4	20.1	0.4	16.2	1.1	10.9	0.7	0.19	0.03	69.0	0.8	0.0026	0.0003	0.9980
PI-7I-CY-5	19.5	0.3	29.2	1.8	12.0	2.5	0.083	0.021	68.5	2.5	0.0024	0.0008	0.9980
PI-7I-CY-BU	6.8	0.2	14.5	1.8	6.4	0.4	0.19	0.03	86.8	0.4	0.0010	0.0001	0.9971
PII-1/2I-CY-2	17.4	0.9	7.8	1.2	4.7	4.6	0.091	0.12	77.9	4.6	0.0022	0.0014	0.9879
PII-1/2I-CY-3	13.2	0.7	15.8	1.5	7.6	0.7	1.1	0.2	89.2	1.0	0.0035	0.00009	0.9987
PII-1/2I-CY-4	25.6	2.0	7.1	1.7	16.8	100	0.039	0.17	57.6	100	0.0024	0.022	0.9757
PII-1/2I-CY-5	26.0	0.1	12.2	0.2	11.2	3.2	0.055	0.013	62.8	3.2	0.0034	0.0008	0.9998
PII-1/2I-CY-BU	14.0	0.4	7.7	0.8	8.8	19.8	0.039	0.067	77.2	20	0.0010	0.0034	0.9949
PIII-2I-CY-4	2.7	0.2	3.8	0.9	7.5	0.4	0.044	0.006	89.8	0.5	0	ND†	0.9950
PIII-2I-CY-5	4.6	0.7	2.8	1.2	80	300	0.0029	0.012	15	300	4E-17	ND†	0.9770
PIII-2I-CY-BU	9.8	0.2	4.8	0.3	4.5	2.5	0.061	0.036	84.7	2.5	0.00041	0.00055	0.9981
DiffBat7	3.1	1.4	2.9	2.8	24.6	21.7	0.049	0.042	72.3	21.7	3.1E-6	0.0048	0.9915
DU cone (unsep)	--		--		--		--		--		--		--
DU cone (separated)	5.7	0.3	20.7	4.7	1.3	0.5	0.23	0.25	93.0	0.6	0.0013	0.0002	0.9817

According to Mercer's theory of aerosol particle dissolution (Mercer 1967), the dissolution of particles is directly proportional to the specific surface area of the particles. For particles having similar shapes (and therefore similar shape factors), the specific surface area will increase with decreasing particle size. Because the cyclone stages selectively collect particles of decreasing size in the progressive stages, it would be expected that the *in vitro* dissolution rates would increase with increasing stage number (i.e., 1<2<3<4<5<backup filter). As will be shown, this trend was sometimes observed, but there were significant exceptions.

The results of dissolution studies of the material collected from the cyclone stages and backup filters are described by target, phase, and shot. Note that Stage 1 was analyzed for PI-7 only. These result descriptions are followed by descriptions of the results of the filter samples and the DU cone sample.

E.3.4.1 Abrams Tank

Phase I, Shots 3/4. The order of increasing dissolution (Figure E.29 and fit parameters from Table E.4) was measured to be backup filter<2<3,4<5. The order of dissolution for the discrete stages showed a trend of increased dissolution with decreasing particle size, as reflected by the stage number order. The results for material found in the backup filter, however, were anomalous, because the backup filter should collect the smallest sized particles of all of the sampling stages. The finding that the material from the backup filter showed the lowest dissolution level is not consistent with Mercer's theory. Additionally, the shapes of the curves did not vary consistently. In particular, both Stage 2 and backup filter curves showed small slopes for the long-term components. The major difference between Stage 2 and backup filter is in the amount dissolving rapidly. The long-term slopes for Stages 3, 4 and 5 were reasonably consistent with default Type M.

Phase I, Shot 7. For this cyclone, all of the stages were analyzed. The order of increasing dissolution (Figure E.30, Table E.4) was found to be backup filter, 2 < 1,3,4,5. This behavior is similar to the grouping noted for PI-3/4. For this shot, very little stage-specific dissolution was observed. The dissolution behavior showed two groupings of data, whose major differences were in the amounts of uranium that dissolved in the first day. For backup filter and Stage 2, 7-10% dissolved by Day 1, whereas, for the remaining group of stages, 18-24% dissolved. The longer-term slopes were reasonably similar for all six of the analyzed samples. As with PI-3/4, the material collected on Stage 2 and the backup filter had the least solubility.

E.3.4.2 Bradley Fighting Vehicle

Phase II, Shots 1/2. Cyclone material from Stages 2 through 5 was analyzed. The order of increasing dissolution (Figure E.31, Table E.4) was found to be backup filter < 2,3 < 4,5. The trend of increasing dissolution with increasing stage number was reasonably consistent for the samples in this series. The major difference seen in dissolution was the fraction of the uranium that dissolved in the first day of the study. The long-term slopes for the backup filter and Stages 2 and 3 were essentially the same; the slopes for Stages 4 and 5 also were also the same but larger than those of the previous grouping. As with the results from the Abrams series (Phase I), material collected on the backup filter showed the least dissolution over the 46-day study period.

E.3.4.3 Abrams Tank with DU Armor

Phase III, Shot 2. Because so little material was collected on cyclone Stages 2 and 3, only Stages 4 and 5 plus the backup filter were analyzed. The uranium collected on the backup filter had the highest solubility of the three samples (Figure E.32, Table E.4), in contrast to previously described data. The results from this test most resembled the dissolution data obtained from the backup filter analysis for PI-7. The dissolution rates for Stages 4 and 5 showed 3 to 5% uranium dissolution during the first day, followed by fairly small slopes for the remaining days. By Day 46, 91% and 87% of the uranium was undissolved for Stages 4 and 5, respectively. This is more reminiscent of Type S dissolution (where 99.4% would be predicted to be undissolved at Day-46) than Type M (about 70% undissolved).

E.3.4.4 Additional Samples

Phase I, Shot 2, Driver's Array Filter Samples. A separate comparison can be made of the five IOM filter samples (1, 3, 4, 6, and 7) that were analyzed for *in vitro* dissolution because the time-sequenced filters should have collected increasingly smaller aerodynamic particle sizes as a function of elapsed time as the larger particles settled out of the atmosphere within the vehicle. In that sense, increasing time would correspond qualitatively to increasing cyclone stage number. The IOM filters operated within these post-shot intervals:

IOM-1	5 to 35 sec
IOM-3	1 min, 30 sec to 3 min, 30 sec
IOM-4	3 min, 30 sec to 7 min, 30 sec
IOM 6	15 min, 30 sec to 31 min, 30 sec
IOM 7	32 min, 30 sec to 1 h, 30 sec

The results (Figure E.33, Table E.4) show the following sequence of increasing dissolution rates (operating times shown as post-shot): $1 < 3,6,7 < 4$. This sequence appears to be almost random, and the range of dissolution only represents a difference of about 20% of the undissolved uranium by the end of the study, ranging from 90% to 70%. In this series of samples, there were differences in initial dissolution (1-d values), ranging from 5% to 15% dissolved, as well as in the long-term slopes, which varied by about a factor of three.

DU Cone Sample. Two samples from a DU "cone" sample, in which a DU metal fragment ignited and burned intact on the floor of Abrams ballistic hull and turret (BHT), were tested for *in vitro* solubility. This powder consisted almost entirely of DU oxide and contained only small amounts of other metal oxides (iron, aluminum, and titanium). The sample designated as unseparated (unsep) was a bulk powder sample, and the separated (sep) sample was size-segregated by sedimentation in alcohol. The results showed that the separated sample had a larger fraction of uranium that dissolved in the first day (6.3% vs. 1.4 %), and its slope was about four times that of the unseparated sample. This finding probably represents the effect of removing the largest particles during the sedimentation procedure and is consistent with a particle-size-dependent effect.

E.3.5 Effect of Target on Aerosol Solubility

A useful approach to evaluating differences in *in vitro* solubility of aerosols produced by DU penetrator impact on different types of armor is to compare the measured solubilities for samples having similar size

characteristics (i.e., from the same cyclone stages from different shots). This approach was used to generate the data shown in Figures E.35 through E.39. For cyclone stages 2 and 3, only data from two Abrams shots and one Bradley vehicle shot were available; additional data were available from Phase III (DU penetrator impacting DU armor) for cyclone stages 4 and 5 and the backup filter.

The results for Stages 2 and 3 were disparate. For stage 2, the Phase-II sample was more soluble than both of the Phase-I samples, which were essentially the same. The differences were due to a somewhat larger fraction of uranium dissolved in the Day-1 sample and a larger long-term slope for the Phase-II sample. In comparison, the opposite was noted for Stage 3; the Phase-II sample dissolved more slowly than either of the Phase-I samples. In this case, the differences were mainly in the magnitude of the long-term slopes. It is interesting that the "role reversal" was due to differences in the Phase-I samples, as the *in vitro* dissolution of the Phase-II samples for Stages 2 and 3 were essentially the same. It is not clear whether this similarity was a true characteristic of these samples or random variability due to the small samples analyzed. Replicate analyses would be needed to clarify this question. However, the results from Stages 4 and 5 are reasonably consistent. The solubility of the aerosol particles collected for the Phase-III shot were substantially less soluble than those from either of the Phase-I shots or the Phase-II shot. The principal difference appears to be in the fraction of U dissolving in the first day, although the long-term slopes for the Phase-I and II samples were also greater than that for the Phase-III sample. This was not the case for the backup filter samples, where the PI-3/4 sample was least soluble. As in earlier comparisons it is difficult to discern uniformly consistent trends. Nevertheless, it does appear that the Phase-III smaller-sized aerosols resulting from interaction of a DU penetrator with DU armor were less soluble than those produced by the interaction of a DU penetrator with either Abrams or Bradley side armor. There do not appear to be consistent differences in solubility between the aerosols produced from Abrams or Bradley side armors.

E.4 Discussion

Visual inspection of the goodness of fit of the two- and three-component functions, as well as the standard errors for the fitted parameters, shows that for the most part the three-component fits were better. As pointed out previously, there would be no impact of either function at relatively early times after inhalation exposure on biokinetics or the uranium urinary excretion curve. However, at longer times (i.e., greater than 1 year after exposure), differences would be seen in the urinary excretion functions. It is likely that intake interpretation based on using the three-component functions as drivers of *in vivo* solubility would provide better estimates. It should be pointed out, however, that there were occasions where a third fitted component was either not justified (e.g., DU cone [unsep], PI-3/4 BU, PIII-2, Stage 5) or that the third component parameters (usually the intermediate dissolution component) were unstable despite the goodness-of-fit of the total function (e.g., PIII-2 BU, DU cone [sep], PII-1/2 Stage 4). The dose assessment portion of this study will need to address the uncertainties and sensitivities of the dose estimates on assumptions of *in vivo* solubility.

In general, most of the *in vitro* solubility functions resembled most closely the Type-M absorption behavior as defined in Publication 66 of the International Commission of Radiation Protection (ICRP) Human Respiratory Tract Dosimetry Model (HRTM) (ICRP 1994). Some samples, such as PI-3/4-CY-BU and U(unsep) samples more resembled Type-S behavior, which is the least soluble category of the HRTM, and some showed Type-S, long-term behavior coupled with significant solubility

over the first day (e.g., PI-7 Stage 2, PI-7 BU). Considering the heterogeneity of both physical and chemical forms of the U-containing aerosols, these combinations are not surprising.

None of the aerosol samples showed the most rapid Type-F behavior, suggesting that the conditions of aerosol formation were not conducive to formation of large amounts of the higher oxides of uranium such as UO_3 or UO_4. However, this does not preclude the possibility that subsequent additional oxidation could not happen as a function of time after impact, which could result in a shift to more soluble forms as a result of environmental weathering. Thus the results of this study should be constrained to apply to exposures that occur relatively soon after a DU impact event (minutes to weeks); correspondingly, the time frame for potential changes in solubility would probably be extensive—that is, months to years depending on environmental conditions.

Despite the preponderance of Type-M-like behavior, significant differences were seen among the various samples. The most significant differences noted were in the fraction of DU that dissolved rapidly, usually within 1 day. This ranged from about 4% to as much as 30%. There also appeared to be a correlation between the initial rate of dissolution and the subsequent dissolution rate; the more U dissolving in the first day, the more rapid the long-term dissolution. This behavior is exemplified reasonably well in Figure E.29.

The dissolution behavior of the various aerosol samples tested is most likely to be influenced by the article shapes and sizes, which affect the specific surface area, the chemical form of the uranium within the particles, and the degree of heterogeneity of the various elements comprising the particles. Focusing first on the influence of particle size, it must be noted that the size cutoff curves, expressed as effective cutoff diameters (ECD), are not as steep as those for cascade impactors (CIs). This means that the segregation of particles by aerodynamic size on the various cyclone stages is not as marked as for a size-separating device with sharper ECD curves. Thus, it is as probable that larger particles will be found on stages with small ECDs as smaller particles on stages with larger ECDs, particularly for particles that agglomerate after collection. This blending of particles of apparently widely varying physical size on the different cyclone stages was observed in the scanning electron micrographs (see Appendix D).

As mentioned previously, the heterogeneity of the aerosol particles probably significantly influenced the particle-size-specific dissolution rates observed in this study. Review of the scanning electron microscopy (SEM) micrographs showed the presence of several discrete forms of uranium in the aerosol cloud formed as a result of the DU penetration of armor (micrographs of aerosol cloud formations in Appendix D). One form consisted of irregularly shaped particles with sizes in the tens of :m and with surfaces that appeared to be fracture surfaces (Figure D.2). These particles typically had very high uranium contents and low oxygen contents, and are believed to be uranium metal particles that were spalled from the surface of the DU penetrator during perforation. A second type of particle, typically spherical, between 1 and about 12 µm in diameter, and with high uranium and oxygen contents, had what appeared to be a highly vesiculated or compartmented surfaces with well-defined, cell-like features (e.g., see Figure D.3). The surfaces of these particles were often irregularly coated with relatively electron-lucent material having the appearance of a moldy growth. This latter material had little or no uranium elemental signature. A third type of particle, which predominated in number particularly in cyclone Stages 4 and 5, consisted of ill-defined agglomerates of relatively electron-lucent materials (Figure D.13, a-d). Embedded within this flocculent-appearing matrix were numerous micrometer- and submicrometer-sized spherical uranium particles. The physical sizes of the aggregates ranged from a few micrometers to several tens of micrometers.

The presence of these different types of particles confounds the relationship between uranium dissolution and aerodynamic particle size. For example, the aggregate particles have varying amounts of uranium particles embedded within them, and the relative proportions of the different types of particles captured in an analyzed sample will likely influence its measured solubility. Thus the relationship between aerodynamic particle size and uranium content is probably highly variable. That a relationship between solubility and cyclone stage number was observed in many cases probably suggests that 1) there were different proportions of the different morphologically identifiable uranium-containing particles on the different stages, and 2) the different particles had different dissolution characteristics. This relationship might be further investigated by performing SEM analysis on a population of particles both before and after (undissolved) *in vitro* dissolution, and determining if there is a change in the population and/or size distribution of the particles.

A second factor that confounds the relationship between aerodynamic particle size and solubility is the fact that the stage collection efficiency curves for a cyclone are not as distinct as those for a CI. This leads necessarily to overlaps in size-specific collections of particles on adjacent stages of the cyclone, which in turn will tend to blur differences in particle-specific solubility. If it becomes important to define the size-solubility relationship more carefully, it might be possible to resuspend some of the dry powders collected by the cyclone and collect them on CI substrates. This approach would refine the particle size separation, and would allow follow-up *in vitro* dissolution studies to be done. However, this should not be considered until a sensitivity analysis of dose on solubility has been done in the dose assessment portion of this study.

In terms of inter-armor comparison of *in vitro* solubility, there did not appear to be consistent differences between the aerosols resulting from the Abrams and Bradley side-armor shots when compared on a stage-by-stage basis (Figures E.35 through E.39). The Bradley-derived aerosols were sometimes more soluble than those from the Abrams tests (Figures E.35 and E.39), sometimes less (Figure E.36), and sometimes the same (Figures E.37 and E.38). The aerosols from Phase III (DU penetrator against DU armor), however, appeared to be less soluble than those of either Phase I (Abrams side armor) or Phase II (Bradley side armor). Whether this was due to differences in interacting materials, particle size/morphology, or to differences in temperature and pressure history as the DU munition penetrated the armor is not known.

Reproducibility of *in vitro* dissolution for different shots from the same target (Phase) can be compared from the data obtained from PI-3/4 and PI-7. Although there may be differences in armor compositions between these two shots (Shots 3/4 were turret shots on an Abrams and Shot 7 was a hull shot), the majority of the cyclone stages (2, 3, 4) showed similar dissolution patterns. Stage 5 showed about a 10% greater amount of uranium dissolved in the first day for PI-3/4, and substantially less uranium dissolved on the backup filter. Although the comparison lacks consistency across stages, it appears that different shots produced aerosols with similar *in vitro* dissolution behavior. This seems logical if the paths of DU penetrators result in interaction with similar metals in the armor, although armor thickness may vary.

Because the regulatory framework of radiation protection for both the U.S. Nuclear Regulatory Commission (NRC) and U.S. Department of Energy (DOE) is based on biokinetic models from Publication 30 of the ICRP (1979), the *in vitro* results can be used to assign proportionate amounts of DU to the default clearance Classes D, W, and Y according to the following criteria: the fraction of dissolved DU associated with half-times ($T_{1/2}$) < 10 days are assigned to Class D; fractions associated with 10 d # $T_{1/2}$ # 100 d as Class W; and fractions associated with $T_{1/2}$ > 100 d as Class Y. Accordingly, Table E.6

summarizes the D, W, and Y classification for the 27 *in vitro* samples analyzed in this study. Note that, when possible, the results of the three-component exponential fits were used. In all cases, more than 50% of the DU aerosol sample was assigned to Class Y clearance. In some cases, the Class Y fraction was >90%. From 1% to about 30% of the DU aerosols dissolved rapidly enough to be considered Class D. Seven of the samples had amounts ranging from 4% to 25% assigned to Class W. It thus appears that there is significant variability among the various samples analyzed in terms of their assignments to the default clearance classes. This variability was certainly highlighted by the fitted curves and is reinforced here.

Table E.6. Assignment of ICRP 30 Clearance Class Based on *In Vitro* Solubility Measurements (three-component fits)

Sample ID	Class D	Class W	Class Y
PI-2I-D-1-FS	9.4	--	90.6
PI-2I-D-3-FS	16.8	--	83.2
PI-2I-D-4-FS	22.4	--	77.6
PI-2I-D-6-FS	17.0	--	83.0
PI-2I-D-7-FS	11.4	--	88.6
PI-3/4I-CY-2	15.8	--	84.2
PI-3/4I-CY-3	35.8	--	64.2
PI-3/4I-CY-4	20.0	21.3	58.7
PI-3/4I-CY-5	29.3	--	70.7
PI-3/4-CY-BU	1.0	--	99
PI-7I-CY-1	35.1	--	64.9
PI-7I-CY-2	15.2	--	84.8
PI-7I-CY-3	31.0	--	69.0
PI-7I-CY-4	31.0	--	69.0
PI-7I-CY-5	31.5	--	68.5
PI-7I-CY-BU	13.2	--	86.8
PII-1/2I-CY-2	22.1	--	77.9
PII-1/2I-CY-3	20.8	--	89.2
PII-1/2I-CY-4	25.6	16.8	57.6
PII-1/2I-CY-5	26.0	11.2	62.8
PII-1/2I-CY-BU	14.0	8.8	77.2
PIII-2I-CY-4	2.7	7.5	89.8
PIII-2I-CY-5	4.6	--	95.4
PIII-2I-CY-BU	9.8	4.5	84.7
DiffBat7	3.1	24.6	72.3
DU cone (unsep)	1.4	--	98.6
DU cone (separated)	7.0	--	93.0

The categorization of the *in vitro* results in terms of solubility depends strongly on which model is selected (i.e., the ICRP 30 model or the ICRP 66 model [1994]). There is a general equivalence between the absorption Types (F, M, S) and the clearance Classes (D, W, Y), but the numerical values that define the respective categories for a given set of data are different. Because Type F represents absorption that is significantly more rapid than for Class D, and Type S is significantly slower than Class Y, the consequence is that more results end up as Type M. In other words, the Type-M "box" is larger than the corresponding Class-W "box." However, the classes and types are used differently in their respective model structures, so it is not appropriate to simply compare them one-to-one. Specifically the absorption types represent the transfer of material via a dissolution pathway mainly to blood, and this pathway competes in the HRTM with mechanical clearance of particulate material either up the conducting airways to the gastrointestinal tract or via the lymph nodes draining the lung. On the other hand, the clearance classes of ICRP 30 represent the combined effects of mechanical clearance and dissolution/ absorption. In any case, for this report, it is adequate to simply compare the results obtained with the *in vitro* solubility tests with the ICRP models, recognizing that more detailed exposure-dose assessment will be forthcoming.

E.5 References

Brina, R. and A. G. Miller. 1992. "Direct Detection of Trace Levels of Uranium by Laser-Induced Kinetic Phosphorimetry," *Anal. Chem.*, 64, 1413-1418.

Eidson, A. F. and W. C. Griffith, Jr. 1984. "Techniques for Yellowcake Dissolution Studies In Vitro and Their Use in Bioassay Interpretation," *Health Physics*, 46, 151-173.

Eidson, A. F. and J. A. Mewhinney. 1980. "In Vitro Solubility of Yellowcake Samples from Four Uranium Mills and the Implications for Bioassay Interpretation," *Health Physics*, 39, 893-902.

International Commission on Radiological Protection (ICRP). 1979. *Limits for Intakes of Radionuclides by Workers.* Publication 30, Ann. 2, Nos. 3/4, Pergamon Press, Oxford.

International Commission on Radiological Protection (ICRP). 1994. *Human Respiratory Tract Model for Radiological Protection*. Publication 66, Ann. 24, Nos. 1-3, Pergamon Press, Oxford.

Mercer, T. 1967. "On the Role of Particle Size in the Dissolution of Lung Burdens," *Health Physics*, 13, 1211-1221.

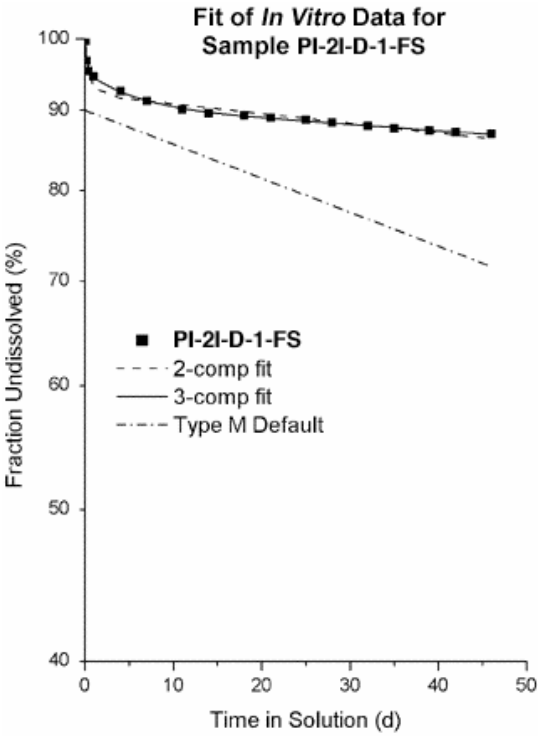

Figure E.2. Fit of *In Vitro* Data for Sample PI-2I-D-1-FS

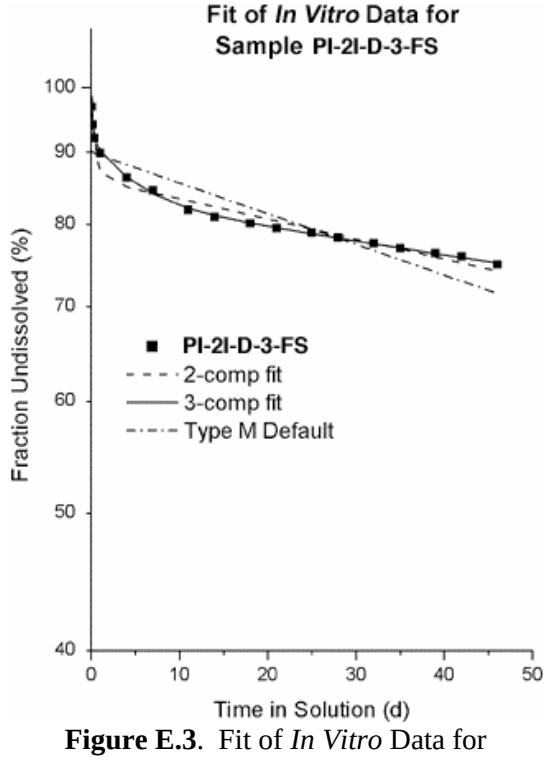

Figure E.3. Fit of *In Vitro* Data for Sample PI-2I-D-3-FS

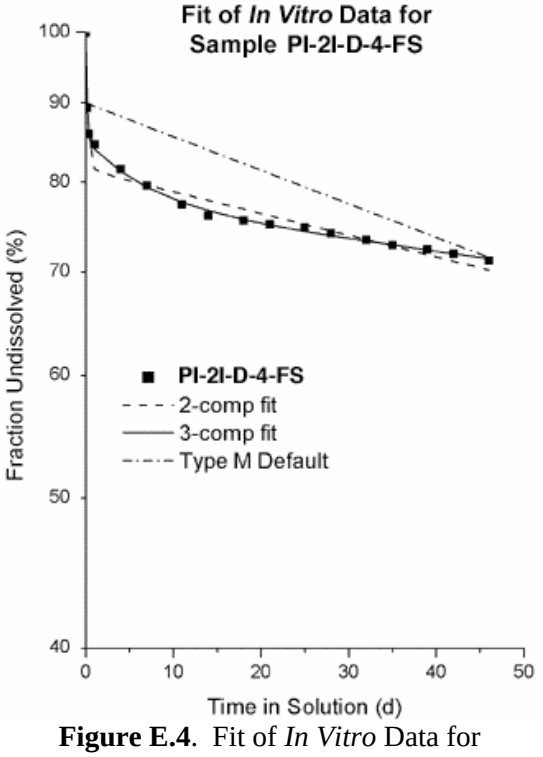

Figure E.4. Fit of *In Vitro* Data for Sample PI-2I-D-4-FS

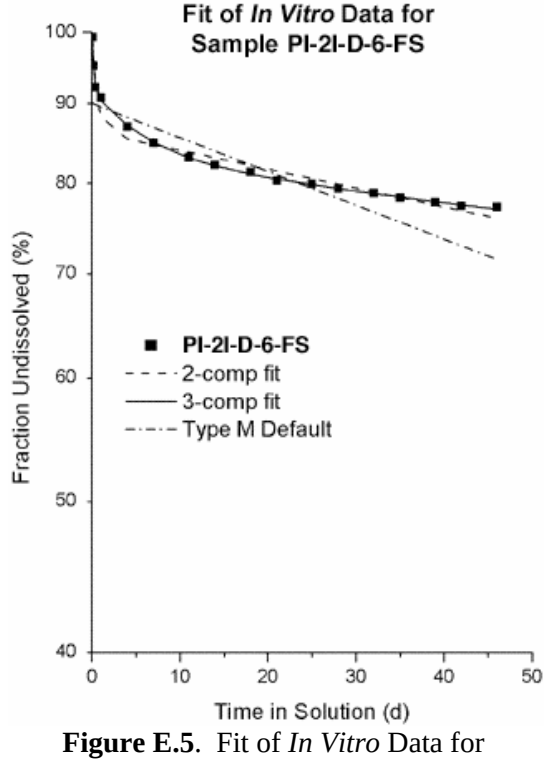

Figure E.5. Fit of *In Vitro* Data for Sample PI-2I-D-6-FS

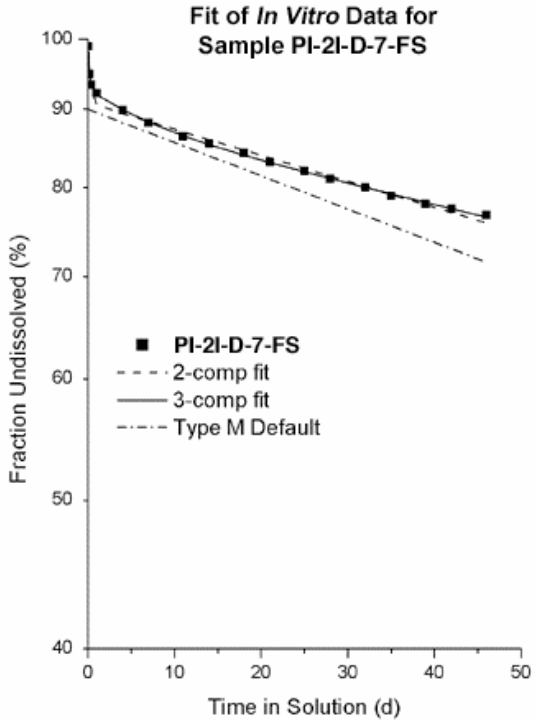

Figure E.6. Fit of *In Vitro* Data for Sample PI-2I-D-7-FS

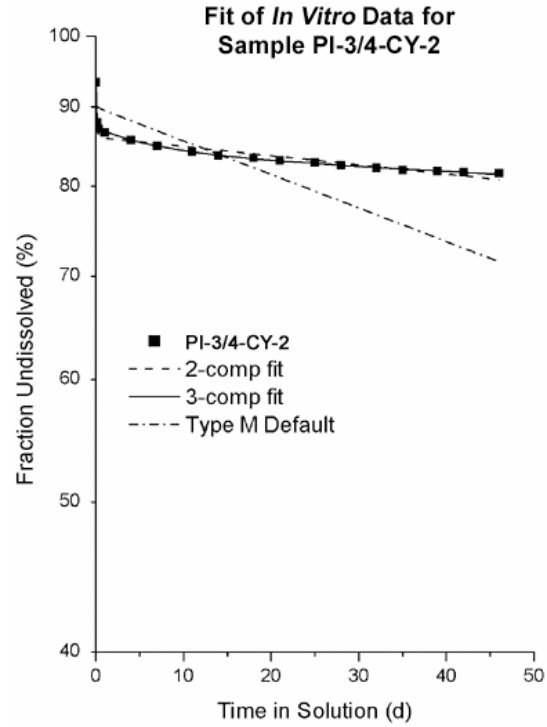

Figure E.7. Fit of *In Vitro* Data for Sample PI-3/4-CY-2

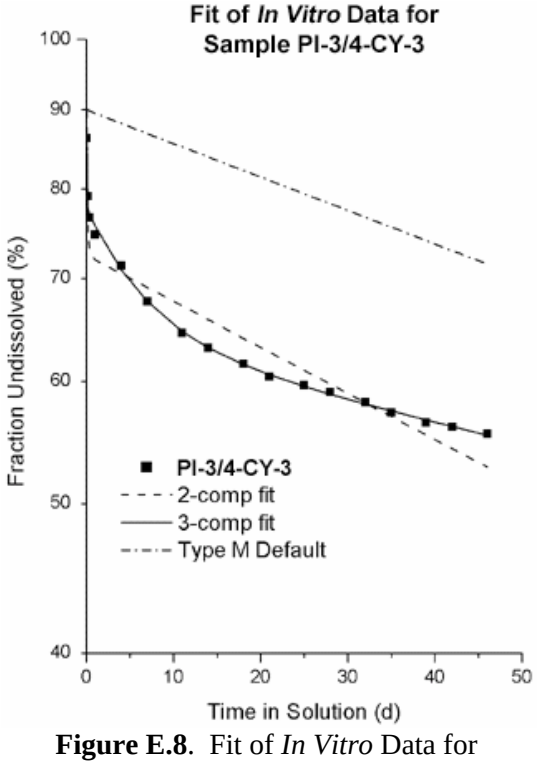

Figure E.8. Fit of *In Vitro* Data for Sample PI-3/4-CY-3

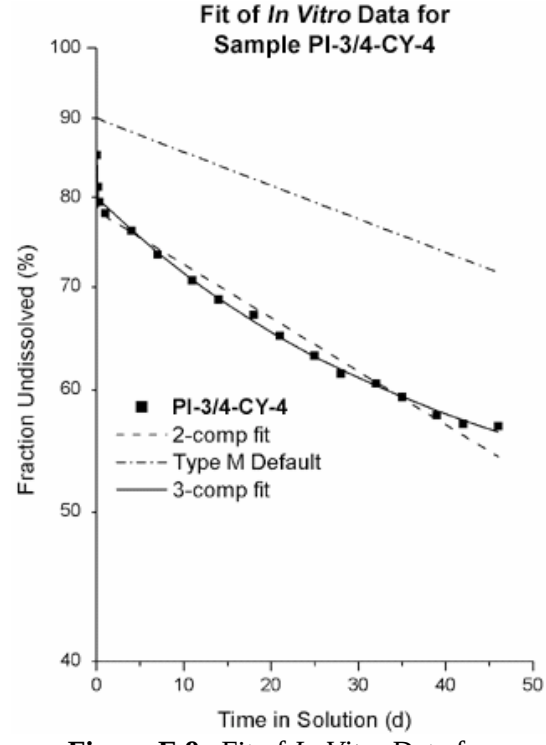

Figure E.9. Fit of *In Vitro* Data for Sample PI-3/4-CY-4

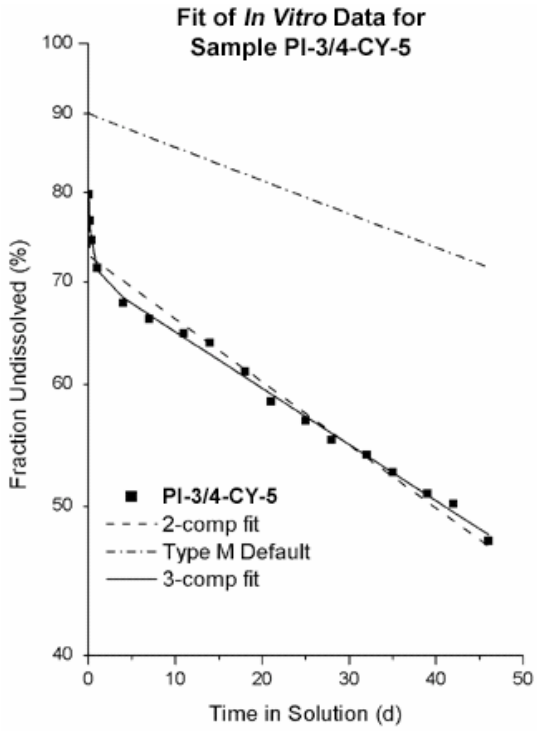

Figure E.10. Fit of *In Vitro* Data for Sample PI-3/4-CY-5

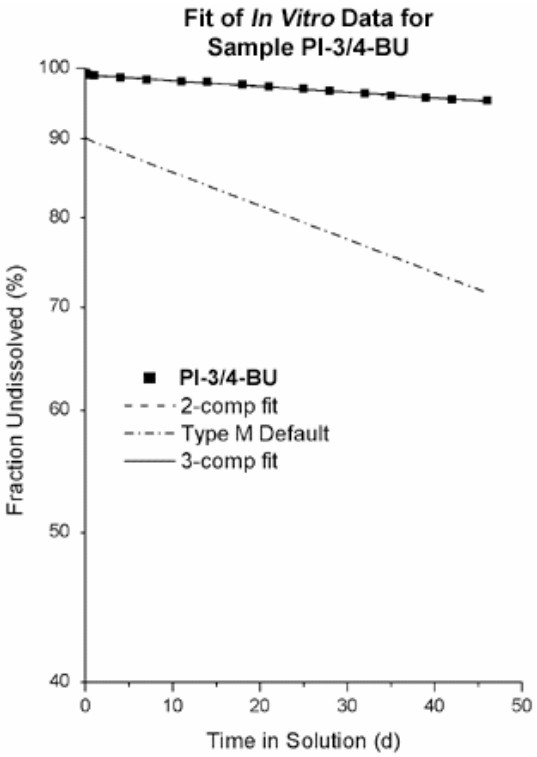

Figure E.11. Fit of *In Vitro* Data for Sample PI-3/4-BU

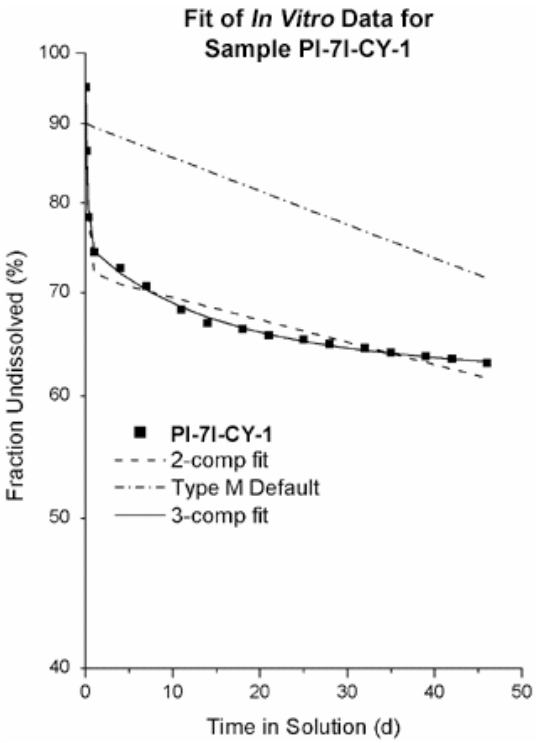

Figure E.12. Fit of *In Vitro* Data for Sample PI-7I-CY-1

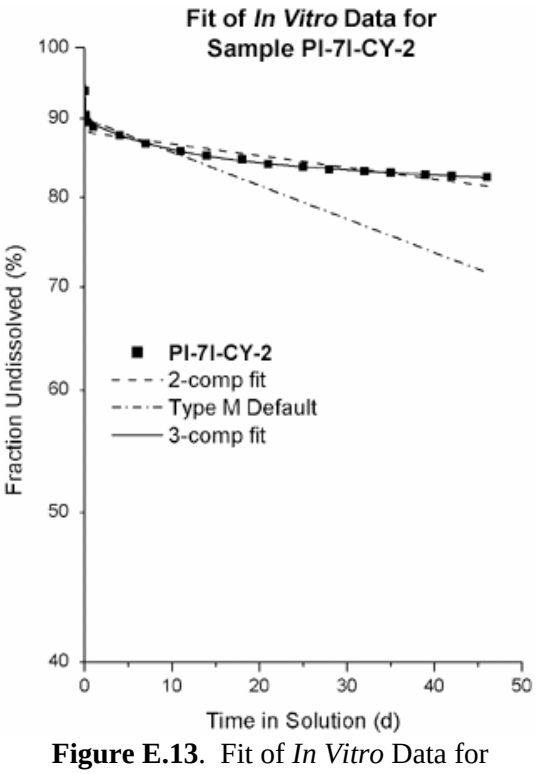

Figure E.13. Fit of *In Vitro* Data for Sample PI-7I-CY-2

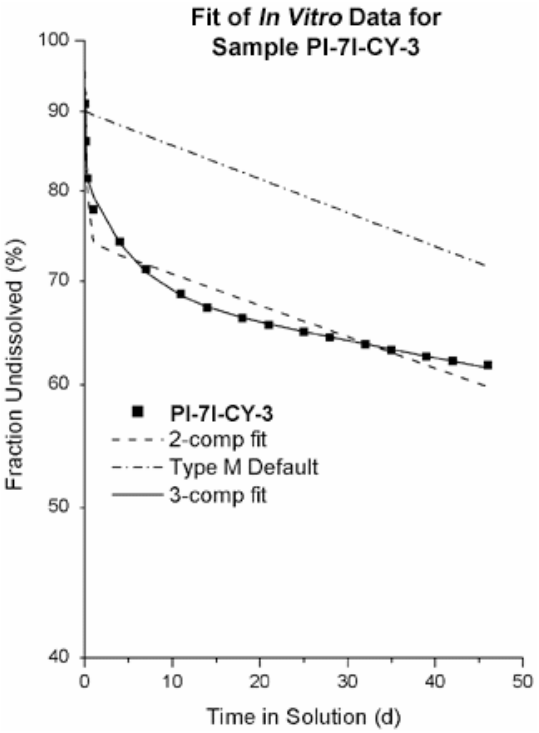

Figure E.14. Fit of *In Vitro* Data for Sample PI-7I-CY-3

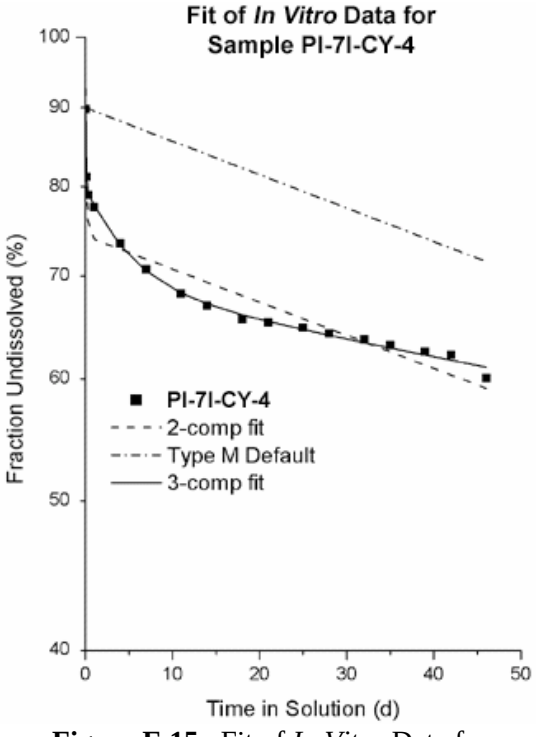

Figure E.15. Fit of *In Vitro* Data for Sample PI-7I-CY-4

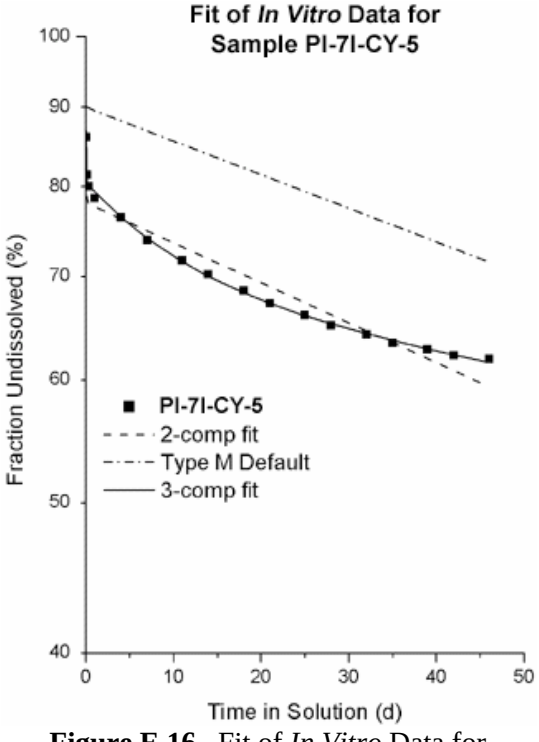

Figure E.16. Fit of *In Vitro* Data for Sample PI-7I-CY-5

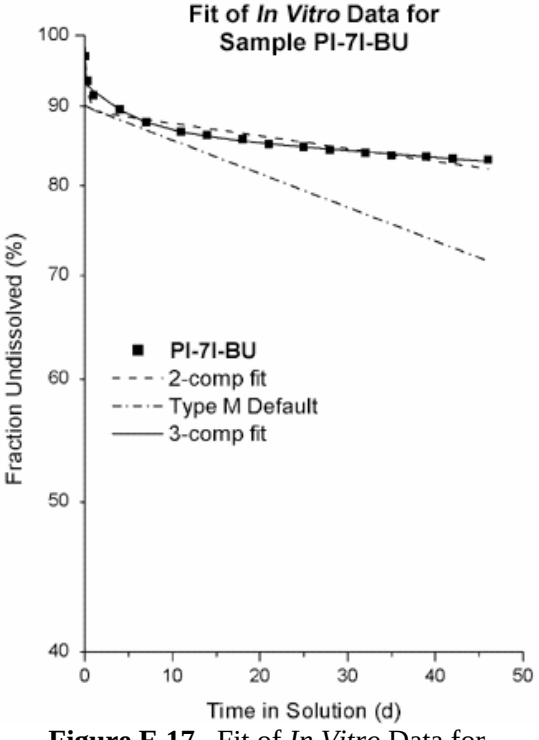

Figure E.17. Fit of *In Vitro* Data for Sample PI-7I-BU

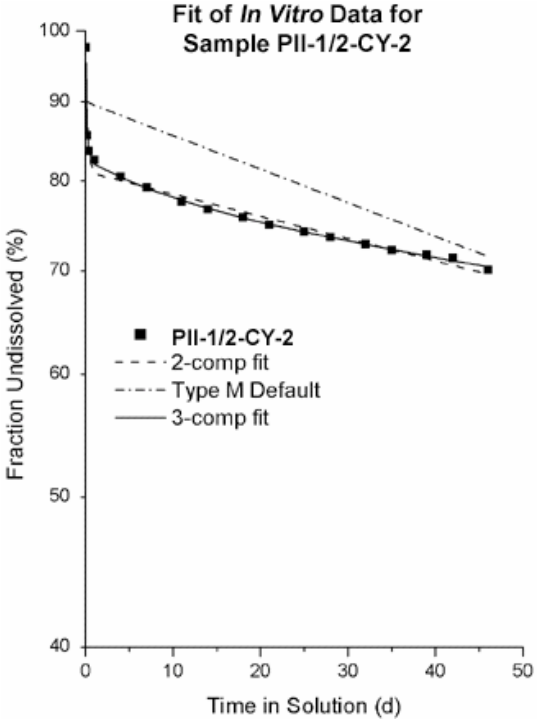

Figure E.18. Fit of *In Vitro* Data for Sample PII-1/2-CY-2

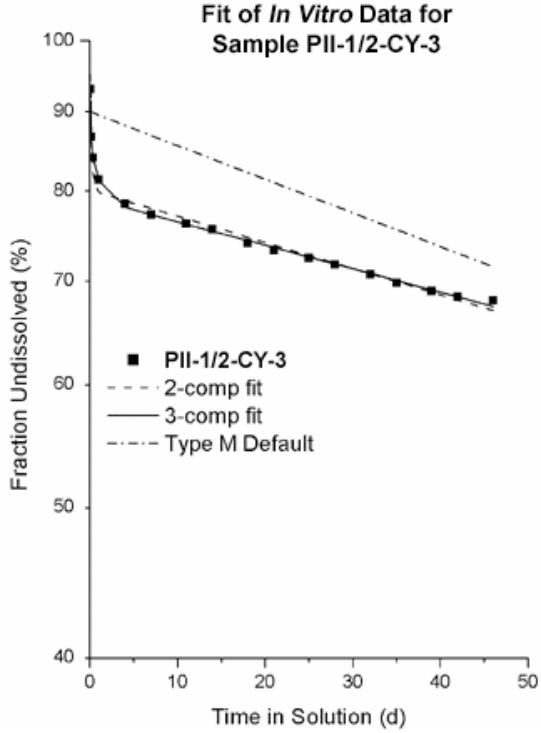

Figure E.19. Fit of *In Vitro* Data for Sample PII-1/2-CY-3

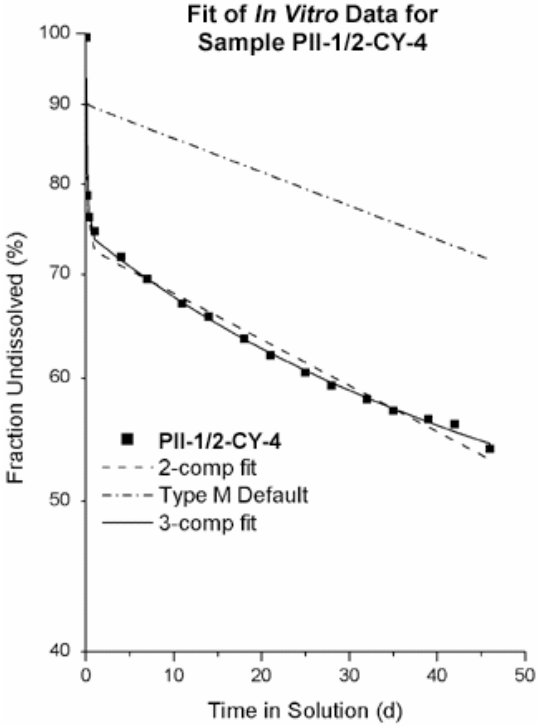

Figure E.20. Fit of *In Vitro* Data for Sample PII-1/2-CY-4

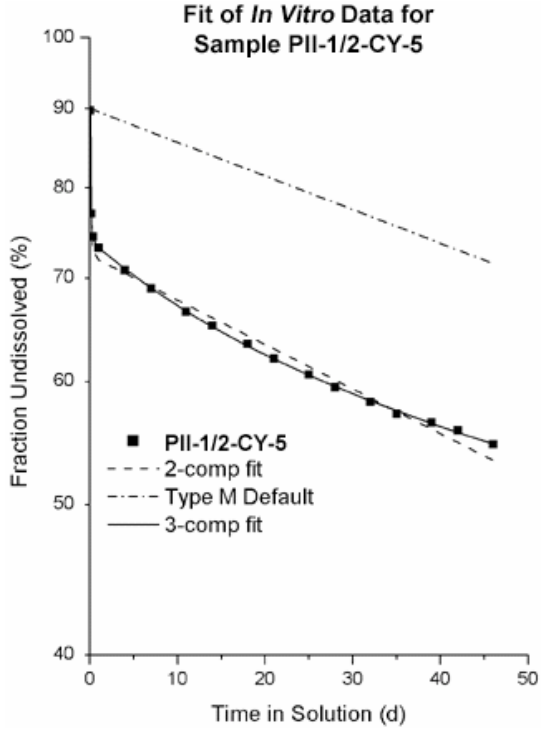

Figure E.21. Fit of *In Vitro* Data for Sample PII-1/2-CY-5

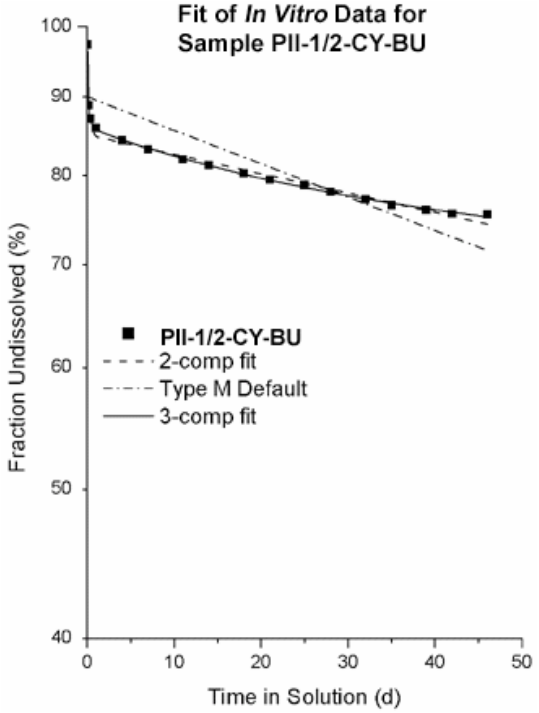

Figure E.22. Fit of *In Vitro* Data for Sample PII-1/2-CY-BU

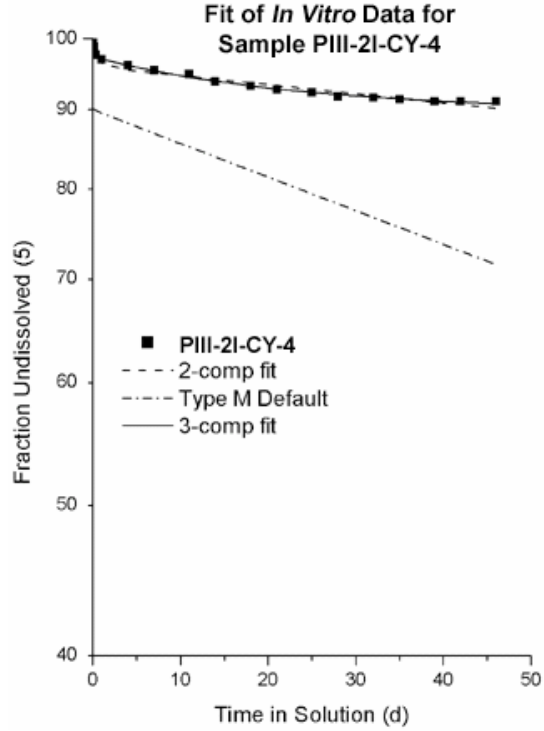

Figure E.23. Fit of *In Vitro* Data for Sample PIII-2I-CY-4

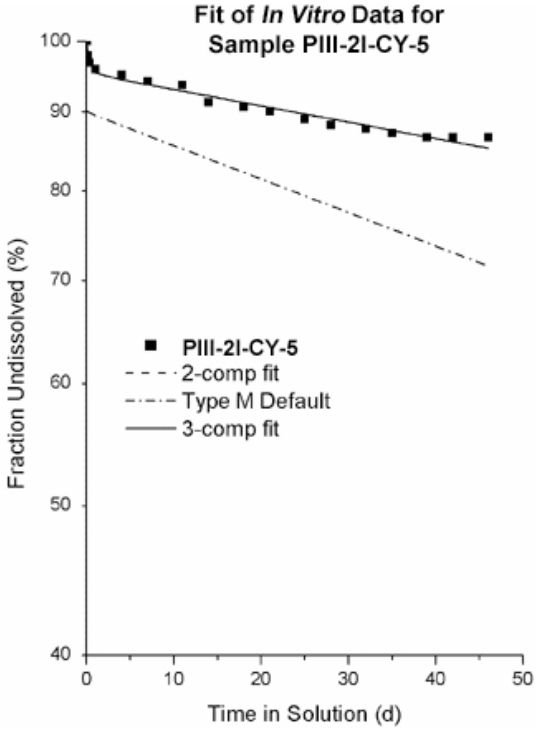

Figure E.24. Fit of *In Vitro* Data for Sample PIII-2I-CY-5

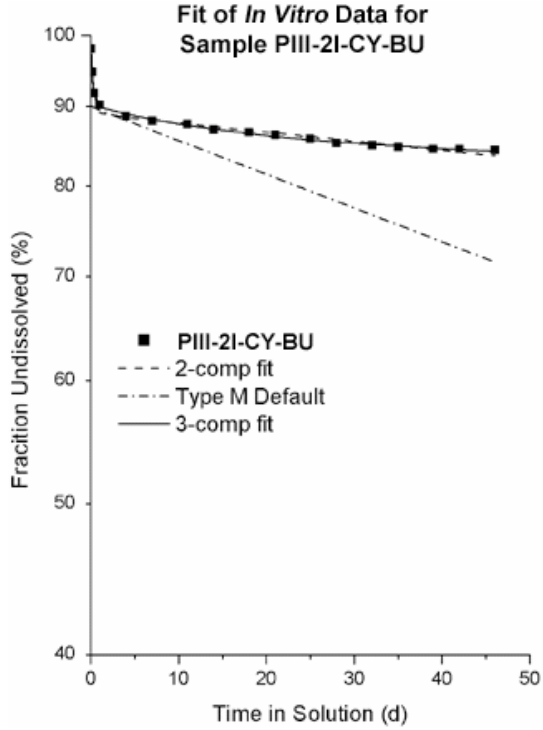

Figure E.25. Fit of *In Vitro* Data for Sample PIII-2I-CY-BU

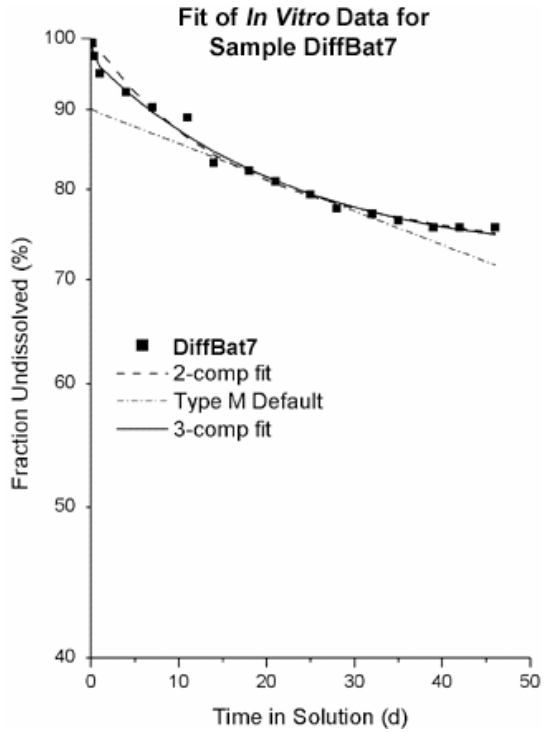

Figure E.26. Fit of *In Vitro* Data for Sample DiffBat7

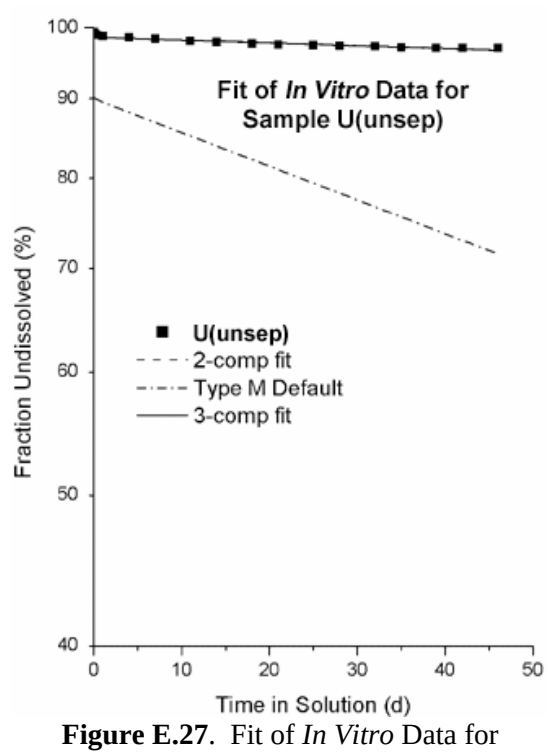

Figure E.27. Fit of *In Vitro* Data for Sample U(unsep)

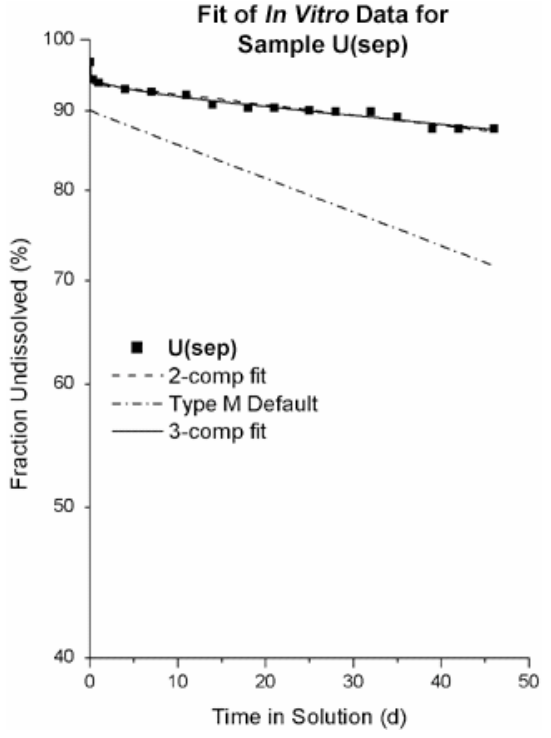

Figure E.28. Fit of *In Vitro* Data for Sample U(sep)

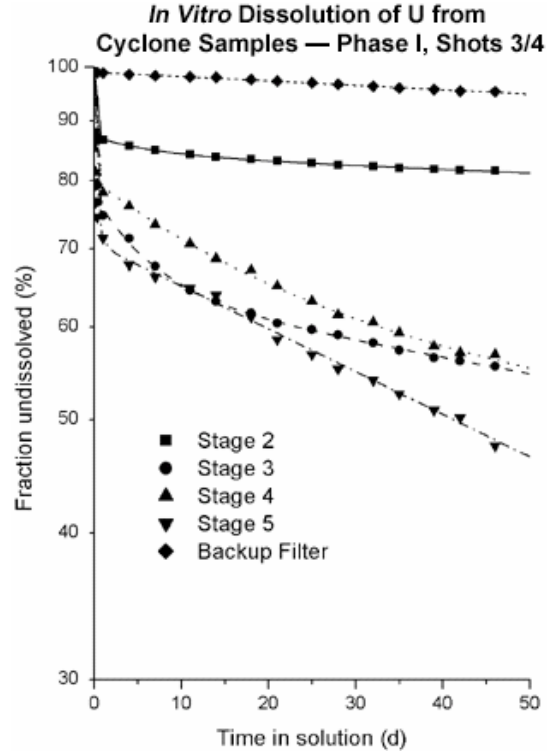

Figure E.29. *In Vitro* Dissolution of U from Cyclone Samples—PI-3/4

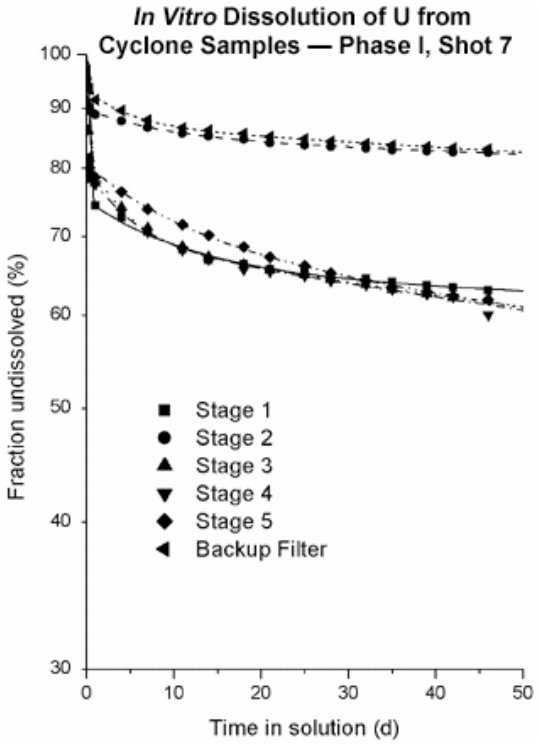

Figure E.30. *In Vitro* Dissolution of U from Cyclone Samples—PI-7

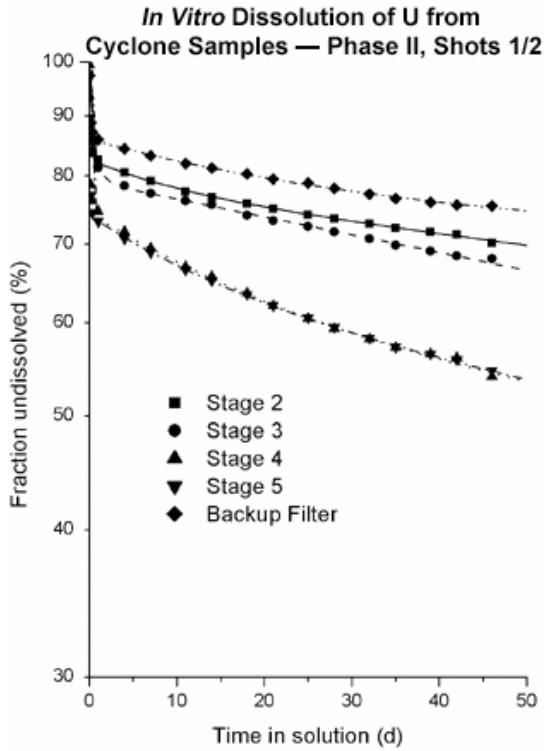

Figure E.31. *In Vitro* Dissolution of U from Cyclone Samples—PII-1/2

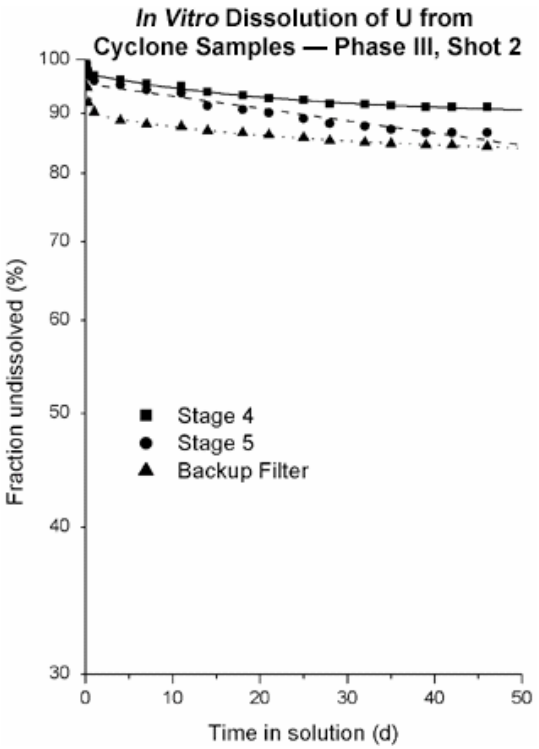

Figure E.32. *In Vitro* Dissolution of U from Cyclone Samples—PIII-2

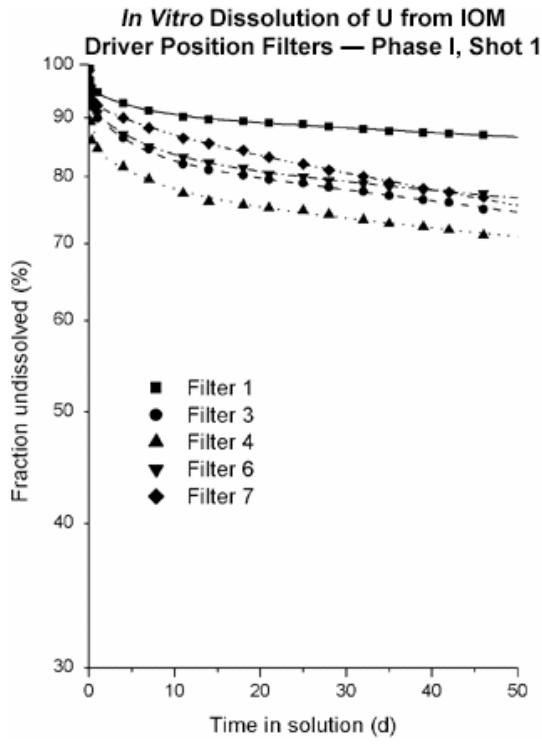

Figure E.33. *In Vitro* Dissolution of U from IOM Driver Position Filters—PI-3/4

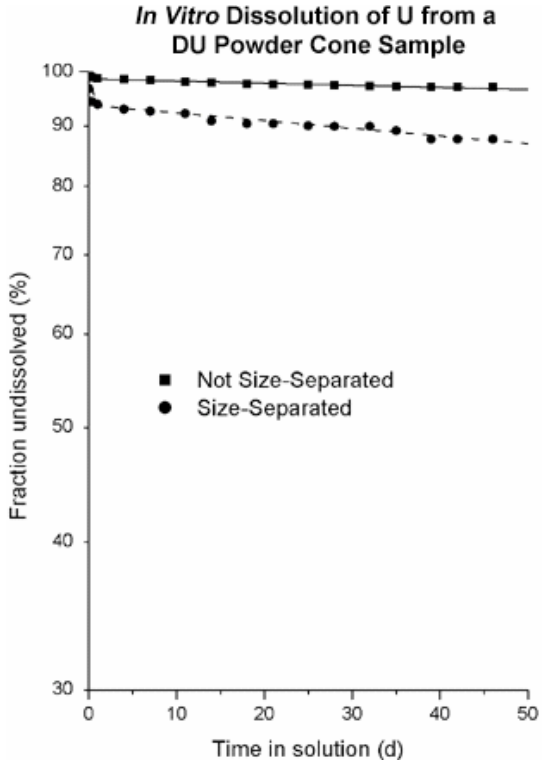

Figure E.34. *In Vitro* Dissolution of U from a DU Powder Cone Sample

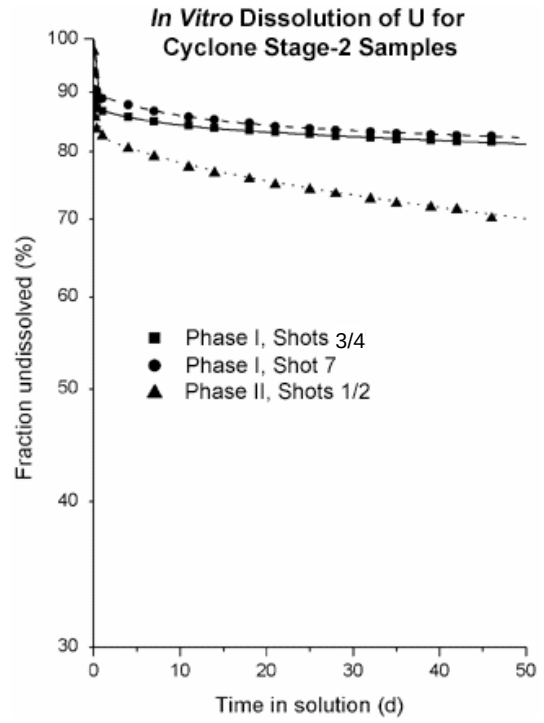

Figure E.35. *In Vitro* Dissolution of U for Cyclone Stage-2 Samples

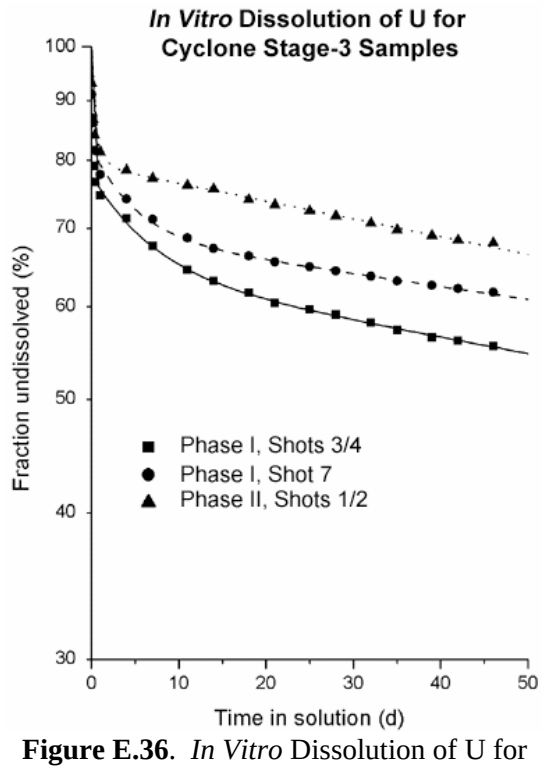

Figure E.36. *In Vitro* Dissolution of U for Cyclone Stage-3 Samples

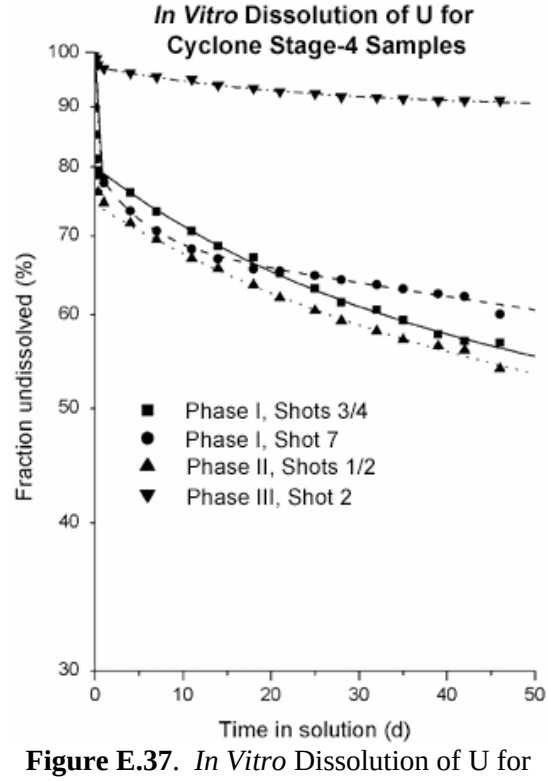

Figure E.37. *In Vitro* Dissolution of U for Cyclone Stage-4 Samples

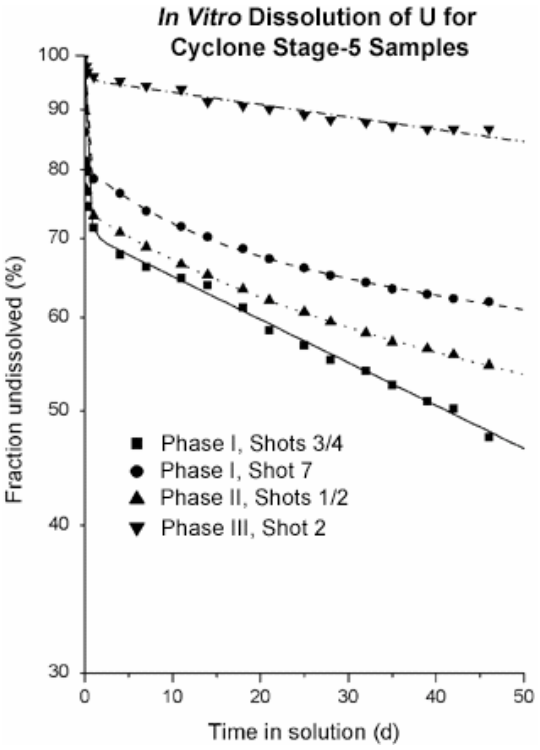

Figure E.38. *In Vitro* Dissolution of U for Cyclone Stage-5 Samples

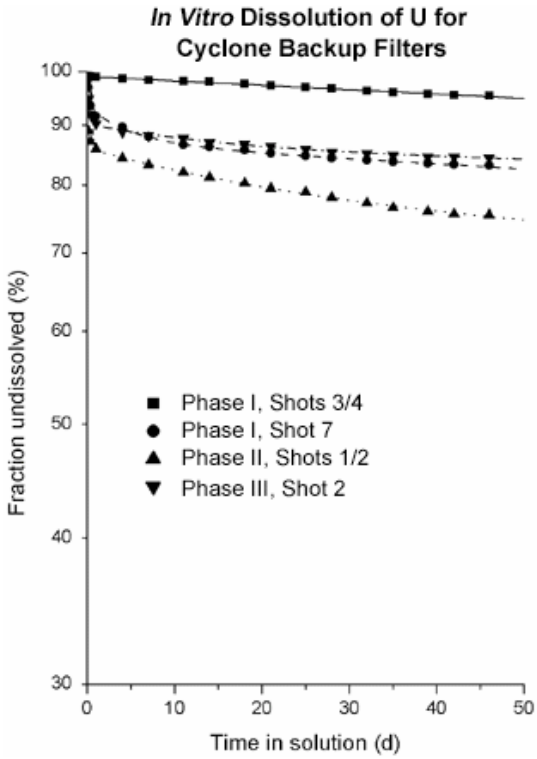

Figure E.39. *In Vitro* Dissolution of U for Cyclone Backup Filters

Appendix F

Wipe Surveys

Appendix F

Wipe Surveys

Wipe surveys were conducted inside target vehicles and on exterior surfaces to evaluate surface deposition. This information will be used in future analyses to determine potential contamination that could be ingested through the hand-to-mouth pathway by first responders and others climbing on or entering a vehicle recently perforated by depleted uranium (DU) munitions. Some instrument surveys were taken in conjunction with the wipe surveys to evaluate how well the wipe versus instrument survey results were correlated. This appendix presents example schematics of the sampling locations used and lists the mass of uranium in the samples derived from beta activity adjusted for ingrowth. It also includes a section on exhaustive wipes and their relationship to surveys conducted with radiation detection instrumentation. Summaries of these data are provided in Section 5.3.

F.1 Baseline and Post-Shot Wipe Surveys

Data tables containing surface contamination wipe data by phase and by shot are presented in Table F.1, which lists the results of interior surveys, and Table F.2, which contains the results of the exterior surveys. Both baseline and post-shot wipe data are presented for comparison. The baseline results are not subtracted from the post-shot wipes. Each wipe location is presented in the first column labeled "Specific Features." Each sample collected as part of the Capstone DU Aerosol Study was assigned a unique code, and the code for each individual wipe is presented in the columns labeled "Field ID." The remaining columns list the mass of DU in micrograms (μg) and the 1-sigma level of uncertainty associated with the mass. This uncertainty is a measure of the counting error and the error in applying an ingrowth factor. See Appendix A, Section A.2.1, for further detail on the derivation and application of this factor. Data were copied into Tables F.1 and F.2 from spreadsheets, and the number of figures provided is not intended as an indication of significant figures. The tables are presented in order of the actual events rather than numerical order (i.e., Phase III tables follow Phase I tables).

The sample numbers at the far right of the column titled "Field ID" correspond to the wipe survey locations that are documented schematics of the floor plan (Figures F.1 through F.13, beginning on page F.22) and of the exterior surfaces of the vehicles (Figure F.14 through F.57, beginning on page F.29). Deposition tray positions also are shown in the schematics of overhead views.

Several data sets are listed in the tables with a notation in the columns of "N/A." This notation indicates that data are not available for these entries. Specifically, baseline wipes were not taken before the first shot. Additionally, post-impact wipes after shots PI-2 and PI-5 were taken but were incompletely analyzed before becoming cross-contaminated. Therefore, these data are not included in this data set. Fortunately, surveys were conducted on replicate shots (PI-1 and PI-6), so the missing data did not prevent analysis of the wipes by respective and prospective scenarios.

F.2 Instrumentation Surveys

Various instrument surveys were performed using currently fielded U.S. Army radiation, detection, indication, and computation (RADIAC) equipment. The RADIAC instrument selected for these surveys was the AN/PDR-77, mated with either a 100-cm^2 zinc sulfide alpha probe, a 15-cm^2 beta-gamma "pancake" probe, or a 5-cm^2 beta-gamma end-window probe. Operational checks to include background readings were completed before and after the surveys were performed.

F.2.1 Instrument Readings

Instrument readings were taken at designated locations inside and outside the vehicle, usually in conjunction with removable "exhaustive" wipes. These readings were taken prior to associated wipe-test surveys. Instrument probes were held as close as possible to the survey location (approximately 1 cm) without contaminating the probe and without puncturing the active area of the probe. Instrument readings were recorded after a preset time (integrated counts for alpha and beta-gamma pancake probes) or the when the rate meter stabilized (beta-gamma end-window). Instrument readings were obtained from the entry and exit holes made by the penetrator; however, wipe test samples were not collected from these locations. Instrument readings were not taken on all shots.

Instrument readings on interior vehicle surfaces are presented in Table F.3 (beginning on page F.51). Instrument readings on surfaces exterior to the vehicle are presented in Table F.4. Table F.5 presents alpha and beta-gamma (pancake) integrated counts on interior surfaces shot PI-1. Table F.6 presents alpha and beta-gamma (pancake) integrated counts exterior to the vehicle for PI-1. Column 1 in Tables F.3 and F.4 identifies the phase and shot; Column 2 describes the specific feature associated with the reading; Column 3 lists the integrated gross alpha counts; Column 4 lists the integrated gross beta counts; Column 5 lists the dose rate with the detector shield open; and Column 6 lists the dose rate with the detector shield closed. For PI-1, gross alpha and gross beta counts are presented in Table F.5. The notation N/A in these tables indicates that readings were not attempted. All beta pancake counts were 1-min counts, while alpha count times for PI-1 through PI-3/4 were 30 seconds. All other alpha count times were 1 min.

F.2.2 Instrument Response versus Removable Beta Activity

Instrument readings coupled with "exhaustive" wipe-test surveys were also performed. The exhaustive wipe-test surveys were performed after several of the shots following the interior and exterior removable wipe-test surveys were completed. A delineated area of 100 cm^2 was surveyed with the RADIAC instrument prior to removing DU contamination with five successive wipe-test samples. The wipe-test sample identification was appended with an "a" to "e" to indicate which exhaustive wipe, with "a" being the first exhaustive wipe and "e" being the last exhaustive wipe. After the last wipe-test another instrument reading was taken. The differences in the instrument readings were plotted against the total amount of removable beta activity for the various instruments used. The beta-gamma end-window, and beta-gamma pancake probes were used. There were three interior and three exterior exhaustive wipe locations. Figure F.58 (page F.57) shows the relationship between removable DU contamination and beta-gamma pancake probe instrument readings. Figure F.59 (page F.58) shows the relationship between removable DU contamination and beta-gamma end-window probe instrument readings. Good

correlations were observed between the removable beta activity and the beta-gamma pancake probe and the removable beta activity and the "open" window beta/gamma end-window probe.

Table F.1. Interior Wipes

PI-1 Interior Wipes (μg per 100 cm^2)						
	Baseline Wipe			Post-shot		
Specific Features	Field ID	Mass of DU (μg)	1 sigma (μg)	Field ID	Mass of DU (μg)	1 sigma (μg)
Floor driver's area	PI-1I-BW-1	N/A	N/A	PI-1I-IW-1	1130.97	225.94
Wall in driver's area	PI-1I-BW-2	N/A	N/A	PI-1I-IW-2	1456.83	290.02
Floor loader's area	PI-1I-BW-3	N/A	N/A	PI-1I-IW-3	1005.18	201.14
Wall loader's area	PI-1I-BW-4	N/A	N/A	PI-1I-IW-4	1637.55	326.45
Wall loader's area	PI-1I-BW-5	N/A	N/A	PI-1I-IW-5	2096.28	418.57
Ledge loader's area	PI-1I-BW-6	N/A	N/A	PI-1I-IW-6	1464.39	292.64
Floor loader's area	PI-1I-BW-7	N/A	N/A	PI-1I-IW-7	974.51	195.05
Top of louver - loader	PI-1I-BW-8	N/A	N/A	PI-1I-IW-8	1827.74	364.48
Face of louver - loader	PI-1I-BW-9	N/A	N/A	PI-1I-IW-9	2065.06	411.48
Wall brace facing loader	PI-1I-BW-10	N/A	N/A	PI-1I-IW-10	4996.58	993.31
Wall under camera - commander	PI-1I-BW-11	N/A	N/A	PI-1I-IW-11	9670.59	1919.67
Foot rest commander	PI-1I-BW-12	N/A	N/A	PI-1I-IW-12	896.04	179.58
Ledge commander's area	PI-1I-BW-13	N/A	N/A	PI-1I-IW-13	599.36	120.60
Hull floor in commander's area	PI-1I-BW-14	N/A	N/A	PI-1I-IW-14	562.69	113.54
Top of louver - commander	PI-1I-BW-15	N/A	N/A	PI-1I-IW-15	2695.58	536.62
Face of louver - commander	PI-1I-BW-16	N/A	N/A	PI-1I-IW-16	3809.34	757.46
Next to exit hole (wall)	PI-1I-BW-17	N/A	N/A	PI-1I-IW-17	2045.45	408.44
Wall gunner's area	PI-1I-BW-18	N/A	N/A	PI-1I-IW-18	4322.57	860.57
Floor gunner's area	PI-1I-BW-19	N/A	N/A	PI-1I-IW-19	1425.65	284.58
Ledge gunner's area	PI-1I-BW-20	N/A	N/A	PI-1I-IW-20	2226.75	443.39
Hull floor gunner's area	PI-1I-BW-21	N/A	N/A	PI-1I-IW-21	799.91	160.60
Top of louver - gunner	PI-1I-BW-22	N/A	N/A	PI-1I-IW-22	1831.99	365.27
Face of louver - gunner	PI-1I-BW-23	N/A	N/A	PI-1I-IW-23	2230.49	444.06
Top of breech	PI-1I-BW-24	N/A	N/A	PI-1I-IW-24	23811.57	4724.42
Impact side of breech	PI-1I-BW-25	N/A	N/A	PI-1I-IW-25	4664.47	927.00
Hull floor impact side	PI-1I-BW-26	N/A	N/A	PI-1I-IW-26	2231.33	444.07
Ledge impact side	PI-1I-BW-27	N/A	N/A	PI-1I-IW-27	4678.81	930.02
Wall impact side	PI-1I-BW-28	N/A	N/A	PI-1I-IW-28	1966.84	393.66
Wall impact side	PI-1I-BW-29	N/A	N/A	PI-1I-IW-29	1593.18	318.02
Entry impact hole	PI-1I-BW-30	N/A	N/A	PI-1I-IW-30	1322.61	264.84
Ceiling	PI-1I-BW-31	N/A	N/A	PI-1I-IW-31	1456.42	291.34
Lower wall impact side	PI-1I-BW-32	N/A	N/A	PI-1I-IW-32	1236.77	247.15

PI-2 Interior Wipes (μg per 100 cm^2)						
	Baseline Wipe			Post-shot		
Specific Features	Field ID	Mass of DU (μg)	1 sigma (μg)	Field ID	Mass of DU (μg)	1 sigma (μg)
Floor driver's area	PI-2I-BW-1	441.60	88.45	PI-2I-W-1	N/A	N/A
Wall in driver's area	PI-2I-BW-2	577.79	115.57	PI-2I-IW-2	N/A	N/A
Floor loader's area	PI-2I-BW-3	723.40	144.83	PI-2I-IW-3	N/A	N/A
Wall loader's area	PI-2I-BW-4	4059.56	804.84	PI-2I-IW-4	N/A	N/A
Wall loader's area	PI-2I-BW-5	36.44	10.64	PI-2I-IW-5	N/A	N/A
Ledge loader's area	PI-2I-BW-6	109.90	23.05	PI-2I-IW-6	N/A	N/A
Floor loader's area	PI-2I-BW-7	321.20	65.11	PI-2I-IW-7	N/A	N/A
Top of louver - loader	PI-2I-BW-8	48.45	12.01	PI-2I-IW-8	N/A	N/A
Face of louver - loader	PI-2I-BW-9	99.04	23.06	PI-2I-IW-9	N/A	N/A
Wall brace facing loader	PI-2I-BW-10	64.48	15.45	PI-2I-IW-10	N/A	N/A
Wall under camera - commander's area	PI-2I-BW-11	186.91	39.28	PI-2I-IW-11	N/A	N/A
Foot rest commander	PI-2I-BW-12	743.28	148.49	PI-2I-IW-12	N/A	N/A

PI-2 Interior Wipes (μg per 100 cm^2)						
Ledge commander's area	PI-2I-BW-13	500.26	101.49	PI-2I-IW-13	N/A	N/A
Hull floor in commander's area	PI-2I-BW-14	316.53	63.26	PI-2I-IW-14	N/A	N/A
Top of louver commander	PI-2I-BW-15	299.94	61.33	PI-2I-IW-15	N/A	N/A
Face of louver - commander	PI-2I-BW-16	386.21	78.73	PI-2I-IW-16	N/A	N/A
Next to exit hole	PI-2I-BW-17	30.80	8.48	PI-2I-IW-17	N/A	N/A
Wall gunner's area	PI-2I-BW-18	1500.10	300.15	PI-2I-IW-18	N/A	N/A
Floor gunner's area	PI-2I-BW-19	453.01	91.05	PI-2I-BW-19	N/A	N/A
Ledge gunner's area	PI-2I-BW-20	79.26	18.99	PI-2I-IW-20	N/A	N/A
Hull floor gunner's area	PI-2I-BW-21	103.90	22.33	PI-2I-IW-21	N/A	N/A
Top of louver - gunner	PI-2I-BW-22	52.59	13.35	PI-2I-IW-22	N/A	N/A
Face of louver - gunner	PI-2I-BW-23	374.13	75.00	PI-2I-IW-23	N/A	N/A
Top of breech	PI-2I-BW-24	143.21	30.34	PI-2I-IW-24	N/A	N/A
Impact side of breech	PI-2I-BW-25	105.02	21.94	PI-2I-IW-25	N/A	N/A
Hull floor impact side	PI-2I-BW-26	357.14	72.56	PI-2I-IW-26	N/A	N/A
Ledge impact side	PI-2I-BW-27	63.47	14.80	PI-2I-IW-27	N/A	N/A
Wall impact side	PI-2I-BW-28	23.29	8.05	PI-2I-IW-28	N/A	N/A
Wall impact side	PI-2I-BW-29	36.31	10.05	PI-2I-IW-29	N/A	N/A
Entry impact hole	PI-2I-BW-30	21.03	5.89	PI-2I-IW-30	N/A	N/A
Ceiling	PI-2I-BW-31	29.17	8.60	PI-2I-IW-31	N/A	N/A
Lower wall impact side	PI-2I-BW-32	1066.72	212.44	PI-2I-IW-32	N/A	N/A

PI-3/4 Interior Wipes (μg per 100 cm^2)						
	Baseline Wipe			Post-shot		
Specific Features	Field ID	Mass of DU (μg)	1 sigma (μg)	Field ID	Mass of DU (μg)	1 sigma (μg)
Floor driver's area	PI-3/4I-BW-1	2150.89	427.77	PI-3/4I-W-1	2242.43	447.93
Wall in driver's area	PI-3/4I-BW-2	474.44	96.07	PI-3/4I-IW-2	2410.84	479.74
Floor loader's area	PI-3/4I-BW-3	742.55	148.94	PI-3/4I-IW-3	11851.80	2352.04
Hull wall (lower) gunner's area	PI-3/4I-BW-4	3166.73	629.64	PI-3/4I-IW-4	12773.79	2535.36
Wall loader's area	PI-3/4I-BW-5	132.71	29.35	PI-3/4I-IW-5	4968.45	987.15
Ledge loader's area	PI-3/4I-BW-6	218.94	45.09	PI-3/4I-IW-6	2224.17	443.12
Floor loader's area	PI-3/4I-BW-7	742.42	148.87	PI-3/4I-IW-7	936.85	187.69
Top of louver - loader	PI-3/4I-BW-8	89.64	20.17	PI-3/4I-IW-8	11565.47	2297.68
Face of louver -loader	PI-3/4I-BW-9	1074.16	215.98	PI-3/4I-IW-9	12914.35	2565.82
Wall brace facing loader	PI-3/4I-BW-10	127.69	27.60	PI-3/4I-IW-10	24311.38	4824.32
Wall under camera - commander	PI-3/4I-BW-11	199.59	43.40	PI-3/4I-IW-11	15428.27	3063.82
Foot rest commander	PI-3/4I-BW-12	792.76	159.00	PI-3/4I-IW-12	3753.36	746.26
Ledge commander's area	PI-3/4I-BW-13	649.91	132.04	PI-3/4I-IW-13	3213.17	639.28
Hull floor forward of loader's area	PI-3/4I-BW-14	393.81	79.72	PI-3/4I-IW-14	1559.01	311.29
Top of louver - commander	PI-3/4I-BW-15	307.19	62.64	PI-3/4I-IW-15	3841.94	763.73
Face of louver - commander	PI-3/4I-BW-16	72.36	16.96	PI-3/4I-IW-16	17039.25	3382.10
Next to entry hole	PI-3/4I-BW-17	313.31	63.56	PI-3/4I-IW-17	3423.28	681.23
Wall gunner's area	PI-3/4I-BW-18	424.27	86.64	PI-3/4I-IW-18	12075.31	2396.65
Floor gunner's area	PI-3/4I-BW-19	794.86	159.18	PI-3/4I-BW-19	4307.36	856.52
Ledge gunner's area	PI-3/4I-BW-20	139.21	30.11	PI-3/4I-IW-20	8378.13	1663.98
Hull floor loader's area	PI-3/4I-BW-21	212.30	43.65	PI-3/4I-IW-21	1776.39	354.16
Top of louver - gunner	PI-3/4I-BW-22	168.89	36.09	PI-3/4I-IW-22	3580.87	713.39
Face of louver - gunner	PI-3/4I-BW-23	987.27	197.44	PI-3/4I-IW-23	14019.94	2782.46
Top of breech	PI-3/4I-BW-24	423.74	85.91	PI-3/4I-IW-24	15904.46	3157.82
Exit side of breech	PI-3/4I-BW-25	199.66	41.27	PI-3/4I-IW-25	17209.20	3417.67
Hull floor commander's area	PI-3/4I-BW-26	2401.22	476.93	PI-3/4I-IW-26	1206.73	241.21
Ledge exit side	PI-3/4I-BW-27	130.57	28.23	PI-3/4I-IW-27	7713.90	1531.33
Wall exit side	PI-3/4I-BW-28	43.34	13.39	PI-3/4I-IW-28	5698.45	1135.38
Wall exit side	PI-3/4I-BW-29	70.35	15.72	PI-3/4I-IW-29	5522.50	1100.23
Exit impact hole	PI-3/4I-BW-30	102.04	22.95	PI-3/4I-IW-30	3478.65	691.14
Ceiling	PI-3/4I-BW-31	296.72	61.69	PI-3/4I-IW-31	3563.30	711.35
Lower wall entry side	PI-3/4I-BW-32	1141.72	228.02	PI-3/4I-IW-32	3041.41	605.13

PI-5 and PI-6 (Wipe results not available)

PI-7 Interior Wipes (μg per 100 cm^2)						
	Baseline Wipe			Post-shot		
Specific Features	Field ID	Mass of DU (μg)	1 sigma (μg))	Field ID	Mass of DU (μg)	1 sigma (μg)
Floor driver's area	PI-7I-BW-1	800.21	220.27	PI-7I-IW-1	6107.68	1206.70
Wall in driver's area	PI-7I-BW-2	2309.84	632.34	PI-7I-IW-2	3912.49	773.53
Floor loader's area	PI-7I-BW-3	736.98	202.85	PI-7I-IW-3	4298.93	849.91
Hull wall (lower) driver's area	PI-7I-BW-4	1033.21	283.56	PI-7I-IW-4	2457.58	486.20
Wall loader's area	PI-7I-BW-5	1372.61	376.60	PI-7I-IW-5	726.60	147.44
Ledge loader's area	PI-7I-BW-6	201.59	56.13	PI-7I-IW-6	2945.67	583.16
Floor loader's area	PI-7I-BW-7	371.39	103.04	PI-7I-IW-7	1276.05	253.44
Top of array - loader	PI-7I-BW-8	1478.32	405.09	PI-7I-IW-8	4548.77	900.77
Face of array -loader	PI-7I-BW-9	2412.59	659.94	PI-7I-IW-9	3722.93	737.66
Wall brace facing loader	PI-7I-BW-10	635.66	174.88	PI-7I-IW-10	4110.06	813.45
Wall under camera - commander	PI-7I-BW-11	809.24	222.49	PI-7I-IW-11	3416.59	676.64
Foot rest commander	PI-7I-BW-12	303.71	84.45	PI-7I-IW-12	2501.18	495.48
Ledge commander's area	PI-7I-BW-13	570.24	157.59	PI-7I-IW-13	1982.91	392.99
Hull floor in commander's area	PI-7I-BW-14	322.50	89.20	PI-7I-IW-14	1129.11	224.60
Side of array - commander	PI-7I-BW-15	1994.47	545.75	PI-7I-IW-15	4900.97	969.70
Side of array - commander	PI-7I-BW-16	1319.58	361.66	PI-7I-IW-16	4395.11	870.22
Upper wall commander's	PI-7I-BW-17	501.29	138.35	PI-7I-IW-17	1859.35	369.21
Wall gunner's area	PI-7I-BW-18	1478.22	404.92	PI-7I-IW-18	3000.41	594.62
Floor gunner's area	PI-7I-BW-19	927.16	255.03	PI-7I-IW-19	1836.53	363.80
Ledge gunner's area	PI-7I-BW-20	330.91	91.45	PI-7I-IW-20	6731.59	1329.98
Hull floor loader's area	PI-7I-BW-21	1062.78	291.81	PI-7I-IW-21	1830.78	362.74
Support bracket - gunner	PI-7I-BW-22	706.05	194.40	PI-7I-IW-22	2920.00	578.59
Support bracket - gunner	PI-7I-BW-23	882.52	242.42	PI-7I-IW-23	2152.48	426.85
Top of breech	PI-7I-BW-24	2446.74	669.43	PI-7I-IW-24	15043.90	2971.18
Impact side of breech	PI-7I-BW-25	172.77	48.84	PI-7I-IW-25	7654.33	1512.61
Hull floor exit side - commander	PI-7I-BW-26	1139.24	312.83	PI-7I-IW-26	935.56	186.20
Ledge impact side	PI-7I-BW-27	957.04	262.86	PI-7I-IW-27	7601.41	1501.69
Wall impact side	PI-7I-BW-28	1412.20	387.14	PI-7I-IW-28	1257.25	252.62
Wall impact side	PI-7I-BW-29	1314.85	360.65	PI-7I-IW-29	1628.10	324.94
Impact hole	PI-7I-BW-30	350.54	96.95	PI-7I-IW-30	934.68	187.16
Ceiling	PI-7I-BW-31	2536.16	693.58	PI-7I-IW-31	2307.32	458.63
Lower hull wall exit side	PI-7I-BW-32	2653.01	725.60	PI-7I-IW-32	5612.01	1109.18

Phase III-1 Interior Wipes (μg per 100 cm^2)						
	Baseline Wipe			Post-shot		
Specific Features	Field ID	Mass of DU (μg)	1 sigma (μg)	Field ID	Mass of DU (μg)	1 sigma (μg)
Floor driver's area	PIII-1I-BW-1	437.37	120.61	PIII-1I-IW-1	7729.16	1528.48
Wall in driver's area	PIII-1I-BW-2	47.57	14.77	PIII-1I-IW-2	1810.26	359.10
Floor loader's area	PIII-1I-BW-3	290.05	80.64	PIII-1I-IW-3	9200.16	1817.61
Ledge gunner's area	PIII-1I-BW-4	46.32	14.06	PIII-1I-IW-4	no sample collected	
Wall loader's area	PIII-1I-BW-5	472.44	130.35	PIII-1I-IW-5	8367.91	1653.55
Ledge loader's area	PIII-1I-BW-6	75.35	21.53	PIII-1I-IW-6	35026.04	6919.36
Floor loader's area	PIII-1I-BW-7	161.87	45.85	PIII-1I-IW-7	6446.31	1274.09
Wall loader's area	PIII-1I-BW-8	13.65	5.04	PIII-1I-IW-8	20014.27	3954.80
Wall loader's area	PIII-1I-BW-9	26.04	7.88	PIII-1I-IW-9	18201.18	3596.68
Wall brace facing loader	PIII-1I-BW-10	50.57	14.32	PIII-1I-IW-10	10484.59	2072.12
Wall under camera - commander	PIII-1I-BW-11	12.14	3.73	PIII-1I-IW-11	5299.96	1048.14
Floor commander's area	PIII-1I-BW-12	158.72	44.39	PIII-1I-IW-12	12867.39	2542.97
Ledge commander's area	PIII-1I-BW-13	64.47	18.95	PIII-1I-IW-13	16815.21	3323.68
Ledge commander's area	PIII-1I-BW-14	28.04	8.55	PIII-1I-IW-14	13814.37	2731.20
Wall commander's area	PIII-1I-BW-15	4.63	3.63	PIII-1I-IW-15	2198.13	436.76
Ledge commander's area	PIII-1I-BW-16	29.04	9.58	PIII-1I-IW-16	7199.52	1423.50
Upper wall commander's	PIII-1I-BW-17	202.93	56.92	PIII-1I-IW-17	517.84	103.72
Wall gunner's area	PIII-1I-BW-18	17.27	5.56	PIII-1I-IW-18	937.14	188.68
Floor gunner's area	PIII-1I-BW-19	75.48	21.84	PIII-1I-IW-19	7476.75	1477.02
Floor under breech	PIII-1I-BW-20	120.31	34.45	PIII-1I-IW-20	9245.59	1827.52
Hull floor forward from loader	PIII-1I-BW-21	257.23	71.21	PIII-1I-IW-21	9514.25	1879.87

Side support bracket - gunner	PIII-1I-BW-22	127.80	35.91	PIII-1I-IW-22	2734.73	541.57
Ledge gunner's area	PIII-1I-BW-23	78.11	22.12	PIII-1I-IW-23	12935.70	2556.82
Impact side of breech	PIII-1I-BW-24	64.34	18.61	PIII-1I-IW-24	16879.84	3335.49
Impact side of breech	PIII-1I-BW-25	64.09	18.62	PIII-1I-IW-25	18113.03	3579.06
Commander's foot rest	PIII-1I-BW-26	50.57	15.21	PIII-1I-IW-26	no sample collected	
Wall impact side	PIII-1I-BW-27	121.05	34.52	PIII-1I-IW-27	1785.65	353.27
Wall impact side	PIII-1I-BW-28	7.39	3.14	PIII-1I-IW-28	5721.19	1130.74
Wall impact side	PIII-1I-BW-29	4.63	3.63	PIII-1I-IW-29	8173.24	1615.19
Upper wall	PIII-1I-BW-30	25.05	9.81	PIII-1I-IW-30	23169.14	4578.13
Ceiling	PIII-1I-BW-31	35.05	10.15	PIII-1I-IW-31	1162.96	232.96
Upper wall commander's area	PIII-1I-BW-32	9.01	2.46	PIII-1I-IW-32	7717.52	1666.06

*There was no wipe #4 or #26 collected.

Phase III-2 Interior Wipes (μg per 100 cm^2)						
	Baseline Wipe			Post-shot		
Specific Features	**Field ID**	**Mass of DU (μg)**	**1 sigma (μg)**	**Field ID**	**Mass of DU (μg)**	**1 sigma (μg)**
Floor driver's area	PIII-2I-BW-1	2103.00	571.89	PIII-2I-IW-1	16278.24	3217.58
Wall in driver's area	PIII-2I-BW-2	107.90	30.41	PIII-2I-IW-2	1622.03	322.06
Floor loader's area	PIII-2I-BW-3	1134.40	308.78	PIII-2I-IW-3	16780.16	3316.64
Ledge gunner's area	PIII-2I-BW-4	78.36	22.85	PIII-2I-IW-4	3361.57	665.40
Wall loader's area	PIII-2I-BW-5	169.25	47.45	PIII-2I-IW-5	7869.95	1556.02
Ledge loader's area	PIII-2I-BW-6	176.25	48.99	PIII-2I-IW-6	3580.32	708.86
Floor loader's area	PIII-2I-BW-7	828.61	225.70	PIII-2I-IW-7	2713.55	537.29
Wall loader's area	PIII-2I-BW-8	22.91	7.67	PIII-2I-IW-8	5086.23	1006.68
Wall loader's area	PIII-2I-BW-9	145.71	41.12	PIII-2I-IW-9	7552.84	1493.27
Wall brace facing loader	PIII-2I-BW-10	861.72	235.18	PIII-2I-IW-10	2951.80	584.99
Wall under camera - commander	PIII-2I-BW-11	991.37	270.18	PIII-2I-IW-11	5634.94	1114.97
Floor commander's area	PIII-2I-BW-12	1198.26	326.19	PIII-2I-IW-12	7207.15	1425.01
Ledge commander's area	PIII-2I-BW-13	127.55	35.87	PIII-2I-IW-13	4637.04	917.39
Ledge commander's area	PIII-2I-BW-14	30.67	10.20	PIII-2I-IW-14	13920.73	2751.67
Wall commander's area	PIII-2I-BW-15	28.16	8.37	PIII-2I-IW-15	9235.25	1827.44
Ledge commander's area	PIII-2I-BW-16	23.91	8.77	PIII-2I-IW-16	2855.84	565.31
Upper wall commander's	PIII-2I-BW-17	133.19	37.35	PIII-2I-IW-17	2776.29	549.77
Wall gunner's area	PIII-2I-BW-18	46.32	14.40	PIII-2I-IW-18	3634.43	720.52
Floor gunner's area	PIII-2I-BW-19	628.10	171.35	PIII-2I-IW-19	22315.05	4410.39
Floor under breech	PIII-2I-BW-20	1234.98	336.41	PIII-2I-IW-20	18126.88	3582.70
Hull floor forward from loader	PIII-2I-BW-21	1551.62	422.15	PIII-2I-IW-21	12114.31	2393.98
Side support bracket - gunner	PIII-2I-BW-22	19.03	7.26	PIII-2I-IW-22	9513.72	1881.84
Ledge gunner's area	PIII-2I-BW-23	54.20	16.30	PIII-2I-IW-23	7580.65	1498.80
Impact side of breech	PIII-2I-BW-24	3715.72	1009.79	PIII-2I-IW-24	2240.20	443.95
Impact side of breech	PIII-2I-BW-25	927.78	252.88	PIII-2I-IW-25	14489.10	2864.32
Commander's foot rest	PIII-2I-BW-26	80.87	23.43	PIII-2I-IW-26	10390.72	2053.58
Wall impact side	PIII-2I-BW-27	103.77	29.48	PIII-2I-IW-27	3274.00	648.25
Wall impact side	PIII-2I-BW-28	22.28	7.14	PIII-2I-IW-28	4539.57	899.30
Wall impact side	PIII-2I-BW-29	22.66	7.81	PIII-2I-IW-29	5895.89	1167.09
Upper wall	PIII-2I-BW-30	17.77	6.14	PIII-2I-IW-30	6859.71	1359.19
Ceiling	PIII-2I-BW-31	81.49	23.71	PIII-2I-IW-31	7605.66	1507.76
Upper wall commander's area	PIII-2I-BW-32	19.15	6.21	PIII-2I-IW-32	6300.67	1247.31

Phase II-1/2 Interior Wipes (μg per 100 cm^2)						
	Baseline Wipe			Post-shot		
Specific Features	Field ID	Mass of DU (μg)	1 sigma (μg))	Field ID	Mass of DU (μg)	1 sigma (μg)
Floor engine compartment	PII-1/2I-BW-1	107.52	29.64	PII-1/2I-IW-1	940.79	187.13
Wall engine compartment	PII-1/2I-BW-2	20.03	5.64	PII-1/2I-IW-2	143.60	30.95
Side of bench - driver	PII-1/2I-BW-3	5.38	2.23	PII-1/2I-IW-3	284.47	59.45
Floor driver's area	PII-1/2I-BW-4	112.78	31.30	PII-1/2I-IW-4	1378.61	274.24
Wall driver's area	PII-1/2I-BW-5	0.63	2.41	PII-1/2I-IW-5	465.60	94.63
Wall driver's area	PII-1/2I-BW-6	4.01	2.63	PII-1/2I-IW-6	327.28	67.93
Bench driver's area	PII-1/2I-BW-7	21.03	7.01	PII-1/2I-IW-7	1390.24	276.49
Upper wall driver's area	PII-1/2I-BW-8	4.01	2.63	PII-1/2I-IW-8	198.68	41.67
Bench between driver's and crew area	PII-1/2I-BW-9	5.13	2.77	PII-1/2I-IW-9	671.30	133.88
Turret shroud assembly	PII-1/2I-BW-10	3.76	3.11	PII-1/2I-IW-10	729.32	146.13
Upper wall (left scout position)	PII-1/2I-BW-11	-2.75	2.52	PII-1/2I-IW-11	140.23	30.79
Bench (left scout position)	PII-1/2I-BW-12	21.53	6.70	PII-1/2I-IW-12	2084.99	413.26
Lower wall under bench (left scout position)	PII-1/2I-BW-13	-4.13	3.15	PII-1/2I-IW-13	839.44	167.53
Floor (left scout position)	PII-1/2I-BW-14	16.15	5.24	PII-1/2I-IW-14	2056.07	407.50
Ceiling left scout position	PII-1/2I-BW-15	4.51	1.21	PII-1/2I-IW-15	546.79	111.81
Ceiling left scout position	PII-1/2I-BW-16	-2.75	2.52	PII-1/2I-IW-16	1467.76	292.05
Floor right scout position	PII-1/2I-BW-17	165.48	45.43	PII-1/2I-IW-17	3484.21	689.53
Upper wall right scout position	PII-1/2I-BW-18	5.63	1.51	PII-1/2I-IW-18	1852.20	367.43
Upper wall right scout position	PII-1/2I-BW-19	-1.87	2.99	PII-1/2I-IW-19	1427.89	282.95
Bench right scout position	PII-1/2I-BW-20	11.89	4.00	PII-1/2I-IW-20	2902.25	574.82
Between hull and turret right scout position	PII-1/2I-BW-21	12.77	4.52	PII-1/2I-IW-21	1626.88	322.83
Turret shroud assembly right scout position	PII-1/2I-BW-22	-3.00	3.05	PII-1/2I-IW-22	2452.87	486.49
Upper wall right scout position	PII-1/2I-BW-23	4.26	2.05	PII-1/2I-IW-23	1009.57	201.23
Floor in turret	PII-1/2I-BW-24	55.96	16.40	PII-1/2I-IW-24	1879.36	372.79
Floor under breech – turret	PII-1/2I-BW-25	33.42	9.89	PII-1/2I-IW-25	3586.47	710.12
Ledge turret	PII-1/2I-BW-26	89.51	25.48	PII-1/2I-IW-26	3550.98	702.88
Lower wall turret	PII-1/2I-BW-27	2.38	3.46	PII-1/2I-IW-27	1109.21	220.95
Ledge above wall in turret	PII-1/2I-BW-28	17.77	5.06	PII-1/2I-IW-28	3458.92	684.91
Upper wall turret	PII-1/2I-BW-29	-1.00	3.41	PII-1/2I-IW-29	802.82	160.83
Ceiling turret	PII-1/2I-BW-30	6.26	2.93	PII-1/2I-IW-30	519.51	106.63

Phase II shot 3 Interior Wipes (μg per 100 cm^2)						
	Baseline Wipe			Post-shot		
Specific Features	Field ID	Mass of DU (μg)	1 sigma (μg)	Field ID	Mass of DU (μg)	1 sigma (μg)
Floor engine compartment	PII-3I-BW-1	293.41	59.25	PII-3I-IW-1	1469.86	292.74
Wall engine compartment	PII-3I-BW-2	106.90	22.75	PII-3I-IW-2	417.49	84.86
Side of bench - driver	PII-3I-BW-3	70.73	16.00	PII-3I-IW-3	122.43	26.42
Floor driver's area	PII-3I-BW-4	240.85	49.54	PII-3I-IW-4	1358.98	270.85
Wall driver's area	PII-3I-BW-5	183.55	39.33	PII-3I-IW-5	235.35	48.92
Wall driver's area	PII-3I-BW-6	274.70	57.46	PII-3I-IW-6	152.10	32.47
Bench driver's area	PII-3I-BW-7	1025.18	203.82	PII-3I-IW-7	789.88	158.43
Upper wall driver's area	PII-3I-BW-8	23.53	6.47	PII-3I-IW-8	88.87	19.05
Bench between driver's and crew area	PII-3I-BW-9	185.38	37.79	PII-3I-IW-9	130.68	27.61
Turret shroud assembly	PII-3I-BW-10	39.56	10.22	PII-3I-IW-10	191.89	39.34
Upper wall (left scout position)	PII-3I-BW-11	26.79	7.92	PII-3I-IW-11	11.26	4.07
Bench (left scout position)	PII-3I-BW-12	86.12	18.47	PII-3I-IW-12	2305.60	458.47
Lower wall under bench (left scout position)	PII-3I-BW-13	29.79	7.78	PII-3I-IW-13	745.65	149.28
Floor (left scout position)	PII-3I-BW-14	72.10	16.14	PII-3I-IW-14	2383.94	473.95
Ceiling left scout position	PII-3I-BW-15	395.86	80.80	PII-3I-IW-15	567.12	115.17
Ceiling left scout position	PII-3I-BW-16	765.68	153.87	PII-3I-IW-16	801.45	161.36
Floor right scout position	PII-3I-BW-17	344.22	69.17	PII-3I-IW-17	1256.47	250.50

Upper wall right scout position	PII-3I-BW-18	1177.60	234.50	PII-3I-IW-18	811.74	162.34
Upper wall right scout position	PII-3I-BW-19	738.80	147.51	PII-3I-IW-19	432.72	87.21
Bench right scout position	PII-3I-BW-20	346.89	70.54	PII-3I-IW-20	1655.39	329.67
Floor right scout position	PII-3I-BW-21	158.72	32.87	PII-3I-IW-21	1697.42	337.85
Turret shroud assembly right scout position	PII-3I-BW-22	35.68	9.95	PII-3I-IW-22	865.57	173.11
Upper wall right scout position	PII-3I-BW-23	192.03	39.94	PII-3I-IW-23	630.48	126.25
Floor in turret	PII-3I-BW-24	52.83	12.45	PII-3I-IW-24	409.44	82.55
Floor under breech – turret	PII-3I-BW-25	147.72	31.19	PII-3I-IW-25	658.28	131.89
Ledge turret	PII-3I-BW-26	115.17	25.00	PII-3I-IW-26	976.31	194.72
Lower wall turret	PII-3I-BW-27	35.05	8.07	PII-3I-IW-27	389.53	78.56
Ledge above wall in turret	PII-3I-BW-28	203.07	42.69	PII-3I-IW-28	1437.46	286.38
Upper wall turret	PII-3I-BW-29	427.62	86.36	PII-3I-IW-29	574.06	115.49
Ceiling turret	PII-3I-BW-30	180.04	38.54	PII-3I-IW-30	318.74	65.74

PIV-1 Interior Wipes (μg per 100 cm^2)

	Baseline Wipe			Post-shot		
Specific Features	**Field ID**	**Mass of DU (μg)**	**1 sigma (μg)**	**Field ID**	**Mass of DU (μg)**	**1 sigma (μg)**
Driver's throttle control	PIV-1I-BW-1	1.13	0.23	PIV-1I-IW-1	9.14	3.85
Driver's integrated display	PIV-1I-BW-2	6.51	2.13	PIV-1I-IW-2	6.51	2.13
Ready rack - loader	PIV-1I-BW-3	6.01	3.17	PIV-1I-IW-3	16.15	4.34
Loader's ammo door knee switch (90^o elbow)	PIV-1I-BW-4	0.00	0.00	PIV-1I-IW-4	3.76	3.04
Front face of Loader's panel	PIV-1I-BW-5	2.00	1.75	PIV-1I-IW-5	1.75	2.43
GPS guard above radio	PIV-1I-BW-6	0.88	1.71	PIV-1I-IW-6	1.13	0.23
Top of breech	PIV-1I-BW-7	0.88	1.71	PIV-1I-IW-7	7.39	2.81
Ceiling in between hatch openings	PIV-1I-BW-8	4.01	2.53	PIV-1I-IW-8	-1.13	0.23
Floor behind breech	PIV-1I-BW-9	4.26	1.90	PIV-1I-IW-9	6.64	4.02
Commander's rear most vision block	PIV-1I-BW-10	5.13	2.61	PIV-1I-IW-10	2.25	0.45
Commander's "joy stick" control forearm rest	PIV-1I-BW-11	4.26	1.90	PIV-1I-IW-11	5.38	2.01
Commander's display unit	PIV-1I-BW-12	-0.75	2.95	PIV-1I-IW-12	2.38	3.43
Commander's goggles	PIV-1I-BW-13	5.63	1.11	PIV-1I-IW-13	3.13	1.81
Backrest of Gunner's seat	PIV-1I-BW-14	2.25	0.45	PIV-1I-IW-14	0.88	1.71
Commander's GPS extension (back plate)	PIV-1I-BW-15	1.13	0.23	PIV-1I-IW-15	6.51	2.13

PIV-2 Interior Wipes (μg per 100 cm^2)

	Baseline Wipe			Post-shot		
Specific Features	**Field ID**	**Mass of DU (μg)**	**1 sigma (μg)**	**Field ID**	**Mass of DU (μg)**	**1 sigma (μg)**
Driver's throttle control	PIV-2I-BW-1	8.51	2.95	PIV-2I-IW-1	Sample not collected	
Driver's integrated display	PIV-2I-BW-2	2.25	0.45	PIV-2I-IW-2	Sample not collected	
Ready rack - loader	PIV-2I-BW-3	5.13	2.62	PIV-2I-IW-3	7.39	3.71
Loader's ammo door knee switch (90^o elbow)	PIV-2I-BW-4	6.26	2.71	PIV-2I-IW-4	9.26	2.52
Front face of Loader's panel	PIV-2I-BW-5	2.00	1.75	PIV-2I-IW-5	9.01	3.01
GPS guard above radio	PIV-2I-BW-6	1.13	0.23	PIV-2I-IW-6	3.13	3.01
Top of breech	PIV-2I-BW-7	7.88	1.58	PIV-2I-IW-7	4.51	2.57
Ceiling in between hatch openings	PIV-2I-BW-8	2.38	3.43	PIV-2I-IW-8	-1.00	4.17
Floor behind breech	PIV-2I-BW-9	4.26	1.90	PIV-2I-IW-9	0.25	1.70
Commander's rear most vision block	PIV-2I-BW-10	5.13	2.62	PIV-2I-IW-10	1.75	3.42
Commander's "joy stick" control forearm rest	PIV-2I-BW-11	15.90	4.66	PIV-2I-IW-11	11.64	4.46
Commander's display unit	PIV-2I-BW-12	32.54	7.55	PIV-2I-IW-12	3.38	2.50

Commander's goggles	PIV-2I-BW-13	15.65	4.93	PIV-2I-IW-13	2.00	2.97
Backrest of Gunner's seat	PIV-2I-BW-14	23.78	5.85	PIV-2I-IW-14	4.51	2.57
Commander's GPS extension (back plate)	PIV-2I-BW-15	0.88	1.71	PIV-2I-IW-15	3.51	4.22

PIV-3 Interior Wipes (μg per 100 cm^2)

	Baseline Wipe			Post-shot		
Specific Features	**Field ID**	**Mass of DU (μg)**	**1 sigma (μg)**	**Field ID**	**Mass of DU (μg)**	**1 sigma (μg)**
Driver's throttle control	PIV-3I-BW-1	14.14	3.69	PIV-3I-IW-1	33.42	7.81
Driver's integrated display	PIV-3I-BW-2	1.13	0.23	PIV-3I-IW-2	8.26	3.37
Ready rack - loader	PIV-3I-BW-3	11.64	3.74	PIV-3I-IW-3	-0.50	2.41
Loader's ammo door knee switch (90° elbow)	PIV-3I-BW-4	1.13	0.23	PIV-3I-IW-4	140.19	28.98
Front face of Loader's panel	PIV-3I-BW-5	0.88	1.71	PIV-3I-IW-5	5.13	2.61
GPS guard above radio	PIV-3I-BW-6	5.63	1.11	PIV-3I-IW-6	5.38	2.01
Top of breech	PIV-3I-BW-7	5.13	2.61	PIV-3I-IW-7	35.42	8.32
Ceiling in between hatch openings	PIV-3I-BW-8	3.38	0.67	PIV-3I-IW-8	7.64	2.27
Floor behind breech	PIV-3I-BW-9	4.63	3.52	PIV-3I-IW-9	9.39	3.48
Commander's rear most vision block	PIV-3I-BW-10	-0.37	4.17	PIV-3I-IW-10	5.13	2.61
Commander's "joy stick" control forearm rest	PIV-3I-BW-11	13.65	4.34	PIV-3I-IW-11	20.15	5.51
Commander's display unit	PIV-3I-BW-12	4.26	1.90	PIV-3I-IW-12	19.03	5.35
Commander's goggles	PIV-3I-BW-13	1.75	2.43	PIV-3I-IW-13	10.52	3.60
Backrest of Gunner's seat	PIV-3I-BW-14	0.00	0.00	PIV-3I-IW-14	6.01	3.18
Commander's GPS extension (back plate)	PIV-3I-BW-15	9.64	3.07	PIV-3I-IW-15	27.16	6.35

PIV-4 Interior Wipes (μg per 100 cm^2)

	Baseline Wipe			Post-shot		
Specific Features	**Field ID**	**Mass of DU (μg)**	**1 sigma (μg)**	**Field ID**	**Mass of DU (μg)**	**1 sigma (μg)**
Driver's throttle control	PIV-4I-BW-1	3.13	1.81	PIV-4I-IW-1	127.93	27.06
Driver's integrated display	PIV-4I-BW-2	-5.88	2.06	PIV-4I-IW-2	16.53	5.31
Ready rack - loader	PIV-4I-BW-3	8.01	3.76	PIV-4I-IW-3	979.22	196.06
Loader's ammo door knee switch (90° elbow)	PIV-4I-BW-4	4.01	2.53	PIV-4I-IW-4	297.54	60.62
Front face of Loader's panel	PIV-4I-BW-5	0.00	0.00	PIV-4I-IW-5	41.06	9.33
GPS guard above radio	PIV-4I-BW-6	2.25	0.45	PIV-4I-IW-6	137.93	28.27
Top of breech	PIV-4I-BW-7	0.38	2.95	PIV-4I-IW-7	1340.18	267.68
Ceiling in between hatch openings	PIV-4I-BW-8	-0.25	1.70	PIV-4I-IW-8	57.46	13.53
Floor behind breech	PIV-4I-BW-9	5.63	1.12	PIV-4I-IW-9	1186.59	237.05
Commander's rear most vision block	PIV-4I-BW-10	6.01	3.18	PIV-4I-IW-10	467.81	95.08
Commander's "joy stick" control forearm rest	PIV-4I-BW-11	3.38	0.68	PIV-4I-IW-11	978.46	195.86
Commander's display unit	PIV-4I-BW-12	-3.63	1.85	PIV-4I-IW-12	844.78	169.32
Commander's goggles	PIV-4I-BW-13	-0.25	1.70	PIV-4I-IW-13	704.01	141.77
Backrest of Gunner's seat	PIV-4I-BW-14	-5.00	2.60	PIV-4I-IW-14	660.78	132.70
Commander's GPS extension (back plate)	PIV-4I-BW-15	-3.38	0.67	PIV-4I-IW-15	863.92	173.01

PIV-4 Interior Wipes (μg per 100 cm^2)

	Post-shot A			Post-shot B		
Specific Features	**Field ID**	**Mass of DU (μg)**	**1 sigma (μg)**	**Field ID**	**Mass of DU (μg)**	**1 sigma (μg)**
Driver's integrated display	PIV-4I-IW-1A	48.19	10.94	PIV-4I-IW-1B	22.66	6.11
Loader's ready rack	PIV-4I-IW-2A	1898.08	376.19	PIV-4I-IW-2B	1165.57	231.12
Left of breech	PIV-4I-IW-3A	315.18	63.34	PIV-4I-IW-3B	205.91	42.01

Right top of breech	PIV-4I-IW-4A	922.14	183.46	PIV-4I-IW-4B	411.21	82.82
Front face of Loader’s panel	PIV-4I-IW-5A	181.63	37.28	PIV-4I-IW-5B	55.58	12.68
Ceiling above breech	PIV-4I-IW-6A	489.45	98.32	PIV-4I-IW-6B	500.82	100.23
Floor under breech	PIV-4I-IW-7A	1152.44	228.87	PIV-4I-IW-7B	744.27	148.14
Vision block - removed	PIV-4I-IW-8A	918.05	183.01	PIV-4I-IW-8B	546.60	108.73
Right side of commander's seat on flat panel	PIV-4I-IW-9A	136.44	28.12	PIV-4I-IW-9B	150.20	30.75
Wall behind commander's seat	PIV-4I-IW-10A	1092.36	216.98	PIV-4I-IW-10B	1107.54	219.99
Commander keyboard top	PIV-4I-IW-11A	797.28	158.18	PIV-4I-IW-11B	1146.78	227.26
Commander's seat ledge	PIV-4I-IW-12A	438.71	87.70	PIV-4I-IW-12B	452.74	90.49
GPS screen	PIV-4I-IW-13A	661.44	132.27	PIV-4I-IW-13B	769.28	152.84
Floor gunner's left side	PIV-4I-IW-14A	16838.67	3329.14	PIV-4I-IW-14B	9227.87	1822.07
Loader's seat	PIV-4I-IW-15A	850.34	168.57	PIV-4I-IW-15B	944.98	187.16

Table F.2. Exterior Wipes

PI-1 Exterior Wipes (μg per 100 cm^2)						
	Baseline Wipe			Post-shot		
Specific Features	Field ID	Mass of DU (μg)	1 sigma (μg)	Field ID	Mass of DU (μg)	1 sigma (μg)
Front glacis turret impact side	N/A	N/A	N/A	PI-1E-IW-1	361.25	72.92
Front glacis turret impact side	N/A	N/A	N/A	PI-1E-IW-2	143.33	30.28
Side glacis turret impact side	N/A	N/A	N/A	PI-1E-IW-3	249.46	50.53
Rear turret impact side	N/A	N/A	N/A	PI-1E-IW-4	214.79	43.79
Rear turret impact side	N/A	N/A	N/A	PI-1E-IW-5	80.48	16.76
Hull horizontal surface under turret	N/A	N/A	N/A	PI-1E-IW-6	-0.25	2.94
Hull metal plate horizontal	N/A	N/A	N/A	PI-1E-IW-7	44.94	11.22
Hull horizontal surface on top of fender	N/A	N/A	N/A	PI-1E-IW-8	81.00	18.19
Hull metal plate horizontal surface	N/A	N/A	N/A	PI-1E-IW-9	65.35	15.04
Hull metal plate horizontal surface	N/A	N/A	N/A	PI-1E-IW-10	87.25	18.76
Front glacis turret exit side	N/A	N/A	N/A	PI-1E-IW-11	227.08	46.90
Side glacis turret exit side	N/A	N/A	N/A	PI-1E-IW-12	244.59	50.04
Side glacis turret exit side	N/A	N/A	N/A	PI-1E-IW-13	131.56	27.72
Rear turret exit side	N/A	N/A	N/A	PI-1E-IW-14	86.38	19.22
Rear turret exit side	N/A	N/A	N/A	PI-1E-IW-15	178.02	37.58
Hull metal plate horizontal surface	N/A	N/A	N/A	PI-1E-IW-16	139.70	29.65
Hull metal plate horizontal surface	N/A	N/A	N/A	PI-1E-IW-17	83.25	18.59
Hull top of fender horizontal	N/A	N/A	N/A	PI-1E-IW-18	56.46	13.00
Hull metal plate	N/A	N/A	N/A	PI-1E-IW-19	77.49	17.24
Hull metal plate	N/A	N/A	N/A	PI-1E-IW-20	87.62	19.06
Rear hull top impact side	N/A	N/A	N/A	PI-1E-IW-21	54.07	12.12
Rear hull top exit side	N/A	N/A	N/A	PI-1E-IW-22	54.58	13.02
Top front turret top impact side	N/A	N/A	N/A	PI-1E-IW-23	286.54	58.58
Top front turret over breech	N/A	N/A	N/A	PI-1E-IW-24	344.61	69.86
Top front turret exit side	N/A	N/A	N/A	PI-1E-IW-25	162.72	33.47
Top back turret impact side	N/A	N/A	N/A	PI-1E-IW-26	721.00	144.46
Top turret on commander's hatch	N/A	N/A	N/A	PI-1E-IW-27	660.30	132.49
Top rear turret blow-off panels	N/A	N/A	N/A	PI-1E-IW-28	961.95	192.16
Top hull impact side	N/A	N/A	N/A	PI-1E-IW-29	102.52	21.72
Top hull exit side	N/A	N/A	N/A	PI-1E-IW-30	33.69	10.84

PI- 2 Exterior Wipes (μg per 100 cm^2)						
	Baseline Wipe			Post-shot		
Specific Features	Field ID	Mass of DU (μg)	1 sigma (μg)	Field ID	Mass of DU (μg)	1 sigma (μg)
Turret impact side	PI-2E-BW-1	1240.41	246.50	PI-2E-IW-1	3937.55	779.06
Turret impact side	PI-2E-BW2	562.88	112.42	PI-2E-IW-2	4165.23	824.04
Turret impact side	PI-2E-BW-3	157.10	32.65	PI-2E-IW-3	2877.06	569.32
Turret impact side	PI-2E-BW-4	483.77	96.67	PI-2E-IW-4	2551.05	505.09
Turret impact side	PI-2E-BW-5	73.47	15.32	PI-2E-IW-5	2036.61	403.41
Hull horizontal under turret	PI-2E-BW-6	4.63	3.52	PI-2E-IW-6	165.96	33.57
Hull metal plate horizontal	PI-2E-BW-7	403.93	81.13	PI-2E-IW-7	397.17	79.78
Hull horizontal on top of fender	PI-2E-BW-8	50.20	11.43	PI-2E-IW-8	572.80	114.63
Hull metal plate horizontal	PI-2E-BW-9	154.47	32.02	PI-2E-IW-9	921.03	183.45
Hull metal plate horizontal	PI-2E-BW-10	339.71	68.24	PI-2E-IW-10	745.05	148.85

Turret exit side	PI-2E-BW-11	500.69	100.40	PI-2E-IW-11	3930.11	777.44
Turret exit side	PI-2E-BW-12	836.85	166.37	PI-2E-IW-12	4192.79	829.55
Turret exit side	PI-2E-BW-13	149.08	30.52	PI-2E-IW-13	269.89	55.25
Turret exit side	PI-2E-BW-14	550.46	109.49	PI-2E-IW-14	2039.25	404.03
Turret exit side	PI-2E-BW-15	531.93	105.75	PI-2E-IW-15	3386.70	670.26
Hull metal plate	PI-2E-BW-16	166.46	33.38	PI-2E-IW-16	1014.03	201.77
Hull metal plate	PI-2E-BW-17	366.48	73.31	PI-2E-IW-17	908.26	180.83
Hull top of fender horizontal	PI-2E-BW-18	165.48	34.15	PI-2E-IW-18	870.85	173.69
Hull metal plate	PI-2E-BW-19	194.90	39.91	PI-2E-IW-19	1167.00	232.06
Hull metal plate	PI-2E-BW-20	181.63	37.34	PI-2E-IW-20	656.77	131.05
Rear hull top impact side	PI-2E-BW-21	14.77	4.49	PI-2E-IW-21	845.77	168.27
Rear hull top exit side	PI-2E-BW-22	40.05	8.28	PI-2E-IW-22	1900.38	376.89
Top front turret top impact side	PI-2E-BW-23	170.37	35.20	PI-2E-IW-23	5451.25	1078.23
Top front turret over breech	PI-2E-BW-24	485.43	97.53	PI-2E-IW-24	1655.18	328.54
Top front turret exit side	PI-2E-BW-25	217.68	44.55	PI-2E-IW-25	4162.75	823.63
Top back turret impact side	PI-2E-BW-26	132.44	27.78	PI-2E-IW-26	9392.56	1856.60
Top turret on commander's hatch	PI-2E-BW-27	251.72	51.06	PI-2E-IW-27	6235.15	1233.07
Top rear turret center	PI-2E-BW-28	45.07	11.49	PI-2E-IW-28	325.19	65.53
Top hull impact side	PI-2E-BW-29	91.25	19.45	PI-2E-IW-29	604.33	120.66
Top hull exit side	PI-2E-BW-30	97.62	19.76	PI-2E-IW-30	611.20	121.94

PI-3/4 Exterior Wipes (μg per 100 cm^2)

	Baseline Wipe			Post-shot		
Specific Features	**Field ID**	**Mass of DU (μg)**	**1 sigma (μg)**	**Field ID**	**Mass of DU (μg)**	**1 sigma (μg)**
Turret exit side	PI-3/4E-BW-1	N/A	N/A	PI-3/4E-IW-1	7640.16	1517.12
Turret exit side	PI-3/4E-BW-2	N/A	N/A	PI-3/4E-IW-2	8098.87	1607.84
Turret exit side	PI-3/4E-BW-3	N/A	N/A	PI-3/4E-IW-3	7935.34	1575.52
Turret exit side	PI-3/4E-BW-4	N/A	N/A	PI-3/4E-IW-4	3922.58	779.79
Turret exit side	PI-3/4E-BW-5	N/A	N/A	PI-3/4E-IW-5	3181.04	632.21
Hull horizontal under turret	PI-3/4E-BW-6	N/A	N/A	PI-3/4E-IW-6	115.65	23.99
Hull metal plate horizontal	PI-3/4E-BW-7	N/A	N/A	PI-3/4E-IW-7	4669.33	927.90
Hull horizontal on top of fender	PI-3/4E-BW-8	N/A	N/A	PI-3/4E-IW-8	1704.93	340.01
Hull metal plate horizontal	PI-3/4E-BW-9	N/A	N/A	PI-3/4E-IW-9	3352.15	666.57
Hull metal plate horizontal	PI-3/4E-BW-10	N/A	N/A	PI-3/4E-IW-10	3362.17	667.80
Turret impact side	PIB3/4E-BW-11	N/A	N/A	PI-3/4E-IW-11	6585.75	1307.70
Turret impact side	PIB3/4E-BW-1B	N/A	N/A	PI-3/4E-IW-12	5528.59	1097.99
Turret impact side	PI-3/4E-BW-13	N/A	N/A	PI-3/4E-IW-13	2658.39	528.69
Turret impact side	PI-3/4E-BW-14	N/A	N/A	PI-3/4E-IW-14	1800.81	358.37
Turret impact side	PI-3/4E-BW-15	N/A	N/A	PI-3/4E-IW-15	4038.28	802.52
Hull metal plate	PI-3/4E-BW-16	N/A	N/A	PI-3/4E-IW-16	3748.61	745.35
Hull metal plate	PI-3/4E-BW-17	N/A	N/A	PI-3/4E-IW-17	1653.47	329.78
Hull top of fender horizontal	PI-3/4E-BW-18	N/A	N/A	PI-3/4E-IW-18	1845.37	367.85
Hull metal plate	PI-3/4E-BW-19	N/A	N/A	PI-3/4E-IW-19	725.91	145.76
Hull metal plate	PI-3/4E-BW-20	N/A	N/A	PI-3/4E-IW-20	1864.75	371.58
Rear hull top impact side	PI-3/4E-BW-21	N/A	N/A	PI-3/4E-IW-21	2929.79	582.66
Rear hull top exit side	PI-3/4E-BW-22	N/A	N/A	PI-3/4E-IW-22	1746.66	347.88
Top front turret exit side	PI-3/4E-BW-23	N/A	N/A	PI-3/4E-IW-23	3485.90	693.32
Top front turret above breech	PI-3/4E-BW-24	N/A	N/A	PI-3/4E-IW-24	5440.06	1080.94
Top front turret impact side	PI-3/4E-BW-25	N/A	N/A	PI-3/4E-IW-25	3743.89	744.13

Top front turret exit side	PI-3/4E-BW-26	N/A	N/A	PI-3/4E-IW-26	6303.55	1251.85
Top back turret impact side	PI-3/4E-BW-27	N/A	N/A	PI-3/4E-IW-27	5471.06	1086.69
Top turret on commander's hatch	PI-3/4E-BW-28	N/A	N/A	PI-3/4E-IW-28	6883.05	1366.51
Top rear turret center	PI-3/4E-BW-29	N/A	N/A	PI-3/4E-IW-29	1598.38	318.78
Top hull exit side	PI-3/4E-BW-30	N/A	N/A	PI-3/4E-IW-30	985.87	197.02

PI-5 Exterior Wipes (μg per 100 cm^2)

	Baseline Wipe			Post-shot		
Specific Features	**Field ID**	**Mass of DU (μg)**	**1 sigma (μg)**	**Field ID**	**Mass of DU (μg)**	**1 sigma (μg)**
Turret exit side	PI-5E-BW-1	876.22	174.27	PI-5E-IW-1	N/A	N/A
Turret exit side	PI-5E-BW-2	461.40	92.51	PI-5E-IW-2	N/A	N/A
Turret exit side	PI-5E-BW-3	96.76	20.12	PI-5E-IW-3	N/A	N/A
Turret exit side	PI-5E-BW-4	271.39	55.38	PI-5E-IW-4	N/A	N/A
Turret exit side	PI-5E-BW-5	870.83	173.12	PI-5E-IW-5	N/A	N/A
Hull horizontal under turret	PI-5E-BW-6	11.27	5.57	PI-5E-IW-6	N/A	N/A
Hull metal plate horizontal	PI-5E-BW-7	98.03	21.90	PI-5E-IW-7	N/A	N/A
Hull horizontal on top of fender	PI-5E-BW-8	61.09	13.95	PI-5E-IW-8	N/A	N/A
Hull metal plate horizontal	PI-5E-BW-9	46.08	12.23	PI-5E-IW-9	N/A	N/A
Hull metal plate horizontal	PI-5E-BW-10	15.78	5.98	PI-5E-IW-10	N/A	N/A
Turret impact side	PI-5E-BW-11	930.76	184.69	PI-5E-IW-11	N/A	N/A
Turret impact side	PI-5E-BW-12	336.59	67.60	PI-5E-IW-12	N/A	N/A
Turret impact side	PI-5E-BW-13	44.07	10.64	PI-5E-IW-13	N/A	N/A
Turret impact side	PI-5E-BW-14	290.29	59.02	PI-5E-IW-14	N/A	N/A
Turret impact side	PI-5E-BW-15	187.52	38.66	PI-5E-IW-15	N/A	N/A
Hull metal plate	PI-5E-BW-16	8.89	4.19	PI-5E-IW-16	N/A	N/A
Hull metal plate	PI-5E-BW-17	113.80	24.68	PI-5E-IW-17	N/A	N/A
Hull top of fender horizontal	PI-5E-BW-18	82.00	18.53	PI-5E-IW-18	N/A	N/A
Hull metal plate	PI-5E-BW-19	316.22	64.42	PI-5E-IW-19	N/A	N/A
Hull metal plate	PI-5E-BW-20	204.92	42.20	PI-5E-IW-20	N/A	N/A
Rear hull top impact side	PI-5E-BW-21	81.12	18.30	PI-5E-IW-21	N/A	N/A
Rear hull top exit side	PI-5E-BW-22	86.00	18.68	PI-5E-IW-22	N/A	N/A
Top front turret top impact side	PI-5E-BW-23	157.99	33.58	PI-5E-IW-23	N/A	N/A
Top front turret over breech	PI-5E-BW-24	476.82	96.05	PI-5E-IW-24	N/A	N/A
Top front turret exit side	PI-5E-BW-25	257.63	52.79	PI-5E-IW-25	N/A	N/A
Top back turret impact side	PI-5E-BW-26	96.89	21.07	PI-5E-IW-26	N/A	N/A
Top turret on commander's hatch	PI-5E-BW-27	256.12	52.42	PI-5E-IW-27	N/A	N/A
Top rear turret center	PI-5E-BW-28	392.68	79.04	PI-5E-IW-28	N/A	N/A
Top hull impact side	PI-5E-BW-29	101.02	21.61	PI-5E-IW-29	N/A	N/A
Top hull exit side	PI-5E-BW-30	136.64	28.96	PI-5E-IW-30	N/A	N/A

PI-6 Exterior Wipes (μg per 100 cm^2)

	Baseline Wipe			Post-shot		
Specific Features	**Field ID**	**Mass of DU (μg)**	**1 sigma (μg)**	**Field ID**	**Mass of DU (μg)**	**1 sigma (μg)**
Turret impact side	PI-6E-IW-1	N/A	N/A	PI-6E-IW-1	3551.91	702.49
Turret impact side	PI-6E-IW-2	N/A	N/A	PI-6E-IW-2	3318.38	656.09
Turret impact side	PI-6E-IW-3	N/A	N/A	PI-6E-IW-3	2439.42	482.56
Turret impact side	PI-6E-IW-4	N/A	N/A	PI-6E-IW-4	2084.32	412.47
Turret impact side	PI-6E-IW-5	N/A	N/A	PI-6E-IW-5	2563.92	506.98

Hull horizontal under turret	PI-6E-IW-6	N/A	N/A	PI-6E-IW-6	88.37	18.72
Hull metal plate horizontal	PI-6E-IW-7	N/A	N/A	PI-6E-IW-7	244.22	49.85
Hull horizontal on top of fender	PI-6E-IW-8	N/A	N/A	PI-6E-IW-8	479.17	96.01
Hull metal plate horizontal	PI-6E-IW-9	N/A	N/A	PI-6E-IW-9	1269.87	251.91
Hull metal plate horizontal	PI-6E-IW-10	N/A	N/A	PI-6E-IW-10	1065.94	211.43
Turret exit side	PI-6E-IW-11	N/A	N/A	PI-6E-IW-11	2415.46	477.61
Turret exit side	PI-6E-IW-12	N/A	N/A	PI-6E-IW-12	3075.91	608.18
Turret exit side	PI-6E-IW-13	N/A	N/A	PI-6E-IW-13	2022.72	400.24
Turret exit side	PI-6E-IW-14	N/A	N/A	PI-6E-IW-14	1909.57	377.37
Turret exit side	PI-6E-IW-15	N/A	N/A	PI-6E-IW-15	3188.44	630.41
Hull metal plate	PI-6E-IW-16	N/A	N/A	PI-6E-IW-16	1190.78	236.40
Hull metal plate	PI-6E-IW-17	N/A	N/A	PI-6E-IW-17	1068.13	212.40
Hull top of fender horizontal	PI-6E-IW-18	N/A	N/A	PI-6E-IW-18	628.38	125.54
Hull metal plate	PI-6E-IW-19	N/A	N/A	PI-6E-IW-19	1830.78	362.72
Hull metal plate	PI-6E-IW-20	N/A	N/A	PI-6E-IW-20	1627.17	322.78
Rear hull top exit side	PI-6E-IW-21	N/A	N/A	PI-6E-IW-21	1395.54	275.93
Rear hull top impact side	PI-6E-IW-22	N/A	N/A	PI-6E-IW-22	813.36	161.67
Top front turret top impact side	PI-6E-IW-23	N/A	N/A	PI-6E-IW-23	1377.17	273.25
Top front turret over breech	PI-6E-IW-24	N/A	N/A	PI-6E-IW-24	1242.10	246.54
Top front turret exit side	PI-6E-IW-25	N/A	N/A	PI-6E-IW-25	1764.09	349.67
Top back turret impact side	PI-6E-IW-26	N/A	N/A	PI-6E-IW-26	3201.72	633.09
Top turret on commander's hatch	PI-6E-IW-27	N/A	N/A	PI-6E-IW-27	1596.28	316.14
Top rear turret center	PI-6E-IW-28	N/A	N/A	PI-6E-IW-28	3760.93	743.32
Top hull exit side	PI-6E-IW-29	N/A	N/A	PI-6E-IW-29	670.42	133.56
Top hull impact side	PI-6E-IW-30	N/A	N/A	PI-6E-IW-30	777.54	154.37

PI-7 Exterior Wipes (μg per 100 cm^2)

	Baseline Wipe			Post-shot		
Specific Features	**Field ID**	**Mass of DU (μg)**	**1 sigma (μg)**	**Field ID**	**Mass of DU (μg)**	**1 sigma (μg)**
Turret impact side	PI-7E-BW-1	151.61	43.54	PI-7E-IW-1	2221.95	582.76
Turret impact side	PI-7E-BW-2	60.00	19.43	PI-7E-IW-2	2884.72	756.10
Turret impact side	PI-7E-BW-3	78.95	23.11	PI-7E-IW-3	2236.42	586.53
Turret impact side	PI-7E-BW-4	86.11	25.78	PI-7E-IW-4	1785.00	467.95
Turret impact side	PI-7E-BW-5	78.80	22.87	PI-7E-IW-5	2042.73	535.60
Hull horizontal under turret	PI-7E-BW-6	34.96	11.01	PI-7E-IW-6	897.81	236.36
Hull metal plate horizontal	PI-7E-BW-7	57.32	17.21	PI-7E-IW-7	2371.61	622.11
Hull horizontal on top of fender	PI-7E-BW-8	27.72	9.98	PI-7E-IW-8	1604.29	421.35
Hull metal plate horizontal	PI-7E-BW-9	69.37	20.54	PI-7E-IW-9	559.93	148.12
Hull metal plate horizontal	PI-7E-BW-10	61.46	19.93	PI-7E-IW-10	381.91	101.34
Turret exit side	PI-7E-BW-11	39.49	13.18	PI-7E-IW-11	1652.53	433.72
Turret exit side	PI-7E-BW-12	72.89	22.06	PI-7E-IW-12	3340.38	875.43
Turret exit side	PI-7E-BW-13	66.61	19.77	PI-7E-IW-13	4359.30	1142.03
Turret exit side	PI-7E-BW-14	12.76	5.50	PI-7E-IW-14	2000.54	524.79
Turret exit side	PI-7E-BW-15	157.20	44.43	PI-7E-IW-15	2351.73	616.77
Hull metal plate	PI-7E-BW-16	148.01	41.50	PI-7E-IW-16	82.41	22.65
Hull metal plate	PI-7E-BW-17	55.13	16.39	PI-7E-IW-17	537.28	141.94
Hull top of fender horizontal	PI-7E-BW-18	144.63	41.58	PI-7E-IW-18	575.51	152.27
Hull metal plate	PI-7E-BW-19	73.72	21.57	PI-7E-IW-19	261.55	69.63
Hull metal plate	PI-7E-BW-20	29.02	10.10	PI-7E-IW-20	271.09	72.82

Turret impact side	PI-7E-BW-21	12.76	5.50	PI-7E-IW-21	664.32	175.37
Rear hull top exit side	PI-7E-BW-22	84.03	24.40	PI-7E-IW-22	685.78	180.99
Rear hull top impact side	PI-7E-BW-23	59.38	18.31	PI-7E-IW-23	882.51	232.39
Top front turret top impact side	PI-7E-BW-24	191.38	54.25	PI-7E-IW-24	806.70	212.88
Top front turret over breech	PI-7E-BW-25	128.31	36.50	PI-7E-IW-25	1956.92	513.72
Top front turret exit side	PI-7E-BW-26	280.44	77.94	PI-7E-IW-26	2205.86	578.52
Top back turret impact side	PI-7E-BW-27	121.57	35.62	PI-7E-IW-27	2466.77	646.90
Top turret on commander's hatch	PI-7E-BW-28	137.63	39.34	PI-7E-IW-28	3121.82	818.10
Top rear turret center	PI-7E-BW-29	175.66	49.63	PI-7E-IW-29	413.34	109.44
Top hull exit side	PI-7E-BW-30	77.39	23.31	PI-7E-IW-30	524.17	138.62

PIII-1 Exterior Wipes (μg per 100 cm^2)

	Baseline Wipe			Post-shot		
Specific Features	**Field ID**	**Mass of DU (μg)**	**1 sigma (μg)**	**Field ID**	**Mass of DU (μg)**	**1 sigma (μg)**
Front turret opposite impact side	PIII-1E-BW-1	28.79	8.22	PIII-1E-BW-1	628.75	172.68
Side turret opposite impact side	PIII-1E-BW-2	28.17	9.23	PIII-1E-BW-2	497.19	136.73
Side turret opposite impact side	PIII-1E-BW-3	29.66	8.62	PIII-1E-BW-3	372.76	102.60
Hull metal plate horizontal surface	PIII-1E-BW-4	80.61	22.72	PIII-1E-BW-4	327.09	90.52
Hull metal plate horizontal surface	PIII-1E-BW-5	132.81	37.16	PIII-1E-BW-5	331.96	91.58
Front turret impact side	PIII-1E-BW-6	13.02	4.29	PIII-1E-BW-6	240.96	66.68
Side turret impact side	PIII-1E-BW-7	12.14	3.72	PIII-1E-BW-7	710.48	194.88
Side turret impact side	PIII-1E-BW-8	14.77	5.28	PIII-1E-BW-8	663.90	182.05
Hull metal plate horizontal impact side	PIII-1E-BW-9	76.23	21.83	PIII-1E-BW-9	265.63	73.80
Hull metal plate horizontal impact side	PIII-1E-BW-10	225.21	62.87	PIII-1E-BW-10	384.04	105.91
Floor impact side	PIII-1E-BW-11	203.66	56.55	PIII-1E-BW-11	680.70	186.81
Floor impact side	PIII-1E-BW-12	102.40	29.12	PIII-1E-BW-12	488.41	134.13
Top front turret opposite impact side	PIII-1E-BW-13	65.72	18.88	PIII-1E-BW-13	816.40	223.99
Top front turret above breech	PIII-1E-BW-14	32.54	9.66	PIII-1E-BW-14	737.05	202.40
Top front turret impact side	PIII-1E-BW-15	136.57	38.28	PIII-1E-BW-15	288.03	79.74
Top front turret impact side	PIII-1E-BW-16	77.11	22.12	PIII-1E-BW-16	469.79	129.38
Top rear turret impact side	PIII-1E-BW-17	25.17	9.06	PIII-1E-BW-17	1127.80	308.80
Top rear turret impact side	PIII-1E-BW-18	19.28	6.27	PIII-1E-BW-18	1197.55	328.00
Top turret blow-off panels	PIII-1E-BW-19	92.64	26.74	PIII-1E-BW-19	1050.83	287.85
Top rear turret opposite impact side	PIII-1E-BW-20	9.89	3.19	PIII-1E-BW-20	833.13	228.25
Top rear turret opposite impact side	PIII-1E-BW-21	37.05	10.80	PIII-1E-BW-21	574.57	158.04
Top turret Commander's hatch	PIII-1E-BW-22	54.70	15.96	PIII-1E-BW-22	338.71	93.26
Top front turret opposite impact side	PIII-1E-BW-23	31.67	9.29	PIII-1E-BW-23	488.93	134.46
Top front turret over breech	PIII-1E-BW-24	38.43	11.03	PIII-1E-BW-24	765.81	210.01
Top hull impact side	PIII-1E-BW-25	6.14	4.80	PIII-1E-BW-25	85.75	24.74
Top hull impact side	PIII-1E-BW-26	31.17	9.47	PIII-1E-BW-26	252.47	69.76
Top hull impact side	PIII-1E-BW-27	14.77	5.28	PIII-1E-BW-27	95.89	27.37
Top hull opposite impact side	PIII-1E-BW-28	15.65	5.72	PIII-1E-BW-28	83.75	24.16
Top hull opposite impact side	PIII-1E-BW-29	27.54	8.76	PIII-1E-BW-29	121.42	34.35
Top hull impact side	PIII-1E-BW-30	24.66	7.73	PIII-1E-BW-30	50.82	15.17

PIII-2 Exterior Wipes (μg per 100 cm^2)						
	Baseline Wipe			Post-shot		
Specific Features	Field ID	Mass of DU (μg)	1 sigma (μg)	Field ID	Mass of DU (μg)	1 sigma (μg)
Front turret opposite impact side	PIII-2E-BW-1	99.13	27.96	PIII-2E-IW-1	3209.15	634.70
Side turret opposite impact side	PIII-2E-BW-2	94.65	27.08	PIII-2E-IW-2	2564.00	507.29
Side turret opposite impact side	PIII-2E-BW-3	212.18	58.63	PIII-2E-IW-3	3234.77	639.60
Hull metal plate horizontal surface	PIII-2E-BW-4	219.94	61.19	PIII-2E-IW-4	2124.64	420.52
Hull metal plate horizontal surface	PIII-2E-BW-5	136.33	38.55	PIII-2E-IW-5	2216.99	439.18
Front turret impact side	PIII-2E-BW-6	338.09	92.55	PIII-2E-IW-6	2582.53	510.49
Side turret impact side	PIII-2E-BW-7	169.67	47.21	PIII-2E-IW-7	6055.82	1196.38
Side turret impact side	PIII-2E-BW-8	196.35	54.27	PIII-2E-IW-8	6109.27	1206.68
Hull metal plate horizontal impact side	PIII-2E-BW-9	265.29	72.97	PIII-2E-IW-9	2794.47	552.89
Hull metal plate horizontal impact side	PIII-2E-BW-10	192.32	53.40	PIII-2E-IW-10	2761.83	546.57
Floor impact side	PIII-2E-BW-11	324.69	89.33	PIII-2E-IW-11	2001.05	396.47
Floor impact side	PIII-2E-BW-12	303.84	83.92	PIII-2E-IW-12	2360.12	467.15
Top front turret opposite impact side	PIII-2E-BW-13	137.47	38.69	PIII-2E-IW-13	5512.44	1089.38
Top front turret above breech	PIII-2E-BW-14	211.56	59.18	PIII-2E-IW-14	3537.74	699.61
Top front turret impact side	PIII-2E-BW-15	147.78	41.51	PIII-2E-IW-15	2363.06	467.96
Top front turret impact side	PIII-2E-BW-16	268.23	73.99	PIII-2E-IW-16	3157.96	624.60
Top rear turret impact side	PIII-2E-BW-17	269.14	74.47	PIII-2E-IW-17	6808.67	1345.13
Top rear turret impact side	PIII-2E-BW-18	146.45	40.93	PIII-2E-IW-18	4972.68	982.46
Top turret blow-off panels	PIII-2E-BW-19	195.13	54.58	PIII-2E-IW-19	4108.89	811.98
Top rear turret opposite impact side	PIII-2E-BW-20	176.21	49.01	PIII-2E-IW-20	4585.79	906.43
Top rear turret opposite impact side	PIII-2E-BW-21	160.22	44.50	PIII-2E-IW-21	4913.37	971.12
Top turret Commander's hatch	PIII-2E-BW-22	169.18	47.84	PIII-2E-IW-22	2681.17	530.45
Top front turret opposite impact side	PIII-2E-BW-23	111.23	32.02	PIII-2E-IW-23	4352.04	860.16
Top front turret over breech	PIII-2E-BW-24	211.82	59.04	PIII-2E-IW-24	6143.80	1214.26
Top hull impact side	PIII-2E-BW-25	209.45	58.06	PIII-2E-IW-25	1361.81	270.50
Top hull impact side	PIII-2E-BW-26	105.53	29.95	PIII-2E-IW-26	440.87	88.42
Top hull impact side	PIII-2E-BW-27	50.81	15.26	PIII-2E-IW-27	887.20	176.16
Top hull opposite impact side	PIII-2E-BW-28	56.75	16.45	PIII-2E-IW-28	868.95	172.85
Top hull opposite impact side	PIII-2E-BW-29	145.85	41.04	PIII-2E-IW-29	975.48	193.89
Top hull impact side	PIII-2E-BW-30	143.15	40.32	PIII-2E-IW-30	690.85	137.91

PII-1/2 Exterior Wipes (μg per 100 cm^2)						
	Baseline Wipe			Post-shot		
Specific Features	Field ID	Mass of DU (μg)	1 sigma (μg)	Field ID	Mass of DU (μg)	1 sigma (μg)
Exit side hull vertical surface	PII-1/2E-BW-1	11.89	3.36	PII-1/2E-IW-1	69.59	14.75
Exit side hull vertical surface	PII-1/2E-BW-2	8.51	2.93	PII-1/2E-IW-2	416.98	84.14
Exit side hull vertical surface	PII-1/2E-BW-3	4.26	1.90	PII-1/2E-IW-3	1916.26	379.50
Rear on backplate	PII-1/2E-BW-4	9.01	1.78	PII-1/2E-IW-4	10.02	4.29
Rear on backplate	PII-1/2E-BW-5	38.06	9.24	PII-1/2E-IW-5	24.79	7.07
Impact side hull vertical surface	PII-1/2E-BW-6	2.88	2.47	PII-1/2E-IW-6	16.40	4.03
Impact side hull vertical surface	PII-1/2E-BW-7	10.52	3.60	PII-1/2E-IW-7	271.49	54.54
Impact side hull vertical surface	PII-1/2E-BW-8	8.51	2.93	PII-1/2E-IW-8	236.94	47.68
Impact side hull vertical surface	PII-1/2E-BW-9	7.39	2.81	PII-1/2E-IW-9	6.51	2.13

Impact side hull vertical surface	PII-1/2E-BW-10	15.52	3.50	PII-1/2E-IW-10	19.15	3.78
Floor impact side	PII-1/2E-BW-11	225.83	46.54	PII-1/2E-IW-11	317.07	63.99
Floor impact side	PII-1/2E-BW-12	43.56	9.55	PII-1/2E-IW-12	304.67	61.38
Rear Turret shroud vertical surface	PII-1/2E-BW-13	10.76	3.21	PII-1/2E-IW-13	171.35	34.75
Top rear hull	PII-1/2E-BW-14	407.80	81.45	PII-1/2E-IW-14	2592.21	512.56
Top rear turret	PII-1/2E-BW-15	30.42	7.88	PII-1/2E-IW-15	2066.67	409.01
Top exit side turret	PII-1/2E-BW-16	31.42	7.27	PII-1/2E-IW-16	1199.98	237.82
Commander's hatch	PII-1/2E-BW-17	24.66	6.18	PII-1/2E-IW-17	3133.19	619.33
Loader's hatch	PII-1/2E-BW-18	15.90	4.63	PII-1/2E-IW-18	2157.59	426.60
Top TOW launcher horizontal surface	PII-1/2E-BW-19	23.78	5.80	PII-1/2E-IW-19	1206.35	238.99
Impact side hull horizontal surface	PII-1/2E-BW-20	509.70	101.87	PII-1/2E-IW-20	2068.50	409.16
Top front turret	PII-1/2E-BW-21	81.86	17.45	PII-1/2E-IW-21	3665.30	724.09
Top front turret	PII-1/2E-BW-22	17.02	4.78	PII-1/2E-IW-22	1583.81	313.26
Top middle turret	PII-1/2E-BW-23	224.57	45.88	PII-1/2E-IW-23	2023.98	400.51
Front turret	PII-1/2E-BW-24	280.90	56.92	PII-1/2E-IW-24	1935.53	383.27
Front turret	PII-1/2E-BW-25	44.81	10.35	PII-1/2E-IW-25	2262.55	447.61
Top front hull	PII-1/2E-BW-26	23.53	6.00	PII-1/2E-IW-26	2243.01	443.68
Top front hull under gun	PII-1/2E-BW-27	16.15	4.34	PII-1/2E-IW-27	738.15	147.04
Hull under front turret	PII-1/2E-BW-28	3.38	0.67	PII-1/2E-IW-28	46.94	10.16
Top front turret	PII-1/2E-BW-29	64.96	13.48	PII-1/2E-IW-29	2643.87	522.62
Top front hull	PII-1/2E-BW-30	179.75	37.01	PII-1/2E-IW-30	1051.43	208.68

PII-3 Exterior Wipes (μg per 100 cm^2)

	Baseline Wipe			Post-shot		
Specific Features	**Field ID**	**Mass of DU (μg)**	**1 sigma (μg)**	**Field ID**	**Mass of DU (μg)**	**1 sigma (μg)**
Exit side hull vertical surface	PII-3E-BW-1	123.04	25.28	PII-3E-IW-1	2266.20	450.74
Exit side hull vertical surface	PII-3E-BW-2	116.42	24.81	PII-3E-IW-2	5753.89	1142.97
Exit side hull vertical surface	PII-3E-BW-3	709.96	141.23	PII-3E-IW-3	3242.40	644.06
Rear on backplate	PII-3E-BW-4	23.41	7.10	PII-3E-IW-4	25.04	6.92
Rear on backplate	PII-3E-BW-5	32.92	8.09	PII-3E-IW-5	38.31	9.16
Impact side hull vertical surface	PII-3E-BW-6	14.27	5.03	PII-3E-IW-6	1489.77	296.68
Impact side hull vertical surface	PII-3E-BW-7	135.81	27.86	PII-3E-IW-7	2349.42	467.19
Impact side hull vertical surface	PII-3E-BW-8	102.89	21.76	PII-3E-IW-8	2503.65	497.89
Impact side hull vertical surface	PII-3E-BW-9	9.14	3.85	PII-3E-IW-9	2206.33	439.25
Impact side hull vertical surface	PII-3E-BW-10	40.31	9.61	PII-3E-IW-10	1426.95	284.32
Floor impact side	PII-3E-BW-11	559.73	111.11	PII-3E-IW-11	2727.98	542.49
Floor impact side	PII-3E-BW-12	454.75	91.02	PII-3E-IW-12	2470.99	491.43
Rear hull exit side	PII-3E-BW-13	99.90	22.03	PII-3E-IW-13	1029.13	205.15
Rear hull impact side	PII-3E-BW-14	246.47	50.00	PII-3E-IW-14	4596.07	912.63
Rear turret	PII-3E-BW-15	1461.21	289.41	PII-3E-IW-15	7050.50	1399.93
Exit side turret	PII-3E-BW-16	1879.08	371.58	PII-3E-IW-16	8075.74	1602.89
Commander's hatch	PII-3E-BW-17	632.69	125.44	PII-3E-IW-17	4194.85	833.19
Loader's hatch	PII-3E-BW-18	478.39	95.33	PII-3E-IW-18	4470.14	887.93
Front turret	PII-3E-BW-19	437.55	86.76	PII-3E-IW-19	4134.33	821.03

Impact side hull	PII-3E-BW-20	1054.67	209.22	PII-3E-IW-20	3497.50	695.09
Top of turret	PII-3E-BW-21	285.14	57.53	PII-3E-IW-21	7011.37	1391.78
Front turret	PII-3E-BW-22	264.60	53.10	PII-3E-IW-22	5864.66	1164.40
Top of turret middle	PII-3E-BW-23	876.42	173.95	PII-3E-IW-23	2349.73	467.50
Top of turret	PII-3E-BW-24	171.99	35.33	PII-3E-IW-24	7074.62	1404.20
Front turret	PII-3E-BW-25	343.09	68.91	PII-3E-IW-25	7775.97	1543.62
Front top hull	PII-3E-BW-26	791.68	157.17	PII-3E-IW-26	1937.52	385.62
Under the gun	PII-3E-BW-27	850.41	168.98	PII-3E-IW-27	878.48	175.77
Under front turret	PII-3E-BW-28	16.40	4.03	PII-3E-IW-28	3751.98	745.62
Front top turret	PII-3E-BW-29	141.07	29.17	PII-3E-IW-29	2835.82	563.67
Front top hull	PII-3E-BW-30	482.42	96.58	PII-3E-IW-30	1521.96	303.21

PIV-1 Exterior Wipes (μg per 100 cm^2)

	Baseline Wipe			Post-shot				
Specific Features	**Field ID**	**Mass of DU (μg)**	**1 sigma (μg)**	**Field ID**	**Mass of DU (μg) (Group A)**	**1 sigma (μg)**	**Mass of DU (μg) (Group B)**	**1 sigma (μg)**
Floor	PIV-1E-BW-1	288.16	58.50	PIV-1E-IW-1	1601.62	316.96	N/A	N/A
Right front glacis	PIV-1E-BW-2	1.13	0.23	PIV-1E-IW-2	602.19	119.98	N/A	N/A
Right side glacis	PIV-1E-BW-3	4.39	3.90	PIV-1E-IW-3	492.01	97.78	N/A	N/A
Right front skirt vertical surface	PIV-1E-BW-4	-2.50	1.77	PIV-1E-IW-4	10.52	3.60	N/A	N/A
Right rear skirt vertical surface	PIV-1E-BW-5	-2.25	0.45	PIV-1E-IW-5	6.51	2.13	N/A	N/A
Left front glacis	PIV-1E-BW-6	13.40	4.63	PIV-1E-IW-6	857.64	170.13	N/A	N/A
Left side glacis	PIV-1E-BW-7	20.90	4.77	PIV-1E-IW-7	674.78	134.15	N/A	N/A
Left front skirt	PIV-1E-BW-8	6.51	2.13	PIV-1E-IW-8	24.16	6.56	N/A	N/A
Left middle skirt	PIV-1E-BW-9	0.88	1.71	PIV-1E-IW-9	15.27	3.86	N/A	N/A
Left rear skirt	PIV-1E-BW-10	-2.25	0.45	PIV-1E-IW-10	8.14	5.08	N/A	N/A
Left front hull (top)	PIV-1E-BW-11	-1.38	1.72	PIV-1E-IW-11	279.86	55.88	N/A	N/A
Left front turret (top of GPS)	PIV-1E-BW-12	9.89	2.59	PIV-1E-IW-12	476.64	95.10	N/A	N/A
Left rear turret blow-off panel	PIV-1E-BW-13	-1.62	2.43	PIV-1E-IW-13	231.81	46.62	N/A	N/A
Commander's hatch	PIV-1E-BW-14	1.13	0.23	PIV-1E-IW-14	188.89	38.54	N/A	N/A
Top front turret above breech	PIV-1E-BW-15	2.00	1.75	PIV-1E-IW-15	212.79	43.09	N/A	N/A

PIV-2 Exterior Wipes (μg per 100 cm^2)

	Baseline Wipe			Post-shot				
Specific Features	**Field ID**	**Mass of DU (μg)**	**1 sigma (μg)**	**Field ID**	**Mass of DU (μg) (Group A)**	**1 sigma (μg)**	**Mass of DU (μg) (Group B)**	**1 sigma (μg)**
Floor	PIV-2E-BW-1	457.90	93.38	PIV-2E-IW-1	227.09	47.63	1243.73	250.68
Right front glacis	PIV-2E-BW-2	666.94	135.20	PIV-2E-IW-2	228.58	47.44	473.04	96.30
Right side glacis	PIV-2E-BW-3	8.38	2.93	PIV-2E-IW-3	263.48	53.97	226.19	46.85
Right front skirt vertical surface	PIV-2E-BW-4	32.17	7.67	PIV-2E-IW-4	2137.17	429.53	107.41	23.59
Right rear skirt vertical surface	PIV-2E-BW-5	29.53	6.61	PIV-2E-IW-5	2198.21	441.56	1855.26	372.90
Left front glacis	PIV-2E-BW-6	12.39	4.21	PIV-2E-IW-6	3678.50	737.68	84.86	18.16
Left side glacis	PIV-2E-BW-7	1.62	2.43	PIV-2E-IW-7	172.11	35.73	32.54	7.92
Left front skirt	PIV-2E-BW-8	23.53	6.95	PIV-2E-IW-8	379.78	77.60	413.57	84.25

Left middle skirt	PIV-2E-BW-9	29.04	6.95	PIV-2E-IW-9	1895.89	380.79	1397.98	281.04
Left rear skirt	PIV-2E-BW-10	39.17	8.72	PIV-2E-IW-10	3487.79	699.93	1684.02	338.53
Left front hull (top)	PIV-2E-BW-11	52.44	11.30	PIV-2E-IW-11	4303.19	863.48	418.60	85.53
Left front turret (top of GPS)	PIV-2E-BW-12	1.13	3.41	PIV-2E-IW-12	494.14	99.65	17.78	6.89
Left rear turret blow-off panel	PIV-2E-BW-13	28.67	8.05	PIV-2E-IW-13	3623.05	727.24	150.46	31.61
Commander's hatch	PIV-2E-BW-14	38.43	9.08	PIV-2E-IW-14	1310.16	263.74	93.51	20.23
Top front turret above breech	PIV-2E-BW-15	23.65	5.83	PIV-2E-IW-15	490.67	99.59	137.81	28.80

PIV-3 Exterior Wipes (μg per 100 cm^2)

	Baseline Wipe			Post-shot				
Specific Features	**Field ID**	**Mass of DU (μg)**	**1 sigma (μg)**	**Field ID**	**Mass of DU (μg) (Group A)**	**1 sigma (μg)**	**Mass of DU (μg) (Group B)**	**1 sigma (μg)**
Floor	PIV-3E-BW-1	181.39	37.94	PIV-3E-IW-1	117.29	24.51	161.72	33.33
Right front glacis	PIV-3E-BW-2	171.73	35.31	PIV-3E-IW-2	71.10	15.33	346.34	69.37
Right side glacis	PIV-3E-BW-3	5.25	3.94	PIV-3E-IW-3	389.17	78.39	59.96	13.01
Right front skirt vertical surface	PIV-3E-BW-4	40.43	10.07	PIV-3E-IW-4	231.94	46.83	13.15	5.47
Right rear skirt vertical surface	PIV-3E-BW-5	16.27	5.26	PIV-3E-IW-5	677.39	134.64	41.80	9.25
Left front glacis	PIV-3E-BW-6	10.89	4.37	PIV-3E-IW-6	626.97	124.96	37.56	9.78
Left side glacis	PIV-3E-BW-7	24.78	6.86	PIV-3E-IW-7	18.53	5.80	15.77	3.94
Left front skirt	PIV-3E-BW-8	5.88	4.64	PIV-3E-IW-8	102.40	21.82	30.92	7.96
Left middle skirt	PIV-3E-BW-9	17.77	6.19	PIV-3E-IW-9	1145.79	227.39	1408.31	279.55
Left rear skirt	PIV-3E-BW-10	11.13	4.05	PIV-3E-IW-10	1521.95	301.92	1360.61	270.04
Left front hull (top)	PIV-3E-BW-11	59.83	13.20	PIV-3E-IW-11	2477.58	490.56	140.70	29.53
Left front turret (top of GPS)	PIV-3E-BW-12	5.88	4.64	PIV-3E-IW-12	118.66	24.17	48.19	11.20
Left rear turret blow-off panel	PIV-3E-BW-13	12.26	4.18	PIV-3E-IW-13	1555.49	308.52	88.12	18.93
Commander's hatch	PIV-3E-BW-14	37.42	8.65	PIV-3E-IW-14	510.95	102.15	144.81	29.26
Top front turret above breech	PIV-3E-BW-15	17.14	5.63	PIV-3E-IW-15	487.90	97.26	19.78	5.18

PIV-4 Exterior Wipes (μg per 100 cm^2)

	Baseline Wipe			Post-shot				
Specific Features	**Field ID**	**Mass of DU (μg)**	**1 sigma (μg)**	**Field ID**	**Mass of DU (μg) (Group A)**	**1 sigma (μg)**	**Mass of DU (μg) (Group B)**	**1 sigma (μg)**
Floor	PIV-4E-BW-1	113.43	25.15	PIV-4E-IW-1	423.97	85.66	494.83	100.21
Right front glacis	PIV-4E-BW-2	214.29	43.81	PIV-4E-IW-2	253.88	52.65	582.27	117.29
Right side glacis	PIV-4E-BW-3	2.25	0.45	PIV-4E-IW-3	0.57	3.48	5.23	3.19
Right front skirt vertical surface	PIV-4E-BW-4	80.11	17.08	PIV-4E-IW-4	451.05	91.45	1261.61	252.46
Right rear skirt vertical surface	PIV-4E-BW-5	59.46	13.00	PIV-4E-IW-5	67.03	14.78	106.99	23.14
Left front glacis	PIV-4E-BW-6	45.94	10.61	PIV-4E-IW-6	61.23	13.63	86.94	18.89
Left side glacis	PIV-4E-BW-7	0.88	1.71	PIV-4E-IW-7	27.31	9.01	29.05	8.36
Left front skirt	PIV-4E-BW-8	26.91	6.57	PIV-4E-IW-8	1294.49	259.78	605.51	121.49

PIV-4 Exterior Wipes (μg per 100 cm^2)								
	Baseline Wipe			Post-shot				
Specific Features	Field ID	Mass of DU (μg)	1 sigma (μg)	Field ID	Mass of DU (μg) (Group A)	1 sigma (μg)	Mass of DU (μg) (Group B)	1 sigma (μg)
Left middle skirt	PIV-4E-BW-9	67.09	14.49	PIV-4E-IW-9	268.17	54.89	595.60	119.86
Left rear skirt	PIV-4E-BW-10	29.66	6.60	PIV-4E-IW-10	122.76	25.95	419.99	84.88
Left front hull (top)	PIV-4E-BW-11	72.97	15.48	PIV-4E-IW-11	1077.05	216.58	213.17	43.55
Left front turret (top of GPS)	PIV-4E-BW-12	19.53	4.88	PIV-4E-IW-12	302.67	61.44	55.60	12.96
Left rear turret blow-off panel	PIV-4E-BW-13	55.70	11.96	PIV-4E-IW-13	382.45	77.26	587.76	118.30
Commander's hatch	PIV-4E-BW-14	3.51	3.47	PIV-4E-IW-14	243.94	50.06	556.32	112.22
Top front turret above breech	PIV-4E-BW-15	33.92	7.56	PIV-4E-IW-15	728.98	146.56	727.34	145.55

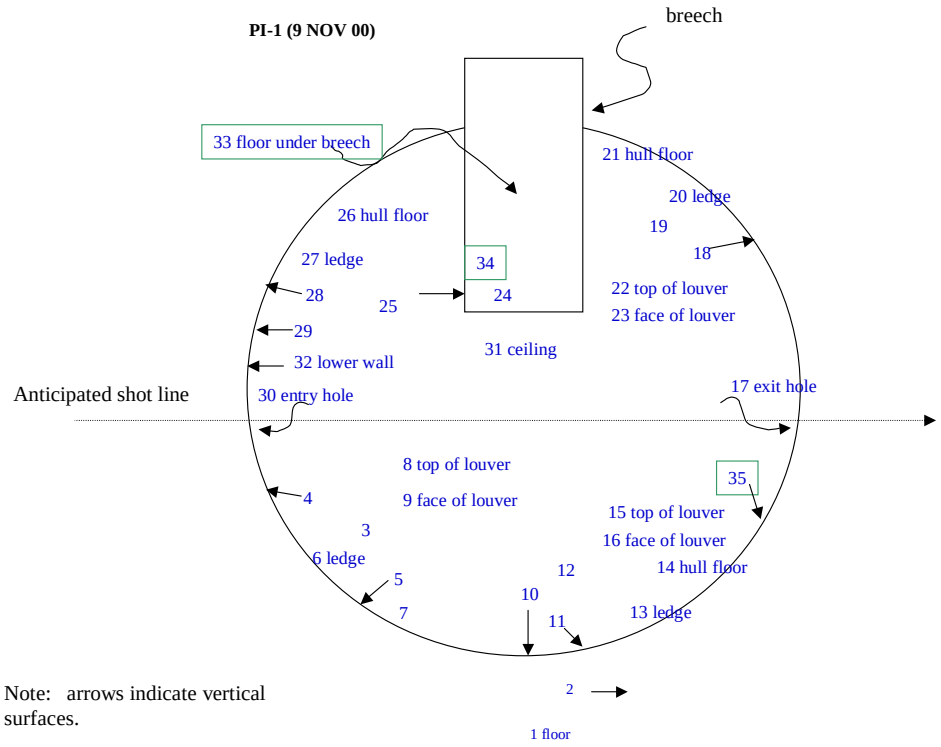

Figure F.1. PI-1 Interior Survey Locations

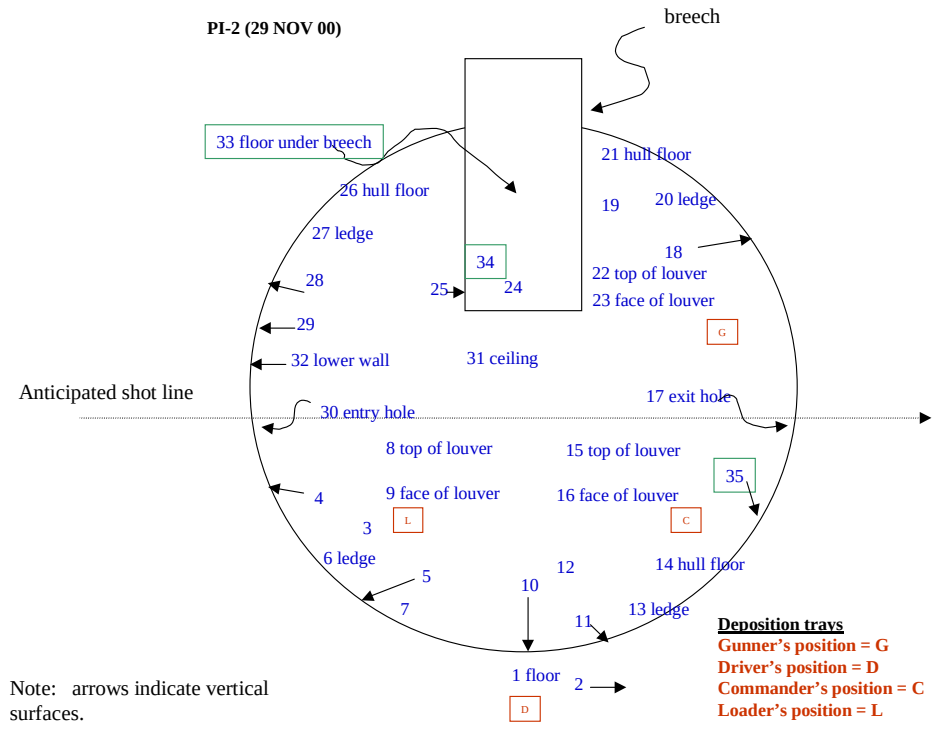

Figure F.2. PI-2 Interior Survey Locations

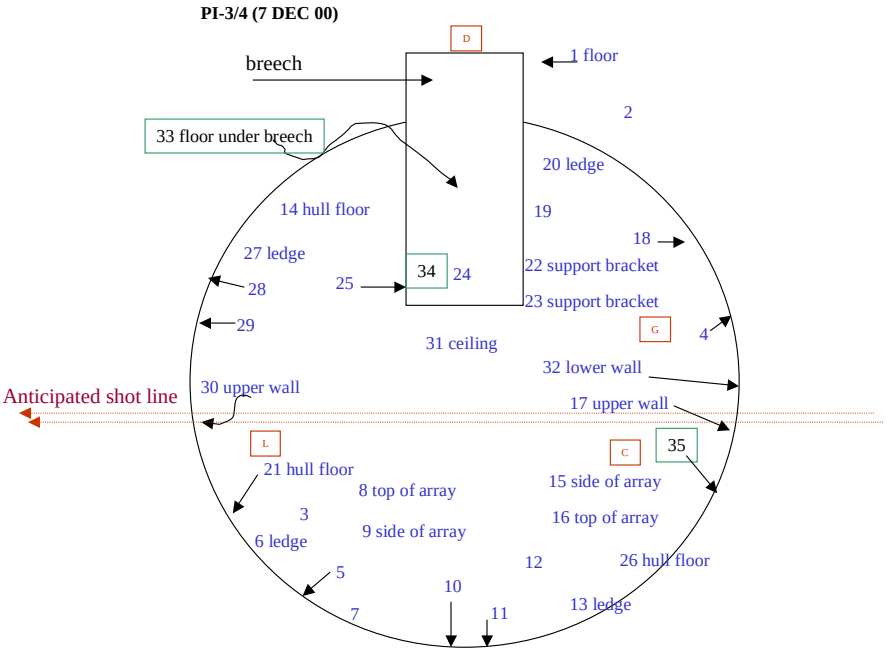

Note: arrows indicate vertical surfaces.

Deposition trays
Gunner's position = G
Driver's position = D
Commander's position = C
Loader's position = L

Figure F.3. PI-3/4 Interior Survey Locations

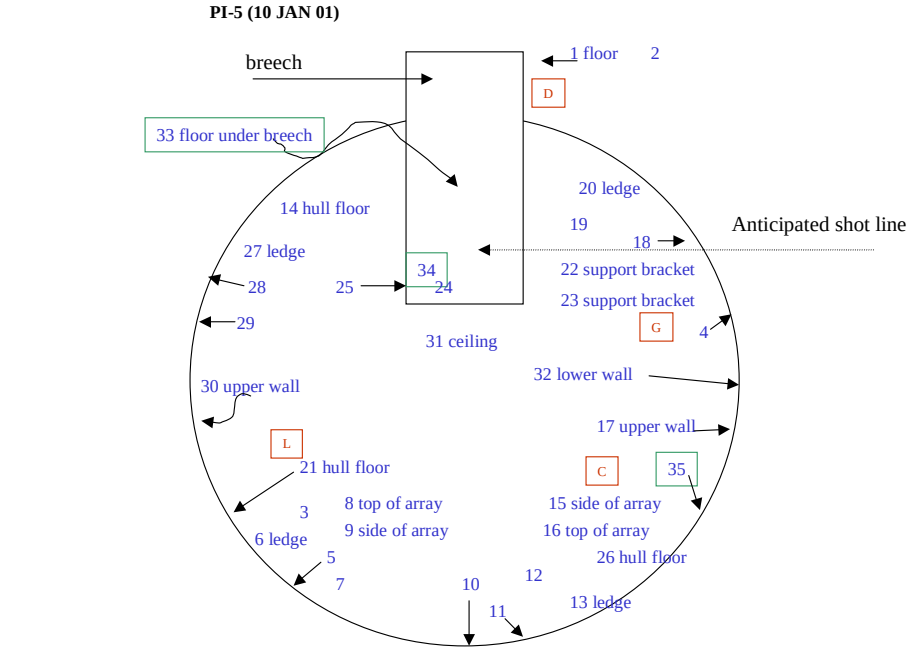

Note: arrows indicate vertical surfaces.

Deposition trays
Gunner's position = G
Driver's position = D
Commander's position = C
Loader's position = L

Figure F.4. PI-5 Interior Survey Locations

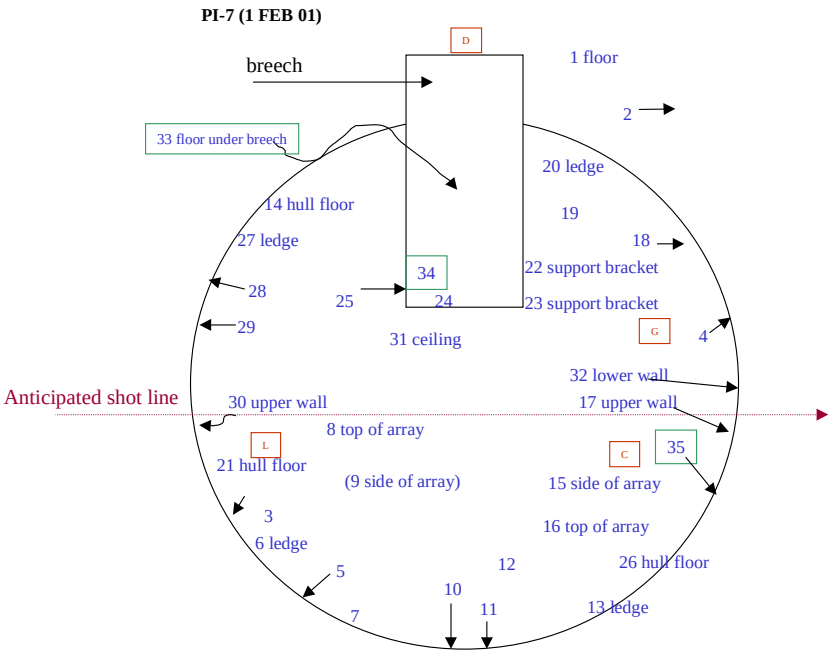

Note: arrows indicate vertical surfaces.

Deposition trays
Gunner's position = G
Driver's position = D
Commander's position = C
Loader's position = L

Figure F.5. PI-7 Interior Survey Locations

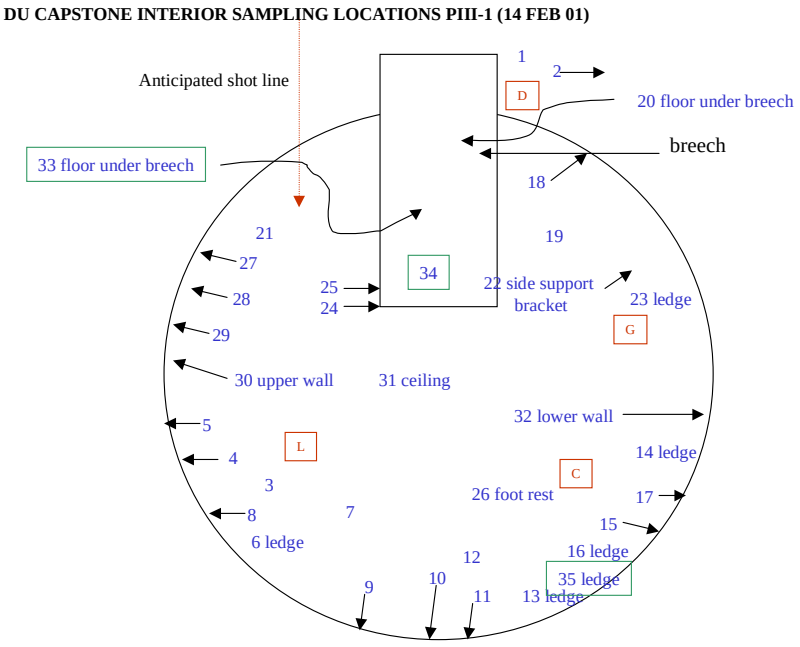

Note: arrows indicate vertical surfaces.
Mark location of discretionary samples

Deposition trays
Gunner's position = G
Driver's position = D
Commander's position = C
Loader's position = L

Figure F.6. PIII-1 Interior Survey Locations

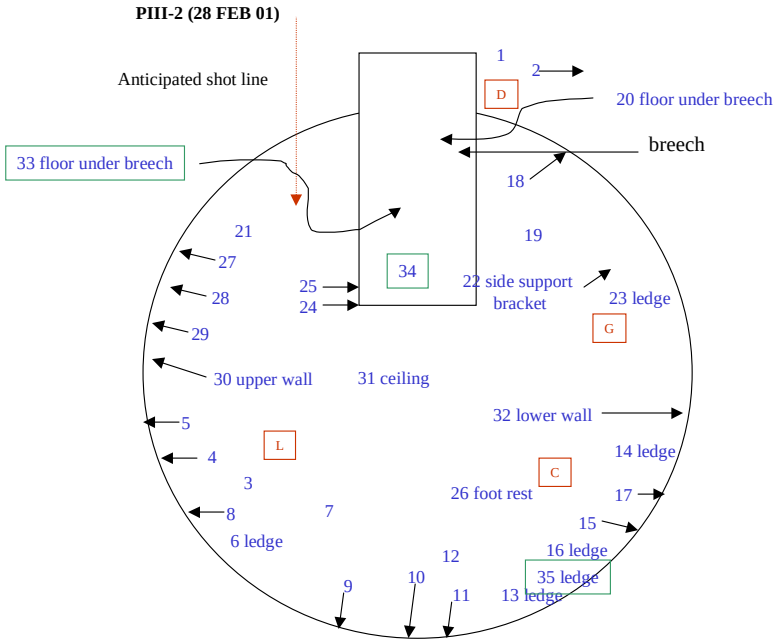

Note: arrows indicate vertical surfaces.

Deposition trays
Gunner's position = G
Driver's position = D
Commander's position = C
Loader's position = L

Figure F.7. PIII-2 Interior Survey Locations

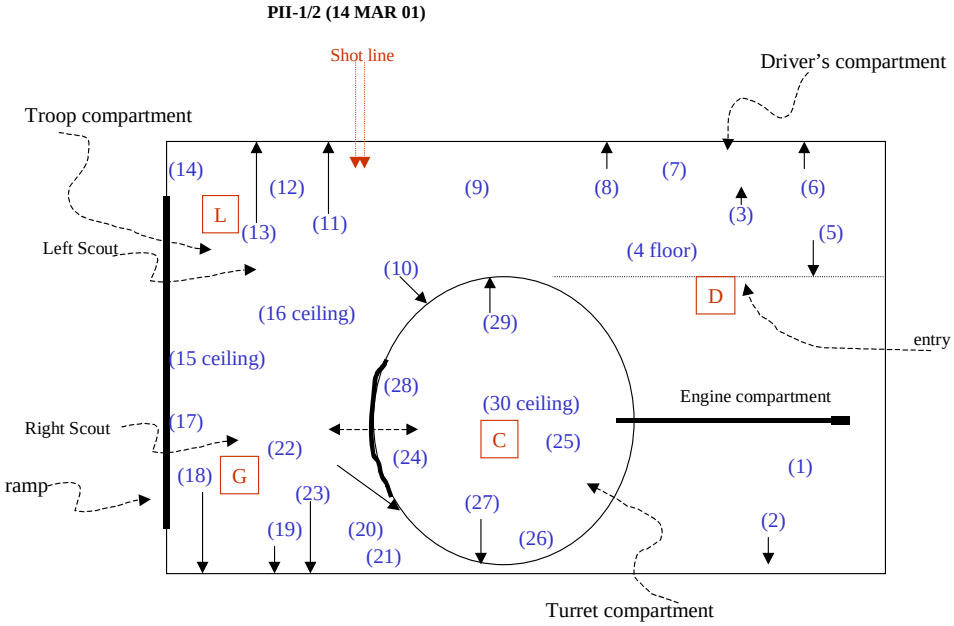

Note: Arrows indicate vertical surfaces.

Deposition trays
Gunner's position (right Scout) = G
Driver's position = D
Commander's position = C
Loader's position (left Scout) = L

Figure F.8. PII-1/2 Interior Survey Locations

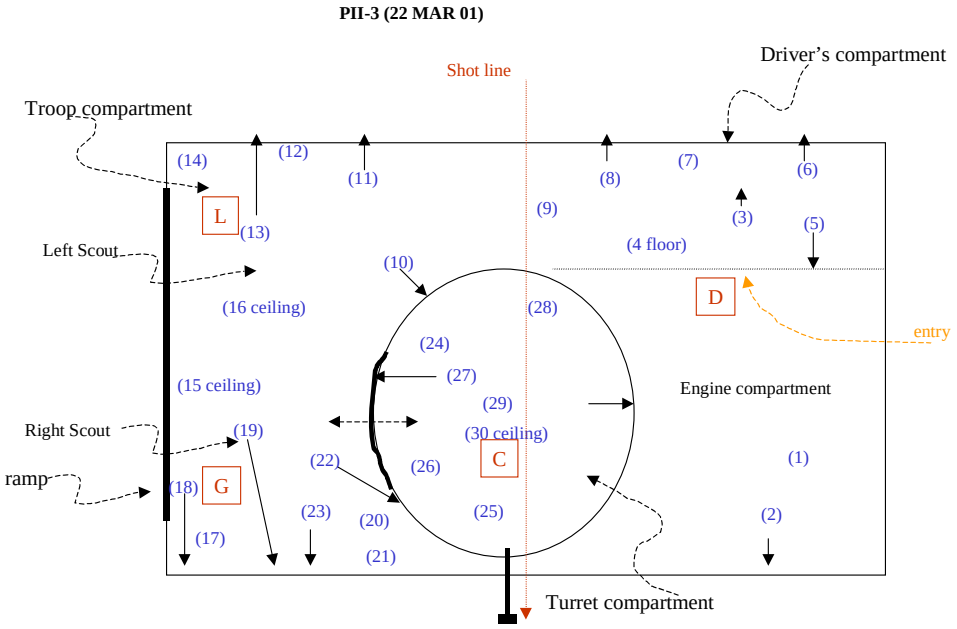

Note: Arrows indicate vertical surfaces. Post-shot values are in green and are reported in DPM per 100 sq cm

Figure F.9. PII-3 Interior Survey Locations

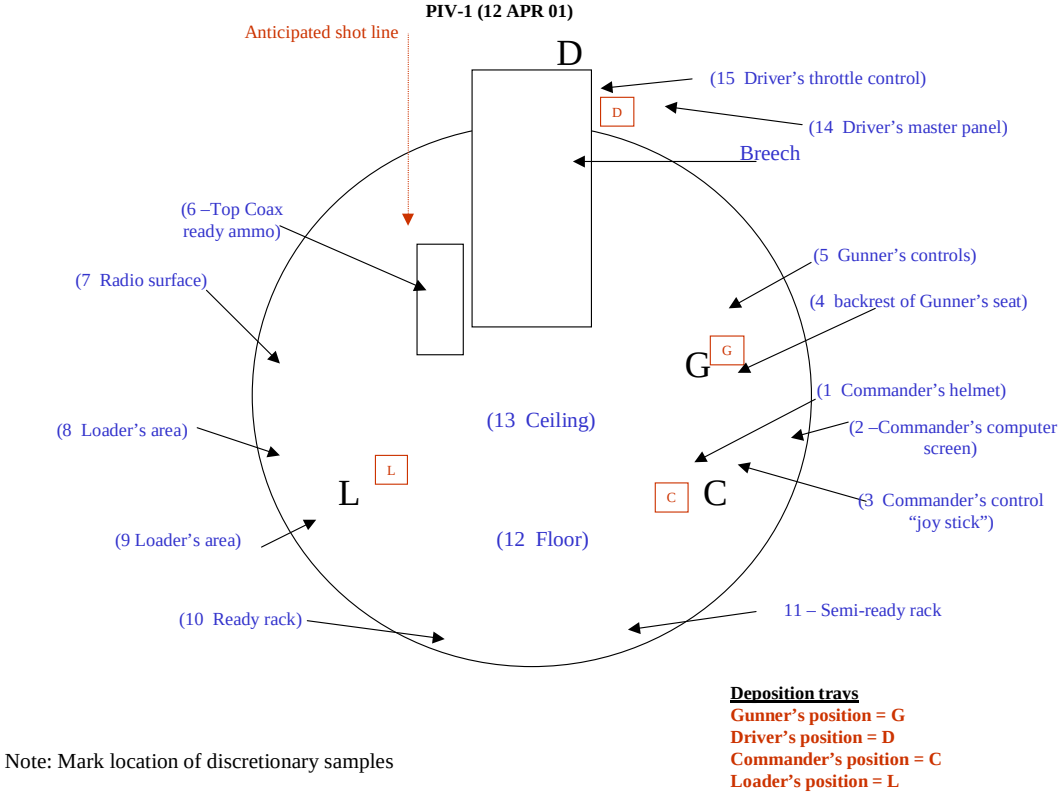

Note: Mark location of discretionary samples

Figure F.10. PIV-1 Interior Survey Locations

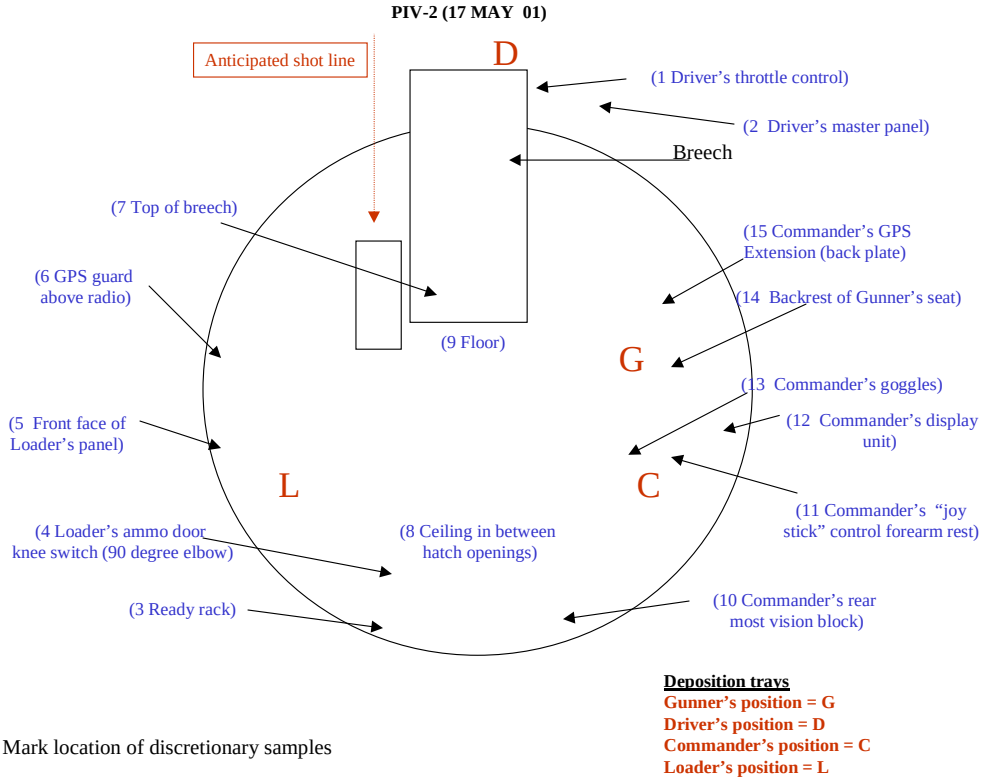

Note: Mark location of discretionary samples

Figure F.11. PIV-2 Interior Survey Locations

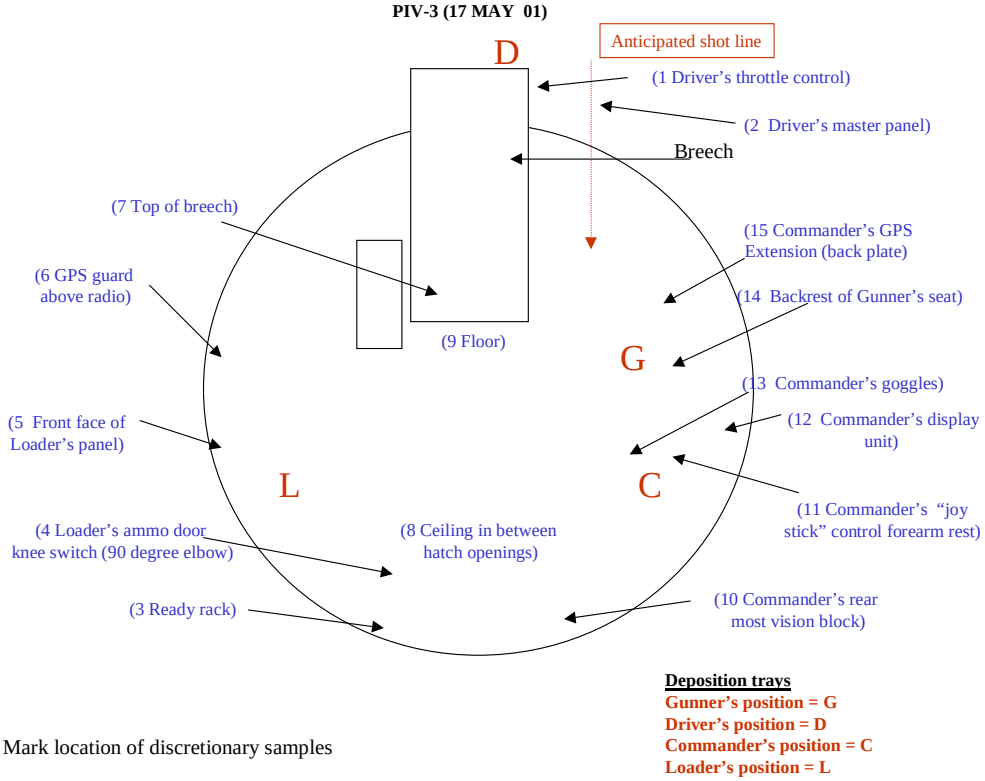

Note: Mark location of discretionary samples

Figure F.12. PIV-3 Interior Survey Locations

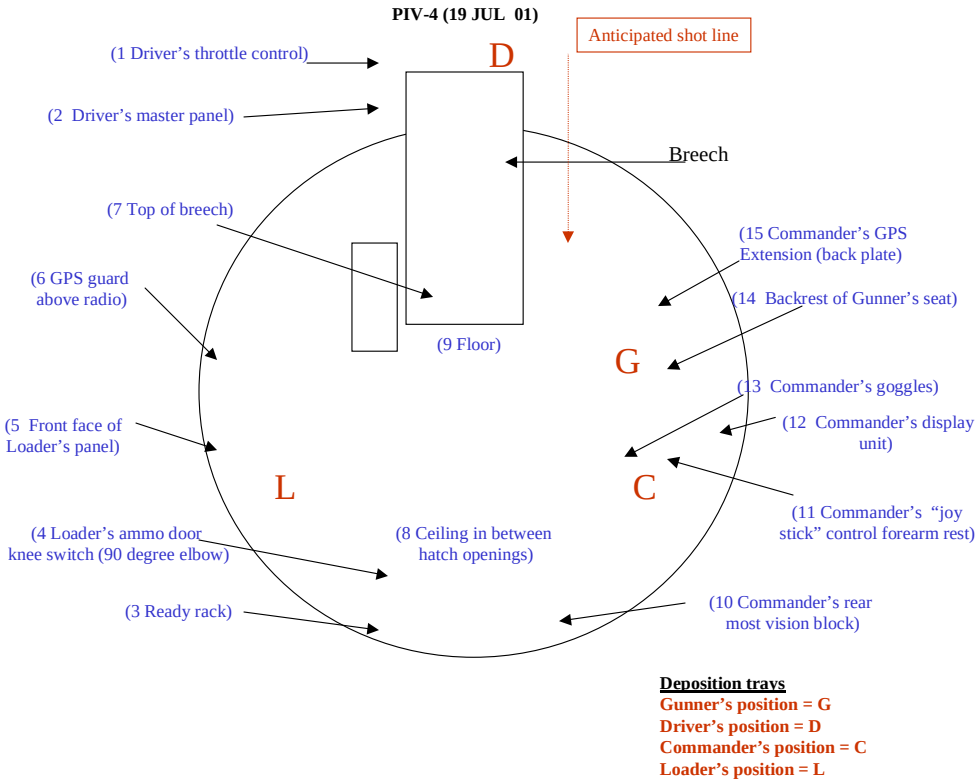

Figure F.13. PIV-4 Interior Survey Locations

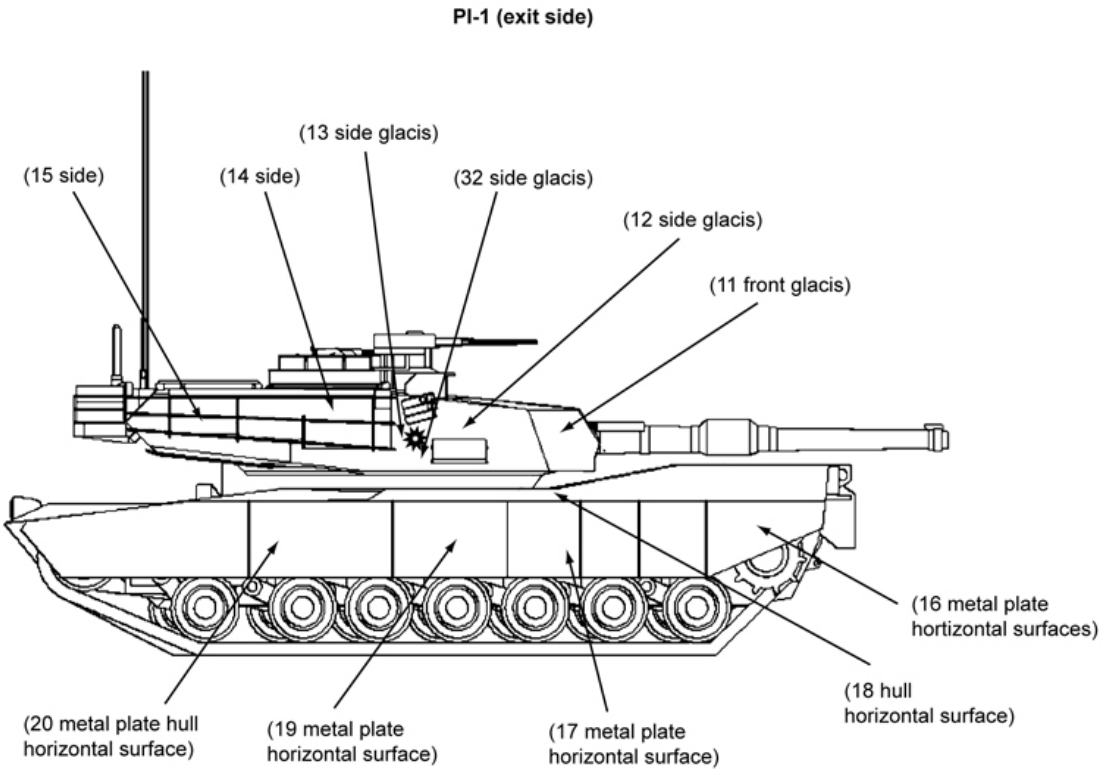

Figure F.14. PI-1 Exterior Survey, Exit Side

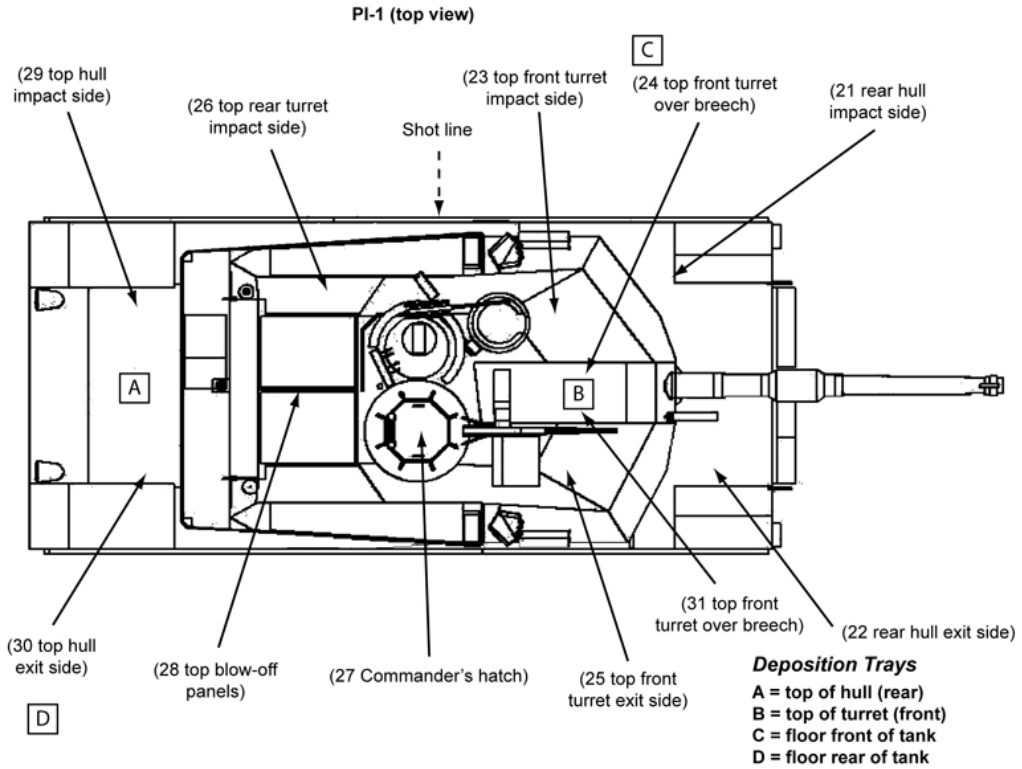

Figure F.15. PI-1 Exterior Survey, Top View

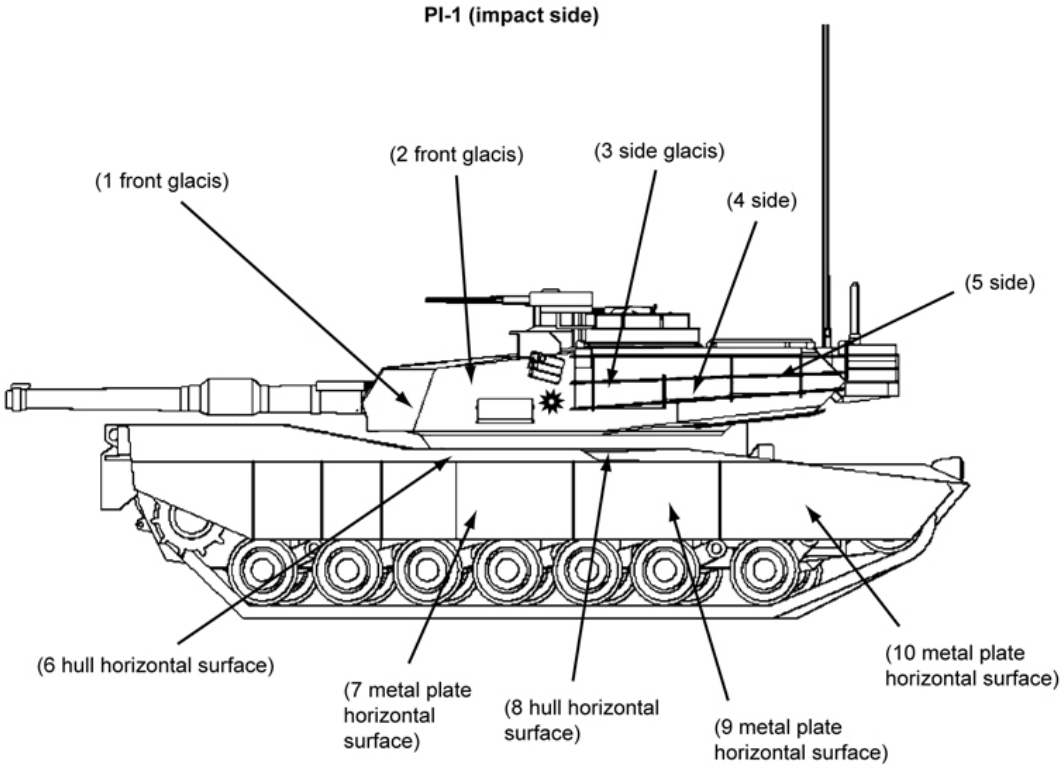

Figure F.16. PI-1 Exterior Survey, Impact Side

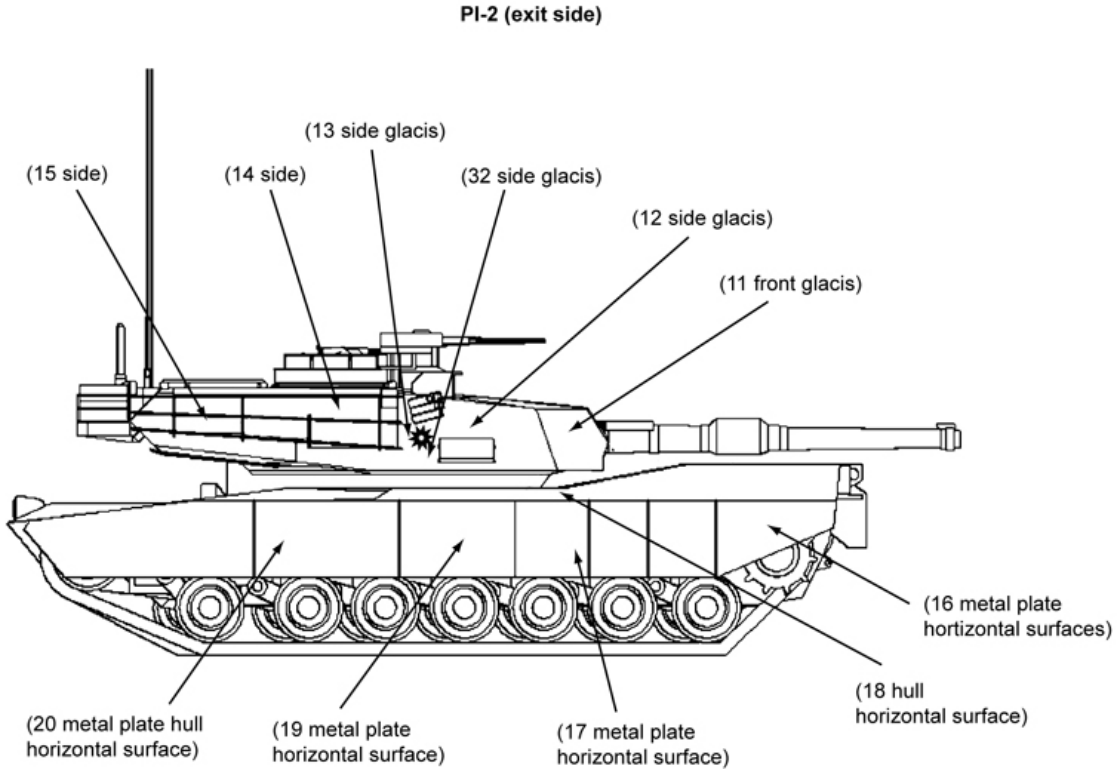

Figure F.17. PI-2 Exterior Survey, Exit Side

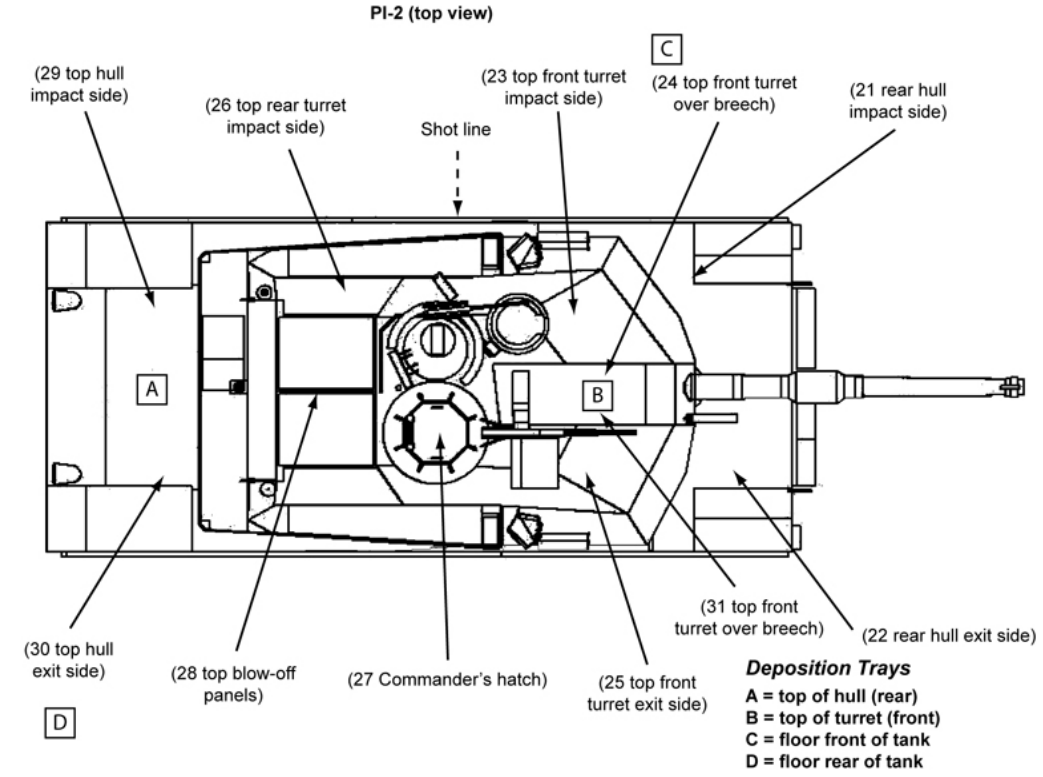

Figure F.18. PI-2 Exterior Survey, Top View

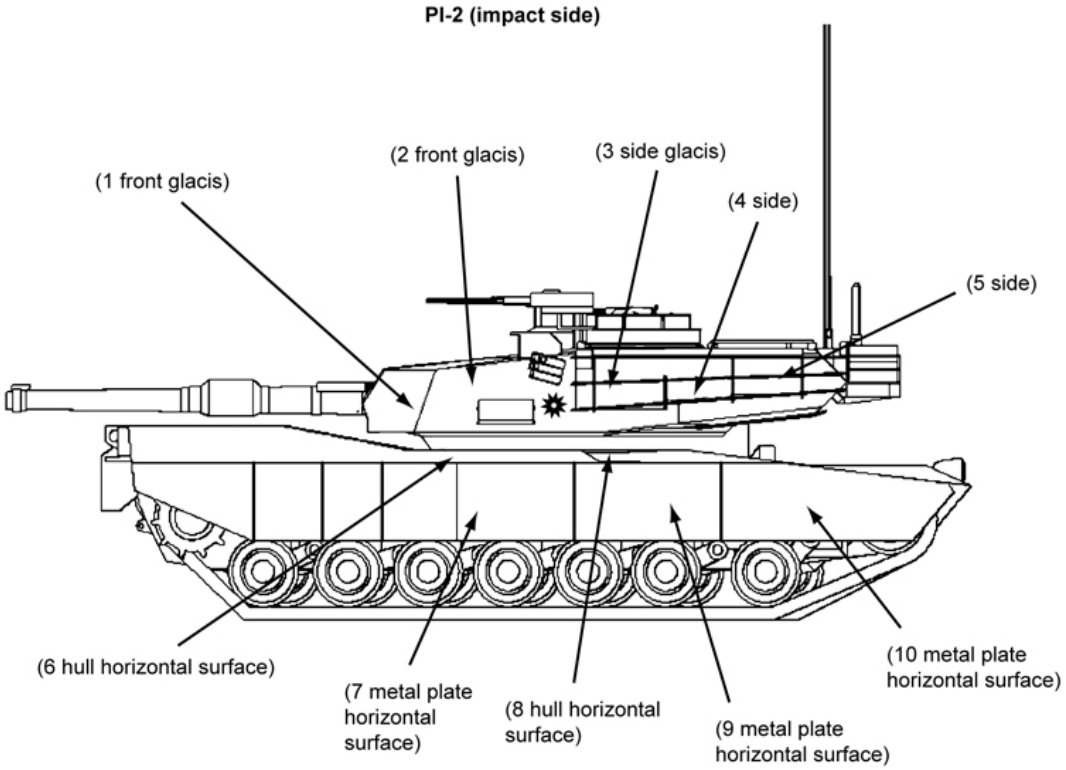

Figure F.19. PI-2 Exterior Survey, Impact Side

Figure F.20. PI-3/4 Exterior Survey, Impact Side

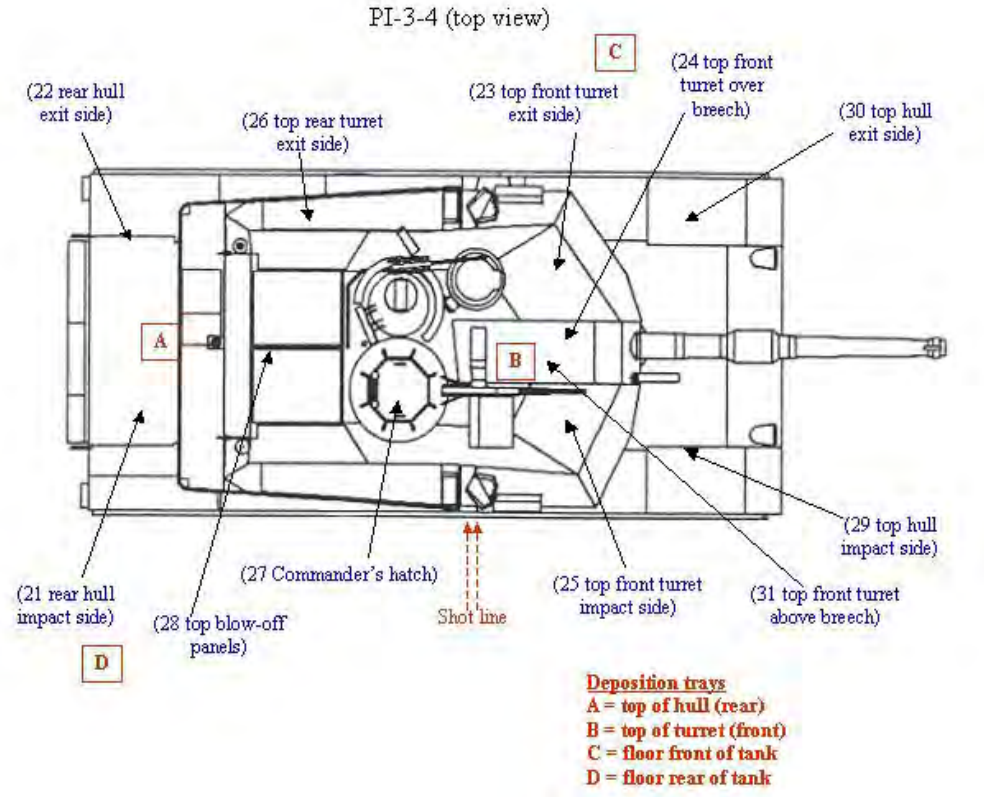

Figure F.21. PI-3/4 Exterior Survey, Top View

Figure F.22. PI-3/4 Exterior Survey, Exit Side

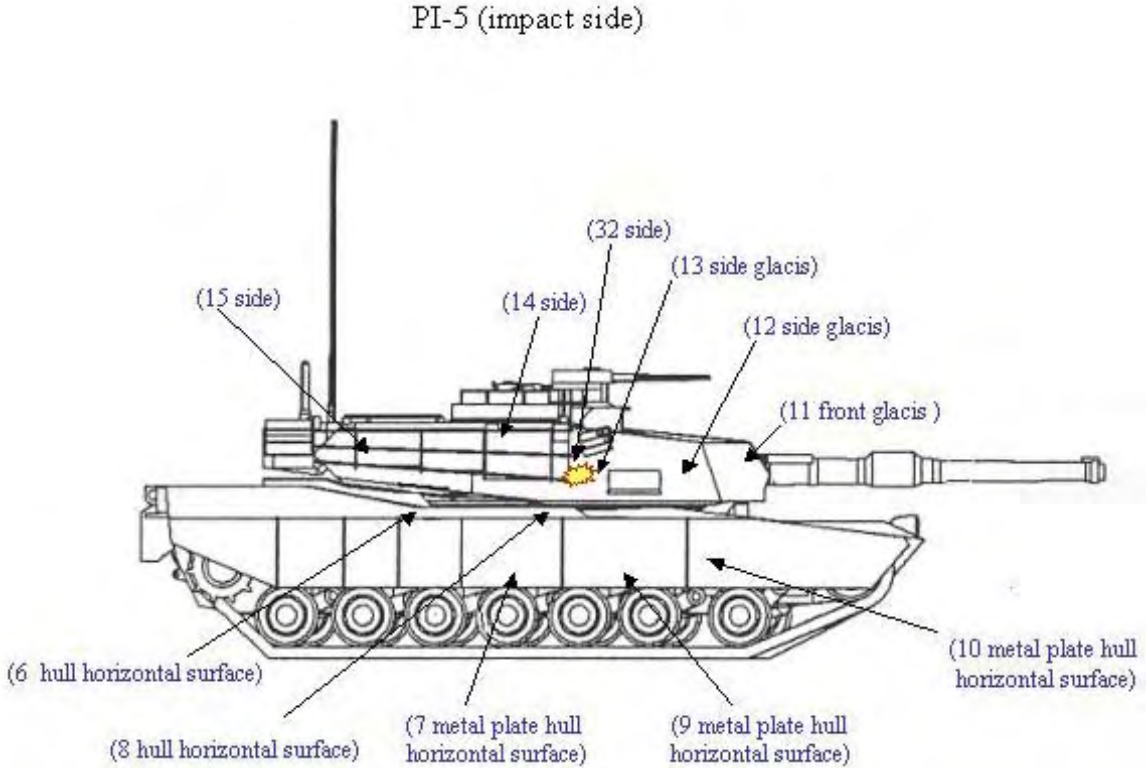

Figure F.23. PI-5 Exterior Survey, Impact Side

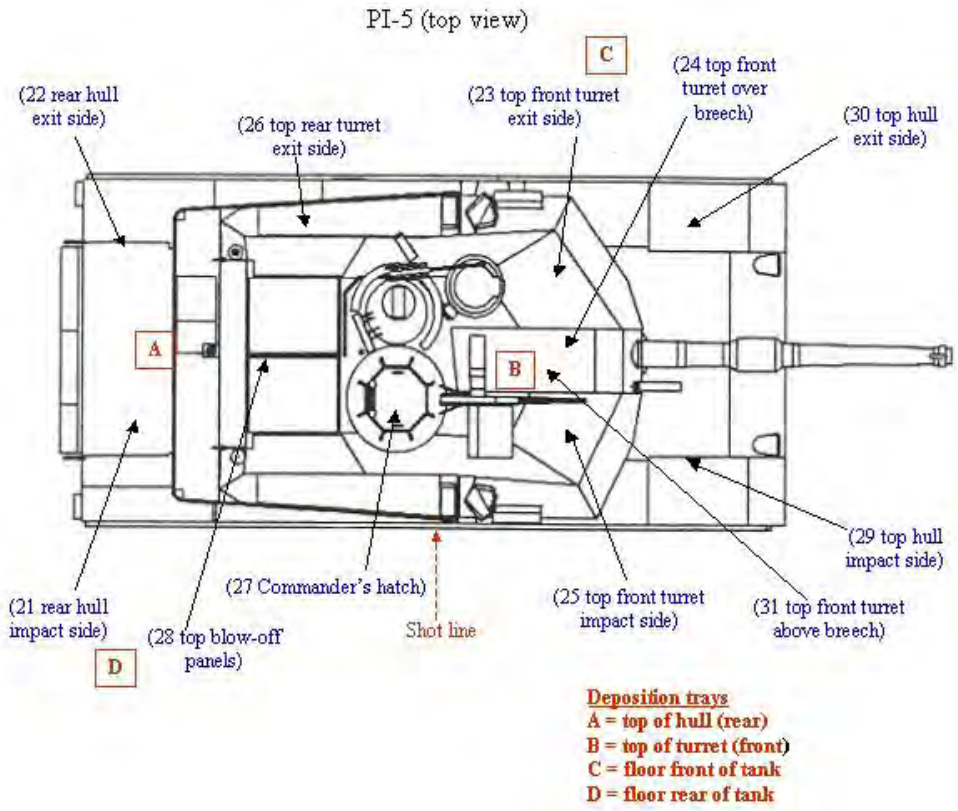

Figure F.24. PI-5 Exterior Survey, Top View

Figure F.25. PI-5 Exterior Survey, Exit Side

Figure F.26. PI-6 Exterior Survey, Exit Side

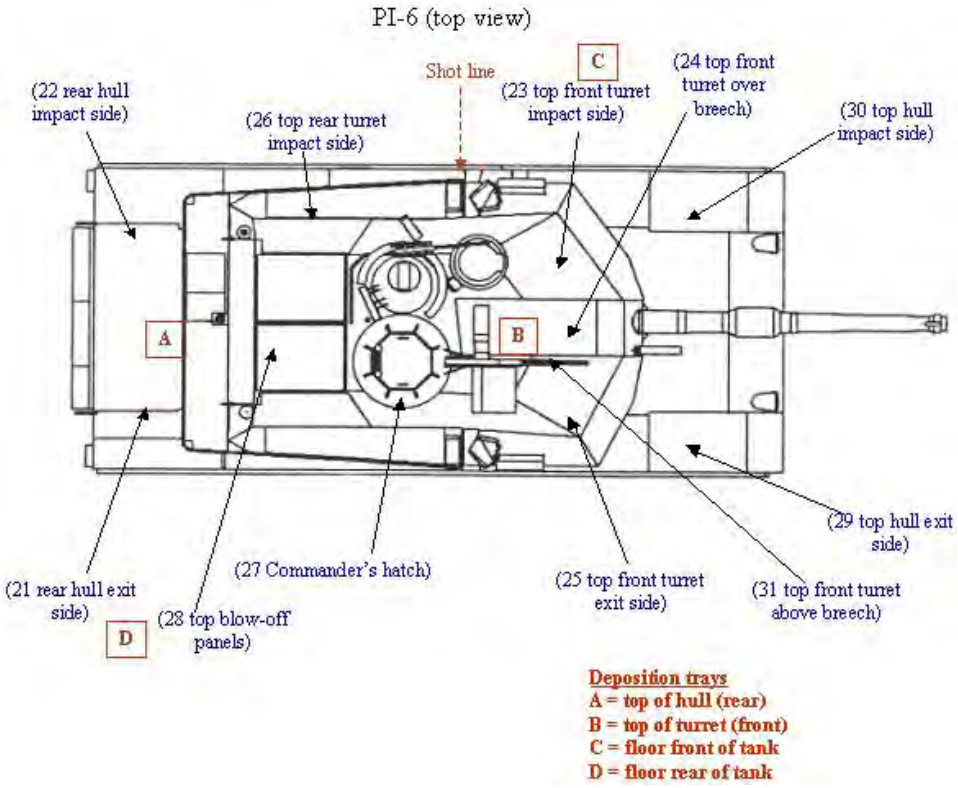

Figure F.27. PI-6 Exterior Survey, Top View

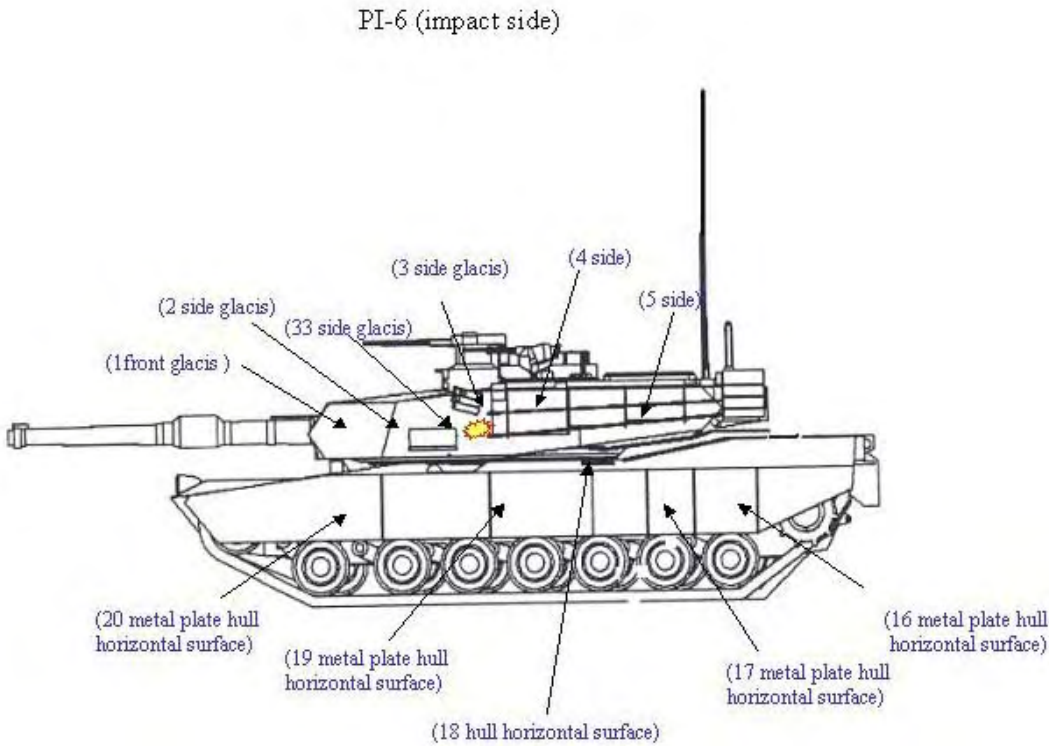

Figure F.28. PI-6 Exterior Survey, Impact Side

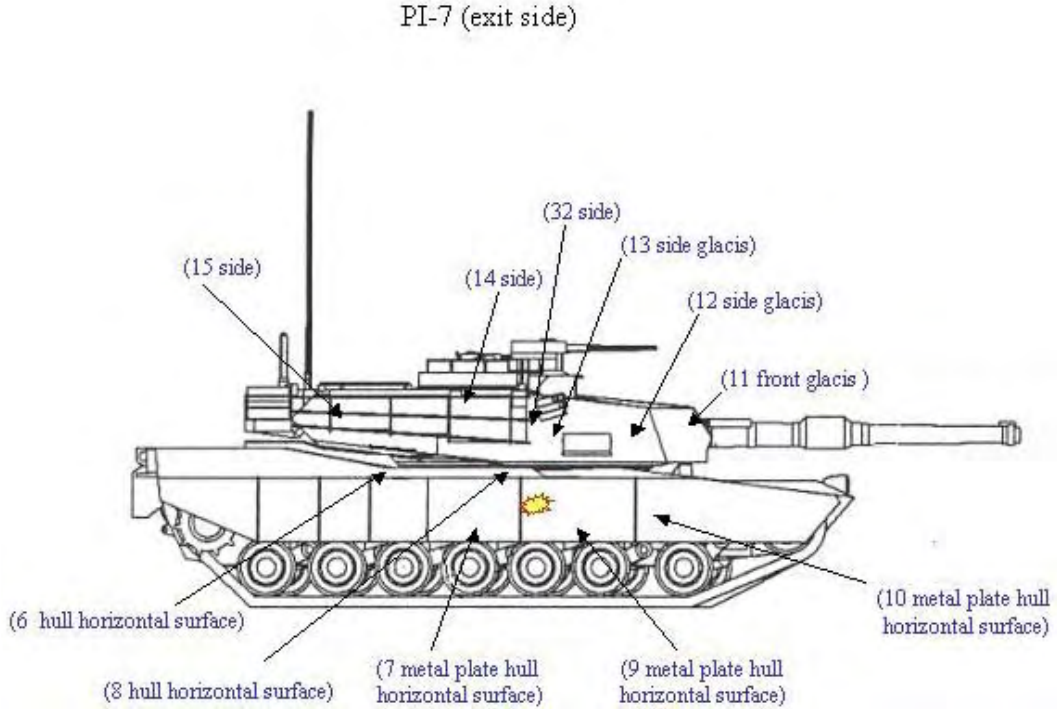

Figure F.29. PI-7 Exterior Survey, Exit Side

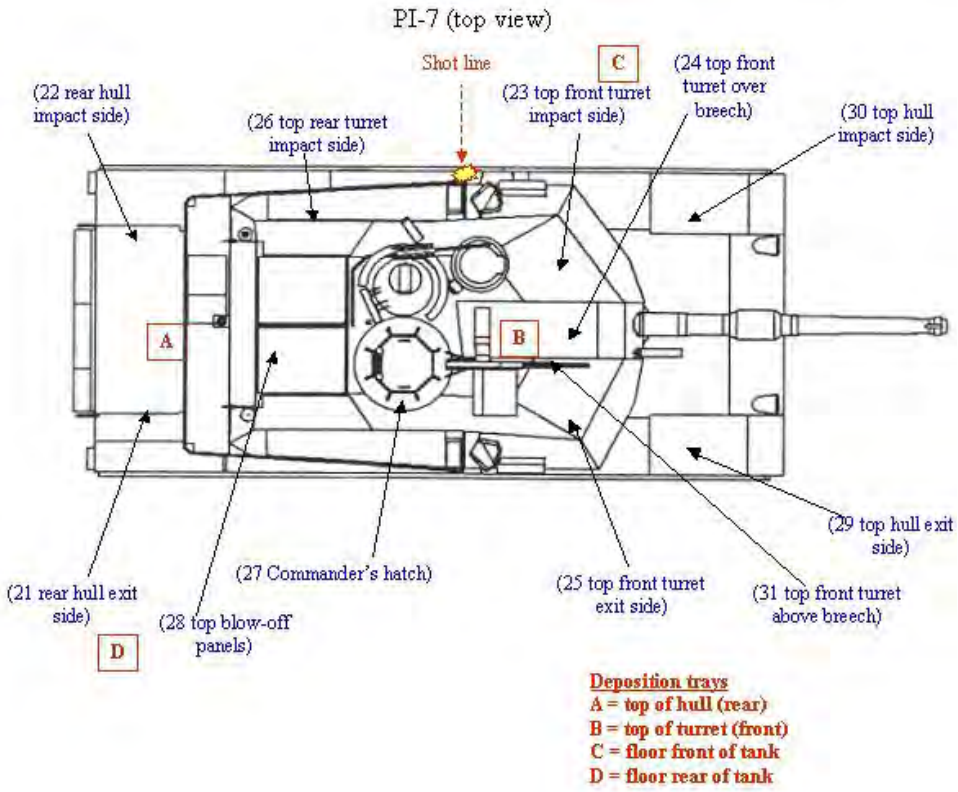

Figure F.30. PI-7 Exterior Survey, Top View

Figure F.31. PI-7 Exterior Survey, Impact Side

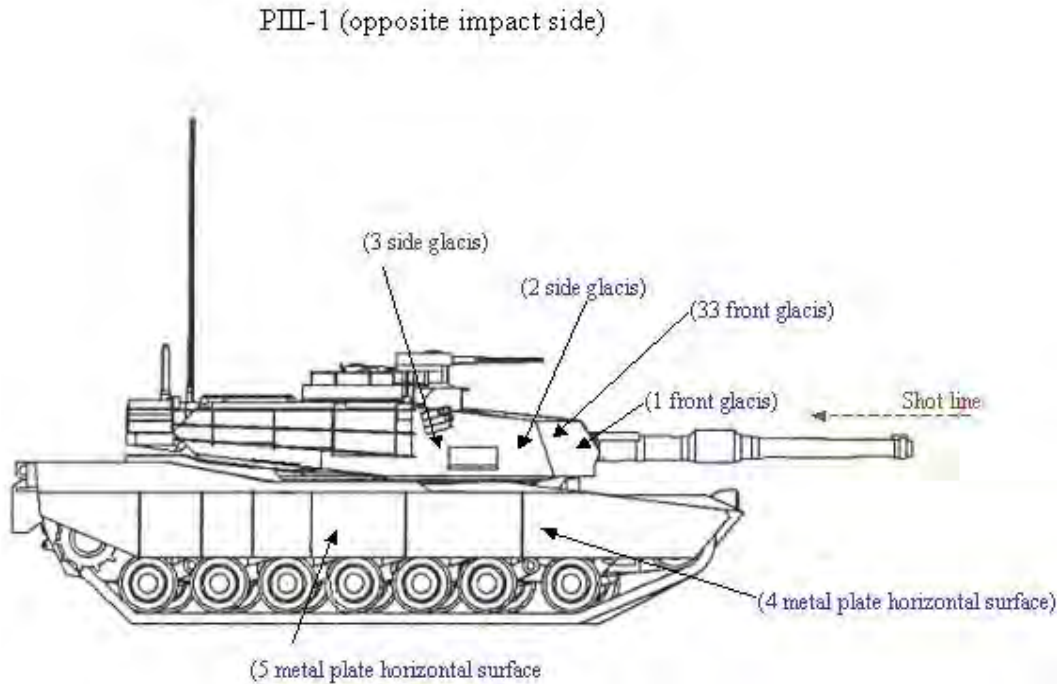

Figure F.32. PIII-1 Exterior Survey, Side Opposite Impact

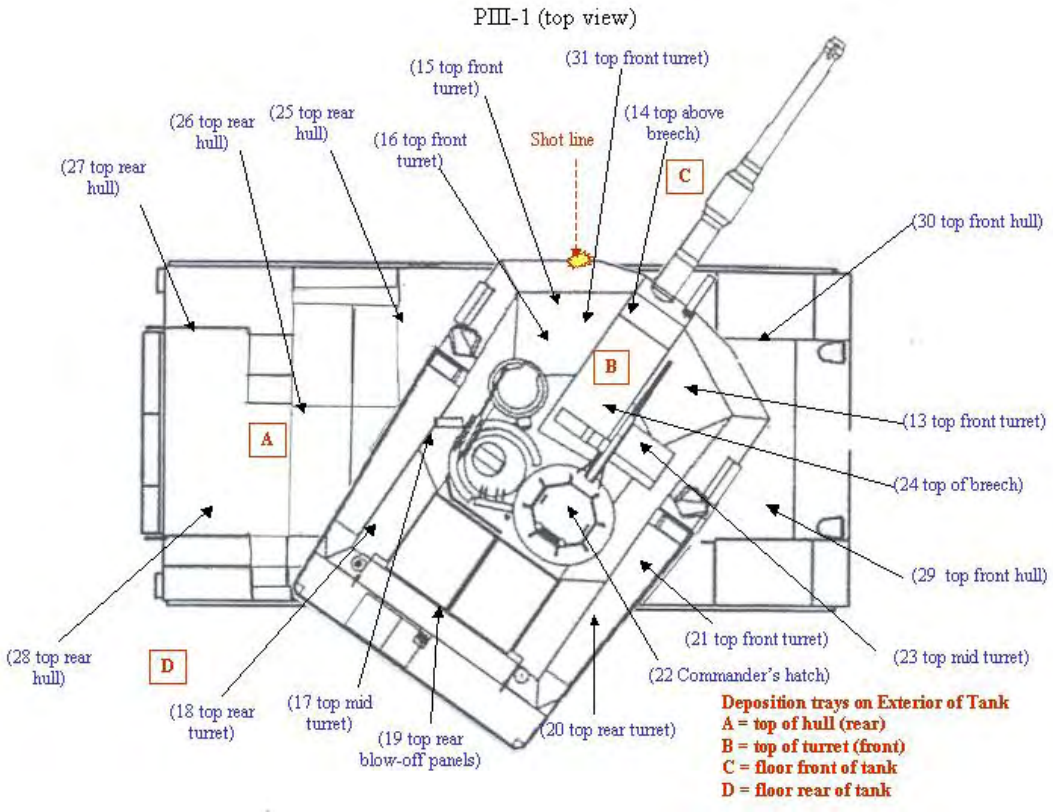

Figure F.33. PIII-1 Exterior Survey, Top View

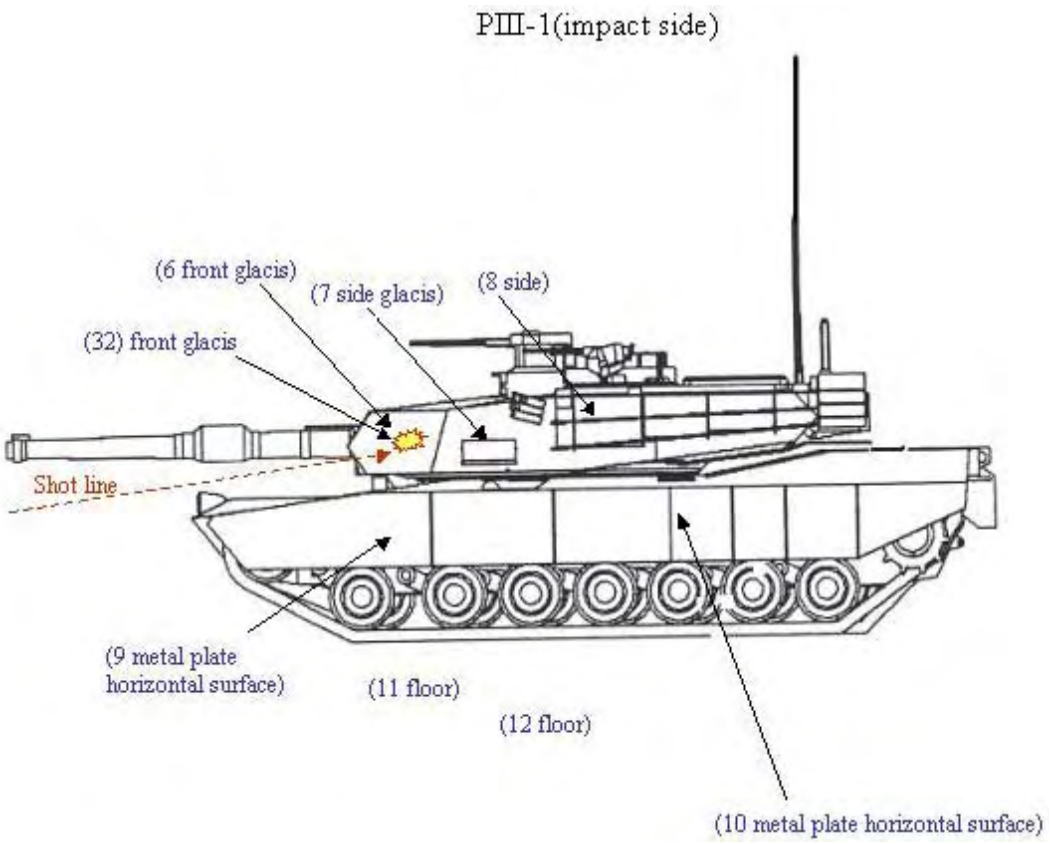

Figure F.34. PIII-1 Exterior Survey, Impact Side

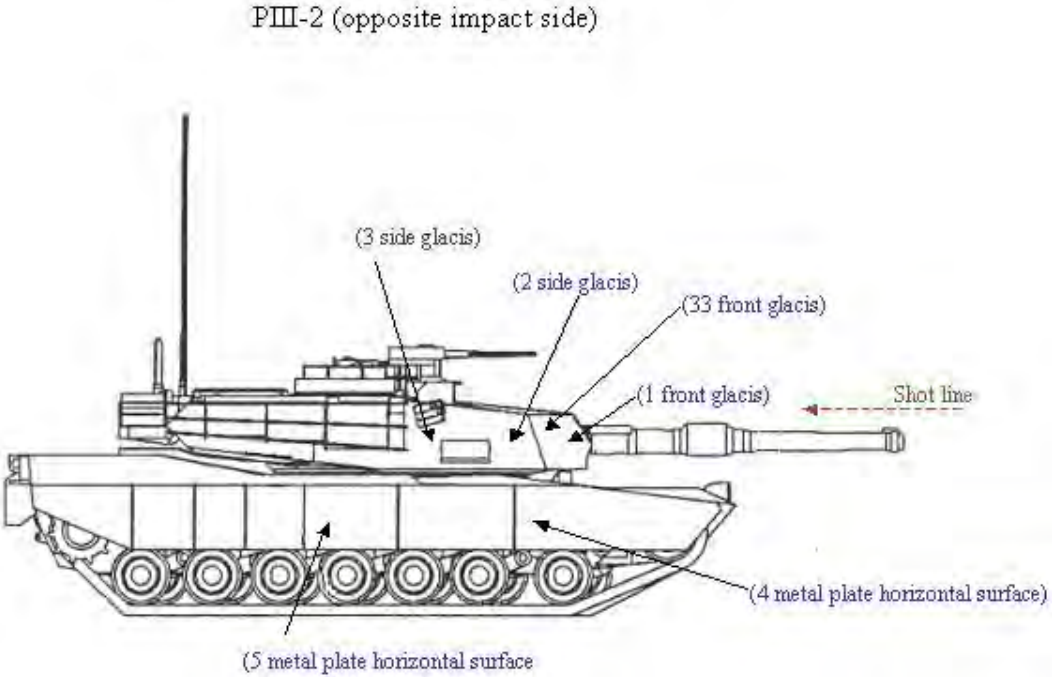

Figure F.35. PIII-2 Exterior Survey, Side Opposite Impact

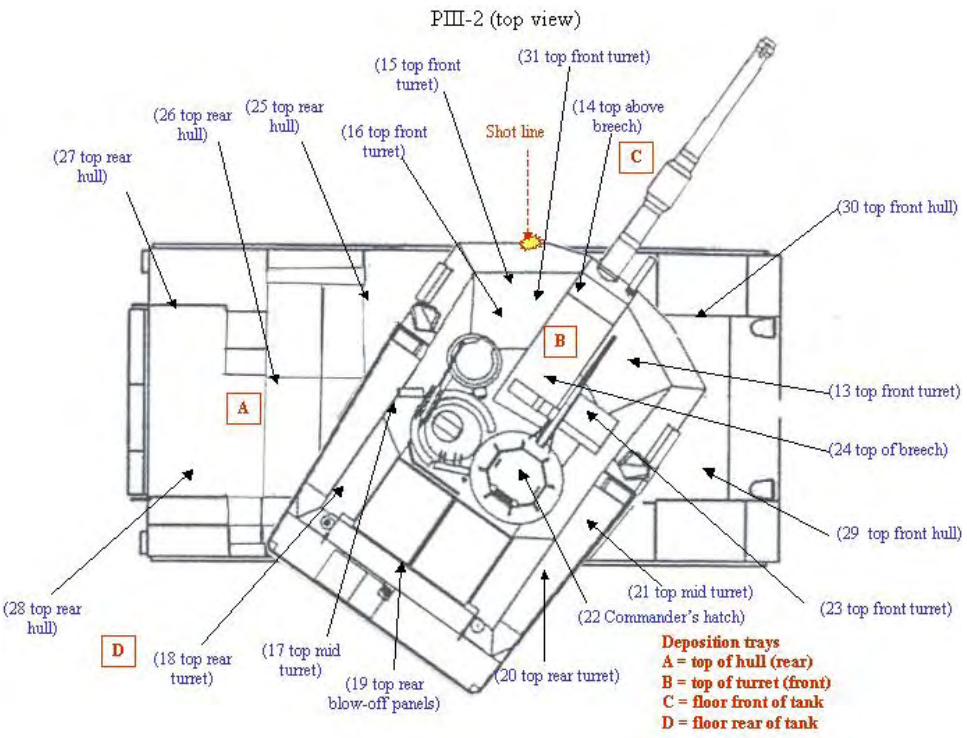

Figure F.36. PIII-2 Exterior Survey, Top View

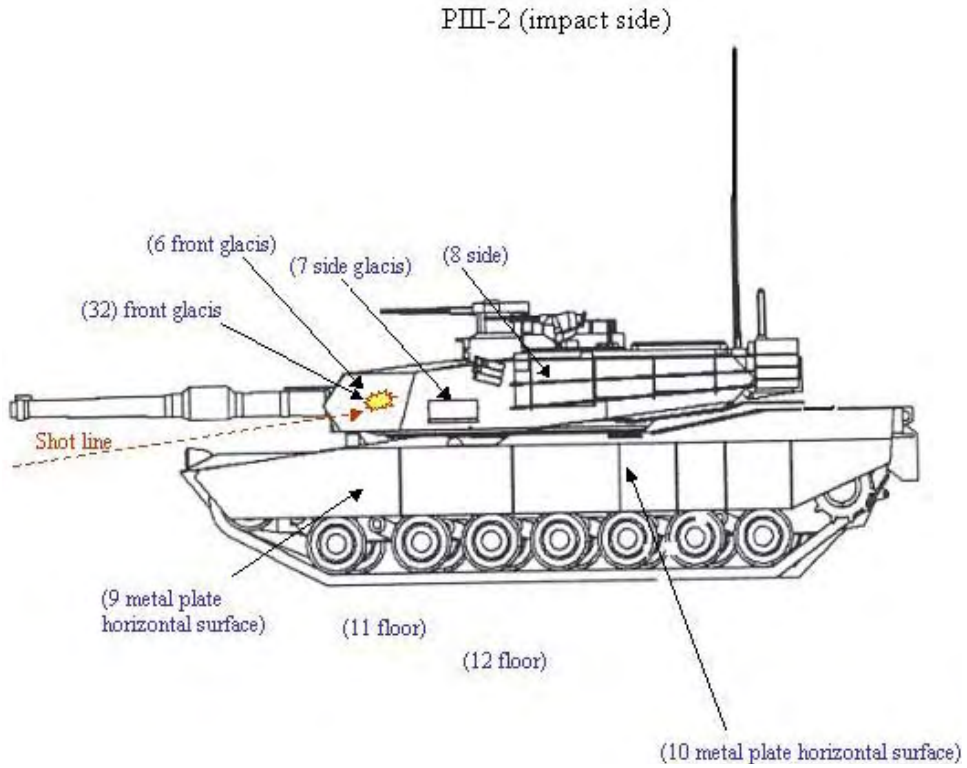

Figure F.37. PIII-2 Exterior Survey, Impact Side

Figure F.38. PII-1/2 Exterior Survey, Impact Side

Figure F.39. PII-1/2 Exterior Survey, Exit Side

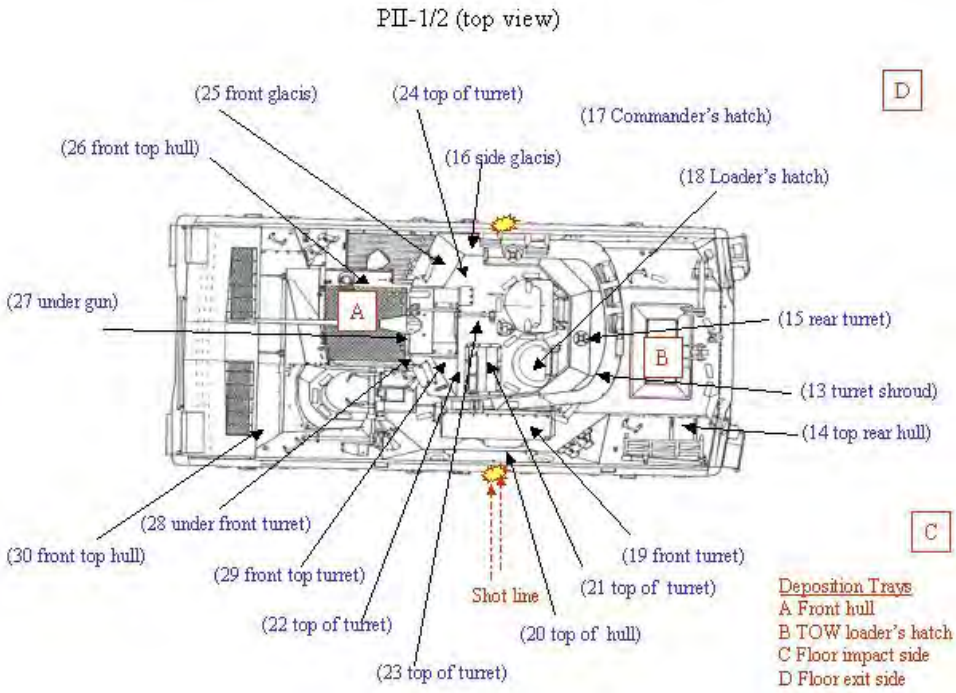

Figure F.40. PII-1/2 Exterior Survey, Top View

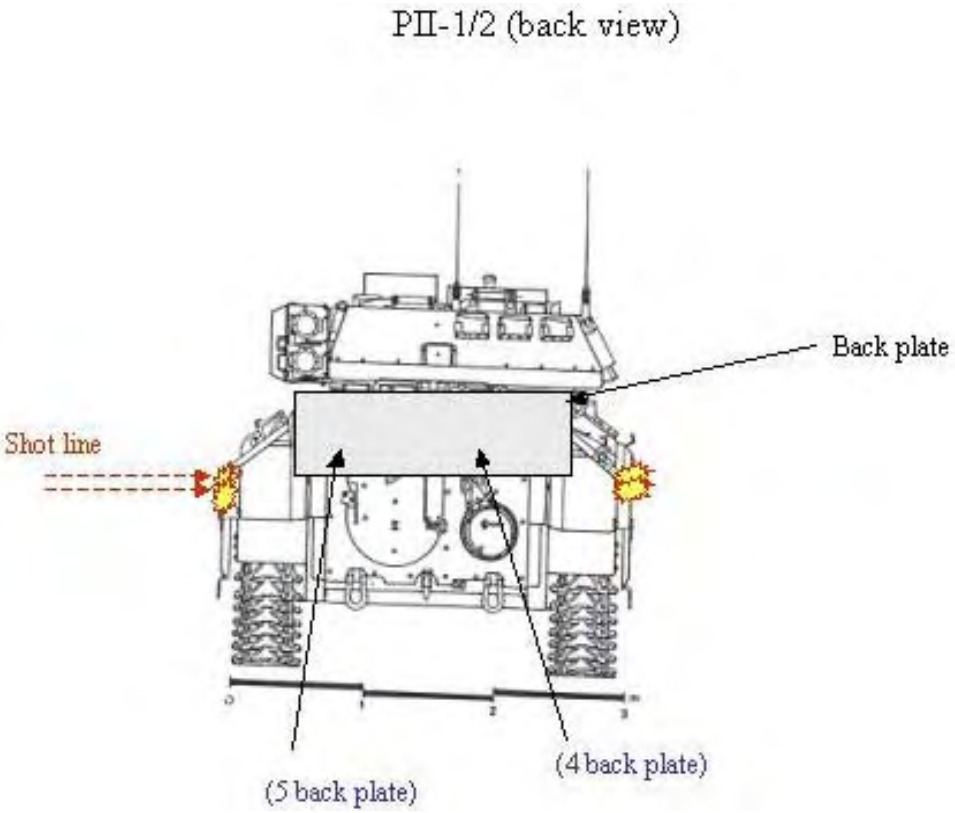

Figure F.41. PII-1/2 Exterior Survey, Back View

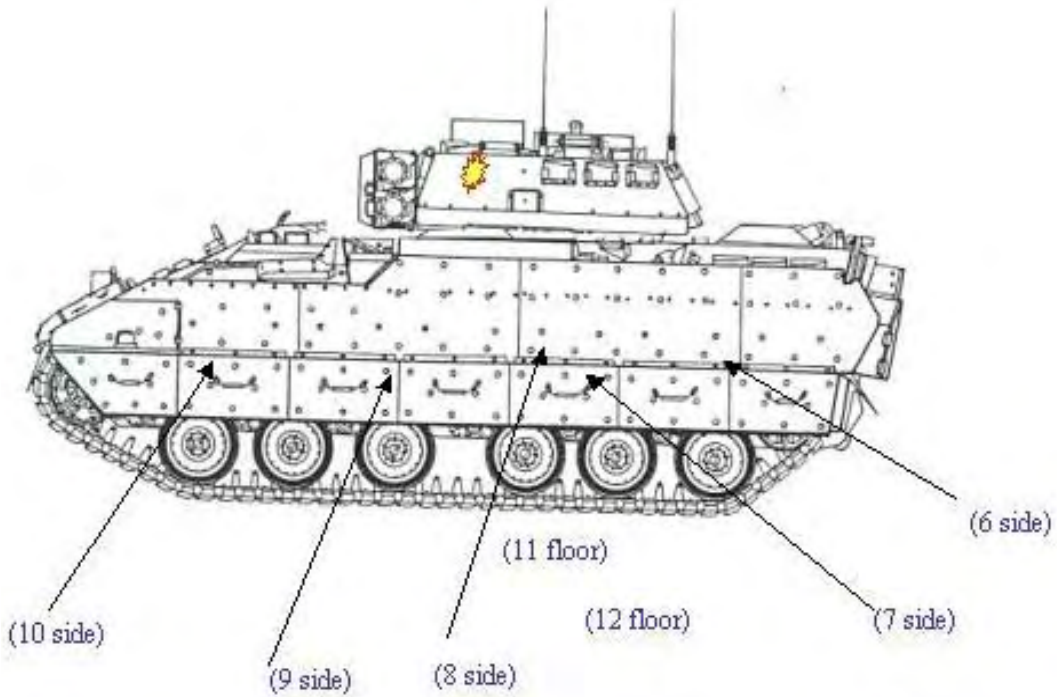

Figure F.42. PII-3 Exterior Survey, Impact Side

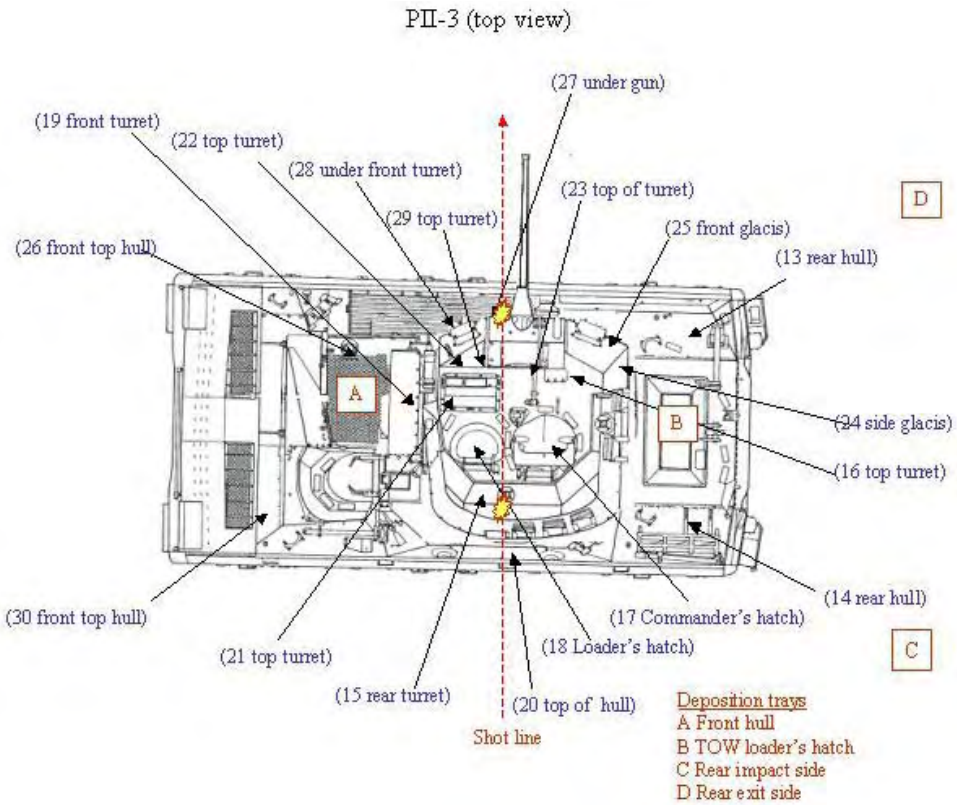

Figure F.43. PII-3 Exterior Survey, Top View

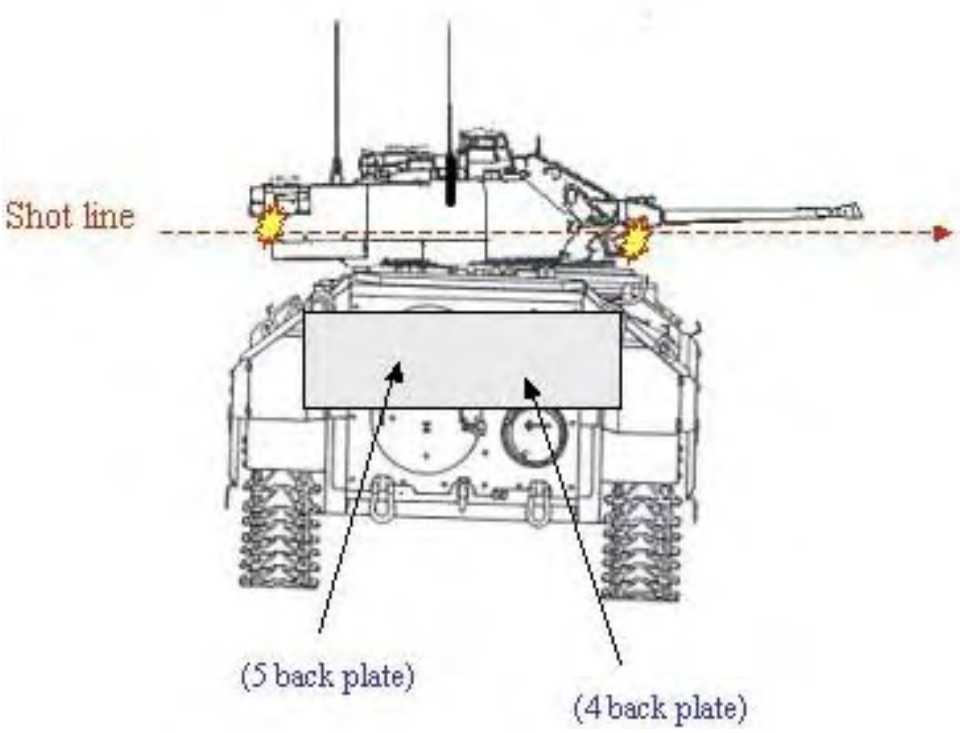

Figure F.44. PII-3 Exterior Survey, Back View

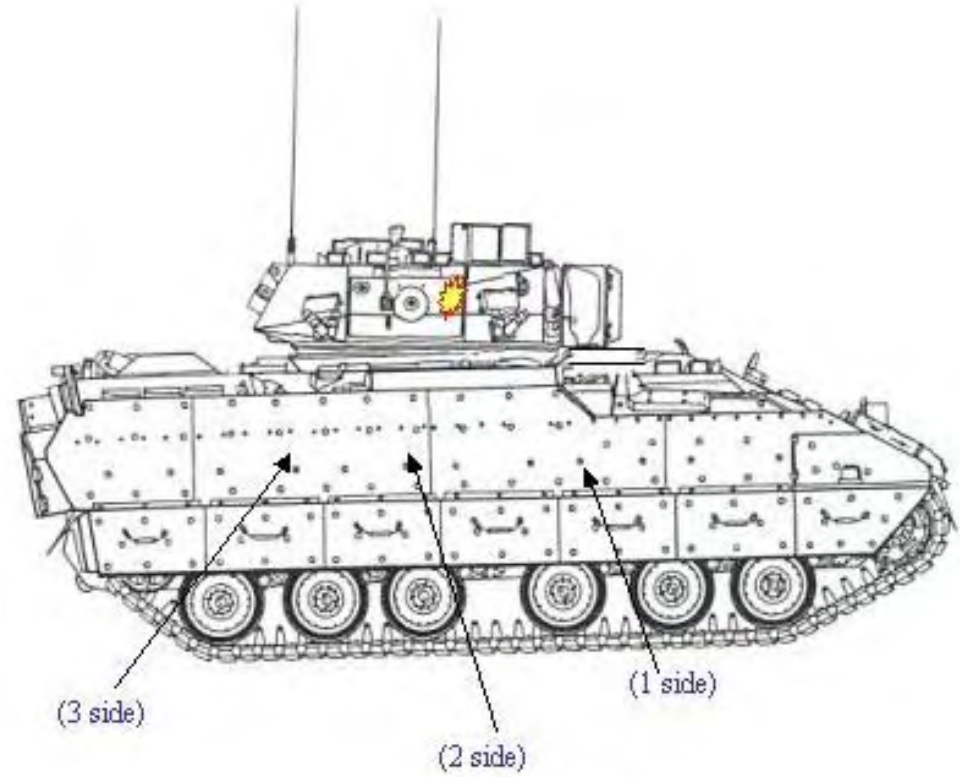

Figure F.45. PII-3 Exterior Survey, Exit Side

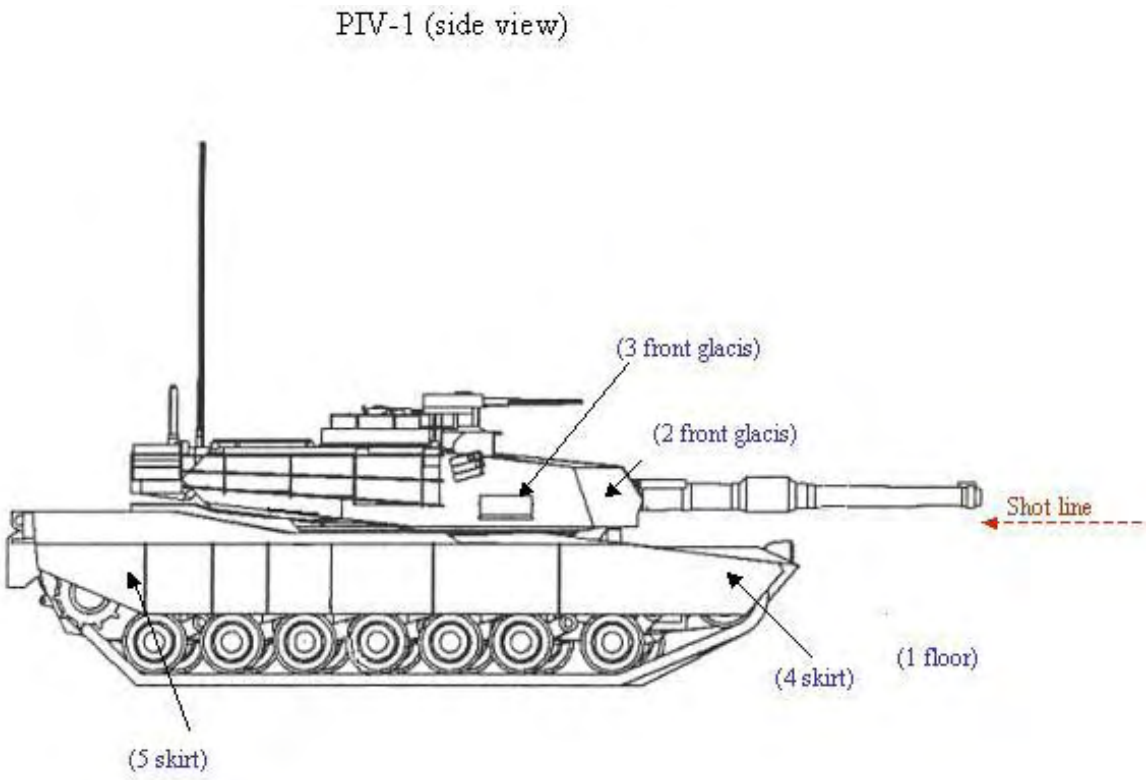

Figure F.46. PIV-1 Exterior Survey, Side Opposite Impact

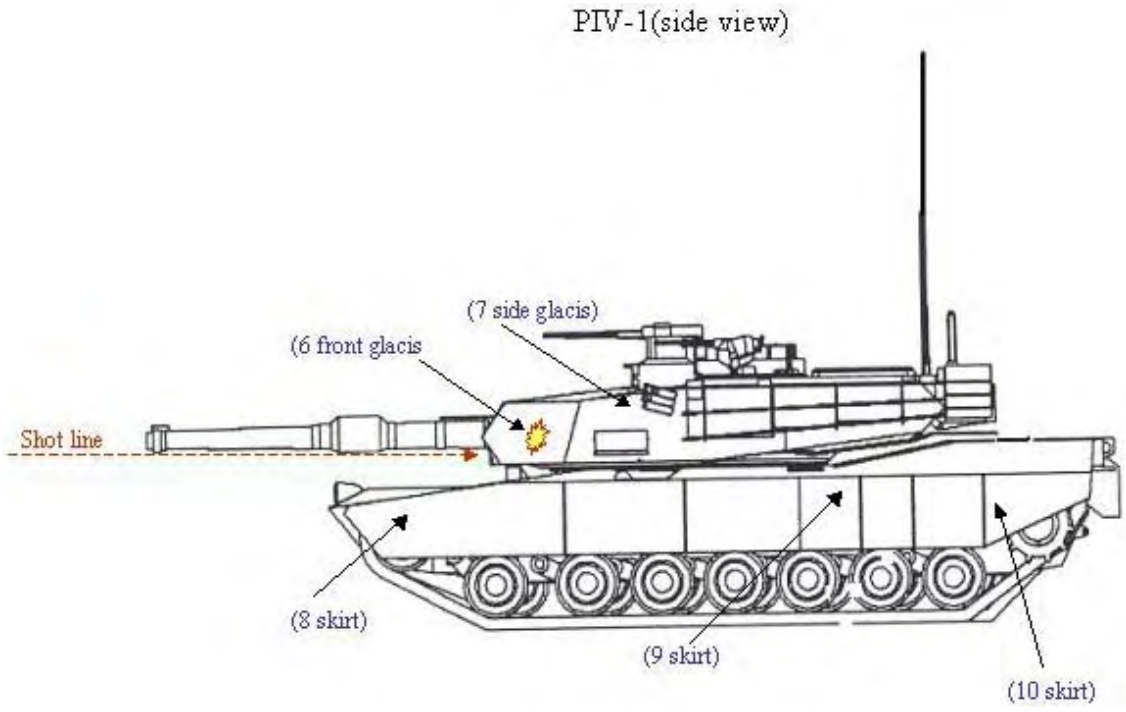

Figure F.47. PIV-1 Exterior Survey, Impact Side

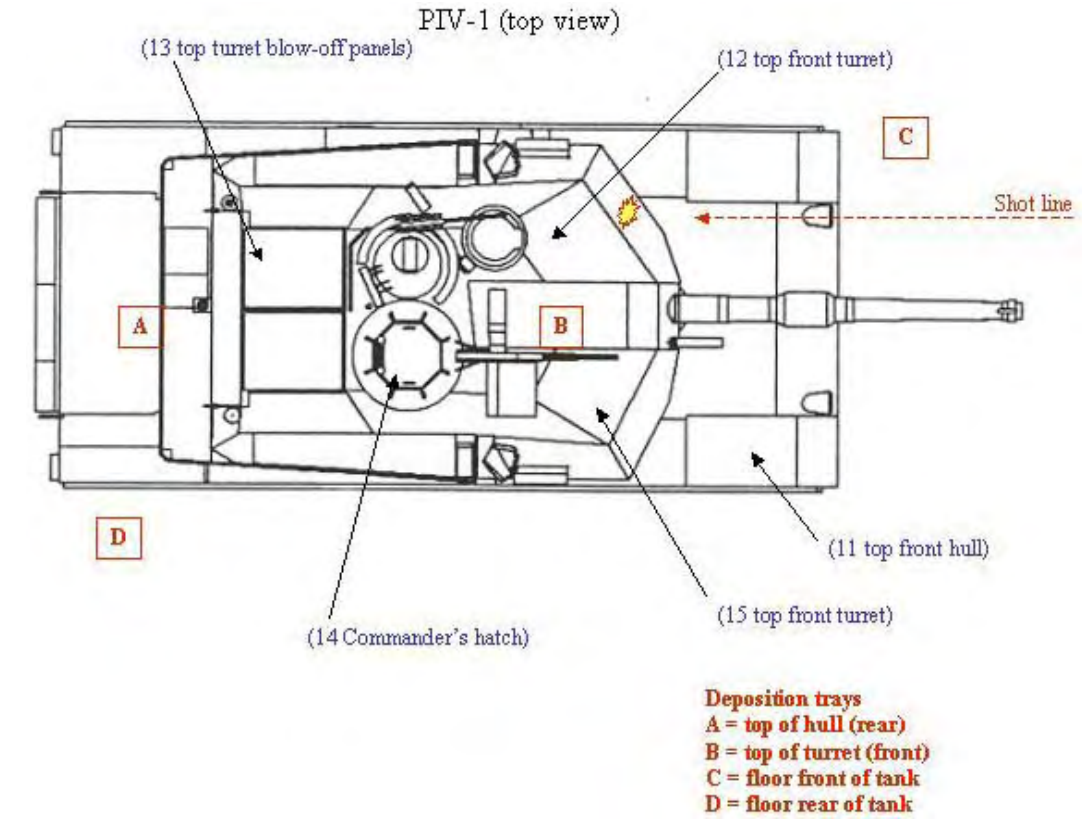

Figure F.48. PIV-1 Exterior Survey, Top View

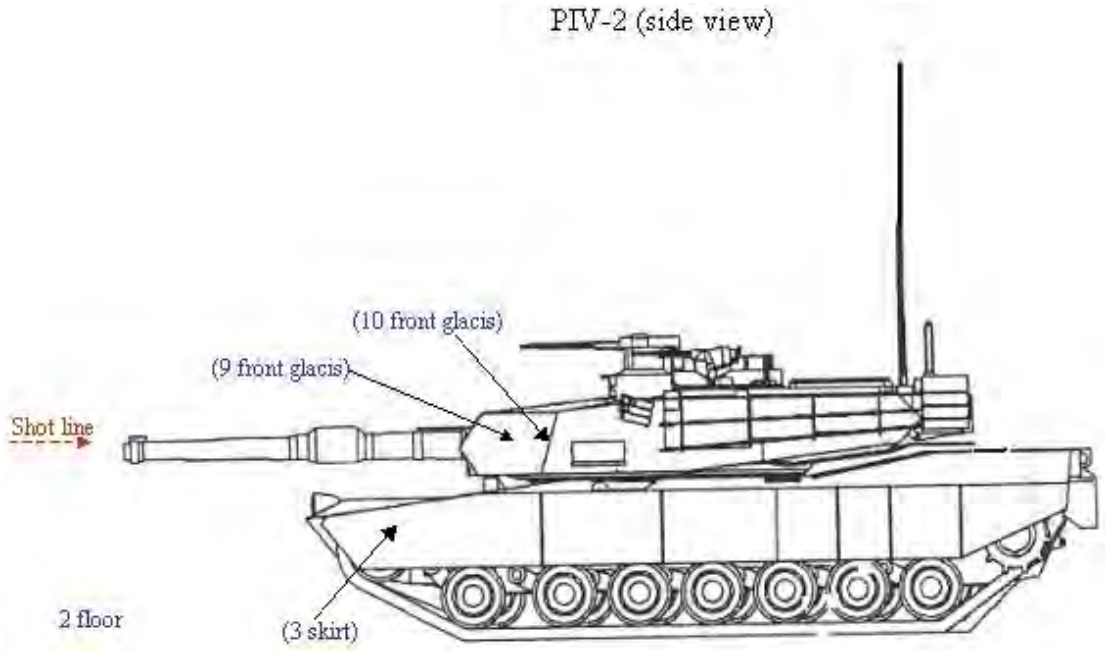

Figure F.49. PIV-2 Exterior Survey, Side View

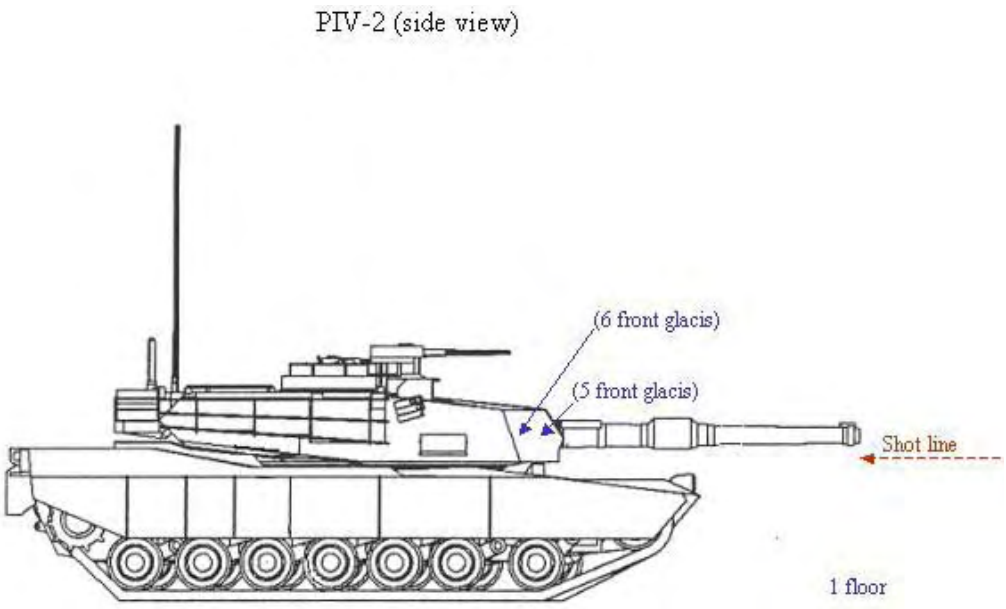

Figure F.50. PIV-2 Exterior Survey, Impact Side

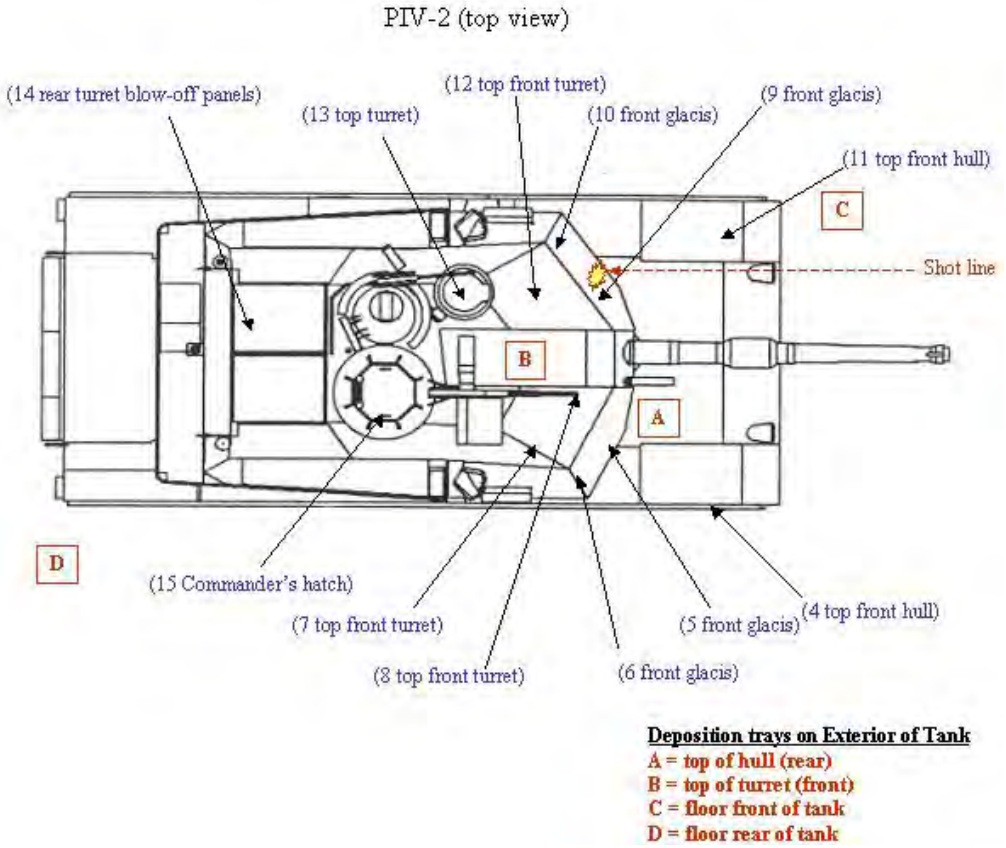

Figure F.51. PIV-2 Exterior Survey, Top View

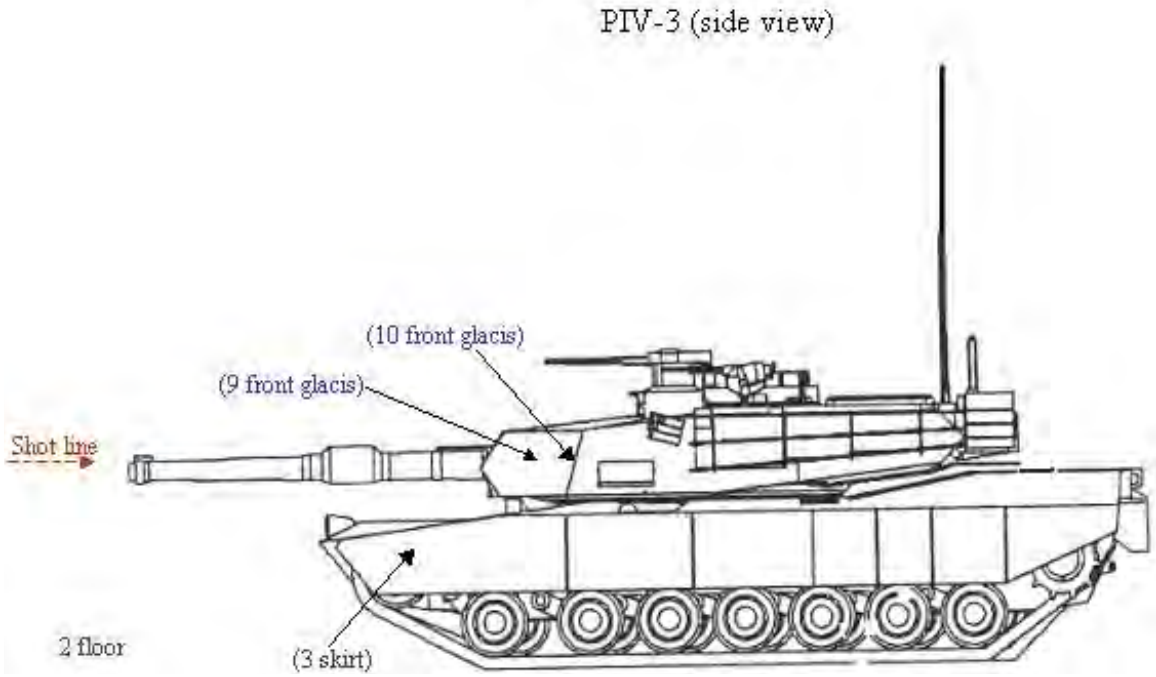

Figure F.52. PIV-3 Exterior Survey, Side View

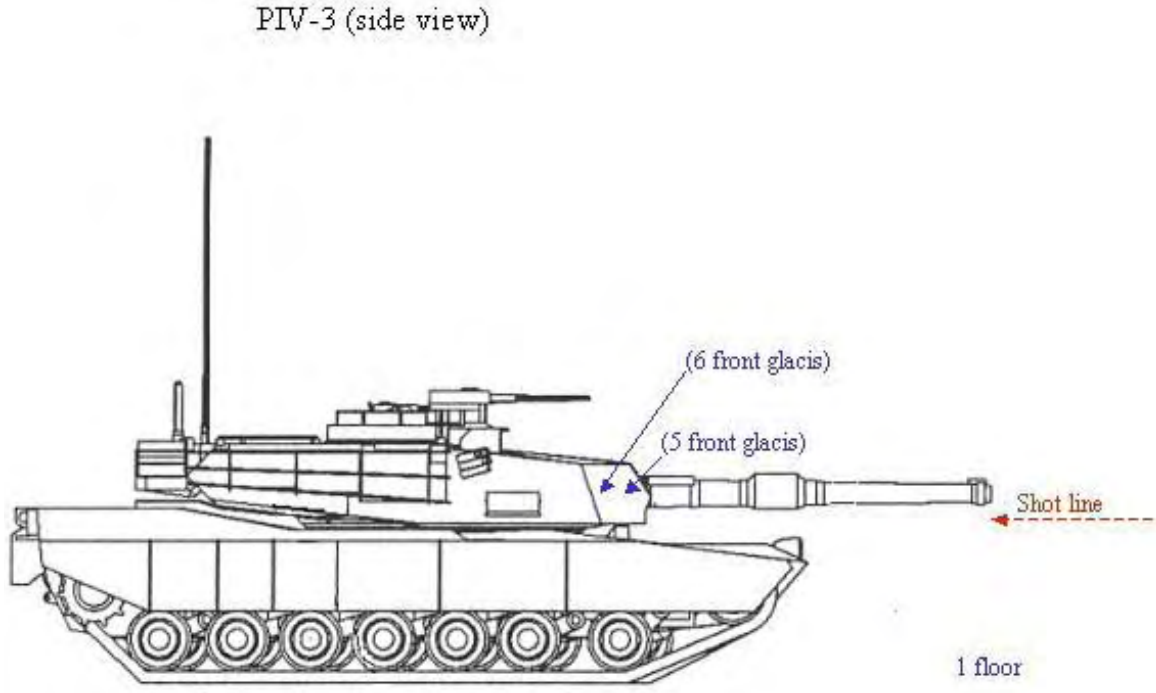

Figure F.53. PIV-3 Exterior Survey, Impact Side

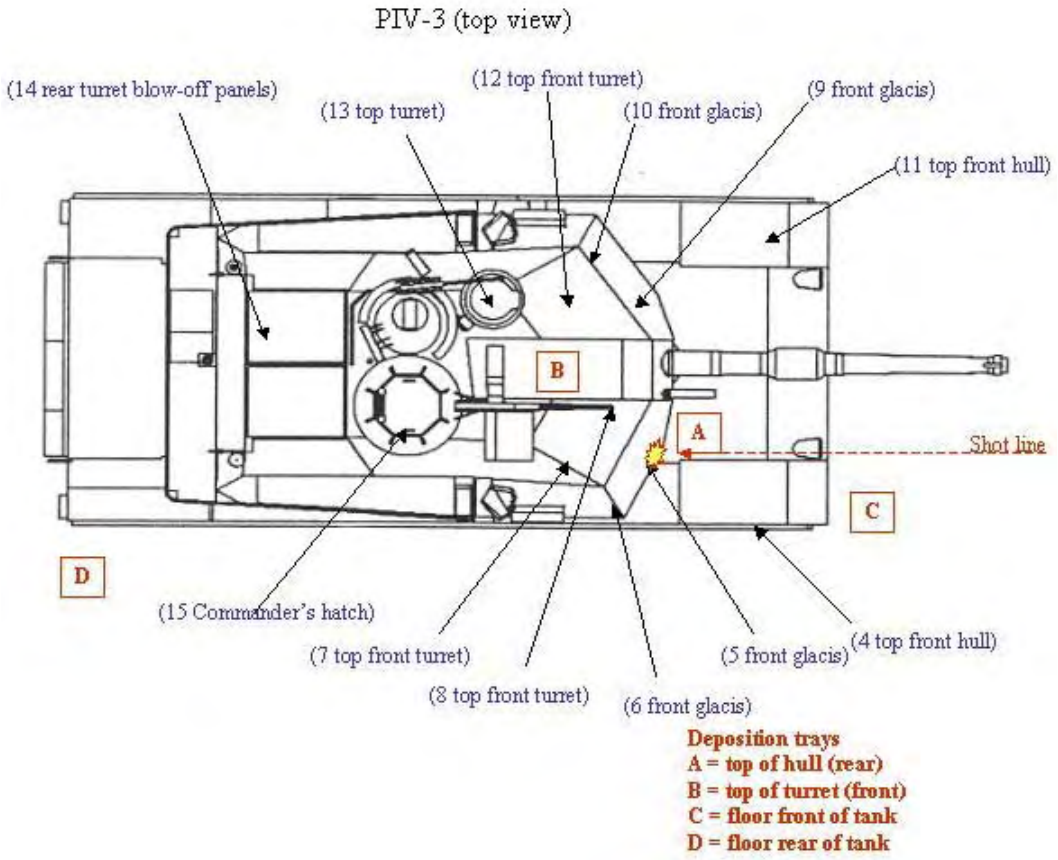

Figure F.54. PIV-3 Exterior Survey, Top View

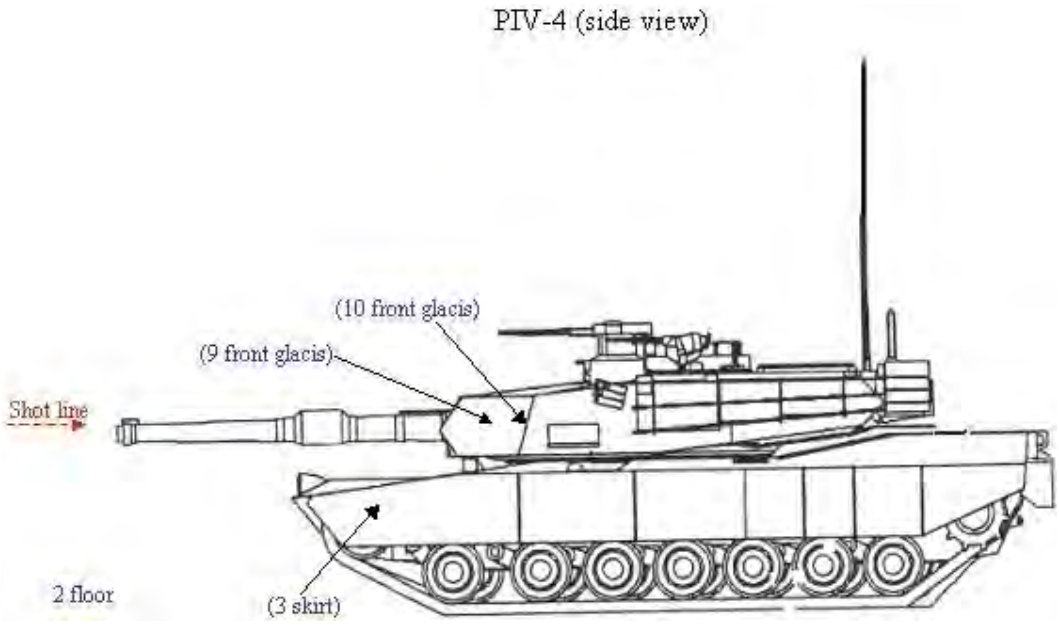

Figure F.55. PIV-4 Exterior Survey, Side View

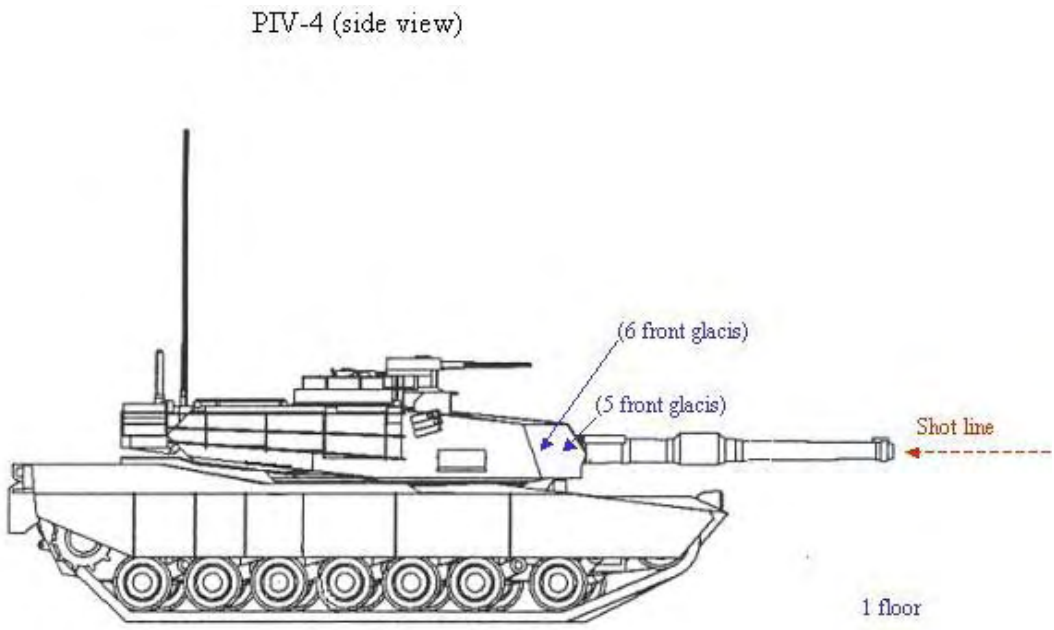

Figure F.56. PIV-4 Exterior Survey, Impact View

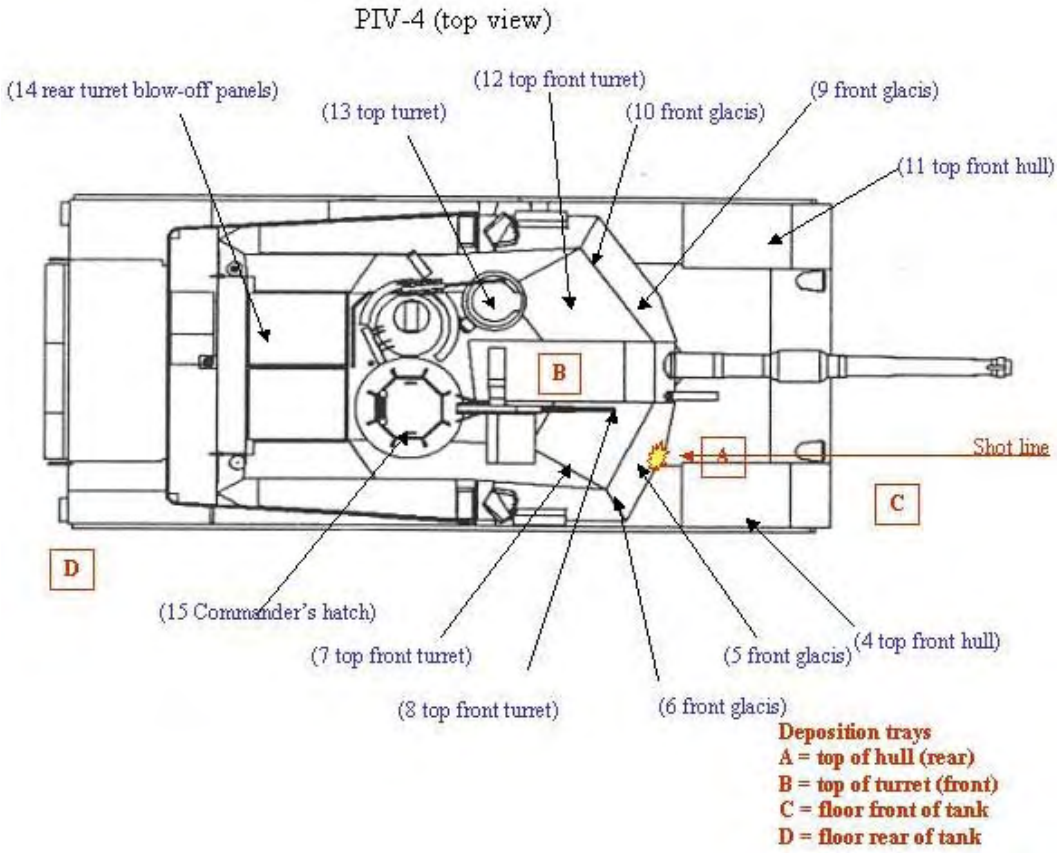

Figure F.57. PIV-4 Exterior Survey, Top View

Table F.3. Instrument Readings on Interior Vehicle Surfaces

Shot	Specific Feature	Alpha (counts)	Beta Pancake (counts)	Beta end-window open shield (mrad/hr)	Beta end-window closed shield (mrad/hr)
Phase I, Shot 1	See Table	See Table	See Table	N/A	N/A
Phase I, Shot 2	Floor under breech	316*	9,002	N/A	N/A
	Top of breech impact side	341*	300	N/A	N/A
	Ledge commander's area exit side	303*	5,960	N/A	N/A
Phase I, Shot 3/4	Floor under breech	N/A	3,003	0.201	N/A
	Top of breech exit side	N/A	3,870	0.108	N/A
	Ledge commander's area impact side	N/A	2,710	0.102	N/A
	Entry hole top	N/A	140,000	4.19	0.038
	Exit hole top	N/A	184,000	5.4	0.017
	Entry hole bottom	N/A	102,000	3.59	0.044
	Exit hole bottom	N/A	203,000	6.66	0.025
Phase I, Shot 5	Floor under breech	N/A	18,000	0.848	0.034
	Top of breech exit side	N/A	8,640	0.165	0.067
	Ledge commander's area impact side	N/A	3,220	0.104	0.09
	Hole impact side	N/A	121,000	2.43	0.026
	Hole exit side	N/A	666,000	22.1	0.058
	Breech entrance hole	N/A	493,000	16.4	0.071
	Breech exit hole	N/A	314,000	11.7	0.063
Phase I, Shot 6	Floor under breech	N/A	N/A	0.911	0.108
	Top of breech impact side	N/A	N/A	0.729	0.066
	Ledge commander's area exit side	N/A	N/A	0.398	0.022
	Hole impact side	N/A	N/A	5.29	0.069
	Hole exit side	N/A	N/A	15	0.09
	Breech entrance hole	N/A	N/A	16.2	0.173
	Breech exit hole	N/A	N/A	10.5	0.042
Phase I, Shot 7	Floor under breech	N/A	N/A	0.511	0.039
	Top of breech impact side	N/A	N/A	0.451	0.067
	Ledge commander's area exit side	N/A	N/A	0.092	0.032
	Entrance hole	N/A	N/A	2.58	0.023
	Exit hole	N/A	N/A	7.31	0.051
Phase III, Shot I	Floor under breech	N/A	N/A	1.03	0.022
	Top breech exit side	N/A	4,740	0.098	0.087
	Wall commander's area impact side	N/A	8,960	0.206	0.026
	Entrance impact hole	N/A	306,000	15.4	0.204
	Breech (gouge)	N/A	N/A	4.98	0.051
	Entrance hole on breech	N/A	320,000	10.2	0.183
	Ledge loader's area under camera window	N/A	49,800	N/A	N/A
Phase III, Shot 2	Floor under breech	N/A	25,800	1.39	0.027
	Top of breech impact side	N/A	6,160	0.377	0.048
	Wall near commander's area	N/A	8,940	0.589	0.045

Shot	Specific Feature	Alpha (counts)	Beta Pancake (counts)	Beta end-window open shield (mrad/hr)	Beta end-window closed shield (mrad/hr)
Phase III, Shot 2, cont.	Entrance hole	N/A	100,000	11.8	0.047
	Ledge next to #11 commander's area	N/A	30,500	2.41	0.048
	Breech next to #24 exit side	N/A	65,900	6.11	0.034
	Breech next to #24 entrance side	N/A	120,000	10.4	0.083
Phase II, Shot 1/2	Impact hole top	N/A	1,100	0.075	0.017
	Exit hole top	N/A	8,330	1.12	0.064
	Impact hole bottom	N/A	N/A	N/A	N/A
	Exit hole bottom	N/A	1,090	0.381	0.036
Phase II, Shot 3	Impact hole	N/A	N/A	0.028	0.031
	Exit hole	N/A	N/A	7.14	0.036
Phase IV, Shot 1	Impact hole	N/A	N/A	16.4	0.770
Phase IV, Shot 2	Next to impact hole on armor	N/A	N/A	0.34	0.28
Phase IV, Shot 3	N/A	N/A	N/A	N/A	N/A
Phase IV, Shot 4	N/A	N/A	N/A	N/A	N/A

N/A = Not Applicable. No instrument readings were attempted.

* Denotes counts in 30 sec.

Table F.4. Instrument Readings Exterior to Vehicle

Shot	Specific Feature	Alpha (counts)	Beta Pancake (counts)	Beta end-window open shield (mRad/hr)	Beta end-window closed shield (mRad/hr)
Phase I, Shot 1	See Table	See Table	See Table	N/A	N/A
Phase I, Shot 2	Top of turret above breech	148	2,004	N/A	N/A
	Exit side of turret	12	128	N/A	N/A
	Impact side of turret	75	1,007	N/A	N/A
	8:00 position between fragmentation shield and dome	21	168	N/A	N/A
	11:00 position between fragmentation shield and dome	208	1,420	N/A	N/A
	2:00 position between fragmentation shield and dome	238	1,830	N/A	N/A
	4:00 position between fragmentation shield and dome	183	1,780	N/A	N/A
	8:00 position between fragmentation shield and dome (repeat)	161	1,008	N/A	N/A
Phase I, Shot 3/4	Top of turret above breech	N/A	3,830	0.73	N/A
	Impact side of turret	N/A	1,730	0.048	N/A
	Exit side of turret	N/A	2,170	0.079	N/A
Phase I, Shot 3/4	8:00 position between fragmentation shield and dome	N/A	2,450	0.031	N/A

Shot	Specific Feature	Alpha (counts)	Beta Pancake (counts)	Beta end-window open shield (mRad/hr)	Beta end-window closed shield (mRad/hr)
	11:00 position between fragmentation shield and dome	N/A	1,280	0.044	N/A
	2:00 position between fragmentation shield and dome	N/A	2,390	0.043	N/A
	4:00 position between fragmentation shield and dome	N/A	1,860	0.047	N/A
	Top entrance hole	N/A	14,500	0.721	0.021
	Top exit hole	N/A	114,000	4.70	0.062
	Bottom entrance hole	N/A	10,400	0.385	0.013
	Bottom exit hole	N/A	65,000	234	0.046
Phase I, Shot 5	Top of turret above breech	N/A	2,720	0.065	0.056
	Impact side of turret	N/A	721	0.046	0.042
	Exit side of turret	N/A	1,870	0.048	0.048
	8:00 position between fragmentation shield and dome	N/A	1,440	0.055	0.045
	11:00 position between fragmentation shield and dome	N/A	1,360	0.043	0.042
	2:00 position between fragmentation shield and dome	N/A	1,800	0.054	0.052
	4:00 position between fragmentation shield and dome	N/A	1,850	0.048	0.045
	Entrance hole	N/A	1,340	0.252	0.016
	Exit hole	N/A	38,800	1.24	0.054
Phase I, Shot 6	Top of turret above breech	N/A	N/A	0.063	0.058
	Impact side of turret	N/A	N/A	0.037	0.033
	Exit side of turret	N/A	N/A	0.036	0.062
	8:00 position between fragmentation shield and dome	N/A	N/A	0.027	0.027
	11:00 position between fragmentation shield and dome	N/A	N/A	0.035	0.030
	2:00 position between fragmentation shield and dome	N/A	N/A	0.03	0.03
	4:00 position between fragmentation shield and dome	N/A	N/A	0.042	0.035
	Entrance hole	N/A	N/A	0.404	0.024
Phase I, Shot 6	Exit hole	N/A	N/A	0.372	0.043
Phase I, Shot 7	Top of turret above breech	N/A	N/A	0.073	0.028
	Exit side of turret	N/A	N/A	0.124	0.023
	Impact side of turret	N/A	N/A	0.066	0.021

Shot	Specific Feature	Alpha (counts)	Beta Pancake (counts)	Beta end-window open shield (mRad/hr)	Beta end-window closed shield (mRad/hr)
	8:00 position between fragmentation shield and dome	N/A	N/A	0.041	0.016
	11:00 position between fragmentation shield and dome	N/A	N/A	0.042	0.022
	2:00 position between fragmentation shield and dome	N/A	N/A	0.025	0.025
	4:00 position between fragmentation shield and dome	N/A	N/A	0.027	0.020
	Entrance hole	N/A	N/A	2.33	0.036
	Exit hole	N/A	N/A	3.80	0.065
Phase III, Shot I	Top of turret above breech	N/A	1,660	0.155	0.130
	Impact side of turret	N/A	1,780	0.324	0.249
	Opposite impact side of turret	N/A	N/A	0.045	0.035
	Entrance hole	N/A	288,000	13.6	1.30
Phase III, Shot 2	Top of turret above breech	N/A	2,150	0.272	0.163
	Impact side of turret	N/A	127,000	0.350	0.319
	Opposite impact side of turret	N/A	185	0.026	0.025
	8:00 position between fragmentation shield and dome	N/A	472	0.031	0.018
	4:00 position between fragmentation shield and dome	N/A	742	0.029	0.024
	Entrance hole	N/A	93,900	11.7	0.895
Phase II Shot 1/2	Impact side hull	N/A	154	0.021	0.022
	Exit side hull	N/A	740	0.042	0.040
	Top entrance hole	N/A	2,670	0.314	0.026
	Top exit hole	N/A	23,700	2.43	0.064
	Bottom entrance hole	N/A	2,100	0.261	0.023
	Bottom exit hole	N/A	14,200	1.26	0.057
Phase II, Shot 3	Entrance hole	N/A	N/A	0.07	2.8
	Exit hole	N/A	N/A	0.052	0.02
Phase IV, Shot 1	Entrance hole	N/A	N/A	N/A	N/A
Phase IV, Shot 2	Entrance hole	N/A	N/A	12.7	0.541
	Gouge	N/A	N/A	0.461	0.474
Phase IV, Shot 3	Front turret near impact	N/A	N/A	0.4	0.37
Phase IV, Shot 4	Front turret near impact	N/A	147	0.037	0.036

N/A = Not Applicable. No instrument readings were attempted.

Table F.5. Phase I, Shot 1, Instrument Readings Vehicle Interior

Location	Specific Feature	Alpha (counts)	Beta Pancake (counts)
PI-1I-IW-1	Floor driver's area	12	6,680
PI-1I-IW-2	Wall in drivers' area	16	822
PI-1I-IW-3	Floor loader's area	33	9,340
PI-1I-IW-4	Wall loader's area	16	4,020
PI-1I-IW-5	Wall loader's area	8	2,240
PI-1I-IW-6	Ledge loader's area	8	1,610
PI-1I-IW-7	Floor loader's area	N/A	N/A
PI-1I-IW-8	Top of louver	N/A	N/A
PI-1I-IW-9	Face of louver	N/A	N/A
PI-1I-IW-10	Wall brace facing loader	16	1,380
PI-1I-IW-11	Wall under camera	37	2,000
PI-1I-IW-12	Foot rest commander	24	11,500
PI-1I-IW-13	Ledge commander's area	N/A	N/A
PI-1I-IW-14	Hull floor in commander's area	24	14,400
PI-1I-IW-15	Top of louver	N/A	N/A
PI-1I-IW-16	Face of louver	N/A	N/A
PI-1I-IW-17	Next to exit hole	8	37,800
PI-1I-IW-18	Wall gunner's area	8	2,400
PI-1I-IW-19	Floor gunner's area	41	17,800
PI-1I-IW-20	Ledge gunner's area	288	15,700
PI-1I-IW-21	Floor gunner's area	N/A	N/A
PI-1I-IW-22	Top of louver	N/A	N/A
PI-1I-IW-23	Face of louver	N/A	N/A
PI-1I-IW-24	Top of breech	N/A	N/A
PI-1I-IW-25	Impact side of breech	N/A	N/A
PI-1I-IW-26	Hull floor impact side	92	16,100
PI-1I-IW-27	Ledge impact side	16	16,000
PI-1I-IW-28	Wall impact side	96	902
PI-1I-IW-29	Wall impact side	N/A	N/A
PI-1I-IW-30	Entry impact hole	N/A	N/A
PI-1I-IW-31	Ceiling	N/A	N/A
PI-1I-IW-32	Lower wall impact side	N/A	N/A

N/A = Not Applicable. No instrument readings were attempted.

Table F.6. Phase I, Shot 1, Instrument Reading Exterior to the Vehicle

Location	Specific Feature	Alpha (counts)	Beta Pancake (counts)
PI-1E-IW-1	Turret impact side	29	496
PI-1E-IW-2	Turret impact side	71	638
PI-1E-IW-3	Turret impact side	70	1,420
PI-1E-IW-4	Turret impact side	N/A	N/A
PI-1E-IW-5	Turret impact side	N/A	N/A
PI-1E-IW-6	Hull horizontal under turret	N/A	N/A
PI-1E-IW-7	Hull metal plate horizontal	37	732
PI-1E-IW-8	Hull horizontal on top of fender	45	999
PI-1E-IW-9	Hull metal plate horizontal	N/A	N/A
PI-1E-IW-10	Hull metal plate horizontal	N/A	N/A
PI-1E-IW-11	Turret exit side	N/A	N/A
PI-1E-IW-12	Turret exit side	N/A	N/A
PI-1E-IW-13	Turret exit side	88	1,310
PI-1E-IW-14	Turret exit side	N/A	N/A
PI-1E-IW-15	Turret exit side	N/A	N/A
PI-1E-IW-16	Hull metal plate	N/A	N/A
PI-1E-IW-17	Hull metal plate	41	626
PI-1E-IW-18	Hull top of fender horizontal	113	906
PI-1E-IW-19	Hull metal plate	N/A	N/A
PI-1E-IW-20	Hull metal plate	152	1,700
PI-1E-IW-21	Rear hull top impact side	88	1,350
PI-1E-IW-22	Rear hull top exit side	164	1,530
PI-1E-IW-23	Top front turret top impact side	N/A	N/A
PI-1E-IW-24	Top front turret over breech	198	1,180
PI-1E-IW-25	Top front turret exit side	N/A	N/A
PI-1E-IW-26	Top back turret impact side	N/A	N/A
PI-1E-IW-27	Top turret on commander's hatch	25	1,720
PI-1E-IW-28	Top rear turret center	N/A	N/A
PI-1E-IW-29	Top hull impact side	58	1,840
PI-1E-IW-30	Top hull exit side	N/A	N/A

N/A = Not Applicable. No instrument readings were attempted.

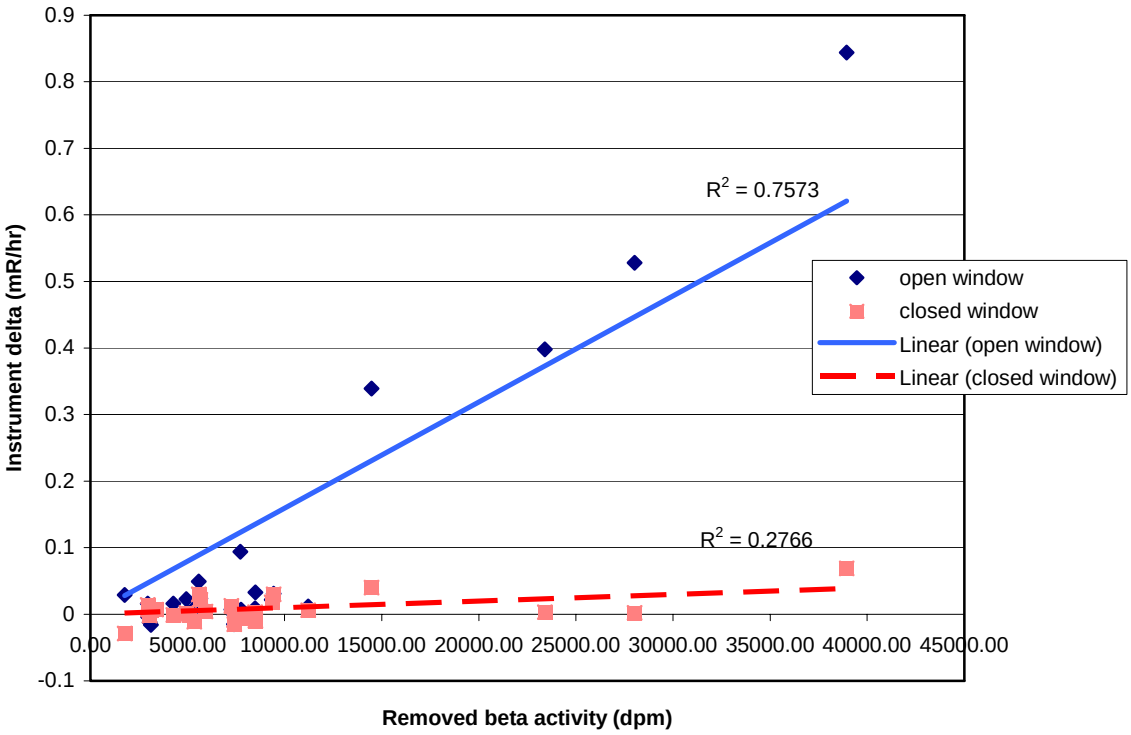

Figure F.58. Relationship Between Readings Using an AN/PDR-77 Beta-Gamma Pancake Probe and Gross Beta Removable Wipes

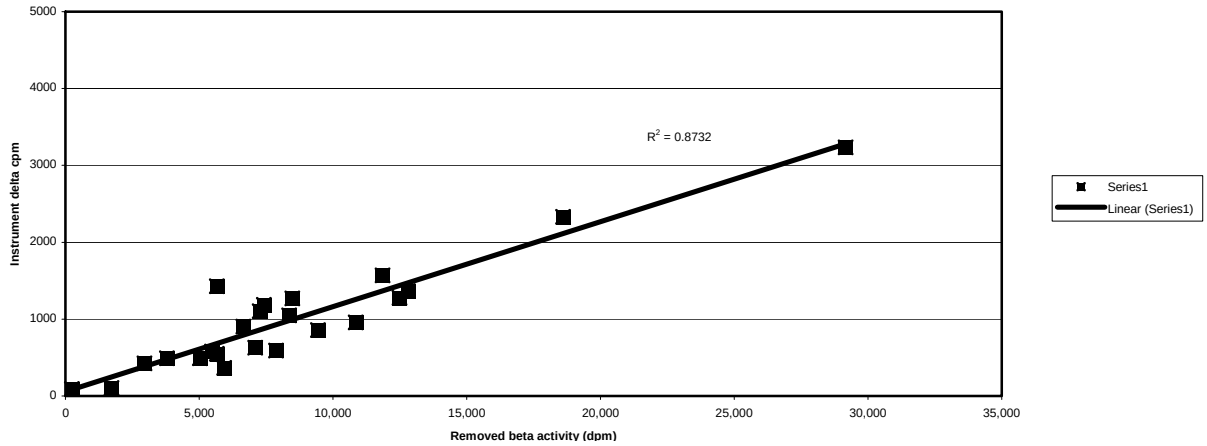

Figure F.59. Relationship Between Readings Using AN/PDR-77 End-Window Beta-Gamma Probe and Gross Beta Removable Wipes

Appendix G

Target Vehicle Ventilation

Appendix G

Target Vehicle Ventilation

The target vehicles used in the Capstone DU Aerosol Study were ballistic hulls and turrets (BHTs) that had been stripped of instrumentation, flammable material, and fixtures that would impede access to aerosol samplers (e.g., seats). As a result, the air volume inside the turret (and passenger compartment in the Bradley vehicle) was considerably larger inside the test BHT than in functional vehicles. To assist with extrapolation of the volume of air exchange of the BHTs to functional vehicles, the volume change per hour was measured for in BHT and in functional Abrams tanks and a Bradley vehicle. In addition, the volume changes per hour were measured for the functional vehicles both with and without ventilation systems operating and hatches open to determine the impact of these conditions on air exchange rates. Results of these analyses are summarized in Section 4.5.6.

The air exchange rates were measured by introducing a small quantity of an inert tracer gas (sulfur hexafluoride [SF_6)]) into the containment in which the air exchange is to be measured. The concentration of the SF_6 is measured *in situ* using a dedicated electron-capture gas chromatograph.[a] By serially measuring the concentration of SF_6, the decay rate can be calculated from the equation $I=1/t \ln(C_0/C_t)$, where I is the containment air exchange rate, t is time of measurement, and C_0 and C_t are the initial and final tracer concentrations, respectively.

Functional Vehicle Testing. The ventilation rates were measured using the SF_6 trace-gas technique in three Abrams tanks (M1, M1A1, and M1A2 models) and in a Bradley vehicle. Measurements also were performed in test vehicles during each shot. Figures G.1 to G.3 show SF_6 decay as a function of time in the tests with the M1, M1A1, and M1A2 Abrams tanks. Fast decay indicates higher ventilation rates because the SF_6 was removed from the vehicle by air exchanged with the outside atmosphere. The ventilation rate constant in terms of the vehicle volume per hour was estimated by fitting data with the exponential decay function. The rate constant of the exponential function was the ventilation or air exchange rate. Ventilation rates for the Abrams tanks are listed in Table G.1 (also shown in Table 4.23). The ventilation rates were lowest when the fan was off and the hatches were closed, thus restricting the airflow. Ventilation rates were higher when either the fan was on or the hatch was open. Of the three Abrams tanks, the M1A1 and M1A2 models had much lower ventilation rates than the M1 model when the hatches were closed.

The Bradley vehicle was tested under three conditions: 1) with the internal fan off and the hatches closed, 2) with the fan on and the hatches closed, and 3) with the fan off and the commander's hatches open. Figure G.4 shows SF_6 decay as a function of time for the test, and Table G.1 lists the estimated ventilation rates for the Bradley vehicle. Even when the hatches were closed and the internal fan was off, the ventilation in the Bradley vehicle was greater than in the Abrams tanks. When the internal fan was on, the ventilation rates were significantly higher than when the fans were off.

BHT Vehicle Testing. During the penetrator test inside the Superbox, SF_6 was released about 40 to 60 min prior to the shot. Figure G.5 shows the recorded SF_6 concentrations. In the first 20 min, the concentration increased with time after the SF_6 was injected into the vehicle. The concentration

[a] Model 101 Autotrac; Lagus Applied Technology Inc., San Diego, California.

decreased between 20 min to 1 h and 10 min, because of the air exchange. At 1 h, 10 min, the shot was fired, and the SF_6 concentration increased rather than decreased. This result was totally unexpected. It may have been caused by interference from combustion gases or vapors after the penetrator entered the vehicle. However, the real reason is not known. The concentration decreased at 3 h and 20 min after the test shot was fired and the ventilation system inside the Superbox was turned on. Similar curves were obtained in every test as shown in Figures G.6 and G.7 for the Phase-II and Phase-III tests. Therefore, the ventilation rate after the shot was fired could not be estimated although the ventilation rate before the impact could be estimated as shown in Table G.2 (also shown in Table 4.24). The Phase-I and -III studies used an Abrams BHT. The measured ventilation rate was between 2.7 and 7.2 volume exchanges per hour, which were in the same range as those for the M1A1 and M1A2 vehicles when the hatch was open (Table G.1). On the other hand, the Phase-II study used a Bradley vehicle, and the only measured ventilation rate of 33.9 exchanges per hour was similar to test results with the fan on and the hatch closed.

Table G.1. Ventilation Rate (1/h) for Abrams Tanks and Bradley Vehicle

G.1.1 M1 Tank					
Fan OFF	**Exchange**	**Fan ON**	**Exchange**	**Fan OFF**	**Exchange**
Hatches Closed	**Rate**	**Hatches Closed**	**Rate**	**Hatches Open**	**Rate**
1	6.02	1	7.51	1	19.69
2	3.90	2	7.38	2	18.23
3	4.18	--	--	--	--
G.1.2 M1A1 Tank					
1	1.17	1	6.59	1	2.96
2	1.09	2	6.58	2	2.86
G.1.3 M1A2 Tank					
1	0.27	1	n/a	1	4.83
2	0.23	2	n/a	2	5.63
G.1.4 Bradley Fighting Vehicle					
1	7.66	1	45.27	1	7.14
2	11.51	2	34.57	2	9.21

Table G.2. Ventilation Rate (1/h) for Phases I, II, and III

G.1.5 Phase/Shot	**Air Exchange Rate (volumes per hour)**
PI-1	2.98
PI-2	3.49
PI-3/4	2.70
PI-5	n/a
PI-6	n/a
PI-7	7.15
PII-1/2	n/a
PII-3	33.86
PIII-1	5.55
PIII-2	6.28

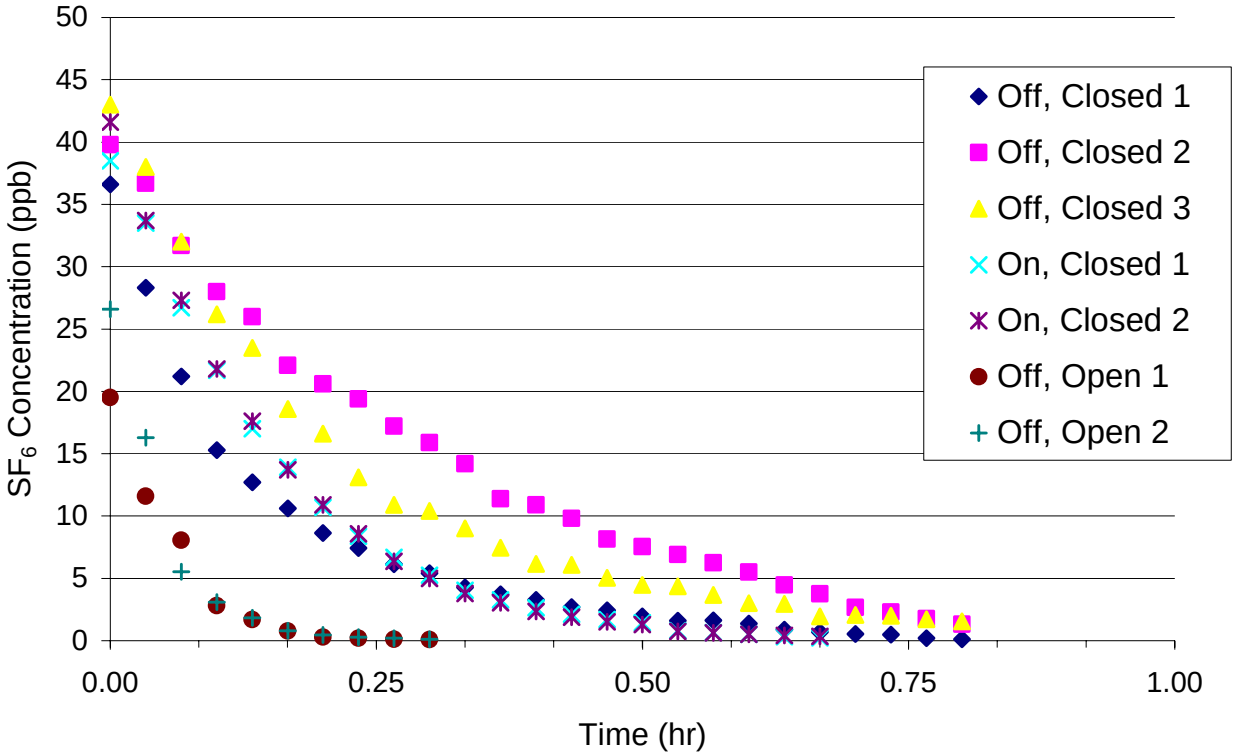

Figure G.1. SF_6 Decay with Time in the M1 Abrams Tank

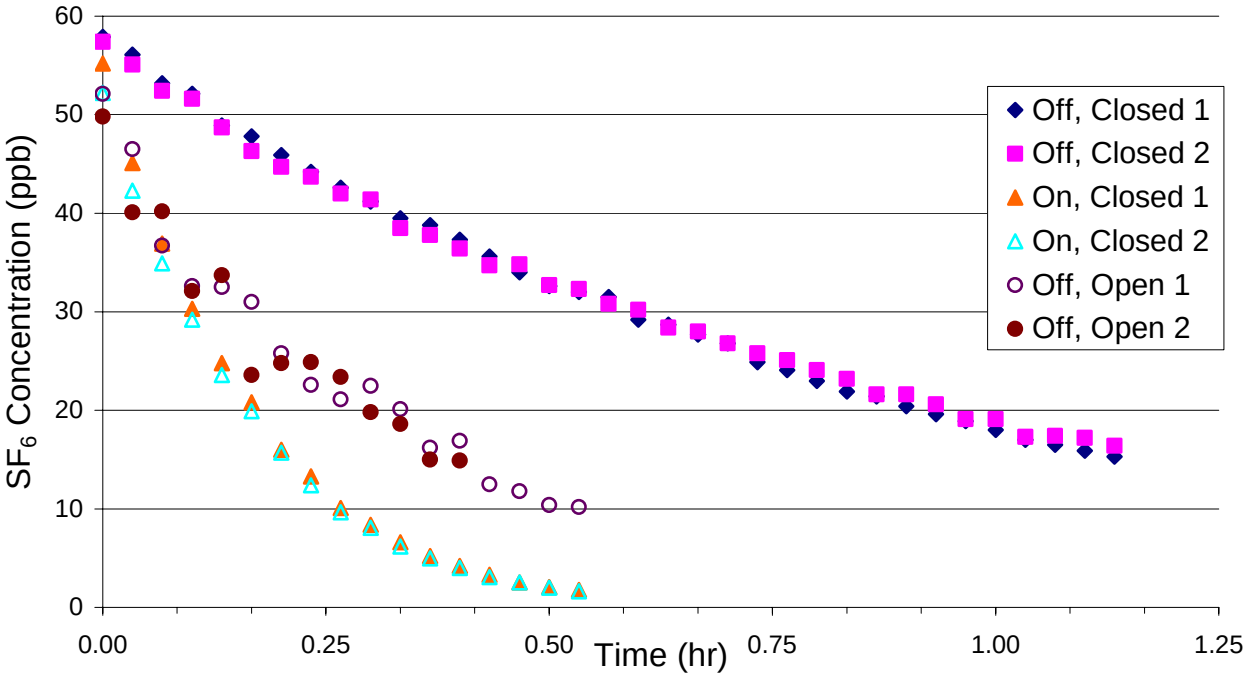

Figure G.2. SF_6 Decay with Time in the M1A1 Abrams Tank

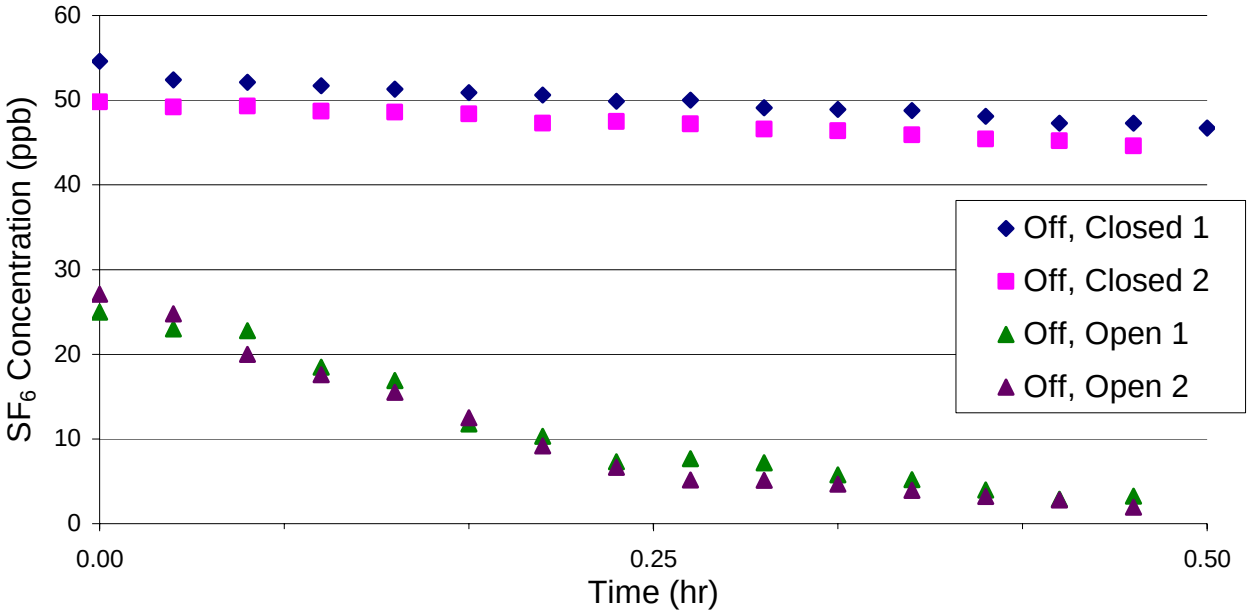

Figure G.3. SF_6 Decay with Time in the M1A2 Abrams Tank

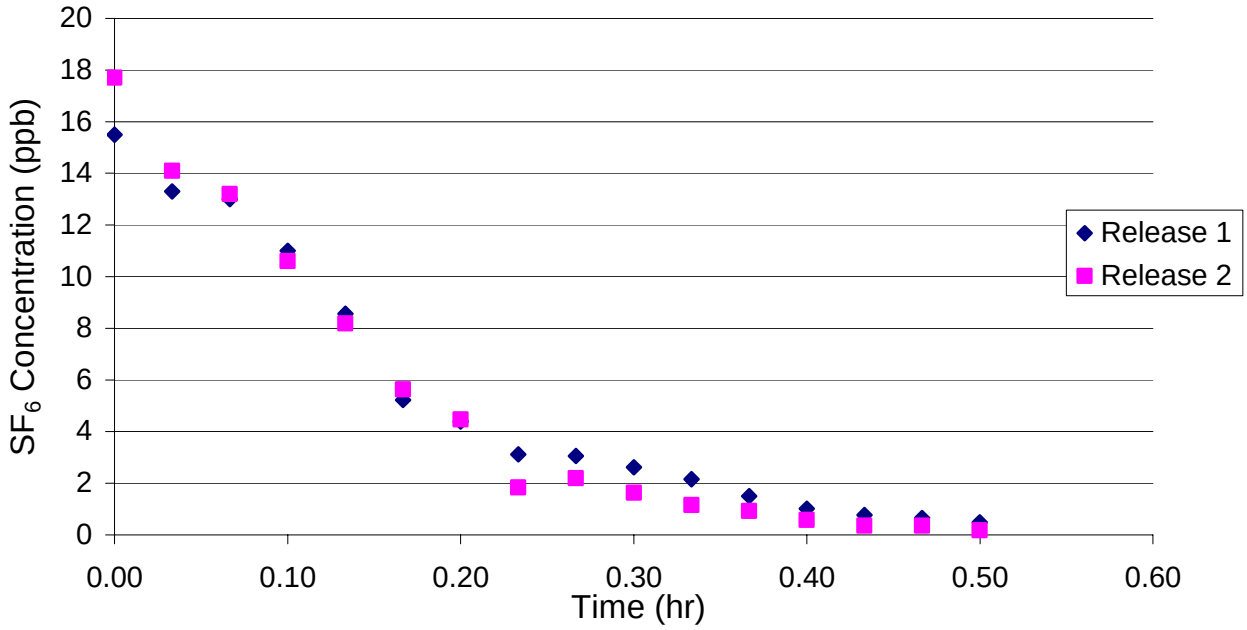

Figure G.4. SF_6 Decay with Time in the Bradley Vehicle, Fan Off, Commander's Hatch Open

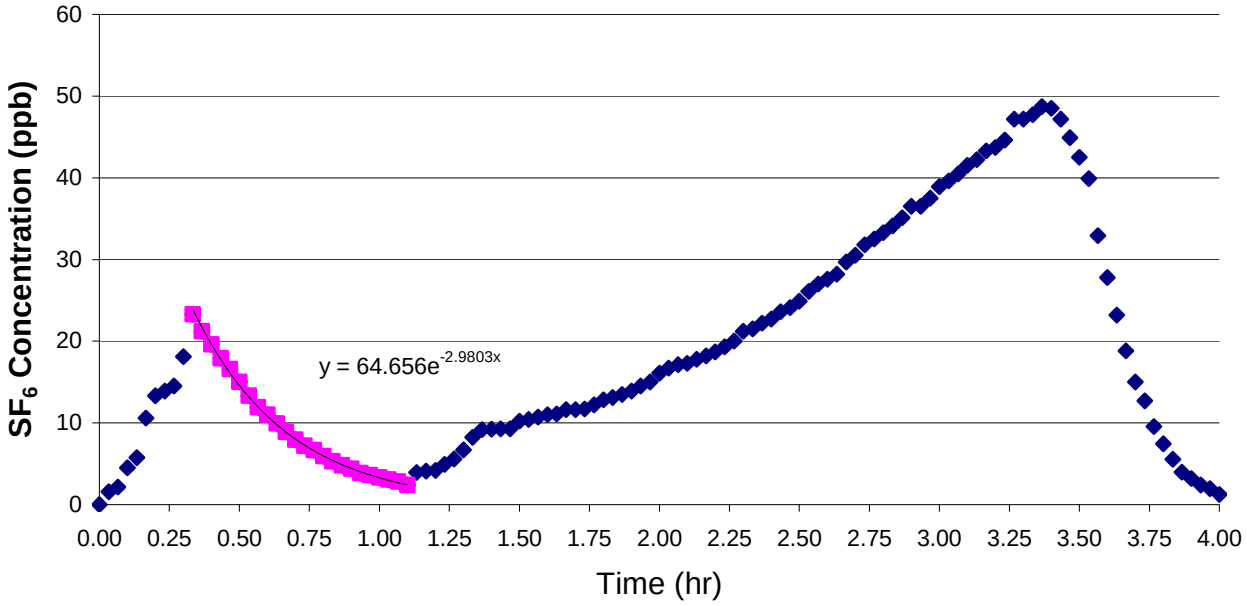

Figure G.5. SF_6 Decay as a Function of Time during the PI-1 Test

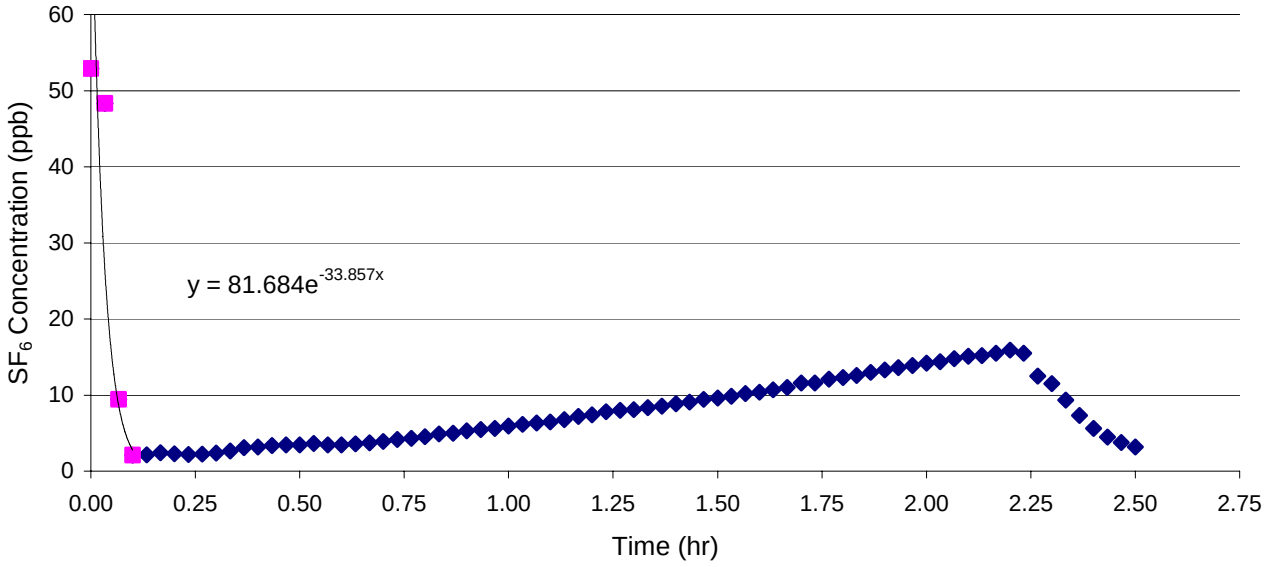

Figure G.6. SF_6 Decay as a Function of Time during the PII-3 Test

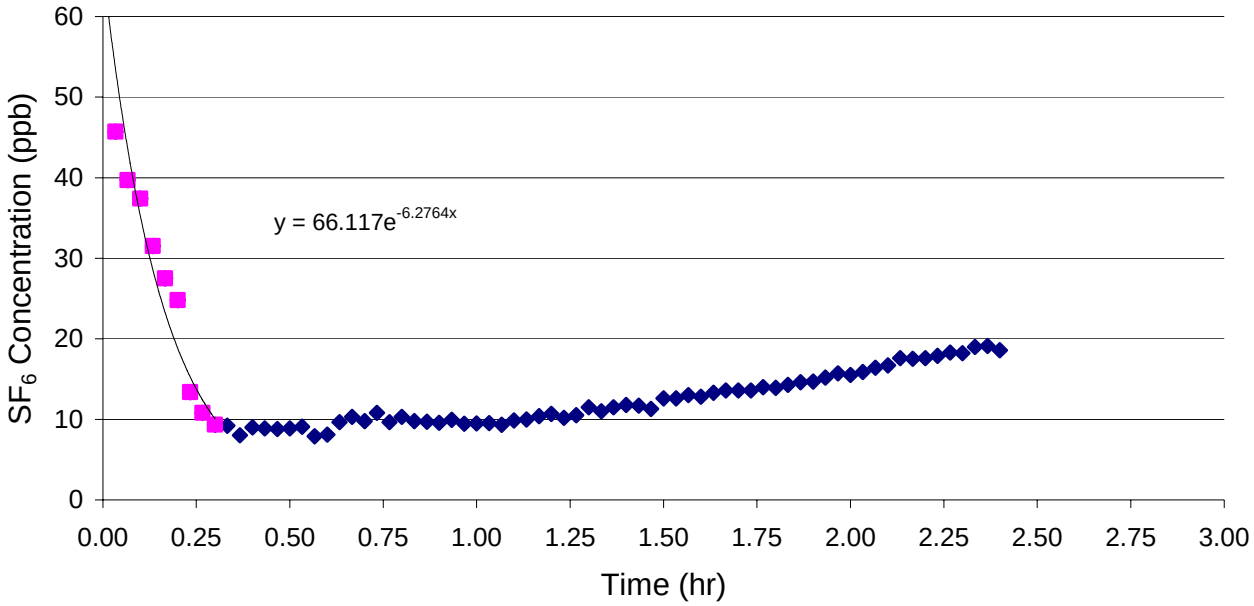

Figure G.7. SF_6 Decay as a Function of Time During the PIII-2 Test